VOLUME 28 / NUMBER 5
MARCH 8, 1990
ACC. NOS. N90-13323 TO N90-14183

STAR

AN ABSTRACT JOURNAL

Scientific and Technical Aerospace Reports

PRODUCED BY THE
SCIENTIFIC AND TECHNICAL
INFORMATION
DIVISION

NASA

NATIONAL AERONAUTICS AND SPACE ADMINISTRATION

WHAT YOU CAN DO FOR *STAR*

All users of this abstract service are urged to forward reports to be considered for announcement in *STAR*. This will aid NASA in its efforts to provide the fullest possible coverage of all scientific and technical publications that might support aeronautics and space research and development. If you have prepared relevant reports (other than those that you will transmit to NASA, DOD, or DOE through the usual contract- or grant-reporting channels), please send them for consideration to the NASA Scientific and Technical Information Facility, P.O. Box 8757, BWI Airport, MD 21240.

Reprints of journal articles, book chapters, and conference papers are also welcome. These will be considered for announcement in *STAR's* companion journal, *International Aerospace Abstracts*.

You may specify a particular source to be included in a report announcement if you wish; otherwise the report will be placed on public sale at the National Technical Information Service. Copyrighted publications will be announced but not distributed or sold.

PURCHASE OF *STAR*

The semimonthly issues are available to registered users on annual subscription from the NASA Scientific and Technical Information Facility, ATTN: Registration Services, P.O. Box 8757, BWI Airport, MD 21240. *STAR* is publicly available on annual subscription from the Superintendent of Documents, U.S. Government Printing Office, Washington, DC 20402.

PUBLISHED BY:

UNITED STATES GOVERNMENT
NATIONAL AERONAUTICS AND SPACE ADMINISTRATION
SCIENTIFIC AND TECHNICAL INFORMATION DIVISION
Scientific and Technical Aerospace Reports, Volume 28, is prepared by the NASA Scientific and Technical Information Facility operated for the National Aeronautics and Space Administration by RMS Associates.

The Administrator of the National Aeronautics and Space Administration has determined that the publication of this periodical is necessary in the transaction of the public business required by law of this agency. Use of funds for printing this periodical has been approved by the Director of the Office of Management and Budget through March 22, 1991.

US ISSN 0036-8741

Scientific and Technical Aerospace Reports (STAR) is issued twice a month and contains abstracts and indexes of meeting papers, conference proceedings, and unlimited distribution reports that have been added to the NASA Scientific and Technical Information Database during the preceding period. These citations may also be accessed online via NASA/RECON or via AIAA's Aerospace Database (File 108) through Dialog Information Services, Inc.

STAR subject coverage includes all aerospace-related areas that will help NASA achieve its mission. Material is gathered from all over the world and includes significant input from many countries under exchange and access agreements.

Consult the indexes at the back of this volume to help zero in on what you are looking for. These include:

Subject Index
Personal Author Index
Corporate Source Index
Contract Number Index
Report/Accession Number Index

STAR's companion abstract journal *International Aerospace Abstracts* should be used if you are looking for references to periodicals, books, and published meeting papers or conference proceedings.

Questions and comments should be addressed to:

NASA Scientific and Technical Information Facility
User Services
P.O. Box 8757
BWI Airport, MD 21240
301-621-0150

VOLUME 28 NUMBER 5 / MARCH 8, 1990

TABLE OF CONTENTS

AERONAUTICS

Includes aeronautics (general); aerodynamics; air transportation and safety; aircraft communications and navigation; aircraft design, testing and performance; aircraft instrumentation; aircraft propulsion and power; aircraft stability and control; and research and support facilities (air).

For related information see also *Astronautics.*

01 AERONAUTICS (GENERAL) 571

02 AERODYNAMICS 571

Includes aerodynamics of bodies, combinations, wings, rotors, and control surfaces; and internal flow in ducts and turbomachinery.

For related information see also *34 Fluid Mechanics and Heat Transfer.*

03 AIR TRANSPORTATION AND SAFETY 576

Includes passenger and cargo air transport operations; and aircraft accidents.

For related information see also *16 Space Transportation* and *85 Urban Technology and Transportation.*

04 AIRCRAFT COMMUNICATIONS AND NAVIGATION 577

Includes digital and voice communication with aircraft; air navigation systems (satellite and ground based); and air traffic control.

For related information see also *17 Space Communications, Spacecraft Communications, Command and Tracking* and *32 Communications and Radar.*

05 AIRCRAFT DESIGN, TESTING AND PERFORMANCE 578

Includes aircraft simulation technology.

For related information see also *18 Spacecraft Design, Testing and Performance* and *39 Structural Mechanics.* For land transportation vehicles see *85 Urban Technology and Transportation.*

06 AIRCRAFT INSTRUMENTATION 580

Includes cockpit and cabin display devices; and flight instruments.

For related information see also *19 Spacecraft Instrumentation* and *35 Instrumentation and Photography.*

07 AIRCRAFT PROPULSION AND POWER 581

Includes prime propulsion systems and systems components, e.g., gas turbine engines and compressors; and onboard auxiliary power plants for aircraft.

For related information see also *20 Spacecraft Propulsion and Power, 28 Propellants and Fuels,* and *44 Energy Production and Conversion.*

08 AIRCRAFT STABILITY AND CONTROL 583

Includes aircraft handling qualities; piloting; flight controls; and autopilots.

For related information see also *05 Aircraft Design, Testing and Performance.*

09 RESEARCH AND SUPPORT FACILITIES (AIR) 584

Includes airports, hangars and runways; aircraft repair and overhaul facilities; wind tunnels; shock tubes; and aircraft engine test stands.

For related information see also *14 Ground Support Systems and Facilities (Space).*

ASTRONAUTICS

Includes astronautics (general); astrodynamics; ground support systems and facilities (space); launch vehicles and space vehicles; space transportation; space communications, spacecraft communications, command and tracking; spacecraft design, testing and performance; spacecraft instrumentation; and spacecraft propulsion and power.

For related information see also *Aeronautics.*

12 ASTRONAUTICS (GENERAL) 585

For extraterrestrial exploration see *91 Lunar and Planetary Exploration.*

13 ASTRODYNAMICS 586

Includes powered and free-flight trajectories; and orbital and launching dynamics.

14 GROUND SUPPORT SYSTEMS AND FACILITIES (SPACE) 593

Includes launch complexes, research and production facilities; ground support equipment, e.g., mobile transporters; and simulators.

For related information see also *09 Research and Support Facilities (Air).*

15 LAUNCH VEHICLES AND SPACE VEHICLES N.A.

Includes boosters; operating problems of launch/space vehicle systems; and reusable vehicles.

For related information see also *20 Spacecraft Propulsion and Power.*

16 SPACE TRANSPORTATION 593

Includes passenger and cargo space transportation, e.g., shuttle operations; and space rescue techniques.

For related information see also *03 Air Transportation and Safety* and *18 Spacecraft Design, Testing and Performance.* For space suits see *54 Man/System Technology and Life Support.*

17 SPACE COMMUNICATIONS, SPACECRAFT COMMUNICATIONS, COMMAND AND TRACKING N.A.

Includes telemetry; space communications networks; astronavigation and guidance; and radio blackout.

For related information see also *04 Aircraft Communications and Navigation* and *32 Communications and Radar.*

18 SPACECRAFT DESIGN, TESTING AND PERFORMANCE 594

Includes satellites; space platforms; space stations; spacecraft systems and components such as thermal and environmental controls; and attitude controls.

For life support systems see *54 Man/System Technology and Life Support.* For related information see also *05 Aircraft Design, Testing and Performance, 39 Structural Mechanics,* and *16 Space Transportation.*

19 SPACECRAFT INSTRUMENTATION N.A.

For related information see also *06 Aircraft Instrumentation* and *35 Instrumentation and Photography.*

20 SPACECRAFT PROPULSION AND POWER 614

Includes main propulsion systems and components, e.g. rocket engines; and spacecraft auxiliary power sources.

For related information see also *07 Aircraft Propulsion and Power, 28 Propellants and Fuels, 44 Energy Production and Conversion,* and *15 Launch Vehicles and Space Vehicles.*

CHEMISTRY AND MATERIALS

Includes chemistry and materials (general); composite materials; inorganic and physical chemistry; metallic materials; nonmetallic materials; propellants and fuels; and materials processing.

23 CHEMISTRY AND MATERIALS (GENERAL) 617

24 COMPOSITE MATERIALS 617

Includes physical, chemical, and mechanical properties of laminates and other composite materials.

For ceramic materials see *27 Nonmetallic Materials.*

25 INORGANIC AND PHYSICAL CHEMISTRY 620

Includes chemical analysis, e.g., chromatography; combustion theory; electrochemistry; and photochemistry.

For related information see also *77 Thermodynamics and Statistical Physics.*

26 METALLIC MATERIALS 623

Includes physical, chemical, and mechanical properties of metals, e.g., corrosion; and metallurgy.

27 NONMETALLIC MATERIALS 626

Includes physical, chemical, and mechanical properties of plastics, elastomers, lubricants, polymers, textiles, adhesives, and ceramic materials.

For composite materials see *24 Composite Materials.*

28 PROPELLANTS AND FUELS 629

Includes rocket propellants, igniters and oxidizers; their storage and handling procedures; and aircraft fuels.

For related information see also *07 Aircraft Propulsion and Power, 20 Spacecraft Propulsion and Power,* and *44 Energy Production and Conversion.*

29 MATERIALS PROCESSING 630

Includes space-based development of products and processes for commercial application.

For biological materials see *55 Space Biology.*

ENGINEERING

Includes engineering (general); communications and radar; electronics and electrical engineering; fluid mechanics and heat transfer; instrumentation and photography; lasers and masers; mechanical engineering; quality assurance and reliability; and structural mechanics.

For related information see also *Physics.*

31 ENGINEERING (GENERAL) 630

Includes vacuum technology; control engineering; display engineering; cryogenics; and fire prevention.

32 COMMUNICATIONS AND RADAR 631

Includes radar; land and global communications; communications theory; and optical communications.

For related information see also *04 Aircraft Communications and Navigation* and *17 Space Communications, Spacecraft Communications, Command and Tracking.* For search and rescue see *03 Air Transportation and Safety,* and *16 Space Transportation.*

33 ELECTRONICS AND ELECTRICAL ENGINEERING 633

Includes test equipment and maintainability; components, e.g., tunnel diodes and transistors; microminiaturization; and integrated circuitry.

For related information see also *60 Computer Operations and Hardware* and *76 Solid-State Physics.*

34 FLUID MECHANICS AND HEAT TRANSFER 637

Includes boundary layers; hydrodynamics; fluidics; mass transfer and ablation cooling.

For related information see also *02 Aerodynamics* and *77 Thermodynamics and Statistical Physics.*

35 INSTRUMENTATION AND PHOTOGRAPHY 644

Includes remote sensors; measuring instruments and gauges; detectors; cameras and photographic supplies; and holography.

For aerial photography see *43 Earth Resources and Remote Sensing.* For related information see also *06 Aircraft Instrumentation* and *19 Spacecraft Instrumentation.*

36 LASERS AND MASERS 647

Includes parametric amplifiers.

For related information see also *76 Solid-State Physics.*

37 MECHANICAL ENGINEERING 649

Includes auxiliary systems (nonpower); machine elements and processes; and mechanical equipment.

38 QUALITY ASSURANCE AND RELIABILITY 653

Includes product sampling procedures and techniques; and quality control.

39 STRUCTURAL MECHANICS 653

Includes structural element design and weight analysis; fatigue; and thermal stress.

For applications see *05 Aircraft Design, Testing and Performance* and *18 Spacecraft Design, Testing and Performance.*

GEOSCIENCES

Includes geosciences (general); earth resources and remote sensing; energy production and conversion; environment pollution; geophysics; meteorology and climatology; and oceanography.

For related information see also *Space Sciences.*

42 GEOSCIENCES (GENERAL) 656

43 EARTH RESOURCES AND REMOTE SENSING 663

Includes remote sensing of earth resources by aircraft and spacecraft; photogrammetry; and aerial photography.

For instrumentation see *35 Instrumentation and Photography.*

44 ENERGY PRODUCTION AND CONVERSION 665

Includes specific energy conversion systems, e.g., fuel cells; global sources of energy; geophysical conversion; and windpower.

For related information see also *07 Aircraft Propulsion and Power, 20 Spacecraft Propulsion and Power,* and *28 Propellants and Fuels.*

45 ENVIRONMENT POLLUTION 665

Includes atmospheric, noise, thermal, and water pollution.

46 GEOPHYSICS 666

Includes aeronomy; upper and lower atmosphere studies; ionospheric and magnetospheric physics; and geomagnetism.

For space radiation see *93 Space Radiation.*

47 METEOROLOGY AND CLIMATOLOGY 670

Includes weather forecasting and modification.

48 OCEANOGRAPHY 671

Includes biological, dynamic, and physical oceanography; and marine resources.

For related information see also *43 Earth Resources and Remote Sensing.*

LIFE SCIENCES

Includes life sciences (general); aerospace medicine; behavioral sciences; man/system technology and life support; and space biology.

51 LIFE SCIENCES (GENERAL) 672

52 AEROSPACE MEDICINE 672

Includes physiological factors; biological effects of radiation; and effects of weightlessness on man and animals.

53 BEHAVIORAL SCIENCES 674

Includes psychological factors; individual and group behavior; crew training and evaluation; and psychiatric research.

54 MAN/SYSTEM TECHNOLOGY AND LIFE SUPPORT 675

Includes human engineering; biotechnology; and space suits and protective clothing.

For related information see also *16 Space Transportation.*

55 SPACE BIOLOGY 676

Includes exobiology; planetary biology; and extraterrestrial life.

MATHEMATICAL AND COMPUTER SCIENCES

Includes mathematical and computer sciences (general); computer operations and hardware; computer programming and software; computer systems; cybernetics; numerical analysis; statistics and probability; systems analysis; and theoretical mathematics.

59 MATHEMATICAL AND COMPUTER SCIENCES (GENERAL) N.A.

60 COMPUTER OPERATIONS AND HARDWARE 680

Includes hardware for computer graphics, firmware, and data processing.

For components see *33 Electronics and Electrical Engineering.*

61 COMPUTER PROGRAMMING AND SOFTWARE 681

Includes computer programs, routines, algorithms, and specific applications, e.g., CAD/CAM.

62 COMPUTER SYSTEMS 685

Includes computer networks and special application computer systems.

63 CYBERNETICS 686

Includes feedback and control theory, artificial intelligence, robotics and expert systems.

For related information see also *54 Man/System Technology and Life Support.*

64 NUMERICAL ANALYSIS 687

Includes iteration, difference equations, and numerical approximation.

65 STATISTICS AND PROBABILITY 693

Includes data sampling and smoothing; Monte Carlo method; and stochastic processes.

66 SYSTEMS ANALYSIS 694

Includes mathematical modeling; network analysis; and operations research.

67 THEORETICAL MATHEMATICS 695

Includes topology and number theory.

PHYSICS

Includes physics (general); acoustics; atomic and molecular physics; nuclear and high-energy physics; optics; plasma physics; solid-state physics; and thermodynamics and statistical physics.

For related information see also *Engineering.*

70 PHYSICS (GENERAL) 696

For precision time and time interval (PTTI) see *35 Instrumentation and Photography;* for geophysics, astrophysics or solar physics see *46 Geophysics, 90 Astrophysics,* or *92 Solar Physics.*

71 ACOUSTICS 696
Includes sound generation, transmission, and attenuation.
For noise pollution see *45 Environment Pollution.*

72 ATOMIC AND MOLECULAR PHYSICS 697
Includes atomic structure, electron properties, and molecular spectra.

73 NUCLEAR AND HIGH-ENERGY PHYSICS 699
Includes elementary and nuclear particles; and reactor theory.
For space radiation see *93 Space Radiation.*

74 OPTICS 699
Includes light phenomena and optical devices.
For lasers see *36 Lasers and Masers.*

75 PLASMA PHYSICS 701
Includes magnetohydrodynamics and plasma fusion.
For ionospheric plasmas see *46 Geophysics.* For space plasmas see *90 Astrophysics.*

76 SOLID-STATE PHYSICS 702
Includes superconductivity.
For related information see also *33 Electronics and Electrical Engineering* and *36 Lasers and Masers.*

77 THERMODYNAMICS AND STATISTICAL PHYSICS 704
Includes quantum mechanics; theoretical physics; and Bose and Fermi statistics.
For related information see also *25 Inorganic and Physical Chemistry* and *34 Fluid Mechanics and Heat Transfer.*

SOCIAL SCIENCES

Includes social sciences (general); administration and management; documentation and information science; economics and cost analysis; law, political science, and space policy; and urban technology and transportation.

80 SOCIAL SCIENCES (GENERAL) 705
Includes educational matters.

81 ADMINISTRATION AND MANAGEMENT 705
Includes management planning and research.

82 DOCUMENTATION AND INFORMATION SCIENCE 706
Includes information management; information storage and retrieval technology; technical writing; graphic arts; and micrography.
For computer documentation see *61 Computer Programming and Software.*

83 ECONOMICS AND COST ANALYSIS N.A.
Includes cost effectiveness studies.

84 LAW, POLITICAL SCIENCE AND SPACE POLICY 709
Includes NASA appropriation hearings; aviation law; space law and policy; international law; international cooperation; and patent policy.

85 URBAN TECHNOLOGY AND TRANSPORTATION 709
Includes applications of space technology to urban problems; technology transfer; technology assessment; and surface and mass transportation.
For related information see *03 Air Transportation and Safety, 16 Space Transportation,* and *44 Energy Production and Conversion.*

SPACE SCIENCES

Includes space sciences (general); astronomy; astrophysics; lunar and planetary exploration; solar physics; and space radiation.
For related information see also *Geosciences.*

88 SPACE SCIENCES (GENERAL) 710

89 ASTRONOMY 710
Includes radio, gamma-ray, and infrared astronomy; and astrometry.

90 ASTROPHYSICS 712
Includes cosmology; celestial mechanics; space plasmas; and interstellar and interplanetary gases and dust.
For related information see also *75 Plasma Physics.*

91 LUNAR AND PLANETARY EXPLORATION 714
Includes planetology; and manned and unmanned flights.
For spacecraft design or space stations see *18 Spacecraft Design, Testing and Performance.*

92 SOLAR PHYSICS 715
Includes solar activity, solar flares, solar radiation and sunspots.
For related information see *93 Space Radiation.*

93 SPACE RADIATION 715
Includes cosmic radiation; and inner and outer earth's radiation belts.
For biological effects of radiation see *52 Aerospace Medicine.* For theory see *73 Nuclear and High-Energy Physics.*

GENERAL

Includes aeronautical, astronautical, and space science related histories, biographies, and pertinent reports too broad for categorization; histories or broad overviews of NASA programs.

99 GENERAL 716

Note: N.A. means that no abstracts were assigned to this category for this issue.

SUBJECT INDEX I-1
PERSONAL AUTHOR INDEX I-53
CORPORATE SOURCE INDEX I-61
CONTRACT NUMBER INDEX I-71
REPORT/ACCESSION NUMBER INDEX .. I-73
APPENDIX—ABOUT STAR A-1

TYPICAL CITATION AND ABSTRACT

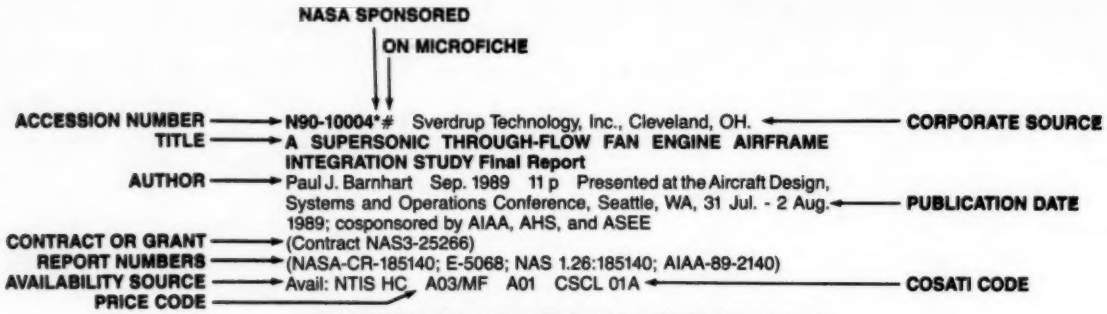
NASA SPONSORED
ON MICROFICHE
ACCESSION NUMBER
N90-10004*# Sverdrup Technology, Inc., Cleveland, OH.
CORPORATE SOURCE
TITLE
A SUPERSONIC THROUGH-FLOW FAN ENGINE AIRFRAME INTEGRATION STUDY Final Report
AUTHOR
Paul J. Barnhart Sep. 1989 11 p Presented at the Aircraft Design, Systems and Operations Conference, Seattle, WA, 31 Jul. - 2 Aug. 1989; cosponsored by AIAA, AHS, and ASEE
PUBLICATION DATE
CONTRACT OR GRANT
(Contract NAS3-25266)
REPORT NUMBERS
(NASA-CR-185140; E-5068; NAS 1.26:185140; AIAA-89-2140)
AVAILABILITY SOURCE
Avail: NTIS HC A03/MF A01 CSCL 01A
COSATI CODE
PRICE CODE

Engine airframe integration effects are investigated for superonsic through-flow fan engines installed on a Mach 3.20 supersonic cruise vehicle. Six different supersonic through-flow fan engine installations covering the effects of engine size, nacelle contour, nacelle placement, and approximate bypass plume effects are presented. The different supersonic through-flow fan installations are compared with a conventional turbine bypass engine configuration on the same basic airframe. The supersonic through-flow fan engine integrations are shown to be comparable to the turbine bypass engine configuration on the basis of installed nacelle wave drag. The supersonic through-flow fan engine airframe integrated vehicles have superior aerodynamic performance on the basis of maximum lift-to-drag ratio than the turbine bypass engine installation over the entire operating Mach number range from 1.10 to 3.20. When approximate bypass plume modeling is included, the supersonic through-flow fan engine configuration shows even larger improvements over the turbine bypass engine configuration. Author

VOLUME 28 NUMBER 5 / MARCH 8, 1990

Scientific and Technical Aerospace Reports

A Semimonthly Publication of the National Aeronautics and Space Administration

01 AERONAUTICS (GENERAL)

N90-13323*# Sverdrup Technology, Inc., Cleveland, OH.
MULTIGRID CALCULATIONS OF 3-D TURBULENT VISCOUS FLOWS Final Report
Jeffrey W. Yokota Oct. 1989 18 p Presented at the 1st Canadian Symposium on Aerodynamics, Ottawa, Ontario, 4-5 Dec. 1989; sponsored by Canadian Aeronautics and Space Inst.
(Contract NAS3-25266)
(NASA-CR-185154; E-5116; NAS 1.26:185154) Avail: NTIS HC A03/MF A01 CSCL 01B

Convergence properties of a multigrid algorithm, developed to calculate compressible viscous flows, are analyzed by a vector sequence eigenvalue estimate. The full 3-D Reynolds-averaged Navier-Stokes equations are integrated by an implicit multigrid scheme while a k-epsilon turbulence model is solved, uncoupled from the flow equations. Estimates of the eigenvalue structure for both single and multigrid calculations are compared in an attempt to analyze the process as well as the results of the multigrid technique. The flow through an annular turbine is used to illustrate the scheme's ability to calculate complex 3-D flows. Author

N90-13324*# National Aeronautics and Space Administration. Ames Research Center, Moffett Field, CA.
APPLICATION OF A SELF-ADAPTIVE GRID METHOD TO COMPLEX FLOWS
G. S. Deiwert, E. Venkatapathy, C. Davies, J. Djomehri, and K. Abrahamson (Boeing Military Airplane Development, Wichita, KS.) Jul. 1989 20 p
(NASA-TM-102223; A-89172; NAS 1.15:102223) Avail: NTIS HC A03/MF A01 CSCL 01B

A directional-split, modular, user-friendly grid point distribution code is applied to several test problems. The code is self-adaptive in the sense that grid point spacing is determined by user-specified constants denoting maximum and minimum grid spacings and constants relating the relative influence of smoothness and orthogonality. Estimates of truncation error, in terms of flow-field gradients and/or geometric features, are used to determine the point distribution. Points are redistributed along grid lines in a specified direction in an elliptic manner over a user-specified subdomain, while orthogonality and smoothness are controlled in a parabolic (marching) manner in the remaining directions. Multidirectional adaption is achieved by sequential application of the method in each coordinate direction. The flow-field solution is redistributed onto the newly distributed grid points after each unidirectional adaption by a simple one-dimensional interpolation scheme. For time-accurate schemes such interpolation is not necessary and time-dependent metrics are carried in the fluid dynamic equations to account for grid movement. Author

02 AERODYNAMICS

Includes aerodynamics of bodies, combinations, wings, rotors, and control surfaces; and internal flow in ducts and turbomachinery.

For related information see also *34 Fluid Mechanics and Heat Transfer.*

N90-13325 Arizona Univ., Tucson.
INFLUENCE OF VANE SWEEP ON ROTOR-STATOR INTERACTION NOISE Ph.D. Thesis
Edmane Envia 1988 169 p
Avail: Univ. Microfilms Order No. DA8907954

The influence of vane sweep on rotor-stator interaction noise is investigated. In an analytical approach, the interaction of a convected gust, representing the rotor viscous wake, with a cascade of finite span swept airfoils, representing the stator, is analyzed. The analysis is based on the solution of the exact linearized equations of motion. High-frequency convected gusts for which noise generation is concentrated near the leading edge of the airfoils are considered. In a preliminary study, the problem of an isolated finite span swept airfoil interacting with a convected gust is analyzed. Using Fourier transform methods and the Wiener-Hopf technique, an approximate solution for this problem is developed. Closed form expressions for the acoustic farfield are obtained and used in a parametric study to assess the effect of airfoil sweep on noise generation. Utilizing the single airfoil model, an approximate solution to the problem of noise radiation from a cascade of finite span swept airfoils interacting with a convected gust is derived. A parametric study of noise generated by gust-cascade interaction is then performed to assess the effectiveness of vane sweep in reducing rotor-stator interaction noise. Dissert. Abstr.

N90-13326# National Aeronautical Establishment, Ottawa (Ontario).
ANALYSIS OF EXPERIMENTAL DATA FOR CAST 10-2/DOA 2 SUPERCRITICAL AIRFOIL AT LOW REYNOLDS NUMBERS AND APPLICATION TO HIGH REYNOLDS NUMBER FLOW
Y. Y. Chan Jan. 1989 42 p
(AD-A211654; NAE-AN-60; NRC-30268) Avail: NTIS HC A03/MF A01 CSCL 01/3

The experimental investigation of CAST 10-2/DOA 2 supercritical airfoil previously conducted in the NAE Two-Dimensional Test Facility has been extended to low Reynolds number range at the design Mach number 0.765. The results indicate that with forward transition fixing, the data trend at low Reynolds number is different from that at high Reynolds number with the former more sensitive to the Reynolds number variation. The dividing Reynolds number for these two regions is about 10 million. With aft fixing, the low Reynolds number data approach those at higher Reynolds numbers for cruise conditions. However, at high list conditions the thin boundary layer delays separation and higher maximum lift is obtained. The characteristics of the Reynolds number dependency obtained from the analysis substantiate the principle of the simulation/extrapolation methodology for data obtained from low Reynolds number to flight Reynolds number as proposed by the AGARD/Fluid Dynamics Panel. GRA

N90-13327*# Army Aviation Systems Command, Moffett Field, CA.
CORRELATION OF PUMA AIRLOADS: LIFTING-LINE AND WAKE CALCULATION
William G. Bousman, Colin Young, Neil Gilbert, Francois Toulmay, Wayne Johnson, and M. J. Riley (Royal Aerospace Establishment, Bedford, England) Nov. 1989 31 p Presented at the 15th European Rotorcraft Forum, Amsterdam, The Netherlands, 12-15 Sep. 1989
(NASA-TM-102212; USAAVSCOM-TR-89-A-006; A-89209; NAS 1.15:102212) Avail: NTIS HC A03/MF A01 CSCL 01A

A cooperative program undertaken by organizations in the United States, England, France, and Australia has assessed the strengths and weaknesses of four lifting-line/wake methods and three CFD methods by comparing their predictions with the data obtained in flight trials of a research Puma. The Puma was tested in two configurations: a mixed bladed rotor with instrumented rectangular tip blades, and a configuration with four identical swept tip blades. The results are examined of the lifting-line predictions. The better lifting-line methods show good agreement with lift at the blade tip for the configuration with four swept tips; the moment is well predicted at 0.92 R, but deteriorates outboard. The predictions for the mixed bladed rotor configuration range from fair to good. The lift prediction is better for the swept tip blade than for the rectangular tip blade, but the reasons for this cannot be determined because of the unmodeled effects of the mixed bladed rotor. Author

N90-13328*# Purdue Univ., West Lafayette, IN. School of Mechanical Engineering.
APPLICATION OF LARGE EDDY INTERACTION MODEL TO A MIXING LAYER Final Report
S. N. B. Murthy Nov. 1989 50 p
(Grant NAG3-592)
(NASA-CR-185123; NAS 1.26:185123; M/NA/TURB-1) Avail: NTIS HC A03/MF A01 CSCL 01A

The large eddy interaction model (LEIM) is a statistical model of turbulence based on the interaction of selected eddies with the mean flow and all of the eddies in a turbulent shear flow. It can be utilized as the starting point for obtaining physical structures in the flow. The possible application of the LEIM to a mixing layer formed between two parallel, incompressible flows with a small temperature difference is developed by invoking a detailed similarity between the spectra of velocity and temperature. Author

N90-13329*# National Aeronautics and Space Administration. Ames Research Center, Moffett Field, CA.
COMPUTATION OF VISCOUS INCOMPRESSIBLE FLOWS
Dochan Kwak Mar. 1989 116 p Presented at the von Karman Inst. for Fluid Dynamics Lecture Series 1989-04, 6-10 Mar. 1989
(NASA-TM-101090; A-89094; NAS 1.15:101090) Avail: NTIS HC A06/MF A01 CSCL 01A

Incompressible Navier-Stokes solution methods and their applications to three-dimensional flows are discussed. A brief review of existing methods is given followed by a detailed description of recent progress on development of three-dimensional generalized flow solvers. Emphasis is placed on primitive variable formulations which are most promising and flexible for general three-dimensional computations of viscous incompressible flows. Both steady- and unsteady-solution algorithms and their salient features are discussed. Finally, examples of real world applications of these flow solvers are given. Author

N90-13330# Indiana Univ.-Purdue Univ., Indianapolis. School of Engineering and Technology.
BLOCK-STRUCTURED SOLUTION OF THREE-DIMENSIONAL TRANSONIC FLOWS USING PARALLEL PROCESSING Final Report, 1 Jun. 1987 - 31 May 1989
Akin Ecer Aug. 1989 20 p
(Grant AF-AFOSR-0184-87; AF Proj. 2307)
(AD-A212851; AFOSR-89-1256TR) Avail: NTIS HC A03/MF A01 CSCL 20/4

The main objective of the program has been to implement and test the three-dimensional, block-structured Euler solver on computers with multiple processors. The developed scheme involves the partitioning of a large aerodynamics problem into several smaller problems where each represents a particular flow region. Each of these problems are solved on an Intel-IPSC computer with sixteen processors and an IBM 3090 computer with four processors. In the case of IPSC, the memory is distributed between sixteen processors (4.5 megabytes each). In the case of IBM 3090, all four processors share the same large memory. Several test cases have been run on these computers and basic considerations for analyzing large problems on parallel computers have been investigated. GRA

N90-13331# Air Force Avionics Lab., Wright-Patterson AFB, OH.
TRANSONIC EULER SOLUTIONS ON MUTUALLY INTERFERING FINNED BODIES Final Report, Oct. 1983 - Sep. 1989
Lawrence E. Lijewski Sep. 1989 7 p Previously announced in IAA as A89-25222
(AD-A213395; AFATL-TP-89-18) Avail: NTIS HC A02/MF A01 CSCL 01/1

The ability of an Euler code to predict mutual aerodynamic interference in the transonic regime was investigated. One, two, and three body combinations of a cruciform finned configuration were examined at Mach numbers from 0.80 to 1.20 and angles of attack up to ten degrees. Predicted surface pressure distributions were compared with wind tunnel data or the first time on three finned bodies with success. The Euler code was found to predict body pressures well in many interference regions, although shock location often was less accurate due to viscous effects in the strongest interference flow field near Mach 1. Rigid body physics of the three body combination was investigated from integrated pressure distributions. Force and moment behavior was found to be strongly dependent upon Mach number. GRA

N90-13332*# National Aeronautics and Space Administration. Ames Research Center, Moffett Field, CA.
STUDY OF THE INTEGRATION OF WIND TUNNEL AND COMPUTATIONAL METHODS FOR AERODYNAMIC CONFIGURATIONS
Lindsey E. Browne and Dale L. Ashby Oct. 1989 69 p
(NASA-TM-102196; A-89148; NAS 1.15:102196) Avail: NTIS HC A04/MF A01 CSCL 01A

A study was conducted to determine the effectiveness of using a low-order panel code to estimate wind tunnel wall corrections. The corrections were found by two computations. The first computation included the test model and the surrounding wind tunnel walls, while in the second computation the wind tunnel walls were removed. The difference between the force and moment coefficients obtained by comparing these two cases allowed the determination of the wall corrections. The technique was verified by matching the test-section, wall-pressure signature from a wind tunnel test with the signature predicted by the panel code. To prove the viability of the technique, two cases were considered. The first was a two-dimensional high-lift wing with a flap that was tested in the 7- by 10-foot wind tunnel at NASA Ames Research Center. The second was a 1/32-scale model of the F/A-18 aircraft which was tested in the low-speed wind tunnel at San Diego State University. The panel code used was PMARC (Panel Method Ames Research Center). Results of this study indicate that the proposed wind tunnel wall correction method is comparable to other methods and that it also inherently includes the corrections due to model blockage and wing lift. Author

N90-13333# Deutsche Forschungsanstalt fuer Luft- und Raumfahrt, Brunswick (Germany, F.R.). Abteilung Unterschall-Entwurfsaerodynamik.
COMPUTATION OF FLOW FIELDS AROUND PROPELLERS AND HOVERING ROTORS BASED ON THE SOLUTION OF THE EULER EQUATIONS Ph.D. Thesis - Tech. Univ. Brunswick
Norbert Kroll Jun. 1989 134 p In GERMAN; ENGLISH

summary
(DLR-FB-89-37; ISSN-0171-1342; ETN-90-95051) Avail: NTIS HC A07/MF A01; DLR, VB-PL-DO, Postfach 90 60 58, 5000 Cologne, Fed. Republic of Germany, 43.50 DM

A numerical method for the calculation of inviscid flow fields around propellers in axial uniform onflow and around hovering rotors is described. The method is based on the solution of the Euler equations in a blade-attached Cartesian reference frame. The solution method presented here is an extension of the finite volume method for nonrotating coordinate systems outlined by Jameson et al. Due to a suitable choice of the dependent variables for the system of the Euler equations, it is guaranteed that important properties of the discrete system known in the nonrotating coordinate system are preserved in the blade-attached rotating reference frame. In order to verify the solution method computations for a two-blade propeller and rotor in hover are carried out. The numerical results show good agreement with the experiment. Since the Euler equations are solved in the whole computational domain, a modeling of the wake geometry is not necessary. ESA

N90-13334# Von Karman Inst. for Fluid Dynamics, Rhode-Saint-Genese (Belgium).
AN INTRODUCTION TO HYPERSONIC AERODYNAMICS
1989 422 p Lecture series held in Rhode-Saint-Genese, Belgium, 13-15 Dec. 1988
(VKI-LS-1989-01; D/1989/0238/367; ISSN-0377-8312; ETN-90-95737) Avail: NTIS HC A18/MF A03

Studies on hypersonic aerodynamics are presented. The basic concepts of the hypersonic flow phenomena are reviewed, together with the inviscid and viscous flow solutions equations. The Navier-Stokes, Euler and boundary layer equations are analyzed. The effect of coupled chemical rate processes in the external inviscid airflows, at high enthalpy levels, are discussed. The development of boundary layer equations, for the case of very high speed flight (where the external flow is in a dissociated state) is presented. The rate of recombination of the dissociated air behind the detached shock wave is examined. For individual titles, see N90-13335 through N90-13338.

N90-13335# Maryland Univ., College Park. Dept. of Aerospace Engineering.
HYPERSONIC AERODYNAMICS
John D. Anderson, Jr. *In* VKI, An Introduction to Hypersonic Aerodynamics 1989 171 p (For primary document see N90-13334 05-02)
Avail: NTIS HC A18/MF A03

The basic concepts of the hypersonic flow phenomena are reviewed. The inviscid, viscous, high temperature and low density flows are analyzed. Concerning the inviscid flow, the following topics are considered: the basic hypersonic shock relations, the Newtonian flow, the tangent wedge/tangent cone methods, the shock expansion theory, the Euler equation, the Mach number independence, the concept of hypersonic similarity, the thin shock layer theory, and the influence of the vehicles blunt nose shape. In the analysis of the viscous effects prevailing in hypersonic flight conditions, the Navier-Stokes and the boundary layer equations, and the weak and strong viscous interaction theories, are examined. ESA

N90-13336# State Univ. of New York, Buffalo. Cornell Aeronautical Lab.
BLUNT-NOSE INVISCID AIRFLOWS WITH COUPLED NONEQUILIBRIUM PROCESSES
J. Gordon Hall, Alan Q. Eschenroeder, and Paul V. Marrone *In* VKI, An Introduction to Hypersonic Aerodynamics 1989 20 p Revised Sponsored in part by the DOE and CAL Internal Research (For primary document see N90-13334 05-02)
(Contract AF 49(638)-792)
Avail: NTIS HC A18/MF A03

The effect of coupled chemical rate processes in external inviscid hypersonic airflows, at high enthalpy levels, is discussed. Exact numerical solutions are obtained, for nose radii about 1 ft, at an altitude of 250,000 ft, and velocities of 15,000 and 23,000 ft/s. The importance of the coupling among the reactions considered is demonstrated. The dissociation-recombination, the bimolecular-exchange and ionization reactions, are included. The gasdynamic expansion in the curved shock layer in the blunt nose flow is observed. The inviscid nose flow is shown to be amenable to binary scaling for a given velocity. ESA

N90-13337# Avco-Everett Research Lab., MA.
THEORY OF STAGNATION POINT HEAT TRANSFER IN DISSOCIATED AIR
J. A. Fay and F. R. Riddell *In* VKI, An Introduction to Hypersonic Aerodynamics 1989 13 p Repr. from Journal of the Aeronautical Sciences, v. 25, no. 2, Feb. 1958 p 73-85 (For primary document see N90-13334 05-02)
(Contract AF 04(645)-18)
Avail: NTIS HC A18/MF A03

Boundary layer equations are developed for the case of very high speed flight, where the external flow is in a dissociated state. The effects of diffusion and of atom recombination in the boundary layer are included. It is shown that at the stagnation point, the equations can be reduced to a set of nonlinear differential equations. The numerical solutions for the equilibrium and nonequilibrium cases are presented. It is concluded that the heat transfer through the equilibrium stagnation point boundary layer can be computed by a simple correlation formula. Moreover, the heat transfer is almost unaffected by a nonequilibrium state of boundary layer provided the wall is catalytic and the Lewis number near unity. ESA

N90-13338# Purdue Univ., West Lafayette, IN.
ON CATALYTIC RECOMBINATION RATES IN HYPERSONIC STAGNATION HEAT TRANSFER
R. Goulard *In* VKI, An Introduction to Hypersonic Aerodynamics 1989 58 p Presented at the 12th ARS Annual Meeting, New York, NY, 2-5 Dec. 1957 Revised Sponsored in part by the Army Office of Ordnance Research and McDonnell Aircraft Corp. (For primary document see N90-13334 05-02)
Avail: NTIS HC A18/MF A03

The rate of recombination of the dissociated air behind the detached shock wave is investigated. Large recombination times, compared to the time of diffusion across the boundary layer, are considered. The conditions for the existence of a frozen flow and its dissociation log behind the shock wave are discussed. The heat transfer solutions are shown to correspond to the limiting case of an infinitely fast catalysis. For a given nose material, the percentage of the heat transfer is found to increase with the velocity, the nose diameter and the wall temperature, and to decrease with altitude. The experimental values obtained for the recombination rates of oxygen and nitrogen atoms are presented. ESA

N90-13339# Von Karman Inst. for Fluid Dynamics, Rhode-Saint-Genese (Belgium).
MEASUREMENT TECHNIQUES IN AERODYNAMICS
1989 547 p Lecture series held in Rhode-Saint-Genese, Belgium, 10-13 Apr. 1989
(VKI-LS-1989-05; D/1989/0238/371; ISSN-0377-8312; ETN-90-95739) Avail: NTIS HC A23/MF A03

The measurement techniques used in fluid dynamics are reviewed. The unsteady aspects occurring in a periodic, transitional or turbulent flow, are emphasized. The data acquisition principles, the sampling techniques, the filtering and the averaging methods are presented. Concerning the flow probing, single and wire techniques, film sensors and pressure probes are considered. The two and three dimensional flow investigations are performed, applying the laser two forms techniques the laser Doppler anemometer and the particle image displacement velocimeter. Examples related to low and high speed unsteady flow, strong vortical flow, blade wakes in a centrifugal field, transition and boundary layer flow, are given. For individual titles, see N90-13340 through N90-13348.

N90-13340# Oxford Univ. (England). Dept. of Engineering Sciences.
DATA ACQUISITION IN AERODYNAMIC RESEARCH
R. W. Ainsworth *In* VKI, Measurement Techniques in Aerodynamics 1989 78 p (For primary document see N90-13339 05-02)
Avail: NTIS HC A23/MF A03

The data acquisition technology in aerodynamic research, from transducer performance through signal conditioning to digitization and processing, is discussed. The construction, the excitation, and the signal response of typical transducers used in aerodynamic research, is reviewed. The waveform of a continuous time or analog signal is presented. Emphasis is given to the digital manipulation of output signals involving frequency time transformations, Fourier analysis and correlation functions. Examples of applications in the field of turbomachinery are given. ESA

N90-13341# Essen Univ. (Germany, F.R.).
PRACTICAL SYSTEMS FOR SPECKLE VELOCIMETRY
W. Merzkirch *In* VKI, Measurement Techniques in Aerodynamics 1989 14 p Previously announced as N89-17185 (For primary document see N90-13339 05-02)
Avail: NTIS HC A23/MF A03

Three dimensional flow visualization, applying a thin light sheet method of illumination, is presented. The speckle velocimetry technique is described. The combination of the cylindrical lens with two telescope lenses is used. Concerning the specklegram, the length and the number of exposures is discussed. The illumination of the system, applying white light speckle patterns, is included. The importance and influences of the photographic film on the speckle velocimetry is emphasized. The direct visualization of the velocity field, by analyzing the spatial filtering of the developed specklegram, is emphasized. ESA

N90-13342# Aix-Marseilles Univ. (France). Inst. de Mecanique Statistique de la Turbulence.
LOW SPEED HOT AND COLD WIRE TECHNIQUES FOR UNSTEADY FLOW **c35**
F. Anselmet *In* VKI, Measurement Techniques in Aerodynamics 1989 36 p (For primary document see N90-13339 05-02)
Avail: NTIS HC A23/MF A03

Unsteady flow temperature and velocity measurements are discussed. Cold and hot wire anemometry techniques are applied. Concerning the measurement problems, the constant current of the cold and hot wires, and the constant temperature amplifier, are emphasized. The dynamic nonlinearity is shown to be critical for the constant current hot wire method. The measurements performed apply constant resistance amplifiers for the hot wire probes. The results obtained with the cold and hot wire probes seem correct. The study leads to the conclusion that the hot and cold wire anemometry and optical methods are complementary techniques. ESA

N90-13343# Aix-Marseilles Univ. (France). Inst. de Mecanique Statistique de la Turbulence.
HOT AND COLD WIRE APPLICATIONS IN SUPERSONIC FLOWS: INTRODUCTORY NOTES **c35**
J. P. Dussauge *In* VKI, Measurement Techniques in Aerodynamics 1989 30 p (For primary document see N90-13339 05-02)
Avail: NTIS HC A23/MF A03

The basic rules for the measurement of fluctuations in supersonic flows is studied. Hot and cold wire anemometry is applied. The properties of the constant current and constant temperature anemometers are compared. Recommendations for the probe designs and the form of sensitivity coefficients are given. Examples of simple and asymptotic situations are presented. The dynamic response of the anemometer is shown to be crucial for the reliability of the turbulence measurements performance. The determination of velocity and temperature measurements is described. Applications of hot wire anemometry to transonic flows and to the measurement of the transverse velocity component are provided. ESA

N90-13344# Aix-Marseilles Univ. (France). Inst. de Mecanique Statistique de la Turbulence.
LASER APPLICATIONS IN SUPERSONIC UNSTEADY FLOW **c36**
M. Elena *In* VKI, Measurement Techniques in Aerodynamics 1989 20 p (For primary document see N90-13339 05-02)
Avail: NTIS HC A23/MF A03

The measurements of supersonic unsteady flow velocities, applying laser Doppler anemometry, are dicussed. This method allows the study of high turbulence levels. The advantages and disadvantages of the method are given. The difficulties created by high velocities and rapid spatial changes in velocity or flow direction are considered. Three dimensional flow measurements are shown to be difficult with this technique. Moreover, the deterioration of the signal to noise ratio is observed near the walls. It is suggested that the seeding effect and the particle response be checked for a given wind tunnel and laser Doppler anemometry system. ESA

N90-13345# Centre d'Etudes et de Recherches, Toulouse (France).
SKIN FRICTION MEASUREMENTS WITH HOT ELEMENTS **c35**
R. Houdeville and J. C. Juillen *In* VKI, Measurement Techniques in Aerodynamics 1989 71 p (For primary document see N90-13339 05-02)
Avail: NTIS HC A23/MF A03

The description of skin friction gauges, using the heated element technique, is presented. Adapted efficient gauge and the corresponding analysis are studied. The accuracy is shown to be improved by using temperature compensated wirings. The unsteady response of the gauges is analyzed. The performances of fiber gauges, three wire gauges, and two wire or two film gauges are compared. It is shown that the calibration of the gauges, in the heated element technique, depends neither on the nature of the boundary layer (laminar, turbulent and compressible), nor on the pressure gradients. ESA

N90-13346# Deutsche Forschungsanstalt fuer Luft- und Raumfahrt, Goettingen (Germany, F.R.). Inst. fuer Experimentelle Stroemungsmechanik.
THE 3D LDA TECHNIQUES IN VORTEX STUDIES AND BOUNDARY LAYER SURVEYS **c35**
Karl-Aloys Buetefisch *In* VKI, Measurement Techniques in Aerodynamics 1989 45 p (For primary document see N90-13339 05-02)
Avail: NTIS HC A23/MF A03

The physical background of laser Doppler anemometry (LDA) is studied. The parameters influencing the proper operation of such an instrument in large wind tunnels to obtain the local flow velocity is discussed. The aspects for designing a three component laser Doppler anemometry system, to get the time dependent velocity vector, are treated. A three component system operated in backscatter and off-axis mode is described. Three component velocity and turbulence results, obtained in a 3 sqm subsonic and 1 sqm transonic wind tunnel are presented. ESA

N90-13347# Royal Aerospace Establishment, Bedford (England). Aerodynamics Div.
PRESSURE MEASUREMENT TECHNIQUES IN USE AT THE ROYAL AEROSPACE ESTABLISHMENT **c35**
B. L. Welsh and P. R. Ashill *In* VKI, Measurement Techniques in Aerodynamics 1989 108 p (For primary document see N90-13339 05-02)
Avail: NTIS HC A23/MF A03

Pressure measurement techniques for both steady and unsteady flows in use in wind tunnel tests at the Royal Aerospace Establishment (RAE) are reviewed. Methods for measuring static pressure, stagnation pressure, and flow direction, on the surface of models and in the flowfield, are included. The accuracy of pressure measurement and the problems experienced in making the measurements are included. The accuracy improvements and the increase of the data acquisition speed are described. ESA

N90-13348# Deutsche Forschungs- und Versuchsanstalt fuer Luft- und Raumfahrt, Cologne (Germany, F.R.). Inst. fuer Antriebstechnik.

LASER TWO FOCUS TECHNIQUES **c35**

R. Schodl *In* VKI, Measurement Techniques in Aerodynamics 1989 96 p (For primary document see N90-13339 05-02)
Avail: NTIS HC A23/MF A03

The development of the laser two focus velocimetry are reviewed. The fundamentals of this nonintrusive fluid flow velocity measurement technique are described. Emphasis is placed upon the advances of this technique. Results of measurements in a very small flow channel and in a small turbocharger compressor rotor are presented. The influence of beam diameter - beam separation ratio on the measuring accuracy and on the measuring time is treated. A multicolor two dimensional system with selectable beam separation is presented. The laser Doppler and the laser two focus techniques are compared. ESA

N90-13349*# Stanford Univ., CA. Dept. of Aeronautics and Astronautics.

A CFD STUDY OF TILT ROTOR FLOWFIELDS

Ian Fejtek and Leonard Roberts Oct. 1989 101 p
(NASA-CR-186116; JIAA-TR-96; NAS 1.26:186116) Avail: NTIS HC A06/MF A01 CSCL 01A

The download on the wing produced by the rotor wake of a tilt rotor vehicle in hover is of major concern because of its severe impact on payload-carrying capability. In a concerted effort to understand the fundamental fluid dynamics that cause this download, and to help find ways to reduce it, computational fluid dynamics (CFD) is employed to study this problem. The thin-layer Navier-Stokes equations are used to describe the flow, and an implicit, finite difference numerical algorithm is the method of solution. The methodology is developed to analyze the tilt rotor flowfield. Included are discussions of computations of an airfoil and wing in freestream flows at -90 degrees, a rotor alone, and wing/rotor interaction in two and three dimensions. Preliminary results demonstrate the feasibility and great potential of the present approach. Recommendations are made for both near-term and far-term improvements to the method. Author

N90-13350 Manchester Univ. (England).

STUDY OF FORCES AND MOMENTS ON WING-BODIES AT HIGH INCIDENCE, VOLUMES 1 AND 2 Ph.D. Thesis

G. A. Johnson 1987 555 p
Avail: Univ. Microfilms Order No. BRD-85587

A systematic experimental study of the forces and moments on a wing-body combination at high incidence is reported. The effect of several parameters, such as wing planform, wing axial location, and wing roll angle were investigated. Throughout the tests the basic body used was a three diameter tangent-ogive forebody with a nine diameter cylindrical afterbody. Flow visualization tests were also done using the smoke-wire and oil-surface flow techniques, this enabled the leeward flow structure of the wing-body to be studied, particularly in the vital region near the wings. The results of these tests showed that the overall out-of-plane forces and moments were more dependent on incidence and the structure of the body asymmetric flow than on the parameters of wing planform, wing axial location, and wing roll angle. The flow visualization results showed several important changes to the flow structure compared to a body-alone case.
Dissert. Abstr.

N90-13351*# Institute for Computer Applications in Science and Engineering, Hampton, VA.

OPTIMUM SHAPE OF A BLUNT FOREBODY IN HYPERSONIC FLOW Final Report

L. Maestrello and L. Ting (New York Univ., New York.) Dec. 1989 22 p
(Contract NAS1-18605)
(NASA-CR-181955; NAS 1.26:181955; ICASE-89-51) Avail: NTIS HC A03/MF A01 CSCL 01A

The optimum shape of a blunt forebody attached to a symmetric wedge or cone is determined. The length of the forebody, its semi-thickness or base radius, the nose radius and the radius of the fillet joining the forebody to the wedge or cone are specified. The optimum shape is composed of simple curves. Thus experimental models can be built readily to investigate the utilization of aerodynamic heating for boundary layer control. The optimum shape based on the modified Newtonian theory can also serve as the preliminary shape for the numerical solution of the optimum shape using the governing equations for a compressible inviscid or viscous flow. Author

N90-13352*# National Aeronautics and Space Administration. Lewis Research Center, Cleveland, OH.

EFFECT OF REDUCED AFT DIAMETER AND INCREASED BLADE NUMBER ON HIGH-SPEED COUNTERROTATION PROPELLER PERFORMANCE

Gayle E. Rose (Sverdrup Technology, Inc., Cleveland, OH.) and Robert J. Jeracki 1989 31 p Presented at the 27th Aerospace Sciences Meeting, Reno, NV, 9-12 Jan. 1989; sponsored by AIAA
(NASA-TM-102077; E-4837; NAS 1.15:102077; AIAA-89-0438)
Avail: NTIS HC A03/MF A01 CSCL 01A

Performance data of 0.17-scale model counterrotation pusher propeller configurations were taken in the NASA Lewis 8- by 6-Foot Supersonic Wind Tunnel at Mach numbers of 0.66, 0.71, 0.75, and 0.79. These tests investigated the aerodynamic performance of the unducted fan (UDF) demonstrator propeller engine developed in a joint program by General Electric and NASA. Data were recorded to show the effect on counterrotation propeller cruise efficiency of two takeoff noise-reduction concepts. These two concepts are reduced aft blade diameter and increased forward blade number. The four configurations tested were a baseline (F1/A1 8/8) configuration, a reduced aft diameter (F1/A3 8/8) configuration, an increase forward blade number (F1/A1 9/8) configuration, and a combination of the latter two (F1/A3 9/8) configurations. Data were collected with a complex counterrotation propeller test rig via rotating thrust and torque balances and pressure instrumentation. Data comparisons documented the power differences between the baseline and the reduced aft diameter concepts. Performance comparisons to the baseline configuration showed that reducing the aft blade diameter reduced the net efficiency, and adding a blade to the front rotor increased the net efficiency. The combination of the two concepts showed only slightly lower net efficiency than the baseline configuration. It was also found that the counterrotation demonstrator propeller model (F7/A7 8/8) configuration outperformed the baseline (F1/A1 8/8) configuration. Author

N90-13353*# National Aeronautics and Space Administration. Ames Research Center, Moffett Field, CA.

COMPUTATION OF NAVIER-STOKES EQUATIONS FOR THREE-DIMENSIONAL FLOW SEPARATION

Ching-Mao Hung Dec. 1989 22 p
(NASA-TM-102266; A-90036; NAS 1.15:102266) Avail: NTIS HC A03/MF A01 CSCL 01A

Supersonic flows over a sharp and a flat-faced blunt fin mounted on a flat plate are simulated numerically. Several basic issues involved in the resultant three-dimensional steady flow separation are studied. Using the same number of grid points, different grid spacings are employed to investigate the effects of a grid resolution on the origin of the line of separation. Various shock strengths are used to study the so-called separated and unseparated boundary layer and to establish the existence or absence of secondary separation. The length of separation ahead of the flat-faced blunt fin, bifurcation of a horseshoe vortex, and the accessibility of a closed-type separation are investigated. The usual interpretation of the flow field from previous studies and new interpretations arising from the present simulation are discussed. Author

N90-13354*# Kansas Univ. Center for Research, Inc., Lawrence. Flight Research Lab.

AERODYNAMICS OF THRUST VECTORING Semiannual Status Report, 11 Jun. - 10 Dec. 1989

J. B. Tseng and C. Edward Lan Dec. 1989 50 p

(Grant NAG1-837)
(NASA-CR-185074; NAS 1.26:185074) Avail: NTIS HC A03/MF A01 CSCL 01A

Thrust vectoring as a means to enhance maneuverability and aerodynamic performane of a tactical aircraft is discussed. This concept usually involves the installation of a multifunction nozzle. With the nozzle, the engine thrust can be changed in direction without changing the attitude of the aircraft. Change in the direction of thrust induces a significant change in the aerodynamic forces on the aircraft. Therefore, this device can be used for lift-augmenting as well as stability and control purposes. When the thrust is deflected in the longitudinal direction, the lift force and the pitching stability can be manipulated, while the yawing stability can be controlled by directing the thrust in the lateral direction. Author

N90-13355*# National Aeronautics and Space Administration. Lewis Research Center, Cleveland, OH.
APPLICATION OF AN EFFICIENT HYBRID SCHEME FOR AEROELASTIC ANALYSIS OF ADVANCED PROPELLERS
R. Srivastava, N. L. Sankar, T. S. R. Reddy (Toledo Univ., OH.), and D. L. Huff [1989] 30 p Presented at the 28th Aerospace Sciences Meeting, Reno, NV, 8-11 Jan. 1990; sponsored by AIAA
(NASA-TM-102428; E-5196; NAS 1.15:102428; AIAA-90-0028) Avail: NTIS HC A03/MF A01 CSCL 01A

An efficient 3-D hybrid scheme is applied for solving Euler equations to analyze advanced propellers. The scheme treats the spanwise direction semi-explicitly and the other two directions implicitly, without affecting the accuracy, as compared to a fully implicit scheme. This leads to a reduction in computer time and memory requirement. The calculated power coefficients for two advanced propellers, SR3 and SR7L, and various advanced ratios showed good correlation with experiment. Spanwise distribution of elemental power coefficient and steady pressure coefficient differences also showed good agreement with experiment. A study of the effect of structural flexibility on the performance of the advanced propellers showed that structural deformation due to centrifugal and aero loading should be included for better correlation. Author

N90-13356# Institut de Mecanique des Fluides de Lille (France). Groupe Mecanique des Fluides Fondamentales.
REDUCTION OF PROFILE DRAG BY MODIFYING THE STRUCTURE NEXT TO THE WAKE AREA [REDUCTION DE LA TRAINEE DE CULOT D'UN PROFIL PAR MODIFICATION DE LA STRUCTURE DU SILLAGE PROCHE]
O. Rodriguez and J. Pruvost 13 Dec. 1988 48 p In FRENCH
(Contract DRET-87-003)
(IMFL-88/35; ETN-90-95269) Avail: NTIS HC A03/MF A01

Drag reduction of two dimensional profiles with thick trailing edges in subsonic flow is experimentally studied by carrying out performance tests in subsonic wind tunnel with the help of a variable shape three dimensional auxiliary device to determine optimum drag reduction. The study leads to the design of a dented trailing edge characterized by the inclusion of a solid angle. The device allows a reduction of 49 percent of the drag in a profile with 0.036 relative thickness. ESA

N90-13357# Technische Univ., Delft (Netherlands). Dept. of Aerospace Engineering.
INDUCED DRAG FOR NON-PLANAR WINGS
H. J. Bos Aug. 1987 69 p
(LR-521; ETN-90-95980) Avail: NTIS HC A04/MF A01

Induced drag for nonplanar wings is studied with the rolling-up process of the wake and its influence on lift and drag particularly analyzed. Important conclusions are given with examples, including that in general it is favorable to extend a lift generating geometry in vertical or horizontal direction since the induced mass is increased in this way. The most favorable way to enlarge the induced mass is by increasing the span. ESA

03 AIR TRANSPORTATION AND SAFETY

Includes passenger and cargo air transport operations; and aircraft accidents.

For related information see also *16 Space Transportation* and *85 Urban Technology and Transportation.*

N90-13358# Advisory Group for Aerospace Research and Development, Neuilly-Sur-Seine (France).
THE HUMAN FACTORS RELATING TO ESCAPE AND SURVIVAL FROM HELICOPTERS DITCHING IN WATER
C. J. Brooks (Defence and Civil Inst. of Environmental Medicine, Downsview, Ontario) Aug. 1989 71 p
(AGARD-AG-305(E); ISBN-92-835-0522-0) Copyright Avail: NTIS HC A04/MF A01

The worldwide incidence of military and civilian over-water helicopter accidents and the problems related to survival are described. Typical accident scenarios are reviewed from the moment the occupant steps on board a helicopter to the pre-flight briefing through to the accident itself, to the difficulties with escape (commonly from underwater and in darkness), to the rescue and return safely to dry land. Improvements to crashworthiness and life support equipment in current in-service and future helicopters are proposed. A syllabus for underwater escape training is also discussed. Author

N90-13359# Southwest Research Inst., San Antonio, TX.
NDI (NONDESTRUCTIVE INSPECTION) ORIENTED CORROSION CONTROL FOR ARMY AIRCRAFT. PHASE 1: INSPECTION METHODS Final Report
F. A. Iddings Jul. 1989 253 p
(Contract DLA900-84-C-0910; SwRI Proj. 17-7958-843)
(AD-A213368) Avail: NTIS HC A12/MF A02 CSCL 11/6

The purpose of the work in this project was to assess the extent of corrosion in Army aircraft and its cost, to investigate nondestructive inspection (NDI) methods of corrosion control, and to formulate specific recommendations for detecting corrosion in new and fielded Army aircraft. The work focused on corrosion detection based on techniques in place and on the latest NDI techniques taking into account the type and stage of corrosion. Included was investigation of the application of NDI methods at critical points in the Corpus Christi Army Depot (CCAD) operation in order to better detect, prevent, and control corrosion in aircraft components as a result of depot maintenance. A key task involved determining how to proceed in developing an NDI oriented manufacturing model for CCAD into which can be incorporated candidate NDI methods that would improve the prevention of corrosion during CCAD's depot maintenance/NDI operations. Effort was concentrated on structuring a flexible manufacturing system (FMS) model for CCAD, including the defining of an FMS cell for support of corrosion control. The report contains a summary of the NTIAC State-of-the-Art (SOAR) on Nondestructive Evaluation methods for Characterization of Corrosion. GRA

N90-13360# Dayton Univ., OH. Structural Integrity Div.
STUDY OF THE ENGINE BIRD INGESTION EXPERIENCE OF THE BOEING 737 AIRCRAFT Interim Report, Oct. 1986 - Sep. 1987
Peter W. Hovey and Donald A. Skinn Oct. 1989 106 p Prepared in cooperation with Federal Aviation Administration, Atlantic City, NJ
(Contract DTFA03-88-C-00024)
(DOT/FAA/CT-89/16; UDR-TR-88-137) Avail: NTIS HC A06/MF A01

The Federal Aviation Administration (FAA) Technical Center initiated a study in October 1986 to determine the numbers, stress, and types of birds which are being ingested into medium and large inlet area turbofan engines and to determine what damage, if any, results. Bird ingestion data are being collected for the Boeing 737 model aircraft which uses either the Pratt and Whitney JT8D medium inlet area turbofan engine or the CFM International CFM56 large inlet area turbofan engine. The first of 3 years of

data collection are analyzed. The first year extends from October 1986 through September 1987. Author

04 AIRCRAFT COMMUNICATIONS AND NAVIGATION

Includes digital and voice communication with aircraft; air navigation systems (satellite and ground based); and air traffic control.

For related information see also *17 Space Communications, Spacecraft Communications, Command and Tracking* and *Communications and Radar.*

N90-13361# Mitre Corp., McLean, VA.
NATIONAL AIRSPACE SYSTEM AIRSPACE MANAGEMENT OPERATIONAL CONCEPT
Stephanie B. Fraser Sep. 1989 81 p
(Contract DTFA01-89-C-00001)
(DOT/FAA/DS-89/29; NAS-SR-1321) Avail: NTIS HC A05/MF A01

This concept of operations describes the operation of the National Airspace System (NAS), as it will be in the projected upgrade, i.e., end state. The requirements specified in NAS System Requirements Specification (NASSRS) is linked with the NAS design. The NASSRS addresses airspace management requirements. Airspace management serves to organize air traffic in the aggregate so that it can be managed with maximum safety and throughput, while minimizing delays, controller stress, and interference with pilot intent. Operational concepts are provided for airspace management, as it is described in the NASSRS. Author

N90-13362# Mitre Corp., McLean, VA.
NATIONAL AIRSPACE SYSTEM FLIGHT PLANNING OPERATIONAL CONCEPT
Alexandra Argyropoulos Oct. 1989 57 p
(Contract DTFA01-89-C-00001)
(DOT/FAA/DS-89/30; NAS-SR-1310) Avail: NTIS HC A04/MF A01

An operational concept of the flight planning processing system which will be in place upon implementation of the Federal Aviation Administration (FAA) National Airspace System (NAS) Plan is presented. Flight planning includes all activities involved in the preparation of a flight, that is the information retrieved by the pilot prior to the flight and used to make go/no go decisions; the information conveyed by the pilot to the NAS in the form of a flight plan; and all NAS related services which support these activities. The objective is to describe the relationship between subsystems, facilities, information, and operators/users involved in the flight planning process. In addition, the elements and operations of the NAS Plan are mapped into the flight planning requirements stated in the National Airspace System Requirement Specification. Several types of block diagrams are used to illustrate systems connectivity and operational flow. Scenarios are also derived to describe the flight planning process from a user's perspective. Author

N90-13363# Mitre Corp., McLean, VA. Civil Systems Div.
AN UPDATE TO THE SYSTEM SAFETY STUDY OF TCAS 2 Final Report
Ned A. Spencer Jun. 1989 87 p
(Contract DTFA01-89-C-00001)
(DOT/FAA/SA-89/3; MTR-88W115) Avail: NTIS HC A05/MF A01

An update to the System Safety Study of the Traffic Alert and Collision Avoidance System TCAS 2 is given. Since the time of the original study, and its companion study for instrument weather conditions, new data and new concepts have become available. Recent measurements of the Mode C reported altitude in general aviation aircraft strongly indicate that the errors assumed in the previous studies were overly conservative. On the other hand, new data on the vertical separation of aircraft at their closest point of approach indicates that this factor may have been too optimistic. The Advisory Invalid feature of the collision avoidance logic, which would provide a warning against an intruder's sudden levelling-off maneuver, was replaced with an explicit reversal or increase rate, as the case may require. These and other new concepts in the collision avoidance logic greatly reduce the computed susceptibility to a sudden intruder maneuver, given reasonable pilot reaction. Several features were also introduced into the modified logic to improve interaction with the ATC system. The effects of all of these changes are taken into account in this update. Author

N90-13364# Federal Aviation Administration, Atlantic City, NJ. Technical Center.
LORAN C STABILITY INTEGRITY ASSURANCE
Thomas Wisser Jun. 1989 40 p
(AD-A212663; DOT/FAA/CT-TN88/13) Avail: NTIS HC A03/MF A01 CSCL 17/7

A program is described which determines if an operational integrity check is necessary before beginning a Loran C nonprecision approach. Simulation testing and a questionnaire distributed to Loran C receiver manufacturers were used to determine if present state-of-the-art receivers could reliably acquire the Loran C signal. The questionnaire was designed to solicit from manufacturers the probability of reliable acquisition for state-of-the-art receivers and if improvements are possible. Flight tests were also conducted to gather preliminary information related to employing Loran C operational integrity checks prior to initiating a nonprecision approach. GRA

N90-13365# Technische Univ., Delft (Netherlands). Faculty of Geodesy.
TEST NETWORK DELFT Thesis
W. H. vanOoijen Aug. 1988 109 p
(ETN-90-96009) Avail: NTIS HC A06/MF A01

The accuracy of relative positioning with the Global Positioning System (GPS), using Trimble 4000SX receivers and the Trimble supplied baseline calculation software is tested. The test consists of the comparison of the network measured with the GPS system and the same network terrestrially surveyed with conventional surveying methods. The observations were made at five stations simultaneously. It is shown that it is not allowed to perform a network adjustment using the baselines that close a traverse one. Treatment of the eventually existing misclosure vectors in the closed traverses is studied. A procedure handling the correlated nature of the independently calculated baselines is suggested. The coordinate sets obtained from the GPS measurements and from conventional surveying are compared. It is concluded that there are no biases in the GPS derived coordinates in this network. ESA

N90-13366# Royal Signals and Radar Establishment, Malvern (England).
COMPUTER-BASED TOOLS FOR ASSISTING AIR TRAFFIC CONTROLLERS WITH ARRIVALS FLOW MANAGEMENT
S. A. N. Magill, A. C. F. Tyler, E. T. Wilkinson, and W. Finch Sep. 1988 110 p Sponsored by Civil Aviation Authority
(RSRE-88001; BR108480; ETN-90-94833) Copyright Avail: NTIS HC A06/MF A01

The use of computer based tools for arrivals flow management at major airports is reported. Two experimental prototype tools are described in detail. They were constructed and exercised in a real time simulation environment. The tools were a landing order calculator and a speed control adviser. Both give advice to air traffic controllers for aircraft which are in the vicinity of their top-of-descent points. The underlying concepts and the methods used in the tools are described. The real time simulation environment is discussed. ESA

N90-13367# Stuttgart Univ. (Germany, F.R.). Inst. of Geodesy.
GEODETIC NETWORK ADJUSTMENT USING GPS TRIPLE DIFFERENCE OBSERVATIONS AND A PRIORI STOCHASTIC INFORMATION

K. Eren Oct. 1987 56 p Sponsored by the Alexander von Humboldt Foundation
(TR-1-1987; ISSN-0933-2839; ETN-90-95861) Avail: NTIS HC A04/MF A01

A triple difference network adjustment software is presented which provides the option of introducing a priori information for the associated parameters for processing of GPS (global positioning system) observations. Triple differences are selected because they contain no bias parameters except receiver clock errors and the magnitude of clock terms is so small that a linear function can be easily substituted for the adjustment purpose. The receiver clock parameters and all the receiver and satellite positions are considered as parameters with their a priori stochastic information. Since the triple difference observations are correlated in terms of time, satellites, and receivers, the derivation and coding of these correlations is described. GPS satellites and positioning are reviewed, and GPS observations, and partials for triple difference observations and their correlations are explained. The adjustment models, mathematical derivations, and final expressions as used in the software are presented. Some case studies are provided. The approach is proposed as improving precision of adjusted quantities and yielding realistic values of uncertainties. ESA

N90-13368# Stuttgart Univ. (Germany, F.R.). Inst. of Geodesy.
PROCESSING OF UNDIFFERENCES GPS CARRIER BEAT PHASE MEASUREMENTS AND ADJUSTMENT COMPUTATIONS
W. Lindlohr 1988 66 p
(TR-5-1988; ISSN-0933-2839; ETN-90-95863) Avail: NTIS HC A04/MF A01; Institute of Geodesy, Stuttgart University, Keplerstr. 11, P.O. Box 560, D-7000 Stuttgart 1, Fed. Republic of Germany, 10 DM

A prototype software product is presented which is created to gain a some parts per mission relative accuracy in the processing of undifferenced GPS (global positioning system) carrier beat phase measurements as an alternative concept for high precision static relative positioning. System concept, program structure and computer configuration is reviewed. Conclusions on, the development of the observation equation and use of original undifferenced GPS carrier phase, the application of prediction methods in the mixed model and of estimation procedures in the Gauss-Markov-model, and their applicability on a dynamical analysis of the local displacement field, are given. ESA

05 AIRCRAFT DESIGN, TESTING AND PERFORMANCE

Includes aircraft simulation technology.

For related information see also *18 Spacecraft Design, Testing and Performance* and *39 Structural Mechanics*.For land transportation vehicles see *85 Urban Technology and Transportation*.

N90-13369*# Princeton Univ., NJ. Dept. of Mechanical and Aerospace Engineering.
TRAJECTORY OPTIMIZATION AND GUIDANCE FOR AN AEROSPACE PLANE Final Report, Sept. 1988 - Aug. 1989
Kenneth D. Mease and Mark A. VanBuren Sep. 1989 42 p
(Grant NAG1-907)
(NASA-CR-185884; NAS 1.26:185884) Avail: NTIS HC A03/MF A01 CSCL 01C

The first step in the approach to developing guidance laws for a horizontal take-off, air breathing single-stage-to-orbit vehicle is to characterize the minimum-fuel ascent trajectories. The capability to generate constrained, minimum fuel ascent trajectories for a single-stage-to-orbit vehicle was developed. A key component of this capability is the general purpose trajectory optimization program OTIS. The pre-production version, OTIS 0.96 was installed and run on a Convex C-1. A propulsion model was developed covering the entire flight envelope of a single-stage-to-orbit vehicle. Three separate propulsion modes, corresponding to an after burning turbojet, a ramjet and a scramjet, are used in the air breathing propulsion phase. The Generic Hypersonic Aerodynamic Model Example aerodynamic model of a hypersonic air breathing single-stage-to-orbit vehicle was obtained and implemented. Preliminary results pertaining to the effects of variations in acceleration constraints, available thrust level and fuel specific impulse on the shape of the minimum-fuel ascent trajectories were obtained. The results show that, if the air breathing engines are sized for acceleration to orbital velocity, it is the acceleration constraint rather than the dynamic pressure constraint that is active during ascent. Author

N90-13370*# Douglas Aircraft Co., Inc., Long Beach, CA. New Commercial Programs.
STUDY OF HIGH-SPEED CIVIL TRANSPORTS Final Report
Washington NASA Dec. 1989 182 p
(Contract NAS1-18378)
(NASA-CR-4235; NAS 1.26:4235) Avail: NTIS HC A09/MF A01 CSCL 01C

A systems study to identify the economic potential for a high-speed commercial transport (HSCT) has considered technology, market characteristics, airport infrastructure, and environmental issues. Market forecasts indicate a need for HSCT service in the 2000/2010 time frame conditioned on economic viability and environmental acceptability. Design requirements focused on a 300 passenger, 3 class service, and 6500 nautical mile range based on the accelerated growth of the Pacific region. Compatibility with existing airports was an assumed requirement. Mach numbers between 2 and 25 were examined in conjunction with the appropriate propulsion systems, fuels, structural materials, and thermal management systems. Aircraft productivity was a key parameter with aircraft worth, in comparison to aircraft price, being the airline-oriented figure of merit. Aircraft screening led to determination that Mach 3.2 (TSJF) would have superior characteristics to Mach 5.0 (LNG) and the recommendation that the next generation high-speed commercial transport aircraft use a kerosene fuel. The sensitivity of aircraft performance and economics to environmental constraints (e.g., sonic boom, engine emissions, and airport/community noise) was identified together with key technologies. In all, current technology is not adequate to produce viable HSCTs for the world marketplace. Technology advancements must be accomplished to meet environmental requirements (these requirements are as yet undetermined for sonic boom and engine emissions). High priority is assigned to aircraft gross weight reduction which benefits both economics and environmental aspects. Specific technology requirements are identified and national economic benefits are projected. Author

N90-13371# National Aerospace Lab., Amsterdam (Netherlands). Structures and Materials Div.
THE S.D.G., P.S.D. AND THE NONLINEAR AIRPLANE
R. Noback 23 Feb. 1988 26 p Presented at the Gust Specialists Research Workshop, Williamsburg, VA, 21 Apr. 1988
(Contract OV/RLD-837)
(NLR-MP-88018-U; ETN-89-95053) Avail: NTIS HC A03/MF A01

The Power Spectral Density (PSD) method and Statistical Discrete Gust (SDG) method of calculating airplane loads due to atmospheric turbulence are compared. They tend to produce the same design loads and can be regarded as equivalent. The SDG method is capable of handling calculations for nonlinear air planes. Determination of design loads using SDG however leads to prohibitively long simulation times. A method is developed which allows the PSD model to define nonlinear airplane design loads. The simulation times are thus reduced. ESA

N90-13372*# National Aeronautics and Space Administration. Hugh L. Dryden Flight Research Facility, Edwards, CA.
A SMOKE GENERATOR SYSTEM FOR AERODYNAMIC FLIGHT RESEARCH
David M. Richwine, Robert E. Curry, and Gene V. Tracy Sep. 1989 26 p
(NASA-TM-4137; H-1515; NAS 1.15:4137) Avail: NTIS HC A03/MF A01 CSCL 01C

A smoke generator system was developed for in-flight vortex flow studies on the F-18 high alpha research vehicle (HARV). The development process included conceptual design, a survey of existing systems, component testing, detailed design, fabrication, and functional flight testing. Housed in the forebody of the aircraft, the final system consists of multiple pyrotechnic smoke cartridges which can be fired simultaneously or in sequence. The smoke produced is ducted to desired locations on the aircraft surface. The smoke generator system (SGS) has been used successfully to identify vortex core and core breakdown locations as functions of flight condition. Although developed for a specific vehicle, this concept may be useful for other aerodynamic flight research which requires the visualization of local flows. Author

N90-13373# Department of the Navy, Washington, DC.
APPARATUS FOR COOLING ELECTRONIC COMPONENTS IN AIRCRAFT Patent Application
F. E. Altoz, inventor (to Navy) 25 Jan. 1989 27 p Filed 25 Jan. 1989
(AD-D014207; US-Patent-Appl-SN-304048) Avail: NTIS HC A03/MF A01 CSCL 13/1

A ram air cooling system for cooling electronic components in an aircraft provides automatic switching from a high ram air speed cooling mode (ACM) to a low ram air speed cooling mode (RAM). The cooling system receives variable speed ram air during the flight of the aircraft and includes an automatically controlled valve for either directing high speed ram air to a precooling means prior to cooling the electronic components or directing low speed ram air directly to the electronic components without precooling. The automatically controlled valve is controlled by programmable logic module means for comparing the cooling efficiency of the electronic components by precooled ram air with the cooling efficiency of the electronic components by the non-precooled ram air. The cooling efficiencies are calculated from temperature measurements of the ram air at several locations in the system of the invention. Preferably, the ram air cooling means is an air turbine which extracts energy from the ram air to drive a compressor that compresses and discharges heated air that exists from the housing for the electronic components after the ram air has performed its cooling function. GRA

N90-13374# Army Aviation Engineering Flight Activity, Edwards AFB, CA.
PRELIMINARY AIRWORTHINESS EVALUATION OF THE AH-64A EQUIPPED WITH THE AIR TO AIR STINGER (ATAS) MISSILE SYSTEM Final Report, 18 Jul. - 28 Jul. 1988
John S. Lawrence, Joseph A. Lyle, and Gerald J. Hopkins Dec. 1988 118 p
(AD-A213030) Avail: NTIS HC A06/MF A01 CSCL 01/2

A Preliminary Airworthiness Evaluation was conducted for the AH-64A equipped with the Air-To-Air Stinger (ATAS) missile system. The first phase was an evaluation of the effects of the ATAS installation on the handling qualities on the AH-64A. The second phase was a human factors evaluation of the installation of a fully operational preproduction ATAS system using captive flight training Stinger missiles, Tests were flown in the eight Hellfire missile configuration. Two Stinger missiles with launcher and mounting hardware were mounted at each wing tip. Test results were compared with data obtained during previous testing and evaluated against the AH-64 System Specification. Handling qualities of the AH-64A with the ATAS system installed were quantitatively and qualitatively evaluated and found to be essentially the same as the basic AH-64A. Specific shortcomings associated with the ATAS system were: poor integration of the Air-to-Air Stinger missile system, which is not directly compatible with the MIL STD 1553 data bus of the AH-64; insufficient ATAS sighting symbology, which does not provide the copilot/gunner with accurate missile seeker line of sight relative to the selected sight line of sight except in FLIR wide field of view; reduction in storage space imposed by the ATAS installation in the aft storage bay; location of the repositioned chaff fire switch on the cyclic hand grip; and the manual reset feature of the ATAS missile sequencing logic. The absence of an altitude encoding feature in the installation of the AN/APX-100(V) transponder was a shortcoming not associated with the ATAS modification. Nine previously reported shortcomings were evaluated during this test and still exist. GRA

N90-13375# Human Engineering Labs., Aberdeen Proving Ground, MD.
SOFTWARE AND HARDWARE DESCRIPTION OF THE HELICOPTER MOTION EQUATIONS FOR VAX COMPUTERS Final Report
Maria delCLopez Aug. 1989 101 p
(AD-A213248; HEL-TN-8-89) Avail: NTIS HC A06/MF A01 CSCL 12/5

The Human Factors Cockpit Research, Experimentation, and Workload (CREW) Simulator is a fixed base, generic helicopter simulator that provides the flexibility to explore state-of-the-art aircrew/display/control interaction. The CREW simulator involves four major components: the visual system, the graphics system, the data collection, and the flight equations. HEL uses the UH60 Blackhawk version of the standard kinematic equations for an aircraft (herein called HAC equations) when conducting experiments on the CREW simulator. The HAC equations were acquired from NASA Ames, in Mountain View, California, with the objective of simulating aerodynamic characteristics of a helicopter in a part-task simulator for human factors studies related to displays and controls. The HAC equations also allows the simulation of nap-of-the-earth (NOE) flight. The software design and the hardware configuration used to execute the HAC equations on a MicroVAX II VAXLab computer under the VMS operating system using VAX FORTRAN is described. The HAC equations are not described in detail. For more detailed information, refer to McFarland (1975). The objective is to provide internal documentation and also to provide a description of design for others desiring to implement these or similar equations of motion under the VAX/VMS (Virtual Address EXtension/Virtual Memory System) operating system in a real-time, manned interactive simulation. GRA

N90-13376 Virginia Polytechnic Inst. and State Univ., Blacksburg.
EFFICIENT METHODS FOR INTEGRATED STRUCTURAL-AERODYNAMIC WING OPTIMUM DESIGN Ph.D. Thesis
Pi-Jen Kao 1989 140 p
Avail: Univ. Microfilms Order No. DA8915725

The large computational costs of integrated multidisciplinary design is analyzed. Efficient techniques are developed to reduce the computational costs associated with integrated structural-aerodynamic design. First, efficient methods for the calculations of the derivatives of the flexibility matrix and the aerodynamic influence coefficient matrix are developed. An adjoint method is used for the flexibility sensitivity, and a perturbation method is used for the aerodynamic sensitivity. Second, a sequential optimization algorithm that employes approximate analysis methods is implemented. Finally, a modular sensitivity analysis, corresponding to the abstraction of a system as an assembly of interacting black boxes, is applied. This method was developed for calculating system sensitivity without modifying disciplinary black box software packages. The modular approach permits the calculation of aeroelastic sensitivities without the expensive calculation of the derivatives of the flexibility matrix and the aerodynamic influence coefficient matrix. Dissert. Abstr.

N90-13377 Georgia Inst. of Tech., Atlanta.
A TECHNIQUE FOR THE PREDICTION OF AERODYNAMICS AND AEROELASTICITY OF ROTOR BLADES Ph.D. Thesis
Oh Joon Kwon 1988 199 p
Avail: Univ. Microfilms Order No. DA8916159

Some of the computational issues related to coupling of a three-dimensional lifting surface method with an elastic rotor blade model were explored. A thick panel method based on piecewise constant distribution of source and doublet singularities with prescribed tip-vortex geometry and calculated inner wake is used to predict the steady-state response and aeroelastic stability of hingeless rotor blades in the hovering flight conditions. The blade

is represented by a geometrically nonlinear beam model which accounts for coupled flap bending, lead-lag bending, and torsion, and allows for moderately large displacements and rotations due to structural deformation. The analysis was carried out for the blade configuration having uniform mass and stiffness, no twist, and no chordwise offsets of the elastic axis, two-dimensional Greenberg theory which uses the simple momentum wake model. Some calculations were done to predict the aerodynamic loads of wings and rigid rotors in hover and in low-speed forward flight for code validation. The flows past two-dimensional airfoils in steady and unsteady harmonic motions were also calculated.
Dissert. Abstr.

N90-13378# Centre d'Essais Aeronautique Toulouse (France). Lab. d'Analyses non Destructives.
NONDESTRUCTIVE ANALYSIS OF AILERON FATIGUE AND AGING IN A MIRAGE F1 [ANALYSE NON DESTRUCTIVE DE COLLAGES AILERON DE FATIGUE VIEILLISSEMENT MIRAGE F1]
Ia. Armando Feb. 1989 73 p In FRENCH
(Rept-M6-594000; ETN-90-95715) Avail: NTIS HC A04/MF A01

A signal recognition method used to analyze adhesion efficiency of composite materials used in an aileron is described. Test trials were carried out on a representative test sample. The composite material was investigated using longitudinal ultrasound techniques. The development of the analysis technique is described and the limitations of the method are identified. ESA

N90-13379# Technische Univ., Delft (Netherlands). Dept. of Aerospace Engineering.
SOME NEW TECHNIQUES FOR AIRCRAFT FUSELAGE SKIN TESTS
D. Chen Jun. 1987 12 p
(LR-547; ETN-90-95990) Avail: NTIS HC A03/MF A01

The fatigue behavior of an aircraft fuselage skin is investigated. Two major aspects of the loading conditions existing in the skin are considered. The biaxial load condition and the curvature effect, are reviewed. Some new testing techniques are introduced. Further studies of these techniques are proposed. ESA

06 AIRCRAFT INSTRUMENTATION

Includes cockpit and cabin display devices; and flight instruments.

For related information see also *19 Spacecraft Instrumentation* and *35 Instrumentation and Photography.*

N90-13380*# General Dynamics Corp., San Diego, CA. Space Systems Div.
DEFINITION OF AVIONICS CONCEPTS FOR A HEAVY LIFT CARGO VEHICLE, APPENDIX A Final Report
Sep. 1989 38 p
(Contract NAS8-37578)
(NASA-CR-183817; NAS 1.26:183817) Avail: NTIS HC A03/MF A01 CSCL 01D

The major objective of the study task was to define a cost effective, multiuser simulation, test, and demonstration facility to support the development of avionics systems for future space vehicles. This volume provides the results of the main simulation processor selection study and describes some proof-of-concept demonstrations for the avionics test bed facility. Author

N90-13381*# National Aeronautics and Space Administration. Lewis Research Center, Cleveland, OH.
SILICON-ETALON FIBER-OPTIC TEMPERATURE SENSOR
Glenn Beheim, Klaus Fritsch, Joseph M. Flatico, and Massood Tabib Azar (Case Western Reserve Univ., Cleveland, OH.) 1989 8 p Presented at the Fiber Optic and Laser Sensors 7 Conference of the OE/Fibers '89 Symposium, Boston, MA, 5-8 Sep. 1989; sponsored by Society of Photo-Optical Instrumentation Engineers
(NASA-TM-102389; E-5130; NAS 1.15:102389) Avail: NTIS HC A02/MF A01 CSCL 01D

A temperature sensor is described which consists of a silicon etalon that is sputtered directly onto the end of an optical fiber. A two-layer protective cap structure is used to improve the sensor's long-term stability. The sensor's output is wavelength encoded to provide a high degree of immunity from cable and connector effects. This sensor is extremely compact and potentially inexpensive.
Author

N90-13382# RAND Corp., Santa Monica, CA.
A NEW VIEW OF WEAPON SYSTEM RELIABILITY AND MAINTAINABILITY Interim Report
J. R. Gebman, D. W. McIver, and H. L. Shulman Jan. 1989 108 p
(Contract F49620-86-C-0008)
(AD-A213281; RAND/R-3604/2-AF) Avail: NTIS HC A06/MF A01 CSCL 15/5

This report presents a new approach for evaluating weapon system reliability and maintainability. The following recommendations were made to strengthen the support process: (1) debrief pilots for all indications of faults; (2) track performance of avionics by equipment serial number; (3) share information about fault symptoms across maintenance levels (flight line to shop to depot); and (4) establish a special program to repair problem units or components. In addition to changes in the support process, some adjustments to the product improvement process and the acquisition process are suggested. GRA

N90-13383# RAND Corp., Santa Monica, CA.
A NEW VIEW OF WEAPON SYSTEM RELIABILITY AND MAINTAINABILITY: EXECUTIVE SUMMARY Interim Report
J. R. Gebman, D. W. McIver, and H. L. Shulman Jan. 1989 27 p
(Contract F49620-86-C-0008)
(AD-A213282; RAND/R-3604/1-AF) Avail: NTIS HC A03/MF A01 CSCL 15/5

The final results of the project Methods and Strategies for Improving Weapon System Reliability and Maintainability conducted within RAND's Project Air Force Resource Management Program are summarized. This project, sponsored by the Air Force Special Assistant for Reliability and Maintainability, examined tactical aircraft weapon systems. The Air Force Special Assistant for Reliability and Maintainability and The RAND Corporation jointly developed the research plan that called for RAND to develop methods and strategies for improving weapon system reliability and maintainability (R and M). GRA

N90-13384*# National Aeronautics and Space Administration. Ames Research Center, Moffett Field, CA.
FLIGHT DECK AUTOMATION: PROMISES AND REALITIES
Susan D. Norman, ed. and Harry W. Orlady, ed. (Orlady Associates, Inc., Los Gatos, CA.) Sep. 1989 200 p Proceedings of a NASA/FAA/Industry Workshop, Carmel Valley, CA, 1-4 Aug. 1988
(NASA-CP-10036; A-89196; NAS 1.55:10036) Avail: NTIS HC A09/MF A02 CSCL 01D

Issues of flight deck automation are multifaceted and complex. The rapid introduction of advanced computer-based technology onto the flight deck of transport category aircraft has had considerable impact both on aircraft operations and on the flight crew. As part of NASA's responsibility to facilitate an active exchange of ideas and information among members of the aviation community, a NASA/FAA/Industry workshop devoted to flight deck automation, organized by the Aerospace Human Factors Research Division of NASA Ames Research Center. Participants were invited from industry and from government organizations responsible for design, certification, operation, and accident investigation of transport category, automated aircraft. The goal of the workshop was to clarify the implications of automation, both positive and negative. Workshop panels and working groups identified issues regarding the design, training, and procedural aspects of flight deck automation, as well as the crew's ability to interact and perform effectively with the new technology. The proceedings

include the invited papers and the panel and working group reports, as well as the summary and conclusions of the conference.
Author

07 AIRCRAFT PROPULSION AND POWER

Includes prime propulsion systems and systems components, e.g., gas turbine engines and compressors; and onboard auxilliary power plants for aircraft.

For related information see also *20 Spacecraft Propulsion and Power, 28 Propellants and Fuels,* and *44 Energy Production and Conversion.*

N90-13385*# PDA Engineering, Santa Ana, CA.
THE APPLICATION OF CAST SiC/Al TO ROTARY ENGINE COMPONENTS Final Report
H. M. Stoller, J. R. Carluccio, and J. P. Norman 15 Aug. 1986 101 p
(Contract NAS3-24847)
(NASA-CR-179610; NAS 1.26:179610; PDA-86-FR-5333-00-06) Avail: NTIS HC A06/MF A01 CSCL 21E

A silicon carbide reinforced aluminum (SiC/Al) material fabricated by Dural Aluminum Composites Corporation was tested for various components of rotary engines. Properties investigated included hardness, high temperature strength, wear resistance, fatigue resistance, thermal conductivity, and expansion. SiC/Al appears to be a viable candidate for cast rotors, and may be applicable to other components, primarily housings. J.P.S.

N90-13386# Advanced Structures Technology, Inc., Phoenix, AZ.
DEVELOPMENT OF AN ADVANCED FAN BLADE CONTAINMENT SYSTEM Final Report, 11 Oct. 1988 - 7 Apr. 1989
Alan D. Lane Aug. 1989 34 p
(Contract DTRS-57-88-C-00117)
(DOT/FAA/CT-89/20; AST-89-004) Avail: NTIS HC A03/MF A01

The objective was to investigate potential weight savings using a ceramic-based blade containment system. Technology developed to provide light-weight armor for aircraft and aircrew members has shown that systems using ceramics (Al2O3, SiC, and B4C) are more weight efficient than metals (steel, titanium, and aluminum), or polymer fibers (fiberglass and Kevlar). Three primary subtasks were performed: design a ceramic-based fan blade containment system to achieve the maximum possible weight effectiveness; compare the ceramic containment system with current metal and Kevlar systems to quantify the potential weight improvement and corresponding cost impact; and develop a test plan, including the design of test fixtures and test articles to allow verification of improved weight effectiveness of ceramic-based systems. Author

N90-13387*# National Aeronautics and Space Administration. Lewis Research Center, Cleveland, OH.
APPLICATION OF A TWO-DIMENSIONAL UNSTEADY VISCOUS ANALYSIS CODE TO A SUPERSONIC THROUGHFLOW FAN STAGE
Ronald J. Steinke Nov. 1989 18 p
(NASA-TM-4141; E-4848; NAS 1.15:4141) Avail: NTIS HC A03/MF A01 CSCL 21E

The Rai ROTOR1 code for two-dimensional, unsteady viscous flow analysis was applied to a supersonic throughflow fan stage design. The axial Mach number for this fan design increases from 2.0 at the inlet to 2.9 at the outlet. The Rai code uses overlapped O- and H-grids that are appropriately packed. The Rai code was run on a Cray XMP computer; then data postprocessing and graphics were performed to obtain detailed insight into the stage flow. The large rotor wakes uniformly traversed the rotor-stator interface and dispersed as they passed through the stator passage. Only weak blade shock losses were computerd, which supports the design goals. High viscous effects caused large blade wakes and a low fan efficiency. Rai code flow predictions were essentially steady for the rotor, and they compared well with Chima rotor viscous code predictions based on a C-grid of similar density.
Author

N90-13388*# Pratt and Whitney Aircraft, East Hartford, CT. Commercial Engine Business.
THERMAL BARRIER COATING LIFE PREDICTION MODEL DEVELOPMENT, PHASE 1 Final Report
Jeanine T. DeMasi and Milton Ortiz Dec. 1989 338 p
(Contract NAS3-23944)
(NASA-CR-182230; NAS 1.26:182230; PWA-5970-40) Avail: NTIS HC A15/MF A02 CSCL 21E

The objective of this program was to establish a methodology to predict thermal barrier coating (TBC) life on gas turbine engine components. The approach involved experimental life measurement coupled with analytical modeling of relevant degradation modes. Evaluation of experimental and flight service components indicate the predominant failure mode to be thermomechanical spallation of the ceramic coating layer resulting from propagation of a dominant near interface crack. Examination of fractionally exposed specimens indicated that dominant crack formation results from progressive structural damage in the form of subcritical microcrack link-up. Tests conducted to isolate important life drivers have shown MCrAlY oxidation to significantly affect the rate of damage accumulation. Mechanical property testing has shown the plasma deposited ceramic to exhibit a non-linear stress-strain response, creep and fatigue. The fatigue based life prediction model developed accounts for the unusual ceramic behavior and also incorporates an experimentally determined oxide rate model. The model predicts the growth of this oxide scale to influence the intensity of the mechanic driving force, resulting from cyclic strains and stresses caused by thermally induced and externally imposed mechanical loads. Author

N90-13389*# National Aeronautics and Space Administration. Lewis Research Center, Cleveland, OH.
STOVL AIRCRAFT SIMULATION FOR INTEGRATED FLIGHT AND PROPULSION CONTROL RESEARCH
James R. Mihaloew and Colin K. Drummond 1989 23 p
Presented at the 10th Applied Dynamics International Users Society Annual Conference, Keystone, CO, 25-28 Jun. 1989
(NASA-TM-102419; E-5185; NAS 1.15:102419) Avail: NTIS HC A03/MF A01 CSCL 21E

The United States is in the initial stages of committing to a national program to develop a supersonic short takeoff and vertical landing (STOVL) aircraft. The goal of the propulsion community in this effort is to have the enabling propulsion technologies for this type aircraft in place to permit a low risk decision regarding the initiation of a research STOVL supersonic attack/fighter aircraft in the late mid-90's. This technology will effectively integrate, enhance, and extend the supersonic cruise, STOVL and fighter/attack programs to enable U.S. industry to develop a revolutionary supersonic short takeoff and vertical landing fighter/attack aircraft in the post-ATF period. A joint NASA Lewis and NASA Ames research program, with the objective of developing and validating technology for integrated-flight propulsion control design methodologies for short takeoff and vertical landing (STOVL) aircraft, was planned and is underway. This program, the NASA Supersonic STOVL Integrated Flight-Propulsion Controls Program, is a major element of the overall NASA-Lewis Supersonic STOVL Propulsion Technology Program. It uses an integrated approach to develop an integrated program to achieve integrated flight-propulsion control technology. Essential elements of the integrated controls research program are realtime simulations of the integrated aircraft and propulsion systems which will be used in integrated control concept development and evaluations. This paper describes pertinent parts of the research program leading up to the related realtime simulation development and remarks on the simulation structure to accommodate propulsion system hardware drop-in for real system evaluation. Author

N90-13390*# Southwest Research Inst., San Antonio, TX.
CONSTITUTIVE MODELING FOR ISOTROPIC MATERIALS (HOST) Annual Status Report No. 3
Kwai S. Chan, Ulric S. Lindholm, S. R. Bodner, Jeff T. Hill, R. M. Weber, and T. G. Meyer (Pratt and Whitney Aircraft, East Hartford, CT.) Aug. 1986 129 p
(Contract NAS3-23925; SwRI Proj. 06-7576)
(NASA-CR-179522; SwRI-7576/45; NAS 1.26:179522) Avail: NTIS HC A07/MF A01 CSCL 21E

The results of the third year of work on a program which is part of the NASA Hot Section Technology program (HOST) are presented. The goals of this program are: (1) the development of unified constitutive models for rate dependent isotropic materials; and (2) the demonstration of the use of unified models in structural analyses of hot section components of gas turbine engines. The unified models selected for development and evaluation are those of Bodner-Partom and of Walker. A test procedure was developed for assisting the generation of a data base for the Bodner-Partom model using a relatively small number of specimens. This test procedure involved performing a tensile test at a temperature of interest that involves a succession of strain-rate changes. The results for B1900+Hf indicate that material constants related to hardening and thermal recovery can be obtained on the basis of such a procedure. Strain aging, thermal recovery, and unexpected material variations, however, preluded an accurate determination of the strain-rate sensitivity parameter is this exercise. The effects of casting grain size on the constitutive behavior of B1900+Hf were studied and no particular grain size effect was observed. A systematic procedure was also developed for determining the material constants in the Bodner-Partom model. Both the new test procedure and the method for determining material constants were applied to the alternate material, Mar-M247 . Test data including tensile, creep, cyclic and nonproportional biaxial (tension/torsion) loading were collected. Good correlations were obtained between the Bodner-Partom model and experiments. A literature survey was conducted to assess the effects of thermal history on the constitutive behavior of metals. Thermal history effects are expected to be present at temperature regimes where strain aging and change of microstructure are important. Possible modifications to the Bodner-Partom model to account for these effects are outlined. The use of a unified constitutive model for hot section component analyses was demonstrated by applying the Walker model and the MARC finite-element code to a B1900+Hf airfoil problem. Author

N90-13391*# Southwest Research Inst., San Antonio, TX.
CONSTITUTIVE MODELING FOR ISOTROPIC MATERIALS (HOST) Annual Report No. 1
Ulric S. Lindholm, Kwai S. Chan, S. R. Bodner, R. M. Weber (Pratt and Whitney Aircraft, East Hartford, CT.), K. P. Walker, and B. N. Cassenti May 1984 127 p
(Contract NAS3-23925; SwRI Proj. 06-7576)
(NASA-CR-174718; SwRI-06-7576/13; NAS 1.26:174718) Avail: NTIS HC A07/MF A01 CSCL 21E

The results of the first year of work on a program to validate unified constitutive models for isotropic materials utilized in high temperature regions of gas turbine engines and to demonstrate their usefulness in computing stress-strain-time-temperature histories in complex three-dimensional structural components. The unified theories combine all inelastic strain-rate components in a single term avoiding, for example, treating plasticity and creep as separate response phenomena. An extensive review of existing unified theories is given and numerical methods for integrating these stiff time-temperature-dependent constitutive equations are discussed. Two particular models, those developed by Bodner and Partom and by Walker, were selected for more detailed development and evaluation against experimental tensile, creep and cyclic strain tests on specimens of a cast nickel base alloy, B19000+Hf. Initial results comparing computed and test results for tensile and cyclic straining for temperature from ambient to 982 C and strain rates from 10(exp-7) 10(exp-3) s(exp-1) are given. Some preliminary date correlations are presented also for highly non-proportional biaxial loading which demonstrate an increase in biaxial cyclic hardening rate over uniaxial or proportional loading conditions. Initial work has begun on the implementation of both constitutive models in the MARC finite element computer code. Author

N90-13392*# National Aeronautics and Space Administration. Lewis Research Center, Cleveland, OH.
TWO-DIMENSIONAL ANALYSIS OF TWO-PHASE REACTING FLOW IN A FIRING DIRECT-INJECTION DIESEL ENGINE
H. Lee Nguyen Dec. 1989 21 p
(NASA-TM-102069; E-4826; NAS 1.15:102069) Avail: NTIS HC A03/MF A01 CSCL 21E

The flow field, spray penetration, and combustion in two-stroke diesel engines are described. Fuel injection begins at 345 degrees after top dead center (ATDC) and n-dodecane is used as the liquid fuel. Arrhenius kinetics is used to calculate the reaction rate term in the quasi-global combustion model. When the temperature, fuel, and oxygen mass fraction are within suitable flammability limits, combustion begins spontaneously. No spark is necessary to ignite a localized high temperature region. Compression is sufficient to increase the gaseous phase temperature to a point where spontaneous chemical reactions occur. Results are described for a swirl angle of 22.5 degrees. Author

N90-13393*# National Aeronautics and Space Administration. Lewis Research Center, Cleveland, OH.
A PLANAR REACTING SHEAR LAYER SYSTEM FOR THE STUDY OF FLUID DYNAMICS-COMBUSTION INTERACTION
C. J. Marek, C. T. Chang, B. Ghorashi, C. C. Wey, C. Wey, and E. J. Mularz (Army Aviation Research and Development Command, Cleveland, OH.) [1989] 21 p Proposed for presentation at the 23rd International Symposium on Combustion, Orleans, France, 22-27 Jul. 1990; sponsored by Orleans Univ. Prepared in cooperation with Army Aviation Research and Development Command, Cleveland, OH
(DA Proj. 1L1-61102-AH-45)
(NASA-TM-102422; E-5063; NAS 1.15:102422; AVSCOM-TR-89-C-013) Avail: NTIS HC A03/MF A01 CSCL 21E

A versatile planar reacting shear layer facility is constructed at NASA-Lewis. The research objectives, as well as design, instrumentations and the operational procedures developed for the system are described. The fundamental governing equations and the type of quantitative information that are needed from experiments are described. Additionally, a review of earlier work is presented. Whenever appropriate, comparisons are made with similar systems in other facilities and the main differences are described. Finally, the nonintrusive measurement techniques (PLIF, PMS, LDV, and Schlieren photography) and the type of experiments that are planned are described. Author

N90-13394*# National Aeronautics and Space Administration. Lewis Research Center, Cleveland, OH.
RECENT PROGRESS IN RESEARCH PERTAINING TO ESTIMATES OF GAS-SIDE HEAT TRANSFER IN AN AIRCRAFT GAS TURBINE
Robert W. Graham [1989] 9 p Proposed for presentation at the Turbo Expo, Brussels, Belgium, 11-14 Jun. 1990; sponsored by ASME
(NASA-TM-102460; E-5247; NAS 1.15:102460) Avail: NTIS HC A02/MF A01 CSCL 21E

A decade ago several important fundamental heat transfer phenomena were identified which were considered basic to the ability to predict heat transfer loads in aircraft gas turbines. The progress in addressing these fundamentals over the past ten years is assessed. Much reseach effort has been devoted to their study in university, industry and government labs and significant progress has been achieved. Advances in computer technology have enabled the modeling of complex 3-D fluid flow in gas turbines so necessary for heat transfer calculations. Advances in instrumentation plus improved data acquisition have brought about more reliable data sets. While much has advanced in the 1980's,

much challenging research remains to be done. Several of these areas are suggested. Author

N90-13395# Technische Univ., Delft (Netherlands). Dept. of Aerospace Engineering.
AIRCRAFT PROPULSION: LEADING THE WAY IN AVIATION
H. Wittenberg Sep. 1987 37 p
(LR-532; ETN-90-95981) Avail: NTIS HC A03/MF A01

Some fundamental aspects of airbreathing propulsion systems are considered with emphasis on fuel economy in relation to the thermal and the propulsion efficiency. The state of the art of piston-engines in general aviation is surveyed and the application of gas turbines in civil transports at high-subsonic speeds is considered. Trends of future developments with respect to ducted- and unducted (propulsion) concepts are discussed. Some features of the propulsion of supersonic transports are reviewed, based on the Concorde, and future developments, and propulsion concepts for hypervelocity vehicles are reviewed. The leading role of propulsion in aviation is emphasized. ESA

08 AIRCRAFT STABILITY AND CONTROL

Includes aircraft handling qualities; piloting; flight controls; and autopilots.

For related information see also *05 Aircraft Design, Testing and Performance.*

N90-13396 Ohio State Univ., Columbus.
AEROELASTIC CONTROL OF COMPOSITE LIFTING SURFACES: INTEGRATED AEROELASTIC CONTROL OPTIMIZATION Ph.D. Thesis
Theodore Nicolas Dracopoulos 1988 131 p
Avail: Univ. Microfilms Order No. DA8907212

A new design method for aeroelastic control of composite lifting surfaces is developed and demonstrated. The design is posed as an optimization problem to determine the laminate design and the control law which maximize the critical aeroelastic speed of an actively controlled composite lifting surface without excessive expenditure of control energy. Aeroelastic tailoring and optimum control design are investigated in a formal optimization procedure. An analytical investigation, preliminary to the development of the integrated aeroelastic control optimization method, was conducted to study the effects of the interaction between laminate and active control designs on the aeroelastic stability and control performance of actively controlled composite plates. The integrated aeroelastic control optimization method is formulated and illustrated for composite lifting surfaces simulated by rectangular symmetric cantilevered composite plates, with structural and control constraints. The formulation incorporated the Rayleigh-Ritz theory, and optimum control design. The effectiveness of the method was evaluated by comparing the optimum designs obtained by the method with designs obtained by a design procedure using aeroelastic tailoring and optimum control design as well but in a non-integrated fashion. Dissert. Abstr.

N90-13397 Purdue Univ., West Lafayette, IN.
DISCRETIZATION AND MODEL REDUCTION FOR A CLASS OF NONLINEAR SYSTEMS Ph.D. Thesis
Andrew Mark King 1988 160 p
Avail: Univ. Microfilms Order No. DA8911935

Nonlinear analysis for control design is required in many modern engineering systems. Strict performance requirements over wide ranges of operation cannot be met using linear models. The lack of structure in nonlinear models has hindered the development of analysis techniques. Many engineering systems are computer controlled so that methods of attaining structured discrete-time nonlinear models are needed. Many of these nonlinear models have high model order, and effective methods for order reduction need to be developed. Both the discretization problem and the model reduction problem for a large class of nonlinear systems are addressed. A method was developed for discretizing linear-analytic continuous-time systems. The solution for the class of nonlinear systems can be expressed as a Volterra series. The result is a state-affine discrete-time system that represents an exact discretization of a specific number of terms in the Volterra series solution of a given linear-analytic continuous-time system. An algorithm is present for constructing low order approximations of state-affine discrete-time systems. The model reduction algorithm for state-affine systems is based on a new approach for constructing q-Markov covariance equivalent realizations of linear discrete-time systems. In the linear discrete-time case, the algorithm solves a model reduction problem and a partial realization problem. Dissert. Abstr.

N90-13398# Dynamic Controls, Inc., Dayton, OH.
ADVANCED ACTUATION SYSTEMS DEVELOPMENT, VOLUME 2 Final Report, May 1983 - Jan. 1987
Gavin D. Jenney, Harry W. Schreadley, John A. Anderson, William G. Talley, and Carl A. Allbright Aug. 1989 374 p
(Contract F33615-83-C-3600; AF Proj. 2403)
(AD-A213378; WRDC-TR-89-3076-Vol-2) Avail: NTIS HC A16/MF A02 CSCL 01/4

This report describes six different research and development activities in flight control actuation. The activities are: (1) the development and test of a unique linear actuator sealing system for high pressure systems, (2) the development and test of a digital servovalve using piezo-controlled high speed solenoid valves, (3) the performance evaluation of an F-15 rudder actuator under applied loads, (4) the performance evaluation of a Mission Adaptive Wing section under different load conditions, (5) the evaluation of output impedance modification of an electrohydraulic actuator for flutter suppression, and (6) the development and test of a direct drive valve and electronics (analog and digital) for an F-16 Horizontal Tail/Flaperon actuator. GRA

N90-13399# Air Force Armament Lab., Eglin AFB, FL.
AN AUTOPILOT DESIGN METHODOLOGY FOR BANK-TO-TURN MISSILES Interim Report, Mar. 1988 - Apr. 1989
Roger L. Smith Aug. 1989 108 p
(AD-A213379; AD-E801979; AFATL-TR-89-49) Avail: NTIS HC A06/MF A01 CSCL 16/2

Complete use of the multiinput/multioutput (MIMO) capability of modern control theory is utilized by employing a 3-axis, fully coupled autopilot design for the extended medium range air-to-air technology (EMRAAT) airframe. With the exception of the drag equation, all nonlinear dynamics (including coriolis and gyroscopic terms) are retained prior to model linearization. Discrete linear quadratic regulator theory is used for controller designs. Gain scheduling is addressed in a stochastic manner allowing large random parametric variations in missile roll, pitch, yaw rates, angle-of-attack, and sideslip. This is in contrast to most modern methodologies which in spite of the MIMO capability of modern control separate one axis from the other two (either roll from yaw/pitch or pitch from yaw/roll) in a decoupled design strategy. GRA

N90-13400# Cranfield Inst. of Tech., Bedford (England). College of Aeronautics.
ON THE APPLICATION OF MODIFIED STEPWISE REGRESSION FOR THE ESTIMATION OF AIRCRAFT STABILITY AND CONTROL PARAMETERS Quarterly Report No. 2, Jan. - Apr. 1989
H. A. Hinds and M. V. Cook Apr. 1989 48 p
(Contract MOD-2082/192)
(Rept-8905; ISBN-1-871315-03-4; ETN-90-95932) Avail: NTIS HC A03/MF A01

Progress made during the quarter Jan. to Apr. 1989 on research into a modified stepwise regression method for estimating the stability and control derivatives of a British Aerospace Hawk aircraft, from data obtained by use of a scaled model on a dynamic wind tunnel test rig, is discussed. The objectives are described and the program status is reported as running on schedule. Future objectives are outlined. ESA

09 RESEARCH AND SUPPORT FACILITIES (AIR)

Includes airports, hangars and runways; aircraft repair and overhaul facilities; wind tunnels; shock tubes; and aircraft engine test stands.

For related information see also *14 Ground Support Systems and Facilities (Space).*

N90-13401*# Tennessee Univ., Tullahoma. Center for Aerospace Research.

A WALL INTERFERENCE ASSESSMENT/CORRECTION INTERFACE MEASUREMENT SYSTEM FOR THE NASA/ARC 12-FT PWT Final Report

31 Jul. 1989 44 p

(Grant NAG2-551)

(NASA-CR-185474; NAS 1.26:185474) Avail: NTIS HC A03/MF A01 CSCL 14B

Development of complex air vehicle configurations is placing increasing demands on wind tunnel testing capabilities. A major area of concern is wall induced interference. Recent developments in wall interference technology provide a means for assessing and correcting for the wall induced interference using information contained in the distribution of flow variables measured at, or near, the wall. The restoration of the NASA-ARC 12-ft pressure wind tunnel (PWT) provides an opportunity to incorporate a measurement system with which wall interference assessment/correction (WIAC) technology can be applied. In this first phase of the development of a WIAC system for the PWT, the design criteria for the placement and the geometry of wall static pressure orifices were determined with a three step approach. First, the operational environment of the PWT was analyzed as to the requirements for the WIAC system. Second, appropriate wall interference theories were evaluated against the requirements determined from the operational environment. Third, the flow about representative models in the PWT was calculated and, specifically, the pressure signatures at the location of the test section wall were obtained. The number of discrete pressure measurements and their locations were determined by curve fitting the pressure distribution through the discrete measurements and evaluating the resulting error. K.C.D.

N90-13402# Army Tank-Automotive Command, Warren, MI.

USER'S MANUAL FOR THE RIDE MOTION SIMULATOR Final Report, Sep. 1988 - Aug. 1989

Alexander A. Reid Aug. 1989 119 p

(AD-A212855; TACOM-TR-13464) Avail: NTIS HC A06/MF A01 CSCL 13/6

This report presents a complete user's manual for the Ride Motion Simulator (RMS). The report details the system description, hazard controls, facility configuration and maintenance, standard operating procedures and proficiency of operator's criteria. This report contains the following information: a physical description of the simulator with emphasis upon the safety features; and a description of system operation including safety procedures. The RMS is a four degree of freedom simulator capable of recreating the ride of any army vehicle. GRA

N90-13403*# National Aeronautics and Space Administration. Langley Research Center, Hampton, VA.

A VAPOR GENERATOR FOR TRANSONIC FLOW VISUALIZATION

Robert A. Bruce, Robert W. Hess, and Jose A. Rivera, Jr. Oct. 1989 19 p

(NASA-TM-101670; NAS 1.15:101670) Avail: NTIS HC A03/MF A01 CSCL 14B

A vapor generator was developed for use in the NASA Langley Transonic Dynamics Tunnel (TDT). Propylene glycol was used as the vapor material. The vapor generator system was evaluated in a laboratory setting and then used in the TDT as part of a laser light sheet flow visualization system. The vapor generator provided satisfactory seeding of the air flow with visible condensate particles, smoke, for tests ranging from low subsonic through transonic speeds for tunnel total pressures from atmospheric pressure down to less than 0.1 atmospheric pressure. Author

N90-13404*# Thiokol Corp., Brigham City, UT. Space Operations.

SYSTEMS TUNNEL LINEAR SHAPED CHARGE LIGHTNING STRIKE Final Test Report

M. Cook Aug. 1989 26 p

(Contract NAS8-30490)

(NASA-CR-183832; NAS 1.26:183832; TWR-19872) Avail: NTIS HC A03/MF A01 CSCL 14B

Simulated lightning strike testing of the systems tunnel linear shaped charge (LSC) was performed at the Thiokol Lightning Test Complex in Wendover, Utah, on 23 Jun. 1989. The test article consisted of a 160-in. section of the LSC enclosed within a section of the systems tunnel. The systems tunnel was bonded to a section of a solid rocket motor case. All test article components were full scale. The systems tunnel cover of the test article was subjected to three discharges (each discharge was over a different grounding strap) from the high-current generator. The LSC did not detonate. All three grounding straps debonded and violently struck the LSC through the openings in the systems tunnel floor plates. The LSC copper surface was discolored around the areas of grounding strap impact, and arcing occurred at the LSC clamps and LSC ends. This test verified that the present flight configuration of the redesigned solid rocket motor systems tunnel, when subjected to simulated lightning strikes with peak current levels within 71 percent of the worst-case lightning strike condition of NSTS-07636, is adequate to prevent LSC ignition. It is therefore recommended that the design remain unchanged. Author

N90-13405*# Thiokol Corp., Brigham City, UT. Space Operations.

CABLE COUPLING LIGHTNING TRANSIENT QUALIFICATION Final Test Report

M. Cook Sep. 1989 156 p Revised

(Contract NAS8-30490)

(NASA-CR-183826; NAS 1.26:183826; TWR-17796-Rev-A) Avail: NTIS HC A08/MF A01 CSCL 14B

Simulated lightning strike testing of instrumentation cabling on the redesigned solid rocket motor was performed. Testing consisted of subjecting the lightning evaluation test article to simulated lightning strikes and evaluating the effects of instrumentation cable transients on cables within the system tunnel. The maximum short-circuit current induced onto a United Space Boosters, Inc., operational flight cable within the systems tunnel was 92 A, and the maximum induced open-circuit voltage was 316 V. These levels were extrapolated to the worst-case (200 kA) condition of NASA specification NSTS 07636 and were also scaled to full-scale redesigned solid rocket motor dimensions. Testing showed that voltage coupling to cables within the systems tunnel can be reduced 40 to 90 dB and that current coupling to cables within the systems tunnel can be reduced 30 to 70 dB with the use of braided metallic sock shields around cables that are external to the systems tunnel. Testing also showed that current and voltage levels induced onto cables within the systems tunnel are partially dependant on the cables' relative locations within the systems tunnel. Results of current injections to the systems tunnel indicate that the dominant coupling mode on cables within the systems tunnel is not from instrumentation cables but from coupling through the systems tunnel cover seam apertures. It is recommended that methods of improving the electrical bonding between individual sections of the systems tunnel covers be evaluated. Further testing to better characterize redesigned solid rocket motor cable coupling effects as an aid in developing methods to reduce coupling levels, particularly with respect to cable placement within the systems tunnel, is also recommended. Author

N90-13406 Georgia Inst. of Tech., Atlanta.

DYNAMIC TESTING TECHNIQUES AND APPLICATIONS FOR AN AEROELASTIC ROTOR TEST FACILITY Ph.D. Thesis

Mostafa Hashemi-Kia 1988 319 p
Avail: Univ. Microfilms Order No. DA8916156

A package is produced which provides operational capabilities for the new Georgia Tech Aeroelastic Rotor Test Facility. This package is constructed in a manner such that it: (1) provides sufficient and accurate calibration data for all the facility components that can be used for current and future applications; (2) illustrates test procedures for various dynamic tests for a variety of controlled test conditions; (3) validates test procedures by performing dynamic tests on a scaled model rotor; and (4) complements the experimental data by performing correlations with an analytical model. Various analytical tools and experimental test setups are used to calibrate and make major changes in the loop gain setting of the hydraulic actuator-servo systems to satisfy the test requirements. Different procedures are used to calibrate the data acquisition path, swashplate, and the rotor system. Test procedures for four types of dynamic tests are developed. These test procedures are checked through experiments on a scale model rotor. Extensive analysis and tests are performed to determine both the theoretical and experimental natural frequencies, mode shapes, and dampings of the rotor test stand. Dissert. Abstr.

N90-13407*# National Aeronautics and Space Administration. Ames Research Center, Moffett Field, CA.
A TWO-DIMENSIONAL ADAPTIVE-WALL TEST SECTION WITH VENTILATED WALLS IN THE AMES 2- BY 2-FOOT TRANSONIC WIND TUNNEL
Edward T. Schairer, George Lee, and T. Kevin McDevitt (Complere, Inc., Palo Alto, CA.) Aug. 1989 59 p
(NASA-TM-102207; A-89195; NAS 1.15:102207) Avail: NTIS HC A04/MF A01 CSCL 14B

The first tests conducted in the adaptive-wall test section of the Ames Research Center's 2- by 2-Foot Transonic Wind Tunnel are described. A procedure was demonstrated for reducing wall interference in transonic flow past a two-dimensional airfoil by actively controlling flow through the slotted walls of the test section. Flow through the walls was controlled by adjusting pressures in compartments of plenums above and below the test section. Wall interference was assessed by measuring (with a laser velocimeter) velocity distributions along a contour surrounding the model, and then checking those measurements for their compatibility with free-air far-field boundary conditions. Plenum pressures for minimum wall interference were determined from empirical influence coefficients. An NACA 0012 airfoil was tested at angles of attach of 0 and 2, and at Mach numbers between 0.70 and 0.85. In all cases the wall-setting procedure greatly reduced wall interference. Wall interference, however, was never completely eliminated, primarily because the effect of plenum pressure changes on the velocities along the contour could not be accurately predicted.
Author

N90-13408# Royal Aircraft Establishment, Farnborough (England).
HELICOPTER ROTOR TEST RIG (RoTeSt) IN DNW: APPLICATION AND RESULTS
H.-J. Langer, G. Braun, B. Junker, R. W. Quartermaine, ed., and R. J. Marshall, ed. Feb. 1989 18 p Transl. into ENGLISH from DGLR, Jahrestagung, Bonn, West Germany, 30 Sep. - 2 Oct. 1985 Original language document was announced in IAA as A86-35166
(RAE-Trans-2171; BR112013; DGLR-Paper-85-113) Avail: NTIS HC A03/MF A01

The model standardization and functioning of the helicopter test installation RoTeSt in DNW is discussed. The choice of standardization factors for the different aspects of the installation is addressed, and a block diagram of the installation signal flow is given. Tests conducted on various rotors in the installation's wind tunnel are reviewed, showing results on the relation between model rotor operation points and flight states, on the derivative of the longitudinal angle of control as a function of velocity, on correction values for rotor angle of attack for various measuring section configurations and mast angles of inclination, and on the effect of tunnel temperature on the rotor thrust for constant rotational speed. Comparison results for various rotors are given, including accelerations, dynamic momentum behavior, and measurements of downwash. IAA

N90-13409# Loughborough Univ. of Technology (England). Dept. of Transport Technology.
AIRCRAFT/AIRPORT COMPATIBILITY: SOME STRATEGIC, TACTICAL, AND OPERATIONAL ISSUES
Robert Caves Jun. 1989 28 p Presented at the 3rd National Seminar on Airports and Air Transport, Sao Jose dos Campos, Brazil, 26-28 Apr. 1989
(TT-8902; ISBN-0-904947-14-9; ETN-90-95935) Copyright
Avail: NTIS HC A03/MF A01

Strategic and operational aspects of the relationship between aircraft and airports are examined. Strategically, historic difficulties in achieving compatibility are discussed and careful attention to controlling the use of ever larger aircraft is suggested. Further potential in vertical and short takeoff and landing aircraft, for solving the long term pressures of system capacity, total system cost, noise and safety, is proposed. Operationally, runway safety, accommodating larger aircraft and apron space efficiency, are highlighted. Minimization of problems of both airside geometry and apron space efficiency are proposed by development of aircraft with high ratios of payload to span. ESA

N90-13410# Technische Univ., Delft (Netherlands). Dept. of Aerospace Engineering.
MATHEMATICAL MODEL IDENTIFICATION FOR FLIGHT SIMULATION, BASED ON FLIGHT AND TAXI TESTS
M. Baarspul, J. A. Mulder, A. H. M. Nieuwpoort, and J. H. Breeman Feb. 1989 33 p Presented at the International Conference on Flight Simulation: Recent Developments in Technology and Use, London, England, 12-13 Apr. 1988 Previously announced in IAA as A89-48833
(LR-550; ETN-90-95993) Avail: NTIS HC A03/MF A01

Tasks carried out to develop the mathematical model and data package for the Citation 500 full flight simulator are described. The a priori models of the aerodynamics, engines, mass properties, flight control system and landing gear are outlined. The high accuracy measurement system and the flight test program are discussed. The data analysis and mathematical model development are described using the aerodynamic lift coefficient as an example. Offline and online flight simulation used for model evaluation are discussed and model validation is described with some results outlined. ESA

12 ASTRONAUTICS (GENERAL)

For extraterrestrial exploration see *91 Lunar and Planetary Exploration.*

N90-13411 Institut d'Aeronomie Spatiale de Belgique, Brussels.
A SUMMARY OF 30 YEARS OF SPACE LAUNCHES [BILAN DE 30 ANS DE LANCEMENTS SPATIAUX]
J. Vercheval 1989 359 p In FRENCH; ENGLISH summary
(Aeronomica-Acta-F-39-1989; ISSN-0065-3713; ETN-90-95930)
Avail: Institut d'Aeronomie Spatiale de Belgique, 3 Avenue Circulaire, B-1180 Brussels, Belgium

A general report of space flights concluded on 31 December 1987 is made, with a distinction between launches and satellites with payloads (including space probes). A table is given with the orbital elements drawn as an alphabetical classification of the satellites. The nature of the missions is explained in a glossary. A chronological list is given of the manned space flights. ESA

N90-13412*# Jet Propulsion Lab., California Inst. of Tech., Pasadena.
THE VOYAGER NEPTUNE TRAVEL GUIDE
Charles Kohlhase, ed. 1 Jun. 1989 292 p
(Contract NAS7-918)
(NASA-CR-186108; JPL-Publ-89-24; NAS 1.26:186108) Avail: NTIS HC A13/MF A02 CSCL 22A

The Voyager mission to the giant outer planets of our solar system is described. Scientific highlights include interplanetary cruise, Jupiter, Saturn, Uranus, and their vast satellite and ring systems. Detailed plans are provided for the August 1989 Neptune encounter and subsequent interstellar journey to reach the heliopause. As background, the elements of an unmanned space mission are explained, with emphasis on the capabilities of the spacecraft and the scientific sensors. Other topics include the Voyager Grand Tour trajectory design, deep-space navigation, and gravity-assist concepts. The Neptune flyby is animated through the use of computer-generated, flip-page movie frames that appear in the corners of the publication. Useful historical information is also presented, including facts associated with the Voyager mission. Finally, short summaries are provided to describe the major objectives and schedules for several space missions planned for the remainder of the 20th century. Author

N90-13524# European Space Agency, Paris (France).
LAUNCH AND EARLY ORBIT
K. Clausen *In its* The Hipparcos Mission. Prelaunch Status. Volume 1: The Hipparcos Satellite Jun. 1989 p 265-269 (For primary document see N90-13499 05-18)
Copyright Avail: NTIS HC A16/MF A02; ESA Publications Div., ESTEC, Noordwijk, Netherlands, 80 Dutch guilders

N90-13525# European Space Agency, Paris (France).
THE IN-ORBIT INITIALIZATION PHASE
J. vanderHa *In its* The Hipparcos Mission. Prelaunch Status. Volume 1: The Hipparcos Satellite Jun. 1989 p 271-282 (For primary document see N90-13499 05-18)
Copyright Avail: NTIS HC A16/MF A02; ESA Publications Div., ESTEC, Noordwijk, Netherlands, 80 Dutch guilders

N90-13526# European Space Agency, Paris (France).
IN-ORBIT PAYLOAD CALIBRATION
R. D. Wills *In its* The Hipparcos Mission. Prelaunch Status. Volume 1: The Hipparcos Satellite Jun. 1989 p 283-295 (For primary document see N90-13499 05-18)
Copyright Avail: NTIS HC A16/MF A02; ESA Publications Div., ESTEC, Noordwijk, Netherlands, 80 Dutch guilders

N90-13532# European Space Agency, Paris (France).
MISSION SIMULATIONS
M. Creze, B. Nicolet, and M. Chareton *In its* The Hipparcos Mission. Prelaunch Status. Volume 2: The Input Catalog Jun. 1989 p 47-64 Original contains color illustrations (For primary document see N90-13529 05-18)
Copyright Avail: NTIS HC A13/MF A02; ESA Publications Div., ESTEC, Noordwijk, Netherlands, 80 Dutch guilders

13 ASTRODYNAMICS

Includes powered and free-flight trajectories; and orbital and launching dynamics.

N90-13413*# National Aeronautics and Space Administration. Goddard Space Flight Center, Greenbelt, MD.
FLIGHT MECHANICS/ESTIMATION THEORY SYMPOSIUM, 1989
Thomas Stengle, ed. Washington Oct. 1989 466 p Symposium held in Greenbelt, MD, 23-24 May 1989
(NASA-CP-3050; Rept-89B00261; NAS 1.55:3050) Avail: NTIS HC A20/MF A03 CSCL 22A

Numerous topics in flight mechanics and estimation were discussed. Satellite attitude control, quaternion estimation, orbit and attitude determination, spacecraft maneuvers, spacecraft navigation, gyroscope calibration, spacecraft rendevous, and atmospheric drag model calculations for spacecraft lifetime prediction are among the topics covered. For individual titles, see N90-13414 through N90-13440.

N90-13414*# Computer Sciences Corp., Silver Spring, MD.
THE EFFECTS OF SEASONAL AND LATITUDINAL EARTH INFRARED RADIANCE VARIATIONS ON ERBS ATTITUDE CONTROL
M. C. Phenneger, J. Dehen, D. Foch, E. Harvie, and M. Virdy *In* NASA, Goddard Space Flight Center, Flight Mechanics/Estimation Theory Symposium, 1989 Oct. 1989 p 3-22 (For primary document see N90-13413 05-13)
(Contract NAS5-31500)
Avail: NTIS HC A20/MF A03 CSCL 22A

Analysis performed in the Flight Dynamics Facility by the Earth Radiation Budget Satellite (ERBS) Attitude Determination Support team illustrates the pitch attitude control motion and roll attitude errors induced by Earth infrared (IR) horizon radiance variations. IR scanner and inertial reference unit (IRU) pitch and roll flight data spanning 4 years of the ERBS mission are analyzed to illustrate the changes in the magnitude of the errors on time scales of the orbital period, months, and seasons. The analysis represents a unique opportunity to compare prelaunch estimates of radiance-induced attitude errors with flight measurements. As a consequence of this work the following additional information is obtained: an assessment of an average model of these errors and its standard deviation, a measurement to determine and verify previously proposed corrections to the current Earth IR radiance data base, and the possibility of a mean motion model derived from flight data in place of IRU data for ERBS fine attitude determination. Author

N90-13415*# Johns Hopkins Univ., Laurel, MD. Applied Physics Lab.
AUTONOMOUS SPACECRAFT ATTITUDE CONTROL USING MAGNETIC TORQUING ONLY **c18**
Keith L. Musser and Ward L. Ebert *In* NASA, Goddard Space Flight Center, Flight Mechanics/Estimation Theory Symposium, 1989 Oct. 1989 p 23-38 (For primary document see N90-13413 05-13)
Avail: NTIS HC A20/MF A03 CSCL 22B

Magnetic torquing of spacecraft has been an important mechanism for attitude control since the earliest satellites were launched. Typically a magnetic control system has been used for precession/nutation damping for gravity-gradient stabilized satellites, momentum dumping for systems equipped with reaction wheels, or momentum-axis pointing for spinning and momentum-biased spacecraft. Although within the small satellite community there has always been interest in expensive, light-weight, and low-power attitude control systems, completely magnetic control systems have not been used for autonomous three-axis stabilized spacecraft due to the large computational requirements involved. As increasingly more powerful microprocessors have become available, this has become less of an impediment. These facts have motivated consideration of the all-magnetic attitude control system presented here. The problem of controlling spacecraft attitude using only magnetic torquing is cast into the form of the Linear Quadratic Regulator (LQR), resulting in a linear feedback control law. Since the geomagnetic field along a satellite trajectory is not constant, the system equations are time varying. As a result, the optimal feedback gains are time-varying. Orbit geometry is exploited to treat feedback gains as a function of position rather than time, making feasible the onboard solution of the optimal control problem. In simulations performed to date, the control laws have shown themselves to be fairly robust and a good candidate for an onboard attitude control system. Author

N90-13416*# National Aeronautics and Space Administration. Lyndon B. Johnson Space Center, Houston, TX.
PERIODIC-DISTURBANCE ACCOMMODATING CONTROL OF THE SPACE STATION FOR ASYMPTOTIC MOMENTUM MANAGEMENT **c18**
Wayne Warren, Bong Wie (Texas Univ., Austin.), and David Geller *In* NASA, Goddard Space Flight Center, Flight Mechanics/Estimation Theory Symposium, 1989 Oct. 1989

p 39-50 Previously announced in IAA as A89-52570 (For primary document see N90-13413 05-13)
Avail: NTIS HC A20/MF A03 CSCL 22B

Periodic-disturbance accommodating control is investigated for asymptotic momentum management of control moment gyros used as primary actuating devices for the Space Station. The proposed controller utilizes the concepts of quaternion feedback control and periodic-disturbance accommodation to achieve oscillations about the constant torque equilibrium attitude, while minimizing the control effort required. Three-axis coupled equations of motion, written in terms of quaternions, are derived for roll/yaw controller design and stability analysis. The quaternion feedback controller designed using the linear-quadratic regulator synthesis technique is shown to be robust for a wide range of pitch angles. It is also shown that the proposed controller tunes the open-loop unstable vehicle to a stable oscillatory motion which minimizes the control effort needed for steady-state operations. Author

N90-13417*# National Aeronautics and Space Administration. Goddard Space Flight Center, Greenbelt, MD.
SIMULTANEOUS QUATERNION ESTIMATION (QUEST) AND BIAS DETERMINATION
F. Landis Markley *In its* Flight Mechanics/Estimation Theory Symposium, 1989 Oct. 1989 p 51-63 (For primary document see N90-13413 05-13)
Avail: NTIS HC A20/MF A03 CSCL 22A

Tests of a new method for the simultaneous estimation of spacecraft attitude and sensor biases, based on a quaternion estimation algorithm minimizing Wahba's loss function are presented. The new method is compared with a conventional batch least-squares differential correction algorithm. The estimates are based on data from strapdown gyros and star trackers, simulated with varying levels of Gaussian noise for both inertially-fixed and Earth-pointing reference attitudes. Both algorithms solve for the spacecraft attitude and the gyro drift rate biases. They converge to the same estimates at the same rate for inertially-fixed attitude, but the new algorithm converges more slowly than the differential correction for Earth-pointing attitude. The slower convergence of the new method for non-zero attitude rates is believed to be due to the use of an inadequate approximation for a partial derivative matrix. The new method requires about twice the computational effort of the differential correction. Improving the approximation for the partial derivative matrix in the new method is expected to improve its convergence at the cost of increased computational effort. Author

N90-13418*# Computer Sciences Corp., Silver Spring, MD.
COBE NONSPINNING ATTITUDE PROPAGATION
D. Chu *In* NASA, Goddard Space Flight Center, Flight Mechanics/Estimation Theory Symposium, 1989 Oct. 1989 p 65-73 (For primary document see N90-13413 05-13)
(Contract NAS5-31500)
Avail: NTIS HC A20/MF A03 CSCL 22A

The Cosmic Background Explorer (COBE) spacecraft will exhibit complex attitude motion consisting of a spin rate of approximately -0.8 revolution per minute (rpm) about the x-axis and simultaneous precession of the spin axis at a rate of one revolution per orbit (rpo) about the nearly perpendicular spacecraft-to-Sun vector. The effect of the combined spinning and precession is to make accurate attitude propagation difficult and the 1-degree (3 sigma) solution accuracy goal problematic. To improve this situation, an intermediate reference frame is introduced, and the angular velocity divided into two parts. The nonspinning part is that which would be observed if there were no rotation about the X-axis. The spinning part is simply the X-axis component of the angular velocity. The two are propagated independently and combined whenever the complete attitude is needed. This approach is better than the usual one-step method because each of the two angular velocities look nearly constant in their respective reference frames. Since the angular velocities are almost constant, the approximations made in discrete time propagation are more nearly true. To demonstrate the advantages of this nonspinning method, attitude is propagated as outlined above and is then compared with the results of the one-step method. Over the 100-minute COBE orbit, the one-step error grows to several degrees while the nonspinning error remains negligible. Author

N90-13419*# Auburn Univ., AL. Dept. of Aerospace Engineering.
SIMULATION OF SPACECRAFT ATTITUDE DYNAMICS USING TREETOPS AND MODEL-SPECIFIC COMPUTER CODES c18
John E. Cochran, T. S. No, and Norman G. Fitz-Coy *In* NASA, Goddard Space Flight Center, Flight Mechanics/Estimation Theory Symposium, 1989 Oct. 1989 p 75-95 (For primary document see N90-13413 05-13)
Avail: NTIS HC A20/MF A03 CSCL 22B

The simulation of spacecraft attitude dynamics and control using the generic, multi-body code called TREETOPS and other codes written especially to simulate particular systems is discussed. Differences in the methods used to derive equations of motion--Kane's method for TREETOPS and the Lagrangian and Newton-Euler methods, respectively, for the other two codes--are considered. Simulation results from the TREETOPS code are compared with those from the other two codes for two example systems. One system is a chain of rigid bodies; the other consists of two rigid bodies attached to a flexible base body. Since the computer codes were developed independently, consistent results serve as a verification of the correctness of all the programs. Differences in the results are discussed. Results for the two-rigid-body, one-flexible-body system are useful also as information on multi-body, flexible, pointing payload dynamics. Author

N90-13420*# MCI Telecommunications Corp., Clarksburg, MD.
ORBIT AND ATTITUDE DETERMINATION RESULTS DURING LAUNCH SUPPORT OPERATIONS FOR SBS-5
K. R. Hartman and P. J. Iano *In* NASA, Goddard Space Flight Center, Flight Mechanics/Estimation Theory Symposium, 1989 Oct. 1989 p 97-116 (For primary document see N90-13413 05-13)
(Paper-7) Avail: NTIS HC A20/MF A03 CSCL 22A

Presented are orbit and attitude determination results from the launch of Satellite Business Systems (SBS)-5 satellite on September 8, 1988 by Arianespace. SBS-5 is a (HS-376) spin stabilized spacecraft. The launch vehicle injected the spacecraft into a low inclination transfer orbit. Apogee motor firing (AMF) attitude was achieved with trim maneuvers. An apogee kick motor placed the spacecraft into drift orbit. Postburn, reorientation and spindown maneuvers were performed during the next 25 hours. The spacecraft was on-station 19 days later. The orbit and attitude were determined by both an extended Kalman filter and a weighted least squares batch processor. Although the orbit inclination was low and the launch was near equinox, post-AMF analysis indicated an attitude declination error of 0.034 deg., resulting in a saving of 8.5 pounds of fuel. The AMF velocity error was 0.4 percent below nominal. The post-AMF drift rate was determined with the filter only 2.5 hours after motor firing. The filter was used to monitor and retarget the reorientation to orbit normal in real time. Author

N90-13421*# National Aeronautics and Space Administration. Goddard Space Flight Center, Greenbelt, MD.
GOES-I/M ASCENT MANEUVERS FROM TRANSFER ORBIT TO STATION
S. Abeyagunawardene, S. Devlin, D. Elkin (Computer Sciences Corp., Silver Spring, MD.), and R. DeFazio *In its* Flight Mechanics/Estimation Theory Symposium, 1989 Oct. 1989 p 117-127 (For primary document see N90-13413 05-13)
(Contract NAS5-31500)
Avail: NTIS HC A20/MF A03 CSCL 22A

The Geostationary Operational Environmental Satellite (GOES)-I/M station acquisition sequence consists nominally of three in-plane/out-of-plane maneuvers at apogee on the line of relative nodes and a small in-plane maneuver at perigee. Existing software to determine maneuver attitude, ignition time, and burn duration required modification to optimize the out-of-plane parts and admit the noninertial, three-axis stabilized attitude. The Modified

Multiple Impulse Station Acquisition Maneuver Planning Program (SENARIO2) was developed from its predecessor, SCENARIO, to optimize the out-of-plane components of the impulsive delta-V vectors. Additional new features include commputation of short term J sub 2 perturbations and output of all premaneuver and postmaneuver orbit elements, coarse maneuver attitudes, propellant usage, spacecraft antenna aspect angles, and ground station coverage. The output data are intended to be used in the launch window computation and by the maneuver targeting computation (General Maneuver (GMAN) Program) software. The maneuver targeting computation in GMAN was modified to admit the GOES-I/M maneuver attitude. Appropriate combinations of ignition time, burn duration, and attitude enable any reasonable target orbit to be achieved. Author

N90-13422*# Computer Sciences Corp., Silver Spring, MD.
GOES I/M IMAGE NAVIGATION AND REGISTRATION
J. L. Fiorello, Jr., I. H. Oh, K. A. Kelly, and L. Ranne (National Oceanic and Atmospheric Administration, Suitland, MD.) *In* NASA, Goddard Space Flight Center, Flight Mechanics/Estimation Theory Symposium, 1989 Oct. 1989 p 129-147 (For primary document see N90-13413 05-13)
(Contract NOAA-50-DGNE-6-00003)
Avail: NTIS HC A20/MF A03 CSCL 22A

Image Navigation and Registration (INR) is the system that will be used on future Geostationary Operational Environmental Satellite (GOES) missions to locate and register radiometric imagery data. It consists of a semiclosed loop system with a ground-based segment that generates coefficients to perform image motion compensation (IMC). The IMC coefficients are uplinked to the satellite-based segment, where they are used to adjust the displacement of the imagery data due to movement of the imaging instrument line-of-sight. The flight dynamics aspects of the INR system is discussed in terms of the attitude and orbit determination, attitude pointing, and attitude and orbit control needed to perform INR. The modeling used in the determination of orbit and attitude is discussed, along with the method of on-orbit control used in the INR system, and various factors that affect stability. Also discussed are potential error sources inherent in the INR system and the operational methods of compensating for these errors.
Author

N90-13423*# McDonnell-Douglas Astronautics Co., Houston, TX. Engineering Services Div.
SHUTTLE RELATIVE NAVIGATION OF A TETHERED SATELLITE MISSION WITH CURRENT ON BOARD SOFTWARE
Kevin A. Lee *In* NASA, Goddard Space Flight Center, Flight Mechanics/Estimation Theory Symposium, 1989 Oct. 1989 p 149-168 (For primary document see N90-13413 05-13)
Avail: NTIS HC A20/MF A03 CSCL 22A

A Shuttle mission planned in 1991 will test the feasibility of tethers in space. This mission, a joint effort between Italy and the United States, will connect a satellite (built by the Italians) to the Shuttle with a 20 km long tether. This mission poses unique navigation problems. The flight software on the Shuttle was never designed to account for the low level acceleration that is generated by the gravity gradient. IMUs on the Shuttle was never designed to account for the low level acceleration that is generated by the gravity gradient. Inertial Maneuvering Units on the shuttle will sense the acceleration of the tether but it turns out that incorporating the continuous accelerometer noise also generates large error growth. Relative navigation is another important issue since the majority of the mission will be conducted while the satellite is out of the visual range of the crew. Some kind of feedback on the motion of the satellite will be desirable. Feedback of the satellite motion can be generated by using the rendezvous radar. To process the radar measurements, the flight software uses a 13 state Kalman Filter, but unfortunately with the filter currently tuned as it is, valid measurements tend to be ignored. This is due to the constraint of the tether on the satellite, which is an unmodeled force. Analysis shows that with proper tuning, relative navigation is possible.
Author

N90-13424*# McDonnell-Douglas Astronautics Co., Houston, TX. Engineering Services Div.
IMPACT OF TETHER CUTTING ON ONBOARD NAVIGATION DURING THE TETHERED SATELLITE MISSION-1
Dana M. Pirker *In* NASA, Goddard Space Flight Center, Flight Mechanics/Estimation Theory Symposium, 1989 Oct. 1989 p 169-180 (For primary document see N90-13413 05-13)
Avail: NTIS HC A20/MF A03 CSCL 22A

The first Tethered Satellite System mission (TSS-1) is manifested for Shuttle Flight STS-44 in January of 1991. The TSS mission presents a new challenge to engineers, requiring advanced guidance, navigation and control concepts. Current NASA flight rules require that the navigational state of the Orbiter at deorbit burn be known to an accuracy of 20 nautical miles. Response of the Shuttle crew to this contingency may involve cutting the tether prior to a complete retrieval. The degradation of the navigational state accuracy as modelled by Shuttle navigation system is examined. Responses to the loss of communication scenario are proposed for two cases. The first case examines navigational performance during a nominal attitude profile. The second case is identical to the first, with the inclusion of modelled tether electrodynamical forces. Comparisons of trajectories propagated from the onboard navigational state vector and a reference ephemeris state vector were performed, with the tether cut simulated at various points during the mission. Additionally, updates to the onboard navigational state via ground uplinks were provided prior to the assumed loss of communication. Through these comparisons, the onboard navigation state error was determined. Alternative responses result from efforts to minimize this error during the various phases of TSS-1 deployment. These results demonstrated existing NASA flight rules could be violated by cutting the tether, and suggests reponses to a loss of communications contingency to maintain a more accurate navigational state.
Author

N90-13425*# McDonnell-Douglas Astronautics Co., Houston, TX. Guidance and Control Mechanics.
SHUTTLE TETHERED OPERATIONS: THE EFFECT ON ORBITAL TRAJECTORY AND INERTIAL NAVIGATION
Mark N. Lardas *In* NASA, Goddard Space Flight Center, Flight Mechanics/Estimation Theory Symposium, 1989 Oct. 1989 p 181-199 (For primary document see N90-13413 05-13)
Avail: NTIS HC A20/MF A03 CSCL 22A

The first full scale test of a large tethered satellite system is planned. The Orbiter will be linked to a 500 kg payload by a 20 km tether, an action with a profound effect on the trajectory of the Orbiter. For the first time in the history of the Shuttle program, the vehicle will conduct prolonged operations with the center of mass of the orbiting system a significant distance from the center of mass of the Space Shuttle Orbiter, a violation of the fundamental assumption made in both the Orbiter ground-based and onboard navigation software. Inertial navigation of tethered operations with the Shuttle is further complicated by the presence of non-conservative forces in the system: Reaction Control System (RCS) translational effects, atmospheric drag, and electro-magnetic dynamics. These can couple with the conservative tether dynamics effects, and degrade the navigation software performance. The primary effects are examined on the Orbiter's trajectory, coupling by conservative forces during tethered operations, and the impact of both on the ability to meet inertial navigation constraints. The impact of electrodynamics, different RCS control modes, commanded attitudes, and attitude deadbands are presented. Operational guidelines which optimize successful mission navigation, and necessary navigation constraints are discussed.
Author

N90-13426*# Computer Sciences Corp., Silver Spring, MD.
TEMPERATURE DEPENDENCE OF ATTITUDE SENSOR COALIGNMENTS ON THE SOLAR MAXIMUM MISSION (SMM)
D. S. Pitone, A. H. Eudell, and F. S. Patt (Applied Research Corp., Greenbelt, MD.) *In* NASA, Goddard Space Flight Center, Flight Mechanics/Estimation Theory Symposium, 1989 Oct. 1989

p 201-219 (For primary document see N90-13413 05-13)
(Contract NAS5-31500)
Avail: NTIS HC A20/MF A03 CSCL 22A

Results are presented on the temperature correlation of the relative coalignment between the fine pointing sun sensor (FPSS) and fixed head star trackers (FHSTs) on the Solar Maximum Mission (SMM). This correlation can be caused by spacecraft electronic and mechanical effects. Routine daily measurements reveal a time dependent sensor coalignment variation. The magnitude of the alignment variation is on the order of 120 arc seconds (arc sec), which greatly exceeds the prelaunch thermal structural analysis estimate of 15 acr sec. Differences between FPSS-only and FHST-only yaw solutions as a function of mission day are correlated with the relevant spacecraft temperature. If unaccounted for, the sensor misalignments due to thermal effects are a significant source of error in attitude determination accuracy. Prominent sources of temperature variation are identified and correlated with the temperature profile observed on the SMM. It was determined that even relatively small changes in spacecraft temperature can affect the coalignments between the attitude hardware on the SMM and the science instrument support plate and that frequent recalibration of sensor alignments is necessary to compensate for this effect. An alterntive to frequent recalibration is to model the variation of alignments as a function of temperature and use this to maintain accurate ground or onboard alignment estimates. These flight data analysis results may be important consierations for prelaunch analysis of future missions. Author

N90-13427*# National Aeronautics and Space Administration. Goddard Space Flight Center, Greenbelt, MD.
TRUE COVARIANCE SIMULATION OF THE EUVE UPDATE FILTER
Itzhack Y. Bar-Itzhack (Technion - Israel Inst. of Tech., Haifa.) and R. R. Harman *In its* Flight Mechanics/Estimation Theory Symposium, 1989 Oct. 1989 p 223-235 (For primary document see N90-13413 05-13)
Avail: NTIS HC A20/MF A03 CSCL 22A

A covariance analysis of the performance and sensitivity of the attitude determination Extended Kalman Filter (EKF) used by the On Board Computer (OBC) of the Extreme Ultra Violet Explorer (EUVE) spacecraft is presented. The linearized dynamics and measurement equations of the error states are derived which constitute the truth model describing the real behavior of the systems involved. The design model used by the OBC EKF is then obtained by reducing the order of the truth model. The covariance matrix of the EKF which uses the reduced order model is not the correct covariance of the EKF estimation error. A true covariance analysis has to be carried out in order to evaluate the correct accuracy of the OBC generated estimates. The results of such analysis are presented which indicate both the performance and the sensitivity of the OBC EKF. Author

N90-13428*# National Aeronautics and Space Administration. Goddard Space Flight Center, Greenbelt, MD.
A GYROSCOPE CALIBRATION ANALYSIS FOR THE GAMMA RAY OBSERVATORY (GRO) **c35**
Eleanor A. Ketchum and Michael H. Lee (Computer Sciences Corp., Silver Spring, MD.) *In its* Flight Mechanics/Estimation Theory Symposium, 1989 Oct. 1989 p 237-253 (For primary document see N90-13413 05-13)
(Contract NAS5-31500)
Avail: NTIS HC A20/MF A03 CSCL 14B

Current documentation and software do not adequately address the calculation and use of the optimal weight matrices involved in calibrating inertial reference units (IRU). Several facets of the GRO IRU calibration as it relates to the bias and misalignment weighting matrices are investigated. The physical meaning and use of the bias and misalignment weight matrices in IRU calibration are examined. The relation of the weighting and the final biases, misalignments, and their corrections are pursued. Methods for determining reliable, realistic weighting matrices to be used in the GRO IRU calibration (IRUCAL) utility are determined. Possible correlations among observation uncertainties are also explored. For the undetermined case where the maneuvers are insufficient to identify all calibration parameters, the weighting matrices allow as much information as possible to be extracted from the measurements. Finally, applicable simulated flight data are used, incorporating the appropriate calibration maneuvers, to test the weighting matrices in the IRUCAL utility, and examine correlation effects. Author

N90-13429*# OAO Corp., Greenbelt, MD.
SPACECRAFT ATTITUDE DETERMINATION USING THE EARTH'S MAGNETIC FIELD
David G. Simpson *In* NASA, Goddard Space Flight Center, Flight Mechanics/Estimation Theory Symposium, 1989 Oct. 1989 p 255-274 (For primary document see N90-13413 05-13)
(Contract NAS5-29320)
Avail: NTIS HC A20/MF A03 CSCL 22A

A method is presented by which the attitude of a low-Earth orbiting spacecraft may be determined using a vector magnetometer, a digital Sun sensor, and a mathematical model of the Earth's magnetic field. The method is currently being implemented for the Solar Maximum Mission spacecraft (as a backup for the failing star trackers) as a way to determine roll gyro drift. Author

N90-13430*# Illinois Univ., Urbana. Dept. of Aeronautical and Astronautical Engineering.
BILINEAR MODELING AND NONLINEAR ESTIMATION **c64**
Thomas A. W. Dwyer, III, Fakhreddine Karray, and William H. Bennett *In* NASA, Goddard Space Flight Center, Flight Mechanics/Estimation Theory Symposium, 1989 Oct. 1989 p 275-297 (For primary document see N90-13413 05-13)
(Grants NAG1-613; F49620-87-C-0103)
Avail: NTIS HC A20/MF A03 CSCL 12A

New methods are illustrated for online nonlinear estimation applied to the lateral deflection of an elastic beam on board measurements of angular rates and angular accelerations. The development of the filter equations, together with practical issues of their numerical solution as developed from global linearization by nonlinear output injection are contrasted with the usual method of the extended Kalman filter (EKF). It is shown how nonlinear estimation due to gyroscopic coupling can be implemented as an adaptive covariance filter using off-the-shelf Kalman filter algorithms. The effect of the global linearization by nonlinear output injection is to introduce a change of coordinates in which only the process noise covariance is to be updated in online implementation. This is in contrast to the computational approach which arises in EKF methods arising by local linearization with respect to the current conditional mean. Processing refinements for nonlinear estimation based on optimal, nonlinear interpolation between observations are also highlighted. In these methods the extrapolation of the process dynamics between measurement updates is obtained by replacing a transition matrix with an operator spline that is optimized off-line from responses to selected test inputs. Author

N90-13431*# National Aeronautics and Space Administration. Goddard Space Flight Center, Greenbelt, MD.
EXTENSION TO EULERS'S THEOREM TO n-DIMENSIONAL SPACES **c64**
Itzhack Y. Bar-Itzhack (Technion - Israel Inst. of Tech., Haifa.) *In its* Flight Mechanics/Estimation Theory Symposium, 1989 Oct. 1989 p 299-315 (For primary document see N90-13413 05-13)
Avail: NTIS HC A20/MF A03 CSCL 12A

Euler's theorem states that any sequence of finite rotations of a rigid body can be described as a single rotation of the body about a fixed axis in three-dimensional Euclidean space. The usual statement of the theorem in the literature cannot be extended to Euclidean spaces of other dimensions. Equivalent formulations of the theorem are given in this paper and proven in a way which does not limit them to the three-dimensional Euclidean space. Thus, the equivalent theorems hold in other dimensions. The proof

of one formulation presents an algorithm which shows how to compute an angular-difference matrix that represents a single rotation which is equivalent to the sequence of rotations that have generated the final n-D orientation. This algorithm results also in a constant angular-velocity which, when applied to the initial orientation, yields eventually the final orientation regardless of what angular velocity generated the latter. Finally, the extension of the theorem is demonstrated in a four-dimensional numerical example. Author

N90-13432*# Computer Sciences Corp., Silver Spring, MD.
ANALYSIS OF THE FLIGHT DYNAMICS OF THE SOLAR MAXIMUM MISSION (SMM) OFF-SUN SCIENTIFIC POINTING
D. S. Pitone and J. R. Klein *In* NASA, Goddard Space Flight Center, Flight Mechanics/Estimation Theory Symposium, 1989 Oct. 1989 p 317-332 (For primary document see N90-13413 05-13)
(Contract NAS5-31500)
Avail: NTIS HC A20/MF A03 CSCL 22A

Algorithms are presented which were created and implemented by the Goddard Space Flight Center's (GSFC's) Solar Maximum Mission (SMM) attitude operations team to support large-angle spacecraft pointing at scientific objectives. The mission objective of the post-repair SMM satellite was to study solar phenomena. However, because the scientific instruments, such as the Coronagraph/Polarimeter (CP) and the Hard X ray Burst Spectrometer (HXRBS), were able to view objects other than the Sun, attitude operations support for attitude pointing at large angles from the nominal solar-pointing attitudes was required. Subsequently, attitude support for SMM was provided for scientific objectives such as Comet Halley, Supernova 1987A, Cygnus X-1, and the Crab Nebula. In addition, the analysis was extended to include the reverse problem, computing the right ascension and declination of a body given the off-Sun angles. This analysis led to the computation of the orbits of seven new solar comets seen in the field-of-view (FOV) of the CP. The activities necessary to meet these large-angle attitude-pointing sequences, such as slew sequence planning, viewing-period prediction, and tracking-bias computation are described. Analysis is presented for the computation of maneuvers and pointing parameters relative to the SMM-unique, Sun-centered reference frame. Finally, science data and independent attitude solutions are used to evaluate the large-angle pointing performance. Author

N90-13433*# National Aeronautics and Space Administration. Goddard Space Flight Center, Greenbelt, MD.
EXTENDED KALMAN FILTER FOR ATTITUDE ESTIMATION OF THE EARTH RADIATION BUDGET SATELLITE
Julie Deutschmann and Itzhack Y. Bar-Itzhack (Technion - Israel Inst. of Tech., Haifa.) *In its* Flight Mechanics/Estimation Theory Symposium, 1989 Oct. 1989 p 333-346 (For primary document see N90-13413 05-13)
Avail: NTIS HC A20/MF A03 CSCL 22A

The design and testing of an Extended Kalman Filter (EKF) for ground attitude determination, misalignment estimation and sensor calibration of the Earth Radiation Budget Satellite (ERBS) are described. Attitude is represented by the quaternion of rotation and the attitude estimation error is defined as an additive error. Quaternion normalization is used for increasing the convergence rate and for minimizing the need for filter tuning. The development of the filter dynamic model, the gyro error model and the measurement models of the Sun sensors, the IR horizon scanner and the magnetometers which are used to generate vector measurements are also presented. The filter is applied to real data transmitted by ERBS sensors. Results are presented and analyzed and the EKF advantages as well as sensitivities are discussed. On the whole the filter meets the expected synergism, accuracy and robustness. Author

N90-13434*# National Aeronautics and Space Administration. Goddard Space Flight Center, Greenbelt, MD.
AUTOMATION OF ORBIT DETERMINATION FUNCTIONS FOR NATIONAL AERONAUTICS AND SPACE ADMINISTRATION (NASA)-SUPPORTED SATELLITE MISSIONS
H. Mardirossian, K. Heuerman, A. Beri, M. V. Samii (Computer Sciences Corp., Silver Spring, MD.), and C. E. Doll *In its* Flight Mechanics/Estimation Theory Symposium, 1989 Oct. 1989 p 349-366 (For primary document see N90-13413 05-13)
(Contract NAS5-31500)
Avail: NTIS HC A20/MF A03 CSCL 22A

The Flight Dynamics Facility (FDF) at Goddard Space Flight Center (GSFC) provides spacecraft trajectory determination for a wide variety of National Aeronautics and Space Administration (NASA)-supported satellite missions, using the Tracking Data Relay Satellite System (TDRSS) and Ground Spaceflight and Tracking Data Network (GSTDN). To take advantage of computerized decision making processes that can be used in spacecraft navigation, the Orbit Determination Automation System (ODAS) was designed, developed, and implemented as a prototype system to automate orbit determination (OD) and orbit quality assurance (QA) functions performed by orbit operations. Based on a machine-resident generic schedule and predetermined mission-dependent QA criteria, ODAS autonomously activates an interface with the existing trajectory determination system using a batch least-squares differential correction algorithm to perform the basic OD functions. The computational parameters determined during the OD are processed to make computerized decisions regarding QA, and a controlled recovery process isactivated when the criteria are not satisfied. The complete cycle is autonomous and continuous. ODAS was extensively tested for performance under conditions resembling actual operational conditions and found to be effective and reliable for extended autonomous OD. Details of the system structure and function are discussed, and test results are presented. Author

N90-13435*# Computer Sciences Corp., Silver Spring, MD.
CALCULATION OF DOUBLE-LUNAR SWINGBY TRAJECTORIES: I. KEPLERIAN FOUNDATION
Stephen Stalos *In* NASA, Goddard Space Flight Center, Flight Mechanics/Estimation Theory Symposium, 1989 Oct. 1989 p 367-379 (For primary document see N90-13413 05-13)
(Contract NAS5-31500)
Avail: NTIS HC A20/MF A03 CSCL 22A

Scientific satellites may require translunar orbits aligned with the Sun-Earth line, with most of the period spent in either the sunward or antisunward direction. To maintain alignment, the orbit's line of apsides must rotate at a rate equal to mean angular motion of the Earth about the Sun. To maintain this rotation of the line of apsides by use of fuel onboard the spacecraft is prohibitively expensive. Farquhar and Dunham proposed a method for maintaining the desired alignment by gaining momentum at the expense of the Moon during a close approach (a lunar swingby) as the spacecraft passes beyond lunar orbit, then returning the momentum at the second lunar swingby as the spacecraft returns within the lunar orbit. The cycle of double-lunar swingbys may then be repeated. Dunham presented the orbit parameters necessary to achieve double-lunar swingby orbits which will maintain Sun-Earth line alignment. The details of the Keplerian approach to calculation of these parameters are presented. Methods for solution of the necessary equations for these parameters are presented. Author

N90-13436*# Computer Sciences Corp., Silver Spring, MD.
ACTIVE RENDEZVOUS BETWEEN A LOW-EARTH ORBIT USER SPACECRAFT AND THE SPACE TRANSPORTATION SYSTEM (STS) SHUTTLE
H. L. Hooper and J. R. Herrnstein *In* NASA, Goddard Space Flight Center, Flight Mechanics/Estimation Theory Symposium, 1989 Oct. 1989 p 381-401 (For primary document see N90-13413 05-13)
(Contract NAS5-31500)
Avail: NTIS HC A20/MF A03 CSCL 22A

Active rendezvous of an unmanned spacecraft with the Space Transportation System (STS) Shuttle is considered. The various operational constraints facing both the maneuvering spacecraft and the Shuttle during such a rendezvous sequence are discussed. Specifically, the actively rendezvousing user spacecraft must arrive in the generic Shuttle control box at a specified time after Shuttle launch. In so doing it must at no point violate Shuttle separation requirements. In addition, the spacecraft must be able to initiate the transfer sequence from any point in its orbit. The four-burn rendezvous sequence incorporating two Hohmann transfers and an intermediate phasing orbit as a low-energy solution satisfying the above requirements are discussed. The general characteristics of the four-burn sequence are discussed, with emphasis placed on phase orbit altitude and delta-velocity requirements. The planning and execution of such a sequence in the operational environment are then considered. Factor crucial in maintaining the safety of both spacecraft, such as spacecraft separation and contingency analysis, are considered in detail. Author

N90-13437*# National Aeronautics and Space Administration. Goddard Space Flight Center, Greenbelt, MD.

OPTIMUM DATA WEIGHTING AND ERROR CALIBRATION FOR ESTIMATION OF GRAVITATIONAL PARAMETERS

Francis J. Lerch *In its* Flight Mechanics/Estimation Theory Symposium, 1989 Oct. 1989 p 403-430 (For primary document see N90-13413 05-13)

Avail: NTIS HC A20/MF A03 CSCL 22A

A new technique was developed for the weighting of data from satellite tracking systems in order to obtain an optimum least-squares solution and an error calibration for the solution parameters. Data sets from optical, electronic, and laser systems on 17 satellites in GEM-T1 Goddard Earth Model-T1 (GEM-T1) were employed toward application of this technique for gravity field parameters. Also GEM-T2 (31 satellites) was recently computed as a direct application of the method and is summarized. The method employs subset solutions of the data associated with the complete solution to agree with their error estimates. With the adjusted weights the process provides for an automatic calibration of the error estimates for the solution parameters. The data weights derived are generally much smaller than corresponding weights obtained from nominal values of observation accuracy or residuals. Independent tests show significant improvement for solutions with optimal weighting. The technique is general and may be applied to orbit parameters, station coordinates, or other parameters than the gravity model. Author

N90-13438*# McDonnell-Douglas Astronautics Co., Houston, TX. Engineering Services Div.

THE CONTROLLABILITY OF THE AEROASSIST FLIGHT EXPERIMENT ATMOSPHERIC SKIP TRAJECTORY

R. Wood *In* NASA, Goddard Space Flight Center, Flight Mechanics/Estimation Theory Symposium, 1989 Oct. 1989 p 431-443 (For primary document see N90-13413 05-13)

Avail: NTIS HC A20/MF A03 CSCL 22A

The Aeroassist Flight Experiment (AFE) will be the first vehicle to simulate a return from geosynchronous orbit, deplete energy during an aerobraking maneuver, and navigate back out of the atmosphere to a low earth orbit It will gather scientific data necessary for future Aeroasisted Orbitl Transfer Vehicles (AOTV's). Critical to mission success is the ability of the atmospheric guidance to accurately attain a targeted post-aeropass orbital apogee while nulling inclination errors and compensating for dispersions in state, aerodynamic, and atmospheric parameters. In typing to satisfy mission constraints, atmospheric entry-interface (EI) conditions, guidance gains, and trajectory. The results of the investigation are presented; emphasizing the adverse effects of dispersed atmospheres on trajectory controllability. Author

N90-13439*# Computer Sciences Corp., Silver Spring, MD.

ATMOSPHERIC DRAG MODEL CALIBRATIONS FOR SPACECRAFT LIFETIME PREDICTION

A. L. Binebrink, M. S. Radomski, and M. V. Samii *In* NASA, Goddard Space Flight Center, Flight Mechanics/Estimation Theory Symposium, 1989 Oct. 1989 p 445-458 (For primary document see N90-13413 05-13)

(Contract NAS5-31500)

Avail: NTIS HC A20/MF A03 CSCL 22A

Although solar activity prediction uncertainty normally dominates decay prediction error budget for near-Earth spacecraft, the effect of drag force modeling errors for given levels of solar activity needs to be considered. Two atmospheric density models, the modified Harris-Priester model and the Jacchia-Roberts model, to reproduce the decay histories of the Solar Mesosphere Explorer (SME) and Solar Maximum Mission (SMM) spacecraft in the 490- to 540-kilometer altitude range were analyzed. Historical solar activity data were used in the input to the density computations. For each spacecraft and atmospheric model, a drag scaling adjustment factor was determined for a high-solar-activity year, such that the observed annual decay in the mean semimajor axis was reproduced by an averaged variation-of-parameters (VOP) orbit propagation. The SME (SMM) calibration was performed using calendar year 1983 (1982). The resulting calibration factors differ by 20 to 40 percent from the predictions of the prelaunch ballistic coefficients. The orbit propagations for each spacecraft were extended to the middle of 1988 using the calibrated drag models. For the Jaccia-Roberts density model, the observed decay in the mean semimajor axis of SME (SMM) over the 4.5-year (5.5-year) predictive period was reproduced to within 1.5 (4.4) percent. The corresponding figure for the Harris-Priester model was 8.6 (20.6) percent. Detailed results and conclusions regarding the importance of accurate drag force modeling for lifetime predictions are presented. Author

N90-13440*# National Aeronautics and Space Administration. Goddard Space Flight Center, Greenbelt, MD.

LIFETIME PREDICTIONS FOR THE SOLAR MAXIMUM MISSION (SMM) AND SAN MARCO SPACECRAFT

E. A. Smith, D. T. Ward, M. W. Schmitt, M. C. Phenneger (Computer Sciences Corp., Silver Spring, MD.), F. J. Vaughn, and M. L. Lupisella *In its* Flight Mechanics/Estimation Theory Symposium, 1989 Oct. 1989 p 459-476 (For primary document see N90-13413 05-13)

(Contract NAS5-31500)

Avail: NTIS HC A20/MF A03 CSCL 22A

Lifetime prediction techniques developed by the Goddard Space Flight Center (GSFC) Flight Dynamics Division (FDD) are described. These techniques were developed to predict the Solar Maximum Mission (SMM) spacecraft orbit, which is decaying due to atmospheric drag, with reentry predicted to occur before the end of 1989. Lifetime predictions were also performed for the Long Duration Exposure Facility (LDEF), which was deployed on the 1984 SMM repair mission and is scheduled for retrieval on another Space Transportation System (STS) mission later this year. Concepts used in the lifetime predictions were tested on the San Marco spacecraft, which reentered the Earth's atmosphere on December 6, 1988. Ephemerides predicting the orbit evolution of the San Marco spacecraft until reentry were generated over the final 90 days of the mission when the altitude was less than 380 kilometers. The errors in the predicted ephemerides are due to errors in the prediction of atmospheric density variations over the lifetime of the satellite. To model the time dependence of the atmospheric densities, predictions of the solar flux at the 10.7-centimeter wavelength were used in conjunction with Harris-Priester (HP) atmospheric density tables. Orbital state vectors, together with the spacecraft mass and area, are used as input to the Goddard Trajectory Determination System (GTDS). Propagations proceed in monthly segments, with the nominal atmospheric drag model scaled for each month according to the predicted monthly average value of F10.7. Calibration propagations are performed over a period of known orbital decay to obtain the effective ballistic coefficient. Progagations using plus or minus 2 sigma solar flux predictions are also generated to estimate the despersion in expected reentry dates. Definitive orbits are compared with these predictions as time expases. As updated vectors are received, these are also propagated to reentryto continually update the lifetime predictions. Author

N90-13441*# Rice Univ., Houston, TX. Aero-Astronautics Group.
OPTIMAL TRAJECTORIES FOR THE AEROASSISTED FLIGHT EXPERIMENT. PART 1: EQUATIONS OF MOTION IN AN EARTH-FIXED SYSTEM
A. Miele, Z. G. Zhao, and W. Y. Lee 1989 41 p Sponsored in part by Boeing Military Airplane Co., Seattle, WA
(Contract JPL-956415; NAG8-755)
(NASA-CR-186134; NAS 1.26:186134; AAR-238-Pt-1) Avail: NTIS HC A03/MF A01 CSCL 22A

The determination of optimal trajectories for the aeroassisted flight experiment (AFE) is discussed. The AFE refers to the study of the free flight of an autonomous spacecraft, shuttle-launched and shuttle-recovered. Its purpose is to gather atmospheric entry environmental data for use in designing aeroassisted orbital transfer vehicles (AOTV). It is assumed that: (1) the spacecraft is a particle of constant mass; (2) the Earth is rotating with constant angular velocity; (3) the Earth is an oblate planet, and the gravitational potential depends on both the radial distance and the latitude (harmonics of order higher than four are ignored); and (4) the atmosphere is at rest with respect to the Earth. Under these assumptions, the equations of motion for hypervelocity atmospheric flight (which can be used not only for AFE problems, but also for AOT problems and space shuttle problems) are derived in an Earth-fixed system. Transformation relations are supplied which allow one to pass from quantities computed in an Earth-fixed system to quantities computed in an inertial system, and vice versa.
Author

N90-13442*# Rice Univ., Houston, TX. Aero-Astronautics Group.
OPTIMAL TRAJECTORIES FOR THE AEROASSISTED FLIGHT EXPERIMENT. PART 2: EQUATIONS OF MOTION IN AN INERTIAL SYSTEM
A. Miele, Z. G. Zhao, and W. Y. Lee 1989 50 p Sponsored in part by Boeing Military Airplane Co., Seattle, WA
(Contract JPL-956415; NAG8-755)
(NASA-CR-186135; NAS 1.26:186135; AAR-239-Pt-2) Avail: NTIS HC A03/MF A01 CSCL 22A

The determination of optimal trajectories for the aeroassisted flight experiment (AFE) is discussed. The AFE refers to the study of the free flight of an autonomous spacecraft, shuttle-launched and shuttle-recovered. Its purpose is to gather atmospheric entry environmental data for use in designing aeroassisted orbital transfer vehicles (AOTV). It is assumed that: (1) the spacecraft is a particle of constant mass; (2) the Earth is rotating with constant angular velocity; (3) the Earth is an oblate planet, and the gravitational potential depends on both the radial distance and the latitude (harmonics of order higher than four are ignored); and (4) the atmosphere is at rest with respect to the Earth. Under these assumptions, the equations of motion for hypervelocity atmospheric flight (which can be used not only for AFE problems, but also for AOT problems and space shuttle problems) are derived in an inertial system. Transformation relations are supplied which allow one to pass from quantities computed in an inertial system to quantities computed in an Earth-fixed system and vice versa.
Author

N90-13443*# Rice Univ., Houston, TX. Dept. of Mechanical Engineering.
OPTIMAL TRAJECTORIES FOR THE AEROASSISTED FLIGHT EXPERIMENT, 1988-89 Final Report
A. Miele 1989 21 p
(Grant NAG8-755)
(NASA-CR-186132; NAS 1.26:186132; AAR-245) Avail: NTIS HC A03/MF A01 CSCL 22A

Research is summarized on optimal trajectories for the aeroassisted flight experiment, performed by the Aero-Astronautics Group of Rice University during the period 1988 through 1989. This research includes the following topics: (1) equations of motion in an Earth-fixed system; (2) equations of motion in an inertial system; (3) formultion of the optimal trajectory problem; (4) results on the optimal trajectory problem; and (5) guidance implications.
Author

N90-13444*# National Aeronautics and Space Administration. Marshall Space Flight Center, Huntsville, AL.
A TRANSIENT RESPONSE METHOD FOR LINEAR COUPLED SUBSTRUCTURES
J. R. Admire and J. A. Brunty Dec. 1989 26 p
(NASA-TP-2926; NAS 1.60:2926) Avail: NTIS HC A03/MF A01 CSCL 22A

A method is presented for determining the transient response of a discrete coordinate model of a linear structural system composed of substructures. The method is applicable to systems consisting of any number of substructures, both determinate and indeterminate interface boundaries, and any topological arrangement of the substructures. The method is simple to implement from a computational point of view because the equations of motion of each of the substructures are solved independently, and the interface boundary compatibility conditions are enforced at each integration time step by a matrix multiplication. The method is demonstrated for a structural system consisting of two beam segments and acted upon by a time dependent force. The numerical results from the demonstration problem validates the accuracy of the method. The application of this method to structural systems with changing interface boundary conditions between substructures is discussed.
Author

N90-13552# European Space Agency, Paris (France).
ON-GROUND ATTITUDE DETERMINATION
F. Donati, E. Canuto, P. Belforte, D. Carlucci, and F. vanLeeuwen *In its* The Hipparcos Mission. Prelaunch Status. Volume 3: The Data Reductions Jun. 1989 p 73-91 Original contains color illustrations (For primary document see N90-13548 05-18)
Copyright Avail: NTIS HC A22/MF A03; ESA Publications Div., ESTEC, Noordwijk, Netherlands, 80 Dutch guilders

N90-13553# European Space Agency, Paris (France).
THE GREAT CIRCLE REDUCTIONS
H. vanderMarel, D. vanDaalen, and C. Petersen *In its* The Hipparcos Mission. Prelaunch Status. Volume 3: The Data Reductions Jun. 1989 p 93-115 (For primary document see N90-13548 05-18)
Copyright Avail: NTIS HC A22/MF A03; ESA Publications Div., ESTEC, Noordwijk, Netherlands, 80 Dutch guilders

N90-13554# European Space Agency, Paris (France).
GREAT CIRCLE INTERACTIONS: ATTITUDE SMOOTHING AND GRID-STEP INCONSISTENCIES
H. vanderMarel, D. vanDaalen, and C. Petersen *In its* The Hipparcos Mission. Prelaunch Status. Volume 3: The Data Reductions Jun. 1989 p 117-140 (For primary document see N90-13548 05-18)
Copyright Avail: NTIS HC A22/MF A03; ESA Publications Div., ESTEC, Noordwijk, Netherlands, 80 Dutch guilders

N90-13555# European Space Agency, Paris (France).
GENERAL AND NUMERICAL APPROACH TO THE SPHERE SOLUTION IN FAST
I. Galligani, M. Lattanzi, B. Bucciarelli, T. Tommasini, and P. L. Bernacca *In its* The Hipparcos Mission. Prelaunch Status. Volume 3: The Data Reductions Jun. 1989 p 141-162 (For primary document see N90-13548 05-18)
Copyright Avail: NTIS HC A22/MF A03; ESA Publications Div., ESTEC, Noordwijk, Netherlands, 80 Dutch guilders

N90-13557# European Space Agency, Paris (France).
THE SPHERE SOLUTION AND ASTROMETRIC PARAMETER DETERMINATION IN NDAC
L. Lindegren *In its* The Hipparcos Mission. Prelaunch Status. Volume 3: The Data Reductions Jun. 1989 p 171-181 (For primary document see N90-13548 05-18)
Copyright Avail: NTIS HC A22/MF A03; ESA Publications Div., ESTEC, Noordwijk, Netherlands, 80 Dutch guilders

N90-13565# European Space Agency, Paris (France).
LINKING HIPPARCOS TO A QUASI-INERTIAL SYSTEM
J. Kovalevsky, J. F. Lestrade, and R. A. Preston *In its* The Hipparcos Mission. Prelaunch Status. Volume 3: The Data Reductions Jun. 1989 p 297-309 (For primary document see N90-13548 05-18)
Copyright Avail: NTIS HC A22/MF A03; ESA Publications Div., ESTEC, Noordwijk, Netherlands, 80 Dutch guilders

N90-13569# European Space Agency, Paris (France).
GREAT CIRCLE REDUCTIONS: IMPLEMENTATION AND SIMULATIONS
H. vanderMarel and C. Petersen *In its* The Hipparcos Mission. Prelaunch Status. Volume 3: The Data Reductions Jun. 1989 p 343-363 (For primary document see N90-13548 05-18)
Copyright Avail: NTIS HC A22/MF A03; ESA Publications Div., ESTEC, Noordwijk, Netherlands, 80 Dutch guilders

N90-13570# European Space Agency, Paris (France).
IMPLEMENTATION AND SIMULATIONS OF THE SPHERE SOLUTION IN FAST
F. P. Murgolo, M. G. Schirone, M. Lattanzi, and P. L. Bernacca *In its* The Hipparcos Mission. Prelaunch Status. Volume 3: The Data Reductions Jun. 1989 p 365-372 (For primary document see N90-13548 05-18)
Copyright Avail: NTIS HC A22/MF A03; ESA Publications Div., ESTEC, Noordwijk, Netherlands, 80 Dutch guilders

14 GROUND SUPPORT SYSTEMS AND FACILITIES (SPACE)

Includes launch complexes, research and production facilities; ground support equipment, e.g., mobile transporters; and simulators.

For related information see also *09 Research and Support Facilities (Air).*

N90-13445# Army Military Personnel Center, Alexandria, VA.
CURRENT MANAGEMENT FOR IMPROVED RAILGUN PERFORMANCE Ph.D. Thesis
Joseph Henry Beno, Jr. 1989 240 p
(AD-A212887) Avail: NTIS HC A11/MF A02 CSCL 19/6

Continued railgun development toward high energy devices that launch useful projectiles and have a lifetime of hundreds to thousands of shots, requires progress in two related aspects of accelerator design: (1) rail containment structures must be made capable of withstanding greater rail repulsion forces, without causing accelerators to become too bulky for their intended use; and (2) rails must sustain very minor heat-related damage during projectile launch. The potential for managing rail current and its distribution to alleviate the two aforementioned problems is investigated. Techniques for calculating pulsed, rail current distribution, in the infinite conductivity approximation, and resultant projectile force are developed. Then, passive, current management methods -- involving multiple rail pairs to distribute currents and rail-repulsive forces in a few, evenly-spaced, radial directions, for easier rail containment -- are explored. Optimized multi-rail, railgun cross sectional shapes that produce more projectile force than conventional two-rail railguns operating under the same local peak current density constraints are determined. These railguns have nontraditional bore shapes, i.e., not square or round. The use of neighboring, current-carrying conductors to actively influence rail current distribution is then studied. GRA

N90-13527# European Space Agency, Paris (France).
THE ROLE OF THE GROUND SEGMENT
J. vanderHa *In its* The Hipparcos Mission. Prelaunch Status. Volume 1: The Hipparcos Satellite Jun. 1989 p 297-304 (For primary document see N90-13499 05-18)
Copyright Avail: NTIS HC A16/MF A02; ESA Publications Div., ESTEC, Noordwijk, Netherlands, 80 Dutch guilders

N90-13528# European Space Agency, Paris (France).
THE INTERFACE WITH THE DATA REDUCTION CONSORTIA
J. vanderHa *In its* The Hipparcos Mission. Prelaunch Status. Volume 1: The Hipparcos Satellite Jun. 1989 p 305-315 (For primary document see N90-13499 05-18)
Copyright Avail: NTIS HC A16/MF A02; ESA Publications Div., ESTEC, Noordwijk, Netherlands, 80 Dutch guilders

N90-13859# Norwegian Space Center, Oslo. Andoya Rocket Range.
ANDOYA ROCKET RANGE: NEW INSTALLATIONS, FUTURE PLANS, AND INVESTMENTS
K. Adolfsen, P. A. Mikalsen, and I. Nyheim *In* ESA, European Rocket and Balloon Programs and Related Research Jun. 1989 p 203-208 (For primary document see N90-13826 05-42)
Copyright Avail: NTIS HC A15/MF A02

N90-13876# Swedish Space Corp., Esrange.
ESRANGE
J. Englund, A. Helger, A. Wikstroem, and L. Marcus *In* ESA, European Rocket and Balloon Programs and Related Research Jun. 1989 p 293-298 (For primary document see N90-13826 05-42)
Copyright Avail: NTIS HC A15/MF A02

15 LAUNCH VEHICLES AND SPACE VEHICLES

Includes boosters; operating problems of launch/space vehicle systems; and reusable vehicles.

For related information see also *20 Spacecraft Propulsion and Power.*

N90-13860# Centro Tecnico Aerospacial, San Jose dos Campos (Brazil). Inst. de Atividades Espaciais.
QUALIFICATION OF THE 4TH STAGE PROPULSOR OF THE BRAZILIAN LAUNCHER. SLV: A NEW SOUNDING ROCKET [QUALIFICATION DU PROPULSEUR 4EME ETAGE DU LANCEUR BRESILIEN. VLS: UNE NOUVELLE FUSEE SONDE]
Jayme Boscov and Wilson Katsumi Toyama *In* ESA, European Rocket and Balloon Programs and Related Research Jun. 1989 p 209-212 In FRENCH (For primary document see N90-13826 05-42)
Copyright Avail: NTIS HC A15/MF A02

N90-13861# Centro Tecnico Aerospacial, San Jose dos Campos (Brazil). Inst. de Atividades Espaciais.
THE BRAZILIAN SPACE PROGRAM: ACTUAL STATE OF THE ART
A. C. F. Pedrosa, T. S. Ribeiro, and Jayme Boscov *In* ESA, European Rocket and Balloon Programs and Related Research Jun. 1989 p 213-218 (For primary document see N90-13826 05-42)
Copyright Avail: NTIS HC A15/MF A02

16 SPACE TRANSPORTATION

Includes passenger and cargo space transportation, e.g., shuttle operations; and space rescue techniques.

For related information see also *03 Air Transportation and Safety* and *18 Spacecraft Design, Testing and Performance.* For space suits see *54 Man/System Technology and Life Support.*

N90-13446*# National Aeronautics and Space Administration, Washington, DC.
ON THE WINGS OF A DREAM: THE SPACE SHUTTLE
[1988] 31 p Original contains color illustrations
(NASA-EP-269; NAS 1.19:269) Avail: NTIS HC A03/MF A01 CSCL 22B

Described are the organization and some of the interests and

missions of NASA, the Space Transportation System, the Space Shuttle orbiter Enterprise, astronaut training and clothing, being launched into space, living and working in weightlessness, extravehicular activity, and the return from space to Earth. The various aspects of living in space are treated in considerable detail. This includes how the astronauts prepare food, how they eat and drink, how they sleep, exercise, change clothes and handle personal hygiene when in space. J.P.S.

N90-13447*# National Aeronautics and Space Administration. John F. Kennedy Space Center, Cocoa Beach, FL.
DEBRIS/ICE/TPS ASSESSMENT AND PHOTOGRAPHIC ANALYSIS FOR SHUTTLE MISSION STS-34
Charles G. Stevenson, Gregory N. Katnik, and Scott A. Higginbotham Nov. 1989 235 p
(NASA-TM-102153; NAS 1.15:102153) Avail: NTIS HC A11/MF A02 CSCL 22A

A Debris/Ice/Thermal Protection System (TPS) assessment and photographic analysis was conducted for Space Shuttle Mission STS-34. Debris inspections of the flight elements and launch pad are performed before and after launch. Ice/frost conditions on the External Tank are assessed by the use of computer programs, nomographs, and infrared scanner data during cryogenic loading of the vehicle followed by on-pad visual inspection. High speed photography is analyzed after launch to identify ice/debris sources and evaluate potential vehicle damage and/or in-flight anomalies. The debris/ice/TPS conditions and photographic analysis of Mission STS-34, and their overall effect on the Space Shuttle Program are documented. Author

N90-13448* National Aeronautics and Space Administration, Washington, DC.
SYNCOM 4 DEPLOY, LDEF RETRIEVAL HIGHLIGHT 10-DAY COLUMBIA FLIGHT
Dec. 1989 32 p
(NASA-News-Release-89-180; P89-10180) Avail: NASA Scientific and Technical Information Facility, PO Box 8757, BWI Airport, MD 21240 CSCL 22A

The objectives of Space Shuttle Mission STS-32 are described along with major flight activities, prelaunch and launch operations, trajectory sequence of events, and landing and post-landing operations. The primary objectives of STS-32 are the deployment of a Navy synchronous communications satellite (Syncom 4) and the retrieval of the Long Duration Exposure Facility (LDEF) launched from the Challenger in April 1984. Secondary STS-32 payloads include a protein crystal growth experiment, the Fluids Experiment Apparatus (FEA) for the investigation of microgravity materials processing, the Mesoscale Lighting Experiment, the Latitude-Longitude Locator Experiment, the Americal Flight Echocardiograph, and an experiment to investigate neurospora circadian rhythms in a microgravity environment. M.G.

17 SPACE COMM., SPACECRAFT COMM., COMMAND & TRACKING

Includes telemetry; space communications networks; astronavigation and guidance; and radio blackout.

For related information see also *04 Aircraft Communications and Navigation* and *32 Communications and Radar.*

N90-13875# Max-Planck-Inst. fuer Physik und Astrophysik, Garching (Germany, F.R.). Inst. fuer Extraterrestrische Physik.
SN 1987: A TELEMETRY DECODING SYSTEM
Siegfried Mueller *In* ESA, European Rocket and Balloon Programs and Related Research Jun. 1989 p 289-291 (For primary document see N90-13826 05-42)
Copyright Avail: NTIS HC A15/MF A02

18 SPACECRAFT DESIGN, TESTING AND PERFORMANCE

Includes satellites; space platforms; space stations; spacecraft systems and components such as thermal and environmental controls; and attitude controls.

For life support systems see *54 Man/System Technology and Life Support.* For related information see also *05 Aircraft Design, Testing and Performance, 39 Structural Mechanics,* and *16 Space Transportation.*

N90-13449*# Jet Propulsion Lab., California Inst. of Tech., Pasadena.
REPORT OF THE ASILOMAR 3 LDR WORKSHOP
M. J. Mahoney, ed. 15 Aug. 1988 153 p Workshop held in Asilomar, CA, 7-10 Sep. 1987
(NASA-CR-184656; JPL-Publ-88-23; NAS 1.26:184656) Avail: NTIS HC A08/MF A01 CSCL 22B

The conclusions and recommendations of the workshop held to study technology development issues critical to the Large Deployable Reflector (LDR) are summarized. LDR is to be a dedicated, orbiting, astronomical observatory, operating at wavelengths from 30 to 1000 microns, a spectral region where the Earth's atmosphere is almost completely opaque. Because it will have a large, segmented, passively cooled aperture, LDR addresses a wide range of technology areas. These include lightweight, low cost, structural composite reflector panels, primary support structures, wavefront sensing and adaptive optics, thermal background management, and integrated vibration and pointing control systems. The science objectives for LDR present instrument development challenges for coherent and direct arrayed detectors which can operate effectively at far infrared and submillimeter wavelengths, and for sub-Kelvin cryogenic systems. For individual titles, see N90-13450 through N90-13490.

N90-13450*# Jet Propulsion Lab., California Inst. of Tech., Pasadena.
INTRODUCTION TO THE REPORT OF THE ASILOMAR 3 LDR WORKSHOP
In its Report of the Asilomar 3 LDR Workshop 15 Aug. 1988 p 1-49 (For primary document see N90-13449 05-18)
Avail: NTIS HC A08/MF A01 CSCL 22B

The Large Deployable Reflector (LDR) is a system concept for a dedicated, orbiting, submillimeter, far infrared, astronomical observatory. The purpose of the 3rd conference was to review the latest system concepts for LDR, update the science requirements, and assess the status of the technology development that was recommended at Asilomar 2. The technology development assessment included ongoing work within NASA, the DOD, and various universities. Problem areas and technologies not being adequately addressed were to be identified and prioritized. In particular, the CSTI program in Sensors and Precision Segmented Reflectors was reviewed for appropriateness and progress relative to LDR technology needs. Author

N90-13451*# Jet Propulsion Lab., California Inst. of Tech., Pasadena.
A FIGURE CONTROL SENSOR FOR THE LARGE DEPLOYABLE REFLECTOR (LDR)
R. Bartman and S. Dubovitsky *In its* Report of the Asilomar 3 LDR Workshop 15 Aug. 1988 p 50-51 (For primary document see N90-13449 05-18)
Avail: NTIS HC A08/MF A01 CSCL 22B

A sensing and control system is required to maintain high optical figure quality in a segmented reflector. Upon detecting a deviation of the segmented surface from its ideal form, the system drives segment mounted actuators to realign the individual segments and thereby return the surface to its intended figure. When the reflector is in use, a set of figure sensors will determine positions of a number of points on the back surface of each of the reflector's segments, each sensor being assigned to a single point. By measuring the positional deviations of these points from previously established nominal values, the figure sensors provide the control

system with the information required to maintain the reflector's optical figure. The optical lever, multiple wavelength interferometer, and electronic capacitive sensor, the most promising technologies for the development of the figure sensor, are illustrated. It is concluded that to select a particular implementation of the figure sensors, performance requirement will be refined and relevant technologies investigated further. Author

N90-13452*# General Research Corp., McLean, VA.
EXPERT SYSTEMS FOR ADAPTIVE CONTROL OF LARGE SPACE STRUCTURES
Charles F. Gartrell *In* Jet Propulsion Lab., California Inst. of Tech., Report of the Asilomar 3 LDR Workshop 15 Aug. 1988 p 52-53 (For primary document see N90-13449 05-18)
Avail: NTIS HC A08/MF A01 CSCL 22B

It is expected that space systems for the future will evolve to structures of unprecedented size with associated extreme control requirements. A method is necessary that is sufficiently general to initiate stable control of a vehicle and subsequently learn the true nature of the structure. It is suggested that a suitable constructed expert system (ES) would be capable of learning by appending observations to a knowledge base. To verify that an ES can control a large space structure, numerical simulations of a simple structure subjected to periodic vibrations and the performance of a classical controllers were performed. The ES was then exercised to show its ability to truthfully mimic nominal control and to demonstrate its superiority to the classical controller, given sensor failures. An ES generating software package, The Intelligent Machine Model, was employed. It uses the pattern matching technique. Results of this program are discussed.
Author

N90-13453*# Jet Propulsion Lab., California Inst. of Tech., Pasadena.
POINTING CONTROL FOR LDR
Y. Yam and C. Briggs *In its* Report of the Asilomar 3 LDR Workshop 15 Aug. 1988 p 54-55 (For primary document see N90-13449 05-18)
Avail: NTIS HC A08/MF A01 CSCL 22B

One important aspect of the LDR control problem is the possible excitations of structural modes due to random disturbances, mirror chopping, and slewing maneuvers. An analysis was performed to yield a first order estimate of the effects of such dynamic excitations. The analysis involved a study of slewing jitters, chopping jitters, disturbance responses, and pointing errors, making use of a simplified planar LDR model which describes the LDR dynamics on a plane perpendicular to the primary reflector. Briefly, the results indicate that the command slewing profile plays an important role in minimizing the resultant jitter, even to a level acceptable without any control action. An optimal profile should therefore be studied. Author

N90-13454*# Lockheed Missiles and Space Co., Sunnyvale, CA.
SPACE TELESCOPE POINTING CONTROL
Hugh Dougherty *In* Jet Propulsion Lab., California Inst. of Tech., Report of the Asilomar 3 LDR Workshop 15 Aug. 1988 p 56-57 (For primary document see N90-13449 05-18)
Avail: NTIS HC A08/MF A01 CSCL 22B

The Space Telescope pointing control system is designed to meet the fine pointing performance of 0.007 arc-sec stability, maneuver the telescope 90 deg in 18 min, or less, and provide the capability for deployment from, and retrieval by, the space shuttle. The pointing control system objectives are met using fine guidance sensors for attitude information, reaction wheel assemblies sized to provide both the torque required for pointing, and magnetometers and magnetic torquers for momentum management. A digital computer is used to calculate the control law, attitude reference, momentum management law, and command generator. The command generator shapes the acceleration and incremental angle commands to the control system to limit structural mode excitation. The control techniques are briefly discussed. Author

N90-13455*# Jet Propulsion Lab., California Inst. of Tech., Pasadena.
WAVEFRONT ERROR SENSING FOR LDR
Eldred F. Tubbs and T. A. Glavich *In its* Report of the Asilomar 3 LDR Workshop 15 Aug. 1988 p 58-59 (For primary document see N90-13449 05-18)
Avail: NTIS HC A08/MF A01 CSCL 22B

Wavefront sensing is a significant aspect of the LDR control problem and requires attention at an early stage of the control system definition and design. A combination of a Hartmann test for wavefront slope measurement and an interference test for piston errors of the segments was examined and is presented as a point of departure for further discussion. The assumption is made that the wavefront sensor will be used for initial alignment and periodic alignment checks but that it will not be used during scientific observations. The Hartmann test and the interferometric test are briefly examined. Author

N90-13456*# TRW Space Technology Labs., Redondo Beach, CA.
AN APPROACH TO OPTICAL STRUCTURES CONTROL
R. P. Iwens, R. J. Benhabib, and C. S. Major *In* Jet Propulsion Lab., California Inst. of Tech., Report of the Asilomar 3 LDR Workshop 15 Aug. 1988 p 60-61 (For primary document see N90-13449 05-18)
Avail: NTIS HC A08/MF A01 CSCL 22B

The stabilization of a large, spaceborne Cassegrain telescope is examined. Modal gain factors and known characteristics of disturbances are used to determine which structural model affect line of sight (LOS) the most and are candidates for active control. THe approach is to: (1) actively control and maintain alignment of optical components; (2) place structural control actuators for optimum impact on the selected modes for active vibration control; and (3) feed back the best available estimate of LOS error for direct LOS control. Local analog loops are used for lower bandwidth control and multivariable digital control for lower bandwidth control. The control law is synthesized in the frequency domain using the characteristic gain approach. Robustness is measured by employing conicity, which is an outgrowth of the positivity approach to robust feedback system design. The feasibility of the design approach will be demonstrated by conducting a lab experiment on a structure similar to a scaled version of the telescope. Author

N90-13457*# Lockheed Missiles and Space Co., Palo Alto, CA.
SEGMENT ALIGNMENT CONTROL SYSTEM
Jean-N. Aubrun and Ken R. Lorell *In* Jet Propulsion Lab., California Inst. of Tech., Report of the Asilomar 3 LDR Workshop 15 Aug. 1988 p 62-64 (For primary document see N90-13449 05-18)
Avail: NTIS HC A08/MF A01 CSCL 22B

The segmented primary mirror for the LDR will require a special segment alignment control system to precisely control the orientation of each of the segments so that the resulting composite reflector behaves like a monolith. The W.M. Keck Ten Meter Telescope will utilize a primary mirror made up of 36 actively controlled segments. Thus the primary mirror and its segment alignment control system are directly analogous to the LDR. The problems of controlling the segments in the face of disturbances and control/structures interaction, as analyzed for the TMT, are virtually identical to those for the LDR. The two systems are briefly compared. Author

N90-13458*# Jet Propulsion Lab., California Inst. of Tech., Pasadena.
COMPOSITE PANEL DEVELOPMENT AT JPL
Paul McElroy and Rich Helms *In its* Report of the Asilomar 3 LDR Workshop 15 Aug. 1988 p 66-67 (For primary document see N90-13449 05-18)
Avail: NTIS HC A08/MF A01 CSCL 22B

Parametric computer studies can be use in a cost effective manner to determine optimized composite mirror panel designs. An InterDisciplinary computer Model (IDM) was created to aid in the development of high precision reflector panels for LDR. The

materials properties, thermal responses, structural geometries, and radio/optical precision are synergistically analyzed for specific panel designs. Promising panels designs are fabricated and tested so that comparison with panel test results can be used to verify performance prediction models and accomodate design refinement. The iterative approach of computer design and model refinement with performance testing and materials optimization has shown good results for LDR panels. Author

N90-13459*# United Technologies Corp., West Palm Beach, FL. Optics and Applied Technology Lab.
STATUS OF Gr/GLASS COMPOSITES TECHNOLOGY AT UTOS **c24**
Ramon A. Mayor *In* Jet Propulsion Lab., California Inst. of Tech., Report of the Asilomar 3 LDR Workshop 15 Aug. 1988 p 68-69 (For primary document see N90-13449 05-18)
Avail: NTIS HC A08/MF A01 CSCL 11D

The TSC (Thermally Stable Composite) refers to a family of graphite reinforced glass matrix composite materials developed by UTOS. This fiber matrix combination exhibits low coefficients of thermal expansion (CTE), exceptional dimensional stability, high specific strength and stiffness, adequate fracture toughness, and space environment compatibility. The dimensional stability of a TSC mirror structure was experimentally characterized at the Steward Observatory. Preliminary results indicate that TSC is significantly more thermally stable than most current structural composite materials. In addition, the use of lower CTE glass matrix materials, such as 96 percent silica glass, have the potential for producing graphite/glass panels with expansion rates and stability comparable to that of fused silica. Author

N90-13460*# Jet Propulsion Lab., California Inst. of Tech., Pasadena.
LARGE DEPLOYABLE REFLECTOR (LDR) THERMAL CHARACTERISTICS
R. N. Miyake and Y. C. Wu *In its* Report of the Asilomar 3 LDR Workshop 15 Aug. 1988 p 70-71 (For primary document see N90-13449 05-18)
Avail: NTIS HC A08/MF A01 CSCL 22B

The thermal support group, which is part of the lightweight composite reflector panel program, developed thermal test and analysis evaluation tools necessary to support the integrated interdisciplinary analysis (IIDA) capability. A detailed thermal mathematical model and a simplified spacecraft thermal math model were written. These models determine the orbital temperature level and variation, and the thermally induced gradients through and across a panel, for inclusion in the IIDA. Author

N90-13461*# National Aeronautics and Space Administration. Langley Research Center, Hampton, VA.
ADVANCED COMPOSITE MATERIALS FOR PRECISION SEGMENTED REFLECTORS **c24**
Bland A. Stein and David E. Bowles *In* Jet Propulsion Lab., California Inst. of Tech., Report of the Asilomar 3 LDR Workshop 15 Aug. 1988 p 72-73 (For primary document see N90-13449 05-18)
Avail: NTIS HC A08/MF A01 CSCL 11D

The objective in the NASA Precision Segmented Reflector (PSR) project is to develop new composite material concepts for highly stable and durable reflectors with precision surfaces. The project focuses on alternate material concepts such as the development of new low coefficient of thermal expansion resins as matrices for graphite fiber reinforced composites, quartz fiber reinforced epoxies, and graphite reinforced glass. Low residual stress fabrication methods will be developed. When coupon specimens of these new material concepts have demonstrated the required surface accuracies and resistance to thermal distortion and microcracking, reflector panels will be fabricated and tested in simulated space environments. An important part of the program is the analytical modeling of environmental stability of these new composite materials concepts through constitutive equation development, modeling of microdamage in the composite matrix, and prediction of long term stability (including viscoelasticity). These analyses include both closed form and finite element solutions at the micro and macro levels. Author

N90-13462*# Jet Propulsion Lab., California Inst. of Tech., Pasadena.
LIGHTWEIGHT COMPOSITE REFLECTOR PANELS **c24**
R. E. Freeland and P. M. McElroy *In its* Report of the Asilomar 3 LDR Workshop 15 Aug. 1988 p 74-75 (For primary document see N90-13449 05-18)
Avail: NTIS HC A08/MF A01 CSCL 11D

The Hexel Corp. has produced additional composite panels, based on JPL designs, that: (1) have increased the panel size from 0.15 to 0.40 meters, (2) have improved the as-manufactured surface precision 3.0 to approx. 1.0 micron RMS, (3) have utilized different numbers of face sheet plys, (4) have improved face sheet fiber orientation, (5) have variations of aluminum honeycomb core cell size, (6) have combined graphite/epoxy (Gr/Ep) face sheets with E-glass honeycomb cores, and (7) have used standard aluminum core with face sheets composed of combinations of glass, Kevlar, and carbon fibers. Additionally, JPL has identified candidate alternate materials for the facesheets and core, modified the baseline polymer panel matrix material, and developed new concepts for panel composite cores. Dornier designed and fabricated three 0.6 meter Gr/Ep panels, that were evaluated by JPL. Results of both the Hexel and Dornier panel work were used to characterize the state-of-the-art for Gr/Ep mirrors. Author

N90-13463*# Arizona Univ., Tucson. Steward Observatory.
LOW TEMPERATURE OPTICAL TESTING OF CFRP TELESCOPE PANELS **c74**
William F. Hoffmann, Patrick Woida, and Thomas Tysenn *In* Jet Propulsion Lab., California Inst. of Tech., Report of the Asilomar 3 LDR Workshop 15 Aug. 1988 p 76-77 (For primary document see N90-13449 05-18)
Avail: NTIS HC A08/MF A01 CSCL 20F

Since 1984, low temperature optical tests were made of very lightweight mirror panels for use in balloon and space infrared and submillimeter telescopes. In order to accomplish this testing, an ambient pressure 0.5 meter test chamber operating from 20 to -80 C, developed techniques for measuring non-optical quality mirrors with phase modulation 10.6 micron interferometry, and created the interferogram reduction program. During the course of the program, nineteen mirrors from four manufactures were tested: carbon fiber reinforced plastic (CFRP) aluminum honeycomb sandwich panel mirrors, a CFRP sandwich panel with an added glass facesheet, and carbon fiber reinforced glass panels. The results of the panel development and test program are summarized. Author

N90-13464*# National Aeronautics and Space Administration. Ames Research Center, Moffett Field, CA.
STATUS OF DIRECT DETECTOR AND ARRAY DEVELOPMENT
Craig R. McCreight *In* Jet Propulsion Lab., California Inst. of Tech., Report of the Asilomar 3 LDR Workshop 15 Aug. 1988 p 80-82 (For primary document see N90-13449 05-18)
Avail: NTIS HC A08/MF A01 CSCL 22B

Programs are now underway to develop and demonstrate the detector/array technology needed for the Space Infrared Telescope Facility (SIRTF), Large Deployable Reflector (LDR), and other future NASA missions. The development goal is to achieve focal plane sensitivities, at extended integration times over the 2 to 700 microns range, limited only by the low astrophysical backgrounds encountered in cryogenic telescopes such as SIRTF. Dramatic progress has been made in the last 2 to 3 years in integrated array and detector systems for low background astronomical applications. With the broadly based developments and lab characterizations now underway for SIRTF and similar space applications, coupled with the rapidly expanding art and science of ground based astronomical imagery with arrays, the potential for effective utilization of arrays with LDR appears to be very good. Author

N90-13465*# California Univ., Berkeley.
FAR-INFRARED HETERODYNE RECEIVERS c32
Albert Betz *In* Jet Propulsion Lab., California Inst. of Tech., Report of the Asilomar 3 LDR Workshop 15 Aug. 1988 p 83-85 (For primary document see N90-13449 05-18)
Avail: NTIS HC A08/MF A01 CSCL 17B

The development of open resonator mixer structures and laser local oscillators has made heterodyne spectroscopy at far infrared (FIR) wavelengths between 150 and 400 microns a reality. Several laser based receivers are now part of the instrument complement flown aboard the Kuiper Airborne Observatory. Lasers are eminently practical as FIR local oscillators whenever there is close frequency coincidence between a strong laser transition and the Doppler-shifted astronomical line. While it is desirable to have continuous frequency coverage in a spectrometer, it should be recognized that most astronomers will focus their interest on the few spectral lines deemed optimum for probing the cosmos. Ultimately, the development of a reliable thin film technology for the new high temperature oxide superconductors may favor SIS-type devices for all wavelengths in future space based FIR receivers. Author

N90-13466*# Jet Propulsion Lab., California Inst. of Tech., Pasadena.
ADVANCES IN SIS RECEIVER TECHNOLOGY c32
M. A. Frerking *In its* Report of the Asilomar 3 LDR Workshop 15 Aug. 1988 p 86-87 (For primary document see N90-13449 05-18)
Avail: NTIS HC A08/MF A01 CSCL 17B

Significant advances in SIS receiver technology since the last Asilomar meeting include: superconductor materials, integrated inductive tuning elements, and planar mounting structures. The effect of these advances is to push the upper frequency operating limit from about 600 to 1500 GHz, and to enhance the feasibility of focal plane arrays of heterodyne receivers. A fundamental high frequency operating limit of SIS mixers is set by the superconducting energy gap. A practical limitation for high frequency operation of SIS junctions is their parasitic capacitance and resistance. The performance of the mixer will be degraded by the Resistor-Capacitor rolloff. Several designs were reported for inductive elements integrated on the same substrate as the SIS junctions to tune out the bulk junction capacitance. Most millimeter SIS-based heterodyne receivers have used waveguide coupling structures. Technology has advanced to the state where programs that have a high probability of success can be defined to produce arrays of SIS receivers for frequencies as high as 1500 GHz. Author

N90-13467*# Massachusetts Inst. of Tech., Lexington. Lincoln Lab.
RESONANT-TUNNELING OSCILLATORS AND MULTIPLIERS FOR SUBMILLIMETER RECEIVERS c33
T. C. L. Gerhard Sollner *In* Jet Propulsion Lab., California Inst. of Tech., Report of the Asilomar 3 LDR Workshop 15 Aug. 1988 p 88-89 (For primary document see N90-13449 05-18)
Avail: NTIS HC A08/MF A01 CSCL 09A

Resonant tunneling through double-barrier heterostructures has attracted increasing interest recently, largely because of the fast charge transport it provides. In addition, the negative differential resistance regions that exist in the current-voltage (I-V) curve (peak-to-valley ratios of 3.5:1 at room temperature, and nearly 10:1 at 77 K, were measured) suggest that high-speed devices based on the character of the I-V curve should be possible. For example, the negative differential resistance region is capable of providing the gain necessary for high-frequency oscillations. In the laboratory attempts were made to increase the frequency and power of these oscillators and to demonstrate several different high-frequency devices. Author

N90-13468*# Jet Propulsion Lab., California Inst. of Tech., Pasadena.
SPECTROMETER TECHNOLOGY RECOMMENDATIONS c35
William J. Wilson *In its* Report of the Asilomar 3 LDR Workshop 15 Aug. 1988 p 90-91 (For primary document see N90-13449 05-18)
Avail: NTIS HC A08/MF A01 CSCL 14B

A typical heterodyne remote sensing system contains three major elements: the antenna, the radiometer, and the spectrometer. The radiometer consists of the local oscillator, the mixer, and the intermediate frequency amplifiers. This subsystem performs the function of down converting the high frequency incident thermal emission signal to a lower intermediate frequency. The spectrometer measures the power spectrum of the down-converted signal simultaneously in many contiguous frequency channels. Typical spectrum analysis requirements involve measurement of signal bandwidths of 100 to 1000 MHz with a channel resolution of 0.5 to 10 MHz. Three general approaches are used for spectrometers: (1) filter banks, (2) Acousto-Optic Spectrometers (AOS's), and (3) digital autocorrelators. In contrast to the two frequency domain techniques, an autocorrelator works in the time domain. The autocorrelation function (ACF) of the incoming signal is computed and averaged over the integration time. The averaged ACF is then Fourier transformed to obtain the signal power spectrum. Significant progress was made in the development of sub mm antennas and radiometers. It is now time to begin research in the development of low power spaceborne spectrometers and to reduce their size and weight. The near-term research goal will be to develop a prototype digital autocorrelation spectrometer, using VLSI gate array technology, which will have a small size, low power requirements, and can be used in spacecraft mm and sub mm radiometer systems. The long-range objective of this technology development is to make extremely low power, less than 10 mW/channel, small and stable wideband spectrometers which can be used in future mm and sub mm wavelength space missions such as the Large Deployable Reflector. Author

N90-13469*# Massachusetts Inst. of Tech., Cambridge.
A FOUR CHANNEL HE-3 COOLED BALLOON-BORNE BOLOMETER RADIOMETER c35
Stephan Meyer *In* Jet Propulsion Lab., California Inst. of Tech., Report of the Asilomar 3 LDR Workshop 15 Aug. 1988 p 92-93 (For primary document see N90-13449 05-18)
Avail: NTIS HC A08/MF A01 CSCL 14B

A four channel He-3 cooled balloon-borne bolometer radiometer was constructed. The principal goal of the instrument is to measure the anisotropy of the 3 K cosmic background radiation on angular scales of 4 to 180 deg. The goal is to improve the sensitivity of the measurements to Delta T/T is less than .00001. A secondary goal is to survey the galactic thermal dust emission in the submillimeter range. Author

N90-13470*# Jet Propulsion Lab., California Inst. of Tech., Pasadena.
CRYOGENIC SYSTEMS FOR THE LARGE DEPLOYABLE REFLECTOR
Peter V. Mason *In its* Report of the Asilomar 3 LDR Workshop 15 Aug. 1988 p 94-95 (For primary document see N90-13449 05-18)
Avail: NTIS HC A08/MF A01 CSCL 22B

There are five technologies which may have application for Large Deployable Reflector (LDR), one passive and four active. In order of maturity, they are passive stored cryogen systems, and mechanical, sorption, magnetic, and pulse-tube refrigerators. In addition, deep space radiators will be required to reject the heat of the active systems, and may be useful as auxiliary coolers for the stored cryogen systems. Hybrid combinations of these technologies may well be more efficient than any one alone, and extensive system studies will be required to determine the best trade-offs. Stored cryogen systems were flown on a number of missions. The systems are capable of meeting the temperature requirements of LDR. The size and weight of stored cryogen systems are proportional to heat load and, as a result, are applicable only if the low-temperature heat load can be kept small. Systems using chemisorption and physical adsorption for compressors and pumps have received considerable attention in the past few years. Systems based on adiabatic demagnetization

of paramagnetic salts were used for refrigeration for many years. Pulse-tube refrigerators were recently proposed which show relatively high efficiency for temperatures in the 60 to 80 K range. The instrument heat loads and operating temperatures are critical to the selection and design of the cryogenic system. Every effort should be made to minimize heat loads, raise operating temperatures, and to define these precisely. No one technology is now ready for application to LDR. Substantial development efforts are underway in all of the technologies and should be monitored and advocated. Magnetic and pulse-tube refrigerators have high potential. Author

N90-13471*# National Aeronautics and Space Administration. Ames Research Center, Moffett Field, CA.
CRYOGENICS FOR LDR
Peter Kittel *In* Jet Propulsion Lab., California Inst. of Tech., Report of the Asilomar 3 LDR Workshop 15 Aug. 1988 p 96-97 (For primary document see N90-13449 05-18)
Avail: NTIS HC A08/MF A01 CSCL 22B

Three cryogenic questions of importance to Large Deployable Reflector (LDR) are discussed: the primary cooling requirement, the secondary cooling requirement, and the instrument changeout requirement. Author

N90-13472*# Lockheed Missiles and Space Co., Palo Alto, CA.
LDR CRYOGENICS
T. Nast *In* Jet Propulsion Lab., California Inst. of Tech., Report of the Asilomar 3 LDR Workshop 15 Aug. 1988 p 98-99 (For primary document see N90-13449 05-18)
Avail: NTIS HC A08/MF A01 CSCL 22B

A brief summary from the 1985 Large Deployable Reflector (LDR) Asilomar 2 workshop of the requirements for LDR cryogenic cooling is presented. The heat rates are simply the sum of the individual heat rates from the instruments. Consideration of duty cycle will have a dramatic effect on cooling requirements. There are many possible combinations of cooling techniques for each of the three temperatures zones. It is clear that much further system study is needed to determine what type of cooling system is required (He-2, hybrid or mechanical) and what size and power is required. As the instruments, along with their duty cycles and heat rates, become better defined it will be possible to better determine the optimum cooling systems. Author

N90-13473*# Arizona Univ., Tucson. Steward Observatory.
DEVELOPMENT OF FIR ARRAYS WITH INTEGRATING AMPLIFIERS **c33**
Erick T. Young *In* Jet Propulsion Lab., California Inst. of Tech., Report of the Asilomar 3 LDR Workshop 15 Aug. 1988 p 100 (For primary document see N90-13449 05-18)
Avail: NTIS HC A08/MF A01 CSCL 09A

The development of optimized photoconductor arrays suitable for far infrared space astronomical applications are described. Although the primary impetus is the production of a 16 by 16 element Ge:Ga demonstration array for SIRTF, the extension of this technology to Large Deployable Reflector (LDR) is considered. The optimization of Ge:Ga and Ge:Be photoconductor materials is discussed. In collaboration with Lawrence Berkeley Laboratory, measurements of FIR photoconductors with quantum efficiencies greater than 20 percent at 100 micrometers, and dark currents below 300 electrons/s are presented. Integrating J-FET amplifier technology is discussed. The current generation of integrating amplifiers has a demonstrated read noise of less than 20 electrons for an integration time of 100 s. The design is shown for a stackable 16 x n Ge:Ga array that utilizes a 16-channel monolithic version of the J-FET integrator. A part of the design is the use of a thin, thermally insulating substrate that allows the electronics to operate at the optimum temperature of 50 K while maintaining thermal and optical isolation from the detectors at 2 K. The power dissipation for the array is less than 16 mW. The array design may particularly be applicable to high resolution imaging spectrometers for LDR. Author

N90-13474*# Eastman Kodak Co., Rochester, NY. Federal Systems Div.
COHERENT PHASING OF SEGMENTED MIRRORS **c74**
Peter A. Jones *In* Jet Propulsion Lab., California Inst. of Tech., Report of the Asilomar 3 LDR Workshop 15 Aug. 1988 p 102-103 (For primary document see N90-13449 05-18)
Avail: NTIS HC A08/MF A01 CSCL 20F

The technical issues associated with a coherently phased segmented mirror can be divided into two types. The first involves the issues of manufacturing the surface quality of the mirror segments themselves (coherent phasing of individual segments). The second involves assembly issues of initializing in 1 G and retaining in 0 G an aggregate segmented mirror (coherent phasing between individual segments). Using a rectangular coordinate system at the vertex of a mirror segment, the rigid body motions are the six translational and rotational degrees of freedom. A first cut primary mirror wavefront error budget is presented. For a minimum operational wavelength of 30 micrometers, the derived values from the budget are: segment surface quality (0.45 micrometers RMS), radius mismatch (50 PPM), segment piston error (1.3 micrometers, segment tip/tilt error (0.6 microrad). Either active or passive segmented mirrors can be addressed, but if the surface quality of the off-axis segment and the radius matching requirements can be passively met, then only segment alignment need be sensed and controlled during operation in orbit. For the active mirror case, dimensional stability of the mirror material during operation is a key factor in establishing the degree of active figure control required. Author

N90-13475*# Jet Propulsion Lab., California Inst. of Tech., Pasadena.
EFFECT OF CENTRAL OBSCURATION ON THE LDR POINT SPREAD FUNCTION **c74**
Jakob J. vanZyl *In its* Report of the Asilomar 3 LDR Workshop 15 Aug. 1988 p 104-105 (For primary document see N90-13449 05-18)
Avail: NTIS HC A08/MF A01 CSCL 20F

It is well known that Gaussian apodization of an aperture reduces the sidelobe levels of its point spread function (PSF). In the limit where the standard deviation of the Gaussian function is much smaller than the diameter of the aperture, the sidelobes completely disappear. However, when Gaussian apodization is applied to the Large Deployable Reflector (LDR) array consisting of 84 hexagonal panels, it is found that the sidelobe level only decreases by about 2.5 dB. The reason for this is explained. The PSF is shown for an array consisting of 91 uniformly illuminated hexagonal apertures; this array is identical to the LDR array, except that the central hole in the LDR array is filled with seven additional panels. For comparison, the PSF of the uniformly illuminated LDR array is shown. Notice that it is already evident that the sidelobe structure of the LDR array is different from that of the full array of 91 panels. The PSF's of the same two arrays are shown, but with the illumination apodized with a Gaussian function to have 20 dB tapering at the edges of the arrays. While the sidelobes of the full array have decreased dramatically, those of the LDR array changed in structure, but stayed at almost the same level. This result is not completely surprising, since the Gaussian apodization tends to emphasize the contributions from the central portion of the array; exactly where the hole in the LDR array is located. The two most important conclusions are: the size of the central hole should be minimized, and a simple Gaussian apodization scheme to suppress the sidelobes in the PSF should not be used. A more suitable apodization scheme would be a Gaussian annular ring. Author

N90-13476*# California Univ., Los Angeles.
DIFFRACTION, CHOPPING, AND BACKGROUND SUBTRACTION FOR LDR **c74**
Edward L. Wright *In* Jet Propulsion Lab., California Inst. of Tech., Report of the Asilomar 3 LDR Workshop 15 Aug. 1988 p 106-109 (For primary document see N90-13449 05-18)
Avail: NTIS HC A08/MF A01 CSCL 20F

The Large Deployable Reflector (LDR) will be an extremely

sensitive infrared telescope if the noise due to the photons in the large thermal background is the only limiting factor. For observations with a 3 arcsec aperture in a broadband at 100 micrometers, a 20-meter LDR will emit 10(exp 12) per second, while the photon noise limited sensitivity in a deep survey observation will be 3,000 photons per second. Thus the background subtraction has to work at the 1 part per billion level. Very small amounts of scattered or diffracted energy can be significant if they are modulated by the chopper. The results are presented for 1-D and 2-D diffraction calculations for the lightweight, low-cost LDR concept that uses an active chopping quaternary to correct the wavefront errors introduced by the primary. Fourier transforms were used to evaluate the diffraction of 1 mm waves through this system. Unbalanced signals due to dust and thermal gradients were also studied. Author

N90-13477*# Jet Propulsion Lab., California Inst. of Tech., Pasadena.
A LABORATORY VERIFICATION SENSOR c35
Arthur H. Vaughan *In its* Report of the Asilomar 3 LDR Workshop 15 Aug. 1988 p 110-111 (For primary document see N90-13449 05-18)
Avail: NTIS HC A08/MF A01 CSCL 14B

The use of a variant of the Hartmann test is described to sense the coalignment of the 36 primary mirror segments of the Keck 10-meter Telescope. The Shack-Hartmann alignment camera is a surface-tilt-error-sensing device, operable with high sensitivity over a wide range of tilt errors. An interferometer, on the other hand, is a surface-height-error-sensing device. In general, if the surface height error exceeds a few wavelengths of the incident illumination, an interferogram is difficult to interpret and loses utility. The Shack-Hartmann aligment camera is, therefore, likely to be attractive as a development tool for segmented mirror telescopes, particularly at early stages of development in which the surface quality of developmental segments may be too poor to justify interferometric testing. The constraints are examined which would define the first-order properties of a Shack-Hartmann alignment camera and the precision and range of measurement one could expect to achieve with it are investigated. Fundamental constraints do arise, however, from consideration of geometrical imaging, diffraction, and the density of sampling of images at the detector array. Geometrical imagining determines the linear size of the image, and depends on the primary mirror diameter and the f-number of a lenslet. Diffraction is another constraint; it depends on the lenslet aperture. Finally, the sampling density at the detector array is important since the number of pixels in the image determines how accurately the centroid of the image can be measured. When these factors are considered under realistic assumptions it is apparent that the first order design of a Shack-Hartmann alignment camera is completely determined by the first-order constraints considered, and that in the case of a 20-meter telescope with seeing-limited imaging, such a camera, used with a suitable detector array, will achieve useful precision. Author

N90-13478*# Arizona Univ., Tucson. Steward Observatory
SiO OVERCOATING AND POLISHING OF CFRP TELESCOPE PANELS c27
Patrick Woida and William F. Hoffmann *In* Jet Propulsion Lab., California Inst. of Tech., Report of the Asilomar 3 LDR Workshop 15 Aug. 1988 p 112-113 (For primary document see N90-13449 05-18)
Avail: NTIS HC A08/MF A01 CSCL 11C

Development of carbon fiber reinforces plastic (CFRP) panel overcoating and polishing is structured in two parts. The first part utilized a short series of experiments to determine the feasibility of overcoating and polishing CFRP panels, and the second part employes a systematic approach to optimize techniques learned. Questions which required answers in the initial investigation are summarized. Tests were performedin the Steward Observatory's 2.2 Meter Vacuum Coating Chamber and began with 3 cm square pieces of CFRP facesheet material. Next, a 10 cm square and one-inch-thick CFPR-Aluminum core panel was tested. Tests were then conducted on a 0.5-meter-square Dornier panel (QUAD 4) with CFRP facesheets on two-inch aluminum Flexcore. To complete the initial study, a previously characterized 0.5 m Dornier panel (QUAD 23) was coated and hand polished. The mirror's optical performance was not affected by the SiO coating. Author

N90-13479*# Perkin-Elmer Corp., Danbury, CT.
REAL-TIME SENSING OF OPTICAL ALIGNMENT c74
Mark T. Stier and Alan B. Wissinger *In* Jet Propulsion Lab., California Inst. of Tech., Report of the Asilomar 3 LDR Workshop 15 Aug. 1988 p 114-116 (For primary document see N90-13449 05-18)
Avail: NTIS HC A08/MF A01 CSCL 20F

The Large Deployable Reflector and other future segmented optical systems may require autonomous, real-time alignment of their optical surfaces. Researchers have developed gratings located directly on a mirror surface to provide interferometric sensing of the location and figure of the mirror. The grating diffracts a small portion of the incident beam to a diffractive focus where the designed diagnostics can be performed. Mirrors with diffraction gratings were fabricated in two separate ways. The formation of a holographic grating over the entire surface of a mirror, thereby forming a Zone Plate Mirror (ZPM) is described. Researchers have also used computer-generated hologram (CGH) patches for alignment and figure sensing of mirrors. When appropriately illuminated, a grid of patches spread over a mirror segment will yield a grid of point images at a wavefront sensor, with the relative location of the points providing information on the figure and location of the mirror. A particular advantage of using the CGH approach is that the holographic patches can be computed, fabricated, and replicated on a mirror segment in a mass production 1-g clean room environment. Author

N90-13480*# National Aeronautics and Space Administration. Langley Research Center, Hampton, VA.
ASSEMBLY CONSIDERATIONS FOR LARGE REFLECTORS
H. Bush *In* Jet Propulsion Lab., California Inst. of Tech., Report of the Asilomar 3 LDR Workshop 15 Aug. 1988 p 118-119 (For primary document see N90-13449 05-18)
Avail: NTIS HC A08/MF A01 CSCL 22B

The technologies developed at LaRC in the area of erectable instructures are discussed. The information is of direct value to the Large Deployable Reflector (LDR) because an option for the LDR backup structure is to assemble it in space. The efforts in this area, which include development of joints, underwater assembly simulation tests, flight assembly/disassembly tests, and fabrication of 5-meter trusses, led to the use of the LaRC concept as the baseline configuration for the Space Station Structure. The Space Station joint is linear in the load and displacement range of interest to Space Station; the ability to manually assemble and disassemble a 45-foot truss structure was demonstrated by astronauts in space as part of the ACCESS Shuttle Flight Experiment. The structure was built in 26 minutes 46 seconds, and involved a total of 500 manipulations of untethered hardware. Also, the correlation of the space experience with the neutral buoyancy simulation was very good. Sections of the proposed 5-meter bay Space Station truss have been built on the ground. Activities at LaRC have included the development of mobile remote manipulator systems (which can traverse the Space Station 5-meter structure), preliminary LDR sun shield concepts, LDR construction scenarios, and activities in robotic assembly of truss-type structures. Author

N90-13481*# TRW Space Technology Labs., Redondo Beach, CA.
EXPLICIT MODELING AND CONCURRENT PROCESSING IN THE SIMULATION OF MULTIBODY DYNAMIC SYSTEMS
R. Gluck *In* Jet Propulsion Lab., California Inst. of Tech., Report of the Asilomar 3 LDR Workshop 15 Aug. 1988 p 120-121 (For primary document see N90-13449 05-18)
Avail: NTIS HC A08/MF A01 CSCL 22B

The objective is to present the activities at TRW in developing the capability to simulate the behavior of large flexible multibody space structures. The features of the simulation tools are: (1) to

accommodate all rigid/flexible body degrees-of-freedom which incorporate the control system models and external forces, (2) to provide the flexibility to incorporate engineering-defined models and to retain parameters of significance to the engineer, (3) to reduce the computation cost by one order of magnitude (two orders of magnitude compared to a CRAY 1S), and (4) to keep it versatile so that radical variations in anticipated space structures can be accommodated. The current computer tools to simulate multibody systems appear not only to be very costly and time consuming, but also do not produce the desired fidelity of the mathematical models. In summary, a multibody simulation tool will be developed in the near future which will allow solution of the dynamics and controls of the deployment of the LDR backup structure, or the problem associated with the robotic assembly of the structure. The tools will allow the engineer to define the modeling technique and solve problems in less time and at reduced cost. Author

N90-13482*# National Aeronautics and Space Administration. Langley Research Center, Hampton, VA.
INITIAL TEST RESULTS FOR THE MINI-MAST
L. Horta and G. Horner *In* Jet Propulsion Lab., California Inst. of Tech., Report of the Asilomar 3 LDR Workshop 15 Aug. 1988 p 122-123 (For primary document see N90-13449 05-18)
Avail: NTIS HC A08/MF A01 CSCL 22B

The objectives of the 20-meter Mini-Mast were: (1) to learn how to efficiently test this type of large truss structure, (2) to relate component testing to the overall behavior of the structure, and (3) to update the associated analytical model based upon the experimental data. The Mini-Mast represents structural characteristics similar to the COFS beam which is planned to be flown on Shuttle to perform on-orbit structures and controls experiments. The information is of interest to LDR because it represents analysis and test information on a truss-type structure which may be similar to the Large Deployable Reflector (LDR) backup structure. The structure has a total of 111 titanium joints; the joint in the center of the truss element is a near-center latch joint. The results of this research indicate that linear deployable-type structures can be built, but difficulties do exist in extracting modes with identical frequencies; gravitational loading does affect the ground test results; and prediction of truss-type-structure dynamic characteristics is not trivial. Author

N90-13483*# National Aeronautics and Space Administration. Langley Research Center, Hampton, VA.
LDR STRUCTURAL EXPERIMENT DEFINITION
R. A. Russell *In* Jet Propulsion Lab., California Inst. of Tech., Report of the Asilomar 3 LDR Workshop 15 Aug. 1988 p 124-125 (For primary document see N90-13449 05-18)
Avail: NTIS HC A08/MF A01 CSCL 22B

A system study to develop the definition of a structural flight experiment for a large precision segmented reflector on the Space Station was accomplished by the Boeing Aerospace Company for NASA's Langley Research Center. The objective of the study was to use a Large Deployable Reflector (LDR) baseline configuration as the basis for focusing an experiment definition, so that the resulting accommodation requirements and interface constraints could be used as part of the mission requirements data base for Space Station. The primary objectives of the first experiment are to construct the primary mirror support truss and to determine its structural and thermal characteristics. Addition of an optical bench, thermal shield and primary mirror segments, and alignment of the optical components, would occur on a second experiment. The structure would then be moved to the payload point system for pointing, optical control, and scientific optical measurement for a third experiment. Experiment 1 will deploy the primary support truss while it is attached to the instrument module structure. The ability to adjust the mirror attachment points and to attach several dummy primary mirror segments with a robotic system will also be demonstrated. Experiment 2 will be achieved by adding new components and equipment to experiment one. Experiment 3 will demonstrate advanced control strategies, active adjustment of the primary mirror alignment, and technologies associated with optical sensing. Author

N90-13484*# Air Force Systems Command, Kirtland AFB, NM.
CONTROL OF OPTICAL SYSTEMS **c37**
D. Founds *In* Jet Propulsion Lab., California Inst. of Tech., Report of the Asilomar 3 LDR Workshop 15 Aug. 1988 p 126-127 (For primary document see N90-13449 05-18)
Avail: NTIS HC A08/MF A01 CSCL 13I

Some of the current and planned activities at the Air Force Systems Command in structures and controls for optical-type systems are summarized. Many of the activities are contracted to industry; one task is an in-house program which includes a hardware test program. The objective of the in-house program, referred to as the Aluminum Beam Expander Structure (ABES), is to address issues involved in on-orbit system identification. The structure, which appears similar to the LDR backup structure, is about 35 feet tall. The activity to date has been limited to acquisition of about 250 hours of test data. About 30 hours of data per excitation force is gathered in order to obtain sufficient data for a good statistical estimate of the structural parameters. The development of an Integrated Structural Modeling (ISM) computer program is being done by Boeing Aerospace Company. The objective of the contracted effort is to develop a combined optics, structures, thermal, controls, and multibody dynamics simulation code. Author

N90-13485*# Astro Aerospace Corp., Santa Barbara, CA.
HYBRID DEPLOYABLE SUPPORT TRUSS DESIGNS FOR LDR **c31**
J. Hedgepeth *In* Jet Propulsion Lab., California Inst. of Tech., Report of the Asilomar 3 LDR Workshop 15 Aug. 1988 p 128-129 (For primary document see N90-13449 05-18)
Avail: NTIS HC A08/MF A01 CSCL 13B

Concepts for a 20-meter diameter Large Deployable Reflector (LDR) deployable truss backup structure, and analytical predictions of its structural characteristics are discussed. The concept shown is referred to as the SIXPAC; It is a combination of the PACTRUSS concept and a single-fold beam, which would make up the desired backup structure. One advantage of retaining the PACTRUSS concept is its packaging density and its capability for synchronous deployment. Various 2-meter hexagonal panel arrangements are possible for this Hybrid PACTRUSS structure depending on the panel-to-structure attachment strategies used. Static analyses of the SIXPAC using various assumptions for truss designs and panel masses of 10 kg sq meters were performed to predict the tip displacement of the structure when supported at the center. The tip displacement ranged from 0.20 to 0.44 mm without the panel mass, and from 0.9 to 3.9 mm with the panel mass (in a 1-g field). The data indicate that the structure can be adequately ground tested to validate its required performance in space, assuming the required performance in space is approximately 100 microns. The static displacement at the tip of the structure when subjected to an angular acceleration of 0.001 rad/sec squared were estimated to range from 0.8 to 7.5 microns, depending on the type of truss elements. Author

N90-13486*# Boeing Aerospace Co., Seattle, WA.
EFFECTS OF JOINTS IN TRUSS STRUCTURES **c31**
R. Ikegami *In* Jet Propulsion Lab., California Inst. of Tech., Report of the Asilomar 3 LDR Workshop 15 Aug. 1988 p 130-131 (For primary document see N90-13449 05-18)
Avail: NTIS HC A08/MF A01 CSCL 13B

The response of truss-type structures for future space applications, such as Large Deployable Reflector (LDR), will be directly affected by joint performance. Some of the objectives of research at BAC were to characterize structural joints, establish analytical approaches that incorporate joint characteristics, and experimentally establish the validity of the analytical approaches. The test approach to characterize joints for both erectable and deployable-type structures was based upon a Force State Mapping Technique. The approach pictorially shows how the nonlinear joint results can be used for equivalent linear analysis. Testing of the

Space Station joints developed at LaRC (a hinged joint at 2 Hz and a clevis joint at 2 Hz) successfully revealed the nonlinear characteristics of the joints. The Space Station joints were effectively linear when loaded to plus or minus 500 pounds with a corresponding displacement of about plus or minus 0.0015 inch. It was indicated that good linear joints exist which are compatible with errected structures, but that difficulty may be encountered if nonlinear-type joints are incorporated in the structure. Author

N90-13487*# Martin Marietta Aerospace, Denver, CO.
PACOSS PROGRAM
K. E. Richards, Jr. *In* Jet Propulsion Lab., California Inst. of Tech., Report of the Asilomar 3 LDR Workshop 15 Aug. 1988 p 132-133 (For primary document see N90-13449 05-18)
Avail: NTIS HC A08/MF A01 CSCL 22B

The objectives of the PACOSS program were to demonstrate the respective roles of passive and active control for structures that represented future Large Space Structures (LSS), to develop means to introduce passive vibration control, and to experimentally verify the damping predictions and the control algorithms. In order to meet the objectives, the program was divided into an analytical simulation phase to establish the respective roles of passive and active damping on a LSS-type structure, and a design, analysis, and test phase to validate the passive damping and the control algorithm performance for a structure. Predictable amounts of damping can be designed into a LSS structure, the best control strategy uses a combination of passive damping and active controls, and a more optimum system can be achieved by an early interaction between the structural designer, controls engineer, and the damping designer. Author

N90-13488*# Jet Propulsion Lab., California Inst. of Tech., Pasadena.
LDR STRUCTURAL TECHNOLOGY ACTIVITIES AT JPL
Ben Wada *In its* Report of the Asilomar 3 LDR Workshop 15 Aug. 1988 p 134-135 (For primary document see N90-13449 05-18)
Avail: NTIS HC A08/MF A01 CSCL 22B

The status of the Large Deployable Reflector (LDR) technology requirements and the availability of that technology in the next few years are summarized. The research efforts at JPL related to these technology needs are also discussed. LDR requires that a large and relatively stiff truss-type backup structure have a surface accurate to 100 microns in space (initial position with thermal distortions) and the dynamic characteristics predictable and/or measurable by on-orbit system identification for micron level motion. This motion may result from the excitation of the lower modes or from wave-type motions. It is also assumed that the LDR structure can be ground tested to validate its ability to meet mission requirements. No program manager will commit a structural design based solely on analysis, unless the analysis is backed by a validation test program. Author

N90-13489*# National Aeronautics and Space Administration. Langley Research Center, Hampton, VA.
JOINTS IN DEPLOYABLE SPACE TRUSS STRUCTURES
M. Rhodes *In* Jet Propulsion Lab., California Inst. of Tech., Report of the Asilomar 3 LDR Workshop 15 Aug. 1988 p 136-137 (For primary document see N90-13449 05-18)
Avail: NTIS HC A08/MF A01 CSCL 22B

Since the response of deployable structural concepts being considered for the Large Deployable Reflector (LDR) backup structure will be dominated by the response of joints, the joint characteristics are significant. An overview is given of the research activities at LaRC on the static behavior of joints for deployable space truss structures. Since a pin-clevis-type joint will be utilized in deployable structures, an experimental research program to characterize the joint parameters which affect stiffness was conducted. An experimental research program was conducted on a second type of joint, referred to as a near-center latch joint. It was used in the center of members on the deployable truss structure for the Control of Flexible Structures (COFS) flight experiment. The test results of the near-center latch joint and the member with the joints indicated that the stiffness of the near-center joint is linear and stiffer than the stiffness of the total member, and that non-linearities in the stiffness characteristics of the total member were due to bending introduced at the ends of the member. The resulting data indicates that stiff linear folding joints can be designed and that bending load paths should be avoided whenever possible. In summary, for deployable structures, special attention to the joint and the structure design is required to minimize the undesirable structural non-linearities. Author

N90-13490*# Arizona Univ., Tucson.
THREE-METER BALLOON-BORNE TELESCOPE **c74**
William F. Hoffmann, G. G. Fazio, and D. A. Harper (Chicago Univ., IL.) *In* Jet Propulsion Lab., California Inst. of Tech., Report of the Asilomar 3 LDR Workshop 15 Aug. 1988 p 138-139 (For primary document see N90-13449 05-18)
Avail: NTIS HC A08/MF A01 CSCL 20F

The Three-Meter Balloon-Borne Telescope is planned as a general purpose facility for making far-infrared and submillimeter astronomical observations from the stratosphere. It will operate throughout the spectral range 30 microns to 1 millimeter which is largely obscurred from the ground. The design is an f/13.5 Cassegrain telescope with an f/1.33 3-meter primary mirror supported with a 3-axis gimbal and stabilization system. The overall structure is 8.0 m high by 5.5 m in width by 4.0 m in depth and weighs 2000 kg. This low weight is achieved through the use of an ultra lightweight primary mirror of composite construction. Pointing and stabilization are achieved with television monitoring of the star field, flex-pivot bearing supports, gyroscopes, and magnetically levitated reaction wheels. Two instruments will be carried on each flight; generally a photometric camera and a spectrometer. A 64-element bolometer array photometric camera operating from 30 to 300 microns is planned as part of the facility. Additional instruments will be derived from KAO and other development programs. Author

N90-13491*# Allied-Signal Aerospace Co., Torrance, CA. AiResearch Div.
SPACE STATION GAS COMPRESSOR TECHNOLOGY STUDY PROGRAM, PHASE 1 Final Report
B. W. Hafele and R. R. Rapozo 16 Jun. 1989 76 p
(Contract NAS8-37747)
(NASA-CR-183758; NAS 1.26:183758; Rept-89-62104(5)) Avail: NTIS HC A05/MF A01 CSCL 22B

The objectives were to identify the space station waste gases and their characteristics, and to investigate compressor and dryer types, as well as transport and storage requirements with tradeoffs leading to a preliminary system definition. Author

N90-13492*# National Academy of Sciences - National Research Council, Washington, DC.
SPACE STATION ENGINEERING DESIGN ISSUES
Duane T. McRuer, Barry W. Boehm, Daniel B. Debra, C. Cordell Green, Richard C. Henry, Paul D. Maycock, John H. McElroy, Chester M. Pierce, Thomas P. Stafford, and Laurence R. Young (Massachusetts Inst. of Tech., Cambridge.) et al 1989 85 p Workshop presented in Irvine, CA, 7-11 Nov. 1988
(Contract NASw-4003)
(NASA-CR-185978; NAS 1.26:185978; LC-89-62778; ISBN-0-309-04083-3) Avail: NTIS HC A05/MF A01 CSCL 22B

Space Station Freedom topics addressed include: general design issues; issues related to utilization and operations; issues related to systems requirements and design; and management issues relevant to design. B.G.

N90-13493*# National Aeronautics and Space Administration, Washington, DC.
SCIENCE AND APPLICATIONS ON THE SPACE STATION: A STRATEGIC VISION
Mar. 1988 18 p
(NASA-TM-101863; NAS 1.15:101863) Avail: NTIS HC A03/MF A01 CSCL 22B

The central themes relating to science and applications on the Space Station for fiscal year 1989 are discussed. Materials science research is proposed in a wide variety of subfields including protein crystal growth, metallurgy, and properties of fluids. Also proposed are the U.S. Polar Platform, an Extended Duration Crew Operations Project, and a long-range Space Biology Research Project to investigate plant and animal physiology, gravitational biology, life support systems, and exobiology. The exterior of the Space Station will provide attachment points for payloads to study subjects such as the earth and its environment, the sun, other bodies in the solar system, and cosmic objects. Examples of such attached payloads are given. They include a plasma interaction monitoring system, observation of solar features and properties, studies of particle radiation from the sun, cosmic dust collection and analysis, surveys of various cosmic and solar rays, measurements of rainfall and wind and the study of global changes on earth. J.P.S.

N90-13494*# Howard Univ., Washington, DC. Dept. of Mechanical Engineering.
THE DYNAMICS AND CONTROL OF LARGE FLEXIBLE SPACE STRUCTURES - 12, SUPPLEMENT 11 Final Report
Peter M. Bainum, A. S. S. R. Reddy, Feiyue Li, and Jianke Xu Sep. 1989 67 p
(Grant NsG-1414)
(NASA-CR-185966; NAS 1.26:185966) Avail: NTIS HC A04/MF A01 CSCL 22B

The rapid 2-D slewing and vibrational control of the unsymmetrical flexible SCOLE (Spacecraft Control Laboratory Experiment) with multi-bounded controls is considered. Pontryagin's Maximum Principle is applied to the nonlinear equations of the system to derive the necessary conditions for the optimal control. The resulting two point boundary value problem is then solved by using the quasilinearization technique, and the near minimum time is obtained by sequentially shortening the slewing time until the controls are near the bang-bang type. The tradeoff between the minimum time and the minimum flexible amplitude requirements is discussed. The numerical results show that the responses of the nonlinear system are significantly different from those of the linearized system for rapid slewing. The SCOLE station-keeping closed loop dynamics are re-examined by employing a slightly different method for developing the equations of motion in which higher order terms in the expressions for the mast modal shape functions are now included. A preliminary study on the effect of actuator mass on the closed loop dynamics of large space systems is conducted. A numerical example based on a coupled two-mass two-spring system illustrates the effect of changes caused in the mass and stiffness matrices on the closed loop system eigenvalues. In certain cases the need for redesigning control laws previously synthesized, but not accounting for actuator masses, is indicated. Author

N90-13495*# Rensselaer Polytechnic Inst., Troy, NY. Dept. of Electrical, Computer and Systems Engineering.
A PRACTICAL APPROACH FOR MINIMUM TIME CONTROL OF THE SPACECRAFT CONTROL LABORATORY EXPERIMENT (SCOLE), APPENDIX A
H. Kaufman and K. J. Kyriakopoulos 1989 26 p
(Grant NAG1-515)
(NASA-CR-186008; NAS 1.26:186008) Avail: NTIS HC A03/MF A01 CSCL 22B

The Space COntrol Laboratory Experiment (SCOLE) is a challenge for control engineering applications. This is a result of the system dynamics, the available measurement information, the actuator capabilities and finally the specified performance requirements set. Results on the use of Model Reference Adaptive Control were reported. In view of the necessity for rapid response, this work deals with an optimal control formulation, with a minimum time requirement and constrained input. A mathematical statement of the problem is presented. The time optimal control formulation is presented and the reasons that make such an approach not promising are discussed. As a result, a pseudo time-optimal control algorithm is discussed. The proposed approach is tested to see if it satisfies the design specifications, and finally a discussion and suggestions for further research are provided. Author

N90-13496*# Southwest Research Inst., San Antonio, TX.
THE ROLE OF THE HOST IN A COOPERATING MAINFRAME AND WORKSTATION ENVIRONMENT, VOLUMES 1 AND 2 Final Report
Antone Kusmanoff and Nancy L. Martin 12 Oct. 1989 144 p
(Grant NAG9-341; SwRI Proj. 05-0769)
(NASA-CR-185463-Vol-1/2; NAS 1.26:185463-Vol-1/2) Avail: NTIS HC A07/MF A01 CSCL 22B

In recent years, advancements made in computer systems have prompted a move from centralized computing based on timesharing a large mainframe computer to distributed computing based on a connected set of engineering workstations. A major factor in this advancement is the increased performance and lower cost of engineering workstations. The shift to distributed computing from centralized computing has led to challenges associated with the residency of application programs within the system. In a combined system of multiple engineering workstations attached to a mainframe host, the question arises as to how does a system designer assign applications between the larger mainframe host and the smaller, yet powerful, workstation. The concepts related to real time data processing are analyzed and systems are displayed which use a host mainframe and a number of engineering workstations interconnected by a local area network. In most cases, distributed systems can be classified as having a single function or multiple functions and as executing programs in real time or nonreal time. In a system of multiple computers, the degree of autonomy of the computers is important; a system with one master control computer generally differs in reliability, performance, and complexity from a system in which all computers share the control. This research is concerned with generating general criteria principles for software residency decisions (host or workstation) for a diverse yet coupled group of users (the clustered workstations) which may need the use of a shared resource (the mainframe) to perform their functions. Author

N90-13497*# Mississippi State Univ., Mississippi State. Dept. of Electrical Engineering.
SPACELAB SYSTEM ANALYSIS: THE MODIFIED FREE ACCESS PROTOCOL: AN ACCESS PROTOCOL FOR COMMUNICATION SYSTEMS WITH PERIODIC AND POISSON TRAFFIC Final Report
Frank Ingels, John Owens, and Steven Daniel 31 Oct. 1989 261 p
(Contract NAS8-36717)
(NASA-CR-183805; NAS 1.26:183805; MSU-EE-FIN-20A-89)
Avail: NTIS HC A12/MF A02 CSCL 22B

The protocol definition and terminal hardware for the modified free access protocol, a communications protocol similar to Ethernet, are developed. A MFA protocol simulator and a CSMA/CD math model are also developed. The protocol is tailored to communication systems where the total traffic may be divided into scheduled traffic and Poisson traffic. The scheduled traffic should occur on a periodic basis but may occur after a given event such as a request for data from a large number of stations. The Poisson traffic will include alarms and other random traffic. The purpose of the protocol is to guarantee that scheduled packets will be delivered without collision. This is required in many control and data collection systems. The protocol uses standard Ethernet hardware and software requiring minimum modifications to an existing system. The modification to the protocol only affects the Ethernet transmission privileges and does not effect the Ethernet receiver. Author

N90-13498# Naval Postgraduate School, Monterey, CA.
INEXPENSIVE GLOBAL LOCATION AND TRACKING SYSTEMS USING GEOSTATIONARY SATELLITES M.S. Thesis
Danny L. DeFries Jun. 1989 43 p
(AD-A213025) Avail: NTIS HC A03/MF A01 CSCL 17/7

Inexpensive Global Location and Tracking Systems are currently being designed to provide the civilian market low-cost

radio position determination. This paper discusses two possible designs. The first design employs 3 or 4 satellites, depending on whether altitude is known a priori, each transmitting continuous ranging signals. The user transceiver receives the ranging signals, measures the time differentials of the receipt of the signals and transfers this information to a control station via a satellite link. The control station computes the user position from this data and sends the position coordinates back to the user via another satellite link. In the second design, each user transceiver transmits a unique code to the control station via the 3 or 4 satellite links, again depending on whether the altitude is known a priori. The control station measures the time differentials of the receipt of the signals and determines the user position. This position information is then transmitted back to the user via a satellite link. GRA

N90-13499# European Space Agency, Paris (France).
THE HIPPARCOS MISSION. PRELAUNCH STATUS. VOLUME 1: THE HIPPARCOS SATELLITE
M. A. C. Perryman, H. Hassan, T. Batut, K. D. Bock, C. J. Burrows, K. Clausen, P. E. Davies, A. Dherbecourt, H. Eggel, and A. Errington et al Jun. 1989 360 p Original contains color illustrations (ESA-SP-1111-Vol-1; ISBN-92-9092-016-5; ISSN-0379-6566; ETN-90-95527) Copyright Avail: NTIS HC A16/MF A02; ESA Publications Div., ESTEC, Noordwijk, Netherlands, 80 Dutch guilders

The Hipparcos project is reported. In particular, the design, development and performance tests of the prelaunching phase are presented. The following topics are included: the operating principle, the payload structure, the telescope mirrors and related optical equipment, the thermal control, the baffles and the detectors. The spacecraft structure, along with thermal, mechanical and electrical subsystems, is described. The data handling systems, and the attitude and orbit control systems are analyzed. The tests carried out for the calibration of the payload and to ascertain the influence of the performance in orbit on the ultimate accuracy of the measurements are included. For individual titles, see N90-13500 through N90-13528.

N90-13500# European Space Agency, Paris (France).
OPERATING PRINCIPLE
M. A. C. Perryman and S. Vaghi *In its* The Hipparcos Mission. Prelaunch Status. Volume 1: The Hipparcos Satellite Jun. 1989 p 11-22 (For primary document see N90-13499 05-18)
Copyright Avail: NTIS HC A16/MF A02; ESA Publications Div., ESTEC, Noordwijk, Netherlands, 80 Dutch guilders

The operating principle of the Hipparcos satellite is presented. The key features of the payload design, the way in which the satellite scans the sky, and the way in which the stars present in the combined field of view are observed, are described. In the scope of the work, the following topics are included: the optimization of the star observations, the star dependent parameters, the fully and partially observable stars, the star selection, the observation time allocation and the execution of the observing sequence. ESA

N90-13501# European Space Agency, Paris (France).
ERROR ALLOCATION AND ACCURACY ASSESSMENT
C. J. Burrows, P. E. Davies, and R. D. Wills *In its* The Hipparcos Mission. Prelaunch Status. Volume 1: The Hipparcos Satellite Jun. 1989 p 23-42 (For primary document see N90-13499 05-18)
Copyright Avail: NTIS HC A16/MF A02; ESA Publications Div., ESTEC, Noordwijk, Netherlands, 80 Dutch guilders

The concepts of error allocation, performance verification and accuracy assessment of the measurements to be effectuated by Hipparcos satellite are discussed. The total system required accuracy concerning data reduction (sub) systems are considered. The individual components are measured and modeled. The estimation of the component performances is given. The results of the image location stage program, the great circle reduction program and the expected mission accuracy are analyzed. ESA

N90-13502# European Space Agency, Paris (France).
OVERVIEW OF THE HIPPARCOS SATELLITE
K. Clausen and R. D. Wills *In its* The Hipparcos Mission. Prelaunch Status. Volume 1: The Hipparcos Satellite Jun. 1989 p 43-55 (For primary document see N90-13499 05-18)
Copyright Avail: NTIS HC A16/MF A02; ESA Publications Div., ESTEC, Noordwijk, Netherlands, 80 Dutch guilders

Several aspects of the Hipparcos satellite are presented. In particular the orbit, the environmental conditions, the attitude control concept, the data handling and processing, and the operational concept, are described. The actual design of the satellite, is presented. The satellite payload, dedicated to the on board experiments, is given. The satellite characteristics, the mass budget, the power budget for preoperational and operational periods, and the electrical subsystems are listed. A block diagram of the main measurement and operational functions involved during mission, is shown. ESA

N90-13503# European Space Agency, Paris (France).
OVERVIEW OF THE HIPPARCOS PAYLOAD
K. vanKatwijk *In its* The Hipparcos Mission. Prelaunch Status. Volume 1: The Hipparcos Satellite Jun. 1989 p 57-66 Original contains color illustrations (For primary document see N90-13499 05-18)
Copyright Avail: NTIS HC A16/MF A02; ESA Publications Div., ESTEC, Noordwijk, Netherlands, 80 Dutch guilders

The hardware elements constituting the onboard experiments are described. The payload characteristics concerning the reflective Schmidt telescope, the primary detection system and the star mapper system are listed. The payload main assemblies are the two baffle assemblies, the telescope assembly, the focal plane assembly and the service electronics units. The payload functional and electrical block diagrams are presented. The spectral transmittance of the main detection chain, for lambda between 350 and 825 nanometers, is shown. ESA

N90-13504# European Space Agency, Paris (France).
THE TELESCOPE MIRRORS **c74**
G. Ratier and T. Batut *In its* The Hipparcos Mission. Prelaunch Status. Volume 1: The Hipparcos Satellite Jun. 1989 p 67-73 (For primary document see N90-13499 05-18)
Copyright Avail: NTIS HC A16/MF A02; ESA Publications Div., ESTEC, Noordwijk, Netherlands, 80 Dutch guilders

The optical and mechanical characteristics of the Hipparcos telescope mirrors are studied. The telescope contains three mirrors: a beam combiner, a primary spherical mirror and a flat folding mirror. The beam combiner functions concerning the combination of the two fields of view, the definition of the entrance pupil, and the correction of the aberrations of the spherical mirror are discussed. The spherical and the flat mirrors are made of light weight zerodur blanks and measure 393 and 356 mm respectively. The steps in the manufacture of the beam combiner are included. ESA

N90-13505# European Space Agency, Paris (France).
THE MODULATING GRID **c74**
G. Ratier and T. Batut *In its* The Hipparcos Mission. Prelaunch Status. Volume 1: The Hipparcos Satellite Jun. 1989 p 75-84 (For primary document see N90-13499 05-18)
Copyright Avail: NTIS HC A16/MF A02; ESA Publications Div., ESTEC, Noordwijk, Netherlands, 80 Dutch guilders

The modulating grid of the Hipparcos satellite, applied to bring the star images to a focal surface, is analyzed. It is formed by a main grid and a star grid. The main grid consists of 2688 parallel slits, with a projected spacing of 1.208 arc sec, and the star mapper grids each consisting of two sets of four slits each set of four slits being spaced in the ratio 1:3:2. The results of the main grid calibration, concerning the slit geometry, the medium and small scale grid irregularities, and the grid reference marks are given. ESA

N90-13506# European Space Agency, Paris (France).
THE RELAY LENS SYSTEMS **c74**
G. Ratier and T. Batut *In its* The Hipparcos Mission. Prelaunch Status. Volume 1: The Hipparcos Satellite Jun. 1989 p 85-94

(For primary document see N90-13499 05-18)
Copyright Avail: NTIS HC A16/MF A02; ESA Publications Div., ESTEC, Noordwijk, Netherlands, 80 Dutch guilders

The relay lens assembly used in the Hipparcos satellite is studied. It is applied to transfer the modulated light from the grid to the image dissector tube detector, as well as from the star mapper grid to the photomultiplier detectors. The design of the image dissector relay lens assembly, is presented. The requirements concerning the image quality are discussed. The chromaticity, the wide band, and the dichroic filters are presented. ESA

N90-13507# European Space Agency, Paris (France).
THE DETECTORS **c74**
H. Eggel *In its* The Hipparcos Mission. Prelaunch Status. Volume 1: The Hipparcos Satellite Jun. 1989 p 95-100 (For primary document see N90-13499 05-18)
Copyright Avail: NTIS HC A16/MF A02; ESA Publications Div., ESTEC, Noordwijk, Netherlands, 80 Dutch guilders

The detectors used for Hipparcos satellite are studied. The image dissector tube detector which samples the modulated images of the stars as they cross the main field of view, and the star mapper (photomultiplier) detectors, which sample the entire field of the star mapper, are presented. In the scope of the work, the following topics are included: the main detector assembly, the detection subsystem block diagram, the operating principle of the image dissector tube, and the detection electronics box and signal coding. ESA

N90-13508# European Space Agency, Paris (France).
PAYLOAD ELECTRONICS AND MECHANISMS **c33**
T. vanderLaan, E. Jaekel, and H. Eggel *In its* The Hipparcos Mission. Prelaunch Status. Volume 1: The Hipparcos Satellite Jun. 1989 p 101-105 (For primary document see N90-13499 05-18)
Copyright Avail: NTIS HC A16/MF A02; ESA Publications Div., ESTEC, Noordwijk, Netherlands, 80 Dutch guilders

The mechanisms and the electronic payload used for Hipparcos are presented. The mechanism drive electronics unit, applied to supply suitable pulses for the motors of the mechanisms, is examined. The thermal control electronics are described. The refocusing, the switching mirror, the two chromaticity, and the four shutter mechanisms are outlined. Moreover the operational modes for each mechanism are given. ESA

N90-13509# European Space Agency, Paris (France).
THE BAFFLES **c37**
G. Ratier and T. Batut *In its* The Hipparcos Mission. Prelaunch Status. Volume 1: The Hipparcos Satellite Jun. 1989 p 107-111 Original contains color illustrations (For primary document see N90-13499 05-18)
Copyright Avail: NTIS HC A16/MF A02; ESA Publications Div., ESTEC, Noordwijk, Netherlands, 80 Dutch guilders

The baffles applied to protect the Hipparcos telescope field of view are examined. External and internal baffles are responsible for reducing both the overall mission dead time, and the duration and number of great circle interruptions. The major constituents, which are the support structure, the baffle tube, and the front aperture assembly, are indicated. The straylight test configuration and attenuation curves are included. ESA

N90-13510# European Space Agency, Paris (France).
THE PAYLOAD STRUCTURE
T. vanderLaan and E. Jaekel *In its* The Hipparcos Mission. Prelaunch Status. Volume 1: The Hipparcos Satellite Jun. 1989 p 113-116 (For primary document see N90-13499 05-18)
Copyright Avail: NTIS HC A16/MF A02; ESA Publications Div., ESTEC, Noordwijk, Netherlands, 80 Dutch guilders

The design analysis and the manufacturing solutions for the Hipparcos payload structure are examined. Special attention is paid to the thermal and temporal stability of the relative positions of the optical components. The requirements concerning the mechanical interfaces with the satellite, the focal assembly units and harness, the variation and the effect of the gravity release are considered. The following telescope structure subassemblies are analyzed: the main structure, the mirror mounts, the focal plane assembly platform, and the Cherenkov shielding. ESA

N90-13511# European Space Agency, Paris (France).
PAYLOAD THERMAL CONTROL
E. Jaekel *In its* The Hipparcos Mission. Prelaunch Status. Volume 1: The Hipparcos Satellite Jun. 1989 p 117-119 (For primary document see N90-13499 05-18)
Copyright Avail: NTIS HC A16/MF A02; ESA Publications Div., ESTEC, Noordwijk, Netherlands, 80 Dutch guilders

The Hipparcos payload thermal control is presented. It ensures the active and passive thermal control with a temperature stability better than 0.05C over short periods, and about 2C over the entire mission duration. The payload structure, manufactured from carbon fiber reinforced plastic, is described. The principles of the active thermal control system are indicated, and its characteristics are listed. ESA

N90-13512# European Space Agency, Paris (France).
THE SPACECRAFT STRUCTURE
T. vanderLaan and E. Jaekel *In its* The Hipparcos Mission. Prelaunch Status. Volume 1: The Hipparcos Satellite Jun. 1989 p 121-125 (For primary document see N90-13499 05-18)
Copyright Avail: NTIS HC A16/MF A02; ESA Publications Div., ESTEC, Noordwijk, Netherlands, 80 Dutch guilders

The spacecraft structure for the Hipparcos program is presented. The mass budget of this aluminum made structure is given. The central thrust tube, which carries the satellite assemblies and forms the interface to the Ariane launcher, is examined. The secondary structure, which consists of the shade structure, the fill-in antenna boom and the support structures for the cold gas and hydrazine tanks, is outlined. ESA

N90-13513# European Space Agency, Paris (France).
SPACECRAFT THERMAL CONTROL
E. Jaekel *In its* The Hipparcos Mission. Prelaunch Status. Volume 1: The Hipparcos Satellite Jun. 1989 p 127-129 (For primary document see N90-13499 05-18)
Copyright Avail: NTIS HC A16/MF A02; ESA Publications Div., ESTEC, Noordwijk, Netherlands, 80 Dutch guilders

The spacecraft thermal control, applied to the Hipparcos mission, is analyzed. The principal elements, the functional requirements during the launch and on-station configurations, and the corresponding performances are examined. The objectives of the thermal control system are reviewed. The elements of the spacecraft accounting for the overall thermal design are presented. The spacecraft heating strategies, developed on the basis of flight performance predictions, are discussed. ESA

N90-13514# European Space Agency, Paris (France).
DATA HANDLING AND TELECOMMUNICATIONS **c32**
A. Errington *In its* The Hipparcos Mission. Prelaunch Status. Volume 1: The Hipparcos Satellite Jun. 1989 p 131-146 (For primary document see N90-13499 05-18)
Copyright Avail: NTIS HC A16/MF A02; ESA Publications Div., ESTEC, Noordwijk, Netherlands, 80 Dutch guilders

The data handling and the telecommunications subsystems, applied in the Hipparcos mission, are discussed. The data handling subsystem manages the interface with the ground segment, the acquisition of science and housekeeping data, and the maintenance of an on board time reference. It provides star mapper data acquisition and processing for attitude reference, and image dissector tube piloting. The design, the unit descriptions, the operational modes and the performances of the data handling subsystem are presented. Concerning the telecommunication subsystem, the unit and the operational mode are described and the performances are given. ESA

N90-13515# European Space Agency, Paris (France).
POWER GENERATION AND DISTRIBUTION **c20**
H. K. Fiebrich *In its* The Hipparcos Mission. Prelaunch Status.

Volume 1: The Hipparcos Satellite Jun. 1989 p 147-164 (For primary document see N90-13499 05-18)
Copyright Avail: NTIS HC A16/MF A02; ESA Publications Div., ESTEC, Noordwijk, Netherlands, 80 Dutch guilders

The three subsystems involved in the generation and distribution of electrical power of the Hipparcos mission, are presented. The mechanical and electrical properties of the solar generator subsystem are summarized. The operational concept of the electrical power subsystem, which provides 50V main direct current bus to all satellite power users, is detailed. The spacecraft harness subsystem, which provides all the electrical connections for all electrical units of the payload, is described. Moreover, the following topics are included: the shint regulator unit, the batteries, the batteries unit control and discharge regulator, the electrical integration unit, the auxiliary power supply, and the pyrotechnic relay unit. ESA

N90-13516# European Space Agency, Paris (France).
THE ATTITUDE AND ORBIT CONTROL SYSTEM
P. Strada *In its* The Hipparcos Mission. Prelaunch Status. Volume 1: The Hipparcos Satellite Jun. 1989 p 165-196 (For primary document see N90-13499 05-18)
Copyright Avail: NTIS HC A16/MF A02; ESA Publications Div., ESTEC, Noordwijk, Netherlands, 80 Dutch guilders

The Hipparcos attitude and orbit control system is presented. It performs two major tasks: during the spin stabilized phase, it provides a reference for the control of most of the flight related functions, such as pointing antennas or solar panels, or orienting the apogee boost motor for orbit maneuvers. The attitude and orbit control equipment is detailed and an overall block diagram is given. The reaction control assembly, which provides impulses for velocity corrections is examined. The active nutation damping, the spin adjustment with hydrazine and the spin axis orientation are covered. The maneuvers concerning the station acquisition and the pointing of the spin axis to the sun are discussed. The deployment of the solar arrays and the hydrazine tank depletion procedures are included. ESA

N90-13517# European Space Agency, Paris (France).
THE APOGEE BOOST MOTOR **c20**
P. Strada *In its* The Hipparcos Mission. Prelaunch Status. Volume 1: The Hipparcos Satellite Jun. 1989 p 197-203 (For primary document see N90-13499 05-18)
Copyright Avail: NTIS HC A16/MF A02; ESA Publications Div., ESTEC, Noordwijk, Netherlands, 80 Dutch guilders

The apogee boost motor, used in the Hipparcos satellite, is presented. It is applied to circularize the satellite's initial elliptical transfer orbit, determined by the launch vehicle, into a circular near geosynchronous orbit. The solid propellant MAGE 2 motor (European geostationary apogee motor), is described. The operating mode for the injection into a geostationary orbit is examined. The motor thrust curve and pressure curve during firing as a function of time are given. The apogee boost motor mass budget and the mechanical interfaces to the spacecraft are summarized. ESA

N90-13518# European Space Agency, Paris (France).
ON-BOARD SOFTWARE **c61**
C. Rolls and A. Dherbecourt *In its* The Hipparcos Mission. Prelaunch Status. Volume 1: The Hipparcos Satellite Jun. 1989 p 205-219 (For primary document see N90-13499 05-18)
Copyright Avail: NTIS HC A16/MF A02; ESA Publications Div., ESTEC, Noordwijk, Netherlands, 80 Dutch guilders

The Hipparcos onboard software is presented. The software residing in the central terminal unit of the data handling system, and the software residing in the attitude and orbit control system are described. The central onboard software, in addition to providing data handling services, provides specific support for payload operation and controls the payload's thermal state. The central onboard software functions are summarized. The Hipparcos data handling architecture, with the location of the software and their processing units, is given. The various functions of the attitude control software are described. ESA

N90-13519# European Space Agency, Paris (France).
ASSEMBLY, INTEGRATION, AND VERIFICATION
M. Setzke and O. Pace *In its* The Hipparcos Mission. Prelaunch Status. Volume 1: The Hipparcos Satellite Jun. 1989 p 221-225 (For primary document see N90-13499 05-18)
Copyright Avail: NTIS HC A16/MF A02; ESA Publications Div., ESTEC, Noordwijk, Netherlands, 80 Dutch guilders

The approaches adopted for the tasks of the Hipparcos satellite assembly, concerning performance and functional verification, are examined. The philosophy of the satellite model development is explained. The industrial development of the Hipparcos satellite and the activities of the test program are described. The purposes and the management of the verification program are reviewed. The launch range operations, which include satellite preparation, satellite filling and integration and combined launcher/satellite operations, are summarized. ESA

N90-13520# European Space Agency, Paris (France).
ELECTRICAL TESTING **c33**
M. Setzke, O. Pace, and G. Jung *In its* The Hipparcos Mission. Prelaunch Status. Volume 1: The Hipparcos Satellite Jun. 1989 p 227-239 (For primary document see N90-13499 05-18)
Copyright Avail: NTIS HC A16/MF A02; ESA Publications Div., ESTEC, Noordwijk, Netherlands, 80 Dutch guilders

The electrical testing of the Hipparcos satellite component units is described. The electromagnetic compatibility tests, and the electrical ground support equipment required for the tests are given. Hipparcos integrated system test is effectuated in the various operational modes to be experienced during its lifetime. The integrated subsystem tests, performed on the main as well as on the redundant units of each system, are listed. The payload checkout equipment and the software validation facility are included. ESA

N90-13521# European Space Agency, Paris (France).
MECHANICAL AND THERMAL TESTING
K. D. Bock *In its* The Hipparcos Mission. Prelaunch Status. Volume 1: The Hipparcos Satellite Jun. 1989 p 241-245 (For primary document see N90-13499 05-18)
Copyright Avail: NTIS HC A16/MF A02; ESA Publications Div., ESTEC, Noordwijk, Netherlands, 80 Dutch guilders

The mechanical and thermal qualification of the Hipparcos satellite are described. The following tests are carried out: static load, modal survey, sine and random vibration, acoustic test, pyrorelease, and shock separation. Concerning the thermal tests, the qualification and acceptance for the spacecraft and the payload are separated. The purposes of the tests at unit, subsystem and system level are described. The qualification of the mechanical ground support equipment is summarized. ESA

N90-13522# European Space Agency, Paris (France).
PRODUCT ASSURANCE **c38**
K. Huehn *In its* The Hipparcos Mission. Prelaunch Status. Volume 1: The Hipparcos Satellite Jun. 1989 p 247-250 (For primary document see N90-13499 05-18)
Copyright Avail: NTIS HC A16/MF A02; ESA Publications Div., ESTEC, Noordwijk, Netherlands, 80 Dutch guilders

The procedures and implementation of the product assurance program applied in the Hipparcos satellite development are described. The top level requirements for the product assurance program include: the product assurance management; the quality assurance (hardware); the reliability assurance; the safety assurance; the maintainability and availability assurance; the components selection, procurement, and control; the materials and processes control; and the software quality assurance. Concerning the implementation, the prime contractor's commitments and objectives are detailed. ESA

N90-13523# European Space Agency, Paris (France).
ON-GROUND PHOTOMETRIC CALIBRATION **c35**
T. Batut *In its* The Hipparcos Mission. Prelaunch Status. Volume 1: The Satellite Jun. 1989 p 251-263 (For primary document

see N90-13499 05-18)
Copyright Avail: NTIS HC A16/MF A02; ESA Publications Div., ESTEC, Noordwijk, Netherlands, 80 Dutch guilders

The on-ground photometric calibration of the Hipparcos satellite payload is reported. The aim of the tests is to obtain knowledge of the instrument's photometric parameters to a specific accuracy to provide the basis for the prediction of in-orbit parameters. The experiments are carried out under representative thermal and vacuum conditions. The calibration sequences are given. The calibration results for the main field of view and for the star mappers are shown. They give a good indication of the inflight performance, especially for the homogeneity and uniformity of the payload responses. ESA

N90-13524# European Space Agency, Paris (France).
LAUNCH AND EARLY ORBIT **c12**
K. Clausen *In its* The Hipparcos Mission. Prelaunch Status. Volume 1: The Hipparcos Satellite Jun. 1989 p 265-269 (For primary document see N90-13499 05-18)
Copyright Avail: NTIS HC A16/MF A02; ESA Publications Div., ESTEC, Noordwijk, Netherlands, 80 Dutch guilders

The launch and early orbit phase of the Hipparcos mission are studied. This comprises the launch, the highly eccentric transfer orbit, the firing of the satellite's solid rocket motor at the transfer orbit apogee to boost it into a circular near synchronous orbit, the drift to the final geosynchronous station at 12 degrees west, and the sun acquisition. All the steps between the launcher separation up to the station acquisition are analyzed. The initial steps for the sun acquisition, and for the initialization of the normal mode attitude control and real time attitude determination, are included. ESA

N90-13525# European Space Agency, Paris (France).
THE IN-ORBIT INITIALIZATION PHASE **c12**
J. vanderHa *In its* The Hipparcos Mission. Prelaunch Status. Volume 1: The Hipparcos Satellite Jun. 1989 p 271-282 (For primary document see N90-13499 05-18)
Copyright Avail: NTIS HC A16/MF A02; ESA Publications Div., ESTEC, Noordwijk, Netherlands, 80 Dutch guilders

The initialization of the onboard real time attitude determination loop of the Hipparcos satellite is presented. It initializes the autonomous onboard operation of the payload functions. The normal mode real time attitude determination processing is summarized. The ground capabilities needed, and the interaction with the two onboard computers during the critical mission phases are listed. The functional tasks distribution between control law electronics and onboard computer during normal mode operations are presented. The star pattern recognition algorithm is examined. ESA

N90-13526# European Space Agency, Paris (France).
IN-ORBIT PAYLOAD CALIBRATION **c12**
R. D. Wills *In its* The Hipparcos Mission. Prelaunch Status. Volume 1: The Hipparcos Satellite Jun. 1989 p 283-295 (For primary document see N90-13499 05-18)
Copyright Avail: NTIS HC A16/MF A02; ESA Publications Div., ESTEC, Noordwijk, Netherlands, 80 Dutch guilders

The Hipparcos payload calibration activities during the commissioning period of the inorbit operations are discussed. Both geometrical and photometric calibration tasks are performed. The aim of the payload calibration during the commissioning phase include: calibration of parameters that are used in the operation of the satellite; preliminary calibration to establish the feasibility of the definitive calibration to be performed by the data reduction consortia; and verification that the payload and appropriate satellite performances are within specification. Concerning the calibration performance, the predicted accuracies and the specifications are compared, and the corresponding individual measurement times are shown. ESA

N90-13527# European Space Agency, Paris (France).
THE ROLE OF THE GROUND SEGMENT **c14**
J. vanderHa *In its* The Hipparcos Mission. Prelaunch Status. Volume 1: The Hipparcos Satellite Jun. 1989 p 297-304 (For primary document see N90-13499 05-18)
Copyright Avail: NTIS HC A16/MF A02; ESA Publications Div., ESTEC, Noordwijk, Netherlands, 80 Dutch guilders

The ground segment operations during the Hipparcos mission are discussed. The ground segment must ensure that the inputs are properly communicated to the satellite, and guarantee that the data products delivered meet the expectations. In the scope of the analysis, the following topics are considered: the early operational activities, the initialization of payload operations, the calibration operations, the scientific mission support, the program star file, the telemetry processing, and the data validation. ESA

N90-13528# European Space Agency, Paris (France).
THE INTERFACE WITH THE DATA REDUCTION CONSORTIA **c14**
J. vanderHa *In its* The Hipparcos Mission. Prelaunch Status. Volume 1: The Hipparcos Satellite Jun. 1989 p 305-315 (For primary document see N90-13499 05-18)
Copyright Avail: NTIS HC A16/MF A02; ESA Publications Div., ESTEC, Noordwijk, Netherlands, 80 Dutch guilders

The scientific data flow and associated monitoring during Hipparcos normal operations is presented. It comprises preparatory, monitoring, and processing tasks. The activities related to the execution of payload functions, including the input catalog, the nominal scanning law, and the program star file, are described. The monitoring of the data reduction and the telemetry data processing are examined. ESA

N90-13529# European Space Agency, Paris (France).
THE HIPPARCOS MISSION. PRELAUNCH STATUS. VOLUME 2: THE INPUT CATALOG
M. A. C. Perryman, C. Turon, F. Arenou, A. N. Argue, A. Bec-Borsenberger, M. Chareton, M. Creze, F. Crifo, J. Dommanget, and D. Egret et al Jun. 1989 298 p Original contains color illustrations
(ESA-SP-1111-Vol-2; ISBN-92-9092-016-5; ISSN-0379-6566; ETN-90-95528) Copyright Avail: NTIS HC A13/MF A02; ESA Publications Div., ESTEC, Noordwijk, Netherlands, 80 Dutch guilders

The work performed for the Hipparcos input catalog (INCA) construction is described. An astrometric data base providing data on distances and motions is presented. The two hundred proposals for inclusion of objects are examined. The simulation of ground based programs is detailed. In particular, the following tasks are considered: the proximity effects on adjacent and multiple stars, the successive interactions of the input catalog, the compilation of astrometric data, the standard stars photometric calibration, the double and the variable stars, the choice of stars in open clusters and in the Magellanic clouds, the link to extragalactic objects, the minor planets, and other solar systems objects. For individual titles, see N90-13530 through N90-13547.

N90-13530# European Space Agency, Paris (France).
FROM SCIENTIFIC PROPOSALS TO THE INCA DATA BASE **c81**
C. Turon, A. Gomez, F. Crifo, and M. Grenon *In its* The Hipparcos Mission. Prelaunch Status. Volume 2: The Input Catalog Jun. 1989 p 7-22 Original contains color illustrations (For primary document see N90-13529 05-18)
Copyright Avail: NTIS HC A13/MF A02; ESA Publications Div., ESTEC, Noordwijk, Netherlands, 80 Dutch guilders

The Hipparcos mission input catalog (INCA), to establish a stellar data base, is presented. Duplicated entries and entries containing inadequate astrometric on photometric information are identified. The implementation of Hipparcos observing mode for double and variable stars is effectuated. The procedure for processing the 500,000 proposed stars is explained. The different categories of double and multiple systems in the INCA data base is shown. Concerning variable stars, the observing time is established on the basis of the magnitude retained in the final input catalog. ESA

N90-13531# European Space Agency, Paris (France).
THE INCA DATA BASE **c82**
A. Gomez, D. Morin, and F. Arenou *In its* The Hipparcos Mission. Prelaunch Status. Volume 2: The Input Catalog Jun. 1989 p 23-45 Original contains color illustrations (For primary document see N90-13529 05-18)
Copyright Avail: NTIS HC A13/MF A02; ESA Publications Div., ESTEC, Noordwijk, Netherlands, 80 Dutch guilders

The construction and the contents of the input catalog (INCA) data base are presented. It contains the compiled data on all stars processed by the INCA Consortium, which are about 215,000. The specific software developed for handling the data base, is outlined. Examples of the data base interrogation for a single and nonvariable star, for the components of a double star, and for a variable star, are given. Due to the structure of the Inca data base continuous updating of data during and after the Hipparcos mission is possible. ESA

N90-13532# European Space Agency, Paris (France).
MISSION SIMULATIONS **c12**
M. Creze, B. Nicolet, and M. Chareton *In its* The Hipparcos Mission. Prelaunch Status. Volume 2: The Input Catalog Jun. 1989 p 47-64 Original contains color illustrations (For primary document see N90-13529 05-18)
Copyright Avail: NTiS HC A13/MF A02; ESA Publications Div., ESTEC, Noordwijk, Netherlands, 80 Dutch guilders

The simulation software for the automatic selection of stars of the Hipparcos mission is presented. The software tools allowing the derivation of the expected accuracy, and the types of detailed and statistical information generated by the various simulation runs, are shown. The INCA Consortium tasks, concerning the selection of a subset of the 200,000 proposed objects to be retained, is included. A collection of simulation programs reflecting observational considerations and scientific requirements are included. ESA

N90-13533# European Space Agency, Paris (France).
PROXIMITY EFFECTS ON ADJACENT AND MULTIPLE STARS **c89**
C. Turon, J. Kovalevsky, and L. Lindegren *In its* The Hipparcos Mission. Prelaunch Status. Volume 2: The Input Catalog Jun. 1989 p 65-71 Original contains color illustrations (For primary document see N90-13529 05-18)
Copyright Avail: NTIS HC A13/MF A02; ESA Publications Div., ESTEC, Noordwijk, Netherlands, 80 Dutch guilders

The response profile of the main Hipparcos detector, related to the observed star signal perturbation, is discussed. The perturbing signal is due to the proximity effect from brighter stars, in the instantaneous field of view. The different treatments of these objects, according to the magnitude difference and separations of the considered stars or components, is summarized. The numerical studies carried out to derive the optimum methods for the observations of components of double, multiple systems, and of stars in the vicinity of other stars, are outlined. ESA

N90-13534# European Space Agency, Paris (France).
SUCCESSIVE ITERATIONS OF THE INPUT CATALOG **c89**
C. Turon *In its* The Hipparcos Mission. Prelaunch Status. Volume 2: The Input Catalog Jun. 1989 p 73-87 Original contains color illustrations (For primary document see N90-13529 05-18)
Copyright Avail: NTIS HC A13/MF A02; ESA Publications Div., ESTEC, Noordwijk, Netherlands, 80 Dutch guilders

The successive simulations carried out to validate the distribution of the selected program stars for the Hipparcos mission are examined. The satellite observing constraints and the goals of the scientific program are included. The test of the efficiency of the procedure, the identification of the quality and the limitations of each step, the calibration of the selection criteria, and the warning criteria, are considered. The results of the simulation runs and the sky distribution of the final catalog, are presented. ESA

N90-13535# European Space Agency, Paris (France).
STELLAR CONTENT OF THE INPUT CATALOG **c89**
A. Gomez, F. Crifo, and C. Turon *In its* The Hipparcos Mission. Prelaunch Status. Volume 2: The Input Catalog Jun. 1989 p 89-106 Original contains color illustrations (For primary document see N90-13529 05-18)
Copyright Avail: NTIS HC A13/MF A02; ESA Publications Div., ESTEC, Noordwijk, Netherlands, 80 Dutch guilders

The astrometric and astrophysical contents of the Hipparcos mission input catalog are summarized. The extent to which the different inclusion proposals are satisfied, is also considered. Tables are given which show the percentage of stars from major astrometric catalogs which have passed the simulations, and the statistics according to spectral type, the magnitude, and heliocentric distance, are given. The completeness of the magnitude limited survey is analyzed. The final retained survey is presented. It contains 53,000 stars, 95 percent of them are closer than 500 parsecs. ESA

N90-13536# European Space Agency, Paris (France).
GROUND-BASED ASTROMETRIC MEASUREMENTS **c89**
Y. Requieme *In its* The Hipparcos Mission. Prelaunch Status. Volume 2: The Input Catalog Jun. 1989 p 107-114 (For primary document see N90-13529 05-18)
Copyright Avail: NTIS HC A13/MF A02; ESA Publications Div., ESTEC, Noordwijk, Netherlands, 80 Dutch guilders

The ground based astrometric observations in the scope of the Hipparcos mission are reported. They are applied to improve the knowledge of both position and proper motion of the stars. The stars submitted to the catalog from scientific proposals are overviewed. The choice of efficient methods of obtaining accurate star positions are discussed. The observing and measuring tasks, as well as the difficulties encountered in identifying and retrieving the positions of each of the proposed stars are emphasized. ESA

N90-13537# European Space Agency, Paris (France).
THE COMPILATION OF ASTROMETRIC DATA **c89**
H. Jahreiss *In its* The Hipparcos Mission. Prelaunch Status. Volume 2: The Input Catalog Jun. 1989 p 115-127 (For primary document see N90-13529 05-18)
Copyright Avail: NTIS HC A13/MF A02; ESA Publications Div., ESTEC, Noordwijk, Netherlands, 80 Dutch guilders

The creation of the best available astrometric data compilation for the Hipparcos mission is presented. It combines the ground based measurements with the already available proper motions and summarizes the accuracy of the included catalogs. The final position accuracy of the Hipparcos input catalog is shown to be better than 0.5 arcsec in the Northern Hemisphere and 0.7 arcsec in the Southern Hemisphere. Details and results of the systematic data corrections are given. ESA

N90-13538# European Space Agency, Paris (France).
NEW GROUND-BASED PHOTOMETRIC MEASUREMENTS **c35**
M. Grenon *In its* The Hipparcos Mission. Prelaunch Status. Volume 2: The Input Catalog Jun. 1989 p 129-140 (For primary document see N90-13529 05-18)
Copyright Avail: NTIS HC A13/MF A02; ESA Publications Div., ESTEC, Noordwijk, Netherlands, 80 Dutch guilders

The work undertaken on the ground based photometric measurements for the Hipparcos program is presented. The purposes of the work are, an input to the definition of the observing program, optimization of the observations by allocating observing time according to the stars' magnitudes, and the photometric reductions and calibrations of the satellite data. In the scope of the study the following topics are included: the prediction of the H(sub p) magnitude, the evaluation of the necessity of new photometric data, the choice of photometric systems, the organization, and the program management. ESA

N90-13539# European Space Agency, Paris (France).
STANDARD STARS AND PHOTOMETRIC CALIBRATION **c35**
M. Grenon *In its* The Hipparcos Mission. Prelaunch Status. Volume 2: The Input Catalog Jun. 1989 p 141-147 (For

primary document see N90-13529 05-18)
Copyright Avail: NTIS HC A13/MF A02; ESA Publications Div., ESTEC, Noordwijk, Netherlands, 80 Dutch guilders

The set of photometric standard stars, and the requirements to achieve a self consistent photometric system for the Hipparcos mission, are presented. The reduction of the photometric data contained in the main grid and star mapper data streams is effectuated. The magnitude uncertainties concerning the noise of the collected photons, the pointing errors, the errors on the detection efficiency mapping and the drift of the transmission of the optics are analyzed. It is concluded that the applied procedure removes the erratic errors, and preserves the original definition of the magnitude scales. ESA

N90-13540# European Space Agency, Paris (France).
DOUBLE STARS **c89**
J. Dommanget *In its* The Hipparcos Mission. Prelaunch Status. Volume 2: The Input Catalog Jun. 1989 p 149-162 (For primary document see N90-13529 05-18)
Copyright Avail: NTIS HC A13/MF A02; ESA Publications Div., ESTEC, Noordwijk, Netherlands, 80 Dutch guilders

The work devoted to the identification of double and multiple stars for the Hipparcos input catalog is presented. Ground based observations, and photometric and astrometric aspects are included. The aim of the work is to improve the main stream of the data reduction. The tasks performed by the input catalog (INCA) double star working groups are reported. The contents of the catalog of the components of double and multiple stars is given. The search for the over abundant and missing entries in the INCA data base is included. ESA

N90-13541# European Space Agency, Paris (France).
VARIABLE STARS **c89**
M. O. Mennessier and F. Figueras *In its* The Hipparcos Mission. Prelaunch Status. Volume 2: The Input Catalog Jun. 1989 p 163-176 (For primary document see N90-13529 05-18)
Copyright Avail: NTIS HC A13/MF A02; ESA Publications Div., ESTEC, Noordwijk, Netherlands, 80 Dutch guilders

The work performed on the identification of the variable stars for the photometric calibration of the Hipparcos satellite data is reported. Investigations to assess the accuracy on measurements of variable stars, which can be expected at the end of the 2.5 year mission, are undertaken. The observation and classification of the variable stars, as well as the magnitudes used in the simulations, are included. The prediction of the light curve of a variable star and the construction of final ephemerides are discussed. ESA

N90-13542# European Space Agency, Paris (France).
THE CHOICE OF STARS IN OPEN CLUSTERS **c89**
J. C. Mermilliod and C. Turon *In its* The Hipparcos Mission. Prelaunch Status. Volume 2: The Input Catalog Jun. 1989 p 177-190 Original contains color illustrations (For primary document see N90-13529 05-18)
Copyright Avail: NTIS HC A13/MF A02; ESA Publications Div., ESTEC, Noordwijk, Netherlands, 80 Dutch guilders

The tasks performed and the results obtained by the input catalog (INCA) working group on the selection of stars in open clusters are reported. The characteristics and evolution of the stars in open clusters are summarized. The problem relating to the accurate identification of stars to their clusters is considered. On the basis of the ten selected proposals of the astronomical community and the principle of the Hipparcos measurements, the star selection rules are established. The statistics on the number of stars selected per cluster, and the magnitude histogram of the proposed and selected stars, are given. ESA

N90-13543# European Space Agency, Paris (France).
THE CHOICE OF STARS IN THE MAGELLANIC CLOUDS **c89**
L. Prevot *In its* The Hipparcos Mission. Prelaunch Status. Volume 2: The Input Catalog Jun. 1989 p 191-198 (For primary document see N90-13529 05-18)
Copyright Avail: NTIS HC A13/MF A02; ESA Publications Div., ESTEC, Noordwijk, Netherlands, 80 Dutch guilders

The work performed on the selection of stars in the Magellanic clouds, for the Hipparcos data base, is reported. The scientific interest of the Hipparcos measurements of the cloud star parameters is considered. On account of the scientific requirements identified by the proposers, and the technical constraints imposed by the satellite operations, the star selection is performed. For both Magellanic clouds, the statistics of the star selection and the distribution of stars, according to their V magnitudes and their spectral types, are given. ESA

N90-13544# European Space Agency, Paris (France).
THE LINK TO EXTRAGALACTIC OBJECTS **c90**
A. N. Argue *In its* The Hipparcos Mission. Prelaunch Status. Volume 2: The Input Catalog Jun. 1989 p 199-211 Original contains color illustrations (For primary document see N90-13529 05-18)
Copyright Avail: NTIS HC A13/MF A02; ESA Publications Div., ESTEC, Noordwijk, Netherlands, 80 Dutch guilders

The work performed to ensure the Hipparcos catalog optimal link, to both the radio reference frame and a quasi inertial frame, is reported. The review of the observational proposals and the identification of shortcomings are effectuated. Two kinds of links are considered: the coordinates at a state epoch, and the proper motions. The proper motions are measured relative to extragalactic objects. The methods applied by the input catalog (INCA) working group include the direct observations by Hipparcos, the use of a Hubble space telescope, and the direct photography established by a ground based link. ESA

N90-13545# European Space Agency, Paris (France).
MINOR PLANETS AND OTHER SOLAR SYSTEM OBJECTS **c89**
A. Bec-Borsenberger *In its* The Hipparcos Mission. Prelaunch Status. Volume 2: The Input Catalog Jun. 1989 p 213-223 (For primary document see N90-13529 05-18)
Copyright Avail: NTIS HC A13/MF A02; ESA Publications Div., ESTEC, Noordwijk, Netherlands, 80 Dutch guilders

The work performed to include observable planets and planet satellites in the Hipparcos input catalog is presented. The preparatory astrometric and photometric work needed to prepare the observations, and the considerations applied to their selection, are discussed. The magnitude of the minor planets proposed for observation by Hipparcos is analyzed, and those retained for observation are given. The position of minor planets in the input catalog is given by using their ephemerides, and examples of plots for Hebe and Flora planets, are given. Moreover, it is shown that Europa and Titan satellites can be adequately modulated by the Hipparcos main grid. ESA

N90-13546# European Space Agency, Paris (France).
THE CATALOGS PRODUCED BY THE INCA CONSORTIUM **c89**
C. Turon *In its* The Hipparcos Mission. Prelaunch Status. Volume 2: The Input Catalog Jun. 1989 p 225-232 (For primary document see N90-13529 05-18)
Copyright Avail: NTIS HC A13/MF A02; ESA Publications Div., ESTEC, Noordwijk, Netherlands, 80 Dutch guilders

The work performed by the Input Catalog (INCA) Consortium to provide the definitive star list and associated data necessary for the Hipparcos satellite operations and data reductions, is summarized. The catalog unification, and the error identification and correction is discussed. The systematic improvement in ground based astrometric, photometric and double star data for Hipparcos candidate stars, is underlined. The four annex catalog and their contents are listed. The solar system objects included in the catalog are reviewed. ESA

N90-13547# European Space Agency, Paris (France).
THE SIMBAD DATA BASE **c82**
D. Egret and M. Wenger *In its* The Hipparcos Mission. Prelaunch Status. Volume 2: The Input Catalog Jun. 1989 p 233-236

(For primary document see N90-13529 05-18)
Copyright Avail: NTIS HC A13/MF A02; ESA Publications Div., ESTEC, Noordwijk, Netherlands, 80 Dutch guilders

The Set of Identifications, Measurements, and Bibliography for Astronomical Data (SIMBAD) data base, applied by the input catalog (INCA) Consortium for the creation of the INCA data base, is described. The SIMBAD present status, which includes galaxies and other astronomical objects outside the solar system, is given. The SIMBAD data base information availability, and the data, the measurements and bibliographic retrieval are underlined. The applied methods and cooperation with persons or institutes for the data base updating, are reviewed. ESA

N90-13548# European Space Agency, Paris (France).
THE HIPPARCOS MISSION. PRELAUNCH STATUS. VOLUME 3: THE DATA REDUCTIONS
M. A. C. Perryman, L. Lindegren, C. A. Murray, E. Hog, J. Kovalevsky, M. Amoretti, G. K. Andreasen, M. Badiali, P. Belforte, and P. L. Bernacca et al Jun. 1989 513 p Original contains color illustrations
(ESA-SP-1111-Vol-3; ISBN-92-9092-016-5; ISSN-0379-6566; ETN-90-95529) Copyright Avail: NTIS HC A22/MF A03; ESA Publications Div., ESTEC, Noordwijk, Netherlands, 80 Dutch guilders

The methods adopted for the reduction of the Hipparcos data are described. The astrometric and photometric measurements constituting the Tycho program, and the measurements of double and multiple stars are discussed. The variations in the geometric and photometric parameters of the instrument are considered. The methods and the reduction scheme adopted by the Fundamental Astronomy by Space Techniques (FAST) and the Northern Data Analysis Consortium (NDAC) teams are shown and compared. The data simulation and error analysis are performed. The modeling of the attitude evolution, to provide precise estimates of the satellite attitude, is reported. The estimates of the achievable precision are given. For individual titles, see N90-13549 through N90-13576.

N90-13549# European Space Agency, Paris (France).
OVERVIEW OF THE DATA ACQUISITION AND REDUCTIONS **c82**
L. Lindegren and J. Kovalevsky *In its* The Hipparcos Mission. Prelaunch Status. Volume 3: The Data Reductions Jun. 1989 p 1-32 Original contains color illustrations (For primary document see N90-13548 05-18)
Copyright Avail: NTIS HC A22/MF A03; ESA Publications Div., ESTEC, Noordwijk, Netherlands, 80 Dutch guilders

The measurement principles of the Hipparcos satellite are reviewed with particular reference to the data reductions. The main stages of the reduction procedure are summarized. The reference frames adopted by the two data reduction consortia, and the relationship between them are outlined. In the scope of the report, the following topics are considered: the optical instrument, the sky scanning, the image dissector tube detector, the star observations, the data compression, the attitude determination, the star mapper detectors, the scientific data stream, the celestial and instrumental reference frames. An example of the star observing strategy and the comparison with the construction of other astrometric catalogs are included. ESA

N90-13550# European Space Agency, Paris (France).
ANALYSIS OF THE IMAGE DISSECTOR TUBE DATA **c82**
C. A. Murray, F. vanLeeuwen, L. Lindegren, F. Donati, and B. Fassino *In its* The Hipparcos Mission. Prelaunch Status. Volume 3: The Data Reductions Jun. 1989 p 33-49 Original contains color illustrations (For primary document see N90-13548 05-18)
Copyright Avail: NTIS HC A22/MF A03; ESA Publications Div., ESTEC, Noordwijk, Netherlands, 80 Dutch guilders

The image dissector tube data of the Hipparcos satellite, and the procedures for data handling, are described. The purpose of the image dissector tube data analysis is to determine the instantaneous and simultaneous locations of several program star images relative to the slits on the main grid. The estimation procedure (based on the maximum likelihood principles) and its implementation, the calculation of reference phases, and the program testing are examined. The three parameter model and statistical tests are applied. The results of the tests and the computing time are given. ESA

N90-13551# European Space Agency, Paris (France).
ANALYSIS OF THE STAR MAPPER DATA **c82**
E. Canuto, F. Donati, P. Belforte, P. L. Bernacca, and F. vanLeeuwen *In its* The Hipparcos Mission. Prelaunch Status. Volume 3: The Data Reductions Jun. 1989 p 51-72 (For primary document see N90-13548 05-18)
Copyright Avail: NTIS HC A22/MF A03; ESA Publications Div., ESTEC, Noordwijk, Netherlands, 80 Dutch guilders

The star mapper, located to one side of the main Hipparcos grid, is discussed. It provides real time information about the satellite's three axis attitude with a precision of about 1 arcsec. The data handling of information from bright stars transiting across the star mapper grid is discussed. Details of the star mapper reduction is given. Problems related to the photon noise, instrumental defects, measurement noise, and the superposition of two areas of the sky on the same star mapper grid, are considered. The photometric estimates, the simulation experiments, the accurate determination of transit times, the statistical tests and the applications are included. ESA

N90-13552# European Space Agency, Paris (France).
ON-GROUND ATTITUDE DETERMINATION **c13**
F. Donati, E. Canuto, P. Belforte, D. Carlucci, and F. vanLeeuwen *In its* The Hipparcos Mission. Prelaunch Status. Volume 3: The Data Reductions Jun. 1989 p 73-91 Original contains color illustrations (For primary document see N90-13548 05-18)
Copyright Avail: NTIS HC A22/MF A03; ESA Publications Div., ESTEC, Noordwijk, Netherlands, 80 Dutch guilders

The on-ground attitude determination of the Hipparcos satellite, is examined. It is based on the information from the star mapper transits, and the satellite's gyroscopes. According to the physical perturbations, such as solar radiation pressure, acting on the satellite, models of the satellite attitude are developed. Concerning the attitude estimation, the body rigidity, the disturbance and control torques, the gyro and star mapper measurements are discussed. The adopted procedures for star coordinates and attitude improvements are given. ESA

N90-13553# European Space Agency, Paris (France).
THE GREAT CIRCLE REDUCTIONS **c13**
H. vanderMarel, D. vanDaalen, and C. Petersen *In its* The Hipparcos Mission. Prelaunch Status. Volume 3: The Data Reductions Jun. 1989 p 93-115 (For primary document see N90-13548 05-18)
Copyright Avail: NTIS HC A22/MF A03; ESA Publications Div., ESTEC, Noordwijk, Netherlands, 80 Dutch guilders

The great circle reduction step of the Hipparcos data processing, is presented. The great circle reductions yield improved information on the along scan satellite attitude, and information on the geometrical transformation between the coordinates on the sky and coordinates on the primary modulating grid. In order to solve the resulting observation equations, a method based on Cholesky factorization of the large, sparse matrices and on techniques developed for geodetic applications, is used. Moreover, the reordering of the star parameters and the rank deficiencies are included. ESA

N90-13554# European Space Agency, Paris (France).
GREAT CIRCLE INTERACTIONS: ATTITUDE SMOOTHING AND GRID-STEP INCONSISTENCIES **c13**
H. vanderMarel, D. vanDaalen, and C. Petersen *In its* The Hipparcos Mission. Prelaunch Status. Volume 3: The Data Reductions Jun. 1989 p 117-140 (For primary document see N90-13548 05-18)
Copyright Avail: NTIS HC A22/MF A03; ESA Publications Div., ESTEC, Noordwijk, Netherlands, 80 Dutch guilders

The algorithms used in the Hipparcos satellite data reduction

are presented. The differences in the adopted data treatments are shown. The validation of the great circle reduction numerical is effectuated. The outcomes of the statistical tests, which include the correction of slit numbers, skipping of doubtful observations or skipping stars from the normal equation solution stars, are considered. In particular, the following topics are discussed: the setting up of the equations for smoothing, the smoothing with B-splines, the gridstep errors and inconsistensies and their corrections, and the passive stars treatment and reweighting. ESA

N90-13555# European Space Agency, Paris (France).
GENERAL AND NUMERICAL APPROACH TO THE SPHERE SOLUTION IN FAST **c13**
I. Galligani, M. Lattanzi, B. Bucciarelli, T. Tommasini, and P. L. Bernacca *In its* The Hipparcos Mission. Prelaunch Status. Volume 3: The Data Reductions Jun. 1989 p 141-162 (For primary document see N90-13548 05-18)
Copyright Avail: NTIS HC A22/MF A03; ESA Publications Div., ESTEC, Noordwijk, Netherlands, 80 Dutch guilders

The general approach to the sphere solution problem, as adopted by the FAST (fundamental astronomy by space techniques) consortium, for the Hipparcos satellite data reduction, is presented. It consists in the combination of the reference great circle data sets accumulated throughout the mission, and the solution for the great circle zero points, and is carried out on a subset of 40 to 60,000 of the program stars. In the scope of the analysis the following tasks are discussed: the nonlinear least squares problem; the system resolution; the computational complexity, the feasibility and the choice of the method; the variance-covariance matrix; and the numerical features of the system. Simulations show that, based on only half a year of data, program star positions with an accuracy of about 10 milli arcsec is achieved. Moreover, the full astrometric accuracy results from a treatment of the full 2.5 years of mission data. ESA

N90-13556# European Space Agency, Paris (France).
ASTROMETRIC PARAMETER DETERMINATION IN FAST **c89**
H. G. Walter *In its* The Hipparcos Mission. Prelaunch Status. Volume 3: The Data Reductions Jun. 1989 p 163-169 (For primary document see N90-13548 05-18)
Copyright Avail: NTIS HC A22/MF A03; ESA Publications Div., ESTEC, Noordwijk, Netherlands, 80 Dutch guilders

The astrometric parameter determination, as adopted by the FAST (fundamental astronomy by space techniques) consortium, for the Hipparcos satellite data reduction, is presented. The objective is the improvement of the approximate positions, proper motion and parallaxes of the program stars provided in the input catalog. The results for single stars on reference great circles accumulated throughout the mission, are discussed. The attempt to derive information on the individual components from the double and multiple star systems, is made. The grid step errors are identified. ESA

N90-13557# European Space Agency, Paris (France).
THE SPHERE SOLUTION AND ASTROMETRIC PARAMETER DETERMINATION IN NDAC **c13**
L. Lindegren *In its* The Hipparcos Mission. Prelaunch Status. Volume 3: The Data Reductions Jun. 1989 p 171-181 (For primary document see N90-13548 05-18)
Copyright Avail: NTIS HC A22/MF A03; ESA Publications Div., ESTEC, Noordwijk, Netherlands, 80 Dutch guilders

The approach for the sphere solution and the astrometric parameter determination of the Hipparcos satellite data reduction adopted by NDAC (Northern Data Analysis Consortium), is presented. Data for the remaining stars, of which many are double, multiple or disturbed by veiling glare, are also studied. An updated version of the input catalog is applied for stellar data derivation. Concerning the observation model, the theoretical abcissa and the global unknowns are examined. Observation and normal equations are studied. The main output stellar data and the organization of the programs are included. ESA

N90-13558# European Space Agency, Paris (France).
OVERVIEW OF THE TYCHO DATA ANALYSIS **c82**
E. Hog *In its* The Hipparcos Mission. Prelaunch Status. Volume 3: The Data Reductions Jun. 1989 p 183-194 (For primary document see N90-13548 05-18)
Copyright Avail: NTIS HC A22/MF A03; ESA Publications Div., ESTEC, Noordwijk, Netherlands, 80 Dutch guilders

The Tycho data reduction applied in the Hipparcos data processing is discussed. By treatment of continuous data records from satellite mappers, astrometric and two colored photometric data of about 400,000 stars to a magnitude limit of about B = 11 magnitude, is derived. The Tycho data analysis architecture and the recognition processes, are given. Concerning the details of the strategy, the terminology, the steps in the data processing, the attitude and geometric calibration, the prediction of star transits, the stellar photon flux, and the stellar position measurements are discussed. ESA

N90-13559# European Space Agency, Paris (France).
TYCHO ASTROMETRY **c89**
E. Hog, P. C. Hansen, and L. Lindegren *In its* The Hipparcos Mission. Prelaunch Status. Volume 3: The Data Reductions Jun. 1989 p 195-204 (For primary document see N90-13548 05-18)
Copyright Avail: NTIS HC A22/MF A03; ESA Publications Div., ESTEC, Noordwijk, Netherlands, 80 Dutch guilders

The Tycho astrometric data processing for Hipparcos satellite data reduction in described. It deals with the transit times to the astrometric parameters of the Tycho stars. The observed transit time and the predicted values are compared. A mathematical formulation of the astrometry task is outlined. The positions for some 500,000 stars with an accuracy of about 0.03 arcsec root mean square for the majority of faint stars at about B = 11 magnitude are obtained. Double stars with separations larger than about 2 arcsec are resolved. ESA

N90-13560# European Space Agency, Paris (France).
PHOTOMETRY: MAIN MISSION AND TYCHO **c35**
F. Mignard, M. Froeschle, J. L. Falin, G. K. Andreasen, E. Hog, M. Grewing, and D. Scales *In its* The Hipparcos Mission. Prelaunch Status. Volume 3: The Data Reductions Jun. 1989 p 205-223 (For primary document see N90-13548 05-18)
Copyright Avail: NTIS HC A22/MF A03; ESA Publications Div., ESTEC, Noordwijk, Netherlands, 80 Dutch guilders

The photometric reductions and calibrations of the Hipparcos satellite, for both the main mission and the star mapper data, are described. The principles of the Hipparcos and Tycho photometric systems are presented along with their relation to those in ground based photometry. The efficiency of the detection chain as a function of the wavelength of the light is considered. The problems arising with the star mapper chain are included. The following subjects are also included: the scientific aspects of the photometry, the image dissector tube and Tycho data processing algorithms. The simulation results for the main detection chain are given. ESA

N90-13561# European Space Agency, Paris (France).
DOUBLE STAR REDUCTIONS IN NDAC **c89**
S. Soderhjelm *In its* The Hipparcos Mission. Prelaunch Status. Volume 3: The Data Reductions Jun. 1989 p 225-241 (For primary document see N90-13548 05-18)
Copyright Avail: NTIS HC A22/MF A03; ESA Publications Div., ESTEC, Noordwijk, Netherlands, 80 Dutch guilders

The approach adopted by the Northern Data Analysis Consortium (NDAC) for the double star data treatment, to be applied in Hipparcos data reduction, is presented. Accurate orbit sizes and parallaxes for nearby binaries are obtained. The phase shift between the first and second harmonics of the primary grid modulated signal is applied to the recognition and parameter determination for non single objects. The goals of the strategy of the reductions are underlined. The method of solution and the standard reduction programs are described. ESA

N90-13562# European Space Agency, Paris (France).
DOUBLE STAR REDUCTIONS IN FAST **c89**
F. Mignard, L. Borriello, J. Kovalevsky, N. Prezioso, and P. L. Bernacca *In its* The Hipparcos Mission. Prelaunch Status. Volume 3: The Data Reductions Jun. 1989 p 243-267 (For primary document see N90-13548 05-18)
Copyright Avail: NTIS HC A22/MF A03; ESA Publications Div., ESTEC, Noordwijk, Netherlands, 80 Dutch guilders

The approach adopted by the Fundamental Astronomy by Space Techniques (FAST) consortium for double star data reduction is described. It is to be applied in Hipparcos satellite data processing. The organization of the work by FAST is given. The double star recognition and the data processing is discussed. For a multiple star system, an imaging approach is developed. The steps required to find the parameters describing the double system, after data compression, are outlined. ESA

N90-13563# European Space Agency, Paris (France).
THE TREATMENT OF MINOR PLANETS AND PLANETARY SATELLITES **c89**
B. Morando and L. Lindegren *In its* The Hipparcos Mission. Prelaunch Status. Volume 3: The Data Reductions Jun. 1989 p 269-281 (For primary document see N90-13548 05-18)
Copyright Avail: NTIS HC A22/MF A03; ESA Publications Div., ESTEC, Noordwijk, Netherlands, 80 Dutch guilders

The reduction considerations needed for the minor planets, taking into account their proximity, high apparent motion, and their surface properties, are summarized. Of the 60 bright minor planets, 40 show the most favorable conditions to be observed by Hipparcos satellite. The reasons for, the conditions of, and what can be expected from, the minor planets observations, are presented. The image of a minor planet in the focal plane of Hipparcos, and the modulation curves for a star and for a minor planet are included. The importance of light curves obtained from earth measurement to improve the ephemerides of minor planets is underlined. Concerning natural satellites, only Europa and Titan are adequately modulated by Hipparcos. ESA

N90-13564# European Space Agency, Paris (France).
VALIDATION OF THE HIPPARCOS CATALOG **c82**
L. Lindegren, J. Kovalevsky, H. vanderMarel, M. A. C. Perryman, and S. Roeser *In its* The Hipparcos Mission. Prelaunch Status. Volume 3: The Data Reductions Jun. 1989 p 283-295 (For primary document see N90-13548 05-18)
Copyright Avail: NTIS HC A22/MF A03; ESA Publications Div., ESTEC, Noordwijk, Netherlands, 80 Dutch guilders

The principal differences in the data treatment by the Fundamental Astronomy by Space Techniques (FAST) consortium and the Northern Data Analysis Consortium (NDAC) teams, are presented. The current plans for comparing certain intermediate quantities throughout and at the end of the Hipparcos mission are given. The aim of such a parallel data processing is to obtain a single agreed astrometric catalog to be released to the scientific community. The comparisons include: the approaches and procedures, the image dissector tube data, the star mapper data, the attitude data, the great circle results, and the sphere solution. ESA

N90-13565# European Space Agency, Paris (France).
LINKING HIPPARCOS TO A QUASI-INERTIAL SYSTEM **c13**
J. Kovalevsky, J. F. Lestrade, and R. A. Preston *In its* The Hipparcos Mission. Prelaunch Status. Volume 3: The Data Reductions Jun. 1989 p 297-309 (For primary document see N90-13548 05-18)
Copyright Avail: NTIS HC A22/MF A03; ESA Publications Div., ESTEC, Noordwijk, Netherlands, 80 Dutch guilders

The external observations and the associated reduction procedures applied to transform the final Hipparcos catalog in a self consistent reference frame are presented. The Earth's equatorial plane position in the year 2000 is extrapolated from present and past positions and applying Hipparcos reduction algorithms. Optical and radio methods are used in the linking techniques. The astrometry techniques and the synthesis of the results are included. ESA

N90-13566# European Space Agency, Paris (France).
ACCURACY AND CHARACTERISTICS OF THE HIPPARCOS CATALOG **c82**
L. Lindegren *In its* The Hipparcos Mission. Prelaunch Status. Volume 3: The Data Reductions Jun. 1989 p 311-323 (For primary document see N90-13548 05-18)
Copyright Avail: NTIS HC A22/MF A03; ESA Publications Div., ESTEC, Noordwijk, Netherlands, 80 Dutch guilders

The best available predictions of the final astrometric results, including estimates of the 5 x 5 variance-covariance matrix and the expected correlation between different stars, are presented. The estimates are shown to depend on the satellite detection efficiency, performance of the attitude control system and the instrumental stability. The estimated accuracy of the astrometric parameters, and the expected correlations between the astrometric data and the systematic errors are examined. ESA

N90-13567# European Space Agency, Paris (France).
DATA PROCESSING IN THE FAST CONSORTIUM **c82**
J. L. Pieplu, C. Huc, and A. Vargas *In its* The Hipparcos Mission. Prelaunch Status. Volume 3: The Data Reductions Jun. 1989 p 325-334 (For primary document see N90-13548 05-18)
Copyright Avail: NTIS HC A22/MF A03; ESA Publications Div., ESTEC, Noordwijk, Netherlands, 80 Dutch guilders

A description of the implementation of the data reduction algorithms within the Fundamental Astronomy by Space Techniques (FAST) consortium is provided. The logistics of the data flow and the administrative aspects of the data handling are included. The FAST and the main reduction structures, as well as the operation scheme are given. The purpose and the steps of the scientific data processing are explained. An example of the data management and command software is given. The operations and the size of the main reductions performed by the computing centers are included. ESA

N90-13568# European Space Agency, Paris (France).
DATA PROCESSING IN THE NDAC CONSORTIUM **c82**
F. vanLeeuwen, E. Hog, C. Petersen, and L. Lindegren *In its* The Hipparcos Mission. Prelaunch Status. Volume 3: The Data Reductions Jun. 1989 p 335-341 (For primary document see N90-13548 05-18)
Copyright Avail: NTIS HC A22/MF A03; ESA Publications Div., ESTEC, Noordwijk, Netherlands, 80 Dutch guilders

A description of the implementation of the data reduction algorithms in the Northern Data Analysis Consortium (NDAC) team is provided. The logistics of the data flow and the administrative aspects of the data handling are included. The main flow of data between the institutes and the different reduction processes are given. The computer systems, the size of the source code and estimated processing times are summarized. The steps concerning the reception and the processing of the tapes is examined. The tasks concerning data reduction (including great circle reduction), interaction steps, and preparation for the double star analysis, are described. ESA

N90-13569# European Space Agency, Paris (France).
GREAT CIRCLE REDUCTIONS: IMPLEMENTATION AND SIMULATIONS **c13**
H. vanderMarel and C. Petersen *In its* The Hipparcos Mission. Prelaunch Status. Volume 3: The Data Reductions Jun. 1989 p 343-363 (For primary document see N90-13548 05-18)
Copyright Avail: NTIS HC A22/MF A03; ESA Publications Div., ESTEC, Noordwijk, Netherlands, 80 Dutch guilders

The details of the implementation of the great circle reduction software in both the Fundamental Astronomy by Space Techniques (FAST) consortium and the Northern Data Analysis Consortium (NDAC) teams, for the Hipparcos data processing, are presented. The results of simulations carried out with the great circle reduction software, are included. These simulations indicate the results

expected for the precision of the star abscissae along the reference great circles, as a function of star magnitude, both with and without attitude smoothing. The parameters describing the transformation between geometrical sky and instrument coordinates as a function of star color, grid position and time, are also given. ESA

N90-13570# European Space Agency, Paris (France).
IMPLEMENTATION AND SIMULATIONS OF THE SPHERE SOLUTION IN FAST **c13**
F. P. Murgolo, M. G. Schirone, M. Lattanzi, and P. L. Bernacca *In its* The Hipparcos Mission. Prelaunch Status. Volume 3: The Data Reductions Jun. 1989 p 365-372 (For primary document see N90-13548 05-18)
Copyright Avail: NTIS HC A22/MF A03; ESA Publications Div., ESTEC, Noordwijk, Netherlands, 80 Dutch guilders

The details of the implementation of the sphere solution software in the Fundamental Astronomy by Space Techniques (FAST) consortium, are described. The simulation results for realistic data sets, both with and without grid-step errors are given. Expected errors on the astrometric parameters of the primary stars and the precision of the reference great circle zero points, are provided as a function of mission duration. The design matrix, the diagrams of the context processor and the processors experimental results are given. ESA

N90-13571# European Space Agency, Paris (France).
THE FIRST-LOOK DATA ANALYSIS AT UTRECHT **c82**
H. Schrijver *In its* The Hipparcos Mission. Prelaunch Status. Volume 3: The Data Reductions Jun. 1989 p 373-388 (For primary document see N90-13548 05-18)
Copyright Avail: NTIS HC A22/MF A03; ESA Publications Div., ESTEC, Noordwijk, Netherlands, 80 Dutch guilders

The calibration tasks to be performed during the reduction of the Hipparcos data are described. One reference great circle (about 12 hours) of data per week is analyzed. The data and the tape quality are inspected. Initial calibration parameters are derived as input to subsequent stages of the data reductions. The large scale geometric and photometric calibrations of the main grid field of view, and geometric and photometric calibrations of the star mapper are carried out. Short term variations of the basic angle and medium scale calibrations are included. The tools developed to assist the evaluation of the reduction of the star mapper data and for the image dissector tube processing are given. ESA

N90-13572# European Space Agency, Paris (France).
MODELING OF THE HIPPARCOS OPTICAL SYSTEM **c74**
D. Iorio-Fili, M. Badiali, M. Cetica, M. Amoretti, D. Bertani, D. Cardini, and A. Emanuele *In its* The Hipparcos Mission. Prelaunch Status. Volume 3: The Data Reductions Jun. 1989 p 389-407 (For primary document see N90-13548 05-18)
Copyright Avail: NTIS HC A22/MF A03; ESA Publications Div., ESTEC, Noordwijk, Netherlands, 80 Dutch guilders

A modeling of the Hipparcos satellite optical system, carried out by the Fundamental Astronomy by Space Techniques (FAST) consortium, is described. The Hipparcos signal structure and the meaning of chromaticity are recalled. The simulation of the performance of the Hipparcos is carried out, taking into account the optical system in its nominal and real configurations. The results of the simulations concerning the modeling of the nominal and real telescope optical elements are provided. The double star signals obtained by complete simulation of light propagation through telescopes are investigated. ESA

N90-13573# European Space Agency, Paris (France).
DATA SIMULATIONS IN THE FAST CONSORTIUM **c61**
M. Froeschle, J. L. Falin, J. Kovalevsky, F. Mignard, and J. Dupic *In its* The Hipparcos Mission. Prelaunch Status. Volume 3: The Data Reductions Jun. 1989 p 409-421 (For primary document see N90-13548 05-18)
Copyright Avail: NTIS HC A22/MF A03; ESA Publications Div., ESTEC, Noordwijk, Netherlands, 80 Dutch guilders

The data simulation carried out by the Fundamental Astronomy by Space Techniques (FAST) consortium is reported. It concerns the final stages of the software preparation and is generated in a format specified by ESA. The combined effects of all the physical parameters involved in the data production is taken into account. The simulation of the events occuring during the mission (time sequence of the transits of stars, of the Earth and Moon through the fields of view) and the observing time of allotment, are described. The statistical and instrumental effects as modeled for the generation of photon counts for the star mapper and for the main grid are discussed. ESA

N90-13574# European Space Agency, Paris (France).
DATA SIMULATIONS IN THE NDAC CONSORTIUM **c61**
F. vanLeeuwen *In its* The Hipparcos Mission. Prelaunch Status. Volume 3: The Data Reductions Jun. 1989 p 423-426 (For primary document see N90-13548 05-18)
Copyright Avail: NTIS HC A22/MF A03; ESA Publications Div., ESTEC, Noordwijk, Netherlands, 80 Dutch guilders

The data simulation carried out by the Northern Data Analysis Consortium (NDAC) is reported. It includes software for the data interface, the data display, the data reduction and the administration. The simulation of the data stream is obtained by means of a numerical integration of the external and internal forces working on the satellite. Extensive intervals of star mapper data and software validation are provided by an extension of the NDAC simulation facilities. ESA

N90-13575# European Space Agency, Paris (France).
THE TYCHO INPUT CATALOG **c82**
D. Egret, P. Didelon, and B. J. McLean *In its* The Hipparcos Mission. Prelaunch Status. Volume 3: The Data Reductions Jun. 1989 p 427-435 (For primary document see N90-13548 05-18)
Copyright Avail: NTIS HC A22/MF A03; ESA Publications Div., ESTEC, Noordwijk, Netherlands, 80 Dutch guilders

The production of a specific Tycho input catalog for data reduction is presented. It contains about 2,000,000 objects at a magnitude value of B = 12.5 magnitude. The expected external errors of the Tycho input catalog positions are in the range of 1 to 2 arcsec. The identification of the Hipparcos star mapper transits are allowed at the epochs when a Tycho star is predicted to be transiting either the vertical or chevron star mapper slits. The Tycho input catalog contents and format are described. The additional files and the features of the revised catalog are given. ESA

N90-13576# European Space Agency, Paris (France).
EXPERIMENTS TOWARDS A GLOBAL SPHERE SOLUTION **c61**
F. Sanso, B. Betti, and F. Migliaccio *In its* The Hipparcos Mission. Prelaunch Status. Volume 3: The Data Reductions Jun. 1989 p 437-455 (For primary document see N90-13548 05-18)
Copyright Avail: NTIS HC A22/MF A03; ESA Publications Div., ESTEC, Noordwijk, Netherlands, 80 Dutch guilders

An alternative and more rigorous approach to the sphere solution problem, for the Hipparcos mission, is described. The simulation results, involving 2,000 stars, using this method, are presented. The reasons for considering a global approach are given. The attitude and the instrumental polynomials are kept fixed, and a solution is made only for the astrometric parameters of each star. The result of the studies allow the following conclusions to be formulated: the problem of estimating the parameters and attitude parameters is reduced to the solution of a block diagonal normal system; the system can give rise to a convergence sequence; the procedure is not affected by the presence of a rank deficiency; the computing time seems to be acceptable; and the use of a parallel computer to reduce computing times by a factor of 10. ESA

N90-13577# Deutsche Forschungsanstalt fuer Luft- und Raumfahrt, Brunswick (Germany, F.R.). Abteilung Verbundstrukturen.
THERMAL PROTECTION SYSTEMS FOR REENTRY AND HYPERSONIC FLIGHT
Harald Twardy Apr. 1989 48 p In GERMAN; ENGLISH summary Report will also be announced as translation (ESA-TT-1179)
(DLR-Mitt-89-14; ISSN-0176-7739; ETN-90-95848) Avail: NTIS HC A03/MF A01; DLR, VB-PL-DO, Postfach 90 60 58, 5000 Cologne, Fed. Republic of Germany, 21 DM

Different concepts and specific problems of thermal protection systems needed for reentry and during hypersonic flight are described. In future hydrogen-propelled hypersonic aircraft, the cryogenic storage temperature of the hydrogen fuel must be maintained when the skin is heated. A regenerative method for cooling the covering skin using the high heat capacity of the liquid hydrogen is described. Other so-called hot structures and thermal protection systems are described. These are either made of insulating materials or a combination of insulation with reradiating surfaces. ESA

N90-13578 Southampton Univ. (England).
MODELLING OF SATELLITE CONTROL THRUSTER PLUMES Ph.D. Thesis
Iain Boyd 1988 218 p
Avail: Univ. Microfilms Order No. BRDX85534

Deleterious effects such as surface heating and turning moments can arise as a consequence of the impingement of thruster plumes with spacecraft surfaces. Such thrusters are normally fired for altitude control. The prediction of such effects must be undertaken at the design stage of the vehicle. The modeling of such plumes was studied. The following prediction techniques were implemented into computer programs: (1) Simons model; (2) Method of Characteristics; and (3) Direct Simulation Monte Carlo method. The first two methods are derived from continuum equations while the third adopts a discrete particle approach. The three modeling techniques were then applied to the isentropic core expansion of a small hydrazine thruster plume. It was found that significant errors occur in the determination of impingement quantities through application of the continuum methods in the flow regime lying between the continuum and free molecular limits. Dissert. Abstr.

N90-13579 Howard Univ., Washington, DC.
ATTITUDE AND SHAPE CONTROL OF OPTIMALLY DESIGNED LARGE SPACE STRUCTURES Ph.D. Thesis
Satyanarayana Kotaru 1989 187 p
Avail: Univ. Microfilms Order No. DA8921109

The equations of motion of flexible structures such as cantilever beams and free-free beams are taken as a basis to study the uncontrolled dynamics and to synthesize control laws using linear regulator theory. Such control laws must meet the design specification levels for shape and orientation control purposes. Point actuators that are used for control purposes are incorporated into the linear dynamic models of the beams. The focus is on the design of minimum weight structures for space applications satisfying mission requirements such as frequency and other constraints. The stepped configurations obtained by implementing the finite element method during the optimization process are considered as they represent a class of optimally designed structures. A comparison of the control system designs and requirement of control efforts is studied for the weight optimized stepped beams and the corresponding uniform beams. Examples of stepped configurations obtained by both rigorous optimization procedures and trial and error designs are examined. Control laws are also developed for both uniform and stepped structures with inherent structural damping which is additive to the control efforts in suppressing the vibrations of the cantilever beams. The use of optimality criteria methods for optimizing the combined cost function including the structural dynamicist's objective function and a form of the control designer's objective function taken from the linear regulator theory is studied with a numerical example applied to a long orbiting beam. Dissert. Abstr.

N90-13580*# National Aeronautics and Space Administration, Washington, DC.
SPACE STATION SYSTEMS: A BIBLIOGRAPHY WITH INDEXES (SUPPLEMENT 9)
Nov. 1989 325 p
(NASA-SP-7056(09); NAS 1.21:7056(09)) Avail: NTIS HC A13 CSCL 22B

This bibliography lists 1,313 reports, articles, and other documents introduced into the NASA scientific and technical information system between January 1, 1989 and June 30, 1989. Its purpose is to provide helpful information to researchers, designers and managers engaged in Space Station technology development and mission design. Coverage includes documents that define major systems and subsystems related to structures and dynamic control, electronics and power supplies, propulsion, and payload integration. In addition, orbital construction methods, servicing and support requirements, procedures and operations, and missions for the current and future Space Station are included. Author

N90-13581*# National Aeronautics and Space Administration. Lewis Research Center, Cleveland, OH.
THE SPACE STATION PHOTOVOLTAIC PANELS PLASMA INTERACTION TEST PROGRAM: TEST PLAN AND RESULTS
Henry K. Nahra, Marian C. Felder, Bernard L. Sater, and John V. Staskus [1989] 11 p Presented at the 28th Aerospace Sciences Meeting, Reno, NV, 8-11 Jan. 1990; sponsored by AIAA
(NASA-TM-102474; E-5261; NAS 1.15:102474; AIAA-90-0722)
Avail: NTIS HC A03/MF A01 CSCL 22B

The Plasma Interaction Test performed on two space station solar array panels is addressed. This includes a discussion of the test requirements, test plan, experimental set-up, and test results. It was found that parasitic current collection was insignificant (0.3 percent of the solar array delivered power). The measured arcing threshold ranged from -210 to -457 V with respect to the plasma potential. Furthermore, the dynamic response of the panels showed the panel time constant to range between 1 and 5 microsec, and the panel capacitance to be between .01 and .02 microF. Author

N90-13582# Centre National d'Etudes Spatiales, Toulouse (France).
CHOICE OF A DIFFERENTIAL METHOD FOR THE ATTITUDE RESTITUTION IN DYNAMIC UNBALANCE [CHOIX D'UNE METHODE DIFFERENTIELLE POUR LA RESTITUTION D'ATTITUDE AVEC BALOURD DYNAMIQUE]
E. Cazala-Hourcade 19 Oct. 1988 56 p In FRENCH
(CNES-CT/DTI/MS/CM/290; ETN-90-95281) Avail: NTIS HC A04/MF A01

The Van der Ha formalism used to calculate the sensitivity of the pseudo-measurements to the unbalance is applied to develop a differential pseudo-measurements correction method to take into account dynamic unbalance in spin restitution procedures. The method is limited to first order analysis. The total error depends on amplitude unbalance, sensor configurations, distribution of unbalance between axes and geometric configuration of sensor visibilities. ESA

N90-13583# Swedish Defence Research Establishment, Linkoeping. Dept. of Information Technology.
RE-ENTRY HAZARDS AND COSMOS 1900
Ulf Ekblad Jun. 1989 41 p
(FOA-C-30535-9.4; ISSN-0347-3708; ETN-90-95921) Avail: NTIS HC A03/MF A01; Swedish Defence Research Establishment, Box 1165, S-581 11 Linkoeping, Sweden, 50 Swedish crowns

A report is presented which attempts to clarify some of the questions about hazards in connection with satellites using nuclear reactors. It is prompted by the reaction of the press when it became clear in the spring of 1988 that the Soviet satellite Cosmos 1900 was to enter the atmosphere later in the year. The usefulness of

analyzing orbital elements is demonstrated. Basically only one of the six orbital elements necessary to completely describe the orbit of a satellite is used in the analysis of what happened to Cosmos 1900. Information about when the satellite malfunction occurred and when and what happened at the final phase of the re-entry are examples of what can be deduced from just one orbital element. The example of information drawn from the analysis of basically one orbital element shows that some space surveillance can be done by analysis of orbital elements, and even non-compliance with outer space treaties might be detectible. ESA

N90-13415*# Johns Hopkins Univ., Laurel, MD. Applied Physics Lab.
AUTONOMOUS SPACECRAFT ATTITUDE CONTROL USING MAGNETIC TORQUING ONLY
Keith L. Musser and Ward L. Ebert *In* NASA, Goddard Space Flight Center, Flight Mechanics/Estimation Theory Symposium, 1989 Oct. 1989 p 23-38 (For primary document see N90-13413 05-13)
Avail: NTIS HC A20/MF A03 CSCL 22B

N90-13416*# National Aeronautics and Space Administration. Lyndon B. Johnson Space Center, Houston, TX.
PERIODIC-DISTURBANCE ACCOMMODATING CONTROL OF THE SPACE STATION FOR ASYMPTOTIC MOMENTUM MANAGEMENT
Wayne Warren, Bong Wie (Texas Univ., Austin.), and David Geller *In* NASA, Goddard Space Flight Center, Flight Mechanics/Estimation Theory Symposium, 1989 Oct. 1989 p 39-50 Previously announced in IAA as A89-52570 (For primary document see N90-13413 05-13)
Avail: NTIS HC A20/MF A03 CSCL 22B

N90-13419*# Auburn Univ., AL. Dept. of Aerospace Engineering.
SIMULATION OF SPACECRAFT ATTITUDE DYNAMICS USING TREETOPS AND MODEL-SPECIFIC COMPUTER CODES
John E. Cochran, T. S. No, and Norman G. Fitz-Coy *In* NASA, Goddard Space Flight Center, Flight Mechanics/Estimation Theory Symposium, 1989 Oct. 1989 p 75-95 (For primary document see N90-13413 05-13)
Avail: NTIS HC A20/MF A03 CSCL 22B

19 SPACECRAFT INSTRUMENTATION

For related information see also *06 Aircraft Instrumentation* and *35 Instrumentation and Photography.*

No abstracts in this category.

20 SPACECRAFT PROPULSION AND POWER

Includes main propulsion systems and components, e.g., rocket engines; and spacecraft auxilliary power sources.

For related information see also *07 Aircraft Propulsion and Power, 28 Propellants and Fuels, 44 Energy Production and Conversion,* and *15 Launch Vehicles and Space Vehicles.*

N90-13584*# Remtech, Inc., Huntsville, AL.
DEVELOPMENT OF A SHUTTLE PLUME RADIATION HEATING INDICATOR Final Report
John E. Reardon Nov. 1988 19 p
(Contract NAS8-35671)
(NASA-CR-183679; NAS 1.26:183679; RTR-109-02) Avail: NTIS HC A03/MF A01 CSCL 21H

The primary objectives were to develop a Base Heating Indicator Code and a new plume radiation code for the Space Shuttle. Additional work included: revision of the Space Shuttle plume radiation environment for changes in configuration and correction of errors, evaluation of radiation measurements to establish a plume radiation model for the SRB High Performance Motor (HPM) plume, radiation predictions for preliminary designs, and participation in hydrogen disposal analysis and testing for the VAFB Shuttle launch site. The two most significant accomplishments were the development of the Base Heating Indicator Code and the Shuttle Engine Plume Radiation (SEPRAD) Code. The major efforts in revising the current Shuttle plume radiation environment were for the Orbiter base heat shield and the ET components in the Orbiter-ET interface region. The work performed is summarized in the technical discussion section with references to the documents containing detailed results. The technical discussion is followed by a summary of conclusions and recommendations for future work. Author

N90-13585*# Aerojet TechSystems Co., Sacramento, CA.
SPACE TRANSPORTATION ENGINE PROGRAM (STEP). PHASE B: PROJECT STUDY AND MANAGEMENT PLAN-INGREDIENTS FOR STEP SUCCESS
Ron Newton 28 Aug. 1989 97 p
(Contract NAS8-38150)
(NASA-CR-183770; NAS 1.26:183770) Avail: NTIS HC A05/MF A01 CSCL 21H

This Project Study and Management Plan serves as the primary control document for NASA and Aerojet for the Space Transportation Engine Program (STEP)-Phase B. It defines the method of accomplishing the Statement of Work (SOW) tasks and is fully responsive to the scope and objectives stated in NASA-MSFC RFP No. 8-1-8-PP-01836 (Ref. 1). The plan defines a disciplined process to meet program objectives of delivering credible, on-time, quality products defining designs, implementation plans, and costs for safe, reliable, low cost Space Transportation Main Engine (STME) and Space Transportation Booster Engine (STBE) systems. These will effectively and efficiently interface with Advanced Launch System (ALS) vehicles, facilities, and operations to support a first flight in the 1998 to 2000 timeframe. Author

N90-13586*# Morton Thiokol, Brigham City, UT. Space Div.
QM-8 FIELD JOINT PROTECTION SYSTEM, VOLUME 7 Final Report
Elgie Hale Jun. 1989 23 p
(Contract NAS8-30490)
(NASA-CR-183748; NAS 1.26:183748; TWR-17591-Vol-7) Avail: NTIS HC A03/MF A01 CSCL 21H

The pre-launch functioning data of the Field Joint Protection System (JPS) used on QM-8 are presented. Also included is the post fire condition of the JPS components following the test firing of the motor. The JPS components are: field joint heaters; field joint sensors; field joint moisture seal; moisture seal kevlar retaining straps; field joint external extruded cork insulation; vent valve; power cables; and igniter heater. Author

N90-13587*# Morton Thiokol, Brigham City, UT. Aerospace Group.
RSRM NOZZLE FIXED HOUSING COOLDOWN TEST Final Report
D. J. Bolieau May 1989 45 p
(Contract NAS8-30490)
(NASA-CR-183741; NAS 1.26:183741; TWR-19322) Avail: NTIS HC A03/MF A01 CSCL 21H

Flight 5 aft segments with nozzles were exposed to -17 F temperatures while awaiting shipment to KSC in February, 1989. No records were found which show that any previous nozzles were exposed to air temperatures as low as those seen by the Flight 5 nozzles. Thermal analysis shows that the temperature of the fixed housing, and forward and aft exit cone components dropped as low as -10 F. Structural analysis of the nozzles at these low temperatures show the forward and aft exit cone adhesive bonds to have a positive margin of safety, based on a 2.0 safety factor. These analyses show the normal and shear stresses in the fixed housing bond as low values. However, the

hoop and meridinal stresses were predicted to be in the 4000 psi range; the failure stress allowable of EA913NA adhesive at -7 F. If the bonds did break in directions perpendicular to the surfaces, called bond crazing, no normal bond strength would be lost. Testing was conducted in two phases, showing that no degradation to the adhesive bonds occurred while the Flight 5 nozzles were subjected to subzero temperatures. The results of these tests are documented. Phase 1 testing cooled a full-scale RSRM insulated fixed housing to -13 F, with extensive bondline inspections. Phase 2 testing cooled the witness panel adhesive tensile buttions to -13 F, with failure strengths recorded before, during, and after the cooldown. Author

N90-13588*# Thiokol Corp., Brigham City, UT. Space Operations.
FLIGHT MOTOR SET 360L001 (STS-26R). VOLUME 5: NOZZLE COMPONENT Final Report
Russell J. George Jul. 1989 371 p
(Contract NAS8-30490)
(NASA-CR-183771; NAS 1.26:183771; TWR-17272-Vol-5) Avail: NTIS HC A16/MF A02 CSCL 21H

A review of the performance and post-flight condition of the STS-26 Redesigned Solid Rocket Motor (RSRM) nozzles is presented. The nozzle assemblies, flown on the Space Shuttle Discovery on 29 September 1988, were tested to demonstrate flex bearing system reusability. The evaluation indicated no condition that would adversely affect the reusability of the flex bearing system. Inspection showed that the flex bearings did not leak, were not damaged by water impact, had the expected erosion profiles, and that the remaining ablative liner thicknesses met the performance margin of safety. Applicable Discrepancy Reports and Process Departures, the Nozzle Component Program Team performance evaluation, and the Redesign Program Review Board assessment are included. J.P.S.

N90-13589*# Rockwell International Corp., Canoga Park, CA. Rocketdyne Div.
LOX/HYDROCARBON COMBUSTION INSTABILITY INVESTIGATION Final Report
R. J. Jensen, H. C. Dodson, and S. E. Claflin Jul. 1989 177 p
(Contract NAS3-24612)
(NASA-CR-182249; RI/RD-89-179; NAS 1.26:182249) Avail: NTIS HC A09/MF A02 CSCL 21B

The LOX/Hydrocarbon Combustion Instability Investigation Program was structured to determine if the use of light hydrocarbon combustion fuels with liquid oxygen (LOX) produces combustion performance and stability behavior similar to the LOX/hydrogen propellant combination. In particular methane was investigated to determine if that fuel can be rated for combustion instability using the same techniques as previously used for LOX/hydrogen. These techniques included fuel temperature ramping and stability bomb tests. The hot fire program probed the combustion behavior of methane from ambient to subambient temperatures. Very interesting results were obtained from this program that have potential importance to future LOX/methane development programs. A very thorough and carefully reasoned documentation of the experimental data obtained is contained. The hot fire test logic and the associated tests are discussed. Subscale performance and stability rating testing was accomplished using 40,000 lb. thrust class hardware. Stability rating tests used both bombs and fuel temperature ramping techniques. The test program was successful in generating data for the evaluation of the methane stability characteristics relative to hydrogen and to anchor stability models. Data correlations, performance analysis, stability analyses, and key stability margin enhancement parameters are discussed. Author

N90-13590*# National Aeronautics and Space Administration. Lewis Research Center, Cleveland, OH.
TANK PRESSURE CONTROL EXPERIMENT ON THE SPACE SHUTTLE
1989 11 p
(NASA-TM-102313; E-5007; NAS 1.15:102313) Avail: NTIS HC A03/MF A01 CSCL 22B

The tank pressure control experiment is a demonstration of NASA intent to develop new technology for low-gravity management of the cryogenic fluids that will be required for future space systems. The experiment will use freon as the test fluid to measure the effects of jet-induced fluid mixing on storage tank pressure and will produce data on low-gravity mixing processes critical to the design of on-orbit cryogenic storage and resupply systems. Basic data on fluid motion and thermodynamics in low gravity is limited, but such data is critical to the development of space transfer vehicles and spacecraft resupply facilities. An in-space experiment is needed to obtain reliable data on fluid mixing and pressure control because none of the available microgravity test facilities provide a low enough gravity level for a sufficient duration to duplicate in-space flow patterns and thermal processes. Normal gravity tests do not represent the fluid behavior properly; drop-tower tests are limited in length of time available; aircraft low-gravity tests cannot provide the steady near-zero gravity level and long duration needed to study the subtle processes expected in space. Author

N90-13591# Pennsylvania State Univ., University Park. Dept. of Mechanical Engineering.
GAS FLOWS IN ROCKET MOTORS, VOLUME 1 Final Report, Jul. 1988 - Mar. 1989
Yigal Kronzon, Chau Lyan-Chang, and Charles L. Merkle Jun. 1989 84 p Prepared for Science Applications Engineering Corp., Torrance, CA
(Contract F04611-88-C-0014)
(AD-A213348; AL-TR-89-011-Vol-1) Avail: NTIS HC A05/MF A01 CSCL 20/4

A supersonic nozzle analysis for both perfect and real gases and for viscous and inviscid flows is presented. The primary focus was to develop an accurate, efficient procedure for computing nozzle flows with careful attention to global mass conservation. In general, the goal was to demonstrate computations with mass flux errors of less than 1 percent on moderately resolved grids. Calculation procedures for both viscous and inviscid flows and for parabolized Navier-Stokes (PNS) algorithms have consistently demonstrated this goal. Primary emphasis was developed and demonstrated to a lesser degree. Also included in the effort was a procedure for coupling the nozzle wall cooling flow with the nozzle flowfield so that both nozzle wall temperature and heat flux were simultaneously determined by the calculation. Finally, a procedure for determining the effect of small variations in back pressure on the nozzle flowfield was developed. A Ph.D. thesis which describes the detail of the perfect gas work is presented as Appendix C. In particular, this appendix includes the coupled nozzle wall cooling and nozzle back pressure calculations. GRA

N90-13592# Pennsylvania State Univ., University Park. Dept. of Mechanical Engineering.
GAS FLOWS IN ROCKET MOTORS. VOLUME 2, APPENDIX C: TIME ITERATIVE SOLUTION OF VISCOUS SUPERSONIC FLOW Final Report, Jul. 1988 - Mar. 1989
Yigal Kronzon, Chau Lyan-Chang, and Charles L. Merkle Aug. 1989 233 p Prepared for Science Applications International Corp., Torrance, CA
(Contract F04611-88-C-0014)
(AD-A213349; AL-TR-89-011-Vol-2-App-C) Avail: NTIS HC A11/MF A02 CSCL 20/4

Numerical solutions of supersonic viscous flows are studied by applying an implicit time-dependent scheme to the thin-layer Navier-Stokes (TLNS) equations. The alternating direction implicit (ADI) scheme is first formulated to solve transonic viscous axisymmetric flows in two dimensions. The results indicate that the ADI scheme is not efficient enough for supersonic viscous calculations. A spatial discretization scheme using upwind flux-vector split differencing in the streamwise direction and central differencing in the cross-stream direction is chosen. Three approximate factorization schemes and one fully implicit direct solver are considered. Of them, the diagonally dominant ADI(DDADI) and the parabolized ADI are found to be much faster than the standard ADI procedure. These numerical algorithms are

applied to solve supersonic flows through conical and high expansion ratio contoured nozzles for different Reynolds numbers, wall temperatures, and back pressures. Proper downstream boundary conditions for the subsonic portion of the outflow are shown to allow variations of the boundary layer thickness at the exit plane and recirculating separated flows for sufficiently high back pressure. Parabolized Navier-Stokes (PNS) procedures are also studied. Swirling viscous flows in transonic and supersonic propulsive nozzles have been investigated numerically. The algorithms developed for axisymmetric two-dimensional flows are extended to solve the three-dimensional TLNS equations. GRA

N90-13593# Pennsylvania State Univ., University Park. Dept. of Mechanical Engineering.
GAS FLOWS IN ROCKET MOTORS. VOLUME 3, APPENDIX D: COMPUTER CODE LISTINGS Final Report, Jul. 1988 - Mar. 1989
Yigal Kronzon, Chau Lyan-Chang, and Charles L. Merkle Aug. 1989 180 p Prepared for Science Applications International Corp., Torrance, CA
(Contract F04611-88-C-0014)
(AD-A213350; AL-TR-89-011-Vol-3-App-D) Avail: NTIS HC A09/MF A01 CSCL 20/4

Detailed descriptions of the governing equations, the method of solution, and the computer code for calculating perfect gas or real gas flow in axisymmetric nozzles are given. The codes permit calculation of a perfect gas or a real gas for inviscid flow by solving the Euler equations, and for viscous flow by solving the thin layer Navier-Stokes equations. These equations are written in a conservative form and solved implicitly in body-fitted coordinates. The solution obtained by the conservative variables is expressed in terms of the density, rho, the momentum parallel to the axis of symmetry (rho(u)), the momentum perpendicular to the axis (rho(v)), and the total internal energy, e(o). These variables are then used to calculate the nonconservative primitive variables, the velocity components, u and v, the pressure, p, and the temperature, T. The nozzle performance including the rate of mass flow, m, the thrust, T, and the specific impulse are also computed. The codes were written in FORTRAN V and ran on the CYBER 180/840, NOS/BE system which limited the number of grid points to 20 x 44 for solving the Euler equations and 60 x 40 for the TLNS equations. The results obtained for the nozzle flowfield showed maximum global mass flux errors of less than + or - 1 percent for the Euler equations and less than + or - 2 percent for the TLNS equations. Solutions with more dense grids (typically 100 x 50 or higher) consistently showed global mass conservation of better than one percent. GRA

N90-13594*# Thiokol Corp., Brigham City, UT. Space Operations.
QUALIFICATION OF IMPROVED JOINT HEATERS Final Test Report
M. Cook 14 Sep. 1989 18 p
(Contract NAS8-30490)
(NASA-CR-183827; NAS 1.26:183827; TWR-19899) Avail: NTIS HC A03/MF A01 CSCL 21H

Qualification testing of the Redesigned Solid Rocket Motor improved igniter-to-case joint and field joint heaters was conducted on the fired TEM-04 static test motor and was completed on 7 Sep. 1989. The purpose of the test was to certify the installation and performance of the improved joint heaters for use on flight motors. The changes incorporated in the improved heaters improve durability and should reduce handling damage. The igniter-to-case joint and field joint primary heater circuits were subjected to five 20-hr ON cycles. The heater redundant circuits were then subjected to one 20-hr ON cycle. Voltage, current, and temperature set point values were maintained within the specified limits for both heaters during each ON cycle. When testing was complete, both heaters were removed and inspected. No discolorations or any other anomalies were found on either of the heaters. Based on the successful completion of this test, it is recommended that the improved igniter-to-case joint and field joint heaters be used on future flight motors. Author

N90-13595*# National Aeronautics and Space Administration. Lewis Research Center, Cleveland, OH.
THIN-FILM SENSORS FOR REUSABLE SPACE PROPULSION SYSTEMS
Aloysius F. Hepp and Walter S. Kim 1989 10 p Presented at the Sensors Expo International, Cleveland, OH, 12-14 Sep. 1989; sponsored by Sensors Magazine
(NASA-TM-102383; E-5122; NAS 1.15:102383) Avail: NTIS HC A02/MF A01 CSCL 21H

Thin-film thermocouples (TFTCs) were developed for aircraft gas turbine engines and are in use for temperature measurement on turbine blades up to 1800 F. Established aircraft engine gas turbine technology is currently being adapted to turbine engine blade materials and the environment encountered in the Space Shuttle Main Engine (SSME)-severe thermal shock from cryogenic fuel to combustion temperatures. Initial results with coupons of MAR M-246 (+Hf) and PWA 1480 were followed by fabrication of TFTC on SSME turbine blades. Current efforts are focused on preparation for testing in the Turbine Blade Tester at NASA Marshall Space Flight Center. Author

N90-13596*# National Aeronautics and Space Administration. Lewis Research Center, Cleveland, OH.
THE US SPACE STATION AND ITS ELECTRIC POWER SYSTEM
Ronald L. Thomas 1988 26 p Presented at the 10th South Pacific Electrical International Convention, Brisbane, Australia, 2-5 May 1988; sponsored by the Electrical Development Association of Queensland, Inc.
(NASA-TM-101974; E-4674; NAS 1.15:101974) Avail: NTIS HC A03/MF A01 CSCL 10B

The United States has embarked on a major development program to have a space station operating in low earth orbit by the mid-1990s. This endeavor draws on the talents of NASA and most of the aerospace firms in the U.S. Plans are being pursued to include the participation of Canada, Japan, and the European Space Agency in the space station. From the start of the program these was a focus on the utilization of the space station for science, technology, and commercial endeavors. These requirements were utilized in the design of the station and manifest themselves in: pressurized volume; crew time; power availability and level of power; external payload accommodations; microgravity levels; servicing facilities; and the ability to grow and evolve the space station to meet future needs. President Reagan directed NASA to develop a permanently manned space station in his 1984 State of the Union message. Since then the definition phase was completed and the development phase initiated. A major subsystem of the space station is its 75 kW electric power system. The electric power system has characteristics similar to those of terrestrial power systems. Routine maintenance and replacement of failed equipment must be accomplished safely and easily and in a minimum time while providing reliable power to users. Because of the very high value placed on crew time it is essential that the power system operate in an autonomous mode to minimize crew time required. The power system design must also easily accommodate growth as the power demands by users are expected to grow. An overview of the U.S. space station is provided with special emphasis on its electrical power system. Author

N90-13515# European Space Agency, Paris (France).
POWER GENERATION AND DISTRIBUTION
H. K. Fiebrich *In its* The Hipparcos Mission. Prelaunch Status. Volume 1: The Hipparcos Satellite Jun. 1989 p 147-164 (For primary document see N90-13499 05-18)
Copyright Avail: NTIS HC A16/MF A02; ESA Publications Div., ESTEC, Noordwijk, Netherlands, 80 Dutch guilders

N90-13517# European Space Agency, Paris (France).
THE APOGEE BOOST MOTOR
P. Strada *In its* The Hipparcos Mission. Prelaunch Status. Volume 1: The Hipparcos Satellite Jun. 1989 p 197-203 (For primary document see N90-13499 05-18)

Copyright Avail: NTIS HC A16/MF A02; ESA Publications Div., ESTEC, Noordwijk, Netherlands, 80 Dutch guilders

N90-13844# Technische Univ., Brunswick (Germany, F.R.). Inst. fuer Geophysik und Meteorologie.
HIGH PRECISION ROCKET ATTITUDE RECONSTRUCTION USING STAR SENSOR AND MAGNETOMETER DATA
A. Muschinski and H. Luehr *In* ESA, European Rocket and Balloon Programs and Related Research Jun. 1989 p 111-116 (For primary document see N90-13826 05-42)
Copyright Avail: NTIS HC A15/MF A02

N90-13845# Deutsche Forschungs- und Versuchsanstalt fuer Luft- und Raumfahrt, Oberpfaffenhofen (Germany, F.R.). Hauptabteilung Angewandte Datentechnik.
THE SN 1987A ATTITUDE CONTROL SYSTEM
J. Turner *In* ESA, European Rocket and Balloon Programs and Related Research Jun. 1989 p 117-122 (For primary document see N90-13826 05-42)
Copyright Avail: NTIS HC A15/MF A02

N90-13866# Max-Planck-Inst. fuer Physik und Astrophysik, Garching (Germany, F.R.). Inst. fuer Extraterrestrische Physik.
PROJECT SUPERNOVA 1987
Horst Hippmann *In* ESA, European Rocket and Balloon Programs and Related Research Jun. 1989 p 239-240 (For primary document see N90-13826 05-42)
Copyright Avail: NTIS HC A15/MF A02

N90-13867# Max-Planck-Inst. fuer Physik und Astrophysik, Garching (Germany, F.R.). Inst. fuer Extraterrestrische Physik.
THE X RAY MIRROR AND THE PSPC OF THE SUPERNOVA-ROCKET-PROJECT
U. G. Briel, E. Pfeffermann, H. Braeuninger, W. Burkert, G. Kettenring, and G. Metzner *In* ESA, European Rocket and Balloon Programs and Related Research Jun. 1989 p 241-244 (For primary document see N90-13826 05-42)
Copyright Avail: NTIS HC A15/MF A02

23 CHEMISTRY AND MATERIALS (GENERAL)

N90-13597*# National Aeronautics and Space Administration. Lewis Research Center, Cleveland, OH.
THE MATERIALS DIVISION: A CASE STUDY
Salvatore J. Grisaffe and Carl E. Lowell 1989 13 p Presented at the Quality Improvement Prototype Workshop, Washington, DC, 6 Sep. 1989
(NASA-TM-102380; E-5119; NAS 1.15:102380) Avail: NTIS HC A03/MF A01 CSCL 07A

The Materials Division at NASA's Lewis Research Center has been engaged in a program to improve the quality of its output. The division, its work, and its customers are described as well as the methodologies developed to assess and improve the quality of the Division's staff and output. Examples of these methodologies are presented and evaluated. An assessment of current progress is also presented along with a summary of future plans. Author

24 COMPOSITE MATERIALS

Includes physical, chemical, and mechanical properties of laminates and other composite materials.

For ceramic materials see *27 Nonmetallic Materials.*

N90-13598 Virginia Polytechnic Inst. and State Univ., Blacksburg.
FAILURE PROCESSES IN UNIDIRECTIONAL COMPOSITE MATERIALS Ph.D. Thesis
Mannur Jaganathan Sundaresan 1988 164 p
Avail: Univ. Microfilms Order No. DA8907520

Failure processes in unidirectional composite materials subjected to quasi-static tensile load along the fiber direction are investigated. The emphasis in this investigation is to identify the physical processes taking place during the evolution of failure in these materials. An extensive literature review is conducted and the information relevant to the present topic is summarized. The nature of damage growth in five different commercially available composite systems is studied. In-situ scanning electron microscopy is employed for identifying the failure events taking place at the microscopic level. Acoustic emission monitoring is used for estimating the rate of damage growth on a global scale and determining the size of individual failure events. The results of this study has shown the important roles of the matrix material and the interphase in determining the tensile strength of unidirectional composite materials. Several failure modes occurring at the microscopic scale are revealed for the first time. Further, the results indicate that dynamic fracture participates to a significant extent in determining the failure process in these materials. Based on the results of this study the influence of various parameters in determining the composite strength is described. Dissert. Abstr.

N90-13599*# Utah Univ., Salt Lake City. Dept. of Materials Science and Engineering.
FRACTOGRAPHY OF COMPOSITE DELAMINATION Final Report
W. D. Bascom 15 Oct. 1989 99 p
(Grant NAG1-705)
(NASA-CR-183291; NAS 1.26:183291) Avail: NTIS HC A05/MF A01 CSCL 11D

Delamination is a major failure mode of carbon fiber organic matrix composites. It can occur under a variety of loading conditions. Efforts to develop predictive models of the delamination of carbon fiber composites are hampered by a lack of information about the micromechanics of impact damage and delamination growth. Crack formation and propagation in these materials cannot be observed in sufficient detail to determine micro-damage using currently available nondestructive methods such as acoustic backscattering or x ray imaging. Consequently, destructive methods are required. Delamination of composites in Mode I, Mode II and after low energy impact loads were investigated using metallographic techniques of potting the failed specimens, sectioning and examining the cut sections for damage modes.
Author

N90-13600*# Virginia Polytechnic Inst. and State Univ., Blacksburg. Center for Composite Materials and Structures.
STATIC AND FREE-VIBRATIONAL RESPONSE OF SEMI-CIRCULAR GRAPHITE-EPOXY FRAMES WITH THIN-WALLED OPEN SECTIONS
J. Scott Collins and Eric R. Johnson Oct. 1989 218 p
(Grant NAG1-343)
(NASA-CR-186097; NAS 1.26:186097; CCMS-89-21; VPI-E-89-19)
Avail: NTIS HC A10/MF A02 CSCL 11D

Experiments were conducted to measure the three-dimensional static and free vibrational response of two graphite-epoxy, thin-walled, open section frames. The frames are semi-circular with a radius of three feet, and one specimen has an I cross section and the other has a channel cross section. The flexibility influence coefficients were measured in static tests for loads applied at midspan with the ends of the specimens clamped. Natural frequencies and modes were determined from vibrational tests for free and clamped end conditions. The experimental data is used to evaluate a new finite element which was developed specifically for the analysis of curved, thin-walled structures. The formulation of the element is based on a Vlasov-type, thin-walled, curved beam theory. The predictions from the finite element program generally correlated well with the experimental data for the symmetric I-specimen. Discrepancies in some of the data were found to be due to flexibility in the clamped end conditions. With respect to the data for the channel specimen, the correlation was less satisfactory. The finite element analysis predicted the

out-of-plane response of the channel specimen reasonably well, but large discrepancies occurred between the predicted in-plane response and the experimental data. The analysis predicted a much more compliant in-plane response than was observed in the experiments. Author

N90-13601# Brown Univ., Providence, RI.
DUCTILE FAILURE Final Report
A. Needleman Sep. 1989 5 p
(Contract N00014-86-K-0262)
(AD-A212975) Avail: NTIS HC A01/MF A01 CSCL 11/4

Work under this contract has proceeded in three areas: (1) analyses of ductile fracture processes, with the aim of assessing the capability of analyses carried out within the Gurson constitutive framework for progressively cavitating solids to provide quantitative predictions of ductile fracture; (2) the development of a finite element methodology for localization and failure analysis in order to carry out fully three dimensional finite element analyses of ductile failure processes; and (3) studies of the effects of fiber volume fraction, geometry and spacing on plastic response and ductile failure in metal matrix composites. GRA

N90-13602# Northwestern Univ., Evanston, IL. Center for Quality Engineering and Failure Prevention.
LOCALIZATION OF ULTRASOUND IN THICK COMPOSITES Interim Report
Yichi Lu and Jan D. Achenbach 15 Aug. 1989 10 p
(Contract N00014-89-J-1362)
(AD-A212994; NU-CENTER-QEFP-1989-2) Avail: NTIS HC A02/MF A01 CSCL 11/4

The propagation of ultrasound in fiber reinforced composites is controlled by the relative magnitudes of characteristic length variables. These length variables are the wavelength (Lambda), the fiber diameter (a), the thicknesses of plies (h), and the overall thickness of the component (H). The propagation of longitudinal waves is considered in a cross-ply fiber reinforced composite. Since Lambda is much less than a, an effective modulus representation is used for the mechanical behavior of the plies. This means that in the direction normal to the plies longitudinal waves will propagate with a wave speed which is independent of the fiber direction. Hence the problem considered here is a 1-D problem of wave propagation through layers with identical mechanical impedances which are separated by interfaces. Since the interfaces of the plies and/or laminates may reflect sound, a composite may display some of the features that are characteristic of the propagation of ultrasound in periodic media, such as passing and stopping bands in the frequency spectrum. Strict structural periodicity is, however, an idealization. In reality there will be random deviations from periodicity, which will in fact destroy the passing bands, and will give rise to attenuation at all frequencies. This attenuation is often referred to as localization. Such localization is analyzed. GRA

N90-13603# Naval Air Development Center, Warminster, PA. Air Vehicle and Crew Systems Technology Dept.
FATIGUE BEHAVIOR OF SILICON CARBIDE WHISKER/ALUMINUM COMPOSITE Final Report
Eun E. Lee 1 Oct. 1988 23 p
(AD-A213094; NADC-89037-60) Avail: NTIS HC A03/MF A01 CSCL 11/4

Specimens of an extruded 19.8 vol percent SiCw/2124 aluminum alloy composite were subjected to constant amplitude loading of stress ratio 0.1 at room temperature in a laboratory atmosphere. The fatigue crack growth path is tortuous and much of it is nearly parallel to the extrusion direction of the specimen. This is attributable to the SiCw aligned in the extrusion direction. The logarithm of fatigue fracture life, NF, increases linearly with decreasing stress range, within the limits of the applied stress range. The observed fractographic features are facets and steps in the initial stage, striations in the subsequent stage, and dimples in the final stage of fatigue. GRA

N90-13604# Washington Univ., Seattle. Dept. of Mechanical Engineering.
TOUGHENING OF A PARTICULATE-REINFORCED/CERAMIC-MATRIX COMPOSITE
M. Taya, S. Hayashi, A. S. Kobayashi, and H. S. Yoon Sep. 1989 37 p
(Contract N00014-87-K-0326)
(AD-A213180; UWA/DME/TR-89/2) Avail: NTIS HC A03/MF A01 CSCL 11/4

The toughening mechanism of particulate-reinforced ceramic-matrix composites was attributed to the thermal residual stress field induced by the differential thermal expansions of the matrix and the particulate when the composite is cooled from the processing to room temperature. The measured increase of 77 percent in toughness in a TiB2-particulate SiC-matrix ceramic composite compared well with the predicted increase of 52 percent. GRA

N90-13605# Imperial Coll. of Science and Technology, London (England). Dept. of Mechanical Engineering.
THE ADHESIVE BONDING OF THERMOPLASTIC COMPOSITES Final Report, 23 Jul. 1986 - 23 Sep. 1989
A. J. Kinloch and G. K. A. Kodokian 19 Sep. 1989 335 p
(Contract DAJA45-86-C-0037; DA Proj. 1L1-61102-BH-57)
(AD-A213358) Avail: NTIS HC A15/MF A01 CSCL 11/4

This thesis discusses the problems that occur when thermo plastic-based fiber-composite materials are bonded using structural engineering adhesives, such as epoxy and acrylic adhesives. A double-cantilever beam joint has been employed and it is shown that the value of the adhesive fracture energy, G(c), is very low when a simple abrasion/solvent-wipe surface pretreatment is used for the thermoplastic fiber-composites. This arises from crack growth occurring along the adhesive/composite interface, which is relatively weak when such a pretreatment is employed. Secondly, the surfaces of the corona-discharge treated composites have been characterised using x ray photoelectron spectroscopy, contact angle analysis and scanning electron microscopy. These studies revealed that the strong adhesion associated with corona pretreatment is via increasing the wettability and intrinsic adhesion of the thermoplastic fibre-composite materials. Thirdly, it is demonstrated how very effective a corona-discharge surface pretreatment may be for these materials. Indeed, when such a pretreatment is used, interfacial crack growth is no longer observed but the crack now propagates either cohesively in the adhesive or through the composite substate; both failure modes lead to relatively high values of G(c), with the former resulting in the highest values of G(c) being recorded. The thesis concludes by describing a study on designing efficient lap joints. GRA

N90-13606# Deutsche Forschungsanstalt fuer Luft- und Raumfahrt, Brunswick (Germany, F.R.). Abteilung Strukturberechnung.
MEASURING OF THE COMPLETE STIFFNESS MATRIX FOR ANISOTROPIC LAMINATED MATERIALS
Hermann Klein Apr. 1989 38 p In GERMAN; ENGLISH summary
(DLR-Mitt-89-11; ISSN-0176-7739; ETN-90-95845) Avail: NTIS HC A03/MF A01; DLR, VB-PL-DO, Postfach 90 60 58, 5000 Cologne, Fed. Republic of Germany, 17 Deutsche Marks

A method is presented to calculate the whole stiffness matrix for anisotropic layered materials from test results. The stiffnesses are the transfer matrix from strains to stresses. If strains and stresses in several useful tests are measured, the 18 different unknown stiffnesses can be calculated from at least 18 relations as a regression problem. Some examples of stiffness tests are described. ESA

N90-13607# Deutsche Forschungsanstalt fuer Luft- und Raumfahrt, Brunswick (Germany, F.R.). Abteilung Strukturberechnung.
MEASURING OF THE COMPLETE STIFFNESS MATRIX FOR ANISOTROPIC LAMINATED MATERIALS
Hermann Klein Apr. 1989 37 p

(DLR-Mitt-89-12; ISSN-0176-7739; ETN-90-95846) Avail: NTIS HC A03/MF A01; DLR, VB-PL-DO, Postfach 90 60 58, 5000 Cologne, Fed. Republic of Germany, 16.50 Deutsche Marks

A method is presented to calculate the whole stiffness matrix for anisotropic layered materials from test results. The stiffnesses are the transfer matrix from strains to stresses. If strains and stresses in several useful tests are measured, the 18 different unknown stiffnesses can be calculated from at least 18 relations as a regression problem. Some examples of stiffness tests are described. ESA

N90-13608# Massachusetts Inst. of Tech., Cambridge. Advanced Construction Materials Lab.

FIBER REINFORCED CEMENTITIOUS COMPOSITES TECHNOLOGY Final Technical Report, 15 Oct. 1986 - 31 Sep. 1989

Victor C. Li, Stanley Backer, and Youjiang Wang Jun. 1989 308 p Sponsored in part by Shimizu Corp., Japan and E.I. du Pont de Nemours and Co.

(Grant NSF ECE-86-05159)

(PB89-227813; NSF/ENG-89015) Avail: NTIS HC A14/MF A02 CSCL 11D

The tensile and structural behavior of fiber reinforced cementitious composites (FRC) was studied. A model was developed to predict fiber pull-out response. Experiments of fiber pull-out at inclined angles show that the pull-out load and energy increase with the inclining angle but the increases are limited by the strength of the matrix. Fiber bundle pull-out tests reveal that fiber bundles reduce the efficiency of fiber reinforcement. A theoretical model was developed to relate FRC tensile behavior to the parameters of fiber reinforcement including properties of fibers, matrix, and the fiber/matrix interface. A method of direct tensile test which needs only a simple loading fixture was used to study the tensile behavior of FRC containing various synthetic fibers. The failure mechanisms of these synthetic FRC were studied with optical and scanning electron microscopes. Directions for improvement in properties and cost/effectiveness of each FRC were indicated. GRA

N90-13609*# National Aeronautics and Space Administration. Goddard Space Flight Center, Greenbelt, MD.

GRAVIMETRIC MEASUREMENTS OF MATERIALS OUTGASSING APPLIED TO GRAPHITE-EPOXY LAMINATES

John J. Scialdone Dec. 1989 27 p

(NASA-TM-100753; Rept-90B00039; NAS 1.15:100753) Avail: NTIS HC A03/MF A01 CSCL 11D

The outgassing rates of two graphite-epoxy laminates, American Cyanamide 985B-626 and HST-7B-112, were obtained using a gravimetric method. The rates as a function of time and temperature were derived from the measurements of their mass losses at temperatures varying from 25 to 150 C and for a time span of up to 400 hours in a vacuum. The data from those measurements were reduced to obtain the outgassing activation energies, the mass losses per unit mass or area, and the corresponding outgassing rates. The rates are expressed in closed-form equations and are directly usable for medling computations. The procedures to obtain these parameters are shown and may be used for the evaluation of other materials. The results of the tests show that the activation energies of the two materials are: 4630 cal/mole for the 985B-626 materials and 4791 cal/mole for the HST-7B-112 sample no. 10 Graphite Exoxy. The outgassing rates of these materials are in the 10E-5 g/sq cm/hr range and they decay according to a power of time of 0.60 at 25 C, indicating that the outgassing process is mainly a diffusion at that temperature. The normalized mass losses versus time obtained from these tests were compared to the discrete results obtained from the ASTM-E595 tests. The comparison provides general indications on the effects of temperature and time in relation to the ASTM test values obtained at 125 C for a 24-hour test duration. Author

N90-13610# Centre d'Essais Aeronautique Toulouse (France). Lab. des Materiaux Composites et Organiques.

IMPACT TESTS OF THREE COMPOSITE MATERIALS WITH CARBON FIBER CORES [ESSAI DE CHOC INSTRUMENTE SUR TROIS MATERIAUX COMPOSITES A BASE DE FIBRES DE CARBONE]

11 Apr. 1988 57 p In FRENCH

(Rept-M6-582500; ETN-90-95716) Avail: NTIS HC A04/MF A01

A series of low impact tests carried out on the three carbon fiber composite materials most commonly used in aerospace construction are described. These tests seek to determine the amount of structural damage due to small accidental impact. This damage is often invisible to the naked eye, but is the cause of substantial decrease in residual mechanical strength. Ultrasound, computer aided tomography, and microstructural analysis are used to visualize the structural damages. Results of such tests and comparisons of the impact damage on the three different composite materials are presented. ESA

N90-13611# Ecole Centrale de Lyon (France). Lab. de Mecanique des Solides.

STUDY OF FATIGUE DEGRADATION MECHANISMS IN UNIDIRECTIONAL COMPOSITE MATERIALS. APPLICATION TO CUMULATIVE DAMAGE Ph.D. Thesis [ETUDE DES MECANISMES DE DEGRADATION EN FATIGUE DE MATERIAUX COMPOSITES UNIDIRECTIONNELS: APPLICATION AU CUMUL DE DOMMAGE]

Pascale Puget 1988 155 p In FRENCH

(ECL-88-12; ETN-90-95767) Avail: NTIS HC A08/MF A01

The influence of the glass fiber concentration parameter in fatigue damage of unidirectional glass fiber reinfored plastics under flexing load is studied. The degradation mechanisms were followed using optical damage tracers. It is found that static fatigue can lead to faster damage degradation than dynamic fatigue, particularly for high fatigue levels. Different modes of damage initiation and evolution are described. ESA

N90-13612# Ecole Centrale de Lyon (France). Dept. de Mecanique des Solides.

CONTRIBUTION TO THE FATIGUE BEHAVIOR STUDY OF COMPOSITE MATERIALS REINFORCED WITH UNIDIRECTIONAL GLASS FIBERS Ph.D. Thesis [CONTRIBUTION A L'ETUDE DU COMPORTEMENT EN FATIGUE DE MATERIAUX COMPOSITES A RENFORT VERRE UNIDIRECTIONNEL]

Lucien Fiore 1988 158 p In FRENCH

(ECL-88-20; ETN-90-95773) Avail: NTIS HC A08/MF A01

Fatigue damage in flexing tests of unidirectional glass fiber reinforced plastics is studied. The design of a test bench capable of testing, visualizing and registering acoustic emissions is described. The notion of defect tolerance is applied to the characterization of specimens. It is shown that parameters are significant only when related to initial states and evolution status. ESA

N90-13613# Technische Univ., Delft (Netherlands). Dept. of Aerospace Engineering.

IMPACT TESTS ON ALUMINUM 2024 T3, ARAMID AND GLASS REINFORCED ALUMINUM LAMINATES AND THERMOPLASTIC COMPOSITES

A. Vlot Oct. 1987 42 p

(LR-534; ETN-90-95982) Avail: NTIS HC A03/MF A01

Efforts to improve the impact properties of Arall laminates by using aramid weaves instead of unidirectional prepeg, and by using S-glass fibers instead of aramid fibers are described. The impact properties are compared with the behavior of thermoplastic composites. Conclusions are outlined and discussed. ESA

N90-13614# Technische Univ., Delft (Netherlands). Dept. of Aerospace Engineering.

BUCKLING OF DELAMINATIONS IN ARALL LAMINATES

A. Vlot Oct. 1987 55 p
(LR-535; ETN-90-95983) Avail: NTIS HC A04/MF A01

ARALL specimens made with prepared delamination zones and bonded to a thick backing of an aluminum alloy are studied under compressive and bending loads. Tests are carried out under fatigue loads and equations are derived in order to compare the results with theoretical predictions on the buckling strengths of the buckling modes considered. The theoretical model proved to give accurate results. Conclusions are detailed. ESA

N90-13615# Technische Univ., Delft (Netherlands). Faculty of Aerospace Engineering.
CONSTANT AMPLITUDE FATIGUE OF ARALL-2 LAMINATES
G. H. J. J. Roebroeks Oct. 1987 58 p
(LR-539; ETN-90-95985) Avail: NTIS HC A04/MF A01

Typical failure mechanisms observed in the prepeg layer of as-cured material in experiments on ARALL laminates are studied, fiber failure under cyclic load and prepeg splitting in the fiber direction in the delaminated area. Aspects covered are the effect of post-stretching, different types of fatigue loads, frequency effect, biaxial loading, environmental aspects and different types of fibers (aramide, carbon, glass). S-glass appears to be the most interesting substitute for aramid fibers so the name ALGLA laminates is used. Conclusions are detailed. ESA

N90-13616# Technische Univ., Delft (Netherlands). Dept. of Aerospace Engineering.
SOME ASPECTS OF TEST FREQUENCY INFLUENCE ON THE FATIGUE BEHAVIOR OF ARALL
D. Chen Dec. 1987 19 p
(LR-549; ETN-90-95992) Avail: NTIS HC A03/MF A01

Applications of Arall laminates as a highly fatigue insensitive aircraft material for various aircraft structures are studied. The influence of the loading frequency on the crack growth behavior is addressed. Materials and type of load wave shapes are discussed and test results are outlined with graphics. Several conclusions and future recommendations are described. ESA

N90-13617# Technische Univ., Delft (Netherlands). Dept. of Aerospace Engineering.
REPAIR OF COMPOSITES BY MEANS OF WET-LAY-UP
J. A. Krebbekx Mar. 1988 52 p
(LR-551; ETN-90-95994) Avail: NTIS HC A04/MF A01

The repair of damaged composites used in airplanes at a reasonable cost is studied. Theoretical aspects of repair such as, types of damage, repair methods, and parameters influencing the optimum wet-lay-up repair, are considered. Practical aspects of reparation, including the sanding of carbon-epoxy laminates and the wet-lay-up of the patches are discussed. A specimen fabrication procedure and forces working therein, and results of testing of undamaged and damaged panels, are described. Comparison of results is given. The results are concluded as being better in reality by a better redistribution of the stresses due to the better dimensions of the part in which the repair is made. ESA

N90-13459*# United Technologies Corp., West Palm Beach, FL. Optics and Applied Technology Lab.
STATUS OF Gr/GLASS COMPOSITES TECHNOLOGY AT UTOS
Ramon A. Mayor *In* Jet Propulsion Lab., California Inst. of Tech., Report of the Asilomar 3 LDR Workshop 15 Aug. 1988 p 68-69 (For primary document see N90-13449 05-18)
Avail: NTIS HC A08/MF A01 CSCL 11D

N90-13461*# National Aeronautics and Space Administration. Langley Research Center, Hampton, VA.
ADVANCED COMPOSITE MATERIALS FOR PRECISION SEGMENTED REFLECTORS
Bland A. Stein and David E. Bowles *In* Jet Propulsion Lab., California Inst. of Tech., Report of the Asilomar 3 LDR Workshop 15 Aug. 1988 p 72-73 (For primary document see N90-13449 05-18)
Avail: NTIS HC A08/MF A01 CSCL 11D

N90-13462*# Jet Propulsion Lab., California Inst. of Tech., Pasadena.
LIGHTWEIGHT COMPOSITE REFLECTOR PANELS
R. E. Freeland and P. M. McElroy *In its* Report of the Asilomar 3 LDR Workshop 15 Aug. 1988 p 74-75 (For primary document see N90-13449 05-18)
Avail: NTIS HC A08/MF A01 CSCL 11D

25 INORGANIC AND PHYSICAL CHEMISTRY

Includes chemical analysis, e.g., chromatography; combustion theory; electrochemistry; and photochemistry.

For related information see also *77 Thermodynamics and Statistical Physics.*.

N90-13618*# Old Dominion Univ., Norfolk, VA. Dept. of Chemical Sciences.
COMPUTATIONAL SOLUTION OF CHEMISTRY PROBLEMS
Final Report, period ending 30 Jun. 1988
Robert L. Ake Nov. 1989 26 p
(Grant NAG1-596)
(NASA-CR-186000; NAS 1.26:186000) Avail: NTIS HC A03/MF A01 CSCL 07D

AB initio quantum chemical techniques have been used to investigate weakly bound complexes of H2O and SO2. An energy gradient program was used to locate stable structures for the H2O, SO2 complexes, and SCF calculations were carried out to determine the binding energies of complexes with multiple water molecules. A 4-31G basis set was used for most potential energy searches. More accurate basis sets including a generally contracted basis set with d orbitals on the sulfur were used for geometry and binding energy verification. For single water complexes, five different stable geometries were located with binding energies between 4 and 11 Kcal mol(-1), suggesting a binding shell for H2O around SO2 and a mechanism for the formation of an SO2-containing water droplet. Calculations on one of the complexes utilizing a larger double zeta basis and d functions on the sulfur atom lead to adjusted binding energies in the range 3 to 8 Kcal mol(-1). Very little charge transfer between SO2 and H2O was present. Addition of more than one H2O was found to be energetically favorable although the addition of the fourth water in certain geometries did not increase the stability of the complex. An alternative mechanism for the tropospheric gas phase production of acid rain is suggested. Author

N90-13619# ESDU International Ltd., London (England).
THERMOPHYSICAL PROPERTIES OF BUTA-1,3-DIENE
Mar. 1989 15 p Supersedes ESDU-87021
(ESDU-89005; ESDU-87021; ISBN-0-85679-676-X; ISSN-0141-4062) Avail: ESDU

ESDU 89005 gives equations obtained from a critical evaluation of experimental data in the literature for the variation along the saturation line with temperature, for both the liquid and the vapor, of: density, enthalpy, heat capacity at constant pressure, dynamic viscosity and thermal conductivity. Also given are equations for the variation with temperature along the saturation line of vapor pressure, latent heat of vaporization and surface tension, together with equations for the variation with temperature for the ideal gas of specific heat capacity at constant pressure, enthalpy, dynamic viscosity and thermal conductivity. Results on the saturation line evaluated in SI units using the equations are tabulated at 5 K intervals from the melting point to the critical point, or as close as possible for some properties. Results for the ideal gas evaluated also in SI units using the equations are tabulated at 10 K intervals from the melting point to 1000 K. In the absence of experimental values some of these results involve extrapolation and they are indicated in the tables. Conversion factors to facilitate use of the data in British Units are included. Author

N90-13620# Yale Univ., New Haven, CT. High Temperature Chemical Reaction Engineering Lab.
TRANSPORT PHENOMENA AND INTERFACIAL KINETICS IN MULTIPHASE COMBUSTION SYSTEMS Final Report, 1 Dec. 1983 - 31 Dec. 1988
Daniel E. Rosner Feb. 1989 15 p
(Grant AF-AFOSR-0034-84; AF Proj. 2308)
(AD-A212932; AFOSR-89-1240TR) Avail: NTIS HC A03/MF A01 CSCL 21/2

This final report summarizes Yale High Temperature Chemical Reaction Engineering Laboratory research methods/results (Grant AFOSR 84-0034) for the ca. five year period ending 12/31/88. Our techniques and results are outlined in the areas of: (1) laser-based real-time optical techniques for measuring soot particle thermophoretic diffusivities in combustion gases; (2) role of thermophoresis and photophoresis in the capture of soot particles; (3) boundary layer computational methods and correlations for vapor and small particle transports, including the effects of particle size polydispersity, high mass loading and dopant redistribution; and (4) use of microwave-induced plasma emission spectroscopic (MIPES) methods to follow boron surface gasification kinetics in gaseous streams containing OBOBO(g). Presentations and archive publications describing these techniques and findings are documented, along with examples of impact of our results on research programs elsewhere. GRA

N90-13621# Defence Research Establishment Suffield, Ralston (Alberta).
RECOVERY OF PARTICLE SIZE DISTRIBUTION OF ULTRAFINE AEROSOLS FROM DIFFUSIONAL DECAY MEASUREMENTS Final Report, Jan. - Jun. 1989
Eugene C. Yee Aug. 1989 36 p
(AD-A213006; DRES-SR-527) Avail: NTIS HC A03/MF A01 CSCL 07/4

An important aspect in the assessment of the hazard posed by the dissemination of chemical and biological warfare agents, including toxins, involves the characterization of the distribution of toxic material as a function of the size of the toxic particles. Diffusion batteries are perhaps one of the best devices for the measurements of the size distribution of ultrafine aerosols with radii in the interval from 0.001 to 0.1 micrometer. A new procedure is presented for reconstruction a submicron aerosol particle size distribution function (PSDF) from a finite number of noisy diffusion battery measurements. This ill-posed problem is solved by utilizing a maximum entropy approach to select, as the solution, that unique PSDF which maximizes the Shannon-Jaynes entropy subject to the constraints imposed by the given measurements. The utility of the method is demonstrated by a number of numerical examples with both noise-free and noisy synthetic diffusion battery data. This new method is compared to two existing inversion procedures and is shown to have superior performance is almost all of the simulated data examples test. GRA

N90-13622# Army Lab. Command, Watertown, MA. Material Technology Lab.
STUDIES OF AFLAS FLUOROELASTOMERS Final Report
Catherine A. Byrne Jul. 1989 24 p
(AD-A213046; MTL-TR-89-69) Avail: NTIS HC A03/MF A01 CSCL 11/10

This report includes studies of Aflas, a family of Japanese fluoroelastomers, and comparison of these materials with two important fluoroelastomers manufactured in the United States. While Fluorel and Viton are prepared from only fluorinated monomers, Aflas is an alternating copolymer of tetrafluoroethylene and propylene. Because of the alternating character of the polymer, Aflas possesses many of the desireable properties of Fluorel and Viton and also has some unique properties which might make it useful in applications where the other two are inferior. Differences noted in this work include dielectric constants in the range of 10 to 11 for Fluorel and Viton and 2.6 for Aflas. GRA

N90-13623# State Univ. of New York, Buffalo. Dept. of Chemistry.
ELECTROCHEMISTRY AT VERY SMALL ELECTRODES Final Report, 1 Oct. 1983 - 30 Sep. 1989
Janet G. Osteryoung 30 Sep. 1989 8 p
(Contract N00014-84-K-0052; NR Proj. 051-855)
(AD-A213156) Avail: NTIS HC A02/MF A01 CSCL 09/1

Microelectrodes have been fabricated as cylinders and as disks or arrays of disks, by employing both conventional and e-beam lithography techniques. Theory has been developed for diffusion to a disk for a variety of electrochemical techniques, especially square wave voltammetry. Cylindrical carbon fiber electrodes have been used as substrates for anodic stripping voltammetry. Small mercury electrodes have been used as tools for investigating anodization reactions in the absence of supporting electrolyte. The properties of low current at high current density and short diffusional relaxation times have been used for applications to corrosion problems. GRA

N90-13624# Illinois Univ., Urbana. Dept. of Materials Science and Engineering.
EFFECT OF ADSORBED ARSENIC ON THE DECOMPOSITION RATE OF NICKEL HYDRIDE
A. Kimura and H. K. Birnbaum 22 Aug. 1989 31 p
(Contract N00014-83-K-0468)
(AD-A213245; MRL-89-015) Avail: NTIS HC A03/MF A01 CSCL 11/6

The decomposition rate of nickel hydride was studied using x ray, Auger spectroscopy, and Secondary Ion Mass Spectrometry (SIMS) techniques. In high purity nickel, which was cathodically charged with hydrogen, deposition of arsenic on the nickel surface considerably decreased the decomposition rate of nickel hydride. This effect of arsenic on the egress of hydrogen from nickel is related to the influence of adsorbed arsenic on the entry of hydrogen into nickel during cathodic charging. Both effects result from inhibition of the recombination of hydrogen atoms at the surface thus resulting in a higher effective hydrogen fugacity at the surface. The effects of adsorbed arsenic on the decomposition of nickel hydride was influenced by alloying elements such as carbon and sulfur in the nickel, with the arsenic effect being greater in Ni-S alloys and smaller in Ni-C alloys than in high purity nickel. GRA

N90-13625# Massachusetts Inst. of Tech., Cambridge. Lab. of Electronics.
CHEMICAL BEAM EPITAXY OF ZnSe Semiannual Report, 1 Feb. - 31 Jul. 1989
Leslie A. Kolodziejski 31 Jul. 1989 7 p
(Contract N00014-88-K-0564)
(AD-A213265) Avail: NTIS HC A02/MF A01 CSCL 07/2

The objective of the program is to determine optimum growth parameters for the chemical beam epitaxy of ZnSe. In addition microstructural, optical, and electrical characterization of the material will be performed to assess the material's quality and potential. Comparisons will be made with material grown by molecular beam epitaxy. GRA

N90-13626# Ballistic Research Labs., Aberdeen Proving Ground, MD.
THE MOBILE COMBUSTION DIAGNOSTIC FIXTURE AND ITS APPLICATION TO THE STUDY OF PROPELLANT COMBUSTION. PART 1: INVESTIGATION OF THE LOW PRESSURE COMBUSTION OF LOVA XM39 PROPELLANT Technical Report, Oct. 1987 - Oct. 1988
J. O. Doali, Robert A. Fifer, David L. Kruczynski, and Bonita J. Nelson Aug. 1989 35 p
(AD-A213272; BRL-MR-3785) Avail: NTIS HC A03/MF A01 CSCL 19/1

A Mobile Combustion Diagnostic Fixture (MCDF) was fabricated to investigate the chemical products produced from the combustion of propellants at pressures below 16 MPa. These data are required in order to better understand the combustion phenomenology of propellants at low pressures. The design and capabilities of the

MCDF as well as preliminary chemical analysis of nonequilibrium ignition/combustion products using gas chromatography (GC) and Fourier transform infrared (FTIR) techniques from hot wire initiated LOVA XM39 propellant are presented. The experiments were performed in both a closed bomb mode and vented chamber mode at various loading densities and pressures. It was found that greater amounts of nonequilibrium combustion products were produced under interrupted burning conditions than under closed bomb conditions and that these products decreased with increasing burst disc pressure and increased with higher loading density. GRA

N90-13627# Carnegie-Mellon Univ., Pittsburgh, PA. Intelligent Sensors Lab.

GAS IDENTIFICATION SYSTEM USING GRADED TEMPERATURE SENSOR AND NEURAL NET INTERPRETATION

Lanwai Wong, Toshikazu Takemori, and M. W. Siegel Jul. 1989 19 p

(AD-A213359; CMU-RI-TR-89-20) Avail: NTIS HC A03/MF A01 CSCL 13/12

The demand for selectively sensing vapors and gases is keen. For example, it would be valuable to distinguish toxic exhaust gases from fuel vapors and warn of either of these in the passenger compartment of automobiles, boats, and airplanes. Similarly, it is important for a domestic gas leakage detection system to avoid false alarms by differentiating between the odors of alcoholic beverages and the utility gases. An innovative approach is described for enhancing the selectively of an integrated multi-element thick film gas sensor. A temperature gradient maintained along the sensor surface induces spatial sensitivity and selectivity gradients. The response map of the sensor is examined in the vapor of several organic compounds and their binary mixtures. Subtle but recognizable and separable signatures are observed. Emphasis is on identification, since quantitation of identified mixtures is straightforward. An effective and robust classification technique using a neural network trained via the back propagation method is described. GRA

N90-13628# San Diego State Univ., CA.

NUCLEAR MAGNETIC RESONANCE SIGNATURES OF NITROGEN-CONTAINING COMPOUNDS Final Report, Oct. 1987 - May 1988

L. J. Burnett, J. P. Sanders, and M. A. Fineman Aug. 1989 96 p

(Contract N66001-87-D-0136)

(AD-A213375; NOSC/TD-1632) Avail: NTIS HC A05/MF A01 CSCL 20/5

Experiments were conducted to determine if unique NMR signatures can be detected and defined for the proton NMR signals of nitrogen-containing compounds. Compounds of particular interest include explosives and explosive stimulants. The effects of off resonance radio frequency (RF) irradiation, or pumping, were observed in three nitrogen-containing compounds: HMT, TNT, and PETN. Similar effects were observed in mannitol and in the plastic explosive C-4 but dielectric heating of the sample C-4 made it impossible to apply the required sequence of RF pulses. The NMR FID signal from C-4 contains two distinct components. At present, methods to enhance the effects of off-resonance irradiation and improve the NMR signature are not obvious. With proper design, it may be possible to take advantage of the observed effects in field-usuable NMR explosive detectors. GRA

N90-13629# Deutsche Forschungsanstalt fuer Luft- und Raumfahrt, Stuttgart (Germany, F.R.). Inst. fuer Technische Thermodynamik.

GAS EVOLUTION AND BUBBLE FORMATION ON ELECTRODES Ph.D. Thesis - Stuttgart Univ.

Michael Dinkelacker May 1989 150 p In GERMAN; ENGLISH summary Report will also be announced as translation (ESA-TT-1191)

(DLR-FB-89-35; ISSN-0171-1342; ETN-90-95844) Avail: NTIS HC A08/MF A01; DLR, VB-PL-DO, Postfach 90 60 58, 5000 Cologne, Fed. Republic of Germany, 47 Deutsche Marks

The influence of bubble formation on the electrode overvoltages in alkaline water electrolysis is investigated. Fundamental phenomena of the electrolytic gas generation and bubble formation are examined. Similarities and differences to thermal boiling are discussed. It is shown experimentally and theoretically that gas generation and bubble formation cause not only an ohmic potential drop but also an increase in electrochemical overvoltage and the thermodynamical potential. The experimental and theoretical results show that in the range of little current densities the bubble behavior is governed by diffusion and is therefore similar to that of thermal boiling. In extremely high current density ranges a thermal boiling phenomena occurs in the limit case electrode due to high heat evolution. In the intermediate technical current density range the gas generation and bubble formation is governed by increasing current density and by electrochemical coherence. ESA

N90-13630 Institut d'Aeronomie Spatiale de Belgique, Brussels.

ULTRAVIOLET ABSORPTION CROSS-SECTIONS OF BROMOFORM IN THE TEMPERATURE RANGE 295-240 K

D. Gillotay, A. Jenouvrier, B. Coquart, M. F. Merienne (Reims Univ., France.), and P. C. Simon 1989 26 p Prevoiusly announced in IAA as A90-12722 Submitted for publication

(Aeronomica-Acta-A-348-1989; ISSN-0065-3713; ETN-90-96032) Avail: Institut d'Aeronomie Spatiale de Belgique, 3 Avenue Circulaire, B-1180 Brussels, Belgium

Ultraviolet absorption cross-sections of bromoform (CHBr3) are measured for temperatures ranging from 295 to 240 K with two different types of experimental equipment: one with a fixed optical path of 200 cm for wavelengths ranging from 170 to 300 nm and one with a multiple reflection cell in the wavelength region of 252 to 310 nm. These two sets of data are in very close agreement (better than the uncertainties quoted for each measurement) in the overlap region. The full compatibility and complementarity of the two experimental devices in determining absorption cross-section of atmospheric constituents are demonstrated. ESA

N90-13631# Kernforschungsanlage, Juelich (Germany, F.R.). Inst. fuer Chemie 1: Nuklearchemie.

PREPARATION OF BINARY ICE LAYERS BY CONDENSATION FROM GAS PHASE

E. Biel, A. Patnaik, and K. Roessler Dec. 1988 66 p In GERMAN; ENGLISH summary

(Juel-2248; ISSN-0366-0885; ETN-90-95327) Avail: NTIS HC A04/MF A01

Binary ice layers of H2O/NH3, H2O/CO2, NH3/CO2 (77 K), and H2O/CH4 (10 K) are prepared by condensing gas mixtures of defined composition onto a cold KBr plate in a cryostat at a vacuum of about 0.00001 mbar. Layer thickness and composition are determined via infrared spectroscopy in transmission. It is shown that in the CO2 spectrum (13)CO2 possesses other transmission characteristics than (12)CO2, most probably due to lesser amounts of phonon coupling in the (13)CO2. For all systems, the condensates show a depletion of the more volatile component with respect to the gas phase. The relative depletion is maximum for about 1:2 (heavy:light volatile) gas mixtures and more expressed for 77 K than for 10 K. The condensation behavior is not always regular due to thermal effects of the warm gas and varying crystallization seed effects by impurities. The layers are stable at 10 or 77 K over a period exceeding 7 h. During layer growth the composition did not change with condensation time. ESA

N90-13632# Office National d'Etudes et de Recherches Aerospatiales, Paris (France). Direction de la Physique Generale.

STUDY OF THE HYDROXYL RADICAL BY DRASC RESONANCE IN A HIGH PRESSURE FLAME Final Report [ETUDE DU RADICAL OH DANS UNE FLAMME A HAUTE PRESSION PAR DRASC RESONNANTE]

B. Tretout Feb. 1989 75 p In FRENCH

(Contract DRET-BC-88-001-16)

(ONERA-RS-53/7131-PY; ETN-90-95717) Avail: NTIS HC A04/MF A01

Research carried out with a high pressure flame facility using Diffusion Raman Anti-Stokes Coherence (DRASC) is described. Study of the spatial distribution of hydroxyl radicals in the flame of a premixed methane/air mixture is described. Different pressures from one to ten bar are used. Triple resonance spectroscopy and laser techniques are used to analyze concentrations just above the reaction area. The maximum detection sensitivity at one bar is approximately 6 ppm at 2200K. This figure is one hundred times greater at ten bar. The maximum detection sensitivity is calculated to be reached at thirty bar due to limitations in the power of the lasers used. ESA

N90-13633# Technische Univ., Eindhoven (Netherlands).
ELECTROCHEMICAL STUDY OF THE ETCHING OF III TO V SEMICONDUCTORS Ph.D. Thesis
Petrus Henricus Laur Notten 1989 309 p Sponsored by the Philips International B.V., Eindhoven, Netherlands
(ETN-90-96015) Avail: NTIS HC A14/MF A02

The use of semiconductors, composed of group III to V elements, in etching is studied. The etching properties of GaAs and InP in the dark in a large number of aqueous solutions is analyzed. The dependence of the dissolution rate of the semiconductor, on the applied potential is examined. A model, in which a simultaneous rupture of the bonds in the solid and in the bifunctional etching agent is followed by the instantaneous of new surface bonds, is proposed. The results lead to the conclusion that the electrochemical measurements are suitable for the semiconductor compounds etching investigations. ESA

N90-13634 National Physical Lab., Teddington (England). Div. of Materials Applications.
QUANTITATIVE AES AND XPS: DETERMINATION OF THE ELECTRON SPECTROMETER TRANSMISSION FUNCTION AND THE DETECTOR SENSITIVITY ENERGY DEPENDENCIES FOR THE PRODUCTION OF TRUE ELECTRON EMISSION SPECTRA IN AES AND XPS
G. C. Smith and M. P. Seah Aug. 1989 49 p
(NPL-DMA(A)-194; ISSN-0143-7313; ETN-90-96018) Copyright Avail: National Physical Laboratory, Teddington, Middlesex TW11 OLW, United Kingdom

The energy dependance of both the spectrometer transmission function and the detector sensitivity, in Auger Electron Spectroscopy (AES) and X rays Photoelectron Spectroscopy (XPS), is investigated. Measurements for a modified metrology spectrometer, operated in both the constant delta E/E and constant delta E modes, are presented and compared with theoretical estimates. It is shown that an electron-optical calculation is required to match the accuracy of the experimental procedures. Removal of the spectrometer transmission function and the detector sensitivity terms allows the measured spectrum to be converted to the true electron emission spectrum irrespective of the mode of operation. ESA

26 METALLIC MATERIALS

Includes physical, chemical, and mechanical properties of metals, e.g., corrosion; and metallurgy.

N90-13635# Stuttgart Univ. (Germany, F.R.). Staatlichen Materialpruefungsanstalt.
EXPERIMENTAL AND NUMERICAL INVESTIGATIONS OF THE CRACK ARREST BEHAVIOR OF STEELS AND CAST IRON MATERIALS [EXPERIMENTELLE UND NUMERISCHE UNTERSUCHUNGEN ZUM RISSSTOPP-- VERHALTEN VON STAEHLEN UND GUSSEISENWERKSTOFFEN]
Rainer Gillot Apr. 1988 195 p In GERMAN Original contains color illustrations
(Contract BMFT-FK-150-0304-B)
(MPA-TWB-88-03; ETN-89-94604; ISSN-0721-4529) Avail: NTIS HC A09/MF A01

The crack arrest toughness of different container steels is investigated, and the applicability of proposals for standards for cast iron materials is examined. A test set up for the temperature range between -200 and 450 C for different sample dimensions is built. A measuring system for the determination of sample opening, test temperature and crack propagation is presented. After tempering of the sample, the crack length and crack structure are determined. The stress-strain behavior of compact samples is calculated using the finite element method. The transferability of the obtained characteristics to real components is verified. ESA

N90-13636*# National Aeronautics and Space Administration. Lewis Research Center, Cleveland, OH.
THERMAL BARRIER COATINGS FOR GAS TURBINE AND DIESEL ENGINES
Robert A. Miller, William J. Brindley, and M. Murray Bailey 1989 9 p Presented at the 11th Workshop on Ceramic Coatings for Wear and Thermal Applications, Edmonton, Alberta, 16-17 Oct. 1989; sponsored by the Canadian Univ.-Industry-Council on Advanced Ceramics
(NASA-TM-102408; E-5160; NAS 1.15:102408) Avail: NTIS HC A02/MF A01 CSCL 11F

The present state of development of thin thermal barrier coatings for aircraft gas turbine engines and thick thermal barrier coatings for truck diesel engines is assessed. Although current thermal barrier coatings are flying in certain gas turbine engines, additional advances will be needed for future engines. Thick thermal barrier coatings for truck diesel engines have advanced to the point where they are being seriously considered for the next generation of engine. Since coatings for truck engines is a young field of inquiry, continued research and development efforts will be required to help bring this technology to commercialization. Author

N90-13637# Army Lab. Command, Watertown, MA. Material Technology Lab.
MECHANICAL PROPERTY CHARACTERIZATION OF VASCOMAX T-300 Final Report
Charles F. Hickey, Jr., David W. Dix, and David Kagan Aug. 1989 16 p
(AD-A212950; MTL-TR-89-81) Avail: NTIS HC A03/MF A01 CSCL 11/6

This report addresses a mechanical property characterization of 18 percent Nickel 300 grade cobalt-free maraging steel (T-300). Hardness, tensile, Charpy V-notch impact energy, and fracture toughness data were obtained for a 2-3/8-inch-diameter forged bar. These data are presented along with existing data on stress corrosion, microstructure, and ballistic performance for this and other maraging steels. The results indicated that the mechanical properties are more dependent on the aging temperature than on the aging time for the temperatures of 900 F and 950 F, and times of 3 and 4 hours. Both hardness and Charpy impact energy were unaffected by varying the aging temperatures and times, while the tensile properties and fracture toughness increased in response to the increase in aging temperature. Based on the information obtained in this study and the existing information available on this alloy, the recommended aging treatment is 950 F for 4 hours. GRA

N90-13638# Northwestern Univ., Evanston, IL. Center for Quality Engineering and Failure Prevention.
REFLECTION BY DEFECTIVE DIFFUSION BONDS Interim Report
Jan D. Achenbach and Yonglin Xu 15 Aug. 1989 7 p
(Contract N00014-89-J-1362)
(AD-A212995; NU-CENTER-QEFP-1989-3) Avail: NTIS HC A02/MF A01 CSCL 11/6

The reflection of ultrasonic wave motion by planar defect distributions is investigated, with a view towards a method to detect and characterize bond-plane defects and with an ultimate objective of providing information on the bond strength of metal to metal bonds. The primary concern is with an approximate approach to analyze reflection by cavities and cracks which are distributed in

a bond plane. The results show some of the characteristic features of reflection with variation of such parameters as angle of incidence, frequency, defect size, defect shape and defect spacing. Metal to metal bonds by the diffusion welding process are becoming more frequently used for the fabrication of complicated parts, such as integrally bladed compressor and turbine rotors in gas turbine engines. Diffusion bonds may, however, have three kinds of defects: volumetric defects (voids, inclusions), crack-like defects, and crystalline grains. GRA

N90-13639# Naval Air Development Center, Warminster, PA. Air Vehicle and Crew Systems Technology Dept.
QUENCH SENSITIVITY IN Al-Cu-Li ALLOYS Final Report, 1 Oct. 1988 - 1 Oct. 1989
Mary E. Donnellan and William E. Frazier 14 Feb. 1989 33 p (Proj. RS34A50)
(AD-A213055; NADC-89046-60) Avail: NTIS HC A03/MF A01 CSCL 11/6

The quench sensitivity of an aluminum-copper-lithium alloy, 2090 was characterized. The mechanical properties were evaluated from samples subjected to different quench conditions and heat treatments. Transmission electron microscopy (TEM) was used to examine the microstructural characteristics of the alloy. The results are described with respect to correlations between microstructural characteristics and strength. A range for the critical quench rate of alloy 2090 was established. The effect of quench sensitivity on hardness and conductivity is also discussed. GRA

N90-13640# Army Lab. Command, Watertown, MA. Material Technology Lab.
THE EFFECT OF COMPOSITION AND AGING TREATMENT ON THE MICROSTRUCTURE AND MECHANICAL PROPERTIES OF ALUMINUM-LITHIUM-TITANIUM ALLOYS Final Report
Marietta R. Cappucci Aug. 1989 104 p
(AD-A213144; MTL-TR-89-78) Avail: NTIS HC A06/MF A01 CSCL 11/6

Aluminum lithium alloys have recently been recognized for their potential as aerospace alloys. Al-Li alloys offer the combination of high strength and elastic modulus with low density, thereby resulting in substantial weight and cost savings. The precipitation of the metastable delta' (Al3Li) phase upon aging provides considerable increases in strength. The major problem encountered thus far is that the delta' phase, due to its shearable nature, causes slip localization, reducing ductility and fracture toughness. The present study is based on the theory that by altering the precipitation behavior and characteristics by additions of titanium it will be possible to disperse slip and consequently increase fracture toughness. Titanium has been selected as the alloying element because in the Al-Ti binary system Al3Ti forms with lattice parameter and crystal structure similar to those of Al3Li. The mechanical properties of the alloys have been determined at several aging conditions. The strength of the alloy increases significantly at each aging condition as titanium is added to the system. Elongation to failure remains fairly constant with titanium additions, but fracture toughness drops as higher amounts of titanium are added. The 3Li to 0.2Ti alloy shows the best combination of strength and toughness. GRA

N90-13641# Illinois Univ., Urbana. Dept. of Materials Science and Engineering.
ANOMALOUS STRAIN RATE DEPENDENCE OF THE SERRATED FLOW IN Ni-H AND Ni-C-H ALLOYS
A. Kimura and H. K. Birnbaum Sep. 1989 27 p
(Contract N00014-83-K-0468)
(AD-A213244; MRL-88-0007) Avail: NTIS HC A03/MF A01 CSCL 11/6

Serrated flow in Ni-H, Ni-C-H, and Ni-C alloys was studied over a wide range of temperature and strain rates. The results for C related serrated flow in Ni-C or Ni-C-H alloys were in excellent agreement with previous results and were consistent with dislocation pinning by C solutes at the dislocation cores. Hydrogen related serrated yielding was observed in Ni-H and Ni-H-C alloys. Solute C had only a small effect on the temperature range of this H related serrated flow. The results could be interpreted on the basis of hydride formation at the dislocation cores and diffusion of H in these hydrides. GRA

N90-13642# Westinghouse Electric Corp., Middletown, RI. Hydrothermodynamics Research and Technology.
METAL TRANSFER IN GAS METAL ARC WELDING Final Report, 21 Sep. 1988 - 30 Sep. 1989
Donald M. McEligot 30 Sep. 1989 124 p
(Contract N00014-88-C-0393)
(AD-A213390; WNSD/HYDRO-89-06) Avail: NTIS HC A06/MF A01 CSCL 11/6

The ultimate goal of the present work is to develop sufficient fundamental understanding of generic GMA welding to enable prediction of the weld quality to be made in terms of the material properties and control parameters. Evidence from experiments and simple analyses shows that the melting rate is controlled by the thermofluid mechanic behavior of the solid electrode and the molten electrode tip. Consequently, an analytical and numerical study of the transient, thermalfluid mechanic behavior of the electrode region in GMA welding continues. Two idealized regions separately are discussed: steady thermal conduction in a moving solid electrode and transient droplet formation. The method of superposition and classical techniques were used to describe the temperature distribution in an electrode heated on the side by electron condensation. A transient numerical analysis for the liquid droplet or streaming jet is being developed using LaGrangian governing equations. GRA

N90-13643 British Petroleum Co. Ltd., London (England).
WEAR-RESISTANT COATED OBJECT Patent Application
Nigel Keith Gibbs, inventor 14 Apr. 1988 6 p
(EP-Patent-0-289-173-A1; EP-Patent-Appl-SN-88-303394-6; Int-Patent-Class-C23C-28/00; Int-Patent-Class-C23C-14/02; ETN-90-95241) Avail: European Patent Office, Erhardtstr. 27, 8000 Munich 2, Fed. Republic of Germany

The invention of a wear resistant coated object and its preparation are described. The coating comprises a series of layers of titanium nitride, interspersed with alternate layers of titanium. The total thickness of the composite coating is at least ten microns. The performance of the proposed titanium composite coating, concerning toughness, hardness, strength and adhesion, is tested. It is to be applied in abrasive wear conditions such as: hydraulic piston rams in abrasive liquid environment; gate, ball and choke values in oil fields; thrust bearing in down hole turbo drills; mud pump cylinder lines; seals; turbine blades; pump impellers/housings; extrusion dies; thread guides; cutting blades; and bearings. The coating making method comprises the physical vapor deposition of titanium and titanium nitride layers on the substrate. ESA

N90-13644# Deutsche Forschungsanstalt fuer Luft- und Raumfahrt, Cologne (Germany, F.R.). Inst. fuer Raumsimulation.
NUCLEATION KINETICS IN UNDERCOOLED, GLASS-FORMING METALLIC MELTS Ph.D. Thesis - Ruhr Univ.
Friedhelm Gillessen Jun. 1989 103 p In GERMAN; ENGLISH summary
(DLR-FB-89-32; ISSN-0171-1342; ETN-90-95841) Avail: NTIS HC A06/MF A01; DLR, VB-PL-DO, Postfach 90 60 58, 5000 Cologne, Fed. Republic of Germany, 32.50 Deutsche Marks

A quasi-containerless technique by fluxing the melt in B2O3 and containerless solidification in a drop tube is used to undercool melts. The results of the experiments indicate a dependence of both, the glass-forming ability and the undercooling behavior, on the cooling rate and overheating temperature of the melt. It is assumed that associates of intermetallic compound exist in the melt, which can act as heterogeneous nucleation sites. Overheating the melt above the melting temperature of the corresponding intermetallic phase dissolves the nucleants. This, in connection with reduced surface-induced nucleation, leads to an extension of undercooling and an improvement of the glass-forming ability. In the case of Pd40Ni40P20 such conditions enable even the

preparation of bulk amorphous spheres in diameters as large as 5 mm at extremely low cooling rate of 1 to 3 K/s. Using an isothermal approach, the nucleation kinetics are analyzed in the framework of classical nucleation theory allowing the quantitative development of so-called temperature time nucleation diagrams for various nucleation processes. ESA

N90-13645# Deutsche Forschungsanstalt fuer Luft- und Raumfahrt, Brunswick (Germany, F.R.). Inst. fuer Raumsimulation.
CONTAINERLESS PROCESSING OF METALS: UNDERCOOLING AND SOLIDIFICATION
Ivan Egry and Jochen Laakmann (Aachener Centrum fuer Erstarrung unter Schwerelosigkeit e.V., Germany, F.R.) Apr. 1989 92 p Proceedings of an International Conference held in Cologne, Fed. Republic of Germany, 12-13 Dec. 1988; Sponsored by NASA and Bundesministerium fuer Forschung und Technologie
(DLR-Mitt-89-15; ISSN-0176-7739; ETN-90-95849) Avail: NTIS HC A05/MF A01; DLR, VB-PL-DO, Postfach 90 60 58, 5000 Cologne, Fed. Republic of Germany, 28 DM

A workshop aimed at exploring the possibilities of containerless processing under microgravity with respect to studies of undercooling and solidification of metals is described. If a controlled solidification from the undercooled melt can be achieved, production of materials with tailored properties would become possible. On the ground, the electromagnetic levitation technique can be used to undercool metallic melts. Applying this technique under microgravity conditions, only the small residual accelerations need to be compensated. This leads to much smaller positioning fields, and, correspondingly, to improved processing conditions and an extended range of parameters. In particular, lower temperatures can be achieved. In order to exploit this potential, Dornier has built the TEMPUS facility, an electromagnetic heating and positioning system, designed to operate in microgravity. Abstracts of the papers presented at the workshop, and when available, copies of the viewgraphs are included. ESA

N90-13646# Technische Univ., Delft (Netherlands). Heat Treatment Science and Technology Div.
INTERNAL AND EXTERNAL NITRIDING AND NITROCARBURIZING OF IRON AND IRON-BASED ALLOYS Ph.D. Thesis
Marcel Adrianus Joha Somers 1989 285 p Sponsored by the Stichting voor Fundamenteel Onderzoek der Materie, Netherlands
(ETN-90-96012) Avail: NTIS HC A13/MF A02

The phenomena occurring during thermochemical surface treatments, such as nitriding and nitrocarburizing on iron and iron based alloys, are investigated. The solid state precipitation phenomena, the development, the relaxation of residual stresses in surface layers and the kinetics of diffusion layer growth, are considered. The internal nitriding of (originally) binary iron-metal alloys is studied. The external nitriding of pure iron, in particular the development and relaxation of residual stresses in the nitride surface layer, is discussed. The determination of residual stress-depth and composition-depth profiles, using x ray diffraction techniques, is shown. The influence of phase transformations on residual stresses in the gamma prime layer, and the role of carbon during nitrocarburizing, are reported. ESA

N90-13647# Kernforschungszentrum G.m.b.H., Karlsruhe (Germany, F.R.). Inst. fuer Material- und Festkoeperforschung.
CORRELATION BETWEEN MICROSTRUCTURE AND MAGNETIC PROPERTIES OF POROUS SINTERED IRON AND POROUS IRON CONTAINING COMPOSITES Ph.D. Thesis - Tech. Hochschule, Aachen
E. Remane May 1989 73 p In GERMAN; ENGLISH summary
(KfK-4522; ISSN-0303-4003; ETN-90-95328) Copyright Avail: NTIS HC A04/MF A01

The dependence of magnetic induction on the microstructure of two-phase materials is investigated. Investigations based on the microstructure-field property correlation by Ondracek are described. Sintered iron toroids show different microstructures when analyzed by an image analyzing computer. Theoretical values are in good accordance with the experimental results. Iron powder and NiZn-ferrite powder of different mixtures are pressed at different compacting pressures and sintered at 850 C and 950 C. At these temperatures the material is thermodynamically unstable. Independent of the amount of iron powder, the spinel lattice of the ferrite is destroyed and several unmagnetic phases are produced. By means of the microstructure-field property correlation the induction behavior of the material is calculated. ESA

N90-13648# Institut National des Sciences Appliquees de Lyon, Villeurbanne (France). Lab. de Physicochimie Industrielle.
CONTRIBUTION TO THE ELECTROCHEMICAL STUDY OF CORROSION IN THE LOW CONDUCTIVITY MEDIA: APPLICATION TO THE STUDY OF THE BEHAVIOR OF AUSTENITIC STAINLESS STEELS IN CONCENTRATED SOLUTIONS OF ACETIC ACID Ph.D. Thesis [CONTRIBUTION A L'ETUDE ELECTROCHIMIQUE DE LA CORROSION DANS LES MILIEUX A FAIBLE CONDUCTIVITE: APPLICATION A L'ETUDE DU COMPORTEMENT D'ACIERS INOXYDABLES AUSTENITIQUES DANS LES SOLUTIONS CONCENTREES D'ACIDE ACETIQUE]
Serge Chechirlian 1989 220 p In FRENCH
(ISAL-89-0014; ETN-90-95513) Avail: NTIS HC A10/MF A02

The experimental difficulties for the study of the corrosion in concentrated solutions of acetic acid are studied. Stainless steels corrosion is studied with the help of experimental devices which are described. The favorable effect of molybdenum and the negative effects of sulphur and silicon are demonstrated. ESA

N90-13649# Centre de Recherches Scientifiques et Techniques de l'Industrie des Fabrications Metalliques, Brussels (Belgium).
[ACTIVITIES REPORT OF THE METALLIC MANUFACTURING INDUSTRY] Annual Report, 1988 [RAPPORT ANNUEL DU COMITE PERMANENT AU CONSEIL GENERAL]
Jun. 1989 62 p In FRENCH
(ISSN-0524-7705; ETN-90-95743) Avail: NTIS HC A04/MF A01

The research and development studies, carried out in 1988, on the research center of the metallic manufacturing industry, are reported. The report content includes: metal casting, bridges and basic structure, boiler making, welding, mechanical construction, industrial computer applications, plastics, surface covering, local projects of global interest, standardization and specifications, materials data base, ceramic-metal joints and robots in the industry. ESA

N90-13650# Rome Univ. (Italy). Dipt. di Fisica.
ENERGY CONCENTRATION INDUCED BY PHASE TRANSITIONS IN HYDROGENATED METALS
M. Cassandro, G. Gallavotti, and G. Jona-Lasinio 12 May 1989 8 p
(Preprint-672; ETN-90-95800) Avail: NTIS HC A02/MF A01

A mechanism capable of producing, at least in principle, a considerable energy concentration in a space of the order of a single crystal cell in hydrogenated (or deuterated) metals is discussed. It is based on a release of elastic energy in the lattice of the host metal as a consequence of a phase separation of the absorbed gas in non equilibrium conditions. Quantitative estimates and experimental consequences are discussed. ESA

N90-13651# Technical Research Centre of Finland, Espoo. Metallurgy Lab.
THE EFFECTS OF ALLOYING AND THERMAL FACTORS ON THE SOLIDIFICATION AND MECHANICAL PROPERTIES OF GRAY IRON
Yunfeng Yang, Arno Luovo, and Tapio Rantala May 1989 35 p Sponsored by the Nordisk Industrifond
(VTT-619; ISBN-951-38-3428-X; ISSN-0358-5077; ETN-90-96022) Copyright Avail: NTIS HC A03/MF A01; Government Printing Center, P.O. Box 516, SF-00101 Helsinki, Finland, 40 Finnish marks

The quantitative studies of the combined effects of thermal

factors and alloying on the solidification processes and properties of low alloy gray iron, are presented. A derivative thermal analysis system and several computer programs are established and the cooling rate at 900 C provides the best prediction of the final properties and microstructures under fixed composition. The use of solidification simulation in property prediction is possible. Some alloying effects of molybdenum, chromium and vanadium are revealed, taking the cooling rate into consideration. The combined effects of both the alloying and the cooling rate are approximated in mathematical expressions. ESA

27 NONMETALLIC MATERIALS

Includes physical, chemical, and mechanical properties of plastics, elastomers, lubricants, polymers, textiles, adhesives, and ceramic materials.

For composite materials see *24 Composite Materials*.

N90-13652*# Morton Thiokol, Brigham City, UT. Space Div.
CONTAMINATION REMOVAL USING VARIOUS SOLVENTS AND METHODOLOGIES
J. C. Jeppsen May 1989 29 p Revised
(Contract NAS8-30490)
(NASA-CR-183747; NAS 1.26:183747; TWR-18445-Rev-A) Avail: NTIS HC A03/MF A01 CSCL 11G

Critical and non-critical bonding surfaces must be kept free of contamination that may cause potential unbonds. For example, an aft-dome section of a redesigned solid rocket motor that had been contaminated with hydraulic oil did not appear to be sufficiently cleaned when inspected by the optically stimulated electron emission process (Con Scan) after it had been cleaned using a hand double wipe cleaning method. As a result, current and new cleaning methodologies as well as solvent capability in removing various contaminant materials were reviewed and testing was performed. Bonding studies were also done to verify that the cleaning methods used in removing contaminants provide an acceptable bonding surface. The removal of contaminants from a metal surface and the strength of subsequent bonds were tested using the Martin Marietta and double-wipe cleaning methods. Results are reported. Author

N90-13653*# Morton Thiokol, Brigham City, UT. Space Div.
EFFECTS OF TACKY MAT CONTAMINATION ON BOND DEGRADATION FOR CHEMLOK/LINER AND NBR/LINER BONDS Final Report
A. M. Padilla Jun. 1989 9 p
(Contract NAS8-30490)
(NASA-CR-183742; NAS 1.26:183742; TWR-19544) Avail: NTIS HC A02/MF A01 CSCL 11C

Tacky mats are placed by the rubber lay-up areas for the solid rocket motor segments. These mats dust off the shoes prior to entering the platform where the lay-up work is performed. The possibility exists that a tacky mat could be touched with gloved hands prior to handling the uncured nitride butadiene rubber (NBR). Tests were run to determine if NBR were accidentally touched would there be any degradation of the liner/NBR bond. The tacky mats were judged solely on the basis of bond degradation caused by either direct or indirect contamination. Test results all indicate that there was no notable NBR/Chemlok or liner/NBR bond degradation on samples that came into contact with the tacky mat material. Testing procedures are described. The tacky mat adhesive composition does not contain fluorocarbons or release agents that would affect bonding. J.P.S.

N90-13654*# Morton Thiokol, Brigham City, UT. Space Div.
EVALUATION OF A METERING, MIXING, AND DISPENSING SYSTEM FOR MIXING POLYSULFIDE ADHESIVE Final Report
Kurt B. Evans Jun. 1989 26 p
(Contract NAS8-30490)
(NASA-CR-183749; NAS 1.26:183749; TWR-16417) Avail: NTIS HC A03/MF A01 CSCL 11C

Tests were performed to evaluate whether a metered mixing system can mix PR-1221 polysulfide adhesive as well as or better than batch-mixed adhesive; also, to evaluate the quality of meter-mixed PR-1860 and PS-875 polysulfide adhesives. These adhesives are candidate replacements for PR-1221 which will not be manufactured in the future. The following material properties were evaluated: peel strength, specific gravity and adhesive components of mixed adhesives, Shore A hardness, tensile adhesion strength, and flow rate. Finally, a visual test called the butterfly test was performed to observe for bubbles and unmixed adhesive. The results of these tests are reported and discussed. Author

N90-13655# Washington Univ., Seattle. Dept. of Materials Science and Engineering.
SYNTHESIS OF INORGANIC POLYMERS AS GLASS PRECURSORS AND FOR OTHER USES. PRECERAMIC BLOCK OR GRAFT COPOLYMERS AS POTENTIAL PRECURSORS TO NANOCOMPOSITE MATERIALS
Kay A. Youngdahl, Martin L. Hoppe, Richard M. Laine, Jeffrey A. Rahn, and John F. Harrod 1989 13 p
(Contract N00014-88-K-0305)
(AD-A211978; TR-17) Avail: NTIS HC A03/MF A01 CSCL 07/6

Preceramic block or graft copolymers may offer entree into nanocomposite ceramics provided the two homopolymers are immiscible and one can carefully control the size of the blocks or grafts. We are exploring the possibility of making copolymers from methylsilsesquioxane, (MeSiO1.5)(x)(SiO), a precursor to black glass and the polysilazane, (MeHSiNH)(x)(SiMe), a precursor to silicon carbide nitride. Our initial efforts have been directed towards delineating the chemical transformations that SiO, prepared by room temperature catalytic redistribution of (MeHSiO)(x) using Cp2TiMe2 as the catalyst (0.1 wt pct), undergoes as it is heated to 900 C in N2. We find that Cp2TiMe2 will not catalyze the redistribution of SiMe at room temperature; but, in the presence of even small amounts of (MeHSiO)(x), it is an active catalyst precursor and copolymer can be formed. Spectral and chemical composition studies on the pyrolysis products of the copolymers and SiO are described. GRA

N90-13656# National Inst. of Standards and Technology, Gaithersburg, MD. Ceramics Div.
TOUGHENING MECHANISMS IN CERAMIC COMPOSITES Semiannual Interim Progress Report, period ending 31 Mar. 1989
E. R. Fuller, Jr., E. P. Butler, R. F. Krause, Jr., and M. D. Vaudin Jul. 1989 29 p
(Contract DE-AI05-80OR-20679)
(PB89-235907; NISTIR-89/4111) Avail: NTIS HC A03/MF A01 CSCL 11C

A silicon carbide fiber used as reinforcement in a boro-silicate glass matrix has been shown to enhance the fracture toughness of the glass by as much as 22 percent. A ductile nickel coating on the fiber was found to reduce the interfacial shear strength and the frictional sliding between the fibers and the glass matrix, but any influence that the thickness of the nickel coating has on toughening was not conclusive. Time functions of creep strain and creep times to failure were measured for a 25 wt percent SiC whisker-reinforced Al2O3 composite with 4.9 percent porosity. Beam specimens were used in four-point flexure with variously fixed bending moments and fixed temperatures between 1100 and 1300 C. The secondary creep-strain rates of specimens tested at lower stresses did not follow a power-law function of stress which was fitted to the high stress data. The microstructure of as-received specimens and specimens crept to failure were studied using optical and electron microscopy to determine the mechanisms of creep in the two stress regimes. Both kind of specimens contained cavitation at the whisker/Al2O3 grain boundary intersections to varying degrees. However, high stress specimens contained broken whiskers whereas those from low stress regime did not. Author

N90-13657# Centre National de la Recherche Scientifique, Dijon (France).
SURFACES AND INTERFACES OF CERAMIC MATERIALS
Louis C. Dufour, Claude Monty, and Georgette Petot-Ervas Sep. 1988 87 p
(AD-A212417; R/D-6143-MS-02) Avail: NTIS HC A05/MF A01 CSCL 11/2

Materials science of ceramic interfaces; Atomic structure of ceramic surfaces; Structure and microstructure of grain boundaries in ceramic materials; Ceramic-metal interfaces; The role of surfaces in ceramic processes; Segregation at ceramic surface and effects on mass transport; Grain boundary diffusion; Thermodynamics and chemistry of ceramic-metal interfaces; Intergranular phases in polycrystalline ceramics; Microstructure of composite interfaces and its relation to interfacial strength; The role of grain boundaries and interfaces on superconductivity; The theory of dopant and impurity segregation in ceramic oxides; The role of defects in the electronic structure of and chemisorption on oxide surfaces; Solid-gas and solid-solid interactions of ceramic materials at high temperatures; Structure of ceramic oxide-water interfaces; Reactions of ceramic oxides with aqueous solutions (including dissolution); Ionic conductivity and the role of surfaces and interface in ceramic electrolytes; Interfacial tension and contact angle in immiscible systems; Residual stresses in porous plasma-sprayed alumina coatings on titanium alloy for medical applications; Physical and chemical properties of sillicate materials; Characterization, properties and processing of ceramic powders; and sintering processes are discussed. GRA

N90-13658# Endochronics, Inc., Vancouver, WA.
A THEORY OF DAMAGE IN BRITTLE AND CEMENTITIOUS MATERIALS, PART 1 Final Report, 15 Jan. 1988 - 15 May 1989
K. C. Valanis and Khalid Khan (Portland Univ., OR.) 17 Jul. 1989 137 p
(Contract F49620-88-C-0038)
(AD-A212940; ENDIC-007-AFOSR-1989-Pt-1; AFOSR-89-1212TR-Pt-1) Avail: NTIS HC A07/MF A01 CSCL 11/2

The purpose of the present study was to develop a local three-dimensional continuum theory of damage. Two materials were investigated: grey cast iron and plane concrete. The basic concepts (such as the form of the free energy in the presence of damage) were tested on cast iron, which is a brittle substantially elastic material. This approach was very fruitful. The free energy representation proved correct in view of the excellent agreement between the calculated and experimental results in elastic domains with a sharp geometric discontinuity (a crack). Since in endochronic plasticity the free energy is the basis for the derivation of the constitutive equation, this result was instrumental in the development of a damage sensitive constitutive theory for concrete where the interaction between plasticity and damage posed complex questions. GRA

N90-13659# Chicago Univ., IL. Dept. of Chemistry.
A NEW MODEL FOR THE STRUCTURE OF SILICA GLASS Annual Report, 15 Apr. 1988 - 1 Aug. 1989
Carol S. Marians and Jeremy K. Burdett 20 Sep. 1989 48 p
(Contract N00014-85-K-0354)
(AD-A212972) Avail: NTIS HC A03/MF A01 CSCL 11/2

A new model is presented for the structure of silica glass. This modulated network model is a direct heir not only to the continuous random network model of Zachariasen, but also to the microcrystalline model of Phillips. It consists of domains of six-ring networks linked by interfacial material containing rings of other sizes. The model is supported by some new geometrical theorems which lead to important restrictions on the network topology. GRA

N90-13660# University of Southern California, Los Angeles. Dept. of Chemical Engineering.
MODEL FILLED POLYMERS I. SYNTHESIS OF CROSSLINKED MONODISPERSE POLYSTYRENE BEADS Technical Report No. 1, 1 May 1988 - 15 Aug. 1989
D. Zou, K. Gandhi, M. Park, L. Sun, D. Kriz, Y. D. Lee, G. Kim, J. J. Aklonis, and R. Salovey 16 Aug. 1989 29 p Submitted for publication
(Contract N00014-88-K-0302)
(AD-A213228) Avail: NTIS HC A03/MF A01 CSCL 07/6

Monodisperse crosslinked polystyrene beads of varied size and crosslink density are prepared by emulsion copolymerization of styrene and divinylbenzene in the absence of emulsifier. Tumbling and internally stirred reactors were used for synthesis, with minimal agglomeration for at least 0.22 weight percent potassium persulfate and up to 10 percent by weight of styrene in aqueous emulsion in the absence of oxygen. Particle sizes decreased from 800 to 200 nm on raising the polymerization temperature form 60 to 95 C. The glass transition temperature of the beads increased from 104.4 to 133 C by the inclusion of up to 10 percent by weight of divinylbenzene. The thermal stability of the beads was higher for peroxide than for persulfate initiation. The crosslink density estimated from the degree of swelling was about one third that expected from stoichiometry. The polystyrene beads are used as filler particles in polymer composites. GRA

N90-13661*# Thiokol Corp., Brigham City, UT. Space Operations.
EVALUATION OF NEWLY FORMULATED DOW CORNING 321 DRY FILM LUBRICANT Final Test Report
M. Cook 29 Sep. 1989 18 p
(Contract NAS8-30490)
(NASA-CR-183828; NAS 1.26:183828; TWR-19912; TWR-Publ-90197) Avail: NTIS HC A03/MF A01 CSCL 11C

An evaluation of the newly formulated Dow Corning 321 dry film lubricant was performed. The purpose of the evaluation was to compare lubricating characteristics of Dow Corning 321 (STW4-2955, SCN No. 3) to those of Molykote 321R (STW4-2955). Ten igniter bolts were installed and torqued on test plates using the old formulation thread lubricant (Molykote 321R), and 10 bolts were installed using the new formulation (Dow Corning 321). After bolt removal, no signs of galling were found on any of the bolts or test plates threaded holes. Average torque-load values for each formulation were very close. Test results showed there are no significant differences in lubrication abilities between Molykote 321R and Dow Corning 321. It is recommended that, once current supplies of Molykote 321R are depleted, Dow Corning 321 dry film lubricant be used in place of Molykote 321R as a thread lubricant on redesigned solid rocket motor assemblies. Author

N90-13662 British Petroleum Co. Ltd., London (England).
PROCESS FOR PRODUCING A SHAPED, EXTRUDED PRODUCT FROM A CROSSLINKABLE POLYMERIC COMPOSITION Patent Application
Antti Tapani Mattila, inventor, James Elliott Robinson, inventor, and Jeffrey David Umpleby, inventor 14 Feb. 1987 20 p
(GB-Patent-2-201-677-A; GB-Patent-Appl-SN-8703469; Int-Patent-Class-B29C-47/08; Int-Patent-Class-C08J-3/24; Int-Patent-Class-H01B-3/44; ETN-90-95244) Avail: UK Patent Office, 25 Southampton Buildings, London WC2A 1AY, United Kingdom

The invention of a process for producing a shaped, extruded product from a crosslinkable polymeric composition is described. The polymer composition comprises a copolymer of an alpha olefin with a hydrolysable ethylenically unsaturated silane compound. The process includes: introducing the copolymer compound into the feed zone of an extruder; compacting and melting the copolymer in the extruder; passing the compacted, molten copolymer through a distributive mixer positioned at the discharge end of the extruder; injecting a silanol condensation catalyst into the compacted, molten copolymer after compacting and melting in the extruder; blending the compacted, molten copolymer and the silanol condensation catalyst in the distributive mixer, and extruding the resulting blend

out of the distributive mixer through an extrusion die to form a shaped, crosslinkable, extruded product. The distributive mixer is preferably a cavity transfer mixer. The process is particularly useful for coating wires and cables and overcomes the problem of precuring the thermoformed copolymer. ESA

N90-13663 British Petroleum Co. Ltd., London (England).
CROSSLINKABLE POLYMER Patent Application
Jeffrey David Umpleby, inventor 9 Jun. 1988 10 p
(GB-Patent-2-205-846-A; GB-Patent-Appl-SN-8813692; Int-Patent-Class-C08F-230/08; ETN-90-95245) Avail: UK Patent Office, 25 Southampton Buildings, London WC2A 1AY, United Kingdom

The invention and the preparation process of crosslinkable thermoplastic organic and similar composition polymers are presented. The objective is to provide a product with improved properties. The water crosslinkable thermoplastic random interpolymer is prepared by radical interpolymerization, the interpolymer comprising: 78 to 98 weight percent of units derived from ethylene; 1.0 to 20 weight percent of units derived from ethyl acrylate and/or butyl acrylate; and 1.0 to 2.0 weight percent of units derived from an ethylenically unsaturated hydrolyzable silane compound (e.g. vinyltrimethoxy silane, a vinyl methyl dimethoxy silane). ESA

N90-13664# Helsinki Univ. of Technology, Espoo (Finland). Lab. of Physics.
COMPUTATIONAL STUDIES OF STRUCTURAL AND TRANSPORT PROPERTIES OF AMORPHOUS SOLIDS Ph.D. Thesis
Jari Laakkonen 1989 22 p Sponsored by the Finnish Cultural Foundation
(ETN-90-96027) Avail: NTIS HC A03/MF A01

The transport properties of simple metallic glasses and the structure and defects of amorphous solids, are studied. The transport properties are considered within the diffraction model. The electrical resistivity and the thermopower are examined. The MgZn and CaAl metallic glasses are studied. Some aspects of the fabrication technology are presented. For the structural analysis, measurements applying the Extended X ray Absorption Fine Structure (EXAFS), the nuclear magnetic resonance, the Moessbauer techniques are considered. The structural studies include generation of amorphous samples by computer simulation, development of methods to identify point defects in a one component amorphous solid and their use in analyzing radiation damage collision cascades. ESA

N90-13665# Pennsylvania Dept. of Transportation, Harrisburg. Bureau of Bridge and Roadway Technology.
EVALUATION OF A NEOPRENE LATEX MODIFIED SAMI (STRESS ABSORBING MEMBRANE INTERLAYER) Construction Report, Sep. 1987 - Apr. 1989
Dale B. Mellott Apr. 1989 14 p Sponsored by DOT, Washington, DC
(PB89-226435; FHWA/PA-87/03+85-107) Avail: NTIS HC A03/MF A01 CSCL 11C

The use of stress absorbing membrane interlayer (SAMI) is not a new concept. The SAMI usually consists of a seal coat with a modified asphalt. Numerous applications of asphalt and rubber were completed by contractors and by PennDOT (Pennsylvania Department of Transportation) maintenance forces. The main purpose of this type of installation was to evaluate the ability of a seal coat or modified seal coat to extend the service life of the bituminous overlay to the extent that the method would be economical. To date, no significant differences were noted. GRA

N90-13666*# National Aeronautics and Space Administration. Lewis Research Center, Cleveland, OH.
THERMODYNAMIC PROPERTIES OF SOME METAL OXIDE-ZIRCONIA SYSTEMS
Nathan S. Jacobson Dec. 1989 63 p
(NASA-TM-102351; E-5060; NAS 1.15:102351) Avail: NTIS HC A04/MF A01 CSCL 11C

Metal oxide-zirconia systems are a potential class of materials for use as structural materials at temperatures above 1900 K. These materials must have no destructive phase changes and low vapor pressures. Both alkaline earth oxide (MgO, CaO, SrO, and BaO)-zirconia and some rare earth oxide (Y_2O_3, Sc_2O_3, La_2O_3, CeO_2, Sm_2O_3, Gd_2O_3, Yb_2O_3, Dy_2O_3, Ho_2O_3, and Er_2O_3)-zirconia system are examined. For each system, the phase diagram is discussed and the vapor pressure for each vapor species is calculated via a free energy minimization procedure. The available thermodynamic literature on each system is also surveyed. Some of the systems look promising for high temperature structural materials. Author

N90-13667# Ecole Centrale de Lyon (France). Lab. de Metallurgie Physique-Materiaux.
IMPLEMENTATION AND ANALYSIS OF ADHESION IN MULTIMATERIALS OF THE TYPE Al(Si)-ZrO2 AND GRAPHITE, METAL OR CERAMICS Ph.D. Thesis [REALISATION ET ANALYSE DE L'ADHERENCE DANS DES MULTIMATERIAUX TYPE AL(SI)-ZRO2 ET GRAPHITE-METAL OU CERAMIQUE]
Nadir Mesrati 1989 255 p In FRENCH
(ECL-89-004; ETN-90-95779) Avail: NTIS HC A12/MF A02

Material obtained by plasma projection of oxide type ceramic powders on aluminum alloys and graphite are studied. The substrate was treated with interfacial tension reducing agents. The contribution of the preliminary destruction of the Al_2O_3 surface layer to improve the adherence of aluminum alloy is demonstrated. In the case of graphite, the dominant function of chrome to obtain the adhesion of metal and oxides is shown. ESA

N90-13668# Swedish Defence Research Establishment, Stockholm.
A LITERATURE SURVEY OF INHERENTLY CONDUCTING POLYMERS
Tom Karlsson Jul. 1989 39 p In SWEDISH; ENGLISH summary
(FOA-C-20763-2.4; ISSN-0347-3694; ETN-90-95919) Avail: NTIS HC A03/MF A01

Electrical conducting polymers, and in particular inherently (molecular) conducting ones, were rapidly developed during the last few years. The literature of synthesis, structure, mechanical and optical properties, conductance, and stability of polyacetylene, polyaniline, polypyrrole, and polythiophene and their derivates and copolymers is reported. The doping processes are described for all these substances with the corresponding additives. Short notices about some other inherently conducting polymers are also included. ESA

N90-13669# Technische Univ., Delft (Netherlands). Dept. of Aerospace Engineering.
PRELIMINARY EXPERIMENTS ON FILAMENT WINDING NYLON IMPREGNATED GLASS FIBERS (FIT)
L. G. Meyers Aug. 1987 15 p
(LR-545; ETN-90-95988) Avail: NTIS HC A03/MF A01

Some preliminary experiments conducted on the fiber impregnated thermoplastic (FIT) material, or nylon pre-impregnated glass-fibers, and the advantages of this type of material, mainly focussed on manufacturing technology, are described. Filament-winding, flexible braids, and weaves are given as some of the possibilities. A characterization of the material is given with respect to its basic properties. Some filament winding experiments are described with regard to a number of important parameters. ESA

N90-13478*# Arizona Univ., Tucson. Steward Observatory
SiO OVERCOATING AND POLISHING OF CFRP TELESCOPE PANELS
Patrick Woida and William F. Hoffmann *In* Jet Propulsion Lab., California Inst. of Tech., Report of the Asilomar 3 LDR Workshop 15 Aug. 1988 p 112-113 (For primary document see N90-13449 05-18)
Avail: NTIS HC A08/MF A01 CSCL 11C

28 PROPELLANTS AND FUELS

Includes rocket propellants, igniters, and oxidizers; their storage and handling procedures; and aircraft fuels.

For related information see also *07 Aircraft Propulsion and Power, 20 Spacecraft Propulsion and Power,* and *44 Energy Production and Conversion.*

N90-13670# Air Force Space Technology Center, Edwards AFB, CA. Astronautics Lab.
PROCEEDINGS OF THE HIGH ENERGY DENSITY MATTER (HEDM) CONFERENCE Special Report, Mar. 1988 - Mar. 1989
Timothy G. Wiley, ed. and Roeland A. vanOpijnen, ed. Jul. 1989 388 p Conference held in New Orleans, LA, 12-15 Mar. 1989
(AF Proj. 5730)
(AD-A212314; AL-CP-89-002) Avail: NTIS HC A17/MF A03 CSCL 07/4

This program is specifically targeted at identifying and developing new high energy molecular systems which will substantially exceed the energetics of current propulsion systems. Such systems must have a large ratio of energy to molecular weight (energy density). Molecular systems that are currently being examined include chemically bound excited states (CBES), high energy ground states, hypervalent molecules and strained compounds. The goal of the program is to develop these and other chemical systems as propellants resulting in increased specific impulse, with a concomitant increase in payload, and more versatile space capability. Other Air Force payoffs from the HEDM program's investigation of energetic molecules include spinoffs in lasers, explosives, and power generation. GRA

N90-13671# Naval Ordnance Station, Indian Head, MD.
EVALUATION OF SELECTED COMPUTER MODELS FOR MODELING PYROTECHNIC AND PROPELLANT DEVICES Final Report
Leo V. DeYong (Materials Research Labs., Melbourne, Australia) and Frank J. Valenta 8 Sep. 1989 32 p Presented at the Annual Meeting of the Pyrotechnics and Explosives Application Section of the ADPA, Shreveport, LA, 25-27 Oct. 1988 Submitted for publication
(AD-A213003; NOS-IHTR-1279) Avail: NTIS HC A03/MF A01 CSCL 19/1

A variety of analytic computer models are available and have been used successfully to predict performance in pyrotechnic systems, providing an inexpensive and quick method for initial validation of the performance of a system design. The authors have assessed several of those available at Naval Ordnance Station, Indian Head, MD, including several of the standard thermodynamic codes (NASA-Lewis, PEP, BLAKE, TIGER) as well as lumped parameter ballistic codes (CADPROG, EBED, ROCIGN), delay burn rate codes (HARDT), and ignition requirements analysis (Bryan-Lawrence). The use, characteristics, and outputs of the various codes are discussed with emphasis on limitations and cautions required when applying these techniques to predict performance of pyrotechnic systems. GRA

N90-13672# Office National d'Etudes et de Recherches Aerospatiales, Paris (France). Direction de l'Energetique.
A THEORETICAL MODEL OF DOUBLE BASE PROPELLANT COMBUSTION Final Report [MODELISATION DE LA COMBUSTION DES PROPERGOLS SOLIDES]
Alain Bizot 25 Apr. 1989 38 p Partly in FRENCH and ENGLISH
(Contract DRET-86-34-1390)
(ONERA-RTF-23/7128-EY; ETN-90-95928) Avail: NTIS HC A03/MF A01

The special behavior of double base propellants in condensed and gas phases are taken into account in making a comprehensive model of double base propellent combustion. A continuous temperature profile is calculated through both phases. The model solves the energy and species equations for both gas phases separately, then matches the boundary conditions between the two phases. The gas phase kinetics are summarized for four reactions. The burning rate is determined as a function of pressure, initial temperature, and heat of propulsion. ESA

N90-13673# Princeton Univ., NJ. Dept. of Mechanical and Aerospace Engineering.
EXPERIMENTAL AND COMPUTATIONAL STUDY OF COMBUSTION LIMITS IN NATURAL-GAS FUELED INTERNAL COMBUSTION ENGINES Annual Report, May 1988 - Apr. 1989
Paul D. Ronney May 1989 39 p Sponsored in part by NSF
(Contract GRI-5088-260-1688)
(PB89-235196; GRI-89/0142) Avail: NTIS HC A03/MF A01 CSCL 07D

The mechanisms of flame propagation and combustion limits relevant to natural-gas fueled internal combustion engines are studied. The progress of work performed during the first year of a two-year grant are summarized. GRA

N90-13674# Environmental Protection Agency, Ann Arbor, MI. Emission Control Technology Div.
MOBILE4 OXYGENATED FUELS VERSION USER'S GUIDE
Edward L. Glover Aug. 1989 8 p
(PB89-230700; EPA/AA/TSS/IM-89/1) Avail: NTIS HC A02/MF A01 CSCL 07D

Changes are described which were made to the standard MOBILE4 emission factors program to create a special version which facilitates modeling the effect of the use of oxygenated fuel on carbon monoxide (CO) emissions from mobile sources. The changes made to the MOBILE4 input and output formats is explained to allow user input of oxygenated fuel use. Finally, examples of input and output files for the model are provided. GRA

N90-13675*# National Aeronautics and Space Administration. Lewis Research Center, Cleveland, OH.
BUOYANCY EFFECTS ON THE VAPOR CONDENSATION RATE ON A HORIZONTAL LIQUID SURFACE
Mohammad M. Hasan and Chin-Shun Lin (Analex Corp., Cleveland, OH.) [1989] 14 p Presented at the 28th Aerospace Sciences Meeting, Reno, NV, 8-11 Jan. 1990; sponsored by AIAA
(NASA-TM-102437; E-5206; NAS 1.15:102437; AIAA-90-0353) Avail: NTIS HC A03/MF A01 CSCL 21I

The results are presented of a numerical study of the effects of buoyancy on the direct condensation of saturated or nearly saturated vapor on a horizontal liquid surface in a cylindrical tank. The liquid motion beneath the liquid-vapor interface is induced by an axisymmetric laminar jet of subcooled liquid. Analysis and numerical results show that the dominant parameter which determines the influence of buoyancy on the condensation rate is the Richardson number. However, the effect of buoyancy on the condensation rate cannot be quantified in terms of the Richardson number alone. The critical value of the Richardson number below which the condensation rate is not significantly reduced depends on the Reynolds number as well as the Prandtl number. Author

N90-13676 British Petroleum Co. Ltd., London (England).
NOVEL CARBAMATES, THEIR PRODUCTION AND THEIR USE AS FUELS ADDITIVES Patent Application
Richard ACourt, inventor, John Edward Hamlin, inventor, William Joseph Fox, inventor, and Sean Patrick OConnor, inventor 23 Jun. 1988 14 p
(EP-Patent-0-298-636-A-1; EP-Patent-Appl-SN-88-305799; Int-Patent-Class-C07C-125/06; Int-Patent-Class-C10L-1/22; Int-Patent-Class-C08G-65/32; ETN-90-95240) Avail: European Patent Office, Erhardjstr. 27, 8000 Munich 2, Fed. Republic of Germany

A patent is claimed for an invention relating to novel carbamates, their production, and their use as fuel additives. An improved process for the production of carbamates wherein strong organic bases are used as the catalyst is presented. The invention is described and illustrated by way of example. ESA

N90-13677# Swedish Defence Research Establishment, Stockholm.
THERMOCHEMICAL CALCULATIONS WITH INERT COMPOUNDS
Torsten Liljegren Jun. 1989 28 p In SWEDISH; ENGLISH summary
(FOA-C-20759-2.1; ISSN-0347-3694; ETN-90-95523) Avail: NTIS HC A03/MF A01

The combustion of fuel-rich propellants can often be incomplete due to low reaction rate of any component. A method is described to compute the combustion temperature if a component is inert or reacts only partly, whereas equilibrium between the combustion products is assumed. Examples of computations are given: composite propellants with high contents of aluminum; fuel-rich boron propellants for ramjet engines; incomplete combustion of carbon in ramjet engines. The results of such computations are valuable for judgment of the feasibility of efficient combustion and for design of combustion chambers. ESA

29 MATERIALS PROCESSING

Includes space-based development of products and processes for commercial applications.
For biological materials see *55 Space Biology.*

N90-13678*# Wyle Labs., Inc., Huntsville, AL.
DEVELOPMENT OF A SHUTTLE RECOVERY COMMERCIAL MATERIALS PROCESSING IN SPACE (CMPS) PROGRAM Final Report
Jun. 1989 194 p
(Contract NAS8-36109)
(NASA-CR-183720; NAS 1.26:183720) Avail: NTIS HC A09/MF A02 CSCL 22A

The work performed has covered the following tasks: update commercial users requirements; assess availability of carriers and facilities; shuttle availability assessment; development of optimum accommodations plan; and payload documentation requirements assessment. The results from the first four tasks are presented. To update commercial user requirements, contacts were made with the JEA and CCDS partners to obtain copies of their most recent official flight requests. From these requests the commercial partners' short and long range plans for flight dates, flight frequency, experiment hardware and carriers was determined. A 34 by 44 inch chart was completed to give a snapshot view of the progress of commercialization in space. Further, an assessment was made of the availability of carriers and facilities. Both existing carriers and those under development were identified for use by the commercial partners. A data base was compiled to show the capabilities of the carriers. A shuttle availability assessment was performed using the primary and secondary shuttle manifests released by NASA. Analysis of the manifest produced a flight-by-flight list of flight opportunities available to commercial users. Using inputs from the first three tasks, an Optimum Accommodations Plan was developed. The Accommodation Plan shows the commercial users manifested by flight, the experiment flown, the carrier used and complete list of commercial users that could not be manifested in each calendar year. Author

N90-13679*# National Aeronautics and Space Administration. Lewis Research Center, Cleveland, OH.
FACILITIES FOR MICROGRAVITY COMBUSTION RESEARCH
Kurt R. Sacksteder 1988 20 p Presented at the 39th Annual Astronautical Congress of the International Astronautical Federation, Bangalore, India, 8-15 Oct. 1988
(NASA-TM-102014; E-4726; NAS 1.15:102014; IAF-88-355)
Avail: NTIS HC A03/MF A01 CSCL 21B

Combustion science and applications have benefited in unforeseen ways from experimental research performed in the low-gravity environment. The capability to control for the first time the influence of gravitational buoyancy has provided some insight into soot formation in droplet combustion, the nature of flammability limits in premixed gases, and the relationship between normal-gravity and low-gravity material flammability that may influence how materials are best selected for routine use in habitable spacecraft. The opportunity to learn about these complex phenomena is derived from the control of the ambient body-force field and, perhaps as importantly, the simplified boundary conditions that can be established in well designed low-gravity combustion experiments. A description of the test facilities and typical experimental apparatus are provided; and conceptual plans for a Space Station Freedom capability, the Modular Combustion Facility, are described. Author

N90-13680*# National Aeronautics and Space Administration. Lewis Research Center, Cleveland, OH.
AN INVESTIGATION OF FLAME SPREAD OVER SHALLOW LIQUID POOLS IN MICROGRAVITY AND NONAIR ENVIRONMENTS
Howard D. Ross and Raymond G. Sotos [1989] 19 p Proposed for presentation at the 23rd International Symposium on Combustion, Orleans, France, 22-27 Jul. 1990; sponsored by Orleans Univ.
(NASA-TM-102425; E-5190; NAS 1.15:102425) Avail: NTIS HC A03/MF A01 CSCL 21B

Experiments of interest to combustion fundamentals and spacecraft fire safety investigated flame spread of alcohol fuels over shallow, 15 cm diameter pools in a 5.2 sec free-fall, microgravity facility. Results showed that, independent O2 concentration, alcohol fuel, and diluent types, microgravity flame spread rates were nearly identical to those corresponding normal-gravity flames for conditions where the normal gravity flames spread uniformly. This similarity indicated buoyancy-related convection in either phase does not affect flame spread, at least for the physical scale of the experiments. However, microgravity extinction coincided with the onset conditions for pulsating spread in normal gravity, implicating gas phase, buoyant flow as a requirement for pulsating spread. When the atmospheric nitrogen was replaced with argon, the conditions for the onset of normal-gravity pulsating flame spread and microgravity flame extinction were changed, in agreement with the expected lowering of the flash point through the thermal properties of the diluent. Helium-diluted flames, however, showed unexpected results with a shift to apparently higher flash-point temperatures and high normal gravity pulsation amplitudes. Author

31 ENGINEERING (GENERAL)

Includes vacuum technology; control engineering; display engineering; cryogenics; and fire prevention.

N90-13681*# Morton Thiokol, Brigham City, UT. Aerospace Group.
EVALUATION OF COPPER SLAG BLAST MEDIA FOR RAILCAR MAINTENANCE Final Report
N. W. Sagers and Mack H. Finlayson Jun. 1989 11 p
(Contract NAS8-30490)
(NASA-CR-183744; NAS 1.26:183744; TWR-19105) Avail: NTIS HC A03/MF A01 CSCL 13B

Copper slag was tested as a blasting substitute for zirconium silicate which is used to remove paint from railroad cars. The copper slag tested is less costly, strips paint faster, is produced near the point of need, provides a good bonding surface for paint, and permits the operator to work in a more comfortable position, i.e., standing nearly erect instead of having to crouch. Outdoor blasting with the tested Blackhawk (20 to 40 mesh) copper slag is also environmentally acceptable to the State of Utah. Results of tests for the surface erosion rate with copper slag blasting are included. J.P.S.

N90-13682# Carnegie-Mellon Univ., Pittsburgh, PA. Robotics Inst.
THE ECONOMIC IMPACT OF AUTOMATION TECHNOLOGY
Aydan Kutay Jul. 1989 29 p

(AD-A213363; CMU-RI-TR-89-13) Avail: NTIS HC A03/MF A01 CSCL 05/3

There is a growing consensus among academicians, business leaders and government officials that the American competitive problem rests centrally on the slowing rate of investment to integrate new automation technology into manufacturing operations. Although the source of major innovations in automation technology is from United States universities and research centers, American firms have been too slow in adopting these technologies. One of the major factors underlying this problem is the lack of an economic analysis technique specifically aimed at estimating the benefits of automation technology. This paper offers an economic analysis technique based upon the premise of increased probability of capturing the market segments through economies of scope. The paper first demonstrates the inadequacy of current economic analysis techniques to assess the benefits of automation technology, then proposes a new methodology which can be integrated to an expert system to assess the economic impact of various types of automation technology. GRA

N90-13683# Massachusetts Inst. of Tech., Cambridge. Dept. of Ocean Engineering.

AN ALGORITHM FOR CONTROL VOLUME ANALYSIS OF CRYOGENIC SYSTEMS M.S. Thesis

Michael B. Stanton Jun. 1989 72 p

(Contract N00228-89-G-0580)

(AD-A213394) Avail: NTIS HC A04/MF A01 CSCL 13/1

This thesis presents an algorithm suitable for numerical analysis of cryogenic refrigeration systems. Preliminary design of a cryogenic system commences with a number of decoupling assumptions with regard to the process variables of heat and work transfer (e.g., work input rate, heat loading rates) and state variables (pinch points, momentum losses). Making preliminary performance estimations minimizes the effect of component interactions which is inconsistent with the intent of analysis. A more useful design and analysis tool is one in which no restrictions are applied to the system - interactions become absolutely coupled and governed by the equilibrium state variables. Such a model would require consideration of hardware specifications and performance data and information with respect to the thermal environment. Model output would consist of the independent thermodynamic state variables from which process variables and performance parameters may be computed. This model will have a framework compatible for numerical solution on a digital computer so that it may be interfaced with graphic symbology for user interaction. This algorithm approaches cryogenic problems in a highly-coupled state-dependent manner. The framework for this algorithm revolves around the revolutionary thermodynamic solution technique for computer Aided Thermodynamics (CAT). Fundamental differences exist between the Control Volume (CV) algorithm and CAT, which will be discussed where appropriate. GRA

N90-13485*# Astro Aerospace Corp., Santa Barbara, CA.

HYBRID DEPLOYABLE SUPPORT TRUSS DESIGNS FOR LDR

J. Hedgepeth *In* Jet Propulsion Lab., California Inst. of Tech., Report of the Asilomar 3 LDR Workshop 15 Aug. 1988 p 128-129 (For primary document see N90-13449 05-18)

Avail: NTIS HC A08/MF A01 CSCL 13B

N90-13486*# Boeing Aerospace Co., Seattle, WA.

EFFECTS OF JOINTS IN TRUSS STRUCTURES

R. Ikegami *In* Jet Propulsion Lab., California Inst. of Tech., Report of the Asilomar 3 LDR Workshop 15 Aug. 1988 p 130-131 (For primary document see N90-13449 05-18)

Avail: NTIS HC A08/MF A01 CSCL 13B

32 COMMUNICATIONS AND RADAR

Includes radar; land and global communications; communications theory; and optical communications.

For related information see also *04 Aircraft Communications and Navigation* and *17 Space Communications, Spacecraft Communications, Command and Tracking.* For search and rescue see *03 Air Transportation and Safety,* and *16 Space Transportation.*

N90-13684 Council for National Academic Awards (England).

THE USE OF DIGITAL SIGNAL PROCESSING IN SATELLITE COMMUNICATION Ph.D. Thesis

Jonathan Richard Bramwell 1988 346 p

Avail: Univ. Microfilms Order No. BRDX84848

The recent emphasis on information technology has increased the need for methods of data communications with a greater interest in the areas of satellite communications. Data communications over a satellite can be easily achieved by the use of excessive power and bandwidth but efficient management of the satellite resource requires more elegant means of transmission. The optimum modulator and demodulator can be described by mathematical expressions to represent the physical processes that are required to transmit and receive a signal. Digital signal processing circuits can be used to implement these mathematical functions and once correctly designed are not susceptible to variations in accuracy and hence can maintain an accurate representation of the mathematical model. This thesis documents an investigation into the algorithms and techniques that can be used in the digital implementation of a satellite data modem. The technique used for carrier phase recovery and data decoding is a major variation on a method proposed by Viterbi and Viterbi and relies on phase estimation instead of the more common carrier regeneration techniques. A computer simulation of this algorithm and its performance is described and the overall performance of the simulation is compared to theoretical analysis and experimental performance of a multi-data rate satellite modem covering data rates in the range of 16 Ksymbol/sec to 256 Ksymbol/sec in both the BPSK and QPSK data formats.

Dissert. Abstr.

N90-13685*# Notre Dame Univ., IN. Dept. of Electrical and Computer Engineering.

ERROR CONTROL TECHNIQUES FOR SATELLITE AND SPACE COMMUNICATIONS Annual Status Report

Daniel J. Costello, Jr. Oct. 1989 126 p

(Grant NAG5-557)

(NASA-CR-182751; NAS 1.26:182751) Avail: NTIS HC A07/MF A01 CSCL 17B

Two aspects of the work for NASA are examined: the construction of multi-dimensional phase modulation trellis codes and a performance analysis of these codes. A complete list is contained of all the best trellis codes for use with phase modulation. LxMPSK signal constellations are included for M = 4, 8, and 16 and L = 1, 2, 3, and 4. Spectral efficiencies range from 1 bit/channel symbol (equivalent to rate 1/2 coded QPSK) to 3.75 bits/channel symbol (equivalent to 15/16 coded 16-PSK). The parity check polynomials, rotational invariance properties, free distance, path multiplicities, and coding gains are given for all codes. These codes are considered to be the best candidates for implementation of a high speed decoder for satellite transmission. The design of a hardware decoder for one of these codes, viz., the 16-state 3x8-PSK code with free distance 4.0 and coding gain 3.75 dB is discussed. An exhaustive simulation study of the multi-dimensional phase modulation trellis codes is contained. This study was motivated by the fact that coding gains quoted for almost all codes found in literature are in fact only asymptotic coding gains, i.e., the coding gain at very high signal to noise ratios (SNRs) or very low BER. These asymptotic coding gains can be obtained directly from a knowledge of the free distance of the code. On the other hand, real coding gains at BERs in the range of 10(exp -2) to 10(exp -6), where these codes are most

likely to operate in a concatenated system, must be done by simulation. Author

N90-13686 Princeton Univ., NJ.
MAGNETO-ELASTIC INTERACTIONS IN CONDUCTING STRUCTURES IN TRANSIENT MAGNETIC FIELDS Ph.D. Thesis
Jong Seh Lee 1989 208 p
Avail: Univ. Microfilms Order No. DA8910883

The theory of electrodynamics of deformable continua is reviewed and the pertinent coupled field equations and boundary conditions in magneto-elasticity for non-ferrous conductors are developed. In order to clarify the basic tenets of the interaction between the electromagnetic field and the mechanical response, thickness vibrations of a magneto-elastic plate in strong magnetic fields are investigated. Exact closed form solutions of the three-dimensional field equations are obtained for both free and forced vibrations and numerical results are presented. Magnetic damping and electromagnetic radiation effects are identified and examined in detail. A general and efficient finite element is proposed for analysis transient magneto-elastic interactions in conducting structures and corroborated numerically. Accuracy and versatility of the method are demonstrated by applying it to various magnetic induction problems with different geometries and field configurations. The numerical results are shown to be in very good agreement with known analytical solutions or experimental results. Then the electromagnetic finite elements are coupled to structural finite elements including beam and plate elements to investigate magneto-elastic interaction effects in structures. An efficient partitioned time integration for the coupled nonlinear system of equations is proposed. The applicability of the suggested numerical model is examined by applying it to analyze fully coupled vibrations of structural components excited by transient magnetic fields. Finally, the Fusion Electromagnetic Induction Experiments (FELIX) are modeled and the numerical results are shown to be in very good agreement with measured field data. Dissert. Abstr.

N90-13687# General Accounting Office, Washington, DC. National Security and International Affairs Div.
ELECTRONIC WARFARE: RELIABLE EQUIPMENT NEEDED TO TEST AIR FORCE'S ELECTRONIC WARFARE SYSTEMS
Aug. 1989 27 p
(AD-A212952; GAO/NSIAD-89-137) Avail: NTIS HC A03/MF A01 CSCL 17/4

The Air Force equips its tactical aircraft with electronic warfare systems such as the ALR-56A radar warning receiver and the ALQ-135 jammer. The receiver alerts the pilot that the airplane is being tracked by enemy radar and the jammer transmits electronic signals to deceive enemy radars. The combat readiness of tactical aircraft and the capability to sustain combat operations has been impaired because of faulty and unreliable test equipment used to identify malfunctions in electronic warfare systems. The Air Force has not adhered to policies requiring that test equipment be developed and deployed simultaneously with electronic warfare systems. To deploy the warfare systems as quickly as possible, the Air Force has not taken steps to assure that the electronic warfare system can be adequately maintained in an operational environment. The Air Force's strategy may result in additional cost and will continue to place combat readiness at risk. In addition, the Air Force cannot perform its maintenance functions without relying extensively on civilian contractor technical assistance, which might not be available during combat operations. GRA

N90-13688# Army Construction Engineering Research Lab., Champaign, IL.
ELECTROMAGNETIC WAVE PROPAGATION THROUGH CIRCULAR WAVEGUIDES CONTAINING RADIALLY INHOMOGENEOUS LOSSY MEDIA Final Report
Keith W. Whites Aug. 1989 167 p
(AD-A213062; CERL-TM-M-89/11) Avail: NTIS HC A08/MF A01 CSCL 20/14

Propagation characteristics of an electromagnetic (EM) wave inside a waveguide are greatly modified by the introduction of dielectrics into the guide. Frequency of cutoff, attenuation, and power flow distribution are all properties of the EM wave that are highly dependent on the physical structural and composition within the guide. Shielding applications take advantage of the large amount of attenuation provided by a waveguide when the incident EM wave has a frequency lower than the cutoff frequency of the waveguide. In practice, small sections of waveguides are inserted through the metal walls of a shielded enclosure to construct an air passage that does not compromise the shielding effectiveness of the shelter. Typically, however, other fluids and materials besides air must be transferred inside the enclosure. Therefore, hoses are sometimes inserted through these waveguides, which can reduce the shielding provided by the waveguide above and below cutoff. GRA

N90-13689# Systems Engineering Labs., Inc., Greenbelt, MD.
STOCHASTIC MODELLING OF EM SCATTERING FROM FOLIAGE Final Report, Sep. 1985 - Oct. 1988
Gilmore L. Blankenship Mar. 1989 112 p
(Contract F19628-85-C-0180)
(AD-A213118; RADC-TR-89-22) Avail: NTIS HC A06/MF A01 CSCL 20/3

This project focused on the development and evaluation of analytical methods for the description of scattering and absorption of electromagnetic radiation by dense foliage. The key consideration has been the description of multiple scattering processes in a random medium. Three different techniques for the description of microscopic scattering processes are discussed in this report. The T-matrix approach to multiple scattering represents the field at an individual scattering center in terms of an equivalent field produced by the other scatterers. It supports several natural approximations for this equivalent field which take multiple scattering processes into account at various levels of detail. The Coherent Potential Approximation is developed in detail. The homogenization method is a technique for the derivation of an equivalent representation of the scattering process in terms of an asymptotic analysis of Maxwell's equations in the limit as the separation between the scattering centers approaches zero. Bounds for the effective parameter representations are also discussed. Scattering from foliage covered terrain on a macroscopic scale is treated by using the approximations to develop effective media representations of the foliage. These are used in combination with an analytical methodology based on the method of smoothing perturbation to treat the foliage as an interface region with a very rough boundary. GRA

N90-13690# Massachusetts Inst. of Tech., Cambridge. Lincoln Lab.
EFFICIENT DETECTION OF SMALL MOVING OBJECTS
Peter L. Chu 21 Jul. 1989 81 p Sponsored by AFSC
(AD-A213314; TR-846; ESD-TR-89-104) Avail: NTIS HC A05/MF A01 CSCL 17/11

A signal processing problem encountered with many sensor systems having a wide field-of-view is detection of small, unresolved objects moving in a straight line amid stationary clutter. The wide field-of-view combined with the need to accurately pinpoint object positions imply that these sensors must have hundreds of thousands of samples in their output. To process this amount of data in a timely fashion, computationally efficient algorithms are a necessity. In this report, a computationally efficient set of algorithms is described for detecting satellites, meteorites, and other moving objects using data from an optical telescope charge-coupled device (CCD) focal plane in the MIT Lincoln Laboratory Demonstration Surveillance System (DSS). The trade-off of reduced detection sensitivity for lower computational cost in the algorithm is quantitatively discussed. Major techniques employed are: (1) sample normalization by temporal mean and standard deviation to suppress clutter; (2) maximum value projection to reduce the dimensionality of the data; (3) a two-stage matched filter detector which first nominates and then confirms signal candidates; and (4) two-dimensional binary velocity filtering. The techniques should have practical application to other wide field-of-view sensors where moving object detection is important. GRA

N90-13691# Defence Research Establishment Pacific, Victoria (British Columbia).
FIRST-ORDER BRAGG SAR IMAGERY OF KELVIN WAKES AND MOVING INTERNAL WAVE FIELDS
Blyth A. Hughes Jun. 1989 57 p
(AD-A213361; DREP-TM-89-13) Avail: NTIS HC A04/MF A01 CSCL 17/9

Two theoretical investigations are given relating to SAR imaging of perturbed surface waves. The first is an analysis of the effect of a long wavelength corrugation on the SAR image formed by 1st order Bragg scattering from a deterministic sea wave pattern such as a Kelvin wake. A standard SAR processor is assumed. The second is a stochastic treatment of the SAR imagery formed by a first order Bragg scattering process from surface waves modulated by the horizontal surface currents of internal waves. Propagational velocities (normalized by the SAR platform velocity) are included to first order. For the Kelvin wake analysis it is shown that the vertical curvature of the corrugating wave can rotate the effective Bragg acceptance angle by up to about .000001 for typical wave parameters. For the internal wave analysis, SAR resolutions are given, and in particular it is shown that typical azimuthal velocity components are important in determining the azimuthal resolution dimension of the scene, especially for resolutions of a few meters size. GRA

N90-13692 Institute for Perception RVO-TNO, Soesterberg (Netherlands). Audiology Group.
SPEECH RECEPTION IN QUIET AND IN NOISY CONDITIONS BY INDIVIDUALS WITH NOISE-INDUCED HEARING LOSS IN RELATION TO THEIR AUDIOGRAM
G. F. Smoorenburg Mar. 1989 57 p Sponsored by the Netherlands Ministry of Social Affairs Directorate General of Labor
(IZF-1989-11; TD89-1534; ETN-90-96006) Copyright Avail: TNO Institute for Perception, P.O. Box 23, 3769 ZG Soesterberg, Netherlands

Tone thresholds and speech reception thresholds are measured in 200 individuals (400 ears) with noise induced hearing loss. The speech-reception thresholds are measured in a quiet condition and in noise. The tone audiograms can be described by three components: hearing loss in the regions above 3 kHz, from 1 to 3 kHz and below 1 kHz. The speech thresholds can be described by two components: speech reception in quiet and speech reception in noise. Hearing loss above 1 kHz is related to speech reception in noise; hearing loss at and below 1 kHz to speech reception in quiet. The correlation between the speech thresholds in quiet and in noise was only $R = 0.45$. The minimum value of the prediction error for any tone audiometric predictor of this speech threshold is 1.2 dB. The prediction cannot be improved by taking into account the critical ratio for low frequency noise nor by its upward spread of masking. ESA

N90-13693# National Telecommunications and Information Administration, Washington, DC.
LONG-RANGE PLAN FOR MANAGEMENT AND USE OF THE RADIO SPECTRUM BY AGENCIES AND ESTABLISHMENTS OF THE FEDERAL GOVERNMENT Special Report
Jun. 1989 154 p
(PB89-232367; NTIA-SP-89-22) Avail: NTIS HC A08/MF A01 CSCL 17B

Federal Government electromagnetic spectrum planning issues are addressed in a long range plan. This plan will be used in U.S. preparations for international spectrum negotiations and conferences. In addition, a plan for improved spectrum management procedures is provided which includes information related to spectrum-use plans of the Federal Government. The material is divided into four major topics: (1) a description of the national spectrum resource; (2) a plan for national spectrum management; (3) a plan for international radiocommunications activities; and (4) a plan for spectrum use. GRA

N90-13694*# National Aeronautics and Space Administration. Langley Research Center, Hampton, VA.
CHARACTERISTIC IMPEDANCE OF MICROSTRIP LINES
M. C. Bailey and M. D. Deshpande (Vigyan Research Associates, Inc., Hampton, VA.) Nov. 1989 59 p
(NASA-TM-101581; NAS 1.15:101581) Avail: NTIS HC A04/MF A01 CSCL 17B

The dyadic Green's function for a current embedded in a grounded dielectric slab is used to analyze microstrip lines at millimeter wave frequencies. The dyadic Green's function accounts accurately for fringing fields and dielectric cover over the microstrip line. Using Rumsey's reaction concept, an expression for the characteristic impedance is obtained. The numerical results are compared with other reported results. Author

N90-13465*# California Univ., Berkeley.
FAR-INFRARED HETERODYNE RECEIVERS
Albert Betz *In* Jet Propulsion Lab., California Inst. of Tech., Report of the Asilomar 3 LDR Workshop 15 Aug. 1988 p 83-85 (For primary document see N90-13449 05-18)
Avail: NTIS HC A08/MF A01 CSCL 17B

N90-13466*# Jet Propulsion Lab., California Inst. of Tech., Pasadena.
ADVANCES IN SIS RECEIVER TECHNOLOGY
M. A. Frerking *In its* Report of the Asilomar 3 LDR Workshop 15 Aug. 1988 p 86-87 (For primary document see N90-13449 05-18)
Avail: NTIS HC A08/MF A01 CSCL 17B

N90-13514# European Space Agency, Paris (France).
DATA HANDLING AND TELECOMMUNICATIONS
A. Errington *In its* The Hipparcos Mission. Prelaunch Status. Volume 1: The Hipparcos Satellite Jun. 1989 p 131-146 (For primary document see N90-13499 05-18)
Copyright Avail: NTIS HC A16/MF A02; ESA Publications Div., ESTEC, Noordwijk, Netherlands, 80 Dutch guilders

33 ELECTRONICS AND ELECTRICAL ENGINEERING

Includes test equipment and maintainability; components, e.g., tunnel diodes and transistors; microminiaturization; and integrated circuitry.

For related information see also *60 Computer Operations and Hardware* and *76 Solid-State Physics.*

N90-13695 Michigan State Univ., East Lansing.
ON THE DESIGN OF A COMPUTER-AIDED DESIGN SYSTEM FOR DIGITAL CIRCUITS Ph.D. Thesis
Tao Shinn Chen 1988 103 p
Avail: Univ. Microfilms Order No. DA8912560

A methodology for automating the design processes for digital circuits is investigated. Tools are developed to illustrate this methodology. There is a graphic tool with interactive visualization for design capture, a logic-timing simulator at the MOS transistor-switch level, and a verification tool for circuit layout. The embedded theory for the methodology and tools is established and proven. For the graphic tool, the major endeavor focuses on developing efficient data structures for any circuit schematic with unlimited drawing size and only having fastest graphic operations executed to obtain the shortest computer response time. Next, a totally new method is used for switch-level simulation. This approach not only has linear-time complexity but also obeys the law of excluded middle. Moreover, the bidirectional problem for simulating MOS transistors at pure logic level is solved. The performance analysis shows that this tool can simulate a 15,000-transistor circuit with the speed of less than 25 seconds per clock on a workstation. A rule-based verification approach provides a static way to validate circuit structures from the layout level to a system level without specifying the inputs. The fundamental work which verifies a transistor network by its Boolean

functions is developed. This method ensures full correctness of the circuit topology because it takes all components into account.
Dissert. Abstr.

N90-13696# Massachusetts Inst. of Tech., Cambridge. Microsystems Research Center.
RESISTIVE FUSES: ANALOG HARDWARE FOR DETECTING DISCONTINUITIES IN EARLY VISION
John Harris, Christof Koch, Jin Luo, and John Wyatt Jun. 1989 31 p Submitted for publication Sponsored in part by Du Pont de Nemours (E. I.) and Co., Wilmington, DE
(Contract N00014-87-K-0825; NSF MIP-88-14612)
(AD-A211891; VLSI-MEMO-89-551) Avail: NTIS HC A03/MF A01 CSCL 09/1

The detection of discontinuities in motion, intensity, color, and depth is a well-studied but difficult problem in computer vision. We discuss our resistive fuse circuit--the first hardware circuit that explicitly implements either analog or binary line processes in a controlled fashion. We have successfully designed and tested an analog CMOS VLSI circuit that contains a 1-D resistive network of fuses implementing piece-wise smooth surface interpolation. The segmentation ability of this network is demonstrated for a noisy step-edge input. We derive the specific current-voltage relationship of the resistive fuse from a number of computational considerations, closely related to the early vision algorithms of Koch, Marroquin and Yuille (1986) and Blake and Zisserman (1987). We discuss the circuit implementation and the performance of the chip. In the last section, we show that a model of our resistive network--in which the resistive fuses have no internal dynamics--has an associated Lyapunov function, the co-content. The network will thus converge, without oscillations, to a stable solution, even in the presence of arbitrary parasitic capacitances throughout the network.
GRA

N90-13697# Massachusetts Inst. of Tech., Cambridge. Microsystems Research Center.
DELAY TEST GENERATION FOR SYNCHRONOUS SEQUENTIAL CIRCUITS
Srinivas Devadas May 1989 11 p
(Contract N00014-87-K-0825)
(AD-A211917; VLSI-MEMO-89-539) Avail: NTIS HC A03/MF A01 CSCL 09/1

We address the problem of generating tests for delay faults in non-scan synchronous sequential circuits. Delay test generation for sequential circuits is a considerably more difficult problem than delay testing of combinational circuits and has received much less attention. In this paper, we present a method for generating test sequences to detect delay faults in sequential circuits using the stuck-at fault sequential test generator STALLION. The method is complete in that it will generate a delay test sequence for a targeted fault given sufficient CPU time, if such a sequence exists. We term faults for which no delay test sequence exists, under out test methodology, sequentially delay redundant. We describe means of eliminating sequential delay redundancies in logic circuits. We present a partial-scan methodology for enhancing the testability of difficult-to-test of untestable sequential circuits, wherein a small number of flip-flops are selected and made controllable/observable. The selection process guarantees the elimination of all sequential delay redundancies. We show that an intimate relationship exists between state assignment and delay testability of a sequential machine. We describe a state assignment algorithm for the synthesis of sequential machines with maximal delay fault testability. Preliminary experimental results using the test generation, partial-scan and synthesis algorithm are presented.
GRA

N90-13698# Massachusetts Inst. of Tech., Cambridge. Microsystems Research Center.
TEST GENERATION FOR HIGHLY SEQUENTIAL CIRCUITS
Abhijit Ghosh, Srinivas Devadas, and A. Richard Newton Aug. 1989 6 p Presented at the International Conference of Computer Aided Design (ICCAD '89), Nov. 1989 Sponsored in part by Digital Equipment Corp., Maynard, MA; Bell Telephone Labs., Murray Hill, NJ and Semiconductor Research Corp., Research Triangle Park, NC
(Contracts N00014-87-K-0825; N00039-87-C-0182)
(AD-A211932; VLSI-MEMO-89-553) Avail: NTIS HC A02/MF A01 CSCL 09/1

We address the problem of generating test sequences for stuck-at faults in non-scan synchronous sequential circuits. We present a novel test procedure that exploits both the structure of the combinational logic in the circuit as well as the sequential behavior of the circuit. In contrast to previous approaches, we decompose the problem of sequential test generation into three subproblems of combinational test generation, fault-free state justification and fault-free state differentiation. We describe fast algorithms for state justification and state differentiation using the ON-sets and OFF-sets of flip-flop inputs and primary outputs. The decomposition of the testing problems into three subproblems rather than the traditional two, performing the justification and differentiation steps on the fault free rather than the faulty machine and the use of efficient techniques for cube intersection results in significant performance improvements over previous approaches.
GRA

N90-13699# Harvard Univ., Cambridge, MA. Div. of Applied Sciences.
JOINT SERVICES ELECTRONICS PROGRAM Annual Progress Report No. 103, 1 Oct. 1988 - 31 Jul. 1989
Michael Tinkham 31 Jul. 1989 108 p
(Contract N00014-89-J-1023)
(AD-A213015) Avail: NTIS HC A06/MF A01 CSCL 02/3

Topics addressed include: Electronic Theory of Semiconductor Alloys and Superlattices; Pressure Dependence of Photo Luminescence Excitation in GaAs/Al(x)Ga(1-x)As Multi-Quantum Wells; X Ray Surface Characterization; High Temperature Superconductivity; Quantum and Charging Phenomena in Mesoscopic Josephson Junctions; Nonlinear Dynamics of Electronic Neural Networks; Structural and Electronic Studies of Semiconductor Interfaces and Surfaces; Interaction of Ultrashort Laser Pulses with Semiconductor Surfaces; Multiphoton Vibrational Excitation of Molecules; Analytical and Numerical Determination of the Fields of Antennas near an Interface Between Two Half-Spaces with Significantly Different Wave Numbers; Theoretical Study of Lateral-Wave Propagation in Horizontally-Layered Media; Lateral Electromagnetic Waves from a Horizontal Antenna for Remote Sensing in the Ocean; Lateral Electromagnetic Pulses Generated by Horizontal and Vertical Dipoles on the Boundary Between Two Dielectrics; Theoretical Study of Isolated and Coupled Strip Antennas; Theoretical Study of Electromagnetic Pulses with a Slow Rate of Decay; Experimental Study of Electromagnetic Pulses with a Slow Rate of Decay; Properties of Closed Loops of Pseudodipoles; Asymptotic Solution for the Charge and Current Near the Open End of a Linear Tubular Antenna; Closed Loops of Parallel Coplanar Dipoles - Electrically Short Elements; Harmonic Generation in High-Temperature Superconductors and Resonant Closed Loops of Dipoles.
GRA

N90-13700# Cincinnati Univ., OH. Nanoelectronics Lab.
MECHANISMS IN REACTIVE ION ETCHING OF SILICON CARBIDE THIN FILMS
W.-S. Pan (INTEL Corp., Santa Clara, CA.) and A. J. Steckl 1989 9 p Submitted for publication
(Contract N00014-81-K-0605)
(AD-A213018; UC-TR-18) Avail: NTIS HC A02/MF A01 CSCL 09/1

The etching mechanisms for the reactive ion etching of SiC thin films were investigated using fluorinated gases, such as SF6/O2, CHF3/O2, CBrF3/O2. The major mechanisms involved are: (1) physical removal by sputtering due to ionized particles within the plasma, and (2) chemical reaction of active plasma species with C and Si with the generation of volatile products. The self-induced DC Bias has been shown to have a very strong effect up to a certain crossover value of around 300 V. The effect is related to the rate-limiting removal of the C-rich surface layer. We have confirmed that the chemical reaction process proceeds

by removal of Si through reactions with F species (to generate SIF4) while C is removed by reactions with O2 (to generate COx) only. No reaction between C and F was observed in the experimental results. GRA

N90-13701# TRW Space and Defense Sector, Redondo Beach, CA. Electronics and Technology Div.
DEVELOPMENT OF HIGH GAIN THREE TERMINAL DEVICES - AT MILLIMETER WAVE FREQUENCIES Program Status Report No. 14-16, 30 Jun. - 31 Aug. 1989
E. K. Hsieh 31 Aug. 1989 16 p
(Contract N00014-88-C-2088)
(AD-A213089) Avail: NTIS HC A03/MF A01 CSCL 09/1

The objectives of this program are: to develop high gain three terminal devices at millimeter wave frequencies. Specifically, InGaAs pseudomorphic high electron mobility transistors (HEMT) will be developed in four key areas: materials, device models, processing, and characterization. The 36 month program consists of two tasks. Task I is to develop the high gain transistor with 6 dB gain, 0.3 W/mm power density, and 20 percent efficiency at 60 GHz in the first 12 months. Task II is to develop transistor with at least 6 dB of gain, 0.25 W/mm power density and 15 percent efficiency at 94 GHz and to assess the reliability of the transistor in the next 24 months. GRA

N90-13702# Illinois Univ., Urbana. Coordinated Science Lab.
AN ACCURATE TIMING MODEL FOR FAULT SIMULATION IN MOS CIRCUITS M.S. Thesis
Sungho Kim Sep. 1989 45 p Sponsored in cooperation with the Semiconductor Research Corp. and the Joint Services Electronics Program
(Contract N00014-84-C-0149)
(AD-A213153; UILU-ENG-89-2229; CSG-106) Avail: NTIS HC A03/MF A01 CSCL 09/1

With the increasing need for manufacturers to maintain quality requirements for high performance and high density MOS VLSI integrated circuits and the multitude of physical failures and defects that can occur in such circuits, delay fault testing is gaining importance. An extremely important component of such a delay test generation environment is an accurate yet fast delay fault simulator. The goal of fault simulation is to generate the responses of digital circuits under both fault and fault-free conditions, without prohibitive cost. Most simulators available today either sacrifice accuracy or are very time consuming. Therefore, choosing the right simulation model is the key in fault simulation. MOS circuit models that were previously developed for true value simulation, after being modified to accommodate fault models, have been used by fault simulators, such as FMOSSIM. These fault simulators are incapable of detecting timing errors and even some logic errors, both of which occur in actual failures in the MOS circuits. Others have shown that some faults only affect the circuit timing and the delay may invalidate test sets. Therefore, fault simulators must consider the circuit delay in order to evaluate test sets accurately. FAUST is one such fault simulator which very accurately detects timing as well as logical errors. It was based on using a combination of table lookup and numerical integration techniques to solve differential equations. GRA

N90-13703# Texas Instruments, Inc., Dallas.
MM AND T FOR VHSIC MULTICHIP PACKAGES Final Report, Sep. 1985 - Sep. 1989
Ron Natali and Edwin Case 20 Sep. 1989 371 p
(Contract DAAL01-85-C-0442)
(AD-A213259; SLCET-TR-85-0442-F) Avail: NTIS HC A16/MF A02 CSCL 09/1

The objective of the LABCOM Multichip Packaging program was to develop hermetic ceramic packages suitable for interconnection of up to nine VHSIC chips operating at 100 MHz clock rates. Two packages have been designed and fabricated. One design (196 I/O) accommodated 2 to 4 VHSIC devices, while the other (308 I/O) accommodated 5 to 9 VHSIC devices. A populated 196 I/O quad SRAM module has been delivered and also five (5) each unpopulated 196 and 308 I/O packages. All electrical testing, data fixtures, methods, etc., relative to the packages and module have been delivered per Phase 1 contractual requirements. The program was divided into three phases. Phase 1, originally scheduled to complete Sept. '87, was put on an accelerated schedule and completed December 31, 1986. It included design and fabrication of both package types in prototype quantities, selection of appropriate interconnect schemes, and full electrical evaluation of a populated four chip module. Also included was a survey of VHSIC community packaging requirements and development of domestic sources for package production. Phase 3 was scheduled to complete the project with a demonstration of limited production capability. GRA

N90-13704*# National Aeronautics and Space Administration. Lyndon B. Johnson Space Center, Houston, TX.
MICROWAVE MICROSTRIP RESONATOR MEASUREMENTS OF Y1Ba2Cu3O(7-x) AND Bi2Sr2Ca1Cu2O(8-y) THIN FILMS
Christopher L. Lichtenberg, Jaroslaw Wosik, Matthew Davis, and J. C. Wolfe (Houston Univ., TX.) Nov. 1989 9 p
(NASA-TM-102159; S-601; NAS 1.15:102159) Avail: NTIS HC A02/MF A01 CSCL 09C

Radio frequency (RF) surface resistance measurement experiments on high T(sub c) thin films were performed. The method uses a microstrip resonator comprising a top gold conductor strip, an alumina dielectric layer, and a separate superconductivity ground plane. The surface resistance of the superconducting ground plane can be determined, with reference to a gold calibration standard, from the measured quality factor of the half-wave resonator. Initial results near 7 GHz over the temperature range from 25 to 300 K are presented for YBa2Cu3O(7-x) and Bi2Sr2CaCu2O(8-y) thin film samples deposited by an electron beam flash evaporation process. The RF surface resistance at 25 K for both materials in these samples was found to be near 25 milliohms. Author

N90-13705# Helsinki Univ. of Technology, Espoo (Finland). Dept. of Mathematics.
PARAMETER ESTIMATION FOR THE GUMMEL-POON TRANSISTOR MODEL
S. Granlund, P. Lindqvist, and M. Vuorinen 1989 23 p Sponsored by the Academy of Finland and Nokia-Mobira
(Ma-53; ISBN-951-666-282-X; ISSN-0355-2713; ETN-90-96028)
Avail: NTIS HC A03/MF A01

An account of the Gummel-Poon transistor model, is given. A series of measurements, which provides data for the estimation of the model parameters are described. Algorithms for the practical evaluation of the model parameters in the personnel computer environment are suggested by exploiting and improving the graphical methods of Getreu. The algorithms are intended mainly for the computer assisted design of circuits in industrial applications and they provide estimates for the input parameters of circuit analyzing programs such as SPICE. The algorithms are implemented on an IBM PC in the Turbo PASCAL language. ESA

N90-13706*# Clemson Univ., SC. Dept. of Computer Science.
SUFFICIENCY AND NECESSITY IN RELIABILITY MODELING Progress Report
Robert Geist 1989 16 p
(Grant NAG1-755)
(NASA-CR-186119; NAS 1.26:186119) Avail: NTIS HC A03/MF A01 CSCL 09C

Limitations of current analytic techniques in estimating the reliability of life-critical electronics systems are discussed. A new framework for specification of recovery and fault-handling submodels is suggested, and is shown through several examples to provide substantially improved modeling accuracy and flexibility. Implementation of the new technique in an X-windows based system, XHARP, is also described. The implementation allows for an automated behavioral decomposition of full system models, heretofore unavailable in such tools. Author

N90-13707# Grenoble-1 Univ. (France). Lab. des Tech. de l'Informatique, des Math., de la Microelectronique et de la Microscopie Quant.

ELECTRON BEAM SENSITIVE DEVICES FOR CONTROLLABILITY

Dominique Micollet Dec. 1988 108 p

(IMAG-RR-761-I; ETN-90-95695) Avail: NTIS HC A06/MF A01

Electron beam controllability is approached from two points of view: the physical use of the phenomenon, the Electron Beam Induced Current (EBIC), and the integrated devices which allow the controllability. The general laws of the EBIC are applied to the case of a diffused diode and show that the energy needed for the controllability is greater than that for the observability. Microscope specifications are outlined. The range of possible induced currents used to integrate the amplifiers of the control circuit is described. The general structure of these amplifiers is detailed, followed by analysis of each of their parts. Design methods and numerical results are presented. ESA

N90-13708# Institut National Polytechnique, Grenoble (France). Techniques de l'Informatique, des Mathematiques, de la Microelectronique et de la Microscopie Quanti

RESEARCH ON THE CONTROLLABILITY OF INTEGRATED CIRCUITS BY MEANS OF ELECTRON BEAMS Ph.D. Thesis [ETUDE DE LA CONTROLLABILITE DES CIRCUITS INTEGRES PAR FAISCEAUX D'ELECTRONS]

Dominique Micollet 1988 241 p In FRENCH; ENGLISH summary

(ETN-90-95710) Avail: NTIS HC A11/MF A01

Solutions for the implementation of integrated circuit controllability using an electron beam tester are outlined. The various phenomena which can be applied to the electron beam controllability from the physical and technological points of view are reviewed. A parallel is drawn with the photon beam. The EBIC (electron beam induced current) phenomenon is chosen for the particular case of a diffused planar junction. This theoretical and experimental study concludes that controllability requires a higher beam energy than the observability. This difference induces some important perturbations on the beam. These are analyzed and solutions are proposed to reduce them. It is shown that in most cases, the electron beam will be unable to control a circuit without on chip amplification. Devices designed to control any circuit in the same technology, without interfacing problems, are described. ESA

N90-13709# Ecole Centrale de Lyon (France). Lab. d'Electronique, Automatique et Mesures Electriques.

ELABORATION AND CHARACTERIZATION OF MISFET TRANSISTORS ON InP Ph.D. Thesis [ELABORATION ET CARACTERISATION DE TRANSISTORS MISFET SUR INP]

Bruno Commere 1988 200 p In FRENCH

(ECL-88-19; ETN-90-95772) Avail: NTIS HC A09/MF A02

The manufacturing procedures of MISFET (metal-insulator-semiconductor field effect transistor) transistors on InP are reviewed and original methods of passivation are proposed. During the deposition of a silicon nitride layer, a small quantity of AsO3 is introduced. The optimal heat treatment conditions are studied using a photoluminescence method. It is shown that photoluminescence imagery is very useful in optimizing the technological steps and chemical treatments. ESA

N90-13710# Ecole Centrale de Lyon (France).

DESIGN OF A POWER COMPONENT WITH IGBT INSULATED GRID. STATIC AND DYNAMIC STUDY Ph.D. Thesis [CONCEPTION D'UN COMPOSANT DE PUISSANCE A GRILLE ISOLEE IGBT ETUDE STATIQUE ET DYNAMIQUE]

G. Rouault 1988 125 p In FRENCH

(ECL-88-22; ETN-90-95774) Avail: NTIS HC A06/MF A01

Design rules for first and second generation IGBT (insulated gate bipolar transistors) for more than 400 volt power applications are derived from theoretical and simulation analysis. Implementation experiments including specifically designed manufacturing masks are described. Manufacturing feasibility is demonstrated. It is suggested that this type of component is to replace VDMOS transistors in the near future. ESA

N90-13711# Ecole Centrale de Lyon (France). Dept. d'Electrotechnique.

CONTRIBUTION TO THE STUDY OF A SELF-PROTECTED STATIC SWITCH AND ITS COMMAND STRATEGY Ph.D. Thesis [CONTRIBUTION A L'ETUDE DU CONTACTEUR STATIQUE AUTOPROTEGE ET DE SA STRATEGIE DE COMMANDE]

Guy Clerc 1989 216 p In FRENCH

(ECL-89-002; ETN-90-95778) Avail: NTIS HC A10/MF A02

Different implementations of static power switches are discussed, including a voltage commanded cascade GTO-MOS and a circuit designed on the basis of an insulated gate bipolar transistor. The behavior of static switches commanding a synchronous motor is described. A program to choose the command strategy in order to minimize thermal and electric constraints is presented. A microprocessor based system to manage the connection of a load to an electric network is also described. The command system assures protection against short-circuits and overheating. ESA

N90-13712# Rome Univ. (Italy). Dipt. di Fisica.

LOW RESISTIVITY ELECTRODELESS STREAMER TUBES

F. Ferrarotto and B. Stella 20 Jun. 1989 18 p Submitted for publication

(Preprint-685-89; ETN-90-95805) Avail: NTIS HC A03/MF A01

A set of bottomless coverless plastic streamer tubes with a low surface resistivity coating, arranged with both digital and analogical external pickup electrodes read out were made and tested. The tests performed at the CERN (Centre Europeen de Recherche Nucleaire) SpS using high energy pion beams, in strict correlation with normal coverless plastic streamer tubes with high resistivity coating are described. Their performances under experimental conditions are compared. The results show that they are comparable both for tracking and calorimetry, though the low resistivity electrodeless models have many practical advantages. ESA

N90-13713# Allgemeine Elektrizitaets-Gesellschaft, Ulm (Germany, F.R.). Fachbereich Mikrowellen- und Hochspannungsroehren.

DEVELOPMENT OF A TRAVELING WAVE TUBE FOR THE PROJECT X-SAR. CONSTRUCTION AND TESTING OF A BREADBOARD MODEL Final Report, Sep. 1987

Gerold Lippert Dec. 1988 51 p In GERMAN; ENGLISH summary

(Contract BMFT-01-TH-8503-AK/RT)

(ETN-90-95900) Avail: NTIS HC A04/MF A01

Earth remote sensing with SAR (synthetic aperture radar) satellites is tested at the frequencies 1.4 GHz, 5.3 GHz and 9.6 GHz by space shuttle missions. For this purpose pulsed power amplifiers of high reliability, equipped with Traveling Wave Tubes (TWTs) are needed. In accordance with the design of a similar tube at 5.3 GHz (320 W average) previously developed by AEG, the development of a 9.6 GHz TWT with an average power of about 275 W is described. This development includes design, construction and testing of a first breadboard model. The essential features of the design are described. ESA

N90-13714# Helsinki Univ. of Technology, Espoo (Finland). Electronic Circuit Design Lab.

MODELING AND MEASUREMENT METHODS FOR HIGH SPEED BIPOLAR TRANSISTORS Ph.D. Thesis

Markku Sipilae May 1989 113 p

(Rept-11; ISBN-951-754-881-8; ISSN-0783-9448; ETN-90-96025)

Avail: NTIS HC A06/MF A01

The modeling problems in high speed bipolar transistors are discussed. The dynamic modeling of carrier distribution in the base, the parameter determination for a multisection model, model verification in the time domain, and the determination of parasitics

are considered. Special emphasis is placed on the possible use of a new time domain measurement technique for model verification and parameter determination. An improved nonlinear high frequency model, and a model for doping density are presented. A system for the accurate measurement of high frequency periodic time domain voltage and current waveforms of a nonlinear microwave device is shown. The determination of package parasitic series inductances of microwave bipolar transistor is performed. ESA

N90-13467*# Massachusetts Inst. of Tech., Lexington. Lincoln Lab.
RESONANT-TUNNELING OSCILLATORS AND MULTIPLIERS FOR SUBMILLIMETER RECEIVERS
T. C. L. Gerhard Sollner *In* Jet Propulsion Lab., California Inst. of Tech., Report of the Asilomar 3 LDR Workshop 15 Aug. 1988 p 88-89 (For primary document see N90-13449 05-18)
Avail: NTIS HC A08/MF A01 CSCL 09A

N90-13473*# Arizona Univ., Tucson. Steward Observatory.
DEVELOPMENT OF FIR ARRAYS WITH INTEGRATING AMPLIFIERS
Erick T. Young *In* Jet Propulsion Lab., California Inst. of Tech., Report of the Asilomar 3 LDR Workshop 15 Aug. 1988 p 100 (For primary document see N90-13449 05-18)
Avail: NTIS HC A08/MF A01 CSCL 09A

N90-13508# European Space Agency, Paris (France).
PAYLOAD ELECTRONICS AND MECHANISMS
T. vanderLaan, E. Jaekel, and H. Eggel *In its* The Hipparcos Mission. Prelaunch Status. Volume 1: The Hipparcos Satellite Jun. 1989 p 101-105 (For primary document see N90-13499 05-18)
Copyright Avail: NTIS HC A16/MF A02; ESA Publications Div., ESTEC, Noordwijk, Netherlands, 80 Dutch guilders

N90-13520# European Space Agency, Paris (France).
ELECTRICAL TESTING
M. Setzke, O. Pace, and G. Jung *In its* The Hipparcos Mission. Prelaunch Status. Volume 1: The Hipparcos Satellite Jun. 1989 p 227-239 (For primary document see N90-13499 05-18)
Copyright Avail: NTIS HC A16/MF A02; ESA Publications Div., ESTEC, Noordwijk, Netherlands, 80 Dutch guilders

34 FLUID MECHANICS AND HEAT TRANSFER

Includes boundary layers; hydrodynamics; fluidics; mass transfer; and ablation cooling.

For related information see also *02 Aerodynamics* and *77 Thermodynamics and Statistical Physics.*

N90-13715*# Lockheed Missiles and Space Co., Huntsville, AL. Engineering Center.
SSME LOX POST FLOW ANALYSIS/FLUID STRUCTURE INTERACTION. VOLUME 1: FLOW ANALYSIS Final Report
Roger W. Burke Jun. 1989 32 p
(Contract NAS8-37361)
(NASA-CR-183677; NAS 1.26:183677;
LMSC-HEC-TR-F268618-Vol-1) Avail: NTIS HC A03/MF A01 CSCL 20D

The realization of measures to improve the performance of the Space Shuttle is, to a large extent, dependent on an improved understanding of the fluid flow phenomena occurring in the main engine. The overall arrangement of the primary components of the Space Shuttle Main Engine (SSME) are presented. The impingement of the hot gases from the transfer ducts onto the LOX posts causes them to be subjected to severe thermal and gas dynamic loads, which in the past have resulted in the occasional breakage of some elements of the outer row of posts during test firings of the engine, particularly at higher power levels. Large velocities in the gap between the LOX posts may also be a contributing factor in causing dynamic stability problems. The deforming structural response of the posts to the pressure loading may likely affect the gas flowfield by producing a moving flowfield boundary, thereby creating a dynamically coupled unsteady fluid-structure system. The objective was to investigate the three-dimensional, turbulent flow around a simplified SSME LOX post array using an existing Reynolds averaged Navier-Stokes flow solver and a suitable turbulence model to parameterize the turbulent shear stresses. Numerical computations were performed to analyze the effect on the flowfield of varying the spacing between the LOX posts, which were modeled as rigid, three-dimensional circular cylinders. The methodology used in the computations is described. Results are presented. Author

N90-13716*# Computational Mechanics Co., Austin, TX.
SSME LOX POST FLOW ANALYSIS/FLUID STRUCTURE INTERACTION. VOLUME 2: FLUID STRUCTURE INTERACTION Final Report
Jun. 1989 130 p Prepared in cooperation with Lockheed Missiles and Space Co., Inc.
(Contract NAS8-37361)
(NASA-CR-183678; NAS 1.26:183678;
LMSC-HEC-TR-F268618-Vol-2) Avail: NTIS HC A07/MF A01 CSCL 20D

The progress made in resolving the computational issues associated with modeling high temperature and pressure viscous flows in advanced propulsion systems is documented. An overview of adaptive computational methods for various classes of fluid-structure interaction problems is presented. The key features associated with several approaches are outlined and the advantages/disadvantages of each are summarized. A mathematical formulation is presented for general fluid-structure interaction problems with a moving domain. The two adaptive approaches are discussed used in solving the benchmark problems. The first scheme is a user interactive scheme which is quite versatile and easy to implement but requires an excessive amount of monitoring by the operator and is computationally inefficient. The second method is a new, local remeshing method for handling a general class of fluid-structure interaction problems. This method couples many of the attractive features of other approaches into a computationally efficient and versatile method. The results obtained for two test cases are presented. Results from both the user interactive and local remeshing procedure are described. The current status of the project and future goals to be completed are summarized. Author

N90-13717 Virginia Univ., Charlottesville.
A THREE-DIMENSIONAL POTENTIAL FLOW ANALYSIS OF DYNAMIC FLUID FORCES ACTING ON A WHIRLING CENTRIFUGAL IMPELLER BOUNDED BY A VOLUTE Ph.D. Thesis
David Marc Waite 1988 390 p
Avail: Univ. Microfilms Order No. DA8913939

An unsteady three-dimensional potential flow model was developed. The panel method, as developed by Hess and Smith, formed the basis for this model. Instantaneous and time-averaged dynamic fluid forces, acting on whirling centrifugal impellers, were computed. Unbounded impellers and impellers bounded by a volute were analyzed. Inertial, damping, and stiffness matrices were presented for both types of impellers. For the unbounded impeller, the radial and tangential forces remained constant in time. Therefore, the rotor dynamic matrices possessed skew-symmetry. When bounded impellers were operated at design flows and beyond, the rotor dynamic matrices could be approximated by skew-symmetry matrices. For both the unbound and bound impeller analyses, the panel method correctly predicted radial force trends with increasing flow. However, for negative whirl speed ratios, the radial force predictions were underestimated. In the case of the unbound impeller, cross-coupling stiffness coefficients were accurately predicted at design flows and above. The destabilizing cross-coupling stiffness coefficients, which were found experimentally at flows below the design point, were not predicted by the panel method. The computational technique developed has

the capability of assessing dynamic fluid forces acting on a single stage centrifugal pump. It provides analytical verification of the existence of a subsynchronous whirl instability region for centrifugal pumps bounded by a volute. Dissert. Abstr.

N90-13718*# Texas A&M Univ., College Station. Surface Electrochemistry Lab.

MODERN BIOFUEL CELLS FOR WASTE RECYCLING IN LIFE SUPPORT SYSTEMS Final Report

L. Chen and J. OM. Bockris Sep. 1989 44 p
(Grant NAG9-283)
(NASA-CR-185963; NAS 1.26:185963) Avail: NTIS HC A03/MF A01 CSCL 20D

Innovative ways of treating urea in waste water reprocessing for long duration space exploration are being considered. Urea is very stable and therefore there are few effective ways for its decomposition. The feasibility of the use of the enzyme urease is to catalyze the hydrolysis of urea to ammonia and carbon dioxide is discussed, including a methodology, potential problems, the capabilities and advantages of such a system. J.P.S.

N90-13719*# National Aeronautics and Space Administration. Lewis Research Center, Cleveland, OH.

EFFECT OF SPATIAL RESOLUTION ON APPARENT SENSITIVITY TO INITIAL CONDITIONS OF A DECAYING FLOW AS IT BECOMES TURBULENT

Robert G. Deissler and Frank B. Molls Nov. 1989 8 p Submitted for publication
(NASA-TM-102377; E-5115; NAS 1.15:102377) Avail: NTIS HC A02/MF A01 CSCL 20D

Grids with 32(exp 3), 64(exp 3), and 128(exp 3) points are used in numerical solutions for a decaying flow. The sensitivity of initially neighboring solutions to small changes in initial conditions increases as the spatial resolution improves. A fourth-order finite-difference method is used for the solutions with 32(exp 3) and 64(exp 3) grid points, and a pseudospectral method is used for 128(exp 3) grid points. The latter solutions appear to be rather well-resolved, in spite of the formation of steep velocity gradients in the flow. Author

N90-13720# Wisconsin Univ., Madison. Center for Mathematical Studies.

QUADRATIC DYNAMICAL SYSTEMS DESCRIBING SHEAR FLOW OF NON-NEWTONIAN FLUIDS Technical Summary Report

David S. Malkus, John A. Nohel, and Bradley J. Plohr Aug. 1989 19 p
(Contract DAAL03-87-K-0036; NSF DMS-87-12058; NSF DMS-86-20303; AF-AFOSR-0191-87; AF-AFOSR-0141-85)
(AD-A212892; CMS-TSR-90-7) Avail: NTIS HC A03/MF A01 CSCL 20/4

Phase-plane techniques are used to analyze a quadratic system of ordinary differential equations that approximates a single relaxation-time system of partial differential equations used to model transient behavior of highly elastic non-Newtonian liquids in shear flow through slit dies. The latter one-dimensional model is derived from three-dimensional balance laws coupled with differential constitutive relations well-known by rheologists. The resulting initial-boundary-value problem is globally well-posed and possesses the key feature that the steady shear stress is a non-monotone function of the strain rate. Results of the global analysis of the quadratic system of ordinary differential equations lead to the same qualitative features as those obtained recently by numerical simulation of the governing partial differential equations for realistic data for polymer melts used in rheological experiments. The analytical results provide an explanation of the experimentally observed phenomenon called spurt; they also predict new phenomena discovered in the numerical simulation; these phenomena should also be observable in experiments. GRA

N90-13721# Wisconsin Univ., Madison. Center for Mathematical Sciences.

ANALYSIS OF NEW PHENOMENA IN SHEAR FLOW OF NON-NEWTONIAN FLUIDS Technical Summary Report

David S. Malkus, John A. Nohel, and Bradley J. Plohr Aug. 1989 38 p
(Contract DAAL03-87-K-0036; NSF DMS-87-12058; NSF DMS-86-20303; AF-AFOSR-0191-87; AF-AFOSR-0141-85)
(AD-A212893; CMS-TSR-90-6) Avail: NTIS HC A03/MF A01 CSCL 20/4

Phase-plane and small-parameter asymptotic techniques are used to analyze systems of ordinary differential equations that describe the transient behavior of non-Newtonian fluids in shear flow. These systems approximate the partial differential equations that derive from three-dimensional balance laws and from differential constitutive models for highly elastic liquids. Two models are considered: one with a single relaxation time and small Newtonian viscosity; the other with two relaxation times and no Newtonian viscosity. Both possess the key feature that the variation of steady shear stress with strain rate is not monotone. The analysis shows that both models exhibit several distinctive phenomena: spurt, shape memory, hysteresis, latency, and normal stress oscillations. The predictions for the spurt phenomenon agree quantitatively with experimental results for polymer melts; the other new phenomena, which were discovered recently in numerical simulation, should also be observable in rheological experiments. GRA

N90-13722*# Institute for Computer Applications in Science and Engineering, Hampton, VA.

MULTIPLE PATHS TO SUBHARMONIC LAMINAR BREAKDOWN IN A BOUNDARY LAYER Final Report

Thomas A. Zang (National Aeronautics and Space Administration. Langley Research Center, Hampton, VA.) and M. Yousuff Hussaini Oct. 1989 15 p Submitted for publication
(Contract NAS1-18605)
(NASA-CR-181948; NAS 1.26:181948; ICASE-89-78) Avail: NTIS HC A03/MF A01 CSCL 20D

Numerical simulations demonstrate that laminar breakdown in a boundary layer induced by the secondary instability of two-dimensional Tollmien-Schlichting waves to three-dimensional subharmonic disturbances need not take the conventional lambda vortex/high-shear layer path. Author

N90-13723*# National Aeronautics and Space Administration. Ames Research Center, Moffett Field, CA.

A REVIEW OF QUASI-COHERENT STRUCTURES IN A NUMERICALLY SIMULATED TURBULENT BOUNDARY LAYER

S. K. Robinson, S. J. Kline, and P. R. Spalart May 1989 36 p Presented at the Quasi-Coherent Structures in the Turbulent Boundary Layer, part 2. Verification and New Inform. from a Numerically Simulated Flat-Plate Layer at Memorial Intern. Seminar on Near-Wall Turbulence, Dubrovnik, Yugoslavia, 16-20 May 1988
(NASA-TM-102191; A-88294; NAS 1.15:102191) Avail: NTIS HC A03/MF A01 CSCL 20D

Preliminary results of a comprehensive study of the structural aspects of a numerically simulated number turbulent boundary layer are presented. A direct Navier-Stokes simulation of a flat-plate, zero pressure gradient boundary layer at Re0 = 670 was used. Most of the known nonrandom, coherent features of turbulent boundary layers are confirmed in the simulation, and several new aspects of their spatial character are reported. The spatial relationships between many of the various structures are described, forming the basis for a more complete kinematical picture of boundary layer physics than has been previously known. In particular, the importance of vortex structures of various forms to the generation of Reynolds shear stress is investigated. Author

N90-13724# Deutsche Forschungsanstalt fuer Luft- und Raumfahrt, Goettingen (Germany, F.R.). Abteilung Grenzschichten und Unterschallstroemung.

THE INFLUENCE OF MULTIPLE HOT-WIRE PROBE GEOMETRY ON THE RESULTS OF MEASUREMENTS IN TURBULENT FLOWS Ph.D. Thesis - Tech. Univ. Clausthal

Henning Rosemann May 1989 119 p In GERMAN; ENGLISH summary Report will also be announced as translation (ESA-TT-1182)

(DLR-FB-89-26; ISSN-0171-1342; ETN-90-95835) Avail: NTIS HC A06/MF A01; DLR, VB-PL-DO, Postfach 90 60 58, 5000 Cologne, Fed. Republic of Germany, 35 DM

An analytical evaluation method to compute the instantaneous velocity vector from the signals of triple and quadruple hot-wire probes with nearly arbitrary geometry is developed. The domain of flow angles, in which a unique relationship between the measured values and the velocity vector exists, is determined for several probe geometries. Measurement errors, which occur in the time-averaged velocity components and in the Reynolds stress tensor are estimated theoretically and checked experimentally. A comparison of different three-sensor probes with a four-sensor Kovasznay-type probe shows that, with the latter, better accuracy in turbulence measurements should be attainable. ESA

N90-13725# Deutsche Forschungsanstalt fuer Luft- und Raumfahrt, Goettingen (Germany, F.R.). Abteilung Instabilitaeten und Abloesung.

GENERALIZED SIMILARITY SOLUTIONS FOR THREE DIMENSIONAL, LAMINAR, STEADY, COMPRESSIBLE BOUNDARY LAYER FLOWS ON SWEPT PROFILE CYLINDERS

Viktor Saljnikov and Uwe Dallmann Jan. 1928 103 p In GERMAN; ENGLISH summary Report will also be announced as translation (ESA-TT-1190)

(DLR-FB-89-34; ISSN-0171-1342; ETN-90-95843) Avail: NTIS HC A06/MF A01; DLR, VB-PL-DO, Postfach 90 60 58, 5000 Cologne, Fed. Republic of Germany, 34.50 DM

A method of generalized similarity which allows one to derive solutions of the laminar, steady, compressible, and 3-D boundary layer equations for swept wing configurations is presented. The model configuration is an infinitely long swept profile cylinder within ideal gas flow with a dynamic viscosity which depends linearly on the temperature. The pressure distribution, Pr and Ma numbers, as well as the sweep angle and temperature boundary conditions, can be chosen arbitrarily. A universal mathematical model is derived which is integrated numerically. In view of transonic swept wings these numerical calculations are performed for various values. The influence of Mach number, sweep angle, and changes of wall temperature on the characteristic boundary layer properties between the stagnation and the separation points are investigated. ESA

N90-13726# Universiteit Twente, Enschede (Netherlands). Faculty of Applied Mathematics.

BALANCE LAWS AND CENTRO VELOCITY IN DISSIPATIVE SYSTEMS

E. vanGroesen and F. Mainardi (Bologna Univ., Italy) Jul. 1989 18 p

(MEMO-797; ISSN-0169-2690; ETN-90-95964) Avail: NTIS HC A03/MF A01

Starting with a density that is conserved for a dynamical system when dissipation is ignored, a local conservation law is derived for which the total flux (integrated over the spatial domain) is unique. When dissipation is incorporated, the conservation law is shown to become a balance law. The contribution due to dissipation in this balance law is split in a unique way in a part that is proportional to the density and in a divergence expression which adds to the original (conservative) flux density. The total additional flux is uniquely defined, and these total fluxes are shown to appear in the expression for the centro velocity, i.e. in the velocity of the center of gravity of the density, which shows that this velocity can be defined in a unique way (in contrast to a local velocity). Applications to the Korteweg-de Vries-Burgers and to the incompressible Navier-Stokes equations are given. ESA

N90-13727# Technische Univ., Delft (Netherlands).

MULTIGRID AND DEFECT CORRECTION FOR THE STEADY NAVIER-STOKES EQUATIONS: APPLICATIONS TO AERODYNAMICS Ph.D. Thesis

Barend Koren 1989 132 p

(ETN-90-96011) Avail: NTIS HC A07/MF A01

High speed gas flows, applying the steady Navier-Stokes equations, are described. On the basis of the Hemker-Sperkreijse method, a procedure which is suitable for an accurate and efficient computation of Euler and Navier-Stokes equations, is proposed. The transonic wind tunnel flow, and transonic, subsonic and supersonic airfoil flows are studied, from the steady Euler equations concept. The practical interest of the Navier-Stokes method is analyzed. Subsonic and supersonic flat plate flows and hypersonic flat plate flow, are examined. It is shown that the method does not have an upper bound in Reynolds number. ESA

N90-13728# Deutsche Forschungsanstalt fuer Luft- und Raumfahrt, Goettingen (Germany, F.R.). Gruppe Transition und Turbulenz.

NUMERICAL SIMULATION OF TRANSITION IN THREE-DIMENSIONAL BOUNDARY LAYERS Ph.D. Thesis - Karlsruhe Univ.

Friedrich Meyer Jun. 1989 104 p In GERMAN; ENGLISH summary Original contains color illustrations

(DLR-FB-89-12; ISSN-0171-1342; ETN-90-96049) Avail: NTIS HC A06/MF A01; DLR, VB-PL-DO, Postfach 90 60 58, 5000 Cologne, Fed. Republic of Germany, 40 DM

Linear and nonlinear stages of laminar-turbulent transition in three-dimensional boundary-layers, initiated by crossflow instability, are investigated by linear stability analysis and numerical simulation of the incompressible Navier-Stokes equations. The conditions in the numerical calculations are adapted to the DLR (Deutsche forschungsanstalt fur Luft und Raumfahrt) swept flat plate transition experiment. Falkner-Skan-Cooke similarity profiles are used to describe the parallel basic flow. A quasi-two-dimensional treatment of the problem yields nonlinear saturation of the stationary crossflow vortices. The nonlinear interaction of stationary vortices with traveling disturbances is then investigated. The evolution of the mean flow, fluctuations and instantaneous velocity is documented. The development of the disturbances strongly depends on the initial disturbances. Good agreement is observed between simulation and experiment. The nonlinear development initiates a marked deformation of the streamwise and crossflow profiles and an increase of the mean wall shear. ESA

N90-13729# Deutsche Forschungsanstalt fuer Luft- und Raumfahrt, Brunswick (Germany, F.R.). Abteilung Unterschall-Entwurfsaerodynamik.

CALCULATION OF FLOW FIELDS BY THE SOLUTION OF THE EULER EQUATIONS USING AN EXTENDED FINITE VOLUME DISCRETIZATION SCHEME Ph.D. Thesis - Tech. Univ. Brunswick

Cord-Christian Rossow Jun. 1989 150 p In GERMAN; ENGLISH summary

(DLR-FB-89-38; ISSN-0171-1342; ETN-90-96052) Avail: NTIS HC A08/MF A01; DLR, VB-PL-DO, Postfach 90 60 58, 5000 Cologne, Fed. Republic of Germany, 48 DM

Different two-dimensional finite volume schemes for the spatial discretization of the Euler equations are outlined. The accuracy of these schemes is investigated by theoretical analysis. With the discretization schemes discussed calculations are performed in order to demonstrate the influence of the different discretization errors. Comparison of the results shows that in the case of discontinuities in the computational mesh only a cell vertex scheme is capable to ensure a consistent discretization of the governing equations. The higher accuracy of the cell vertex method is retained for three-dimensional problems by the use of an appropriate formulation derived in the present study. This is proven by theoretical analysis and confirmed by the calculation of three-dimensional flow fields. ESA

N90-13730# Von Karman Inst. for Fluid Dynamics, Rhode-Saint-Genese (Belgium).
TURBULENT SHEAR FLOWS
1989 488 p Lecture series held in Rhode-Saint-Genese, Belgium, 6-10 Feb. 1989
(VKI-LS-1989-03; D/1989/0238/369; ISSN-0377-8312; ETN-90-95738) Avail: NTIS HC A21/MF A03

Studies on turbulent shear flow are presented. The following subjects are covered: (1) the current understanding of the shear layer phenomena; (2) the prospects of direct and large eddy simulation; (3) the transport of scalars in turbulent shear flow; and (4) the nature of coherent structures and their influence on the turbulent transport. The dynamics of coherent structures in an excited jet and the transport of heat by coherent structures are considered. Applications of homogeneous flows, and datasets of turbulent shear flows, are given. For individual titles, see N90-13731 through N90-13734.

N90-13731# Cambridge Univ. (England). Dept. of Applied Mathematics and Theoretical Physics.
AN INTRODUCTION VIA VORTICITY DYNAMICS AND STATISTICAL THEORY
J. C. R. Hunt *In* VKI, Turbulent Shear Flows 1989 189 p (For primary document see N90-13730 05-34)
Avail: NTIS HC A21/MF A03

Some aspects of the mathematical description of the velocity fields in turbulent flow are presented. The definition of the different flow regions, their statistical distribution and dependence on the nature of the flow, as well as the means to measure them, are discussed. Numerical simulations, probe measurements or image analysis can be applied to analyze the different flow regions. The general features of the results are in agreement, but precise definition of these structures is needed. Experimental studies of shear flows show that the nature and form of these structures differ between one flow and another. Moreover, measurements of coherent structures in the free shear layer show how the spectrum evolves as the pairing and splitting of vortices proceeds. Applications and practical problems are given. ESA

N90-13732# Centre d'Etudes et de Recherches, Toulouse (France).
APPLICATION OF TWO-POINT CLOSURES TO SUBGRID SCALE MODELING FOR HOMOGENEOUS, 3D TURBULENCE
B. Aupoix *In* VKI, Turbulent Shear Flows 1989 58 p (For primary document see N90-13730 05-34)
Avail: NTIS HC A21/MF A03

The subgrid scale modeling in homogeneous, incompressible, three dimensional turbulence, is presented. The concept of homogeneous turbulence is described. Large eddy simulation and the problem of subgrid scale modeling are introduced. The role of the subgrid terms is analyzed and various approaches for subgrid scale modeling are reviewed. Attention is paid to the application of two point closures. Coupling of a statistical resolution for the subgrid scales with a large eddy simulation is introduced for homogeneous, isotropic turbulence. Derivations of eddy viscosity models are presented. A model to account for the energy backscatter from the subgrid scales is detailed. Homogeneous flow applications are discussed. ESA

N90-13733# Institut de Mecanique de Grenoble (France).
COHERENT STRUCTURES IN A ROUND JET
M. Favre-Marinet *In* VKI, Turbulent Shear Flows 1989 78 p (For primary document see N90-13730 05-34)
Avail: NTIS HC A21/MF A03

The main features of the mean flow in the round jet are viewed, and the observations of coherent structures are described. The three regions of the mean flow are analyzed. The visualization of the flow issue from a nozzle is presented. The theoretical background on the non-random velocity fluctuations and the experimental results are compared. The axisymmetric mode is shown to be dominant in the first two or three diameters. Detailed quantitative measurements are shown to be needed to elucidate the role of coherent structures in turbulent transport. An experiment on a heated jet with weak excitation is described. The dynamics of coherent structures in an excited jet and the transport of heat by coherent structures are discussed. ESA

N90-13734# Brunel Univ., Uxbridge (England). Dept. of Mathematics and Statistics.
SCALAR TRANSPORT IN TURBULENT SHEAR FLOWS
P. C. Chatwin *In* VKI, Turbulent Shear Flows 1989 71 p (For primary document see N90-13730 05-34)
Avail: NTIS HC A21/MF A03

The transport phenomena in turbulent shear flows are studied. The statistical description of turbulent diffusion and the importance of the probability density function in pratical problems are reviewed. The equations and the quantification of the turbulent diffusion of fluid elements are presented. Taylor and Lagrangian analysis are included. The research performed and the interpretation of data and datasets, concerning turbulent diffusion in shear flows, are presented. In particular, a framework development, the intermittency factor, and the structure of the probability density function are considered. ESA

N90-13735# Von Karman Inst. for Fluid Dynamics, Rhode-Saint-Genese (Belgium).
NUMERICAL METHODS FOR FLOWS IN TURBOMACHINERY, VOLUME 1
1989 305 p Lecture series held in Rhode-Saint-Genese, Belgium, 22-26 May 1989
(VKI-LS-1989-06-Vol-1; D/1989/0238/372-Vol-1; ISSN-0377-8312; ETN-90-95740) Avail: NTIS HC A14/MF A02

Studies in the advances in the application of Euler and Navier-Stokes equations to flows in turbomachinery bladings are presented. The methods to solve the Euler equations (in particular the Runge-Kutta scheme), methods to accelerate the convergence rate (vectorization, multiprocessing, multigrid, implicit residual smoothing, etc.) and methods to improve the accuracy of the solution through the use of adaptive, unstructured grids, are discussed. The various issues related to the solution of Navier-Stokes equations are analyzed. The viscous flow calculations without numerical mixing is emphasized. The numerical problems related to the coupling of turbulence models with Navier-Stokes solvers and the treatment of non-conservative equations are included. For individual titles, see N90-13736 through N90-13740.

N90-13736# General Electric Co., Schenectady, NY. Research and Development Center.
INVISCID 3D SOLUTION METHODS
D. Graham Holmes *In* VKI, Numerical Methods for Flows in Turbomachinery, Volume 1 1989 58 p (For primary document see N90-13735 05-34)
Avail: NTIS HC A14/MF A02

An approach to modeling the flow through turbomachinery is described. It consists of modeling a single blade row and solving the equations for compressible, inviscid, rotational, steady, three dimensional flow, which are known as steady Euler equations. The advantages of applying three dimensional solutions (in particular the fact that no increase in computational cost is observed) over the standard one blade row model are considered. The basic algorithm used to solve the Euler equations is presented. For discretizing the spatial derivatives in partial differential equations the finite volume scheme is applied. Moreover, the steady state convergence acceleration, the vector computer processing, and the modification of the algorithms to handle the modeling of propellors, multiple blade rows and part-span shrouds, are given. ESA

N90-13737# General Electric Co., Schenectady, NY. Research and Development Center.
INVISCID 2D SOLUTIONS ON UNSTRUCTURED, ADAPTIVE GRIDS
D. Graham Holmes *In* VKI, Numerical Methods for Flows in Turbomachinery, Volume 1 1989 39 p (For primary document

see N90-13735 05-34)
Avail: NTIS HC A14/MF A02

The approach to solving two dimensional Euler equations, applying an unstructured, adaptive triangular grid, is presented. The distinction between structured and unstructured grids is discussed. The main steps of the solution algorithm, which is based on a standard Runge-Kutta model and is able to run on an unstructured grid, are outlined. Concerning the process of grid generation, the basic ideas underlying Delaunay triangulation, and the creation of the boundary and interior points, are discussed. The adaptive refinement to obtain good solutions is considered. Application examples are supplied and improvements are suggested. ESA

N90-13738# Virginia Polytechnic Inst. and State Univ., Blacksburg. Dept. of Mechanical Engineering.
PRESSURE CORRECTION CALCULATION PROCEDURES FOR 3D VISCOUS FLOW
Joan G. Moore *In* VKI, Numerical Methods for Flows in Turbomachinery, Volume 1 1989 54 p (For primary document see N90-13735 05-34)
Avail: NTIS HC A14/MF A02

Pressure correction calculation procedures for three dimensional viscous flow are described. The conservation equations and the types of pressure correction methods, are given. The advantages of the pressure correction approach are discussed. The calculations with measurements for several three dimensional turbulent flows are compared. An elliptic calculation procedure is described by using a simple example. A variety of calculation procedures are explored with the aid of a hand held calculator or small personal computer. An explicit procedure which parallels time marching methods is presented. The necessary modifications to extend the pressure correction method to transonic flow, including shock capturing, are described. ESA

N90-13739# Virginia Polytechnic Inst. and State Univ., Blacksburg. Dept. of Mechanical Engineering.
THREE D FLOWS IN TURBINE BLADE ROWS
John Moore *In* VKI, Numerical Methods for Flows in Turbomachinery, Volume 1 1989 92 p (For primary document see N90-13735 05-34)
Avail: NTIS HC A14/MF A02

The numerical methods to solve three dimensional flows in turbine blade rows are discussed. The results from the application of a three dimensional Navier-Stokes code to flow in turbine blade rows, and the two linear turbine rotor case, are included. Predictions of the losses produced through the cascades and the exit angles resulting from the secondary flows are given. The contributions of secondary kinetic energy to the overall losses in turbine blade rows are discussed. The mechanisms for the dissipation of mean kinetic energy in swirling three dimensional passage vortex flow, quantified through measurements of Reynolds stresses and mean velocities, are presented. ESA

N90-13740# Virginia Polytechnic Inst. and State Univ., Blacksburg. Dept. of Mechanical Engineering.
FLOWS WITH TIP LEAKAGE
John Moore *In* VKI, Numerical Methods for Flows in Turbomachinery, Volume 1 1989 45 p Presented at the Gas Turbine and Aeroengine Congress and Exposition, Amsterdam, Netherlands, 5-9 Jun. 1989 (For primary document see N90-13735 05-34)
Avail: NTIS HC A14/MF A02

The flow development within the tip gap and the flow tip leakage, applying Navier-Stokes codes, are discussed. The loss production, the turbine inefficiency and the heat transfer to the blade tip, are considered. The measurements and calculations used demonstrate features of the flow, such as separation and reattachment on the blade tip, shock formation in the tip gap, and formation and dissipation of tip gap secondary kinetic energy. A procedure for calculating turbine blade tip temperatures is included. The results for a centrifugal compressor show the interaction of the tip leakage and passage flows. The radial blackflow near the shroud wall at low off-design flow rates is considered. The calculations demonstrate the potential use of a computational fluid dynamics code for predicting a centrifugal compressor map. ESA

N90-13741# Von Karman Inst. for Fluid Dynamics, Rhode-Saint-Genese (Belgium).
NUMERICAL METHODS FOR FLOWS IN TURBOMACHINERY, VOLUME 2
1989 317 p Lecture series held in Rhode-Saint-Genese, Belgium, 22-26 May 1989
(VKI-LS-1989-06-Vol-2; D/1989/0238/372-Vol-2; ISSN-0377-8312; ETN-90-95741) Avail: NTIS HC A14/MF A02

The calculation of flows in turbomachinery is discussed. Different ways to get a suitable solution, by presenting a given problem, and the drawbacks attached to it, are considered. A basic review of turbulence models, the coupling problems and the implicit treatment of non-conservative equations, are included. In particular, the turbulence modeling and the implementation in solving Navier-Stokes equation is discussed. Concerning the unsteady flow in turbomachinery, the different approaches of the problem are reviewed. For individual titles, see N90-13742 through N90-13743.

N90-13742# Rouen Univ. (France). Faculte des Sciences et Techniques.
TURBULENCE MODELING AND IMPLEMENTATION IN NAVIER-STOKES SOLVERS
Dany Vandromme *In* VKI, Numerical Methods for Flows in Turbomachinery, Volume 2 1989 58 p (For primary document see N90-13741 05-34)
Avail: NTIS HC A14/MF A02

A general survey on the tools available to perform basic turbulence modeling of compressible flow is given. The following topics are discussed: the basic features of compressible flows, the Cebeci-Smith-Mosinski and the Baldwin-Lomax models, and the turbulence transport equations. The topic of the second order closure is touched through the problem of the Reynolds stress modeling. It is shown that for the variable density problems, the low speed, the weakly compressible and the strongly compressible flows, must be distinguished. ESA

N90-13743# Massachusetts Inst. of Tech., Cambridge. Dept. of Aeronautics and Astronautics.
NUMERICAL METHODS FOR UNSTEADY TURBOMACHINERY FLOW
Michael Giles *In* VKI, Numerical Methods for Flows in Turbomachinery, Volume 2 1989 52 p (For primary document see N90-13741 05-34)
Avail: NTIS HC A14/MF A02

The approaches to calculating the unsteady flow in turbomachinery are reviewed. The formulation of the mathematical models, and the assumptions, approximations and circumstances under which they remain valid, are emphasized. The tradeoffs in time and accuracy between different methods are considered. The key features of the numerical methods are underlined. The sources of unsteadiness in turbomachinery are discussed. The linear method, the nonlinear unsteady Euler method, and the unsteady Navier-Stokes method are studied. ESA

N90-13744*# Arizona State Univ., Tempe. Dept. of Mechanical and Aerospace Engineering.
NAVIER-STOKES SIMULATION OF THE CROSSFLOW INSTABILITY IN SWEPT-WING FLOWS Final Report
Helen L. Reed Oct. 1989 59 p
(Grant NAG1-874)
(NASA-CR-186122; NAS 1.26:186122) Avail: NTIS HC A04/MF A01 CSCL 20D

The computational modeling of the transition process characteristic of flows over swept wings are described. Specifically, the crossflow instability and crossflow/T-S wave interactions are analyzed through the numerical solution of the full three-dimensional Navier-Stokes equations including unsteadiness, curvature, and sweep. This approach is chosen because of the complexity of the problem and because it appears that linear

stability theory is insufficient to explain the discrepancies between different experiments and between theory and experiments. The leading edge region of a swept wing is considered in a three-dimensional spatial simulation with random disturbances as the initial conditions. The work has been closely coordinated with the experimental program of Professor William Saric, examining the same problem. Comparisons with NASA flight test data and the experiments at Arizona State University were a necessary and an important integral part of this work. Author

N90-13745 Virginia Polytechnic Inst. and State Univ., Blacksburg.
EFFECT OF SUCTION AND COOLING ON THE STABILITY OF SUBSONIC AND SUPERSONIC BOUNDARY LAYERS Ph.D. Thesis
Ayman Adnan Al-Maaitah 1989 154 p
Avail: Univ. Microfilms Order No. DA8915715

The effect of cooling and suction on the stability of subsonic flow over two-dimensional roughness elements and supersonic flow over flat plates is investigated. First, the effect of wall cooling on the two-dimensional linear stability of subsonic flows over two-dimensional surface imperfections is investigated. Results are presented for flows over smooth humps and backward-facing steps with Mach numbers up to 0.8. Second, the effect of suction on the stability of compressible flows over backward-facing steps is investigated. As expected, suction considerably reduces the separation region. The results show that continuous suction stabilizes the flow outside the separation bubble, as expected, but it destabilizes the flow inside it. Third, the effect of suction on the stability of supersonic and hypersonic boundary layers is investigated. Calculations are performed for non-similar and self-similar boundary layers. The variation of the maximum growth rate with Mach number at low levels of suction is different from that at high levels of suction. This is due to the coexistence of viscous and inviscid instability mechanisms in supersonic and hypersonic boundary layers. Dissert. Abstr.

N90-13746 Arizona State Univ., Tempe.
UNSTEADY FORCES INDUCED ON FINITE-SPAN CYLINDERS IN A CROSS-FLOW Ph.D. Thesis
Farzad Baban 1989 210 p
Avail: Univ. Microfilms Order No. DA8919587

A three axis piezoelectric load cell was used to measure the local unsteady forces induced on cylinders placed in a cross flow. In conjunction, a laser Doppler anemometer along with a single hot wire were used to traverse the wake so that correlations between the induced forces on the cylinder and the wake velocity could be calculated to provide insight into the character of the flow induced unsteady forces. Experiments were carried out for 2-D as well as for several finite span cylinders with different aspect ratios at a Reynolds number of 46,000 and a free stream turbulence level of approx. 2 percent. For the 2-D cylinder case, substantial evidence was obtained to demonstrate that the strength of the vortex roll-up along the span was quite uniform. As a result, the lift-velocity correlation along the span remained unchanged. In all the finite span cylinder cases, the separated flow from the top edge of the cylinder suppressed vortex shedding along the span of the cylinder and destroyed its coherence. Dissert. Abstr.

N90-13747*# North Carolina State Univ., Raleigh. Dept. of Mechanical and Aerospace Engineering.
NUMERICAL SOLUTIONS OF THE COMPLETE NAVIER-STOKES EQUATIONS Progress Report No. 16, 1 Jul. 1988 - 31 Dec. 1989
H. A. Hassan 18 Dec. 1989 16 p
(Grant NAG1-244)
(NASA-CR-186102; NAS 1.26:186102) Avail: NTIS HC A03/MF A01 CSCL 20D

A hybrid Reynolds averaged/assumed probability density function (PDF) approach was developed and applied to the study of turbulent combustion in a supersonic mixing layer. This approach was used to address the laminar-like treatment of the thermochemical terms that appear in the conservation equations. Calculations were carried out for two experiments involving H2-air supersonic turbulent mixing. A SPARK combustion model was employed. In general, the approach shows modest improvement over previous calculations. Author

N90-13748*# Sverdrup Technology, Inc., Cleveland, OH.
AN IMPROVED ALGORITHM FOR THE MODELING OF VAPOR FLOW IN HEAT PIPES Final Report
Leonard K. Tower and Donald C. Hainley Dec. 1989 12 p Proposed for presentation at the 7th International Heat Pipe Conference, Minsk, USSR, 21-25 May 1990; sponsored by Luikov Heat and Mass Transfer Inst.
(Contract NAS3-25266)
(NASA-CR-185179; E-5195; NAS 1.26:185179) Avail: NTIS HC A03/MF A01 CSCL 20D

A heat pipe vapor flow algorithm suitable for use in codes on microcomputers is presented. The incompressible heat pipe vapor flow studies of Busse are extended to incorporate compressibility effects. The Busse velocity profile factor is treated as a function of temperature and pressure. The assumption of a uniform saturated vapor temperature determined by the local pressure at each cross section of the pipe is not made. Instead, a mean vapor temperature, defined by an energy integral, is determined in the course of the solution in addition to the pressure, saturation temperature at the wall, and the Busse velocity profile factor. For alkali metal working fluids, local species equilibrium is assumed. Temperature and pressure profiles are presented for several cases involving sodium heat pipes. An example for a heat pipe with an adiabatic section and two evaporators in sequence illustrates the ability to handle axially varying heat input. A sonic limit plot for a short evaporator falls between curves for the Busse and Levy inviscid sonic limits. Author

N90-13749*# National Aeronautics and Space Administration. Lewis Research Center, Cleveland, OH.
ANALYSIS OF ROTARY ENGINE COMBUSTION PROCESSES BASED ON UNSTEADY, THREE-DIMENSIONAL COMPUTATIONS
M. S. Raju (Sverdrup Technology, Inc., Cleveland, OH.) and E. A. Willis [1989] 37 p Presented at the 28th Aerospace Sciences Meeting, Reno, NV, 8-11 Jan. 1990; sponsored by AIAA
(NASA-TM-102469; E-5249; NAS 1.15:102469; AIAA-90-0643)
Avail: NTIS HC A03/MF A01 CSCL 20D

A new computer code was developed for predicting the turbulent, and chemically reacting flows with sprays occurring inside of a stratified charge rotary engine. The solution procedure is based on an Eulerian Lagrangian approach where the unsteady, 3-D Navier-Stokes equations for a perfect gas mixture with variable properties are solved in generalized, Eulerian coordinates on a moving grid by making use of an implicit finite volume, Steger-Warming flux vector splitting scheme, and the liquid phase equations are solved in Lagrangian coordinates. Both the details of the numerical algorithm and the finite difference predictions of the combustor flow field during the opening of exhaust and/or intake, and also during fuel vaporization and combustion, are presented. Author

N90-13750*# National Aeronautics and Space Administration. Lewis Research Center, Cleveland, OH.
CONVECTIVE HEAT TRANSFER MEASUREMENTS FROM A NACA 0012 AIRFOIL IN FLIGHT AND IN THE NASA LEWIS ICING RESEARCH TUNNEL
Philip E. Poinsatte, G. James VanFossen, and Kenneth J. DeWitt (Toledo Univ., OH.) [1989] 20 p Presented at the 28th Aerospace Sciences Meeting, Reno, NV, 8-11 Jan. 1990; sponsored by AIAA
(NASA-TM-102448; E-5232; NAS 1.15:102448) Avail: NTIS HC A03/MF A01 CSCL 20D

Local heat transfer coefficients were measured on a smooth and roughened NACA 0012 airfoil. Heat transfer measurements on the 0.533 m chord airfoil were made both in flight on the NASA Lewis Twin Otter Icing Research Aircraft and in the NASA Lewis Icing Research Tunnel (IRT). Roughness was obtained by

the attachment of uniform 2 mm diameter hemispheres to the airfoil surface in 4 distinct patterns. Flight data were taken for the smooth and roughened airfoil at various Reynolds numbers based on chord in the range 1.24 to 2.50 x 10(exp 6) and at various angles of attack up to 4 deg. During these flight tests, the free stream velocity turbulence intensity was found to be very low (less than 0.1 percent). Wind tunnel data were acquired in the Reynolds number range 1.20 to 4.25 x 10(exp 6) and at angles of attack from -4 to 8 deg. The turbulence intensity in the IRT was 0.5 to 0.7 percent with the cloud generating sprays off. A direct comparison was made between the results obtained in flight and in the IRT. The higher level of turbulence in the IRT vs. flight had little effect on the heat transfer for the lower Reynolds numbers but caused a moderate increase in heat transfer at the high Reynolds numbers. Roughness generally increased the heat transfer. Author

N90-13751*# National Aeronautics and Space Administration. Lewis Research Center, Cleveland, OH.
VAPOR CONDENSATION ON LIQUID SURFACE DUE TO LAMINAR JET-INDUCED MIXING: THE EFFECTS OF SYSTEM PARAMETERS
Chin-Shun Lin (Analex Corp., Cleveland, OH.) and Mohammad M. Hasan [1989] 21 p Presented at the 28th Aerospace Sciences Meeting, Reno, NV, 8-11 Jan. 1990; sponsored by AIAA
(NASA-TM-102433; E-5201; NAS 1.15:102433; AIAA-90-0354)
Avail: NTIS HC A03/MF A01 CSCL 20D

The effects of system parameters on the interface condensation rate in a laminar jet induced mixing tank are numerically studied. The physical system consists of a partially filled cylindrical tank with a slightly subcooled jet discharged from the center of the tank bottom toward the liquid-vapor interface which is at a saturation temperature corresponding to the constant tank pressure. Liquid is also withdrawn from the outer part of the tank bottom to maintain the constant liquid level. The jet velocity is selected to be low enough such that the free surface is approximately flat. The effect of vapor superheat is assumed to be negligible. Therefore, the interface condensation rate can be determined from the resulting temperature field in the liquid region alone. The nondimensional form of the steady state conservation equations are solved by a finite difference method for various system parameters including liquid height to tank diameter ratio, tank to jet diameter ratio, liquid inflow to outflow area ratio, and a heat leak parameter which characterizes the uniform wall heat flux. Detailed analyses based on the numerical solutions are performed and simplified equations are suggested for the prediction of condensation rate. Author

N90-13752# Admiralty Research Establishment, Teddington (England).
COMPARISON OF INTEGRAL AND FINITE-DIFFERENCE METHODS FOR PREDICTING THE TURBULENT BOUNDARY LAYER ON AXISYMMETRIC BODIES
D. J. Atkins Oct. 1988 18 p
(ARE-TM(UHA)-88512; BR108415; ETN-90-94845) Copyright
Avail: NTIS HC A03/MF A01

The predictions of the attached turbulent boundary layer on three axisymmetric bodies are examined. Integral and finite difference methods are applied. Both methods take into account viscous-inviscid interaction effects. The finite difference method takes account of the variation of static pressure across the boundary layer. Comparisons with experimental data show both methods to be of similar accuracy over all but the last few percent of the body length. The finite difference method gives information on the individual velocity components and the Reynolds shear stress. ESA

N90-13753# Ecole Centrale de Lyon (France).
SPECTRAL STUDY OF A COMPRESSIBLE ISOTROPIC TURBULENCE Ph.D. Thesis [ETUDE SPECTRALE D'UNE TURBULENCE ISOTROPE COMPRESSIBLE]
Jean-Denis Marion 1988 164 p In FRENCH; ENGLISH summary Sponsored by Avions Marcel Dassault - Breguet Aviation, Saint Cloud, France and CNRS
(ECL-88-16; ETN-90-95770) Avail: NTIS HC A08/MF A01

Compressibility of a barotropic fluid (weak compressibility) is studied in the case of homogeneous isotropic turbulence. A two point description is adopted to allow the knowledge of energy transfer among eddies of different size. In this frame, a two-time closure, DIA (Direct Interaction Approximation), is derived. This work is a basis for developing, a one-time closure, an EDQNM (eddy damping quasi-normal Markov). Both closures reveal the existence of waves and the complex nature of the non-linear interactions between modes. A simplified model of the EDQNM closure is then derived. The EDQNM model is numerically solved. An asymptotic behavior of the compressible spectrum is found. This spectrum displays a -7/2 slope and an energetic level proportional to the square of the turbulent Mach number. The compressible modes tend towards an equipartition of energy between compressible velocity and pressure. Their energy decay is found to be slower than the incompressible one, especially for the large scales. ESA

N90-13754# Ecole Centrale de Lyon (France).
LARGE EDDY SIMULATION OF HOMOGENEOUS TURBULENCE UNDERGOING SHEAR AND THERMAL GRADIENTS. APPLICATION TO ONE POINT CLOSING MODELS Ph.D. Thesis
Mohammed Khoudli 1988 269 p In ENGLISH and FRENCH Original contains color illustrations
(ECL-88-23; ETN-90-95775) Avail: NTIS HC A12/MF A02

The macrosimulation numerical approach was employed, consisting of simulating the large eddies, resolving their evolution equations and modeling the small vortices to allow the analysis of higher Reynolds numbers. The numerical method used is described. Simulations in laminar and turbulent flows are used to evaluate the quality of the method. The results show that the described approach allows the same conclusions as the transportation of Reynolds tensions method. The counter gradient flow is predicted by both models as well as the oscillations of thermal flow. ESA

N90-13755# Ecole Centrale de Lyon (France). Lab. de Mecanique des Fluides.
MODEL AND COMPUTATION OF THREE-DIMENSIONAL TURBULENT JETS IN A CROSSFLOW Ph.D. Thesis
Guang-Ping Huang 1989 157 p In FRENCH; ENGLISH summary
(ECL-89-007; ETN-90-95782) Avail: NTIS HC A08/MF A01

An analysis of the transport phenomena between the jet and the external flow is presented. The analysis leads to the definition of particular closure relationships associated with the external fluid transfer in the jet. The conservation equation of the mass momentum and energy are written in a curvilinear coordinate system, tied on the jet trajectory. The model is capable of giving global jet information such as the trajectory, the levels of the maximum velocity and temperature, as well as local information. ESA

N90-13756# Rome Univ. (Italy). Dipt. di Fisica.
THE INITIAL-BOUNDARY VALUE PROBLEM FOR THE DAVEY-STEWARTSON 1 EQUATION; HOW TO GENERATE AND DRIVE LOCALIZED COHERENT STRUCTURES IN MULTIDIMENSIONS
P. M. Santini and A. S. Fokas (Clarkson Univ., Potsdam, NY.) 26 Jun. 1989 37 p Submitted for publication
(Preprint-684; ETN-90-95804) Avail: NTIS HC A03/MF A01

The initial-boundary value problem for the Davey-Stewartson 1 equation is linearized using the inverse scattering transform method. The genericity and the spectral interpretation of multidimensional localized coherent structures are established. These structures upon interaction not only exhibit a two dimensional phase shift, but also change form and exchange energy. They can be driven everywhere in the plane choosing a suitable motion of the boundaries. If this motion is not uniform, energy is lost through

radiation. These are called novel, localized, coherent, traveling structures dromions, to emphasize their ability to be driven by the boundaries. ESA

N90-13757# Heidelberg Univ. (Germany, F.R.). Sonderforschungsbereich 123.
COMPUTATION OF NONEQUILIBRIUM GAS FLOW PAST BLUNT BODIES
Youlan Zhu, Xionghua Wu (Tongji Univ., Shanghai, China), and J. Warnatz Nov. 1988 28 p Sponsored in part by the AvH Foundation and the Chinese National Natural Science Foundation
(Preprint-488; ETN-90-95875) Avail: NTIS HC A03/MF A01

A straight line method is used for the computation of nonequilibrium gas flow past blunt bodies. The boundary value problem is turned into an initial value problem by introducing an iterative method. Both explicit and semi-implicit schemes are used for solving the problem with chemical reactions. Many satisfying numerical results, including the case that some concentrations of species vary rapidly behind the shock wave, are obtained. ESA

N90-13758# Technische Univ., Delft (Netherlands). Faculty of Aerospace Engineering.
ON THE TOPOLOGY OF THREE-DIMENSIONAL VISCOUS FLOW STRUCTURES NEAR A PLANE WALL. A CLASSIFICATION AND NON-HYPERBOLIC SINGULARITIES ON THE WALL
M. E. M. deWinkel and P. G. Bakker Mar. 1988 48 p
(LR-541; ETN-90-95986) Avail: NTIS HC A03/MF A01

Flow structures near a plane wall are investigated by consideration of local solutions of the continuity equation and the Navier-Stokes equations. The flow is assumed to be steady, incompressible and satisfies the no-slip boundary conditions at the wall. The local solutions are obtained by performing series expansions near a point at the wall and they are used to classify the topology of the three-dimensional steady streamline patterns near the wall. ESA

35 INSTRUMENTATION AND PHOTOGRAPHY

Includes remote sensors; measuring instruments and gages; detectors; cameras and photographic supplies; and holography.

For aerial photography see *43 Earth Resources and Remote Sensing*. For related information see also *06 Aircraft Instrumentation*, and *19 Spacecraft Instrumentation*.

N90-13759*# Cornell Univ., Ithaca, NY. Dept. of Astronomy.
THE INFRARED SPECTROGRAPH DURING THE SIRTF PRE-DEFINITION PHASE Final Report, Nov. 1984 - Sep. 1987
James R. Houck 30 Sep. 1988 234 p
(Grant NAG2-317)
(NASA-CR-183234; NAS 1.26:183234) Avail: NTIS HC A11/MF A02 CSCL 14B

A test facility was set up to evaluate back-illuminated impurity band detectors constructed for an infrared spectrograph to be used on the Space Infrared Telescope Facility (SIRTF). Equipment built to perform the tests on these arrays is described. Initial tests have been geared toward determining dark current and read noise for the array. Four prior progress reports are incorporated into this report. They describe the first efforts in the detector development and testing effort; testing details and a new spectrograph concept; a discussion of resolution issues raised by the new design; management activities; a review of computer software and testing facility hardware; and a review of the preamplifier constructed as well as a revised schematic of the detector evaluation facility. J.P.S.

N90-13760*# HITEC Products, Inc., Ayer, MA. Strain Gage Development Lab.
HIGH TEMPERATURE CAPACITIVE STRAIN GAGE Final Report, 21 Mar. 1988 - 20 June 1989
Stephen P. Wnuk, Jr., Stephen P. Wnuk, III, and V. P. Wnuk Washington NASA Jan. 1990 50 p
(Contract NAS1-18668)
(NASA-CR-4266; NAS 1.26:4266) Avail: NTIS HC A03/MF A01 CSCL 14B

Capacitive strain gages designed for measurements in wind tunnels to 2000 F were built and evaluated. Two design approaches were followed. One approach was based on fixed capacitor plates with a movable ground plane inserted between the plates to effect differential capacitive output with strain. The second approach was based on movable capacitor plates suspended between sapphire bearings, housed in a rugged body, and arranged to operate as a differential capacitor. A sapphire bearing gage (1/4 in. diameter x 1 in. in size) was built with a range of 50,000 and a resolution of 200 microstrain. Apparent strain on Rene' 41 was less than + or - 1000 microstrain from room temperature to 2000 F. Three gage models were built from the Ground Plane Differential concept. The first was 1/4 in. square by 1/32 in. high and useable to 700 F. The second was 1/2 in. square by 1/16 in. high and useable to 1440 F. The third, also 1/2 in. square by 1/16 in. high was expected to operate in the 1600 to 2000 F range, but was not tested because time and funding ended. Author

N90-13761*# Sverdrup Technology, Inc., Cleveland, OH.
DEVELOPMENT AND CHARACTERIZATION OF PdCr TEMPERATURE-COMPENSATED WIRE RESISTANCE STRAIN GAGE Final Report
Jih-Fen Lei Oct. 1989 9 p Presented at the Sensors Expo International, Cleveland, OH, 12-14 Sep. 1989; sponsored by Sensors Magazine
(Contract NAS3-25266)
(NASA-CR-185153; E-5112; NAS 1.26:185153) Avail: NTIS HC A02/MF A01 CSCL 14B

A temperature-compensated resistance static strain gage with potential to be used to 600 C was recently developed. Gages were fabricated from specially developed palladium-13 w/o chromium (Pd-13Cr) wire and platinum (Pt) compensator. When bonded to high temperature Hastelloy X, the apparent strain from room temperature to 600 C was within 400 microstrain for gages with no preheat treatment and within 3500 microstrain for gages with 16 hours prestabilization at 640 C. The apparent strain versus temperature relationship of stabilized PdCr gages were repeatable with the reproducibility within 100 microstrain during three thermal cycles to 600 C and an 11 hours soak at 600 C. The gage fabrication, construction and installation is described. Also, the coating system used for this compensated resistance strain gage is explained. The electrical properties of the strain sensing element and main characteristics of the compensated gage including apparent strain, drift and reproducibility are discussed. Author

N90-13762# Diamond Materials, Inc., State College, PA.
NOVEL IN SITU SPECTROSCOPIC ELLIPSOMETER FOR REAL TIME ANALYSIS OF CVD DIAMOND FILMS Final Technical Report, 30 Sep. 1988 - 30 Aug. 1989
Richard J. Koba 4 Oct. 1989 45 p
(Contract DAAH01-88-C-0899)
(AD-A213218; DMI-TR-89010) Avail: NTIS HC A03/MF A01 CSCL 14/2

A split reflected beam spectroscopic ellipsometer (SRBSE) was designed, assembled and used to perform elliposmetric measurements on four different samples. The four samples were: (1) a base silicon wafer, (2) a silicon wafer coated with diamond-like carbon, (3) a silicon wafer coated with diamond of 70 percent of its surface area, and (4) a silicon wafer coated with a fully dense diamond film. The purpose of the program was to determine whether SRBSE could distinguish between different carbon films deposited on silicon substrates, thereby serving as a low cost alternative to more expensive spectroscopic techniques. The SRBSE could not provide accurate ellipsometric results over the range of light wavelengths investigated. The SRBSE could distinguish a coated substrate from an uncoated substrate. The measurements were too inaccurate to distinguish between the various types of carbon coatings on silicon. The lack of accuracy

was attributed to sensitivity of SRBSE to slight changes in optical beam alignment, polarization, and monochromaticity of the incident beam. GRA

N90-13763*# Thiokol Corp., Brigham City, UT. Space Operations.
THE EVALUATION OF A METERED MIXER FOR RTV SILICONE FOR RSRM NOZZLE BACKFILL OPERATIONS Final Report
T. C. Wardell Sep. 1989 11 p
(Contract NAS8-30490)
(NASA-CR-183831; NAS 1.26:183831; TWR-19968) Avail: NTIS HC A03/MF A01 CSCL 14B

Metered mixing specifically for the RSRM backfill operation was investigated. Projected advantages were the elimination of waste RTV silicone produced in the operation and the elimination of entrapped air during the mix. Although metered mixing proved to be a viable method for mixing the Dow Corning DC 90-0006 rubber with its catalyst, applying the technology to the RSRM backfill operation has several disadvantages that are decisive. Use of a metered mixer would increase the amount of material that was being scraped for each backfill and increase the amount of time required to clean up the equipment after each operation. Therefore, use of metered static mixers is not recommended for use in the RSRM nozzle backfill operations. Because metered mixers proved to have significant disadvantages other methods of mixing and dispensing the RTV during the backfill operation are being investigated, and will be reported in a separate document. Author

N90-13764# Aeronautical Research Labs., Melbourne (Australia).
A SLOW STRAIN-RATE TENSILE TESTING MACHINE
M. R. Kindermann, B. Cave, and D. R. Arnott Aug. 1989 15 p
(ARL-MAT-TM-399; AR-005-648) Avail: NTIS HC A03/MF A01

A slow strain-rate tensile testing machine intended for use in investigations into adhesive-bond durability and hydrogen embrittlement in metals is described. It is a basically simple design to facilitate ease of manufacture and its stepping-motor drive permits electronic control of the straining control of the straining rate over a range of several orders of magnitude. The driving circuitry provides a high degree of stability in the straining rate over extended periods and the entire system may be adapted to computer control if desired. Author

N90-13765# Helsinki Univ. of Technology, Espoo (Finland). Dept. of Technical Physics.
CONSTRUCTION OF THE ROTATING CRYOSTAT ROTA2, ITS USE FOR ZERO SOUND EXPERIMENTS IN (3)He-B, AND CALCULATIONS OF ION MOBILITY IN (3)He-A AND (3)He-P Ph.D. Thesis
Riitta Salmelin 1989 46 p
(ISBN-952-90091-3-5; ETN-90-96026) Avail: NTIS HC A03/MF A01

The construction of a new rotating demagnetization cryostat ROTA2, for research on superfluid He-3, is described. The first experiments employing this apparatus are presented. The effect of rotation on the real squashing collective mode in superfluid (3)He-B, is measured. The calculations of the multiple scattering of quasiparticles in superfluid He-3 from a microscope impurity, leading to the high mobility of negative ions, are discussed in the anisotropic A and P (polar) phases. The concept of quasiparticles, elementary excitations in the ground state of the Fermi system, is employed. When the critical temperature 0.93 mK is reached, this quantum fluid (He-3) is found to enter a regime of frictionless flow. ESA

N90-13766# Mosaic Industries, Inc., Mountain View, CA.
MULTISENSOR TECHNOLOGIES FOR LOW COST METHANE DETECTION Final Report, Apr. - Nov. 1987
P. K. Clifford and M. G. Dorman Nov. 1988 79 p
(Contract GRI-5087-254-1472)
(PB89-235188; GRI-88/0293) Avail: NTIS HC A05/MF A01 CSCL 14B

The study lays the technical foundation necessary to quantitatively characterize array performance and to determine the number of sensors needed for false-alarm-free methane detection. A technique was developed to quantitate the performances of sensor arrays. This technique was verified using data from a series of experiments that measured the responses of metal oxide semiconductor sensing arrays to methane and representative interfering gases, carbon monoxide and ammonia. Arrays of as few as two or three properly chosen sensors exhibit excellent immunity to false alarms. Further experiments show that arrays demonstrate good selectivity and low false alarm rates even after significant drift of sensor characteristics. GRA

N90-13767*# National Aeronautics and Space Administration. Goddard Space Flight Center, Greenbelt, MD.
ANALYTICAL DERIVATION AND VERIFICATION OF ZERO-GYRO CONTROL FOR THE IUE SATELLITE
Tiffany Bowles and John Croft Nov. 1989 48 p
(NASA-TM-100748; Rept-89B00245; NAS 1.15:100748) Avail: NTIS HC A03/MF A01 CSCL 14B

The International Ultraviolet Explorer (IUE) satellite was launched January 26, 1978 into a geosynchronous orbit over South America. From its stationary position, the telescope maintains continuous communication with the control centers at NASA's Goddard Space Flight Center in Greenbelt, Maryland, and at the European Space Agency's (ESA's) Villagranca del Castillo Satellite Tracking Station in Spain. Since its launch in 1978, the satellite has gradually lost four of the original six gyroscopes in the Inertial Reference Assembly (IRA). In August 1985, the fourth of the original six gyros failed and a two-gyro system developed by NASA-GSFC was uplinked to the satellite and is currently in use. A one-gyro system also developed by NASA-GSFC is ready for use in case of another gyro failure. In the event that the sixth gyro should also fail, a zero-gyro system is being developed. The goal of this system is to provide interial target pointing without the use of gyroscopes. The satellite has sun sensors to provide attitude information about two of the three axes. It relies upon the exchange of reaction wheel momenta to determine angular position and rate of the third axis. Author

N90-13768# Swedish Defence Research Establishment, Stockholm. Dept. of Weapons Technology.
CONSTRUCTION OF A SQUID MAGNETOMETER FOR INVESTIGATION OF SCREENING PROPERTIES OF HIGH-T(SUB c) SUPERCONDUCTORS
Johan Mattsson Sep. 1989 26 p In SWEDISH; ENGLISH summary
(FOA-C-20765-2.2; ISSN-0347-3694; ETN-90-96020) Avail: NTIS HC A03/MF A01

A SQUID (Superconducting QUantum Interferens Device) magnetometer, constructed for investigations of screening properties of high-T(sub c) superconductors, is described. The instrument is capable of detecting extremely small changes in magnetic flux. The temperature of the sample can be varied in the interval 4.2 to 300 K. with a temperature stability of 1 mk or better. Two superconducting NbTi coils are used to magnetize the sample. One is operating in persistant mode generating a constant magnetic field in the range 0 to 1000 gauss, and the other is generating an ac-field in the range 0 to 2 gauss and in frequency range 0.01 to 10.000 Hz. The effect of a coaxial superconducting shield on the sample signal detected by the pickup coils, often called the image effect, is theoretically studied. The reaction field of a superconducting shield in the presence of a coaxial magnet is studied. ESA

N90-13769# Technical Research Centre of Finland, Espoo. Lab. of Electrical and Automation Engineering.
ANALYSIS OF AN R-SQUID NOISE THERMOMETER Ph.D. Thesis - Helsinki Univ. of Technology
Heikki Seppa May 1989 91 p
(VTT-Publ-54; ISBN-951-38-3435-2; ISSN-0358-5069;

ETN-90-96024) Copyright Avail: NTIS HC A05/MF A01; Government Printing Center, P.O. Box 516, SF-00101 Helsinki, Finland, 74 Finnish marks

The metrological performances of the resistive ring superconducting quantum interference device (R-SQUID) is verified. It is intended to be used as a cryogenic thermometer. The R-SQUID consists of the Josephson junction which converts voltage noise from the shunt resistor into frequency fluctuations. Measuring the value of the shunt resistor and the variance of the frequency fluctuations, the temperature of the bath are determined. The influence of the post detection filter and the additive noise on the frequency variance is analyzed. The analytic models for the dc impedance and the noise performances of the R-SQUID are derived. All theoretical models are experimentally verified and some of the experiments are reported. It is shown that the R-SQUID is a complex gauge to maintain a cryogenic temperature scale. However, the careful choice of the device parameter and the point of operation, the use of the low noise cooled preamplifier, and the operation at high pump frequencies, enable accurate determination of the temperature of the bath in which the R-SQUID is immersed. ESA

N90-13342# Aix-Marseilles Univ. (France). Inst. de Mecanique Statistique de la Turbulence.
LOW SPEED HOT AND COLD WIRE TECHNIQUES FOR UNSTEADY FLOW
F. Anselmet *In* VKI, Measurement Techniques in Aerodynamics 1989 36 p (For primary document see N90-13339 05-02)
Avail: NTIS HC A23/MF A03

N90-13343# Aix-Marseilles Univ. (France). Inst. de Mecanique Statistique de la Turbulence.
HOT AND COLD WIRE APPLICATIONS IN SUPERSONIC FLOWS: INTRODUCTORY NOTES
J. P. Dussauge *In* VKI, Measurement Techniques in Aerodynamics 1989 30 p (For primary document see N90-13339 05-02)
Avail: NTIS HC A23/MF A03

N90-13345# Centre d'Etudes et de Recherches, Toulouse (France).
SKIN FRICTION MEASUREMENTS WITH HOT ELEMENTS
R. Houdeville and J. C. Juillen *In* VKI, Measurement Techniques in Aerodynamics 1989 71 p (For primary document see N90-13339 05-02)
Avail: NTIS HC A23/MF A03

N90-13346# Deutsche Forschungsanstalt fuer Luft- und Raumfahrt, Goettingen (Germany, F.R.). Inst. fuer Experimentelle Stroemungsmechanik.
THE 3D LDA TECHNIQUES IN VORTEX STUDIES AND BOUNDARY LAYER SURVEYS
Karl-Aloys Buetefisch *In* VKI, Measurement Techniques in Aerodynamics 1989 45 p (For primary document see N90-13339 05-02)
Avail: NTIS HC A23/MF A03

N90-13347# Royal Aerospace Establishment, Bedford (England). Aerodynamics Div.
PRESSURE MEASUREMENT TECHNIQUES IN USE AT THE ROYAL AEROSPACE ESTABLISHMENT
B. L. Welsh and P. R. Ashill *In* VKI, Measurement Techniques in Aerodynamics 1989 108 p (For primary document see N90-13339 05-02)
Avail: NTIS HC A23/MF A03

N90-13348# Deutsche Forschungs- und Versuchsanstalt fuer Luft- und Raumfahrt, Cologne (Germany, F.R.). Inst. fuer Antriebstechnik.
LASER TWO FOCUS TECHNIQUES
R. Schodl *In* VKI, Measurement Techniques in Aerodynamics 1989 96 p (For primary document see N90-13339 05-02)
Avail: NTIS HC A23/MF A03

N90-13428*# National Aeronautics and Space Administration. Goddard Space Flight Center, Greenbelt, MD.
A GYROSCOPE CALIBRATION ANALYSIS FOR THE GAMMA RAY OBSERVATORY (GRO)
Eleanor A. Ketchum and Michael H. Lee (Computer Sciences Corp., Silver Spring, MD.) *In its* Flight Mechanics/Estimation Theory Symposium, 1989 Oct. 1989 p 237-253 (For primary document see N90-13413 05-13)
(Contract NAS5-31500)
Avail: NTIS HC A20/MF A03 CSCL 14B

N90-13468*# Jet Propulsion Lab., California Inst. of Tech., Pasadena.
SPECTROMETER TECHNOLOGY RECOMMENDATIONS
William J. Wilson *In its* Report of the Asilomar 3 LDR Workshop 15 Aug. 1988 p 90-91 (For primary document see N90-13449 05-18)
Avail: NTIS HC A08/MF A01 CSCL 14B

N90-13469*# Massachusetts Inst. of Tech., Cambridge.
A FOUR CHANNEL HE-3 COOLED BALLOON-BORNE BOLOMETER RADIOMETER
Stephan Meyer *In* Jet Propulsion Lab., California Inst. of Tech., Report of the Asilomar 3 LDR Workshop 15 Aug. 1988 p 92-93 (For primary document see N90-13449 05-18)
Avail: NTIS HC A08/MF A01 CSCL 14B

N90-13477*# Jet Propulsion Lab., California Inst. of Tech., Pasadena.
A LABORATORY VERIFICATION SENSOR
Arthur H. Vaughan *In its* Report of the Asilomar 3 LDR Workshop 15 Aug. 1988 p 110-111 (For primary document see N90-13449 05-18)
Avail: NTIS HC A08/MF A01 CSCL 14B

N90-13523# European Space Agency, Paris (France).
ON-GROUND PHOTOMETRIC CALIBRATION
T. Batut *In its* The Hipparcos Mission. Prelaunch Status. Volume 1: The Satellite Jun. 1989 p 251-263 (For primary document see N90-13499 05-18)
Copyright Avail: NTIS HC A16/MF A02; ESA Publications Div., ESTEC, Noordwijk, Netherlands, 80 Dutch guilders

N90-13538# European Space Agency, Paris (France).
NEW GROUND-BASED PHOTOMETRIC MEASUREMENTS
M. Grenon *In its* The Hipparcos Mission. Prelaunch Status. Volume 2: The Input Catalog Jun. 1989 p 129-140 (For primary document see N90-13529 05-18)
Copyright Avail: NTIS HC A13/MF A02; ESA Publications Div., ESTEC, Noordwijk, Netherlands, 80 Dutch guilders

N90-13539# European Space Agency, Paris (France).
STANDARD STARS AND PHOTOMETRIC CALIBRATION
M. Grenon *In its* The Hipparcos Mission. Prelaunch Status. Volume 2: The Input Catalog Jun. 1989 p 141-147 (For primary document see N90-13529 05-18)
Copyright Avail: NTIS HC A13/MF A02; ESA Publications Div., ESTEC, Noordwijk, Netherlands, 80 Dutch guilders

N90-13560# European Space Agency, Paris (France).
PHOTOMETRY: MAIN MISSION AND TYCHO
F. Mignard, M. Froeschle, J. L. Falin, G. K. Andreasen, E. Hog, M. Grewing, and D. Scales *In its* The Hipparcos Mission. Prelaunch Status. Volume 3: The Data Reductions Jun. 1989 p 205-223 (For primary document see N90-13548 05-18)
Copyright Avail: NTIS HC A22/MF A03; ESA Publications Div., ESTEC, Noordwijk, Netherlands, 80 Dutch guilders

N90-13847# Dornier System G.m.b.H., Friedrichshafen (Germany, F.R.). Space Div.
DESIGN AND TECHNICAL ASPECTS OF THE SOLLY INSTRUMENT
M. Boison and E. Weber *In* ESA, European Rocket and Balloon

Programs and Related Research Jun. 1989 p 125-128 (For primary document see N90-13826 05-42)
Copyright Avail: NTIS HC A15/MF A02

N90-13848# Bern Univ. (Switzerland). Inst. of Physics.
A DOUBLE FOCUSING MASS-SPECTROMETER FOR SIMULTANEOUS ION MEASUREMENTS IN THE STRATOSPHERE
R. Moor, E. Kopp, U. Jenzer, H. Ramseyer, U. Waelchli, E. Arijs, D. Nevejans, J. Ingels, D. Fussen, and A. Barassin (Centre National de la Recherche Scientifique, Orleans, France) et al *In* ESA, European Rocket and Balloon Programs and Related Research Jun. 1989 p 129-134 Sponsored by Swiss National Science Foundation; Belgian National Science Foundation; and CNES, France (For primary document see N90-13826 05-42)
Copyright Avail: NTIS HC A15/MF A02

N90-13849*# National Aeronautics and Space Administration. Wallops Flight Facility, Wallops Island, VA.
APPLICATION OF AN OPTIMAL FILTER FOR INFLATABLE SPHERE DATA PROCESSING
H. S. Lee, F. J. Schmidlin, and W. Michel (Dayton Univ., Wallops Island, VA.) *In* ESA, European Rocket and Balloon Programs and Related Research Jun. 1989 p 135-138 (For primary document see N90-13826 05-42)
Copyright Avail: NTIS HC A15/MF A02 CSCL 14B

36 LASERS AND MASERS

Includes parametric amplifiers.
For related information see also *76 Solid-State Physics.*

N90-13770*# Johns Hopkins Univ., Baltimore, MD. Dept. of Electrical and Computer Engineering.
OPTICAL COMMUNICATION WITH SEMICONDUCTOR LASER DIODE Interim Progress Report, 1 Mar. - 31 Aug. 1989
Frederic Davidson and X. Sun Sep. 1989 13 p
(Grant NAG5-356)
(NASA-CR-185886; NAS 1.26:185886) Avail: NTIS HC A03/MF A01 CSCL 20E

This interim report describes the progress in the construction of a 220 Mbps Q=4 PPM optical communication system that uses a semiconductor laser as the optical transmitter and an avalanche photodiode (APD) as the photodetector. The transmitter electronics have been completed and contain both GaAs and ECL III IC's. The circuit was able to operate at a source binary data rate from 75 Mbps to 290 Mbps with pulse rise and fall times of 400 ps. The pulse shapes of the laser diode and the response from the APD/preamplifier module were also measured. Author

N90-13771*# California Univ., Los Angeles. Dept. of Electrical Engineering.
ON-LINE RANGE PREDICTION SYSTEM, PART 2
Nhan Levan Sep. 1988 24 p
(Grant NAG2-303)
(NASA-CR-185889; NAS 1.26:185889) Avail: NTIS HC A03/MF A01 CSCL 20E

The on-line range prediction system is designed for providing a prediction of the target range in the case of a laser data dropout. It consists of real time implementation of a Kalman filter on an IBM PC/AT equipped with necessary hardware. The system was set up and tested at Crows Landing in the Fall of 1987. The improvements made on the on-line range prediction system during 1988 are examined. Solutions are proposed and discussed to the several problems encountered during system tests. Then, the improvements made on the filter software are explained, namely, accounting for the time lag and providing data continously. Finally, the ideas are mentioned that can be considered in the future. Author

N90-13772*# Hampton Inst., VA. Dept. of Physics.
DEVELOPMENT OF MID-INFRARED SOLID STATE LASERS FOR SPACEBORNE LIDAR Final Report, 13 Apr. 1988 - 15 Oct. 1989
Donald A. Whitney and Kyong H. Kim Oct. 1989 52 p
(Grant NAG1-877)
(NASA-CR-183290; NAS 1.26:183290) Avail: NTIS HC A04/MF A01 CSCL 20E

Laser performance of Ho(3+):Tm(3+):Cr(3+):YAG crystals was investigated under both Cr:GSAG laser and flashlamp pumping. A flashlamp pumped Cr:GSAG laser was built to simulate high power quasi-CW laser diode pumping of a 2.1 micrometer holmium laser. The 2.1 micrometer output laser energy exceeded more than 14 mJ, the highest value reported to date under laser pumping near 785 nm. This was obtained in a pulse length of nearly 650 microsec from a 3 x 3 mm Ho:Tm:Cr:YAG rod by using the flashlamp-pumped Cr:CSAG laser as a pumping source at the diode laser wavelength, 785 micrometers. In addition, Ho:Tm:Cr:YAG crystals with various Tm(3+) concentrations were evaluated for flashlamp-pumped normal mode and Q-switched 2.1 micrometer laser operations under a wide variety of experimental conditions in order to understand internal dynamic processes among the ions and to determine an optimum lasing condition. An increase of the laser slope efficiency was observed with the increase of the Tm(3+) concentration from 2.5 to 4.5 atomic percent. The thermal dependence of the laser performance was also investigated. Q-switched laser output energies corresponding to nearly 100 percent of the normal-mode laser energies were obtained in a strong single spike of 200 ns pulse length by optimizing the opening time of a lithium niobate Q-switch. Author

N90-13773# Princeton Univ., NJ. Dept. of Electrical Engineering and Computer Science.
ULTRAFAST PROCESSES AND SPECTROSCOPY WITH FREE ELECTRON LASERS Annual Report, 1 Jun. 1988 - 31 May 1989
Philippe M. Fauchet 20 Sep. 1989 6 p
(Contract N00014-86-K-0711)
(AD-A212889) Avail: NTIS HC A02/MF A01 CSCL 20/5

The goal of this project is twofold: (1) to demonstrate that the SCA Free Electron Laser (FEL) is a useful tool for time-resolved spectroscopy; and (2) to use the FEL with other ultrashort pulse sources to uncover the electronic processes in disordered semiconductors. Potentially, the SCA FEL is a near-ideal source for ultrashort time-spectroscopy. It delivers widely tunable, psec pulses with high peak power and at high repetition rate. However, pulse-to-pulse variations in duration, wavelength and phase within one micropulse may be a limitation for high quality spectroscopy. In addition, pulses below one picosecond and tunability around the laser wavelength are desirable. Essential experiments will demonstrate how useful the SCA FEL is in ultrashort time resolved spectroscopy, including pulse compression and generation of white light continuum. The second goal is to uncover the electronic processes in disorder materials. Understanding these processes is the key to understanding the physics in materials such as amorphous semiconductors or liquid semiconductors. In turn, understanding the physics of these materials will lead to novel devices or improved device operation and will impact on our models for other materials. Picosecond and femtosecond time-resolved measurements are carried out on a Si:H and its alloys with Ge and C. The electronic properties of carriers in the vicinity of the mobility edge are emphasized. GRA

N90-13774# Air Force Weapons Lab., Kirtland AFB, NM.
GENERATION OF IODINE MONOFLUORIDE IN A SUPERSONIC MULTIPURPOSE FLOWTUBE FACILITY Final Report, May - Oct. 1988
Charles A. Helms Aug. 1989 56 p
(AD-A213082; WL-TR-89-29) Avail: NTIS HC A04/MF A01 CSCL 07/2

Iodine monofluoride, a promising visible chemical laser candidate, has been chemically produced at number densities

exceeding 1x10 exp 15 molecules/cu cm in a supersonic flow. The low pressure (3 torr), low temperature (300 K) flow environment should be suitable for lasing. GRA

N90-13775# Textron Lycoming, Stratford, CT.
MM AND T ADVANCED BALANCING/MACHINING
Albert Kalbfleisch, Charles Turcotte, Alex Ballantyne, and Henry Eppich (Avco-Everett Research Lab., MA.) Nov. 1988 149 p
(Contract DAAE07-85-C-R163)
(AD-A213103; TACOM-TR-13315) Avail: NTIS HC A07/MF A01 CSCL 09/3

A laser balancing system was developed and successfully demonstrated. The system uses a pulsed Nd:YAG laser to remove metal from the part while it is rotating in the balancing machine. Computer algorithms were developed which accepted imbalance information from the balancing machine and generated firing signals for the laser. This system balanced AGT1500 compressor impellers to less than one half the allowable imbalance under full computer control. Preliminary low cycle fatigue testing showed no major differences between laser irradiated test bar, and hand ground and burnished test bars. GRA

N90-13776# Naval Research Lab., Washington, DC. Applied Optics Branch.
A REVIEW OF LASER FILTER MATERIALS Final Report, Oct. 1987 - Sep. 1988
Jeanne A. Welch 26 Sep. 1989 28 p
(AD-A213134; NRL-R-9226) Avail: NTIS HC A03/MF A01 CSCL 09/3

This report presents a discussion of laser eye-protection filtering materials. Four classes of filters are evaluated for immediate and future filtering capabilities. Salient features required for near-term multiwavelength filtering are discussed in general, and the effectiveness of several filter materials as laser protection is assessed. Spectral illuminances for the most promising eye-protection filters are computed for representative day- and night-lighting conditions to approximate visual acuity. GRA

N90-13777# Naval Research Lab., Washington, DC. Beam Physics Branch.
SYNCHROTRON-BETATRON PARAMETRIC INSTABILITY IN FREE-ELECTRON LASERS Interim Report
B. Hafizi (Science Applications International Corp., McLean, VA.) and A. Ting 5 Oct. 1989 21 p
(AD-A213373; NRL-MR-6550) Avail: NTIS HC A03/MF A01 CSCL 09/3

Analysis of the synchrotron betatron coupling in a free electron laser indicates that the particle motion is susceptible to an instability which is of a fundamentally different physical character to those examined previously. The domain of this instability, which is of a parametric type and causes an exponential growth of the betatron amplitude, is identified and the growth rate therein determined. GRA

N90-13778# Deutsche Forschungsanstalt fuer Luft- und Raumfahrt, Oberpfaffenhofen (Germany, F.R.). Abteilung Lasertechnik.
A STOCHASTIC MODEL FOR THE CALCULATION OF MULTIPLE SCATTERED LIDAR RETURNS
Ulrich G. Oppel, Andreas Findling, Wilhelm Krichbaumer, Sigrid Krieglmeier, and Masoud Noormohammadian (Ludwig-Masimilians-Universitaet, Munich, Germany, F.R.) Apr. 1989 223 p
(DLR-FB-89-36; ISSN-0171-1342; ETN-90-96050) Avail: NTIS HC A11/MF A01; DLR, VB-PL-DO, Postfach 90 60 58, 5000 Cologne, Fed. Republic of Germany, 70 DM

A model is developed for the calculation and simulation of multiple scattered Light Detection And Ranging (LIDAR) return signals. A universal and exact LIDAR equation is presented including all orders of scattering, from which approximations can be derived for different geometrical and atmospheric situations and different orders of scattering. An inversion procedure for the reconstruction of the phase function from the double scattering part of the LIDAR equation is given, and relations to transport theory are presented. ESA

N90-13779 California Univ., Davis.
AN EXPERIMENTAL ANALYSIS OF THE WAVEGUIDE MODES IN A HIGH-GAIN FREE-ELECTRON LASER AMPLIFIER Ph.D. Thesis
Bruce Robert Anderson 1989 262 p
Avail: Univ. Microfilms Order No. DA8919529

The presence, growth, and interaction of transverse waveguide modes in high-gain free electron laser (FEL) amplifiers was observed and studied. A 3 MeV, 800 A electron beam generated by the Experimental Test Accelerator was injected into a planar wiggler. Power was then extracted and measured in the fundamental and higher-order modes under various sets of operating conditions. Horizontal focusing through the wiggler was provided by external quadrupole magnets. The input microwave signal for amplification was generated by a 100 kW magnetron operating at 34.6 GHz. Power measurements were taken for both flat and tapered wigglers, for two sizes of waveguide, and for both fundamental and higher mode injection. Mode content was determined by sampling the radiated signal at specific points in the radiation pattern. For the flat wiggler and with the large waveguide the power in the higher modes was comparable to power in the fundamental. Both exhibited gains greater than 30 dB/m prior to saturation and both reached powers in excess of 80 MW. Choice of injection mode had little effect on the operation of the system. Operation with the smaller guide provided much better mode selectivity. The fundamental mode continued to show optimum gain in excess of 30 dB/m while the higher-mode gain was of the order of 20 dB/m. As expected, power output increased significantly with the tampered wigglers. The relative mode content depended on the specific taper used. Operation with a linear taper resulted in both modes showing significant power increases at 3 m to about 400 MW each. However, an optimized nonlinear taper resulted in an increase in power in the fundamental to 750 MW while power in the high-order modes was unchanged.
Dissert. Abstr.

N90-13780# Institut National des Sciences Appliquees de Lyon, Villeurbanne (France). Lab. d'Etude des Procedes de Fabrication.
CHARACTERIZATION OF SURFACES CUT WITH A LASER BEAM AND THERMAL MODEL OF THE PROCESS Ph.D. Thesis [CARACTERISATION DES SURFACES DECOUPEES PAR LASER ET MODELISATION THERMIQUE DU PROCESSUS]
Shifeng Yuan 1989 164 p In FRENCH
(ISAL-89-0008; ETN-90-95265) Avail: NTIS HC A08/MF A01

The morphology of a surface cut by a laser beam is studied. The influence of the machining parameters on the cut quality are experimentally determined. A model of the thermal phenomena is developed. It is shown that cut surface smoothness has a maximum, usually in the median zone. The applicability of a finite element model to the cutting process is demonstrated. ESA

N90-13781# Deutsche Forschungs- und Versuchsanstalt fuer Luft- und Raumfahrt, Stuttgart (Germany, F.R.). Inst. fuer Technische Physik.
MICROWAVE EXCITED EXCIMER LASER Final Report
Hans H. Klingenberg 20 Jul. 1987 27 p In GERMAN; ENGLISH summary
(Contract BMFT-13-EU-0023/10)
(ETN-90-95909) Avail: NTIS HC A03/MF A01

Microwave excitation is studied as an alternative means to standard excitation schemes of excimer lasers within the framework of the EUROLASER definition phase. A summary of the published work in this field is presented. Special emphasis is given to the evaluation of the scaling of the excitation volume from three cubic centimeters to larger discharge volumes. Whether a microwave excited excimer laser can be realized is investigated. It is concluded

that the technical and physical problems of a microwave excited rare gas halide gas mixture require more experimental work.
ESA

N90-13782# Centro Informazioni Studi Esperienze, Milan (Italy).
OUTLINE ON THE FUTURE ITALIAN TRANSPORTABLE LASER RANGING STATION
P. L. Pizzolati and I. Gianioni 1988 20 p Repr. from the Proceedings of the 3rd International Conference on the Wegener/Medlas Project, 1988 p 395-412 Presented at the 3rd International Conference on the Wegener/Medlas Project, Bologna, Italy, 25-27 May 1987
(CISE-4845; ETN-90-96030) Avail: NTIS HC A03/MF A01

The design of the future Italian transportable laser ranging station is presented. Design criteria and station main specifications are described. The characteristics of the main components, are discussed. A layout of the station is illustrated. The internal calibration path philosophy and the list of participants are given. The main features of the station are: single or multiphotoelectron working capability, internal calibration path, transportability, night and day measuring capability. ESA

N90-13344# Aix-Marseilles Univ. (France). Inst. de Mecanique Statistique de la Turbulence.
LASER APPLICATIONS IN SUPERSONIC UNSTEADY FLOW
M. Elena *In* VKI, Measurement Techniques in Aerodynamics 1989 20 p (For primary document see N90-13339 05-02)
Avail: NTIS HC A23/MF A03

37 MECHANICAL ENGINEERING

Includes auxiliary systems (nonpower); machine elements and processes; and mechanical equipment.

N90-13783*# Georgia Inst. of Tech., Atlanta. School of Mechanical Engineering.
ADAPTIVE STRATEGIES FOR CONTROLS OF FLEXIBLE ARMS Ph.D. Thesis
Bau-San Yuan Apr. 1989 192 p
(Grant NAG1-623)
(NASA-CR-185868; NAS 1.26:185868) Avail: NTIS HC A09/MF A01 CSCL 13I

An adaptive controller for a modern manipulator has been designed based on asymptotical stability via the Lyapunov criterion with the output error between the system and a reference model used as the actuating control signal. Computer simulations were carried out to test the design. The combination of the adaptive controller and a system vibration and mode shape estimator show that the flexible arm should move along a pre-defined trajectory with high-speed motion and fast vibration setting time. An existing computer-controlled prototype two link manipulator, RALF (Robotic Arm, Large Flexible), with a parallel mechanism driven by hydraulic actuators was used to verify the mathematical analysis. The experimental results illustrate that assumed modes found from finite element techniques can be used to derive the equations of motion with acceptable accuracy. The robust adaptive (modal) control is implemented to compensate for unmodelled modes and nonlinearities and is compared with the joint feedback control in additional experiments. Preliminary results show promise for the experimental control algorithm. J.P.S.

N90-13784 Iowa State Univ. of Science and Technology, Ames.
SIMULATION OF THE CONTROL CHARACTERISTICS OF AN AXIAL PISTON PUMP AND A FLAPPER-NOZZLE VALVE COMBINATION Ph.D. Thesis
Shir-Tau Tsai 1988 89 p
Avail: Univ. Microfilms Order No. DA8909197

This research was aimed to develop and simulate the mathematical model for the control of an axial piston pump using a flapper-nozzle valve. It was assumed that all the state variables are defined as the perturbations in the physical quantities; therefore, linearized relations were used. These linearized relations were combined to form the state-variable representation of the model. The model was then simulated to investigate the control characteristics of the proposed system. The responses of a stand along flapper-nozzle valve were evaluated first. Excellent agreement between the experimental data and theoretical data of output pressure rise of the valve was found. The open-loop system performance of the axial piston pump and flapper-nozzle valve combination was unstable. To enhance the stability of the system, an optimal control design was applied. It was found that the computed results of the nonaugmented optimal design lack robustness for improving the existing control system. Thus the augmented optimal control method was used to enhance the system performances. Time responses of the augmented optimal control system were evaluated. It was observed that the increase of input current had little effect on the system responses. Doubling the discharge flow rate also doubled the overshoot. Whereas increasing the discharge volume tended to slow down the system responses. Finally, the increase of the rotational speed of the pump shaft produced a higher overshoot and a slower response of the system. The performances of the control of an axial piston pump using a flapper-nozzle valve as a controller were compared to the performances of using a four-way hydraulic valve, a single-stage electrohydraulic servovalve, and a two-stage electrohydraulic servovalve as controllers. It was concluded that the system of a flapper-nozzle valve and an axial piston pump combination was superior to other combinations in terms of the balance between pressure-time response and maximum pressure overshoot. Dissert. Abstr.

N90-13785*# National Aeronautics and Space Administration. Lewis Research Center, Cleveland, OH.
AN INVESTIGATION OF GEAR MESH FAILURE PREDICTION TECHNIQUES M.S. Thesis - Cleveland State Univ.
James J. Zakrajsek Nov. 1989 100 p Prepared in cooperation with Army Aviation Systems Command, Cleveland, OH
(DA Proj. 1L1-62209-A4-7A)
(NASA-TM-102340; E-5049; NAS 1.15:102340;
AVSCOM-TM-89-C-005) Avail: NTIS HC A05/MF A01 CSCL 13I

A study was performed in which several gear failure prediction methods were investigated and applied to experimental data from a gear fatigue test apparatus. The primary objective was to provide a baseline understanding of the prediction methods and to evaluate their diagnostic capabilities. The methods investigated use the signal average in both the time and frequency domain to detect gear failure. Data from eleven gear fatigue tests were recorded at periodic time intervals as the gears were run from initiation to failure. Four major failure modes, consisting of heavy wear, tooth breakage, single pits, and distributed pitting were observed among the failed gears. Results show that the prediction methods were able to detect only those gear failures which involved heavy wear or distributed pitting. None of the methods could predict fatigue cracks, which resulted in tooth breakage, or single pits. It is suspected that the fatigue cracks were not detected because of limitations in data acquisition rather than in methodology. Additionally, the frequency response between the gear shaft and the transducer was found to significantly affect the vibration signal. The specific frequencies affected were filtered out of the signal average prior to application of the methods. Author

N90-13786*# National Aeronautics and Space Administration. Lewis Research Center, Cleveland, OH.
ELASTICITY EFFECTS ON CAVITATION IN A SQUEEZE FILM DAMPER UNDERGOING NONCENTERED CIRCULAR WHIRL
David E. Brewe (Army Aviation Research and Development Command, Cleveland, OH.) 1988 20 p Presented at the Nordic Symposium on Tribology, Trondheim, Norway, 26-29 Jun. 1988; sponsored by Wear Magazine
(DA Proj. 1L1-61102-AH-45)
(NASA-TM-102392; E-4224; NAS 1.15:102392;
AVSCOM-TM-89-C-012) Avail: NTIS HC A03/MF A01 CSCL 13I

Elasticity of the liner and its effects on cavitation were

numerically determined for a squeeze film damper subjected to dynamic loading. The loading was manifested as a prescribed motion of the rotor undergoing noncentered circular whirl. The boundary conditions were implemented using Elrod's algorithm which conserves lineal mass flux through the moving cavitation bubble as well as the oil film region of the damper. Computational movies were used to analyze the rapidly changing pressures and vapor bubble dynamics throughout the dynamic cycle for various flexibilities in the damper liner. The effects of liner elasticity on cavitation were only noticeable for the intermediate and high values of viscosity used in this study. Author

N90-13787# Naval Postgraduate School, Monterey, CA.
REVIEW AND EVALUATION OF A TURBOMACHINERY THROUGHFLOW FINITE ELEMENT CODE M.S. Thesis
Peng Hian Yeo (Singapore Univ.) Jun. 1989 81 p
(AD-A213058) Avail: NTIS HC A05/MF A01 CSCL 13/7

The finite element code Q3DFLO 81 was evaluated to determine its suitability for use in a program to investigate axial compressor tip clearance effects. The code was first applied to Dring's fully comprehensive benchmark data set in order to validate the numerical modelling free of experimental uncertainties. It was then applied to the Naval Postgraduate School axial research compressor with which tip clearance effects were to be investigated experimentally. The evaluation identified both limitations in the code and limitations in the data which could be obtained in the experiment. It was recommended that provision be made to accommodate peripherally non-uniform flow effects (blockage) in the throughflow code calculation, and that provision be made to obtain adequate peripheral flow surveys in the experiment. GRA

N90-13788# Illinois Univ., Urbana. Coordinated Science Lab.
ARC CURRENT CONTROL OF A ROBOTIC WELDING SYSTEM: MODELING AND CONTROL SYSTEM DESIGN M.S. Thesis
Bruce William Greene Sep. 1989 53 p
(Contract DACA88-88-M-1554)
(AD-A213150; UILU-ENG-89-2227; DC-114) Avail: NTIS HC A04/MF A01 CSCL 11/6

The ultimate objective of the program is to develop an automated welding system that produces consistently good welds despite variations in material parameters and other disturbances. The scope of the research is limited to consumable electrode gas metal are welding (GMAW) since this is one of the most frequently employed and economically important welding processes. Arc current is one of the key process variables that must be controlled if weld quality is to be maintained. This aspect of weld quality control is the focus. GRA

N90-13789# Dayton Univ., OH.
PROBABILISTIC FINITE ELEMENT ANALYSIS OF DYNAMIC STRUCTURAL RESPONSE Final Report, Oct. 1985 - Oct. 1987
R. A. Brockman, F. Y. Lung, and W. R. Braisted Mar. 1989 216 p
(Contract F33615-85-C-2585)
(AD-A213249; UDR-TR-87-130; AFWAL-TR-88-2149) Avail: NTIS HC A10/MF A01 CSCL 20/11

Turbomachinery components exhibit more diverse and complex structural behavior than most classes of engineering structures. Stress analysis of rotating propulsion system components has been a driving force in the development of many of the most sophisticated numerical methods in common use: substructuring and cyclic symmetry techniques, large scale eigensolution algorithms, creep and thermoplasticity models, and modal and reduced basis methods. Even with the powerful analytical tools and software which exist today, the stress and vibration analysis of turbomachine components is usually a challenging task. The most important contributors to this analytical complexity are: intricacy of the structure geometry and properties; nonlinearity and its influence on other responses; and uncertainty in properties, loading, and other variables. Applied research in finite element methods and numerical solution algorithms at the present time is concerned, in large measure, with addressing these problems areas. The issue of uncertainty in defining a structural analysis model is addressed and the results are interpreted. A bladed disk is useful example of the sources of uncertainty which may exist for a single model. GRA

N90-13790# Carnegie-Mellon Univ., Pittsburgh, PA. Robotics Inst.
DESIGN AND CONTROL OF A TWO-DEGREE-OF-FREEDOM LIGHTWEIGHT FLEXIBLE ARM
Vicente Feliu, H. Benjamin Brown, Jr., and Kuldip S. Rattan (Wright State Univ., Dayton, OH.) Jul. 1989 42 p
(AD-A213335; CMU-RI-TR-89-21) Avail: NTIS HC A03/MF A01 CSCL 13/7

This report describes the design and control of a two-joint, two-link flexible arm. Our purpose has been to build an efficient arm in the sense that most of the energy provided by the motors is spent in doing the task (moving the tip mass) instead of moving the arm structure. In order to achieve that, we designed a flexible arm that has most of its mass concentrated on the tip. We wanted also to decouple radial tip motions from angular tip motions. The special mechanical configuration that fulfills all these specifications is described in Section 2. Section 3 describes the control scheme of this arm, an important problem when controlling it was the large Coulomb friction of the motors. A two-nested-loop multivariable controller has been used. The inner loop controls the position of the motors while the outer loop controls the tip position. The resolved acceleration method is generalized to control this flexible arm. The compliance matrix was used to model the oscillations of the structure, and was included in the decoupling/linearizing term of this controller. GRA

N90-13791# Carnegie-Mellon Univ., Pittsburgh, PA. Robotics Inst.
ACCELERATION SETS OF PLANAR MANIPULATORS. PART 2: APPLICATIONS AND EXPERIMENTS
Yong-yil Kim (IBM Research Lab., Yorktown Heights, NY.) and Subhas Desa Jul. 1989 41 p
(AD-A213336; CMU-RI-TR-89-17-Pt-2) Avail: NTIS HC A03/MF A01 CSCL 13/9

The acceleration set theory developed in the companion report is applied to two important problems which arise in the design of manipulator systems for performance: manipulator type selection and actuator size determination. A systematic procedure is given for the comparison of the performance, based on acceleration, of a set of alternative manipulator types. This procedure is then used to compare the performance of three well-known manipulator designs which have been proposed for high performance. Simple algorithms, based on the acceleration set theory, are given for the determination of the minimum actuator sizes to obtain a specific isotropic acceleration. The ease of implementation of these algorithms is demonstrated by actual examples. The experimental determination of acceleration sets is also addressed and simple experimental results are presented and compared with those predicted by the theory. GRA

N90-13792# Carnegie-Mellon Univ., Pittsburgh, PA. Robotics Inst.
A NEW APPROACH TO CONTROL SINGLE-LINK FLEXIBLE ARMS. PART 3: ADAPTIVE CONTROL OF THE TIP POSITION WITH PAYLOAD CHANGES
Vicente Feliu, Kuldip S. Rattan (Wright State Univ., Dayton, OH.), and H. Benjamin Brown, Jr. Jul. 1989 34 p
(AD-A213337; CMU-RI-TR-89-15-Pt-3) Avail: NTIS HC A03/MF A01 CSCL 12/9

The third report describes a new method to control single-link lumped-mass flexible arms in the case of having friction in the joint and changes in the payload. Both linear and nonlinear friction components are overcome by using the very robust control scheme developed in the second report which is based on two nested feedback loops: an inner one that controls the motor position and an outer one that controls the tip position. In order to compensate for changes in the payload, an adaptive control scheme is used. Two cases are considered when compensating for changes in

the tip payload: the arm is a minimum phase system or a non-minimum phase one. Different adaptive control schemes are proposed in each case. In them, compensation for changes in the load is achieved in two steps: first the tip payload is estimated from a very simple procedure proposed here, and then the feedforward and feedback controllers are tuned according to this estimated value. It results in a quite simple control law that can be used for real-time control of flexible arms, and that needs minimal computing effort. Experimental results are shown. GRA

N90-13793# Carnegie-Mellon Univ., Pittsburgh, PA. Robotics Inst.
DEFINITION, DETERMINATION AND CHARACTERIZATION OF ACCELERATION SETS FOR SPATIAL MANIPULATORS
Yong-yil Kim and Subhas Desa Jul. 1989 70 p
(AD-A213366; CMU-RI-TR-89-18) Avail: NTIS HC A04/MF A01 CSCL 12/9

The approach developed for systematically studying the acceleration capabilities and acceleration properties of the end effector of a planar 2 degree of freedom manipulator, is extended to the general spatial manipulator with three degrees of freedom. A central feature is the determination of the properties of the quadratic mapping between the joint-velocity space and the acceleration space of P which then makes it possible to obtain analytical solutions for most acceleration properties of interest.It is shown that a fundamental way of studying these quadratic mappings is in terms of the mapping of (input) line congruences into (output) line congruences. GRA

N90-13794*# Teledyne Brown Engineering, Huntsville, AL.
USER NEEDS, BENEFITS, AND INTEGRATION OF ROBOTIC SYSTEMS IN A SPACE STATION LABORATORY Final Report, Oct. 1987 - Oct. 1989
W. R. Dodd, M. B. Badgley, and C. R. Konkel Oct. 1989 78 p
(Contract NAS3-25278)
(NASA-CR-185150; NAS 1.26:185150; TBE-SSD-P601-89-191)
Avail: NTIS HC A05/MF A01 CSCL 13I

The methodology, results and conclusions of all tasks of the User Needs, Benefits, and Integration Study (UNBIS) of Robotic Systems in a Space Station Laboratory are summarized. Study goals included the determination of user requirements for robotics within the Space Station, United States Laboratory. In Task 1, three experiments were selected to determine user needs and to allow detailed investigation of microgravity requirements. In Task 2, a NASTRAN analysis of Space Station response to robotic disturbances, and acceleration measurement of a standard industrial robot (Intelledex Model 660) resulted in selection of two ranges of microgravity manipulation: Level 1 (10-3 to 10-5 G at greater than 1 Hz) and Level 2 (less than equal 10-6 G at 0.1 Hz). This task included an evaluation of microstepping methods for controlling stepper motors and concluded that an industrial robot actuator can perform milli-G motion without modification. Relative merits of end-effectors and manipulators were studied in Task 3 in order to determine their ability to perform a range of tasks related to the three microgravity experiments. An Effectivity Rating was established for evaluating these robotic system capabilities. Preliminary interface requirements for an orbital flight demonstration were determined in Task 4. Task 5 assessed the impact of robotics. Author

N90-13795# Technische Univ., Eindhoven (Netherlands). Dept. of Mathematics and Computing Science.
CONJUGATE PROFILES ON MATING GEAR TEETH
D. A. Overdijk Jan. 1989 13 p
(MEMO-COSOR-89-01; ETN-90-95946) Avail: NTIS HC A03/MF A01

Profiles on a pair of gears such that the mating teeth produce rotary motion are studied. An alternative method for calculating the envelope of a one-parameter family of surfaces is presented, which simplifies the analytic description of conjugate profiles in cartesian coordinates. A description of rotation in terms of antisymmetric matrices is given which enables concise transformation formulation of the coordinates in various coordinate systems. An analytic description of conjugates profiles is presented and the application of the formulas to a pair of parallel helical gears, a pair of straight-toothed bevel gears and to the face gear transmission is described. ESA

N90-13796*# Jet Propulsion Lab., California Inst. of Tech., Pasadena.
PERFORMANCE EVALUATION OF A SIX-AXIS GENERALIZED FORCE-REFLECTING TELEOPERATOR
B. Hannaford, L. Wood, B. Guggisberg, D. McAffee, and H. Zak
15 Jun. 1989 141 p
(Contract NAS7-918)
(NASA-CR-186106; JPL-Publ-89-18; NAS 1.26:186106) Avail: NTIS HC A07/MF A01 CSCL 13I

Work in real-time distributed computation and control has culminated in a prototype force-reflecting telemanipulation system having a dissimilar master (cable-driven, force-reflecting hand controller) and a slave (PUMA 560 robot with custom controller), an extremely high sampling rate (1000 Hz), and a low loop computation delay (5 msec). In a series of experiments with this system and five trained test operators covering over 100 hours of teleoperation, performance was measured in a series of generic and application-driven tasks with and without force feedback, and with control shared between teleoperation and local sensor referenced control. Measurements defining task performance included 100-Hz recording of six-axis force/torque information from the slave manipulator wrist, task completion time, and visual observation of predefined task errors. The task consisted of high precision peg-in-hole insertion, electrical connectors, velcro attach-de-attach, and a twist-lock multi-pin connector. Each task was repeated three times under several operating conditions: normal bilateral telemanipulation, forward position control without force feedback, and shared control. In shared control, orientation was locally servo controlled to comply with applied torques, while translation was under operator control. All performance measures improved as capability was added along a spectrum of capabilities ranging from pure position control through force-reflecting teleoperation and shared control. Performance was optimal for the bare-handed operator. Author

N90-13797*# National Aeronautics and Space Administration. Lewis Research Center, Cleveland, OH.
LIQUID WATER CONTENT AND DROPLET SIZE CALIBRATION OF THE NASA LEWIS ICING RESEARCH TUNNEL
Robert F. Ide (Army Aviation Research and Development Command, Cleveland, OH.) [1989] 28 p Presented at the 28th Aerospace Sciences Meeting, Reno, NV, 8-11 Jan. 1990; sponsored by AIAA Prepared in cooperation with Army Aviation Research and Development Command, Cleveland, OH
(DA Proj. 1L1-62209-A47-A)
(NASA-TM-102447; E-5231; NAS 1.15:102447;
AVSCOM-TM-89-C-014; AIAA-90-0669) Avail: NTIS HC A03/MF A01 CSCL 14B

The icing research tunnel at the NASA Lewis Research Center underwent a major rehabilitation in 1986 to 1987, necessitating recalibration of the icing cloud. The methods used in the recalibration, including the procedure used to establish a uniform icing cloud and the use of a standard icing blade technique for measurement of liquid water content are described. PMS Forward Scattering Spectrometer and Optical Array probes were used for measurement of droplet size. Examples of droplet size distributions are shown for several median volumetric diameters. Finally, the liquid water content/droplet size operating envelopes of the icing tunnel are shown for a range of airspeeds and are compared to the FAA icing certification criteria. Author

N90-13798# Centre de Recherches Scientifiques et Techniques de l'Industrie des Fabrications Metalliques, Brussels (Belgium). Afdeling: Ketelbouw.
THEORETICAL EVALUATION OF DEFECTS IN PRESSURE VESSELS AND PIPINGS
J. Decock Dec. 1988 44 p Sponsored by the Institut pour

l'Encouragement de la Recherche Scientifique dans l'Industrie et l'Agriculture
(CRIF-MT-174; ETN-90-94558) Avail: NTIS HC A03/MF A01

The validity and the field of application of some of the assessment methods used for the evaluation of defects in pressure vessels and piping, are discussed. The existing acceptance theories and methods are based on fracture mechanics studies. The result of a parametric study is presented. Several defects are assumed in welded joints of plates and pipelines. Seven different materials for pressure vessel and pipeline manufacturing are selected. The following assessment methodologies are used: PD 6493, WES 2805, API 1104, BS 4515, CSA Z184 and the line-spring or modified critical crack-opening displacement model. It is shown that the BS 4515 and the API 1104 are simple methods that are generally (but not always) conservative. The other methods are flexible and more correct from the theoretical point of view. ESA

N90-13799# Centre de Recherches Scientifiques et Techniques de l'Industrie des Fabrications Metalliques, Brussels (Belgium). Afdeling: Ketelbouw.
FATIGUE RESISTANCE OF PRESSURE VESSELS IN HIGH STRENGTH STEELS EFFECT OF SOME IMPROVEMENT TECHNIQUES
A. Sys May 1989 26 p Sponsored by the State Univ. of Ghent Belgium
(CRIF-MT-176; ETN-90-95186) Avail: NTIS HC A03/MF A01

Fatigue tests by external cyclic loading on nozzles in heavy pressurized vessel models are performed. Twelve models are tested. They are manufactured under industrial conditions from a high tensile pipe material API X60. One third are reference specimens for which the fatigue strength is compared with those made from mild steels. To the other models tungsten-inert gas (TIG) dressing and burr grinding techniques are applied to improve the fatigue resistance. During testing computer aided control measurements are applied to ensure correct loading conditions. The fatigue properties of the higher tensile material in untreated conditions are found to be lower than those of mild steel. TIG dressing of a higher strength material always has a favorable effect on the fatigue properties compared with those of mild steels. With burr grinding the same fatigue properties as for mild steel can only be got in the low cycle region. ESA

N90-13800# Office National d'Etudes et de Recherches Aerospatiales, Paris (France). Direction des Etudes de Synthese.
IMAGE SEGMENTATION FOR THE STEREOSCOPIC VISION OF A MOBILE ROBOT [VISION STEREO POUR ROBOT MOBILE. SEGMENTATION D'IMAGE]
S. J. Lagarde 1 Mar. 1989 103 p In FRENCH
(Contract DRET-87-34-001)
(ONERA-RT-1/3692-SY; ETN-90-95718) Avail: NTIS HC A06/MF A01

Tools used in the segmentation of external images for use in developing stereoscopic vision for an autonomous robot are described. The importance of image edge correlation between the two images is stressed. The algorithms used, based on local statistical properties of image texture, are outlined. ESA

N90-13801# Ecole Centrale de Lyon (France).
THE LIMITING FRICTION FORCE Ph.D. Thesis [LA FORCE DE FROTTEMENT LIMITE]
Denis Mazuyer 1989 78 p In FRENCH Original contains color illustrations
(ECL-89-005; ETN-90-95780) Avail: NTIS HC A05/MF A01

Friction forces are studied. The relation between interfacial film rheology and the friction coefficient is analyzed. The effects of the agglomeration of wear products is discussed. A two dimensional model of a soap bubble system is developed to relate the shear behavior of an amorphous film to the rate thickness to length of the sheared layer (Hill number). For low Hill numbers the movement of elementary groups of five or six bubbles control the shearing of the layer. ESA

N90-13802# Kernforschungszentrum G.m.b.H., Karlsruhe (Germany, F.R.). Inst. fuer Mikrostrukturtechnik.
DEVELOPMENT AND TESTING OF A CONTACTLESS STATIC/DYNAMIC SHAFT SEAL WITH LITTLE SEALING GAS REQUIREMENT Thesis - Karlsruhe Univ.
W. Ehrfeld, W. Keller, and D. Seidel Jul. 1989 64 p In GERMAN; ENGLISH summary
(KfK-4599; ISSN-0303-4003; ETN-90-95871) Avail: NTIS HC A04/MF A01

Development of a shaft seal which ensures safe seal operation while requiring a minimum volume of sealing gas and which operates without contact during startup and shutdown and is, consequently, free of wear is described. A novel combination of static and dynamic modes of operation is used to obtain this type of seal. Dynamic effects at higher speeds cause a pressure buildup in the sealing gap and hence the sealing effect of the shaft seal. The dynamically operating shaft seal, compared to a static one allows for a substantial decrease in the width of the sealing gap. Several test specimens are fabricated and tested. The results show that dependable predictions can be made on the basis of the operating variables. It is demonstrated that the sealing gas demands for the static/dynamic shaft seal under comparable boundary conditions amount to about one fifth of those of the static seals used in the separation nozzle compressors. ESA

N90-13803 Technische Univ., Delft (Netherlands). Dept. of Mechanical Engineering and Marine Technology.
KINEMATICS AND CONTROL OF MANIPULATION ROBOTS
S. P. Patarinski Mar. 1988 64 p
(WTHD-187; ISBN-90-370-0020-7; ETN-90-96001) Copyright Avail: S. P. Patarinski, Faculty of Mechanical Engineering and Marine Technology, Technische Universitaet Delft, 2628 BL Delft, Netherlands

The research carried out on the kinematics and the control of Manipulation Robots (MR) is reported. A unified algebric approach is applied. The concept of structural regularity is introduced. It is shown that the MR with six and more degrees of mobility are at least three structurally regular. Moreover, the transformation off line provides a way for the reduction of the number of elementary calculations for real time control. The model referenced adaptive disturbances are discussed. The developed method is shown to be effective from a computational point of view and suitable for digital or analog servoing MR independent controllers. Application examples are given. ESA

N90-13804# Technische Univ., Eindhoven (Netherlands).
ON CONTROL OF MANIPULATORS Ph.D. Thesis
Theodorus Antonius G Heeren 1989 126 p
(ISBN-90-9002789-7; ETN-90-96017) Avail: NTIS HC A07/MF A01

The control of mechanical manipulators is studied. A model derivation procedure is proposed, and a control law is obtained. Three strategies for nonlinear manipulator models are discussed. The reduction of the online computational effort and the improvement of the controlled manipulator robustness is considered. The development of an optical system for direct measurement of the end effector position in the online control situation is studied. A case study on flexible manipulator control with end effector position feedback is included. The controller hardware design and the control algorithm for XY-table are discussed. It is shown that the effect of elastic deformations on the end effector position can be compensated while external forces are exerted on the end effector. ESA

N90-13484*# Air Force Systems Command, Kirtland AFB, NM.
CONTROL OF OPTICAL SYSTEMS
D. Founds *In* Jet Propulsion Lab., California Inst. of Tech., Report of the Asilomar 3 LDR Workshop 15 Aug. 1988 p 126-127 (For primary document see N90-13449 05-18)
Avail: NTIS HC A08/MF A01 CSCL 13I

N90-13509# European Space Agency, Paris (France).
THE BAFFLES

G. Ratier and T. Batut *In its* The Hipparcos Mission. Prelaunch Status. Volume 1: The Hipparcos Satellite Jun. 1989 p 107-111 Original contains color illustrations (For primary document see N90-13499 05-18)
Copyright Avail: NTIS HC A16/MF A02; ESA Publications Div., ESTEC, Noordwijk, Netherlands, 80 Dutch guilders

38 QUALITY ASSURANCE AND RELIABILITY

Includes product sampling procedures and techniques; and quality control.

N90-13805 Hull Univ. (England).
QUANTITATIVE NON-DESTRUCTIVE EVALUATION USING LASER GENERATED ULTRASONIC PULSES Ph.D. Thesis
Ross Andrew Crosbie 1987 261 p
Avail: Univ. Microfilms Order No. BRDX85343

Features of laser generated ultra-sound are utilized for the detection of defects in solids. Ultrasound is generated non-contactively by this method and likewise many of the detection devices used do not require direct coupling to the test pieces, thus acoustic pulses with high frequency components are able to be produced and monitored on a range of samples. Steel samples coated with between 3 and 7 mm of plasma-transferred arc depositions are examined for bond quality via measurements of attenuation caused by porosity in the coatings, found to be related to weld current. Surface breaking cracks in such claddings are quantitatively detected by a method which utilizes Rayleigh pulses. A two sided automated scanning system is described which examines samples for subsurface defects. Results from the examinations of a dural test piece, plasma sprayed steel bars and carbon fiber composite samples are presented. A second scanning technique, requiring access to only one sample face, is presented which employs an interferometer for detection and is thus a truly remote system. Laminar flaws are modeled using flat-bottomed holes, the dimensions of which are measured using the resonance of the bodies. A theoretical investigation using boundary conditions suggests possible applications for quantitative NDE of structures with well defined natural vibration frequencies. The propagation of acoustic transients in plates is also examined. Possible future work concerning laser/ultrasonic NDE is discussed. Dissert. Abstr.

N90-13806# Centre de Recherches Scientifiques et Techniques de l'Industrie des Fabrications Metalliques, Brussels (Belgium). Metallic Construction Div.
CONSIDERATIONS ABOUT THE ACCEPTANCE INSPECTION OF HS FASTENERS INTENDED FOR CONTROLLED TIGHTENING
E. Dehan and E. Piraprez Mar. 1989 38 p
(CRIF-MT-175; ETN-90-94559) Avail: NTIS HC A03/MF A01

The rules for acceptance inspection of fasteners with reference to the Belgian standard NBN E 27/073 are proposed. European and ISO standards were taken into account. Theoretical and experimental research was undertaken to verify a proposal or to seek better specifications for particular characteristics. The following steps of the work are presented: the division of the supply into lots; the test programs for mechanical and dimensional properties of the components; the supplementary controls for the fasteners to be tightened by nut rotation; the clamping force durability of fasteners tightened over the yielding point; the appreciation of the fitness of a fastener for a controlled tightening by nut rotation; and lubrication. It is concluded that the information content of the work can be applied as a draft of a European standard. ESA

N90-13522# European Space Agency, Paris (France).
PRODUCT ASSURANCE
K. Huehn *In its* The Hipparcos Mission. Prelaunch Status. Volume 1: The Hipparcos Satellite Jun. 1989 p 247-250 (For primary document see N90-13499 05-18)
Copyright Avail: NTIS HC A16/MF A02; ESA Publications Div., ESTEC, Noordwijk, Netherlands, 80 Dutch guilders

39 STRUCTURAL MECHANICS

Includes structural element design and weight analysis; fatigue; and thermal stress.

For applications see *05 Aircraft Design, Testing and Performance* and *18 Spacecraft Design, Testing and Performance.*

N90-13807*# National Aeronautics and Space Administration. Langley Research Center, Hampton, VA.
A STUDY ON THE SENSITIVITY AND SIMULTANEOUS ADJUSTMENT OF A HOOP-COLUMN ANTENNA SURFACE
Kyong Been Lim, Jer-Nan Juang, and Peiman Maghami (Old Dominion Univ., Norfolk, VA.) Jan. 1989 15 p
(NASA-TM-101538; NAS 1.15:101538) Avail: NTIS HC A03/MF A01 CSCL 20K

The results of a recent surface adjustment of the 15-meter diameter hoop-column antenna are presented. A least-squares differential algorithm is used to adjust the surface shape as close as possible to a perfect parabola. Since the desired perfect parabola is not uniquely known a priori, parameters of the perfect parabola are included in the design vector along with the cable length changes. As an extension to an earlier study, lateral sensitivity is included in the least-squares adjustment procedure. In addition, the effect of cable length uncertainties on the surface RMS error is considered and an error bound is derived. The results in this study indicate an improvement over earlier studies. The sensitivity analysis provided a quantitative measure of the needed accuracy of the cable adjustments in the laboratory. Recommendations are included to further enhance shape adjustment. Author

N90-13808# Aeronautical Research Labs., Melbourne (Australia).
A COUNTER GATING CIRCUIT FOR ACOUSTIC EMISSION MONITORING OF STRUCTURES CRACKING UNDER REPETITIVE ALTERNATING LOADS
M. R. Kindermann Sep. 1989 14 p
(ARL-MAT-TM-398; AR-005-647) Avail: NTIS HC A03/MF A01

A circuit for gating the input to an electronic counter used in the acoustic emission monitoring of cyclically loaded propagating cracks is described. The circuit ensures that acoustic emission signals registered by the counter arise principally from propagating cracks and that the counting of extraneous signals such as those occurring as a result of rubbing and fretting of contacting surfaces are minimized. Author

N90-13809# Oxford Univ. (England). Dept. of Engineering Science.
THE FOURTH OXFORD INTERNATIONAL CONFERENCE ON THE MECHANICAL PROPERTIES OF MATERIALS AT HIGH RATES OF STRAIN
22 Mar. 1989 119 p Conference held in Oxford, England, 19-22 Mar. 1989; sponsored by US Army European Research Office
(Contract DAJA45-89-M-0358)
(AD-A212293; R/D-6154-MS-02) Avail: NTIS HC A06/MF A01 CSCL 11/4

This document is a compilation of reports presented at the conference on the mechanical properties of materials at high rate of strain. Titles include: On the reliability of experimental measurements in dynamic fracture; A map for impact induced ductile failure; Evolution of thermo-visco-plastic shearing; Experimental methods of material characterization; The development of constitutive relationships for material behavior at high rates of strain; Numerical modelling; Discussion of microstructural effects at its modelling at rates of strain; Overview of the impact of monolithic ceramics; Overview of impact of composites; Some comments on the modelling of material

properties for dynamic structural plasticity; Applications in the nuclear industry; and Aerospace applications of materials at high strain rates. GRA

N90-13810# Northwestern Univ., Evanston, IL. Center for Quality Engineering and Failure Prevention.
NUMERICAL ANALYSIS OF SCATTERING BY INTERFACE FLAWS Interim Report
Yonglin Xu and Jan D. Achenbach 15 Aug. 1989 10 p
(Contract N00014-89-J-1362)
(AD-A212996; NU-CENTER-QEFP-1989-1) Avail: NTIS HC A02/MF A01 CSCL 20/11

Scattering by inhomogeneities in homogeneous media can be analyzed in an elegant manner by reducing the problem statement to the solution of a system of singular integral equations over the surface of the scatterer. This system can be solved in a relatively straight forward manner by the use of the boundary element method. An inhomogeneity in an interface between two solids of different mechanical properties presents some additional complications to the numerical analyst. These complications are discussed. In deriving the system of singular integral equations, it was decided to use the Green's function for the unbounded regions of the two materials, rather than the single Green's function for the space of the joined half spaces. This approach introduces a considerable simplification in the integrands, but at the expense of the addition of a set of boundary integral equations over the interface between the two solids, outside of the inhomogeneity. In the boundary element approach the domain of these equations has to be truncated. Specific results are presented for backscattering by a spherical cavity in the interface of solids of different elastic moduli and mass densities. GRA

N90-13811# Naval Civil Engineering Lab., Port Hueneme, CA.
TIME DOMAIN COUPLING OF THE BOUNDARY AND FINITE ELEMENT METHODS FOR ELASTODYNAMICS Final Report, Oct. 1986 - Apr. 1988
J. Cox Aug. 1989 72 p
(AD-A213243; NCEL-TN-1799) Avail: NTIS HC A04/MF A01 CSCL 12/1

The time domain coupling of the boundary and finite element methods for elastodynamics is investigated. The study is motivated by the need for a silent boundary in nonlinear problems with infinite domains. Of the boundary element methods (BEMs) considered, formulations based on the Stokes solution appear to be the best suited. The theoretical and numerical bases for the indirect and direct BEMs using the Stokes solution are presented. The integral equation statements of the boundary-initial value problem included a convolution of the time variable and thus appear to be computationally intense. A coupling algorithm which treats the BEM region as a nonlinear boundary condition to the finite element region is presented. The potential of the coupled approach might be realized by exploiting special properties of Stoke's solution and designing the algorithm to use the advances in computer hardware (e.g. parallel processing). GRA

N90-13812# Structureal Integrity Associates, Inc., San Jose, CA.
STRESS INTENSITY FACTORS FOR CRACKING METAL STRUCTURES UNDER RAPID THERMAL LOADING. VOLUME 2: THEORETICAL BACKGROUND Final Report, Oct. 1987 - Apr. 1989
An-Yu Kuo, Peter C. Riccardella, Shu S. Tang, Curtis S. Carney, and Reji John Aug. 1989 452 p Prepared in cooperation with Dayton Univ., OH
(Contract F33615-87-C-3250)
(AD-A213297; SIR-89-023-Vol-2; WRDC-TR-89-3074-Vol-2)
Avail: NTIS HC A20/MF A03 CSCL 13/13

An SBIR Phase 2 study has been conducted on a novel method of calculating cracktip stress intensity factors for cracked metal structures under rapid thermal pulse loadings. The work couples a Green's function integration technique for transient thermal stresses with the well-known influence function approach for calculating stress intensity factors. A total of seven most commonly used crack models were investigated in this study. A computer program implementing the methodology designated THERMO-K, was developed and delivered with the Phase 2 project report. Temperature, stress and stress intensity factor solutions predicted by THERMO-K for all seven crack models have been verified by comparing them with finite element results or experimental measurements. Operable on an IBM-pc or compatible, the program demonstrates the ability to accurately calculate stress intensity factors, with very short turnaround times, and immediate graphics visualization of the results. Based on the success of this Phase 2 study, it is concluded that the computer program THERMO-K resulting from this study is an easy to use, fast, and accurate tool, for predicting stress intensity factors for a wide range of metallic (or other) structures of interest to the Air Force, under rapid thermal pulses. GRA

N90-13813*# National Aeronautics and Space Administration. John F. Kennedy Space Center, Cocoa Beach, FL.
COMPARISON OF ANALYTICAL METHODS FOR CALCULATION OF WIND LOADS
Donald J. Minderman and Larry L. Schultz Sep. 1989 50 p
(NASA-TM-102782; KSC-DM-3282; NAS 1.15:102782) Avail: NTIS HC A03/MF A01 CSCL 20K

The following analysis is a comparison of analytical methods for calculation of wind load pressures. The analytical methods specified in ASCE Paper No. 3269, ANSI A58.1-1982, the Standard Building Code, and the Uniform Building Code were analyzed using various hurricane speeds to determine the differences in the calculated results. The winds used for the analysis ranged from 100 mph to 125 mph and applied inland from the shoreline of a large open body of water (i.e., an enormous lake or the ocean) a distance of 1500 feet or ten times the height of the building or structure considered. For a building or structure less than or equal to 250 feet in height acted upon by a wind greater than or equal to 115 mph, it was determined that the method specified in ANSI A58.1-1982 calculates a larger wind load pressure than the other methods. For a building or structure between 250 feet and 500 feet tall acted upon by a wind rangind from 100 mph to 110 mph, there is no clear choice of which method to use; for these cases, factors that must be considered are the steady-state or peak wind velocity, the geographic location, the distance from a large open body of water, and the expected design life and its risk factor. Author

N90-13814*# Textron Bell Helicopter, Fort Worth, TX.
INVESTIGATION OF DIFFICULT COMPONENT EFFECTS ON FINITE ELEMENT MODEL VIBRATION PREDICTION FOR THE BELL AG-1G HELICOPTER. VOLUME 2: CORRELATION RESULTS Final Report
R. V. Dompka Oct. 1989 211 p
(Contract NAS1-17496)
(NASA-CR-181916-Vol-2; NAS 1.26:181916-Vol-2; BHT-699-099-251-Vol-2) Avail: NTIS HC A10/MF A02 CSCL 20K

Under the NASA-sponsored DAMVIBS (Design Analysis Methods for VIBrationS) program, a series of ground vibration tests and NASTRAN finite element model (FEM) correlations were conducted on the Bell AH-1G helicopter gunship to investigate the effects of difficult components on the vibration response of the airframe. Previous correlations of the AG-1G showed good agreement between NASTRAN and tests through 15 to 20 Hz, but poor agreement in the higher frequency range of 20 to 30 Hz. Thus, this effort emphasized the higher frequency airframe vibration response correlations and identified areas that need further R and T work. To conduct the investigations, selected difficult components (main rotor pylon, secondary structure, nonstructural doors/panels, landing gear, engine, furl, etc.) were systematically removed to quantify their effects on overall vibratory response of the airframe. The entire effort was planned and documented, and the results reviewed by NASA and industry experts in order to ensure scientific control of the testing, analysis, and correlation exercise. In particular, secondary structure and damping had significant effects on the frequency response of the airframe above

15 Hz. Also, the nonlinear effects of thrust stiffening and elastomer mounts were significant on the low frequency pylon modes below main rotor 1p (5.4 Hz). The results of the NASTRAN FEM correlations are given. Author

N90-13815# Deutsche Forschungsanstalt fuer Luft- und Raumfahrt, Cologne (Germany, F.R.). Abteilung Bruchvorgaenge und Mechanische Eigenschaften.

THRESHOLD FOR FATIGUE CRACK PROPAGATION Ph.D. Thesis

Daniel C. Castro Apr. 1989 105 p In GERMAN; ENGLISH summary

(DLR-FB-89-33; ISSN-0171-1342; ETN-90-95842) Avail: NTIS HC A06/MF A01; DLR, VB-PL-DO, Postfach 90 60 58, 5000 Cologne, Fed. Republic of Germany, 35.50 Deutsche Marks

The influence of the loading history on the threshold for fatigue crack propagation by the alloys Inconel 617 and Ti-6Al-4V is investigated. Measurements of the crack opening stress intensity factor K sub op are carried out in order to judge the influence of this parameter on delta K sub th. The results show that the threshold always exists independent of the prior loading condition. The value of Delta K sub th decreases with increasing delta K and increasing maximal stress intensity factor K sub max of the prior loading. The results are discussed in terms of crack closure and changes of the microstructure in the plastic zone. ESA

N90-13816# Deutsche Forschungsanstalt fuer Luft- und Raumfahrt, Brunswick (Germany, F.R.). Abteilung Strukturberechnung.

GENERAL BUCKLING TESTS WITH THIN-WALLED SHELLS

Hermann Klein Apr. 1989 23 p

(DLR-Mitt-89-13; ISSN-0176-7739; ETN-90-95847) Avail: NTIS HC A03/MF A01; DLR, VB-PL-DO, Postfach 90 60 58, 5000 Cologne, Fed. Republic of Germany, 18 Deutsche Marks

Hints are given for the preparation, execution and evaluation of buckling tests with thin-walled shells. Controlling of load, displacement, and boundary conditions are discussed. Buckling tests in the Deutsche Forschungsanstalt fur Luft-und Raumfahrt (DLR) are given as examples for the buckling behavior of real shells. The role of imperfections and load interferences in influencing behavior and why their sensitivity depends on the properties of the shell and the test are discussed. ESA

N90-13817*# Florida Atlantic Univ., Boca Raton. Center for Acoustics and Vibrations.

MOBILITY POWER FLOW ANALYSIS OF AN L-SHAPED PLATE STRUCTURE SUBJECTED TO ACOUSTIC EXCITATION Progress Report, Jun. - Dec. 1989

J. M. Cuschieri Dec. 1989 35 p

(Grant NAG1-685)

(NASA-CR-186130; NAS 1.26:186130) Avail: NTIS HC A03/MF A01 CSCL 20K

An analytical investigation based on the Mobility Power Flow method is presented for the determination of the vibrational response and power flow for two coupled flat plate structures in an L-shaped configuration, subjected to acoustical excitation. The principle of the mobility power flow method consists of dividing the global structure into a series of subsystems coupled together using mobility functions. Each separate subsystem is analyzed independently to determine the structural mobility functions for the junction and excitation locations. The mobility functions, together with the characteristics of the junction between the subsystems, are then used to determine the response of the global structure and the power flow. In the coupled plate structure considered here, mobility power flow expressions are derived for excitation by an incident acoustic plane wave. In this case, the forces (acoustic pressures) acting on the structure are dependent on the response of the structure because of the scattered pressure component. The interaction between the structure and the fluid leads to the derivation of a corrected mode shape for the plates' normal surface velocity and also for the structure mobility functions. The determination of the scattered pressure components in the expressions for the power flow represents an additional component in the power flow balance for the source plate and the receiver plate. This component represents the radiated acoustical power from the plate structure. Author

N90-13818*# National Aeronautics and Space Administration. Langley Research Center, Hampton, VA.

THE COMPUTATIONAL STRUCTURAL MECHANICS TESTBED USER'S MANUAL

Caroline B. Stewart, comp. (Analytical Services and Materials, Inc., Hampton, VA.) Oct. 1989 668 p

(NASA-TM-100644; NAS 1.15:100644) Avail: NTIS HC A99/MF A04 CSCL 20K

The Computational Structural Mechanics (CSM) Testbed software system is a highly modular and flexible structural analysis system for research in computational methods and for exploitation of new multiprocessor and vector computer hardware. This structural analysis system is based on Level 13 of the SPAR finite element code and the NICE System with extensions provided for specific analysis capabilities. NICE contains data management utilities, a command language interpreter, and a command language definition for integrating engineering computational modules. SPAR is a system of programs used for finite element structural analysis. It includes many complementary structural and thermal analysis and utility functions which communicate through a common database. It was extended to include additional analysis functions required for nonlinear analysis capability, and several new element families were installed to replace the SPAR element library. The purpose of this manual is to document the processors of the Computational Structural Mechanics Testbed software system. A description of each processor including its function, commands, data interface, and use is presented. Author

N90-13819*# National Aeronautics and Space Administration. Lewis Research Center, Cleveland, OH.

MEAN STRESS AND THE EXHAUSTION OF FATIGUE-DAMAGE RESISTANCE

Avraham Berkovits Nov. 1989 18 p

(NASA-TM-101311; E-4307; NAS 1.15:101311) Avail: NTIS HC A03/MF A01 CSCL 20K

Mean-stress effects on fatigue life are critical in isothermal and thermomechanically loaded materials and composites. Unfortunately, existing mean-stress life-prediction methods do not incorporate physical fatigue damage mechanisms. An objective is to examine the relation between mean-stress induced damage (as measured by acoustic emission) and existing life-prediction methods. Acoustic emission instrumentation has indicated that, as with static yielding, fatigue damage results from dislocation buildup and motion until dislocation saturation is reached, after which void formation and coalescence predominate. Correlation of damage processes with similar mechanisms under monotonic loading led to a reinterpretation of Goodman diagrams for 40 alloys and a modification of Morrow's formulation for life prediction under mean stresses. Further testing, using acoustic emission to monitor dislocation dynamics, can generate data for developing a more general model for fatigue under mean stress. Author

N90-13820*# National Aeronautics and Space Administration. Hugh L. Dryden Flight Research Facility, Edwards, CA.

APPLICATION OF FRACTURE MECHANICS AND HALF-CYCLE METHOD TO THE PREDICTION OF FATIGUE LIFE OF B-52 AIRCRAFT PYLON COMPONENTS

W. L. Ko, A. L. Carter, W. W. Totton, and J. M. Ficke Sep. 1989 80 p

(NASA-TM-88277; H-1383; NAS 1.15:88277) Avail: NTIS HC A05/MF A01 CSCL 20K

Stress intensity levels at various parts of the NASA B-52 carrier aircraft pylon were examined for the case when the pylon store was the space shuttle solid rocket booster drop test vehicle. Eight critical stress points were selected for the pylon fatigue analysis. Using fracture mechanics and the half-cycle theory (directly or indirectly) for the calculations of fatigue-crack growth ,the remaining fatigue life (number of flights left) was estimated for each critical part. It was found that the two rear hooks had relatively short

fatigue life and that the front hook had the shortest fatigue life of all the parts analyzed. The rest of the pylon parts were found to be noncritical because of their extremely long fatigue life associated with the low operational stress levels. Author

N90-13821# Ecole Centrale de Lyon (France).
IDENTIFICATION OF EQUIVALENT MODULUS OF A COMPOSITE BEAM FROM NONMODAL VIBRATORY TESTS Ph.D. Thesis [IDENTIFICATION DES MODULES EQUIVALENTS D'UNE POUTRE COMPOSITE A PARTIR D'ESSAIS VIBRATOIRES NON-MODAUX]
Somsak Chaiyaporn 1989 198 p In FRENCH; ENGLISH summary
(ECL-89-001; ETN-90-95777) Avail: NTIS HC A09/MF A02

An identification method of dynamic characteristics of material (complex Young's modulus and complex shear modulus), based on an analysis of the response of a forced vibrated beam, is presented. An impedance at the midpoint of a free beam is measured. The moduli are obtained at each frequency of excitation by comparing the experimental impedance with the calculated one. Calculated impedance is obtained by using a development in series of the exact impedance. On application of Euler-Bernoulli approximations with a development limited to the 9th order, the curves obtained cover a large frequency domain including several resonant frequencies. ESA

N90-13822# Technische Univ., Delft (Netherlands). Dept. of Aerospace Engineering.
AN EVALUATION OF A FATIGUE CRACK GROWTH PREDICTION MODEL FOR VARIABLE-AMPLITUDE LOADING (PREFFAS)
J. Schijve Dec. 1987 35 p
(LR-537; ETN-90-95984) Avail: NTIS HC A03/MF A01

A prediction model for fatigue crack growth (PREFFAS) under stationary variable amplitude load histories with a short recurrence (for example flight simulation loading) is described and analyzed. It is a cycle-by-cycle prediction model based on crack closure. Consequences, limitations and possible extensions are discussed. The model is applied to a series of simplified flight simulation tests. ESA

N90-13823# Technische Univ., Delft (Netherlands). Dept. of Aerospace Engineering.
BUCKLING LOAD ANALYSIS FOR IMPERFECT CYLINDRICAL SHELLS, PART 1
M. S. Skowronek (Gdansk Technical Univ., Poland) Oct. 1987 54 p
(LR-543-Pt-1; ETN-90-95987) Avail: NTIS HC A04/MF A01

The nonlinear Novozhilov type shell equations for imperfect stiffened shells are reduced to a set of ordinary differential equations by Galerkin's method. For four modes initial geometrical imperfections, the solution is obtained by the parallel shooting method with Runge-Kutta numerical integration. The SHELL computer code is applied for determination of buckling loads. ESA

N90-13824# Technische Univ., Delft (Netherlands). Dept. of Aerospace Engineering.
DESIGN AND EVALUATION OF A NEW BIAXIAL TESTING METHOD FOR SHEET MATERIAL (SUPERBAT)
D. Chen Dec. 1987 21 p
(LR-548; ETN-90-95991) Avail: NTIS HC A03/MF A01

A new biaxial testing technique, called Specimen Using Poisson's ratio Effect Restraining for BiAxial Testing (SUPERBAT) suitable for testing sheet materials is described. The design and evaluation of the method are outlined. Some preliminary test results are discussed in detail. Theoretical calculations lead to the suggestion for further study. ESA

N90-13825# Technische Univ., Delft (Netherlands). Dept. of Aerospace Engineering.
THE INITIAL IMPERFECTION DATA BANK AT THE DELFT UNIVERSITY OF TECHNOLOGY, PART 2
R. Dancy and D. Jacobs Jun. 1988 167 p
(LR-559-Pt-2; ETN-90-95996-Pt-2) Avail: NTIS HC A08/MF A01

The results of initial imperfection surveys on a series of 33 nominally identical thin walled cylindrical shells are presented. The quasi three-dimensional plots of the initial imperfections show the influence of the production process on the initial imperfections of the shells. The modal components of the measured imperfection surfaces as a function of the circumferential and axial wave numbers are calculated and displayed. ESA

42 GEOSCIENCES (GENERAL)

N90-13826# European Space Agency, Paris (France).
EUROPEAN ROCKET AND BALLOON PROGRAMS AND RELATED RESEARCH
W. R. Burke, comp. Jun. 1989 332 p Partly in ENGLISH and FRENCH Proceedings of the 9th ESA/PAC symposium, Lahnstein, Fed. Republic of Germany, 3-7 Apr. 1989
(ESA-SP-291; ISBN-92-9092-006-8; ISSN-0379-6566; ETN-90-95760) Copyright Avail: NTIS HC A15/MF A02

Investigations on the European rocket, balloon programs and related research are reported. The subject discussions are focused on: the national programs; the studies concerning upper and middle atmosphere, ionosphere and magnetosphere; the Viking related results; the new techniques and instrumentation; the range facilities; astronomy and astrophysics; and telemetry. As concluding remarks, it is noted that: not only new techniques are asked for, but improved or more efficient use of proven techniques is needed. Moreover, the lack of high precision tracking radar is stressed. For individual titles, see N90-13827 through N90-13877.

N90-13827# Geneva Observatory (Switzerland).
SWISS SCIENTIFIC BALLOON AND SOUNDING ROCKET EXPERIMENTS 1987-1989 **c46**
D. Huguenin *In* ESA, European Rocket and Balloon Programs and Related Research Jun. 1989 p 3-6 (For primary document see N90-13826 05-42)
Copyright Avail: NTIS HC A15/MF A02

Swiss laboratories participation in rocket flight and four to five balloon flights, in cooperation with foreign institutes are reported. The fields covered are chemistry and composition of the middle atmosphere, astrophysics (sun, stars, interstellar matter) and life science. A continuation of these programs with Belgium, France, Sweden and the U.S.A. is considered. ESA

N90-13828# Centre National de la Recherche Scientifique, Paris (France).
THE FRENCH BALLOON PROGRAM AND RELATED SPACE RESEARCH **c46**
I. Sadourny *In* ESA, European Rocket and Balloon Programs and Related Research Jun. 1989 p 7-12 (For primary document see N90-13826 05-42)
Copyright Avail: NTIS HC A15/MF A02

The balloon program of the Centre National d'Etudes Spaciales (CNES-France) is reported. The program components, the means developed and the future programs are discussed. The interest in the study of balloon flight in the terrestrial environment or high above the dense layers of the atmosphere, using a wide variety of scientific instruments, is underlined. The balloon has played for more than 20 years a very specific and original part in space research. This is the reason why CNES maintained and developed a very active balloon program for both French and foreign users. ESA

N90-13829# Norwegian Space Center, Oslo.
THE NORWEGIAN BALLOON AND SOUNDING ROCKET PROGRAM 1989-1992 **c46**
B. N. Andersen and A. Gundersen *In* ESA, European Rocket

and Balloon Programs and Related Research Jun. 1989 p 13-16 (For primary document see N90-13826 05-42)
Copyright Avail: NTIS HC A15/MF A02

The Norwegian sounding rocket and balloon programs are reviewed. The aim of these programs is to perform investigations into ionospheric and magnetospheric processes. These investigations are supplemented by a wide range of ground based support instrumentation. Tests with recovery of payloads will be carried out at Andoya Rocket Range, partly as preparation for microgravity experiments. The overall program for the period 1989 to 1992 is reviewed. ESA

N90-13830# Swedish Space Corp., Solna.
THE SWEDISH SOUNDING ROCKET AND BALLOON PROGRAM **c46**
K. Lundahl *In* ESA, European Rocket and Balloon Programs and Related Research Jun. 1989 p 17-22 (For primary document see N90-13826 05-42)
Copyright Avail: NTIS HC A15/MF A02

The Swedish sounding rocket and balloon program is presented. The investigations relate to geophysical disciplines, astrophysics and microgravity research. The planned future scientific projects using sounding rockets and balloons are included. It is to be applied to infrared observations of interstellar medium and studies on nitrogen and oxygen photochemistry and transport in the upper atmosphere. Continued studies on auroral electrodynamics are proposed. A continued investigation on the structure and dynamics of the middle atmosphere above the northern polar region during summer are discussed. ESA

N90-13831# Deutsche Forschungsanstalt fuer Luft- und Raumfahrt, Cologne (Germany, F.R.). Executive Dept. for Space Projects.
THE GERMAN SCIENTIFIC BALLOON AND SOUNDING ROCKET PROGRAM **c46**
A. F. Dahl and Manfred Otterbein (Bundesministerium fuer Forschung und Technologie, Bonn, Germany, F.R.) *In* ESA, European Rocket and Balloon Programs and Related Research Jun. 1989 p 23-31 (For primary document see N90-13826 05-42)
Copyright Avail: NTIS HC A15/MF A02

The German space program which uses scientific balloon and sounding rocket as investigative instruments, is presented. Information on sounding rocket projects in the scientific fields of astronomy, aeronomy, magnetospheric research, and microgravity research, is provided. The scientific balloon projects are performed with emphasis on astronomical and aeronomical research. The projects undertaken after 1987 are identified as are preparations and plans for the future until 1992. ESA

N90-13832# Swedish Inst. of Space Physics, Kiruna.
ENHANCED ELECTRON DENSITY LAYERS IN THE HIGH-LATITUDE LOWER IONOSPHERE **c46**
S. Kirkwood, L. Eliasson, I. Haeggstroem, and P. N. Collis (EISCAT Scientific Association, Kiruna, Sweden) *In* ESA, European Rocket and Balloon Programs and Related Research Jun. 1989 p 35-40 Sponsored by NFR, Sweden (For primary document see N90-13826 05-42)
Copyright Avail: NTIS HC A15/MF A02

Narrow layers of enhanced electron density appearing at altitudes between 90 and 100 km are investigated. They are found to be of at least 3 distinct types: the first type consists of very narrow, short lived, sporadic E type layers, which can be associated with similar layers in neutral sodium, and which may be composed of metallic ions; the second type comprises broader, short lived layers which are seen in the magnetic evening and midnight sectors and which appear to be produced directly by precipitation of energetic electrons from the outer edge of the radiation belts; and the third type comprises persistent daytime/early evening layers which seem to be composed of unusual ion species, with the bulk of the ions having a short lifetime (not longer than a few tens of minutes). ESA

N90-13833# Laboratoire de Meteorologie Dynamique du CNRS, Palaiseau (France).
HUMIDITY LOCAL MEASUREMENTS IN THE MIDDLE ATMOSPHERE [MESURES IN SITU D'HUMIDITE DANS L'ATMOSPHERE MOYENNE] **c46**
J. Ovarlez, J. Capus, M. Forichon, and H. Ovarlez *In* ESA, European Rocket and Balloon Programs and Related Research Jun. 1989 p 43-47 In FRENCH (For primary document see N90-13826 05-42)
Copyright Avail: NTIS HC A15/MF A02

The development of a hydrometer, to be applied in stratospheric balloons for humidity measurements, is described. The device is also designed for satellite data validation. Data from the experiment carried out in the Southern Hemisphere, in November and December 1988, is discussed. The measurements between 20 and 70 hPa showed a volume mixture ratio from 3 to 6. The mechanism of the equatorial stratosphere drying is considered. ESA

N90-13834# Stockholm Univ. (Sweden). Arrhenius Lab.
NEW CALCULATIONS OF PHOTODISSOCIATION CROSS-SECTIONS IN THE O2 SCHUMANN-RUNGE SYSTEM **c46**
Donal P. Murtagh *In* ESA, European Rocket and Balloon Programs and Related Research Jun. 1989 p 49-53 (For primary document see N90-13826 05-42)
Copyright Avail: NTIS HC A15/MF A02

The recalculation of atomic oxygen production rates by photodissociation in the Schumann-Runge band region, is performed. The results indicate that, on the whole, the new spectroscopic data do not give rise to large changes from the existing recommendations of the World Meteorological Organization. However, high atmospheric transmission in the region 194 to 200 nm, as observed by recent balloon experiments, is indicated. A method based on O2 column density and local atmospheric temperature is presented. The parameterization of the results is also considered. This parameterization is shown to be accurate to better than 5 percent for a wide range of solar zenith angles and atmospheric conditions. ESA

N90-13835*# National Aeronautics and Space Administration. Wallops Flight Facility, Wallops Island, VA.
EVIDENCE FOR ACCURATE TEMPERATURES FROM THE INFLATABLE FALLING SPHERE **c46**
F. J. Schmidlin, H. S. Lee, and W. Michel (Dayton Univ., Wallops Island, VA.) *In* ESA, European Rocket and Balloon Programs and Related Research Jun. 1989 p 55-58 (For primary document see N90-13826 05-42)
Copyright Avail: NTIS HC A15/MF A02 CSCL 04A

The experiments performed with the inflatable falling sphere technique, for middle atmosphere studies, are reported. It is shown to be a potentially high accurate and independent source of temperature measurement and an intrinsic method for establishing accuracy of other atmospheric measurement techniques. Theoretical derivation, simulations, and actual measurements show that the sphere's temperature data are accurate. It is demonstrated that retrieved temperatures from falling spheres are not significantly affected by linear bias in density caused by uncertainties in sphere mass, volume, or cross sectional area. Case studies illustrate the sphere's capability to produce accurate temperatures. Comparisons with Datasonde temperature measurements obtained close in time and space are in agreement below 60 km. ESA

N90-13836# Max-Planck-Inst. fuer Aeronomie, Katlenburg-Lindau (Germany, F.R.).
OBSERVATION OF WIND CORNERS IN THE MIDDLE ATMOSPHERE OVER ANDENES (69 N) DURING WINTER 1983/84, SUMMER 1987 AND SUMMER 1988 **c46**
H. U. Widdel *In* ESA, European Rocket and Balloon Programs and Related Research Jun. 1989 p 59-62 (For primary document see N90-13826 05-42)
(Grants BMFT-01-OE-610; BMFT-01-OE-86033)
Copyright Avail: NTIS HC A15/MF A02

The wind corners measurements, over Andenes (Belgium), in winter and summer, are reported. The height levels at which they are seen in summer are higher than in winter. They appeared at some preferred heights around 86 to 88, 91 to 92 and 95 km. High resolution measurements above 92 to 93 km are possible by a new type of chaff which allows measurements up to about 100 km. This height is rather close to the limit (approximately 105 km) up to which the chaff cloud method can sensibly be used. The experiments are launched in salvos comprising several rockets, and an estimate on the lifetime of some wind corners is possible. Relations to turbulence and results obtained by radars are mentioned. ESA

N90-13837# Bonn Univ. (Germany, F.R.). Inst. fuer Physik.
NEAR-MESOPAUSE TEMPERATURES AT 69 N LATITUDE IN LATE SUMMER **c46**
U. vonZahn and H. Kurzawa *In* ESA, European Rocket and Balloon Programs and Related Research Jun. 1989 p 63-66 (For primary document see N90-13826 05-42)
(Grant DFG-Ho-858/1)
Copyright Avail: NTIS HC A15/MF A02

The measured temperature profiles in the altitude region 80 to 110 km, by probing the Doppler width of the laser excited D2 resonance line of free sodium atoms, are presented. They are obtained by applying a Na lidar. Three difficulties are encountered: the lack of a sufficient sodium density below 88 km altitude; a strongly enhanced background due to scattered solar radiation; and potential Na saturation effects. Trial observations in 12 nights of August and with solar depression angles as small as minus 4 deg are obtained. During these nights temperatures down to 120 K are observed. ESA

N90-13838# Oslo Univ. (Norway). Dept. of Physics.
THE ELECTRODYNAMICS OF THE POLAR IONOSPHERE WITH SPECIAL EMPHASIS ON THE DAYSIDE CLEFT REGION **c46**
A. Egeland *In* ESA, European Rocket and Balloon Programs and Related Research Jun. 1989 p 69-77 (For primary document see N90-13826 05-42)
Copyright Avail: NTIS HC A15/MF A02

The basic equations governing the electrodynamics of the dynamo regions, in the ionosphere, are reviewed. The Harang discontinuity in the premidnight auroral zone is discussed. The conclusion is that this is a dynamic region which requires further combined ground and in situ observations. Special attention is given to the large and small scale dynamics of the dayside cusp/cleft aurora. Their relations to the interplanetary magnetic field, particle precipitations, ionospheric electric fields and Birkeland currents, are considered. The advantage of continuous ground based observations is pointed out. The need for further coordinated ground, balloon and rocket measurements poleward of 70 degrees invariant latitudes is stressed. ESA

N90-13839# Max-Planck-Inst. fuer Aeronomie, Katlenburg-Lindau (Germany, F.R.).
SOME REMARKS ON THE WORKING PRINCIPLE OF THE ROCKETBORNE NOSE TIP dc PROBES IN THE D-REGION OF THE IONOSPHERE **c46**
H. U. Widdel *In* ESA, European Rocket and Balloon Programs and Related Research Jun. 1989 p 79-84 (For primary document see N90-13826 05-42)
(Grants BMFT-WRK-90; ERO-DAERO-75-G076)
Copyright Avail: NTIS HC A15/MF A02

The conversion of the currents measured by rocketborne direct current (dc) probes, in the middle atmosphere, is studied. It is shown that the conversion factors derived for positive ion currents are much more stable than those obtained for electron current. This problem is investigated using results obtained by dc probes which had a well confined collection geometry and were flown at 37 degrees north during autumn, winter, spring and summer. It is shown that the probes work as mobility probes and that the electron current is controlled by the mass of the positive ions and the temperature of the electrons which are at thermal equilibrium at heights below about 90 km at middle latitudes. It is found that, due to a peculiarity in the design, these probes responded to vertical electric fields too. ESA

N90-13840# Kiel Univ. (Germany, F.R.). Inst. fuer Experimentalphysik.
RESONANCE CONE DIAGNOSTICS IN THE MID-LATITUDE IONOSPHERE **c46**
A. Piel, H. Thiemann, and K. I. Oyama (Tokyo Univ., Sagamihara, Japan) *In* ESA, European Rocket and Balloon Programs and Related Research Jun. 1989 p 85-90 (For primary document see N90-13826 05-42)
(Grant BMFT-PA4-010-M-86080)
Copyright Avail: NTIS HC A15/MF A02

The German and Japanese cooperation program, concerning the development of a resonance cone instrument, is presented. The aim of the device is the measurement of the electron density and temperature and the study of the nonthermal plasma properties in the ionosphere. The instrument is launched from Kagashima Space Center (Japan), on the 25th of January 1989. The electron density and temperature profiles are reported. The results show nonreciprocity effects that may be related to non-Maxwellian distribution functions. Nonthermal plasma properties could not be detected, in agreement with the absence of the typical temperature anomaly around 90 to 120 km. ESA

N90-13841# Royal Inst. of Tech., Stockholm (Sweden). Dept. of Plasma Physics.
AURORAL PARTICLE ACCELERATION BY dc AND LOW FREQUENCY ELECTRIC FIELDS **c46**
L. P. Block and C.-G. Faelthammar *In* ESA, European Rocket and Balloon Programs and Related Research Jun. 1989 p 93-95 (For primary document see N90-13826 05-42)
Copyright Avail: NTIS HC A15/MF A02

Six independent methods to determine DC potential drops along auroral magnetic field lines are described. The results indicate that DC acceleration plays a dominant role, and that the accelerated particles are heated by waves, induced by the same particles. Satellite observations show that the field aligned potential drops are made up of hundreds or thousands of weak double layers. It is concluded that the average electric fields are much weaker than the fluctuating fields, as seen on a satellite. Low frequency electric field spectra show characteristic features that support these conclusions. ESA

N90-13842# Swedish Inst. of Space Physics, Uppsala.
OBSERVATIONS OF ELECTROSTATIC HYDROGEN CYCLOTRON WAVES AND ELECTRIC FIELD FLUCTUATIONS NEAR ONE Hz IN AURORAL ACCELERATION REGIONS **c46**
Anders I. Eriksson and Georg Gustafsson *In* ESA, European Rocket and Balloon Programs and Related Research Jun. 1989 p 97-102 Sponsored by the Swedish Board for Space Activities (For primary document see N90-13826 05-42)
Copyright Avail: NTIS HC A15/MF A02

The electrostatic hydrogen cyclotron waves and the electric field fluctuations, below the oxygen gyrofrequency (a few Hz) are studied. Satellite observations in the altitude range 7000 to 13000 km of the electric field in 0.2 to 2 Hz and between 1 and 1.9 of the proton frequency ranges, are studied. Wave data from seven orbits passing through the mid altitude acceleration region are studied. A close correlation between the power in the two frequency ranges is observed, during ion conic events, and in ion beam events. The amount of power, the detailed correlation, and the power ratio between the two frequency ranges indicate the possibility that the low frequency fluctuations may be a source of ion acceleration. ESA

N90-13843# Royal Inst. of Tech., Stockholm (Sweden). Dept. of Plasma Physics.
THE AURORAL CURRENT - VOLTAGE RELATIONSHIP **c46**
Kornelia Bruening *In* ESA, European Rocket and Balloon Programs and Related Research Jun. 1989 p 103-108

Sponsored by ESA (For primary document see N90-13826 05-42)
Copyright Avail: NTIS HC A15/MF A02

The classification of the field aligned current-voltage relationship is effectuated. It is peformed in three parts: the field aligned current without field aligned acceleration; the Ohms law for the current voltage relationship; and the saturation current. It is observed that the linear relationship between the field aligned current and potential drop appears, when the field aligned potential drop is smaller than the critical field aligned potential drop V sub C. Moreover, when the field aligned potential drop is stronger than V sub C a saturation current is flowing. An example from Viking observations of the Ohms law for the current voltage relationship and an example for a saturation current are shown. ESA

N90-13844# Technische Univ., Brunswick (Germany, F.R.). Inst. fuer Geophysik und Meteorologie.
HIGH PRECISION ROCKET ATTITUDE RECONSTRUCTION USING STAR SENSOR AND MAGNETOMETER DATA **c20**
A. Muschinski and H. Luehr *In* ESA, European Rocket and Balloon Programs and Related Research Jun. 1989 p 111-116 (For primary document see N90-13826 05-42)
Copyright Avail: NTIS HC A15/MF A02

A method for the attitude reconstruction of sounding rockets is presented. It is demonstrated how the attitude accuracy achieved with star sensor data can be improved with information from high resolution dc (direct current) magnetometer data. Extensive analytical investigations are performed. The results show that spin frequency and phase can very precisely be determined by the star sensor data; and that the mutation angle and phase are more sensitively monitored by the magnetometer data. ESA

N90-13845# Deutsche Forschungs- und Versuchsanstalt fuer Luft- und Raumfahrt, Oberpfaffenhofen (Germany, F.R.). Hauptabteilung Angewandte Datentechnik.
THE SN 1987A ATTITUDE CONTROL SYSTEM **c20**
J. Turner *In* ESA, European Rocket and Balloon Programs and Related Research Jun. 1989 p 117-122 (For primary document see N90-13826 05-42)
Copyright Avail: NTIS HC A15/MF A02

The development, test, operation and flight performance, of an attitude control system (ACS), and the refurbishment and launch of a payload are described. The system is applied in the German SN (supernovae) 1987A sounding rocket mission. The ACS comprised an inertial platform with a star tracker and two stellar TV cameras with ground based interactive telecommand for update and fine pointing. The ground and flight telecommand systems are based on the 8052 and 8031 microcontrollers respectively and provided precise offsets for: the automatic mode control, the facility for inflight corrections and the remote selection of redundant operational modes. ESA

N90-13846# Deutsche Forschungsanstalt fuer Luft- und Raumfahrt, Cologne (Germany, F.R.).
SOFIA (STRATOSPHERIC OBSERVATORY FOR INFRARED ASTRONOMY): A 3m CLASS AIRBORNE TELESCOPE **c89**
A. F. Dahl, R. Ewald, and A. Himmes *In* ESA, European Rocket and Balloon Programs and Related Research Jun. 1989 p 123-124 (For primary document see N90-13826 05-42)
Copyright Avail: NTIS HC A15/MF A02

The studies to provide a 3m class airborne telescope for SOFIA are presented. It is effectuated by means of cooperation with NASA and the German minister for research and technology. SOFIA can provide a continuing and readily deployable observation possibility at heights above 12.5km for sophisticated instrumentation from the submm well into the optical spectral range. The telescope system definition phase is included. ESA

N90-13847# Dornier System G.m.b.H., Friedrichshafen (Germany, F.R.). Space Div.
DESIGN AND TECHNICAL ASPECTS OF THE SOLLY INSTRUMENT **c35**
M. Boison and E. Weber *In* ESA, European Rocket and Balloon Programs and Related Research Jun. 1989 p 125-128 (For primary document see N90-13826 05-42)
Copyright Avail: NTIS HC A15/MF A02

The Solar Lyman (Solly) spectrometer is described. It is a type of resonance spectrometer for sounding rocket missions (launched on October 24, 1988, and recovered). The instrument is designed to measure the solar line profile and intensity within the core of the solar Lyman alpha line at 121.6 nanometers. The instrument comprises sequentially arranged hydrogen and oxygen cells with two independent detectors. A technical description of the instrument design and layout are presented. ESA

N90-13848# Bern Univ. (Switzerland). Inst. of Physics.
A DOUBLE FOCUSING MASS-SPECTROMETER FOR SIMULTANEOUS ION MEASUREMENTS IN THE STRATOSPHERE **c35**
R. Moor, E. Kopp, U. Jenzer, H. Ramseyer, U. Waelchli, E. Arijs, D. Nevejans, J. Ingels, D. Fussen, and A. Barassin (Centre National de la Recherche Scientifique, Orleans, France) et al *In* ESA, European Rocket and Balloon Programs and Related Research Jun. 1989 p 129-134 Sponsored by Swiss National Science Foundation; Belgian National Science Foundation; and CNES, France (For primary document see N90-13826 05-42)
Copyright Avail: NTIS HC A15/MF A02

A modified Mattauch-Herzog analyzer is developed for positive ion measurements in the mass range 12 to 500 units and is upgraded for negative ions. It is to be applied in the identification of less abundant stratospheric ions. The main characteristics, design parameters and first laboratory test results obtained with it are described. The ions are mass separated in combined toroidal electrostatic and constant magnetic fields. The simultaneous measurement of a spectrum part is achieved with the use of two detectors. They consist of a one inch microchannel plate, an attached phosphor screen, a fiberoptic seal and a linear position sensitive light detector. Ambient atmospheric ions are sampled through a small orifice. The atmospheric air density is reduced in the inlet region of the instrument with a liquid helium cyropump. An octopole HF field is integrated into the ion optics in order to reduce the ion loss. ESA

N90-13849*# National Aeronautics and Space Administration. Wallops Flight Facility, Wallops Island, VA.
APPLICATION OF AN OPTIMAL FILTER FOR INFLATABLE SPHERE DATA PROCESSING **c35**
H. S. Lee, F. J. Schmidlin, and W. Michel (Dayton Univ., Wallops Island, VA.) *In* ESA, European Rocket and Balloon Programs and Related Research Jun. 1989 p 135-138 (For primary document see N90-13826 05-42)
Copyright Avail: NTIS HC A15/MF A02 CSCL 14B

The improvement in the sphere data processing, concerning the signal to noise ratio, is discussed. Frequency analysis of the radar data is effectuated. It reveals a specific frequency component in the radar angle error, which may originate from the tracking radar mechanism itself. An optimal (Wiener) filter is applied to the radar data in order to suppress the systematic angular error components selectively. Using this technique, a significant improvement in the signal to noise ratio is achieved. The resolution of sphere measurements, previously limited by the length of the polynomial filter in the sphere data processing algorithm, is improved. ESA

N90-13850# Max-Planck-Inst. fuer Aeronomie, Katlenburg-Lindau (Germany, F.R.).
PRELIMINARY RESULTS OF THE ROCKET AND SCATTER EXPERIMENTS ROSE: MEASUREMENTS WITH THE NEWLY DESIGNED SPHERICAL PROBE **c46**
G. Rose *In* ESA, European Rocket and Balloon Programs and Related Research Jun. 1989 p 141-147 Sponsored by Bundesminister fuer Forschung und Technologie (For primary document see N90-13826 05-42)
Copyright Avail: NTIS HC A15/MF A02

The Rocket and Scatter Experiments (ROSE) are presented. They are designed to measure the parameters characterizing the

modified two stream and the gradient drift instabilities occurring under radar auroral conditions in the polar E region between 90 km and 120 km. Four rockets are instrumented and launched successfully. Each rocket contained nine different experiments and a star sensor. Some of the measurements in the frequency range from 120 Hz to 3.5 kHz, obtained with the small, newly designed spherical probe, are presented. ESA

N90-13851# Auroral Observatory, Tromso (Norway).
BACKGROUND ELECTRODYNAMICS MEASURED BY EISCAT DURING THE NEED CAMPAIGN **c46**
C. Hall, A. Brekke, M. T. Rietveld, U. P. Lovhaug, and B. N. Maehlum (Norwegian Defence Research Establishment, Kjeller.) *In* ESA, European Rocket and Balloon Programs and Related Research Jun. 1989 p 153-157 Sponsored by Norges Almenvitenskapelige Foskningsradet, Norway; Science and Engineering Research, England; CNRS, France; Max-Planck Gesellschaft, Fed. Republic of Germany; Suomen Akatemia, Finland; and Naturvitenskapeliga Forskningsradet, Sweden (For primary document see N90-13826 05-42)
Copyright Avail: NTIS HC A15/MF A02

Data obtained during the Non-Maxwellian Electron Energy Distribution (NEED) flight, are discussed. The measurements are effectuated by the European Incoherent Scatter (EISCAT) ultra high frequency radar. Information on the background ionosphere before and during the flight, is provided. The study is focused on electron densities, electron and ion temperatures and line of sight ion velocities. Electrodynamics and particle energy determination, are discussed. ESA

N90-13852# Norwegian Defence Research Establishment, Kjeller.
THE EFFECTS OF GRAVITY WAVES ON HORIZONTAL LAYERS: SIMULATION AND INTERPRETATION **c46**
U.-P. Hoppe *In* ESA, European Rocket and Balloon Programs and Related Research Jun. 1989 p 161-166 (For primary document see N90-13826 05-42)
Copyright Avail: NTIS HC A15/MF A02

The results of the simulation of the gravity wave activity are discussed. A luminous layer of given finite thickness and profile is assumed. It is modulated with gravity waves of typical wavelengths and amplitudes representative of the gravity wave spectrum. The image is generated by integrating the luminous intensity along the line of sight, through the layer at the angles representing each picture element. The obtained results and published observations are compared. It is shown which waves of the spectrum are most prominent in the images. Ground-based imaging and imaging from space are also compared. ESA

N90-13853# Stockholm Univ. (Sweden). Arrhenius Lab.
A SELF-CONSISTENT MODEL OF THE MOST COMMON NIGHTGLOW EMISSIONS **c46**
Donal P. Murtagh *In* ESA, European Rocket and Balloon Programs and Related Research Jun. 1989 p 167-171 (For primary document see N90-13826 05-42)
Copyright Avail: NTIS HC A15/MF A02

A model for the nightglow emissions, applying an empirical approach, is presented. A Barth mechanism is assumed for the excitation of O(1S) and a similar mechanism, with O2 as the transfer agent, is used for the production of O2 (b to the 1st power Sigma plus sub g). In these cases laboratory rates are used for the quenching of the emitting states by atmospheric constituents. Empirical coefficients are derived for the production and loss of the precursor states. A rigorous test of the model is provided by rocket observations made under different geophysical conditions. In these flights the atomic oxygen green line intensity varied from 30 to 400 Rayleighs. The model is used to derive an atomic oxygen profile by inversion of the (0-0) atmospheric band measurement. The expected height profiles of the other emissions is calculated. The agreement with observation is satisfactory. ESA

N90-13854# Bonn Univ. (Germany, F.R.). Inst. fuer Astrophysik und Extraterrestrische Forschung.
INTERZODIAK 2: OBSERVATION OF EUV-RESONANCE RADIATION **c46**
G. Lay, H. J. Fahr, and H. U. Nass *In* ESA, European Rocket and Balloon Programs and Related Research Jun. 1989 p 173-176 Sponsored by the Bundesministerium fuer Forschung und Technologie (For primary document see N90-13826 05-42)
Copyright Avail: NTIS HC A15/MF A02

The results of the Extraterrestrial Ultra Violet (EUV) radiation measurements, are reported. The observations are effectuated by means of Interzodiak 2 sounding rocket, launched on board of Skylark 12. A total of 13 different celestial targets in the vicinity of the Sun are observed during the 16 minute flight. EUV radiation from interplanetary space and the geocorona is measured with several spectrophotometric sensors at the resonance wavelengths 58.4 nanometers (He) and 121.6 nanometers (H). ESA

N90-13855# Bonn Univ. (Germany, F.R.). Inst. fuer Physik.
NEUTRAL AIR TURBULENCE IN THE MIDDLE AND UPPER ATMOSPHERE OBSERVED DURING THE MAC/EPSILON CAMPAIGN **c46**
W. Hillert and F.-J. Luebken *In* ESA, European Rocket and Balloon Programs and Related Research Jun. 1989 p 179-186 (For primary document see N90-13826 05-42)
(Grant BMFT-01-OE-8604-6)
Copyright Avail: NTIS HC A15/MF A02

An instrument, developed for the measurement of small scale fluctuations of the total air density, is described. It consists of an ionization gauge with a neutral gas mass spectrometer. The measurements are effectuated in the altitude range from 60 to 115 km at 69 N, 16 E. Measurements of the number densities of nitrogen and argon are performed by a mass spectrometer in the altitude range from 95 to 125 km. From the spectral analysis of the measured density fluctuations altitude profiles of turbulent parameters, mean turbulent velocity and energy dissipation rate are derived, with one kilometer altitude resolution. ESA

N90-13856# Coleg Prifysgol Cymru, Aberystwyth (Wales).
POLAR MESOSPHERE SUMMER ECHOES AND ASSOCIATED ATMOSPHERIC GRAVITY WAVES **c46**
P. J. S. Williams, A. P. vanEyken, C. Hall, and J. Roettger (EISCAT Scientific Association, Kiruna, Sweden) *In* ESA, European Rocket and Balloon Programs and Related Research Jun. 1989 p 187-191 Sponsored in part by the United Kingdom Science and Engineering Research Council; Suomen Akatemia, Finland; CNRS, France; Max-Planck Gesellschaft, Fed. Republic of Germany; NAF, Norway; and NVF, Sweden (For primary document see N90-13826 05-42)
Copyright Avail: NTIS HC A15/MF A02

Mesospheric observations made with the European Incoherent Scatter (EISCAT) very high frequency radar are reported. A correlator program to determine pulse-to-pulse correlation functions for Barker coded double pulses is applied. During a total of 5 hours a relatively weak Polar Mesosphere Summer Echo (PMSE) is observed at a height of 85 km with its intensity increasing to a maximum at intervals of approximately 27 minutes. In the region below the PMSE layer, height profiles of vertical velocity showed an atmospheric gravity wave, also with a period of about 27 minutes. In most cases the maximum intensity of the PMSE corresponded to the maximum upward velocity associated with the wave. It is suggested that particle precipitation, adiabatic cooling, and breaking at the mesopause, play a role in creating the conditions for PMSEs to be observed. ESA

N90-13857# Centre National d'Etudes Spatiales, Toulouse (France).
OPERATIONAL ACTIVITY IN FRANCE AND A NEW METHOD OF BALLOON TEMPERATURE PILOTING **c46**
P. Faucon *In* ESA, European Rocket and Balloon Programs and Related Research Jun. 1989 p 195-200 (For primary document see N90-13826 05-42)
Copyright Avail: NTIS HC A15/MF A02

The French balloon activities and a method of temperature piloting are presented. This procedure concerns balloon flights in cold atmospheres. The stratospheric balloon activities for 1982 are evaluated. The evolution of the payloads since 1982 is discussed. The flight duration for each type of balloon is shown. The failure rate of the transport system is shown to be in the order of 6 percent. The temperature piloting procedure allows more reliable results in cold atmospheres flights. ESA

N90-13858# Centre National d'Etudes Spatiales, Toulouse (France).

LARGE HEAVY DUTY BALLOONS IN EUROPE c46

A. Soubrier *In* ESA, European Rocket and Balloom Programs and Related Research Jun. 1989 p 201-202 (For primary document see N90-13826 05-42)

Copyright Avail: NTIS HC A15/MF A02

The large heavy duty balloons, regularly operated in Europe, are considered. The development of materials allows technical difficulties to be overcome. The transmediterranean flights campaign, of 1987, is discussed. The balloons activity extended to the Southern Hemisphere. The Australian government cooperation are included. The overall efficiency of these flights is underlined. ESA

N90-13859# Norwegian Space Center, Oslo. Andoya Rocket Range.

ANDOYA ROCKET RANGE: NEW INSTALLATIONS, FUTURE PLANS, AND INVESTMENTS c14

K. Adolfsen, P. A. Mikalsen, and I. Nyheim *In* ESA, European Rocket and Balloon Programs and Related Research Jun. 1989 p 203-208 (For primary document see N90-13826 05-42)

Copyright Avail: NTIS HC A15/MF A02

The installations and the investments concerning the Andoya rocket range (Norway) are presented. The extensive 1987 campaign with 108 launched rockets, the launch criteria, and the performance and recovery of payloads are discussed. The science operation center, which enables access to real time data from ground based support instrumentation, is described. A historical review and launch possibilities are included. ESA

N90-13860# Centro Tecnico Aerospacial, San Jose dos Campos (Brazil). Inst. de Atividades Espaciais.

QUALIFICATION OF THE 4TH STAGE PROPULSOR OF THE BRAZILIAN LAUNCHER. SLV: A NEW SOUNDING ROCKET [QUALIFICATION DU PROPULSEUR 4EME ETAGE DU LANCEUR BRESILIEN. VLS: UNE NOUVELLE FUSEE SONDE] c15

Jayme Boscov and Wilson Katsumi Toyama *In* ESA, European Rocket and Balloon Programs and Related Research Jun. 1989 p 209-212 In FRENCH (For primary document see N90-13826 05-42)

Copyright Avail: NTIS HC A15/MF A02

The development of the Satellite Launcher Vehicle (SLV) is presented. In particular, the attention is focused on the acquisition of the propulsion parameters of the 4th stage propulsor. The device feasibility analysis is considered. The system consists of a two staged sounding rocket. Its second stage contains the SVL, which can be launched by the 4th stage propulsor to a height range of about 50 to 60 km. ESA

N90-13861# Centro Tecnico Aerospacial, San Jose dos Campos (Brazil). Inst. de Atividades Espaciais.

THE BRAZILIAN SPACE PROGRAM: ACTUAL STATE OF THE ART c15

A. C. F. Pedrosa, T. S. Ribeiro, and Jayme Boscov *In* ESA, European Rocket and Balloon Programs and Related Research Jun. 1989 p 213-218 (For primary document see N90-13826 05-42)

Copyright Avail: NTIS HC A15/MF A02

The activities of the Institute for Space Activities, related to the sounding rockets and the satellite launcher programs, are presented. The Brazilian Space Program, MECB, comprises the satellite launcher, the satellite itself, and the launching range. The difficulties found in the development of the satellite launcher program, concerning the recent policy of export restriction of materials and services imposed, are discussed. ESA

N90-13862# Centre d'Etude Spatiale des Rayonnements, Toulouse (France).

INTERSTELLAR MEDIUM AND INFRARED EMISSION OF THE GALACTIC DISK c90

Guy Serra *In* ESA, European Rocket and Balloon Programs and Related Research Jun. 1989 p 221-228 (For primary document see N90-13826 05-42)

Copyright Avail: NTIS HC A15/MF A02

The measurements of the galactic disc infrared emission are summarized. The empirical models made to explain the spatial distribution of the infrared fluxes emitted by the galactic disc are recalled. The dust models are reviewed. Special emphasis is given to the difficulties in accounting for dust models. The proposition of a new component of the interstellar matter, the Polycyclic Aromatic Molecules (PAHs) is discussed. The results obtained using balloon-borne instruments are reported. The identification of the galactic interstellar very small grains to PAH molecules is strengthened. The present vision of the interstellar medium is described. ESA

N90-13863# Bonn Univ. (Germany, F.R.). Inst. fuer Astrophysik und Extraterrestrische Forschung.

OPTICAL OBSERVATIONS OF INTERPLANETARY PICK-UP IONS: THE EXPERIMENT HELLY c90

H. J. Fahr, G. Lay, and H. U. Nass *In* ESA, European Rocket and Balloon Programs and Related Research Jun. 1989 p 229-232 (For primary document see N90-13826 05-42)

Copyright Avail: NTIS HC A15/MF A02

A rocket mission, called HELLY (helium-Lyman alpha line), devoted to the observation of solar He II 304 angstrom photons resonantly scattered at plasmaspheric and interplanetary He II ions is described. Such observations are carried out at the night side of the Earth. In these conditions, a scan out of the sunlit part of the terrestrial plasmasphere into the antisolar core shadow region can be carried out. The 304 angstroms signal strength is sensitively determined by the shape of the velocity distribution function of interplanetary He II pickup ions. ESA

N90-13864# Ruhr Univ., Bochum (Germany, F.R.). Bereich Extraterrestrische Physik.

INTERPLANETARY DUST CLOSE TO THE SUN (F CORONA): ITS OBSERVATION IN THE VISIBLE AND INFRARED BY A ROCKET-BORNE CORONAGRAPH c90

B. Kneissel, I. Mann, and H. vanderMeer *In* ESA, European Rocket and Balloon Programs and Related Research Jun. 1989 p 233-235 (For primary document see N90-13826 05-42)

Copyright Avail: NTIS HC A15/MF A02

The observation of the Frauenhofer corona (F corona) is discussed. It provides the opportunity for studying the annihilation and creation of dust within circumstellar dust clouds. The specific patterns of scattering light and thermal radiation in the infrared, are studied. A spaceborne remote sensing experiment regarding the radiation properties of dust, in the visible for scattered sunlight, and in the infrared for the thermal emission of grains, is effectuated. It allows the analysis of this complex scenario. A rocketborne twin coronagraph is shown to be needed. ESA

N90-13865# Laboratoire d'Astronomie Spatiale, Marseille (France).

DEEP DETECTION OF HOT STAR POPULATIONS AT BALLOON ULTRAVIOLET WAVELENGTHS c90

B. Milliard, M. Laget, J. Donas, D. Burgarella, H. Moulinec, and D. Huguenin (Geneva Observatory, Switzerland) *In* ESA, European Rocket and Balloon Programs and Related Research Jun. 1989 p 237-238 (For primary document see N90-13826 05-42)

Copyright Avail: NTIS HC A15/MF A02

The observations of the imaging program, concerning a total of approximately 50 sq. degrees of the sky, are reported. The observations are performed with a 40 cm balloon borne telescope.

It has a limit of visual magnitude above 20 for blue objects. For an inflight image resolution of 13 arcsec the bulk of the observations concern field galaxies, cluster of galaxies and a few galactic globular clusters. An automated reduction technique allows numeric summation of night sky limited individual exposures to reach an equivalent observing time which may reach one hour. Results concerning the space distribution of horizontal branch stars up to the central part of the globular cluster M13 and the star formation activity of galaxies member of the cluster Abell 1367 are presented. ESA

N90-13866# Max-Planck-Inst. fuer Physik und Astrophysik, Garching (Germany, F.R.). Inst. fuer Extraterrestrische Physik.
PROJECT SUPERNOVA 1987 **c20**
Horst Hippmann *In* ESA, European Rocket and Balloon Programs and Related Research Jun. 1989 p 239-240 (For primary document see N90-13826 05-42)
Copyright Avail: NTIS HC A15/MF A02

The project concerning the supernova investigations in the soft x ray radiation range on a sounding rocket experiment, is discussed. On the basis of a recovered payload, a new one is designed and built. The project results lead to the conclusion that astronomical x ray experiments request conditions, to which sounding rockets are not suited for, in particular for long observation time and low particle background. However, the supernova results are still the best obtained in this energy band. ESA

N90-13867# Max-Planck-Inst. fuer Physik und Astrophysik, Garching (Germany, F.R.). Inst. fuer Extraterrestrische Physik.
THE X RAY MIRROR AND THE PSPC OF THE SUPERNOVA-ROCKET-PROJECT **c20**
U. G. Briel, E. Pfeffermann, H. Braeuninger, W. Burkert, G. Kettenring, and G. Metzner *In* ESA, European Rocket and Balloon Programs and Related Research Jun. 1989 p 241-244 (For primary document see N90-13826 05-42)
Copyright Avail: NTIS HC A15/MF A02

The payload for the German supernova rocket project, the Astro 4/2, is presented. The payload consists of a 32 cm x ray telescope with a focal length of 143 cm and an effective collecting area of 23 sqcm. A position sensitive proportional counter (PSPC) with an aperture of 23 mm, is used. The PSPC is designed for an energy range from 0.2 to 2.0 KeV and has an energy resolution of 45 percent at 1 KeV. Its positional resolution is 300 micrometers at 1 KeV. The half power width of the telescope-detector combination is approximately 1.4 arc min. With its high quantum efficiency and its good background rejection of about 95 percent, the PSPC is especially suited for low surface brightness extended x ray sources. ESA

N90-13868# Bonn Univ. (Germany, F.R.). Inst. fuer Astronomie.
OBSERVATION OF THE SOLAR LYMAN-ALPHA LINE **c92**
H. U. Nass, G. Lay, and H. J. Fahr *In* ESA, European Rocket and Balloon Programs and Related Research Jun. 1989 p 245-249 (For primary document see N90-13826 05-42)
Copyright Avail: NTIS HC A15/MF A02

The first results of the Solar Lyman (Solly) observations, are presented. The Solly payload was launched on October 24, 1988, and reached an apogee of about 350 km. The experiment Solly consists of a hydrogen cell containing molecular hydrogen at low pressure and is sealed by magnesium fluoride windows. A hot filament dissociates the molecules into hydrogen atoms. By measuring the scattered Ly-alpha photons with a sideways mounted detector, the core region of the solar Ly-alpha line can be studied. Another detector is positioned along the optic axis at the rear of the instrument and measures the total intensity of the solar photons near 1216 angstroms. ESA

N90-13869# Bonn Univ. (Germany, F.R.). Inst. of Physics.
DIURNAL VARIATION OF THE SODIUM LAYER AT POLAR LATITUDES IN SUMMER **c46**
H. Kurzawa and U. vonZahn *In* ESA, European Rocket and Balloon Programs and Related Research Jun. 1989 p 253-256 (For primary document see N90-13826 05-42)
(Grant DFG-Ho-858/1)
Copyright Avail: NTIS HC A15/MF A02

The sodium lidar measurements under daylight conditions, performed at Andoya, Norway (69 N, 16 E) during the summers 1986 to 1988, are studied. Na density profiles are derived from these measurements. The observations show a significant diurnal variation in the Na column density as well as in the maximum Na density. Part of this diurnal variation is attributed to the occurrence of sudden sodium layers. ESA

N90-13870# Wuppertal Univ. (Germany, F.R.).
THE DYANA CAMPAIGN 1990 **c46**
D. Offermann *In* ESA, European Rocket and Balloon Programs and Related Research Jun. 1989 p 259-267 (For primary document see N90-13826 05-42)
Copyright Avail: NTIS HC A15/MF A02

The international campaign of coordinated ground based, balloon- and rocket-borne experiments at various places on the globe for case studies of Dynamical Analysis of the Middle Atmosphere (DYANA) up to about 100 km is described. The campaign duration is from January to March 1990. Emphasis is given on planetary waves, gravity waves, and turbulence. Relationship to minor constituents distributions is studied. The campaign relies on meteorological rockets (plus radiosondes) and ground based lidars and radars for measurements of density, temperature and wind. The measurement sites form a network with varying mesh width, adapted to the horizontal scales of the dynamical features studied. ESA

N90-13871# British Aerospace Public Ltd. Co., Bristol (England). Space Systems Div.
THE SKYLARK SOUNDING ROCKET PROGRAM AND FUTURE LAUNCHER DEVELOPMENTS BY BRITISH AEROSPACE (SPACE SYSTEMS) LTD. **c46**
J. A. Ellis *In* ESA, European Rocket and Balloon Programs and Related Research Jun. 1989 p 269-271 (For primary document see N90-13826 05-42)
Copyright Avail: NTIS HC A15/MF A02

The past history of the Skylark sounding rocket, is reported. A background to the rationalization of the variations of rocket now available, is provided. The last two years launch program, with a summary of future scheduled programs, is listed. The future interests of British Aerospace in rocket launchers, in particular LittLEO (the small launcher for payloads into low earth orbit), are described. ESA

N90-13872# Observatoire de Paris-Meudon (France). Forecasting Center.
PREDICTION OF THE 10 cm SOLAR FLUX INDEX **c92**
P. Lantos *In* ESA, European Rocket and Balloon Programs and Related Research Jun. 1989 p 277-278 (For primary document see N90-13826 05-42)
Copyright Avail: NTIS HC A15/MF A02

The 10.7 cm solar flux index is analyzed. The solar radiation in the X and UV range, is forecasted and evaluated. The effects on the terrestrial atmosphere are predicted. The origin of the centimeter emission is reviewed. The operational, short term prediction method (a few days in advance) is evaluated. Long term predictions for the next solar cycle maximum (in 1990) are given. The results lead to the conclusion that the present cycle is one of the strongest solar activity cycles. ESA

N90-13873# Deutsche Forschungsanstalt fuer Luft- und Raumfahrt, Cologne (Germany, F.R.).
THE GERMAN SPACE SCIENCE PROGRAM **c88**
Ferdinand Dahl and Manfred Otterbein (Bundesministerium fuer Forschung und Technologie, Bonn, Germany, F.R.) *In* ESA, European Rocket and Balloon Programs and Related Research Jun. 1989 p 279-283 (For primary document see N90-13826 05-42)
Copyright Avail: NTIS HC A15/MF A02

A survey of the ongoing and planned projects of extraterrestrial

research within the German space program is given. Distinction between astronomy and exploration of the solar system, is made. In the scope of the report, the following topics are considered: the national, bilateral and European programs; the astronomy and astrophysics current programs; the ESA infrared observatory; the German x ray satellite; the exploration of the solar system; the aeronomy research; the use of solar probes; and instrument development. ESA

N90-13874# Centre National d'Etudes Spatiales, Toulouse (France). Div. Ballons.
LONG DURATION BALLOON FLIGHTS IN THE MIDDLE STRATOSPHERE **c46**
Pierre Malaterre *In* ESA, European Rocket and Balloon Programs and Related Research Jun. 1989 p 285-287 (For primary document see N90-13826 05-42)
Copyright Avail: NTIS HC A15/MF A02

The results of a series of long duration flights, carried out in the Southern Hemisphere, at levels of 25 to 32 kms are reported. The scientific experiments concerning stratospheric water vapor measurements are performed with an experiment from the Laboratoire de Meteorologie Dynamique, Paris. An experiment of geophysics with the measurement of magnetic crustal anomalies over the Atlantic and Pacific oceans are prepared by the Institut de Physique du Globe, Paris. ESA

N90-13875# Max-Planck-Inst. fuer Physik und Astrophysik, Garching (Germany, F.R.). Inst. fuer Extraterrestrische Physik.
SN 1987: A TELEMETRY DECODING SYSTEM **c17**
Siegfried Mueller *In* ESA, European Rocket and Balloon Programs and Related Research Jun. 1989 p 289-291 (For primary document see N90-13826 05-42)
Copyright Avail: NTIS HC A15/MF A02

The Supernova telemetry data decoding and display system is described. It is realized by means of personal computers with a special interface card. The software supports: data recording on hard disk, individual color screen layouts for the different payload units, serveral data display types, limit checks and screen hard copies. A playback version is available to review, after flight, data stored on hard disk at variable speed or in single steps. ESA

N90-13876# Swedish Space Corp., Esrange.
ESRANGE **c14**
J. Englund, A. Helger, A. Wikstroem, and L. Marcus *In* ESA, European Rocket and Balloon Programs and Related Research Jun. 1989 p 293-298 (For primary document see N90-13826 05-42)
Copyright Avail: NTIS HC A15/MF A02

The international space operations center for sounding rockets, named Esrange (Sweden), is presented. The range of services offered to users is stressed. Experiments carried out include microgravity, geophysics, space physics, astronomy and the chemistry of the upper atmosphere. Data from the extensive network of ground based scientific instruments in northern Scandinavia can be displayed at Esrange. The high performance vehicles and the balloon payloads, which can be launched at Esrange are listed. The land recovery operations, concerning rockets and balloons, are shown to be reliable at Esrange. ESA

N90-13877# Swedish Inst. of Space Physics, Kiruna.
ALIS: AN AURORAL LARGE IMAGING SYSTEM IN NORTHERN SCANDINAVIA **c46**
A. Steen *In* ESA, European Rocket and Balloon Programs and Related Research Jun. 1989 p 299-303 (For primary document see N90-13826 05-42)
Copyright Avail: NTIS HC A15/MF A02

A complementary (to satellite imaging) ground based imaging system, Auroral Large Imaging System (ALIS) is presented. The proposed system consists of a two dimensional array of 28 monochromatic imagers and a Control Center (CC). Each station images with a medium field of view (90 degrees) and transfers the image data in real time to CC. A grand image is constructed with 300 km coverage in latitude and 600 km in longitude, and 2000 and 4000 pixels resolution respectively. The parameters derived from the grand image are available at CC for telescience applications. ESA

43 EARTH RESOURCES AND REMOTE SENSING

Includes remote sensing of earth resources by aircraft and spacecraft; photogrammetry; and aerial photography.

For instrumentation see *35 Instrumentation and Photography.*

N90-13878*# Utah Univ., Salt Lake City. Dept. of Geography.
LATE QUATERNARY GEOMORPHOLOGY OF THE GREAT SALT LAKE REGION, UTAH, AND OTHER HYDROGRAPHICALLY CLOSED BASINS IN THE WESTERN UNITED STATES: A SUMMARY OF OBSERVATIONS Final Report
Donald R. Currey 25 Jul. 1989 78 p
(Contract NAS5-28753)
(NASA-CR-185912; NAS 1.26:185912; LLTR-89-3) Avail: NTIS HC A05/MF A01 CSCL 08B

Attributes of Quaternary lakes and lake basins which are often important in the environmental prehistory of semideserts are discussed. Basin-floor and basin-closure morphometry have set limits on paleolake sizes; lake morphometry and basin drainage patterns have influenced lacustrine processes; and water and sediment loads have influenced basin neotectonics. Information regarding inundated, runoff-producing, and extra-basin spatial domains is acquired directly from the paleolake record, including the littoral morphostratigraphic record, and indirectly by reconstruction. Increasingly detailed hypotheses regarding Lake Bonneville, the largest late Pleistocene paleolake in the Great Basin, are subjects for further testing and refinement. Oscillating transgression of Lake Bonneville began about 28,000 yr B.P.; the highest stage occurred about 15,000 yr B.P., and termination occurred abruptly about 13,000 yr B.P. A final resurgence of perennial lakes probably occurred in many subbasins of the Great Basin between 11,000 and 10,000 yr B.P., when the highest stage of Great Salt Lake (successor to Lake Bonneville) developed the Gilbert shoreline. The highest post-Gilbert stage of Great Salt Lake, which has been one of the few permanent lakes in the Great Basin during Holocene time, probably occurred between 3,000 and 2,000 yr B.P. Author

N90-13879*# Massachusetts Inst. of Tech., Cambridge. Dept. of Civil Engineering.
PHYSICALLY-BASED PARAMETERIZATION OF SPATIALLY VARIABLE SOIL AND VEGETATION USING SATELLITE MULTISPECTRAL DATA
Michael F. Jasinski and Peter S. Eagleson Sep. 1989 261 p
(Grants NAG5-510; NAGw-1696)
(NASA-CR-185957; NAS 1.26:185957; R89-22; MIT-324) Avail: NTIS HC A12/MF A02 CSCL 08B

A stochastic-geometric landsurface reflectance model is formulated and tested for the parameterization of spatially variable vegetation and soil at subpixel scales using satellite multispectral images without ground truth. Landscapes are conceptualized as 3-D Lambertian reflecting surfaces consisting of plant canopies, represented by solid geometric figures, superposed on a flat soil background. A computer simulation program is developed to investigate image characteristics at various spatial aggregations representative of satellite observational scales, or pixels. The evolution of the shape and structure of the red-infrared space, or scattergram, of typical semivegetated scenes is investigated by sequentially introducing model variables into the simulation. The analytical moments of the total pixel reflectance, including the mean, variance, spatial covariance, and cross-spectral covariance, are derived in terms of the moments of the individual fractional cover and reflectance components. The moments are applied to the solution of the inverse problem: The estimation of subpixel landscape properties on a pixel-by-pixel basis, given only one

multispectral image and limited assumptions on the structure of the landscape. The landsurface reflectance model and inversion technique are tested using actual aerial radiometric data collected over regularly spaced pecan trees, and using both aerial and LANDSAT Thematic Mapper data obtained over discontinuous, randomly spaced conifer canopies in a natural forested watershed. Different amounts of solar backscattered diffuse radiation are assumed and the sensitivity of the estimated landsurface parameters to those amounts is examined. Author

N90-13880*# Environmental Research Inst. of Michigan, Ann Arbor.

SUMMARIES OF THE THEMATIC CONFERENCES ON REMOTE SENSING FOR EXPLORATION GEOLOGY

Oct. 1989 290 p Sponsored in part by ARCO Oil and Gas Co.; Chevron Overseas Petroleum, Inc.; Earth Observation Satellite Co.; Environmental Research Inst. of Michigan; Exxon Production Research Co., INTERA Technologies, Ltd.; NASA; and PCI, Inc.
(NASA-CR-185321; NAS 1.26:185321) Avail: NTIS HC A13/MF A02 CSCL 05B

The Thematic Conference series was initiated to address the need for concentrated discussion of particular remote sensing applications. The program is primarily concerned with the application of remote sensing to mineral and hydrocarbon exploration, with special emphasis on data integration, methodologies, and practical solutions for geologists. Some fifty invited papers are scheduled for eleven plenary sessions, formulated to address such important topics as basement tectonics and their surface expressions, spectral geology, applications for hydrocarbon exploration, and radar applications and future systems. Other invited presentations will discuss geobotanical remote sensing, mineral exploration, engineering and environmental applications, advanced image processing, and integration and mapping. Author

N90-13881# Deutsche Forschungsanstalt fuer Luft- und Raumfahrt, Oberpfaffenhofen (Germany, F.R.). Abteilung Optische Fernerkundung.

THE USE OF LANDSAT-TM DATA FOR THE MANAGEMENT OF PINE FORESTATIONS IN CENTRAL CHILE

Wilfried Endlicher (Marburg Univ., Germany, F.R.) and Werner Kirchhof Oct. 1988 61 p In GERMAN; ENGLISH summary Original contains color illustrations
(DLR-FB-89-44; ISSN-0171-1342; ETN-90-96053) Avail: NTIS HC A04/MF A01; DLR, VB-PL-DO, Postfach 90 60 58, 5000 Cologne, Fed. Republic of Germany, 36 DM

Data from a LANDSAT thematic mapper (TM) quarter scene from 21 Dec. 1986 over central Chile is investigated for possible use in detailed forest inventories. Visual and automatic classification methods are applied. Pine plantations are mapped by visual as well as by automatic classification methods. A distinction between tree species and young, middle aged and mature stands of pine is possible. Thirteen land-use classes are distinguished by maximum likelihood classification. Problems occurred with very young plantations and new clearcuts which did not always form homogeneous spectral classes. ESA

N90-13882# Deutsche Forschungsanstalt fuer Luft- und Raumfahrt, Oberpfaffenhofen (Germany, F.R.). Abteilung Meteorologische Fernerkundung.

REFLECTION INDICATRICES OF NATURAL SURFACES FOR AVHRR CHANNELS 1 AND 2

Reinhold Busen May 1989 119 p In GERMAN; ENGLISH summary
(DLR-Mitt-89-16; ISSN-0176-7739; ETN-90-96054) Avail: NTIS HC A06/MF A01; DLR, VP-PL-DO, Postfach 90 60 58, 5000 Cologne, Fed. Republic of Germany, 39 DM

Reflection indicatrices for different types of natural or vegetated surfaces are presented. These indicatrices describe relative angular distributions of the reflected radiation. They are dependent on the solar and the observer zenith angle and on the relative azimuth of the direction of observation. The data presented here are valid in the channels 1 and 2 of the AVHRR (advanced very high resolution radiometer), i.e., between 0.58 and 0.68 microns and between 0.725 and 1.1 microns respectively. The results are placed as data sets at general disposal. The data handling is described. ESA

N90-13883*# Research Triangle Inst., Research Triangle Park, NC.

SENEGALESE LAND SURFACE CHANGE ANALYSIS AND BIOPHYSICAL PARAMETER ESTIMATION USING NOAA AVHRR SPECTRAL DATA Final Report

Fred M. Vukovich, David L. Toll, and Ruth L. Kennard (ST Systems Corp., Lanham, MD.) Dec. 1989 54 p
(Grant NAG5-1068)
(NASA-CR-186120; NAS 1.26:186120) Avail: NTIS HC A04/MF A01 CSCL 08B

Surface biophysical estimates were derived from analysis of NOAA Advanced Very High Spectral Resolution (AVHRR) spectral data of the Senegalese area of west Africa. The parameters derived were of solar albedo, spectral visible and near-infrared band reflectance, spectral vegetative index, and ground temperature. Wet and dry linked AVHRR scenes from 1981 through 1985 in Senegal were analyzed for a semi-wet southerly site near Tambacounda and a predominantly dry northerly site near Podor. Related problems were studied to convert satellite derived radiance to biophysical estimates of the land surface. Problems studied were associated with sensor miscalibration, atmospheric and aerosol spatial variability, surface anisotropy of reflected radiation, narrow satellite band reflectance to broad solar band conversion, and ground emissivity correction. The middle-infrared reflectance was approximated with a visible AVHRR reflectance for improving solar albedo estimates. In addition, the spectral composition of solar irradiance (direct and diffuse radiation) between major spectral regions (i.e., ultraviolet, visible, near-infrared, and middle-infrared) was found to be insensitive to changes in the clear sky atmospheric optical depth in the narrow band to solar band conversion procedure. Solar albedo derived estimates for both sites were not found to change markedly with significant antecedent precipitation events or correspondingly from increases in green leaf vegetation density. The bright soil/substrate contributed to a high albedo for the dry related scenes, whereas the high internal leaf reflectance in green vegetation canopies in the near-infrared contributed to high solar albedo for the wet related scenes. The relationship between solar albedo and ground temperature was poor, indicating the solar albedo has little control of the ground temperature. The normalized difference vegetation index (NDVI) and the derived visible reflectance were more sensitive to antecedent rainfall amounts and green vegetation changes than were near-infrared changes. The information in the NDVI related to green leaf density changes primarily was from the visible reflectance. The contribution of the near-infrared reflectance to explaining green vegetation is largely reduced when there is a bright substrate. Author

N90-13884# Grenoble-1 Univ. (France). Lab. des Techniques de l'Informatique, des Mathematiques, de la Microelectronique et de la Microscop

THE USE OF A DEFORMATION MODEL FOR SAMPLING DIGITALIZED STEREOSCOPIC IMAGES [UTILISATION D'UN MODELE DE DEFORMATION POUR LE REECHANTILLONNAGE D'IMAGES NUMERIQUES STEREOSCOPIQUES]

M. Memier Nov. 1988 18 p In FRENCH
(IMAG-RR-753-I; ETN-90-95691) Avail: NTIS HC A03/MF A01

The use of teledetection in determining surface geometry for cartographic purposes is described. A universally applicable image sampling method is presented. Such a method is the preliminary step in three-dimensional image reconstruction. The goal of the research is to apply the method to images from the SPOT satellite. The physical characteristics of its probe and its particular type of orbit allow it to collect data particularly well adapted for geometric analysis. ESA

N90-13885# Technische Univ., Delft (Netherlands). Satellite Geodesy Section.
PRECISION OF SEMI-GEOMETRICALLY DETERMINED SLR BASELINES VS. SITE OCCUPATION TIME Thesis
H. E. deZwijger Jul. 1988 63 p
(ETN-90-96007) Avail: NTIS HC A04/MF A01

The precision and stability of the baselines of the Satellite Laser Ranging (SLR) are investigated. The aim is to indicate that the inaccuracy in SLR data does not necessarily imply a change in the length of the site occupation time, at least for short arc analysis methods. This is done by working out the requirements of a dedicated experiment. The mathematical model is elucidated, and parameters with their influence on the satellite orbit are discussed. A formula indicating the influence of some parameters is derived. The final analysis includes: the use of one, two or three months of data, and the adjustment of inter-station baselines in one run; 10, 15, 20 or more basic analysis units (spirals). A short arc analysis is performed by using for each baseline, 5, 10 or 15 spirals. The results of the analysis and recommendations for the dedicated experiment, including site occupation time are presented. ESA

44 ENERGY PRODUCTION AND CONVERSION

Includes specific energy conversion systems, e.g., fuel cells; global sources of energy; geophysical conversion; and windpower.

For related information see also *07 Aircraft Propulsion and Power, 20 Spacecraft Propulsion and Power,* and *28 Propellants and Fuels.*

N90-13886*# Arizona State Univ., Tempe.
THE PHOTOVOLTAIC PROPERTIES OF AN Al In As/InP HETEROJUNCTIONS GROWN BY LPE METHOD Final Technical Report
Edward Y. Wang 27 Oct. 1989 18 p
(Grant NAG3-383)
(NASA-CR-185996; NAS 1.26:185996) Avail: NTIS HC A03/MF A01 CSCL 10A

Work is presented on heterojunction solar cells which were studied under the NASA/Arizona State University intern program. The heterojunction solar cells were fabricated by the liquid phase epitaxy method. The basic conversion efficiency was measured at 5 percent. It was determined that a thicker epilayer is needed, and that the density of recombination center should be reduced to give a smaller saturation current and hence a larger open-circuit voltage. J.P.S.

N90-13887# AiResearch Mfg. Co., Los Angeles, CA.
ADVANCED ENERGY SYSTEM PROGRAM Annual Report, Mar. 1987 - Oct. 1988
K. Trester Feb. 1989 109 p Sponsored in part by Southern California Gas Co., Los Angeles; Brooklyn Union Gas Co., NY; and Pacific Gas and Electric Co., San Francisco, CA
(Contract GRI-5084-243-1028)
(PB89-235170; DOC-89-62095; GRI-89/0080) Avail: NTIS HC A06/MF A01 CSCL 10A

The objectives of the program are to design, develop and demonstrate a natural-gas-fueled, highly recuperated, 50 kW Brayton-cycle cogeneration system for commercial, institutional, and multifamily residential applications. Marketing studies have shown that this Advanced Energy System (AES), with its many unique and cost-effective features, has the potential to offer significant reductions in annual electrical and thermal energy costs to the consumer. Specific advantages of the system that result in low cost of ownership are high electrical efficiency (30 percent, HHV), low maintenance, high reliability and long life (20 years). GRA

N90-13888# Institut National des Sciences Appliquees de Lyon, Villeurbanne (France). Lab. de Physique de la Matiere.
EVOLUTION OF THE EPR PROCEDURE FOR POLYCRYSTALLINE Si RIBBON DRAWING FOR PHOTOVOLTAIC CELL MANUFACTURING Ph.D. Thesis [EVOLUTION DE LA METHODE DE TIRAGE EPR DE RUBANS DE Si POLYCRISTALLIN DESTINES A LA PRODUCTION DE PHOTOPHILES]
Ridha MGhaieth 1989 152 p In FRENCH Original contains color illustrations
(ISAL-89-0027; ETN-90-95708) Avail: NTIS HC A08/MF A01

A detailed analysis of the EPR (electron powder ribbon) manufacturing method is presented including the zone fusion method, the magnetic deflection of the electron beam and the minimization of residual stress. The mechanical and electrical characterization of the ribbon is described. The cells manufactured from the ribbons have a yield rate of 6.5 percent. Hydrogen passivation does not significantly improve the photoelectric efficiency. The characterization shows a potential for yield improvement. ESA

45 ENVIRONMENT POLLUTION

Includes atmospheric, noise, thermal, and water pollution.

N90-13889# Virginia Polytechnic Inst. and State Univ., Blacksburg. Center for Environmental/Hazardous Materials Studies.
ADAPTATION AND RESISTANCE OF ECOSYSTEMS TO STRESS Annual Technical Report No. 1, 1 Aug. 1988 - 1 Aug. 1989
John Cairns, Jr. and B. R. Niederlehner 30 Aug. 1989 42 p
(Grant AF-AFOSR-0263-88; AF Proj. 2312)
(AD-A212999; AFOSR-89-1244TR) Avail: NTIS HC A03/MF A01 CSCL 08/1

Naturally derived, microbial microcosms are employed to evaluate the ability of aquatic communities to adapt to stress. A series of laboratory toxicity tests were conducted examining structural and functional responses of microbial communities to a sequence of stresses. Tentative conclusions from early research suggest that there is no detectable acclimation at the community level after low level cadmium exposure. More severe stress appears to be necessary to produce detectable increases in tolerance to subsequent stress. Acclimation was observed for net daily metabolism of communities developed in zinc and subsequently exposed to zinc, for gross primary production and respiration in communities colonized in zinc and then exposed to cadmium, and for species richness of communities colonized in zinc and then explosed to acidic pH. GRA

N90-13890# Systems Applications, Inc., San Rafael, CA.
AIR QUALITY SIMULATION MODEL PERFORMANCE FOR ONE-HOUR AVERAGES
G. E. Moore, T. E. Stoeckenius, Steve Hanna, and D. Strimitas Aug. 1989 150 p Prepared in cooperation with Sigma Research, Inc., Lexington, MA
(Contract EPA-68-02-4352)
(PB89-233506; EPA/600/3-89/071) Avail: NTIS HC A07/MF A01 CSCL 13B

If a one-hour standard for sulfur dioxide were promulgated, air quality dispersion modeling in the vicinity of major point sources would be an important air quality management tool. It is questioned whether currently available dispersion models would be suitable for use in demonstrating attainment of such a standard in the vicinity of large, elevated, buoyant point sources such as utility power plants. The results summarized in the report suggest that using these models in connection with an hourly average standard does not present the regulatory community with any significant additional uncertainties that are not already being dealt with in connection with the current 3- and 24-hour standards. This review of the results of model evaluation studies was restricted to some fairly simple analyses. Additional analyses are recommended.

Recommendations to improve model formulations are made regarding the treatment of plume behavior in the vicinity of the mixing height and the simulation of plume dispersion within the mixed layer during convective conditions. GRA

N90-13891# Environmental Protection Agency, Research Triangle Park, NC. Atmospheric Research and Exposure Assessment Lab.
PROCEEDINGS: US/FRG (FEDERAL REPUBLIC OF GERMANY) WORKSHOP ON PHOTOCHEMICAL OZONE PROBLEM AND ITS CONTROL: US EXPERIENCES AND THE SITUATION IN EUROPE
Basil Dimitriades, ed., K. Becker, K. Demerjian, H. Jeffries, and U. Schurath Mar. 1989 79 p Workshop held in Cologne, Fed. Republic of Germany, 4-6 May 1988 Prepared in cooperation with Umweltbundesamt, Berlin, Fed. Republic of Germany
(PB89-233514; EPA/600/9-89/058) Avail: NTIS HC A05/MF A01 CSCL 13B

Concern for the photochemical ozone problems in the U.S. and Europe led the U.S. and FRG Governments to organize and conduct the subject workdshop in May 1988, in Cologne, FRG, to review the magnitude of the problem, underlying science, and outstanding technical issues. Discussions focused on the pervasiveness, cause/effect, and control aspects of the problem. Issues and information gaps were identified in the atmospheric chemistry and transport and ozone modeling areas, and recommendations for future research activities were formulated including one for a 2nd workshop to be conducted in the U.S. GRA

N90-13892 Institut d'Aeronomie Spatiale de Belgique, Brussels.
OBSERVATIONS OF STRATOSPHERIC HCl: 1975-1985
M. DeMaziere, C. Lippens, and C. Muller 1989 15 p Presented at the 28th Liege International Astrophysical Colloquium on Our Changing Atmosphere, Liege, Belgium, 26-30 Jun. 1989
(Aeronomica-Acta-A-349-1989; ISSN-0065-3713; ETN-90-96033) Avail: Institut d'Aeronomie Spatiale de Belgique, 3 Avenue Circulaire, B-1180 Brussels, Belgium

Observations of HCl in the stratosphere are reported. Infrared absorption spectroscopy data from balloonborne, airborne, and spaceborne spectrometers are presented. The first spectra are reinterpreted using more sophisticated spectroscopic parameters in order to check for a secular trend of stratospheric HCl and compare it with the known variations of the main chlorine source gas concentrations. No significant variation can be deduced from the data and an upper limit of three percent of annual increase in HCl abundance is proposed. ESA

46 GEOPHYSICS

Includes aeronomy; upper and lower atmosphere studies; ionospheric and magnetospheric physics; and geomagnetism.

For space radiation see *93 Space Radiation.*

N90-13893*# Jet Propulsion Lab., California Inst. of Tech., Pasadena.
A HIGH-RESOLUTION ATLAS OF THE INFRARED SPECTRUM OF THE SUN AND THE EARTH ATMOSPHERE FROM SPACE: A COMPILATION OF ATMOS SPECTRA OF THE REGION FROM 650 TO 4800 cm (2.3 TO 16 MICRON). VOLUME 1: THE SUN
Crofton B. Farmer and Robert H. Norton 1989 535 p
(Contract NAS7-918)
(NASA-RP-1224-Vol-1; NAS 1.61:1224-Vol-1; JPL-400-370-Vol-1) Avail: NTIS HC A23/MF A03 CSCL 04A

During the period April 29 through May 2, 1985, the Atmospheric Trace Molecular Spectroscopy experiment was operated as part of the Spacelab-3 payload of the shuttle Challenger. The instrument, a modified Michelson Interferometer covering the frequency range from 600 to 5000/cm, at a spectral resolution of 0.01/cm, recorded infrared spectra of the Sun and of the Earth's atmosphere at times close to entry into and exit from occultation by the Earth's limb as seen from the shuttle orbit of 360 km. Spectra were obtained that are free from absorptions due to constituents of the atmosphere (i.e., solar pure spectra), as well as spectra of the atmosphere itself, covering line-of-sight tangent altitudes that span the range from the lower thermosphere to the bottom of the troposphere. This atlas, believed to be the first record of observations of the continuous high resolution infrared spectrum of the Sun and the Earth's atmosphere from space, provides a compilation of these spectra arranged in a hardcopy format suitable for quick-look reference purposes; the data are also available in digital form. Author

N90-13894*# Massachusetts Inst. of Tech., Cambridge.
STRAIN ACCUMULATION AND SURFACE DEFORMATION ALONG THE SAN ANDREAS, CALIFORNIA Semiannual Technical Report, 1 Jan. - 30 Jun. 1989
Victor C. Li 1 Oct. 1989 13 p
(Grant NAG5-740)
(NASA-CR-185893; NAS 1.26:185893) Avail: NTIS HC A03/MF A01 CSCL 08G

The goal of this project remains to be the achievement of a better understanding of the regional and local deformation and crustal straining processes in western North America, particularly the effect of the San Andreas and nearby faults on the spatial and temporal crustal deformation behavior. Construction of theoretical models based on the mechanics of coupled elastic plate/viscoelastic foundation and large scale crack mechanics provide a rational basis for the interpretation of seismic and aseismic anomalies and expedite efforts in forecasting the stability of plate boundary deformations. In the present period, special focus is placed on the 3-D effect of irregular fault locked patches on the ground measured deformation fields. Specifically, use is made of a newly developed 3-D boundary element program to analyze the fault slip and vertical ground motion in the Parkfield area on the San Andreas. Author

N90-13895# Alaska Univ., Fairbanks.
CRUSTAL STRUCTURE STUDIES UTILIZING EARTHQUAKE SEQUENCES Final Report, 1 Sep. 1985 - 31 Aug. 1988
Larry D. Gedney, David B. Stone, and John N. Davies Aug. 1989 106 p
(Grant AF-AFOSR-0266-85; AF Proj. 2309)
(AD-A212916; AFOSR-89-1231TR) Avail: NTIS HC A06/MF A01 CSCL 08/11

The original goal was to use the Dall City earthquake sequence of February and March 1985 to investigate the crustal structure of north-central Alaska. The scope was later modified to include studies of some earthquakes just north of the Alaska Range, the Gold King earthquakes, and later still to include data gathered from chemical explosions detonated by USGS as part of their Trans-Alaska Crustal Transect (TACT) program. The work divided roughly into Dall City events, Gold King events, Yukon Flats Experiment, permanent network/explosion data, and Barter Island - Fairbanks refraction. The models used in this study were applied to most of Alaska, and thus large differences were expected. In general the models for the areas north of Fairbanks are reasonably similar which is consistent with the fact that relocations of events using these different models don't produce any clear preference; and south is expectedly much more complex, given young accreted terranes with an underthrusting Pacific plate. GRA

N90-13896# Boston Univ., MA. Dept. of Astronomy.
AURORAL AND SUB-AURORAL INTERACTION AT THE F REGION IONOSPHERE Final Report, 1 Jun. 1987 - 30 Jun. 1989
Jules Aarons and Michael Mendillo 31 Aug. 1989 18 p
(Contract N00014-87-K-0158)
(AD-A213284) Avail: NTIS HC A03/MF A01 CSCL 04/1

Deterioration of satellite signals and fading on HF are results of the appearance of intense irregularities of the order of meters to several hundred meters in the F layer. At auroral and sub-auroral latitudes the irregularities become intense and create serious

problems. The interaction of the ionosphere during magnetic storms has been studied at auroral and subauroral latitudes. Results include a model which shows the expansion during the injection phase of the magnetic storm and the effect of storm effects of the stored up energy in the ring current during the recovery phase. In comparing observations with incoherent scatter data from Millstone Hill the total convection velocity appears to be the dominating parameter in the injection phase creation of irregularities. The work will move to studying the global effects of individual storms since the storms can inhibit irregularities at the equator while creating them at auroral and sub-auroral latitudes. GRA

N90-13897# Physical Sciences, Inc., Andover, MA.
CANOES 2: DYNAMICS OF ATMOSPHERIC INFRARED THERMOCHEMICAL EXCITATION, VOLUME 1 Final Report, 24 Mar. 1985 - 24 May 1989
Wilson T. Rawlins, Lawrence G. Piper, Mark E. Fraser, Henry C. Murphy, Thomas R. Tucker, and A. Gelb Mar. 1989 101 p
(Contract F19628-85-C-0032; AF Proj. 2310)
(AD-A213341; PSI-9032/TR-901-Vol-1; GL-TR-89-0124-Vol-1)
Avail: NTIS HC A06/MF A01 CSCL 04/1

In the electron disturbed upper atmosphere, electronically excited metastable forms of oxygen and nitrogen are formed by electron impact processes. These species dissipate their energy into the atmosphere largely by collisional quenching and chemical reaction. Specific species and reactions of interest include: (1) electronically and/or vibrationally excited nitrogen, its spectroscopy, energy pooling and interactions with O, O2, and trace, infrared-active atmospheric species such as CO, CO2, and N2O; (2) metastable atomic nitrogen, N(2D, 2P), reaction kinetics and product branching ratios in interactions with the above atmospheric species; (3) various metastable states of O2, excited O2, and their potential as auroral precursors of infrared radiation from other atmospheric species; and (4) the role of metastable-metastable O2/N2 interactions as potential sources for non-linear infrared effects which might occur in strong aurorae. GRA

N90-13898# Physical Sciences, Inc., Andover, MA.
CANOES 2: DYNAMICS OF ATMOSPHERIC INFRARED THERMOCHEMICAL EXCITATION, VOLUME 2 Final Report, 24 Mar. 1985 - 24 May 1989
Wilson T. Rawlins, Lawrence G. Piper, Mark E. Fraser, Henry C. Murphy, Thomas R. Tucker, and A. Gelb Mar. 1989 263 p
(Contract F19628-85-C-0032; AF Proj. 2310)
(AD-A213342; PSI-9032/TR-901-Vol-2; GL-TR-89-0124-Vol-2)
Avail: NTIS HC A12/MF A02 CSCL 04/1

In the electron disturbed upper atmosphere, electronically excited metastable forms of oxygen and nitrogen are formed by electron impact processes. These species dissipate their energy into the atmosphere largely by collisional quenching and chemical reaction. Specific species and reactions of interest include: (1) electronically and/or vibrationally excited nitrogen, its spectroscopy, energy pooling and interactions with O, O2 and trace, infrared-active atmospheric species such as CO, CO2, and N2O; (2) metastable atomic nitrogen, N(2D, 2P), reaction kinetics and product branching ratios in interactions with the above atmospheric species; (3) various metastable states of O2, excited oxygen, and their potential as auroral precursors of infrared radiation from other atmospheric species; and (4) the role of metastable-metastable O2/N2 interactions as potential sources for non-linear infrared effects which might occur in strong aurorae. Results are reported from a four-year coupled experimental program using the COCHISE and FAKIR facilities to investigate these issues in fundamental detail. GRA

N90-13899# Physical Sciences, Inc., Andover, MA.
CANOES 2: DYNAMICS OF ATMOSPHERIC INFRARED THERMOCHEMICAL EXCITATION, VOLUME 3 Final Report, 24 Mar. 1985 - 24 May 1989
Wilson T. Rawlins, Lawrence G. Piper, Mark E. Fraser, Henry C. Murphy, Thomas R. Tucker, and A. Gelb Mar. 1989 241 p
(Contract F19628-85-C-0032; AF Proj. 2310)
(AD-A213343; PSI-9032/TR-901-Vol-3; GL-TR-89-0124-Vol-3)
Avail: NTIS HC A11/MF A02 CSCL 04/1

In the electron disturbed upper atmosphere, electronically excited metastable forms of oxygen and nitrogen are formed by electron impact processes. These species dissipate their energy into the atmosphere largely by collisional quenching and chemical reaction. Specific species and reactions of interest include: (1) electronically and/or vibrationally excited nitrogen, its spectroscopy, energy pooling and interactions with atomic oxygen, O2 and trace, infrared-active atmospheric species such as carbon monoxide, carbon dioxide, and nitric oxide; (2) metastable atomic nitrogen, (2D, 2P), reaction kinetics and product branching ratios in interactions with the above atmospheric species; (3) various metastable states of O2, excited O2, and their potential as auroral precursors of infrared radiation from other atmospheric species; and (4) the role of metastable-metastable O2/N2 interactions as potential sources for non-linear infrared effects which might occur in strong aurorae. Results are reported for a four-year coupled experimental program using the COCHISE and FAKIR facilities to investigate these issues in fundamental detail. GRA

N90-13900# Physical Sciences, Inc., Andover, MA.
CANOES 2: DYNAMICS OF ATMOSPHERIC INFRARED THERMOCHEMICAL EXCITATION, VOLUME 4 Final Report, 24 Mar. 1985 - 24 May 1989
Wilson T. Rawlins, Lawrence G. Piper, Mark E. Fraser, Henry C. Murphy, Thomas R. Tucker, and A. Gelb Mar. 1989 224 p
(Contract F19628-85-C-0032; AF Proj. 2310)
(AD-A213344; PSI-9032/TR-901-Vol-4; GL-TR-89-0124-Vol-4)
Avail: NTIS HC A10/MF A02 CSCL 04/1

In the electron disturbed upper atmosphere, electronically excited metastable forms of oxygen and nitrogen are formed by electron impact processes. These species dissipate their energy into the atmosphere largely by collisional quenching and chemical reaction. Specific species and reactions of interest include: (1) electronically and/or vibrationally excited nitrogen, its spectroscopy, energy pooling and interactions with atomic oxygen, O2 and trace, infrared-active atmospheric species such as carbon monoxide, and carbon dioxide; (2) metastable atomic nitrogen, N(2D, 2P), reaction kinetics and product branching ratios in interactions with the above atmospheric species; (3) various metastable states of O2, excited O2, and their potential as auroral precursors of infrared radiation from other atmospheric species; and (4) the role of metastable-metastable O2/N2 interactions as potential sources for non-linear infrared effects which might occur in strong aurorae. Results are reported for a four-year coupled experimental program using COCHISE and FAKIR facilities to investigate these issues in fundamental detail. GRA

N90-13901# Technische Univ., Delft (Netherlands). Faculty of Geodesy.
GRADIO: AN ERROR ANALYSIS OF THE SPACEBORNE GRAVITY GRADIOMETER Thesis
M. Hofman May 1988 67 p
(ETN-90-96010) Avail: NTIS HC A04/MF A01

The spaceborne gravity gradiometer project is described. The purpose of the instrument is the determination of the Earth's gravity field by means of measuring gravity gradients through differential accelerometry. The accuracy of the measurements are expected to be 0.01 to 0.001 E.U.Hz(exp -1/2). The influence of the fuel mass variations during flight is studied. An analysis of the errors that can occur in the configuration of the gradiometer and of the onboard calibrating system is performed. The principle of the calibration is the generation of known accelerations which can be separated from the accelerations due to the gravity field, atmospheric drag, and rotation of the spacecraft. It is shown that the errors coming from either the rotation of one accelerometer or a nonorthogonality of the axes of an accelerometer do not cause relatively large errors and can be removed by the calibration with sufficient accuracy. Moreover, the perpendicularity of the gradiometer axes is shown to depend on the precision of an optical cube in the center of the instrument. ESA

N90-13902 Reading Univ. (England).
THE LINEAR STUDY OF ZONALLY ASYMMETRIC BAROTROPIC FLOWS Ph.D. Thesis
Zuojun Zhang 1988 191 p
Avail: Univ. Microfilms Order No. BRDX85669

The loss of orthogonality between unstable normal modes is general for any kind of eigen analysis. In particular, for an observed climatological mean flow, this is found to be very significant for the development of perturbations. A small perturbation can have a very large projection onto the most unstable normal mode. The adjoint eigenmode is most efficient at exciting the normal mode. The gain on projection is described by the projectibility. In general, growth rate and frequency information should be augmented with the projectibility and eigenvectors should be augmented by the corresponding adjoint eigenvectors. For the 300 mb January climatological mean flow, the maximum projectibility is found to be 7.8 and the adjoint mode corresponding to the most unstable normal mode has large amplitude over the subtropical Indian Ocean and southeast Asia. The adjoint mode when used as an initial perturbation yields an energy increase of a factor of 50 within 10 days even when a damping is added to make the system stable. Both the initial value problems and forcing problems show that the linear barotropic vorticity equation gives important ideas on atmospheric low-frequency variability and the role of the tropics. The sensitivity of linear analysis to details of flow is studied. The sensitivity to basic states maintained by a divergent wind forcing and an equivalent orographic forcing are studied. Dissert. Abstr.

N90-13903# Bureau of Reclamation, Denver, CO. Research and Lab. Services Div.
APPLIED ATMOSPHERIC RESOURCES RESEARCH PROGRAM IN THAILAND
J. G. Medina, R. M. Rasmussen, A. S. Dennis, and B. A. Silverman Aug. 1989 137 p
(Contract AID/ANE-0337-P-IZ-8021-00)
(PB89-235402; R-89-10) Avail: NTIS HC A07/MF A01 CSCL 04A

The Royal Thai Government requested assistance of the United States Agency for International Development for the development and implementation of a more comprehensive scientific approach to the design, operation, and evaluation of Thailand's weather modification program. Upon visiting Thailand, a team of American scientists recommended a 5-year developmental program to improve Thai technical capabilities through training, additional equipment, and a demonstration cloud seed project. The program will test for an increase in rainfall from: (1) warm clouds seeded with hygroscopic agents; and (2) cold clouds seeded for dynamic effects with glaciogenic materials. The field program will be conducted in the Nam Mae Tun River Watershed of western Thailand. The primary response variable is rainfall measured by rain-gauge-adjusted radar. Given equal numbers of warm and cold cloud units and typical operations problems and weather variability, at least four seasons of field experimentation are required. GRA

N90-13904# Stuttgart Univ. (Germany, F.R.). Inst. of Geodesy.
SUPPLEMENTING GEODETIC DATA WITH PRIOR INFORMATION FOR CRUSTAL DEFORMATION IN THE IMPERIAL VALLEY, CALIFORNIA
Richard A. Snay and Alice R. Drew (National Geodetic Survey, Rockville, MD.) 1988 34 p Submitted for publication
(TR-6-1988; ISSN-0933-2839; ETN-90-95864) Avail: NTIS HC A03/MF A01

The combined data set from a GPS (global positioning system) survey of a 38 station network in Imperial Valley, California, performed by the U.S. National Geodetic Survey, is supplemented with prior information in order to estimate how individual stations have moved from survey epoch to survey epoch. The prior information has the form of quasi-observations that dampen the amount of displacement that can occur at individual stations in the direction perpendicular to the plate boundary. The quasi-observations serve to remove datum defects encountered when estimating displacements from geodetic data and to better resolve attributes of the deformation that are hidden within the noise of the real observations. The derived station displacements indicate that: to the north of the Imperial fault interplate deformation distributes over a zone at least 50 km wide, whereas near the Imperial fault, interplate deformation is concentrated within a 20 km wide zone; strain that had accumulated between the 1940 and 1979 earthquakes has yet to be completely released; and accelerated deformation following the 1940 earthquake was especially significant northwest of the Imperial fault. ESA

N90-13827# Geneva Observatory (Switzerland).
SWISS SCIENTIFIC BALLOON AND SOUNDING ROCKET EXPERIMENTS 1987-1989
D. Huguenin *In* ESA, European Rocket and Balloon Programs and Related Research Jun. 1989 p 3-6 (For primary document see N90-13826 05-42)
Copyright Avail: NTIS HC A15/MF A02

N90-13828# Centre National de la Recherche Scientifique, Paris (France).
THE FRENCH BALLOON PROGRAM AND RELATED SPACE RESEARCH
I. Sadourny *In* ESA, European Rocket and Balloon Programs and Related Research Jun. 1989 p 7-12 (For primary document see N90-13826 05-42)
Copyright Avail: NTIS HC A15/MF A02

N90-13829# Norwegian Space Center, Oslo.
THE NORWEGIAN BALLOON AND SOUNDING ROCKET PROGRAM 1989-1992
B. N. Andersen and A. Gundersen *In* ESA, European Rocket and Balloon Programs and Related Research Jun. 1989 p 13-16 (For primary document see N90-13826 05-42)
Copyright Avail: NTIS HC A15/MF A02

N90-13830# Swedish Space Corp., Solna.
THE SWEDISH SOUNDING ROCKET AND BALLOON PROGRAM
K. Lundahl *In* ESA, European Rocket and Balloon Programs and Related Research Jun. 1989 p 17-22 (For primary document see N90-13826 05-42)
Copyright Avail: NTIS HC A15/MF A02

N90-13831# Deutsche Forschungsanstalt fuer Luft- und Raumfahrt, Cologne (Germany, F.R.). Executive Dept. for Space Projects.
THE GERMAN SCIENTIFIC BALLOON AND SOUNDING ROCKET PROGRAM
A. F. Dahl and Manfred Otterbein (Bundesministerium fuer Forschung und Technologie, Bonn, Germany, F.R.) *In* ESA, European Rocket and Balloon Programs and Related Research Jun. 1989 p 23-31 (For primary document see N90-13826 05-42)
Copyright Avail: NTIS HC A15/MF A02

N90-13832# Swedish Inst. of Space Physics, Kiruna.
ENHANCED ELECTRON DENSITY LAYERS IN THE HIGH-LATITUDE LOWER IONOSPHERE
S. Kirkwood, L. Eliasson, I. Haeggstroem, and P. N. Collis (EISCAT Scientific Association, Kiruna, Sweden) *In* ESA, European Rocket and Balloon Programs and Related Research Jun. 1989 p 35-40 Sponsored by NFR, Sweden (For primary document see N90-13826 05-42)
Copyright Avail: NTIS HC A15/MF A02

N90-13833# Laboratoire de Meteorologie Dynamique du CNRS, Palaiseau (France).
HUMIDITY LOCAL MEASUREMENTS IN THE MIDDLE ATMOSPHERE [MESURES IN SITU D'HUMIDITE DANS L'ATMOSPHERE MOYENNE]
J. Ovarlez, J. Capus, M. Forichon, and H. Ovarlez *In* ESA, European Rocket and Balloon Programs and Related Research Jun. 1989 p 43-47 In FRENCH (For primary document see N90-13826 05-42)
Copyright Avail: NTIS HC A15/MF A02

N90-13834# Stockholm Univ. (Sweden). Arrhenius Lab.
NEW CALCULATIONS OF PHOTODISSOCIATION CROSS-SECTIONS IN THE O2 SCHUMANN-RUNGE SYSTEM
Donal P. Murtagh *In* ESA, European Rocket and Balloon Programs and Related Research Jun. 1989 p 49-53 (For primary document see N90-13826 05-42)
Copyright Avail: NTIS HC A15/MF A02

N90-13835*# National Aeronautics and Space Administration. Wallops Flight Facility, Wallops Island, VA.
EVIDENCE FOR ACCURATE TEMPERATURES FROM THE INFLATABLE FALLING SPHERE
F. J. Schmidlin, H. S. Lee, and W. Michel (Dayton Univ., Wallops Island, VA.) *In* ESA, European Rocket and Balloon Programs and Related Research Jun. 1989 p 55-58 (For primary document see N90-13826 05-42)
Copyright Avail: NTIS HC A15/MF A02 CSCL 04A

N90-13836# Max-Planck-Inst. fuer Aeronomie, Katlenburg-Lindau (Germany, F.R.).
OBSERVATION OF WIND CORNERS IN THE MIDDLE ATMOSPHERE OVER ANDENES (69 N) DURING WINTER 1983/84, SUMMER 1987 AND SUMMER 1988
H. U. Widdel *In* ESA, European Rocket and Balloon Programs and Related Research Jun. 1989 p 59-62 (For primary document see N90-13826 05-42)
(Grants BMFT-01-OE-610; BMFT-01-OE-86033)
Copyright Avail: NTIS HC A15/MF A02

N90-13837# Bonn Univ. (Germany, F.R.). Inst. fuer Physik.
NEAR-MESOPAUSE TEMPERATURES AT 69 N LATITUDE IN LATE SUMMER
U. vonZahn and H. Kurzawa *In* ESA, European Rocket and Balloon Programs and Related Research Jun. 1989 p 63-66 (For primary document see N90-13826 05-42)
(Grant DFG-Ho-858/1)
Copyright Avail: NTIS HC A15/MF A02

N90-13838# Oslo Univ. (Norway). Dept. of Physics.
THE ELECTRODYNAMICS OF THE POLAR IONOSPHERE WITH SPECIAL EMPHASIS ON THE DAYSIDE CLEFT REGION
A. Egeland *In* ESA, European Rocket and Balloon Programs and Related Research Jun. 1989 p 69-77 (For primary document see N90-13826 05-42)
Copyright Avail: NTIS HC A15/MF A02

N90-13839# Max-Planck-Inst. fuer Aeronomie, Katlenburg-Lindau (Germany, F.R.).
SOME REMARKS ON THE WORKING PRINCIPLE OF THE ROCKETBORNE NOSE TIP dc PROBES IN THE D-REGION OF THE IONOSPHERE
H. U. Widdel *In* ESA, European Rocket and Balloon Programs and Related Research Jun. 1989 p 79-84 (For primary document see N90-13826 05-42)
(Grants BMFT-WRK-90; ERO-DAERO-75-G076)
Copyright Avail: NTIS HC A15/MF A02

N90-13840# Kiel Univ. (Germany, F.R.). Inst. fuer Experimentalphysik.
RESONANCE CONE DIAGNOSTICS IN THE MID-LATITUDE IONOSPHERE
A. Piel, H. Thiemann, and K. I. Oyama (Tokyo Univ., Sagamihara, Japan) *In* ESA, European Rocket and Balloon Programs and Related Research Jun. 1989 p 85-90 (For primary document see N90-13826 05-42)
(Grant BMFT-PA4-010-M-86080)
Copyright Avail: NTIS HC A15/MF A02

N90-13841# Royal Inst. of Tech., Stockholm (Sweden). Dept. of Plasma Physics.
AURORAL PARTICLE ACCELERATION BY dc AND LOW FREQUENCY ELECTRIC FIELDS
L. P. Block and C.-G. Faelthammar *In* ESA, European Rocket and Balloon Programs and Related Research Jun. 1989 p 93-95 (For primary document see N90-13826 05-42)
Copyright Avail: NTIS HC A15/MF A02

N90-13842# Swedish Inst. of Space Physics, Uppsala.
OBSERVATIONS OF ELECTROSTATIC HYDROGEN CYCLOTRON WAVES AND ELECTRIC FIELD FLUCTUATIONS NEAR ONE Hz IN AURORAL ACCELERATION REGIONS
Anders I. Eriksson and Georg Gustafsson *In* ESA, European Rocket and Balloon Programs and Related Research Jun. 1989 p 97-102 Sponsored by the Swedish Board for Space Activities (For primary document see N90-13826 05-42)
Copyright Avail: NTIS HC A15/MF A02

N90-13843# Royal Inst. of Tech., Stockholm (Sweden). Dept. of Plasma Physics.
THE AURORAL CURRENT - VOLTAGE RELATIONSHIP
Kornelia Bruening *In* ESA, European Rocket and Balloon Programs and Related Research Jun. 1989 p 103-108 Sponsored by ESA (For primary document see N90-13826 05-42)
Copyright Avail: NTIS HC A15/MF A02

N90-13850# Max-Planck-Inst. fuer Aeronomie, Katlenburg-Lindau (Germany, F.R.).
PRELIMINARY RESULTS OF THE ROCKET AND SCATTER EXPERIMENTS ROSE: MEASUREMENTS WITH THE NEWLY DESIGNED SPHERICAL PROBE
G. Rose *In* ESA, European Rocket and Balloon Programs and Related Research Jun. 1989 p 141-147 Sponsored by Bundesminister fuer Forschung und Technologie (For primary document see N90-13826 05-42)
Copyright Avail: NTIS HC A15/MF A02

N90-13851# Auroral Observatory, Tromso (Norway).
BACKGROUND ELECTRODYNAMICS MEASURED BY EISCAT DURING THE NEED CAMPAIGN
C. Hall, A. Brekke, M. T. Rietveld, U. P. Lovhaug, and B. N. Maehlum (Norwegian Defence Research Establishment, Kjeller.) *In* ESA, European Rocket and Balloon Programs and Related Research Jun. 1989 p 153-157 Sponsored by Norges Almenvitenskapelige Foskningsradet, Norway; Science and Engineering Research, England; CNRS, France; Max-Planck Gesellschaft, Fed. Republic of Germany; Suomen Akatemia, Finland; and Naturvitenskapeliga Forskningsradet, Sweden (For primary document see N90-13826 05-42)
Copyright Avail: NTIS HC A15/MF A02

N90-13852# Norwegian Defence Research Establishment, Kjeller.
THE EFFECTS OF GRAVITY WAVES ON HORIZONTAL LAYERS: SIMULATION AND INTERPRETATION
U.-P. Hoppe *In* ESA, European Rocket and Balloon Programs and Related Research Jun. 1989 p 161-166 (For primary document see N90-13826 05-42)
Copyright Avail: NTIS HC A15/MF A02

N90-13853# Stockholm Univ. (Sweden). Arrhenius Lab.
A SELF-CONSISTENT MODEL OF THE MOST COMMON NIGHTGLOW EMISSIONS
Donal P. Murtagh *In* ESA, European Rocket and Balloon Programs and Related Research Jun. 1989 p 167-171 (For primary document see N90-13826 05-42)
Copyright Avail: NTIS HC A15/MF A02

N90-13854# Bonn Univ. (Germany, F.R.). Inst. fuer Astrophysik und Extraterrestrische Forschung.
INTERZODIAK 2: OBSERVATION OF EUV-RESONANCE RADIATION
G. Lay, H. J. Fahr, and H. U. Nass *In* ESA, European Rocket and Balloon Programs and Related Research Jun. 1989 p 173-176 Sponsored by the Bundesministerium fuer Forschung und Technologie (For primary document see N90-13826 05-42)
Copyright Avail: NTIS HC A15/MF A02

N90-13855# Bonn Univ. (Germany, F.R.). Inst. fuer Physik.
NEUTRAL AIR TURBULENCE IN THE MIDDLE AND UPPER ATMOSPHERE OBSERVED DURING THE MAC/EPSILON CAMPAIGN
W. Hillert and F.-J. Luebken *In* ESA, European Rocket and Balloon Programs and Related Research Jun. 1989 p 179-186 (For primary document see N90-13826 05-42)
(Grant BMFT-01-OE-8604-6)
Copyright Avail: NTIS HC A15/MF A02

N90-13856# Coleg Prifysgol Cymru, Aberystwyth (Wales).
POLAR MESOSPHERE SUMMER ECHOES AND ASSOCIATED ATMOSPHERIC GRAVITY WAVES
P. J. S. Williams, A. P. vanEyken, C. Hall, and J. Roettger (EISCAT Scientific Association, Kiruna, Sweden) *In* ESA, European Rocket and Balloon Programs and Related Research Jun. 1989 p 187-191 Sponsored in part by the United Kingdom Science and Engineering Research Council; Suomen Akatemia, Finland; CNRS, France; Max-Planck Gesellschaft, Fed. Republic of Germany; NAF, Norway; and NVF, Sweden (For primary document see N90-13826 05-42)
Copyright Avail: NTIS HC A15/MF A02

N90-13857# Centre National d'Etudes Spatiales, Toulouse (France).
OPERATIONAL ACTIVITY IN FRANCE AND A NEW METHOD OF BALLOON TEMPERATURE PILOTING
P. Faucon *In* ESA, European Rocket and Balloon Programs and Related Research Jun. 1989 p 195-200 (For primary document see N90-13826 05-42)
Copyright Avail: NTIS HC A15/MF A02

N90-13858# Centre National d'Etudes Spatiales, Toulouse (France).
LARGE HEAVY DUTY BALLOONS IN EUROPE
A. Soubrier *In* ESA, European Rocket and Balloom Programs and Related Research Jun. 1989 p 201-202 (For primary document see N90-13826 05-42)
Copyright Avail: NTIS HC A15/MF A02

N90-13869# Bonn Univ. (Germany, F.R.). Inst. of Physics.
DIURNAL VARIATION OF THE SODIUM LAYER AT POLAR LATITUDES IN SUMMER
H. Kurzawa and U. vonZahn *In* ESA, European Rocket and Balloon Programs and Related Research Jun. 1989 p 253-256 (For primary document see N90-13826 05-42)
(Grant DFG-Ho-858/1)
Copyright Avail: NTIS HC A15/MF A02

N90-13870# Wuppertal Univ. (Germany, F.R.).
THE DYANA CAMPAIGN 1990
D. Offermann *In* ESA, European Rocket and Balloon Programs and Related Research Jun. 1989 p 259-267 (For primary document see N90-13826 05-42)
Copyright Avail: NTIS HC A15/MF A02

N90-13871# British Aerospace Public Ltd. Co., Bristol (England). Space Systems Div.
THE SKYLARK SOUNDING ROCKET PROGRAM AND FUTURE LAUNCHER DEVELOPMENTS BY BRITISH AEROSPACE (SPACE SYSTEMS) LTD.
J. A. Ellis *In* ESA, European Rocket and Balloon Programs and Related Research Jun. 1989 p 269-271 (For primary document see N90-13826 05-42)
Copyright Avail: NTIS HC A15/MF A02

N90-13874# Centre National d'Etudes Spatiales, Toulouse (France). Div. Ballons.
LONG DURATION BALLOON FLIGHTS IN THE MIDDLE STRATOSPHERE
Pierre Malaterre *In* ESA, European Rocket and Balloon Programs and Related Research Jun. 1989 p 285-287 (For primary document see N90-13826 05-42)
Copyright Avail: NTIS HC A15/MF A02

N90-13877# Swedish Inst. of Space Physics, Kiruna.
ALIS: AN AURORAL LARGE IMAGING SYSTEM IN NORTHERN SCANDINAVIA
A. Steen *In* ESA, European Rocket and Balloon Programs and Related Research Jun. 1989 p 299-303 (For primary document see N90-13826 05-42)
Copyright Avail: NTIS HC A15/MF A02

47 METEOROLOGY AND CLIMATOLOGY

Includes weather forecasting and modification.

N90-13905# Texas A&M Univ., College Station. Climate System Research Program.
ESTIMATION OF RAIN RATE USING SPATIAL AND MULTICHANNEL COHERENCE: ANALYSIS OF SSM/I DATA
Jerry Tessendorf and Robert Upson [1989] 6 p
Avail: NTIS HC A02/MF A01

The spatial and multichannel coherence (SMC) properties of the remotely sensed environment derived from microwave radiometry data is investigated. This data is from the Special Sensor Microwave Imager (SSM/I) instrument on the DMSP F8 satellite. Based on preliminary results, it is possible to suppress the environmental background in multichannel microwave images by a factor of 100 to 1000 (20 to 30 dB) even over land. Two processing algorithms are introduced which exploit this coherent suppression potential to extract the rainfield. The analysis is restricted to a simulated rainfield which is injected into apparently rain-free SSM/I data. This allows the algorithms to be illustrated and probably indicates the potential for success under more realistic conditions. The philosopy behind the two processing algorithms is to quantitatively estimate the rainfall by a two-stage process, in which a map is obtained of the regions which have significant levels of rainfall. Primarily results of analysis connected with the first stage are presented, although an algorithm for the second stage is defined. K.C.D.

N90-13906# Control Data Corp., Minneapolis, MN. Meteorology Research Center.
THE INTERACTION AND VARIATION OF WAVES AND TURBULENCE FROM MST RADAR DATA Final Report, 1 Feb. 1986 - 31 Jul. 1989
Miriam R. Peterson 31 Aug. 1989 109 p
(Contract F49620-86-C-0027)
(AD-A212849; AFOSR-89-1242TR) Avail: NTIS HC A06/MF A01 CSCL 17/9

Research results are summarized for the interactions of gravity waves, small-scale turbulence, and the background weather conditions obtained using data from clear-air Doppler profilers (also called MST radars), and from aircraft and balloons. The major results from these studies are as follows: (1) It was found from analysis of a set of aircraft data taken near the tropopause and from MST radar taken in Alaska and Colorado that there is enhanced mesoscale variability over mountains compared to over plains or oceans. These observational results were compared with predictions from the theory of stratified turbulence and theory of Doppler-shifted gravity waves, and it was found that neither theory predicts all of the observed features. (2) Modeling of the refractivity turbulence structure constant (cn2) showed that small-scale shears of the horizontal wind are about twice as large over the mountainous regions of Colorado compared to over the plains of Illinois, presumably due to terrain differences. (3) It was found that gravity wave activity is enhanced near fronts, jet streams, and convective elements. (4) The flatland MST radar was used to monitor tropopause folding events under a variety of background conditions and a preliminary climatology of the occurrence of folds was developed. (5) The spectrum of vertical motions at Flatland was analyzed and was found to closely match predictions for a spectrum of Doppler-shifted gravity waves. (6) Temporal mean vertical velocities measured by the radar reflect the large-scale flow when weather systems are changing slowly enough that the radar sample

is representative of a large area. (7) Finally, it was found that the sampling strategy for vertical motions must be carefully designed to accommodate the frequency spectrum. GRA

N90-13907# Air Force Geophysics Lab., Hanscom AFB, MA.
AN EVALUATION OF THE SMITH-FEDDES MODEL Interim Report
Robert O. Berthel and Yutaka Izumi 13 Mar. 1989 28 p
(AD-A213237; AFGL-TR-89-0079; AFGL-ERP-1024) Avail: NTIS HC A03/MF A01 CSCL 04/2

A model designed to produce estimates of water contents and number density distributions at any time and geographical location was published in 1974. Known by its authors names as the Smith-Feddes, this model is initiated by gridded, data-base information from the 3DNEPH (or RTNEPH) and Hemispherical analyses. The Smith-Feddes has been used periodically with mixed results and the implicit assumption has been that new, more definitive cloud physics information would improve the model's consistency which is investigated to develop it into a useful tool for future Air Force planning and operations. The initial phase of this study was essentially an exercise to gain familiarity with both the Smith-Feddes and the initiating analyses. Three weather situations were defined by water content and temperature-versus-altitude profiles derived from aircraft measurements. The model was then exercised for the same situations and the results of the separate analyses were then compared. This report describes this investigation and details our observations and conclusions based on the results of this comparison study. It is recommended that no further time be expended in an effort to improve the 3DNEPH/RTHNEPH, Smith-Feddes model, as it is unable to consistently produce water-content values within reasonable error bounds. GRA

N90-13908*# National Aeronautics and Space Administration. Goddard Space Flight Center, Greenbelt, MD.
METEOROLOGICAL ATLAS OF THE NORTHERN HEMISPHERE LOWER STRATOSPHERE FOR JANUARY AND FEBRUARY 1989 DURING THE AIRBORNE ARCTIC STRATOSPHERIC EXPEDITION
Paul A. Newman, Leslie R. Lait, Mark R. Schoeberl, Ronald M. Nagatani (National Oceanic and Atmospheric Administration, Washington, DC.), and Arlin J. Krueger Nov. 1989 187 p
(NASA-TM-4145; Rept-89B00264; NAS 1.15:4145) Avail: NTIS HC A09/MF A02 CSCL 04B

Northern Hemisphere meteorological data for the months of January and February 1989 in the lower stratosphere are shown. National Meteorological Center (NMC) data, and Total Ozone Mapping Spectrometer (TOMS) data are used to display polar stereographic projections of 100-mb temperatures, 50-mb temperatures, 50-mb geopotential heights, total ozone, and Ertel's potential vorticity (Epv) on both 400 K and 460 K isentropic surfaces. In addition, latitude/height cross sections at 10 E of balanced wind isotachs, wind vectors, potential temperature, and temperature are also shown. Horizontal traces of NASA ER-2 and DC-8 flight tracks are also included. Vertical profiles of NMC temperatures following flight paths of both aircraft are shown. In addition, vertical profiles of wind speed are contoured following the ER-2 for estimating the lateral penetration into the polar vortex, while vertical profiles of Ertel's potential vorticity are included for estimating the vertical penetration of the DC-8 into the stratosphere. Author

N90-13909 Institut d'Aeronomie Spatiale de Belgique, Brussels.
CLIMATE PREDICTABILITY: A DYNAMICAL VIEW
C. Nicolis and C. L. Keppenne 1989 17 p Submitted for publication
(Aeronomica-Acta-A-347-1989; ISSN-0065-3713; ETN-90-96031) Avail: Institut d'Aeronomie Spatiale de Belgique, 3 Avenue Circulaire, B-1180 Brussels, Belgium

Evidence is reported that the dynamics involved in the 500 mb geopotential record are associated with deterministic chaos. The fractal dimension of the attractor and the average time beyond which predictions on individual trajectories break down are estimated. The possibility of carrying out predictions beyond this limit on the basis of a statistical approach is discussed. ESA

N90-13910# National Weather Service, Salt Lake City, UT. Scientific Services Div.
A COLLECTION OF PAPERS RELATED TO HEAVY PRECIPITATION FORECASTING
Roderick A. Scofield, G. Alan Johnson, Michael Koziara, Henry Law, Dolores B. Taylor, John G. Weikel, and J. Owen Rhea Aug. 1989 81 p
(PB89-230833; NOAA-TM-NWS-WR-206) Avail: NTIS HC A05/MF A01 CSCL 04B

A collection of four papers is presented. The first is a general discussion of the complexity of heavy precipitation within Extratropical Cyclone Systems and the theory of instability bursts. The second is a case study which reveals the usefulness of the AFOS Development Analysis Program mesoscale analysis package in identifying heavy precipitation focusing mechanisms. The third is a thorough overview of the Ventura County, California ALERT flood warning system, including its operation, multipurpose uses, concerns of local sponsors, and its impact on users. The fourth paper discusses the use of an orographic precipitation model in part of the Sierra Nevada mountains as an aid in quantitative precipitation forecasting. Author

N90-13911# Paris VI Univ. (France).
THREE DIMENSIONAL ANALYSIS OF THE STRUCTURE OF THE ATMOSPHERE IN POLAR ENVIRONMENTS BY VERTICAL SATELLITE SOUNDING. INTEREST FOR THE METEOROLOGICAL FORECASTS AT HIGH LATITUDES Ph.D. Thesis [ANALYSE TRIDIMENSIONNELLE DE LA STRUCTURE DE L'ATMOSPHERE EN ENVIRONNEMENT POLAIRE PAR SONDAGE VERTICAL SATELLITAIRE. INTERET POUR LA PREVISION METEOROLOGIQUE AUX HAUTES LATITUDES]
Chantal Claud 1989 208 p In FRENCH
(ETN-90-95506) Avail: NTIS HC A10/MF A01

The Improved Initialization Inversion (3I) method is adapted to polar latitudes. The problem of the sea ices/free water discrimination by determining the emissivity of surface microwaves from satellite observation is discussed. The 3I method is applied to a selection of satellite observations. ESA

N90-13912# World Meteorological Organization, Geneva (Switzerland).
[ACTIVITIES REPORT OF THE WORLD METEOROLOGICAL ORGANIZATION] Annual Report, 1988
1989 235 p Original contains color illustrations
(WMO-713; ISBN-92-63-10713-X; ETN-90-96019) Copyright Avail: MF A01; World Meteorological Organization, Case Postale No. 5, CH-1211 Geneva 20, Switzerland

The 1988 activities of the World Meteorological Organization are reported. Detailed information on the following program areas are given: the world weather watch, the world climate program, the research and development program, the applications of the meteorology, the hydrology and water resources, the education and training program, and the technical cooperation activities. The technical and supporting activities and external relations, and legal and administration matters are included. ESA

48 OCEANOGRAPHY

Includes biological, dynamic, and physical oceanography; and marine resources.

For related information see also *43 Earth Resources and Remote Sensing.*

N90-13913# Rondout Associates, Inc., Stone Ridge, NY.
ULF/VLF (0.001 TO 50 Hz) SEISMO-ACOUSTIC NOISE IN THE OCEAN Final Report
George H. Sutton, ed. 3 Aug. 1989 201 p Proceedings of a

Workshop held in Austin, TX, 29 Nov. - 1 Dec. 1988
(Contract N00014-89-J-1345)
(AD-A212942) Avail: NTIS HC A10/MF A02 CSCL 20/1

The objective of the research in ULF/VLF seismo-acoustic noise in the ocean is to improve our quantitative understanding of the physical processes that generate the acoustic/seismic ambient noise field in the frequency band from 0.001 to 50 Hz as a function of location and time: to experimentally identify and quantitatively define the important noise sources including the discrimination between noise from local and distant sources; where possible, to theoretically establish and describe the physical processes which are the noise source in the ULF/VLF frequency band; and to determine the effects of ocean, bottom, and sub-bottom acoustic/seismic parameters on the observed noise field, i.e., the effects both of propagation and of local site conditions. General characteristics of important noise sources and of the noise power spectrum are already fairly well established over much of the frequency band of interest; most are related to ocean waves and their meteorological sources. Ice motions, earthquakes, volcanic eruptions, turbulent tidal (or other) water currents, and atmospheric acoustic disturbances (also discussed in the Proceedings), are other possible sources that might be considered where appropriate. GRA

N90-13914# Naval Ocean Research and Development Activity, Bay Saint Louis, MS.
FEATURE MODELING: THE INCORPORATION OF A FRONT AND EDDY MAP INTO OPTIMUM INTERPOLATION-BASED THERMAL ANALYSIS Final Report
Theodore J. Bennett, Jr., Michael R. Carnes, Patricia A. Phoebus, and Lancelot M. Riedlinger Apr. 1989 28 p
(AD-A213253; NORDA-242) Avail: NTIS HC A03/MF A01 CSCL 08/3

Ocean acoustics are crucial to modern naval operations. Acoustics constantly change due to the variability in space and in time of the ocean thermal structure. Thus, a thermal analysis system that transforms irregularly sampled data from disparate sources into an analysis of the ocean thermal structure is of increasing importance. In a data-sparse environment such as the ocean, the key to obtaining realistic but cost-effective analyses is the use of all available data sources, as well as the most powerful data assimilation techniques. Feature modeling is a powerful means of supplementing the limited in situ and remotely sensed data with our understanding of the oceanography of mesoscale ocean features. Initially, the data are used to map the location of mesoscale fronts and eddies. Schematic descriptions of the thermal structure of these features, called feature models, are subsequently used to represent them in the first-guess thermal field. In data-sparse areas, features that would otherwise be poorly resolved in the analysis are instead represented by these schematic models. Models are developed for the Gulf Stream front and eddies, as well as an algorithm for the incorporation of the models into the first-guess field. The models were evaluated within the Optimum Thermal Interpolation System (OTIS) framework. Subsurface thermal fields constructed via these feature models agree well with observed fields and are substantially more realistic than analyses produced using the current regional operational system, the Expanded Ocean Thermal Structure (EOTS) analysis. GRA

51 LIFE SCIENCES (GENERAL)

N90-13915# Connecticut Univ., Farmington. Surgical Research Center.
GENERATION OF FREE RADICALS DURING COLD INJURY AND REWARMING
Jaisimha Lyengar, Saswati Samanta, Anna George, John C. Russell, and Dipak K. Das 1988 22 p
(Contract N00014-88-K-0546)
(AD-A213088) Avail: NTIS HC A03/MF A01 CSCL 06/10

Cold injury is often associated with irreversible cell damage. The present study examines the mechanism of such injury. New Zealand white rabbits were anesthetized with ketamine and xylazine, and then ventilated. The femoral artery and vein were exposed. A continuous display of electrocardiogram was obtained. One leg was cooled with a freezing mixture up to 0 C, which was followed by rewarming; the other leg served as control. Blood samples were withdrawn from the femoral artery for analysis of creatine kinase (CK), lactate dehydrogenase (LDH), and malonaldehyde (MDA). At the end, salicylate was injected through the femoral vein to trap any hydroxyl radical (OH) formed. Rabbits were immediately sacrificed, and biopsies were withdrawn and frozen at liquid Nitrogen temperature to analyze OH. Local blood flow in the cold-exposed leg was reduced significantly, suggesting that cold injury was associated with ischemic insult. CK and LDH were increased after cold exposure, then increased further during rewarming. MDA formation followed a similar pattern. OH generated after cooling increased significantly upon rewarming. These results indicate that rewarming is associated with an episode of ischemia/perfusion, with simultaneous generation of free radicals which, at least in part, may be responsible for cellular injury associated with rewarming. GRA

N90-13916*# Pennsylvania State Univ., University Park. Dept. of Agricultural Engineering.
MEASUREMENT OF THE LIGHT FLUX DENSITY PATTERNS FROM LUMINAIRES PROPOSED AS PHOTON SOURCES FOR PHOTOSYNTHESIS DURING SPACE TRAVEL
Paul N. Walker 1 Dec. 1989 57 p
(Grant NAG10-0059)
(NASA-CR-186124; NAS 1.26:186124) Avail: NTIS HC A04/MF A01 CSCL 06B

Two luminaires were evaluated to determine the light flux density pattern on a horizontal plane surface. NASA supplied both luminaires; one was made by NASA and the other is commercially available. Tests were made for three combinations of luminaire height and luminaire lens material using the NASA luminaire; only one configuration of the commercial luminaire was tested. Measurements were made using four sensors with different wavelength range capabilities. The data are presented in graphical and tabular formats. Author

N90-13917# European Space Agency, Paris (France).
LIFE SCIENCE RESEARCH IN SPACE
H. Oser, ed. and B. Battrick, ed. Jul. 1989 137 p Original contains color illustrations
(ESA-SP-1105; ISBN-92-9092-012-2; ISSN-0379-6566; ETN-90-95761) Copyright Avail: NTIS HC A07/MF A01; ESA Publications Division, ESTEC, Noordwijk, Netherlands, 40 Dutch guilders

The life science research carried out to date in low gravity conditions is summarized. The areas of research covered are: human physiology, developmental biology, plant biology, cell biology, radiation biology, exobiology, life support systems for man, and bioprocessing. The direction of future research and possible applications of such research are described. The European Space Agency life science facilities are described. These include the sled facility, the Biorack and the Anthorack facilities. ESA

52 AEROSPACE MEDICINE

Includes physiological factors; biological effects of radiation; and effects of weightlessness on man and animals.

N90-13918# SRI International Corp., Menlo Park, CA. Sensory Sciences Research Lab.
ROLE OF RETINOCORTICAL PROCESSING IN SPATIAL VISION Annual Report No. 2, 1 May 1988 - 1 May 1989
Donald H. Kelly Jun. 1989 35 p
(Contract F49620-87-K-0009; AF Proj. 2313)
(AD-A210995; AFOSR-89-1027TR) Avail: NTIS HC A03/MF A01 CSCL 23/3

The inhomogeneous retinal filtering algorithms is incorporated

into a more general model that includes conformal projection of the retinal filtered outputs into cortical input images, suitable for further processing, such as Gabor filtering. The new cortical images seem to show much less loss of information relative to the retina. No longer is restored some of the dc (zero frequency) component that is filtered out by the (Laplacian/Gaussian) retinal receptive-field model. Both right and left hemisphere images are provided, joined at the fovea for easy comparison with the corresponding retinal image. Study of these cortical images is yielding new insights. Peripheral objects, while remaining otherwise relatively undistorted, will be rotated either clockwise or counterclockwise as for as + or - 90 deg in cortical coordinates if they lie above or below the horizontal meridian. This is consistent with other cortical image models, but it does not bode well for the possibility of creating a stable frame by any known array-processing operation on cortical outputs. Modeling cortical filtering, as by Gabor functions, was examined. It is already clear that a simple, linear convolution without further refinements is not a good model for this process. GRA

N90-13919# Army Aeromedical Research Lab., Fort Rucker, AL. Sensory Research Div.

EVALUATION OF SPEECH INTELLIGIBILITY THROUGH A BONE CONDUCTION STIMULATOR Final Report

Ted L. Langford, Ben T. Mozo, and James H. Patterson, Jr. Jul. 1989 21 p

(AD-A212002; USAARL-89-13) Avail: NTIS HC A03/MF A01 CSCL 20/1

The intelligibility of speech, delivered via a bone-conduction transducer, was measured under simulated combat vehicle noise conditions and compared with the same measurements made with a conventional, air-conduction system. The measurements were made for conditions in which the ear canals were open and in which they were occluded with protective earplugs. The use of the bone-conduction system led to a 25.3-dB improvement over the conventional air-conduction system. GRA

N90-13920# California Univ., Irvine. Public Policy Research Organization.

PILOT INVESTIGATION OF INDOOR-OUTDOOR AND PERSONAL PM10 (THORACIC) AND ASSOCIATED IONIC COMPOUNDS AND MUTAGENIC ACTIVITY Final Report, Feb. 1987 - Apr. 1989

Steven D. Colome, Norman Y. Kado, Michael Kleinman, and Peter Jaques (New York Univ., New York.) 27 Apr. 1989 126 p

(Contract ARB-A6-129-87)

(PB89-222723; ARB-R-89/397) Avail: NTIS HC A07/MF A01 CSCL 06S

A major objective of the pilot study was to evaluate methods of measuring indoor and personal exposures to PM10. Other objectives were to examine the feasibility of measuring particle characteristics (other than mass) that may be useful in relating exposures to PM10 to health effects. The investigators tested several types of particle sampling devices in the homes of eight asthmatic subjects who resided in Orange County. The investigators measured particle mass for levels of sulfate nitrate ions and the mutagenicity of particle extracts. The pilot study demonstrated successfully the use of certain portable sampling devices to measure PM10 exposure and showed that it is feasible to measure levels of ionic species and mutagenic activity in particle samples obtained with these devices. The results of the study can be applied in the design of larger studies of similar nature. Author

N90-13921# Defence and Civil Inst. of Environmental Medicine, Downsview (Ontario).

A PROTOTYPE MICROPROCESSOR BASED AUDIOMETER FOR USE BY THE CF (CANADIAN FORCES) MEDICAL SERVICES FOR PERIODIC HEARING TESTS

S. E. Forshaw, P. C. Odell, and R. B. Crabtree May 1989 56 p

(AD-A212990; DCIEM-89-TR-19) Avail: NTIS HC A04/MF A01 CSCL 12/5

A prototype microcomputer-based audiometer designed to demonstrate the potential of such technology for routine periodic hearing testing in the Canadian Forces (CF) is demonstrated. Besides the microcomputer and its dual-disk drive, display screen and printer, the system is comprised of an interface box containing a crystal clock, frequency synthesizer, digital attenuator, electronic switch, audio amplifier, acoustic earphone calibrators, and patient-response interface circuitry. The threshold-detection paradigms are based on the modified Hughson and Westlake procedure. The associated software provides prompts to the technician for parameters and data for each patient (e.g., age, social insurance number (SIN), military occupation code (MOC)), along with prompts during the testing if problems are encountered. After a test is completed, the patient's CF hearing category is computed and displayed on the screen audiogram form, and the test results are stored automatically in a disk file for future reference. GRA

N90-13922# Defence and Civil Inst. of Environmental Medicine, Downsview (Ontario).

THE RELATIONSHIP BETWEEN SUBJECTIVE AND OBJECTIVE MEASURES OF SIMULATOR-INDUCED ATAXIA

L. Kantor, L. E. Magee, and K. M. Hamilton Jun. 1989 19 p

(AD-A213095; DCIEM-89-RR-28) Avail: NTIS HC A03/MF A01 CSCL 06/10

Flight simulator training sometimes leads to unwanted aftereffects commonly called simulator induced sickness. Subjective reports of simulator-induced sickness include loss of balance (ataxia), dizziness, nausea, headache, eyestrain, and general discomfort. Symptoms of balance loss are particularly worrisome because of their potential to compromise safety following simulator training. While the reason flight simulators produce ataxia in some aircrew is not clear, most investigators speculate that it is caused by readaptation of the human spatial orientation system to the real world following adaptation to the artificial environment provided by the simulator. Subjective reports of simulator-induced ataxia are difficult to corroborate using objective tests of balance. Two reasons for this are ceiling and practice effects that occur with objective tests of balance. An attempt was made to overcome these problems. Postural control was assessed subjectively following exposure to a general purpose flight simulator and objectively using four balance tests specifically designed to avoid celling effects. The experimental design was intended to control for practice. Subjective reports of disequilibrium following training were verified by only one of the balance tests; the Walk On Rail Eyes Open (WOREO) was reliable in showing loss of postural control. The results suggest that the WOREO should be used as an objective test for studying postural disequilibrium following simulator exposure. GRA

N90-13923# Defence and Civil Inst. of Environmental Medicine, Downsview (Ontario).

SIMULATOR INDUCED SICKNESS IN THE CP-140 (AURORA) FLIGHT DECK SIMULATOR

K. M. Hamilton, L. Kantor, R. Heslegrave, L. E. Magee, and K. Hendy May 1989 25 p

(AD-A213096; DCIEM-89-RR-32) Avail: NTIS HC A03/MF A01 CSCL 06/10

Training on modern flight simulators can lead to a condition referred to as simulator induced sickness (SIS) which is characterized by nausea, dizziness and postural instability. It is believed that SIS results from exposure to conflicting sensory information. The present report examined the incidence, severity and duration of SIS as a function of flight experience and aircrew position (pilot/copilot) in 16 aircrew following training on the CP-140 (Aurora) Flight Deck Simulator at Canadian Forces Base Greenwood. The dependent measures included symptomatology and postural stability. In addition, measures of workload were taken to examine the contribution of the high task demands generally associated with simulator training to the development of SIS symptomatology. The results indicated that over 50 percent of tested aircrew experienced increases in symptom frequency following simulator training with the most commonly reported symptoms being mild mental fatigue, physical fatigue, eye strain and after sensations of motion. The workload results confirmed that the simulator imposed high task demands on the aircrew.

Furthermore, the workload results were consistent with the pattern of symptoms observed, suggesting that factors other than sensory conflict may be involved in the development of symptomatology following simulator exposure. Future investigations should attempt to identify these factors so that SIS can be managed more effectively. GRA

N90-13924# California Univ., Berkeley.
COMPUTATIONAL AND PSYCHOPHYSICAL STUDY OF HUMAN VISION USING NEURAL NETWORKS Final Report, 1 Aug. 1985 - 31 Jan. 1989
Donald A. Glaser and Kumar Tribhawan 28 Apr. 1989 66 p
(Contract N00014-85-K-0692; RR04209)
(AD-A213290) Avail: NTIS HC A04/MF A01 CSCL 06/4

The overall goal of our research program is to construct models of the human visual system that can be implemented on available computers and capture essential abilities of the real thing. These models should be useful in understanding how the human visual system works and for practical applications. In order to incorporate some of the known structural features of the brain in our models, we have chosen a neural net paradigm to mimic some aspects of the real nervous system. These networks contain nodes representing simplified nerve cells and can have an enormous variety of structures, some of which are the subjects of intensive study in many laboratories. Since so many different network structures are possible, it is necessary to use as much information as possible to limit the choice of nets to those most likely to be useful models of the human visual system. Our work in psychophysics is designed to provide limits on the choice of architectures for model nets by requiring them to satisfy certain general conditions indicated by these experiments. Several experimental projects will be described concerning perception of relative depth and motion. One generalization that emerges from all of them is that local visual judgements can be grossly influenced by information gleaned from quite distant parts of a scene. To mimic the operation of the human visual system, then, a neural net must collect information from sizeable areas of a scene and use it to influence outputs from local visual processes. GRA

N90-13925*# National Aeronautics and Space Administration, Washington, DC.
AEROSPACE MEDICINE AND BIOLOGY: A CONTINUING BIBLIOGRAPHY WITH INDEXES (SUPPLEMENT 330)
Dec. 1989 62 p
(NASA-SP-7011(330); NAS 1.21:7011(330)) Avail: NTIS HC A11; NTIS standing order as PB89-912300, $10.50 domestic, $21.00 foreign CSCL 06E

This bibliography lists 156 reports, articles, and other documents introduced into the NASA Scientific and Technical Information System during November 1989. Subject coverage includes: aerospace medicine and psychology, life support system and controlled environments, safety equipment, exobiology and extraterrestrial life, and flight crew behavior and performance. Author

N90-13926*# National Aeronautics and Space Administration. Ames Research Center, Moffett Field, CA.
EXERCISE COUNTERMEASURES FOR BED REST DECONDITIONING
John Greenleaf, ed. Oct. 1989 58 p
(NASA-TM-101045; A-88315; NAS 1.15:101045) Avail: NTIS HC A04/MF A01 CSCL 06S

The major objectives were to evaluate the efficiency of different modes of exercise (isotonic and isokinetic) for countering the effects of bed rest deconditioning on work capacity (peak oxygen uptake), muscular strength, orthostatic tolerance, posture, equilibrium and gait; and to collect additional data of a more fundamental nature to help understand how these deconditioning responses occur. These data will be used for writing prescriptions for exercise to be utilized by astronauts for maintaining work capacity and well-being on Freedom Station, and to determine what exercise devices should be place in the station. Author

N90-13927# Centre d'Etudes et de Recherches de Medecine Aerospatiale, Paris (France).
PRELIMINARY STUDY OF PHARMACOLOGICAL CONTROL OF SPACE DISEASE [ETUDES PRELIMINAIRES AU CONTROLE PHARMACOLOGIQUE DU MAL DE L'ESPACE]
C. L. Milhaud, D. P. Lagarde, and G. Florence 19 Dec. 1988 25 p In FRENCH
(Contract DRET-85-1032)
(ETN-90-95015) Avail: NTIS HC A03/MF A01

The design of experiments to implement simulations of low body positive pressure type using Macaque Rhesus animals is described. The same species was employed to study the standard induction of emetic syndromes caused by copper sulfate, Ipecac syrup and Ergotamine. The effects of the three substances on the Macaque Rhesus are characterized. ESA

N90-13928# Toulouse Univ. (France).
WATCHFULNESS AND ATTENTION DURING WEIGHTLESSNESS SIMULATIONS: USE OF COMPUTERIZED PSYCHOMETRIC TESTS Ph.D. Thesis [LA VIGILANCE ET L'ATTENTION AU COURS D'UNE SIMULATION PROLONGEE D'IMPESANTEUR: UTILISATION D'UNE BATTERIE DE TESTS PSYCHOMETRIQUES INFORMATISES]
Alain Cornac 1989 116 p In FRENCH
(Rept-89-TOU-3-1045; ETN-90-95264) Avail: NTIS HC A06/MF A01

Psychometric analysis was carried out on four subjects for 30 days. The position of the body maintained the head 15 cm lower than the feet. This simulation technique allows reproduction of the hemodynamic effects observed in microgravity. Three of the four subjects were subjected to periods of decompression of the lower part of the body (low body negative pressure). The results do not allow positive or negative conclusions. The tests used are sensitive to learning phenomena. ESA

53 BEHAVIORAL SCIENCES

Includes psychological factors; individual and group behavior; crew training and evaluation; and psychiatric research.

N90-13929# SRI International Corp., Menlo Park, CA. Vision Research Program.
SPATIOTEMPORAL CHARACTERISTICS OF VISUAL LOCALIZATION, PHASE 2 Annual Report, Aug. 1988 - Aug. 1989
Christina A. Burbeck, Duane K. Bowman, and Yen Lee Yap Aug. 1989 165 p
(Contract F49620-88-K-0008)
(AD-A212934; AFOSR-89-1246TR) Avail: NTIS HC A08/MF A01 CSCL 06/4

We have conducted psychophysical experiments to determine: (1) the contribution of local spatial filters to separation discrimination, and (2) the properties of mechanisms that enter into subsequent stages of spatial processing i.e., separation discriminators. The separation, eccentricity, spatial extent, exposure duration, and proximity of the targets to other objects were manipulated. The extent of the target was more important for discrimination of relatively small (rather than large) separations at any given eccentricity, supporting the idea that an additional stage beyond the local spatial filters is necessary to explain performance of separation discrimination. The proximity of other spatial features was found to affect thresholds only for briefly exposed targets, implying that subsequent mechanisms can select the frequency content of the information carried by the local spatial filters. Separation discrimination appeared to be performed by two different types of separation discriminators, one largely separation-dependent, and the other separation-independent but strongly eccentricity-dependent. Unlike the local spatial filters the separation discriminator processes information serially, with each separation taking at least 100 ms to encode. GRA

N90-13930# Center for Mathematics and Computer Science, Amsterdam (Netherlands). Computer Science/Dept. of Interactive Systems.

THE STRUCTURAL MEMORY: A NETWORK MODEL FOR HUMAN PERCEPTION OF SERIAL OBJECTS

Jantien vanderVegt, Hans Buffart, and Cees vanLeeuwen Dec. 1988 24 p Submitted for publication Sponsored by the Psychon Foundation

(CWI-CS-R8829; ETN-90-95973) Copyright Avail: NTIS HC A03/MF A01

The Structural Memory, a network model for human perception of serial objects, is presented. Based upon the automatic generation of all representations, G (generation)-relations are defined between the representations, and S (structure)-relations are defined based on the structures described by the representations. The representations and the relations are seen as respectively the modes and the links in a network which is the basis for the Structural Memory. An activation value is assigned to each representation which expresses the strength of the preference for the described structure at a certain moment. A process model predicts strength of the preference for a perceptible structure in an object. Experiments are simulated with two of these process models. ESA

N90-13931*# National Aeronautics and Space Administration. Ames Research Center, Moffett Field, CA.

FUNCTIONAL DECOR IN THE INTERNATIONAL SPACE STATION: BODY ORIENTATION CUES AND PICTURE PERCEPTION

Richard G. Coss, Yvonne A. Clearwater, Christopher G. Barbour, and Steven R. Towers (California Univ., Davis.) Nov. 1989 29 p

(NASA-TM-102242; A-89260; NAS 1.15:102242) Avail: NTIS HC A03/MF A01 CSCL 05I

Subjective reports of American astronauts and their Soviet counterparts suggest that homogeneous, often symmetrical, spacecraft interiors can contribute to motion sickness during the earliest phase of a mission and can also engender boredom. Two studies investigated the functional aspects of Space Station interior aesthetics. One experiment examined differential color brightnesses as body orientation cues; the other involved a large survey of photographs and paintings that might enhance the interior aesthetics of the proposed International Space Station. Ninety male and female college students reclining on their backs in the dark were disoriented by a rotating platform and inserted under a slowly rotating disk that filled their entire visual field. The entire disk was painted the same color but one half had a brightness value that was about 69 percent higher than the other. The effects of red, blue, and yellow were examined. Subjects wearing frosted goggles opened their eyes to view the rotating, illuminated disk, which was stopped when they felt that they were right-side up. For all three colors, significant numbers of subjects said they felt right-side up when the brighter side of the disk filled their upper visual field. These results suggest that color brightness could provide Space Station crew members with body orientation cues as they move about. It was found that subjects preferred photographs and paintings with the greatest depths of field, irrespective of picture topic. Author

N90-13932# Plessey Research Roke Manor Ltd., Romsey (England).

A GUIDE TO REASONING UNDER UNCERTAINTY

D. A. Findlay Nov. 1987 13 p

(Rept-72/87/R486U; ETN-90-94847) Copyright Avail: NTIS HC A03/MF A01

Some aspects of reasoning under uncertainty are discussed. The analysis is structured around the sort of question a prospective reasoner under uncertainty is likely to ask. The situations where the reasoning under uncertainty arises are outlined. The meaning of uncertainty is established. The way of representing uncertainty in a self-consistent manner is considered. The treatments of the approximate and plausible reasoning are given. ESA

N90-13933# Technische Univ., Delft (Netherlands). Dept. of Aerospace Engineering.

COMPENSATORY TRACKING IN DISTURBANCE TASKS AND TARGET FOLLOWING TASKS. THE INFLUENCE OF COCKPIT MOTION ON PERFORMANCE AND CONTROL BEHAVIOR

J. C. vanderVaart and R. J. A. W. Hosman Dec. 1987 55 p

(LR-511; ETN-90-95979) Avail: NTIS HC A04/MF A01

Manned, moving base simulator experiments showing improved tracking performance in disturbance tasks as well as in target following tasks when cockpit motion is added to a basic, visual, artificial horizon display are investigated. The experimental findings are clarified qualitatively and quantitatively by analysis of the differences of the two tasks in terms of classic control theory and by use of experimented data on vestibular motion perception previously obtained. ESA

54 MAN/SYSTEM TECHNOLOGY AND LIFE SUPPORT

Includes human engineering; biotechnology; and space suits and protective clothing.

For related information see also *16 Space Transportation.*

N90-13934*# Life Systems, Inc., Cleveland, OH.

REFURBISHMENT OF ONE-PERSON REGENERATIVE AIR REVITALIZATION SYSTEM Final Report, 22 Jul. 1985 - 3 Apr. 1989

Ferolyn T. Powell Mar. 1989 24 p

(Contract NAS8-36435)

(NASA-CR-183757; NAS 1.26:183757; LSI-TR-875-9) Avail: NTIS HC A03/MF A01 CSCL 05H

Regenerative processes for the revitalization of spacecraft atmospheres and reclamation of waste waters are essential for making long-term manned space missions a reality. Processes studied include: static feed water electrolysis for oxygen generation, Bosch carbon dioxide reduction, electrochemical carbon dioxide concentration, vapor compression distillation water recovery, and iodine monitoring. The objectives were to: provide engineering support to Marshall Space Flight Center personnel throughout all phases of the test program, e.g., planning through data analysis; fabricate, test, and deliver to Marshall Space Flight Center an electrochemical carbon dioxide module and test stand; fabricate and deliver an iodine monitor; evaluate the electrochemical carbon dioxide concentrator subsystem configuration and its ability to ensure safe utilization of hydrogen gas; evaluate techniques for recovering oxygen from a product oxygen and carbon dioxide stream; and evaluate the performance of an electrochemical carbon dioxide concentrator module to operate without hydrogen as a method of safe haven operation. Each of the tasks were related in that all focused on providing a better understanding of the function, operation, and performance of developmental pieces of environmental control and life support system hardware. Author

N90-13935 Wisconsin Univ., Madison.

MEASUREMENT OF MECHANICAL WORK AND ENERGY EXPENDITURE IN RUNNING AND BICYCLING Ph.D. Thesis

David Robinson Bassett, Jr. 1988 148 p

Avail: Univ. Microfilms Order No. DA8824082

Three objectives are fulfilled: to quantitate the differences in oxygen uptake (VO2) and mechanical work in level versus uphill running; to propose two refinements for measuring external power output during the Wingate Anaerobic Test (WAT); and to evaluate the metabolic and thermoregulatory responses to skin wetting during running. Seven males performed overground (OG) and treadmill (TM) running at two grades (0 and 5 percent) over a range of speeds between 136 to 286 m/min. No significant differences were found betwwen the VO2 of TM vs overground running at either of the grades examined. In a subsequent study, 8 males ran at 188 m/min at 0, 5, 10, and 15 percent grades. Internal work, measured by the link segment approach, decreased with increasing grades. The WAT is a 30 s test of external power

output performed on a cycle ergometer. Since flywheel (FW) velocity decreases over the course of the test, kinetic energy stores contribute to the total power output. Correcting for this factor lowered peak power, mean power, and percent fatigue by 6.2, 3.0, and 6.6 percent, respectively in 8 male subjects. The measurement of external power output using a Monark 864 weight ergometer was found to require the placement of a load cell in series with the FW belt. During distance running, the total energy expenditure results in heat production, since no net external work is done. The responses to this treatment during a 2 hr run were examined under two different humidity conditions. Spraying had no effect on rectal temperature, heart rate, VO2, sweat loss, or percent change in plasma volume. Dissert. Abstr.

N90-13936# Air Force Wright Research and Development Center, Wright-Patterson AFB, OH.
CONFERENCE PROCEEDINGS OF THE HUMAN-ELECTRONIC CREW: CAN THEY WORK TOGETHER
Jerry Emerson, ed., John Reising, ed., Robert M. Taylor, ed., and Michael Reinecke, ed. Jul. 1989 171 p Conference held in Ingolstadt, Fed. Republic of Germany, 19-22 Sep. 1988; sponsored by AFWAL, Royal Air Force Inst. of Aviation Medicine, Flugmedizinisches Inst. der Luftwaffe and Air Force European Office of Aerospace Research and Development
(AD-A211871; WRDC-TR-89-7008) Avail: NTIS HC A08/MF A01 CSCL 23/2

Advances in artificial intelligence (AI) will enable future fighter/attack aircraft to have a rather unique crew -- one human and one electronic. The objective of the workshop was to bring together AI specialists and cockpit designers in order to exchange ideas relative to: (1) the state of the art in aircraft applications of AI technology; and (2) the impact on the cockpit of the human/electronic crew. This meeting provided a valuable forum for the experts of several countries to exchange ideas, concepts, and data relative to hardware and software capabilities that can be included in an aircraft system design to aid the human operator in performing the mission. GRA

N90-13937# Defence and Civil Inst. of Environmental Medicine, Downsview (Ontario).
TEST PROCEDURES FOR THE EVALUATION OF HELMET AND HEADSET MOUNTED ACTIVE NOISE REDUCTION SYSTEMS
Stanly E. Forshaw, Julia M. Rylands, and R. B. Crabtree Feb. 1989 22 p
(AD-A212991; DCIEM-89-TR-24) Avail: NTIS HC A03/MF A01 CSCL 06/8

Laboratory and field procedures appropriate for measuring the effectiveness of active noise reduction (ANR) devices mounted in flight helmets, armoured-vehicle crew helmets, communication headsets, and circumaural hearing protectors are described. The procedures described are: ear canal measurements using real subjects or an acoustic test fixture (ATF), masked-threshold and loudness-balance psychophysical procedures, a signal detection procedure, and speech reception procedures using modified rhyme and diagnostic rhyme test (MRT, DRT) and Speech Transmission Index (STI) measures. GRA

N90-13938# Anacapa Sciences, Inc., Fort Rucker, AL.
HUMAN FACTORS RESEARCH IN AIRCREW PERFORMANCE AND TRAINING Final Report, Oct. 1987 - Oct. 1988
Theodore B. Aldrich and D. M. McAnulty Aug. 1989 139 p (Contract MDA903-87-C-0523)
(AD-A213285; ASI-690-319-88; ARI-TR-858) Avail: NTIS HC A07/MF A01 CSCL 23/2

This report presents summaries of the research projects performed by Anacapa Sciences, Inc., for the ARI Aviation R and D Activity (ARIARDA) at Fort Rucker, Alabama. From 9 October 1987 to 8 October 1988, Anacapa personnel worked on 25 research projects and took part in 6 technical advisory services that address emerging aviation weapon systems design, manpower and personnel programs, and aviator training research. The summary for each project and technical advisory service contains: (1) a background section that describes the rational for the project and specifies the research objectives, (2) a research approach section that describes the tasks and activities required to meet the project objectives (3) a results section that describes the research findings or, in the case of developmental activities, the research product, and (4) a project status section that describes the work completed and projections for future research, if any. GRA

55 SPACE BIOLOGY

Includes exobiology; planetary biology; and extraterrestrial life.

N90-13939*# National Aeronautics and Space Administration. Ames Research Center, Moffett Field, CA.
CELLS IN SPACE
Jean D. Sibonga, ed., Richard C. Mains, ed., Thomas N. Fast, ed. (Santa Clara Univ., CA.), Paul X. Callahan, ed., and Charles M. Winget, ed. Aug. 1989 310 p Conference held in San Juan Bautista, CA, 31 Oct. - 4 Nov. 1988
(NASA-CP-10034; A-89131; NAS 1.55:10034) Avail: NTIS HC A14/MF A02 CSCL 06C

Discussions and presentations addressed three aspects of cell research in space: the suitability of the cell as a subject in microgravity experiments, the requirements for generic flight hardware to support cell research, and the potential for collaboration between academia, industry, and government to develop these studies in space. Synopses are given for the presentations and follow-on discussions at the conference and papers are presented from which the presentations were based. An Executive Summary outlines the recommendations and conclusions generated at the conference. For individual titles, see N90-13940 through N90-13958.

N90-13940*# National Aeronautics and Space Administration. Ames Research Center, Moffett Field, CA.
FUNDAMENTAL RESULTS FROM MICROGRAVITY CELL EXPERIMENTS WITH POSSIBLE COMMERICIAL APPLICATIONS
Charles M. Winget, Thomas N. Fast, Williams E. Hinds, R. L. Schaefer (Lockheed Engineering and Sciences Co., Houston, TX.), and Paul X. Callahan *In its* Cells in Space Aug. 1989 p 65-69 (For primary document see N90-13939 05-55)
Avail: NTIS HC A14/MF A02 CSCL 06C

Some of the major milestones are presented for studies in cell biology that were conducted by the Soviet Union and the United States in the upper layers of the atmosphere and in outer space for more than thirty-five years. The goals have changed as new knowledge is acquired and the priorities for the use of microgravity have shifted toward basic research and commercial applications. Certain details concerning the impact of microgravity on cell systems is presented. However, it needs to be emphasized that in planning and conducting microgravity experiments, there are some important prerequisites not normally taken into account. Apart from the required background knowledge of previous microgravity and ground-based experiments, the investigator should have the understanding of the hardware as a physical unit, the complete knowledge of its operation, the range of its capabilities and the anticipation of problems that may occur. Moreover, if the production of commercial products in space is to be manifested, data obtained from previous microgravity experiments must be used to optimize the design of flight hardware. Author

N90-13941*# National Aeronautics and Space Administration. Ames Research Center, Moffett Field, CA.
THE PITUITARY GROWTH HORMONE CELL IN SPACE
Wesley C. Hymer (Pennsylvania State Univ., University Park.) and R. Grindeland *In its* Cells in Space Aug. 1989 p 71-75 (For primary document see N90-13939 05-55)
Avail: NTIS HC A14/MF A02 CSCL 06C

Growth hormone (GH), produced and secreted from specialized cells in the pituitary gland, controls the metabolism of protein, fat,

and carbohydrate. It is also probably involved in the regulation of proper function of bone, muscle and immune systems. The behavior of the GH cell system was studied by flying either isolated pituitary cells or live rats. In the latter case, pituitary GH cells are prepared on return to earth and then either transplanted into hypophysectomized rats or placed into cell culture so that function of GH cells in-vivo vs. in-vitro can be compared. The results from three flights to date (STS-8, 1983; SL-3, 1985; Cosmos 1887, 1987) established that the ability of GH cells to release hormone, on return to earth, is compromised. The mechanism(s) responsible for this attenuation response is unknown. However, the data are sufficiently positive to indicate that the nature of the secretory defect resides directly within the GH cells. Author

N90-13942*# Louisville Univ., KY. Dept. of Microbiology and Immunology.

RESPONSE OF LYMPHOCYTES TO A MITOGENIC STIMULUS DURING SPACEFLIGHT

Gerald Sonnenfeld *In* NASA, Ames Research Center, Cells in Space Aug. 1989 p 77-85 (For primary document see N90-13939 05-55)

(Contract NCC2-213; NAG9-181; NAG9-234)
Avail: NTIS HC A14/MF A02 CSCL 06C

Several studies were performed that demonstrate that immunological activities of lymphocytes can be affected by spaceflight or by models that attempt to simulate some aspects of weightlessness. Included among these are the responses of lymphocytes to external stimuli such as mitogens and viruses. When cultures of lymphocytes were flown in space, the ability of the lymphocytes to respond to mitogens was inhibited. Similar results were obtained when lymphocytes from astronauts or animals just returned from space were placed into culture immediately upon return to earth, and when models of hypogravity were used. Lymphocytes placed in culture during spaceflights produced enhanced levels of interferon compared to control cultures. When cultures of lymphocytes were prepared for cosmonauts or rodents immediately upon return to earth, interferon production was inhibited. These results suggest that space flight can have profound effects on lymphocyte function, and that effects on isolated cells may be different from that on cells in the whole organism.

Author

N90-13943*# State Univ. of New York, Stony Brook. Dept. of Biochemistry.

POLARITY ESTABLISHMENT, MORPHOGENESIS, AND CULTURED PLANT CELLS IN SPACE

Abraham D. Krikorian *In* NASA, Ames Research Center, Cells in Space Aug. 1989 p 87-95 (For primary document see N90-13939 05-55)

(Grant NsG-7270)
Avail: NTIS HC A14/MF A02 CSCL 06C

Plant development entails an orderly progression of cellular events both in terms of time and geometry. There is only circumstantial evidence that, in the controlled environment of the higher plant embryo sac, gravity may play a role in embryo development. It is still not known whether or not normal embryo development and differentiation in higher plants can be expected to take place reliably and efficiently in the micro g space environment. It seems essential that more attention be given to studying aspects of reproductive biology in order to be confident that plants will survive seed to seed to seed in a space environment. Until the time arrives when successive generations of plants can be grown, the best that can be done is utilize the most appropriate systems and begin, piece meal, to accumulate information on important aspects of plant reproduction. Cultured plant cells can play an important role in these activities since they can be grown so as to be morphogenetically competent, and thus can simulate those embryogenic events more usually identified with fertilized eggs in the embryo sac of the ovule in the ovary. Also, they can be manipulated with relative ease. The extreme plasticity of such demonstrably totipotent cell systems provides a means to test environmental effects such as micro g on a potentially free-running entity. The successful manipulation and management of plant cells and propagules in space also has significance for exploitation of biotechnologies in space since such systems, perforce, are an important vehicle whereby many genetic engineering manipulations are achieved. Author

N90-13944*# Loma Linda Univ., CA. Dept. of Microbiology.

THE SENSORY TRANSDUCTION PATHWAYS IN BACTERIAL CHEMOTAXIS

Barry L. Taylor *In* NASA, Ames Research Center, Cells in Space Aug. 1989 p 97-102 (For primary document see N90-13939 05-55)

Avail: NTIS HC A14/MF A02 CSCL 06C

Bacterial chemotaxis is a useful model for investigating in molecular detail the behavioral response of cells to changes in their environment. Peritrichously flagellated bacteria such as coli and typhimurium swim by rotating helical flagella in a counterclockwise direction. If flagellar rotation is briefly reversed, the bacteria tumble and change the direction of swimming. The bacteria continuously sample the environment and use a temporal sensing mechanism to compare the present and immediate past environments. Bacteria respond to a broad range of stimuli including changes in temperature, oxygen concentration, pH and osmotic strength. Bacteria are attracted to potential sources of nutrition such as sugars and amino acids and are repelled by other chemicals. In the methylation-dependent pathways for sensory transduction and adaptation in E. coli and S. typhimurium, chemoeffectors bind to transducing proteins that span the plasma membrane. The transducing proteins are postulated to control the rate of autophosphorylation of the CheA protein, which in turn phosphorylates the CheY protein. The phospho-CheY protein binds to the switch on the flagellar motor and is the signal for clockwise rotation of the motor. Adaptation to an attractant is achieved by increasing methylation of the transducing protein until the attractant stimulus is cancelled. Responses to oxygen and certain sugars involve methylation-independent pathways in which adaption occurs without methylation of a transducing protein. Taxis toward oxygen is mediated by the electron transport system and changes in the proton motive force. Recent studies have shown that the methylation-independent pathway converges with the methylation-dependent pathway at or before the CheA protein.

Author

N90-13945*# National Inst. of Standards and Technology, Boulder, CO. Chemical Engineering Science Div.

PHYSICAL PHENOMENA AND THE MICROGRAVITY RESPONSE

Paul Todd *In* NASA, Ames Research Center, Cells in Space Aug. 1989 p 103-116 (For primary document see N90-13939 05-55)

Avail: NTIS HC A14/MF A02 CSCL 06C

The living biological cell is not a sack of Newtonian fluid containing systems of chemical reactions at equilibrium. It is a kinetically driven system, not a thermodynamically driven system. While the cell as a whole might be considered isothermal, at the scale of individual macromolecular events there is heat generated, and presumably sharp thermal gradients exist at the submicron level. Basic physical phenomena to be considered when exploring the cell's response to inertial acceleration include particle sedimentation, solutal convection, motility electrokinetics, cytoskeletal work, and hydrostatic pressure. Protein crystal growth experiments, for example, illustrate the profound effects of convection currents on macromolecular assembly. Reaction kinetics in the cell vary all the way from diffusion-limited to life-time limited. Transport processes vary from free diffusion, to facilitated and active transmembrane transport, to contractile-protein-driven motility, to crystalline immobilization. At least four physical states of matter exist in the cell: aqueous, non-aqueous, immiscible-aqueous, and solid. Levels of order vary from crystalline to free solution. The relative volumes of these states profoundly influence the cell's response to inertial acceleration. Such subcellular phenomena as stretch-receptor activation, microtubule re-assembly, synaptic junction formation, chemotactic receptor activation, and statolith sedimentation were studied recently with

respect to both their basic mechanisms and their responsiveness to inertial acceleration. From such studies a widespread role of cytoskeletal organization is becoming apparent. Author

N90-13946*# Washington Univ., Seattle. Dept. of Botany.
HOW TO DETECT WHEN CELLS IN SPACE PERCEIVE GRAVITY
Thomas Bjoerkman *In* NASA, Ames Research Center, Cells in Space Aug. 1989 p 117-120 (For primary document see N90-13939 05-55)
Avail: NTIS HC A14/MF A02 CSCL 06C

It is useful to be able to measure when and whether cells detect gravity during spaceflights. For studying gravitational physiology, gravity perception is the response the experimentalist needs to measure. Also, for growing plants in space, plant cells may have a non-directional requirement for gravity as a development cue. The main goals of spaceflight experiments in which gravity perception would be measured are to determine the properties of the gravity receptor and how it is activated, and to determine fundamental characteristics of the signal generated. The main practical difficulty with measuring gravity sensing in space is that gravity sensing cannot be measured with certainty on earth. Almost all experiments measure gravitropic curvature. Reciprocity and intermittent stimulation are measurements which were made to some degree on earth using clinostatting, but which would provide clearer results if done with microgravity rather than clinostatting. These would be important uses of the space laboratory for determining the nature of gravity sensing in plants. Those techniques which do not use gravitropic curvature to measure gravity sensing are electrophysiological. The vibrating probe would be somewhat easier to adapt to space conditions than the intracellular microelectrode because it can be positioned with less precision. Ideally, a non-invasive technique would be best suited if an appropriate measure could be developed. Thus, the effect of microgravity on cultured cells is more likely to be by large-scale physical events than gravity sensing in the culture cells. It is not expected that it will be necessary to determine whether individual cultured cells perceive gravity unless cells grow abnormally even after the obvious microgravity effects on the culture as a whole can be ruled out as the cause. Author

N90-13947*# Michigan State Univ., East Lansing. Dept. of Botany.
EFFECTS OF MICROGRAVITY ON GROWTH HORMONE CONCENTRATION AND DISTRIBUTION IN PLANTS
Aga Schulze, Philip Jensen, Mark Desrosiers, and Robert S. Bandurski *In* NASA, Ames Research Center, Cells in Space Aug. 1989 p 121-131 (For primary document see N90-13939 05-55)
Avail: NTIS HC A14/MF A02 CSCL 06C

On earth, gravity affects the distribution of the plant growth hormone, indole-3-acetic acid (IAA), in a manner such that the plant grows into a normal vertical orientation (shoots up, roots down). How the plant controls the amount and distribution of IAA is only partially understood and is currently under investigation in this laboratory. The question to be answered in the flight experiment concerns the effect of gravity on the concentration, turn over, and distribution of the growth hormone. The answer to this question will aid in understanding the mechanism by which plants control the amount and distribution of growth hormone. Such knowledge of a plant's hormonal metabolism may aid in the growth of plants in space and will lead to agronomic advances. Author

N90-13948*# University City Science Center, Philadelphia, PA. Gravitational Plant Physiology Lab.
GRAVITY RECEPTORS AND RESPONSES
Allan H. Brown *In* NASA, Ames Research Center, Cells in Space Aug. 1989 p 133-138 (For primary document see N90-13939 05-55)
Avail: NTIS HC A14/MF A02 CSCL 06C

The overall process of gravity sensing and response processes in plants may be divided conveniently into at least four components or stages: Stimulus susception (a physical event, characteristically the input to the G receptor system of environmental information about the G force magnitude, its vector direction, or both); information perception (an influence of susception on some biological structure or process that can be described as the transformation of environmental information into a biologicallly meaningful change); information transport (the export, if required, of an influence (often chemical) to cells and organs other than those at the sensor location); and biological response (almost always (in plants) a growth change of some kind). Some analysts of the process identify, between information perception and information transport, an additional stage, transduction, which would emphasize the importance of a transformation from one form of information to another, for example from mechanical statolith displacement to an electric, chemical, or other alteration that was its indirect result. These four (or five) stages are temporally sequential. Even if all that occurs at each stage can not be confidently identified, it seems evident that during transduction and transport, matters dealt with are found relatively late in the information flow rather than at the perception stage. As more and more is learned about the roles played by plant hormones which condition the G responses, the mechanism(s) of perception which should be are not necessarily better understood. However, if by asking the right questions and being lucky with experiments perhaps the discovery of how some process (such as sedimentation of protoplasmic organelles) dictates what happens down stream in the information flow sequence may be made. Author

N90-13949*# Arizona Univ., Tucson. Dept. of Physics.
FREE SWIMMING ORGANISMS: MICROGRAVITY AS AN INVESTIGATIVE TOOL
John O. Kessler *In* NASA, Ames Research Center, Cells in Space Aug. 1989 p 139-152 (For primary document see N90-13939 05-55)
Avail: NTIS HC A14/MF A02 CSCL 06C

On earth, micro-organisms are in the grip of gravitational and viscous forces. These forces, in combination with sensory stimuli, determine the average orientation of the organisms' swimming trajectories relative to the fluid environment. Microgravity provides the opportunity to study the rules which govern the summation or orienting influences and to develop quantitative physical measurements of sensory responses, e.g. the measurement of phototactic orientation tendency in torque units. Also, by reducing or eliminating density anisotropy-driven buoyant convection, it will be possible to study illumination, temperature gradient and concentration gradient-mediated collective dynamics. Author

N90-13950*# Pennsylvania State Univ., University Park. Dept. of Biology.
GRAVITROPISM IN PLANTS: HYDRAULICS AND WALL GROWTH PROPERTIES OF RESPONDING CELLS
Daniel J. Cosgrove *In* NASA, Ames Research Center, Cells in Space Aug. 1989 p 153-156 (For primary document see N90-13939 05-55)
Avail: NTIS HC A14/MF A02 CSCL 06C

Gravitropism is the asymmetrical alteration of plant growth in response to a change in the gravity vector, with the typical result that stems grow up and roots grow down. The gravity response is important for plants because it enables them to grow their aerial parts in a mechanically stable (upright) position and to develop their roots and leaves to make efficient use of soil nutrients and sunlight. The elucidation of gravitropic responses will tell much about how gravity exerts its morphogenetic effects on plants and how plants regulate their growth at the cellular and molecular levels. Author

N90-13951*# California Univ., Davis.
GRAVITY AND ANIMAL EMBRYOS
Lynn M. Wiley *In* NASA, Ames Research Center, Cells in Space Aug. 1989 p 157-160 (For primary document see N90-13939 05-55)
Avail: NTIS HC A14/MF A02 CSCL 06C

Out of more than 4,500 rat hours in space there was only one experimental attempt (Cosmos 1129) at mating with an

apparent absence of fertilization, implantation and subsequent development to term and partuition. Portions of this process were successfully flown, however, including the major portion of organogenesis in the rat (Cosmos 1524). These observations show that the cellular and molecular events underlying morphogenesis and differentiation in a small mammal can proceed normally in-utero under microgravity and other conditions encountered during short-duration flight. However, it is not known whether this situation will hold for larger mammals over several generations during extended missions that venture outside of near Earth. Furthermore, it is not understood why the previous attempt at obtaining copulation, fertilization and implantation in orbit failed but may be related to limitations of the rat habitat for meeting the preconditions for reproductive behavior. With respect to mammalian development it is important to appreciate that fertilization and development occur internally within the female and take a long time to complete and their success will, therefore, be contingent upon the maternal response to the space environment. One process central to development (the establishment of cell lines) is initiated prior to implantation by environmental asymmetries preceived by progenitor cells. These asymmetries appear to result from the formation of asymmetric cell-cell contacts and the concommitant development of an electrical axis across the progenitor cells. Other asymmetries were also documented. It is not known whether any of the known asymmetries perceived by progenitor cells are influenced by gravity vectors and/or by the maternal response to microgravity and other conditions encountered in space. Author

N90-13952*# Lockheed Missiles and Space Co., Sunnyvale, CA. Bioastronautics Div.

HUMAN FACTORS ISSUES IN PERFORMING LIFE SCIENCE EXPERIMENTS IN A 0-G ENVIRONMENT

Wayne Gonzalez *In* NASA, Ames Research Center, Cells in Space Aug. 1989 p 161-165 (For primary document see N90-13939 05-55)

Avail: NTIS HC A14/MF A02 CSCL 06C

An overview of the environmental conditions within the Spacelab and the planned Space Station Freedom is presented. How this environment causes specific Human Factors problems and the nature of design solutions are described. The impact of these problems and solutions on the performance of life science activities onboard Spacelab (SL) and Space Station Freedom (SSF) is discussed. The first area highlighted is contamination. The permanence of SSF in contrast to the two-week mission of SL has significant impacts on crew and specimen protection requirements and, thus, resource utilization. These requirements, in turn impose restrictions on working volumes, scheduling, training, and scope of experimental procedures. A second area is microgravity. This means that all specimens, materials, and apparatus must be restrained and carefully controlled. Because so much of the scientific activity must occur within restricted enclosures (gloveboxes), the provisions for restraint and control are made more complex. The third topic is crewmember biomechanics and the problems of movement and task performance in microgravity. In addition to the need to stabilize the body for the performance of tasks, performance of very sensitive tasks such as dissection is difficult. The issue of space sickness and adaption is considered in this context. Author

N90-13953*# Pennsylvania Univ., Philadelphia.

DO THE DESIGN CONCEPTS USED FOR THE SPACE FLIGHT HARDWARE DIRECTLY AFFECT CELL STRUCTURE AND/OR CELL FUNCTION GROUND BASED SIMULATIONS

David K. Chapman *In* NASA, Ames Research Center, Cells in Space Aug. 1989 p 167-176 (For primary document see N90-13939 05-55)

Avail: NTIS HC A14/MF A02 CSCL 06C

The use of clinostats and centrifuges to explore the hypogravity range between zero and 1 g is described. Different types of clinostat configurations and clinostat-centrifuge combinations are compared. Some examples selected from the literature and current research in gravitational physiology are presented to show plant responses in the simulated hypogravity region of the g-parameter (0 is greater than g is greater than 1). The validation of clinostat simulation is discussed. Examples in which flight data can be compared to clinostat data are presented. The data from 3 different laboratories using 3 different plant species indicate that clinostat simulation in some cases were qualitatively similar to flight data, but that in all cases were quantitatively different. The need to conduct additional tests in weightlessness is emphasized. Author

N90-13954*# Jet Propulsion Lab., California Inst. of Tech., Pasadena.

MODEL SYSTEM STUDIES WITH A PHASE SEPARATED MEMBRANE BIOREACTOR

G. R. Petersen, P. K. Seshan, and Eric H. Dunlop (Colorado State Univ., Fort Collins.) *In* NASA, Ames Research Center, Cells in Space Aug. 1989 p 177-185 (For primary document see N90-13939 05-55)

Avail: NTIS HC A14/MF A02 CSCL 06C

The operation and evaluation of a bioreactor designed for high intensity oxygen transfer in a microgravity environment is described. The reactor itself consists of a zero headspace liquid phase separated from the air supply by a long length of silicone rubber tubing through which the oxygen diffuses in and the carbon dioxide diffuses out. Mass transfer studies show that the oxygen is film diffusion controlled both externally and internally to the tubing and not by diffusion across the tube walls. Methods of upgrading the design to eliminate these resistances are proposed. Cell growth was obtained in the fermenter using Saccharomyces cerevisiae showing that this concept is capable of sustaining cell growth in the terrestial simulation. Author

N90-13955*# Jet Propulsion Lab., California Inst. of Tech., Pasadena.

DESIGN CHALLENGES FOR SPACE BIOREACTORS

P. K. Seshan and G. R. Petersen *In* NASA, Ames Research Center, Cells in Space Aug. 1989 p 187-205 (For primary document see N90-13939 05-55)

Avail: NTIS HC A14/MF A02 CSCL 06C

The design of bioreactors for operation under conditions of microgravity presents problems and challenges. Absence of a significant body force such as gravity can have profound consequences for interfacial phenomena. Marangoni convection can no longer be overlooked. Many speculations on the advantages and benefits of microgravity can be found in the literature. Initial bioreactor research considerations for space applications had little regard for the suitability of the designs for conditions of microgravity. Bioreactors can be classified in terms of their function and type of operation. The complex interaction of parameters leading to optimal design and operation of a bioreactor is illustrated by the JSC mammalian cell culture system. The design of a bioreactor is strongly dependent upon its intended use as a production unit for cell mass and/or biologicals or as a research reactor for the study of cell growth and function. Therefore a variety of bioreactor configurations are presented in rapid summary. Following this, a rationale is presented for not attempting to derive key design parameters such as the oxygen transfer coefficient from ground-based data. A set of themes/objectives for flight experiments to develop the expertise for design of space bioreactors is then proposed for discussion. These experiments, carried out systematically, will provide a database from which engineering tools for space bioreactor design will be derived. Author

N90-13956*# Colorado State Univ., Fort Collins. Dept. of Chemical Engineering.

FERMENTATION AND OXYGEN TRANSFER IN MICROGRAVITY

Eric H. Dunlop *In* NASA, Ames Research Center, Cells in Space Aug. 1989 p 207-211 (For primary document see N90-13939 05-55)

Avail: NTIS HC A14/MF A02 CSCL 06C

The need for high rate oxygen transfer in microgravity for a Controlled Ecological Life Support System (CELSS) environment offers a number of difficulties and challenges. The use of a phase

separated bioreactor appears to provide a way of overcoming these problems resulting in a system capable of providing high cell densities with rapid fermentation rates. Some of the key design elements are discussed. Author

N90-13957*# Colorado Univ., Boulder. Aerospace Engineering Sciences and Bioserve Space Technologies.
COUNTERMEASURES TO MICROGRAVITY
Marvin W. Luttges *In* NASA, Ames Research Center, Cells in Space Aug. 1989 p 213-220 (For primary document see N90-13939 05-55)
Avail: NTIS HC A14/MF A02 CSCL 06C

Biological systems ranging from the most simple to the most complex generally survive exposure to microgravity. Changes in many characteristics of biological systems are well documented as a consequence of space flight. Attempts to devise countermeasures to microgravity may have direct pragmatic consequences for crew protection and may provide additional insights into the nature of microgravity influences on biological systems. Some of the most well documented changes occur in humans who have experienced space flight. Changes appear to be transient. Space adaption syndrome occurs relatively briefly whereas bone deterioration may require months of postflight time for restoration. It seems critical to recognize that these changes and others may derive from rather passive, active or even reactive changes in the biological systems that are hosts to them. For example, hydrostatic fluid redistributions may be quite passive occurrences that are realized through extensive fluid channels. Changes occur in cell metabolism because of fluid, nutrient and gas redistributions. Equally important are the misconstrued messages likely to be carried by fluid redistributions. These reactive events can trigger, for example, loss of fluids and electrolytes through altered kidney function. Each of these considerations must be evaluated in regard to the biological site affected. Countermeasures to the vast range of biological changes and sites are difficult to envision. The most obvious countermeasure is the restoration of gravity-like influences. Some options are discussed. Recent work has focussed on the use of magnetic fields. Pulsed electromagnetic fields (PEMF) are shown to alleviate bone deterioration produced in rodents exposed to tail suspension. Methods of PEMF exposure are consistent with human use in space. Related methods may provide muscular and neural benefits. Author

N90-13958*# Lunar Radiation Corp., Madison, WI.
BONE MINERAL MEASUREMENT USING DUAL ENERGY X RAY DENSITOMETRY
Steven W. Smith *In* NASA, Ames Research Center, Cells in Space Aug. 1989 p 221-224 (For primary document see N90-13939 05-55)
Avail: NTIS HC A14/MF A02 CSCL 06C

Bone mineral measurements before and after space missions have shown that weightlessness greatly accelerates bone demineralization. Bone mineral losses as high as 1 to 3 percent per month were reported. Highly precise instrumentation is required to monitor this loss and thereby test the efficacy of treatment. During the last year, a significant improvement was made in Dual-Photon Absorptiometry by replacing the radioactive source with an x ray tube. Advantages of this system include: better precision, lower patient dose, better spacial resolution, and shorter scan times. The high precision and low radiation dose of this technique will allow detection of bone mineral changes of less than 1 percent with measurements conducted directly at the sites of interest. This will allow the required bone mineral studies to be completed in a shorter time with greater confidence. Author

59 MATHEMATICAL AND COMPUTER SCIENCES (GENERAL)

No abstracts in this category.

60 COMPUTER OPERATIONS AND HARDWARE

Includes hardware for computer graphics, firmware, and data processing.

For components see *33 Electronics and Electrical Engineering.*

N90-13959# Naval Postgraduate School, Monterey, CA.
PROJECT ORION MICROCOMPUTER MANAGEMENT SYSTEM M.S. Thesis
Richard B. Darden Sep. 1988 64 p
(AD-A212945) Avail: NTIS HC A04/MF A01 CSCL 12/7

This thesis describes the development of a microcomputer project management system for the Space Systems Academic Group (SSAG) at the Naval Postgraduate School. The focus of the paper is on system requirements and implementation to manage Project ORION. Project ORION is a high technology mini-satellite venture under direction of the SSAG. It involves the design, procurement, fabrication and testing of the satellite in the planning, scheduling and controlling phases of project management. Conclusions define key factors important in the implementation process such as organizational responsibilities, quantification of planning detail, personnel training and operating procedures. GRA

N90-13960# Illinois Univ., Urbana. Coordinated Science Lab.
EFFICIENT ON-LINE SIMULATIONS OF TREE MACHINES AND MULTIDIMENSIONAL TURING MACHINES BY RANDOM ACCESS MACHINES
Michael C. Loui and David R. Luginbuhl 24 Aug. 1989 33 p
Sponsored in cooperation with the AF Inst. of Tech.
(Contract N00014-85-K-0570)
(AD-A213152; UILU-ENG-89-2222; ACT-108) Avail: NTIS HC A03/MF A01 CSCL 12/6

The random access machine (RAM) and the Turing machine (TM) are the standard models for sequential computation. Research into the use to time and space by these and other models gives insight into their computational power. How two different models use time and space is analyzed, and time and space utilization is compared within a single model. Another avenue of investigation is determining how altering the definitions of time and space (for example, log-cost versus unit-cost) for a model affects its computational power. Slot and van Emde Boas (1988), for example, showed how space equivalence of RAMs and Turing machines is affected by varying the definition of space complexity for RAMs. An on-line systems simulation is presented of a tree machine of time complexity t by a log-cost RAM of time complexity O((T log T)/log log t). Using the notion of incompressibility from Kolmogorov complexity (Li and Vitanyi, 1988), it is shown that this simulation is optimal. This appears to be the first application of Kolmogorov complexity to sequential RAMs. It is significant because few algorithms have been shown to be optimal. This work is a complement to Loui's (1983) simulation of tree machines by multidimensional Turing machines and Reischuk's (1982) simulation of multidimensional Turing machines by tree machines. GRA

N90-13961 British Petroleum Co. Ltd., London (England).
MEMORY MATRIX Patent Application
Peter Brian Denyer, inventor and Keith Allen Sabine, inventor 17 Nov. 1987 18 p
(WO-Patent-88/04096; WO-Patent-Appl-SN-PCT/G-B87/00;

Int-Patent-Class-G11C-11/34; ETN-90-95243) Avail: World Intellectual Property Organization, 34 Chemin des Colombettes, CH-1211 Geneva 20, Switzerland

A patent application concerning an electrical programmable memory matrix is discussed. It comprises a plurality of memory cells of layered amorphous or microcrystalline semiconductor (silicon). These can be repeatedly switched between high and low conductance states by voltages of alternate polarity. For each cell there is a single row line and a pair of column lines. The matrix comprises write-enable means and means for maintaining voltage difference between paris of column lines below that sufficient to write to a cell in the absence of a write-enable signal. ESA

61 COMPUTER PROGRAMMING AND SOFTWARE

Includes computer programs, routines, alogorithms, and specific applications, e.g., CAD/CAM.

N90-13962*# Auburn Univ., AL. Dept. of Computer Science and Engineering.

THE DEVELOPMENT OF A PROGRAM ANALYSIS ENVIRONMENT FOR Ada

David B. Brown, Homer W. Carlisle, Kai-Hsiung Chang, James H. Cross, William H. Deason, Kevin D. Haga, John R. Huggins, William R. A. Keleher, Benjamin B. Starke, and Orville R. Weyrich et al 1 Jun. 1989 155 p

(Contract NCC8-14)

(NASA-CR-185860; NAS 1.26:185860) Avail: NTIS HC A08/MF A01 CSCL 09B

A unit level, Ada software module testing system, called Query Utility Environment for Software Testing of Ada (QUEST/Ada), is described. The project calls for the design and development of a prototype system. QUEST/Ada design began with a definition of the overall system structure and a description of component dependencies. The project team was divided into three groups to resolve the preliminary designs of the parser/scanner: the test data generator, and the test coverage analyzer. The Phase 1 report is a working document from which the system documentation will evolve. It provides history, a guide to report sections, a literature review, the definition of the system structure and high level interfaces, descriptions of the prototype scope, the three major components, and the plan for the remainder of the project. The appendices include specifications, statistics, two papers derived from the current research, a preliminary users' manual, and the proposal and work plan for Phase 2. J.P.S.

N90-13963*# Nebraska Univ., Lincoln. Dept. of Electrical Engineering.

IMPLEMENTATION ISSUES IN SOURCE CODING Semiannual Status Report

Khalid Sayood, Yun-Chung Chen, and A. C. Hadenfeldt 6 Oct. 1989 123 p

(Grant NAG5-916)

(NASA-CR-185327; NAS 1.26:185327) Avail: NTIS HC A06/MF A01 CSCL 09B

An edge preserving image coding scheme which can be operated in both a lossy and a lossless manner was developed. The technique is an extension of the lossless encoding algorithm developed for the Mars observer spectral data. It can also be viewed as a modification of the DPCM algorithm. A packet video simulator was also developed from an existing modified packet network simulator. The coding scheme for this system is a modification of the mixture block coding (MBC) scheme described in the last report. Coding algorithms for packet video were also investigated. K.C.D.

N90-13964*# Alabama Univ., Huntsville. Dept. of Electrical and Computer Engineering.

SOFTWARE DEVELOPMENT FOR AVIONICS SSME CONTROL AND DIAGNOSTICS Final Report

A. Choudry Aug. 1989 34 p

(Contract NCC8-13)

(NASA-CR-184894; NAS 1.26:184894; UAH-RR-810) Avail: NTIS HC A03/MF A01 CSCL 09B

A study was made of software to integrate data from about 500 sensors that monitor the Space Shuttle Main Engine (SSME) and to make decisions for real-time control. Such software is expected to be applicable to other distributed systems as well. This study investigated the use of pattern recognition and other techniques to detect trends that could lead to major damage to the SSME and which would allow an orderly shutdown of the SSME before such damage could occur. J.P.S.

N90-13965*# Alabama Univ., Huntsville.

METHODOLOGY FOR AUTOMATING SOFTWARE SYSTEMS. TASK 1 OF THE FOUNDATIONS FOR AUTOMATING SOFTWARE SYSTEMS Final Report

Warren Moseley 1989 63 p

(Contract NCC8-13)

(NASA-CR-180499; NAS 1.26:180499; UA-Rept-814) Avail: NTIS HC A04/MF A01 CSCL 09B

The early stages of a research program designed to establish an experimental research platform for software engineering are described. Major emphasis is placed on Computer Assisted Software Engineering (CASE). The Poor Man's CASE Tool is based on the Apple Macintosh system, employing available software including Focal Point II, Hypercard, XRefText, and Macproject. These programs are functional in themselves, but through advanced linking are available for operation from within the tool being developed. The research platform is intended to merge software engineering technology with artificial intelligence (AI). In the first prototype of the PMCT, however, the sections of AI are not included. CASE tools assist the software engineer in planning goals, routes to those goals, and ways to measure progress. The method described allows software to be synthesized instead of being written or built. J.P.S.

N90-13966*# Houston Univ., Clear Lake, TX. Research Inst. for Computing and Information Systems.

SOFTWARE ENGINEERING AND ADA (TRADEMARK) TRAINING: AN IMPLEMENTATION MODEL FOR NASA

Sue LeGrand (Softech, Inc., Houston, TX.) and Glenn Freedman 27 Jun. 1988 26 p Presented at the Washington Ada (Trademark) Symposium, Washington, DC, 27 Jun. 1988

(Contract NCC9-16)

(NASA-CR-186071; NAS 1.26:186071) Avail: NTIS HC A03/MF A01 CSCL 09B

The choice of Ada for software engineering for projects such as the Space Station has resulted in government and industrial groups considering training programs that help workers become familiar with both a software culture and the intricacies of a new computer language. The questions of how much time it takes to learn software engineering with Ada, how much an organization should invest in such training, and how the training should be structured are considered. Software engineering is an emerging, dynamic discipline. It is defined by the author as the establishment and application of sound engineering environments, tools, methods, models, principles, and concepts combined with appropriate standards, guidelines, and practices to support computing which is correct, modifiable, reliable and safe, efficient, and understandable throughout the life cycle of the application. Neither the training programs needed, nor the content of such programs, have been well established. This study addresses the requirements for training for NASA personnel and recommends an implementation plan. A curriculum and a means of delivery are recommended. It is further suggested that a knowledgeable programmer may be able to learn Ada in 5 days, but that it takes 6 to 9 months to evolve into a software engineer who uses the

language correctly and effectively. The curriculum and implementation plan can be adapted for each NASA Center according to the needs dictated by each project. J.P.S.

N90-13967*# Houston Univ., Clear Lake, TX. Research Inst. for Computing and Information Systems.
ADA TASK SCHEDULING: A FOCUSED ADA INVESTIGATION Final Report
Sue LeGrand (Softech, Inc., Houston, TX.) 5 Oct. 1988 37 p Prepared for NASA, Washington, DC
(Contract NCC9-16)
(NASA-CR-186072; NAS 1.26:186072) Avail: NTIS HC A03/MF A01 CSCL 09B

The types of control that are important for real time task scheduling are discussed. Some closely related real time issues are mentioned and major committee and research activities in this area are delineated. Although there are some problems with Ada and its real time task scheduling, Ada presents fewer than any known alternative. Ada was designed for the domain of real time embedded systems, but Ada compilers may not contain a level of task scheduling support that is adequate for all real time applications. The question addressed is which implementations of Ada's task scheduling are adequate for effective real time systems for NASA applications. J.P.S.

N90-13968*# Sverdrup Technology, Inc., Cleveland, OH.
AN INTERACTIVE GRID GENERATION PROCEDURE FOR AXIAL AND RADIAL FLOW TURBOMACHINERY Final Report
Timothy A. Beach Nov. 1989 13 p Presented at the 28th Aerospace Sciences Meeting, Reno, NV, 8-11 Jan. 1990; sponsored by AIAA
(Contract NAS3-25266)
(NASA-CR-185167; E-5151; NAS 1.26:185167; AIAA-90-0344)
Avail: NTIS HC A03/MF A01 CSCL 09B

A combination algebraic/elliptic technique is presented for the generation of three dimensional grids about turbo-machinery blade rows for both axial and radial flow machinery. The technique is built around use of an advanced engineering workstation to construct several two dimensional grids interactively on predetermined blade-to-blade surfaces. A three dimensional grid is generated by interpolating these surface grids onto an axisymmetric grid. On each blade-to-blade surface, a grid is created using algebraic techniques near the blade to control orthogonality within the boundary layer region and elliptic techniques in the mid-passage to achieve smoothness. The interactive definition of bezier curves as internal boundaries is the key to simple construction. This procedure lends itself well to zonal grid construction, an important example being the tip clearance region. Calculations done to date include a space shuttle main engine turbopump blade, a radial inflow turbine blade, and the first stator of the United Technologies Research Center large scale rotating rig. A finite Navier-Stokes solver was used in each case. Author

N90-13969# Massachusetts Inst. of Tech., Cambridge. Microsystems Research Center.
COMPUTER-AIDED FABRICATION SYSTEM IMPLEMENTATION Final Technical Report, 1 Apr. 1985 - 31 Dec. 1988
Paul Penfield, Jr., Dimitri A. Antoniadis, Stanley B. Gershwin, Emanuel M. Sachs, Stephen D. Senturia, and Donald E. Troxel 31 Dec. 1988 30 p
(Contract N00014-85-K-0213; ARPA Order 5339)
(AD-A213005) Avail: NTIS HC A03/MF A01 CSCL 09/1

The major objective of this contract was to develop a computer system to aid the fabrication of VLSI integrated circuits. Particular attention was paid to use of university and industry standards in the system, and an open architecture. Other objectives of this contract were to extend the system architecture to encompass mechanical properties of integrated circuits, particularly as these may affect reliability, and to incorporate models for VLSI fabrication equipment. GRA

N90-13970# University of Southern California, Marina del Rey. Information Sciences Inst.
PARALLELISM IN THE DISCRETE-EVENT SIMULATION ALGORITHM
Walid Najjar, Jean-Luc Jezouin, and Jean-Luc Gaudiot Jul. 1989 15 p
(Contract N00014-87-K-0022; NSF CCR-86-03772)
(AD-A213060; ISI/RR-89-227) Avail: NTIS HC A03/MF A01 CSCL 12/7

With the increasing complexity of very large scale integrate circuits, simulation on a digital computer system has become a primary means of low cost testing of new designs. However, a detailed behavioral simulation can be highly expensive in terms of computation loads. Simulation time can be reduced by distributing the problem over several processors. Indeed, the availability of commercial multiprocessors gives a new importance to parallel and distributed simulation. The techniques are surveyed that have been proposed to deal with this problem and then a new scheme is presented based on a consistent description of the system to be simulated, which allows a maximum exploitation of the parallelism inherent in the system. GRA

N90-13971# LNK Corp., Riverdale, MD.
NOVEL GRAPH SEARCHING METHODS FOR IMAGE ANALYSIS Final Report
Aug. 1989 60 p
(Contract N00014-87-C-0689)
(AD-A213065) Avail: NTIS HC A04/MF A01 CSCL 12/5

A generalization of the Artificial search algorithm, SSS asterisk, is given, allowing it to handle incomplete and inconsistent data. A parallel formulation of the generalized SSS asterisk is developed and implemented on a BBN Butterfly Plus parallel processor. In order to make the parallel version of SSS asterisk as efficient as possible, a concurrent heap data structure (based on the work of Nageshwara and Kumar) is utilized. Theoretical speedup due to the use of the concurrent heap is shown. An automatic tree generator is developed to allow the testing of parallel SSS asterisk on multiple trees. Empirical results are given for testing SSS asterisk on 1 to 40 processors. Speedup proportional to the number of processors for up to 24 processors is achieved depending on the size of the search space. A procedure for achieving rapid output of solutions by using a tradeoff between the estimated complexity and quality of solutions was developed. Finally, future directions for research are presented. GRA

N90-13972# Naval Postgraduate School, Monterey, CA.
A FAULT-TOLERANT SOFTWARE ALGORITHM FOR A NETWORK OF TRANSPUTERS M.S. Thesis
William Fred Benage, Jr. Jun. 1989 60 p
(AD-A213092) Avail: NTIS HC A04/MF A01 CSCL 12/5

This thesis presents a software algorithm that resends work packages to processors when one or more of the worker processors fails or when the link with one or more processors fails. There are two resend criteria used in this algorithm: resend at end of initial assignment and resend at time out. The work, divided into several packages in order to run on several processors in parallel, will be completed as long as at least one worker processor remains working and communicating with the main processor. This algorithm could add some fault-tolerance to computer processing equipment in embedded systems. GRA

N90-13973# Royal Signals and Radar Establishment, Malvern (England).
SIMOGEN: AN OBJECT-ORIENTED LANGUAGE FOR SIMULATION
C. A. Arthur Mar. 1989 26 p
(AD-A213129; RSRE-Memo-4279; DRIC-BR-110829) Avail: NTIS HC A03/MF A01 CSCL 12/5

The Simogen language has been designed specifically to provide a user-friendly environment for computer modellers. It is a heavily object-oriented language, but has been designed to be easy to pick up for the most inexperienced of users, rather than to exploit the full power of the object-oriented paradigm in all

cases. This paper looks at the reasons why it was felt necessary to create a new language, and considers the reasons behind the particular design chosen. It also describes the language in outline, and discusses briefly to what extent the language can be said to be object-oriented. Finally, an outline is given of a possible iconic interface for the language, to ease it's use still further. GRA

N90-13974# Naval Postgraduate School, Monterey, CA.
COMPRESSION OF BITMAPPED GRAPHIC DATA M.S. Thesis
Jane Lee Kretzmann Jun. 1989 90 p
(AD-A213141) Avail: NTIS HC A05/MF A01 CSCL 12/5

This paper explores the general topic of data compression, with emphasis on application of the techniques to graphic bitmapped data. Run-length encoding, statistical encoding (including Huffman codes), and relative encoding are examined and evaluated. A compression application of the Huffman coding of a run-length encoded file is designed and partially implemented in Chapter 7. A listing of the computer program which performs the compression is included as an appendix. Possibilities for further study are suggested. GRA

N90-13975# Thomson-CSF, Palo Alto, CA. Pacific Rim Operations.
MULTI-LEVEL SPECIFICATION AND VERIFICATION OF REAL-TIME SOFTWARE
Armen Gabrielian and Matthew K. Franklin Jul. 1989 22 p
(Contract N00014-89-C-0022)
(AD-A213227; TR-89-14) Avail: NTIS HC A03/MF A01 CSCL 12/5

A state based approach is presented for specification of real-time software at multiple levels of abstraction. In this approach, specification at each level is performed in terms of a Hierarchical Multi-State (HMS) machine, with the higher levels defining requirements and the lower levels indicating methods of achieving the requirements. This leads to a considerable simplification of the specification process, can lead to reusability of specifications and is fundamentally different from the refinement approach to specification. A restricted method of verifying the consistency of multi-level specifications is also presented. By the use of this method, necessary scheduling of concurrent tasks to satisfy a complex set of logical and temporal constraints can be derived. GRA

N90-13976*# National Aeronautics and Space Administration. Goddard Space Flight Center, Greenbelt, MD.
ALGORITHM FOR ATMOSPHERIC CORRECTIONS OF AIRCRAFT AND SATELLITE IMAGERY
Robert S. Fraser, Yoram J. Kaufman, Richard A. Ferrare, and Shana Mattoo (Applied Research Corp., Landover, MD.) Dec. 1989 105 p
(Contract NAS5-30430; NAG5-203)
(NASA-TM-100751; Rept-90B00032; NAS 1.15:100751) Avail: NTIS HC A06/MF A01 CSCL 09B

A simple and fast atmospheric correction algorithm is described which is used to correct radiances of scattered sunlight measured by aircraft and/or satellite above a uniform surface. The atmospheric effect, the basic equations, a description of the computational procedure, and a sensitivity study are discussed. The program is designed to take the measured radiances, view and illumination directions, and the aerosol and gaseous absorption optical thickness to compute the radiance just above the surface, the irradiance on the surface, and surface reflectance. Alternatively, the program will compute the upward radiance at a specific altitude for a given surface reflectance, view and illumination directions, and aerosol and gaseous absorption optical thickness. The algorithm can be applied for any view and illumination directions and any wavelength in the range 0.48 micron to 2.2 micron. The relation between the measured radiance and surface reflectance, which is expressed as a function of atmospheric properties and measurement geometry, is computed using a radiative transfer routine. The results of the computations are presented in a table which forms the basis of the correction algorithm. The algorithm can be used for atmospheric corrections in the presence of a rural aerosol. The sensitivity of the derived surface reflectance to uncertainties in the model and input data is discussed. Author

N90-13977# Universiteit Twente, Enschede (Netherlands). Faculty of Applied Mathematics.
STOPPING RULES FOR A CLASS OF RANDOM METHODS FOR DETECTING NECESSARY LINEAR INEQUALITY CONSTRAINTS
R. J. Caron, J. F. McDonald, R. L. Smith (Michigan Univ., Ann Arbor.), and J. Telgen Mar. 1989 22 p
(MEMO-777; ISSN-0169-2690; ETN-90-95668) Avail: NTIS HC A03/MF A01

Random methods for detecting necessary linear inequality constraints, which produce a sequence of points in the polyhedral set represented by the contraints, are considered. A condition is given under which the points have a stationary limiting distribution on the interior of the polyhedral set. Under an additional condition, the limiting distribution is uniform. These results are used to justify the analysis used to develop two new stopping rules. The first stopping rule is based upon the number of iterations required to guarantee that, within a prespecified probability, all necessary constraints will have been identified. The second stopping rule is based upon the number of iterations required to identify a prespecified percentage of the necessary constraints. Computational results are given which validate the reliability of the stopping rules. ESA

N90-13978# Center for Mathematics and Computer Science, Amsterdam (Netherlands). Computer Science/Dept. of Software Technology.
ON THE SAFE APPROXIMATION OF PROLOG PROGRAMS
Kryzysztof R. Apt, Roland N. Bol, and Jan Willem Klop Apr. 1989 19 p Presented at the 6th International Conference on Logic Programming Submitted for publication
(CWI-CS-R8913; ETN-90-95657) Copyright Avail: NTIS HC A03/MF A01

Loop checking mechanisms for logic programs are systematically studied by considering their soundness, completeness, relative strength and related concepts. A natural concept of a simple loop check is introduced and it is proved that no sound and complete simple loop check exists, even for programs without function symbols. A number of sound simple loop checks are introduced, and a natural class of PROLOG programs for which they are complete are identified. In this class a limited form of recursion is allowed. As a by-product, an implementation of the closed world assumption of Reiter and a query evaluation algorithm for a class of logic programs without function symbols are obtained. ESA

N90-13979# Center for Mathematics and Computer Science, Amsterdam (Netherlands). Computer Science/Dept. of Software Technology.
CONSTRUCTING A CALCULUS OF PROGRAMS
Lambert G. L. T. Meertens Apr. 1989 28 p Presented at the International Conference on Mathematics of Program Construction Submitted for publication Sponsored by the Dutch National Facility for Infomratics and the Netherlands Organization for Scientific Research
(CWI-CS-R8914; ETN-90-95658) Copyright Avail: NTIS HC A03/MF A01

Program construction as a mathematical activity is studied. The need for powerful theories is discussed, and algorithmics, type system, functions, serial and parallel composition input sharing, combination laws, and locking and unlocking are addressed. An attempt is made to construct a system of combinators that is more amenable to manipulation than the classical ones. ESA

N90-13980# Technische Univ., Eindhoven (Netherlands). Dept. of Mathematics and Computing Science.
THE CELLULAR APPROACH: A NEW METHOD TO SPEED UP SIMULATED ANNEALING FOR MACRO PLACEMENT

Peter C. Schuur Oct. 1988 24 p
(MEMO-COSOR-88-29; ETN-90-95942) Avail: NTIS HC A03/MF A01

Considerable reduction in the computation time associated with the standard annealing algorithm for the macro placement problem is demonstrated. The most time consuming part of this algorithm is the evaluation of the difference in cost between the present and a candidate configuration. A cellular approach that greatly simplifies this calculation is introduced. If the number of rectangles is large compared to the average number of rectangle cells, then an annealing program based on the cellular approach is shown to perform significantly better. ESA

N90-13981*# Houston Univ., Clear Lake, TX. Research Inst. for Computing and Information Systems.
MICRO-BASED FACT COLLECTION TOOL USER'S MANUAL
Richard Mayer (Texas A&M Univ., College Station.) Nov. 1988 19 p
(Contract NCC9-16)
(NASA-CR-180414; NAS 1.26:180414) Avail: NTIS HC A03/MF A01 CSCL 09B

A procedure designed for use by an analyst to assist in the collection and organization of data gathered during the interview processes associated with system analysis and modeling task is described. The basic concept behind the development of this tool is that during the interview process an analyst is presented with assertions of facts by the domain expert. The analyst also makes observations of the domain. These facts need to be collected and preserved in such a way as to allow them to serve as the basis for a number of decision making processes throughout the system development process. This tool can be thought of as a computerization of the analysts's notebook. Author

N90-13982*# Houston Univ., Clear Lake, TX. Research Inst. for Computing and Information Systems.
Ada PROGRAMMING GUIDELINES FOR DETERMINISTIC STORAGE MANAGEMENT
David Auty (Softech, Inc., Houston, TX.) 29 Jan. 1988 65 p
(Contract NCC9-16)
(NASA-CR-181308; NAS 1.26:181308) Avail: NTIS HC A04/MF A01 CSCL 09B

Previous reports have established that a program can be written in the Ada language such that the program's storage management requirements are determinable prior to its execution. Specific guidelines for ensuring such deterministic usage of Ada dynamic storage requirements are described. Because requirements may vary from one application to another, guidelines are presented in a most-restrictive to least-restrictive fashion to allow the reader to match appropriate restrictions to the particular application area under investigation. Author

N90-13983# Grenoble-1 Univ. (France). Lab. des Techniques de l'Informatique, des Mathematiques, de la Microelectronique et de la Microscop
IMPLEMENTING THE DISCRETE FOURIER TRANSFORM ON THE HYPERCUBE FPS T40
Laurent Desbat and Denis Trystram (Institut National Polytechnique, Grenoble, France) Apr. 1989 22 p
(IMAG-RR-773-I; ETN-90-95702) Avail: NTIS HC A03/MF A01

The implementation of the fast Fourier transforms on the FPS T40, a vector-parallel hypercube with 32 processors, is described. The implementation is based on a repartition of work over the processor network, and refers directly to successive steps in the elementary perfect shuffle transformation, each step corresponding to a direction in the hypercube. After dispatching the data in respect to the usual bit reverse order of the binary representation of the indices, the algorithm involves two phases: local computation using the vector processing unit (which is in fact successive direct Fourier transform and fast Fourier transform) as efficiently as possible and global computaton with interprocessor communications. Many experiments are done to measure the speed-up (in the extended sense of distributed memory architectures) and to compare computation times with communication times. A theoretical model of execution time, which allows for study of the optimal length of the vector registers of a vector process unit is derived. ESA

N90-13984# Technische Univ., Eindhoven (Netherlands). Dept. of Mathematics and Computing Science.
ON THE ASYMPTOTIC CONVERGENCE OF THE SIMULATED ANNEALING ALGORITHM IN THE PRESENCE OF A PARAMETER DEPENDENT PENALIZATION
Peter C. Schuur Jun. 1989 21 p
(MEMO-COSOR-89-16; ETN-90-95957) Avail: NTIS HC A03/MF A01

Asymptotic convergence of the standard simulated annealing algorithm, when used with a parameter dependent penalization, to the set of globally optimal solutions of the original combinatorial optimization problem is established. Precise and explicit asymptotic estimates are given. The asymptotic behavior of the expected cost, the variance of the cost, and the entropy are explicitly described. Familiar properties like monotonicity of the expected cost and the entropy are shown to be no longer guaranteed in the penalized case, and the practical consequences of the results are discussed. ESA

N90-13985# Technische Univ., Delft (Netherlands). Dept. of Aerospace Engineering.
INTERFACE BETWEEN MEDUSA AND GIFTS FOR SHELL STRUCTURES
Ronald P. Notenboom Mar. 1988 52 p
(LR-553; ETN-90-95995) Avail: NTIS HC A04/MF A01

A method to convert data from a drawing sheet to finite element preprocessor input is described as an essential to an optimal working Computer Aided Design (CAD) system. The MEDUSA CAD program is used to generate the drawing data base, containing the geometrical data to be converted into a Graphical Interactive Finite-element Total System (GIFTS) file. The GIFTS program used consists of separate modules using a common database. Program use and preprocessing modules for three dimensional shell models are described. The simplicity and speed of use of the GIFTS preprocessing modules are discussed in conclusion. ESA

N90-13986# Swedish Defence Research Establishment, Linkoeping. Dept. of Information Technology.
AN EDITOR FOR 3D-MODELS FOR IMAGE ANALYSIS
Bengt Rosen Jun. 1989 19 p In SWEDISH; ENGLISH summary
(Grant STU-SS-01693P)
(FOA-C-30534-3.4; ISSN-0347-3694; ETN-90-96021) Avail: NTIS HC A03/MF A01; Swedish Defence Research Establishment, Box 1165, S-58111 Linkoeping, Sweden, 50 Swedish crowns

The model editor is a program for manual, interactive removal of hidden lines in geometrical object models. A coordinate transformation from cartesian coordinates is used, for determining in what angle interval segments of the figure are visible, these segments are marked on the screen with a black line. Hidden segments are marked light grey. A Texas Explorer Lisp machine is utilized, and the operating method is described. A model based image analysis is presented, which could also be used in other applications. ESA

N90-13987# Technical Research Centre of Finland, Espoo. Lab. of Electrical and Automation Engineering.
THE APROS SOFTWARE FOR PROCESS SIMULATION AND MODEL DEVELOPMENT
Eero Silvennoinen, Kaj Juslin, Markku Haenninen, Olli Tiihonen, Jorma Kurki, and Kari Porkholm (Imatran Voima Oy, Helsinki, Finland) May 1989 129 p
(VTT-618; ISBN-951-38-3468-8; ISSN-0358-5077; ETN-90-96023) Copyright Avail: NTIS HC A07/MF A01; Government Prinding Centre, P.O. Box 516, SF-00101 Helsinki, Finland, 84 Finnish marks

The advanced process simulator (APROS) software environment, designed for process simulation and model development, is presented. The procedure of model development

in general and the software used in model development are reviewed. The principles of the APROS software system are discussed. The structure of the real time database and the tools for model development are presented. The already implemented APROS software packages and some larger application examples currently under development are described. ESA

N90-13518# European Space Agency, Paris (France).
ON-BOARD SOFTWARE
C. Rolls and A. Dherbecourt *In its* The Hipparcos Mission. Prelaunch Status. Volume 1: The Hipparcos Satellite Jun. 1989 p 205-219 (For primary document see N90-13499 05-18)
Copyright Avail: NTIS HC A16/MF A02; ESA Publications Div., ESTEC, Noordwijk, Netherlands, 80 Dutch guilders

N90-13573# European Space Agency, Paris (France).
DATA SIMULATIONS IN THE FAST CONSORTIUM
M. Froeschle, J. L. Falin, J. Kovalevsky, F. Mignard, and J. Dupic *In its* The Hipparcos Mission. Prelaunch Status. Volume 3: The Data Reductions Jun. 1989 p 409-421 (For primary document see N90-13548 05-18)
Copyright Avail: NTIS HC A22/MF A03; ESA Publications Div., ESTEC, Noordwijk, Netherlands, 80 Dutch guilders

N90-13574# European Space Agency, Paris (France).
DATA SIMULATIONS IN THE NDAC CONSORTIUM
F. vanLeeuwen *In its* The Hipparcos Mission. Prelaunch Status. Volume 3: The Data Reductions Jun. 1989 p 423-426 (For primary document see N90-13548 05-18)
Copyright Avail: NTIS HC A22/MF A03; ESA Publications Div., ESTEC, Noordwijk, Netherlands, 80 Dutch guilders

N90-13576# European Space Agency, Paris (France).
EXPERIMENTS TOWARDS A GLOBAL SPHERE SOLUTION
F. Sanso, B. Betti, and F. Migliaccio *In its* The Hipparcos Mission. Prelaunch Status. Volume 3: The Data Reductions Jun. 1989 p 437-455 (For primary document see N90-13548 05-18)
Copyright Avail: NTIS HC A22/MF A03; ESA Publications Div., ESTEC, Noordwijk, Netherlands, 80 Dutch guilders

62 COMPUTER SYSTEMS

Includes computer networks and special application computer systems.

N90-13988*# National Aeronautics and Space Administration. Lewis Research Center, Cleveland, OH.
FLIGHT SOFTWARE DEVELOPMENT FOR THE ISOTHERMAL DENDRITIC GROWTH EXPERIMENT
Laurie H. Levinson, Edward A. Winsa, and Martin E. Glicksman (Rensselaer Polytechnic Inst., Troy, NY.) 1989 11 p Proposed for presentation at the 28th Aerospace Sciences Meeting, Reno, NV, 8-11 Jan. 1990; sponsored by AIAA
(NASA-TM-102412; E-5170; NAS 1.15:102412; AIAA-90-0744) Avail: NTIS HC A03/MF A01 CSCL 09B

The Isothermal Dendritic Growth Experiment (IDGE) is a microgravity materials science experiment scheduled to fly in the cargo bay of the shuttle on the United States Microgravity Payload (USMP) carrier. The experiment will be operated by real-time control software which will not only monitor and control onboard experiment hardware, but will also communicate, via downlink data and uplink commands, with the Payload Operaticns Control Center (POCC) at NASA George C. Marshall Space Flight Center (MSFC). The software development approach being used to implement this system began with software functional requirements specification. This was accomplished using the Yourdon/DeMarco methodology as supplemented by the Ward/Mellor real-time extensions. The requirements specification in combination with software prototyping was then used to generate a detailed design consisting of structure charts, module prologues, and Program Design Language (PDL) specifications. This detailed design will next be used to code the software, followed finally by testing against the functional requirements. The result will be a modular real-time control software system with traceability through every phase of the development process. Author

N90-13989# Center for Mathematics and Computer Science, Amsterdam (Netherlands). Dept. of Operations Research, Statistics, and System Theory.
WAITING TIMES IN POLLING SYSTEMS WITH MARKOVIAN SERVER ROUTING
O. J. Boxma and J. A. Weststrate (Tilburg Univ., Netherlands) Mar. 1989 18 p Sponsored by Netherlands Organization for the Advancement of Research
(CWI-BS-R8905; ETN-90-95615) Copyright Avail: NTIS HC A03/MF A01

Queueing analysis of polling systems with a probabilistic server routing mechanism is studied. A single server serves a number of queues, switching between the queues according to a discrete time parameter Markov chain. The switchover times between queues are nonnegligible. It is observed that the total amount of work in this Markovian polling system can be decomposed into two independent parts, the total amount of work in the corresponding system without switchover times and the amount of work in the system at some epoch covered by a switching interval. This work decomposition leads to a pseudoconservation law for mean waiting times, i.e., an exact expression for a weighted sum of the mean waiting times at all queues. The results generalize known results for polling systems with strictly cyclic service. ESA

N90-13990*# National Aeronautics and Space Administration. Hugh L. Dryden Flight Research Facility, Edwards, CA.
A KNOWLEDGE-BASED SYSTEM DESIGN/INFORMATION TOOL FOR AIRCRAFT FLIGHT CONTROL SYSTEMS
Dale A. Mackall and James G. Allen (Draper, Charles Stark Lab., Inc., Cambridge, MA) Oct. 1989 19 p Presented at the 7th AIAA Computers in Aerospace Conference, Monterey, CA, 4-6 Oct. 1989 Previously announced in IAA as A90-10491
(NASA-TM-101704; H-1546; NAS 1.15:101704) Avail: NTIS HC A03/MF A01 CSCL 09B

Research aircraft have become increasingly dependent on advanced control systems to accomplish program goals. These aircraft are integrating multiple disciplines to improve performance and satisfy research objectives. This integration is being accomplished through electronic control systems. Because of the number of systems involved and the variety of engineering disciplines, systems design methods and information management have become essential to program success. The primary objective of the system design/information tool for aircraft flight control system is to help transfer flight control system design knowledge to the flight test community. By providing all of the design information and covering multiple disciplines in a structured, graphical manner, flight control systems can more easily be understood by the test engineers. This will provide the engineers with the information needed to thoroughly ground test the system and thereby reduce the likelihood of serious design errors surfacing in flight. The secondary objective is to apply structured design techniques to all of the design domains. By using the techniques in the top level system design down through the detailed hardware and software designs, it is hoped that fewer design anomalies will result. The flight test experiences of three highly complex, integrated aircraft programs are reviewed: the X-29 forward-swept wing, the advanced fighter technology integration (AFTI) F-16, and the highly maneuverable aircraft technology (HiMAT) program. Significant operating anomalies and the design errors which cause them, are examined to help identify what functions a system design/information tool should provide to assist designers in avoiding errors. Author

63 CYBERNETICS

Includes feedback and control theory, artificial intelligence, robotics and expert systems.

For related information see also *54 Man/System Technology and Life Support.*

N90-13991*# Alabama Univ., Huntsville.
APPLICATIONS OF ARTIFICIAL INTELLIGENCE TO SPACE STATION AND AUTOMATED SOFTWARE TECHNIQUES: HIGH LEVEL ROBOT COMMAND LANGUAGE Final Report, 1 Jun. 1988 - 31 May 1989
James W. McKee Jun. 1989 116 p
(Contract NCC8-13)
(NASA-CR-182997; NAS 1.26:182997; UAH-RR-803) Avail: NTIS HC A06/MF A01 CSCL 09B

The objective is to develop a system that will allow a person not necessarily skilled in the art of programming robots to quickly and naturally create the necessary data and commands to enable a robot to perform a desired task. The system will use a menu driven graphical user interface. This interface will allow the user to input data to select objects to be moved. There will be an imbedded expert system to process the knowledge about objects and the robot to determine how they are to be moved. There will be automatic path planning to avoid obstacles in the work space and to create a near optimum path. The system will contain the software to generate the required robot instructions. Author

N90-13992# Naval Research Lab., Washington, DC. Center for Applied Research in Artificial Intelligence.
AN ARTIFICIAL INTELLIGENCE APPROACH TO ANALOG SYSTEM DIAGNOSIS Interim Report, Oct. 1985 - Sep. 1988
F. J. Pipitone, K. A. DeJong, and W. M. Spears 22 Sep. 1989 29 p
(AD-A213135; NRL-R-9219) Avail: NTIS HC A03/MF A01 CSCL 14/2

This report describes techniques for the automatic diagnosis of primarily analog systems. These results were obtained after several years of work at NRL in this area, along with a fully implemented research prototype diagnosis system, FIS (Fault Isolation System). Key features are a local qualitative causal model of replaceable module behavior, the absence of the single fault assumption, a rigorous probabilistic treatment of fault probabilities, dynamic best test selection based on heuristics or entropy, and efficient algorithms for computing the probability and the entropy of Boolean expressions. GRA

N90-13993# Universiteit Twente, Enschede (Netherlands). Faculty of Applied Mathematics.
MODEL REDUCTION OF WEAKLY DAMPED MECHANICAL SYSTEMS
A. J. vanderSchaft Jul. 1989 8 p
(MEMO-798; ISSN-0169-2690; ETN-90-95965) Avail: NTIS HC A02/MF A01

An approach to model reduction of weakly damped linear mechanical systems is studied and elaborated on. The approach is based on the balancing of a gradient system which can be naturally associated with the conservative idealization of the system. Connections to model reduction based on modal analysis are indicated. ESA

N90-13994*# California Univ., San Diego, La Jolla. Inst. for Cognitive Science.
THE PROBLEM OF AUTOMATION: INAPPROPRIATE FEEDBACK AND INTERACTION, NOT OVERAUTOMATION
Donald A. Norman Jul. 1989 14 p Presented at the Discussion Meeting on Human Factors in High-Risk Situations, London, England, 28-29 Jun. 1989 Submitted for publication Sponsored in part by Apple Computer Co. and Digital Equipment Corp.
(Contract NCC2-591)
(NASA-CR-186126; NAS 1.26:186126; ICS-8904) Avail: NTIS HC A03/MF A01 CSCL 09B

As automation increasingly takes its place in industry, especially high-risk industry, it is often blamed for causing harm and increasing the chance of human error when failures occur. It is proposed that the problem is not the presence of automation, but rather its inappropriate design. The problem is that the operations are performed appropriately under normal conditions, but there is inadequate feedback and interaction with the humans who must control the overall conduct of the task. When the situations exceed the capabilities of the automatic equipment, then the inadequate feedback leads to difficulties for the human controllers. The problem is that the automation is at an intermediate level of intelligence, powerful enough to take over control that which used to be done by people, but not powerful enough to handle all abnormalities. Moreover, its level of intelligence is insufficient to provide the continual, appropriate feedback that occurs naturally among human operators. To solve this problem, the automation should either be made less intelligent or more so, but the current level is quite inappropriate. The overall message is that it is possible to reduce error through appropriate design considerations. Author

N90-13995*# National Aeronautics and Space Administration. Hugh L. Dryden Flight Research Facility, Edwards, CA.
A KNOWLEDGE-BASED FLIGHT STATUS MONITOR FOR REAL-TIME APPLICATION IN DIGITAL AVIONICS SYSTEMS
E. L. Duke, J. D. Disbrow, and G. F. Butler (Royal Aerospace Establishment, Farnborough, England) Oct. 1989 14 p Presented at the MILCOMP'89 Conference, London, England, 26-28 Sep. 1989
(NASA-TM-101710; H-1568; NAS 1.15:101710) Avail: NTIS HC A03/MF A01 CSCL 09B

The Dryden Flight Research Facility of the National Aeronautics and Space Administration (NASA) Ames Research Center (Ames-Dryden) is the principal NASA facility for the flight testing and evaluation of new and complex avionics systems. To aid in the interpretation of system health and status data, a knowledge-based flight status monitor was designed. The monitor was designed to use fault indicators from the onboard system which are telemetered to the ground and processed by a rule-based model of the aircraft failure management system to give timely advice and recommendations in the mission control room. One of the important constraints on the flight status monitor is the need to operate in real time, and to pursue this aspect, a joint research activity between NASA Ames-Dryden and the Royal Aerospace Establishment (RAE) on real-time knowledge-based systems was established. Under this agreement, the original LISP knowledge base for the flight status monitor was reimplemented using the intelligent knowledge-based system toolkit, MUSE, which was developed under RAE sponsorship. Details of the flight status monitor and the MUSE implementation are presented. Author

N90-13996# Technische Univ., Eindhoven (Netherlands). Dept. of Mathematics and Computing Science.
A PRIORI RESULTS IN LINEAR QUADRATIC OPTIMAL CONTROL THEORY Preliminary Draft
Ton Geerts Jan. 1989 6 p
(MEMO-COSOR-89-02; ETN-90-95947) Avail: NTIS HC A02/MF A01

A linear-quadratic control problem (LQCP) with a stability modulo is defined from consideration of a linear time-invariant finite-dimensional system together with the quadratic cost criterion. A theorem is presented which is a powerful instrument in obtaining a priori results on LQCPs and examples are given. ESA

N90-13997# Technische Univ., Eindhoven (Netherlands). Dept. of Mathematics and Computing Science.
THE QUADRATIC MATRIX INEQUALITY IN SINGULAR H INFINITY CONTROL WITH STATE FEEDBACK
A. A. Stoorvogel and Harry L. Trentelman Feb. 1989 31 p
(MEMO-COSOR-89-03; ETN-90-95948) Avail: NTIS HC A03/MF A01

The standard infinity H control problem using state feedback is addressed. Given a linear, time-invariant, finite-dimensional system this problem consists of finding a static state feedback such that the resulting closed loop transfer matrix has infinity H norm smaller than some a priori given upper bound and in addition

the closed loop system is required to be internally stable. Conditions for the existence of a suitable state feedback are formulated in terms of a quadratic matrix inequality, reminiscent of the dissipation inequality of singular linear quadratic optimal control. In the case that the direct feedthrough matrix of the control input is injective the results are specialized to known results in terms of solvability of a certain indefinite algebraic Riccati equation. ESA

N90-13998# Technische Univ., Eindhoven (Netherlands). Dept. of Mathematics and Computing Science.
THE TOTALLY SINGULAR LINEAR QUADRATIC PROBLEM WITH INDEFINITE COST
Harry L. Trentelman Mar. 1989 27 p
(MEMO-COSOR-89-05; ETN-90-95950) Avail: NTIS HC A03/MF A01

The most general version of the stationary, infinite horizon linear quadratic optimal control problem is studied. In previous studies either both or one of two assumptions are made, that the integrand of the cost criterion is given by a positive semi-definite quadratic form, and that the latter quadratic form is positive definite in the control variable alone. A problem formulation for the case that neither assumption is imposed is proposed. The case when the problem is completely singular is described. ESA

N90-13999# Technische Univ., Eindhoven (Netherlands). Dept. of Mathematics and Computing Science.
THE SINGULAR ZERO SUM DIFFERENTIAL GAME WITH STABILITY USING H INFINITY CONTROL THEORY
A. A. Stoorvogel 13 Apr. 1989 26 p
(MEMO-COSOR-89-09; ETN-90-95954) Avail: NTIS HC A03/MF A01

The time-invariant, finite-dimensional, infinite-horizon, linear quadratic differential game is considered. Sufficient conditions for the existence of (almost) equilibria, and necessary conditions, are derived. Allowances are made for singular weighting on the minimizing player in the cost-criterion. This problem has a strong relation with the singular infinity H problem with state feedback where the direct feedthrough matrix from control input to output is not necessarily injective. ESA

N90-14000# Technische Univ., Eindhoven (Netherlands). Dept. of Mathematics and Computing Science.
THE SINGULAR H INFINITY CONTROL PROBLEM WITH DYNAMIC MEASUREMENT FEEDBACK
A. A. Stoorvogel 2 Jun. 1989 40 p
(MEMO-COSOR-89-14; ETN-90-95955) Avail: NTIS HC A03/MF A01

The infinity H problem with measurement feedback is described and addressed. Necessary and sufficient conditions are given under which such a feedback exists. The only assumptions made are that there are no invariant zeros on the imaginary axis for two subsystems. No assumptions are made on the direct feedthrough matrices of the plant. This problem is reduced to an almost disturbance decoupling problem with measurement feedback and internal stability. ESA

N90-14001# Technische Univ., Eindhoven (Netherlands). Dept. of Mathematics and Computing Science.
THE OUTPUT-STABILIZABLE SUBSPACE AND LINEAR OPTIMAL CONTROL
A. H. W. Geerts and M. L. J. Hautus Jun. 1989 12 p Sponsored by the Netherlands Organization for Scientific Research
(MEMO-COSOR-89-15; ETN-90-95956) Avail: NTIS HC A03/MF A01

Properties of a certain subspace are linked to well-known problems in system theory. Output stabilizability is shown to be difficult to prove as necessary and sufficient for solvability of linear-quadratic problems. The theorems and propositions are detailed. ESA

64 NUMERICAL ANALYSIS

Includes iteration, difference equations, and numerical approximation.

N90-14002*# National Aeronautics and Space Administration. Lewis Research Center, Cleveland, OH.
APPLICATION OF MULTI-GRID METHODS FOR SOLVING THE NAVIER-STOKES EQUATIONS
A. O. Demuren Oct. 1989 23 p Reprint from the Proceedings of the Inst. of Mechanical Engineers, Part C, 1989, by permission of the Council of the Inst. Previously announced in IAA as A89-53172 Prepared in cooperation with Lagos Univ., Nigeria (NASA Order C-99066-G)
(NASA-TM-102359; ICOMP-89-24; E-4655; NAS 1.15:102359) Avail: NTIS HC A03/MF A01 CSCL 12A

The application of a class of multi-grid methods to the solution of the Navier-Stokes equations for two-dimensional laminar flow problems is discussed. The methods consist of combining the full approximation scheme-full multi-grid technique (FAS-FMG) with point-, line-, or plane-relaxation routines for solving the Navier-Stokes equations in primitive variables. The performance of the multi-grid methods is compared to that of several single-grid methods. The results show that much faster convergence can be procured through the use of the multi-grid approach than through the various suggestions for improving single-grid methods. The importance of the choice of relaxation scheme for the multi-grid method is illustrated. Author

N90-14003# Universiteit Twente, Enschede (Netherlands). Faculty of Applied Mathematics.
ON SMALLEST NONHAMILTONIAN REGULAR ROUGH GRAPHS
Douglas Bauer (Stevens Inst. of Tech., Hoboken, NJ.), H. J. Broersma, and Henk Jan Veldman May 1989 9 p
(Contract MDA904-89-H-2008)
(Memo-788; ISSN-0169-2690; ETN-89-95678) Avail: NTIS HC A02/MF A01

Theorems on hamiltonian and nonhamiltonian graphs are studied. The problem of finding the minimum order of a nonhamiltonian K-regulator 1-tough graph (K greater than or equal to 3) is addressed. Different classes of graphs are discussed and representations of graphs are included. ESA

N90-14004# Wisconsin Univ., Madison. Center for Mathematical Sciences.
PARABOLIC EQUATIONS FOR CURVES ON SURFACES. 2: INTERSECTIONS, BLOW UP AND GENERALIZED SOLUTIONS Technical Summary Report
Sigurd Angenent Jan. 1989 35 p
(Grants NSF DMS-88-01486; AF-AFOSR-0202-87)
(AD-A212890; CMS-TSR-89-24-2) Avail: NTIS HC A03/MF A01 CSCL 12/1

This paper describes a theory for parabolic differential equations for immersed curves on surfaces, which generalizes the curve shortening or flow by mean curvature problem, as well as several models in the theory of phase transitions in two dimensions. The author describes a class of equations for which the initial value problem is well posed for rough initial data, for which one define generalized solutions, i.e., solutions which are smooth, except at a discrete set of times. The methods which are used in this paper are more geometrical than those of part 1. By comparing arbitrary solutions with certain special solutions, and by considering the way they intersect, estimates for the curvature and the tangent are derived, which allow one to study the initial value problem, and the way solutions become singular. GRA

N90-14005# Wisconsin Univ., Madison. Center for Mathematical Sciences.
PERIODIC SOLUTIONS OF HAMILTONIAN SYSTEMS OF 3-BODY TYPE Technical Summary Report
Abbas Bahri (Rutgers Univ., New Brunswick, NJ.) and Paul H. Rabinowitz Aug. 1989 107 p Sponsored in part by the Sloan Foundation

(Contracts DAAL03-87-K-0043; N00014-88-K-0134; NSF MCS-81-10556)
(AD-A212891; CMS-TSR-90-8) Avail: NTIS HC A06/MF A01 CSCL 12/2

The study of time periodic solutions of the n-body problem is a classical one. The authors' goal in this paper is to present some new variational approaches of a global nature to a class of problems of 3-body type. GRA

N90-14006# Naval Research Lab., Washington, DC. Beam Physics Branch.
A SOLVABLE SELF-SIMILAR MODEL OF THE SAUSAGE INSTABILITY IN A RESISTIVE Z-PINCH Interim Report
Martin Lampe 20 Sep. 1989 38 p
(AD-A213137; NRL-MR-6549) Avail: NTIS HC A03/MF A01 CSCL 20/9

A solvable model is developed for the linearized sausage mode within the context of resistive magnetohydrodynamics (MHD). The model is based on the assumption that the fluid motion of the plasma is self-similar, as well as several assumptions pertinent to the long-wavelength limit. The perturbations to the magnetic field are not assumed to be self-similar, but rather are calculated. Effects arising from time dependences of the equilibrium, e.g., current rising as T (sup alpha), ohmic heating, and time variation of the pinch radius, are included in the analysis. The formalism appears to provide a good representation of those modes that involve coherent sausage distortion of the entire cross section of the pinch, but excludes modes that are localized radially, and higher radial eigenmodes. for this and other reasons, it is expected that the model underestimates the maximum instability growth rates, but is reasonable for global sausage modes. The net effect of resistivity and time variation of the equilibrium is to decrease the growth rate if alpha is approx. less than 1, but never by more than a factor of about two. The effect is to increase the growth rate if alpha is somewhat greater than 1. GRA

N90-14007# Naval Postgraduate School, Monterey, CA.
WHY STOCHASTIC MODELING IS ESSENTIAL IN ANALYZING INTERDICTED TRANSPORTATION NETWORK PERFORMANCE M.S. Thesis
Byung Kwon Choi Jun. 1989 70 p
(AD-A213140) Avail: NTIS HC A04/MF A01 CSCL 15/5

In this thesis, we use simulation to study the probabilistic dynamics of a military road transportation network when the network is subjected to interdiction by aircraft. We consider several road interdiction schemes. The simulation results are compared to those obtained by using deterministic expected value optimization techniques. This latter approach has been used by other researchers in studies of interdictions of networks. We demonstrate, through the use of two realistic military examples, that the deterministic result poorly predicts the performance of the stochastic systems and that the bias incurred by using deterministic methods is significant. Therefore, the stochastic model should be used in the real situation. GRA

N90-14008# Illinois Univ., Urbana. Coordinated Science Lab.
A MULTILEVEL PARALLEL SOLVER FOR BLOCK TRIDIAGONAL AND BANDED LINEAR SYSTEMS
Ibrahim N. Hajj and Stig Skelboe (Copenhagen Univ., Denmark) 25 Aug. 1989 31 p
(Contract N00014-84-C-0149)
(AD-A213151; UILU-ENG-89-2223; DAC-15) Avail: NTIS HC A03/MF A01 CSCL 12/3

An efficient algorithm is described for the parallel solution of systems of linear equations with a block tridiagonal coefficient matrix. The algorithm comprises a multilevel LU-factorization based on block cyclic reduction and a corresponding solution algorithm. A general presentation is included of the parallel multilevel LU-factorization and solution algorithms, but the main emphasis is on implementation principles for a message passing computer with hypercube topology. Problem partitioning, processor allocation and communication requirements are discussed for the general block tridiagonal algorithm. GRA

N90-14009# Illinois Univ., Urbana. Coordinated Science Lab.
IDENTIFICATION OF IMPULSIVE INTERFERENCE CHANNELS Ph.D. Thesis
Serena M. Zabin Jul. 1989 126 p
(Contract N00014-84-C-0149)
(AD-A213154; UILU-ENG-89-2224) Avail: NTIS HC A07/MF A01 CSCL 12/9

In this work, the problem of optimum and near-optimum identification of the parameters of the Middleton Class A impulsive interference model is considered. In particular, under the assumption of the availability of a set of independent samples from the Class A envelope distribution, the problems of basic batch estimation of the Class A parameters, recursive identification of the parameters, and efficient estimation of the parameters for small sample sizes, are investigated. Within the context of basic batch estimation, several estimators of the parameters are proposed and their asymptotic performances explored. From this analysis, estimates based on the method of moments are seen to be consistent and computationally desirable but highly inefficient, whereas more efficient likelihood-based estimators are seen to be computationally unwieldy. However, an estimator that initiates likelihood iteration with the method-of-moments estimates is seen to overcome these difficulties in its asymptotic performance. Unfortunately, simulation of this third estimator for moderate sample sizes reveals poor performance under these conditions. To overcome this lack of moderate-sample-size efficiency, a similar estimator that initiates likelihood iteration with physically motivated (but nonoptimal) estimates is also proposed. Simulation of this latter estimator for moderate sample sizes indicates that near-optimal performance is obtained by this technique. GRA

N90-14010# Naval Ocean Systems Center, San Diego, CA.
USING BROYDEN UPDATES TO APPROXIMATE THE JACOBIAN IN A SEMI-IMPLICIT BACKWARD DIFFERENTIATION CODE Final Report
Laura D. Knight Sep. 1989 51 p
(AD-A213239; NOSC/TD-1652) Avail: NTIS HC A04/MF A01 CSCL 12/1

If one wishes to solve a system of stiff ordinary differential equations (ODEs), which are generally large and sparse, one requires the solution of a nonlinear equation involving the ODE Jacobian at each time step. This Jacobian is often formed by finite differences. Here Broyden's Method is discussed which will update the Jacobian as we go using information available in order to avoid the cost of recomputing the Jacobian. The update is a rank-one update. This method is implemented in the code STRUT. STRUT is the original code STEP which implements an Adams predictor-corrector for solving nonstiff problems coupled with Stewart's implementation of a Semi-Implicit Backward Differentiation Formula (SIBDF) predictor-corrector for solving stiff problems. Two models are discussed for implementing Broyden's Method over different time steps. A Method of Lines semidiscretization of Burgers' equation and a reaction-diffusion model are used as our test problems. Results are given for each model and are compared with the original STRUT code, LSODE and LSODA. GRA

N90-14011# Ballistic Research Labs., Aberdeen Proving Ground, MD.
PROGRAM TRANSFORMATION WITH ABSTRACT RELATION ALGEBRAS
Paul Broome Oct. 1989 23 p
(AD-A213270; BRL-MR-3784) Avail: NTIS HC A03/MF A01 CSCL 12/5

Our objective is to satisfy two seemingly opposing constraints on program design. We want to begin a program as an obvious formal specification but also insist upon efficient execution. Our approach is to find expressive, model independent program constructs with algebraic properties that can show logical equivalence between a clear specification and an efficient program. Our solution is an implementation of some of the relations, relation operators, and equations that comprise Tarski's Q-relation algebra. The key to this solution is a single operator for linear recursions

that satisfies two equations. The first merges recursions and the second propagates constraints for early pruning of the nonproductive branches of the computation tree. GRA

N90-14012# Naval Postgraduate School, Monterey, CA. Dept. of Mathematics.
FORTRAN SUBROUTINES FOR THE EVALUATION OF THE CONFLUENT HYPERGEOMETRIC FUNCTIONS Technical Report, Feb. - Aug. 1989
William Gragg and Beny Neta 14 Aug. 1989 16 p
(AD-A213308; NPS53-89-014) Avail: NTIS HC A03/MF A01 CSCL 05/9

The FORTRAN subroutines for evaluating the confluent hypergeometric functions M(a,b;x) and U(a,b;x) are listed. These subroutines use the stable recurrence relations given e.g., in Wimp. GRA

N90-14013# Universiteit Twente, Enschede (Netherlands). Faculty of Applied Mathematics.
HAMILTONIAN PROPERTIES OF GRAPHS WITH LARGE NEIGHBORHOOD UNIONS
Douglas Bauer, Genghua Fan (Waterloo Univ., Ontario), and Henk Jan Veldman Apr. 1989 30 p
(Contract NSA MDA904-89-H-2008)
(MEMO-779; ISSN-0169-2690; ETN-90-95670) Avail: NTIS HC A03/MF A01

Results in Hamiltonian graph theory involving degree-sums or cardinalities of neighborhood unions are compared in terms of generality. Results are proved including those concerning the lower bound and length of cycle. Sufficient conditions of Lindquester for the existence of Hamilton cycles and paths are extended to D-cycles and D-paths. ESA

N90-14014# Universiteit Twente, Enschede (Netherlands). Faculty of Applied Mathematics.
USING THE PHYSICAL STRUCTURE OF A SYSTEM FOR CONTROL: AN ILLUSTRATION
H. J. C. Huijberts Apr. 1989 10 p Presented at the COMCON Workshop on Stabilization of Flexible Structures Submitted for publication
(MEMO-782; ISSN-0169-2690; ETN-90-95673) Avail: NTIS HC A02/MF A01

The importance of using the physical structure of a system for solving control problems is illustrated by means of the input-output decoupling problem with stability for Hamiltonian systems. With the decoupling feedback chosen, critical stability can be achieved, and asymptotic stability only under conditions. It is suggested that further research for the achievement of asymptotic stability remains by the choice of a different type of decoupling feedback. ESA

N90-14015# Universiteit Twente, Enschede (Netherlands). Faculty of Applied Mathematics.
ON THE PERFORMANCE OF ON-LINE ALGORITHMS FOR PARTITION PROBLEMS
U. Faigle, W. Kern, and G. Turan (Chicago Univ., IL.) Apr. 1989 29 p
(MEMO-784; ISSN-0169-2690; ETN-90-95675) Avail: NTIS HC A03/MF A01

The performance of the greedy algorithm and of on-line algorithms for partition problems in combinatorial optimization is considered. After a survey of known results bounds are given for matroid and graph partitioning, and the power of non-adaptive adversaries for proving lower bounds is discussed. ESA

N90-14016# Universiteit Twente, Enschede (Netherlands). Faculty of Applied Mathematics.
OPTIMAL PROCESSES DESCRIBED BY A PARABOLIC DIFFERENTIAL EQUATION WITH CONTROL IN THE COEFFICIENTS, PART 4
E. A. vanMarle and R. Nottrot May 1989 14 p
(MEMO-785-Pt-4; ISSN-0169-2690; ETN-90-95676-Pt-4) Avail: NTIS HC A03/MF A01

In the preceding papers, a continuous distillation-column was obtained by continuizing the mass balances. These balances might be considered as the process equations of a discrete distillation column. The optimization of discrete columns is studied. By discretizing the partial differential equation describing the continuous column, agreement between the discrete column and the discretized continuous column is obtained. ESA

N90-14017# Universiteit Twente, Enschede (Netherlands). Faculty of Applied Mathematics.
ON THE RECURRENCE RELATION FOR MULTIVARIATE B-SPLINES WITH RESPECT TO DIMENSION
M. Neamtu May 1989 29 p Sponsored by the Netherlands Organization for the Advancement of Research
(MEMO-786; ISSN-0169-2690; ETN-90-95677) Avail: NTIS HC A03/MF A01

A new recurrence relation for derived multivariate B-splines is studied. Its algorithmical and numerical properties are discussed and a comparison with the derived classical recurrence relation is given. The new recurrence relation is shown to provide in general a plausible alternative for the numerical evaluation of multivariate B-splines. ESA

N90-14018# Center for Mathematics and Computer Science, Amsterdam (Netherlands). Dept. of Operations Research, Statistics, and System Theory.
ON THE NONEXISTENCE OF A STRONG SOLUTION IN THE BOUNDARY PROBLEM FOR A STICKY BROWNIAN MOTION
R. J. Chitashvili (Academy of Sciences of the Georgian SSR, Tbilisi.) Jan. 1989 13 p Submitted for publication Sponsored by the Netherlands Organization for the Advancement of Research
(CWI-BS-R8901; ETN-90-95612) Copyright Avail: NTIS HC A03/MF A01

A sticky Brownian motion is proven not measurable with respect to a driving Wiener process and the conjecture of Skorokhod is thereby verified. The methods involved in the theorem are detailed and a proof is presented. ESA

N90-14019# Center for Mathematics and Computer Science, Amsterdam (Netherlands). Dept. of Operations Research, Statistics, and System Theory.
MONOTONICITY OF PERFORMANCE MEASURES IN A PROCESSOR SHARING QUEUE
P. R. deWaal and N. M. vanDijk Jan. 1989 14 p Submitted for publication Sponsored by Netherlands Organization for the Advancement of Research
(CWI-BS-R8902; ETN-90-95613) Copyright Avail: NTIS HC A03/MF A01

The monotonicity of performance measures in a processor sharing queue with two types of customers is studied. The access control law is such that when a new customer arrives he is admitted only if the number of customers of the same type that is already present in the queue does not exceed a predefined critical level. Performance measures, such as throughput, mean queue length and mean sojourn time are shown to be monotonic functions of the critical level for one type if the critical level for the other type is held constant. Monotonicity of throughput and means queue length is proven by comparing policies for discrete time Markov processes. Monotonicity of the mean sojourn time is proven directly with the closed form formula for this measure, using the existence of a product-form equilibrium distribution for the queuing system. ESA

N90-14020# Center for Mathematics and Computer Science, Amsterdam (Netherlands). Dept. of Operations Research, Statistics, and System Theory.
WORKLOADS AND WAITING TIMES IN SINGLE-SERVER SYSTEMS WITH MULTIPLE CUSTOMER CLASSES
O. J. Boxma (Tilburg Univ., Netherlands) Mar. 1989 26 p Submitted for publication Sponsored by Netherlands Organization for the Advancement of Research
(CWI-BS-R8906; ETN-90-95616) Copyright Avail: NTIS HC A03/MF A01

Single-server multi-class service systems, in which work conservation is violated in the sense that the server's activities may be interrupted although work is still present, are studied. For a large class of such systems with interruptions, a decomposition of the amount of work into two independent components is obtained. One of these components is the amount of work in the corresponding system without interruptions. The work decomposition gives rise to a (pseudo) conservation law for mean waiting times, just as work conservation did for the system without interruptions. Problems in relation to conservation principles in service systems are listed. ESA

N90-14021# Center for Mathematics and Computer Science, Amsterdam (Netherlands). Dept. of Operations Research, Statistics and System Theory.
RANDOM MARKOV PROCESSES AND UNIFORM MARTINGALES
Steven Kalikow May 1989 19 p
(CWI-BS-R8908; ETN-90-95618) Copyright Avail: NTIS HC A03/MF A01

A certain generalization of an n-step Markov chain is shown to be equivalent to the uniform convergence of the martingale. Results are stated and discussed, and theorems presented, including the theorem that a process has a random Markov representation if it has a uniform martingale condition, the latter being simple to verify. Evidence is given which suggests that random Markov representation does not satisfy uniqueness but a vigorous proof for this is lacking. Proofs of theorems are given and examples demonstrated. ESA

N90-14022# Technische Univ., Eindhoven (Netherlands). Dept. of Mathematics and Computing Science.
THE REGULAR INDEFINITE LINEAR QUADRATIC PROBLEM WITH LINEAR ENDPOINT CONSTRAINTS
J. M. Soethoudt and Harry L. Trentelman Jun. 1988 14 p
(MEMO-COSOR-88-15; ETN-90-95936) Avail: NTIS HC A03/MF A01

The infinite horizon linear quadratic problem with indefinite cost is addressed. Given a linear system, a quadratic cost functional and a subspace of the state space, the problem of minimizing the cost functional over all inputs for which the state trajectory converges to that subspace is considered. Classical results on the zero-endpoint version of the linear quadratic problem, and results on the free-endpoint version of this problem, are generalized by the results. ESA

N90-14023# Technische Univ., Eindhoven (Netherlands). Faculty of Mathematics and Computing Sciences.
STABILIZABILITY AND DETECTABILITY OF DISCRETE-TIME TIME-VARYING SYSTEMS
J. C. Engwerda Jul. 1988 19 p
(MEMO-COSOR-88-16; ETN-90-95937) Avail: NTIS HC A03/MF A01

Some notions of stabilizability and detectability for discrete time-varying systems are introduced by state-space decompositions of the system. This allows an intuitive interpretation and shows the difficulties which occur if general stabilizability and detectability properties are attempted. A counterexample is given which shows that the notions of uniform stabilizability and uniform detectability, as defined by Anderson and Moore, do not imply stabilizability respectively detectability of the system. ESA

N90-14024# Technische Univ., Eindhoven (Netherlands). Dept. of Mathematics and Computing Science.
CONTINUITY PROPERTIES OF ONE-PARAMETER FAMILIES OF LINEAR-QUADRATIC PROBLEMS WITHOUT STABILITY
Ton Geerts Aug. 1988 27 p Sponsored by the Netherlands Organization for Scientific Research
(MEMO-COSOR-88-17; ETN-90-95938) Avail: NTIS HC A03/MF A01

Given one-parameter families of linear-quadratic control problems are studied, with reference to the absence of continuity properties for problems without stability, and as a continuation of a previous study. The definition of a new type of control problem with partial stability is demonstrated as necessary. The optimal cost for the perturbed problem is shown to converge to the cost for this problem. Additional results are found for inputs, states and outputs in case of left-invertibility. These results are established only by applying the assumptions made in the previous study. ESA

N90-14025# Technische Univ., Eindhoven (Netherlands). Dept. of Mathematics and Computing Science.
GLOBAL OPTIMIZATION AND SIMULATED ANNEALING
A. Dekkers and E. Aarts Oct. 1988 37 p
(MEMO-COSOR-88-21; ETN-90-95939) Avail: NTIS HC A03/MF A01

The problem of global optimization is addressed via a stochastic approach which is based on the simulated annealing algorithm. The approach closely follows the formulation of the simulated annealing algorithm as originally given for discrete optimization problems. The mathematic formulation is extended to continuous optimization problems and asymptotic convergence to the set of global optima is proved. An implementation of the algorithm is discussed and its performance is compared with other well known algorithms. The performance evaluation is carried out for a standard set of test functions from the literature. ESA

N90-14026# Technische Univ., Eindhoven (Netherlands). Dept. of Mathematics and Computing Science.
CONVERGENCE PROPERTIES OF INDEFINITE LINEAR QUADRATIC PROBLEMS WITH RECEDING HORIZON
Harry L. Trentelman and J. M. Soethoudt Oct. 1988 17 p
(MEMO-COSOR-88-25; ETN-90-95940) Avail: NTIS HC A03/MF A01

The following question is addressed: given a finite dimensional linear system together with a finite horizon (possibly indefinite) quadratic cost functional, when does the corresponding optimal cost converge to the optimal cost of the corresponding infinite horizon problem, as the length of the horizon tends to infinity. For the case that the linear quadratic problems are regular, necessary and sufficient conditions are established for this convergence to hold. ESA

N90-14027# Technische Univ., Eindhoven (Netherlands). Dept. of Mathematics and Computing Science.
ON THE OUTPUT-STABILIZABLE SUBSPACE
A. H. W. Geerts and M. L. J. Hautus Oct. 1988 16 p
(MEMO-COSOR-88-27; ETN-90-95941) Avail: NTIS HC A03/MF A01

Properties of a certain subspace are investigated and linked to well-known problems in system theory. The output-stabilizable subspace and ways of characterizing the optimal controls are discussed, including a characterization expressed in terms of the dissipation inequality. A condition for output stability is allowable by the results and a general formulation given. ESA

N90-14028# Technische Univ., Eindhoven (Netherlands). Dept. of Mathematics and Computing Science.
THE ALGEBRAIC RICCATI EQUATION AND SINGULAR OPTIMAL CONTROL Preliminary Draft
Ton Geerts Nov. 1988 11 p
(MEMO-COSOR-88-31; ETN-90-95943) Avail: NTIS HC A03/MF A01

The class of non-negative definite linear quadratic control problems is linked to a subset of all real symmetric equations that satisfy a dissipation inequality. This linking is of interest since symmetric matrices that represent optimal costs for linear quadratic problems necessarily turn out to be elements of this subset. A straightforward characterization of the set of rank minimizing solutions of the dissipation inequality in terms of an algebraic Riccati equation and a linear condition is presented. ESA

N90-14029# Technische Univ., Eindhoven (Netherlands). Dept. of Mathematics and Computing Science.
SOME REMARKS ON THE GAP METRIC

S. Q. Zhu and M. L. J. Hautus Dec. 1988 15 p
(MEMO-COSOR-88-34; ETN-90-95945) Avail: NTIS HC A03/MF A01

Results on the gap metric defined on the space of closed linear operators are presented. The topology introduced by the gap metric is shown to be a diagonal product topology. If the gap of two closed operators is smaller than one, then the two directed gaps are shown to be the same. A normalized right coprime factorization is constructed for given densely defined closed linear operators, and using this result an equivalent form of the gap metric is presented. ESA

N90-14030# Universiteit Twente, Enschede (Netherlands). Faculty of Applied Mathematics.
ON GEOMETRY OF INHOMOGENEOUS HEISENBERG FERROMAGNET: NONINTEGRABLE CASE
Jan Cieslinski, Antoni Sym (Warsaw Univ., Poland), and Willem Wesselius May 1989 19 p
(MEMO-789; ISSN-0169-2690; ETN-90-95958) Avail: NTIS HC A03/MF A01

New classes of exact solutions of the inhomogeneous Heisenberg ferromagnet equation are found by means of geometrical technique. This technique consists in calculating one-parameter families of geodesics on surfaces in E3. The solutions given correspond to geodesics on surfaces of rotation. ESA

N90-14031# Universiteit Twente, Enschede (Netherlands). Faculty of Applied Mathematics.
THE WEIGHTED SUM OF TWO S-UNITS BEING A SQUARE
B. M. M. deWeger Jun. 1989 28 p
(MEMO-792; ISSN-0169-2690; ETN-90-95959) Avail: NTIS HC A03/MF A01

A specific diophantine equation is proved to have essentially only finitely many solutions. The variables in the equation are S-units, i.e., rationals whose numerators and denominators have prime divisors from a fixed finite set of primes only. Using the theory of p-adic linear forms in logarithms an effectively computable upper bound for the solutions is given, and an outline of how to reduce this upper bound by computational p-adic diophantine approximation, is presented. ESA

N90-14032# Universiteit Twente, Enschede (Netherlands). Faculty of Applied Mathematics.
SOLVING A SPECIFIC THUE-MAHLER EQUATION
N. Tzanakis (Crete Univ., Iraklion, Greece) and B. M. M. deWeger Jun. 1989 42 p Sponsored in part by Netherlands Foundation for Mathematics and Netherlands Organization for the Advancement of Pure Research
(MEMO-793; ISSN-0169-2690; ETN-90-95960) Avail: NTIS HC A03/MF A01

A specific diophantine equation is proved to have essentially 156 solutions, and these are listed. It is only a paradigmatic example of the general Thue-Mahler equation, and is studied to show that any Thue-Mahler equation can in practice be solved by the same method. The method used is the theory of p-adic linear forms in logarithms, which is used for obtaining an explicit upper bound for the solutions, together with a computational technique to reduce this bound considerably. This is done by a combination of real and p-adic diophantine approximation computations, based on the L3-algorithm. ESA

N90-14033# Universiteit Twente, Enschede (Netherlands). Faculty of Applied Mathematics.
ANOTHER APPROACH TO THE LOCAL DISTURBANCE DECOUPLING PROBLEM WITH STABILITY FOR NONLINEAR SYSTEMS
Leo vanderWegen Jul. 1989 12 p
(MEMO-799; ISSN-0169-2690; ETN-90-95966) Avail: NTIS HC A03/MF A01

The local disturbance decoupling problem with stability which is the problem of finding a regular state feedback such that for the feedback system the outputs are decoupled from the disturbances and the equilibrium (x sub e), is locally exponentially stabilized. A crucial role in the solution of this problem is played by a distribution that is in some sense the smallest locally controlled invariant distribution containing the disturbance vector fields. Essential in order that the problem is solvable is that the drift dynamics restricted to the leaf of this distribution through (x sub e) is locally exponentially stabilizable. Conditions for solvability of the local disturbance decoupling problem with stability for a nonlinear system are given in terms of conditions for the linearization of such a system around (x sub e). ESA

N90-14034# Universiteit Twente, Enschede (Netherlands). Faculty of Applied Mathematics.
PRACTICE OF BIVARIATE QUADRATIC SIMPLICIAL SPLINES
C. R. Traas Jul. 1989 44 p
(MEMO-800; ISSN-0169-2690; ETN-90-95967) Avail: NTIS HC A03/MF A01

A study on bivariate simplicial splines (B-splines) is presented from the point of view of the user. A recapitulation of the relevant parts of the theory is given. A number of processes are described which are fundamental in applications: evaluating and differentiating B-splines, constructing approximation spaces, satisfying boundary conditions, and using control points and inner products. Each of these items is extensively illustrated. A test problem from the field of finite elements is presented. ESA

N90-14035# Universiteit Twente, Enschede (Netherlands). Dept. of Computer Science.
ANALYSIS OF THREE APPROACHES TO QUALITATIVE SIMULATION
A. Makarovic Jun. 1989 51 p
(Memo-INF-89-32; UT-KBS-89-02; ISBN-90-365-0288-8; ISSN-0923-1714; ETN-90-95969) Avail: NTIS HC A04/MF A01

Three approaches in the area of qualitative simulation developed by Knipers, De Kleer, and Forbus are analyzed to provide insight into the main techniques used, problems encountered, and the way these problems are addressed. Serious deficiences in the approaches are described. The Forbus approach is suggested as suitable for representing a wide class of physical systems, while the other two approaches are suggested as intended for prediction of behavior which the model builder did not foresee. Particular problems are outlined and further research is advised to make qualitative simulation useful for real world problems. ESA

N90-14036# Center for Mathematics and Computer Science, Amsterdam (Netherlands). Dept. of Pure Mathematics.
LINEAR GROUPS AND DISTANCE-TRANSITIVE GRAPHS
John T. M. vanBon and Arjeh M. Cohen Jun. 1989 14 p
(CWI-PM-R8805; ETN-90-95971) Copyright Avail: NTIS HC A03/MF A01

In a continuing study, a detailed treatment is presented of the graphs on which a group with simple socle PSL(n,q) acts distance-transitively. Theorems and proofs are outlined. ESA

N90-14037# Center for Mathematics and Computer Science, Amsterdam (Netherlands). Dept. of Pure Mathematics.
ON DISTANCE-TRANSITIVE GRAPHS AND INVOLUTIONS
John T. M. vanBon Jul. 1988 16 p
(CWI-PM-R8808; ETN-90-95972) Copyright Avail: NTIS HC A03/MF A01

A result on distance-transitive graphs is presented, concerning the case where there is a suborbit on which a maximal subgroup of a finite group acts unfaithfully. The use of the result in the case where the vertex stabilizer is the centralizer of some construction is demonstrated. ESA

N90-14038*# Institute for Computer Applications in Science and Engineering, Hampton, VA.
COMPUTATIONAL ASPECTS OF PSEUDOSPECTRAL LAGUERRE APPROXIMATIONS Final Report
Daniele Funaro (Pavia Univ., Italy) Oct. 1989 16 p Submitted for publication

(Contract NAS1-18605)
(NASA-CR-181934; NAS 1.26:181934; ICASE-89-72) Avail: NTIS HC A03/MF A01 CSCL 12A

Pseudospectral approximations in unbounded domains by Laguerre polynomials lead to ill-conditioned algorithms. Introduced are a scaling function and appropriate numerical procedures in order to limit these unpleasant phenomena. Author

N90-14039# Grenoble-1 Univ. (France). Lab. des Tech. de l'Informatique, des Math., de la Microelectronique et de la Microscopie Quant.

MEASUREMENT OF ARITHMETIC ERROR AND CALCULATION PERTURBATIONS [MESURE DE L'ERREUR ARITHMETIQUE ET PERTURBATION DES CALCULS]

Philippe Francois Feb. 1989 43 p In FRENCH; ENGLISH summary
(IMAG-RR-767-M; ETN-90-95698) Avail: NTIS HC A03/MF A01

The concepts of arithmetic stability and conditioning, and the regularity of an algorithm, are formulated. The usefulness of stochastic arithmetic in stability analysis of an algorithm is explained. A perturbed arithmetic package is proposed. It consists of a methodology for analyzing the potential arithmetic instabilities of an algorithm. Examples are given. ESA

N90-14040# Grenoble-1 Univ. (France). Lab. des Techniques de l'Informatique, des Mathematiques, de la Microelectronique et de la Microscop

DISTRIBUTION OF A SUM OF n RANDOM VARIABLES AND A CENTRAL LIMIT THEOREM BASED ON MOMENTS OR ON COEFFICIENTS OF POLYNOMIAL DEPENDENCE [LOI DE LA SOMME DE N VARIABLES ALEATOIRES ET THEOREME DE LA LIMITE CENTRALE PAR LES COEFFICIENTS DE DEPENDANCE POLYNOMIALE ET LES MOMENTS]

R. Blacher Feb. 1989 100 p In FRENCH; ENGLISH summary
(IMAG-RR-768-M; ETN-90-95699) Avail: NTIS HC A05/MF A01

The law pertaining to the sum of n random variables is obtained by rewriting the laws of probability as expansions of Hermite or Laguerre polynomials. The Fourier transforms of orthogonal polynomials, are presented as a demonstration. The Fourier transforms are calculated for a variety of orthogonal polynomials. The results are used in developing a central limit theorem. A different version of this theorem is thus obtained. This alternate version is presented. ESA

N90-14041# Grenoble-1 Univ. (France). Lab. des Techniques de l'Informatique, des Mathematiques, de la Microelectronique et de la Microscop

DESCRIPTION AND MANIPULATION OF CONVEX POLYGONS USING POLARITY [REPRESENTATION ET LA MANIPULATION DE POLYGONES CONVEXES DANS IR2 DUALITE]

M. Duc-Jacquet, A. Eberhard, and B. Lacolle Mar. 1989 40 p In FRENCH; ENGLISH summary
(IMAG-RR-771-M; ETN-90-95700) Avail: NTIS HC A03/MF A01

Using the geometric transform known as polarity, two dual descriptions of convex polygons are developed: the usual standard form and the minimal ordered writing form. The concept of duality leads to the generalized standard form for unbounded convex polygons. For such unbounded polygons, generalized versions of optimal algorithms for intersecting half-planes and for intersecting two convex polygons are developed. An original algorithm is used to determine for a given direction of parallel planes, any plane section on the convex polyhedron which is given by the intersection on half-planes. ESA

N90-14042# Grenoble-1 Univ. (France). Lab. des Techniques de l'Informatique, des Mathematiques, de la Microelectronique et de la Microscop

DATA STRUCTURES FOR THE REPRESENTATION AND MANIPULATION OF POLYHEDRONS [STRUCTURE DE DONNEES POUR LA REPRESENTATION ET LA MANIPULATION DES POLYEDRES]

Thierry Carlier and Nicolas Szafran Mar. 1989 43 p In FRENCH; ENGLISH summary
(IMAG-RR-772-M; ETN-90-95701) Avail: NTIS HC A03/MF A01

Techniques for computing the manipulation of polyhedrons are presented. The steps involved in finding the best data structure to be used in representing all convex polyhedrons are described. Four algorithms used to manipulate these polyhedrons are presented. These algorithms are sufficiently general and take into account most of the situations that can occur. Two of them find the convex hull of a set of points in three-dimensional space. The other two calculate the intersections of two convex polyhedrons. ESA

N90-14043# Rome Univ. (Italy). Dipt. di Fisica.

ON A NEW INTEGRABLE HAMILTONIAN SYSTEM WITH NEAREST NEIGHBORS INTERACTION

M. Bruschi and Orlando Ragnisco 28 Apr. 1989 24 p Sponsored in part by the Italian Ministry of Public Education
(Preprint-667; ETN-90-95795) Avail: NTIS HC A03/MF A01

An integrable system with nearest neighbor interaction is described. The system is shown to be completely integrable and explicitly solvable by a suitable change of variables. A spectral transform approach is presented and the infinity limit is tersely investigated. The apparent redundancy of the approach is defended as providing a nontrivial example of a system where all the various techniques employed to deal with nonlinear integrable Hamiltonian systems can be shown at work simultaneously. ESA

N90-14044# Rome Univ. (Italy). Dipt. di Fisica.

A UNIFIED ALGEBRAIC APPROACH TO INTEGRAL AND DISCRETE EVOLUTION EQUATIONS

Orlando Ragnisco and P. M. Santini 28 Apr. 1989 15 p Sponsored in part by the Italian Ministry of Public Education
(Preprint-668; ETN-90-95796) Avail: NTIS HC A03/MF A01

The integrability properties of discrete systems and singular integral evolution equations are investigated. It is shown that they correspond to different reductions and different concrete constructs of the same abstract algebraic structures. The bi-hamiltonian formulations of prototype examples such as the discrete sine-Gordon and sine-Hibert equations are obtained. ESA

N90-14045 Institut d'Aeronomie Spatiale de Belgique, Brussels.

AN ITERATIVE METHOD TO SOLVE THE NONLINEAR POISSON'S EQUATION IN THE CASE OF PLASMA TANGENTIAL DISCONTINUITIES

M. Roth, J. Lemaire, and A. Misson (Ecole Polytechnique Federale de Lausanne, Switzerland) 1989 43 p Submitted for publication
(Aeronomica-Acta-A-346-1989; ISSN-0065-3713; ETN-90-95931) Avail: Institut d'Aeronomie Spatiale de Belgique, 3 Avenue Circulaire, B-1180 Brussels, Belgium

A nonlinear second order Poisson equation is solved by an iterative method. This solution is used to determine the electric potential of collisionless tangential discontinuities of a magnetized plasma. An ordered sequence of nonlinear algebraic equations for each successive approximation of the actual electrical potential is developed. It is shown that the method holds for transitions as thin as 5 Debye, but fails for thicknesses of 3 Debye or less due to the fact that the iteration procedure no longer converges. ESA

N90-13430*# Illinois Univ., Urbana. Dept. of Aeronautical and Astronautical Engineering.

BILINEAR MODELING AND NONLINEAR ESTIMATION

Thomas A. W. Dwyer, III, Fakhreddine Karray, and William H.

Bennett *In* NASA, Goddard Space Flight Center, Flight Mechanics/Estimation Theory Symposium, 1989 Oct. 1989 p 275-297 (For primary document see N90-13413 05-13)
(Grants NAG1-613; F49620-87-C-0103)
Avail: NTIS HC A20/MF A03 CSCL 12A

N90-13431*# National Aeronautics and Space Administration. Goddard Space Flight Center, Greenbelt, MD.
EXTENSION TO EULERS'S THEOREM TO n-DIMENSIONAL SPACES
Itzhack Y. Bar-Itzhack (Technion - Israel Inst. of Tech., Haifa.) *In its* Flight Mechanics/Estimation Theory Symposium, 1989 Oct. 1989 p 299-315 (For primary document see N90-13413 05-13)
Avail: NTIS HC A20/MF A03 CSCL 12A

65 STATISTICS AND PROBABILITY

Includes data sampling and smoothing; Monte Carlo method; and stochastic processes.

N90-14046# Center for Mathematics and Computer Science, Amsterdam (Netherlands). Dept. of Operations Research, Statistics, and System Theory.
THEORY OF GOODNESS OF FIT TESTS AND SCANNING INNOVATION MARTINGALES
E. V. Khmaladze (Steklov Mathematical Inst., Moscow, USSR) Jan. 1989 31 p Sponsored by Netherlands Organization for the Advancement of Research
(CWI-BS-R8904; ETN-90-95614) Copyright Avail: NTIS HC A03/MF A01

The statistical problem of the construction, in the case of random variables of any finite dimension and both simple or parametric hypotheses, of empirical processes which could provide the basis for goodness of fit tests - more or less in the same way as the uniform empirical process does in the case of simple hypothesis and scalar random variables, is addressed. The solution of this problem is connected with the theory of multiparameter martingales and the theory of function-parametric processes. Namely, for the limiting Gaussian processes some kind of filtration is introduced and so-called scanning innovation processes are constructed - the adapted standard Wiener processes in on-to-one correspondence with initial Gaussian processes. This is done for the function-parametric versions of the processes. Innovation martingale processes with multidimensional time parameter are discussed with reference to their introduction in function-parametric processes. ESA

N90-14047# Rome Univ. (Italy). Dipt. di Fisica.
ON THE EFFECTS OF AN UNCERTAINTY ON EVOLUTION LAW IN DYNAMICAL SYSTEMS
Andrea Crisanti, Massimo Falcioni, and Angelo Vulpiani (Istituto Nazionale di Fisica Nucleare, Rome, Italy) 20 Jul. 1989 36 p Submitted for publication
(Preprint-689; ETN-90-95809) Avail: NTIS HC A03/MF A01

It is shown that a small perturbation of the evolution law of chaotic dynamical systems is practically equivalent to the finite precision on the knowledge of the initial condition. In spite of the short predictability time t sub p on a single trajectory the statistical properties are not sensitive to small changes in the evolution law or initial probability distribution. This feature holds also for correlation functions at a delay larger than t sub p. The roundoff effects on an integrable systems are discussed. ESA

N90-14048# Technische Univ., Eindhoven (Netherlands). Dept. of Mathematics and Computing Science.
COUNTEREXAMPLES TO ROBERTSON'S CONJECTURE
F. W. Steutel Nov. 1988 10 p
(MEMO-COSOR-88-32; ETN-90-95944) Avail: NTIS HC A02/MF A01

Counter examples to Robertson's conjecture are presented which show negative coefficients. The proofs given depend on well known and fairly elementary results on the divisibility of probability distributions, which are discussed. Results from probability theory are shown to be useful. ESA

N90-14049# Grenoble-1 Univ. (France). Lab. des Tech. de l'Informatique, des Math., de la Microelectronique et de la Microscopie Quant.
SOME QUICK AND EFFICIENT METHODS FOR BEARING-ONLY TARGET MOTION ANALYSIS
Pham Dinh Tuan Jan. 1989 45 p
(IMAG-RR-762-M; ETN-90-95696) Avail: NTIS HC A03/MF A01

Estimation methods for the trajectory of a target, assumed to be linear uniform, based on bearing observations only, are described. The observer is assumed to have a linear uniform motion so one can only estimate the relative motion of the target to it, up to a multiplicative constant. This motion is parameterized by three bearings at three judiciously chosen times. Some simple, quick and highly efficient estimators for them are proposed. It is assumed that the observer's motion is composed of constant velocity segments. The results are generalized to obtain two sets of quasi-sufficient statistics, which contain all relevent information. The quadratic estimator, which is similar to the pseudo-linear estimator but has no bias, is introduced. The covariance matrix of the estimator is examined in relation to the Cramer-Rao bound. Some iterative schemes for attaining the latter are discussed. ESA

N90-14050# Rome Univ. (Italy). Dipt. di Fisica.
LARGE DEVIATION ESTIMATES IN THE STOCHASTIC QUANTIZATION OF PHI SUB 2 EXP 4
G. Jona-Lasinio and P. K. Mitter 12 Jul. 1989 20 p
(Preprint-686; ETN-90-95806) Avail: NTIS HC A03/MF A01

The behavior of field trajectories for the process constructed by the authors in connection with the stochastic quantization of phi sub 2 exp 4 is studied. Due to the presence of infinite renormalization, the usual large deviation techniques do not apply immediately and a new strategy has to be developed. Some estimates analogous to the Freidlin-Ventzel inequalities, are proved. It follows that the field trajectories suitably smeared in space over a scale r sub o behave as the projection on the same scale of a field obeying a regularizad stochastic equation with a large cut-off, when the noise is small. Estimates are not uniform in the cut-off and an interesting feature of the problem, that the scale over which the field is smeared determines whether the noise is sufficiently small for the estimates to apply, is investigated. ESA

N90-14051# Technische Univ., Eindhoven (Netherlands). Dept. of Mathematics and Computing Science.
ESTIMATION OF CONVOLUTION TAIL BEHAVIOR
Eric Willekens (Limburg State Univ., Maastricht, Netherlands) and Noeel Veraverbeke Feb. 1989 18 p Sponsored in part by the United States Dept. of Statistics and the Belgian National Fund for Scientific Research
(Contract F49620-85-C-0144)
(MEMO-COSOR-89-04; ETN-90-95949) Avail: NTIS HC A03/MF A01

A statistic which estimates the asymptotic behavior of convolution tails of a given distribution function is introduced which is asymptotically normal under appropriate conditions. An asymptotic representation in probability for intermediate order statistics is presented which is an important tool and a result of independent interest. ESA

N90-14052# Technische Univ., Eindhoven (Netherlands). Dept. of Mathematics and Computing Science.
SELF-DECOMPOSABLE DISTRIBUTIONS AND BRANCHING PROCESSES
Bjorn Garn Hansen Apr. 1989 41 p
(MEMO-COSOR-89-06; ETN-90-95951) Avail: NTIS HC A03/MF A01

The self-decomposable property of a distribution of random variables was studied. A review of some basic properties of

branching process is given, and the results are used to define and characterize an alpha-discounted branching process with immigration. Canonical representations for the F-stable and F, alpha-self-decomposable Laplace-Stieltjes transforms are given. Sets for these transforms are defined and their representations derived. These sets are shown to provide a classification of the set of infinitely divisable Laplace-Stieltjes transforms. Central limit theorems for F, alpha-self-decomposable distributions are given. ESA

N90-14053# Technische Univ., Eindhoven (Netherlands). Dept. of Mathematics and Computing Science.
NOTE ON URBANIK'S CLASS L(SUB n)
Bjorn Garn Hansen Apr. 1989 17 p
(MEMO-COSOR-89-07; ETN-90-95952) Avail: NTIS HC A03/MF A01

The analog of multiple self-decomposability for characteristic functions satisfying a specific condition is considered. Results are obtained which are analogous to those known for multiple self-decomposable characteristic functions. The theorems and proofs are outlined. ESA

N90-14054# Technische Univ., Eindhoven (Netherlands). Dept. of Mathematics and Computing Science.
REVERSE SELF-DECOMPOSABILITY
Bjorn Garn Hansen Apr. 1989 21 p
(MEMO-COSOR-89-08; ETN-90-95953) Avail: NTIS HC A03/MF A01

The analog of multiple self-decomposability for characteristic functions satisfying a given condition is considered. Results are obtained which are analogous to those known for multiple self-decomposable characteristic functions. Theorems and proofs are provided. ESA

66 SYSTEMS ANALYSIS

Includes mathematical modeling; network analysis; and operations research.

N90-14055# Center for Mathematics and Computer Science, Amsterdam (Netherlands). Dept. of Operations Research, Statistics, and System Theory.
SIMPLE APPOXIMATIONS FOR SECOND MOMENT CHARACTERISTICS OF THE SOJURN TIME IN THE M/G/1 PROCESSOR SHARING QUEUE
J. L. vandenBerg Apr. 1989 22 p
(CWI-BS-R8907; ETN-90-95617) Copyright Avail: NTIS HC A03/MF A01

Simple approximations are derived for the second moment of the conditional and unconditional sojourn time in the M/G/1 processor sharing queue. The approximations are mainly based on general asymptotic results (e.g. heavy traffic) and on simple exact expressions for specific service time distributions. They depend on the service time distribution only through its first and second moment. Numerous numerical examples are given which show that these simple approximations are accurate enough for many practical purposes. A refinement of the approximations is obtained by taking the third moment of the service time into account. ESA

N90-14056# Universiteit Twente, Enschede (Netherlands). Faculty of Applied Mathematics.
THE ACTIVITY SELECTION PROBLEM: A NETWORK AND GAME THEORETIC APPROACH
Theo Driessen Jun. 1989 14 p
(MEMO-794; ISSN-0169-2690; ETN-90-95961) Avail: NTIS HC A03/MF A01

The general activity selection problem is described and studied. An example of the special selection problem, in which five layers, three projects and eight resources are involved, is given. The equivalence between the activity selection problem and a minimum-cut problem, is reviewed. For each coalition, and optimal selection and the value of the characteristic function is shown to be found by solving a minimum-cut problem in an associated capacitated network. Due to the convexity of the activity selection game, the core is the most important game theoretic solution concept, and whether a proposed payoff vector belongs to the core is shown to be determined by the solution of a minimum-cut problem. The case of the so-called r-value payoff vector is considered. ESA

N90-14057# Universiteit Twente, Enschede (Netherlands). Faculty of Applied Mathematics.
ON STABILITY OF QUEUEING MODELS OF LOCAL AREA NETWORKS WITH SLOTTED RING PROTOCOLS
B. vanArem Jul. 1989 44 p
(MEMO-795; ISSN-0169-2690; ETN-90-95962) Avail: NTIS HC A03/MF A01

Stability of queueing models of local area networks with slotted ring protocols is considered. The model is described and a study of the queue length process is presented. A special type of stability, called r-stability, is defined. If a process is r-stable, then a steady-state distribution is defined, regardless of whether the process converges in distribution. The r-stability of the queue length processes is shown to be preserved if a station is shifted along the ring, provided it does not overtake any other station. For various protocols, necessary and sufficient conditions under which the queue length process is r-stable are proved. ESA

N90-14058# Universiteit Twente, Enschede (Netherlands). Faculty of Applied Mathematics.
ANALYSIS OF A QUEUEING MODEL FOR SLOTTED RING NETWORKS
B. vanArem and E. A. vanDoorn Jul. 1989 15 p Presented at the 7th ITC Specialists' Seminar, Adelaide, Australia, 1989 Submitted for publication
(MEMO-796; ISSN-0169-2690; ETN-90-95963) Avail: NTIS HC A03/MF A01

A mutli-server multi-queue system which is intended to model a local area network with slotted ring protocol is studied. Two special cases of the model are analyzed and the results are used to motivate an approach to approximate mean queue lengths in the general model. ESA

N90-14059# Universiteit Twente, Enschede (Netherlands).
DYNAMIC WORKLOAD MODELING OF HIGH SPEED TOKEN RINGS IN A METROPOLITAN AREA NETWORK
Boudewijn R. Haverkort and Ignas G. Niemegeers Mar. 1989 23 p Presented at the 3rd IEEE Workshop on Metropolitan Area Networks, San Diego, CA, 28-30 Mar. 1989 and the ACM Symposium, Austin, TX, Sep. 1989
(Memo-INF-89-21; ISSN-0923-1714; ETN-90-95968) Avail: NTIS HC A03/MF A01

The performance modeling of high speed token rings in a dynamically changing environment, as possible candidates for Metropolitan Area Networks (MANs), is studied. The MAN performance is analyzed by two approaches. The first is based on an upper- and a lowerbound load model and the second is based on a Markov model which describes the load changes during the MAN operation. The distributions of the waiting times at time t as perceived by the MAN user are derived due to the unpredictability of the actual load at time t. The upperbound-lowerbound approach is based on the intuitive observation that the workload exhibits some variability with some distribution. The resulting waiting times will therefore conform the same distribution. The Markov modeling approach is based on behavioral decomposition: the steady state behavior of a number of (in itself static) performance models is combined with the transient behavior of the environment (workload) model. This approximation is legitimate since there exist time scale differences between the two mentioned model parts. Both approaches are used for various models of high speed local area networks. Both models indicate that a small deviation in the workload model can

lead to a substantial deviation in the performance. The upperbound/lowerbound model is suggested as the most appropriate for modeling of the two proposed methods. ESA

N90-14060*# National Aeronautics and Space Administration. Lewis Research Center, Cleveland, OH.
MODELING OF POWER ELECTRONIC SYSTEMS WITH EMTP
Kwa-Sur Tam (Virginia Polytechnic Inst. and State Univ., Blacksburg.) and Narayan V. Dravid Dec. 1989 10 p
(NASA-TM-102375; E-5109; NAS 1.15:102375) Avail: NTIS HC A02/MF A01 CSCL 12B

In view of the potential impact of power electronics on power systems, there is need for a computer modeling/analysis tool to perform simulation studies on power systems with power electronic components as well as to educate engineering students about such systems. The modeling of the major power electronic components of the NASA Space Station Freedom Electric Power System is described along with ElectroMagnetic Transients Program (EMTP) and it is demonstrated that EMTP can serve as a very useful tool for teaching, design, analysis, and research in the area of power systems with power electronic components. EMTP modeling of power electronic circuits is described and simulation results are presented. Author

N90-14061*# National Aeronautics and Space Administration. Langley Research Center, Hampton, VA.
LABORATORY TEST METHODOLOGY FOR EVALUATING THE EFFECTS OF ELECTROMAGNETIC DISTURBANCES ON FAULT-TOLERANT CONTROL SYSTEMS
Celeste M. Belcastro Nov. 1989 20 p
(NASA-TM-101665; NAS 1.15:101665) Avail: NTIS HC A03/MF A01 CSCL 12B

Control systems for advanced aircraft, especially those with relaxed static stability, will be critical to flight and will, therefore, have very high reliability specifications which must be met for adverse as well as nominal operating conditions. Adverse conditions can result from electromagnetic disturbances caused by lightning, high energy radio frequency transmitters, and nuclear electromagnetic pulses. Tools and techniques must be developed to verify the integrity of the control system in adverse operating conditions. The most difficult and illusive perturbations to computer based control systems caused by an electromagnetic environment (EME) are functional error modes that involve no component damage. These error modes are collectively known as upset, can occur simultaneously in all of the channels of a redundant control system, and are software dependent. A methodology is presented for performing upset tests on a multichannel control system and considerations are discussed for the design of upset tests to be conducted in the lab on fault tolerant control systems operating in a closed loop with a simulated plant. Author

67 THEORETICAL MATHEMATICS

Includes topology and number theory.

N90-14062# Center for Mathematics and Computer Science, Amsterdam (Netherlands). Computer Science/Dept. of Software Technology.
INDUCTIVE REASONING AND KOLMOGOROV COMPLEXITY (PRELIMINARY VERSION)
Ming Li and Paul M. B. Vitanyi Apr. 1989 25 p Presented at the 4th Annual IEEE Structure in Complexity Theory Conference, 1989 Submitted for publication
(Contracts N00014-85-K-0445; DAAL03-86-K-0171; NSF DCR-86-06366; NSERC-0GP-0036747)
(CWI-CS-R8915; ETN-90-95659) Copyright Avail: NTIS HC A03/MF A01

Inductive reasoning in correspondence with ideas of Solomonoff is studied, with focus on the fact that although his proposals result in perfect procedures, they involve the noncomputable notion of Kolmogorov complexity. The thesis that Solomonoff's method is fundamental, in the sense that many other induction principles can be viewed as particular ways to obtain computable approximations to it, is developed. This is demonstrated explicity in the cases of Gold's paradigm for inductive inference, Valiant's learning (by adding computational requirements), Rissanen's minimum description length (MDL) principle, Fisher's maximum likelihood principle, and Jaynes's maximum entropy principle. Several theorems and derivations to this effect are presented. What can be learned and what cannot be learned in terms of Kolmogorov complexity is presented, and an experiment in machine learning of handwritten characters is described. ESA

N90-14063# Rome Univ. (Italy). Dipt. di Fisica.
FLUCTUATIONS OF THE LYAPUNOV EXPONENT IN DISORDERED SYSTEMS
Stam Nicolis, Giovanni Paladin, and Angelo Vulpiani (Istituto Nazionale di Fisica Nucleare, Rome, Italy) 20 Jul. 1989 17 p
(Preprint-690; ETN-90-95810) Avail: NTIS HC A03/MF A01

The fluctuations of the maximum Lyapunov exponent of a product of random matrices are studied analytically and numerically. It is shown that they may be expressed as a sum of two terms, one related to the order of matrices within the product, the other to fluctuations of the number of matrices of a given type. This result is applied to the one-dimensional random-field Ising model and the discrete Schrodinger equation with a random potential. ESA

N90-14064# Center for Mathematics and Computer Science, Amsterdam (Netherlands). Dept. of Operations Research and System Theory.
A GRAPH THEORETIC CHARACTERIZATION FOR THE RANK OF THE TRANSFER MATRIX OF A STRUCTURED SYSTEM
J. W. vanderWoude Nov. 1988 12 p
(CWI-OS-R8819; ETN-90-95970) Copyright Avail: NTIS HC A03/MF A01

Structured systems are considered and the generic rank of the transfer matrix of such systems is introduced. This rank is shown to equal the maximum number of vertex disjoint paths from the input vertices to the output vertices in the graph that can be associated to the structured system. This maximum number of disjoint paths is calculated using techniques from combinatorics. As an application a structural version is proposed of the well-known almost disturbance decoupling problem. ESA

N90-14065# Center for Mathematics and Computer Science, Amsterdam (Netherlands). Dept. of Applied Mathematics.
THE ALGEBRAIC BASIS OF MATHEMATICAL MORPHOLOGY. PART 1: DILATIONS AND EROSIONS
H. J. A. M. Heijmans and C. Ronse (Philips Research Labs., Brussels, Belgium) Jun. 1988 52 p
(CWI-AM-R8807; ETN-90-95974) Copyright Avail: NTIS HC A04/MF A01

The Mathematical morphology, the theory of image transformations and functionals deriving its tools from set theory and integral geometry, is addressed. A general algebraic approach is presented which both reveals the mathematical structure of morphological operations and unifies several examples into one framework. The main assumption is that the object space is a complete lattice and that the transformations of interest are invariant under a given abelian group of automorphisms on that lattice. The basic operations called dilation and erosion are shown to be adjoints of each other in a very specific lattice sense and can be completely characterized if the automorphism group is assumed to be transitive on a sub-generating subset of the complete lattice. The abstract theory is illustrated by a large variety of examples and applications. ESA

N90-14066# Rome Univ. (Italy). Dipt. di Fisica.
SCALING IN A NON ABELIAN STRING NETWORK
A. M. Allega 31 May 1989 24 p
(ROM1F-89-676; ETN-90-95783) Avail: NTIS HC A03/MF A01

A complete scaling picture for a network of Abelian strings on a torus is presented. A model to study SO(3) strings on the lattice is developed. Non Abelian strings are realized by Kibble's criterion

and a scaling picture comes out with a third phase distinguished by a characteristic length. Topological contributions are discussed with respect to nontrivial ones. Two general classes of topology are selected and the infinite volume limit is analyzed. ESA

N90-14067# Rome Univ. (Italy). Dipt. di Fisica.
CONFIGURATIONAL STATISTICS OF STRINGS, FRACTALS AND POLYMER PHYSICS. PART 2: NON ABELIAN STRINGS
A. M. Allega 20 Jun. 1989 37 p
(ROM1F-89-680-Pt-2; ETN-90-95786) Avail: NTIS HC A03/MF A01

A systematic numerical analysis of Kibble's non abelian strings is presented. A new phase structure determined by three different scaling laws stresses the intrinsic complexity of this statistical system. Strings, like polymers, show a fractal nature which is strongly dependent on their own topology. The main reason for the third new region, a screening phenomenon already present in the topologically trivial sector of the Abelian situation, is described. Correlations become stronger the longer the string length is. An interpretation of correlations as functionally depending on string concentrations is proposed. Global quantities, such as the probability of no return, are clearly evident in diverging aspects of the model. ESA

N90-14068# Rome Univ. (Italy). Dipt. di Fisica.
STATISTICAL MECHANICS OF STRINGS AND TOPOLOGY
A. M. Allega 20 Jun. 1989 14 p
(ROM1F-89-683; ETN-90-95789) Avail: NTIS HC A03/MF A01

A second order phase transition mediated by strings is discussed in the context of statistical mechanics of strings. Criticality for strings is considered versus the manifold topology. Monte Carlo data on Abelian and non Abelian strings is reported. Attention is called to the importance of scaling in the statistical mechanics of strings. ESA

N90-14069# Rome Univ. (Italy). Dipt. di Fisica.
R-MATRICES AND HIGHER POISSON BRACKETS FOR INTEGRABLE SYSTEMS
Walter Oevel and Orlando Ragnisco 8 Apr. 1989 38 p
Sponsored in part by the Italian Ministry of Public Education, and by Italian Istituto Nazionale di Fisica Nucleare
(Preprint-669; ETN-90-95797) Avail: NTIS HC A03/MF A01

Construction on an integrable set of equations from an R-matrix is demonstrated. These equations can be based on any algebra with a symmetric trace form. They are bi-Hamiltonian relative to a linear (modified) Lie-Poisson-bracket and relative to a cubic bracket. With additional assumptions for the R-matrix, a further quadratic bracket is found, leading to a tri-Hamiltonian formulation of these integrable equations. ESA

N90-14070# Rome Univ. (Italy). Dipt. di Fisica.
SOME COMMENTS ON THE SOLVABLE CHIRAL POTTS MODEL
V. B. Matveev (Leningrad State Univ., USSR) and A. O. Smirnov 18 May 1989 10 p
(Preprint-673; ETN-90-95801) Avail: NTIS HC A02/MF A01

A simple proof of the conjecture produced by Baxter, Perk and Au-Yang on the structure of the normalization factor corresponding to their new solution of the star-triangle equation related to the generalized Fermat curve is presented. Some important properties of the underlying curve are established. The matrix of the b-periods for some normalized basis of holomorphic differentials is calculated. Associated four-dimensional theta-function decomposition into a sum containing twelve terms, each term being the product of four one-dimensional theta-functions is shown. Picard-Fuchs equations for the periods of holomorphic differentials of the same curve are derived. The appearance of the hyper-geometric functions in the answers seem to be closely related to an expression for the ground-state energy per site, obtained for the superintegrable case by Albertini, Perk, McCoy and, independently, Baxter. ESA

70 PHYSICS (GENERAL)

For precision time and time interval (PTTI) see *35 Instrumentation and Photography;* for geophysics, astrophysics or solar physics see *46 Geophysics, 90 Astrophysics,* or *92 Solar Physics.*

N90-14071# Rome Univ. (Italy). Dipt. di Fisica.
ENERGY EXCHANGE OF INTERACTING SOLITONS IN MULTIDIMENSIONS
P. M. Santini 9 Mar. 1989 34 p
(Preprint-662; ETN-90-95793) Avail: NTIS HC A03/MF A01

The formalism developed by Fokas and the author for the solution of the initial boundary value problem for the Davey-Stewartson equation is used to study the time evolution of the multisoliton solution, showing in particular that interacting solitions in multidimensions not only exhibit a two-dimensional phase shift, but also exchange energy. Several examples of physically relevant boundary conditions which generate other kinds of explicit, finite energy solitons on the plane are presented. ESA

N90-14072# Technische Univ., Delft (Netherlands).
SURFACE COOLED, VACUUM IMPREGNATED SUPERCONDUCTING MAGNET SYSTEMS: DESIGN, CONSTRUCTION, APPLICATIONS Ph.D. Thesis
Jacobus Adrianus Mar Dam and Karel Pieterman 1989 261 p
Original contains color illustrations
(ETN-90-96014) Avail: NTIS HC A12/MF A01

The design and construction of three superconducting magnet systems for applications in the fields of medical imaging, plasma physics and nuclear physics are described. All three systems have vacuum impregnated, intrinsically stable coils with cooling at the outer surfaces of the winding package with liquid helium, and are all coupled in some way to closed cycle cooling systems. General theories are discussed. The techniques used in both the design and the construction of the different magnet systems, are given. The use of numerical methods for the calculation of thermal and mechanical properties of superconducting coil systems, is emphasized. The experimental results obtained with the Delft magnetic resonance imaging system are described and examples of images showing sagittal sections of the human head, successfully produced with this system, are given. ESA

71 ACOUSTICS

Includes sound generation, transmission and attenuation. For noise pollution see *45 Environmental Pollution.*

N90-14073# Mississippi Univ., University. Physical Acoustics Research Lab.
PROPAGATION OF SOUND IN VIBRATIONALLY EXCITED NITROGEN AND HYDROGEN GAS MIXTURES M.S. Thesis
Timothy H. Ruppel 31 Jul. 1989 50 p
(Contract N00014-84-C-0193)
(AD-A213002; PARGUM-89-02) Avail: NTIS HC A03/MF A01
CSCL 07/4

Measurements of the resonant reverberation of sound in a tube containing N2/H2, N2/He, N2/CH4, and N2/H2O mixtures have shown an amplification of the sound following a rapid excitation of the gas by an electric discharge. This effect has been named SACER (Sound Amplification from Controlled Excitation Reactions). This paper reports similar measurements in N2/CO and in CO/H2/He mixtures. It has been possible in the past to determine vibrational relaxation times and relaxation times for the conduction of translational and vibrational energy to the tube wall from the changes in the translational temperature in the gas following the electric discharge. In the work reported here, these rates have been confirmed by direct measurement of the decay times of the CO infrared emission. GRA

N90-14074# Ecole Centrale de Lyon (France). Lab. de Mecanique des Fluides et d'Acoustique.
A MODEL SUITABLE FOR PREDICTING THE NOISE ASSOCIATED WITH THE DUCTED TAIL ROTOR OF A HELICOPTER Ph.D. Thesis [MISE AU POINT D'UNE METHODE DE CALCUL ADAPTEE AU BRUIT DES FENESTRONS D'HELICOPTERES]
Francette Fournier 1988 162 p In FRENCH
(ECL-88-09; ETN-90-95765) Avail: NTIS HC A08/MF A01

Different fenestron configurations are studied experimentally. The measured acoustical characteristics include frequency spectra and directivity for several pitch angles of the rotor blades. The primary noise sources discussed include the rotor noise due to ingestion of preturbulence, the stator noise due to interaction with rotor created viscous wakes, and the noise due to the presence of transmission shaft and support arm in the stator. A method is developed to take into account the wakes and the potential field. Good agreement is found between experiment and theory. ESA

N90-14075# Ecole Centrale de Lyon (France).
A MIXED FINITE ELEMENT SOLUTION OF THE LINEAR ACOUSTIC EQUATIONS Ph.D. Thesis
Abdelillah Bouizi 1989 133 p In FRENCH; ENGLISH summary Original contains color illustrations
(ECL-89-006; ETN-90-95781) Avail: NTIS HC A07/MF A01

A three dimensional model for the study of the linear problems of indoor acoustics is presented. The variational formulation is solved by means of a mixed procedure which is derived from conservation equations for the fluid. The discretization uses isoparametric finite element based on quadratic shape functions for a twenty noded element. The advantages are that curved boundaries can be closely represented, that good accuracy of sound intensity is attainable, and that the method can be applied in the presence of main flow. The good agreement between compared results illustrates the model validity. ESA

72 ATOMIC AND MOLECULAR PHYSICS

Includes atomic structure, electron properties, and molecular spectra.

N90-14076*# Academy of Sciences (USSR), Moscow.
OBSERVATIONAL PHYSICS OF MIRROR WORLD
M. Ya. Khlopov, G. M. Beskin, N. E. Bochkarev, L. A. Pustilnik, and S. A. Pustilnik (Academy of Sciences, USSR, Arkhys) Sep. 1989 28 p
(Grant NAGw-1340)
(NASA-CR-185923; NAS 1.26:185923; FERMILAB-Pub-89/193-A) Avail: NTIS HC A03/MF A01 CSCL 20H

The existence of the whole world of shadow particles, interacting with each other and having no mutual interactions with ordinary particles except gravity is a specific feature of modern superstring models, being considered as models of the theory of everything. The presence of shadow particles is the necessary condition in the superstring models, providing compensation of the asymmetry of left and right chirality states of ordinary particles. If compactification of additional dimensions retains the symmetry of left and right states, shadow world turns to be the mirror one, with particles and fields having properties strictly symmetrical to the ones of corresponding ordinary particles and fields. Owing to the strict symmetry of physical laws for ordinary and mirror particles, the analysis of cosmological evolution of mirror matter provides rather definite conclusions on possible effects of mirror particles in the universe. A general qualitative discussion of possible astronomical impact of mirror matter is given, in order to make as wide as possible astronomical observational searches for the effects of mirror world, being the unique way to test the existence of mirror partners of ordinary particles in the Nature. Author

N90-14077# Groningen Rijksuniv. (Netherlands). Kernfysisch Versneller Inst.
THE EFFECTIVE (3)He-NUCLEON FORCE IN A MICROSCOPIC DWBA APPROACH TO THE (3)He,T CHARGE EXCHANGE REACTION
S. Y. vanderWerf, S. Brandenburg, P. Grasdijk, W. A. Sterrenburg, M. N. Harakeh, M. B. Greenfield, B. A. Brown, and M. Fujiwara (Osaka Univ., Japan) 1989 46 p Submitted for publication
(KVI-763; ETN-89-95745) Avail: NTIS HC A03/MF A01

The (Helium-3,t) reaction is studied on C-12, O-16, Mg-24, Mg-26, Si-28, S-32, Ca-42, Ca-48, Fe-54, Ni-58, and Zr-90 targets, at incident energies of 66 to 90 MeV. From angular distributions of transitions to selected states, the parameters V(sub tau), V(sub sigma tau), V(sub T tau), and V(sub LS tau) concerning an effective projectile-nucleon force with single Yukawa potentials parameterization is obtained for this energy range. Differences from the force proposed by Schaeffer for a lower energy are found, notably in the tensor component. ESA

N90-14078# New York Univ., New York. Dept. of Physics.
INTERACTION OF RADIATION WITH MATTER: ATOMIC COLLISION PROCESSES OCCURRING IN THE PRESENCE OF RADIATION FIELDS Annual Report, 1 Aug. 1988 - 30 Sep. 1989
P. R. Berman 30 Sep. 1989 13 p
(Contract N00014-87-K-0303)
(AD-A213112) Avail: NTIS HC A03/MF A01 CSCL 20/5

Physics research was carried out in the areas of: (1) Quantum jumps; (2) Coherent transients; (3) laser assisted collisions; (4) Collision induced resonant structures in laser spectroscopy; (5) Collision kernels and transport coefficients; (6) Interactions with broadband noise. A brief synopsis is given in each area. GRA

N90-14079# Rome Univ. (Italy). Dipt. di Fisica.
LATTICE QCD ESTIMATE OF MIXING PARAMETERS FOR HEAVY MESON SYSTEMS
M. Lusignoli, Guido Martinelli, and A. Morelli 20 Jul. 1989 15 p
(Preprint-687; ETN-90-95807) Avail: NTIS HC A03/MF A01

The matrix elements of the two four fermion operators relevant for the calculation of mixing in the D-D system are obtained by a lattice quantum chromodynamics (QCD) calculation in the quenched approximation at beta = 60. The resulting B-parameters are close to each other and not very different from one. The physical implications are discussed, together with a possible extrapolation of the results to the more interesting B-B case. ESA

N90-14080# Rome Univ. (Italy). Dipt. di Fisica.
NONPOTENTIAL SCATTERING FOR THE DENSITY MATRIX AND QUANTUM GRAVITY
R. Mignani 20 Jul. 1989 11 p
(Preprint-688; ETN-90-95808) Avail: NTIS HC A03/MF A01

A Lie-isotopic density operator is constructed, and its main properties derived. A preliminary application is given to the scattering of incoherent beams of particles interacting via nonconservative, nonpotential forces. A possible connection between this formalism and a quantum-gravity model of quantum-mechanics violation, recently discussed by Ellis, Nanopoulos et al., is developed. ESA

N90-14081# Rome Univ. (Italy). Dipartimento di Fisica.
PERFORMANCE OF RESISTIVE PLATE COUNTERS AT BEAM FLUX UP TO 140 Hz/CM2
M. Bertino, R. Cardarelli, M. Iori, F. Massa, R. Santonico, P. Bernadini, E. Gorini, F. Grancagnolo, O. Palmara, and C. Pinto (Lecce Univ., Italy) et al 15 Mar. 1989 12 p Presented at the Wire Chamber Conference, Vienna, Austria, 13-17 Feb. 1989 Submitted for publication
(Nota-Interna-930; ETN-90-95812) Avail: NTIS HC A03/MF A01

The performance of resistive plate counters of the size 1 x 2 sq meters is studied with a 5 GeV/c positive pion beam of the CERN (Centre Europeen de Recherche Nucleaire) PS. Efficiency,

delay and time resolution at local particle rates ranging from approx. 10 Hz/sq cm to approx. 139 Hz/sq cm are reported. ESA

N90-14082# Rome Univ. (Italy). Dipartimento di Fisica.
NUCLEON POLARIZABILITIES IN THE CONSTITUENT QUARK MODEL
M. DeSanctis and D. Prosperi (Istituto Nazionale di Fisica Nucleare, Rome, Italy) 20 Jul. 1989 19 p
(Nota-Interna-936; ETN-90-95818) Avail: NTIS HC A03/MF A01

The spectrum of the non-strange baryons in the constituent quark model is critically analyzed. The electromagnetic properties of the nucleon are calculated with particular emphasis on the electric and magnetic polarizabilities. Relativistic corrections up to order 1/m squared are consistently considered. ESA

N90-14083# Rome Univ. (Italy). Dipartimento di Fisica.
MEASUREMENT OF THE FRACTIONAL MOMENTUM CARRIED BY THE GLUONS IN THE LOW Q2 PHOTON-GLUON FUSION EVENTS AT THE ep HERA COLLIDER
G. DAgostini and D. Monaldi (Istituto Nazionale di Fisica Nucleare, Rome, Italy) 27 Jul. 1989 14 p Presented at the International Europhysics Conference on High Energy Physics, Madrid, Spain, Sep. 1989
(Nota-Interna-937; ETN-90-95819) Avail: NTIS HC A03/MF A01

It is shown that it is possible to perform a determination of the fractional momentum carried by the gluon in a photon-gluon collision from the hadronic information alone. In the photoproduction region, where the x and QZ are badly measured, this could be the only global physical variable of interest, together with the hadronic invariant mass. Study of these quantities would allow a direct measurement of the gluon density of the proton in the range X sub g = 0.002/0.2. ESA

N90-14084*# Jet Propulsion Lab., California Inst. of Tech., Pasadena.
USE OF A KRYPTON ISOTOPE FOR RAPID ION CHANGEOVER AT THE LAWRENCE BERKELEY LABORATORY 88-INCH CYCLOTRON
George A. Soli and Donald K. Nichols 1 Sep. 1989 9 p
(Contract NAS7-918)
(NASA-CR-186107; JPL-Publ-89-28; NAS 1.26:186107) Avail: NTIS HC A02/MF A01 CSCL 20H

An isotope of krypton, Kr86, has been combined with a mix of Ar, Ne, and N ions at the electron cyclotron resonance (ECR) source, at the Lawrence Berkeley Laboratory cyclotron, to provide rapid ion changeover in Single Event Phenomena (SEP) testing. The new technique has been proved out successfully by a recent Jet Propulsion Laboratory (JPL) test in which it was found that there was no measurable contamination from other isotopes. Author

N90-14085# Admiralty Research Establishment, Teddington (England).
RING SOURCE/FORCE EXCITATION OF AXISYMMETRIC SHELL STRUCTURE
J. H. James Nov. 1988 13 p
(ARE-TM(UHA)-88519; BR108610; ETN-90-94846) Copyright Avail: NTIS HC A03/MF A01

The formulation of the near field pressures, far field pressures and acoustic particle displacements of a ring source and a ring axial force is presented. These quantities are necessary ingredients for calculations of far field radiation in the presence of the scattering action of an axisymmetric shell structure. Numerical results for specific spherical and prolate spheroidal shells show that the former amplifies the radiation, at resonance, much more than does the latter. The programs can be used to predict far field sound radiation from branched shells with or without rib stiffening. ESA

N90-14086# Rome Univ. (Italy). Dipt di Fisica.
A LATTICE STUDY OF SEMILEPTONIC DECAYS OF D-MESONS
M. Crisafulli, Guido Martinelli, V. J. Hill, and C. T. Sachrajda (Southampton Univ., England) 9 Feb. 1989 15 p Sponsored in part by the United Kingdom Science and Engineering Research Council
(Preprint-660; SHEP-88/89-6; ETN-90-95792) Avail: NTIS HC A03/MF A01

The results of a computation of the matrix elements of the vector current which are relevant for the semileptonic decays of D-mesons are presented. The computations, performed on a 20 x 100 x 40 lattice at beta=6.0 using Wilson fermions in the quenched approximation are described. The matrix element analysis shows that the form factor at zero momentum transfer is in excellent agreement with the experimental measurement. From a computation of the matrix element, the corresponding form factor at zero momentum transfer is found. Vector dominance gives a good description of the form factor at the values of the momentum transfers accessible on the lattice. ESA

N90-14087# Rome Univ. (Italy). Dipt. di Fisica.
ASPECTS OF THE PHYSICS OF THE STANDARD MODEL
Guido Martinelli 2 May 1989 59 p
(Preprint-670; ETN-90-95798) Avail: NTIS HC A04/MF A01

Selected aspects of the physics of the standard model are reviewed. The present status of the measurement of the basic parameters of the standard model and their comparison with theoretical predictions, including radiative corrections, are discussed, together with W and Z physics at collider energies and hadron production of heavy flavors. ESA

N90-14088# Rome Univ. (Italy). Dipt. di Fisica.
EXOTIC HIGGS PRODUCTION AT e+e- COLLIDERS
M. Lusignoli and S. Petrarca 4 May 1989 9 p Sponsored in part by the Italian Ministry of Public Education
(Preprint-671; ETN-90-95799) Avail: NTIS HC A02/MF A01

The production of exotic, doubly charged, Higgs particles is discussed. Both the pair production via Z formation and the single production through photon exchange are examined. The possibility of experimental detection even for masses larger than half of the Z mass is stressed. The possibility of electron-positron machines to give bounds on the parameters (mass and Yukawa couplings) of the doubly charged Higgs mesons is discussed. In general, the masses of these particles depend on a bunch of unknown couplings in the Higgs potential. They could be such to give a mass considerably lower than the natural scale which is set by the vacuum expectation value. ESA

N90-14089# Rome Univ. (Italy). Dipt. di Fisica.
MODEL-INDEPENDENT ANALYSIS OF THE Z LINE SHAPE IN e+e- ANNIHILATION
A. Borrelli, M. Consoli, L. Maiani, and R. Sisto 21 Jun. 1989 36 p Sponsored in part by the Italian Ministry of Public Education
(Preprint-679; ETN-90-95803) Avail: NTIS HC A03/MF A01

A model independent analysis of the shape and the size of the Z resonant cross section measured in e+e- collisions is performed. The process e+e- giving mu+mu- is concentrated on, but results are also given for the inclusive hadronic cross-section. Explicit calculations in the case of the standard theory and a comparison with existing calculations are presented. ESA

N90-14090# Technische Univ., Berlin (Germany, F.R.).
INVESTIGATIONS OF SPONTANEOUS NUCLEAR ORDER IN COPPER BY NEUTRON DIFFRACTION Ph.D. Thesis
Konrad Siemensmeyer 1989 115 p In GERMAN; ENGLISH summary
(ETN-90-96060) Avail: NTIS HC A06/MF A01

Nuclear antiferromagnetic ordering of Cu nuclei is investigated by means of neutron diffraction at temperatures below 60 nK. The observation of reflection in external fields between B values of 0 and 0.25 mT gives the first direct evidence for the existence of antiferromagnetic order in the nuclear system of a pure metal. In nuclear systems, which are cooled by demagnetization, owing

to the long spin-lattice relaxation time, entropy is constant. The thermodynamics of the nuclear system at constant entropy is investigated by scanning the external field at constant entropy. The time-dependent behavior of the demagnetized nuclear system is studied by varying the sweep rate of the fieldscan. It is concluded that the phase transition between the two antiferromagnetic phases is of first order. ESA

73 NUCLEAR AND HIGH-ENERGY PHYSICS

Includes elementary and nuclear particles; and reactor theory.

For space radiation see *93 Space Radiation.*

N90-14091# Nationaal Inst. voor Kernfysica en Hoge Energiefysica, Amsterdam (Netherlands).

INFLUENCE OF RF-PARAMETERS ON BEAM LIFETIME

F. B. Kroes and R. Maas Aug. 1989 10 p

(NIKHEF-K/AmPS/89-06; ETN-90-95975) Avail: NTIS HC A02/MF A01

The pulse stretcher/storage ring AmPS (Amsterdam Pulse Stretcher) which uses a 2856 MHz RF (radio frequency) system for operation in the stretcher mode is studied. At this frequency a high RF voltage is shown to be required to obtain reasonable lifetimes in storage mode. At a lower frequency the RF voltage is shown to be less to create the same bucket size. The addition of a low-frequency RF system for operation in storage mode is therefore considered. For commissioning purposes the 2856 MHz system is shown to be suitable for energies up to 650 to 700 MeV. ESA

74 OPTICS

Includes light phenomena; and optical devices.

For lasers see *36 Lasers and Masers.*

N90-14092*# Cockerham (John M.) and Associates, Inc., Huntsville, AL.

OPTICAL PROPERTIES MONITOR: EXPERIMENT DEFINITION PHASE Final Report, 16 Sep. 1988 - 29 Sep. 1989

Donald R. Wilkes, Jean M. Bennett, Leigh L. Hummer, Russell A. Chipman, James B. Hadaway, and Larry Pezzaniti Sep. 1989 147 p Prepared in cooperation with Alabama Univ., Huntsville

(Contract NAS8-37755)

(NASA-CR-183836; NAS 1.26:183836) Avail: NTIS HC A07/MF A01 CSCL 20F

The stability of materials used in the space environment will continue to be a limiting technology for space missions. The Optical Properties Monitor (OPM) Experiment provides a comprehensive space research program to study the effects of the space environment-both natural and induced-on optical, thermal and space power materials. The OPM Experiment was selected for definition under the NASA/OAST In-Space Technology Experiment Program. The results of the OPM Definition Phase are presented. The OPM Experiment will expose selected materials to the space environment and measure the effects with in-space optical measurements. In-space measurements include total hemispherical reflectance total integrated scatter and VUV reflectance/transmittance. The in-space measurements will be augmented with extensive pre- and post-flight sample measurements to determine other optical, mechanical, electrical, chemical or surface effects of space exposure. Environmental monitors will provide the amount and time history of the sample exposure to solar irradiation, atomic oxygen and molecular contamination. Author

N90-14093# Rochester Univ., NY. Inst. of Optics.

OPTICS AND OPTO-ELECTRONICS SYSTEMS Final Report, 15 Mar. 1985 - 24 Mar. 1989

Robert W. Boyd and G. Michael Morris 27 Jul. 1989 11 p

(Contract DAAG29-85-K-0073)

(AD-A212340; ARO-22905.14-PH) Avail: NTIS HC A03/MF A01 CSCL 20/6

The development characteristics and analysis of new nonlinear optical materials and nonlinear optical interactions were examined. The primary application was new techniques for use in optical phase conjugation. Nonlinear optical techniques were studied for real-time image processing. Real-time image correlation, nonlinear optical properties of liquid crystal compounds, and spatial resolution of nonlinear optical materials were studied. B.G.

N90-14094# Naval Postgraduate School, Monterey, CA. Dept. of Electrical and Computer Engineering.

IMAGE ENHANCEMENT SOFTWARE FOR UNDERWATER RECOVERY OPERATIONS: USER'S MANUAL Technical Report, Jun. 1988 - Jun. 1989

William J. Partridge and Charles W. Therrien 16 Jun. 1989 25 p

(AD-A212943; NPS62-89-023) Avail: NTIS HC A03/MF A01 CSCL 12/5

This report describes software for performing image enhancement on live or recorded video images. The software was developed for operational use during underwater recovery operations at the Naval Undersea Warfare Engineering Station. The image processing is performed on an IBM-PC/AT compatible computer equipped with hardware to digitize and display video images. The software provides the capability to provide contrast enhancement and other similar functions in real time through hardware lookup tables, to automatically perform histogram equalization, to capture one or more frames and average them or apply one of several different processing algorithms to a captured frame. The report is in the form of a user manual for the software and includes guided tutorial and reference sections. A Digital Image Processing Primer in the appendix serves to explain the principle concepts that are used in the image processing. GRA

N90-14095# Geltech, Inc., Alachua, FL.

SOL-GEL PROCESSING SCIENCE USING A SOL-GEL OPTICS RESEARCH FACILITY (SGORF) Final Report, 1 Sep. 1986 - 30 Sep. 1988

Jean-Luc R. Nogues 10 Sep. 1989 117 p

(Contract F49620-86-C-0120)

(AD-A213056; AFOSR-89-1248TR) Avail: NTIS HC A06/MF A01 CSCL 13/8

The major challenge facing sol-gel processing of advanced materials, and in fact the entire field of chemically derived ceramics, is to relate processing variables to final properties. In order to develop fundamental processing-properties relationships it is essential to characterize the material after each step of the process: mixing, aging, drying, stabilization and densification. Fundamental studies of sol-gel processing science have led to two major accomplishments: development of a generic sol-gel process for producing fully dense silica monoliths (termed GELSIL), and identification of the need for a broad range of characterization methods to apply to processing steps. In order to achieve the production of reliable and reproducible sol-gel monoliths, a series of seven tasks have been identified. These tasks and a summary of results to date are given below: Sol-Gel Processing Science for Continuous Optics; Processing; Fabrication Science for Net Shape Precision Optics; Effects of Ultrastructure on Thermal and Mechanical Properties of Sol-Gel Optics; Effects of Ultrastructure on the Optical Properties and Optical Homogeneity of Gelsil; Radiation and Severe Environment Sensitivity of Gelsil Multicomponent and Gel-Derived Composites; Effects of Multicomponent Species and Multiphase on Processing-Properties Relationships; and Effect of Sample dimensions on Reliability. GRA

N90-14096# Naval Research Lab., Washington, DC. Beam Physics Branch.

SOLUTION OF THE BOLTZMANN EQUATION USING AN ENERGY GROUP METHOD Interim Report

D. Colombant and Martin Lampe 2 Oct. 1989 45 p

(ARPA Order 4395)
(AD-A213138; NRL-MR-6554) Avail: NTIS HC A03/MF A01 CSCL 20/8

A method is explored for solving the nonlocal linear Boltzmann equation by taking velocity moments while retaining the kinetic energy as an independent variable. The six-dimensional Boltzmann equation is reduced to a set of four-dimensional equations that formally resemble fluid equations. A numerical code is implemented for solving these equations. A number of schemes were tried for closing the hierarchy of moment equations. The validity and accuracy of the method has been tested by running a number of test problems for which exact solutions of the Boltzmann equation are available. These test problems all involve one-dimensional collision-free, free-streaming, which is trivial from the viewpoint of the Boltzmann equation, but which poses a severe test to the model, whose accuracy is improved by the smoothing effects of collisions. Satisfactory closure methods may have to become increasingly elaborate as more complicated situations are considered, and thus it is still not clear whether the method will be practical in treating real applications. GRA

N90-14097# Naval Postgraduate School, Monterey, CA.
REAL TIME IMAGE ENHANCEMENT DURING UNDERWATER RECOVERY OPERATIONS M.S. Thesis
William J. Partridge Jun. 1989 64 p
(AD-A213139) Avail: NTIS HC A04/MF A01 CSCL 15/6

The development of a menu-driven real-time image processing program to be used during underwater torpedo recovery operations is described. Included are an analysis of the images to be processed, a description of the hardware and software tools available to solve the problem, the methodology used to select the most effective enhancement functions, and the results of a test of the program conducted in an underwater recovery environment. Appendices include a source code listing for the program and a User's Manual which provides hardware setup instructions, a tutorial on the use of the program, and a quick reference list of the menu options available. GRA

N90-14098# San Diego State Univ., CA.
INTEGRATED OPTOELECTRONIC RECEIVERS Final Report, Jul. 1987 - Jul. 1988
S. R. Forrest Aug. 1989 79 p
(Contract N66001-85-D-0203)
(AD-A213376; NOSC/TD-1631) Avail: NTIS HC A05/MF A01 CSCL 09/1

Described here is the first phase of a 3-year program for the fabrication of highly sensitive, monolithically integrated optical receivers for fiber optic communication systems operating in the 1.3 to 1.55 micron range. The significant progress in this work has been the growth, by liquid phase epitaxy, of high purity, high uniformity InP(0.53)Ga(0.47)As layers suitable for photodiode and field effect transistor (FET) applications, fabrication of a very low dark current, low capacitance In(0.53)Ga(0.47)As p-i-n photodiode, identification, and complete analysis of In(0.53)Ga(0.47)As and InP self-aligned JFET structures. The result is that In(0.53)Ga(0.47)As is identified as the material which is preferable for use in integrated receivers, and the fabrication of a discrete In(0.53)Ga(0.47)As JFET. The progress of this research effort should be continued over the next 2 years such that the initial goals of a fully integrated, high sensitivity receiver can be realized. GRA

N90-14099 British Petroleum Co. Ltd., London (England).
OPTICAL MODULATORS BASED ON POLYMERS Patent Application
Philip Charles Allen, inventor, Richard Henry Friend, inventor, Jeremy Henley Burroughes, inventor, and Alan John Harrison, inventor 19 May 1988 31 p
(EP-Patent-0-294-061-A1; EP-Patent-Appl-SN-88-304554-4; Int-Patent-Class-G02F-1/35; Int-Patent-Class-H01L-29/28; Int-Patent-Class-C08F-138/02; ETN-90-95239) Avail: European Patent Office, Erhardtstr. 27, 8000 Munich 2, Germany, Federal Republic of

A device for electrooptic modulation of an optical beam is described. The device is a laminate comprising a coherent film of a conjugated polymer (semiconducting properties). Two or more layers of electrically conducting, insulating, or semiconducting materials are added. The polymer layer is capable of interacting with the optical beam. The electrical contact established between the layers enables the detection of the beam emerging from the polymers. The design and application examples concerning a rectifier diode modulator, Schottky diodes, a metal insulator semiconductor, and a metal oxide semiconductor field effect transistor are given. ESA

N90-14100# Rome Univ. (Italy). Dipt. di Fisica.
LOW FREQUENCY POLAHIZED AND DEPOLARIZED LIGHT SCATTERING IN H-BONDED LIQUIDS: CH3(CH2)n-1OH (n=1,...5)
P. Benassi, V. Mazzacurati, M. Nardone, G. Ruocco, and G. Signorelli (Aquila Univ., Italy) 2 Aug. 1989 29 p
(Preprint-693; ETN-90-95811) Avail: NTIS HC A03/MF A01

Polarized and depolarized room temperature light scattering spectra of normal alcohols from methanol to pentanol are measured at up to 8 cm frequency shifts. At low frequency shifts (smaller than 0.4 cm), resolutions as high as 0.004 cm were used. The possibility of using the same spectrometer for measuring both low frequency Brillouin structures and high frequency depolarized tails is investigated. This would allow for a precise determination of both lineshapes and relative integrated intensities between the various spectral components. The experimental results are presented and briefly discussed on the basis of the existing theories for depolarized scattering from molecular liquids. ESA

N90-14101# Swedish Defence Research Establishment, Linkoeping. Dept. of Information Technology.
DISCUSSION OF FACTORS AFFECTING THE SENSITIVITY OF IR IMAGING SENSORS, PARTICULARLY FOCAL PLANE MOSAIC ARRAYS
Lennart Holm Jun. 1989 33 p In SWEDISH; ENGLISH summary
(FOA-C-30536-3.1; ISSN-0347-3708; ETN-90-95922) Avail: NTIS HC A03/MF A01; Swedish Defence Research Establishment, Box 1165, S-581 11 Linkoeping, Sweden, 50 Swedish crowns

A description of presently used criteria for determination of the sensitivity of IR sensors is presented. The kinds of noise which determine the sensitivity of apparatus with single element detectors are described. New kinds of noise, introduced when using multi element detectors are analyzed, particularly with respect to staring arrays. A method for describing the performance of the arrays is suggested. ESA

N90-13463*# Arizona Univ., Tucson. Steward Observatory.
LOW TEMPERATURE OPTICAL TESTING OF CFRP TELESCOPE PANELS
William F. Hoffmann, Patrick Woida, and Thomas Tysenn *In* Jet Propulsion Lab., California Inst. of Tech., Report of the Asilomar 3 LDR Workshop 15 Aug. 1988 p 76-77 (For primary document see N90-13449 05-18)
Avail: NTIS HC A08/MF A01 CSCL 20F

N90-13474*# Eastman Kodak Co., Rochester, NY. Federal Systems Div.
COHERENT PHASING OF SEGMENTED MIRRORS
Peter A. Jones *In* Jet Propulsion Lab., California Inst. of Tech., Report of the Asilomar 3 LDR Workshop 15 Aug. 1988 p 102-103 (For primary document see N90-13449 05-18)
Avail: NTIS HC A08/MF A01 CSCL 20F

N90-13475*# Jet Propulsion Lab., California Inst. of Tech., Pasadena.
EFFECT OF CENTRAL OBSCURATION ON THE LDR POINT SPREAD FUNCTION
Jakob J. vanZyl *In its* Report of the Asilomar 3 LDR Workshop 15 Aug. 1988 p 104-105 (For primary document see N90-13449 05-18)
Avail: NTIS HC A08/MF A01 CSCL 20F

N90-13476*# California Univ., Los Angeles.
DIFFRACTION, CHOPPING, AND BACKGROUND SUBTRACTION FOR LDR
Edward L. Wright *In* Jet Propulsion Lab., California Inst. of Tech., Report of the Asilomar 3 LDR Workshop 15 Aug. 1988 p 106-109 (For primary document see N90-13449 05-18)
Avail: NTIS HC A08/MF A01 CSCL 20F

N90-13479*# Perkin-Elmer Corp., Danbury, CT.
REAL-TIME SENSING OF OPTICAL ALIGNMENT
Mark T. Stier and Alan B. Wissinger *In* Jet Propulsion Lab., California Inst. of Tech., Report of the Asilomar 3 LDR Workshop 15 Aug. 1988 p 114-116 (For primary document see N90-13449 05-18)
Avail: NTIS HC A08/MF A01 CSCL 20F

N90-13490*# Arizona Univ., Tucson.
THREE-METER BALLOON-BORNE TELESCOPE
William F. Hoffmann, G. G. Fazio, and D. A. Harper (Chicago Univ., IL.) *In* Jet Propulsion Lab., California Inst. of Tech., Report of the Asilomar 3 LDR Workshop 15 Aug. 1988 p 138-139 (For primary document see N90-13449 05-18)
Avail: NTIS HC A08/MF A01 CSCL 20F

N90-13504# European Space Agency, Paris (France).
THE TELESCOPE MIRRORS
G. Ratier and T. Batut *In its* The Hipparcos Mission. Prelaunch Status. Volume 1: The Hipparcos Satellite Jun. 1989 p 67-73 (For primary document see N90-13499 05-18)
Copyright Avail: NTIS HC A16/MF A02; ESA Publications Div., ESTEC, Noordwijk, Netherlands, 80 Dutch guilders

N90-13505# European Space Agency, Paris (France).
THE MODULATING GRID
G. Ratier and T. Batut *In its* The Hipparcos Mission. Prelaunch Status. Volume 1: The Hipparcos Satellite Jun. 1989 p 75-84 (For primary document see N90-13499 05-18)
Copyright Avail: NTIS HC A16/MF A02; ESA Publications Div., ESTEC, Noordwijk, Netherlands, 80 Dutch guilders

N90-13506# European Space Agency, Paris (France).
THE RELAY LENS SYSTEMS
G. Ratier and T. Batut *In its* The Hipparcos Mission. Prelaunch Status. Volume 1: The Hipparcos Satellite Jun. 1989 p 85-94 (For primary document see N90-13499 05-18)
Copyright Avail: NTIS HC A16/MF A02; ESA Publications Div., ESTEC, Noordwijk, Netherlands, 80 Dutch guilders

N90-13507# European Space Agency, Paris (France).
THE DETECTORS
H. Eggel *In its* The Hipparcos Mission. Prelaunch Status. Volume 1: The Hipparcos Satellite Jun. 1989 p 95-100 (For primary document see N90-13499 05-18)
Copyright Avail: NTIS HC A16/MF A02; ESA Publications Div., ESTEC, Noordwijk, Netherlands, 80 Dutch guilders

N90-13572# European Space Agency, Paris (France).
MODELING OF THE HIPPARCOS OPTICAL SYSTEM
D. Iorio-Fili, M. Badiali, M. Cetica, M. Amoretti, D. Bertani, D. Cardini, and A. Emanuele *In its* The Hipparcos Mission. Prelaunch Status. Volume 3: The Data Reductions Jun. 1989 p 389-407 (For primary document see N90-13548 05-18)
Copyright Avail: NTIS HC A22/MF A03; ESA Publications Div., ESTEC, Noordwijk, Netherlands, 80 Dutch guilders

75 PLASMA PHYSICS

Includes magnetohydrodynamics and plasma fusion.
For ionospheric plasmas see *46 Geophysics*. For space plasmas see *90 Astrophysics*.

N90-14102*# Polytechnic Univ., Farmingdale, NY. Dept. of Electrical Engineering and Computer Science.
EXPERIMENTAL AND THEORETICAL STUDY OF ARTIFICIAL PLASMA LAYERS PRODUCED BY TWO INTERSECTING BEAMS IN A CHAMBER
S. P. Kuo and Y. S. Zhang 6 Oct. 1989 42 p
(Grant NAG5-1051)
(NASA-CR-184598; NAS 1.26:184598) Avail: NTIS HC A03/MF A01 CSCL 20I

The work done on the Bragg scattering of electromagnetic waves by microwave produced plasma layers is reported. Also summarized is the work accomplished on the propagation of high power microwave pulses in an air breakdown environment. Ongoing work on the theoretical model and numerical results of pulse propagation in air is also presented as are the results of studying the decay of plasma density and temperature. K.C.D.

N90-14103# Ceskoslovenska Akademie Ved, Prague. Inst. of Plasma Physics.
HOT SPOTS Ar AND Ne GAS PUFF z-PINCH
A. Krejci, E. Krousky, and O. Renner Feb. 1989 10 p Submitted for publication
(IPPCZ-289) Avail: NTIS HC A02/MF A01

The hot spots in Ar and Ne pinch plasma are investigated. Both pinhole cameras with entrance diameter 13 to 250 microns and flat crystal spectrographs with Si and KAP crystals were used for spatially and spectrally resolved soft x ray diagnostics. The diameters of Ar (25 to 30 microns) and Ne (40 microns) hot spots were found. From x ray spectrum of Ar spots the parameters of plasma were determined: T(sub e) = 1.0 to 1.1 KeV and n(sub e) = (1.8 to 4.0) x 10(27)/cu. m. The validity of the Bennett equilibrium for unstable hot spots is discussed. Author

N90-14104# Georgia Inst. of Tech., Atlanta. School of Mechanical Engineering.
TRUE ASYMPTOTIC PLASMA-SHEATH MATCHING WITH AN ASYMPTOTICALLY CORRECT COLLISIONAL PRESHEATH
Final Report, 1 Sep. 1985 - 31 Oct. 1988
Geoffrey L. Main 30 Jun. 1989 134 p
(Grant AF-AFOSR-0375-85; AF Proj. 2308)
(AD-A212857; AFOSR-89-1237TR) Avail: NTIS HC A07/MF A01 CSCL 20/9

The work on plasma presheaths, which form a transition region between the collisionless electrode sheaths and the plasma, is directed toward the problems of the Thermionic Energy Converter (TEC). A schematic of a TEC is shown in a reactor core for space power applications and for basic physics. Cesium is put into the gap between the emitter and collector for two purposes: (1) to ionize and neutralize the space charge so that a useful electron current density can pass (10 to 100 amps/square cm); and (2) to reduce the electrode work functions by adsorption of cesium. For the plasma physics of the cesium filled gap of the TEC, the plasma-electrode interactions are the most significant part because these regions form boundary conditions which control the plasma density and temperatures of the entire gap. Thus the research was directed toward the study of collisional presheaths which form the layer adjacent to an electrode on the order of one ion mean free path thick. However, the research is not limited in applicability to TECs but is of interest to plasma-surface interactions in general. Other applications include electric propulsion (where electrode erosion is a problem or not fully understood) and more generally, any plasma-surface interaction. This report includes the asymptotic presheath theory developed, and is preceded by the basic theory of the Thermionic Energy Converter (TEC) and is followed by the application of the theory to a time dependent model of the TEC in a program called TEC. GRA

N90-14105 Iowa Univ., Iowa City.
DYNAMICS EXPLORER-1 SATELLITE STUDY OF ELECTROSTATIC ION CYCLOTRON WAVES Ph.D. Thesis
Scott Arnold Boardsen 1988 150 p
Avail: Univ. Microfilms Order No. DA8913158

Representative examples are described for hydrogen cylotron waves detected by Dynamics Explorer-1 (DE-1). Most of the hydrogen cyclotron waves can be classified into two categories: wave events in which the excited harmonics are located below the lower hybrid frequency, and wave events in which the excited harmonics are located at or above the lower hybrid frequency. Wave events satisfying the first category are strongly correlated with the presence of ion beams flowing up the field lines, while events satisfying the second category are associated with loss cone features in the ion distribution functions. The loss cone features usually persist before and after the hydrogen cyclotron wave events. The hydrogen wave emissions that occur below the lower hybrid frequency are found to be a factor of 10 to 100 times more intense than emissions that occur above the lower hybrid frequency. Examples are shown in which the ion cyclotron emissions in the second category have a double peaked spectral characteristic. The double peaked spectrum is shown to be produced by Doppler shifts from a spectrum of wave vectors distributed uniformly in azimuth around the magnetic field. The separation between the double peaks can be used to infer the wavelength of the emissions. The global distribution of hydrogen cyclotron waves is also investigated. Dissert. Abstr.

76 SOLID-STATE PHYSICS

Includes superconductivity.

For related information, see also *33 Electronics and Electrical Engineering* and *36 Lasers and Masers.*

N90-14106# Naval Ocean Systems Center, San Diego, CA.
ANALYTICAL AND COMPUTER-AIDED MODELS OF InP-BASED MISFETs AND HETEROJUNCTION DEVICES
A. J. Shey, W. H. Ku (California Univ., San Diego.), and L. J. Messick Aug. 1989 21 p Submitted for publication
(Contract N66001-85-C-0422)
(AD-A211861) Avail: NTIS HC A03/MF A01 CSCL 09/1

The superior properties of InP material, e.g., higher peak electron drift velocity, thermal conductivity, and breakdown field, to GaAs have made it an attractive alternative for high performance applications in microwave and millimeter-wave regimes as well as high-speed digital circuits. Recently, a high-efficiency InP MISFET has demonstrated 4.5 watts output power with 4 dB gain and 46 percent power-added efficiency at 9.7 GHz by Messick et al. These impressive results clearly confirmed the promising superior performance of InP MISFETs. The main concern in the applications of III-V MISFETs has been the reliability of output characteristics of the devices, which is mainly attributed to the variations of interfacial properties of the gate dielectric layer and the underlying semiconductor active layer. The task of modeling output characteristics of III-V compound-based MISFET devices has become more complex with the possible dominance of the interfacial properties in the devices' performance. Much more attention should be paid to the nonlinear modulation of the surface potential by the external gate voltage due to the presence of an excessive amount of interfacial states, since the accompanying carrier trapping, scattering, and recombination could have altered completely the charge control and transport mechanisms, and consequently the device output characteristics. GRA

N90-14107# Missouri Univ., Saint Louis. Dept. of Physics.
FUNDAMENTAL QUANTUM 1/f NOISE IN ULTRASMALL SEMICONDUCTOR DEVICES AND THEIR OPTIMAL DESIGN PRINCIPLES Final Report, 1 May 1985 - 30 Apr. 1989
Peter H. Handel 26 Jun. 1989 92 p
(Grant AF-AFOSR-0130-85; AF Proj. 2305)
(AD-A211947; AFOSR-89-1024TR) Avail: NTIS HC A05/MF A01 CSCL 12/9

To learn control 1/f noise in electronic devices, the author's Quantum 1/f Noise theory was further developed and applied to pn junctions, junction and MIS infrared detectors, bipolar transistors, FET, BJT, vacuum tubes, secondary emission tubes, SQUIDs, and other devices. The present report gives a review of the progress made in the theory of the Quantum 1/f Effect, including the general derivation of the effect in second quantization, the derivation of quantum 1/f cross-correlations, the effect of a finite mean free path in condensed matter, the characteristic functional, piezoelectric coherent quantum 1/f noise, and an interpolation formula for coherent and conventional quantum 1/f noise. The practical applications presented here are limited here to infrared detectors and SQUIDs, the rest are referenced. Optimal low-noise design principles based on the 1/f theory are formulated. GRA

N90-14108*# Case Western Reserve Univ., Cleveland, OH.
PREPARATION OF 110K (Bi, Pb)-Sr-Ca-Cu-O SUPERCONDUCTOR FROM GLASS PRECURSOR Final Report
Narottam P. Bansal Oct. 1989 14 p Presented at the 1st International Ceramic Science and Technology Congress, Anaheim, CA, 31 Oct. - 3 Nov. 1989; sponsored by the American Ceramic Society
(Contract NCC3-133)
(NASA-CR-185162; E-5131; NAS 1.26:185162) Avail: NTIS HC A03/MF A01 CSCL 20L

The Bi1.5Pb0.5Sr2Ca2Cu3O(x) glass, prepared by rapid quenching of the melt, showed T(sub g) of 383 C, crystallization temperature of approx. 446 C, melting temperature of approx. 855 C, and bulk density of 5.69 g/cu. cm. in air. The as-quenched glass was oxygen deficient. On heating in O2, it showed a slow, irreversible, and continuous weight gain starting at approx. 530 C. The influence of annealing conditions on the formation of various phases was investigated by XRD and electrical resistivity measurements. The 110K-T(sub c) phase did not form below 840 C. The amount of this phase increased with the sintering time at 840 C. A sample annealed at 840 C for 243 h in air and furnace cooled showed the highest T(sub c)(R=0) of 107.2K and transition width delta T(sub c)(10 to 90 percent) of approx. 2 K. Author

N90-14109# Colorado Univ., Boulder. Dept. of Physics.
STUDIES OF STRUCTURE AND SWITCHING DYNAMICS IN FERROELECTRIC CRYSTAL AND LIQUID CRYSTAL THIN FILMS Final Report, 15 Apr. 1986 - 14 Apr. 1989
Noel A. Clark and James F. Scott 13 Jul. 1989 13 p
(Contract DAAL03-86-K-0053)
(AD-A212650; ARO-22758.19-PH) Avail: NTIS HC A03/MF A01 CSCL 07/4

The structure and switching dynamics of ferroelectric solid state and liquid crystal thin films were investigated experimentally using x ray scattering, optical microscopy and microspectroscopy, and by raman spectroscopy. Applications of crystalline piezoelectric ferroelectric films, formed by sol gel and sputter deposition and ferroelectric liquid crystal devices were studied for application. GRA

N90-14110# Harry Diamond Labs., Adelphi, MD.
ELASTIC IMPURITY SCATTERING IN DOUBLE-BARRIER RESONANT TUNNELING STRUCTURES Final Report, Jul. 1988 - Jan. 1989
Thomas B. Bahder and John D. Bruno Sep. 1989 26 p
(HDL Proj. AE1951)
(AD-A212850; HDL-TR-2162) Avail: NTIS HC A03/MF A01 CSCL 20/10

Fermi's golden rule is used to calculate the electron elastic scattering rate due to a single charged impurity in the quantum well region of a double-barrier resonant tunneling structure at zero applied electric field. The impurity is modeled by a screened Coulomb potential, and the scattering rate out of a conduction band eigenstate is calculated as a function of the initial-state electron wave vector and the impurity position. In a finite crystal with a random distribution of impurities, the scattering of resonant electrons can be dominated by impurities in the quantum well

region. For a double-barrier structure embedded in an infinite crystal, impurity scattering of resonant electrons is always dominated by impurities outside the quantum well region. GRA

N90-14111# California Inst. of Tech., Pasadena. Lab. of Chemical Physics.
REORGANIZATION FREE ENERGY FOR ELECTRON TRANSFERS AT LIQUID-LIQUID AND DIELECTRIC SEMICONDUCTOR-LIQUID INTERFACES Technology Report No. 10, 1 Aug. 1988 - 1 Jul. 1989
R. A. Marcus 26 Jul. 1989 27 p
(Contract N00014-89-J-1278)
(AD-A212985) Avail: NTIS HC A03/MF A01 CSCL 07/4

The reorganization free energy is calculated for a reaction between (1) two reactants, each in its own dielectric medium, separated by an interface, and (2) between a reactant and some semiconductors. An expression is also given for the rate constant of an electron transfer reaction at an interface between reactants in two immiscible phases. Under certain conditions it is shown that the reorganization energy for the two immiscible liquid system is the sum of the electrochemical reorganization energies of the two reactants, each in its own respective solvent. The reorganization energy for a semiconductor/liquid system can differ considerably from the corresponding metal/liquid value, even a factor of two. GRA

N90-14112# California Univ., San Diego. Dept. of Electrical and Computer Engineering.
FIELD-EFFECT SPECTROSCOPY OF INTERFACE STATES Final Report, 1 May 1985 - 31 Dec. 1988
H. H. Wieder 31 Dec. 1988 79 p
(Contract N00014-82-K-0455)
(AD-A212998) Avail: NTIS HC A05/MF A01 CSCL 20/12

During the past year the research was concerned principally with the synthesis by MBE of In(x)Al(1-x)As/InP heterojunctions in Strained Layer Structures (SLS). Some of the layers were grown with their lattice constants matched to that of their (100)-oriented InP substrates. Others were chosen deliberately to be in compression or in tension and with appropriate combinations of their fractional indium concentration, x, and thickness, d, were intended to be strained pseudomorphically or strain-relaxed by the generation and/or motion of misfit dislocations. Conventional as well as double crystal rocking curve X ray diffraction of the (400)-reflection plane was used to determine the composition dependent lattice constant and PL spectroscopic measurements at temperatures near 4 and 300 K were used to determine the fundamental bandgap of the various layers. The pseudomorphic strain dependent shifts of the fundamental bandgaps were determined using a linear interpolation between the InAs and AlAs elastic stiffness coefficients, hydrostatic pressure coefficients and shear deformation potentials. These calculations were shown in good agreement with experimental measurements. The calculated composition dependent critical thickness for the onset of plastic deformation and total relaxation of the strain determined from these measurements is in better agreement with the energy balance model than with the mechanical equilibrium model of Matthews and Blakeslee. GRA

N90-14113# State Univ. of New York, Buffalo. Dept. of Chemistry.
LOCAL PAIRING AND ANTIFERROMAGNETISM IN HIGH-T SUB c SUPERCONDUCTORS
H. R. Lee and Thomas F. George Sep. 1989 17 p Submitted for publication
(Contract N00014-86-K-0043)
(AD-A213004; UBAFFALO/DC/89/TR-112) Avail: NTIS HC A03/MF A01 CSCL 20/3

The CuO2 planes in high-temperature superconductors are studied by a two-dimensional Hubbard Hamiltonian with a new proposed vacuum (d sup 9 p sup 6). The superexchange between Cu sites and the hopping parameters of the carriers estimated in this new vacuum has good agreement with the experimental observation as well as numerical calculations with a finite cluster. Single carriers (electrons for n-type or holes for p-type) are localized due to the rigidity of the antiferromagnetic background. Local pairing in the CuO2 plane enables the paired states to move around without disturbing the antiferromagnetic background. The binding energy is estimated from the pair hopping energy, which causes the paired state to be lower in energy than the single carrier state. GRA

N90-14114# Ecole Centrale de Lyon (France).
STUDY OF METAL-INSULATOR-SEMICONDUCTOR STRUCTURES ON INDIUM PHOSPHIDE, IMPLEMENTED BY ANODIC OXIDATION Ph.D. Thesis [ETUDE DES STRUCTURES METAL-ISOLANT-SEMICONDUCTEUR SUR LE PHOSPHURE D'INDIUM ELABOREES PAR OXYDATION ANODIQUE]
Eric Jalaguier 1988 156 p In FRENCH
(ECL-88-10; ETN-90-95766) Avail: NTIS HC A08/MF A01

The manufacturing of metal-insulator-semiconductor (MIS) field effect transistors in liquid media is described. The procedure starts by oxidating an aluminum layer, followed by the oxidation of substrate. The double anodic layer is characterized by ellipsometry and photoelectron spectroscopy. It is shown that the double oxidation appears in two separate phases allowing the existence of an interface composed by a mixture of indium oxide and In(PO4)3, which contributes to a good passivation of the InP interface. An oxidation depth of 15 to 20 nm considerably improves the electric properties. ESA

N90-14115# Ecole Centrale de Lyon (France). Lab. d'Electronique, Automatique et Mesures Electriques
MANUFACTURING AND CHARACTERIZATION OF INSULATOR-GERMANIUM STRUCTURES Ph.D. Thesis [ELABORATION ET CARACTERISATION DES STRUCTURES GERMANIUM-ISOLANT]
Zineb Benamara 1988 115 p In FRENCH
(ECL-88-13; ETN-90-95768) Avail: NTIS HC A06/MF A01

The electronic interface characteristics of experimental devices implemented in Metal-Insulator-Semiconductor (MIS) technology are studied. The goal is the development of integrated detectors for optical telecommunication. The experimental structures studied include Ge/insulator, Ge/GeO2/insulator, Ge/SiNxH and Ge/insulator with an Al2O3 layer deposited with an electron gun. The results show that it is possible to manufacture Ge/insulator structures with a low density of interface states (5 x 10(exp10)/eV/sq cm). ESA

N90-14116# Ecole Centrale de Lyon (France). Lab. d'Electronique d'Automatique et de Mesures Electriques.
STUDY OF SURFACE UNIFORMITY OF SEMICONDUCTORS 3 TO 5 BY PHOTOLUMINESCENCE IMAGERY Ph.D. Thesis [ETUDE DE L'UNIFORMITE DES SURFACES DES SEMICONDUCTEURS 3-5 PAR IMAGERIE DE PHOTOLUMINESCENCE]
Christian Lallemand 1988 170 p In FRENCH Original contains color illustrations
(ECL-88-15; ETN-90-95769) Avail: NTIS HC A08/MF A01

A device is implemented to characterize the surface properties of semiconductors. The automation, sensitivity, resolution, performance and utilization are discussed. Different morphologies existing on InP and GaAs are described. It is shown that there are many inhomogeneities on the photoluminescence images created by dislocations, nonuniform distribution of doping elements, and surface defects attibuted to surface finishing procedures. ESA

N90-14117# Ecole Centrale de Lyon (France). Lab. de Physicochimie des Interfaces.
PHOTOELECTROCHEMICAL BEHAVIOR OF TYPE n OF GaAs IN CONCENTRATED IODIDE MEDIA AND REALIZATION OF AN EXPERIMENTAL DEVICE Ph.D. Thesis [COMPORTEMENT PHOTOELECTROCHIMIQUE DE L'ARSENIURE DE GALLIUM DE TYPE N EN MILIEUX IODURES CONCENTRES ET REALISATION D'UN NOUVEAU DISPOSITIF D'ETUDE]

Charles Amiry 1988 129 p In FRENCH
(ECL-88-18; ETN-90-95771) Avail: NTIS HC A07/MF A01

A device was developed in order to study photoelectrochemical and electrochemical reactions. The cell features laminar flow, double work electrodes, and double reference elctrodes. Experimental data on the photostability of GaAs structures is presented. The influence of electrolyte composition, radiation intensity and doping level on the kinetic mechanisms are discussed. It is shown that the stability of n-GaAs increases with iodide or proton concentration and is independent of the nature of the cationic elements and of the doping level. ESA

N90-14118# Ecole Centrale de Lyon (France).
GaAs AND GaAs:In: INFLUENCE OF SURFACE TREATMENTS AND CHARACTERIZATION OF HOMOGENEITY BY PHOTOLUMINESCENT IMAGERY Ph.D. Thesis [GAAS ET GAAS:IN: INFLUENCE DES TRAITEMENTS DE SURFACE ET CARACTERISATION DE L'HOMOGENEITE PAR IMAGERIE DE LA PHOTOLUMINESCENCE]
Abdelaziz M. Khoukh 1988 131 p In FRENCH Original contains color illustrations
(ECL-88-24; ETN-90-95776) Avail: NTIS HC A07/MF A01

The study includes the characterization of semiconductor crystals under technological treatments such as polishing, chemical attack and thermal treatments, and the optical analysis of the effects of such treatments. It is shown that NaOCl polishing must be modified for polishing GaAs:In. The thermal decomposition of the same material is strongly controlled by the presence of indium. The imagery technique used allows the detection of crystals dislocation, defects and doping nonuninformities. The proposed theoretical model allows the photoluminescent modifications and imagery contrast to be related with the variations in surface recombination velocity. ESA

N90-14119# Rome Univ. (Italy). Dipt. di Fisica.
ENERGY BARRIERS IN SK SPIN-GLASS MODEL
D. Vertechi and M. A. Virasoro 4 Apr. 1989 13 p Sponsored in part by the J. Simon Guggenheim Memorial Foundation
(Preprint-665; ETN-90-95794) Avail: NTIS HC A03/MF A01

The height of barriers separating metastable states for the infinite range Ising spin-glass model is studied. A barrier configuration, corresponding to a saddle point of an energy surface that smoothly interpolates the energy in the hypercube, is identified. For low energy barriers, the number of independent descending directions from the saddle point is determined to be a finite system where N goes to infinity. Numerical estimates are performed using two distinct algorithms and consistent results are obtained. ESA

N90-14120# Hahn-Meitner-Inst. fuer Kernforschung, Berlin (Germany, F.R.). Bereich Datenverarbeitung und Elektronic.
UNIFIED MODEL OF CHARGE BUILD UP AND ANNEALING OF OXIDE CHARGE AND INTERFACE STATES IN SiO2 DUE TO STRESS Ph.D. Thesis - Tech. Univ. Berlin
Friedrich Wulf Apr. 1989 134 p In GERMAN; ENGLISH summary
(HMI-B-465; ETN-90-95826) Avail: NTIS HC A07/MF A01

The build-up of oxide charges, and interface states during stress - irradiation or Bias (BT) Temperatures - and the annealing of these defects are investigated. The post-stress annealing and the degradation process due to BT-stress can be explained by the chemical reaction of the hydrogen in the SiO2. Using this model it becomes possible to describe the correlation of irradiation and BT-stress, the sensitivity of MOS (metal oxide semiconductor) devices against carrier injection, reverse annealing, dose rate effects, and temperature dependent annealing. ESA

N90-14121# Technische Univ., Eindhoven (Netherlands).
TOWARDS AB INITIO CALCULATION OF ELECTRON ENERGIES IN SEMICONDUCTORS Ph.D. Thesis
Benham Farid 21 Mar. 1989 170 p
(ETN-90-96016) Avail: NTIS HC A08/MF A01

The methods and the problems involving the calculation of electron energies in a semiconductor are studied. The effect of electron-electron interaction is taken into account, and the theory of Green functions applied. A representation of the one particle Green function G, in terms of wave functions satisfying Schroedinger wave equations, is given. The self energy function, called GW, is discussed. A decomposition of the expression for the self energy function, in which the Brillouin zone integration can be performed numerically, is proposed. An analysis of the numerical feasibility is given. ESA

77 THERMODYNAMICS AND STATISTICAL PHYSICS

Includes quantum mechanics; theoretical physics; and Bose and Fermi statistics.

For related information see also *25 Inorganic and Physical Chemistry* and *34 Fluid Mechanics and Heat Transfer.*

N90-14122 Aberdeen Univ. (Scotland).
SOME ASPECTS OF CURVATURE IN GENERAL RELATIVITY Ph.D. Thesis
Alan D. Rendall 1987 162 p
Avail: Univ. Microfilms Order No. BRDX85154

The relationship between the curvature of space-time and the other geometrical objects which naturally arise in general relativity is studied in depth. Most of the results obtained apply to the generic case. Certain aspects of fiber bundle theory which may be unfamiliar to many relativists are discussed. Preliminary material on curvature in relativity is contained and a continuity property of the algebraic classification of the Weyl and energy-momentum tensors is proven. The generic behavior of the Riemann, Weyl and energy-momentum tensors are described. This description is used to investigate the relationship of the Riemann tensor to the metric, conformal class and connection of space-time in the generic case. In particular it is proved that the Riemann tensor uniquely and continuously determines the connection. The information obtained on the algebraic type of curvature in the generic case is related to the topology of the underlying manifold. Topology is defined on the set of sectional curvatures of all Lorentz metrics on a given manifold. An attempt was made to do for the sectional curvature what was done for the Riemann tensor, but because sectional curvature is more difficult to handle the results obtained are necessarily more modest. Dissert. Abstr.

N90-14123# Rome Univ. (Italy). Dipartimento di Fisica.
WHERE IS AN OBJECT BEFORE YOU LOOK AT IT
Marcello Cini and Maurizio Serva (Bielefeld Univ., Germany, F.R.) 21 Jun. 1989 26 p Sponsored by the CNR
(Nota-Interna-935; ETN-90-95817) Avail: NTIS HC A03/MF A01

The question of how quantum mechanics becomes a statistical theory, describing a probabilistic knowledge of intrinsically well determined properties of classical objects when a suitable classical limit is established, is addressed. The role of this limit in giving meaning to a variable, independently of being measured, is investigated. It is shown that an inconsistency arises between the conventional interpretation of classical statistical mechanics which presupposes objectively existent Newtonian trajectories, and the standard interpretation of quantum mechanics. It is concluded that the latter needs revising unless a strictly subjective conception of the world is adopted implying that macroscopic objects are not localized anywhere before being viewed. ESA

N90-14124*# Fermi National Accelerator Lab., Batavia, IL. Astrophysics Center.
ON THICK DOMAIN WALLS IN GENERAL RELATIVITY
Guenter Goetz and Dirk Noetzold (Chicago Univ., IL.) Oct. 1989 18 p Submitted for publication Sponsored in part by Alexander-von-Humboldt Foundation
(Grants NAGw-1321; NAGw-1340; NSF AST-88-22595)
(NASA-CR-185926; NAS 1.26:185926; FERMILAB-Pub-89/236-A)
Avail: NTIS HC A03/MF A01 CSCL 20C

Planar scalar field configurations in general relativity differ

considerably from those in flat space. It is shown that static domain walls of finite thickness in curved space-time do not possess a reflection symmetry. At infinity, the space-time tends to the Taub vacuum on one side of the wall and to the Minkowski vacuum (Rindler space-time) on the other. Massive test particles are always accelerated towards the Minkowski side, i.e., domain walls are attractive on the Taub side, but repulsive on the Minkowski side (Taub-vacuum cleaner). It is also proved that the pressure in all directions is always negative. Finally, a brief comment is made concerning the possibility of infinite, i.e., bigger than horizon size, domain walls in our universe. All of the results are independent of the form of the potential V(phi) greater than or equal to 0 of the scalar field phi. Author

80 SOCIAL SCIENCES (GENERAL)

Includes educational matters.

N90-14125*# Alabama A & M Univ., Normal. Dept. of Chemistry.
ELEMENTARY AND MIDDLE SCHOOL SCIENCE IMPROVEMENT PROJECT Final Report, May 1986 - Dec. 1988
Saundra Y. McGuire 1989 124 p
(Contract NAS8-36277)
(NASA-CR-183768; NAS 1.26:183768) Avail: NTIS HC A06/MF A01 CSCL 05I

The Alabama A and M University Elementary and Middle School Science Improvement Project (Project SIP) was instituted to improve the science knowledge of elementary and middle school teachers using the experimental or hands-on approach. Summer workshops were conducted during the summers of 1986, 1987, and 1988 in the areas of biology, chemistry, physics, and electricity, and magnetism. Additionally, a manual containing 43 lessons which included background information, experiments and activities for classroom and home use was provided to each teacher. During the course of the project activities, the teachers interacted with various university faculty members, scientists, and NASA staff. The administrative aspects of the program, the delivery of the services to participating teachers, and the project outcome are addressed. J.P.S.

81 ADMINISTRATION AND MANAGEMENT

Includes management planning and research.

N90-14126*# National Aeronautics and Space Administration, Washington, DC.
SMALL BUSINESS INNOVATION RESEARCH: PROGRAM SOLICITATION
28 Jun. 1989 108 p
(NASA-TM-101869; NAS 1.15:101869; SBIR-89-1) Avail: NTIS HC A06/MF A01 CSCL 05A

This, the seventh annual SBIR solicitation by NASA, describes the program, identifies eligibility requirements, outlines the required proposal format and content, states proposal preparation and submission requirements, describes the proposal evaluation and award selection process, and provides other information to assist those interested in participating in NASA's SBIR program. It also identifies the Technical Topics and Subtopics in which SBIR Phase 1 proposals are solicited in 1989. These Topics and Subtopics cover a broad range of current NASA interests, but do not necessarily include all areas in which NASA plans or currently conducts research. High-risk high pay-off innovations are desired. Author

N90-14127# Defense Logistics Agency, Alexandria, VA.
TOTAL QUALITY MANAGEMENT IMPLEMENTATION STRATEGY: DIRECTORATE OF QUALITY ASSURANCE
May 1989 56 p
(AD-A212863) Avail: NTIS HC A04/MF A01 CSCL 05/1

The Directorate of Quality Assurance strategy for implementing TQM is described. It includes information concerning TQM concepts, methodology for implementation, goals and execution. The primary goal of the DLA-Q implementation strategy is to focus on doing the job right the first time, on time, everytime, and continually improving the way the job is done. GRA

N90-14128# Defense Logistics Agency, Alexandria, VA.
TOTAL QUALITY MANAGEMENT PLAN: TECHNICAL AND LOGISTICS SERVICES
May 1989 29 p
(AD-A212864) Avail: NTIS HC A03/MF A01 CSCL 05/1

The TQM plan for DLA Technical and Logistics Services is described. As a quality provider of technical and logistics services, the Directorate will implement TQM initiatives at Headquarters DLA and at functional counterparts in the Field. The plan requires continuous assessment of customer needs and a systematic evaluation of the processes performed that contribute to customer satisfaction. GRA

N90-14129# Defense Logistics Agency, Alexandria, VA.
TOTAL QUALITY MANAGEMENT IMPLEMENTING PLAN: OFFICE OF SMALL AND DISADVANTAGED BUSINESS UTILIZATION
Jul. 1989 8 p
(AD-A212865) Avail: NTIS HC A02/MF A01 CSCL 05/1

The Office of Small and Disadvantaged Business Utilization plans for implementing TQM is described. A brief discussion is presented of TQM concepts, methodology for implementation and goals. In addition to focusing on internal improvements, DLA-U will provide TQM information to potential small and disadvantaged businesses as part of their implementation efforts. GRA

N90-14130# Defense Logistics Agency, Alexandria, VA.
TOTAL QUALITY MANAGEMENT PLAN: OFFICE OF CONGRESSIONAL AFFAIRS
Jul. 1989 5 p
(AD-A212866) Avail: NTIS HC A02/MF A01 CSCL 05/1

The DLA Office of Congressional Affairs Total Quality Management implementing plan is described. The plan emphasizes five areas: Customer relations, processes, measurement, awards, and training. The plan also includes specific improvement goals and milestones. GRA

N90-14131# Defense Logistics Agency, Alexandria, VA.
TOTAL QUALITY MANAGEMENT: DIRECTORATE OF CONTRACT MANAGEMENT MASTER PLAN
Jul. 1989 18 p
(AD-A212867) Avail: NTIS HC A03/MF A01 CSCL 05/1

This document describes the Directorate of Contracting Management Total Quality Management implementing plan. It includes a description of the TQM concept, the structure established to complement TQM and goals established by the Directorate of Contract Management to implement TQM. TQM goals within the directorate focus on three primary areas: TQM training, harmonizing contract management policies and procedures with the TQM philosophy, and enhancing communication and feedback. GRA

N90-14132# Defense Logistics Agency, Alexandria, VA.
TOTAL QUALITY MANAGEMENT PLAN: OFFICE OF PUBLIC AFFAIRS
Jul. 1989 15 p
(AD-A212868) Avail: NTIS HC A03/MF A01 CSCL 05/1

The Office of Public Affairs TQM implementing plan is described. A description is provided of three concepts considered vital to TQM as it applies to DLA's Public Affairs program: The customers are the first concern, precise measureable goals and teamwork. Public Affairs TQM goals and a methodology for accomplishment are included. GRA

N90-13530# European Space Agency, Paris (France).
FROM SCIENTIFIC PROPOSALS TO THE INCA DATA BASE
C. Turon, A. Gomez, F. Crifo, and M. Grenon *In its* The Hipparcos

Mission. Prelaunch Status. Volume 2: The Input Catalog Jun. 1989 p 7-22 Original contains color illustrations (For primary document see N90-13529 05-18)
Copyright Avail: NTIS HC A13/MF A02; ESA Publications Div., ESTEC, Noordwijk, Netherlands, 80 Dutch guilders

82 DOCUMENTATION AND INFORMATION SCIENCE

Includes information management; information storage and retrieval technology; technical writing; graphic arts; and micrography.

For computer documentation see *61 Computer Programming and Software.*

N90-14133*# Houston Univ., TX. Dept. of Computer Science.
DATABASE INTERFACES ON NASA'S HETEROGENEOUS DISTRIBUTED DATABASE SYSTEM Final Report
Shou-Hsuan Stephen Huang Jul. 1989 11 p
(Grant NAG5-739)
(NASA-CR-185420; NAS 1.26:185420) Avail: NTIS HC
A03/MF A01 CSCL 05B

The syntax and semantics of all commands used in the template are described. Template builders should consult this document for proper commands in the template. Previous documents (Semiannual reports) described other aspects of this project. Appendix 1 contains all substituting commands used in the system. Appendix 2 includes all repeating commands. Appendix 3 is a collection of DEFINE templates from eight different DBMS's.
Author

N90-14134*# National Aeronautics and Space Administration, Washington, DC.
EXECUTIVE OVERVIEW AND INTRODUCTION TO THE SMAP INFORMATION SYSTEM LIFE-CYCLE AND DOCUMENTATION STANDARDS
1989 17 p Original contains color illustrations
(NASA-TM-101765; NAS 1.15:101765) Avail: NTIS HC
A03/MF A01 CSCL 05B

An overview of the five volume set of Information System Life-Cycle and Documentation Standards is provided with information on its use. The overview covers description, objectives, key definitions, structure and application of the standards, and document structure decisions. These standards were created to provide consistent NASA-wide structures for coordinating, controlling, and documenting the engineering of an information system (hardware, software, and operational procedures components) phase by phase. J.P.S.

N90-14135*# National Aeronautics and Space Administration, Washington, DC.
INFORMATION SYSTEM LIFE-CYCLE AND DOCUMENTATION STANDARDS, VOLUME 1
E. David Callender and Jody Steinbacher 28 Feb. 1989 111 p
(NASA-TM-101856; NAS 1.15:101856) Avail: NTIS HC
A06/MF A01 CSCL 05B

The Software Management and Assurance Program (SMAP) Information System Life-Cycle and Documentation Standards Document describes the Version 4 standard information system life-cycle in terms of processes, products, and reviews. The description of the products includes detailed documentation standards. The standards in this document set can be applied to the life-cycle, i.e., to each phase in the system's development, and to the documentation of all NASA information systems. This provides consistency across the agency as well as visibility into the completeness of the information recorded. An information system is software-intensive, but consists of any combination of software, hardware, and operational procedures required to process, store, or transmit data. This document defines a standard life-cycle model and content for associated documentation.
J.P.S.

N90-14136*# National Aeronautics and Space Administration, Washington, DC.
MANAGEMENT PLAN DOCUMENTATION STANDARD AND DATA ITEM DESCRIPTIONS (DID). VOLUME OF THE INFORMATION SYSTEM LIFE-CYCLE AND DOCUMENTATION STANDARDS, VOLUME 2
E. David Callender and Jody Steinbacher 28 Feb. 1989 185 p
(NASA-TM-101857; NAS 1.15:101857) Avail: NTIS HC
A09/MF A01 CSCL 05B

This is the second of five volumes of the Information System Life-Cycle and Documentation Standards. This volume provides a well-organized, easily used standard for management plans used in acquiring, assuring, and developing information systems and software, hardware, and operational procedures components, and related processes. J.P.S.

N90-14137*# National Aeronautics and Space Administration, Washington, DC.
PRODUCT SPECIFICATION DOCUMENTATION STANDARD AND DATA ITEM DESCRIPTIONS (DID). VOLUME OF THE INFORMATION SYSTEM LIFE-CYCLE AND DOCUMENTATION STANDARDS, VOLUME 3
E. David Callender and Jody Steinbacher 28 Feb. 1989 183 p
(NASA-TM-101858; NAS 1.15:101858) Avail: NTIS HC
A09/MF A01 CSCL 05B

This is the third of five volumes on Information System Life-Cycle and Documentation Standards which present a well organized, easily used standard for providing technical information needed for developing information systems, components, and related processes. This volume states the Software Management and Assurance Program documentation standard for a product specification document and for data item descriptions. The framework can be applied to any NASA information system, software, hardware, operational procedures components, and related processes. J.P.S.

N90-14138*# National Aeronautics and Space Administration, Washington, DC.
ASSURANCE SPECIFICATION DOCUMENTATION STANDARD AND DATA ITEM DESCRIPTIONS (DID). VOLUME OF THE INFORMATION SYSTEM LIFE-CYCLE AND DOCUMENTATION STANDARDS, VOLUME 4
E. David Callender and Jody Steinbacher 28 Feb. 1989 93 p
(NASA-TM-101859; NAS 1.15:101859) Avail: NTIS HC
A05/MF A01 CSCL 05B

This is the fourth of five volumes on Information System Life-Cycle and Documentation Standards. This volume provides a well organized, easily used standard for assurance documentation for information systems and software, hardware, and operational procedures components, and related processes. The specifications are developed in conjunction with the corresponding management plans specifying the assurance activities to be performed. J.P.S.

N90-14139*# National Aeronautics and Space Administration, Washington, DC.
MANAGEMENT CONTROL AND STATUS REPORTS DOCUMENTATION STANDARD AND DATA ITEM DESCRIPTIONS (DID). VOLUME OF THE INFORMATION SYSTEM LIFE-CYCLE AND DOCUMENTATION STANDARDS, VOLUME 5
E. David Callender and Jody Steinbacher 28 Feb. 1989 49 p
(NASA-TM-101860; NAS 1.15:101860) Avail: NTIS HC
A03/MF A01 CSCL 05B

This is the fifth of five volumes on Information System Life-Cycle and Documentation Standards. This volume provides a well organized, easily used standard for management control and status reports used in monitoring and controlling the management, development, and assurance of informations systems and software, hardware, and operational procedures components, and related processes. J.P.S.

N90-14140# Massachusetts Inst. of Tech., Cambridge. Microsystems Research Center.
RETRIEVING AND INTEGRATING IC FABRICATION DATA FROM DISSIMILAR DATABASES
Michael P. Ruf Jun. 1989 25 p
(Contract N00014-87-K-0825)
(AD-A211890; VLSI-MEMO-89-552) Avail: NTIS HC A03/MF A01 CSCL 09/1

Factory personnel need to access data from many aspects of the fabrication environment. Many IC fabrication facilities store manufacturing data in distributed, heterogeneous database networks. Retrieval and integration of data can be a cumbersome task due to this configuration. The ideal solution to these problems is to standardize a data model, storing the manufacturing data in a single database. However, since such a standardization is not likely to occur in the near future, a more immediate solution is needed. Discussed here is a system addressing these problems: DRIFS - A Data Retrieval Interface for Integrated Circuit Fabrication Systems. A uniform query interface and data model is defined for heterogeneous, distributed fabrication databases. A DRIFS prototype is described and evaluated. GRA

N90-14141# Defense Technical Information Center, Alexandria, VA.
THE DOD GATEWAY INFORMATION SYSTEM: OPERATIONAL PROTOTYPE AND TRANSITION PERIOD 1987-1988 Final Report
Roberta S. Schoen Mar. 1989 13 p
(AD-A213044; DTIC/TR-89/15) Avail: NTIS HC A03/MF A01 CSCL 05/2

The Defense Technical Center (DTIC) has developed the DOD Gateway Information System (DGIS) as a means for the DOD Scientific and Technical Information (STI) community to access remote heterogeneous databases in a common simplified manner and analyze the information from these databases. The progress on developing and prototyping Phase 1 of DGIS during the 1987 to 1988 time period is explained. The various components covered are the Directory of Resources, post-processing software, the GENIUS document ordering system, user support, SearchMAESTRO menu driven system and the Common Command Language effort. In addition, the effort to transition DGIS from an operational prototype system to an operational system is covered. A bibliography of DGIS-related paper is included. GRA

N90-14142# Air Force Office of Scientific Research, Bolling AFB, Washington, DC. Technical Documents Section.
AFOSR TECHNICAL REPORT SUMMARIES Quarterly Report, Apr. - Jun. 1989
Debra L. Tyrrell Jun. 1989 409 p
(AD-A213148; AFOSR-89-1238TR) Avail: NTIS HC A18/MF A03 CSCL 05/2

The Air Force Office of Scientific Research Technical Report Summaries are published quarterly as of March, June, September, and December of each calendar year. They consist of a brief summary of each AFOSR technical report received in the Technical Information Division and submitted to the Defense Technical Information Center (DTIC) for that quarter. The summaries contain two indexes (Subject Index and Personal Author Index) for easily locating the technical reports that may be of interest to the user. These are followed by abstracts of the reports. This report informs Air Force Laboratories about the science that the Air Force Office of Scientific Research is supporting. GRA

N90-14143# Rutgers - The State Univ., New Brunswick, NJ. Center for Expert Systems Research.
EMPIRICAL ANALYSIS AND REFINEMENT OF EXPERT SYSTEM KNOWLEDGE BASES Quarterly Report
Sholom M. Weiss and Casimir A. Kulikowski 31 Aug. 1989 9 p
(Contract N00014-87-K-0398)
(AD-A213240) Avail: NTIS HC A02/MF A01 CSCL 12/7

Knowledge base refinement is the modification of an existing expert system knowledge base with the goals of localizing specific weaknesses in a knowledge base and improving an expert system's performance. Systems that automate some aspects of knowledge base refinement can have a significant impact on the related problems of knowledge base acquisition, maintenance, verification, and learning from experience. The SEEK system was the first expert system framework to integrate large-scale performance information into all phases of knowledge base development and to provide automatic information about rule refinement. A recently developed successor system, SEEK2 (Ginsberg, Weiss, and Politakis 88) significantly expands the scope of the original system in terms of generality and automated capabilities. Significant progress is expected to be made in automating empirical expert system techniques for knowledge acquisition, knowledge base refinement, maintenance and verification. Also to be demonstrated is a rule refinement system in an application of the diagnosis of complex equipment failure: computer network troubleshooting. GRA

N90-14144# Carnegie-Mellon Univ., Pittsburgh, PA. Robotics Inst.
ERIS: ENGINEERING RESOURCE INFORMATION SYSTEM
Timothy Roth and Jerome Kraitchman Jun. 1989 54 p
(Contract FGD-502-531)
(AD-A213357; CMU-RI-TR-89-11) Avail: NTIS HC A04/MF A01 CSCL 05/2

ERIS (Engineering Resource Information System) is a knowledge base of engineering resources for the design and manufacture of window regulators. It was created with sufficient generality to form the basis for building similar systems for other products. The form of the knowledge base is hierarchical semantic networks of frames or schemas. This form has been shown effective for representation of knowledge ranging from simple facts to classes of parts to manufacturing processes to complex part geometries. The representation of parts in production allows a search for possible carry over parts for a new application. If a carry over part is not adequate, the parametric representation of the geometry of parts allows for redesign of an existing part to meet new specifications. Two different geometric representations were created. One represents the observed features created by a progressive-die press. The other represents the design process as it evolves through the addition of surfaces and edges. Costs for window regulators were studied and broken down into categories that display all significant costs. Labor and raw materials are major contributors to the total cost. Better designed parts and decreased lead time are major payoffs that result when automated design methods are used. GRA

N90-14145# Technische Univ., Delft (Netherlands). Faculty of Geodesy.
NORMAL POINTS: COMPRESSION OF SATELLITE LASER RANGING DATA Thesis
Stefan Pulles Jun. 1988 73 p
(ETN-90-96008) Avail: NTIS HC A04/MF A01

Various aspects related to nomal points, which are a condensed representation of satellite laser ranging full rate data, are described. A most appropriate weight to assign to normal points in parameter estimations is searched for and found. Safe normal points replacement of full rate data in parameter estimation programs, under several option, is studied. This is performed with testing computations, beginning with generated data. The results obtained with full rate data and normal points are compared. It can be concluded that normal points can safely replace full rate data, under the condition that biases are removed from the obervations. Without proper removal of biases the usefulness of normal points becomes uncertain. ESA

N90-14146 Texas Univ., Dallas.
ARCHITECTURE AND LANGUAGE FOR A LAYERED RELATIONAL DATABASE Ph.D. Thesis
Shyam Sundar Sarkar 1989 145 p
Avail: Univ. Microfilms Order No. DA8913600

Issues are investigated which are concerned with complex object representation, object oriented data bases, reasoning on data base objects and suitable languages as an interface to

complex data bases. Data base theory was studied and developed mainly from the perspective of aggregation, logical dependencies, normal forms, and logical query manipulations on flat untypes data bases. A basic motivation for the work was, the need for better data abstraction facilities and adequate data types to represent a wide range of objects in the data base, and existing mismatch between a data base and a high level programming language. To bridge the gap between data bases and high level programming languages, ways were studied to augment the semantic power of data bases so that various objects can be stored. On the other hand, the expressive power of query langauges needs to be developed further in order to offer a better high level interface for the manipulation of data stored at a higher level of abstraction. The following was accomplished: an extension of the relational data base was proposed. This new model has a layered architecture and maintains subtype-supertype links in a complete type lattice over relations. The design of a logical query language on top of the layered relational data base which captures the lattice was also described. This language is similar to typed prolog and its operational semantics are defined to be an amalgamation of reduction and resolution techniques. Dissert. Abstr.

N90-14147# National Weather Service, Silver Spring, MD. Techniques Development Lab.
EXTENDED MEMORY LIBRARY FOR AFOS (AUTOMATION OF FIELD OPERATIONS AND SERVICES) APPLICATIONS
Mark A. Leaphart Jun. 1989 54 p
(PB89-230858; NOAA-NWS-TDL-CP-89-3) Avail: NTIS HC A04/MF A01 CSCL 05B

The Data General Corporation's Eclipse S/230 minicomputer limits every applications program to 32K of logical memory. This is often very burdensome to programmers who are trying to develop software on Automation of Field Operations and Services (AFOS). The Techniques Development Laboratory has developed an extended memory library, XMEM.LB, which provides the programmer with a way of using more than 32K words of logical memory. This collection of FORTRAN 4 callable assembly language routines interfaces with the Real Time Disk Operating System window mapping facility. The document provides information about extended memory and window mapping, including setting up extended memory, handling data in extended memory, definitions of error codes, and a description of the modules in XMEM.LB with examples showing how to use them. GRA

N90-13531# European Space Agency, Paris (France).
THE INCA DATA BASE
A. Gomez, D. Morin, and F. Arenou *In its* The Hipparcos Mission. Prelaunch Status. Volume 2: The Input Catalog Jun. 1989 p 23-45 Original contains color illustrations (For primary document see N90-13529 05-18)
Copyright Avail: NTIS HC A13/MF A02; ESA Publications Div., ESTEC, Noordwijk, Netherlands, 80 Dutch guilders

N90-13547# European Space Agency, Paris (France).
THE SIMBAD DATA BASE
D. Egret and M. Wenger *In its* The Hipparcos Mission. Prelaunch Status. Volume 2: The Input Catalog Jun. 1989 p 233-236 (For primary document see N90-13529 05-18)
Copyright Avail: NTIS HC A13/MF A02; ESA Publications Div., ESTEC, Noordwijk, Netherlands, 80 Dutch guilders

N90-13549# European Space Agency, Paris (France).
OVERVIEW OF THE DATA ACQUISITION AND REDUCTIONS
L. Lindegren and J. Kovalevsky *In its* The Hipparcos Mission. Prelaunch Status. Volume 3: The Data Reductions Jun. 1989 p 1-32 Original contains color illustrations (For primary document see N90-13548 05-18)
Copyright Avail: NTIS HC A22/MF A03; ESA Publications Div., ESTEC, Noordwijk, Netherlands, 80 Dutch guilders

N90-13550# European Space Agency, Paris (France).
ANALYSIS OF THE IMAGE DISSECTOR TUBE DATA
C. A. Murray, F. vanLeeuwen, L. Lindegren, F. Donati, and B. Fassino *In its* The Hipparcos Mission. Prelaunch Status. Volume 3: The Data Reductions Jun. 1989 p 33-49 Original contains color illustrations (For primary document see N90-13548 05-18)
Copyright Avail: NTIS HC A22/MF A03; ESA Publications Div., ESTEC, Noordwijk, Netherlands, 80 Dutch guilders

N90-13551# European Space Agency, Paris (France).
ANALYSIS OF THE STAR MAPPER DATA
E. Canuto, F. Donati, P. Belforte, P. L. Bernacca, and F. vanLeeuwen *In its* The Hipparcos Mission. Prelaunch Status. Volume 3: The Data Reductions Jun. 1989 p 51-72 (For primary document see N90-13548 05-18)
Copyright Avail: NTIS HC A22/MF A03; ESA Publications Div., ESTEC, Noordwijk, Netherlands, 80 Dutch guilders

N90-13558# European Space Agency, Paris (France).
OVERVIEW OF THE TYCHO DATA ANALYSIS
E. Hog *In its* The Hipparcos Mission. Prelaunch Status. Volume 3: The Data Reductions Jun. 1989 p 183-194 (For primary document see N90-13548 05-18)
Copyright Avail: NTIS HC A22/MF A03; ESA Publications Div., ESTEC, Noordwijk, Netherlands, 80 Dutch guilders

N90-13564# European Space Agency, Paris (France).
VALIDATION OF THE HIPPARCOS CATALOG
L. Lindegren, J. Kovalevsky, H. vanderMarel, M. A. C. Perryman, and S. Roeser *In its* The Hipparcos Mission. Prelaunch Status. Volume 3: The Data Reductions Jun. 1989 p 283-295 (For primary document see N90-13548 05-18)
Copyright Avail: NTIS HC A22/MF A03; ESA Publications Div., ESTEC, Noordwijk, Netherlands, 80 Dutch guilders

N90-13566# European Space Agency, Paris (France).
ACCURACY AND CHARACTERISTICS OF THE HIPPARCOS CATALOG
L. Lindegren *In its* The Hipparcos Mission. Prelaunch Status. Volume 3: The Data Reductions Jun. 1989 p 311-323 (For primary document see N90-13548 05-18)
Copyright Avail: NTIS HC A22/MF A03; ESA Publications Div., ESTEC, Noordwijk, Netherlands, 80 Dutch guilders

N90-13567# European Space Agency, Paris (France).
DATA PROCESSING IN THE FAST CONSORTIUM
J. L. Pieplu, C. Huc, and A. Vargas *In its* The Hipparcos Mission. Prelaunch Status. Volume 3: The Data Reductions Jun. 1989 p 325-334 (For primary document see N90-13548 05-18)
Copyright Avail: NTIS HC A22/MF A03; ESA Publications Div., ESTEC, Noordwijk, Netherlands, 80 Dutch guilders

N90-13568# European Space Agency, Paris (France).
DATA PROCESSING IN THE NDAC CONSORTIUM
F. vanLeeuwen, E. Hog, C. Petersen, and L. Lindegren *In its* The Hipparcos Mission. Prelaunch Status. Volume 3: The Data Reductions Jun. 1989 p 335-341 (For primary document see N90-13548 05-18)
Copyright Avail: NTIS HC A22/MF A03; ESA Publications Div., ESTEC, Noordwijk, Netherlands, 80 Dutch guilders

N90-13571# European Space Agency, Paris (France).
THE FIRST-LOOK DATA ANALYSIS AT UTRECHT
H. Schrijver *In its* The Hipparcos Mission. Prelaunch Status. Volume 3: The Data Reductions Jun. 1989 p 373-388 (For primary document see N90-13548 05-18)
Copyright Avail: NTIS HC A22/MF A03; ESA Publications Div., ESTEC, Noordwijk, Netherlands, 80 Dutch guilders

N90-13575# European Space Agency, Paris (France).
THE TYCHO INPUT CATALOG
D. Egret, P. Didelon, and B. J. McLean *In its* The Hipparcos Mission. Prelaunch Status. Volume 3: The Data Reductions Jun. 1989 p 427-435 (For primary document see N90-13548 05-18)

Copyright Avail: NTIS HC A22/MF A03; ESA Publications Div., ESTEC, Noordwijk, Netherlands, 80 Dutch guilders

83 ECONOMICS AND COST ANALYSIS

Includes cost effectiveness studies.

No abstracts in this category.

84 LAW, POLITICAL SCIENCE AND SPACE POLICY

Includes NASA appropriation hearings; aviation law; space law and policy; international law; international cooperation; and patent policy.

N90-14148# Committee on Commerce, Science, and Transportation (U.S. Senate).
NATIONAL AERONAUTICS AND SPACE ADMINISTRATION MULTIYEAR AUTHORIZATION ACT OF 1989
1989 50 p An act, H.R. 1759, referred to the Committee on Commerce, Science and Transportation, 101st Congress, 1st Session, 25 Sep. 1989
Avail: Document Room, House of Representatives, Washington, D.C. 20515 HC free

A bill was submitted to the Senate of the United States to authorize appropriations to the National Aeronautics and Space Administration (NASA) for research and development, space flight, control and data communications, construction of facilities, and research and program management, and for other purposes.
B.G.

N90-14149# Committee on Commerce, Science, and Transportation (U.S. Senate).
NATIONAL AERONAUTICS AND SPACE ADMINISTRATION AUTHORIZATION
1989 594 p
(S-Hrg-101-348; GPO-99-657) Avail: Subcommittee on Science, Technology, and Space, Senate, Washington, D.C. 20510 HC free; SOD HC $17.00 as 552-070-073-40-0

Hearings before a subcommittee of the Senate Commitee on Commerce, Science, and Transportation are presented for the National Aeronautics and Space Administration budget requests for FY 1990 and FY 1991. All written testimony and submittals for the record are also included. The budget estimates provide a detailed outline of budetary information and justifications for reserach and development, construction of facilities, space flight and communications, and research and program management.
B.G.

N90-14150# Technische Univ., Berlin (Germany, F.R.). Inst. fuer Luft- und Raumfahrt.
COMPARISON OF THE SPACE PROGRAM PERFORMANCE OF COUNTRIES WITH SPACE PROGRAMS [LEISTUNGSANALYSE NATIONALER UND REGIONALER RAUMFAHRTPROGRAMME]
Fabian Eilingsfeld 15 Apr. 1989 77 p In GERMAN; ENGLISH summary
(ILR-Mitt-222; ETN-90-95820) Avail: NTIS HC A05/MF A01

A comparison of the space program performance of the U.S., Western Europe, Japan, the USSR, the People's Republic of China, and India is presented. Based on statistical data collected from 1957 to 1987, the actual comparison is conducted in two parts. The first method is based on the dynamic, subjective evaluation of the space sector from the viewpoint of the respective governments which are in charge of the space program. The second method consists of the unweighted combination of suitable objective indicators into a performance index. Both methods show the unchanged superiority in space of the two superpowers. The space budgets of the other four nations are too low to allow them to catch up with the Soviet and American space programs.
ESA

85 URBAN TECHNOLOGY AND TRANSPORTATION

Includes applications of space technology to urban problems; technology transfer; technology assessment; and surface and mass transportation.

For related information see also *03 Air Transportation and Safety, 16 Space Transportation,* and *44 Energy Production and Conversion.*

N90-14151*# National Aeronautics and Space Administration, Washington, DC.
CENTERS FOR THE COMMERCIAL DEVELOPMENT OF SPACE
Susan E. Walker, ed. 1989 22 p Original contains color illustrations
(NASA-PAM-525) Avail: NTIS HC A03/MF A01 CSCL 05A

In 1985, NASA initiated an innovative effort called Centers for the Commercial Development of Space (CCDS). The CCDS program was designed to increase private-sector interest and investment in space-related activities, while encouraging U.S. economic leadership and stimulating advances in promising areas of research and development. Research conducted in the Centers handling the following areas is summarized: materials processing; life sciences; remote sensing; automation and robotics; space propulsion; space structures and materials; and space power.
B.G.

N90-14152*# National Aeronautics and Space Administration, Washington, DC.
NASA COMMERCIAL PROGRAMS Progress Report, 1988
1988 26 p Original contains color illustrations
(NASA-TM-101853; NAS 1.15:101853) Avail: NTIS HC A03/MF A01 CSCL 05A

An expanded role for the U.S. private sector in America's space future has emerged as a key national objective, and NASA's Office of Commercial Programs is providing a focus for action. The Office supports new high technology commercial space ventures, the commercial application of existing aeronautics and space technology, and expanded commercial access to available NASA capabilities and services. The progress NASA has made in carrying out its new assignment is highlighted.
B.G.

N90-14153*# Allied-Signal Aerospace Co., Phoenix, AZ. Garrett Auxiliary Power Div.
ADVANCED TURBINE TECHNOLOGY APPLICATIONS PROJECT (ATTAP) Annual Report, 1988
Apr. 1989 249 p
(Contract DEN3-335)
(NASA-CR-185109; DOE/NASA/0335-1; NAS 1.26:185109; Garrett-31-8071(1)) Avail: NTIS HC A11/MF A02 CSCL 10B

Work to develop and demonstrate the technology of structural ceramics for automotive engines and similar applications is described. Long-range technology is being sought to produce gas turbine engines for automobiles with reduced fuel consumption and reduced environmental impact. The Advanced Turbine Technology Application Project (ATTAP) test bed engine is designed such that, when installed in a 3,000 pound inertia weight automobile, it will provide low emissions, 42 miles per gallon fuel economy on diesel fuel, multifuel capability, costs competitive with current spark ignition engines, and noise and safety characteristics that meet Federal standards.
Author

88 SPACE SCIENCES (GENERAL)

N90-14154*# National Academy of Sciences - National Research Council, Washington, DC.
AN IMPLEMENTATION PLAN FOR PRIORITIES IN SOLAR-SYSTEM SPACE PHYSICS
Stamatios M. Krimigis, R. Grant Athay, Daniel Baker, Lennard A. Fisk, Robert W. Fredricks, John W. Harvey, Jack R. Jokipii, Margaret Kivelson, Michael Mendillo, and Andrew F. Nagy (Michigan Univ., Ann Arbor.) 1985 83 p Prepared in cooperation with National Center for Atmospheric Research, Boulder, CO
(Contract NASw-3482)
(NASA-CR-185375; NAS 1.26:185375) Avail: NTIS HC A05/MF A01 CSCL 03B

The scientific objectives and implementation plans and priorities of the Space Science Board in areas of solar physics, heliospheric physics, magnetospheric physics, upper atmosphere physics, solar-terrestrial coupling, and comparative planetary studies are discussed and recommended programs are summarized. Accomplishments of Skylab, Solar Maximum Mission, Nimbus-7, and 11 other programs are highlighted. Detailed mission plans in areas of solar and heliospheric physics, plasma physics, and upper atmospheric physics are also described. K.C.D.

N90-13873# Deutsche Forschungsanstalt fuer Luft- und Raumfahrt, Cologne (Germany, F.R.).
THE GERMAN SPACE SCIENCE PROGRAM
Ferdinand Dahl and Manfred Otterbein (Bundesministerium fuer Forschung und Technologie, Bonn, Germany, F.R.) *in* ESA, European Rocket and Balloon Programs and Related Research Jun. 1989 p 279-283 (For primary document see N90-13826 05-42)
Copyright Avail: NTIS HC A15/MF A02

89 ASTRONOMY

Includes radio, gamma-ray, and infrared astronomy, and astrometry.

N90-14155 Illinois Univ. at Urbana-Champaign, Savoy.
ORION B: ANATOMY OF A STAR-FORMING REGION Ph.D. Thesis
Peter John Barnes 1988 119 p
Avail: Univ. Microfilms Order No. DA8908619

The compact H II region/molecular cloud Orion B was observed with the Very Large Array (VLA) in the radio continuum and OH absorption line at a frequency of 1667 MHz, in the near-infrared continuum and H2 emission line at a wavelength of 2 micrometers, and in several millimeter wavelength molecular transitions (of HCO+, SO, 13-HCN, and HC(15)N) with the Hat Creek Array. The VLA continuum map has an integrated flux density of 59 + or - 2 Jy, and it is estimated that the total flux density is 63 + or - 4 Jy at this frequency. In OH absorption maps, the eastern loop (EL) shows up near the velocity of the Zeeman-split OH in such a way as to suggest expansion, and a high optical depth cloud appears in the north central part of the nebula at the velocity of the main OH absorption. The infrared source IRS 2, with a strong stellar wind and a location within the EL, is deduced to be the cause of this loop. The IR observations reveal many new sources which together may supply the missing ionizing flux for the nebula. The ionizing front (IF) is traced by the H2 line emission. In the dense molecular core the HCO+ line maps show a centrally located broad line region with an elliptical velocity distribution, a long, quiescent, NS-oriented ridge, an EW ridge which exactly abuts the IF of the adjacent H II region, and a possible one-sided high density outflow to the south with an origin apparently not near any of the IR sources mentioned. These observations support and expand the previously proposed model of the H II region. An improved model and a suggested history for the H II region and the first detailed model for the molecular core are presented.
Dissert. Abstr.

N90-14156*# Max-Planck-Inst. fuer Physik und Astrophysik, Garching (Germany, F.R.). Inst. fuer Extraterrestrische Physik.
FURTHER OBSERVATIONS OF ROTATIONALLY EXCITED FAR INFRARED OH16 AND OH18 EMISSION IN ORION-KL: TIGHTER CONSTRAINTS ON THE NATURE OF THE EMITTING REGION
G. J. Melnick, G. J. Stacey, R. Genzel, J. B. Lugten (California Univ., Berkeley.), and A. Poglitsch Jul. 1989 33 p Submitted for publication
(Grants NAG2-311; NAG2-208)
(NASA-CR-186004; NAS 1.26:186004; MPE-Preprint-156; ETN-89-95858) Copyright Avail: NTIS HC A03/MF A01 CSCL 03A

The Orion-KL region, within 1 arc minute, is observed. The rotational cross ladder (53.351 microns) and rotational ground state (120.1719 microns) transitions are studied. It is shown that these lines exhibit a P-Cygni profile and unambiguously show that the OH gas is expanding out from the central BN-KL infrared cluster. The OH-16 rotational ground state transition (119.234 microns) is velocity resolved and it is found that its intrinsic full width at half maximum is 75 km/s. The line fluxes and line profiles are modeled and it is shown that no single temperature and density component can reproduce the data. Rather, the best fit to the data requires emission from three main components of the gas: post shocked gas with the profiles of temperature, density, and OH abundance; a high density component to the cool post shocked region; and the plateau region. ESA

N90-14157# Stuttgart Univ. (Germany, F.R.). Dept. of Geodetic Science.
STUDY OF MODERN INSTRUMENTATION AND METHODS FOR ASTRONOMIC POSITIONING IN THE FIELD Final Report No. 2, 31 Oct. 1984 - 31 Oct. 1988
E. Grafarend 5 Sep. 1989 128 p
(Contract DAJA45-84-C-0043; DA Proj. 1L1-61102-BH-57)
(AD-A213217; R/D-4618-EN-01) Avail: NTIS HC A07/MF A01 CSCL 22/1

This study was performed to determine, through a literature survey and interviews with appropriate experts, the types and characteristics of instruments and techniques used in Europe for astronomic positioning in the field, and to make recommendations as to the proper direction for future research. The first technical report contained a detailed simulation study about the possible accuracy of astronomic positioning in the field. The simulation study was based on the assumption that the objects of field observations, the stars, are perfectly known, including also the various astronomic reductions such as proper motion, aberration, parallax etc. The second technical report, therefore, allowed some uncertainty of the star position. We present a detailed analysis of how to proceed once only dispersive pior information about star positions is available. The nonlinear condition equations are linearized by a two-step Taylor series expansion accounting for stochastic information 2, delta of right ascension and declination, the parameters of star positions. A numerical analysis is presented in the final report. GRA

N90-14158 Rochester Univ., NY.
AN EXPERIMENT TO SEARCH FOR GALACTIC AXIONS Ph.D. Thesis
Walter Ulrich Wuensch 1989 188 p
Avail: Univ. Microfilms Order No. DA8913598

Results are presented from a search for axions in the mass range of .51 to 1 x 10(exp -5) eV, which may make up the dark matter of the galaxy. The detector used in the search consists of a microwave cavity placed in the strong magnetic field of a superconducting solenoid magnet. The energy in the TM sub 010 mode of the cavity is monitored by a sensitive microwave receiver as the frequency of the mode is swept. The predicted experimental signature of galactic halo axions is a narrow signal, with a Q sub a = f/delta f approx. = 3 x 10(exp 6), which is expected when the resonant frequency of the cavity corresponds to the mass of the axion. An experimental limit on the coupling times the density of (g sub a gamma gamma/m sub a) sq. rho sub a less than or

equal to 2 x 10(exp -40) for an axion linewidth less than or = 400 Hz with a 97 pct confidence level was obtained. The theoretical prediction is (g sub a gamma gamma/m sub a) sq rho sub a approx. 3.9 x 10(exp -44) with rho sub a = 300 MeV/cu cm. The corresponding limit in g sub a gamma gamma is g sub a gamma gamma less than or = 7 x 10(exp -14) GeV(exp -1) at an axion frequency f = 2 GeV and depends linearly on axion mass.
Dissert. Abstr.

N90-13533# European Space Agency, Paris (France).
PROXIMITY EFFECTS ON ADJACENT AND MULTIPLE STARS
C. Turon, J. Kovalevsky, and L. Lindegren *In its* The Hipparcos Mission. Prelaunch Status. Volume 2: The Input Catalog Jun. 1989 p 65-71 Original contains color illustrations (For primary document see N90-13529 05-18)
Copyright Avail: NTIS HC A13/MF A02; ESA Publications Div., ESTEC, Noordwijk, Netherlands, 80 Dutch guilders

N90-13534# European Space Agency, Paris (France).
SUCCESSIVE ITERATIONS OF THE INPUT CATALOG
C. Turon *In its* The Hipparcos Mission. Prelaunch Status. Volume 2: The Input Catalog Jun. 1989 p 73-87 Original contains color illustrations (For primary document see N90-13529 05-18)
Copyright Avail: NTIS HC A13/MF A02; ESA Publications Div., ESTEC, Noordwijk, Netherlands, 80 Dutch guilders

N90-13535# European Space Agency, Paris (France).
STELLAR CONTENT OF THE INPUT CATALOG
A. Gomez, F. Crifo, and C. Turon *In its* The Hipparcos Mission. Prelaunch Status. Volume 2: The Input Catalog Jun. 1989 p 89-106 Original contains color illustrations (For primary document see N90-13529 05-18)
Copyright Avail: NTIS HC A13/MF A02; ESA Publications Div., ESTEC, Noordwijk, Netherlands, 80 Dutch guilders

N90-13536# European Space Agency, Paris (France).
GROUND-BASED ASTROMETRIC MEASUREMENTS
Y. Requieme *In its* The Hipparcos Mission. Prelaunch Status. Volume 2: The Input Catalog Jun. 1989 p 107-114 (For primary document see N90-13529 05-18)
Copyright Avail: NTIS HC A13/MF A02; ESA Publications Div., ESTEC, Noordwijk, Netherlands, 80 Dutch guilders

N90-13537# European Space Agency, Paris (France).
THE COMPILATION OF ASTROMETRIC DATA
H. Jahreiss *In its* The Hipparcos Mission. Prelaunch Status. Volume 2: The Input Catalog Jun. 1989 p 115-127 (For primary document see N90-13529 05-18)
Copyright Avail: NTIS HC A13/MF A02; ESA Publications Div., ESTEC, Noordwijk, Netherlands, 80 Dutch guilders

N90-13540# European Space Agency, Paris (France).
DOUBLE STARS
J. Dommanget *In its* The Hipparcos Mission. Prelaunch Status. Volume 2: The Input Catalog Jun. 1989 p 149-162 (For primary document see N90-13529 05-18)
Copyright Avail: NTIS HC A13/MF A02; ESA Publications Div., ESTEC, Noordwijk, Netherlands, 80 Dutch guilders

N90-13541# European Space Agency, Paris (France).
VARIABLE STARS
M. O. Mennessier and F. Figueras *In its* The Hipparcos Mission. Prelaunch Status. Volume 2: The Input Catalog Jun. 1989 p 163-176 (For primary document see N90-13529 05-18)
Copyright Avail: NTIS HC A13/MF A02; ESA Publications Div., ESTEC, Noordwijk, Netherlands, 80 Dutch guilders

N90-13542# European Space Agency, Paris (France).
THE CHOICE OF STARS IN OPEN CLUSTERS
J. C. Mermilliod and C. Turon *In its* The Hipparcos Mission. Prelaunch Status. Volume 2: The Input Catalog Jun. 1989 p 177-190 Original contains color illustrations (For primary document see N90-13529 05-18)
Copyright Avail: NTIS HC A13/MF A02; ESA Publications Div., ESTEC, Noordwijk, Netherlands, 80 Dutch guilders

N90-13543# European Space Agency, Paris (France).
THE CHOICE OF STARS IN THE MAGELLANIC CLOUDS
L. Prevot *In its* The Hipparcos Mission. Prelaunch Status. Volume 2: The Input Catalog Jun. 1989 p 191-198 (For primary document see N90-13529 05-18)
Copyright Avail: NTIS HC A13/MF A02; ESA Publications Div., ESTEC, Noordwijk, Netherlands, 80 Dutch guilders

N90-13545# European Space Agency, Paris (France).
MINOR PLANETS AND OTHER SOLAR SYSTEM OBJECTS
A. Bec-Borsenberger *In its* The Hipparcos Mission. Prelaunch Status. Volume 2: The Input Catalog Jun. 1989 p 213-223 (For primary document see N90-13529 05-18)
Copyright Avail: NTIS HC A13/MF A02; ESA Publications Div., ESTEC, Noordwijk, Netherlands, 80 Dutch guilders

N90-13546# European Space Agency, Paris (France).
THE CATALOGS PRODUCED BY THE INCA CONSORTIUM
C. Turon *In its* The Hipparcos Mission. Prelaunch Status. Volume 2: The Input Catalog Jun. 1989 p 225-232 (For primary document see N90-13529 05-18)
Copyright Avail: NTIS HC A13/MF A02; ESA Publications Div., ESTEC, Noordwijk, Netherlands, 80 Dutch guilders

N90-13556# European Space Agency, Paris (France).
ASTROMETRIC PARAMETER DETERMINATION IN FAST
H. G. Walter *In its* The Hipparcos Mission. Prelaunch Status. Volume 3: The Data Reductions Jun. 1989 p 163-169 (For primary document see N90-13548 05-18)
Copyright Avail: NTIS HC A22/MF A03; ESA Publications Div., ESTEC, Noordwijk, Netherlands, 80 Dutch guilders

N90-13559# European Space Agency, Paris (France).
TYCHO ASTROMETRY
E. Hog, P. C. Hansen, and L. Lindegren *In its* The Hipparcos Mission. Prelaunch Status. Volume 3: The Data Reductions Jun. 1989 p 195-204 (For primary document see N90-13548 05-18)
Copyright Avail: NTIS HC A22/MF A03; ESA Publications Div., ESTEC, Noordwijk, Netherlands, 80 Dutch guilders

N90-13561# European Space Agency, Paris (France).
DOUBLE STAR REDUCTIONS IN NDAC
S. Soderhjelm *In its* The Hipparcos Mission. Prelaunch Status. Volume 3: The Data Reductions Jun. 1989 p 225-241 (For primary document see N90-13548 05-18)
Copyright Avail: NTIS HC A22/MF A03; ESA Publications Div., ESTEC, Noordwijk, Netherlands, 80 Dutch guilders

N90-13562# European Space Agency, Paris (France).
DOUBLE STAR REDUCTIONS IN FAST
F. Mignard, L. Borriello, J. Kovalevsky, N. Prezioso, and P. L. Bernacca *In its* The Hipparcos Mission. Prelaunch Status. Volume 3: The Data Reductions Jun. 1989 p 243-267 (For primary document see N90-13548 05-18)
Copyright Avail: NTIS HC A22/MF A03; ESA Publications Div., ESTEC, Noordwijk, Netherlands, 80 Dutch guilders

N90-13563# European Space Agency, Paris (France).
THE TREATMENT OF MINOR PLANETS AND PLANETARY SATELLITES
B. Morando and L. Lindegren *In its* The Hipparcos Mission. Prelaunch Status. Volume 3: The Data Reductions Jun. 1989 p 269-281 (For primary document see N90-13548 05-18)
Copyright Avail: NTIS HC A22/MF A03; ESA Publications Div., ESTEC, Noordwijk, Netherlands, 80 Dutch guilders

N90-13846# Deutsche Forschungsanstalt fuer Luft- und Raumfahrt, Cologne (Germany, F.R.).
SOFIA (STRATOSPHERIC OBSERVATORY FOR INFRARED ASTRONOMY): A 3m CLASS AIRBORNE TELESCOPE

A. F. Dahl, R. Ewald, and A. Himmes *In* ESA, European Rocket and Balloon Programs and Related Research Jun. 1989 p 123-124 (For primary document see N90-13826 05-42)
Copyright Avail: NTIS HC A15/MF A02

90 ASTROPHYSICS

Includes cosmology; celestial mechanics; space plasmas; and interstellar and interplanetary gases and dust.
For related information see also *75 Plasma Physics.*

N90-14159# National Academy of Sciences - National Research Council, Washington, DC.
THE EXPLORER PROGRAM FOR ASTRONOMY AND ASTROPHYSICS
Blair D. Savage, Eric E. Becklin, Joseph P. Cassinelli, Andrea K. Dupree, James L. Elliot, William F. Hoffmann, Hugh S. Hudson, Michael Jura, James Kurfess, and Stephen S. Murray (Smithsonian Astrophysical Observatory, Cambridge, MA.) et al 1986 60 p Original contains color illustrations
Avail: NTIS HC A04/MF A01

This report was prepared to provide NASA with a strategy for proceeding with Explorer-class programs for research in space astronomy and astrophysics. The role of Explorers in astronomy and astrophysics and their past accomplishments are discussed, as are current and future astronomy and astrophysics Explorers. Specific cost needs for an effective Explorer program are considered. K.C.D.

N90-14160*# National Aeronautics and Space Administration. Goddard Space Flight Center, Greenbelt, MD.
THE WINDS OF HIGH LUMINOSITY LATE-TYPE BRIGHT STARS Final Report, 15 Jun. 1986 - 14 Jun. 1989
Robert E. Stencel (Colorado Univ., Boulder.) and K. G. Carpenter 1989 9 p
(Grant NAG5-797)
(NASA-CR-182961; NAS 1.26:182961) Avail: NTIS HC A02/MF A01 CSCL 03C

The occurrence and characteristics of the Fe II line asymmetries were studied to determine the radial dependence of the wind velocity for each star. The dependence of the Fe II profiles on spectral type and luminosity class and thus the variation of the velocity fields with stellar type was also investigated. This allows the generality of the results reported for alpha Ori by Carpenter (1984b) to be judged. In addition, new atomic data was used along with observations of the C II (UV 0.01) multiplet to estimate N(sub e) in the stellar winds. Measures of relative Fe II fluxes can be used in a probability-of-escape model to determine the opacity and hydrogen column density versus height in the chromosphere of each star. Finally, analysis of the fluorescent Fe II lines (pumped by Ly alpha) near 2507 A will yield estimates of the intrinsic stellar Ly alpha flux that cannot be measured directly because of interstellar and circumstellar absorption. One important goal of the effort was to acquire high resolution spectra of the whole 2300 to 3200 A region of 13 luminous K and M stars as a data base that will be enormously valuable in planning observations with the Hubble Space Telescope High Resolution Spectrograph. It is also proposed to follow up the recent discovery of significant variations in the Fe II chromospheric emission line profiles from the M-giant Gamma Cru for the purpose of determining the underlying cause of the variations. Author

N90-14161 New Mexico Univ., Albuquerque.
A SEARCH FOR THE EFFECTS OF ACTIVE MAGNETIC FIELDS IN EXTRA-GALACTIC RADIO SOURCES Ph.D. Thesis
David Alan Clarke 1988 482 p
Avail: Univ. Microfilms Order No. DA8905761

In an effort to detect unequivocal signatures of active magnetic fields in extragalactic radio sources, a new three-tiered approach to comparing radio observations with numerical simulations was developed. The three tiers consists of: (1) extensive high resolution, multifrequency radio observations; (2) self-consistent 2D magnetohydrodynamical (MHD) simulations of jets; and (3) computation of the Stokes, I, Q and U parameters along the line-of-sight from the simulations. The latter tier, referred to here as numerical observations, provides for the first time a direct link between the observations and the simulations. The observed sources include the radio galaxies Centaurus A, 3C219, 3C200 and the quasar 1007+417. There are two sets of observations for Centaurus A. The first set includes Very Large Array (VLA) observations of the inner jet. The second set is VLA observations of the inner lobes. The portion of the lobes contained by the optical extent of NGC5128 is the only significant depolarized region and exhibits a rotation measure in excess of +240 rad/sq m. The observed Faraday depth is attributed to the interstellar medium (ISM) of the galaxy. Observations of 3C219 at 6, 18, 20 and 22 cm are presented. The rotation measure image indicates a possible detection of a weak toroidal field in the cocoon surrounding the jet. A model based on the simulations with a passive magnetic field is proposed which explains the lack of a counter jet and the failure of the main jet to reach the southern hotspot. Both 3C200 and 1007+417 were observed. There is evidence that shocks at two of the knots in the jet of 3C200 are responsible for the emission. The jet in 1007+417 is naked and clumpy. It is proposed that an active toroidal field may play a role in the dynamics of this jet.
Dissert. Abstr.

N90-14162 Pittsburgh Univ., PA.
THE LOW-ION QSO ABSORPTION-LINE SYSTEMS Ph.D. Thesis
Kenneth M. Lanzetta 1988 230 p
Avail: Univ. Microfilms Order No. DA8911278

Various techniques are used to investigate the class of quasi-stellar objects (QSO) absorption-line systems that exhibit low-ion absorption lines. Spectroscopy of 32 QSOs at red wavelengths is presented and used to investigate intermediate-redshift Mg II absorption. A total of 22 Mg II doublets are detected, from which properties of the Mg II absorbers are derived. A sample is constructed of 129 QSOs for which published data are available that are suitable for detecting absorption-line systems that are optically thick to Lyman continuum radiation. A total of 53 such Lyman-limit systems are found, from which properties of the Lyman-limit systems are derived. It is found that the rate of incidence of the systems does not strongly evolve with redshift. The result is contrasted with the evolution found previously for systems selected on the basis of Mg II absorption. Spectroscopy at red wavelengths of eight QSOs with known damped Ly alpha absorption systems is presented. These data are combined with existing blue-wavelength observations in order to investigate the metal-line properties of the damped Ly alpha absorption systems. Statistical properties of the lines are derived and compared with other classes of absorption-line systems, and the element abundances of the absorbing gas are investigated. Spectroscopic and spectrophotometric observations aimed at detecting molecular hydrogen and dust in the z = 2.796 damped Ly alpha absorber toward Q1337 + 113 are presented. A model of the equilibrium abundance of H2 is constructed, and the observed limit to the fractional H2 abundance is used to place an upper limit to the dust content of the absorber of less than one third the Galactic value. Dissert. Abstr.

N90-14163*# Lowell Observatory, Flagstaff, AZ.
ARCHIVAL RESEARCH ON ABSORPTION LINES IN VIOLENTLY STAR-FORMING GALAXIES
J. S. Gallagher 22 Sep. 1989 7 p
(Grant NAG5-989)
(NASA-CR-185960; NAS 1.26:185960) Avail: NTIS HC A02/MF A01 CSCL 03B

A computerized analysis of a starburst model is discussed. The model proposes that the absorption line equivalent width should scale with the level of star forming activity. Archival International Ultraviolet Explorer (IUE) data on IUE spectra of luminous blue galaxies were compared with previous IUE observations of extragalactic HII regions and low luminosity

galaxies. The comparisons are summarized and causes for offsets are discussed. J.P.S.

N90-14164*# Fermi National Accelerator Lab., Batavia, IL. Astrophysics Center.
UNITARITY LIMITS ON THE MASS AND RADIUS OF DARK MATTER PARTICLES
Kim Griest and Marc Kamionkowski (Chicago Univ., IL.) Sep. 1989 10 p Sponsored in part by DOE
(Grants NAGw-1340; NSF AST-88-09616)
(NASA-CR-186079; NAS 1.26:186079; FERMILAB-Pub-89/205-A; CFPA-TH-89-013) Avail: NTIS HC A02/MF A01 CSCL 03B

Using partial wave unitarity and the observed density of the Universe, it is show that a stable elementary particle which was once in thermal equilibrium cannot have a mass greater than 340 TeV. An extended object which was once in thermal equilibrium cannot have a radius less than 7.5 x 10(exp -7) fm. A lower limit to the relic abundance of such particles is also found. Author

N90-14165# Rome Univ. (Italy). Dipartimento di Fisica.
CORRELATION AMONG GRAVITATIONAL WAVE AND NEUTRINO DETECTORS DATA DURING SN1987A
Guido Pizzella (Istituto Nazionale di Fisica Nucleare, Rome, Italy) 28 Mar. 1989 27 p Presented at the International Symposium on General Relativity, Relativistic Astrophysics, and Quantum Theory, Jerusalem, Israel, 14 Mar. 1989
(Nota-Interna-932; ETN-90-95814) Avail: NTIS HC A03/MF A01

Data from the gravitational collapse of a supernova, SN1987A, very near the Earth is used in studying the properties of gravitational waves. The velocity, polarization, multipolarity properties, and other properties of these waves are investigated. Neutrino emission from the supernova is also investigated. The fact that the neutrinos reached the earth in one bunch lasting a few seconds tends to support the standard model of gravitational collapse developed by many theoretical physicists. Evidence of a second bunch of neutrinos arriving a few hours earlier has been ignored by many researchers. This initial neutrino bunch is taken into consideration in this research. ESA

N90-14166# Rome Univ. (Italy). Dipartimento di Fisica.
EXPECTED SUPERNOVAE RATES AND GRAVITATIONAL WAVES DETECTION
P. Rapagnani (Istituto Nazionale di Fisica Nucleare, Rome, Italy) 28 Mar. 1989 50 p
(Nota-Interna-933; ETN-90-95815) Avail: NTIS HC A03/MF A01

Data available in the Kraan-Korteweg catalog of 2810 nearby galaxies is used to evaluate the expected rate of supernovae (SN) events according to distance. Three different statistics and two virgocentric flow models for determinating distance of galaxies are used in the evaluation. The results permit calculation of the Expected SN Event Rate (ESNER) according to the sensitivity of a resonant antenna for gravitational radiation detection, considering both an optimistic and a pessimistic theory for the energy converted into gravitational waves during a SN collapse. It is shown that values of the ESNER greater than 1 SN/year can be considered for the ultralow temperature gravitational wave anenna now being constructed by the Rome and Stanford groups, even with pessimistic predictions of the energy emitted as gravitational waves and of the rate of SN explosion. ESA

N90-14167*# Fermi National Accelerator Lab., Batavia, IL. Astrophysics Center.
NUCLEAR PHYSICS AND COSMOLOGY
David N. Schramm (Chicago Univ., IL.) Dec. 1989 13 p Presented at the International Nuclear Physics Conference, Sao Paulo, Brazil, 20-26 Aug. 1989 Sponsored in part by DOE
(Grants NAGw-1321; NAGw-1340; NSF AST-88-22595)
(NASA-CR-186166; NAS 1.26:186166; FERMILAB-Conf-89/254-A) Avail: NTIS HC A03/MF A01 CSCL 03B

Nuclear physics has provided one of two critical observational tests of all Big Bang cosmology, namely Big Bang Nucleosynthesis. Furthermore, this same nuclear physics input enables a prediction to be made about one of the most fundamental physics questions of all, the number of elementary particle families. The standard Big Bang Nucleosynthesis arguments are reviewed. The primordial He abundance is inferred from He-C and He-N and He-O correlations. The strengthened Li constraint as well as D-2 plus He-3 are used to limit the baryon density. This limit is the key argument behind the need for non-baryonic dark matter. The allowed number of neutrino families, N(nu), is delineated using the new neutron lifetime value of tau(n) = 890 + or - 4s (tau(1/2) = 10.3 min). The formal statistical result is N(nu) = 2.6 + or - 0.3 (1 sigma), providing a reasonable fit (1.3 sigma) to three families but making a fourth light (m(nu) less than or equal to 10 MeV) neutrino family exceedly unlikely (approx. greater than 4.7 sigma). It is also shown that uncertainties induced by postulating a first-order quark-baryon phase transition do not seriously affect the conclusions. Author

N90-14168*# Drexel Univ., Philadelphia, PA. Dept. of Physics.
BIG BANG NUCLEOSYNTHESIS AND THE QUARK-HADRON TRANSITION
Hannu Kurki-Suonio, Richard A. Matzner, Keith A. Olive, and David N. Schramm (Chicago Univ., IL.) Dec. 1989 21 p Prepared in cooperation with Texas Univ., Austin, TX, and Fermi National Accelerator Lab., Batavia, IL Submitted for publication
(Grant NAGw-1340)
(NASA-CR-186169; NAS 1.26:186169; Fermilab-Pub-89/252-A) Avail: NTIS HC A03/MF A01 CSCL 03B

An examination and brief review is made of the effects of quark-hadron transistion induced fluctuations on Big Bang nucleosynthesis. It is shown that cosmologically critical densities in baryons are difficult to reconcile with observation, but the traditional baryon density constraints from homogeneous calculations might be loosened by as much as 50 percent, to 0.3 of critical density, and the limit on the number of neutrino flavors remains about N(sub nu) is less than or approximately 4. To achieve baryon densities of greater than or approximately 0.3 of critical density would require initial density contrasts R is much greater the 10(exp 3), whereas the simplest models for the transition seem to restrict R to less than of approximately 10(exp 2). Author

N90-14169*# Chicago Univ., IL.
COSMOLOGY AND THE WEAK INTERACTION
David N. Schramm Dec. 1989 28 p Presented at the Wein 89 International Symposium on Weak and Electromagnetic Interactions in Nuclei, Montreal, Quebec, May 1989 Prepared in cooperation with Fermi National Accellerator Lab., Batavia, IL
(Grant NAGw-1340)
(NASA-CR-186170; NAS 1.26:186170; Fermilab-Conf-89/255-A) Avail: NTIS HC A03/MF A01 CSCL 03B

The weak interaction plays a critical role in modern Big Bang cosmology. Two of its most publicized comological connections are emphasized: big bang nucleosynthesis and dark matter. The first of these is connected to the cosmological prediction of neutrine flavors, N(sub nu) is approximately 3 which in now being confirmed. The second is interrelated to the whole problem of galacty and structure formation in the universe. The role of the weak interaction both for dark matter candidates and for the problem of generating seeds to form structure is demonstrated. Author

N90-14170# Rome Univ. (Italy). Dipt. di Fisica.
STRING CORRELATIONS AND GALAXIES FORMATION
A. M. Allega 31 May 1989 10 p
(ROM1F-89-677; ETN-90-95784) Avail: NTIS HC A02/MF A01

A string network at formation showing scaling laws for different observables is described. An analytical prediction for string-string correlations from des Cloizeaux's law for polymers is outlined. By only using the intrinsic properties of scaling, the two-point correlation function is calculated by fixing lengths and perimeters to compare it with the known large-scale structure of the universe. ESA

N90-14171# Rome Univ. (Italy). Dipt. di Fisica.
NON ABELIAN STRING CORRELATIONS AND GALAXIES FORMATION
A. M. Allega 31 May 1989 10 p
(ROM1F-89-678; ETN-90-95785) Avail: NTIS HC A02/MF A01

A two-point correlation function is numerically computed for a system of non-Abelian strings on a torus by fixing lengths. The large-scale structure given by matter distribution in the universe is predicted by introducing the Cloizeaux's law for a dense polymer system. Scaling in the very intrinsic nature of the string network, which very closely fits the analytical and experimental results, is described. ESA

N90-14172# Rome Univ. (Italy). Dipt. di Fisica.
DES CLOIZEAUX'S LAW FOR STRINGS AND GALAXIES FORMATION. PART 1: ABELIAN CONFIGURATIONS
A. M. Allega 20 Jun. 1989 36 p
(ROM1F-89-681-Pt-1; ETN-90-95787) Avail: NTIS HC A03/MF A01

The configurational critical behavior of a statistical ensemble of strings on a lattice with periodic boundary conditions by a model of polymers at intermediate concentrations is described. The concentration concept is introduced and its phase diagram is presented for different scaling regions. Des Cloizeaux's law for strings is analyzed to gain insight into the intrinsic nature of their correlations. Using power laws without any free parameter of dynamical theories, the two-point correlation function for strings in terms of des Cloizeaux's law for polymers is characterized. An exact prediction of the power law exponent of the self-similarity distribution of matter on large-scale distances into the universe is given and the detailed numerical analysis by a Monte Carlo simulation is reported. ESA

N90-14173# Rome Univ. (Italy). Dipt. di Fisica.
DES CLOIZEAUX'S LAW FOR STRINGS AND GALAXIES FORMATION. PART 2: NON ABELIAN CONFIGURATIONS
A. M. Allega 20 Jun. 1989 21 p
(ROM1F-89-682-Pt-2; ETN-90-95788) Avail: NTIS HC A03/MF A01

Non Abelian strings are described and compared with experimental data. Des Cloizeaux's law is used to study the correlations shown in the string network. Loop correlations are used to describe large-scale matter distribution in the universe. ESA

N90-14174# Rome Univ. (Italy). Dipt. di Fisica.
DETECTABLE GRAVITATIONAL WAVES BY SUPERNOVA SN 1987 A PULSAR RELIC
Daniele Fargion 16 Feb. 1989 17 p
(Preprint-658; ETN-90-95790) Avail: NTIS HC A03/MF A01

The emission of gravitational waves by the ultrafast pulsar relic of supernova SN1987A, at a frequency of 1968.629 Hz is described. Stability and statistical arguments strongly suggest the emission of detectable, periodic gravitational (synchrotron) radiation at first and second harmonic. If these predictions are not experimentally confirmed, an unknown population of ultrafast pulsars in our galaxy should be looked for. ESA

N90-13544# European Space Agency, Paris (France).
THE LINK TO EXTRAGALACTIC OBJECTS
A. N. Argue *In its* The Hipparcos Mission. Prelaunch Status. Volume 2: The Input Catalog Jun. 1989 p 199-211 Original contains color illustrations (For primary document see N90-13529 05-18)
Copyright Avail: NTIS HC A13/MF A02; ESA Publications Div., ESTEC, Noordwijk, Netherlands, 80 Dutch guilders

N90-13862# Centre d'Etude Spatiale des Rayonnements, Toulouse (France).
INTERSTELLAR MEDIUM AND INFRARED EMISSION OF THE GALACTIC DISK
Guy Serra *In* ESA, European Rocket and Balloon Programs and Related Research Jun. 1989 p 221-228 (For primary document see N90-13826 05-42)
Copyright Avail: NTIS HC A15/MF A02

N90-13863# Bonn Univ. (Germany, F.R.). Inst. fuer Astrophysik und Extraterrestrische Forschung.
OPTICAL OBSERVATIONS OF INTERPLANETARY PICK-UP IONS: THE EXPERIMENT HELLY
H. J. Fahr, G. Lay, and H. U. Nass *In* ESA, European Rocket and Balloon Programs and Related Research Jun. 1989 p 229-232 (For primary document see N90-13826 05-42)
Copyright Avail: NTIS HC A15/MF A02

N90-13864# Ruhr Univ., Bochum (Germany, F.R.). Bereich Extraterrestrische Physik.
INTERPLANETARY DUST CLOSE TO THE SUN (F CORONA): ITS OBSERVATION IN THE VISIBLE AND INFRARED BY A ROCKET-BORNE CORONAGRAPH
B. Kneissel, I. Mann, and H. vanderMeer *In* ESA, European Rocket and Balloon Programs and Related Research Jun. 1989 p 233-235 (For primary document see N90-13826 05-42)
Copyright Avail: NTIS HC A15/MF A02

N90-13865# Laboratoire d'Astronomie Spatiale, Marseille (France).
DEEP DETECTION OF HOT STAR POPULATIONS AT BALLOON ULTRAVIOLET WAVELENGTHS
B. Milliard, M. Laget, J. Donas, D. Burgarella, H. Moulinec, and D. Huguenin (Geneva Observatory, Switzerland) *In* ESA, European Rocket and Balloon Programs and Related Research Jun. 1989 p 237-238 (For primary document see N90-13826 05-42)
Copyright Avail: NTIS HC A15/MF A02

91 LUNAR AND PLANETARY EXPLORATION

Includes planetology; and manned and unmanned flights. For spacecraft design or space stations see *18 Spacecraft Design, Testing and Performance.*

N90-14175*# National Aeronautics and Space Administration. Goddard Space Flight Center, Greenbelt, MD.
REEXAMINATION OF DATA FROM THE ASTEROID/METEOROID DETECTOR Semiannual Report
Robert K. Soberman (Pennsylvania Univ., Philadelphia.) and Maurice Dubin 15 Nov. 1989 18 p
(Grant NAGw-1782)
(NASA-CR-185997; NAS 1.26:185997) Avail: NTIS HC A03/MF A01 CSCL 03B

The discovery of the existence of cosmoids, a class of meteoroid in near hyperbolic orbits, was made in a reevaluation of the Sisyphus Experiment on Pioneer 10 and 11. This experiment measured the spontaneous jetting of cosmoids and showed that the dispersion and increase in brightness occurs in microseconds and lasts only briefly. Cosmoid jetting caused multiple telescope thresholds to be exceeded simultaneously which explains the earlier inabilty to compute trajectories from the measured times in the fields of view. A new calculation correlated the Sisyphus individual event measurements with the zodiacal light. That the meteoroid population is dominated by cosmoids is demonstrated. Reported telescopic small comets, measured by a similar optical technique, appear consistent with the Sisyphus results. Characteristic jetting times measured by Sisyphus also show that the volatile cosmoids could not survive in short period orbits. Author

92 SOLAR PHYSICS

Includes solar activity, solar flares, solar radiation and sunspots.

For related information see *93 Space Radiation.*

N90-14176*# Texas Univ., Austin. Dept. of Astronomy.
ANALYSIS OF COORDINATED OBSERVATIONS OF A GIANT STELLAR FLARE Final Technical Report, 1 Mar. 1988 - 31 Aug. 1989
David L. Lambert 21 Oct. 1989 8 p
(Grant NAG5-987)
(NASA-CR-185961; NAS 1.26:185961) Avail: NTIS HC A02/MF A01 CSCL 03B

Multi-wavelength observations of a giant flare on the star AD Leo were obtained with the 2.1 m and 0.9 m telescopes at McDonald Observatory and the International Ultraviolet Explorer satellite. The quality, spectral coverage, and time resolution of the data represented a major improvement over any published stellar flare data. Two theoretical, quantitative flare models were developed. Combining the models, the chromospheric emission model predictions in the hydrogen Balmer lines, Da II K, Mg II h + k and the optical continuum were compared to the observations, with the result that much of the gradual phase flare emission could be produced by the x ray and conductive heated atmospheres. The models lend insight into the impulsive phase flare emission, but do not reproduce it. Soft x ray and conductive heating of the chromosphere is a natural consequence of the coronal temperatures that have been observed during the gradual phase of flares on the sun and on M dwarf stars. The improved flare observations and quantitative flare models presented here show that these heating mechanisms can produce atmospheres whose emission matches many of the observed stellar flare features. Author

N90-14177*# Stanford Univ., CA. Center for Space Science and Astrophysics.
ROTATION OF THE PHOTOSPHERIC MAGNETIC FIELDS: A NORTH-SOUTH ASYMMETRY
E. Antonucci (Turin Univ., Italy), J. T. Hoeksema, and P. H. Scherrer Aug. 1989 15 p Submitted for publication
(Contract NGR-05-020-559; N00014-86-K-0085; NSF ATM-86-18263)
(NASA-CR-186159; NAS 1.26:186159; AD-A213114; SU-CSSA-Astro-89-14) Avail: NTIS HC A03/MF A01 CSCL 03/2

During most of solar cycle 21 the large-scale photospheric field rotated more rapidly in the Northern Hemisphere than in the southern. The large-scale northern field rotated with a 26.9 day period (synodic), was centered at 15 degress N, and covered a latitude zone about 24 degrees wide. The large-scale southern field rotated with a periodicity of 28.1 days, was centered at 26 degrees S, and covered a latitude zone about 32 degrees wide. Our analysis showed rotational power at only a few discrete latitudes and frequencies in each hemisphere. The center of each peak lies near the sunspot differential rotation curve. The largest scale field contributes to the configuration of the coronal and interplanetary magnetic field (IMF). The strength of the first harmonic of the northern field suggests that this structure may be related to the 4-sector pattern observed in the IMF polarity. The southern field had much lower power at the first harmonic of the solar rotation rate and so would contribute only to a 2-sector structure in the IMF. These results were discovered in Fourier analysis of photospheric synoptic charts obtained at the Wilcox Solar Observatory from 1976 to 1986 and confirmed in higher resolution maps from the National Solar Observatory. Mt. Wilson magnetic field measurements from solar cycle 20 show a similar north-south asymmetry. GRA

N90-14178*# Stanford Univ., CA. Center for Space Science and Astrophysics.
SHEAR-INDUCED INFLATION OF CORONAL MAGNETIC FIELDS
James A. Klimchuk 5 Aug. 1989 40 p
(Grant NGL-05-020-272)
(NASA-CR-186103; NAS 1.26:186103; CSSA-Astro-89-11) Avail: NTIS HC A03/MF A01 CSCL 03B

Using numerical models of force-free magnetic fields, the shearing of footprints in arcade geometries leading to an inflation of the coronal magnetic field was examined. For each of the shear profiles considered, all of the field lines become elevated compared with the potential field. This includes cases where the shear is concentrated well away from the arcade axis, such that B(sub z), the component of field parallel to the axis, increases outward to produce an inward B(sub z)squared/8 pi magnetic pressure gradient force. These results contrast with an earlier claim, shown to be incorrect, that field lines can sometimes become depressed as a result of shear. It is conjectured that an inflation of the entire field will always result from the shearing of simple arcade configurations. These results have implications for prominence formation, the interplanetary magnetic flux, and possibly also coronal holes. Author

N90-13868# Bonn Univ. (Germany, F.R.). Inst. fuer Astronomie.
OBSERVATION OF THE SOLAR LYMAN-ALPHA LINE
H. U. Nass, G. Lay, and H. J. Fahr *In* ESA, European Rocket and Balloon Programs and Related Research Jun. 1989 p 245-249 (For primary document see N90-13826 05-42)
Copyright Avail: NTIS HC A15/MF A02

N90-13872# Observatoire de Paris-Meudon (France). Forecasting Center.
PREDICTION OF THE 10 cm SOLAR FLUX INDEX
P. Lantos *In* ESA, European Rocket and Balloon Programs and Related Research Jun. 1989 p 277-278 (For primary document see N90-13826 05-42)
Copyright Avail: NTIS HC A15/MF A02

93 SPACE RADIATION

Includes cosmic radiation; and inner and outer earth's radiation belts.

For biological effects of radiation see *52 Aerospace Medicine.* For theory see *73 Nuclear and High-Energy Physics.*

N90-14179 Nottingham Univ. (England).
THE DETERMINATIN OF THE MUON CONTENT OF EAS FROM CYGNUS X-3 Ph.D. Thesis
A. D. Bullock 1988 374 p
Avail: Univ. Microfilms Order No. BRD-85105

The operation and testing is described of the 40 sq m muon detector and recording system at the Haverah Park Extensive Air Showers (EAS) array. An EAS trigger for the muon detector is provided by the GREX array, which is sensitive to primary energies greater than 2 x 10 (exp 14) eV. GREX, which is an array of scintillator detectors, is operated by the Leeds University EAS group and was specifically designed to look for point sources of cosmic rays. Firstly a brief review of cosmic ray physics is given. Following this, the discovery and subsequent observational details of the x ray binary Cygnus X-3 are outlined. The muon detector is then described along with the results of the testing of its response to EAS muons. A total of approx. 1 million EAS events, for which there are muon density measurements, were accumulated between March 1986 and May 1987. These events comprise the dataset. A mean lateral distribution is generated from the muon density measurements and is shown to be a very good representation of the data set. Dissert. Abstr.

N90-14180*# Fermi National Accelerator Lab., Batavia, IL. Astrophysics Center.
THE GRAND UNIFIED PHOTON SPECTRUM: A COHERENT VIEW OF THE DIFFUSE EXTRAGALACTIC BACKGROUND RADIATION
M. Ted Ressell and Michael S. Turner (Chicago Univ., IL.) Oct.

1989 32 p Submitted for publication Sponsored in part by DOE
(Grant NAGw-1340)
(NASA-CR-186077; NAS 1.26:186077; FERMILAB-Pub-89/214-A) Avail: NTIS HC A03/MF A01 CSCL 03B

The spectrum of diffuse extragalactic background radiation (DEBRA) at wavelengths from 10(exp 5) to 10(exp -24) cm is presented in a coherent fashion. Each wavelength region, from the radio to ultra-high energy photons and cosmic rays, is treated both separately and as part of the grand unified photon spectrum (GUPS). A discussion of, and references to, the relevant literature for each wavelength region is included. This review should provide a useful tool for those interested in diffuse backgrounds, the epoch of galaxy formation, astrophysical/cosmological constraints to particle properties, exotic early Universe processes, and many other astrophysical and cosmological enterprises. As a worked example, researchers derive the cosmological constraints to an unstable-neutrino spies (with arbitrary branching ratio to a radiative decay mode) that follow from the GUPS. Author

99 GENERAL

N90-14181*# Alabama Univ., Huntsville.
ACTION LANGUAGES: DIMENSIONS, EFFECTS
Daniel G. Hayes and Gordon Streeter 31 Aug. 1989 54 p Prepared in cooperation with NASA, Johnson Space Center, Houston, TX
(Contract NCC8-13)
(NASA-CR-183388; NAS 1.26:183388; RR-805) Avail: NTIS HC A04/MF A01 CSCL 05D

Dimensions of action languages are discussed for communication between humans and machines, and the message handling capabilities of object oriented programming systems are examined. Design of action languages is seen to be very contextual. Economical and effective design will depend on features of situations, the tasks intended to be accomplished, and the nature of the devices themselves. Current object oriented systems turn out to have fairly simple and straightforward message handling facilities, which in themselves do little to buffer action or even in some cases to handle competing messages. Even so, it is possible to program a certain amount of discretion about how they react to messages. Such thoughtfulness and perhaps relative autonomy of program modules seems prerequisite to future systems to handle complex interactions in changing situations. Author

N90-14182# Naval Research Lab., Washington, DC.
NRL (NAVAL RESEARCH LABORATORY) REVIEW
Jul. 1989 270 p
(AD-A212886; NRL-PUB-123-1631) Avail: NTIS HC A12/MF A02 CSCL 14/2

In this Review, NRL presents highlights of the unclassified research and development programs for fiscal year 1988. This book provides an exchange of information among scientists, engineerings, scholars, and managers. Partial contents of this review include: Biologically Based Self-Assembly - Bio/Molecular Engineering; New Horizons in Pulsed-Power Research; Research in Ceramic Composites; Radiation Effects in Space Systems; Acoustics; Behavior and Properties of Materials; Chemical Research; Electromagnetic Systems and Sensing; Electronics Research; Energetic Particles and Beams; Information Technology; Numerical Simulation; Optical Systems; Space Research and Technology. GRA

N90-14183# Naval Academy, Annapolis, MD.
SUMMARY OF RESEARCH ACADEMIC DEPARTMENTS, 1987-1988 Annual Report, Jul. 1987 - Jun. 1988
Fred Fetrow Dec. 1988 271 p
(AD-A213252; USNA-3910-3-13) Avail: NTIS HC A12/MF A02 CSCL 05/6

This annual report summarizes the research work of the Naval Academy faculty and midshipmen for the period July 1987 through June 1988. Sponsored and independent research projects are listed by title, followed by the names of the investigators and an abstract. A list of publications and their abstracts are included as well as presentations at professional meetings, conferences, and seminars. Contents include: Division of Engineering and Weapons; Division of English and History; Division of Mathematics and Science; Division of Professional Development and Division of U.S. and International Studies. GRA

Typical Subject Index Listing

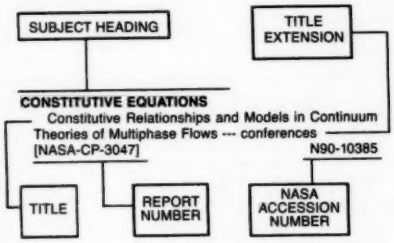

The subject heading is a key to the subject content of the document. Titles, report numbers, and accession numbers of pertinent documents are provided under each subject heading. When the title is insufficiently descriptive of the document content, a title extension has been added, separated from the title by three hyphens. The report number helps to indicate the type of document cited (e.g., NASA report, NASA translation, NASA contractor report). The NASA accession number is the number by which the document abstracts are arranged in this journal and by which the document is sold or requested. The titles, with title extensions if present, are arranged under each subject heading in ascending accession number order. The subject headings have been selected from the latest revision of the *NASA Thesaurus* (NASA SP-7064).

A

ABEL FUNCTION
Scaling in a non Abelian string network
[ROM1F-89-676] N90-14066
Non Abelian string correlations and galaxies formation
[ROM1F-89-678] N90-14171

ABRASION
Evaluation of copper slag blast media for railcar maintenance
[NASA-CR-183744] N90-13681

ABRASIVES
Evaluation of copper slag blast media for railcar maintenance
[NASA-CR-183744] N90-13681

ABSORPTION CROSS SECTIONS
Ultraviolet absorption cross-sections of bromoform in the temperature range 295-240 K
[AERONOMICA-ACTA-A-348-1989] N90-13630
New calculations of photodissociation cross-sections in the O2 Schumann-Runge system N90-13834

ABSORPTION SPECTRA
The low-ion QSO absorption-line systems N90-14162
Archival research on absorption lines in violently star-forming galaxies
[NASA-CR-185960] N90-14163

ABSORPTION SPECTROSCOPY
The low-ion QSO absorption-line systems N90-14162

ABSTRACTS
AFOSR technical report summaries
[AD-A213148] N90-14142

ACCELERATION (PHYSICS)
Acceleration sets of planar manipulators. Part 2: Applications and experiments
[AD-A213336] N90-13791
Definition, determination and characterization of acceleration sets for spatial manipulators
[AD-A213366] N90-13793

ACCESS CONTROL
Long-range plan for management and use of the radio spectrum by agencies and establishments of the Federal Government
[PB89-232367] N90-13693

ACCLIMATIZATION
Adaptation and resistance of ecosystems to stress
[AD-A212999] N90-13889

ACCURACY
Error allocation and accuracy assessment N90-13501
Accuracy and characteristics of the Hipparcos catalog N90-13566
A mixed finite element solution of the linear acoustic equations
[ECL-89-006] N90-14075

ACETIC ACID
Contribution to the electrochemical study of corrosion in the low conductivity media: Application to the study of the behavior of austenitic stainless steels in concentrated solutions of acetic acid
[ISAL-89-0014] N90-13648

ACID RAIN
Computational solution of chemistry problems
[NASA-CR-186000] N90-13618

ACOUSTIC ATTENUATION
Localization of ultrasound in thick composites
[AD-A212994] N90-13602

ACOUSTIC EMISSION
A counter gating circuit for acoustic emission monitoring of structures cracking under repetitive alternating loads
[ARL-MAT-TM-398] N90-13808

ACOUSTIC EXCITATION
Mobility power flow analysis of an L-shaped plate structure subjected to acoustic excitation
[NASA-CR-186130] N90-13817

ACOUSTIC IMPEDANCE
Localization of ultrasound in thick composites
[AD-A212994] N90-13602

ACOUSTIC MEASUREMENT
Test procedures for the evaluation of helmet and headset mounted active noise reduction systems
[AD-A212991] N90-13937
Propagation of sound in vibrationally excited nitrogen and hydrogen gas mixtures
[AD-A213002] N90-14073

ACOUSTIC PROPAGATION
Localization of ultrasound in thick composites
[AD-A212994] N90-13602

ACOUSTIC PROPERTIES
ULF/VLF (0.001 to 50 Hz) Seismo-Acoustic Noise in the Ocean
[AD-A212942] N90-13913

ACOUSTIC SCATTERING
Numerical analysis of scattering by interface flaws
[AD-A212996] N90-13810

ACOUSTICS
A mixed finite element solution of the linear acoustic equations
[ECL-89-006] N90-14075
NRL (Naval Research Laboratory) Review
[AD-A212686] N90-14182

ACOUSTO-OPTICS
Spectrometer technology recommendations N90-13468

ACTIVE CONTROL
An approach to optical structures control N90-13456
Segment alignment control system N90-13457
Control of optical systems N90-13484
PACOSS program N90-13487
LDR structural technology activities at JPL N90-13488
Payload thermal control N90-13511
Spacecraft thermal control N90-13513

ACTUATORS
Advanced actuation systems development, volume 2
[AD-A213378] N90-13398
Evaluation of selected computer models for modeling pyrotechnic and propellant devices
[AD-A213003] N90-13671
Acceleration sets of planar manipulators. Part 2: Applications and experiments
[AD-A213336] N90-13791

ADA (PROGRAMMING LANGUAGE)
The development of a program analysis environment for Ada
[NASA-CR-185860] N90-13962
Software engineering and Ada (Trademark) training: An implementation model for NASA
[NASA-CR-186071] N90-13966
Ada task scheduling: A focused Ada investigation
[NASA-CR-186072] N90-13967
Ada programming guidelines for deterministic storage management
[NASA-CR-181308] N90-13982

ADAPTATION
Advanced actuation systems development, volume 2
[AD-A213378] N90-13398
The relationship between subjective and objective measures of simulator-induced ataxia
[AD-A213095] N90-13922

ADAPTIVE CONTROL
Expert systems for adaptive control of large space structures N90-13452
A practical approach for minimum time control of the Spacecraft Control Laboratory Experiment (SCOLE), appendix A
[NASA-CR-186008] N90-13495
Adaptive strategies for controls of flexible arms
[NASA-CR-185868] N90-13783
A new approach to control single-link flexible arms. Part 3: Adaptive control of the tip position with payload changes
[AD-A213337] N90-13792

ADDITIVES
Novel carbamates, their production and their use as fuels additives
[EP-PATENT-0-298-636-A-1] N90-13676

ADHESION
Implementation and analysis of adhesion in multimaterials of the type Al(Si)-ZrO2 and graphite, metal or ceramics
[ECL-89-004] N90-13667

ADHESION TESTS
Nondestructive analysis of aileron fatigue and aging in a Mirage F1
[REPT-M6-594000] N90-13378
Contamination removal using various solvents and methodologies
[NASA-CR-183747] N90-13652
Effects of tacky mat contamination on bond degradation for Chemlok/liner and NBR/liner bonds
[NASA-CR-183742] N90-13653
Evaluation of a metering, mixing, and dispensing system for mixing polysulfide adhesive
[NASA-CR-183749] N90-13654

ADHESIVE BONDING
RSRM nozzle fixed housing cooldown test
[NASA-CR-183741] N90-13587
The adhesive bonding of thermoplastic composites
[AD-A213358] N90-13605
Effects of tacky mat contamination on bond degradation for Chemlok/liner and NBR/liner bonds
[NASA-CR-183742] N90-13653
Evaluation of a metering, mixing, and dispensing system for mixing polysulfide adhesive
[NASA-CR-183749] N90-13654

ADHESIVES
The adhesive bonding of thermoplastic composites
[AD-A213358] N90-13605
Evaluation of a metering, mixing, and dispensing system for mixing polysulfide adhesive
[NASA-CR-183749] N90-13654

ADJOINTS
The algebraic basis of mathematical morphology. Part 1: Dilations and erosions
[CWI-AM-R8807] N90-14065

ADJUSTING
Geodetic network adjustment using GPS triple difference observations and a priori stochastic information
[TR-1-1987] N90-13367

A study on the sensitivity and simultaneous adjustment of a hoop-column antenna surface [NASA-TM-101536] N90-13807
ADVANCED VERY HIGH RESOLUTION RADIOMETER
Senegalese land surface change analysis and biophysical parameter estimation using NOAA AVHRR spectral data [NASA-CR-186120] N90-13883
AEROASSIST
The controllability of the aeroassist flight experiment atmospheric skip trajectory N90-13438
AERODYNAMIC CHARACTERISTICS
Analysis of experimental data for CAST 10-2/DOA 2 supercritical airfoil at low Reynolds numbers and application to high Reynolds number flow [AD-A211654] N90-13326
Efficient methods for integrated structural-aerodynamic wing optimum design N90-13376
AERODYNAMIC CONFIGURATIONS
Study of the integration of wind tunnel and computational methods for aerodynamic configurations [NASA-TM-102196] N90-13332
Reduction of profile drag by modifying the structure next to the wake area [IMFL-88/35] N90-13356
A model suitable for predicting the noise associated with the ducted tail rotor of a helicopter [ECL-88-09] N90-14074
AERODYNAMIC DRAG
Atmospheric drag model calibrations for spacecraft lifetime prediction N90-13439
AERODYNAMIC HEATING
Optimum shape of a blunt forebody in hypersonic flow [NASA-CR-181955] N90-13351
AERODYNAMIC INTERFERENCE
Transonic Euler solutions on mutually interfering finned bodies [AD-A213395] N90-13331
A wall interference assessment/correction interface measurement system for the NASA/ARC 12-ft PWT [NASA-CR-185474] N90-13401
A two-dimensional adaptive-wall test section with ventilated walls in the Ames 2- by 2-foot transonic wind tunnel [NASA-TM-102207] N90-13407
AERODYNAMIC LOADS
Correlation of Puma airloads: Lifting-line and wake calculation [NASA-TM-102212] N90-13327
AERODYNAMICS
Block-structured solution of three-dimensional transonic flows using parallel processing [AD-A212851] N90-13330
An Introduction to Hypersonic Aerodynamics [VKI-LS-1989-01] N90-13334
Hypersonic aerodynamics N90-13335
Measurement Techniques in Aerodynamics [VKI-LS-1989-05] N90-13339
A technique for the prediction of aerodynamics and aeroelasticity of rotor blades N90-13377
Multigrid and defect correction for the steady Navier-Stokes equations: Applications to aerodynamics [ETN-90-96011] N90-13727
AEROELASTICITY
Application of an efficient hybrid scheme for aeroelastic analysis of advanced propellers [NASA-TM-102428] N90-13355
A technique for the prediction of aerodynamics and aeroelasticity of rotor blades N90-13377
Aeroelastic control of composite lifting surfaces: Integrated aeroelastic control optimization N90-13396
Dynamic testing techniques and applications for an aeroelastic rotor test facility N90-13406
AEROMANEUVERING
Optimal trajectories for the aeroassisted flight experiment, 1988-89 [NASA-CR-186132] N90-13443
AEROSOLS
Transport phenomena and interfacial kinetics in multiphase combustion systems [AD-A212932] N90-13620
Recovery of particle size distribution of ultrafine aerosols from diffusional decay measurements [AD-A213006] N90-13621
Pilot investigation of indoor-outdoor and personal PM10 (thoracic) and associated ionic compounds and mutagenic activity [PB89-222723] N90-13920
AEROSPACE ENGINEERING
Space Station Engineering Design Issues [NASA-CR-185978] N90-13492
The evaluation of a metered mixer for RTV silicone for RSRM nozzle backfill operations [NASA-CR-183831] N90-13763
AEROSPACE ENVIRONMENTS
Development of a shuttle plume radiation heating indicator [NASA-CR-183679] N90-13584
Optical properties monitor: Experiment definition phase [NASA-CR-183836] N90-14092
AEROSPACE MEDICINE
Aerospace medicine and biology: A continuing bibliography with indexes (supplement 330) [NASA-SP-7011(330)] N90-13925
Preliminary study of pharmacological control of space disease [ETN-90-95015] N90-13927
AEROSPACE PLANES
Trajectory optimization and guidance for an aerospace plane [NASA-CR-185884] N90-13369
AEROSPACE SAFETY
Active rendezvous between a low-earth orbit user spacecraft and the Space Transportation System (STS) shuttle N90-13436
AEROSPACE SCIENCES
The French balloon program and related space research N90-13828
AEROSPACE SYSTEMS
Project ORION microcomputer management system [AD-A212945] N90-13959
NRL (Naval Research Laboratory) Review [AD-A212886] N90-14182
AGING (MATERIALS)
Nondestructive analysis of aileron fatigue and aging in a Mirage F1 [REPT-M6-594000] N90-13378
Mechanical property characterization of VascoMax T-300 [AD-A212950] N90-13637
AGING (METALLURGY)
The effect of composition and aging treatment on the microstructure and mechanical properties of aluminum-lithium-titanium alloys [AD-A213144] N90-13640
AH-1G HELICOPTER
Investigation of difficult component effects on finite element model vibration prediction for the Bell AG-1G helicopter: Volume 2: Correlation results [NASA-CR-181916-VOL-2] N90-13814
AH-64 HELICOPTER
Preliminary airworthiness evaluation of the AH-64A equipped with the Air To Air Stinger (ATAS) missile system [AD-A213030] N90-13374
AILERONS
Nondestructive analysis of aileron fatigue and aging in a Mirage F1 [REPT-M6-594000] N90-13378
AIR BREATHING ENGINES
Aircraft propulsion: Leading the way in aviation [LR-532] N90-13395
AIR COOLING
Apparatus for cooling electronic components in aircraft [AD-D014207] N90-13373
AIR POLLUTION
Air quality simulation model performance for one-hour averages [PB89-233506] N90-13890
Observations of stratospheric HCl: 1975-1985 [AERONOMICA-ACTA-A-349-1989] N90-13892
AIR QUALITY
Air quality simulation model performance for one-hour averages [PB89-233506] N90-13890
AIR SAMPLING
Pilot investigation of indoor-outdoor and personal PM10 (thoracic) and associated ionic compounds and mutagenic activity [PB89-222723] N90-13920
AIR TO AIR MISSILES
Preliminary airworthiness evaluation of the AH-64A equipped with the Air To Air Stinger (ATAS) missile system [AD-A213030] N90-13374
An autopilot design methodology for bank-to-turn missiles [AD-A213379] N90-13399
AIR TRAFFIC
National Airspace System airspace management operational concept [DOT/FAA/DS-89/29] N90-13361
AIR TRAFFIC CONTROL
National Airspace System airspace management operational concept [DOT/FAA/DS-89/29] N90-13361
An update to the system safety study of TCAS 2 [DOT/FAA/SA-89/3] N90-13363
Computer-based tools for assisting air traffic controllers with arrivals flow management [RSRE-88001] N90-13366
Flight deck automation: Promises and realities [NASA-CP-10036] N90-13384
AIR TRANSPORTATION
Study of high-speed civil transports [NASA-CR-4235] N90-13370
Flight deck automation: Promises and realities [NASA-CP-10036] N90-13384
AIRBORNE EQUIPMENT
SOFIA (Stratospheric Observatory For Infrared Astronomy): A 3m class airborne telescope N90-13846
AIRBORNE/SPACEBORNE COMPUTERS
Software and hardware description of the helicopter motion equations for VAX computers [AD-A213248] N90-13375
Definition of avionics concepts for a heavy lift cargo vehicle, appendix A [NASA-CR-183817] N90-13380
True covariance simulation of the EUVE update filter N90-13427
A knowledge-based system design/information tool for aircraft flight control systems [NASA-TM-101704] N90-13990
AIRCRAFT ACCIDENTS
The human factors relating to escape and survival from helicopters ditching in water [AGARD-AG-305(E)] N90-13358
AIRCRAFT CONSTRUCTION MATERIALS
Some new techniques for aircraft fuselage skin tests [LR-547] N90-13379
Some aspects of test frequency influence on the fatigue behavior of ARALL [LR-549] N90-13616
Design and evaluation of a new biaxial testing method for sheet material (SUPERBAT) [LR-548] N90-13624
AIRCRAFT CONTROL
Aerodynamics of thrust vectoring [NASA-CR-185074] N90-13354
A knowledge-based system design/information tool for aircraft flight control systems [NASA-TM-101704] N90-13990
Laboratory test methodology for evaluating the effects of electromagnetic disturbances on fault-tolerant control systems [NASA-TM-101665] N90-14061
AIRCRAFT DESIGN
Study of high-speed civil transports [NASA-CR-4235] N90-13370
The S.D.G., P.S.D. and the nonlinear airplane [NLR-MP-88018-U] N90-13371
Efficient methods for integrated structural-aerodynamic wing optimum design N90-13376
AIRCRAFT ENGINES
Effect of reduced aft diameter and increased blade number on high-speed counterrotation propeller performance [NASA-TM-102077] N90-13352
Study of the engine bird ingestion experience of the Boeing 737 aircraft [DOT/FAA/CT-89/16] N90-13360
AIRCRAFT EQUIPMENT
Conference Proceedings of the Human-Electronic Crew: Can They Work Together [AD-A211871] N90-13936
AIRCRAFT GUIDANCE
Trajectory optimization and guidance for an aerospace plane [NASA-CR-185884] N90-13369
AIRCRAFT HAZARDS
The human factors relating to escape and survival from helicopters ditching in water [AGARD-AG-305(E)] N90-13358
AIRCRAFT MAINTENANCE
Repair of composites by means of wet-lay-up [LR-551] N90-13617
AIRCRAFT NOISE
Mobility power flow analysis of an L-shaped plate structure subjected to acoustic excitation [NASA-CR-186130] N90-13817
AIRCRAFT PILOTS
Conference Proceedings of the Human-Electronic Crew: Can They Work Together [AD-A211871] N90-13936
AIRCRAFT RELIABILITY
Preliminary airworthiness evaluation of the AH-64A equipped with the Air To Air Stinger (ATAS) missile system [AD-A213030] N90-13374
AIRCRAFT SAFETY
The human factors relating to escape and survival from helicopters ditching in water [AGARD-AG-305(E)] N90-13358

AIRCRAFT SPECIFICATIONS
Aircraft/airport compatibility: Some strategic, tactical, and operational issues
[TT-8902] N90-13409
AIRCRAFT STABILITY
Aerodynamics of thrust vectoring
[NASA-CR-185074] N90-13354
On the application of modified stepwise regression for the estimation of aircraft stability and control parameters
[REPT-8905] N90-13400
AIRCRAFT STRUCTURES
Investigation of difficult component effects on finite element model vibration prediction for the Bell AG-1G helicopter. Volume 2: Correlation results
[NASA-CR-181916-VOL-2] N90-13814
AIRFOIL OSCILLATIONS
Dynamic testing techniques and applications for an aeroelastic rotor test facility N90-13406
AIRFOILS
Analysis of experimental data for CAST 10-2/DOA 2 supercritical airfoil at low Reynolds numbers and application to high Reynolds number flow
[AD-A211654] N90-13326
Convective heat transfer measurements from a NACA 0012 airfoil in flight and in the NASA Lewis Icing Research Tunnel
[NASA-TM-102448] N90-13750
AIRFRAMES
Investigation of difficult component effects on finite element model vibration prediction for the Bell AG-1G helicopter. Volume 2: Correlation results
[NASA-CR-181916-VOL-2] N90-13814
AIRGLOW
The effects of gravity waves on horizontal layers: Simulation and interpretation N90-13852
AIRLINE OPERATIONS
National Airspace System flight planning operational concept
[DOT/FAA/DS-89/30] N90-13362
AIRPORT PLANNING
Aircraft/airport compatibility: Some strategic, tactical, and operational issues
[TT-8902] N90-13409
ALASKA
Crustal structure studies utilizing earthquake sequences
[AD-A212916] N90-13895
The interaction and variation of waves and turbulence from MST radar data
[AD-A212849] N90-13906
ALBEDO
Senegalese land surface change analysis and biophysical parameter estimation using NOAA AVHRR spectral data
[NASA-CR-186120] N90-13883
ALCOHOLS
An investigation of flame spread over shallow liquid pools in microgravity and nonair environments
[NASA-TM-102425] N90-13680
Low frequency polarized and depolarized light scattering in H-bonded liquids: CH3(CH2)n-1OH (n=1,...5)
[PREPRINT-693] N90-14100
ALGAE
Free swimming organisms: Microgravity as an investigative tool N90-13949
ALGEBRA
Program transformation with abstract relation algebras
[AD-A213270] N90-14011
ALGORITHMS
Automation of orbit determination functions for National Aeronautics and Space Administration (NASA)-supported satellite missions N90-13434
Validation of the Hipparcos catalog N90-13564
Linking Hipparcos to a quasi-inertial system N90-13565
An algorithm for control volume analysis of cryogenic systems
[AD-A213394] N90-13683
Test generation for highly sequential circuits
[AD-A211932] N90-13698
Parameter estimation for the Gummel-Poon transistor model
[MA-53] N90-13705
Inviscid 2D solutions on unstructured, adaptive grids N90-13737
An improved algorithm for the modeling of vapor flow in heat pipes
[NASA-CR-185179] N90-13748
Analysis of rotary engine combustion processes based on unsteady, three-dimensional computations
[NASA-TM-102469] N90-13749
Probabilistic finite element analysis of dynamic structural response
[AD-A213249] N90-13789
Time domain coupling of the boundary and finite element methods for elastodynamics
[AD-A213243] N90-13811
Application of an optimal filter for inflatable sphere data processing N90-13849
Parallelism in the discrete-event simulation algorithm
[AD-A213060] N90-13970
Novel graph searching methods for image analysis
[AD-A213065] N90-13971
A fault-tolerant software algorithm for a network of transputers
[AD-A213092] N90-13972
Algorithm for atmospheric corrections of aircraft and satellite imagery
[NASA-TM-100751] N90-13976
The cellular approach: A new method to speed up simulated annealing for macro placement
[MEMO-COSOR-88-29] N90-13980
On the asymptotic convergence of the simulated annealing algorithm in the presence of a parameter dependent penalization
[MEMO-COSOR-89-16] N90-13984
A multilevel parallel solver for block tridiagonal and banded linear systems
[AD-A213151] N90-14008
FORTRAN subroutines for the evaluation of the confluent hypergeometric functions
[AD-A213308] N90-14012
On the performance of on-line algorithms for partition problems
[MEMO-784] N90-14015
Global optimization and simulated annealing
[MEMO-COSOR-88-21] N90-14025
The weighted sum of two S-units being a square
[MEMO-792] N90-14031
Measurement of arithmetic error and calculation perturbations
[IMAG-RR-767-M] N90-14039
Data structures for the representation and manipulation of polyhedrons
[IMAG-RR-772-M] N90-14042
ALIGNMENT
Extended Kalman filter for attitude estimation of the earth radiation budget satellite N90-13433
Segment alignment control system N90-13457
Real-time sensing of optical alignment N90-13479
ALLOYING
The effects of alloying and thermal factors on the solidification and mechanical properties of gray iron
[VTT-619] N90-13851
ALTERNATING DIRECTION IMPLICIT METHODS
Gas flows in rocket motors. Volume 2, appendix C: Time iterative solution of viscous supersonic flow
[AD-A213349] N90-13592
ALTIMETRY
An update to the system safety study of TCAS 2
[DOT/FAA/SA-89/3] N90-13363
ALUMINUM
Impact tests on aluminum 2024 T3, aramid and glass reinforced aluminum laminates and thermoplastic composites
[LR-534] N90-13613
ALUMINUM ALLOYS
Quench sensitivity in Al-Cu-Li alloys
[AD-A213055] N90-13639
The effect of composition and aging treatment on the microstructure and mechanical properties of aluminum-lithium-titanium alloys
[AD-A213144] N90-13640
Implementation and analysis of adhesion in multimaterials of the type Al(Si)-ZrO2 and graphite, metal or ceramics
[ECL-89-004] N90-13667
Threshold for fatigue crack propagation
[DLR-FB-89-33] N90-13815
ALUMINUM ARSENIDES
Field-effect spectroscopy of interface states
[AD-A212998] N90-14112
ALUMINUM CARBIDES
The application of cast SiC/Al to rotary engine components
[NASA-CR-179610] N90-13385
AMORPHOUS MATERIALS
Computational studies of structural and transport properties of amorphous solids
[ETN-90-96027] N90-13664
AMORPHOUS SEMICONDUCTORS
Ultrafast processes and spectroscopy with free electron lasers
[AD-A212889] N90-13773
AMPLIFIERS
Development of FIR arrays with integrating amplifiers N90-13473
Electron beam sensitive devices for controllability
[IMAG-RR-761-I] N90-13707
An experimental analysis of the waveguide modes in a high-gain free-electron laser amplifier N90-13779
ANALOG DATA
Resistive fuses: Analog hardware for detecting discontinuities in early vision
[AD-A211891] N90-13696
An artificial intelligence approach to analog system diagnosis
[AD-A213135] N90-13992
ANALYTIC FUNCTIONS
Some comments on the solvable Chiral Potts model
[PREPRINT-673] N90-14070
ANGULAR VELOCITY
Extension to Eulers's theorem to n-dimensional spaces N90-13431
ANISOTROPIC PLATES
Measuring of the complete stiffness matrix for anisotropic laminated materials
[DLR-MITT-89-11] N90-13606
Measuring of the complete stiffness matrix for anisotropic laminated materials
[DLR-MITT-89-12] N90-13607
ANISOTROPY
A four channel He-3 cooled balloon-borne bolometer radiometer N90-13469
ANNEALING
Global optimization and simulated annealing
[MEMO-COSOR-88-21] N90-14025
Unified model of charge build up and annealing of oxide charge and interface states in SiO2 due to stress
[HMI-B-485] N90-14120
ANNIHILATION REACTIONS
Model-independent analysis of the Z line shape in e+e- annihilation
[PREPRINT-679] N90-14089
Unitarity limits on the mass and radius of dark matter particles
[NASA-CR-186079] N90-14164
ANODIC COATINGS
Electrochemistry at very small electrodes
[AD-A213156] N90-13623
Study of metal-insulator-semiconductor structures on indium phosphide, implemented by anodic oxidation
[ECL-88-10] N90-14114
ANTENNA DESIGN
Spectrometer technology recommendations N90-13468
Joint Services Electronics Program
[AD-A213015] N90-13699
A study on the sensitivity and simultaneous adjustment of a hoop-column antenna surface
[NASA-TM-101538] N90-13807
ANTIFERROMAGNETISM
Investigations of spontaneous nuclear order in copper by neutron diffraction
[ETN-90-96060] N90-14090
Local pairing and antiferromagnetism in high-T sub c superconductors
[AD-A213004] N90-14113
APEXES
A graph theoretic characterization for the rank of the transfer matrix of a structured system
[CWI-OS-R8819] N90-14064
APOGEE BOOST MOTORS
The apogee boost motor N90-13517
APPLICATIONS PROGRAMS (COMPUTERS)
Gas flows in rocket motors. Volume 3, appendix D: Computer code listings
[AD-A213350] N90-13593
MOBILE4 oxygenated fuels version user's guide
[PB89-230700] N90-13674
Parameter estimation for the Gummel-Poon transistor model
[MA-53] N90-13705
Software development for avionics SSME control and diagnostics
[NASA-CR-184894] N90-13964
Algorithm for atmospheric corrections of aircraft and satellite imagery
[NASA-TM-100751] N90-13976
Extended memory library for AFOS (Automation of Field Operations and Services) applications
[PB89-230858] N90-14147
APPROPRIATIONS
National Aeronautics and Space Administration Multiyear Authorization Act of 1989 N90-14148
National Aeronautics and Space Administration authorization
[S-HRG-101-348] N90-14149
APPROXIMATION
The weighted sum of two S-units being a square
[MEMO-792] N90-14031
Practice of bivariate quadratic simplicial splines
[MEMO-800] N90-14034

Computational aspects of pseudospectral Laguerre approximations
[NASA-CR-181934] N90-14038

ARC MELTING
Metal transfer in gas metal arc welding
[AD-A213390] N90-13642

ARC WELDING
Metal transfer in gas metal arc welding
[AD-A213390] N90-13642
Arc current control of a robotic welding system: Modeling and control system design
[AD-A213150] N90-13788

ARCHITECTURE (COMPUTERS)
Definition of avionics concepts for a heavy lift cargo vehicle, appendix A
[NASA-CR-183817] N90-13380
Overview of the Tycho data analysis N90-13558
Computational and psychophysical study of human vision using neural networks
[AD-A213290] N90-13924
Dynamic workload modeling of high speed token rings in a metropolitan area network
[MEMO-INF-89-21] N90-14059
Architecture and language for a layered relational database N90-14146

ARCTIC REGIONS
Meteorological atlas of the Northern Hemisphere lower stratosphere for January and February 1989 during the Airborne Arctic Stratospheric Expedition
[NASA-TM-4145] N90-13908

ARGON
Hot spots Ar and Ne gas puff z-pinch
[IPPCZ-289] N90-14103

ARITHMETIC
Measurement of arithmetic error and calculation perturbations
[IMAG-RR-767-M] N90-14039

ARITHMETIC AND LOGIC UNITS
Measurement of arithmetic error and calculation perturbations
[IMAG-RR-767-M] N90-14039

ARRAYS
Development of FIR arrays with integrating amplifiers N90-13473

ARRIVALS
Computer-based tools for assisting air traffic controllers with arrivals flow management
[RSRE-88001] N90-13366

ARSENIC
Effect of adsorbed arsenic on the decomposition rate of nickel hydride
[AD-A213245] N90-13624

ARTERIES
Generation of free radicals during cold injury and rewarming
[AD-A213088] N90-13915

ARTIFICIAL INTELLIGENCE
User needs, benefits, and integration of robotic systems in a space station laboratory
[NASA-CR-185150] N90-13794
Conference Proceedings of the Human-Electronic Crew: Can They Work Together
[AD-A211871] N90-13936
A knowledge-based system design/information tool for aircraft flight control systems
[NASA-TM-101704] N90-13990
An artificial intelligence approach to analog system diagnosis
[AD-A213135] N90-13992
The problem of automation: Inappropriate feedback and interaction, not overautomation
[NASA-CR-186126] N90-13994
A knowledge-based flight status monitor for real-time application in digital avionics systems
[NASA-TM-101710] N90-13995

ARTIFICIAL SATELLITES
Auroral and sub-auroral interaction at the F region ionosphere
[AD-A213284] N90-13896

ASCENT TRAJECTORIES
GOES-I/M ascent maneuvers from transfer orbit to station N90-13421

ASPHALT
Evaluation of a neoprene latex modified SAMI (Stress Absorbing Membrane Interlayer)
[PB89-226435] N90-13665

ASSEMBLIES
Assembly, integration, and verification N90-13519

ASSESSMENTS
Error allocation and accuracy assessment N90-13501

ASTEROIDS
The treatment of minor planets and planetary satellites N90-13563

ASTROMETRY
The Hipparcos Mission. Prelaunch status. Volume 2: The input catalog
[ESA-SP-1111-VOL-2] N90-13529
Stellar content of the input catalog N90-13535
Ground-based astrometric measurements N90-13536
The compilation of astrometric data N90-13537
Double stars N90-13540
Minor planets and other solar system objects N90-13545
Overview of the data acquisition and reductions N90-13549
Astrometric parameter determination in FAST N90-13556
The sphere solution and astrometric parameter determination in NDAC N90-13557
Overview of the Tycho data analysis N90-13558
Tycho astrometry N90-13559
Double star reductions in NDAC N90-13561
The treatment of minor planets and planetary satellites N90-13563
Linking Hipparcos to a quasi-inertial system N90-13565

ASTRONAUT PERFORMANCE
On the wings of a dream: The Space Shuttle
[NASA-EP-269] N90-13446

ASTRONAUT TRAINING
On the wings of a dream: The Space Shuttle
[NASA-EP-269] N90-13446

ASTRONAUTS
Exercise countermeasures for bed rest deconditioning
[NASA-TM-101045] N90-13926

ASTRONOMICAL CATALOGS
From scientific proposals to the Inca data base N90-13530
Stellar content of the input catalog N90-13535
The catalogs produced by the Inca consortium N90-13548
Validation of the Hipparcos catalog N90-13564
Accuracy and characteristics of the Hipparcos catalog N90-13566
The Tycho input catalog N90-13575

ASTRONOMICAL COORDINATES
Linking Hipparcos to a quasi-inertial system N90-13565

ASTRONOMICAL MAPS
Analysis of the star mapper data N90-13551
Data processing in the FAST consortium N90-13567
Data processing in the NDAC consortium N90-13568

ASTRONOMICAL MODELS
Orion B: Anatomy of a star-forming region N90-14155
Archival research on absorption lines in violently star-forming galaxies
[NASA-CR-185960] N90-14163
Big Bang nucleosynthesis and the Quark-Hadron transition
[NASA-CR-186169] N90-14168
String correlations and galaxies formation
[ROM1F-89-677] N90-14170
Des Cloizeaux's law for strings and galaxies formation. Part 2: Non Abelian configurations
[ROM1F-89-662-PT-2] N90-14173

ASTRONOMICAL PHOTOMETRY
Reexamination of data from the asteroid/meteoroid detector
[NASA-CR-185997] N90-14175

ASTRONOMICAL SPECTROSCOPY
The low-ion QSO absorption-line systems N90-14162

ASTRONOMY
European Rocket and Balloon Programs and Related Research
[ESA-SP-291] N90-13826
The German space science program N90-13873
The Explorer program for astronomy and astrophysics N90-14159
Analysis of coordinated observations of a giant stellar flare
[NASA-CR-185961] N90-14176

ASTROPHYSICS
Stellar content of the input catalog N90-13535
European Rocket and Balloon Programs and Related Research
[ESA-SP-291] N90-13826
The Swedish sounding rocket and balloon program N90-13830
An implementation plan for priorities in solar-system space physics
[NASA-CR-185375] N90-14154
The Explorer program for astronomy and astrophysics N90-14159

ASYMMETRY
Study of forces and moments on wing-bodies at high incidence, volumes 1 and 2 N90-13350
The linear study of zonally asymmetric barotropic flows N90-13902
Rotation of the photospheric magnetic fields: A north-south asymmetry
[NASA-CR-186159] N90-14177

ASYMPTOTIC PROPERTIES
On the asymptotic convergence of the simulated annealing algorithm in the presence of a parameter dependent penalization
[MEMO-COSOR-89-16] N90-13984
Estimation of convolution tail behavior
[MEMO-COSOR-89-04] N90-14051

ATAXIA
The relationship between subjective and objective measures of simulator-induced ataxia
[AD-A213095] N90-13922
Simulator induced sickness in the CP-140 (Aurora) flight deck simulator
[AD-A213096] N90-13923

ATMOSPHERIC ATTENUATION
Ultraviolet absorption cross-sections of bromoform in the temperature range 295-240 K
[AERONOMICA-ACTA-A-348-1989] N90-13630

ATMOSPHERIC CHEMISTRY
Proceedings: US/FRG (Federal Republic of Germany) Workshop on Photochemical Ozone Problem and Its Control: US Experiences and the Situation in Europe
[PB89-233514] N90-13891
CANOES 2: Dynamics of atmospheric infrared thermochemical excitation, volume 1
[AD-A213341] N90-13897
CANOES 2: Dynamics of atmospheric infrared thermochemical excitation, volume 2
[AD-A213342] N90-13898
CANOES 2: Dynamics of atmospheric infrared thermochemical excitation, volume 3
[AD-A213343] N90-13899

ATMOSPHERIC COMPOSITION
Proceedings: US/FRG (Federal Republic of Germany) Workshop on Photochemical Ozone Problem and Its Control: US Experiences and the Situation in Europe
[PB89-233514] N90-13891
A high-resolution atlas of the infrared spectrum of the Sun and the Earth atmosphere from space: A compilation of ATMOS spectra of the region from 650 to 4800 cm (2.3 to 16 micron). Volume 1: The Sun
[NASA-RP-1224-VOL-1] N90-13893

ATMOSPHERIC CORRECTION
Algorithm for atmospheric corrections of aircraft and satellite imagery
[NASA-TM-100751] N90-13976

ATMOSPHERIC DENSITY
Neutral air turbulence in the middle and upper atmosphere observed during the MAC/EPSILON campaign N90-13855

ATMOSPHERIC EFFECTS
Atmospheric drag model calibrations for spacecraft lifetime prediction N90-13439
Lifetime predictions for the Solar Maximum Mission (SMM) and San Marco spacecraft N90-13440

ATMOSPHERIC ENTRY
Optimal trajectories for the Aeroassisted Flight Experiment. Part 1: Equations of motion in an Earth-fixed system
[NASA-CR-186134] N90-13441
Optimal trajectories for the Aeroassisted Flight Experiment. Part 2: Equations of motion in an inertial system
[NASA-CR-186135] N90-13442
Optimal trajectories for the aeroassisted flight experiment, 1988-89
[NASA-CR-186132] N90-13443

ATMOSPHERIC MODELS
Air quality simulation model performance for one-hour averages
[PB89-233506] N90-13890
An evaluation of the Smith-Feddes model
[AD-A213237] N90-13907
Three dimensional analysis of the structure of the atmosphere in polar environments by vertical satellite sounding. Interest for the meteorological forecasts at high latitudes
[ETN-90-95506] N90-13911

ATMOSPHERIC PHYSICS
An implementation plan for priorities in solar-system space physics
[NASA-CR-185375] N90-14154

ATMOSPHERIC SCATTERING
A stochastic model for the calculation of multiple scattered lidar returns
[DLR-FB-89-36] N90-13778

ATMOSPHERIC SOUNDING
Observation of wind corners in the middle atmosphere over Andenes (69 N) during winter 1983/84, summer 1987 and summer 1988 N90-13836
The electrodynamics of the polar ionosphere with special emphasis on the dayside cleft region N90-13838

Some remarks on the working principle of the rocketborne nose tip dc probes in the D-region of the ionosphere N90-13839
ATMOSPHERIC TEMPERATURE
Evidence for accurate temperatures from the inflatable falling sphere N90-13835
Near-mesopause temperatures at 69 N latitude in late summer N90-13837
ATMOSPHERIC TURBULENCE
The S.D.G., P.S.D. and the nonlinear airplane [NLR-MP-88018-U] N90-13371
ATOM CONCENTRATION
Diurnal variation of the sodium layer at polar latitudes in summer N90-13869
ATOMIC COLLISIONS
CANOES 2: Dynamics of atmospheric infrared thermochemical excitation, volume 1 [AD-A213341] N90-13897
CANOES 2: Dynamics of atmospheric infrared thermochemical excitation, volume 2 [AD-A213342] N90-13898
Interaction of radiation with matter: Atomic collision processes occurring in the presence of radiation fields [AD-A213112] N90-14078
ATOMIC RECOMBINATION
An Introduction to Hypersonic Aerodynamics [VKI-LS-1989-01] N90-13334
On catalytic recombination rates in hypersonic stagnation heat transfer N90-13338
ATOMIC SPECTRA
Interaction of radiation with matter: Atomic collision processes occurring in the presence of radiation fields [AD-A213112] N90-14078
ATTENTION
Watchfulness and attention during weightlessness simulations: Use of computerized psychometric tests [REPT-89-TOU-3-1045] N90-13928
ATTITUDE (INCLINATION)
Simultaneous quaternion estimation (QUEST) and bias determination N90-13417
COBE nonspinning attitude propagation N90-13418
Extension to Eulers's theorem to n-dimensional spaces N90-13431
Analytical derivation and verification of zero-gyro control for the IUE satellite [NASA-TM-100748] N90-13767
ATTITUDE CONTROL
Aerodynamics of thrust vectoring [NASA-CR-185074] N90-13354
The effects of seasonal and latitudinal earth infrared radiance variations on ERBS attitude control N90-13414
Spacecraft attitude determination using the earth's magnetic field N90-13429
Analysis of the flight dynamics of the Solar Maximum Mission (SMM) off-sun scientific pointing N90-13432
Overview of the Hipparcos satellite N90-13502
The attitude and orbit control system N90-13516
High precision rocket attitude reconstruction using star sensor and magnetometer data N90-13844
The SN 1987A attitude control system N90-13845
ATTITUDE GYROS
On-ground attitude determination N90-13552
AUDIO FREQUENCIES
A prototype microprocessor based audiometer for use by the CF (Canadian Forces) medical services for periodic hearing tests [AD-A212990] N90-13921
AUDIOMETRY
Speech reception in quiet and in noisy conditions by individuals with noise-induced hearing loss in relation to their audiogram [IZF-1989-11] N90-13692
Evaluation of speech intelligibility through a bone conduction stimulator [AD-A212002] N90-13919
A prototype microprocessor based audiometer for use by the CF (Canadian Forces) medical services for periodic hearing tests [AD-A212990] N90-13921
AUDITORY PERCEPTION
Speech reception in quiet and in noisy conditions by individuals with noise-induced hearing loss in relation to their audiogram [IZF-1989-11] N90-13692
AUGER SPECTROSCOPY
Quantitative AES and XPS: Determination of the electron spectrometer transmission function and the detector sensitivity energy dependencies for the production of true electron emission spectra in AES and XPS [NPL-DMA(A)-194] N90-13634
AURORAL ZONES
Observations of electrostatic hydrogen cyclotron waves and electric field fluctuations near one Hz in auroral acceleration regions N90-13842
The auroral current - voltage relationship N90-13843
Preliminary results of the rocket and scatter experiments ROSE: Measurements with the newly designed spherical probe N90-13850
ALIS: An Auroral Large Imaging System in northern Scandinavia N90-13877
Auroral and sub-auroral interaction at the F region ionosphere [AD-A213284] N90-13896
AURORAS
Auroral particle acceleration by dc and low frequency electric fields N90-13841
AUSTENITIC STAINLESS STEELS
Contribution to the electrochemical study of corrosion in the low conductivity media: Application to the study of the behavior of austenitic stainless steels in concentrated solutions of acetic acid [ISAL-89-0014] N90-13648
AUTOMATIC CONTROL
Apparatus for cooling electronic components in aircraft [AD-D014207] N90-13373
Flight deck automation: Promises and realities [NASA-CP-10036] N90-13384
The economic impact of automation technology [AD-A213363] N90-13682
Arc current control of a robotic welding system: Modeling and control system design [AD-A213150] N90-13788
Kinematics and control of manipulation robots [WTHD-187] N90-13803
Flight software development for the isothermal dendritic growth experiment [NASA-TM-102412] N90-13988
AUTOMATIC PILOTS
An autopilot design methodology for bank-to-turn missiles [AD-A213379] N90-13399
AUTOMATIC TEST EQUIPMENT
An artificial intelligence approach to analog system diagnosis [AD-A213135] N90-13992
AUTOMORPHISMS
On distance-transitive graphs and involutions [CWI-PM-R8808] N90-14037
The algebraic basis of mathematical morphology. Part 1: Dilations and erosions [CWI-AM-R8807] N90-14065
AUXILIARY POWER SOURCES
Power generation and distribution N90-13515
AVIONICS
Definition of avionics concepts for a heavy lift cargo vehicle, appendix A [NASA-CR-183817] N90-13380
A new view of weapon system reliability and maintainability [AD-A213281] N90-13382
A new view of weapon system reliability and maintainability: Executive summary [AD-A213282] N90-13383
A knowledge-based flight status monitor for real-time application in digital avionics systems [NASA-TM-101710] N90-13995
AXIAL COMPRESSION LOADS
The initial imperfection data bank at the Delft University of Technology, part 2 [LR-559-PT-2] N90-13825
AXIAL FLOW
An interactive grid generation procedure for axial and radial flow turbomachinery [NASA-CR-185167] N90-13968
AXIAL LOADS
Design and evaluation of a new biaxial testing method for sheet material (SUPERBAT) [LR-548] N90-13824
AXISYMMETRIC FLOW
Coherent structures in a round jet N90-13733

B

B-52 AIRCRAFT
Application of fracture mechanics and half-cycle method to the prediction of fatigue life of B-52 aircraft pylon components [NASA-TM-88277] N90-13820
BACKGROUND RADIATION
A four channel He-3 cooled balloon-borne bolometer radiometer N90-13469
Diffraction, chopping, and background subtraction for LDR N90-13476
The grand unified photon spectrum: A coherent view of the diffuse extragalactic background radiation [NASA-CR-186077] N90-14180
BACKSCATTERING
Preliminary results of the rocket and scatter experiments ROSE: Measurements with the newly designed spherical probe N90-13850
BACKWARD DIFFERENCING
Using Broyden updates to approximate the Jacobian in a semi-implicit backward differentiation code [AD-A213239] N90-14010
BAFFLES
The baffles N90-13509
BALANCE
Choice of a differential method for the attitude restitution in dynamic unbalance [CNES-CT/DTI/MS/CM/290] N90-13582
Balance laws and centro velocity in dissipative systems [MEMO-797] N90-13726
The relationship between subjective and objective measures of simulator-induced ataxia [AD-A213095] N90-13922
BALANCING
MM and T advanced balancing/machining [AD-A213103] N90-13775
BALLISTICS
Evaluation of selected computer models for modeling pyrotechnic and propellant devices [AD-A213003] N90-13671
BALLOON FLIGHT
European Rocket and Balloon Programs and Related Research [ESA-SP-291] N90-13826
Swiss scientific balloon and sounding rocket experiments 1987-1989 N90-13827
The French balloon program and related space research N90-13828
The Norwegian balloon and sounding rocket program 1989-1992 N90-13829
The Swedish sounding rocket and balloon program N90-13830
The German scientific balloon and sounding rocket program N90-13831
Evidence for accurate temperatures from the inflatable falling sphere N90-13835
BALLOON SOUNDING
New calculations of photodissociation cross-sections in the O2 Schumann-Runge system N90-13834
BALLOON-BORNE INSTRUMENTS
A four channel He-3 cooled balloon-borne bolometer radiometer N90-13469
Three-meter balloon-borne telescope N90-13490
Deep detection of hot star populations at balloon ultraviolet wavelengths N90-13865
BALLOONS
Operational activity in France and a new method of balloon temperature piloting N90-13857
Large heavy duty balloons in Europe N90-13858
The DYANA campaign 1990 N90-13870
Long duration balloon flights in the middle stratosphere N90-13874
BAROTROPIC FLOW
The linear study of zonally asymmetric barotropic flows N90-13902
BARRIER LAYERS
Elastic impurity scattering in double-barrier resonant tunneling structures [AD-A212850] N90-14110
BATCH PROCESSING
Identification of impulsive interference channels [AD-A213154] N90-14009
BEADS
Model filled polymers I. Synthesis of crosslinked monodisperse polystyrene beads [AD-A213228] N90-13660
BEAM INTERACTIONS
Experimental and theoretical study of artificial plasma layers produced by two intersecting beams in a chamber [NASA-CR-184598] N90-14102
BEAMS (SUPPORTS)
Identification of equivalent modulus of a composite beam from nonmodal vibratory tests [ECL-89-001] N90-13821
BEARING (DIRECTION)
The relationship between subjective and objective measures of simulator-induced ataxia [AD-A213095] N90-13922
BEARINGS
Flight motor set 360L001 (STS-26R). Volume 5: Nozzle component [NASA-CR-183771] N90-13588
BED REST
Exercise countermeasures for bed rest deconditioning [NASA-TM-101045] N90-13926
BEHAVIOR
Analysis of three approaches to qualitative simulation [MEMO-INF-89-32] N90-14035

BEND TESTS
Buckling of delaminations in ARALL laminates
[LR-535] N90-13614
BETATRONS
Synchrotron-betatron parametric instability in free-electron lasers
[AD-A213373] N90-13777
BIAS
Simultaneous quaternion estimation (QUEST) and bias determination N90-13417
BIBLIOGRAPHIES
Space station systems: A bibliography with indexes (supplement 9)
[NASA-SP-7056(09)] N90-13580
Aerospace medicine and biology: A continuing bibliography with indexes (supplement 330)
[NASA-SP-7011(330)] N90-13925
BIG BANG COSMOLOGY
Nuclear physics and cosmology
[NASA-CR-186156] N90-14167
Big Bang nucleosynthesis and the Quark-Hadron transition
[NASA-CR-186169] N90-14168
Cosmology and the weak interaction
[NASA-CR-186170] N90-14169
BINARY MIXTURES
Preparation of binary ice layers by condensation from gas phase
[JUEL-2248] N90-13631
BINARY STARS
Proximity effects on adjacent and multiple stars N90-13533
Double stars N90-13540
Double star reductions in NDAC N90-13561
Double star reductions in FAST N90-13562
BIOASTRONAUTICS
Aerospace medicine and biology: A continuing bibliography with indexes (supplement 330)
[NASA-SP-7011(330)] N90-13925
BIOCHEMISTRY
Response of lymphocytes to a mitogenic stimulus during spaceflight N90-13942
BIOCONVERSION
Modern biofuel cells for waste recycling in life support systems
[NASA-CR-185963] N90-13718
BIOENGINEERING
NRL (Naval Research Laboratory) Review
[AD-A212886] N90-14182
BIOLOGICAL EFFECTS
Aerospace medicine and biology: A continuing bibliography with indexes (supplement 330)
[NASA-SP-7011(330)] N90-13925
BIOPHYSICS
The sensory transduction pathways in bacterial chemotaxis N90-13944
Gravitropism in plants: Hydraulics and wall growth properties of responding cells N90-13950
BIOREACTORS
Model system studies with a phase separated membrane bioreactor N90-13954
Design challenges for space bioreactors N90-13955
Fermentation and oxygen transfer in microgravity N90-13956
BIOTECHNOLOGY
Model system studies with a phase separated membrane bioreactor N90-13954
BIPOLAR TRANSISTORS
Parameter estimation for the Gummel-Poon transistor model
[MA-53] N90-13705
Design of a power component with IGBT insulated grid. Static and dynamic study
[ECL-88-22] N90-13710
Modeling and measurement methods for high speed bipolar transistors
[REPT-11] N90-13714
BIRD-AIRCRAFT COLLISIONS
Study of the engine bird ingestion experience of the Boeing 737 aircraft
[DOT/FAA/CT-89/16] N90-13360
BIRDS
Study of the engine bird ingestion experience of the Boeing 737 aircraft
[DOT/FAA/CT-89/16] N90-13360
BIVARIATE ANALYSIS
Practice of bivariate quadratic simplicial splines
[MEMO-800] N90-14034
BLADE TIPS
Flows with tip leakage N90-13740
BLOCKING
Effect of central obscuration on the LDR point spread function N90-13475
BLOOD CIRCULATION
Generation of free radicals during cold injury and rewarming
[AD-A213066] N90-13915
BLUNT BODIES
Blunt-nose inviscid airflows with coupled nonequilibrium processes N90-13336
Optimum shape of a blunt forebody in hypersonic flow
[NASA-CR-181955] N90-13351
Computation of nonequilibrium gas flow past blunt bodies
[PREPRINT-488] N90-13757
BODY-WING CONFIGURATIONS
Study of forces and moments on wing-bodies at high incidence, volumes 1 and 2 N90-13350
BOLOMETERS
A four channel He-3 cooled balloon-borne bolometer radiometer N90-13469
BOLTZMANN TRANSPORT EQUATION
Solution of the Boltzmann equation using an energy group method
[AD-A213138] N90-14096
BONE MINERAL CONTENT
Bone mineral measurement using dual energy x ray densitometry N90-13958
BOLTS
Evaluation of speech intelligibility through a bone conduction stimulator
[AD-A212002] N90-13919
BOREDOM
Functional decor in the International Space Station: Body orientation cues and picture perception
[NASA-TM-102242] N90-13931
BORN APPROXIMATION
The effective (3)He-nucleon force in a microscopic DWBA approach to the (3)He,t charge exchange reaction --- Distorted Wave-Borne Approximation (DWBA)
[KVI-763] N90-14077
BOROSILICATE GLASS
Toughening mechanisms in ceramic composites
[PB89-235907] N90-13656
BOTANY
Life science research in space
[ESA-SP-1105] N90-13917
BOUNDARIES
Hamiltonian properties of graphs with large neighborhood unions
[MEMO-779] N90-14013
Linear groups and distance-transitive graphs
[CWI-PM-R8805] N90-14036
BOUNDARY ELEMENT METHOD
Numerical analysis of scattering by interface flaws
[AD-A212996] N90-13810
Time domain coupling of the boundary and finite element methods for elastodynamics
[AD-A213243] N90-13811
BOUNDARY LAYER COMBUSTION
Transport phenomena and interfacial kinetics in multiphase combustion systems
[AD-A212932] N90-13620
BOUNDARY LAYER EQUATIONS
An Introduction to Hypersonic Aerodynamics
[VKI-LS-1989-01] N90-13334
Theory of stagnation point heat transfer in dissociated air N90-13337
BOUNDARY LAYER FLOW
Theory of stagnation point heat transfer in dissociated air N90-13337
The 3D LDA techniques in vortex studies and boundary layer surveys N90-13346
Multiple paths to subharmonic laminar breakdown in a boundary layer
[NASA-CR-181948] N90-13722
Generalized similarity solutions for three dimensional, laminar, steady, compressible boundary layer flows on swept profile cylinders
[DLR-FB-89-34] N90-13725
Computation of nonequilibrium gas flow past blunt bodies
[PREPRINT-488] N90-13757
BOUNDARY LAYER SEPARATION
Computation of Navier-Stokes equations for three-dimensional flow separation
[NASA-TM-102266] N90-13353
BOUNDARY LAYER TRANSITION
Multiple paths to subharmonic laminar breakdown in a boundary layer
[NASA-CR-181948] N90-13722
Numerical simulation of transition in three-dimensional boundary layers
[DLR-FB-89-12] N90-13726
BOUNDARY LAYERS
General buckling tests with thin-walled shells
[DLR-MITT-89-13] N90-13816
On the nonexistence of a strong solution in the boundary problem for a sticky Brownian motion
[CWI-BS-R8901] N90-14018
BOUNDARY VALUE PROBLEMS
A practical approach for minimum time control of the Spacecraft Control Laboratory Experiment (SCOLE), appendix A
[NASA-CR-186008] N90-13495
Magneto-elastic interactions in conducting structures in transient magnetic fields N90-13686
The initial-boundary value problem for the Davey-Stewartson 1 equation; how to generate and drive localized coherent structures in multidimensions
[PREPRINT-684] N90-13756
Time domain coupling of the boundary and finite element methods for elastodynamics
[AD-A213243] N90-13811
Parabolic equations for curves on surfaces. 2: Intersections, blow up and generalized solutions
[AD-A212890] N90-14004
The weighted sum of two S-units being a square
[MEMO-792] N90-14031
Solving a specific Thue-Mahler equation
[MEMO-793] N90-14032
Practice of bivariate quadratic simplicial splines
[MEMO-800] N90-14034
Computational aspects of pseudospectral Laguerre approximations
[NASA-CR-181934] N90-14038
Energy exchange of interacting solitons in multidimensions
[PREPRINT-662] N90-14071
BRAGG ANGLE
First-order Bragg SAR imagery of Kelvin wakes and moving internal wave fields
[AD-A213361] N90-13691
BRAIN
Computational and psychophysical study of human vision using neural networks
[AD-A213290] N90-13924
BRANCHING (MATHEMATICS)
Self-decomposeable distributions and branching processes
[MEMO-COSOR-89-06] N90-14052
BRAYTON CYCLE
Advanced energy system program
[PB89-235170] N90-13887
BRAZILIAN SPACE PROGRAM
Qualification of the 4th stage propulsor of the Brazilian launcher. SLV: A new sounding rocket N90-13860
The Brazilian space program: Actual state of the art N90-13861
BREADBOARD MODELS
Development of a traveling wave tube for the project X-SAR. Construction and testing of a breadboard model
[ETN-90-95900] N90-13713
BRIGHTNESS
Functional decor in the International Space Station: Body orientation cues and picture perception
[NASA-TM-102242] N90-13931
Reexamination of data from the asteroid/meteoroid detector
[NASA-CR-185997] N90-14175
BRITTLE MATERIALS
A theory of damage in brittle and cementitious materials, part 1
[AD-A212940] N90-13658
BROMINE COMPOUNDS
Ultraviolet absorption cross-sections of bromoform in the temperature range 295-240 K
[AERONOMICA-ACTA-A-348-1989] N90-13630
BROWNIAN MOVEMENTS
On the nonexistence of a strong solution in the boundary problem for a sticky Brownian motion
[CWI-BS-R8901] N90-14018
BUBBLES
Gas evolution and bubble formation on electrodes
[DLR-FB-89-35] N90-13629
BUCKLING
Buckling of delaminations in ARALL laminates
[LR-535] N90-13614
General buckling tests with thin-walled shells
[DLR-MITT-89-13] N90-13816
Buckling load analysis for imperfect cylindrical shells, part 1
[LR-543-PT-1] N90-13823
The initial imperfection data bank at the Delft University of Technology, part 2
[LR-559-PT-2] N90-13825
BUOYANCY
Buoyancy effects on the vapor condensation rate on a horizontal liquid surface
[NASA-TM-102437] N90-13675
Facilities for microgravity combustion research
[NASA-TM-102014] N90-13679

BUS CONDUCTORS
Power generation and distribution N90-13515
BUTADIENE
Thermophysical properties of buta-1,3-diene [ESDU-89005] N90-13619

C

CALCULUS OF VARIATIONS
Application of a self-adaptive grid method to complex flows [NASA-TM-102223] N90-13324
Periodic solutions of Hamiltonian systems of 3-body type [AD-A212891] N90-14005
CALIBRATING
Dynamic testing techniques and applications for an aeroelastic rotor test facility N90-13406
A gyroscope calibration analysis for the Gamma Ray Observatory (GRO) N90-13428
Extended Kalman filter for attitude estimation of the earth radiation budget satellite N90-13433
The modulating grid N90-13505
On-ground photometric calibration N90-13523
In-orbit payload calibration N90-13526
New ground-based photometric measurements N90-13538
Standard stars and photometric calibration N90-13539
Variable stars N90-13541
The first-look data analysis at Utrecht N90-13571
Liquid water content and droplet size calibration of the NASA Lewis Icing Research Tunnel [NASA-TM-102447] N90-13797
GRADIO: An error analysis of the spaceborne gravity gradiometer [ETN-90-96010] N90-13901
CANTILEVER BEAMS
Attitude and shape control of optimally designed large space structures N90-13579
The adhesive bonding of thermoplastic composites [AD-A213358] N90-13605
CAPACITORS
High temperature capacitive strain gage [NASA-CR-4266] N90-13760
CARBAMATES (TRADENAME)
Novel carbamates, their production and their use as fuels additives [EP-PATENT-0-298-636-A-1] N90-13676
CARBON FIBER REINFORCED PLASTICS
Low temperature optical testing of CFRP telescope panels N90-13463
SiO overcoating and polishing of CFRP telescope panels N90-13478
Fractography of composite delamination [NASA-CR-183291] N90-13599
CARBON FIBERS
Impact tests of three composite materials with carbon fiber cores [REPT-M6-582500] N90-13610
CARBON MONOXIDE
MOBILE4 oxygenated fuels version user's guide [PB89-230700] N90-13674
CARBURIZING
Internal and external nitriding and nitrocarburizing of iron and iron-based alloys [ETN-90-96012] N90-13646
CARRIER DENSITY (SOLID STATE)
Modeling and measurement methods for high speed bipolar transistors [REPT-11] N90-13714
CARRIER FREQUENCIES
Processing of undifferences GPS carrier beat phase measurements and adjustment computations [TR-5-1988] N90-13368
CARTRIDGES
Evaluation of selected computer models for modeling pyrotechnic and propellant devices [AD-A213003] N90-13671
CASSEGRAIN OPTICS
An approach to optical structures control N90-13456
CAST ALLOYS
Constitutive modeling for isotropic materials (HOST) [NASA-CR-179522] N90-13390
Constitutive modeling for isotropic materials (HOST) [NASA-CR-174718] N90-13391
CASTINGS
A theory of damage in brittle and cementitious materials, part 1 [AD-A212940] N90-13658
CATALYSIS
On catalytic recombination rates in hypersonic stagnation heat transfer N90-13338
CATHODES
Gas evolution and bubble formation on electrodes [DLR-FB-89-35] N90-13629
CAVITATION FLOW
Elasticity effects on cavitation in a squeeze film damper undergoing noncentered circular whirl [NASA-TM-102392] N90-13786
CELESTIAL NAVIGATION
Study of modern instrumentation and methods for astronomic positioning in the field [AD-A213217] N90-14157
CELL MEMBRANES (BIOLOGY)
Gravitropism in plants: Hydraulics and wall growth properties of responding cells N90-13950
CELLS (BIOLOGY)
Generation of free radicals during cold injury and rewarming [AD-A213088] N90-13915
Life science research in space [ESA-SP-1105] N90-13917
Cells in Space [NASA-CP-10034] N90-13939
Fundamental results from microgravity cell experiments with possible commericial applications N90-13940
The pituitary growth hormone cell in space N90-13941
Polarity establishment, morphogenesis, and cultured plant cells in space N90-13943
Physical phenomena and the microgravity response N90-13945
How to detect when cells in space perceive gravity N90-13946
Do the design concepts used for the space flight hardware directly affect cell structure and/or cell function ground based simulations N90-13953
CEMENTS
Fiber reinforced cementitious composites technology [PB89-227813] N90-13608
CENTRAL PROCESSING UNITS
Definition of avionics concepts for a heavy lift cargo vehicle, appendix A [NASA-CR-183817] N90-13380
The role of the host in a cooperating mainframe and workstation environment, volumes 1 and 2 [NASA-CR-185463-VOL-1/2] N90-13496
The computational structural mechanics testbed user's manual [NASA-TM-100644] N90-13818
CENTRIFUGAL PUMPS
A three-dimensional potential flow analysis of dynamic fluid forces acting on a whirling centrifugal impeller bounded by a volute N90-13717
CENTROIDS
A laboratory verification sensor N90-13477
CERAMIC COATINGS
Implementation and analysis of adhesion in multimaterials of the type Al(Si)-ZrO2 and graphite, metal or ceramics [ECL-89-004] N90-13667
CERAMIC MATRIX COMPOSITES
Toughening of a particulate-reinforced/ceramic-matrix composite [AD-A213180] N90-13604
CERAMICS
Development of an advanced fan blade containment system [DOT/FAA/CT-89/20] N90-13386
Thermal barrier coatings for gas turbine and diesel engines [NASA-TM-102408] N90-13636
Activities report of the metallic manufacturing industry [ISSN-0524-7705] N90-13649
Synthesis of inorganic polymers as glass precursors and for other uses. Preceramic block or graft copolymers as potential precursors to nanocomposite materials [AD-A211978] N90-13655
Toughening mechanisms in ceramic composites [PB89-235907] N90-13656
Surfaces and interfaces of ceramic materials [AD-A212417] N90-13657
MM and T for VHSIC multichip packages [AD-A213259] N90-13703
Sol-gel processing science using a Sol-Gel Optics Research Facility (SGORF) [AD-A213056] N90-14095
Preparation of 110K (Bi, Pb)-Sr-Ca-Cu-O superconductor from glass precursor [NASA-CR-185162] N90-14108
Advanced Turbine Technology Applications Project (ATTAP) [NASA-CR-185109] N90-14153
NRL (Naval Research Laboratory) Review [AD-A212886] N90-14182
CEREBRAL CORTEX
Role of retinocortical processing in spatial vision [AD-A210995] N90-13918
CESIUM PLASMA
True asymptotic plasma-sheath matching with an asymptotically correct collisional presheath [AD-A212857] N90-14104
CHARACTERIZATION
Characterization of surfaces cut with a laser beam and thermal model of the process [ISAL-89-0008] N90-13780
CHARGE COUPLED DEVICES
Efficient detection of small moving objects [AD-A213314] N90-13690
CHARGE EXCHANGE
The effective (3)He-nucleon force in a microscopic DWBA approach to the (3)He,t charge exchange reaction — Distorted Wave-Borne Approximation (DWBA) [KVI-763] N90-14077
CHARGE TRANSFER
Resonant-tunneling oscillators and multipliers for submillimeter receivers N90-13467
CHARPY IMPACT TEST
Mechanical property characterization of VascoMax T-300 [AD-A212950] N90-13637
CHECKOUT
Qualification of improved joint heaters [NASA-CR-183827] N90-13594
CHEMICAL BONDS
Computational solution of chemistry problems [NASA-CR-186000] N90-13618
CHEMICAL EFFECTS
The sensory transduction pathways in bacterial chemotaxis N90-13944
CHEMICAL LASERS
Generation of iodine monofluoride in a supersonic multipurpose flowtube facility [AD-A213082] N90-13774
CHEMICAL PROPERTIES
Surfaces and interfaces of ceramic materials [AD-A212417] N90-13657
CHEMICAL REACTIONS
Physical phenomena and the microgravity response N90-13945
CHEMICAL WARFARE
Recovery of particle size distribution of ultrafine aerosols from diffusional decay measurements [AD-A213006] N90-13621
CHINESE SPACE PROGRAM
Comparison of the space program performance of countries with space programs [ILR-MITT-222] N90-14150
CHIPS (ELECTRONICS)
Resistive fuses: Analog hardware for detecting discontinuities in early vision [AD-A211891] N90-13696
MM and T for VHSIC multichip packages [AD-A213259] N90-13703
CHIRAL DYNAMICS
Some comments on the solvable Chiral Potts model [PREPRINT-673] N90-14070
CHLOROPRENE RESINS
Evaluation of a neoprene latex modified SAMI (Stress Absorbing Membrane Interlayer) [PB89-226435] N90-13665
CHOLESKY FACTORIZATION
The great circle reductions N90-13553
CHROMOSPHERE
The winds of high luminosity late-type bright stars [NASA-CR-182961] N90-14160
CIRCUIT BREAKERS
Contribution to the study of a self-protected static switch and its command strategy [ECL-89-002] N90-13711
CIRCUIT DIAGRAMS
On the design of a computer-aided design system for digital circuits N90-13695
CIRCUITS
Test generation for highly sequential circuits [AD-A211932] N90-13698
CIRCULAR CYLINDERS
SSME LOX post flow analysis/fluid structure interaction. Volume 1: Flow analysis [NASA-CR-183677] N90-13715
CIRCULAR WAVEGUIDES
Electromagnetic wave propagation through circular waveguides containing radially inhomogeneous lossy media [AD-A213062] N90-13688
CIVIL AVIATION
Study of high-speed civil transports [NASA-CR-4235] N90-13370
CLASSICAL MECHANICS
On a new integrable Hamiltonian system with nearest neighbors interaction [PREPRINT-667] N90-14043

CLASSIFICATIONS
From scientific proposals to the Inca data base N90-13530
Gas identification system using graded temperature sensor and neural net interpretation [AD-A213359] N90-13627
CLEANING
Contamination removal using various solvents and methodologies [NASA-CR-183747] N90-13652
CLIMATE
An evaluation of the Smith-Feddes model [AD-A213237] N90-13907
CLIMATE CHANGE
Climate predictability: A dynamical view [AERONOMICA-ACTA-A-347-1989] N90-13909
CLIMATOLOGY
The interaction and variation of waves and turbulence from MST radar data [AD-A212649] N90-13906
Climate predictability: A dynamical view [AERONOMICA-ACTA-A-347-1989] N90-13909
CLOSED ECOLOGICAL SYSTEMS
Fermentation and oxygen transfer in microgravity N90-13956
CLOSURES
Application of two-point closures to subgrid scale modeling for homogeneous, 3D turbulence N90-13732
Spectral study of a compressible isotropic turbulence [ECL-88-16] N90-13753
Solution of the Boltzmann equation using an energy group method [AD-A213138] N90-14096
CLOTHING
On the wings of a dream: The Space Shuttle [NASA-EP-269] N90-13446
CLOUD PHYSICS
An evaluation of the Smith-Feddes model [AD-A213237] N90-13907
CLOUD SEEDING
Applied atmospheric resources research program in Thailand [PB89-235402] N90-13903
CLUTTER
Stochastic modelling of EM scattering from foliage [AD-A213118] N90-13689
CMOS
Resistive fuses: Analog hardware for detecting discontinuities in early vision [AD-A211891] N90-13696
COATINGS
Evaluation of a neoprene latex modified SAMI (Stress Absorbing Membrane Interlayer) [PB89-226435] N90-13665
Low resistivity electrodeless streamer tubes [PREPRINT-685-89] N90-13712
Novel in situ spectroscopic ellipsometer for real time analysis of CVD diamond films [AD-A213218] N90-13762
COCKPITS
Flight deck automation: Promises and realities [NASA-CP-10036] N90-13384
Conference Proceedings of the Human-Electronic Crew: Can They Work Together [AD-A211871] N90-13936
CODING
Review and evaluation of a turbomachinery throughflow finite element code [AD-A213058] N90-13787
A prototype microprocessor based audiometer for use by the CF (Canadian Forces) medical services for periodic hearing tests [AD-A212990] N90-13921
Implementation issues in source coding [NASA-CR-185327] N90-13963
Compression of bitmapped graphic data [AD-A213141] N90-13974
Surface cooled, vacuum impregnated superconducting magnet systems: Design, construction, applications [ETN-90-96014] N90-14072
COEFFICIENT OF FRICTION
The limiting friction force [ECL-89-005] N90-13801
COEFFICIENTS
Optimal processes described by a parabolic differential equation with control in the coefficients, part 4 [MEMO-785-PT-4] N90-14016
COGENERATION
Advanced energy system program [PB89-235170] N90-13887
COGNITION
A guide to reasoning under uncertainty [REPT-72/87/R486U] N90-13932
COHERENCE
Coherent structures in a round jet N90-13733
COLLISION AVOIDANCE
An update to the system safety study of TCAS 2 [DOT/FAA/SA-89/3] N90-13363
COLLISION PARAMETERS
Aspects of the physics of the standard model [PREPRINT-670] N90-14087
Model-independent analysis of the Z line shape in e+e- annihilation [PREPRINT-679] N90-14089
COLLISIONAL PLASMAS
True asymptotic plasma-sheath matching with an asymptotically correct collisional presheath [AD-A212857] N90-14104
COLOR
Functional decor in the International Space Station: Body orientation cues and picture perception [NASA-TM-102242] N90-13931
COLORADO
The interaction and variation of waves and turbulence from MST radar data [AD-A212849] N90-13906
COLUMBIA (ORBITER)
Syncom 4 deploy, LDEF retrieval highlight 10-day Columbia flight [NASA-NEWS-RELEASE-89-180] N90-13448
COLUMNS (PROCESS ENGINEERING)
Optimal processes described by a parabolic differential equation with control in the coefficients, part 4 [MEMO-785-PT-4] N90-14016
COMBAT
Electronic warfare: Reliable equipment needed to test Air Force's electronic warfare systems [AD-A212952] N90-13687
COMBINATIONS (MATHEMATICS)
On the asymptotic convergence of the simulated annealing algorithm in the presence of a parameter dependent penalization [MEMO-COSOR-89-16] N90-13984
COMBINATORIAL ANALYSIS
Constructing a calculus of programs [CWI-CS-R8914] N90-13979
On the performance of on-line algorithms for partition problems [MEMO-784] N90-14015
COMBUSTIBLE FLOW
A planar reacting shear layer system for the study of fluid dynamics-combustion interaction [NASA-TM-102422] N90-13393
COMBUSTION
Experimental and computational study of combustion limits in natural-gas fueled internal combustion engines [PB89-235196] N90-13673
Thermochemical calculations with inert compounds [FOA-C-20759-2.1] N90-13677
COMBUSTION CHEMISTRY
Transport phenomena and interfacial kinetics in multiphase combustion systems [AD-A212932] N90-13620
A theoretical model of double base propellant combustion [ONERA-RTF-23/7128-EY] N90-13672
COMBUSTION EFFICIENCY
Aircraft propulsion: Leading the way in aviation [LR-532] N90-13395
COMBUSTION PHYSICS
Facilities for microgravity combustion research [NASA-TM-102014] N90-13679
COMBUSTION PRODUCTS
Transport phenomena and interfacial kinetics in multiphase combustion systems [AD-A212932] N90-13620
The mobile combustion diagnostic fixture and its application to the study of propellant combustion. Part 1: Investigation of the low pressure combustion of LOVA XM39 propellant [AD-A213272] N90-13626
COMBUSTION STABILITY
LOX/hydrocarbon combustion instability investigation [NASA-CR-182249] N90-13589
COMBUSTION TEMPERATURE
A theoretical model of double base propellant combustion [ONERA-RTF-23/7128-EY] N90-13672
COMMAND AND CONTROL
Contribution to the study of a self-protected static switch and its command strategy [ECL-89-002] N90-13711
Applications of artificial intelligence to space station and automated software techniques: High level robot command language [NASA-CR-182997] N90-13991
COMMERCE
The economic impact of automation technology [AD-A213363] N90-13682
Small business innovation research: Program solicitation [NASA-TM-101869] N90-14126
Total quality management implementing plan: Office of small and disadvantaged business utilization [AD-A212865] N90-14129
COMMUNICATION NETWORKS
Data handling and telecommunications N90-13514
COMPILERS
The Inca data base N90-13531
The compilation of astrometric data N90-13537
COMPONENT RELIABILITY
Electrical testing N90-13520
Mechanical and thermal testing N90-13521
Sufficiency and necessity in reliability modeling [NASA-CR-186119] N90-13706
Advanced Turbine Technology Applications Project (ATTAP) [NASA-CR-185109] N90-14153
COMPOSITE MATERIALS
Nondestructive analysis of aileron fatigue and aging in a Mirage F1 [REPT-M6-594000] N90-13378
The application of cast SiC/Al to rotary engine components [NASA-CR-179610] N90-13385
Advanced composite materials for precision segmented reflectors N90-13461
The Materials Division: A case study [NASA-TM-102380] N90-13597
Failure processes in unidirectional composite materials N90-13598
Fatigue behavior of silicon carbide Whisker/Aluminum composite [AD-A213094] N90-13603
The adhesive bonding of thermoplastic composites [AD-A213358] N90-13605
Repair of composites by means of wet-lay-up [LR-551] N90-13617
Wear-resistant coated object [EP-PATENT-0-289-173-A1] N90-13643
Toughening mechanisms in ceramic composites [PB89-235907] N90-13656
Model filled polymers I. Synthesis of crosslinked monodisperse polystyrene beads [AD-A213228] N90-13660
NRL (Naval Research Laboratory) Review [AD-A212886] N90-14182
COMPOSITE STRUCTURES
Aeroelastic control of composite lifting surfaces: Integrated aeroelastic control optimization N90-13396
Composite panel development at JPL N90-13458
Status of Gr/glass composites technology at UTOS N90-13459
Large Deployable Reflector (LDR) thermal characteristics N90-13460
Lightweight composite reflector panels N90-13462
Low temperature optical testing of CFRP telescope panels N90-13463
Static and free-vibrational response of semi-circular graphite-epoxy frames with thin-walled open sections [NASA-CR-186097] N90-13600
COMPRESSIBILITY
Spectral study of a compressible isotropic turbulence [ECL-88-16] N90-13753
COMPRESSIBLE BOUNDARY LAYER
Generalized similarity solutions for three dimensional, laminar, steady, compressible boundary layer flows on swept profile cylinders [DLR-FB-89-34] N90-13725
COMPRESSIBLE FLOW
Inviscid 3D solution methods N90-13736
COMPRESSORS
Space station gas compressor technology study program, phase 1 [NASA-CR-183758] N90-13491
COMPUTATION
Thermochemical calculations with inert compounds [FOA-C-20759-2.1] N90-13677
Computation of nonequilibrium gas flow past blunt bodies [PREPRINT-488] N90-13757
Comparison of analytical methods for calculation of wind loads [NASA-TM-102782] N90-13813
On the recurrence relation for multivariate B-splines with respect to dimension [MEMO-786] N90-14017
The weighted sum of two S-units being a square [MEMO-792] N90-14031
Solving a specific Thue-Mahler equation [MEMO-793] N90-14032
Measurement of arithmetic error and calculation perturbations [IMAG-RR-767-M] N90-14039

Towards ab initio calculation of electron energies in semiconductors
[ETN-90-96016] N90-14121

COMPUTATIONAL FLUID DYNAMICS
Analysis of experimental data for CAST 10-2/DOA 2 supercritical airfoil at low Reynolds numbers and application to high Reynolds number flow
[AD-A211654] N90-13326
Correlation of Puma airloads: Lifting-line and wake calculation
[NASA-TM-102212] N90-13327
Computation of viscous incompressible flows
[NASA-TM-101090] N90-13329
Block-structured solution of three-dimensional transonic flows using parallel processing
[AD-A212851] N90-13330
Study of the integration of wind tunnel and computational methods for aerodynamic configurations
[NASA-TM-102196] N90-13332
A CFD study of tilt rotor flowfields
[NASA-CR-186116] N90-13349
Computation of Navier-Stokes equations for three-dimensional flow separation
[NASA-TM-102266] N90-13353
Recent progress in research pertaining to estimates of gas-side heat transfer in an aircraft gas turbine
[NASA-TM-102460] N90-13394
SSME LOX post flow analysis/fluid structure interaction. Volume 2: Fluid structure interaction
[NASA-CR-183678] N90-13716
A three-dimensional potential flow analysis of dynamic fluid forces acting on a whirling centrifugal impeller bounded by a volute N90-13717
Multigrid and defect correction for the steady Navier-Stokes equations: Applications to aerodynamics
[ETN-90-96011] N90-13727
Numerical simulation of transition in three-dimensional boundary layers
[DLR-FB-89-12] N90-13728
Turbulent Shear Flows
[VKI-LS-1989-03] N90-13730
Numerical Methods for Flows in Turbomachinery, volume 1
[VKI-LS-1989-06-VOL-1] N90-13735
Inviscid 3D solution methods N90-13736
Inviscid 2D solutions on unstructured, adaptive grids N90-13737
Flows with tip leakage N90-13740
Navier-Stokes simulation of the crossflow instability in swept-wing flows
[NASA-CR-186122] N90-13744

COMPUTATIONAL GRIDS
Multigrid calculations of 3-D turbulent viscous flows
[NASA-CR-185154] N90-13323
Application of a self-adaptive grid method to complex flows
[NASA-TM-102223] N90-13324
Great circle interactions: Attitude smoothing and grid-step inconsistencies N90-13554
The first-look data analysis at Utrecht N90-13571
Gas flows in rocket motors, volume 1
[AD-A213348] N90-13591
Effect of spatial resolution on apparent sensitivity to initial conditions of a decaying flow as it becomes turbulent
[NASA-TM-102377] N90-13719
Multigrid and defect correction for the steady Navier-Stokes equations: Applications to aerodynamics
[ETN-90-96011] N90-13727
Calculation of flow fields by the solution of the Euler equations using an extended finite volume discretization scheme
[DLR-FB-89-38] N90-13729
Application of two-point closures to subgrid scale modeling for homogeneous, 3D turbulence N90-13732
Application of multi-grid methods for solving the Navier-Stokes equations
[NASA-TM-102359] N90-14002

COMPUTER AIDED DESIGN
Efficient methods for integrated structural-aerodynamic wing optimum design N90-13376
Composite panel development at JPL N90-13458
On the design of a computer-aided design system for digital circuits N90-13695
Parameter estimation for the Gummel-Poon transistor model
[MA-53] N90-13705
Methodology for automating software systems. Task 1 of the foundations for automating software systems
[NASA-CR-180499] N90-13965
The cellular approach: A new method to speed up simulated annealing for macro placement
[MEMO-COSOR-88-29] N90-13980

COMPUTER AIDED MANUFACTURING
Computer-aided fabrication system implementation
[AD-A213005] N90-13969
The problem of automation: Inappropriate feedback and interaction, not overautomation
[NASA-CR-186126] N90-13994

COMPUTER AIDED MAPPING
The Hipparcos Mission. Prelaunch status. Volume 3: The data reductions
[ESA-SP-1111-VOL-3] N90-13548
The use of LANDSAT-TM data for the management of pine forestations in central Chile
[DLR-FB-89-44] N90-13881

COMPUTER GRAPHICS
Resistive fuses: Analog hardware for detecting discontinuities in early vision
[AD-A211891] N90-13696
Interface between MEDUSA and GIFTS for shell structures
[LR-553] N90-13985

COMPUTER NETWORKS
Computational and psychophysical study of human vision using neural networks
[AD-A213290] N90-13924
The structural memory: A network model for human perception of serial objects
[CWI-CS-R8829] N90-13930
Compression of bitmapped graphic data
[AD-A213141] N90-13974
Empirical analysis and refinement of expert system knowledge bases
[AD-A213240] N90-14143

COMPUTER PROGRAMMING
Computer-based tools for assisting air traffic controllers with arrivals flow management
[RSRE-88001] N90-13366
Apparatus for cooling electronic components in aircraft
[AD-D014207] N90-13373
SIMOGEN: An object-oriented language for simulation
[AD-A213129] N90-13973
Multi-level specification and verification of real-time software
[AD-A213227] N90-13975
Ada programming guidelines for deterministic storage management
[NASA-CR-181308] N90-13982
Extended memory library for AFOS (Automation of Field Operations and Services) applications
[PB89-230858] N90-14147

COMPUTER PROGRAMS
Application of a self-adaptive grid method to complex flows
[NASA-TM-102223] N90-13324
Geodetic network adjustment using GPS triple difference observations and a priori stochastic information
[TR-1-1987] N90-13367
Trajectory optimization and guidance for an aerospace plane
[NASA-CR-185884] N90-13369
Software and hardware description of the helicopter motion equations for VAX computers
[AD-A213248] N90-13375
Application of a two-dimensional unsteady viscous analysis code to a supersonic throughflow fan stage
[NASA-TM-4141] N90-13387
Simulation of spacecraft attitude dynamics using TREETOPS and model-specific computer Codes N90-13419
GOES-I/M ascent maneuvers from transfer orbit to station N90-13421
Shuttle relative navigation of a tethered satellite mission with current on board software N90-13423
Automation of orbit determination functions for National Aeronautics and Space Administration (NASA)-supported satellite missions N90-13434
Control of optical systems N90-13484
Validation of the Hipparcos catalog N90-13564
The Tycho input catalog N90-13575
Modelling of satellite control thruster plumes N90-13578
The economic impact of automation technology
[AD-A213363] N90-13682
An improved algorithm for the modeling of vapor flow in heat pipes
[NASA-CR-185179] N90-13748
Analysis of rotary engine combustion processes based on unsteady, three-dimensional computations
[NASA-TM-102469] N90-13749
A prototype microprocessor based audiometer for use by the CF (Canadian Forces) medical services for periodic hearing tests
[AD-A212990] N90-13921
Project ORION microcomputer management system
[AD-A212945] N90-13959
The development of a program analysis environment for Ada
[NASA-CR-185860] N90-13962
A fault-tolerant software algorithm for a network of transputers
[AD-A213092] N90-13972
Constructing a calculus of programs
[CWI-CS-R8914] N90-13979

COMPUTER SYSTEMS DESIGN
A knowledge-based system design/information tool for aircraft flight control systems
[NASA-TM-101704] N90-13990

COMPUTER SYSTEMS PERFORMANCE
Efficient methods for integrated structural-aerodynamic wing optimum design N90-13376
The role of the host in a cooperating mainframe and workstation environment, volumes 1 and 2
[NASA-CR-185483-VOL-1/2] N90-13496
Efficient on-line simulations of tree machines and multidimensional turing machines by random access machines
[AD-A213152] N90-13960
Parallelism in the discrete-event simulation algorithm
[AD-A213060] N90-13970
Monotonicity of performance measures in a processor sharing queue
[CWI-BS-R8902] N90-14019

COMPUTER SYSTEMS PROGRAMS
On-board software N90-13518
Great circle reductions: Implementation and simulations N90-13569
Implementation and simulations of the sphere solution in FAST N90-13570
Data simulations in the fast consortium N90-13573
Data simulations in the NDAC consortium N90-13574
On the design of a computer-aided design system for digital circuits N90-13695
The computational structural mechanics testbed user's manual
[NASA-TM-100644] N90-13818

COMPUTER TECHNIQUES
Recent progress in research pertaining to estimates of gas-side heat transfer in an aircraft gas turbine
[NASA-TM-102460] N90-13394
Space telescope pointing control N90-13454
An algorithm for control volume analysis of cryogenic systems
[AD-A213394] N90-13683
A prototype microprocessor based audiometer for use by the CF (Canadian Forces) medical services for periodic hearing tests
[AD-A212990] N90-13921
Methodology for automating software systems. Task 1 of the foundations for automating software systems
[NASA-CR-180499] N90-13965
Computer-aided fabrication system implementation
[AD-A213005] N90-13969
A fault-tolerant software algorithm for a network of transputers
[AD-A213092] N90-13972
The DOD Gateway Information System: Operational prototype and transition period 1987-1988
[AD-A213044] N90-14141
ERIS: Engineering Resource Information System
[AD-A213357] N90-14144

COMPUTER VISION
Resistive fuses: Analog hardware for detecting discontinuities in early vision
[AD-A211891] N90-13696
Image segmentation for the stereoscopic vision of a mobile robot
[ONERA-RT-1/3692-SY] N90-13800
An editor for 3D-models for image analysis
[FOA-C-30534-3.4] N90-13986

COMPUTERIZED SIMULATION
The S.D.G., P.S.D. and the nonlinear airplane
[NLR-MP-88018-U] N90-13371
STOVL aircraft simulation for integrated flight and propulsion control research
[NASA-TM-102419] N90-13389
Mathematical model identification for flight simulation, based on flight and taxi tests
[LR-550] N90-13410
Explicit modeling and concurrent processing in the simulation of multibody dynamic systems N90-13481
Control of optical systems N90-13484
PACOSS program N90-13487
Mission simulations N90-13532
The Hippercos Mission. Prelaunch status. Volume 3: The data reductions
[ESA-SP-1111-VOL-3] N90-13548
General and numerical approach to the sphere solution in FAST N90-13555
Photometry: Main mission and Tycho N90-13560
Great circle reductions: Implementation and simulations N90-13569
Implementation and simulations of the sphere solution in FAST N90-13570
Modeling of the Hipparcos optical system N90-13572

Data simulations in the fast consortium N90-13573
Data simulations in the NDAC consortium N90-13574
Experiments towards a global sphere solution N90-13576
Evaluation of selected computer models for modeling pyrotechnic and propellant devices [AD-A213003] N90-13671
Sufficiency and necessity in reliability modeling [NASA-CR-186119] N90-13706
A review of quasi-coherent structures in a numerically simulated turbulent boundary layer [NASA-TM-102191] N90-13723
Navier-Stokes simulation of the crossflow instability in swept-wing flows [NASA-CR-186122] N90-13744
Large eddy simulation of homogeneous turbulence undergoing shear and thermal gradients. Application to one point closing models [ECL-88-23] N90-13754
A stochastic model for the calculation of multiple scattered lidar returns [DLR-FB-89-36] N90-13778
The effects of gravity waves on horizontal layers: Simulation and interpretation N90-13852
Methodology for automating software systems. Task 1 of the foundations for automating software systems [NASA-CR-180499] N90-13965
The APROS software for process simulation and model development [VTT-618] N90-13987
Modeling of power electronic systems with EMTP [NASA-TM-102375] N90-14060
Analytical and computer-aided models of InP-based MISFETs and heterojunction devices [AD-A211861] N90-14106

CONCATENATED CODES
Error control techniques for satellite and space communications [NASA-CR-182751] N90-13685

CONCRETES
Fiber reinforced cementitious composites technology [PB89-227813] N90-13608

CONDENSING
Preparation of binary ice layers by condensation from gas phase [JUEL-2248] N90-13631
Buoyancy effects on the vapor condensation rate on a horizontal liquid surface [NASA-TM-102437] N90-13675
Vapor condensation on liquid surface due to laminar jet-induced mixing: The effects of system parameters [NASA-TM-102433] N90-13751

CONDUCTING POLYMERS
Optical modulators based on polymers [EP-PATENT-0-294-061-A1] N90-14099

CONDUCTORS
Magneto-elastic interactions in conducting structures in transient magnetic fields N90-13686

CONFERENCES
Flight deck automation: Promises and realities [NASA-CP-10036] N90-13384
Flight Mechanics/Estimation Theory Symposium, 1989 [NASA-CP-3050] N90-13413
Introduction to the report of the Asilomar 3 LDR workshop N90-13450
Space Station Engineering Design Issues [NASA-CR-185978] N90-13492
The Fourth Oxford International Conference on the Mechanical Properties of Materials at High Rates of Strain [AD-A212293] N90-13809
European Rocket and Balloon Programs and Related Research [ESA-SP-291] N90-13826
Proceedings: US/FRG (Federal Republic of Germany) Workshop on Photochemical Ozone Problem and Its Control: US Experiences and the Situation in Europe [PB89-233514] N90-13891
ULF/VLF (0.001 to 50 Hz) Seismo-Acoustic Noise in the Ocean [AD-A212942] N90-13913
Cells in Space [NASA-CP-10034] N90-13939

CONFIGURATION MANAGEMENT
A figure control sensor for the Large Deployable Reflector (LDR) N90-13451
Expert systems for adaptive control of large space structures N90-13452
Wavefront error sensing for LDR N90-13455
Segment alignment control system N90-13457

CONGRESSIONAL REPORTS
National Aeronautics and Space Administration Multiyear Authorization Act of 1989 N90-14148
National Aeronautics and Space Administration authorization [S-HRG-101-348] N90-14149

CONJUGATES
Conjugate profiles on mating gear teeth [MEMO-COSOR-89-01] N90-13795

CONSERVATION EQUATIONS
Gas flows in rocket motors, volume 1 [AD-A213348] N90-13591

CONSERVATION LAWS
Balance laws and centro velocity in dissipative systems [MEMO-797] N90-13726

CONSTITUTIVE EQUATIONS
Constitutive modeling for isotropic materials (HOST) [NASA-CR-179522] N90-13390
Constitutive modeling for isotropic materials (HOST) [NASA-CR-174718] N90-13391

CONSTRAINTS
Stopping rules for a class of random methods for detecting necessary linear inequality constraints [MEMO-777] N90-13977
The regular indefinite linear quadratic problem with linear endpoint constraints [MEMO-COSOR-88-15] N90-14022

CONSUMABLES (SPACECREW SUPPLIES)
On the wings of a dream: The Space Shuttle [NASA-EP-269] N90-13446

CONTAINERLESS MELTS
Nucleation kinetics in undercooled, glass-forming metallic melts [DLR-FB-89-32] N90-13644
Containerless Processing of Metals: Undercooling and Solidification [DLR-MITT-89-15] N90-13645

CONTAINMENT
Development of an advanced fan blade containment system [DOT/FAA/CT-89/20] N90-13386

CONTAMINANTS
Contamination removal using various solvents and methodologies [NASA-CR-183747] N90-13652

CONTAMINATION
Effects of tacky mat contamination on bond degradation for Chemlok/liner and NBR/liner bonds [NASA-CR-183742] N90-13653
Use of a krypton isotope for rapid ion changeover at the Lawrence Berkeley Laboratory 88-inch cyclotron [NASA-CR-186107] N90-14084
Optical properties monitor: Experiment definition phase [NASA-CR-183836] N90-14092

CONTINUITY (MATHEMATICS)
Continuity properties of one-parameter families of linear-quadratic problems without stability [MEMO-COSOR-88-17] N90-14024

CONTINUUMS
Global optimization and simulated annealing [MEMO-COSOR-88-21] N90-14025

CONTOURS
A two-dimensional adaptive-wall test section with ventilated walls in the Ames 2- by 2-foot transonic wind tunnel [NASA-TM-102207] N90-13407

CONTRACT INCENTIVES
Small business innovation research: Program solicitation [NASA-TM-101869] N90-14126

CONTRACT MANAGEMENT
Total quality management: Directorate of Contract Management master plan [AD-A212867] N90-14131

CONTROL
An algorithm for control volume analysis of cryogenic systems [AD-A213394] N90-13683

CONTROL MOMENT GYROSCOPES
Periodic-disturbance accommodating control of the space station for asymptotic momentum management N90-13416

CONTROL SIMULATION
Computer-based tools for assisting air traffic controllers with arrivals flow management [RSRE-88001] N90-13366
Simulation of spacecraft attitude dynamics using TREETOPS and model-specific computer Codes N90-13419

CONTROL STABILITY
On the application of modified stepwise regression for the estimation of aircraft stability and control parameters [REPT-8905] N90-13400

CONTROL SYSTEMS DESIGN
Discretization and model reduction for a class of nonlinear systems N90-13397
An autopilot design methodology for bank-to-turn missiles [AD-A213379] N90-13399
Report of the Asilomar 3 LDR Workshop [NASA-CR-184656] N90-13449
A figure control sensor for the Large Deployable Reflector (LDR) N90-13451
Space telescope pointing control N90-13454
Wavefront error sensing for LDR N90-13455
An approach to optical structures control N90-13456
Segment alignment control system N90-13457
LDR structural technology activities at JPL N90-13488
A practical approach for minimum time control of the Spacecraft Control Laboratory Experiment (SCOLE), appendix A [NASA-CR-186008] N90-13495
Attitude and shape control of optimally designed large space structures N90-13579
Adaptive strategies for controls of flexible arms [NASA-CR-185868] N90-13783
Arc current control of a robotic welding system: Modeling and control system design [AD-A213150] N90-13788
A knowledge-based system design/information tool for aircraft flight control systems [NASA-TM-101704] N90-13990
Laboratory test methodology for evaluating the effects of electromagnetic disturbances on fault-tolerant control systems [NASA-TM-101685] N90-14061

CONTROL THEORY
An autopilot design methodology for bank-to-turn missiles [AD-A213379] N90-13399
The dynamics and control of large flexible space structures - 12, supplement 11 [NASA-CR-185966] N90-13494
Attitude and shape control of optimally designed large space structures N90-13579
A new approach to control single-link flexible arms. Part 3: Adaptive control of the tip position with payload changes [AD-A213337] N90-13792
On control of manipulators [ISBN-90-9002789-0] N90-13804
Compensatory tracking in disturbance tasks and target following tasks. The influence of cockpit motion on performance and control behavior [LR-511] N90-13933
The cellular approach: A new method to speed up simulated annealing for macro placement [MEMO-COSOR-88-29] N90-13980
Model reduction of weakly damped mechanical systems [MEMO-798] N90-13993
A priori results in linear quadratic optimal control theory [MEMO-COSOR-89-02] N90-13996
The quadratic matrix inequality in singular H infinity control with state feedback [MEMO-COSOR-89-03] N90-13997
The singular zero sum differential game with stability using H infinity control theory [MEMO-COSOR-89-09] N90-13999
The singular H infinity control problem with dynamic measurement feedback [MEMO-COSOR-89-14] N90-14000
The output-stabilizable subspace and linear optimal control [MEMO-COSOR-89-15] N90-14001

CONTROLLABILITY
Preliminary airworthiness evaluation of the AH-64A equipped with the Air To Air Stinger (ATAS) missile system [AD-A213030] N90-13374
Electron beam sensitive devices for controllability [IMAG-RR-761-I] N90-13707

CONTROLLED ATMOSPHERES
Effects of tacky mat contamination on bond degradation for Chemlok/liner and NBR/liner bonds [NASA-CR-183742] N90-13653

CONTROLLERS
Control of optical systems N90-13484
Research on the controllability of integrated circuits by means of electron beams [ETN-90-95710] N90-13708
Design and control of a two-degree-of-freedom lightweight flexible arm [AD-A213335] N90-13790

CONVECTIVE FLOW
Large eddy simulation of homogeneous turbulence undergoing shear and thermal gradients. Application to one point closing models [ECL-88-23] N90-13754

CONVECTIVE HEAT TRANSFER
Convective heat transfer measurements from a NACA 0012 airfoil in flight and in the NASA Lewis Icing Research Tunnel
[NASA-TM-102448] N90-13750
CONVERGENCE
Extended Kalman filter for attitude estimation of the earth radiation budget satellite N90-13433
On the asymptotic convergence of the simulated annealing algorithm in the presence of a parameter dependent penalization
[MEMO-COSOR-89-16] N90-13984
Convergence properties of indefinite linear quadratic problems with receding horizon
[MEMO-COSOR-88-25] N90-14026
CONVEXITY
Description and manipulation of convex polygons using polarity
[IMAG-RR-771-M] N90-14041
CONVOLUTION INTEGRALS
Estimation of convolution tail behavior
[MEMO-COSOR-89-04] N90-14051
COOLING
Cryogenics for LDR N90-13471
Effect of suction and cooling on the stability of subsonic and supersonic boundary layers N90-13745
Generation of free radicals during cold injury and rewarming
[AD-A213088] N90-13915
COOLING SYSTEMS
LDR cryogenics N90-13472
COORDINATES
Conjugate profiles on mating gear teeth
[MEMO-COSOR-89-01] N90-13795
COORDINATION
The interface with the data reduction consortia N90-13528
COPOLYMERIZATION
Model filled polymers I. Synthesis of crosslinked monodisperse polystyrene beads
[AD-A213228] N90-13660
COPOLYMERS
Studies of Aflas fluoroelastomers
[AD-A213046] N90-13622
Synthesis of inorganic polymers as glass precursors and for other uses. Preceramic block or graft copolymers as potential precursors to nanocomposite materials
[AD-A211978] N90-13655
Process for producing a shaped, extruded product from a crosslinkable polymeric composition
[GB-PATENT-2-201-677-A] N90-13662
Crosslinkable polymer
[GB-PATENT-2-205-846-A] N90-13663
COPPER
Investigations of spontaneous nuclear order in copper by neutron diffraction
[ETN-90-96060] N90-14090
COPPER ALLOYS
Quench sensitivity in Al-Cu-Li alloys
[AD-A213055] N90-13639
COPPER OXIDES
Local pairing and antiferromagnetism in high-T sub c superconductors
[AD-A213004] N90-14113
CORNER FLOW
Observation of wind corners in the middle atmosphere over Andenes (69 N) during winter 1983/84, summer 1987 and summer 1988 N90-13836
CORONAL HOLES
Shear-induced inflation of coronal magnetic fields
[NASA-CR-186103] N90-14178
CORRECTION
Pressure correction calculation procedures for 3D viscous flow N90-13738
CORRELATION
On the effects of an uncertainty on evolution law in dynamical systems
[PREPRINT-689] N90-14047
CORROSION
NDI (Nondestructive Inspection) oriented corrosion control for Army aircraft. Phase 1: Inspection methods
[AD-A213368] N90-13359
Contribution to the electrochemical study of corrosion in the low conductivity media: Application to the study of the behavior of austenitic stainless steels in concentrated solutions of acetic acid
[ISAL-89-0014] N90-13648
CORROSION PREVENTION
NDI (Nondestructive Inspection) oriented corrosion control for Army aircraft. Phase 1: Inspection methods
[AD-A213368] N90-13359
CORROSION TESTS
NDI (Nondestructive Inspection) oriented corrosion control for Army aircraft. Phase 1: Inspection methods
[AD-A213368] N90-13359
Contribution to the electrochemical study of corrosion in the low conductivity media: Application to the study of the behavior of austenitic stainless steels in concentrated solutions of acetic acid
[ISAL-89-0014] N90-13648
COSMIC BACKGROUND EXPLORER SATELLITE
COBE nonspinning attitude propagation N90-13418
COSMIC RAY SHOWERS
The determinatin of the muon content of EAS from Cygnus X-3 N90-14179
COSMOLOGY
Observational physics of mirror world
[NASA-CR-185923] N90-14076
On thick domain walls in general relativity
[NASA-CR-185926] N90-14124
Des Cloizeaux's law for strings and galaxies formation. Part 1: Abelian configurations
[ROM1F-89-681-PT-1] N90-14172
Des Cloizeaux's law for strings and galaxies formation. Part 2: Non Abelian configurations
[ROM1F-89-682-PT-2] N90-14173
COSMOS SATELLITES
Re-entry hazards and cosmos 1900
[FOA-C-30535-9.4] N90-13583
COST ANALYSIS
The Explorer program for astronomy and astrophysics N90-14159
COST EFFECTIVENESS
Repair of composites by means of wet-lay-up
[LR-551] N90-13617
COST REDUCTION
Evaluation of copper slag blast media for railcar maintenance
[NASA-CR-183744] N90-13681
COSTS
Convergence properties of indefinite linear quadratic problems with receding horizon
[MEMO-COSOR-88-25] N90-14026
COULOMB COLLISIONS
True asymptotic plasma-sheath matching with an asymptotically correct collisional presheath
[AD-A212857] N90-14104
COUNTER ROTATION
Effect of reduced aft diameter and increased blade number on high-speed counterrotation propeller performance
[NASA-TM-102077] N90-13352
COUNTERMEASURES
Countermeasures to microgravity N90-13957
COUNTERS
A counter gating circuit for acoustic emission monitoring of structures cracking under repetitive alternating loads
[ARL-MAT-TM-398] N90-13808
COVARIANCE
True covariance simulation of the EUVE update filter N90-13427
Bilinear modeling and nonlinear estimation N90-13430
CRACK ARREST
Experimental and numerical investigations of the crack arrest behavior of steels and cast iron materials
[MPA-TWB-88-03] N90-13635
CRACK CLOSURE
Threshold for fatigue crack propagation
[DLR-FB-89-33] N90-13815
CRACK PROPAGATION
Fatigue behavior of silicon carbide Whisker/Aluminum composite
[AD-A213094] N90-13603
The adhesive bonding of thermoplastic composites
[AD-A213358] N90-13605
Some aspects of test frequency influence on the fatigue behavior of ARALL
[LR-549] N90-13616
Threshold for fatigue crack propagation
[DLR-FB-89-33] N90-13815
Application of fracture mechanics and half-cycle method to the prediction of fatigue life of B-52 aircraft pylon components
[NASA-TM-88277] N90-13820
An evaluation of a fatigue crack growth prediction model for variable-amplitude loading (PREFFAS)
[LR-537] N90-13822
CRACKING (FRACTURING)
Stress intensity factors for cracking metal structures under rapid thermal loading. Volume 2: Theoretical background
[AD-A213297] N90-13812
CRACKS
Stress intensity factors for cracking metal structures under rapid thermal loading. Volume 2: Theoretical background
[AD-A213297] N90-13812
CREWS
Conference Proceedings of the Human-Electronic Crew: Can They Work Together
[AD-A211871] N90-13936
CRITICAL PATH METHOD
Project ORION microcomputer management system
[AD-A212945] N90-13959
CROSS FLOW
Unsteady forces induced on finite-span cylinders in a cross-flow N90-13746
CROSSLINKING
Model filled polymers I. Synthesis of crosslinked monodisperse polystyrene beads
[AD-A213228] N90-13660
Process for producing a shaped, extruded product from a crosslinkable polymeric composition
[GB-PATENT-2-201-677-A] N90-13662
Crosslinkable polymer
[GB-PATENT-2-205-846-A] N90-13663
CRUSTAL FRACTURES
Supplementing geodetic data with prior information for crustal deformation in the Imperial Valley, California
[TR-6-1988] N90-13904
CRYOGENIC EQUIPMENT
Cryogenic systems for the large deployable reflector N90-13470
Cryogenics for LDR N90-13471
LDR cryogenics N90-13472
CRYOGENIC FLUIDS
Tank pressure control experiment on the space shuttle
[NASA-TM-102313] N90-13590
CRYOGENIC ROCKET PROPELLANTS
Thermal protection systems for reentry and hypersonic flight
[DLR-MITT-89-14] N90-13577
CRYOGENICS
An algorithm for control volume analysis of cryogenic systems
[AD-A213394] N90-13683
CRYOSTATS
Construction of the rotating cryostat ROTA2, its use for zero sound experiments in (3)He-B, and calculations of ion mobility in (3)He-A and (3)He-P
[ISBN-952-90091-3-5] N90-13765
CRYSTAL DISLOCATIONS
Field-effect spectroscopy of interface states
[AD-A212998] N90-14112
CRYSTAL GROWTH
Flight software development for the isothermal dendritic growth experiment
[NASA-TM-102412] N90-13988
CRYSTAL LATTICES
Energy concentration induced by phase transitions in hydrogenated metals
[PREPRINT-672] N90-13650
CRYSTAL STRUCTURE
Studies of structure and switching dynamics in ferroelectric crystal and liquid crystal thin films
[AD-A212650] N90-14109
CRYSTALLIZATION
A new model for the structure of silica glass
[AD-A212972] N90-13659
CRYSTALS
A prototype microprocessor based audiometer for use by the CF (Canadian Forces) medical services for periodic hearing tests
[AD-A212990] N90-13921
CUES
Functional decor in the International Space Station: Body orientation cues and picture perception
[NASA-TM-102242] N90-13931
CULTURE TECHNIQUES
Response of lymphocytes to a mitogenic stimulus during spaceflight N90-13942
Polarity establishment, morphogenesis, and cultured plant cells in space N90-13943
CUMULATIVE DAMAGE
Failure processes in unidirectional composite materials N90-13598
Study of fatigue degradation mechanisms in unidirectional composite materials. Application to cumulative damage
[ECL-88-12] N90-13611
CURRENT DISTRIBUTION
Characteristic impedance of microstrip lines
[NASA-TM-101581] N90-13694
Some remarks on the working principle of the rocketborne nose tip dc probes in the D-region of the ionosphere N90-13839
CURRENT REGULATORS
Research on the controllability of integrated circuits by means of electron beams
[ETN-90-95710] N90-13708

Arc current control of a robotic welding system: Modeling and control system design
[AD-A213150] N90-13788

CURVATURE
Some aspects of curvature in general relativity N90-14122

CURVES (GEOMETRY)
Parabolic equations for curves on surfaces. 2: Intersections, blow up and generalized solutions
[AD-A212890] N90-14004
On distance-transitive graphs and involutions
[CWI-PM-R8808] N90-14037

CYCLES
Hamiltonian properties of graphs with large neighborhood unions
[MEMO-779] N90-14013

CYCLOTRON FREQUENCY
Observations of electrostatic hydrogen cyclotron waves and electric field fluctuations near one Hz in auroral acceleration regions N90-13842

CYCLOTRON RESONANCE DEVICES
Use of a krypton isotope for rapid ion changeover at the Lawrence Berkeley Laboratory 88-inch cyclotron
[NASA-CR-186107] N90-14084

CYGNUS CONSTELLATION
The determinatin of the muon content of EAS from Cygnus X-3 N90-14179

CYLINDRICAL SHELLS
Unsteady forces induced on finite-span cylinders in a cross-flow N90-13746
The initial imperfection data bank at the Delft University of Technology, part 2
[LR-559-PT-2] N90-13825

CYTOLOGY
Fundamental results from microgravity cell experiments with possible commericial applications N90-13940
Physical phenomena and the microgravity response N90-13945

D

D REGION
Some remarks on the working principle of the rocketborne nose tip dc probes in the D-region of the ionosphere N90-13839

DAMAGE
A theory of damage in brittle and cementitious materials, part 1
[AD-A212940] N90-13658

DAMAGE ASSESSMENT
Study of the engine bird ingestion experience of the Boeing 737 aircraft
[DOT/FAA/CT-89/16] N90-13360
Debris/ice/TPS assessment and photographic analysis for Shuttle Mission STS-34
[NASA-TM-102153] N90-13447
Impact tests of three composite materials with carbon fiber cores
[REPT-M6-582500] N90-13610
Study of fatigue degradation mechanisms in unidirectional composite materials. Application to cumulative damage
[ECL-88-12] N90-13611
Contribution to the fatigue behavior study of composite materials reinforced with unidirectional glass fibers
[ECL-88-20] N90-13612
Mean stress and the exhaustion of fatigue-damage resistance
[NASA-TM-101311] N90-13619

DAMPERS (VALVES)
Elasticity effects on cavitation in a squeeze film damper undergoing noncentered circular whirl
[NASA-TM-102392] N90-13786

DARK MATTER
An experiment to search for galactic axions N90-14158
Unitarity limits on the mass and radius of dark matter particles
[NASA-CR-186079] N90-14164
Cosmology and the weak interaction
[NASA-CR-186170] N90-14169

DATA ACQUISITION
Measurement Techniques in Aerodynamics
[VKI-LS-1989-05] N90-13339
Data acquisition in aerodynamic research N90-13340
Pressure measurement techniques in use at the Royal Aerospace Establishment N90-13347
Control of optical systems N90-13484
Successive iterations of the input catalog N90-13534
The SIMBAD data base N90-13547
Overview of the data acquisition and reductions N90-13549
Analysis of the image disector tube data N90-13550
Analysis of the star mapper data N90-13551
High precision rocket attitude reconstruction using star sensor and magnetometer data N90-13844
Normal points: Compression of satellite laser ranging data
[ETN-90-96008] N90-14145

DATA BASE MANAGEMENT SYSTEMS
The Inca data base N90-13531
Retrieving and integrating IC fabrication data from dissimilar databases
[AD-A211890] N90-14140

DATA BASES
The Hipparcos Mission. Prelaunch status. Volume 2: The input catalog
[ESA-SP-1111-VOL-2] N90-13529
From scientific proposals to the Inca data base N90-13530
The Inca data base N90-13531
Stellar content of the input catalog N90-13535
Variable stars N90-13541
The catalogs produced by the Inca consortium N90-13546
The SIMBAD data base N90-13547
The Hipparcos Mission. Prelaunch status. Volume 3: The data reductions
[ESA-SP-1111-VOL-3] N90-13548
Overview of the Tycho data analysis N90-13558
Tycho astrometry N90-13559
Photometry: Main mission and Tycho N90-13560
Validation of the Hipparcos catalog N90-13564
Implementation and simulations of the sphere solution in FAST N90-13570
The Tycho input catalog N90-13575
The initial imperfection data bank at the Delft University of Technology, part 2
[LR-559-PT-2] N90-13825
Database interfaces on NASA's heterogeneous distributed database system
[NASA-CR-185420] N90-14133
Retrieving and integrating IC fabrication data from dissimilar databases
[AD-A211890] N90-14140
The DOD Gateway Information System: Operational prototype and transition period 1987-1988
[AD-A213044] N90-14141
Architecture and language for a layered relational database N90-14146

DATA COMPRESSION
Overview of the data acquisition and reductions N90-13549
Compression of bitmapped graphic data
[AD-A213141] N90-13974
Normal points: Compression of satellite laser ranging data
[ETN-90-96008] N90-14145

DATA FLOW ANALYSIS
Normal points: Compression of satellite laser ranging data
[ETN-90-96008] N90-14145

DATA LINKS
The role of the ground segment N90-13527
The link to extragalactic objects N90-13544
Linking Hipparcos to a quasi-inertial system N90-13565

DATA MANAGEMENT
The catalogs produced by the Inca consortium N90-13546
Double star reductions in FAST N90-13562
Data processing in the FAST consortium N90-13567
Data processing in the NDAC consortium N90-13568
Implementation and simulations of the sphere solution in FAST N90-13570
The first-look data analysis at Utrecht N90-13571
Data simulations in the fast consortium N90-13573
Data simulations in the NDAC consortium N90-13574

DATA PROCESSING
Data acquisition in aerodynamic research N90-13340
Optimum data weighting and error calibration for estimation of gravitational parameters N90-13437
The in-orbit initialization phase N90-13525
Proximity effects on adjacent and multiple stars N90-13533
Successive iterations of the input catalog N90-13534
The compilation of astrometric data N90-13537
The choice of stars in the Magellanic clouds N90-13543
On-ground attitude determination N90-13552
Data processing in the FAST consortium N90-13567
Data processing in the NDAC consortium N90-13568
Data simulations in the fast consortium N90-13573
Data simulations in the NDAC consortium N90-13574
Application of an optimal filter for inflatable sphere data processing N90-13849
Micro-based fact collection tool user's manual
[NASA-CR-180414] N90-13981
Ada programming guidelines for deterministic storage management
[NASA-CR-181308] N90-13982

DATA PROCESSING EQUIPMENT
SN 1987: A telemetry decoding system N90-13875

DATA REDUCTION
The interface with the data reduction consortia N90-13526
The Hipparcos Mission. Prelaunch status. Volume 2: The input catalog
[ESA-SP-1111-VOL-2] N90-13529
New ground-based photometric measurements N90-13538
Double stars N90-13540
The Hipparcos Mission. Prelaunch status. Volume 3: The data reductions
[ESA-SP-1111-VOL-3] N90-13548
Overview of the data acquisition and reductions N90-13549
The great circle reductions N90-13553
Great circle interactions: Attitude smoothing and grid-step inconsistencies N90-13554
General and numerical approach to the sphere solution in FAST N90-13555
Astrometric parameter determination in FAST N90-13556
The sphere solution and astrometric parameter determination in NDAC N90-13557
Overview of the Tycho data analysis N90-13558
Tycho astrometry N90-13559
Photometry: Main mission and Tycho N90-13560
Double star reductions in NDAC N90-13561
Double star reductions in FAST N90-13562
The treatment of minor planets and planetary satellites N90-13563
Linking Hipparcos to a quasi-inertial system N90-13565
Data processing in the FAST consortium N90-13567
Data processing in the NDAC consortium N90-13568
Great circle reductions: Implementation and simulations N90-13569
The first-look data analysis at Utrecht N90-13571
The Tycho input catalog N90-13575
Micro-based fact collection tool user's manual
[NASA-CR-180414] N90-13981
Ada programming guidelines for deterministic storage management
[NASA-CR-181308] N90-13982

DATA RETRIEVAL
The Inca data base N90-13531
Mission simulations N90-13532
The SIMBAD data base N90-13547

DATA SIMULATION
The APROS software for process simulation and model development
[VTT-618] N90-13987

DATA SMOOTHING
Great circle interactions: Attitude smoothing and grid-step inconsistencies N90-13554

DATA STORAGE
The interface with the data reduction consortia N90-13528
The SIMBAD data base N90-13547

DATA STRUCTURES
Data structures for the representation and manipulation of polyhedrons
[IMAG-RR-772-M] N90-14042

DATA SYSTEMS
The Hipparcos Mission. Prelaunch status. Volume 1: The Hipparcos satellite
[ESA-SP-1111-VOL-1] N90-13499
Data handling and telecommunications N90-13514
On-board software N90-13518
The SIMBAD data base N90-13547
Micro-based fact collection tool user's manual
[NASA-CR-180414] N90-13981
Ada programming guidelines for deterministic storage management
[NASA-CR-181308] N90-13982

DATA TRANSMISSION
Spacelab system analysis: The modified free access protocol: An access protocol for communication systems with periodic and Poisson traffic
[NASA-CR-183805] N90-13497
Data handling and telecommunications N90-13514
The role of the ground segment N90-13527
The interface with the data reduction consortia N90-13528
The use of digital signal processing in satellite communication N90-13684

DEBRIS
Debris/ice/TPS assessment and photographic analysis for Shuttle Mission STS-34
[NASA-TM-102153] N90-13447

DECODING
Error control techniques for satellite and space communications
[NASA-CR-182751] N90-13685
SN 1987: A telemetry decoding system N90-13875
DECOMPOSITION
Effect of adsorbed arsenic on the decomposition rate of nickel hydride
[AD-A213245] N90-13624
DECONTAMINATION
Contamination removal using various solvents and methodologies
[NASA-CR-183747] N90-13652
DECOUPLING
Using the physical structure of a system for control: An illustration
[MEMO-782] N90-14014
DEDUCTION
On the safe approximation of PROLOG programs
[CWI-CS-R8913] N90-13976
DEFECTS
Reflection by defective diffusion bonds
[AD-A212995] N90-13638
Theoretical evaluation of defects in pressure vessels and pipings
[CRIF-MT-174] N90-13798
The initial imperfection data bank at the Delft University of Technology, part 2
[LR-559-PT-2] N90-13825
DEFLECTION
Bilinear modeling and nonlinear estimation N90-13430
DEFORMATION
Anomalous strain rate dependence of the serrated flow in Ni-H and Ni-C-H alloys
[AD-A213244] N90-13641
The use of a deformation model for sampling digitalized stereoscopic images
[IMAG-RR-753-I] N90-13884
DEGREES OF FREEDOM
Design and control of a two-degree-of-freedom lightweight flexible arm
[AD-A213335] N90-13790
DELAMINATING
Fractography of composite delamination
[NASA-CR-183291] N90-13599
Buckling of delaminations in ARALL laminates
[LR-535] N90-13614
DELAY CIRCUITS
Delay test generation for synchronous sequential circuits
[AD-A211917] N90-13697
DENDRITIC CRYSTALS
Flight software development for the isothermal dendritic growth experiment
[NASA-TM-102412] N90-13988
DENSITY (NUMBER/VOLUME)
Nonpotential scattering for the density matrix and quantum gravity
[PREPRINT-688] N90-14080
DENSITY DISTRIBUTION
An evaluation of the Smith-Feddes model
[AD-A213237] N90-13907
DEPOSITION
Effect of adsorbed arsenic on the decomposition rate of nickel hydride
[AD-A213245] N90-13624
Elaboration and characterization of MISFET transistors on InP
[ECL-88-19] N90-13709
DESIGN ANALYSIS
Overview of the Hipparcos satellite N90-13502
The payload structure N90-13510
Spacecraft thermal control N90-13513
Development of a shuttle plume radiation heating indicator
[NASA-CR-183679] N90-13584
Flight motor set 360L001 (STS-26R). Volume 5: Nozzle component
[NASA-CR-183771] N90-13588
Design of a power component with IGBT insulated grid. Static and dynamic study
[ECL-88-22] N90-13710
Design and control of a two-degree-of-freedom lightweight flexible arm
[AD-A213335] N90-13790
On control of manipulators
[ISBN-90-9002789-0] N90-13804
A double focusing mass-spectrometer for simultaneous ion measurements in the stratosphere N90-13848
Bone mineral measurement using dual energy x ray densitometry N90-13958
The problem of automation: Inappropriate feedback and interaction, not overautomation
[NASA-CR-186128] N90-13994
Fundamental quantum 1/f noise in ultrasmall semiconductor devices and their optimal design principles
[AD-A211947] N90-14107
DETECTION
The detectors N90-13507
Stabilizability and detectability of discrete-time time-varying systems
[MEMO-COSOR-88-16] N90-14023
DETERIORATION
Auroral and sub-auroral interaction at the F region ionosphere
[AD-A213284] N90-13896
DEVELOPMENT
Information system life-cycle and documentation standards, volume 1
[NASA-TM-101856] N90-14135
Product specification documentation standard and Data Item Descriptions (DID). Volume of the information system life-cycle and documentation standards, volume 3
[NASA-TM-101858] N90-14137
Assurance specification documentation standard and Data Item Descriptions (DID). Volume of the information system life-cycle and documentation standards, volume 4
[NASA-TM-101859] N90-14138
DEVIATION
Large deviation estimates in the stochastic quantization of phi sub 2 exp 4
[PREPRINT-686] N90-14050
DIAMETERS
Effect of reduced aft diameter and increased blade number on high-speed counterrotation propeller performance
[NASA-TM-102077] N90-13352
DIAMONDS
Novel in situ spectroscopic ellipsometer for real time analysis of CVD diamond films
[AD-A213218] N90-13762
DIELECTRIC PROPERTIES
Characteristic impedance of microstrip lines
[NASA-TM-101581] N90-13694
DIELECTRICS
Joint Services Electronics Program
[AD-A213015] N90-13699
Reorganization free energy for electron transfers at liquid-liquid and dielectric semiconductor-liquid interfaces
[AD-A212985] N90-14111
DIESEL ENGINES
Two-dimensional analysis of two-phase reacting flow in a firing direct-injection diesel engine
[NASA-TM-102069] N90-13392
DIFFERENTIAL EQUATIONS
Using Broyden updates to approximate the Jacobian in a semi-implicit backward differentiation code
[AD-A213239] N90-14010
Analysis of three approaches to qualitative simulation
[MEMO-INF-89-32] N90-14035
DIFFERENTIAL GEOMETRY
On geometry of inhomogeneous Heisenberg ferromagnet: Nonintegrable case
[MEMO-789] N90-14030
DIFFERENTIATION (BIOLOGY)
Polarity establishment, morphogenesis, and cultured plant cells in space N90-13943
Gravity and animal embryos N90-13951
DIFFRACTION
Diffraction, chopping, and background subtraction for LDR N90-13476
DIFFRACTION LIMITED CAMERAS
Introduction to the report of the Asilomar 3 LDR workshop N90-13450
DIFFUSION
Gravimetric measurements of materials outgassing applied to graphite-epoxy laminates
[NASA-TM-100753] N90-13609
Physical phenomena and the microgravity response N90-13945
DIFFUSION WELDING
Reflection by defective diffusion bonds
[AD-A212995] N90-13638
DIGITAL COMPUTERS
Laboratory test methodology for evaluating the effects of electromagnetic disturbances on fault-tolerant control systems
[NASA-TM-101665] N90-14061
DIGITAL ELECTRONICS
On the design of a computer-aided design system for digital circuits N90-13695
DIGITAL SIMULATION
Parallelism in the discrete-event simulation algorithm
[AD-A213060] N90-13970
DIGITAL SYSTEMS
Advanced actuation systems development, volume 2
[AD-A213378] N90-13398
A knowledge-based flight status monitor for real-time application in digital avionics systems
[NASA-TM-101710] N90-13995
DIGITAL TECHNIQUES
The use of digital signal processing in satellite communication N90-13684
DIGITAL TRANSDUCERS
Data acquisition in aerodynamic research N90-13340
DIMENSIONS
On the recurrence relation for multivariate B-splines with respect to dimension
[MEMO-786] N90-14017
DIOPHANTINE EQUATION
The weighted sum of two S-units being a square
[MEMO-792] N90-14031
Solving a specific Thue-Mahler equation
[MEMO-793] N90-14032
DIRECTORIES
The DOD Gateway Information System: Operational prototype and transition period 1987-1988
[AD-A213044] N90-14141
DISCRETE FUNCTIONS
Discretization and model reduction for a class of nonlinear systems N90-13397
A transient response method for linear coupled substructures
[NASA-TP-2926] N90-13444
A unified algebraic approach to integral and discrete evolution equations
[PREPRINT-668] N90-14044
DISCRIMINATION
Gas identification system using graded temperature sensor and neural net interpretation
[AD-A213359] N90-13627
DISCRIMINATORS
Spatiotemporal characteristics of visual localization, phase 2
[AD-A212934] N90-13929
DISEASES
Preliminary study of pharmacological control of space disease
[ETN-90-95015] N90-13927
DISLOCATIONS (MATERIALS)
Anomalous strain rate dependence of the serrated flow in Ni-H and Ni-C-H alloys
[AD-A213244] N90-13641
DISPLAY DEVICES
Image enhancement software for underwater recovery operations: User's manual
[AD-A212943] N90-14094
Studies of structure and switching dynamics in ferroelectric crystal and liquid crystal thin films
[AD-A212650] N90-14109
DISTANCE
Linear groups and distance-transitive graphs
[CWI-PM-R8805] N90-14036
On distance-transitive graphs and involutions
[CWI-PM-R8808] N90-14037
DISTRIBUTED PARAMETER SYSTEMS
Software development for avionics SSME control and diagnostics
[NASA-CR-184894] N90-13964
DISTRIBUTED PROCESSING
Waiting times in polling systems with Markovian server routing
[CWI-BS-R8905] N90-13989
Monotonicity of performance measures in a processor sharing queue
[CWI-BS-R8902] N90-14019
Workloads and waiting times in single-server systems with multiple customer classes
[CWI-BS-R8906] N90-14020
Simple appoximations for second moment characteristics of the sojurn time in the M/G/1 processor sharing queue
[CWI-BS-R8907] N90-14055
Database interfaces on NASA's heterogeneous distributed database system
[NASA-CR-185420] N90-14133
Retrieving and integrating IC fabrication data from dissimilar databases
[AD-A211890] N90-14140
DISTRIBUTION FUNCTIONS
Estimation of convolution tail behavior
[MEMO-COSOR-89-04] N90-14051
Self-decomposable distributions and branching processes
[MEMO-COSOR-89-06] N90-14052
Note on Urbanik's class L(sub n) --- self-decomposability of functions
[MEMO-COSOR-89-07] N90-14053
Reverse self-decomposability --- for characteristic functions
[MEMO-COSOR-89-08] N90-14054

DISTRIBUTION MOMENTS
Simple approximations for second moment characteristics of the sojurn time in the M/G/1 processor sharing queue
[CWI-BS-R8907] N90-14055
DISTURBING FUNCTIONS
Another approach to the local disturbance decoupling problem with stability for nonlinear systems
[MEMO-799] N90-14033
DITCHING (LANDING)
The human factors relating to escape and survival from helicopters ditching in water
[AGARD-AG-305(E)] N90-13358
DIURNAL VARIATIONS
Diurnal variation of the sodium layer at polar latitudes in summer N90-13869
DIVIDING (MATHEMATICS)
Counterexamples to Robertson's conjecture
[MEMO-COSOR-88-32] N90-14048
DOCUMENTATION
Executive overview and introduction to the SMAP information system life-cycle and documentation standards
[NASA-TM-101765] N90-14134
Information system life-cycle and documentation standards, volume 1
[NASA-TM-101856] N90-14135
Management plan documentation standard and Data Item Descriptions (DID). Volume of the information system life-cycle and documentation standards, volume 2
[NASA-TM-101857] N90-14136
Product specification documentation standard and Data Item Descriptions (DID). Volume of the information system life-cycle and documentation standards, volume 3
[NASA-TM-101858] N90-14137
Assurance specification documentation standard and Data Item Descriptions (DID). Volume of the information system life-cycle and documentation standards, volume 4
[NASA-TM-101859] N90-14138
Management control and status reports documentation standard and Data Item Descriptions (DID). Volume of the information system life-cycle and documentation standards, volume 5
[NASA-TM-101860] N90-14139
DOCUMENTS
AFOSR technical report summaries
[AD-A213148] N90-14142
DOMAIN WALL
On thick domain walls in general relativity
[NASA-CR-185926] N90-14124
DOPPLER EFFECT
The interaction and variation of waves and turbulence from MST radar data
[AD-A212849] N90-13906
DOUBLE BASE ROCKET PROPELLANTS
A theoretical model of double base propellant combustion
[ONERA-RTF-23/7128-EY] N90-13672
DRAG
Reduction of profile drag by modifying the structure next to the wake area
[IMFL-88/35] N90-13356
Induced drag for non-planar wings
[LR-521] N90-13357
Lifetime predictions for the Solar Maximum Mission (SMM) and San Marco spacecraft N90-13440
DRAG FORCE ANEMOMETERS
Skin friction measurements with hot elements N90-13345
DRIFT (INSTRUMENTATION)
Simultaneous quaternion estimation (QUEST) and bias determination N90-13417
True covariance simulation of the EUVE update filter N90-13427
DROP SIZE
Liquid water content and droplet size calibration of the NASA Lewis Icing Research Tunnel
[NASA-TM-102447] N90-13797
DROPS (LIQUIDS)
Metal transfer in gas metal arc welding
[AD-A213390] N90-13642
Facilities for microgravity combustion research
[NASA-TM-102014] N90-13679
DRY FRICTION
Evaluation of newly formulated Dow Corning 321 dry film lubricant
[NASA-CR-183828] N90-13661
DUALITY THEOREM
Description and manipulation of convex polygons using polarity
[IMAG-RR-771-M] N90-14041
The algebraic basis of mathematical morphology. Part 1: Dilations and erosions
[CWI-AM-R8807] N90-14065
DUCTILITY
Ductile failure
[AD-A212975] N90-13601
DURABILITY
Considerations about the acceptance inspection of HS fasteners intended for controlled tightening
[CRIF-MT-175] N90-13806
DYADICS
Characteristic impedance of microstrip lines
[NASA-TM-101581] N90-13694
DYNAMIC CHARACTERISTICS
Choice of a differential method for the attitude restitution in dynamic unbalance
[CNES-CT/DTI/MS/CM/290] N90-13582
Design of a power component with IGBT insulated grid. Static and dynamic study
[ECL-88-22] N90-13710
Identification of equivalent modulus of a composite beam from nonmodal vibratory tests
[ECL-89-001] N90-13821
The DYANA campaign 1990 N90-13870
DYNAMIC CONTROL
Using the physical structure of a system for control: An illustration
[MEMO-782] N90-14014
DYNAMIC LOADS
SSME LOX post flow analysis/fluid structure interaction. Volume 1: Flow analysis
[NASA-CR-183677] N90-13715
Elasticity effects on cavitation in a squeeze film damper undergoing noncentered circular whirl
[NASA-TM-102392] N90-13786
Comparison of analytical methods for calculation of wind loads
[NASA-TM-102782] N90-13813
DYNAMIC MODELS
Unified model of charge build up and annealing of oxide charge and interface states in SiO2 due to stress
[HMI-B-465] N90-14120
DYNAMIC RESPONSE
Probabilistic finite element analysis of dynamic structural response
[AD-A213249] N90-13789
DYNAMIC STABILITY
SSME LOX post flow analysis/fluid structure interaction. Volume 1: Flow analysis
[NASA-CR-183677] N90-13715
DYNAMIC STRUCTURAL ANALYSIS
Pointing control for LDR N90-13453
Space telescope pointing control N90-13454
Segment alignment control system N90-13457
Initial test results for the mini-mast N90-13482
Flight motor set 360L001 (STS-26R). Volume 5: Nozzle component
[NASA-CR-183771] N90-13588
Joint Services Electronics Program
[AD-A213015] N90-13899
Investigation of difficult component effects on finite element model vibration prediction for the Bell AG-1G helicopter. Volume 2: Correlation results
[NASA-CR-181916-VOL-2] N90-13814
DYNAMIC TESTS
Dynamic testing techniques and applications for an aeroelastic rotor test facility N90-13406
Static and free-vibrational response of semi-circular graphite-epoxy frames with thin-walled open sections
[NASA-CR-186097] N90-13600
DYNAMICAL SYSTEMS
Explicit modeling and concurrent processing in the simulation of multibody dynamic systems N90-13481
Quadratic dynamical systems describing shear flow of non-Newtonian fluids
[AD-A212892] N90-13720
Balance laws and centro velocity in dissipative systems
[MEMO-797] N90-13726
Climate predictability: A dynamical view
[AERONOMICA-ACTA-A-347-1989] N90-13909
Using the physical structure of a system for control: An illustration
[MEMO-782] N90-14014
On the effects of an uncertainty on evolution law in dynamical systems
[PREPRINT-689] N90-14047
DYNAMO THEORY
The electrodynamics of the polar ionosphere with special emphasis on the dayside cleft region N90-13838

E

E REGION
Preliminary results of the rocket and scatter experiments ROSE: Measurements with the newly designed spherical probe N90-13850
EAR
Test procedures for the evaluation of helmet and headset mounted active noise reduction systems
[AD-A212991] N90-13937
EARTH ATMOSPHERE
European Rocket and Balloon Programs and Related Research
[ESA-SP-291] N90-13826
A self-consistent model of the most common nightglow emissions N90-13853
A high-resolution atlas of the infrared spectrum of the Sun and the Earth atmosphere from space: A compilation of ATMOS spectra of the region from 650 to 4800 cm (2.3 to 16 micron). Volume 1: The Sun
[NASA-RP-1224-VOL-1] N90-13893
EARTH CRUST
Strain accumulation and surface deformation along the San Andreas, California
[NASA-CR-185893] N90-13894
Crustal structure studies utilizing earthquake sequences
[AD-A212916] N90-13895
EARTH ENVIRONMENT
The French balloon program and related space research N90-13828
EARTH IONOSPHERE
The electrodynamics of the polar ionosphere with special emphasis on the dayside cleft region N90-13838
Resonance cone diagnostics in the mid-latitude ionosphere N90-13840
Background electrodynamics measured by EISCAT during the NEED campaign N90-13851
Auroral and sub-auroral interaction at the F region ionosphere
[AD-A213284] N90-13896
EARTH MAGNETOSPHERE
Spacecraft attitude determination using the earth's magnetic field N90-13429
EARTH MOVEMENTS
Supplementing geodetic data with prior information for crustal deformation in the Imperial Valley, California
[TR-6-1988] N90-13904
EARTH OBSERVATIONS (FROM SPACE)
The use of LANDSAT-TM data for the management of pine forestations in central Chile
[DLR-FB-89-44] N90-13881
EARTH OBSERVING SYSTEM (EOS)
Science and applications on the space station: A strategic vision
[NASA-TM-101863] N90-13493
EARTH RADIATION BUDGET
Extended Kalman filter for attitude estimation of the earth radiation budget satellite N90-13433
EARTH RADIATION BUDGET EXPERIMENT
The effects of seasonal and latitudinal earth infrared radiance variations on ERBS attitude control N90-13414
EARTH SURFACE
Senegalese land surface change analysis and biophysical parameter estimation using NOAA AVHRR spectral data
[NASA-CR-186120] N90-13883
EARTH-MOON TRAJECTORIES
Calculation of double-lunar swingby trajectories: I. Keplerian foundation N90-13435
EARTHQUAKES
Crustal structure studies utilizing earthquake sequences
[AD-A212916] N90-13895
ECHO SOUNDING
Polar mesosphere summer echoes and associated atmospheric gravity waves N90-13856
ECONOMIC ANALYSIS
The economic impact of automation technology
[AD-A213363] N90-13682
ECONOMIC IMPACT
The economic impact of automation technology
[AD-A213363] N90-13682
ECOSYSTEMS
Adaptation and resistance of ecosystems to stress
[AD-A212999] N90-13889
EDDY VISCOSITY
Application of large eddy interaction model to a mixing layer
[NASA-CR-185123] N90-13328
EDITING ROUTINES (COMPUTERS)
An editor for 3D-models for image analysis
[FOA-C-30534-3.4] N90-13986
EDUCATION
Software engineering and Ada (Trademark) training: An implementation model for NASA
[NASA-CR-186071] N90-13966
Elementary and middle school science improvement project
[NASA-CR-183768] N90-14125

EFFICIENCY
Large heavy duty balloons in Europe N90-13858
Identification of impulsive interference channels [AD-A213154] N90-14009
EISCAT RADAR SYSTEM (EUROPE)
Enhanced electron density layers in the high-latitude lower ionosphere N90-13832
Background electrodynamics measured by EISCAT during the NEED campaign N90-13851
Polar mesosphere summer echoes and associated atmospheric gravity waves N90-13856
ELASTIC DEFORMATION
Strain accumulation and surface deformation along the San Andreas, California [NASA-CR-185893] N90-13894
Field-effect spectroscopy of interface states [AD-A212998] N90-14112
ELASTIC PROPERTIES
Energy concentration induced by phase transitions in hydrogenated metals [PREPRINT-672] N90-13650
A theory of damage in brittle and cementitious materials, part 1 [AD-A212940] N90-13658
Analysis of new phenomena in shear flow of non-Newtonian fluids [AD-A212893] N90-13721
ELASTIC SCATTERING
Elastic impurity scattering in double-barrier resonant tunneling structures [AD-A212850] N90-14110
ELASTODYNAMICS
Time domain coupling of the boundary and finite element methods for elastodynamics [AD-A213243] N90-13811
ELASTOMERS
Studies of Aflas fluoroelastomers [AD-A213046] N90-13622
ELECTRIC CORONA
The adhesive bonding of thermoplastic composites [AD-A213358] N90-13605
ELECTRIC FIELDS
Auroral particle acceleration by dc and low frequency electric fields N90-13841
ELECTRIC FUSES
Resistive fuses: Analog hardware for detecting discontinuities in early vision [AD-A211891] N90-13696
ELECTRIC NETWORKS
Memory matrix [WO-PATENT-88/04096] N90-13961
ELECTRIC POTENTIAL
An iterative method to solve the nonlinear Poisson's equation in the case of plasma tangential discontinuities [AERONOMICA-ACTA-A-346-1989] N90-14045
ELECTRIC POWER SUPPLIES
The US space station and its electric power system [NASA-TM-101974] N90-13596
ELECTRIC SWITCHES
Contribution to the study of a self-protected static switch and its command strategy [ECL-89-002] N90-13711
ELECTRICAL GROUNDING
Cable coupling lightning transient qualification [NASA-CR-183826] N90-13405
ELECTRICAL INSULATION
Cable coupling lightning transient qualification [NASA-CR-183826] N90-13405
ELECTRICAL MEASUREMENT
Electrochemistry at very small electrodes [AD-A213156] N90-13623
ELECTRICAL PROPERTIES
A literature survey of inherently conducting polymers [FOA-C-20763-2.4] N90-13668
Joint Services Electronics Program [AD-A213015] N90-13699
ELECTRICAL RESISTANCE
A solvable self-similar model of the sausage instability in a resistive Z-pinch [AD-A213137] N90-14006
ELECTRICAL RESISTIVITY
Microwave microstrip resonator measurements of Y1Ba2Cu3O(7-x) and Bi2Sr2Ca1Cu2O(8-y) thin films [NASA-TM-102159] N90-13704
ELECTRO-OPTICS
Optics and opto-electronics systems [AD-A212340] N90-14093
Integrated optoelectronic receivers [AD-A213376] N90-14098
ELECTROCHEMICAL CELLS
Photoelectrochemical behavior of type n of GaAs in concentrated iodide media and realization of an experimental device [ECL-88-18] N90-14117
ELECTROCHEMISTRY
Electrochemistry at very small electrodes [AD-A213156] N90-13623
Electrochemical study of the etching of III to V semiconductors [ETN-90-96015] N90-13633
Refurbishment of one-person regenerative air revitalization system [NASA-CR-183757] N90-13934
ELECTRODELESS DISCHARGES
Low resistivity electrodeless streamer tubes [PREPRINT-685-89] N90-13712
ELECTRODES
Electrochemistry at very small electrodes [AD-A213156] N90-13623
ELECTRODYNAMICS
Magneto-elastic interactions in conducting structures in transient magnetic fields N90-13686
The electrodynamics of the polar ionosphere with special emphasis on the dayside cleft region N90-13838
Background electrodynamics measured by EISCAT during the NEED campaign N90-13851
ELECTROLYSIS
Gas evolution and bubble formation on electrodes [DLR-FB-89-35] N90-13629
ELECTROLYTES
Electrochemistry at very small electrodes [AD-A213156] N90-13623
Surfaces and interfaces of ceramic materials [AD-A212417] N90-13657
ELECTROMAGNETIC COMPATIBILITY
Electrical testing N90-13520
ELECTROMAGNETIC FIELDS
Countermeasures to microgravity N90-13957
ELECTROMAGNETIC INTERFERENCE
Laboratory test methodology for evaluating the effects of electromagnetic disturbances on fault-tolerant control systems [NASA-TM-101665] N90-14061
ELECTROMAGNETIC PROPERTIES
Nucleon polarizabilities in the constituent quark model [NOTA-INTERNA-936] N90-14082
ELECTROMAGNETIC PULSES
Modeling of power electronic systems with EMTP [NASA-TM-102375] N90-14060
ELECTROMAGNETIC RADIATION
Stochastic modelling of EM scattering from foliage [AD-A213118] N90-13689
ELECTROMAGNETIC SCATTERING
Stochastic modelling of EM scattering from foliage [AD-A213118] N90-13689
ELECTROMAGNETIC WAVE TRANSMISSION
Electromagnetic wave propagation through circular waveguides containing radially inhomogeneous lossy media [AD-A213062] N90-13688
ELECTRON BEAMS
Electron beam sensitive devices for controllability [IMAG-RR-761-I] N90-13707
Research on the controllability of integrated circuits by means of electron beams [ETN-90-95710] N90-13708
Evolution of the EPR procedure for polycrystalline Si ribbon drawing for photovoltaic cell manufacturing [ISAL-89-0027] N90-13888
Influence of RF-parameters on beam lifetime [NIKHEF-K/AMPS/89-06] N90-14091
ELECTRON DENSITY (CONCENTRATION)
Resonance cone diagnostics in the mid-latitude ionosphere N90-13840
Background electrodynamics measured by EISCAT during the NEED campaign N90-13851
ELECTRON ENERGY
Some remarks on the working principle of the rocketborne nose tip dc probes in the D-region of the ionosphere N90-13839
Background electrodynamics measured by EISCAT during the NEED campaign N90-13851
Towards ab initio calculation of electron energies in semiconductors [ETN-90-96016] N90-14121
ELECTRON IMPACT
CANOES 2: Dynamics of atmospheric infrared thermochemical excitation, volume 2 [AD-A213342] N90-13898
CANOES 2: Dynamics of atmospheric infrared thermochemical excitation, volume 3 [AD-A213343] N90-13899
CANOES 2: Dynamics of atmospheric infrared thermochemical excitation, volume 4 [AD-A213344] N90-13900
Model-independent analysis of the Z line shape in e+e- annihilation [PREPRINT-679] N90-14089
ELECTRON SCATTERING
Exotic Higgs production at e+e- colliders [PREPRINT-671] N90-14088
Elastic impurity scattering in double-barrier resonant tunneling structures [AD-A212850] N90-14110
ELECTRON SOURCES
CANOES 2: Dynamics of atmospheric infrared thermochemical excitation, volume 4 [AD-A213344] N90-13900
ELECTRON TRANSFER
Reorganization free energy for electron transfers at liquid-liquid and dielectric semiconductor-liquid interfaces [AD-A212985] N90-14111
ELECTRON TRANSITIONS
Quantitative AES and XPS: Determination of the electron spectrometer transmission function and the detector sensitivity energy dependencies for the production of true electron emission spectra in AES and XPS [NPL-DMA(A)-194] N90-13634
ELECTRON TUBES
Low resistivity electrodeless streamer tubes [PREPRINT-685-89] N90-13712
ELECTRONIC CONTROL
Apparatus for cooling electronic components in aircraft [AD-D014207] N90-13373
ELECTRONIC EQUIPMENT
Electronic warfare: Reliable equipment needed to test Air Force's electronic warfare systems [AD-A212952] N90-13687
Joint Services Electronics Program [AD-A213015] N90-13699
Conference Proceedings of the Human-Electronic Crew: Can They Work Together [AD-A211871] N90-13936
Modeling of power electronic systems with EMTP [NASA-TM-102375] N90-14060
ELECTRONIC PACKAGING
MM and T for VHSIC multichip packages [AD-A213259] N90-13703
ELECTRONIC SPECTRA
CANOES 2: Dynamics of atmospheric infrared thermochemical excitation, volume 3 [AD-A213343] N90-13899
CANOES 2: Dynamics of atmospheric infrared thermochemical excitation, volume 4 [AD-A213344] N90-13900
ELECTRONIC WARFARE
Electronic warfare: Reliable equipment needed to test Air Force's electronic warfare systems [AD-A212952] N90-13687
ELECTRONS
Local pairing and antiferromagnetism in high-T sub c superconductors [AD-A213004] N90-14113
ELECTROSTATIC PROBES
Some remarks on the working principle of the rocketborne nose tip dc probes in the D-region of the ionosphere N90-13839
ELECTROSTATIC WAVES
Observations of electrostatic hydrogen cyclotron waves and electric field fluctuations near one Hz in auroral acceleration regions N90-13842
ELECTROSTATICS
Dynamics Explorer-1 satellite study of electrostatic ion cyclotron waves N90-14105
ELEMENTARY PARTICLES
Nuclear physics and cosmology [NASA-CR-186166] N90-14167
ELLIPSOMETERS
Novel in situ spectroscopic ellipsometer for real time analysis of CVD diamond films [AD-A213218] N90-13762
ELLIPTIC FUNCTIONS
On geometry of inhomogeneous Heisenberg ferromagnet: Nonintegrable case [MEMO-789] N90-14030
EMBEDDED COMPUTER SYSTEMS
A fault-tolerant software algorithm for a network of transputers [AD-A213092] N90-13972
Ada programming guidelines for deterministic storage management [NASA-CR-181308] N90-13982
EMBRYOS
Polarity establishment, morphogenesis, and cultured plant cells in space N90-13943
Gravity and animal embryos N90-13951
EMISSION SPECTRA
Auroral particle acceleration by dc and low frequency electric fields N90-13841

EMISSIVITY
Three dimensional analysis of the structure of the atmosphere in polar environments by vertical satellite sounding. Interest for the meteorological forecasts at high latitudes
[ETN-90-95506] N90-13911
EMULSIONS
Model filled polymers I. Synthesis of crosslinked monodisperse polystyrene beads
[AD-A213226] N90-13660
END EFFECTORS
Definition, determination and characterization of acceleration sets for spatial manipulators
[AD-A213366] N90-13793
On control of manipulators
[ISBN-90-9002789-0] N90-13804
ENERGY CONSUMPTION
Measurement of mechanical work and energy expenditure in running and bicycling N90-13935
ENERGY CONVERSION EFFICIENCY
The photovoltaic properties of an Al In As/InP heterojunctions grown by LPE method
[NASA-CR-185996] N90-13888
ENERGY DISSIPATION
Three D flows in turbine blade rows N90-13739
ENERGY DISTRIBUTION
Background electrodynamics measured by EISCAT during the NEED campaign N90-13851
ENERGY GAPS (SOLID STATE)
Local pairing and antiferromagnetism in high-T sub c superconductors
[AD-A213004] N90-14113
ENERGY METHODS
Solution of the Boltzmann equation using an energy group method
[AD-A213136] N90-14096
ENERGY TECHNOLOGY
Advanced energy system program
[PB89-235170] N90-13887
ENERGY TRANSFER
Energy exchange of interacting solitons in multidimensions
[PREPRINT-662] N90-14071
Energy barriers in SK spin-glass model
[PREPRINT-665] N90-14119
ENGINE DESIGN
Space Transportation Engine Program (STEP). Phase B: Project study and management plan-ingredients for STEP success
[NASA-CR-183770] N90-13585
Advanced Turbine Technology Applications Project (ATTAP)
[NASA-CR-185109] N90-14153
ENGINE PARTS
Constitutive modeling for isotropic materials (HOST)
[NASA-CR-179522] N90-13390
Constitutive modeling for isotropic materials (HOST)
[NASA-CR-174718] N90-13391
ENGINE TESTS
Advanced Turbine Technology Applications Project (ATTAP)
[NASA-CR-185109] N90-14153
ENGINEERING
Summary of research academic departments, 1987-1988
[AD-A213252] N90-14183
ENVIRONMENT EFFECTS
Optical properties monitor: Experiment definition phase
[NASA-CR-183836] N90-14092
ENZYMES
Modern biofuel cells for waste recycling in life support systems
[NASA-CR-185963] N90-13718
EPOXY COMPOUNDS
The adhesive bonding of thermoplastic composites
[AD-A213358] N90-13605
EPOXY MATRIX COMPOSITES
Some aspects of test frequency influence on the fatigue behavior of ARALL
[LR-549] N90-13616
EQUATIONS OF MOTION
Software and hardware description of the helicopter motion equations for VAX computers
[AD-A213248] N90-13375
Simulation of spacecraft attitude dynamics using TREETOPS and model-specific computer Codes N90-13419
Optimal trajectories for the Aeroassisted Flight Experiment. Part 1: Equations of motion in an Earth-fixed system
[NASA-CR-186134] N90-13441
Optimal trajectories for the Aeroassisted Flight Experiment. Part 2: Equations of motion in an inertial system
[NASA-CR-186135] N90-13442
Attitude and shape control of optimally designed large space structures N90-13579
EQUIPMENT SPECIFICATIONS
A slow strain-rate tensile testing machine
[ARL-MAT-TM-399] N90-13764
Fundamental results from microgravity cell experiments with possible commericial applications N90-13940
Do the design concepts used for the space flight hardware directly affect cell structure and/or cell function ground based simulations N90-13953
ERROR ANALYSIS
Extended Kalman filter for attitude estimation of the earth radiation budget satellite N90-13433
Error allocation and accuracy assessment N90-13501
Choice of a differential method for the attitude restitution in dynamic unbalance
[CNES-CT/DTI/MS/CM/290] N90-13582
An accurate timing model for fault simulation in MOS circuits
[AD-A213153] N90-13702
GRADIO: An error analysis of the spaceborne gravity gradiometer
[ETN-90-96010] N90-13901
An artificial intelligence approach to analog system diagnosis
[AD-A213135] N90-13992
ERROR CORRECTING DEVICES
Application of an optimal filter for inflatable sphere data processing N90-13649
ERROR DETECTION CODES
Error allocation and accuracy assessment N90-13501
The compilation of astrometric data N90-13537
Standard stars and photometric calibration N90-13539
Multigrid and defect correction for the steady Navier-Stokes equations: Applications to aerodynamics
[ETN-90-96011] N90-13727
ERRORS
The effects of seasonal and latitudinal earth infrared radiance variations on ERBS attitude control N90-13414
Optimum data weighting and error calibration for estimation of gravitational parameters N90-13437
A laboratory verification sensor N90-13477
The problem of automation: Inappropriate feedback and interaction, not overautomation
[NASA-CR-186126] N90-13994
ESCAPE (ABANDONMENT)
The human factors relating to escape and survival from helicopters ditching in water
[AGARD-AG-305(E)] N90-13358
ESCHERICHIA
The sensory transduction pathways in bacterial chemotaxis N90-13944
ESTIMATES
On the application of modified stepwise regression for the estimation of aircraft stability and control parameters
[REPT-8905] N90-13400
Simultaneous quaternion estimation (QUEST) and bias determination N90-13417
Error allocation and accuracy assesament N90-13501
Large deviation estimates in the stochastic quantization of phi sub 2 exp 4
[PREPRINT-686] N90-14050
ESTIMATING
Bilinear modeling and nonlinear estimation N90-13430
Extended Kalman filter for attitude estimation of the earth radiation budget satellite N90-13433
Estimation of rain rate using spatial and multichannel coherence: Analysis of SSM/I data N90-13905
Estimation of convolution tail behavior
[MEMO-COSOR-89-04] N90-14051
ETCHING
Electrochemical study of the etching of III to V semiconductors
[ETN-90-96015] N90-13633
EULER EQUATIONS OF MOTION
Block-structured solution of three-dimensional transonic flows using parallel processing
[AD-A212851] N90-13330
Transonic Euler solutions on mutually interfering finned bodies
[AD-A213395] N90-13331
Computation of flow fields around propellers and hovering rotors based on the solution of the Euler equations
[DLR-FB-89-37] N90-13333
Application of an efficient hybrid scheme for aeroelastic analysis of advanced propellers
[NASA-TM-102428] N90-13355
Gas flows in rocket motors. Volume 3, appendix D: Computer code listings
[AD-A213350] N90-13593
Multigrid and defect correction for the steady Navier-Stokes equations: Applications to aerodynamics
[ETN-90-96011] N90-13727
Calculation of flow fields by the solution of the Euler equations using an extended finite volume discretization scheme
[DLR-FB-89-38] N90-13729
Numerical Methods for Flows in Turbomachinery, volume 1
[VKI-LS-1989-06-VOL-1] N90-13735
Inviscid 3D solution methods N90-13736
EUROPEAN SPACE AGENCY
European Rocket and Balloon Programs and Related Research
[ESA-SP-291] N90-13826
EUROPEAN SPACE PROGRAMS
The Hipparcos Mission. Prelaunch status. Volume 1: The Hipparcos satellite
[ESA-SP-1111-VOL-1] N90-13499
The Norwegian balloon and sounding rocket program 1989-1992 N90-13829
The German scientific balloon and sounding rocket program N90-13831
Large heavy duty balloons in Europe N90-13858
The Skylark sounding rocket program and future launcher developments by British Aerospace (Space Systems) Ltd. N90-13871
The German space science program N90-13873
Comparison of the space program performance of countries with space programs
[ILR-MITT-222] N90-14150
EVALUATION
The infrared spectrograph during the SIRTF pre-definition phase
[NASA-CR-183234] N90-13759
Measurement of the light flux density patterns from luminaires proposed as photon sources for photosynthesis during space travel
[NASA-CR-186124] N90-13916
EXCIMER LASERS
Microwave excited excimer laser
[ETN-90-95909] N90-13781
EXCITATION
Microwave excited excimer laser
[ETN-90-95906] N90-13781
CANOES 2: Dynamics of atmospheric infrared thermochemical excitation, volume 1
[AD-A213341] N90-13897
CANOES 2: Dynamics of atmospheric infrared thermochemical excitation, volume 2
[AD-A213342] N90-13898
CANOES 2: Dynamics of atmospheric infrared thermochemical excitation, volume 3
[AD-A213343] N90-13899
Further observations of rotationally excited far infrared OH16 and OH18 emission in Orion-KL: Tighter constraints on the nature of the emitting region
[NASA-CR-186004] N90-14156
EXERCISE PHYSIOLOGY
Exercise countermeasures for bed rest deconditioning
[NASA-TM-101045] N90-13926
EXHAUST EMISSION
MOBILE4 oxygenated fuels version user's guide
[PB89-230700] N90-13674
EXHAUST GASES
Gas identification system using graded temperature sensor and neural net interpretation
[AD-A213359] N90-13627
EXOBIOLOGY
Life science research in space
[ESA-SP-1105] N90-13917
Aerospace medicine and biology: A continuing bibliography with indexes (supplement 330)
[NASA-SP-7011(330)] N90-13925
EXPANSION
Distribution of a sum of n random variables and a central limit theorem based on moments or on coefficients of polynomial dependence
[IMAG-RR-768-M] N90-14040
EXPERIMENT DESIGN
Cells in Space
[NASA-CP-10034] N90-13939
Fundamental results from microgravity cell experiments with possible commericial applications N90-13940
Effects of microgravity on growth hormone concentration and distribution in plants N90-13947
Gravity receptors and responses N90-13948
Human factors issues in performing life science experiments in a 0-G environment N90-13952
Do the design concepts used for the space flight hardware directly affect cell structure and/or cell function ground based simulations N90-13953

Model system studies with a phase separated membrane bioreactor N90-13954
Design challenges for space bioreactors N90-13955
Fermentation and oxygen transfer in microgravity N90-13956

EXPERT SYSTEMS
Expert systems for adaptive control of large space structures N90-13452
A knowledge-based system design/information tool for aircraft flight control systems [NASA-TM-101704] N90-13990
Applications of artificial intelligence to space station and automated software techniques: High level robot command language [NASA-CR-182997] N90-13991
An artificial intelligence approach to analog system diagnosis [AD-A213135] N90-13992
A knowledge-based flight status monitor for real-time application in digital avionics systems [NASA-TM-101710] N90-13995
Empirical analysis and refinement of expert system knowledge bases [AD-A213240] N90-14143

EXPLORER SATELLITES
The Explorer program for astronomy and astrophysics N90-14159

EXPLOSIONS
Expected supernovae rates and gravitational waves detection [NOTA-INTERNA-933] N90-14166

EXPLOSIVES
Nuclear magnetic resonance signatures of nitrogen-containing compounds [AD-A213375] N90-13628

EXPONENTS
Fluctuations of the Lyapunov exponent in disordered systems [PREPRINT-690] N90-14063

EXPOSURE
Optical properties monitor: Experiment definition phase [NASA-CR-183836] N90-14092

EXTINCTION
An investigation of flame spread over shallow liquid pools in microgravity and nonair environments [NASA-TM-102425] N90-13680

EXTRAGALACTIC RADIO SOURCES
The link to extragalactic objects N90-13544
A search for the effects of active magnetic fields in extra-galactic radio sources N90-14161

EXTRATERRESTRIAL RADIATION
Interzodiak 2: Observation of EUV-resonance radiation N90-13854
A search for the effects of active magnetic fields in extra-galactic radio sources N90-14161

EXTREME ULTRAVIOLET EXPLORER SATELLITE
True covariance simulation of the EUVE update filter N90-13427

EXTRUDING
Process for producing a shaped, extruded product from a crosslinkable polymeric composition [GB-PATENT-2-201-677-A] N90-13662

EYE PROTECTION
A review of laser filter materials [AD-A213134] N90-13776

F

F REGION
Auroral and sub-auroral interaction at the F region ionosphere [AD-A213284] N90-13896

FABRICATION
Activities report of the metallic manufacturing industry [ISSN-0524-7705] N90-13649
Development and characterization of PdCr temperature-compensated wire resistance strain gage [NASA-CR-185153] N90-13761
Computer-aided fabrication system implementation [AD-A213005] N90-13969
Sol-gel processing science using a Sol-Gel Optics Research Facility (SGORF) [AD-A213056] N90-14095
Retrieving and integrating IC fabrication data from dissimilar databases [AD-A211890] N90-14140

FACTORIZATION
Some remarks on the gap metric [MEMO-COSOR-88-34] N90-14029

FAILURE
Ductile failure [AD-A212975] N90-13601
Analytical derivation and verification of zero-gyro control for the IUE satellite [NASA-TM-100748] N90-13767

FAILURE ANALYSIS
Thermal barrier coating life prediction model development, phase 1 [NASA-CR-182230] N90-13388
Re-entry hazards and cosmos 1900 [FOA-C-30535-9.4] N90-13583
Failure processes in unidirectional composite materials N90-13598
Constant amplitude fatigue of ARALL-2 laminates [LR-539] N90-13615
An investigation of gear mesh failure prediction techniques [NASA-TM-102340] N90-13785
Fatigue resistance of pressure vessels in high strength steels effect of some improvement techniques [CRIF-MT-176] N90-13799

FAILURE MODES
An investigation of gear mesh failure prediction techniques [NASA-TM-102340] N90-13785

FAN BLADES
Development of an advanced fan blade containment system [DOT/FAA/CT-89/20] N90-13386

FAR INFRARED RADIATION
Far-infrared heterodyne receivers N90-13465
Development of FIR arrays with integrating amplifiers N90-13473
Further observations of rotationally excited far infrared OH16 and OH18 emission in Orion-KL: Tighter constraints on the nature of the emitting region [NASA-CR-186004] N90-14156

FATIGUE (MATERIALS)
Nondestructive analysis of aileron fatigue and aging in a Mirage F1 [REPT-M6-594000] N90-13378
Measuring of the complete stiffness matrix for anisotropic laminated materials [DLR-MITT-89-11] N90-13606
Measuring of the complete stiffness matrix for anisotropic laminated materials [DLR-MITT-89-12] N90-13607
Some aspects of test frequency influence on the fatigue behavior of ARALL [LR-549] N90-13616
An investigation of gear mesh failure prediction techniques [NASA-TM-102340] N90-13785

FATIGUE LIFE
Fatigue behavior of silicon carbide Whisker/Aluminum composite [AD-A213094] N90-13603
Application of fracture mechanics and half-cycle method to the prediction of fatigue life of B-52 aircraft pylon components [NASA-TM-88277] N90-13820

FATIGUE TESTING MACHINES
Contribution to the fatigue behavior study of composite materials reinforced with unidirectional glass fibers [ECL-88-20] N90-13612

FATIGUE TESTS
Some new techniques for aircraft fuselage skin tests [LR-547] N90-13379
Study of fatigue degradation mechanisms in unidirectional composite materials. Application to cumulative damage [ECL-88-12] N90-13611
Contribution to the fatigue behavior study of composite materials reinforced with unidirectional glass fibers [ECL-88-20] N90-13612
Constant amplitude fatigue of ARALL-2 laminates [LR-539] N90-13615
Mechanical property characterization of VascoMax T-300 [AD-A212950] N90-13637
An investigation of gear mesh failure prediction techniques [NASA-TM-102340] N90-13785
Fatigue resistance of pressure vessels in high strength steels effect of some improvement techniques [CRIF-MT-176] N90-13799
An evaluation of a fatigue crack growth prediction model for variable-amplitude loading (PREFFAS) [LR-537] N90-13822

FAULT TOLERANCE
A fault-tolerant software algorithm for a network of transputers [AD-A213092] N90-13972
Laboratory test methodology for evaluating the effects of electromagnetic disturbances on fault-tolerant control systems [NASA-TM-101665] N90-14061

FAULT TREES
An artificial intelligence approach to analog system diagnosis [AD-A213135] N90-13992

FEDERAL BUDGETS
National Aeronautics and Space Administration Multiyear Authortzation Act of 1989 N90-14148
National Aeronautics and Space Administration authorization [S-HRG-101-348] N90-14149

FEEDBACK CONTROL
Impact of tether cutting on onboard navigation during the Tethered Satellite Mission-1 N90-13424
Adaptive strategies for controls of flexible arms [NASA-CR-185868] N90-13783
A new approach to control single-link flexible arms. Part 3: Adaptive control of the tip position with payload changes [AD-A213337] N90-13792
The problem of automation: Inappropriate feedback and interaction, not overautomation [NASA-CR-186126] N90-13994
The quadratic matrix inequality in singular H infinity control with state feedback [MEMO-COSOR-89-03] N90-13997
The singular H infinity control problem with dynamic measurement feedback [MEMO-COSOR-89-14] N90-14000
Another approach to the local disturbance decoupling problem with stability for nonlinear systems [MEMO-799] N90-14033

FENCES (BARRIERS)
Energy barriers in SK spin-glass model [PREPRINT-665] N90-14119

FERMENTATION
Fermentation and oxygen transfer in microgravity N90-13956

FERMIONS
Lattice QCD estimate of mixing parameters for heavy meson systems [PREPRINT-687] N90-14079
A lattice study of semileptonic decays of D-mesons [PREPRINT-660] N90-14086

FERROELECTRICITY
Studies of structure and switching dynamics in ferroelectric crystal and liquid crystal thin films [AD-A212650] N90-14109

FERROMAGNETIC MATERIALS
On geometry of inhomogeneous Heisenberg ferromagnet: Nonintegrable case [MEMO-789] N90-14030

FIBER COMPOSITES
Status of Gr/glass composites technology at UTOS N90-13459
Failure processes in unidirectional composite materials N90-13598
Localization of ultrasound in thick composites [AD-A212994] N90-13602
Fiber reinforced cementitious composites technology [PB89-227813] N90-13608
Impact tests of three composite materials with carbon fiber cores [REPT-M6-582500] N90-13610
Impact tests on aluminum 2024 T3, aramid and glass reinforced aluminum laminates and thermoplastic composites [LR-534] N90-13613
Constant amplitude fatigue of ARALL-2 laminates [LR-539] N90-13615

FIBER OPTICS
Silicon-etalon fiber-optic temperature sensor [NASA-TM-102389] N90-13381

FIBER ORIENTATION
Study of fatigue degradation mechanisms in unidirectional composite materials. Application to cumulative damage [ECL-88-12] N90-13611
Contribution to the fatigue behavior study of composite materials reinforced with unidirectional glass fibers [ECL-88-20] N90-13612

FIELD ALIGNED CURRENTS
The auroral current - voltage relationship N90-13843

FIELD EFFECT TRANSISTORS
Elaboration and characterization of MISFET transistors on InP [ECL-88-19] N90-13709
Integrated optoelectronic receivers [AD-A213376] N90-14098
Analytical and computer-aided models of InP-based MISFETs and heterojunction devices [AD-A211861] N90-14106
Field-effect spectroscopy of interface states [AD-A212998] N90-14112

FIELD OF VIEW
The baffles N90-13509

FIELD THEORY (PHYSICS)
Large deviation estimates in the stochastic quantization of phi sub 2 exp 4
[PREPRINT-666] N90-14050
FILAMENT WINDING
Preliminary experiments on filament winding nylon impregnated glass fibers (FIT)
[LR-545] N90-13669
FINITE DIFFERENCE THEORY
Computation of viscous incompressible flows
[NASA-TM-101090] N90-13329
Comparison of integral and finite-difference methods for predicting the turbulent boundary layer on axisymmetric bodies
[ARE-TM(UHA)-88512] N90-13752
Using Broyden updates to approximate the Jacobian in a semi-implicit backward differentiation code
[AD-A213239] N90-14010
FINITE ELEMENT METHOD
Constitutive modeling for isotropic materials (HOST)
[NASA-CR-174718] N90-13391
Review and evaluation of a turbomachinery throughflow finite element code
[AD-A213058] N90-13787
Probabilistic finite element analysis of dynamic structural response
[AD-A213249] N90-13789
A study on the sensitivity and simultaneous adjustment of a hoop-column antenna surface
[NASA-TM-101538] N90-13807
Time domain coupling of the boundary and finite element methods for elastodynamics
[AD-A213243] N90-13811
Investigation of difficult component effects on finite element model vibration prediction for the Bell AG-1G helicopter. Volume 2: Correlation results
[NASA-CR-181916-VOL-2] N90-13814
A mixed finite element solution of the linear acoustic equations
[ECL-89-006] N90-14075
FINITE VOLUME METHOD
Computation of flow fields around propellers and hovering rotors based on the solution of the Euler equations
[DLR-FB-89-37] N90-13333
Calculation of flow fields by the solution of the Euler equations using an extended finite volume discretization scheme
[DLR-FB-89-38] N90-13729
FINNED BODIES
Transonic Euler solutions on mutually interfering finned bodies
[AD-A213395] N90-13331
FLAME PROPAGATION
Experimental and computational study of combustion limits in natural-gas fueled internal combustion engines
[PB89-235196] N90-13673
An investigation of flame spread over shallow liquid pools in microgravity and nonair environments
[NASA-TM-102425] N90-13680
FLAME SPECTROSCOPY
Study of the hydroxyl radical by DRASC resonance in a high pressure flame — Diffusion Raman Anti-Stokes Coherence (DRASC)
[ONERA-RS-53/7131-PY] N90-13632
FLAMMABILITY
Experimental and computational study of combustion limits in natural-gas fueled internal combustion engines
[PB89-235196] N90-13673
FLARE STARS
Analysis of coordinated observations of a giant stellar flare
[NASA-CR-185961] N90-14176
FLAT PLATES
Computation of Navier-Stokes equations for three-dimensional flow separation
[NASA-TM-102266] N90-13353
FLAVOR (PARTICLE PHYSICS)
Aspects of the physics of the standard model
[PREPRINT-670] N90-14067
FLEXIBLE BODIES
Adaptive strategies for controls of flexible arms
[NASA-CR-185868] N90-13783
FLEXIBLE SPACECRAFT
Simulation of spacecraft attitude dynamics using TREETOPS and model-specific computer Codes N90-13419
Explicit modeling and concurrent processing in the simulation of multibody dynamic systems N90-13481
The dynamics and control of large flexible space structures - 12, supplement 11
[NASA-CR-185966] N90-13494
FLIGHT CONDITIONS
A technique for the prediction of aerodynamics and aeroelasticity of rotor blades N90-13377
FLIGHT CONTROL
STOVL aircraft simulation for integrated flight and propulsion control research
[NASA-TM-102419] N90-13389
A knowledge-based system design/information tool for aircraft flight control systems
[NASA-TM-101704] N90-13990
FLIGHT CREWS
Test procedures for the evaluation of helmet and headset mounted active noise reduction systems
[AD-A212991] N90-13937
Human factors research in aircrew performance and training
[AD-A213285] N90-13938
FLIGHT FATIGUE
Simulator induced sickness in the CP-140 (Aurora) flight deck simulator
[AD-A213096] N90-13923
FLIGHT MANAGEMENT SYSTEMS
Computer-based tools for assisting air traffic controllers with arrivals flow management
[RSRE-88001] N90-13366
A knowledge-based system design/information tool for aircraft flight control systems
[NASA-TM-101704] N90-13990
A knowledge-based flight status monitor for real-time application in digital avionics systems
[NASA-TM-101710] N90-13995
FLIGHT MECHANICS
Flight Mechanics/Estimation Theory Symposium, 1989
[NASA-CP-3050] N90-13413
Optimal trajectories for the Aeroassisted Flight Experiment. Part 1: Equations of motion in an Earth-fixed system
[NASA-CR-186134] N90-13441
Optimal trajectories for the Aeroassisted Flight Experiment. Part 2: Equations of motion in an inertial system
[NASA-CR-186135] N90-13442
FLIGHT OPTIMIZATION
Induced drag for non-planar wings
[LR-521] N90-13357
FLIGHT PLANS
National Airspace System flight planning operational concept
[DOT/FAA/DS-89/30] N90-13362
FLIGHT SAFETY
National Airspace System airspace management operational concept
[DOT/FAA/DS-89/29] N90-13361
National Airspace System flight planning operational concept
[DOT/FAA/DS-89/30] N90-13362
An update to the system safety study of TCAS 2
[DOT/FAA/SA-89/3] N90-13363
FLIGHT SIMULATION
Mathematical model identification for flight simulation, based on flight and taxi tests
[LR-550] N90-13410
The relationship between subjective and objective measures of simulator-induced ataxia
[AD-A213095] N90-13922
Preliminary study of pharmacological control of space disease
[ETN-90-95015] N90-13927
Human factors research in aircrew performance and training
[AD-A213285] N90-13938
FLIGHT SIMULATORS
Software and hardware description of the helicopter motion equations for VAX computers
[AD-A213248] N90-13375
Simulator induced sickness in the CP-140 (Aurora) flight deck simulator
[AD-A213096] N90-13923
Compensatory tracking in disturbance tasks and target following tasks. The influence of cockpit motion on performance and control behavior
[LR-511] N90-13933
FLIGHT TESTS
Correlation of Puma airloads: Lifting-line and wake calculation
[NASA-TM-102212] N90-13327
LORAN C stability integrity assurance
[AD-A212663] N90-13364
FLIGHT TRAINING
The relationship between subjective and objective measures of simulator-induced ataxia
[AD-A213095] N90-13922
FLOOD PREDICTIONS
A collection of papers related to heavy precipitation forecasting
[PB89-230833] N90-13910
FLOW CHARACTERISTICS
An introduction via vorticity dynamics and statistical theory — turbulent shear flows N90-13731
Coherent structures in a round jet N90-13733
Navier-Stokes simulation of the crossflow instability in swept-wing flows
[NASA-CR-186122] N90-13744
FLOW DISTRIBUTION
Application of a self-adaptive grid method to complex flows
[NASA-TM-102223] N90-13324
Analysis of experimental data for CAST 10-2/DOA 2 supercritical airfoil at low Reynolds numbers and application to high Reynolds number flow
[AD-A211654] N90-13326
Study of the integration of wind tunnel and computational methods for aerodynamic configurations
[NASA-TM-102196] N90-13332
Computation of flow fields around propellers and hovering rotors based on the solution of the Euler equations
[DLR-FB-89-37] N90-13333
Blunt-nose inviscid airflows with coupled nonequilibrium processes N90-13336
A CFD study of tilt rotor flowfields
[NASA-CR-186116] N90-13349
Optimum shape of a blunt forebody in hypersonic flow
[NASA-CR-181955] N90-13351
Computation of Navier-Stokes equations for three-dimensional flow separation
[NASA-TM-102266] N90-13353
Application of an efficient hybrid scheme for aeroelastic analysis of advanced propellers
[NASA-TM-102428] N90-13355
A smoke generator system for aerodynamic flight research
[NASA-TM-4137] N90-13372
A planar reacting shear layer system for the study of fluid dynamics-combustion interaction
[NASA-TM-102422] N90-13393
A wall interference assessment/correction interface measurement system for the NASA/ARC 12-ft PWT
[NASA-CR-185474] N90-13401
Gas flows in rocket motors, volume 1
[AD-A213348] N90-13591
SSME LOX post flow analysis/fluid structure interaction. Volume 1: Flow analysis
[NASA-CR-183677] N90-13715
Calculation of flow fields by the solution of the Euler equations using an extended finite volume discretization scheme
[DLR-FB-89-38] N90-13729
An introduction via vorticity dynamics and statistical theory — turbulent shear flows N90-13731
Numerical Methods for Flows in Turbomachinery, volume 1
[VKI-LS-1989-06-VOL-1] N90-13735
Unsteady forces induced on finite-span cylinders in a cross-flow N90-13746
Convective heat transfer measurements from a NACA 0012 airfoil in flight and in the NASA Lewis Icing Research Tunnel
[NASA-TM-102448] N90-13750
Computation of nonequilibrium gas flow past blunt bodies
[PREPRINT-488] N90-13757
On the topology of three-dimensional viscous flow structures near a plane wall. A classification and non-hyperbolic singularities on the wall
[LR-541] N90-13758
An interactive grid generation procedure for axial and radial flow turbomachinery
[NASA-CR-185167] N90-13968
FLOW EQUATIONS
Balance laws and centro velocity in dissipative systems
[MEMO-797] N90-13726
FLOW GEOMETRY
Block-structured solution of three-dimensional transonic flows using parallel processing
[AD-A212851] N90-13330
The influence of multiple hot-wire probe geometry on the results of measurements in turbulent flows
[DLR-FB-89-26] N90-13724
Numerical Methods for Flows in Turbomachinery, volume 1
[VKI-LS-1989-06-VOL-1] N90-13735
Comparison of integral and finite-difference methods for predicting the turbulent boundary layer on axisymmetric bodies
[ARE-TM(UHA)-88512] N90-13752
FLOW MEASUREMENT
Skin friction measurements with hot elements N90-13345
Pressure measurement techniques in use at the Royal Aerospace Establishment N90-13347
The influence of multiple hot-wire probe geometry on the results of measurements in turbulent flows
[DLR-FB-89-26] N90-13724

On the nonexistence of a strong solution in the boundary problem for a sticky Brownian motion
[CWI-BS-R8901] N90-14018

FLOW STABILITY
Effect of suction and cooling on the stability of subsonic and supersonic boundary layers N90-13745

FLOW VELOCITY
Measurement Techniques in Aerodynamics
[VKI-LS-1989-05] N90-13339
Practical systems for speckle velocimetry N90-13341
Laser two focus techniques N90-13348
Coherent structures in a round jet N90-13733
Numerical Methods for Flows in Turbomachinery, volume 1
[VKI-LS-1989-06-VOL-1] N90-13735
Unsteady forces induced on finite-span cylinders in a cross-flow N90-13746

FLOW VISUALIZATION
Study of forces and moments on wing-bodies at high incidence, volumes 1 and 2 N90-13350
A smoke generator system for aerodynamic flight research
[NASA-TM-4137] N90-13372
A vapor generator for transonic flow visualization
[NASA-TM-101670] N90-13403

FLUID DYNAMICS
A review of quasi-coherent structures in a numerically simulated turbulent boundary layer
[NASA-TM-102191] N90-13723
Application of multi-grid methods for solving the Navier-Stokes equations
[NASA-TM-102359] N90-14002

FLUID FLOW
Application of a self-adaptive grid method to complex flows
[NASA-TM-102223] N90-13324
SSME LOX post flow analysis/fluid structure interaction. Volume 1: Flow analysis
[NASA-CR-183677] N90-13715

FLUID MECHANICS
Tank pressure control experiment on the space shuttle
[NASA-TM-102313] N90-13590

FLUORIDES
Generation of iodine monofluoride in a supersonic multipurpose flowtube facility
[AD-A213082] N90-13774

FLUOROHYDROCARBONS
Studies of Aflas fluoroelastomers
[AD-A213046] N90-13622

FLUOROPOLYMERS
Studies of Aflas fluoroelastomers
[AD-A213046] N90-13622

FLUX DENSITY
Balance laws and centro velocity in dissipative systems
[MEMO-797] N90-13726
Measurement of the light flux density patterns from luminaires proposed as photon sources for photosynthesis during space travel
[NASA-CR-186124] N90-13916

FOCAL PLANE DEVICES
Status of direct detector and array development N90-13464
Advances in SIS receiver technology N90-13466
Discussion of factors affecting the sensitivity of IR imaging sensors, particularly focal plane mosaic arrays --- staring mosaic arrays
[FOA-C-30536-3.1] N90-14101

FOLIAGE
Stochastic modelling of EM scattering from foliage
[AD-A213118] N90-13689

FOREBODIES
Optimum shape of a blunt forebody in hypersonic flow
[NASA-CR-181955] N90-13351

FORTRAN
FORTRAN subroutines for the evaluation of the confluent hypergeometric functions
[AD-A213308] N90-14012

FOURIER ANALYSIS
Data acquisition in aerodynamic research N90-13340
The initial imperfection data bank at the Delft University of Technology, part 2
[LR-559-PT-2] N90-13825

FOURIER TRANSFORMATION
Implementing the discrete Fourier transform on the hypercube FPS T40
[IMAG-RR-773-I] N90-13983
Distribution of a sum of n random variables and a central limit theorem based on moments or on coefficients of polynomial dependence
[IMAG-RR-768-M] N90-14040

FRACTALS
Configurational statistics of strings, fractals and polymer physics. Part 2: Non Abelian strings
[ROM1F-89-680-PT-2] N90-14067

FRACTOGRAPHY
Fractography of composite delamination
[NASA-CR-183291] N90-13599

FRACTURE MECHANICS
Ductile failure
[AD-A212975] N90-13601
Fatigue behavior of silicon carbide Whisker/Aluminum composite
[AD-A213094] N90-13603
The adhesive bonding of thermoplastic composites
[AD-A213358] N90-13605
Toughening mechanisms in ceramic composites
[PB89-235907] N90-13656
Theoretical evaluation of defects in pressure vessels and pipings
[CRIF-MT-174] N90-13798
Stress intensity factors for cracking metal structures under rapid thermal loading. Volume 2: Theoretical background
[AD-A213297] N90-13812
Application of fracture mechanics and half-cycle method to the prediction of fatigue life of B-52 aircraft pylon components
[NASA-TM-88277] N90-13820

FRACTURE STRENGTH
Mechanical property characterization of VascoMax T-300
[AD-A212950] N90-13637
Toughening mechanisms in ceramic composites
[PB89-235907] N90-13656

FRACTURES (MATERIALS)
A theory of damage in brittle and cementitious materials, part 1
[AD-A212940] N90-13658
Theoretical evaluation of defects in pressure vessels and pipings
[CRIF-MT-174] N90-13798
The Fourth Oxford International Conference on the Mechanical Properties of Materials at High Rates of Strain
[AD-A212293] N90-13809

FRAMES (DATA PROCESSING)
Overview of the data acquisition and reductions N90-13549

FREE ELECTRON LASERS
Ultrafast processes and spectroscopy with free electron lasers
[AD-A212869] N90-13773
Synchrotron-betatron parametric instability in free-electron lasers
[AD-A213373] N90-13777
An experimental analysis of the waveguide modes in a high-gain free-electron laser amplifier N90-13779

FREE ENERGY
Reorganization free energy for electron transfers at liquid-liquid and dielectric semiconductor-liquid interfaces
[AD-A212965] N90-14111
Energy barriers in SK spin-glass model
[PREPRINT-665] N90-14119

FREE JETS
Vapor condensation on liquid surface due to laminar jet-induced mixing: The effects of system parameters
[NASA-TM-102433] N90-13751

FREE RADICALS
Generation of free radicals during cold injury and rewarming
[AD-A213088] N90-13915

FREE VIBRATION
Static and free-vibrational response of semi-circular graphite-epoxy frames with thin-walled open sections
[NASA-CR-186097] N90-13800

FREEZING
Generation of free radicals during cold injury and rewarming
[AD-A213088] N90-13915

FRENCH SPACE PROGRAMS
The French balloon program and related space research N90-13828
Operational activity in France and a new method of balloon temperature piloting N90-13857

FREQUENCY MEASUREMENT
Modeling and measurement methods for high speed bipolar transistors
[REPT-11] N90-13714
Analysis of an R-SQUID noise thermometer
[VTT-PUBL-54] N90-13769

FRICTION
A new approach to control single-link flexible arms. Part 3: Adaptive control of the tip position with payload changes
[AD-A213337] N90-13792
The limiting friction force
[ECL-89-005] N90-13801

FUEL COMBUSTION
Two-dimensional analysis of two-phase reacting flow in a firing direct-injection diesel engine
[NASA-TM-102069] N90-13392
An investigation of flame spread over shallow liquid pools in microgravity and nonair environments
[NASA-TM-102425] N90-13680
Analysis of rotary engine combustion processes based on unsteady, three-dimensional computations
[NASA-TM-102469] N90-13749

FUEL CONSUMPTION
Trajectory optimization and guidance for an aerospace plane
[NASA-CR-185884] N90-13369

FUEL INJECTION
Two-dimensional analysis of two-phase reacting flow in a firing direct-injection diesel engine
[NASA-TM-102069] N90-13392
LOX/hydrocarbon combustion instability investigation
[NASA-CR-182249] N90-13589
Analysis of rotary engine combustion processes based on unsteady, three-dimensional computations
[NASA-TM-102469] N90-13749

FUEL-AIR RATIO
A planar reacting shear layer system for the study of fluid dynamics-combustion interaction
[NASA-TM-102422] N90-13393

FUELS
Novel carbamates, their production and their use as fuels additives
[EP-PATENT-0-298-636-A-1] N90-13676

FUSELAGES
Some new techniques for aircraft fuselage skin tests
[LR-547] N90-13379

G

GALACTIC EVOLUTION
An experiment to search for galactic axions N90-14158
String correlations and galaxies formation
[ROM1F-89-677] N90-14170
Non Abelian string correlations and galaxies formation
[ROM1F-89-678] N90-14171
Des Cloizeaux's law for strings and galaxies formation. Part 2: Non Abelian configurations
[ROM1F-89-682-PT-2] N90-14173
The grand unified photon spectrum: A coherent view of the diffuse extragalactic background radiation
[NASA-CR-186077] N90-14180

GALACTIC RADIATION
Interstellar medium and infrared emission of the galactic disk N90-13862

GALACTIC STRUCTURE
Archival research on absorption lines in violently star-forming galaxies
[NASA-CR-185960] N90-14163

GALAXIES
Archival research on absorption lines in violently star-forming galaxies
[NASA-CR-185960] N90-14163

GALLIUM ARSENIDES
Electrochemical study of the etching of III to V semiconductors
[ETN-90-95015] N90-13633
Development of high gain three terminal devices - at millimeter wave frequencies
[AD-A213089] N90-13701
Photoelectrochemical behavior of type n of GaAs in concentrated iodide media and realization of an experimental device
[ECL-88-18] N90-14117
GaAs and GaAs:In: Influence of surface treatments and characterization of homogeneity by photoluminescent imagery
[ECL-88-24] N90-14118

GAME THEORY
The singular zero sum differential game with stability using H infinity control theory
[MEMO-COSOR-89-09] N90-13999
The activity selection problem: A network and game theoretic approach
[MEMO-794] N90-14056

GAMMA RAY OBSERVATORY
A gyroscope calibration analysis for the Gamma Ray Observatory (GRO) N90-13428

GAS ANALYSIS
The mobile combustion diagnostic fixture and its application to the study of propellant combustion. Part 1: Investigation of the low pressure combustion of LOVA XM39 propellant
[AD-A213272] N90-13626

GAS BEARINGS
Development and testing of a contactless static/dynamic shaft seal with little sealing gas requirement
[KFK-4599] N90-13602

GAS COOLING
Gas flows in rocket motors, volume 1
[AD-A213348] N90-13591

GAS DETECTORS
Gas identification system using graded temperature sensor and neural net interpretation
[AD-A213359] N90-13627
Multisensor technologies for low cost methane detection
[PB89-235188] N90-13766

GAS DISSOCIATION
Theory of stagnation point heat transfer in dissociated air N90-13337

GAS EVOLUTION
Gas evolution and bubble formation on electrodes
[DLR-FB-89-35] N90-13629

GAS FLOW
Recent progress in research pertaining to estimates of gas-side heat transfer in an aircraft gas turbine
[NASA-TM-102460] N90-13394
Gas flows in rocket motors. Volume 2, appendix C: Time iterative solution of viscous supersonic flow
[AD-A213349] N90-13592
Gas flows in rocket motors. Volume 3, appendix D: Computer code listings
[AD-A213350] N90-13593

GAS MIXTURES
Gas identification system using graded temperature sensor and neural net interpretation
[AD-A213359] N90-13627
Propagation of sound in vibrationally excited nitrogen and hydrogen gas mixtures
[AD-A213002] N90-14073

GAS TEMPERATURE
Gas identification system using graded temperature sensor and neural net interpretation
[AD-A213359] N90-13627

GAS TURBINE ENGINES
Constitutive modeling for isotropic materials (HOST)
[NASA-CR-179522] N90-13390
Constitutive modeling for isotropic materials (HOST)
[NASA-CR-174718] N90-13391
Recent progress in research pertaining to estimates of gas-side heat transfer in an aircraft gas turbine
[NASA-TM-102460] N90-13394

GAS-SOLID INTERACTIONS
Modelling of satellite control thruster plumes N90-13578

GASEOUS FUELS
Gas identification system using graded temperature sensor and neural net interpretation
[AD-A213359] N90-13627

GASES
Space station gas compressor technology study program, phase 1
[NASA-CR-183758] N90-13491

GASOLINE
MOBILE4 oxygenated fuels version user's guide
[PB89-230700] N90-13674

GATES (CIRCUITS)
A counter gating circuit for acoustic emission monitoring of structures cracking under repetitive alternating loads
[ARL-MAT-TM-398] N90-13808

GEAR TEETH
Conjugate profiles on mating gear teeth
[MEMO-COSOR-89-01] N90-13795

GEARS
An investigation of gear mesh failure prediction techniques
[NASA-TM-102340] N90-13785

GEOCHEMISTRY
Summaries of the thematic conferences on remote sensing for exploration geology
[NASA-CR-185321] N90-13880

GEOCORONAL EMISSIONS
Interzodiak 2: Observation of EUV-resonance radiation N90-13854

GEODESIC LINES
On geometry of inhomogeneous Heisenberg ferromagnet: Nonintegrable case
[MEMO-789] N90-14030

GEOLOGY
Summaries of the thematic conferences on remote sensing for exploration geology
[NASA-CR-185321] N90-13880

GEOMAGNETISM
Spacecraft attitude determination using the earth's magnetic field N90-13429

GEOMETRIC RECTIFICATION (IMAGERY)
Algorithm for atmospheric corrections of aircraft and satellite imagery
[NASA-TM-100751] N90-13976

GEOMETRY
A new model for the structure of silica glass
[AD-A212972] N90-13659

GEOMORPHOLOGY
Late quaternary geomorphology of the Great Salt Lake region, Utah, and other hydrographically closed basins in the western United States: A summary of observations
[NASA-CR-185912] N90-13878

GEOPHYSICS
The Swedish sounding rocket and balloon program N90-13830

GEOPOTENTIAL
Climate predictability: A dynamical view
[AERONOMICA-ACTA-A-347-1989] N90-13909

GERMANIUM
Manufacturing and characterization of insulator-germanium structures
[ECL-88-13] N90-14115

GERMANY
The German space science program N90-13873

GLASS
Synthesis of inorganic polymers as glass precursors and for other uses. Preceramic block or graft copolymers as potential precursors to nanocomposite materials
[AD-A211978] N90-13655
Preparation of 110K (Bi, Pb)-Sr-Ca-Cu-O superconductor from glass precursor
[NASA-CR-185162] N90-14108

GLASS FIBER REINFORCED PLASTICS
Study of fatigue degradation mechanisms in unidirectional composite materials. Application to cumulative damage
[ECL-88-12] N90-13611
Contribution to the fatigue behavior study of composite materials reinforced with unidirectional glass fibers
[ECL-88-20] N90-13612
Preliminary experiments on filament winding nylon impregnated glass fibers (FIT)
[LR-545] N90-13669

GLOBAL POSITIONING SYSTEM
Test network Delft
[ETN-90-96009] N90-13365
Geodetic network adjustment using GPS triple difference observations and a priori stochastic information
[TR-1-1987] N90-13367
Processing of undifferences GPS carrier beat phase measurements and adjustment computations
[TR-5-1988] N90-13368
Supplementing geodetic data with prior information for crustal deformation in the Imperial Valley, California
[TR-6-1988] N90-13904

GLOBULAR CLUSTERS
Deep detection of hot star populations at balloon ultraviolet wavelengths N90-13865

GLUONS
Measurement of the fractional momentum carried by the gluons in the low Q2 photon-gluon fusion events at the ep HERA collider
[NOTA-INTERNA-937] N90-14083

GODDARD TRAJECTORY DETERMINATION SYSTEM
Lifetime predictions for the Solar Maximum Mission (SMM) and San Marco spacecraft N90-13440

GOES SATELLITES
GOES-I/M ascent maneuvers from transfer orbit to station N90-13421

GOODNESS OF FIT
Theory of goodness of fit tests and scanning innovation martingales
[CWI-BS-R8904] N90-14046

GOVERNMENT/INDUSTRY RELATIONS
Small business innovation research: Program solicitation
[NASA-TM-101869] N90-14126

GRAPH THEORY
Novel graph searching methods for image analysis
[AD-A213065] N90-13971
On smallest nonhamiltonian regular rough graphs
[MEMO-788] N90-14003
Hamiltonian properties of graphs with large neighborhood unions
[MEMO-779] N90-14013
A graph theoretic characterization for the rank of the transfer matrix of a structured system
[CWI-OS-R8819] N90-14064

GRAPHITE
Implementation and analysis of adhesion in multimaterials of the type Al(Si)-ZrO2 and graphite, metal or ceramics
[ECL-89-004] N90-13667

GRAPHITE-EPOXY COMPOSITES
Lightweight composite reflector panels N90-13462
Static and free-vibrational response of semi-circular graphite-epoxy frames with thin-walled open sections
[NASA-CR-186097] N90-13600
Gravimetric measurements of materials outgassing applied to graphite-epoxy laminates
[NASA-TM-100753] N90-13609

GRAPHS (CHARTS)
Compression of bitmapped graphic data
[AD-A213141] N90-13974
On smallest nonhamiltonian regular rough graphs
[MEMO-788] N90-14003
Hamiltonian properties of graphs with large neighborhood unions
[MEMO-779] N90-14013
On the performance of on-line algorithms for partition problems
[MEMO-784] N90-14015
Linear groups and distance-transitive graphs
[CWI-PM-R8805] N90-14036
On distance-transitive graphs and involutions
[CWI-PM-R8808] N90-14037

GRATINGS (SPECTRA)
Real-time sensing of optical alignment N90-13479

GRAVIMETERS
GRADIO: An error analysis of the spaceborne gravity gradiometer
[ETN-90-96010] N90-13901

GRAVIMETRY
Gravimetric measurements of materials outgassing applied to graphite-epoxy laminates
[NASA-TM-100753] N90-13609

GRAVIRECEPTORS
Gravity receptors and responses N90-13948

GRAVITATIONAL COLLAPSE
Correlation among gravitational wave and neutrino detectors data during SN1987A
[NOTA-INTERNA-932] N90-14165

GRAVITATIONAL EFFECTS
Optimum data weighting and error calibration for estimation of gravitational parameters N90-13437
Facilities for microgravity combustion research
[NASA-TM-102014] N90-13679
Cells in Space
[NASA-CP-10034] N90-13939
Fundamental results from microgravity cell experiments with possible commericial applications N90-13940
Polarity establishment, morphogenesis, and cultured plant cells in space N90-13943
How to detect when cells in space perceive gravity N90-13946
Effects of microgravity on growth hormone concentration and distribution in plants N90-13947
Free swimming organisms: Microgravity as an investigative tool N90-13949
Human factors issues in performing life science experiments in a 0-G environment N90-13952
Countermeasures to microgravity N90-13957

GRAVITATIONAL FIELDS
GRADIO: An error analysis of the spaceborne gravity gradiometer
[ETN-90-96010] N90-13901

GRAVITATIONAL PHYSIOLOGY
Cells in Space
[NASA-CP-10034] N90-13939
How to detect when cells in space perceive gravity N90-13946
Gravity receptors and responses N90-13948
Do the design concepts used for the space flight hardware directly affect cell structure and/or cell function ground based simulations N90-13953

GRAVITATIONAL WAVE ANTENNAS
Expected supernovae rates and gravitational waves detection
[NOTA-INTERNA-933] N90-14166

GRAVITATIONAL WAVES
Correlation among gravitational wave and neutrino detectors data during SN1987A
[NOTA-INTERNA-932] N90-14165
Detectable gravitational waves by supernova SN 1987 A pulsar relic
[PREPRINT-658] N90-14174

GRAVITROPISM
Gravitropism in plants: Hydraulics and wall growth properties of responding cells N90-13950

GRAVITY WAVES
The effects of gravity waves on horizontal layers: Simulation and interpretation N90-13852
Polar mesosphere summer echoes and associated atmospheric gravity waves N90-13856

GREAT CIRCLES
The great circle reductions N90-13553
Great circle interactions: Attitude smoothing and grid-step inconsistencies N90-13554
General and numerical approach to the sphere solution in FAST N90-13555

Astrometric parameter determination in FAST N90-13556
The sphere solution and astrometric parameter determination in NDAC N90-13557
Great circle reductions: Implementation and simulations N90-13569
Implementation and simulations of the sphere solution in FAST N90-13570
Experiments towards a global sphere solution N90-13576

GREEN'S FUNCTIONS
Characteristic impedance of microstrip lines [NASA-TM-101581] N90-13694
Numerical analysis of scattering by interface flaws [AD-A212996] N90-13810
Towards ab initio calculation of electron energies in semiconductors [ETN-90-96016] N90-14121

GRID GENERATION (MATHEMATICS)
Transonic Euler solutions on mutually interfering finned bodies [AD-A213395] N90-13331
The initial-boundary value problem for the Davey-Stewartson 1 equation; how to generate and drive localized coherent structures in multidimensions [PREPRINT-684] N90-13756
An interactive grid generation procedure for axial and radial flow turbomachinery [NASA-CR-185167] N90-13968

GROUND OPERATIONAL SUPPORT SYSTEM
The Hipparcos Mission. Prelaunch status. Volume 2: The input catalog [ESA-SP-1111-VOL-2] N90-13529
Ground-based astrometric measurements N90-13536
New ground-based photometric measurements N90-13538
The link to extragalactic objects N90-13544
On-ground attitude determination N90-13552

GROUND STATE
Generation of iodine monofluoride in a supersonic multipurpose flowtube facility [AD-A213082] N90-13774

GROUND STATIONS
Test network Delft [ETN-90-96009] N90-13365

GROUND SUPPORT EQUIPMENT
Electrical testing N90-13520
The in-orbit initialization phase N90-13525
Andoya rocket range: New installations, future plans, and investments N90-13859

GROUND SUPPORT SYSTEMS
The role of the ground segment N90-13527
The DYANA campaign 1990 N90-13870
Esrange N90-13876

GROUND TESTS
Helicopter rotor test rig (RoTeSt) in DNW: Application and results [RAE-TRANS-2171] N90-13408
On-ground photometric calibration N90-13523

GUNNERY TRAINING
Human factors research in aircrew performance and training [AD-A213285] N90-13938

GYRATION
Extension to Eulers's theorem to n-dimensional spaces N90-13431

GYROSCOPES
A gyroscope calibration analysis for the Gamma Ray Observatory (GRO) N90-13428
Analytical derivation and verification of zero-gyro control for the IUE satellite [NASA-TM-100748] N90-13767

GYROSCOPIC COUPLING
Bilinear modeling and nonlinear estimation N90-13430

GYROSCOPIC STABILITY
True covariance simulation of the EUVE update filter N90-13427
A gyroscope calibration analysis for the Gamma Ray Observatory (GRO) N90-13428
Spacecraft attitude determination using the earth's magnetic field N90-13429
Extended Kalman filter for attitude estimation of the earth radiation budget satellite N90-13433

H

H II REGIONS
Orion B: Anatomy of a star-forming region N90-14155

HADRONS
Measurement of the fractional momentum carried by the gluons in the low Q2 photon-gluon fusion events at the ep HERA collider [NOTA-INTERNA-937] N90-14083
Aspects of the physics of the standard model [PREPRINT-670] N90-14087
Model-independent analysis of the Z line shape in e+e- annihilation [PREPRINT-679] N90-14089
Big Bang nucleosynthesis and the Quark-Hadron transition [NASA-CR-186169] N90-14168

HALOCARBONS
Ultraviolet absorption cross-sections of bromoform in the temperature range 295-240 K [AERONOMICA-ACTA-A-348-1989] N90-13630

HALOS
An experiment to search for galactic axions N90-14158

HAMILTONIAN FUNCTIONS
Periodic solutions of Hamiltonian systems of 3-body type [AD-A212891] N90-14005
Hamiltonian properties of graphs with large neighborhood unions [MEMO-779] N90-14013
Using the physical structure of a system for control: An illustration [MEMO-782] N90-14014
On a new integrable Hamiltonian system with nearest neighbors interaction [PREPRINT-667] N90-14043
A unified algebraic approach to integral and discrete evolution equations [PREPRINT-668] N90-14044
R-matrices and higher Poisson brackets for integrable systems [PREPRINT-669] N90-14069

HARDNESS
Quench sensitivity in Al-Cu-Li alloys [AD-A213055] N90-13639

HARMONIC ANALYSIS
First-order Bragg SAR imagery of Kelvin wakes and moving internal wave fields [AD-A213361] N90-13691
The initial imperfection data bank at the Delft University of Technology, part 2 [LR-559-PT-2] N90-13825

HAZARDS
Re-entry hazards and cosmos 1900 [FOA-C-30535-9.4] N90-13583

HEARING
Speech reception in quiet and in noisy conditions by individuals with noise-induced hearing loss in relation to their audiogram [IZF-1989-11] N90-13692
Evaluation of speech intelligibility through a bone conduction stimulator [AD-A212002] N90-13919
A prototype microprocessor based audiometer for use by the CF (Canadian Forces) medical services for periodic hearing tests [AD-A212990] N90-13921

HEAT PIPES
An improved algorithm for the modeling of vapor flow in heat pipes [NASA-CR-185179] N90-13748

HEAT RESISTANT ALLOYS
Constitutive modeling for isotropic materials (HOST) [NASA-CR-179522] N90-13390
Constitutive modeling for isotropic materials (HOST) [NASA-CR-174718] N90-13391
Joint Services Electronics Program [AD-A213015] N90-13699

HEAT TRANSFER
An Introduction to Hypersonic Aerodynamics [VKI-LS-1989-01] N90-13334
Theory of stagnation point heat transfer in dissociated air N90-13337
On catalytic recombination rates in hypersonic stagnation heat transfer N90-13338
Recent progress in research pertaining to estimates of gas-side heat transfer in an aircraft gas turbine [NASA-TM-102460] N90-13394
Metal transfer in gas metal arc welding [AD-A213390] N90-13642

HEAT TRANSFER COEFFICIENTS
Convective heat transfer measurements from a NACA 0012 airfoil in flight and in the NASA Lewis Icing Research Tunnel [NASA-TM-102448] N90-13750

HEAT TREATMENT
Quench sensitivity in Al-Cu-Li alloys [AD-A213055] N90-13639

HEATING EQUIPMENT
Qualification of improved joint heaters [NASA-CR-183827] N90-13594

HEAVY LIFT LAUNCH VEHICLES
Definition of avionics concepts for a heavy lift cargo vehicle, appendix A [NASA-CR-183817] N90-13380

HEISENBERG THEORY
On geometry of inhomogeneous Heisenberg ferromagnet: Nonintegrable case [MEMO-789] N90-14030

HELICOPTER CONTROL
Preliminary airworthiness evaluation of the AH-64A equipped with the Air To Air Stinger (ATAS) missile system [AD-A213030] N90-13374

HELICOPTER PERFORMANCE
Correlation of Puma airloads: Lifting-line and wake calculation [NASA-TM-102212] N90-13327
Preliminary airworthiness evaluation of the AH-64A equipped with the Air To Air Stinger (ATAS) missile system [AD-A213030] N90-13374
Software and hardware description of the helicopter motion equations for VAX computers [AD-A213248] N90-13375

HELICOPTER TAIL ROTORS
A model suitable for predicting the noise associated with the ducted tail rotor of a helicopter [ECL-88-09] N90-14074

HELICOPTERS
The human factors relating to escape and survival from helicopters ditching in water [AGARD-AG-305(E)] N90-13358
Helicopter rotor test rig (RoTeSt) in DNW: Application and results [RAE-TRANS-2171] N90-13408
Human factors research in aircrew performance and training [AD-A213285] N90-13938

HELIOSPHERE
An implementation plan for priorities in solar-system space physics [NASA-CR-185375] N90-14154

HELIUM IONS
Optical observations of interplanetary pick-up ions: The experiment Helly N90-13863

HELIUM ISOTOPES
A four channel He-3 cooled balloon-borne bolometer radiometer N90-13469
Construction of the rotating cryostat ROTA2, its use for zero sound experiments in (3)He-B, and calculations of ion mobility in (3)He-A and (3)He-P [ISBN-952-90091-3-5] N90-13765
The effective (3)He-nucleon force in a microscopic DWBA approach to the (3)He,t charge exchange reaction --- Distorted Wave-Borne Approximation (DWBA) [KVI-763] N90-14077

HELMETS
Test procedures for the evaluation of helmet and headset mounted active noise reduction systems [AD-A212991] N90-13937

HERMETIC SEALS
Development and testing of a contactless static/dynamic shaft seal with little sealing gas requirement [KFK-4599] N90-13802

HERMITIAN POLYNOMIAL
Distribution of a sum of n random variables and a central limit theorem based on moments or on coefficients of polynomial dependence [IMAG-RR-768-M] N90-14040

HETEROJUNCTION DEVICES
The photovoltaic properties of an Al In As/InP heterojunctions grown by LPE method [NASA-CR-185996] N90-13886
Analytical and computer-aided models of InP-based MISFETs and heterojunction devices [AD-A211861] N90-14106

HIGH ALTITUDE BALLOONS
Three-meter balloon-borne telescope N90-13490

HIGH ELECTRON MOBILITY TRANSISTORS
Development of high gain three terminal devices - at millimeter wave frequencies [AD-A213089] N90-13701

HIGH GAIN
Development of high gain three terminal devices - at millimeter wave frequencies [AD-A213089] N90-13701

HIGH LEVEL LANGUAGES
Applications of artificial intelligence to space station and automated software techniques: High level robot command language [NASA-CR-182997] N90-13991
Architecture and language for a layered relational database N90-14146

HIGH POWER LASERS
Proceedings of the High Energy Density Matter (HEDM) Conference
[AD-A212314] N90-13670
HIGH RESOLUTION
Reflection indicatrices of natural surfaces for AVHRR channels 1 and 2
[DLR-MITT-89-16] N90-13882
HIGH SPEED
Modeling and measurement methods for high speed bipolar transistors
[REPT-11] N90-13714
HIGH STRENGTH ALLOYS
The effect of composition and aging treatment on the microstructure and mechanical properties of aluminum-lithium-titanium alloys
[AD-A213144] N90-13640
HIGH STRENGTH STEELS
Fatigue resistance of pressure vessels in high strength steels effect of some improvement techniques
[CRIF-MT-176] N90-13799
HIGH TEMPERATURE
High temperature capacitive strain gage
[NASA-CR-4266] N90-13760
Stress intensity factors for cracking metal structures under rapid thermal loading. Volume 2: Theoretical background
[AD-A213297] N90-13812
HIGH TEMPERATURE RESEARCH
The Materials Division: A case study
[NASA-TM-102360] N90-13597
HIGH TEMPERATURE SUPERCONDUCTORS
Microwave microstrip resonator measurements of Y1Ba2Cu3O(7-x) and Bi2Sr2Ca1Cu2O(8-y) thin films
[NASA-TM-102159] N90-13704
Construction of a SQUID magnetometer for investigation of screening properties of high-T(sub c) superconductors
[FOA-C-20765-2.2] N90-13766
Preparation of 110K (Bi, Pb)-Sr-Ca-Cu-O superconductor from glass precursor
[NASA-CR-185162] N90-14108
Local pairing and antiferromagnetism in high-T sub c superconductors
[AD-A213004] N90-14113
HIPPARCOS SATELLITE
The Hipparcos Mission. Prelaunch status. Volume 1: The Hipparcos satellite
[ESA-SP-1111-VOL-1] N90-13499
Operating principle N90-13500
Overview of the Hipparcos satellite N90-13502
Overview of the Hipparcos payload N90-13503
The telescope mirrors N90-13504
Payload thermal control N90-13511
The spacecraft structure N90-13512
Spacecraft thermal control N90-13513
Data handling and telecommunications N90-13514
The attitude and orbit control system N90-13516
The apogee boost motor N90-13517
On-board software N90-13518
Assembly, integration, and verification N90-13519
Mechanical and thermal testing N90-13521
Product assurance N90-13522
On-ground photometric calibration N90-13523
Launch and early orbit N90-13524
The in-orbit initialization phase N90-13525
The role of the ground segment N90-13527
The interface with the data reduction consortia N90-13528
The Hipparcos Mission. Prelaunch status. Volume 2: The input catalog
[ESA-SP-1111-VOL-2] N90-13529
From scientific proposals to the Inca data base N90-13530
The Inca data base N90-13531
Mission simulations N90-13532
Proximity effects on adjacent and multiple stars N90-13533
Successive iterations of the input catalog N90-13534
Ground-based astrometric measurements N90-13536
The compilation of astrometric data N90-13537
New ground-based photometric measurements N90-13538
Standard stars and photometric calibration N90-13539
Double stars N90-13540
Variable stars N90-13541
The choice of stars in open clusters N90-13542
The choice of stars in the Magellanic clouds N90-13543
The link to extragalactic objects N90-13544
Minor planets and other solar system objects N90-13545
The catalogs produced by the Inca consortium N90-13546
The Hipparcos Mission. Prelaunch status. Volume 3: The data reductions
[ESA-SP-1111-VOL-3] N90-13548
Validation of the Hipparcos catalog N90-13564
Linking Hipparcos to a quasi-inertial system N90-13565
Accuracy and characteristics of the Hipparcos catalog N90-13566
The first-look data analysis at Utrecht N90-13571
Modeling of the Hipparcos optical system N90-13572
HOLES (ELECTRON DEFICIENCIES)
Local pairing and antiferromagnetism in high-T sub c superconductors
[AD-A213004] N90-14113
HOLOGRAPHY
Real-time sensing of optical alignment N90-13479
HOMOGENEITY
Numerical analysis of scattering by interface flaws
[AD-A212996] N90-13710
HOMOGENEOUS TURBULENCE
Application of two-point closures to subgrid scale modeling for homogeneous, 3D turbulence N90-13732
Large eddy simulation of homogeneous turbulence undergoing shear and thermal gradients. Application to one point closing models
[ECL-88-23] N90-13754
HOOP COLUMN ANTENNAS
A study on the sensitivity and simultaneous adjustment of a hoop-column antenna surface
[NASA-TM-101538] N90-13807
HORMONES
Effects of microgravity on growth hormone concentration and distribution in plants N90-13947
HOT-WIRE ANEMOMETERS
Low speed hot and cold wire techniques for unsteady flow N90-13342
Hot and cold wire applications in supersonic flows: introductory notes N90-13343
The influence of multiple hot-wire probe geometry on the results of measurements in turbulent flows
[DLR-FB-89-26] N90-13724
HOT-WIRE FLOWMETERS
Low speed hot and cold wire techniques for unsteady flow N90-13342
Hot and cold wire applications in supersonic flows: introductory notes N90-13343
HOUSEKEEPING (SPACECRAFT)
On the wings of a dream: The Space Shuttle
[NASA-EP-269] N90-13446
HOUSINGS
The application of cast SiC/Al to rotary engine components
[NASA-CR-179610] N90-13385
RSRM nozzle fixed housing cooldown test
[NASA-CR-183741] N90-13587
HUBBLE SPACE TELESCOPE
The link to extragalactic objects N90-13544
HUMAN BEHAVIOR
A guide to reasoning under uncertainty
[REPT-72/87/R486U] N90-13932
HUMAN BEINGS
Computational and psychophysical study of human vision using neural networks
[AD-A213290] N90-13924
Spatiotemporal characteristics of visual localization, phase 2
[AD-A212934] N90-13929
HUMAN FACTORS ENGINEERING
The human factors relating to escape and survival from helicopters ditching in water
[AGARD-AG-305(E)] N90-13358
Software and hardware description of the helicopter motion equations for VAX computers
[AD-A213248] N90-13375
Human factors research in aircrew performance and training
[AD-A213285] N90-13938
Human factors issues in performing life science experiments in a 0-G environment N90-13952
HUMIDITY MEASUREMENT
Humidity local measurements in the middle atmosphere N90-13833
Long duration balloon flights in the middle stratosphere N90-13874
HURRICANES
Comparison of analytical methods for calculation of wind loads
[NASA-TM-102782] N90-13813
HYDRATION
Computational solution of chemistry problems
[NASA-CR-186000] N90-13618
HYDRAULIC EQUIPMENT
Review and evaluation of a turbomachinery throughflow finite element code
[AD-A213058] N90-13787
HYDRAULIC TEST TUNNELS
Liquid water content and droplet size calibration of the NASA Lewis Icing Research Tunnel
[NASA-TM-102447] N90-13797
HYDRAULICS
Gravitropism in plants: Hydraulics and wall growth properties of responding cells N90-13950
HYDROCARBONS
Summaries of the thematic conferences on remote sensing for exploration geology
[NASA-CR-185321] N90-13880
HYDROCHLORIC ACID
Observations of stratospheric HCl: 1975-1985
[AERONOMICA-ACTA-A-349-1989] N90-13892
HYDROGEN
Effect of adsorbed arsenic on the decomposition rate of nickel hydride
[AD-A213245] N90-13624
Propagation of sound in vibrationally excited nitrogen and hydrogen gas mixtures
[AD-A213002] N90-14073
Dynamics Explorer-1 satellite study of electrostatic ion cyclotron waves N90-14105
HYDROGEN BONDS
Low frequency polarized and depolarized light scattering in H-bonded liquids: CH3(CH2)n-1OH (n=1,...5)
[PREPRINT-693] N90-14100
HYDROGEN FUELS
Thermal protection systems for reentry and hypersonic flight
[DLR-MITT-89-14] N90-13577
HYDROGEN IONS
Orion B: Anatomy of a star-forming region N90-14155
HYDROGEN PLASMA
Observations of electrostatic hydrogen cyclotron waves and electric field fluctuations near one Hz in auroral acceleration regions N90-13842
HYDROGENATION
Energy concentration induced by phase transitions in hydrogenated metals
[PREPRINT-672] N90-13650
HYDROMETERS
Humidity local measurements in the middle atmosphere N90-13833
HYDROXYL EMISSION
Further observations of rotationally excited far infrared OH16 and OH18 emission in Orion-KL: Tighter constraints on the nature of the emitting region
[NASA-CR-186004] N90-14156
HYDROXYL RADICALS
Study of the hydroxyl radical by DRASC resonance in a high pressure flame — Diffusion Raman Anti-Stokes Coherence (DRASC)
[ONERA-RS-53/7131-PY] N90-13632
HYGIENE
On the wings of a dream: The Space Shuttle
[NASA-EP-269] N90-13446
HYPERCUBE MULTIPROCESSORS
Definition of avionics concepts for a heavy lift cargo vehicle, appendix A
[NASA-CR-183817] N90-13380
Implementing the discrete Fourier transform on the hypercube FPS T40
[IMAG-RR-773-I] N90-13983
A multilevel parallel solver for block tridiagonal and banded linear systems
[AD-A213151] N90-14008
HYPERGEOMETRIC FUNCTIONS
FORTRAN subroutines for the evaluation of the confluent hypergeometric functions
[AD-A213308] N90-14012
Some comments on the solvable Chiral Potts model
[PREPRINT-673] N90-14070
HYPERSONIC FLIGHT
Thermal protection systems for reentry and hypersonic flight
[DLR-MITT-89-14] N90-13577
HYPERSONIC FLOW
An Introduction to Hypersonic Aerodynamics
[VKI-LS-1989-01] N90-13334
Hypersonic aerodynamics N90-13335
On catalytic recombination rates in hypersonic stagnation heat transfer N90-13338
Optimum shape of a blunt forebody in hypersonic flow
[NASA-CR-181955] N90-13351
HYPERSONIC REENTRY
Thermal protection systems for reentry and hypersonic flight
[DLR-MITT-89-14] N90-13577
HYPERSONIC SHOCK
Hypersonic aerodynamics N90-13335
HYPERVELOCITY GUNS
Current management for improved railgun performance
[AD-A212887] N90-13445

HYPOTHERMIA
Generation of free radicals during cold injury and rewarming
[AD-A213088] N90-13915
HYSTERESIS
Analysis of new phenomena in shear flow of non-Newtonian fluids
[AD-A212893] N90-13721

I

ICE
Debris/ice/TPS assessment and photographic analysis for Shuttle Mission STS-34
[NASA-TM-102153] N90-13447
ICE FORMATION
Preparation of binary ice layers by condensation from gas phase
[JUEL-2248] N90-13631
Convective heat transfer measurements from a NACA 0012 airfoil in flight and in the NASA Lewis Icing Research Tunnel
[NASA-TM-102448] N90-13750
Liquid water content and droplet size calibration of the NASA Lewis Icing Research Tunnel
[NASA-TM-102447] N90-13797
ICE NUCLEI
Preparation of binary ice layers by condensation from gas phase
[JUEL-2248] N90-13631
IDENTIFYING
Gas identification system using graded temperature sensor and neural net interpretation
[AD-A213359] N90-13627
Identification of impulsive interference channels
[AD-A213154] N90-14009
IGNITERS
Evaluation of selected computer models for modeling pyrotechnic and propellant devices
[AD-A213003] N90-13671
IGNITION
Systems tunnel linear shaped charge lightning strike
[NASA-CR-183832] N90-13404
The mobile combustion diagnostic fixture and its application to the study of propellant combustion. Part 1: Investigation of the low pressure combustion of LOVA XM39 propellant
[AD-A213272] N90-13626
Evaluation of selected computer models for modeling pyrotechnic and propellant devices
[AD-A213003] N90-13671
IGNITION LIMITS
Experimental and computational study of combustion limits in natural-gas fueled internal combustion engines
[PB89-235196] N90-13673
ILLINOIS
The interaction and variation of waves and turbulence from MST radar data
[AD-A212849] N90-13906
IMAGE ANALYSIS
Analysis of the image dissector tube data N90-13550
Analysis of the star mapper data N90-13551
Overview of the Tycho data analysis N90-13556
Novel graph searching methods for image analysis
[AD-A213065] N90-13971
An editor for 3D-models for image analysis
[FOA-C-30534-3.4] N90-13986
IMAGE CONTRAST
Image enhancement software for underwater recovery operations: User's manual
[AD-A212943] N90-14094
IMAGE DISSECTOR TUBES
The relay lens systems N90-13506
The detectors N90-13507
Analysis of the image dissector tube data N90-13550
IMAGE ENHANCEMENT
Image enhancement software for underwater recovery operations: User's manual
[AD-A212943] N90-14094
Real time image enhancement during underwater recovery operations
[AD-A213139] N90-14097
IMAGE MOTION COMPENSATION
GOES I/M image navigation and registration N90-13422
IMAGE PROCESSING
Effect of central obscuration on the LDR point spread function N90-13475
The Hipparcos Mission. Prelaunch status. Volume 2: The input catalog
[ESA-SP-1111-VOL-2] N90-13529
From scientific proposals to the Inca data base N90-13530
Analysis of the image dissector tube data N90-13550
Photometry: Main mission and Tycho N90-13560
Double star reductions in FAST N90-13562
Summaries of the thematic conferences on remote sensing for exploration geology
[NASA-CR-185321] N90-13880
Estimation of rain rate using spatial and multichannel coherence: Analysis of SSM/I data N90-13905
Implementation issues in source coding
[NASA-CR-185327] N90-13963
Novel graph searching methods for image analysis
[AD-A213065] N90-13971
Algorithm for atmospheric corrections of aircraft and satellite imagery
[NASA-TM-100751] N90-13976
The algebraic basis of mathematical morphology. Part 1: Dilations and erosions
[CWI-AM-R8807] N90-14065
Optics and opto-electronics systems
[AD-A212340] N90-14093
Image enhancement software for underwater recovery operations: User's manual
[AD-A212943] N90-14094
Real time image enhancement during underwater recovery operations
[AD-A213139] N90-14097
IMAGE RECONSTRUCTION
Image segmentation for the stereoscopic vision of a mobile robot
[ONERA-RT-1/3692-SY] N90-13800
IMAGE RESOLUTION
The telescope mirrors N90-13504
The relay lens systems N90-13506
Astrometric parameter determination in FAST N90-13556
Double star reductions in NDAC N90-13561
Data simulations in the fast consortium N90-13573
Data simulations in the NDAC consortium N90-13574
IMAGES
Computational and psychophysical study of human vision using neural networks
[AD-A213290] N90-13924
Spatiotemporal characteristics of visual localization, phase 2
[AD-A212934] N90-13929
Functional decor in the International Space Station: Body orientation cues and picture perception
[NASA-TM-102242] N90-13931
IMAGING TECHNIQUES
Image segmentation for the stereoscopic vision of a mobile robot
[ONERA-RT-1/3692-SY] N90-13800
The effects of gravity waves on horizontal layers: Simulation and interpretation N90-13852
ALIS: An Auroral Large Imaging System in northern Scandinavia N90-13877
Study of surface uniformity of semiconductors 3 to 5 by photoluminescence imagery
[ECL-88-15] N90-14116
GaAs and GaAs:In: Influence of surface treatments and characterization of homogeneity by photoluminescent imagery
[ECL-88-24] N90-14118
IMMUNOLOGY
Response of lymphocytes to a mitogenic stimulus during spaceflight N90-13942
IMPACT DAMAGE
Fractography of composite delamination
[NASA-CR-183291] N90-13599
Impact tests of three composite materials with carbon fiber cores
[REPT-M6-582500] N90-13610
IMPACT TESTS
Impact tests of three composite materials with carbon fiber cores
[REPT-M6-582500] N90-13610
Impact tests on aluminum 2024 T3, aramid and glass reinforced aluminum laminates and thermoplastic composites
[LR-534] N90-13613
IMPEDANCE
Advanced actuation systems development, volume 2
[AD-A213378] N90-13398
IMPELLERS
A three-dimensional potential flow analysis of dynamic fluid forces acting on a whirling centrifugal impeller bounded by a volute N90-13717
MM and T advanced balancing/machining
[AD-A213103] N90-13775
IMPERIAL VALLEY (CA)
Supplementing geodetic data with prior information for crustal deformation in the Imperial Valley, California
[TR-6-1988] N90-13904
IMPINGEMENT
Modelling of satellite control thruster plumes N90-13578
IMPURITIES
Elastic impurity scattering in double-barrier resonant tunneling structures
[AD-A212650] N90-14110
IN-FLIGHT MONITORING
A knowledge-based flight status monitor for real-time application in digital avionics systems
[NASA-TM-101710] N90-13995
INCOMPRESSIBLE FLOW
Computation of viscous incompressible flows
[NASA-TM-101090] N90-13329
INCONEL (TRADEMARK)
Threshold for fatigue crack propagation
[DLR-FB-89-33] N90-13815
INDEXES (DOCUMENTATION)
A summary of 30 years of space launches
[AERONOMICA-ACTA-F-39-1989] N90-13411
Space station systems: A bibliography with indexes (supplement 9)
[NASA-SP-7056(09)] N90-13580
Aerospace medicine and biology: A continuing bibliography with indexes (supplement 330)
[NASA-SP-7011(330)] N90-13925
AFOSR technical report summaries
[AD-A213148] N90-14142
INDIAN SPACE PROGRAM
Comparison of the space program performance of countries with space programs
[ILR-MITT-222] N90-14150
INDICATING INSTRUMENTS
Reflection indicatrices of natural surfaces for AVHRR channels 1 and 2
[DLR-MITT-89-16] N90-13882
INDIUM ARSENIDES
Development of high gain three terminal devices - at millimeter wave frequencies
[AD-A213089] N90-13701
INDIUM COMPOUNDS
Electrochemical study of the etching of III to V semiconductors
[ETN-90-96015] N90-13633
GaAs and GaAs:In: Influence of surface treatments and characterization of homogeneity by photoluminescent imagery
[ECL-88-24] N90-14118
INDIUM PHOSPHIDES
Elaboration and characterization of MISFET transistors on InP
[ECL-88-19] N90-13709
Analytical and computer-aided models of InP-based MISFETs and heterojunction devices
[AD-A211861] N90-14106
Field-effect spectroscopy of interface states
[AD-A212998] N90-14112
Study of metal-insulator-semiconductor structures on indium phosphide, implemented by anodic oxidation
[ECL-88-10] N90-14114
INDOOR AIR POLLUTION
Pilot investigation of indoor-outdoor and personal PM10 (tnoracic) and associated ionic compounds and mutagenic activity
[PB89-222723] N90-13920
INDUCTION (MATHEMATICS)
Inductive reasoning and Kolmogorov complexity (preliminary version)
[CWI-CS-R8915] N90-14062
INDUSTRIAL PLANTS
Retrieving and integrating IC fabrication data from dissimilar databases
[AD-A211890] N90-14140
INDUSTRIES
Centers for the commercial development of space
[NASA-PAM-525] N90-14151
NASA commercial programs
[NASA-TM-101853] N90-14152
INEQUALITIES
The quadratic matrix inequality in singular H infinity control with state feedback
[MEMO-COSOR-89-03] N90-13997
INERTIAL NAVIGATION
Shuttle tethered operations: The effect on orbital trajectory and inertial navigation N90-13425
INERTIAL PLATFORMS
A gyroscope calibration analysis for the Gamma Ray Observatory (GRO) N90-13428
INFERENCE
Inductive reasoning and Kolmogorov complexity (preliminary version)
[CWI-CS-R8915] N90-14062
INFINITY
The quadratic matrix inequality in singular H infinity control with state feedback
[MEMO-COSOR-89-03] N90-13997
The singular zero sum differential game with stability using H infinity control theory
[MEMO-COSOR-89-09] N90-13999

The singular H infinity control problem with dynamic measurement feedback
[MEMO-COSOR-89-14] N90-14000
INFORMATION DISSEMINATION
Activities report of the World Meteorological Organization
[WMO-713] N90-13912
INFORMATION MANAGEMENT
Micro-based fact collection tool user's manual
[NASA-CR-180414] N90-13981
INFORMATION PROCESSING (BIOLOGY)
Role of retinocortical processing in spatial vision
[AD-A210995] N90-13918
Gravity receptors and responses N90-13948
INFORMATION RETRIEVAL
Retrieving and integrating IC fabrication data from dissimilar databases
[AD-A211890] N90-14140
AFOSR technical report summaries
[AD-A213148] N90-14142
INFORMATION SYSTEMS
Executive overview and introduction to the SMAP information system life-cycle and documentation standards
[NASA-TM-101765] N90-14134
Information system life-cycle and documentation standards, volume 1
[NASA-TM-101856] N90-14135
Management plan documentation standard and Data Item Descriptions (DID). Volume of the information system life-cycle and documentation standards, volume 2
[NASA-TM-101857] N90-14136
Product specification documentation standard and Data Item Descriptions (DID). Volume of the information system life-cycle and documentation standards, volume 3
[NASA-TM-101858] N90-14137
Assurance specification documentation standard and Data Item Descriptions (DID). Volume of the information system life-cycle and documentation standards, volume 4
[NASA-TM-101859] N90-14138
Management control and status reports documentation standard and Data Item Descriptions (DID). Volume of the information system life-cycle and documentation standards, volume 5
[NASA-TM-101860] N90-14139
The DOD Gateway Information System: Operational prototype and transition period 1987-1988
[AD-A213044] N90-14141
AFOSR technical report summaries
[AD-A213148] N90-14142
ERIS: Engineering Resource Information System
[AD-A213357] N90-14144
INFORMATION THEORY
Geodetic network adjustment using GPS triple difference observations and a priori stochastic information
[TR-1-1987] N90-13367
Inductive reasoning and Kolmogorov complexity (preliminary version)
[CWI-CS-R8915] N90-14062
INFRARED ASTRONOMY
Three-meter balloon-borne telescope N90-13490
Interstellar medium and infrared emission of the galactic disk N90-13862
Interplanetary dust close to the Sun (F corona): Its observation in the visible and infrared by a rocket-borne coronagraph N90-13864
INFRARED DETECTORS
Status of direct detector and array development N90-13464
The infrared spectrograph during the SIRTF pre-definition phase
[NASA-CR-183234] N90-13759
Discussion of factors affecting the sensitivity of IR imaging sensors, particularly focal plane mosaic arrays — staring mosaic arrays
[FOA-C-30536-3.1] N90-14101
INFRARED IMAGERY
Discussion of factors affecting the sensitivity of IR imaging sensors, particularly focal plane mosaic arrays — staring mosaic arrays
[FOA-C-30536-3.1] N90-14101
INFRARED RADIATION
The effects of seasonal and latitudinal earth infrared radiance variations on ERBS attitude control N90-13414
Development of mid-infrared solid state lasers for spaceborne lidar
[NASA-CR-183290] N90-13772
CANOES 2: Dynamics of atmospheric infrared thermochemical excitation, volume 1
[AD-A213341] N90-13897
CANOES 2: Dynamics of atmospheric infrared thermochemical excitation, volume 2
[AD-A213342] N90-13898
CANOES 2: Dynamics of atmospheric infrared thermochemical excitation, volume 3
[AD-A213343] N90-13899
CANOES 2: Dynamics of atmospheric infrared thermochemical excitation, volume 4
[AD-A213344] N90-13900
INFRARED SPECTRA
A high-resolution atlas of the infrared spectrum of the Sun and the Earth atmosphere from space: A compilation of ATMOS spectra of the region from 650 to 4800 cm (2.3 to 16 micron). Volume 1: The Sun
[NASA-RP-1224-VOL-1] N90-13893
Propagation of sound in vibrationally excited nitrogen and hydrogen gas mixtures
[AD-A213002] N90-14073
INFRARED SPECTROMETERS
The infrared spectrograph during the SIRTF pre-definition phase
[NASA-CR-183234] N90-13759
INFRARED SPECTROSCOPY
Observations of stratospheric HCl: 1975-1985
[AERONOMICA-ACTA-A-349-1989] N90-13892
INFRARED TELESCOPES
Diffraction, chopping, and background subtraction for LDR N90-13476
The infrared spectrograph during the SIRTF pre-definition phase
[NASA-CR-183234] N90-13759
INGESTION (ENGINES)
Study of the engine bird ingestion experience of the Boeing 737 aircraft
[DOT/FAA/CT-89/16] N90-13360
INGOTS
Experimental and numerical investigations of the crack arrest behavior of steels and cast iron materials
[MPA-TWB-86-03] N90-13635
INHOMOGENEITY
Electromagnetic wave propagation through circular waveguides containing radially inhomogeneous lossy media
[AD-A213062] N90-13688
On geometry of inhomogeneous Heisenberg ferromagnet: Nonintegrable case
[MEMO-789] N90-14030
INJURIES
Generation of free radicals during cold injury and rewarming
[AD-A213088] N90-13915
INSPECTION
NDI (Nondestructive Inspection) oriented corrosion control for Army aircraft. Phase 1: Inspection methods
[AD-A213368] N90-13359
Considerations about the acceptance inspection of HS fasteners intended for controlled tightening
[CRIF-MT-175] N90-13806
INSTRUCTORS
Elementary and middle school science improvement project
[NASA-CR-183768] N90-14125
INSTRUMENT ERRORS
A gyroscope calibration analysis for the Gamma Ray Observatory (GRO) N90-13428
INSULATORS
Manufacturing and characterization of insulator-germanium structures
[ECL-88-13] N90-14115
INTEGRAL EQUATIONS
Numerical analysis of scattering by interface flaws
[AD-A212996] N90-13810
A unified algebraic approach to integral and discrete evolution equations
[PREPRINT-668] N90-14044
INTEGRATED CIRCUITS
Research on the controllability of integrated circuits by means of electron beams
[ETN-90-95710] N90-13708
Computer-aided fabrication system implementation
[AD-A213005] N90-13969
Integrated optoelectronic receivers
[AD-A213376] N90-14098
INTELLECT
A guide to reasoning under uncertainty
[REPT-72/87/R486U] N90-13932
INTELLIGIBILITY
Evaluation of speech intelligibility through a bone conduction stimulator
[AD-A212002] N90-13919
Test procedures for the evaluation of helmet and hee]set mounted active noise reduction systems
[AD-A212991] N90-13937
INTERACTIONAL AERODYNAMICS
A model suitable for predicting the noise associated with the ducted tail rotor of a helicopter
[ECL-88-09] N90-14074
INTERFACES
Development of a shuttle plume radiation heating indicator
[NASA-CR-183679] N90-13584
Transport phenomena and interfacial kinetics in multiphase combustion systems
[AD-A212932] N90-13620
Unified model of charge build up and annealing of oxide charge and interface states in SiO2 due to stress
[HMI-B-485] N90-14120
Database interfaces on NASA's heterogeneous distributed database system
[NASA-CR-185420] N90-14133
INTERGALACTIC MEDIA
The link to extragalactic objects N90-13544
INTERLAYERS
Evaluation of a neoprene latex modified SAMI (Stress Absorbing Membrane Interlayer)
[PB89-226435] N90-13665
INTERNAL COMBUSTION ENGINES
Experimental and computational study of combustion limits in natural-gas fueled internal combustion engines
[PB89-235196] N90-13673
INTERNAL WAVES
First-order Bragg SAR imagery of Kelvin wakes and moving internal wave fields
[AD-A213361] N90-13691
INTERNATIONAL COOPERATION
The SIMBAD data base N90-13547
Swiss scientific balloon and sounding rocket experiments 1987-1989 N90-13827
INTERORBITAL TRAJECTORIES
Shuttle tethered operations: The effect on orbital trajectory and inertial navigation N90-13425
INTERPLANETARY DUST
Interplanetary dust close to the Sun (F corona): Its observation in the visible and infrared by a rocket-borne coronagraph N90-13864
INTERPLANETARY MAGNETIC FIELDS
Rotation of the photospheric magnetic fields: A north-south asymmetry
[NASA-CR-186159] N90-14177
INTERPLANETARY MEDIUM
Interzodiak 2: Observation of EUV-resonance radiation N90-13854
Interstellar medium and infrared emission of the galactic disk N90-13862
Optical observations of interplanetary pick-up ions: The experiment Helly N90-13863
Project Supernova 1987 N90-13866
INTERPOLATION
Feature modeling: The incorporation of a front and eddy map into optimum interpolation-based thermal analysis
[AD-A213253] N90-13914
INTERPROCESSOR COMMUNICATION
Implementing the discrete Fourier transform on the hypercube FPS T40
[IMAG-RR-773-I] N90-13983
INVENTIONS
Crosslinkable polymer
[GB-PATENT-2-205-846-A] N90-13663
INVERSE SCATTERING
The initial-boundary value problem for the Davey-Stewartson 1 equation; how to generate and drive localized coherent structures in multidimensions
[PREPRINT-684] N90-13756
INVERSIONS
Three dimensional analysis of the structure of the atmosphere in polar environments by vertical satellite sounding. Interest for the meteorological forecasts at high latitudes
[ETN-90-95506] N90-13911
INVESTMENTS
The economic impact of automation technology
[AD-A213363] N90-13682
INVISCID FLOW
Computation of flow fields around propellers and hovering rotors based on the solution of the Euler equations
[DLR-FB-89-37] N90-13333
Hypersonic aerodynamics N90-13335
Blunt-nose inviscid airflows with coupled nonequilibrium processes N90-13336
Gas flows in rocket motors. Volume 3, appendix D: Computer code listings
[AD-A213350] N90-13593
Inviscid 3D solution methods N90-13736
Inviscid 2D solutions on unstructured, adaptive grids N90-13737
IODINE COMPOUNDS
Generation of iodine monofluoride in a supersonic multipurpose flowtube facility
[AD-A213082] N90-13774

ION BEAMS
Mechanisms in reactive ion etching of silicon carbide thin films
[AD-A213018] N90-13700
ION CYCLOTRON RADIATION
Dynamics Explorer-1 satellite study of electrostatic ion cyclotron waves N90-14105
ION DENSITY (CONCENTRATION)
A double focusing mass-spectrometer for simultaneous ion measurements in the stratosphere N90-13848
ION DISTRIBUTION
Dynamics Explorer-1 satellite study of electrostatic ion cyclotron waves N90-14105
ION TEMPERATURE
Background electrodynamics measured by EISCAT during the NEED campaign N90-13851
IONIC MOBILITY
Construction of the rotating cryostat ROTA2, its use for zero sound experiments in (3)He-B, and calculations of ion mobility in (3)He-A and (3)He-P
[ISBN-952-90091-3-5] N90-13765
IONOSPHERIC ELECTRON DENSITY
Enhanced electron density layers in the high-latitude lower ionosphere N90-13832
IONS
Pilot investigation of indoor-outdoor and personal PM10 (thoracic) and associated ionic compounds and mutagenic activity
[PB89-222723] N90-13920
Use of a krypton isotope for rapid ion changeover at the Lawrence Berkeley Laboratory 88-inch cyclotron
[NASA-CR-186107] N90-14084
IRON
Experimental and numerical investigations of the crack arrest behavior of steels and cast iron materials
[MPA-TWB-88-03] N90-13635
Internal and external nitriding and nitrocarburizing of iron and iron-based alloys
[ETN-90-96012] N90-13646
A theory of damage in brittle and cementitious materials, part 1
[AD-A212940] N90-13658
IRON ALLOYS
Internal and external nitriding and nitrocarburizing of iron and iron-based alloys
[ETN-90-96012] N90-13646
The effects of alloying and thermal factors on the solidification and mechanical properties of gray iron
[VTT-619] N90-13651
IRRADIATION
Nuclear magnetic resonance signatures of nitrogen-containing compounds
[AD-A213375] N90-13628
Optical properties monitor: Experiment definition phase
[NASA-CR-183836] N90-14092
ISCHEMIA
Generation of free radicals during cold injury and rewarming
[AD-A213088] N90-13915
ISING MODEL
Energy barriers in SK spin-glass model
[PREPRINT-665] N90-14119
ISOTOPES
Nonpotential scattering for the density matrix and quantum gravity
[PREPRINT-688] N90-14080
ISOTROPIC MEDIA
The initial imperfection data bank at the Delft University of Technology, part 2
[LR-559-PT-2] N90-13825
ISOTROPIC TURBULENCE
Spectral study of a compressible isotropic turbulence
[ECL-88-16] N90-13753
ITERATION
An iterative method to solve the nonlinear Poisson's equation in the case of plasma tangential discontinuities
[AERONOMICA-ACTA-A-346-1989] N90-14045
ITERATIVE SOLUTION
Gas flows in rocket motors. Volume 2, appendix C: Time iterative solution of viscous supersonic flow
[AD-A213349] N90-13592
An iterative method to solve the nonlinear Poisson's equation in the case of plasma tangential discontinuities
[AERONOMICA-ACTA-A-346-1989] N90-14045
Some quick and efficient methods for bearing-only target motion analysis
[IMAG-RR-762-M] N90-14049
IUE
Analytical derivation and verification of zero-gyro control for the IUE satellite
[NASA-TM-100748] N90-13767
Archival research on absorption lines in violently star-forming galaxies
[NASA-CR-185960] N90-14163

J

JAPANESE SPACE PROGRAM
Comparison of the space program performance of countries with space programs
[ILR-MITT-222] N90-14150
JET FLOW
Coherent structures in a round jet N90-13733
Numerical solutions of the complete Navier-Stokes equations
[NASA-CR-186102] N90-13747
Model and computation of three-dimensional turbulent jets in a crossflow
[ECL-89-007] N90-13755
JET MIXING FLOW
Buoyancy effects on the vapor condensation rate on a horizontal liquid surface
[NASA-TM-102437] N90-13675
Vapor condensation on liquid surface due to laminar jet-induced mixing: The effects of system parameters
[NASA-TM-102433] N90-13751
JET PROPULSION
STOVL aircraft simulation for integrated flight and propulsion control research
[NASA-TM-102419] N90-13389
JOINTS (JUNCTIONS)
Effects of joints in truss structures N90-13486
Joints in deployable space truss structures N90-13489
QM-8 field joint protection system, volume 7
[NASA-CR-183748] N90-13586
Qualification of improved joint heaters
[NASA-CR-183827] N90-13594
The adhesive bonding of thermoplastic composites
[AD-A213358] N90-13605

K

K STARS
The winds of high luminosity late-type bright stars
[NASA-CR-182961] N90-14160
K-EPSILON TURBULENCE MODEL
Multigrid calculations of 3-D turbulent viscous flows
[NASA-CR-185154] N90-13323
KALMAN FILTERS
True covariance simulation of the EUVE update filter N90-13427
Bilinear modeling and nonlinear estimation N90-13430
Extended Kalman filter for attitude estimation of the earth radiation budget satellite N90-13433
On-line range prediction system, part 2
[NASA-CR-185889] N90-13771
KEPLER LAWS
Calculation of double-lunar swingby trajectories: I. Keplerian foundation N90-13435
KINEMATICS
SSME LOX post flow analysis/fluid structure interaction. Volume 2: Fluid structure interaction
[NASA-CR-183678] N90-13716
KINETIC ENERGY
Solution of the Boltzmann equation using an energy group method
[AD-A213138] N90-14096
KNOWLEDGE BASES (ARTIFICIAL INTELLIGENCE)
Expert systems for adaptive control of large space structures N90-13452
A knowledge-based system design/information tool for aircraft flight control systems
[NASA-TM-101704] N90-13990
A knowledge-based flight status monitor for real-time application in digital avionics systems
[NASA-TM-101710] N90-13995
Empirical analysis and refinement of expert system knowledge bases
[AD-A213240] N90-14143
KRYPTON ISOTOPES
Use of a krypton isotope for rapid ion changeover at the Lawrence Berkeley Laboratory 88-inch cyclotron
[NASA-CR-186107] N90-14084

L

LAGUERRE FUNCTIONS
Computational aspects of pseudospectral Laguerre approximations
[NASA-CR-181934] N90-14038
Distribution of a sum of n random variables and a central limit theorem based on moments or on coefficients of polynomial dependence
[IMAG-RR-768-M] N90-14040
LAKES
Late quaternary geomorphology of the Great Salt Lake region, Utah, and other hydrographically closed basins in the western United States: A summary of observations
[NASA-CR-185912] N90-13878
LAMINAR BOUNDARY LAYER
Multiple paths to subharmonic laminar breakdown in a boundary layer
[NASA-CR-181948] N90-13722
LAMINAR FLOW
Generalized similarity solutions for three dimensional, laminar, steady, compressible boundary layer flows on swept profile cylinders
[DLR-FB-89-34] N90-13725
Numerical simulation of transition in three-dimensional boundary layers
[DLR-FB-89-12] N90-13728
Application of multi-grid methods for solving the Navier-Stokes equations
[NASA-TM-102359] N90-14002
LAMINAR MIXING
Buoyancy effects on the vapor condensation rate on a horizontal liquid surface
[NASA-TM-102437] N90-13675
Vapor condensation on liquid surface due to laminar jet-induced mixing: The effects of system parameters
[NASA-TM-102433] N90-13751
LAMINATES
Measuring of the complete stiffness matrix for anisotropic laminated materials
[DLR-MITT-89-11] N90-13606
Measuring of the complete stiffness matrix for anisotropic laminated materials
[DLR-MITT-89-12] N90-13607
Impact tests on aluminum 2024 T3, aramid and glass reinforced aluminum laminates and thermoplastic composites
[LR-534] N90-13613
Buckling of delaminations in ARALL laminates
[LR-535] N90-13614
Constant amplitude fatigue of ARALL-2 laminates
[LR-539] N90-13615
Optical modulators based on polymers
[EP-PATENT-0-294-061-A1] N90-14099
LAND USE
Aircraft/airport compatibility: Some strategic, tactical, and operational issues
[TT-8902] N90-13409
LANDAU-GINZBURG EQUATIONS
Large deviation estimates in the stochastic quantization of phi sub 2 exp 4
[PREPRINT-686] N90-14050
LANDSAT SATELLITES
The use of LANDSAT-TM data for the management of pine forestations in central Chile
[DLR-FB-89-44] N90-13881
LAPLACE TRANSFORMATION
Self-decomposable distributions and branching processes
[MEMO-COSOR-89-06] N90-14052
LARGE DEPLOYABLE REFLECTOR
Report of the Asilomar 3 LDR Workshop
[NASA-CR-184656] N90-13449
Introduction to the report of the Asilomar 3 LDR workshop N90-13450
A figure control sensor for the Large Deployable Reflector (LDR) N90-13451
Pointing control for LDR N90-13453
Space telescope pointing control N90-13454
Wavefront error sensing for LDR N90-13455
Segment alignment control system N90-13457
Composite panel development at JPL N90-13458
Large Deployable Reflector (LDR) thermal characteristics N90-13460
Advanced composite materials for precision segmented reflectors N90-13461
Lightweight composite reflector panels N90-13462
Low temperature optical testing of CFRP telescope panels N90-13463
Status of direct detector and array development N90-13464
Cryogenic systems for the large deployable reflector N90-13470
Cryogenics for LDR N90-13471
LDR cryogenics N90-13472
Development of FIR arrays with integrating amplifiers N90-13473
Effect of central obscuration on the LDR point spread function N90-13475
Diffraction, chopping, and background subtraction for LDR N90-13476
Effects of joints in truss structures N90-13486
LARGE SPACE STRUCTURES
Report of the Asilomar 3 LDR Workshop
[NASA-CR-184656] N90-13449

Expert systems for adaptive control of large space structures N90-13452
Real-time sensing of optical alignment N90-13479
Assembly considerations for large reflectors N90-13480
Explicit modeling and concurrent processing in the simulation of multibody dynamic systems N90-13481
Initial test results for the mini-mast N90-13482
LDR structural experiment definition N90-13483
Control of optical systems N90-13484
Hybrid deployable support truss designs for LDR N90-13485
PACOSS program N90-13487
LDR structural technology activities at JPL N90-13488
Joints in deployable space truss structures N90-13489
The dynamics and control of large flexible space structures - 12, supplement 11
[NASA-CR-185966] N90-13494
Attitude and shape control of optimally designed large space structures N90-13579

LASER ANEMOMETERS
Laser two focus techniques N90-13348

LASER APPLICATIONS
Measurement Techniques in Aerodynamics
[VKI-LS-1989-05] N90-13339
Laser applications in supersonic unsteady flow N90-13344
Laser two focus techniques N90-13348
Optimum data weighting and error calibration for estimation of gravitational parameters N90-13437
Development of mid-infrared solid state lasers for spaceborne lidar
[NASA-CR-183290] N90-13772
MM and T advanced balancing/machining
[AD-A213103] N90-13775
Quantitative non-destructive evaluation using laser generated ultrasonic pulses N90-13805
Precision of semi-geometrically determined SLR baselines vs. site occupation time
[ETN-90-90007] N90-13885

LASER BEAMS
Laser two focus techniques N90-13348

LASER CUTTING
Characterization of surfaces cut with a laser beam and thermal model of the process
[ISAL-89-0008] N90-13780

LASER DOPPLER VELOCIMETERS
Practical systems for speckle velocimetry N90-13341
Laser applications in supersonic unsteady flow N90-13344
The 3D LDA techniques in vortex studies and boundary layer surveys N90-13346

LASER MATERIALS
A review of laser filter materials
[AD-A213134] N90-13776

LASER PROPULSION
Proceedings of the High Energy Density Matter (HEDM) Conference
[AD-A212314] N90-13670

LASER PUMPING
Development of mid-infrared solid state lasers for spaceborne lidar
[NASA-CR-183290] N90-13772
An experimental analysis of the waveguide modes in a high-gain free-electron laser amplifier N90-13779

LASER RANGER/TRACKER
On-line range prediction system, part 2
[NASA-CR-185889] N90-13771
Outline on the future italian transportable laser ranging station
[CISE-4845] N90-13782

LASER SPECTROMETERS
Far-infrared heterodyne receivers N90-13465

LASING
Development of mid-infrared solid state lasers for spaceborne lidar
[NASA-CR-183290] N90-13772

LATE STARS
The winds of high luminosity late-type bright stars
[NASA-CR-182961] N90-14160

LATERAL CONTROL
Periodic-disturbance accommodating control of the space station for asymptotic momentum management N90-13416

LATITUDE
The effects of seasonal and latitudinal earth infrared radiance variations on ERBS attitude control N90-13414

LATTICES (MATHEMATICS)
The algebraic basis of mathematical morphology. Part 1: Dilations and erosions
[CWI-AM-R8807] N90-14065
A lattice study of semileptonic decays of D-mesons
[PREPRINT-660] N90-14086

LAUNCH DATES
A summary of 30 years of space launches
[AERONOMICA-ACTA-F-39-1989] N90-13411

LAUNCH VEHICLE CONFIGURATIONS
Qualification of the 4th stage propulsor of the Brazilian launcher. SLV: A new sounding rocket N90-13860

LAUNCHERS
The Brazilian space program: Actual state of the art N90-13861
The Skylark sounding rocket program and future launcher developments by British Aerospace (Space Systems) Ltd. N90-13871

LAUNCHING
Current management for improved railgun performance
[AD-A212887] N90-13445

LAUNCHING BASES
Andoya rocket range: New installations, future plans, and investments N90-13859
Esrange N90-13876

LEAKAGE
Flows with tip leakage N90-13740

LENSES
The modulating grid N90-13505
The relay lens systems N90-13506

LEPTONS
A lattice study of semileptonic decays of D-mesons
[PREPRINT-660] N90-14086

LEVITATION MELTING
Containerless Processing of Metals: Undercooling and Solidification
[DLR-MITT-89-15] N90-13645

LIAPUNOV FUNCTIONS
Fluctuations of the Lyapunov exponent in disordered systems
[PREPRINT-690] N90-14063

LIE GROUPS
R-matrices and higher Poisson brackets for integrable systems
[PREPRINT-669] N90-14069

LIFE (DURABILITY)
Atmospheric drag model calibrations for spacecraft lifetime prediction N90-13439
Lifetime predictions for the Solar Maximum Mission (SMM) and San Marco spacecraft N90-13440
Cryogenic systems for the large deployable reflector N90-13470
Mean stress and the exhaustion of fatigue-damage resistance
[NASA-TM-101311] N90-13819
Advanced Turbine Technology Applications Project (ATTAP)
[NASA-CR-185109] N90-14153

LIFE SCIENCES
Life science research in space
[ESA-SP-1105] N90-13917
Human factors issues in performing life science experiments in a 0-G environment N90-13952

LIFE SUPPORT SYSTEMS
The human factors relating to escape and survival from helicopters ditching in water
[AGARD-AG-305(E)] N90-13358

LIFT
Correlation of Puma airloads: Lifting-line and wake calculation
[NASA-TM-102212] N90-13327
Induced drag for non-planar wings
[LR-521] N90-13357

LIFT DEVICES
Aeroelastic control of composite lifting surfaces: Integrated aeroelastic control optimization N90-13396

LIGHT CURVE
Variable stars N90-13541

LIGHT EMISSION
Interplanetary dust close to the Sun (F corona): Its observation in the visible and infrared by a rocket-borne coronagraph N90-13864

LIGHT MODULATION
Optical modulators based on polymers
[EP-PATENT-0-294-061-A1] N90-14099

LIGHT SCATTERING
Low frequency polarized and depolarized light scattering in H-bonded liquids: CH3(CH2)n-1OH (n=1,...5)
[PREPRINT-693] N90-14100

LIGHTNING
Systems tunnel linear shaped charge lightning strike
[NASA-CR-183832] N90-13404

LIGHTNING SUPPRESSION
Cable coupling lightning transient qualification
[NASA-CR-183826] N90-13405

LIKELIHOOD RATIO
Software development for avionics SSME control and diagnostics
[NASA-CR-184894] N90-13964

LINE OF SIGHT
An approach to optical structures control N90-13456

LINE SHAPE
Model-independent analysis of the Z line shape in e+e- annihilation
[PREPRINT-679] N90-14089

LINE SPECTRA
Far-infrared heterodyne receivers N90-13465
Archival research on absorption lines in violently star-forming galaxies
[NASA-CR-185960] N90-14163

LINEAR EQUATIONS
Solution of the Boltzmann equation using an energy group method
[AD-A213138] N90-14096

LINEAR OPERATORS
Some remarks on the gap metric
[MEMO-COSOR-88-34] N90-14029

LINEAR PROGRAMMING
Stopping rules for a class of random methods for detecting necessary linear inequality constraints
[MEMO-777] N90-13977
Description and manipulation of convex polygons using polarity
[IMAG-RR-771-M] N90-14041

LINEAR QUADRATIC GAUSSIAN CONTROL
The totally singular linear quadratic problem with indefinite cost
[MEMO-COSOR-89-05] N90-13998

LINEAR QUADRATIC REGULATOR
Autonomous spacecraft attitude control using magnetic torquing only N90-13415
The algebraic Riccati equation and singular optimal control
[MEMO-COSOR-88-31] N90-14028

LINEAR SYSTEMS
Advanced actuation systems development, volume 2
[AD-A213378] N90-13398
A transient response method for linear coupled substructures
[NASA-TP-2926] N90-13444
Model reduction of weakly damped mechanical systems
[MEMO-798] N90-13993
The output-stabilizable subspace and linear optimal control
[MEMO-COSOR-89-15] N90-14001
A multilevel parallel solver for block tridiagonal and banded linear systems
[AD-A213151] N90-14008
The regular indefinite linear quadratic problem with linear endpoint constraints
[MEMO-COSOR-88-15] N90-14022
Stabilizability and detectability of discrete-time time-varying systems
[MEMO-COSOR-88-16] N90-14023
A graph theoretic characterization for the rank of the transfer matrix of a structured system
[CWI-OS-R8819] N90-14064
A mixed finite element solution of the linear acoustic equations
[ECL-89-006] N90-14075

LINEARITY
Linear groups and distance-transitive graphs
[CWI-PM-R8805] N90-14036

LINEARIZATION
Another approach to the local disturbance decoupling problem with stability for nonlinear systems
[MEMO-799] N90-14033

LININGS
Elasticity effects on cavitation in a squeeze film damper undergoing noncentered circular whirl
[NASA-TM-102392] N90-13786

LIQUID CRYSTALS
Studies of structure and switching dynamics in ferroelectric crystal and liquid crystal thin films
[AD-A212650] N90-14109

LIQUID FLOW
Analysis of new phenomena in shear flow of non-Newtonian fluids
[AD-A212893] N90-13721

LIQUID HELIUM
Construction of the rotating cryostat ROTA2, its use for zero sound experiments in (3)He-B, and calculations of ion mobility in (3)He-A and (3)He-P
[ISBN-952-90091-3-5] N90-13765

LIQUID INJECTION
The evaluation of a metered mixer for RTV silicone for RSRM nozzle backfill operations
[NASA-CR-183831] N90-13763

LIQUID OXYGEN
SSME LOX post flow analysis/fluid structure interaction. Volume 1: Flow analysis
[NASA-CR-183677] N90-13715
SSME LOX post flow analysis/fluid structure interaction. Volume 2: Fluid structure interaction
[NASA-CR-183678] N90-13716

LIQUID PHASE EPITAXY
The photovoltaic properties of an Al In As/InP heterojunctions grown by LPE method [NASA-CR-185996] N90-13886
Integrated optoelectronic receivers [AD-A213376] N90-14098
LIQUID-GAS MIXTURES
Preparation of binary ice layers by condensation from gas phase [JUEL-2248] N90-13631
LIQUID-LIQUID INTERFACES
Reorganization free energy for electron transfers at liquid-liquid and dielectric semiconductor-liquid interfaces [AD-A212985] N90-14111
LIQUID-SOLID INTERFACES
Reorganization free energy for electron transfers at liquid-liquid and dielectric semiconductor-liquid interfaces [AD-A212985] N90-14111
LIQUID-VAPOR INTERFACES
Buoyancy effects on the vapor condensation rate on a horizontal liquid surface [NASA-TM-102437] N90-13675
Vapor condensation on liquid surface due to laminar jet-induced mixing: The effects of system parameters [NASA-TM-102433] N90-13751
Model system studies with a phase separated membrane bioreactor N90-13954
LIQUIDS
Thermophysical properties of buta-1,3-diene [ESDU-89005] N90-13619
LITHIUM ALLOYS
Quench sensitivity in Al-Cu-Li alloys [AD-A213055] N90-13639
The effect of composition and aging treatment on the microstructure and mechanical properties of aluminum-lithium-titanium alloys [AD-A213144] N90-13640
LOAD TESTS
Failure processes in unidirectional composite materials N90-13598
Static and free-vibrational response of semi-circular graphite-epoxy frames with thin-walled open sections [NASA-CR-186097] N90-13600
General buckling tests with thin-walled shells [DLR-MITT-89-13] N90-13816
LOADING RATE
An evaluation of a fatigue crack growth prediction model for variable-amplitude loading (PREFFAS) [LR-537] N90-13822
LOADS (FORCES)
Study of forces and moments on wing-bodies at high incidence, volumes 1 and 2 N90-13350
A transient response method for linear coupled substructures [NASA-TP-2926] N90-13444
Cryogenic systems for the large deployable reflector N90-13470
Initial test results for the mini-mast N90-13482
LOCAL AREA NETWORKS
Spacelab system analysis: The modified free access protocol: An access protocol for communication systems with periodic and Poisson traffic [NASA-CR-183805] N90-13497
On stability of queueing models of local area networks with slotted ring protocols [MEMO-795] N90-14057
Analysis of a queueing model for slotted ring networks [MEMO-796] N90-14058
Dynamic workload modeling of high speed token rings in a metropolitan area network [MEMO-INF-89-21] N90-14059
LOGARITHMS
The weighted sum of two S-units being a square [MEMO-792] N90-14031
Solving a specific Thue-Mahler equation [MEMO-793] N90-14032
LOGIC CIRCUITS
Delay test generation for synchronous sequential circuits [AD-A211917] N90-13697
LOGIC DESIGN
Constructing a calculus of programs [CWI-CS-R8914] N90-13979
LOGIC PROGRAMMING
On the safe approximation of PROLOG programs [CWI-CS-R8913] N90-13978
Program transformation with abstract relation algebras [AD-A213270] N90-14011
LOGISTICS
Total quality management plan: Technical and logistics services [AD-A212864] N90-14128
LONG DURATION EXPOSURE FACILITY
Syncom 4 deploy, LDEF retrieval highlight 10-day Columbia flight [NASA-NEWS-RELEASE-89-180] N90-13448
LONG DURATION SPACE FLIGHT
Science and applications on the space station: A strategic vision [NASA-TM-101863] N90-13493
Bone mineral measurement using dual energy x ray densitometry N90-13958
LOOPS
Des Cloizeaux's law for strings and galaxies formation. Part 2: Non Abelian configurations [ROM1F-89-682-PT-2] N90-14173
LORAN C
LORAN C stability integrity assurance [AD-A212663] N90-13364
LOSSES
Speech reception in quiet and in noisy conditions by individuals with noise-induced hearing loss in relation to their audiogram [IZF-1989-11] N90-13692
LOSSLESS MATERIALS
Implementation issues in source coding [NASA-CR-185327] N90-13963
LOSSY MEDIA
Electromagnetic wave propagation through circular waveguides containing radially inhomogeneous lossy media [AD-A213062] N90-13688
Implementation issues in source coding [NASA-CR-185327] N90-13963
LOW FREQUENCIES
Auroral particle acceleration by dc and low frequency electric fields N90-13841
Low frequency polarized and depolarized light scattering in H-bonded liquids: CH3(CH2)n-1OH (n=1,...5) [PREPRINT-693] N90-14100
LOW GRAVITY MANUFACTURING
Containerless Processing of Metals: Undercooling and Solidification [DLR-MITT-89-15] N90-13645
LOW TEMPERATURE
Analysis of an R-SQUID noise thermometer [VTT-PUBL-54] N90-13769
Operational activity in France and a new method of balloon temperature piloting N90-13857
LOW TEMPERATURE TESTS
Low temperature optical testing of CFRP telescope panels N90-13463
LOWER BODY NEGATIVE PRESSURE
Preliminary study of pharmacological control of space disease [ETN-90-95015] N90-13927
LUBRICANT TESTS
Evaluation of newly formulated Dow Corning 321 dry film lubricant [NASA-CR-183828] N90-13661
LUMINAIRES
Measurement of the light flux density patterns from luminaires proposed as photon sources for photosynthesis during space travel [NASA-CR-186124] N90-13916
LUMINOUS INTENSITY
Proximity effects on adjacent and multiple stars N90-13533
LYMAN ALPHA RADIATION
Design and technical aspects of the Solly instrument N90-13847
Observation of the solar Lyman-alpha line N90-13868
The low-ion QSO absorption-line systems N90-14162
LYMAN SPECTRA
The low-ion QSO absorption-line systems N90-14162
LYMPHOCYTES
Response of lymphocytes to a mitogenic stimulus during spaceflight N90-13942

M

M STARS
The winds of high luminosity late-type bright stars [NASA-CR-182961] N90-14160
MACHINE TRANSLATION
Inductive reasoning and Kolmogorov complexity (preliminary version) [CWI-CS-R8915] N90-14062
MACHINING
MM and T advanced balancing/machining [AD-A213103] N90-13775
MAGELLANIC CLOUDS
The choice of stars in the Magellanic clouds N90-13543
MAGNETIC CONTROL
Autonomous spacecraft attitude control using magnetic torquing only N90-13415
Spacecraft attitude determination using the earth's magnetic field N90-13429
MAGNETIC FIELDS
Magneto-elastic interactions in conducting structures in transient magnetic fields N90-13686
A solvable self-similar model of the sausage instability in a resistive Z-pinch [AD-A213137] N90-14006
A search for the effects of active magnetic fields in extra-galactic radio sources N90-14161
MAGNETIC FLUX
Shear-induced inflation of coronal magnetic fields [NASA-CR-186103] N90-14178
MAGNETIC INDUCTION
Correlation between microstructure and magnetic properties of porous sintered iron and porous iron containing composites [KFK-4522] N90-13647
Electron beam sensitive devices for controllability [IMAG-RR-761-I] N90-13707
MAGNETIC RESONANCE
Surface cooled, vacuum impregnated superconducting magnet systems: Design, construction, applications [ETN-90-95014] N90-14072
MAGNETIC STORMS
Auroral and sub-auroral interaction at the F region ionosphere [AD-A213284] N90-13896
MAGNETIC VARIATIONS
A solvable self-similar model of the sausage instability in a resistive Z-pinch [AD-A213137] N90-14006
MAGNETOHYDRODYNAMIC STABILITY
Preliminary results of the rocket and scatter experiments ROSE: Measurements with the newly designed spherical probe N90-13850
A solvable self-similar model of the sausage instability in a resistive Z-pinch [AD-A213137] N90-14006
MAGNETOMETERS
Construction of a SQUID magnetometer for investigation of screening properties of high-T(sub c) superconductors [FOA-C-20765-2.2] N90-13768
High precision rocket attitude reconstruction using star sensor and magnetometer data N90-13844
MAGNETOSTRICTION
Magneto-elastic interactions in conducting structures in transient magnetic fields N90-13686
MAINTAINABILITY
A new view of weapon system reliability and maintainability [AD-A213281] N90-13382
Electronic warfare: Reliable equipment needed to test Air Force's electronic warfare systems [AD-A212952] N90-13687
MAINTENANCE
A new view of weapon system reliability and maintainability [AD-A213281] N90-13382
A new view of weapon system reliability and maintainability: Executive summary [AD-A213282] N90-13383
The US space station and its electric power system [NASA-TM-101974] N90-13596
Electronic warfare: Reliable equipment needed to test Air Force's electronic warfare systems [AD-A212952] N90-13687
MAN MACHINE SYSTEMS
Waiting times in polling systems with Markovian server routing [CWI-BS-R8905] N90-13989
The problem of automation: Inappropriate feedback and interaction, not overautomation [NASA-CR-186126] N90-13994
MAN-COMPUTER INTERFACE
Flight deck automation: Promises and realities [NASA-CP-10036] N90-13384
Conference Proceedings of the Human-Electronic Crew: Can They Work Together [AD-A211871] N90-13936
Workloads and waiting times in single-server systems with multiple customer classes [CWI-BS-R8906] N90-14020
Action languages: Dimensions, effects [NASA-CR-183388] N90-14181
MANAGEMENT ANALYSIS
A guide to reasoning under uncertainty [REPT-72/87/R488U] N90-13932
MANAGEMENT INFORMATION SYSTEMS
The Hipparcos Mission. Prelaunch status. Volume 2: The input catalog [ESA-SP-1111-VOL-2] N90-13529
Project ORION microcomputer management system [AD-A212945] N90-13959

Management control and status reports documentation standard and Data Item Descriptions (DID). Volume of the information system life-cycle and documentation standards, volume 5
[NASA-TM-101660] N90-14139
MANAGEMENT METHODS
Space Station Engineering Design Issues
[NASA-CR-185976] N90-13492
Management control and status reports documentation standard and Data Item Descriptions (DID). Volume of the information system life-cycle and documentation standards, volume 5
[NASA-TM-101660] N90-14139
MANAGEMENT PLANNING
The interface with the data reduction consortia N90-13528
Long-range plan for management and use of the radio spectrum by agencies and establishments of the Federal Government
[PB89-232367] N90-13693
Project ORION microcomputer management system
[AD-A212945] N90-13959
Total quality management implementation strategy: Directorate of Quality Assurance
[AD-A212863] N90-14127
Total quality management plan: Technical and logistics services
[AD-A212864] N90-14128
Total quality management implementing plan: Office of small and disadvantaged business utilization
[AD-A212865] N90-14129
Total quality management plan: Office of Congressional Affairs
[AD-A212866] N90-14130
Total quality management: Directorate of Contract Management master plan
[AD-A212867] N90-14131
Total quality management plan: Office of Public Affairs
[AD-A212868] N90-14132
MANIPULATORS
Assembly considerations for large reflectors N90-13480
Adaptive strategies for controls of flexible arms
[NASA-CR-185868] N90-13783
Design and control of a two-degree-of-freedom lightweight flexible arm
[AD-A213335] N90-13790
Acceleration sets of planar manipulators. Part 2: Applications and experiments
[AD-A213336] N90-13791
Definition, determination and characterization of acceleration sets for spatial manipulators
[AD-A213366] N90-13793
Performance evaluation of a six-axis generalized force-reflecting teleoperator
[NASA-CR-186106] N90-13796
On control of manipulators
[ISBN-90-9002789-0] N90-13804
MANNED SPACE FLIGHT
Cells in Space
[NASA-CP-10034] N90-13939
Countermeasures to microgravity N90-13957
MANUALS
User's manual for the ride motion simulator
[AD-A212855] N90-13402
MANUFACTURING
Activities report of the metallic manufacturing industry
[ISSN-0524-7705] N90-13649
The economic impact of automation technology
[AD-A213363] N90-13682
Evolution of the EPR procedure for polycrystalline Si ribbon drawing for photovoltaic cell manufacturing
[ISAL-89-0027] N90-13888
Study of metal-insulator-semiconductor structures on indium phosphide, implemented by anodic oxidation
[ECL-88-10] N90-14114
Retrieving and integrating IC fabrication data from dissimilar databases
[AD-A211890] N90-14140
MANY BODY PROBLEM
Periodic solutions of Hamiltonian systems of 3-body type
[AD-A212691] N90-14005
MAPPING
Definition, determination and characterization of acceleration sets for spatial manipulators
[AD-A213366] N90-13793
Extended memory library for AFOS (Automation of Field Operations and Services) applications
[PB89-230858] N90-14147
Orion B: Anatomy of a star-forming region N90-14155
MAPS
Feature modeling: The incorporation of a front and eddy map into optimum interpolation-based thermal analysis
[AD-A213253] N90-13914
MARAGING STEELS
Mechanical property characterization of VascoMax T-300
[AD-A212950] N90-13637
MARANGONI CONVECTION
Design challenges for space bioreactors N90-13955
MARINE BIOLOGY
Adaptation and resistance of ecosystems to stress
[AD-A212999] N90-13889
MARINE TECHNOLOGY
NRL (Naval Research Laboratory) Review
[AD-A212886] N90-14182
Summary of research academic departments, 1987-1988
[AD-A213252] N90-14183
MARKOV PROCESSES
Random Markov processes and uniform martingales
[CWI-BS-R8906] N90-14021
MARTINGALES
Random Markov processes and uniform martingales
[CWI-BS-R8906] N90-14021
Theory of goodness of fit tests and scanning innovation martingales
[CWI-BS-R8904] N90-14046
MASS SPECTROMETERS
A double focusing mass-spectrometer for simultaneous ion measurements in the stratosphere N90-13848
Neutral air turbulence in the middle and upper atmosphere observed during the MAC/EPSILON campaign N90-13855
MATCHED FILTERS
Efficient detection of small moving objects
[AD-A213314] N90-13690
MATCHING
Conjugate profiles on mating gear teeth
[MEMO-COSOR-89-01] N90-13795
An editor for 3D-models for image analysis
[FOA-C-30534-3.4] N90-13986
MATHEMATICAL MODELS
Test network Delft
[ETN-90-96009] N90-13365
Thermal barrier coating life prediction model development, phase 1
[NASA-CR-182230] N90-13388
Constitutive modeling for isotropic materials (HOST)
[NASA-CR-179522] N90-13390
Constitutive modeling for isotropic materials (HOST)
[NASA-CR-174718] N90-13391
Discretization and model reduction for a class of nonlinear systems N90-13397
Mathematical model identification for flight simulation, based on flight and taxi tests
[LR-550] N90-13410
GOES I/M image navigation and registration N90-13422
Bilinear modeling and nonlinear estimation N90-13430
Atmospheric drag model calibrations for spacecraft lifetime prediction N90-13439
A transient response method for linear coupled substructures
[NASA-TP-2926] N90-13444
Large Deployable Reflector (LDR) thermal characteristics N90-13460
Advanced composite materials for precision segmented reflectors N90-13461
Explicit modeling and concurrent processing in the simulation of multibody dynamic systems N90-13481
Initial test results for the mini-mast N90-13482
A practical approach for minimum time control of the Spacecraft Control Laboratory Experiment (SCOLE), appendix A
[NASA-CR-186008] N90-13495
Tycho astrometry N90-13559
Modeling of the Hipparcos optical system N90-13572
Modelling of satellite control thruster plumes N90-13578
Fractography of composite delamination
[NASA-CR-183291] N90-13599
A new model for the structure of silica glass
[AD-A212972] N90-13659
Evaluation of selected computer models for modeling pyrotechnic and propellant devices
[AD-A213003] N90-13671
Magneto-elastic interactions in conducting structures in transient magnetic fields N90-13686
Stochastic modelling of EM scattering from foliage
[AD-A213118] N90-13689
A three-dimensional potential flow analysis of dynamic fluid forces acting on a whirling centrifugal impeller bounded by a volute N90-13717
Quadratic dynamical systems describing shear flow of non-Newtonian fluids
[AD-A212892] N90-13720
An improved algorithm for the modeling of vapor flow in heat pipes
[NASA-CR-185179] N90-13748
Large eddy simulation of homogeneous turbulence undergoing shear and thermal gradients. Application to one point closing models
[ECL-88-23] N90-13754
Model and computation of three-dimensional turbulent jets in a crossflow
[ECL-89-007] N90-13755
A stochastic model for the calculation of multiple scattered lidar returns
[DLR-FB-89-36] N90-13778
Characterization of surfaces cut with a laser beam and thermal model of the process
[ISAL-89-0008] N90-13780
The limiting friction force
[ECL-89-005] N90-13801
Quantitative non-destructive evaluation using laser generated ultrasonic pulses N90-13805
A study on the sensitivity and simultaneous adjustment of a hoop-column antenna surface
[NASA-TM-101538] N90-13807
An evaluation of a fatigue crack growth prediction model for variable-amplitude loading (PREFFAS)
[LR-537] N90-13822
Buckling load analysis for imperfect cylindrical shells, part 1
[LR-543-PT-1] N90-13823
Design and evaluation of a new biaxial testing method for sheet material (SUPERBAT)
[LR-548] N90-13824
The use of a deformation model for sampling digitalized stereoscopic images
[IMAG-RR-753-I] N90-13884
Precision of semi-geometrically determined SLR baselines vs. site occupation time
[ETN-90-96007] N90-13885
Strain accumulation and surface deformation along the San Andreas, California
[NASA-CR-185893] N90-13894
The structural memory: A network model for human perception of serial objects
[CWI-CS-R8829] N90-13930
Model reduction of weakly damped mechanical systems
[MEMO-798] N90-13993
A solvable self-similar model of the sausage instability in a resistive Z-pinch
[AD-A213137] N90-14006
Why stochastic modeling is essential in analyzing interdicted transportation network performance
[AD-A213140] N90-14007
Using the physical structure of a system for control: An illustration
[MEMO-782] N90-14014
Analysis of three approaches to qualitative simulation
[MEMO-INF-89-32] N90-14035
A unified algebraic approach to integral and discrete evolution equations
[PREPRINT-668] N90-14044
Self-decomposable distributions and branching processes
[MEMO-COSOR-89-06] N90-14052
On stability of queueing models of local area networks with slotted ring protocols
[MEMO-795] N90-14057
Analysis of a queueing model for slotted ring networks
[MEMO-796] N90-14058
Modeling of power electronic systems with EMTP
[NASA-TM-102375] N90-14060
Some comments on the solvable Chiral Potts model
[PREPRINT-673] N90-14070
Analytical and computer-aided models of InP-based MISFETs and heterojunction devices
[AD-A211861] N90-14106
Shear-induced inflation of coronal magnetic fields
[NASA-CR-186103] N90-14178
MATHEMATICAL PROGRAMMING
Constructing a calculus of programs
[CWI-CS-R8914] N90-13979
MATHEMATICS
Summary of research academic departments, 1987-1988
[AD-A213252] N90-14183
MATRICES (CIRCUITS)
Memory matrix
[WO-PATENT-88/04096] N90-13961
MATRICES (MATHEMATICS)
The quadratic matrix inequality in singular H infinity control with state feedback
[MEMO-COSOR-89-03] N90-13997
A multilevel parallel solver for block tridiagonal and banded linear systems
[AD-A213151] N90-14008

The algebraic Riccati equation and singular optimal control
[MEMO-COSOR-88-31] N90-14028
Fluctuations of the Lyapunov exponent in disordered systems
[PREPRINT-690] N90-14063
A graph theoretic characterization for the rank of the transfer matrix of a structured system
[CWI-OS-R8819] N90-14064
Some comments on the solvable Chiral Potts model
[PREPRINT-673] N90-14070

MATRIX MATERIALS
Status of Gr/glass composites technology at UTOS N90-13459
Failure processes in unidirectional composite materials N90-13598
Toughening of a particulate-reinforced/ceramic-matrix composite
[AD-A213180] N90-13604

MATRIX THEORY
Lattice QCD estimate of mixing parameters for heavy meson systems
[PREPRINT-687] N90-14079

MATTER (PHYSICS)
Interaction of radiation with matter: Atomic collision processes occurring in the presence of radiation fields
[AD-A213112] N90-14078

MAXWELL-BOLTZMANN DENSITY FUNCTION
Solution of the Boltzmann equation using an energy group method
[AD-A213138] N90-14096

MEASURE AND INTEGRATION
On a new integrable Hamiltonian system with nearest neighbors interaction
[PREPRINT-667] N90-14043

MEASUREMENT
Large deviation estimates in the stochastic quantization of phi sub 2 exp 4
[PREPRINT-686] N90-14050

MEASURING INSTRUMENTS
A laboratory verification sensor N90-13477
The evaluation of a metered mixer for RTV silicone for RSRM nozzle backfill operations
[NASA-CR-183831] N90-13763
A slow strain-rate tensile testing machine
[ARL-MAT-TM-399] N90-13764
Bone mineral measurement using dual energy x ray densitometry N90-13958

MECHANICAL PROPERTIES
The application of cast SiC/Al to rotary engine components
[NASA-CR-179610] N90-13385
Mechanical and thermal testing N90-13521
Quench sensitivity in Al-Cu-Li alloys
[AD-A213055] N90-13639
The effect of composition and aging treatment on the microstructure and mechanical properties of aluminum-lithium-titanium alloys
[AD-A213144] N90-13640
The effects of alloying and thermal factors on the solidification and mechanical properties of gray iron
[VTT-619] N90-13651
Considerations about the acceptance inspection of HS fasteners intended for controlled tightening
[CRIF-MT-175] N90-13806
The Fourth Oxford International Conference on the Mechanical Properties of Materials at High Rates of Strain
[AD-A212293] N90-13809
Time domain coupling of the boundary and finite element methods for elastodynamics
[AD-A213243] N90-13811
Sol-gel processing science using a Sol-Gel Optics Research Facility (SGORF)
[AD-A213056] N90-14095

MEMBRANE STRUCTURES
Model system studies with a phase separated membrane bioreactor N90-13954

MEMORY (COMPUTERS)
Memory matrix
[WO-PATENT-88/04096] N90-13961
Extended memory library for AFOS (Automation of Field Operations and Services) applications
[PB89-230858] N90-14147

MENTAL PERFORMANCE
The structural memory: A network model for human perception of serial objects
[CWI-CS-R8829] N90-13930
A guide to reasoning under uncertainty
[REPT-72/87/R486U] N90-13932

MESON-NUCLEON INTERACTIONS
Exotic Higgs production at e+e- colliders
[PREPRINT-671] N90-14088

MESONS
Lattice QCD estimate of mixing parameters for heavy meson systems
[PREPRINT-687] N90-14079
A lattice study of semileptonic decays of D-mesons
[PREPRINT-660] N90-14086
Exotic Higgs production at e+e- colliders
[PREPRINT-671] N90-14088

MESOPAUSE
Near-mesopause temperatures at 69 N latitude in late summer N90-13837

MESOSPHERE
Neutral air turbulence in the middle and upper atmosphere observed during the MAC/EPSILON campaign N90-13855
Polar mesosphere summer echoes and associated atmospheric gravity waves N90-13856
The interaction and variation of waves and turbulence from MST radar data
[AD-A212849] N90-13906

MESSAGE PROCESSING
A multilevel parallel solver for block tridiagonal and banded linear systems
[AD-A213151] N90-14008
Action languages: Dimensions, effects
[NASA-CR-183388] N90-14181

METAL BONDING
Contamination removal using various solvents and methodologies
[NASA-CR-183747] N90-13652

METAL CRYSTALS
Energy concentration induced by phase transitions in hydrogenated metals
[PREPRINT-672] N90-13650

METAL FATIGUE
Threshold for fatigue crack propagation
[DLR-FB-89-33] N90-13815
Mean stress and the exhaustion of fatigue-damage resistance
[NASA-TM-101311] N90-13819

METAL FLUORIDES
Proceedings of the High Energy Density Matter (HEDM) Conference
[AD-A212314] N90-13670

METAL HYDRIDES
Effect of adsorbed arsenic on the decomposition rate of nickel hydride
[AD-A213245] N90-13624
Anomalous strain rate dependence of the serrated flow in Ni-H and Ni-C-H alloys
[AD-A213244] N90-13641

METAL MATRIX COMPOSITES
Ductile failure
[AD-A212975] N90-13601

METAL OXIDE SEMICONDUCTORS
An accurate timing model for fault simulation in MOS circuits
[AD-A213153] N90-13702
Design of a power component with IGBT insulated grid. Static and dynamic study
[ECL-88-22] N90-13710
Multisensor technologies for low cost methane detection
[PB89-235188] N90-13766
Unified model of charge build up and annealing of oxide charge and interface states in SiO2 due to stress
[HMI-B-465] N90-14120

METAL OXIDES
Thermodynamic properties of some metal oxide-zirconia systems
[NASA-TM-102351] N90-13666

METAL PLATES
Mobility power flow analysis of an L-shaped plate structure subjected to acoustic excitation
[NASA-CR-186130] N90-13817

METAL PROPELLANTS
Proceedings of the High Energy Density Matter (HEDM) Conference
[AD-A212314] N90-13670

METAL-METAL BONDING
Reflection by defective diffusion bonds
[AD-A212995] N90-13638

METALLIC GLASSES
Nucleation kinetics in undercooled, glass-forming metallic melts
[DLR-FB-89-32] N90-13644
Computational studies of structural and transport properties of amorphous solids
[ETN-90-96027] N90-13664

METALLIZING
Wear-resistant coated object
[EP-PATENT-0-289-173-A1] N90-13643

METALLOGRAPHY
Internal and external nitriding and nitrocarburizing of iron and iron-based alloys
[ETN-90-96012] N90-13646

METALS
Activities report of the metallic manufacturing industry
[ISSN-0524-7705] N90-13649
Stress intensity factors for cracking metal structures under rapid thermal loading. Volume 2: Theoretical background
[AD-A213297] N90-13812

METASTABLE ATOMS
CANOES 2: Dynamics of atmospheric infrared thermochemical excitation, volume 4
[AD-A213344] N90-13900

METASTABLE STATE
CANOES 2: Dynamics of atmospheric infrared thermochemical excitation, volume 1
[AD-A213341] N90-13897
CANOES 2: Dynamics of atmospheric infrared thermochemical excitation, volume 2
[AD-A213342] N90-13898
CANOES 2: Dynamics of atmospheric infrared thermochemical excitation, volume 3
[AD-A213343] N90-13899

METEOROID CONCENTRATION
Reexamination of data from the asteroid/meteoroid detector
[NASA-CR-185997] N90-14175

METEOROIDS
Reexamination of data from the asteroid/meteoroid detector
[NASA-CR-185997] N90-14175

METEOROLOGICAL FLIGHT
Meteorological atlas of the Northern Hemisphere lower stratosphere for January and February 1989 during the Airborne Arctic Stratospheric Expedition
[NASA-TM-4145] N90-13908

METEOROLOGICAL PARAMETERS
Estimation of rain rate using spatial and multichannel coherence: Analysis of SSM/I data N90-13905

METEOROLOGICAL SATELLITES
A collection of papers related to heavy precipitation forecasting
[PB89-230833] N90-13910

METEOROLOGY
Meteorological atlas of the Northern Hemisphere lower stratosphere for January and February 1989 during the Airborne Arctic Stratospheric Expedition
[NASA-TM-4145] N90-13908
Activities report of the World Meteorological Organization
[WMO-713] N90-13912

METHANE
Multisensor technologies for low cost methane detection
[PB89-235188] N90-13766

METRIC SPACE
Some remarks on the gap metric
[MEMO-COSOR-88-34] N90-14029

MICROCHANNEL PLATES
Outline on the future Italian transportable laser ranging station
[CISE-4845] N90-13782

MICROCRYSTALS
Memory matrix
[WO-PATENT-88/04096] N90-13961

MICROELECTRONICS
Fundamental quantum 1/f noise in ultrasmall semiconductor devices and their optimal design principles
[AD-A211947] N90-14107

MICROGRAVITY APPLICATIONS
Facilities for microgravity combustion research
[NASA-TM-102014] N90-13679

MICROORGANISMS
Adaptation and resistance of ecosystems to stress
[AD-A212999] N90-13889

MICROSTRIP DEVICES
Microwave microstrip resonator measurements of Y1Ba2Cu3O(7-x) and Bi2Sr2Ca1Cu2O(8-y) thin films
[NASA-TM-102159] N90-13704

MICROSTRIP TRANSMISSION LINES
Characteristic impedance of microstrip lines
[NASA-TM-101581] N90-13694

MICROSTRUCTURE
Quench sensitivity in Al-Cu-Li alloys
[AD-A213055] N90-13639
The effect of composition and aging treatment on the microstructure and mechanical properties of aluminum-lithium-titanium alloys
[AD-A213144] N90-13640
Correlation between microstructure and magnetic properties of porous sintered iron and porous iron containing composites
[KFK-4522] N90-13647
Surfaces and interfaces of ceramic materials
[AD-A212417] N90-13657
A new model for the structure of silica glass
[AD-A212972] N90-13659

Computational studies of structural and transport properties of amorphous solids
[ETN-90-96027] N90-13864
MICROWAVE IMAGERY
Estimation of rain rate using spatial and multichannel coherence: Analysis of SSM/I data N90-13905
MICROWAVE RESONANCE
Microwave microstrip resonator measurements of Y1Ba2Cu3O(7-x) and Bi2Sr2Ca1Cu2O(8-y) thin films
[NASA-TM-102159] N90-13704
MICROWAVE SCATTERING
Experimental and theoretical study of artificial plasma layers produced by two intersecting beams in a chamber
[NASA-CR-184598] N90-14102
MICROWAVE SOUNDING
Estimation of rain rate using spatial and multichannel coherence: Analysis of SSM/I data N90-13905
MICROWAVES
Microwave excited excimer laser
[ETN-90-95909] N90-13781
MIDDLE ATMOSPHERE
Evidence for accurate temperatures from the inflatable falling sphere N90-13835
Observation of wind corners in the middle atmosphere over Andenes (69 N) during winter 1983/84, summer 1987 and summer 1988 N90-13836
The DYANA campaign 1990 N90-13870
MILITARY AIRCRAFT
NDI (Nondestructive Inspection) oriented corrosion control for Army aircraft. Phase 1: Inspection methods
[AD-A213368] N90-13359
MILITARY OPERATIONS
Electronic warfare: Reliable equipment needed to test Air Force's electronic warfare systems
[AD-A212952] N90-13687
MILLIMETER WAVES
Development of high gain three terminal devices - at millimeter wave frequencies
[AD-A213089] N90-13701
MINERAL EXPLORATION
Summaries of the thematic conferences on remote sensing for exploration geology
[NASA-CR-185321] N90-13880
MINIMAX TECHNIQUE
The activity selection problem: A network and game theoretic approach
[MEMO-794] N90-14056
MINKOWSKI SPACE
On thick domain walls in general relativity
[NASA-CR-185926] N90-14124
MIRRORS
Composite panel development at JPL N90-13458
Lightweight composite reflector panels N90-13462
Coherent phasing of segmented mirrors N90-13474
Real-time sensing of optical alignment N90-13479
The telescope mirrors N90-13504
The x ray mirror and the PSPC of the supernova-rocket-project N90-13867
MIS (SEMICONDUCTORS)
Elaboration and characterization of MISFET transistors on InP
[ECL-88-19] N90-13709
Study of metal-insulator-semiconductor structures on indium phosphide, implemented by anodic oxidation
[ECL-88-10] N90-14114
Manufacturing and characterization of insulator-germanium structures
[ECL-88-13] N90-14115
MISSILE CONFIGURATIONS
Preliminary airworthiness evaluation of the AH-64A equipped with the Air To Air Stinger (ATAS) missile system
[AD-A213030] N90-13374
MISSION PLANNING
Active rendezvous between a low-earth orbit user spacecraft and the Space Transportation System (STS) shuttle N90-13436
The Hipparcos Mission. Prelaunch status. Volume 1: The Hipparcos satellite
[ESA-SP-1111-VOL-1] N90-13499
Operating principle N90-13500
In-orbit payload calibration N90-13526
MITOSIS
Polarity establishment, morphogenesis, and cultured plant cells in space N90-13943
MIXING
Evaluation of a metering, mixing, and dispensing system for mixing polysulfide adhesive
[NASA-CR-183749] N90-13654
The evaluation of a metered mixer for RTV silicone for RSRM nozzle backfill operations
[NASA-CR-183831] N90-13763
MIXING CIRCUITS
Advances in SIS receiver technology N90-13466
MIXING LAYERS (FLUIDS)
Application of large eddy interaction model to a mixing layer
[NASA-CR-185123] N90-13328
A planar reacting shear layer system for the study of fluid dynamics-combustion interaction
[NASA-TM-102422] N90-13393
Numerical solutions of the complete Navier-Stokes equations
[NASA-CR-186102] N90-13747
MOBILITY
Some remarks on the working principle of the rocketborne nose tip dc probes in the D-region of the ionosphere N90-13839
MODELS
Modeling and measurement methods for high speed bipolar transistors
[REPT-11] N90-13714
MODULATION
The modulating grid N90-13505
MODULATION TRANSFER FUNCTION
The relay lens systems N90-13506
The detectors N90-13507
MODULATORS
Optical modulators based on polymers
[EP-PATENT-0-294-061-A1] N90-14099
MODULES
Apparatus for cooling electronic components in aircraft
[AD-D014207] N90-13373
MODULUS OF ELASTICITY
Identification of equivalent modulus of a composite beam from nonmodal vibratory tests
[ECL-89-001] N90-13821
MOISTURE CONTENT
Liquid water content and droplet size calibration of the NASA Lewis Icing Research Tunnel
[NASA-TM-102447] N90-13797
An evaluation of the Smith-Feddes model
[AD-A213237] N90-13907
MOLECULAR BEAM EPITAXY
Chemical beam epitaxy of ZnSe
[AD-A213265] N90-13625
MOLECULAR CLOUDS
Interstellar medium and infrared emission of the galactic disk N90-13862
Orion B: Anatomy of a star-forming region N90-14155
MOLECULAR COLLISIONS
CANOES 2: Dynamics of atmospheric infrared thermochemical excitation, volume 1
[AD-A213341] N90-13897
CANOES 2: Dynamics of atmospheric infrared thermochemical excitation, volume 2
[AD-A213342] N90-13898
MOLECULAR EXCITATION
CANOES 2: Dynamics of atmospheric infrared thermochemical excitation, volume 4
[AD-A213344] N90-13900
MOLECULAR SPECTRA
A high-resolution atlas of the infrared spectrum of the Sun and the Earth atmosphere from space: A compilation of ATMOS spectra of the region from 650 to 4800 cm (2.3 to 16 micron). Volume 1: The Sun
[NASA-RP-1224-VOL-1] N90-13893
MOMENTS
Study of forces and moments on wing-bodies at high incidence, volumes 1 and 2 N90-13350
MOMENTUM TRANSFER
Periodic-disturbance accommodating control of the space station for asymptotic momentum management N90-13416
A lattice study of semileptonic decays of D-mesons
[PREPRINT-660] N90-14086
MONITORS
Payload electronics and mechanisms N90-13508
Pilot investigation of indoor-outdoor and personal PM10 (thoracic) and associated ionic compounds and mutagenic activity
[PB89-222723] N90-13920
Optical properties monitor: Experiment definition phase
[NASA-CR-183836] N90-14092
MONOTONE FUNCTIONS
Monotonicity of performance measures in a processor sharing queue
[CWI-BS-R8902] N90-14019
MONTE CARLO METHOD
An autopilot design methodology for bank-to-turn missiles
[AD-A213379] N90-13399
MORPHOLOGY
Fundamental results from microgravity cell experiments with possible commericial applications N90-13940
Polarity establishment, morphogenesis, and cultured plant cells in space N90-13943
The algebraic basis of mathematical morphology. Part 1: Dilations and erosions
[CWI-AM-R8807] N90-14065
MOTION SICKNESS
Simulator induced sickness in the CP-140 (Aurora) flight deck simulator
[AD-A213096] N90-13923
Functional decor in the International Space Station: Body orientation cues and picture perception
[NASA-TM-102242] N90-13931
MOTION SIMULATION
Compensatory tracking in disturbance tasks and target following tasks. The influence of cockpit motion on performance and control behavior
[LR-511] N90-13933
MOTION SIMULATORS
User's manual for the ride motion simulator
[AD-A212855] N90-13402
Kinematics and control of manipulation robots
[WTHD-187] N90-13803
Simulator induced sickness in the CP-140 (Aurora) flight deck simulator
[AD-A213096] N90-13923
MOVING TARGET INDICATORS
Efficient detection of small moving objects
[AD-A213314] N90-13690
MULTIPLIERS
Resonant-tunneling oscillators and multipliers for submillimeter receivers N90-13467
MULTIPROCESSING (COMPUTERS)
Parallelism in the discrete-event simulation algorithm
[AD-A213060] N90-13970
A fault-tolerant software algorithm for a network of transputers
[AD-A213092] N90-13972
MULTISENSOR APPLICATIONS
Multisensor technologies for low cost methane detection
[PB89-235188] N90-13766
MULTISPECTRAL PHOTOGRAPHY
Physically-based parameterization of spatially variable soil and vegetation using satellite multispectral data
[NASA-CR-185957] N90-13879
MULTIVARIATE STATISTICAL ANALYSIS
On the recurrence relation for multivariate B-splines with respect to dimension
[MEMO-786] N90-14017
MUONS
The determinatin of the muon content of EAS from Cygnus X-3 N90-14179
MUTAGENS
Pilot investigation of indoor-outdoor and personal PM10 (thoracic) and associated ionic compounds and mutagenic activity
[PB89-222723] N90-13920

N

NASA PROGRAMS
Small business innovation research: Program solicitation
[NASA-TM-101869] N90-14126
National Aeronautics and Space Administration Multiyear Authorization Act of 1989 N90-14148
National Aeronautics and Space Administration authorization
[S-HRG-101-348] N90-14149
Centers for the commercial development of space
[NASA-PAM-525] N90-14151
NASA commercial programs
[NASA-TM-101853] N90-14152
NASA SPACE PROGRAMS
Comparison of the space program performance of countries with space programs
[ILR-MITT-222] N90-14150
An implementation plan for priorities in solar-system space physics
[NASA-CR-185375] N90-14154
The Explorer program for astronomy and astrophysics N90-14158
NASTRAN
Application of an efficient hybrid scheme for aeroelastic analysis of advanced propellers
[NASA-TM-102428] N90-13355
Investigation of difficult component effects on finite element model vibration prediction for the Bell AG-1G helicopter. Volume 2: Correlation results
[NASA-CR-181916-VOL-2] N90-13814
NATIONAL AIRSPACE SYSTEM
National Airspace System airspace management operational concept
[DOT/FAA/DS-89/29] N90-13361
National Airspace System flight planning operational concept
[DOT/FAA/DS-89/30] N90-13362

NATURAL GAS
Experimental and computational study of combustion limits in natural-gas fueled internal combustion engines [PB89-235196] N90-13673
NATURAL SATELLITES
The Voyager Neptune travel guide [NASA-CR-186108] N90-13412
Minor planets and other solar system objects N90-13545
The treatment of minor planets and planetary satellites N90-13563
NAVIER-STOKES EQUATION
Multigrid calculations of 3-D turbulent viscous flows [NASA-CR-185154] N90-13323
Computation of viscous incompressible flows [NASA-TM-101090] N90-13329
An Introduction to Hypersonic Aerodynamics [VKI-LS-1989-01] N90-13334
Gas flows in rocket motors, volume 1 [AD-A213348] N90-13591
Gas flows in rocket motors. Volume 2, appendix C: Time iterative solution of viscous supersonic flow [AD-A213349] N90-13592
Gas flows in rocket motors. Volume 3, appendix D: Computer code listings [AD-A213350] N90-13593
A review of quasi-coherent structures in a numerically simulated turbulent boundary layer [NASA-TM-102191] N90-13723
Multigrid and defect correction for the steady Navier-Stokes equations: Applications to aerodynamics [ETN-90-96011] N90-13727
Numerical simulation of transition in three-dimensional boundary layers [DLR-FB-89-12] N90-13728
Numerical Methods for Flows in Turbomachinery, volume 1 [VKI-LS-1989-06-VOL-1] N90-13735
Three D flows in turbine blade rows N90-13739
Turbulence modeling and implementation in Navier-Stokes solvers N90-13742
Numerical methods for unsteady turbomachinery flow N90-13743
Navier-Stokes simulation of the crossflow instability in swept-wing flows [NASA-CR-186122] N90-13744
Numerical solutions of the complete Navier-Stokes equations [NASA-CR-186102] N90-13747
Analysis of rotary engine combustion processes based on unsteady, three-dimensional computations [NASA-TM-102469] N90-13749
Application of multi-grid methods for solving the Navier-Stokes equations [NASA-TM-102359] N90-14002
NAVIGATION SATELLITES
Inexpensive global location and tracking systems using geostationary satellites [AD-A213025] N90-13498
NAVY
Summary of research academic departments, 1987-1988 [AD-A213252] N90-14183
NEODYMIUM LASERS
MM and T advanced balancing/machining [AD-A213103] N90-13775
NEON
Hot spots Ar and Ne gas puff z-pinch [IPPCZ-289] N90-14103
NEPTUNE (PLANET)
The Voyager Neptune travel guide [NASA-CR-186108] N90-13412
NERVOUS SYSTEM
Computational and psychophysical study of human vision using neural networks [AD-A213290] N90-13924
NETWORK ANALYSIS
Why stochastic modeling is essential in analyzing interdicted transportation network performance [AD-A213140] N90-14007
The activity selection problem: A network and game theoretic approach [MEMO-794] N90-14056
Scaling in a non Abelian string network [ROM1F-89-676] N90-14066
NETWORK CONTROL
Dynamic workload modeling of high speed token rings in a metropolitan area network [MEMO-INF-89-21] N90-14059
NETWORK SYNTHESIS
The structural memory: A network model for human perception of serial objects [CWI-CS-R8829] N90-13930
NEURAL NETS
Gas identification system using graded temperature sensor and neural net interpretation [AD-A213359] N90-13627
Computational and psychophysical study of human vision using neural networks [AD-A213290] N90-13924
NEUROPHYSIOLOGY
Computational and psychophysical study of human vision using neural networks [AD-A213290] N90-13924
NEUTRINOS
Unitarity limits on the mass and radius of dark matter particles [NASA-CR-186079] N90-14164
Correlation among gravitational wave and neutrino detectors data during SN1987A [NOTA-INTERNA-932] N90-14165
Nuclear physics and cosmology [NASA-CR-186166] N90-14167
NEUTRON DIFFRACTION
Investigations of spontaneous nuclear order in copper by neutron diffraction [ETN-90-96060] N90-14090
NEWTON THEORY
Optimum shape of a blunt forebody in hypersonic flow [NASA-CR-181955] N90-13351
NICKEL ALLOYS
Constitutive modeling for isotropic materials (HOST) [NASA-CR-179522] N90-13390
Constitutive modeling for isotropic materials (HOST) [NASA-CR-174718] N90-13391
Effect of adsorbed arsenic on the decomposition rate of nickel hydride [AD-A213245] N90-13624
Anomalous strain rate dependence of the serrated flow in Ni-H and Ni-C-H alloys [AD-A213244] N90-13641
NICKEL COMPOUNDS
Effect of adsorbed arsenic on the decomposition rate of nickel hydride [AD-A213245] N90-13624
NICKEL STEELS
Mechanical property characterization of VascoMax T-300 [AD-A212950] N90-13637
NIGHTGLOW
A self-consistent model of the most common nightglow emissions N90-13853
NITRIDING
Internal and external nitriding and nitrocarburizing of iron and iron-based alloys [ETN-90-96012] N90-13646
NITROGEN
CANOES 2: Dynamics of atmospheric infrared thermochemical excitation, volume 1 [AD-A213341] N90-13897
CANOES 2: Dynamics of atmospheric infrared thermochemical excitation, volume 2 [AD-A213342] N90-13898
CANOES 2: Dynamics of atmospheric infrared thermochemical excitation, volume 3 [AD-A213343] N90-13899
CANOES 2: Dynamics of atmospheric infrared thermochemical excitation, volume 4 [AD-A213344] N90-13900
Propagation of sound in vibrationally excited nitrogen and hydrogen gas mixtures [AD-A213002] N90-14073
NITROGEN COMPOUNDS
Nuclear magnetic resonance signatures of nitrogen-containing compounds [AD-A213375] N90-13628
NITROGEN OXIDES
CANOES 2: Dynamics of atmospheric infrared thermochemical excitation, volume 1 [AD-A213341] N90-13897
CANOES 2: Dynamics of atmospheric infrared thermochemical excitation, volume 2 [AD-A213342] N90-13898
CANOES 2: Dynamics of atmospheric infrared thermochemical excitation, volume 3 [AD-A213343] N90-13899
CANOES 2: Dynamics of atmospheric infrared thermochemical excitation, volume 4 [AD-A213344] N90-13900
NOISE (SOUND)
ULF/VLF (0.001 to 50 Hz) Seismo-Acoustic Noise in the Ocean [AD-A212942] N90-13913
NOISE GENERATORS
Influence of vane sweep on rotor-stator interaction noise N90-13325
NOISE MEASUREMENT
Recovery of particle size distribution of ultrafine aerosols from diffusional decay measurements [AD-A213006] N90-13621
Analysis of an R-SQUID noise thermometer [VTT-PUBL-54] N90-13769
A model suitable for predicting the noise associated with the ducted tail rotor of a helicopter [ECL-88-09] N90-14074
NOISE PREDICTION (AIRCRAFT)
A model suitable for predicting the noise associated with the ducted tail rotor of a helicopter [ECL-88-09] N90-14074
NOISE REDUCTION
Estimation of rain rate using spatial and multichannel coherence: Analysis of SSM/I data N90-13905
Test procedures for the evaluation of helmet and headset mounted active noise reduction systems [AD-A212991] N90-13937
Fundamental quantum 1/f noise in ultrasmall semiconductor devices and their optimal design principles [AD-A211947] N90-14107
NONDESTRUCTIVE TESTS
NDI (Nondestructive Inspection) oriented corrosion control for Army aircraft. Phase 1: Inspection methods [AD-A213368] N90-13359
Nondestructive analysis of aileron fatigue and aging in a Mirage F1 [REPT-M6-594000] N90-13378
Quantitative non-destructive evaluation using laser generated ultrasonic pulses N90-13805
NONLINEAR OPTICS
Optics and opto-electronics systems [AD-A212340] N90-14093
NONLINEAR PROGRAMMING
General and numerical approach to the sphere solution in FAST N90-13555
NONLINEAR SYSTEMS
Correlation of Puma airloads: Lifting-line and wake calculation [NASA-TM-102212] N90-13327
The S.D.G., P.S.D. and the nonlinear airplane [NLR-MP-88018-U] N90-13371
Discretization and model reduction for a class of nonlinear systems N90-13397
Bilinear modeling and nonlinear estimation N90-13430
Using Broyden updates to approximate the Jacobian in a semi-implicit backward differentiation code [AD-A213239] N90-14010
Another approach to the local disturbance decoupling problem with stability for nonlinear systems [MEMO-799] N90-14033
NONNEWTONIAN FLUIDS
Quadratic dynamical systems describing shear flow of non-Newtonian fluids [AD-A212892] N90-13720
Analysis of new phenomena in shear flow of non-Newtonian fluids [AD-A212893] N90-13721
NONUNIFORM FLOW
Review and evaluation of a turbomachinery throughflow finite element code [AD-A213058] N90-13787
NORMALIZING (STATISTICS)
Some remarks on the gap metric [MEMO-COSOR-88-34] N90-14029
NORTHERN HEMISPHERE
Meteorological atlas of the Northern Hemisphere lower stratosphere for January and February 1989 during the Airborne Arctic Stratospheric Expedition [NASA-TM-4145] N90-13908
NOSE CONES
Blunt-nose inviscid airflows with coupled nonequilibrium processes N90-13336
NOZZLE DESIGN
Flight motor set 360L001 (STS-26R). Volume 5: Nozzle component [NASA-CR-183771] N90-13588
NOZZLE FLOW
Gas flows in rocket motors, volume 1 [AD-A213348] N90-13591
Gas flows in rocket motors. Volume 2, appendix C: Time iterative solution of viscous supersonic flow [AD-A213349] N90-13592
Gas flows in rocket motors. Volume 3, appendix D: Computer code listings [AD-A213350] N90-13593
Coherent structures in a round jet N90-13733
NOZZLE THRUST COEFFICIENTS
Aerodynamics of thrust vectoring [NASA-CR-185074] N90-13354

NOZZLES
Simulation of the control characteristics of an axial piston pump and a flapper-nozzle valve combination
N90-13784

NUCLEAR FUSION
Nuclear physics and cosmology
[NASA-CR-186166] N90-14167
Big Bang nucleosynthesis and the Quark-Hadron transition
[NASA-CR-186169] N90-14168
Cosmology and the weak interaction
[NASA-CR-186170] N90-14169

NUCLEAR INTERACTIONS
On a new integrable Hamiltonian system with nearest neighbors interaction
[PREPRINT-667] N90-14043
The effective (3)He-nucleon force in a microscopic DWBA approach to the (3)He,t charge exchange reaction — Distorted Wave-Borne Approximation (DWBA)
[KVI-763] N90-14077

NUCLEAR MAGNETIC RESONANCE
Nuclear magnetic resonance signatures of nitrogen-containing compounds
[AD-A213375] N90-13628

NUCLEAR PHYSICS
Low resistivity electrodeless streamer tubes
[PREPRINT-685-89] N90-13712
Nuclear physics and cosmology
[NASA-CR-186166] N90-14167

NUCLEAR REACTORS
Re-entry hazards and cosmos 1900
[FOA-C-30535-9.4] N90-13583

NUCLEAR STRUCTURE
Investigations of spontaneous nuclear order in copper by neutron diffraction
[ETN-90-96060] N90-14090

NUCLEATION
Nucleation kinetics in undercooled, glass-forming metallic melts
[DLR-FB-89-32] N90-13644

NUCLEON POTENTIAL
Nucleon polarizabilities in the constituent quark model
[NOTA-INTERNA-936] N90-14082

NUCLEON-NUCLEON SCATTERING
The effective (3)He-nucleon force in a microscopic DWBA approach to the (3)He,t charge exchange reaction — Distorted Wave-Borne Approximation (DWBA)
[KVI-763] N90-14077

NUMERICAL ANALYSIS
Study of modern instrumentation and methods for astronomic positioning in the field
[AD-A213217] N90-14157

NUMERICAL FLOW VISUALIZATION
Numerical Methods for Flows in Turbomachinery, volume 2
[VKI-LS-1989-06-VOL-2] N90-13741
Numerical methods for unsteady turbomachinery flow
N90-13743

NUMERICAL INTEGRATION
A transient response method for linear coupled substructures
[NASA-TP-2926] N90-13444

NUTS (FASTENERS)
Considerations about the acceptance inspection of HS fasteners inlanded for controlled tightening
[CRIF-MT-175] N90-13806

O

OBJECT PROGRAMS
SIMOGEN: An object-oriented language for simulation
[AD-A213129] N90-13973
Action languages: Dimensions, effects
[NASA-CR-183388] N90-14181

OCEAN SURFACE
Feature modeling: The incorporation of a front and eddy map into optimum interpolation-based thermal analysis
[AD-A213253] N90-13914

OCEAN TEMPERATURE
Feature modeling: The incorporation of a front and eddy map into optimum interpolation-based thermal analysis
[AD-A213253] N90-13914

OCEANOGRAPHY
Feature modeling: The incorporation of a front and eddy map into optimum interpolation-based thermal analysis
[AD-A213253] N90-13914

OCEANS
ULF/VLF (0.001 to 50 Hz) Seismo-Acoustic Noise in the Ocean
[AD-A212942] N90-13913

ON-LINE SYSTEMS
A practical approach for minimum time control of the Spacecraft Control Laboratory Experiment (SCOLE), appendix A
[NASA-CR-186008] N90-13495
On-line range prediction system, part 2
[NASA-CR-185889] N90-13771
Efficient on-line simulations of tree machines and multidimensional turing machines by random access machines
[AD-A213152] N90-13960
On the performance of on-line algorithms for partition problems
[MEMO-784] N90-14015

ONBOARD DATA PROCESSING
On-board software N90-13518
The in-orbit initialization phase N90-13525
The use of digital signal processing in satellite communication N90-13684

OPEN CIRCUIT VOLTAGE
Cable coupling lightning transient qualification
[NASA-CR-183826] N90-13405

OPERATIONS RESEARCH
In-orbit payload calibration N90-13526

OPERATOR PERFORMANCE
Compensatory tracking in disturbance tasks and target following tasks. The influence of cockpit motion on performance and control behavior
[LR-511] N90-13933

OPERATORS (MATHEMATICS)
Program transformation with abstract relation algebras
[AD-A213270] N90-14011

OPTICAL COMMUNICATION
Optical communication with semiconductor laser diode
[NASA-CR-185886] N90-13770
Integrated optoelectronic receivers
[AD-A213376] N90-14098

OPTICAL DATA PROCESSING
Optics and opto-electronics systems
[AD-A212340] N90-14093
Normal points: Compression of satellite laser ranging data
[ETN-90-96008] N90-14145

OPTICAL DEPOLARIZATION
Low frequency polarized and depolarized light scattering in H-bonded liquids: CH3(CH2)n-1OH (n=1,...5)
[PREPRINT-693] N90-14100

OPTICAL EQUIPMENT
Control of optical systems N90-13484
The modulating grid N90-13505
Modeling of the Hipparcos optical system N90-13572
Efficient detection of small moving objects
[AD-A213314] N90-13690

OPTICAL FILTERS
A review of laser filter materials
[AD-A213134] N90-13776

OPTICAL MEASUREMENT
Optical properties monitor: Experiment definition phase
[NASA-CR-183836] N90-14092
Reexamination of data from the asteroid/meteoroid detector
[NASA-CR-185997] N90-14175

OPTICAL MEASURING INSTRUMENTS
Optical modulators based on polymers
[EP-PATENT-0-294-061-A1] N90-14099

OPTICAL PROPERTIES
A figure control sensor for the Large Deployable Reflector (LDR) N90-13451
Low temperature optical testing of CFRP telescope panels N90-13463
Optical properties monitor: Experiment definition phase
[NASA-CR-183836] N90-14092

OPTICAL RADAR
Development of mid-infrared solid state lasers for spaceborne lidar
[NASA-CR-183290] N90-13772
Near-mesopause temperatures at 69 N latitude in late summer N90-13837
Diurnal variation of the sodium layer at polar latitudes in summer N90-13869

OPTICAL RELAY SYSTEMS
The relay lens systems N90-13506

OPTIMAL CONTROL
Aeroelastic control of composite lifting surfaces: Integrated aeroelastic control optimization N90-13396
The dynamics and control of large flexible space structures - 12, supplement 11
[NASA-CR-185966] N90-13494
Attitude and shape control of optimally designed large space structures N90-13579
Simulation of the control characteristics of an axial piston pump and a flapper-nozzle valve combination
N90-13784
On the asymptotic convergence of the simulated annealing algorithm in the presence of a parameter dependent penalization
[MEMO-COSOR-89-16] N90-13984
A priori results in linear quadratic optimal control theory
[MEMO-COSOR-89-02] N90-13996
The quadratic matrix inequality in singular H infinity control with state feedback
[MEMO-COSOR-89-03] N90-13997
The singular H infinity control problem with dynamic measurement feedback
[MEMO-COSOR-89-14] N90-14000
The output-stabilizable subspace and linear optimal control
[MEMO-COSOR-89-15] N90-14001
Optimal processes described by a parabolic differential equation with control in the coefficients, part 4
[MEMO-785-PT-4] N90-14016
The regular indefinite linear quadratic problem with linear endpoint constraints
[MEMO-COSOR-88-15] N90-14022
Continuity properties of one-parameter families of linear-quadratic problems without stability
[MEMO-COSOR-88-17] N90-14024
Convergence properties of indefinite linear quadratic problems with receding horizon
[MEMO-COSOR-88-25] N90-14026
On the output-stabilizable subspace
[MEMO-COSOR-88-27] N90-14027

OPTIMIZATION
Aeroelastic control of composite lifting surfaces: Integrated aeroelastic control optimization N90-13396
Discretization and model reduction for a class of nonlinear systems N90-13397
Feature modeling: The incorporation of a front and eddy map into optimum interpolation-based thermal analysis
[AD-A213253] N90-13914
Implementing the discrete Fourier transform on the hypercube FPS T40
[IMAG-RR-773-I] N90-13983
Model reduction of weakly damped mechanical systems
[MEMO-798] N90-13993
Identification of impulsive interference channels
[AD-A213154] N90-14009
Global optimization and simulated annealing
[MEMO-COSOR-88-21] N90-14025
Convergence properties of indefinite linear quadratic problems with receding horizon
[MEMO-COSOR-88-25] N90-14026
Fundamental quantum 1/f noise in ultrasmall semiconductor devices and their optimal design principles
[AD-A211947] N90-14107

OPTOELECTRONIC DEVICES
Optical modulators based on polymers
[EP-PATENT-0-294-061-A1] N90-14099

ORBIT CALCULATION
Orbit and attitude determination results during launch support operations for SBS-5
[PAPER-7] N90-13420
GOES I/M image navigation and registration
N90-13422
Automation of orbit determination functions for National Aeronautics and Space Administration (NASA)-supported satellite missions N90-13434
The controllability of the aeroassist flight experiment atmospheric skip trajectory N90-13438
Precision of semi-geometrically determined SLR baselines vs. site occupation time
[ETN-90-96007] N90-13885

ORBIT DECAY
Impact of tether cutting on onboard navigation during the Tethered Satellite Mission-1 N90-13424

ORBIT TRANSFER VEHICLES
Optimal trajectories for the Aeroassisted Flight Experiment. Part 1: Equations of motion in an Earth-fixed system
[NASA-CR-186134] N90-13441
Optimal trajectories for the Aeroassisted Flight Experiment. Part 2: Equations of motion in an inertial system
[NASA-CR-186135] N90-13442
Optimal trajectories for the aeroassisted flight experiment, 1988-89
[NASA-CR-186132] N90-13443

ORBITAL ASSEMBLY
Assembly considerations for large reflectors
N90-13480

ORBITAL MANEUVERS
Orbit and attitude determination results during launch support operations for SBS-5
[PAPER-7] N90-13420
GOES-I/M ascent maneuvers from transfer orbit to station N90-13421
The attitude and orbit control system N90-13516
Launch and early orbit N90-13524

ORBITAL MECHANICS
Flight Mechanics/Estimation Theory Symposium, 1989 [NASA-CP-3050] N90-13413
GOES-I/M ascent maneuvers from transfer orbit to station N90-13421
Shuttle relative navigation of a tethered satellite mission with current on board software N90-13423
Calculation of double-lunar swingby trajectories: I. Keplerian foundation N90-13435
Atmospheric drag model calibrations for spacecraft lifetime prediction N90-13439
ORION NEBULA
Further observations of rotationally excited far infrared OH16 and OH18 emission in Orion-KL: Tighter constraints on the nature of the emitting region [NASA-CR-186004] N90-14156
OSCILLATORS
Resonant-tunneling oscillators and multipliers for submillimeter receivers N90-13487
OUTGASSING
Gravimetric measurements of materials outgassing applied to graphite-epoxy laminates [NASA-TM-100753] N90-13609
OUTPUT
Test generation for highly sequential circuits [AD-A211932] N90-13698
On the output-stabilizable subspace [MEMO-COSOR-88-27] N90-14027
OXIDATION
Study of metal-insulator-semiconductor structures on indium phosphide, implemented by anodic oxidation [ECL-88-10] N90-14114
OXIDES
Preparation of 110K (Bi, Pb)-Sr-Ca-Cu-O superconductor from glass precursor [NASA-CR-185162] N90-14106
OXYGEN
CANOES 2: Dynamics of atmospheric infrared thermochemical excitation, volume 1 [AD-A213341] N90-13897
CANOES 2: Dynamics of atmospheric infrared thermochemical excitation, volume 2 [AD-A213342] N90-13898
Model system studies with a phase separated membrane bioreactor N90-13954
Fermentation and oxygen transfer in microgravity N90-13956
OXYGEN METABOLISM
Measurement of mechanical work and energy expenditure in running and bicycling N90-13935
OXYGEN PRODUCTION
New calculations of photodissociation cross-sections in the O2 Schumann-Runge system N90-13834
OXYGEN RECOMBINATION
CANOES 2: Dynamics of atmospheric infrared thermochemical excitation, volume 4 [AD-A213344] N90-13900
OXYGEN SPECTRA
A self-consistent model of the most common nightglow emissions N90-13853
OXYGEN-HYDROCARBON ROCKET ENGINES
LOX/hydrocarbon combustion instability investigation [NASA-CR-182249] N90-13589
OXYGENATION
MOBILE4 oxygenated fuels version user's guide [PB89-230700] N90-13674
OZONE
Proceedings: US/FRG (Federal Republic of Germany) Workshop on Photochemical Ozone Problem and Its Control: US Experiences and the Situation in Europe [PB89-233514] N90-13891
CANOES 2: Dynamics of atmospheric infrared thermochemical excitation, volume 4 [AD-A213344] N90-13900

P

P-I-N JUNCTIONS
Integrated optoelectronic receivers [AD-A213376] N90-14098
PACKAGES
MM and T for VHSIC multichip packages [AD-A213259] N90-13703
PACKET SWITCHING
Implementation issues in source coding [NASA-CR-185327] N90-13963
PACKET TRANSMISSION
Implementation issues in source coding [NASA-CR-185327] N90-13963
Analysis of a queueing model for slotted ring networks [MEMO-796] N90-14058
PACKINGS (SEALS)
Development and testing of a contactless static/dynamic shaft seal with little sealing gas requirement [KFK-4599] N90-13802
PAIR PRODUCTION
Exotic Higgs production at e+e- colliders [PREPRINT-671] N90-14088
Local pairing and antiferromagnetism in high-T sub c superconductors [AD-A213004] N90-14113
PANEL METHOD (FLUID DYNAMICS)
Study of the integration of wind tunnel and computational methods for aerodynamic configurations [NASA-TM-102196] N90-13332
A technique for the prediction of aerodynamics and aeroelasticity of rotor blades N90-13377
A three-dimensional potential flow analysis of dynamic fluid forces acting on a whirling centrifugal impeller bounded by a volute N90-13717
PANELS
SiO overcoating and polishing of CFRP telescope panels N90-13478
The Space Station Photovoltaic Panels Plasma Interaction Test Program: Test plan and results [NASA-TM-102474] N90-13581
PARABOLIC DIFFERENTIAL EQUATIONS
Parabolic equations for curves on surfaces. 2: Intersections, blow up and generalized solutions [AD-A212890] N90-14004
Optimal processes described by a parabolic differential equation with control in the coefficients, part 4 [MEMO-785-PT-4] N90-14016
PARALLEL PLATES
The modulating grid N90-13505
PARALLEL PROCESSING (COMPUTERS)
Block-structured solution of three-dimensional transonic flows using parallel processing [AD-A212851] N90-13330
Explicit modeling and concurrent processing in the simulation of multibody dynamic systems N90-13481
Parallelism in the discrete-event simulation algorithm [AD-A213060] N90-13970
Implementing the discrete Fourier transform on the hypercube FPS T40 [IMAG-RR-773-I] N90-13983
A multilevel parallel solver for block tridiagonal and banded linear systems [AD-A213151] N90-14008
PARAMETER IDENTIFICATION
Astrometric parameter determination in FAST N90-13556
The sphere solution and astrometric parameter determination in NDAC N90-13557
Double star reductions in FAST N90-13562
Accuracy and characteristics of the Hipparcos catalog N90-13566
Parameter estimation for the Gummel-Poon transistor model [MA-53] N90-13705
Senegalese land surface change analysis and biophysical parameter estimation using NOAA AVHRR spectral data [NASA-CR-186120] N90-13883
Software development for avionics SSME control and diagnostics [NASA-CR-184894] N90-13964
PARAMETERIZATION
Physically-based parameterization of spatially variable soil and vegetation using satellite multispectral data [NASA-CR-185957] N90-13879
Some quick and efficient methods for bearing-only target motion analysis [IMAG-RR-762-M] N90-14049
PARITY
Observational physics of mirror world [NASA-CR-185923] N90-14076
PARTIAL DIFFERENTIAL EQUATIONS
Quadratic dynamical systems describing shear flow of non-Newtonian fluids [AD-A212892] N90-13720
PARTICLE ACCELERATION
Auroral particle acceleration by dc and low frequency electric fields N90-13841
The auroral current - voltage relationship N90-13843
PARTICLE ACCELERATORS
Measurement of the fractional momentum carried by the gluons in the low Q2 photon-gluon fusion events at the ep HERA collider [NOTA-INTERNA-937] N90-14083
Use of a krypton isotope for rapid ion changeover at the Lawrence Berkeley Laboratory 88-inch cyclotron [NASA-CR-186107] N90-14084
PARTICLE BEAMS
Nonpotential scattering for the density matrix and quantum gravity [PREPRINT-668] N90-14080
PARTICLE DIFFUSION
Recovery of particle size distribution of ultrafine aerosols from diffusional decay measurements [AD-A213006] N90-13621
PARTICLE ENERGY
An experiment to search for galactic axions N90-14158
PARTICLE FLUX DENSITY
Performance of resistive plate counters at beam flux up to 140 Hz/cm2 [NOTA-INTERNA-930] N90-14081
PARTICLE INTERACTIONS
Observational physics of mirror world [NASA-CR-185923] N90-14076
Interaction of radiation with matter: Atomic collision processes occurring in the presence of radiation fields [AD-A213112] N90-14078
Measurement of the fractional momentum carried by the gluons in the low Q2 photon-gluon fusion events at the ep HERA collider [NOTA-INTERNA-937] N90-14083
Big Bang nucleosynthesis and the Quark-Hadron transition [NASA-CR-186169] N90-14166
PARTICLE MASS
An experiment to search for galactic axions N90-14158
Unitarity limits on the mass and radius of dark matter particles [NASA-CR-186079] N90-14164
PARTICLE MOTION
Synchrotron-betatron parametric instability in free-electron lasers [AD-A213373] N90-13777
Ring source/force excitation of axisymmetric shell structure [ARE-TM(UHA)-88519] N90-14065
PARTICLE SIZE DISTRIBUTION
Recovery of particle size distribution of ultrafine aerosols from diffusional decay measurements [AD-A213006] N90-13621
PARTICLES
Pilot investigation of indoor-outdoor and personal PM10 (thoracic) and associated ionic compounds and mutagenic activity [PB89-222723] N90-13920
PARTITIONS (MATHEMATICS)
Error control techniques for satellite and space communications [NASA-CR-182751] N90-13685
On the performance of on-line algorithms for partition problems [MEMO-784] N90-14015
PASSIVITY
Elaboration and characterization of MISFET transistors on InP [ECL-88-19] N90-13709
PATTERN RECOGNITION
Software development for avionics SSME control and diagnostics [NASA-CR-184894] N90-13964
PAVEMENTS
Evaluation of a neoprene latex modified SAMI (Stress Absorbing Membrane Interlayer) [PB89-226435] N90-13665
PAYLOAD DELIVERY (STS)
Syncom 4 deploy, LDEF retrieval highlight 10-day Columbia flight [NASA-NEWS-RELEASE-89-180] N90-13448
PAYLOADS
The Hipparcos Mission. Prelaunch status. Volume 1: The Hipparcos satellite [ESA-SP-1111-VOL-1] N90-13499
Overview of the Hipparcos payload N90-13503
Payload electronics and mechanisms N90-13508
The payload structure N90-13510
Payload thermal control N90-13511
In-orbit payload calibration N90-13526
Observation of the solar Lyman-alpha line N90-13868
The Skylark sounding rocket program and future launcher developments by British Aerospace (Space Systems) Ltd. N90-13871
PERCEPTION
The structural memory: A network model for human perception of serial objects [CWI-CS-R8829] N90-13930
PERFORMANCE PREDICTION
On-ground photometric calibration N90-13523
In-orbit payload calibration N90-13526

A three-dimensional potential flow analysis of dynamic fluid forces acting on a whirling centrifugal impeller bounded by a volute N90-13717
An investigation of gear mesh failure prediction techniques
[NASA-TM-102340] N90-13785
PERFORMANCE TESTS
A laboratory verification sensor N90-13477
Electrical testing N90-13520
In-orbit payload calibration N90-13526
LOX/hydrocarbon combustion instability investigation
[NASA-CR-182249] N90-13589
Qualification of improved joint heaters
[NASA-CR-183827] N90-13594
Low resistivity electrodeless streamer tubes
[PREPRINT-685-89] N90-13712
The evaluation of a metered mixer for RTV silicone for RSRM nozzle backfill operations
[NASA-CR-183831] N90-13763
Performance evaluation of a six-axis generalized force-reflecting teleoperator
[NASA-CR-186106] N90-13796
A counter gating circuit for acoustic emission monitoring of structures cracking under repetitive alternating loads
[ARL-MAT-TM-398] N90-13808
Parallelism in the discrete-event simulation algorithm
[AD-A213060] N90-13970
Performance of resistive plate counters at beam flux up to 140 Hz/cm2
[NOTA-INTERNA-930] N90-14081
PERIODIC FUNCTIONS
Periodic solutions of Hamiltonian systems of 3-body type
[AD-A212891] N90-14005
PERTURBATION
First-order Bragg SAR imagery of Kelvin wakes and moving internal wave fields
[AD-A213361] N90-13691
The linear study of zonally asymmetric barotropic flows N90-13902
Measurement of arithmetic error and calculation perturbations
[IMAG-RR-767-M] N90-14039
On the effects of an uncertainty on evolution law in dynamical systems
[PREPRINT-689] N90-14047
PHARMACOLOGY
Preliminary study of pharmacological control of space disease
[ETN-90-95015] N90-13927
PHASE CONJUGATION
Optics and opto-electronics systems
[AD-A212340] N90-14093
PHASE MODULATION
Error control techniques for satellite and space communications
[NASA-CR-182751] N90-13685
PHASE SHIFT
Energy exchange of interacting solitons in multidimensions
[PREPRINT-662] N90-14071
PHASE TRANSFORMATIONS
Statistical mechanics of strings and topology
[ROM1F-89-683] N90-14068
Big Bang nucleosynthesis and the Quark-Hadron transition
[NASA-CR-186169] N90-14168
PHOTOCHEMICAL OXIDANTS
Proceedings: US/FRG (Federal Republic of Germany) Workshop on Photochemical Ozone Problem and Its Control: US Experiences and the Situation in Europe
[PB89-233514] N90-13891
PHOTOCONDUCTORS
Development of FIR arrays with integrating amplifiers N90-13473
PHOTODIODES
Optical communication with semiconductor laser diode
[NASA-CR-185886] N90-13770
PHOTODISSOCIATION
New calculations of photodissociation cross-sections in the O2 Schumann-Runge system N90-13834
PHOTOELECTRIC MATERIALS
Photoelectrochemical behavior of type n of GaAs in concentrated iodide media and realization of an experimental device
[ECL-88-18] N90-14117
PHOTOELECTROCHEMICAL DEVICES
Photoelectrochemical behavior of type n of GaAs in concentrated iodide media and realization of an experimental device
[ECL-88-18] N90-14117
PHOTOLUMINESCENCE
Elaboration and characterization of MISFET transistors on InP
[ECL-88-19] N90-13709
Study of surface uniformity of semiconductors 3 to 5 by photoluminescence imagery
[ECL-88-15] N90-14116
GaAs and GaAs:In: Influence of surface treatments and characterization of homogeneity by photoluminescent imagery
[ECL-88-24] N90-14118
PHOTOMETERS
Optical communication with semiconductor laser diode
[NASA-CR-185886] N90-13770
PHOTOMETRY
On-ground photometric calibration N90-13523
Minor planets and other solar system objects N90-13545
Overview of the Tycho data analysis N90-13558
Photometry: Main mission and Tycho N90-13560
Double star reductions in NDAC N90-13561
PHOTONS
Measurement of the light flux density patterns from luminaires proposed as photon sources for photosynthesis during space travel
[NASA-CR-186124] N90-13916
Measurement of the fractional momentum carried by the gluons in the low Q2 photon-gluon fusion events at the ep HERA collider
[NOTA-INTERNA-937] N90-14083
PHOTOPRODUCTION
Measurement of the fractional momentum carried by the gluons in the low Q2 photon-gluon fusion events at the ep HERA collider
[NOTA-INTERNA-937] N90-14083
PHOTOSPHERE
Rotation of the photospheric magnetic fields: A north-south asymmetry
[NASA-CR-186159] N90-14177
PHOTOSYNTHESIS
Measurement of the light flux density patterns from luminaires proposed as photon sources for photosynthesis during space travel
[NASA-CR-186124] N90-13916
PHYSICAL EXERCISE
Exercise countermeasures for bed rest deconditioning
[NASA-TM-101045] N90-13926
Measurement of mechanical work and energy expenditure in running and bicycling N90-13935
PHYSICS
Elementary and middle school science improvement project
[NASA-CR-183768] N90-14125
PHYSIOLOGICAL RESPONSES
The relationship between subjective and objective measures of simulator-induced ataxia
[AD-A213095] N90-13922
Gravity receptors and responses N90-13948
PILOT PERFORMANCE
Human factors research in aircrew performance and training
[AD-A213285] N90-13938
PILOT SELECTION
Human factors research in aircrew performance and training
[AD-A213285] N90-13938
PILOT TRAINING
Human factors research in aircrew performance and training
[AD-A213285] N90-13938
PILOTS (PERSONNEL)
Human factors research in aircrew performance and training
[AD-A213285] N90-13938
PINCH EFFECT
A solvable self-similar model of the sausage instability in a resistive Z-pinch
[AD-A213137] N90-14006
Hot spots Ar and Ne gas puff z-pinch
[IPPCZ-289] N90-14103
PION BEAMS
Low resistivity electrodeless streamer tubes
[PREPRINT-685-89] N90-13712
Performance of resistive plate counters at beam flux up to 140 Hz/cm2
[NOTA-INTERNA-930] N90-14081
PIPE FLOW
An improved algorithm for the modeling of vapor flow in heat pipes
[NASA-CR-185179] N90-13748
PIPE NOZZLES
Fatigue resistance of pressure vessels in high strength steels effect of some improvement techniques
[CRIF-MT-176] N90-13799
PIPES (TUBES)
Theoretical evaluation of defects in pressure vessels and pipings
[CRIF-MT-174] N90-13798
PISTONS
Simulation of the control characteristics of an axial piston pump and a flapper-nozzle valve combination N90-13784
PITUITARY HORMONES
The pituitary growth hormone cell in space N90-13941
PLANAR STRUCTURES
Acceleration sets of planar manipulators. Part 2: Applications and experiments
[AD-A213336] N90-13791
PLANE WAVES
Mobility power flow analysis of an L-shaped plate structure subjected to acoustic excitation
[NASA-CR-186130] N90-13817
PLANET EPHEMERIDES
Minor planets and other solar system objects N90-13545
The treatment of minor planets and planetary satellites N90-13563
PLANETARY ATMOSPHERES
The Voyager Neptune travel guide
[NASA-CR-186108] N90-13412
PLANETARY MAGNETIC FIELDS
Spacecraft attitude determination using the earth's magnetic field N90-13429
PLANETARY MAGNETOSPHERES
The Voyager Neptune travel guide
[NASA-CR-186108] N90-13412
PLANETARY RINGS
The Voyager Neptune travel guide
[NASA-CR-186108] N90-13412
PLANNING
Space Transportation Engine Program (STEP). Phase B: Project study and management plan-ingredients for STEP success
[NASA-CR-183770] N90-13585
PLANTS (BOTANY)
How to detect when cells in space perceive gravity N90-13946
Effects of microgravity on growth hormone concentration and distribution in plants N90-13947
Gravity receptors and responses N90-13948
Gravitropism in plants: Hydraulics and wall growth properties of responding cells N90-13950
PLASMA CURRENTS
The Space Station Photovoltaic Panels Plasma Interaction Test Program: Test plan and results
[NASA-TM-102474] N90-13581
PLASMA DECAY
Experimental and theoretical study of artificial plasma layers produced by two intersecting beams in a chamber
[NASA-CR-184598] N90-14102
PLASMA DENSITY
Resonance cone diagnostics in the mid-latitude ionosphere N90-13840
Experimental and theoretical study of artificial plasma layers produced by two intersecting beams in a chamber
[NASA-CR-184598] N90-14102
PLASMA DIAGNOSTICS
Resonance cone diagnostics in the mid-latitude ionosphere N90-13840
PLASMA ELECTRODES
True asymptotic plasma-sheath matching with an asymptotically correct collisional presheath
[AD-A212857] N90-14104
PLASMA ETCHING
Mechanisms in reactive ion etching of silicon carbide thin films
[AD-A213018] N90-13700
PLASMA INTERACTIONS
The Space Station Photovoltaic Panels Plasma Interaction Test Program: Test plan and results
[NASA-TM-102474] N90-13581
PLASMA LAYERS
Experimental and theoretical study of artificial plasma layers produced by two intersecting beams in a chamber
[NASA-CR-184598] N90-14102
PLASMA PHYSICS
An implementation plan for priorities in solar-system space physics
[NASA-CR-185375] N90-14154
PLASMA POTENTIALS
An iterative method to solve the nonlinear Poisson's equation in the case of plasma tangential discontinuities
[AERONOMICA-ACTA-A-346-1989] N90-14045
PLASMA RESONANCE
Resonance cone diagnostics in the mid-latitude ionosphere N90-13840
PLASMA SHEATHS
True asymptotic plasma-sheath matching with an asymptotically correct collisional presheath
[AD-A212857] N90-14104
PLASMA SPRAYING
Surfaces and interfaces of ceramic materials
[AD-A212417] N90-13657

PLASMA TEMPERATURE
Experimental and theoretical study of artificial plasma layers produced by two intersecting beams in a chamber [NASA-CR-184598] N90-14102
PLASMAS (PHYSICS)
Mechanisms in reactive ion etching of silicon carbide thin films [AD-A213018] N90-13700
Hot spots Ar and Ne gas puff z-pinch [IPPCZ-289] N90-14103
PLASMASPHERE
Optical observations of interplanetary pick-up ions: The experiment Helly N90-13863
PLASTIC DEFORMATION
Field-effect spectroscopy of interface states [AD-A212998] N90-14112
PLASTIC FLOW
Anomalous strain rate dependence of the serrated flow in Ni-H and Ni-C-H alloys [AD-A213244] N90-13641
Analysis of new phenomena in shear flow of non-Newtonian fluids [AD-A212893] N90-13721
PLASTIC PROPERTIES
A theory of damage in brittle and cementitious materials, part 1 [AD-A212940] N90-13658
PLASTICS
Ductile failure [AD-A212975] N90-13601
PLATES (TECTONICS)
Strain accumulation and surface deformation along the San Andreas, California [NASA-CR-185893] N90-13894
PLUMES
Development of a shuttle plume radiation heating indicator [NASA-CR-183679] N90-13584
Air quality simulation model performance for one-hour averages [PB89-233506] N90-13890
PLY ORIENTATION
Localization of ultrasound in thick composites [AD-A212994] N90-13602
POINT SPREAD FUNCTIONS
Effect of central obscuration on the LDR point spread function N90-13475
POINTING CONTROL SYSTEMS
Analysis of the flight dynamics of the Solar Maximum Mission (SMM) off-sun scientific pointing N90-13432
Report of the Asilomar 3 LDR Workshop [NASA-CR-184656] N90-13449
Pointing control for LDR N90-13453
Space telescope pointing control N90-13454
POISSON DENSITY FUNCTIONS
R-matrices and higher Poisson brackets for integrable systems [PREPRINT-669] N90-14069
POISSON EQUATION
An iterative method to solve the nonlinear Poisson's equation in the case of plasma tangential discontinuities [AERONOMICA-ACTA-A-346-1989] N90-14045
R-matrices and higher Poisson brackets for integrable systems [PREPRINT-669] N90-14069
POISSON RATIO
Design and evaluation of a new biaxial testing method for sheet material (SUPERBAT) [LR-548] N90-13824
POLAR REGIONS
Enhanced electron density layers in the high-latitude lower ionosphere N90-13832
The electrodynamics of the polar ionosphere with special emphasis on the dayside cleft region N90-13838
Polar mesosphere summer echoes and associated atmospheric gravity waves N90-13856
Diurnal variation of the sodium layer at polar latitudes in summer N90-13869
Auroral and sub-auroral interaction at the F region ionosphere [AD-A213284] N90-13896
Three dimensional analysis of the structure of the atmosphere in polar environments by vertical satellite sounding. Interest for the meteorological forecasts at high latitudes [ETN-90-95506] N90-13911
POLARIZATION CHARACTERISTICS
Nucleon polarizabilities in the constituent quark model [NOTA-INTERNA-936] N90-14082
POLARIZED LIGHT
Low frequency polarized and depolarized light scattering in H-bonded liquids: CH3(CH2)n-1OH (n=1,...5) [PREPRINT-693] N90-14100
POLICIES
Electronic warfare: Reliable equipment needed to test Air Force's electronic warfare systems [AD-A212952] N90-13687
Total quality management: Directorate of Contract Management master plan [AD-A212867] N90-14131
POLLUTION CONTROL
Effects of tacky mat contamination on bond degradation for Chemlok/liner and NBR/liner bonds [NASA-CR-183742] N90-13653
Proceedings: US/FRG (Federal Republic of Germany) Workshop on Photochemical Ozone Problem and Its Control: US Experiences and the Situation in Europe [PB89-233514] N90-13891
POLLUTION MONITORING
Air quality simulation model performance for one-hour averages [PB89-233506] N90-13890
POLYACETYLENE
A literature survey of inherently conducting polymers [FOA-C-20763-2.4] N90-13668
POLYCRYSTALS
Surfaces and interfaces of ceramic materials [AD-A212417] N90-13657
POLYGONS
Description and manipulation of convex polygons using polarity [IMAG-RR-771-M] N90-14041
POLYHEDRONS
Data structures for the representation and manipulation of polyhedrons [IMAG-RR-772-M] N90-14042
POLYMER CHEMISTRY
Synthesis of inorganic polymers as glass precursors and for other uses. Preceramic block or graft copolymers as potential precursors to nanocomposite materials [AD-A211978] N90-13655
POLYMER PHYSICS
Configurational statistics of strings, fractals and polymer physics. Part 2: Non Abelian strings [ROM1F-89-680-PT-2] N90-14067
String correlations and galaxies formation [ROM1F-89-677] N90-14170
Non Abelian string correlations and galaxies formation [ROM1F-89-678] N90-14171
Des Cloizeaux's law for strings and galaxies formation. Part 1: Abelian configurations [ROM1F-89-681-PT-1] N90-14172
POLYMERIC FILMS
Optical modulators based on polymers [EP-PATENT-0-294-061-A1] N90-14099
POLYMERIZATION
Synthesis of inorganic polymers as glass precursors and for other uses. Preceramic block or graft copolymers as potential precursors to nanocomposite materials [AD-A211978] N90-13655
POLYMERS
Analysis of new phenomena in shear flow of non-Newtonian fluids [AD-A212893] N90-13721
POLYSTYRENE
Model filled polymers I. Synthesis of crosslinked monodisperse polystyrene beads [AD-A213228] N90-13660
POLYSULFIDES
Evaluation of a metering, mixing, and dispensing system for mixing polysulfide adhesive [NASA-CR-183749] N90-13654
POSITION (LOCATION)
Inexpensive global location and tracking systems using geostationary satellites [AD-A213025] N90-13498
Spatiotemporal characteristics of visual localization, phase 2 [AD-A212934] N90-13929
Where is an object before you look at it [NOTA-INTERNA-935] N90-14123
Study of modern instrumentation and methods for astronomic positioning in the field [AD-A213217] N90-14157
POSITION ERRORS
Wavefront error sensing for LDR N90-13455
POSITION SENSING
A figure control sensor for the Large Deployable Reflector (LDR) N90-13451
POSTLAUNCH REPORTS
Debris/ice/TPS assessment and photographic analysis for Shuttle Mission STS-34 [NASA-TM-102153] N90-13447
POTENTIAL ENERGY
The auroral current - voltage relationship N90-13843
POWER CONDITIONING
The US space station and its electric power system [NASA-TM-101974] N90-13596
POWER LIMITERS
A review of laser filter materials [AD-A213134] N90-13776
POWER SPECTRA
The S.D.G., P.S.D. and the nonlinear airplane [NLR-MP-88018-U] N90-13371
PRECIPITATION (METEOROLOGY)
A collection of papers related to heavy precipitation forecasting [PB89-230833] N90-13910
PRECISION
COBE nonspinning attitude propagation N90-13418
PREDICTION ANALYSIS TECHNIQUES
A technique for the prediction of aerodynamics and aeroelasticity of rotor blades N90-13377
Atmospheric drag model calibrations for spacecraft lifetime prediction N90-13439
Lifetime predictions for the Solar Maximum Mission (SMM) and San Marco spacecraft N90-13440
Effects of joints in truss structures N90-13486
Sufficiency and necessity in reliability modeling [NASA-CR-186119] N90-13706
Mean stress and the exhaustion of fatigue-damage resistance [NASA-TM-101311] N90-13819
An evaluation of a fatigue crack growth prediction model for variable-amplitude loading (PREFFAS) [LR-537] N90-13822
Prediction of the 10 cm solar flux index N90-13872
PREDICTIONS
Thermal barrier coating life prediction model development, phase 1 [NASA-CR-182230] N90-13388
Hybrid deployable support truss designs for LDR N90-13485
On-line range prediction system, part 2 [NASA-CR-185889] N90-13771
Climate predictability: A dynamical view [AERONOMICA-ACTA-A-347-1989] N90-13909
Expected supernovae rates and gravitational waves detection [NOTA-INTERNA-933] N90-14166
Detectable gravitational waves by supernova SN 1987 A pulsar relic [PREPRINT-658] N90-14174
PREIMPREGNATION
Preliminary experiments on filament winding nylon impregnated glass fibers (FIT) [LR-545] N90-13669
PRELAUNCH SUMMARIES
Debris/ice/TPS assessment and photographic analysis for Shuttle Mission STS-34 [NASA-TM-102153] N90-13447
Assembly, integration, and verification N90-13519
PRELAUNCH TESTS
The Hipparcos Mission. Prelaunch status. Volume 1: The Hipparcos satellite [ESA-SP-1111-VOL-1] N90-13499
Electrical testing N90-13520
On-ground photometric calibration N90-13523
The Hipparcos Mission. Prelaunch status. Volume 3: The data reductions [ESA-SP-1111-VOL-3] N90-13548
QM-8 field joint protection system, volume 7 [NASA-CR-183748] N90-13586
PREPROCESSING
Interface between MEDUSA and GIFTS for shell structures [LR-553] N90-13985
PRESSURE DISTRIBUTION
Transonic Euler solutions on mutually interfering finned bodies [AD-A213395] N90-13331
Pressure correction calculation procedures for 3D viscous flow N90-13738
Ring source/force excitation of axisymmetric shell structure [ARE-TM(UHA)-88519] N90-14085
PRESSURE MEASUREMENT
Pressure measurement techniques in use at the Royal Aerospace Establishment N90-13347
A wall interference assessment/correction interface measurement system for the NASA/ARC 12-ft PWT [NASA-CR-185474] N90-13401
PRESSURE REGULATORS
Tank pressure control experiment on the space shuttle [NASA-TM-102313] N90-13590
PRESSURE VESSELS
Theoretical evaluation of defects in pressure vessels and pipings [CRIF-MT-174] N90-13798
Fatigue resistance of pressure vessels in high strength steels effect of some improvement techniques [CRIF-MT-176] N90-13799

PREVENTION
Novel carbamates, their production and their use as fuels additives
[EP-PATENT-0-298-636-A-1] N90-13676
PRINCIPAL COMPONENTS ANALYSIS
Model reduction of weakly damped mechanical systems
[MEMO-798] N90-13993
PROBABILITY DENSITY FUNCTIONS
Counterexamples to Robertson's conjecture
[MEMO-COSOR-88-32] N90-14048
PROBABILITY DISTRIBUTION FUNCTIONS
Theory of goodness of fit tests and scanning innovation martingales
[CWI-BS-R8904] N90-14046
On the effects of an uncertainty on evolution law in dynamical systems
[PREPRINT-669] N90-14047
PROBABILITY THEORY
Probabilistic finite element analysis of dynamic structural response
[AD-A213249] N90-13789
Why stochastic modeling is essential in analyzing interdicted transportation network performance
[AD-A213140] N90-14007
Counterexamples to Robertson's conjecture
[MEMO-COSOR-88-32] N90-14048
Estimation of convolution tail behavior
[MEMO-COSOR-89-04] N90-14051
PROBLEM SOLVING
The relationship between subjective and objective measures of simulator-induced ataxia
[AD-A213095] N90-13922
A priori results in linear quadratic optimal control theory
[MEMO-COSOR-89-02] N90-13996
The totally singular linear quadratic problem with indefinite cost
[MEMO-COSOR-89-05] N90-13998
The output-stabilizable subspace and linear optimal control
[MEMO-COSOR-89-15] N90-14001
Application of multi-grid methods for solving the Navier-Stokes equations
[NASA-TM-102359] N90-14002
Parabolic equations for curves on surfaces. 2: Intersections, blow up and generalized solutions
[AD-A212890] N90-14004
Periodic solutions of Hamiltonian systems of 3-body type
[AD-A212891] N90-14005
Using Broyden updates to approximate the Jacobian in a semi-implicit backward differentiation code
[AD-A213239] N90-14010
On the performance of on-line algorithms for partition problems
[MEMO-784] N90-14015
On the nonexistence of a strong solution in the boundary problem for a sticky Brownian motion
[CWI-BS-R8901] N90-14018
The regular indefinite linear quadratic problem with linear endpoint constraints
[MEMO-COSOR-88-15] N90-14022
Continuity properties of one-parameter families of linear-quadratic problems without stability
[MEMO-COSOR-88-17] N90-14024
Solving a specific Thue-Mahler equation
[MEMO-793] N90-14032
Another approach to the local disturbance decoupling problem with stability for nonlinear systems
[MEMO-799] N90-14033
Practice of bivariate quadratic simplicial splines
[MEMO-800] N90-14034
Theory of goodness of fit tests and scanning innovation martingales
[CWI-BS-R8904] N90-14046
Note on Urbanik's class L(sub n) — self-decomposability of functions
[MEMO-COSOR-89-07] N90-14053
Reverse self-decomposability --- for characteristic functions
[MEMO-COSOR-89-08] N90-14054
The activity selection problem: A network and game theoretic approach
[MEMO-794] N90-14056
PROCESS CONTROL (INDUSTRY)
Optimal processes described by a parabolic differential equation with control in the coefficients, part 4
[MEMO-785-PT-4] N90-14016
PROCUREMENT MANAGEMENT
Project ORION microcomputer management system
[AD-A212945] N90-13959
PRODUCT DEVELOPMENT
Product assurance N90-13522
Process for producing a shaped, extruded product from a crosslinkable polymeric composition
[GB-PATENT-2-201-677-A] N90-13662
Crosslinkable polymer
[GB-PATENT-2-205-846-A] N90-13663
Kinematics and control of manipulation robots
[WTHD-187] N90-13803
PRODUCTION COSTS
ERIS: Engineering Resource Information System
[AD-A213357] N90-14144
PRODUCTION ENGINEERING
Process for producing a shaped, extruded product from a crosslinkable polymeric composition
[GB-PATENT-2-201-677-A] N90-13662
ERIS: Engineering Resource Information System
[AD-A213357] N90-14144
PRODUCTIVITY
The Materials Division: A case study
[NASA-TM-102380] N90-13597
PROGRAM VERIFICATION (COMPUTERS)
Validation of the Hipparcos catalog N90-13564
Data simulations in the NDAC consortium N90-13574
The development of a program analysis environment for Ada
[NASA-CR-185860] N90-13962
Multi-level specification and verification of real-time software
[AD-A213227] N90-13975
PROGRAMMING LANGUAGES
SIMOGEN: An object-oriented language for simulation
[AD-A213129] N90-13973
Action languages: Dimensions, effects
[NASA-CR-183388] N90-14181
PROJECT MANAGEMENT
Assembly, integration, and verification N90-13519
Project ORION microcomputer management system
[AD-A212945] N90-13959
The Explorer program for astronomy and astrophysics N90-14159
PROJECTILES
Current management for improved railgun performance
[AD-A212887] N90-13445
PROLOG (PROGRAMMING LANGUAGE)
On the safe approximation of PROLOG programs
[CWI-CS-R8913] N90-13978
PROPELLANT CHEMISTRY
The mobile combustion diagnostic fixture and its application to the study of propellant combustion. Part 1: Investigation of the low pressure combustion of LOVA XM39 propellant
[AD-A213272] N90-13626
PROPELLANT COMBUSTION
The mobile combustion diagnostic fixture and its application to the study of propellant combustion. Part 1: Investigation of the low pressure combustion of LOVA XM39 propellant
[AD-A213272] N90-13626
PROPELLANT TANKS
Tank pressure control experiment on the space shuttle
[NASA-TM-102313] N90-13590
PROPELLANTS
The mobile combustion diagnostic fixture and its application to the study of propellant combustion. Part 1: Investigation of the low pressure combustion of LOVA XM39 propellant
[AD-A213272] N90-13626
Evaluation of selected computer models for modeling pyrotechnic and propellant devices
[AD-A213003] N90-13671
Thermochemical calculations with inert compounds
[FOA-C-20759-2.1] N90-13677
PROPELLER BLADES
Effect of reduced aft diameter and increased blade number on high-speed counterrotation propeller performance
[NASA-TM-102077] N90-13352
Application of an efficient hybrid scheme for aeroelastic analysis of advanced propellers
[NASA-TM-102428] N90-13355
PROPELLER EFFICIENCY
Application of an efficient hybrid scheme for aeroelastic analysis of advanced propellers
[NASA-TM-102428] N90-13355
PROPORTIONAL COUNTERS
The x ray mirror and the PSPC of the supernova-rocket-project N90-13867
PROPULSION SYSTEM CONFIGURATIONS
SSME LOX post flow analysis/fluid structure interaction. Volume 2: Fluid structure interaction
[NASA-CR-183678] N90-13716
Qualification of the 4th stage propulsor of the Brazilian launcher. SLV: A new sounding rocket N90-13860
PROPULSION SYSTEM PERFORMANCE
SSME LOX post flow analysis/fluid structure interaction. Volume 2: Fluid structure interaction
[NASA-CR-183678] N90-13716
PROPULSIVE EFFICIENCY
Aircraft propulsion: Leading the way in aviation
[LR-532] N90-13395
PROTECTIVE COATINGS
SiO overcoating and polishing of CFRP telescope panels N90-13478
Wear-resistant coated object
[EP-PATENT-0-289-173-A1] N90-13643
PROTOCOL (COMPUTERS)
Spacelab system analysis: The modified free access protocol: An access protocol for communication systems with periodic and Poisson traffic
[NASA-CR-183805] N90-13497
On stability of queueing models of local area networks with slotted ring protocols
[MEMO-795] N90-14057
PROTONS
The grand unified photon spectrum: A coherent view of the diffuse extragalactic background radiation
[NASA-CR-186077] N90-14180
PROTOTYPES
The development of a program analysis environment for Ada
[NASA-CR-185860] N90-13962
PROVING
Assembly, integration, and verification N90-13519
On the safe approximation of PROLOG programs
[CWI-CS-R8913] N90-13978
Counterexamples to Robertson's conjecture
[MEMO-COSOR-88-32] N90-14048
PSYCHOACOUSTICS
Test procedures for the evaluation of helmet and headset mounted active noise reduction systems
[AD-A212991] N90-13937
PSYCHOMETRICS
Watchfulness and attention during weightlessness simulations: Use of computerized psychometric tests
[REPT-89-TOU-3-1045] N90-13928
PSYCHOPHYSICS
Computational and psychophysical study of human vision using neural networks
[AD-A213290] N90-13924
Spatiotemporal characteristics of visual localization, phase 2
[AD-A212934] N90-13929
PULSARS
Detectable gravitational waves by supernova SN 1987 A pulsar relic
[PREPRINT-658] N90-14174
PULSED LASERS
Optical communication with semiconductor laser diode
[NASA-CR-185886] N90-13770
MM and T advanced balancing/machining
[AD-A213103] N90-13775
PULSES
Quantitative non-destructive evaluation using laser generated ultrasonic pulses N90-13805
Countermeasures to microgravity N90-13957
Influence of RF-parameters on beam lifetime
[NIKHEF-K/AMPS/89-06] N90-14091
PUMPS
Simulation of the control characteristics of an axial piston pump and a flapper-nozzle valve combination N90-13784
PYLONS
Application of fracture mechanics and half-cycle method to the prediction of fatigue life of B-52 aircraft pylon components
[NASA-TM-88277] N90-13820
PYROMETALLURGY
Containerless Processing of Metals: Undercooling and Solidification
[DLR-MITT-89-15] N90-13645
Correlation between microstructure and magnetic properties of porous sintered iron and porous iron containing composites
[KFK-4522] N90-13647
PYROTECHNICS
Evaluation of selected computer models for modeling pyrotechnic and propellant devices
[AD-A213003] N90-13671

Q

QUADRATIC EQUATIONS
Quadratic dynamical systems describing shear flow of non-Newtonian fluids
[AD-A212892] N90-13720
Definition, determination and characterization of acceleration sets for spatial manipulators
[AD-A213366] N90-13793

QUALITY CONTROL
NDI (Nondestructive Inspection) oriented corrosion control for Army aircraft. Phase 1: Inspection methods
[AD-A213368] N90-13359
Electrical testing N90-13520
Product assurance N90-13522
The Materials Division: A case study
[NASA-TM-102360] N90-13597
Arc current control of a robotic welding system: Modeling and control system design
[AD-A213150] N90-13788
Total quality management implementation strategy: Directorate of Quality Assurance
[AD-A212863] N90-14127
Total quality management plan: Technical and logistics services
[AD-A212864] N90-14128
Total quality management implementing plan: Office of small and disadvantaged business utilization
[AD-A212865] N90-14129
Total quality management plan: Office of Congressional Affairs
[AD-A212866] N90-14130
Total quality management: Directorate of Contract Management master plan
[AD-A212867] N90-14131
Total quality management plan: Office of Public Affairs
[AD-A212868] N90-14132
Executive overview and introduction to the SMAP information system life-cycle and documentation standards
[NASA-TM-101765] N90-14134
Information system life-cycle and documentation standards, volume 1
[NASA-TM-101856] N90-14135
Management plan documentation standard and Data Item Descriptions (DID). Volume of the information system life-cycle and documentation standards, volume 2
[NASA-TM-101857] N90-14136
Product specification documentation standard and Data Item Descriptions (DID). Volume of the information system life-cycle and documentation standards, volume 3
[NASA-TM-101858] N90-14137
Assurance specification documentation standard and Data Item Descriptions (DID). Volume of the information system life-cycle and documentation standards, volume 4
[NASA-TM-101859] N90-14138
Management control and status reports documentation standard and Data Item Descriptions (DID). Volume of the information system life-cycle and documentation standards, volume 5
[NASA-TM-101860] N90-14139
QUANTUM CHROMODYNAMICS
Lattice QCD estimate of mixing parameters for heavy meson systems
[PREPRINT-687] N90-14079
QUANTUM MECHANICS
Nonpotential scattering for the density matrix and quantum gravity
[PREPRINT-688] N90-14080
Where is an object before you look at it
[NOTA-INTERNA-935] N90-14123
QUANTUM STATISTICS
Where is an object before you look at it
[NOTA-INTERNA-935] N90-14123
QUANTUM THEORY
Fundamental quantum 1/f noise in ultrasmall semiconductor devices and their optimal design principles
[AD-A211947] N90-14107
QUANTUM WELLS
Elastic impurity scattering in double-barrier resonant tunneling structures
[AD-A212850] N90-14110
QUARK MODELS
Nucleon polarizabilities in the constituent quark model
[NOTA-INTERNA-936] N90-14082
QUARKS
Big Bang nucleosynthesis and the Quark-Hadron transition
[NASA-CR-186169] N90-14168
QUASARS
The low-ion QSO absorption-line systems N90-14162
QUATERNIONS
Simultaneous quaternion estimation (QUEST) and bias determination N90-13417
QUENCHING (ATOMIC PHYSICS)
CANOES 2: Dynamics of atmospheric infrared thermochemical excitation, volume 1
[AD-A213341] N90-13897
CANOES 2: Dynamics of atmospheric infrared thermochemical excitation, volume 2
[AD-A213342] N90-13898
CANOES 2: Dynamics of atmospheric infrared thermochemical excitation, volume 3
[AD-A213343] N90-13899
CANOES 2: Dynamics of atmospheric infrared thermochemical excitation, volume 4
[AD-A213344] N90-13900
Lattice QCD estimate of mixing parameters for heavy meson systems
[PREPRINT-687] N90-14079
QUEUEING THEORY
Waiting times in polling systems with Markovian server routing
[CWI-BS-R8905] N90-13989
Monotonicity of performance measures in a processor sharing queue
[CWI-BS-R8902] N90-14019
Workloads and waiting times in single-server systems with multiple customer classes
[CWI-BS-R8906] N90-14020
Simple appoximations for second moment characteristics of the sojurn time in the M/G/1 processor sharing queue
[CWI-BS-R8907] N90-14055
On stability of queueing models of local area networks with slotted ring protocols
[MEMO-795] N90-14057
Analysis of a queueing model for slotted ring networks
[MEMO-796] N90-14058
Dynamic workload modeling of high speed token rings in a metropolitan area network
[MEMO-INF-89-21] N90-14059

R

RADAR DATA
The interaction and variation of waves and turbulence from MST radar data
[AD-A212849] N90-13906
RADAR ECHOES
First-order Bragg SAR imagery of Kelvin wakes and moving internal wave fields
[AD-A213361] N90-13691
RADAR IMAGERY
First-order Bragg SAR imagery of Kelvin wakes and moving internal wave fields
[AD-A213361] N90-13691
RADAR SCATTERING
Stochastic modelling of EM scattering from foliage
[AD-A213118] N90-13689
RADIAL FLOW
An interactive grid generation procedure for axial and radial flow turbomachinery
[NASA-CR-185167] N90-13968
RADIANCE
The effects of seasonal and latitudinal earth infrared radiance variations on ERBS attitude control N90-13414
RADIANT HEATING
Development of a shuttle plume radiation heating indicator
[NASA-CR-183679] N90-13584
RADIATION ABSORPTION
Stochastic modelling of EM scattering from foliage
[AD-A213118] N90-13689
RADIATION COUNTERS
Performance of resistive plate counters at beam flux up to 140 Hz/cm2
[NOTA-INTERNA-930] N90-14081
RADIATION DETECTORS
Observation of the solar Lyman-alpha line N90-13868
Correlation among gravitational wave and neutrino detectors data during SN1987A
[NOTA-INTERNA-932] N90-14165
RADIATION DISTRIBUTION
Interaction of radiation with matter: Atomic collision processes occurring in the presence of radiation fields
[AD-A213112] N90-14078
RADIATION EFFECTS
Life science research in space
[ESA-SP-1105] N90-13917
NRL (Naval Research Laboratory) Review
[AD-A212886] N90-14182
RADIATION SOURCES
Use of a krypton isotope for rapid ion changeover at the Lawrence Berkeley Laboratory 88-inch cyclotron
[NASA-CR-186107] N90-14084
RADIO ASTRONOMY
A search for the effects of active magnetic fields in extra-galactic radio sources N90-14161
RADIO COMMUNICATION
Inexpensive global location and tracking systems using geostationary satellites
[AD-A213025] N90-13496
Long-range plan for management and use of the radio spectrum by agencies and establishments of the Federal Government
[PB88-232367] N90-13693
RADIO FREQUENCIES
Microwave microstrip resonator measurements of Y1Ba2Cu3O(7-x) and Bi2Sr2Ca1Cu2O(8-y) thin films
[NASA-TM-102159] N90-13704
Influence of RF-parameters on beam lifetime
[NIKHEF-K/AMPS/89-06] N90-14091
RADIO SPECTRA
Long-range plan for management and use of the radio spectrum by agencies and establishments of the Federal Government
[PB89-232367] N90-13693
RADIOACTIVE DECAY
Recovery of particle size distribution of ultrafine aerosols from diffusional decay measurements
[AD-A213006] N90-13621
RADIOMETERS
Spectrometer technology recommendations N90-13468
A four channel He-3 cooled balloon-borne bolometer radiometer N90-13469
Reflection indicatrices of natural surfaces for AVHRR channels 1 and 2
[DLR-MITT-89-16] N90-13882
RAILGUN ACCELERATORS
Current management for improved railgun performance
[AD-A212887] N90-13445
RAIN
Applied atmospheric resources research program in Thailand
[PB89-235402] N90-13903
Estimation of rain rate using spatial and multichannel coherence: Analysis of SSM/I data N90-13905
RAMAN SPECTROSCOPY
Study of the hydroxyl radical by DRASC resonance in a high pressure flame — Diffusion Raman Anti-Stokes Coherence (DRASC)
[ONERA-RS-53/7131-PY] N90-13632
RAMJET ENGINES
Apparatus for cooling electronic components in aircraft
[AD-D014207] N90-13373
RANDOM ACCESS MEMORY
Efficient on-line simulations of tree machines and multidimensional turing machines by random access machines
[AD-A213152] N90-13960
RANDOM PROCESSES
Stopping rules for a class of random methods for detecting necessary linear inequality constraints
[MEMO-777] N90-13977
Random Markov processes and uniform martingales
[CWI-BS-R8908] N90-14021
RANDOM VARIABLES
Distribution of a sum of n random variables and a central limit theorem based on moments or on coefficients of polynomial dependence
[IMAG-RR-768-M] N90-14040
Self-decomposable distributions and branching processes
[MEMO-COSOR-89-06] N90-14052
Note on Urbanik's class L(sub n) — self-decomposability of functions
[MEMO-COSOR-89-07] N90-14053
Reverse self-decomposability — for characteristic functions
[MEMO-COSOR-89-08] N90-14054
RANGE (EXTREMES)
The regular indefinite linear quadratic problem with linear endpoint constraints
[MEMO-COSOR-88-15] N90-14022
Convergence properties of indefinite linear quadratic problems with receding horizon
[MEMO-COSOR-88-25] N90-14026
RANGE AND RANGE RATE TRACKING
Precision of semi-geometrically determined SLR baselines vs. site occupation time
[ETN-90-96007] N90-13885
Normal points: Compression of satellite laser ranging data
[ETN-90-96008] N90-14145
RANGE FINDERS
On-line range prediction system, part 2
[NASA-CR-185889] N90-13771
Outline on the future Italian transportable laser ranging station
[CISE-4845] N90-13782
RANK TESTS
A graph theoretic characterization for the rank of the transfer matrix of a structured system
[CWI-OS-R8819] N90-14064

RARE EARTH COMPOUNDS
Thermodynamic properties of some metal oxide-zirconia systems
[NASA-TM-102351] N90-13666
REACTION KINETICS
Transport phenomena and interfacial kinetics in multiphase combustion systems
[AD-A212932] N90-13620
Nucleation kinetics in undercooled, glass-forming metallic melts
[DLR-FB-89-32] N90-13644
Physical phenomena and the microgravity response N90-13645
REACTION WHEELS
Analytical derivation and verification of zero-gyro control for the IUE satellite
[NASA-TM-100748] N90-13767
REACTIVITY
Mechanisms in reactive ion etching of silicon carbide thin films
[AD-A213018] N90-13700
REAL TIME OPERATION
Computer-based tools for assisting air traffic controllers with arrivals flow management
[RSRE-88001] N90-13366
The role of the host in a cooperating mainframe and workstation environment, volumes 1 and 2
[NASA-CR-185483-VOL-1/2] N90-13496
Launch and early orbit N90-13524
The in-orbit initialization phase N90-13525
Novel in situ spectroscopic ellipsometer for real time analysis of CVD diamond films
[AD-A213218] N90-13762
Kinematics and control of manipulation robots
[WTHD-187] N90-13803
ALIS: An Auroral Large Imaging System in northern Scandinavia N90-13877
Ada task scheduling: A focused Ada investigation
[NASA-CR-186072] N90-13967
Multi-level specification and verification of real-time software
[AD-A213227] N90-13975
Flight software development for the isothermal dendritic growth experiment
[NASA-TM-102412] N90-13988
A knowledge-based flight status monitor for real-time application in digital avionics systems
[NASA-TM-101710] N90-13995
Real time image enhancement during underwater recovery operations
[AD-A213139] N90-14097
RECEIVERS
Integrated optoelectronic receivers
[AD-A213376] N90-14098
RECLAMATION
Refurbishment of one-person regenerative air revitalization system
[NASA-CR-183757] N90-13934
RECONSTRUCTION
High precision rocket attitude reconstruction using star sensor and magnetometer data N90-13844
RECRYSTALLIZATION
Containerless Processing of Metals: Undercooling and Solidification
[DLR-MITT-89-15] N90-13645
RECURSIVE FUNCTIONS
Identification of impulsive interference channels
[AD-A213154] N90-14009
REDUCED GRAVITY
An investigation of flame spread over shallow liquid pools in microgravity and nonair environments
[NASA-TM-102425] N90-13680
User needs, benefits, and integration of robotic systems in a space station laboratory
[NASA-CR-185150] N90-13794
The Norwegian balloon and sounding rocket program 1989-1992 N90-13829
The Swedish sounding rocket and balloon program N90-13830
The German scientific balloon and sounding rocket program N90-13831
Watchfulness and attention during weightlessness simulations: Use of computerized psychometric tests
[REPT-89-TOU-3-1045] N90-13928
Response of lymphocytes to a mitogenic stimulus during spaceflight N90-13942
Polarity establishment, morphogenesis, and cultured plant cells in space N90-13943
How to detect when cells in space perceive gravity N90-13946
Effects of microgravity on growth hormone concentration and distribution in plants N90-13947
Free swimming organisms: Microgravity as an investigative tool N90-13949
Gravity and animal embryos N90-13951
Human factors issues in performing life science experiments in a 0-G environment N90-13952
Do the design concepts used for the space flight hardware directly affect cell structure and/or cell function ground based simulations N90-13953
Model system studies with a phase separated membrane bioreactor N90-13954
Design challenges for space bioreactors N90-13955
Fermentation and oxygen transfer in microgravity N90-13956
Countermeasures to microgravity N90-13957
Flight software development for the isothermal dendritic growth experiment
[NASA-TM-102412] N90-13988
REENTRY
Re-entry hazards and cosmos 1900
[FOA-C-30535-9.4] N90-13583
REFERENCE STARS
The Hipparcos Mission. Prelaunch status. Volume 2: The input catalog
[ESA-SP-1111-VOL-2] N90-13529
Successive iterations of the input catalog N90-13534
Standard stars and photometric calibration N90-13539
The choice of stars in open clusters N90-13542
The choice of stars in the Magellanic clouds N90-13543
The catalogs produced by the Inca consortium N90-13546
The Hipparcos Mission. Prelaunch status. Volume 3: The data reductions
[ESA-SP-1111-VOL-3] N90-13548
General and numerical approach to the sphere solution in FAST N90-13555
The sphere solution and astrometric parameter determination in NDAC N90-13557
Tycho astrometry N90-13559
The Tycho input catalog N90-13575
Experiments towards a global sphere solution N90-13576
REFINING
Empirical analysis and refinement of expert system knowledge bases
[AD-A213240] N90-14143
REFLECTING TELESCOPES
An approach to optical structures control N90-13456
REFLECTORS
Real-time sensing of optical alignment N90-13479
Assembly considerations for large reflectors N90-13480
REFRACTORY MATERIALS
Surfaces and interfaces of ceramic materials
[AD-A212417] N90-13657
Thermodynamic properties of some metal oxide-zirconia systems
[NASA-TM-102351] N90-13666
REFRIGERATORS
Cryogenics for LDR N90-13471
An algorithm for control volume analysis of cryogenic systems
[AD-A213394] N90-13683
REGENERATION (ENGINEERING)
Refurbishment of one-person regenerative air revitalization system
[NASA-CR-183757] N90-13934
REGENERATIVE COOLING
Thermal protection systems for reentry and hypersonic flight
[DLR-MITT-89-14] N90-13577
REGRESSION ANALYSIS
On the application of modified stepwise regression for the estimation of aircraft stability and control parameters
[REPT-8905] N90-13400
Measuring of the complete stiffness matrix for anisotropic laminated materials
[DLR-MITT-89-11] N90-13606
Measuring of the complete stiffness matrix for anisotropic laminated materials
[DLR-MITT-89-12] N90-13607
REGULARITY
On smallest nonhamiltonian regular rough graphs
[MEMO-788] N90-14003
REGULATORS
ERIS: Engineering Resource Information System
[AD-A213357] N90-14144
REGULATORY MECHANISMS (BIOLOGY)
The pituitary growth hormone cell in space N90-13941
REINFORCING FIBERS
Fiber reinforced cementitious composites technology
[PB89-227813] N90-13608
REINFORCING MATERIALS
The application of cast SiC/Al to rotary engine components
[NASA-CR-179610] N90-13385
Toughening of a particulate-reinforced/ceramic-matrix composite
[AD-A213180] N90-13604
RELATIVITY
Some aspects of curvature in general relativity N90-14122
On thick domain walls in general relativity
[NASA-CR-185926] N90-14124
RELAXATION OSCILLATORS
Delay test generation for synchronous sequential circuits
[AD-A211917] N90-13697
RELIABILITY
LORAN C stability integrity assurance
[AD-A212663] N90-13364
A new view of weapon system reliability and maintainability
[AD-A213281] N90-13382
A new view of weapon system reliability and maintainability: Executive summary
[AD-A213282] N90-13383
Product assurance N90-13522
Flight motor set 360L001 (STS-26R). Volume 5: Nozzle component
[NASA-CR-183771] N90-13588
Electronic warfare: Reliable equipment needed to test Air Force's electronic warfare systems
[AD-A212952] N90-13687
Operational activity in France and a new method of balloon temperature piloting N90-13857
Sol-gel processing science using a Sol-Gel Optics Research Facility (SGORF)
[AD-A213056] N90-14095
RELIABILITY ANALYSIS
QM-8 field joint protection system, volume 7
[NASA-CR-183746] N90-13586
Sufficiency and necessity in reliability modeling
[NASA-CR-186119] N90-13706
RELIABILITY ENGINEERING
Laboratory test methodology for evaluating the effects of electromagnetic disturbances on fault-tolerant control systems
[NASA-TM-101685] N90-14061
REMOTE CONTROL
Assembly considerations for large reflectors N90-13480
Performance evaluation of a six-axis generalized force-reflecting teleoperator
[NASA-CR-186106] N90-13796
REMOTE SENSING
Spectrometer technology recommendations N90-13468
Summaries of the thematic conferences on remote sensing for exploration geology
[NASA-CR-185321] N90-13880
REMOTE SENSORS
The detectors N90-13507
REPORTS
A summary of 30 years of space launches
[AERONOMICA-ACTA-F-39-1989] N90-13411
REPRODUCTION (BIOLOGY)
Gravity and animal embryos N90-13951
RESEARCH
Summary of research academic departments, 1987-1988
[AD-A213252] N90-14183
RESEARCH AIRCRAFT
STOVL aircraft simulation for integrated flight and propulsion control research
[NASA-TM-102419] N90-13389
RESEARCH AND DEVELOPMENT
Small business innovation research: Program solicitation
[NASA-TM-101869] N90-14126
National Aeronautics and Space Administration Multiyear Authorization Act of 1989 N90-14148
National Aeronautics and Space Administration authorization
[S-HRG-101-348] N90-14149
Centers for the commercial development of space
[NASA-PAM-525] N90-14151
NASA commercial programs
[NASA-TM-101853] N90-14152
RESEARCH FACILITIES
The pituitary growth hormone cell in space N90-13941
Sol-gel processing science using a Sol-Gel Optics Research Facility (SGORF)
[AD-A213056] N90-14095
Centers for the commercial development of space
[NASA-PAM-525] N90-14151
NRL (Naval Research Laboratory) Review
[AD-A212886] N90-14182

RESEARCH MANAGEMENT
A new view of weapon system reliability and maintainability: Executive summary
[AD-A213282] N90-13383
RESONANCE
Study of the hydroxyl radical by DRASC resonance in a high pressure flame — Diffusion Raman Anti-Stokes Coherence (DRASC)
[ONERA-RS-53/7131-PY] N90-13632
Ring source/force excitation of axisymmetric shell structure
[ARE-TM(UHA)-88519] N90-14085
Elastic impurity scattering in double-barrier resonant tunneling structures
[AD-A212850] N90-14110
RESONANT FREQUENCIES
Mobility power flow analysis of an L-shaped plate structure subjected to acoustic excitation
[NASA-CR-186130] N90-13817
RESONANT TUNNELING
Resonant-tunneling oscillators and multipliers for submillimeter receivers N90-13467
Elastic impurity scattering in double-barrier resonant tunneling structures
[AD-A212850] N90-14110
RESONANT VIBRATION
Propagation of sound in vibrationally excited nitrogen and hydrogen gas mixtures
[AD-A213002] N90-14073
RESOURCES
The DOD Gateway Information System: Operational prototype and transition period 1987-1988
[AD-A213044] N90-14141
RETINA
Role of retinocortical processing in spatial vision
[AD-A210995] N90-13918
REVOLVING
COBE nonspinning attitude propagation N90-13418
REYNOLDS NUMBER
Analysis of experimental data for CAST 10-2/DOA 2 supercritical airfoil at low Reynolds numbers and application to high Reynolds number flow
[AD-A211654] N90-13326
REYNOLDS STRESS
A review of quasi-coherent structures in a numerically simulated turbulent boundary layer
[NASA-TM-102191] N90-13723
Turbulence modeling and implementation in Navier-Stokes solvers N90-13742
RHEOLOGY
Quadratic dynamical systems describing shear flow of non-Newtonian fluids
[AD-A212892] N90-13720
Analysis of new phenomena in shear flow of non-Newtonian fluids
[AD-A212893] N90-13721
RIBBONS
Evolution of the EPR procedure for polycrystalline Si ribbon drawing for photovoltaic cell manufacturing
[ISAL-89-0027] N90-13888
RICCATI EQUATION
The singular H infinity control problem with dynamic measurement feedback
[MEMO-COSOR-89-14] N90-14000
The algebraic Riccati equation and singular optimal control
[MEMO-COSOR-88-31] N90-14028
RIGID ROTORS
A technique for the prediction of aerodynamics and aeroelasticity of rotor blades N90-13377
RIGID STRUCTURES
Extension to Eulers's theorem to n-dimensional spaces N90-13431
ROADS
Why stochastic modeling is essential in analyzing interdicted transportation network performance
[AD-A213140] N90-14007
ROBOT DYNAMICS
Applications of artificial intelligence to space station and automated software techniques: High level robot command language
[NASA-CR-182997] N90-13991
ROBOTICS
Adaptive strategies for controls of flexible arms
[NASA-CR-185868] N90-13783
Arc current control of a robotic welding system: Modeling and control system design
[AD-A213150] N90-13788
Design and control of a two-degree-of-freedom lightweight flexible arm
[AD-A213335] N90-13790
A new approach to control single-link flexible arms. Part 3: Adaptive control of the tip position with payload changes
[AD-A213337] N90-13792
User needs, benefits, and integration of robotic systems in a space station laboratory
[NASA-CR-185150] N90-13794
Performance evaluation of a six-axis generalized force-reflecting teleoperator
[NASA-CR-186106] N90-13796
Applications of artificial intelligence to space station and automated software techniques: High level robot command language
[NASA-CR-182997] N90-13991
ROBOTS
Design and control of a two-degree-of-freedom lightweight flexible arm
[AD-A213335] N90-13790
A new approach to control single-link flexible arms. Part 3: Adaptive control of the tip position with payload changes
[AD-A213337] N90-13792
Image segmentation for the stereoscopic vision of a mobile robot
[ONERA-RT-1/3692-SY] N90-13800
Kinematics and control of manipulation robots
[WTHD-187] N90-13803
ROCKET ENGINE CASES
Systems tunnel linear shaped charge lightning strike
[NASA-CR-183832] N90-13404
ROCKET ENGINE CONTROL
High precision rocket attitude reconstruction using star sensor and magnetometer data N90-13844
ROCKET ENGINES
QM-8 field joint protection system, volume 7
[NASA-CR-183748] N90-13586
Gas flows in rocket motors, volume 1
[AD-A213348] N90-13591
Swiss scientific balloon and sounding rocket experiments 1987-1989 N90-13827
ROCKET EXHAUST
Modelling of satellite control thruster plumes N90-13578
ROCKET NOZZLES
RSRM nozzle fixed housing cooldown test
[NASA-CR-183741] N90-13587
Gas flows in rocket motors. Volume 3, appendix D: Computer code listings
[AD-A213350] N90-13593
ROTARY ENGINES
The application of cast SiC/Al to rotary engine components
[NASA-CR-179610] N90-13385
Analysis of rotary engine combustion processes based on unsteady, three-dimensional computations
[NASA-TM-102469] N90-13749
ROTATION
Extension to Eulers's theorem to n-dimensional spaces N90-13431
Rotation of the photospheric magnetic fields: A north-south asymmetry
[NASA-CR-186159] N90-14177
ROTOR AERODYNAMICS
Influence of vane sweep on rotor-stator interaction noise N90-13325
Computation of flow fields around propellers and hovering rotors based on the solution of the Euler equations
[DLR-FB-89-37] N90-13333
ROTOR BLADES
Application of a two-dimensional unsteady viscous analysis code to a supersonic throughflow fan stage
[NASA-TM-4141] N90-13387
ROTORS
Influence of vane sweep on rotor-stator interaction noise N90-13325
The application of cast SiC/Al to rotary engine components
[NASA-CR-179610] N90-13385
Elasticity effects on cavitation in a squeeze film damper undergoing noncentered circular whirl
[NASA-TM-102392] N90-13786
RUBBER
Evaluation of a neoprene latex modified SAMI (Stress Absorbing Membrane Interlayer)
[PB89-226435] N90-13665
RUN TIME (COMPUTERS)
The cellular approach: A new method to speed up simulated annealing for macro placement
[MEMO-COSOR-88-29] N90-13980
RUNGE-KUTTA METHOD
Inviscid 2D solutions on unstructured, adaptive grids N90-13737

S

SADDLE POINTS
Energy barriers in SK spin-glass model
[PREPRINT-665] N90-14119
SAFETY
User's manual for the ride motion simulator
[AD-A212855] N90-13402
Aircraft/airport compatibility: Some strategic, tactical, and operational issues
[TT-8902] N90-13409
SAFETY MANAGEMENT
Product assurance N90-13522
The US space station and its electric power system
[NASA-TM-101974] N90-13596
SALMONELLA
The sensory transduction pathways in bacterial chemotaxis N90-13944
SAMPLING
Identification of impulsive interference channels
[AD-A213154] N90-14009
SAN ANDREAS FAULT
Strain accumulation and surface deformation along the San Andreas, California
[NASA-CR-185893] N90-13894
SATELLITE ATTITUDE CONTROL
Flight Mechanics/Estimation Theory Symposium, 1989
[NASA-CP-3050] N90-13413
Autonomous spacecraft attitude control using magnetic torquing only N90-13415
Simulation of spacecraft attitude dynamics using TREETOPS and model-specific computer Codes N90-13419
Orbit and attitude determination results during launch support operations for SBS-5
[PAPER-7] N90-13420
GOES I/M image navigation and registration N90-13422
Temperature dependence of attitude sensor coalignments on the Solar Maximum Mission (SMM) N90-13426
True covariance simulation of the EUVE update filter N90-13427
A gyroscope calibration analysis for the Gamma Ray Observatory (GRO) N90-13428
Extended Kalman filter for attitude estimation of the earth radiation budget satellite N90-13433
Launch and early orbit N90-13524
The in-orbit initialization phase N90-13525
On-ground attitude determination N90-13552
The great circle reductions N90-13553
Great circle interactions: Attitude smoothing and grid-step inconsistencies N90-13554
Modelling of satellite control thruster plumes N90-13578
Choice of a differential method for the attitude restitution in dynamic unbalance
[CNES-CT/DTI/MS/CM/290] N90-13582
SATELLITE COMMUNICATION
The role of the ground segment N90-13527
The use of digital signal processing in satellite communication N90-13684
SATELLITE IMAGERY
GOES I/M image navigation and registration N90-13422
Proximity effects on adjacent and multiple stars N90-13533
Modeling of the Hipparcos optical system N90-13572
ALIS: An Auroral Large Imaging System in northern Scandinavia N90-13877
Senegalese land surface change analysis and biophysical parameter estimation using NOAA AVHRR spectral data
[NASA-CR-186120] N90-13883
The use of a deformation model for sampling digitalized stereoscopic images
[IMAG-RR-753-I] N90-13884
Estimation of rain rate using spatial and multichannel coherence: Analysis of SSM/I data N90-13905
Algorithm for atmospheric corrections of aircraft and satellite imagery
[NASA-TM-100751] N90-13976
Normal points: Compression of satellite laser ranging data
[ETN-90-96006] N90-14145
SATELLITE NETWORKS
Geodetic network adjustment using GPS triple difference observations and a priori stochastic information
[TR-1-1987] N90-13367
SATELLITE OBSERVATION
Test network Delft
[ETN-90-96009] N90-13365
Geodetic network adjustment using GPS triple difference observations and a priori stochastic information
[TR-1-1987] N90-13367
Precision of semi-geometrically determined SLR baselines vs. site occupation time
[ETN-90-96007] N90-13885

Three dimensional analysis of the structure of the atmosphere in polar environments by vertical satellite sounding, interest for the meteorological forecasts at high latitudes
[ETN-90-95506] N90-13911

SATELLITE ORBITS
Orbit and attitude determination results during launch support operations for SBS-5
[PAPER-7] N90-13420
Automation of orbit determination functions for National Aeronautics and Space Administration (NASA)-supported satellite missions N90-13434
Overview of the Hipparcos satellite N90-13502
Re-entry hazards and cosmos 1900
[FOA-C-30535-9.4] N90-13583
Precision of semi-geometrically determined SLR baselines vs. site occupation time
[ETN-90-96007] N90-13685

SATELLITE ORIENTATION
Choice of a differential method for the attitude restitution in dynamic unbalance
[CNES-CT/DTI/MS/CM/290] N90-13582

SATELLITE SOUNDING
Three dimensional analysis of the structure of the atmosphere in polar environments by vertical satellite sounding, interest for the meteorological forecasts at high latitudes
[ETN-90-95506] N90-13911

SATELLITE TRACKING
Analytical derivation and verification of zero-gyro control for the IUE satellite
[NASA-TM-100748] N90-13767

SATELLITE TRANSMISSION
Error control techniques for satellite and space communications
[NASA-CR-182751] N90-13685

SATELLITE-BORNE RADAR
Development of a traveling wave tube for the project X-SAR. Construction and testing of a breadboard model
[ETN-90-95900] N90-13713

SCALARS
Scalar transport in turbulent shear flows N90-13734

SCALE MODELS
Application of two-point closures to subgrid scale modeling for homogeneous, 3D turbulence N90-13732

SCALING LAWS
Scaling in a non Abelian string network
[ROM1F-89-676] N90-14066
Configurational statistics of strings, fractals and polymer physics. Part 2: Non Abelian strings
[ROM1F-89-680-PT-2] N90-14067
String correlations and galaxies formation
[ROM1F-89-677] N90-14170
Non Abelian string correlations and galaxies formation
[ROM1F-89-678] N90-14171
Des Cloizeaux's law for strings and galaxies formation. Part 1: Abelian configurations
[ROM1F-89-681-PT-1] N90-14172

SCATTERING
Nonpotential scattering for the density matrix and quantum gravity
[PREPRINT-668] N90-14080

SCENE ANALYSIS
Senegalese land surface change analysis and biophysical parameter estimation using NOAA AVHRR spectral data
[NASA-CR-186120] N90-13883

SCHEDULING
Ada task scheduling: A focused Ada investigation
[NASA-CR-186072] N90-13967
Elementary and middle school science improvement project
[NASA-CR-183768] N90-14125

SCHMIDT TELESCOPES
Overview of the Hipparcos payload N90-13503
The telescope mirrors N90-13504
The baffles N90-13509

SCHOOLS
Elementary and middle school science improvement project
[NASA-CR-183768] N90-14125

SCHUMANN-RUNGE BANDS
New calculations of photodissociation cross-sections in the O2 Schumann-Runge system N90-13834

SCIENCE
Summary of research academic departments, 1987-1988
[AD-A213252] N90-14183

SCINTILLATION COUNTERS
The determinatin of the muon content of EAS from Cygnus X-3 N90-14179

SEALING
Development and testing of a contactless static/dynamic shaft seal with little sealing gas requirement
[KFK-4599] N90-13802

SEARCHING
Novel graph searching methods for image analysis
[AD-A213065] N90-13971

SEASONS
The effects of seasonal and latitudinal earth infrared radiance variations on ERBS attitude control N90-13414

SEGMENTS
Coherent phasing of segmented mirrors N90-13474

SEISMIC WAVES
ULF/VLF (0.001 to 50 Hz) Seismo-Acoustic Noise in the Ocean
[AD-A212942] N90-13913

SEISMOLOGY
ULF/VLF (0.001 to 50 Hz) Seismo-Acoustic Noise in the Ocean
[AD-A212942] N90-13913

SELECTION
Stellar content of the input catalog N90-13535
The choice of stars in open clusters N90-13542
The choice of stars in the Magellanic clouds N90-13543
The activity selection problem: A network and game theoretic approach
[MEMO-794] N90-14056

SELECTIVITY
Successive iterations of the input catalog N90-13534

SELF CONSISTENT FIELDS
A self-consistent model of the most common nightglow emissions N90-13853

SEMANTICS
Database interfaces on NASA's heterogeneous distributed database system
[NASA-CR-185420] N90-14133
Architecture and language for a layered relational database N90-14146

SEMICONDUCTING FILMS
Optical modulators based on polymers
[EP-PATENT-0-294-061-A1] N90-14099

SEMICONDUCTOR DEVICES
Fundamental quantum 1/f noise in ultrasmall semiconductor devices and their optimal design principles
[AD-A211947] N90-14107
Manufacturing and characterization of insulator-germanium structures
[ECL-88-13] N90-14115
Study of surface uniformity of semiconductors 3 to 5 by photoluminescence imagery
[ECL-88-15] N90-14116
Photoelectrochemical behavior of type n of GaAs in concentrated iodide media and realization of an experimental device
[ECL-88-18] N90-14117

SEMICONDUCTOR LASERS
Optical communication with semiconductor laser diode
[NASA-CR-185886] N90-13770

SEMICONDUCTORS (MATERIALS)
Electrochemical study of the etching of III to V semiconductors
[ETN-90-96015] N90-13633
Joint Services Electronics Program
[AD-A213015] N90-13699
Ultrafast processes and spectroscopy with free electron lasers
[AD-A212889] N90-13773
Reorganization free energy for electron transfers at liquid-liquid and dielectric semiconductor-liquid interfaces
[AD-A212985] N90-14111
GaAs and GaAs:In: Influence of surface treatments and characterization of homogeneity by photoluminescent imagery
[ECL-88-24] N90-14118
Towards ab initio calculation of electron energies in semiconductors
[ETN-90-96016] N90-14121

SENSITIVITY
Quantitative AES and XPS: Determination of the electron spectrometer transmission function and the detector sensitivity energy dependencies for the production of true electron emission spectra in AES and XPS
[NPL-DMA(A)-194] N90-13634
Quench sensitivity in Al-Cu-Li alloys
[AD-A213055] N90-13639
Effect of spatial resolution on apparent sensitivity to initial conditions of a decaying flow as it becomes turbulent
[NASA-TM-102377] N90-13719
Discussion of factors affecting the sensitivity of IR imaging sensors, particularly focal plane mosaic arrays --- staring mosaic arrays
[FOA-C-30536-3.1] N90-14101

SENSORS
Software development for avionics SSME control and diagnostics
[NASA-CR-184894] N90-13964

SENSORY PERCEPTION
Simulator induced sickness in the CP-140 (Aurora) flight deck simulator
[AD-A213096] N90-13923

SENSORY STIMULATION
Free swimming organisms: Microgravity as an investigative tool N90-13949

SEQUENCING
Test generation for highly sequential circuits
[AD-A211932] N90-13698

SEQUENTIAL CONTROL
Efficient on-line simulations of tree machines and multidimensional turing machines by random access machines
[AD-A213152] N90-13960

SERVICE LIFE
Thermal barrier coating life prediction model development, phase 1
[NASA-CR-182230] N90-13388

SERVOMECHANISMS
Advanced actuation systems development, volume 2
[AD-A213378] N90-13398
Kinematics and control of manipulation robots
[WTHD-187] N90-13803

SET THEORY
Acceleration sets of planar manipulators. Part 2: Applications and experiments
[AD-A213336] N90-13791
The algebraic Riccati equation and singular optimal control
[MEMO-COSOR-88-31] N90-14028

SHAPED CHARGES
Systems tunnel linear shaped charge lightning strike
[NASA-CR-183832] N90-13404

SHEAR FLOW
A planar reacting shear layer system for the study of fluid dynamics-combustion interaction
[NASA-TM-102422] N90-13393
Quadratic dynamical systems describing shear flow of non-Newtonian fluids
[AD-A212892] N90-13720
Analysis of new phenomena in shear flow of non-Newtonian fluids
[AD-A212893] N90-13721
Turbulent Shear Flows
[VKI-LS-1989-03] N90-13730
An introduction via vorticity dynamics and statistical theory --- turbulent shear flows N90-13731
Scalar transport in turbulent shear flows N90-13734
Large eddy simulation of homogeneous turbulence undergoing shear and thermal gradients. Application to one point closing models
[ECL-88-23] N90-13754

SHEAR LAYERS
A planar reacting shear layer system for the study of fluid dynamics-combustion interaction
[NASA-TM-102422] N90-13393
Field-effect spectroscopy of interface states
[AD-A212998] N90-14112

SHEAR PROPERTIES
Identification of equivalent modulus of a composite beam from nonmodal vibratory tests
[ECL-89-001] N90-13821

SHEARING
Shear-induced inflation of coronal magnetic fields
[NASA-CR-186103] N90-14178

SHELL STABILITY
Buckling load analysis for imperfect cylindrical shells, part 1
[LR-543-PT-1] N90-13823

SHELLS (STRUCTURAL FORMS)
Buckling load analysis for imperfect cylindrical shells, part 1
[LR-543-PT-1] N90-13823
Interface between MEDUSA and GIFTS for shell structures
[LR-553] N90-13985

SHIELDING
The baffles N90-13509

SHOCK WAVE PROFILES
Computation of nonequilibrium gas flow past blunt bodies
[PREPRINT-488] N90-13757

SHORELINES
Comparison of analytical methods for calculation of wind loads
[NASA-TM-102782] N90-13813

SHORT CIRCUITS
Test generation for highly sequential circuits
[AD-A211932] N90-13698

SHORT TAKEOFF AIRCRAFT
STOVL aircraft simulation for integrated flight and propulsion control research
[NASA-TM-102419] N90-13389

SIGNAL DETECTION
Test procedures for the evaluation of helmet and headset mounted active noise reduction systems [AD-A212991] N90-13937
SIGNAL DISTORTION
Proximity effects on adjacent and multiple stars N90-13533
SIGNAL PROCESSING
Spectrometer technology recommendations N90-13468
The use of digital signal processing in satellite communication N90-13684
Efficient detection of small moving objects [AD-A213314] N90-13690
An experimental analysis of the waveguide modes in a high-gain free-electron laser amplifier N90-13779
A counter gating circuit for acoustic emission monitoring of structures cracking under repetitive alternating loads [ARL-MAT-TM-398] N90-13808
SIGNAL TO NOISE RATIOS
Application of an optimal filter for inflatable sphere data processing N90-13849
SIGNATURES
Nuclear magnetic resonance signatures of nitrogen-containing compounds [AD-A213375] N90-13628
SILANES
Synthesis of inorganic polymers as glass precursors and for other uses. Preceramic block or graft copolymers as potential precursors to nanocomposite materials [AD-A211978] N90-13655
SILICA GLASS
A new model for the structure of silica glass [AD-A212972] N90-13659
SILICON
Silicon-etalon fiber-optic temperature sensor [NASA-TM-102389] N90-13381
Evolution of the EPR procedure for polycrystalline Si ribbon drawing for photovoltaic cell manufacturing [ISAL-89-0027] N90-13888
SILICON CARBIDES
Fatigue behavior of silicon carbide Whisker/Aluminum composite [AD-A213094] N90-13603
Toughening of a particulate-reinforced/ceramic-matrix composite [AD-A213180] N90-13604
Toughening mechanisms in ceramic composites [PB89-235907] N90-13656
Mechanisms in reactive ion etching of silicon carbide thin films [AD-A213018] N90-13700
SILICON DIOXIDE
Unified model of charge build up and annealing of oxide charge and interface states in SiO2 due to stress [HMI-B-465] N90-14120
SILICON FILMS
Novel in situ spectroscopic ellipsometer for real time analysis of CVD diamond films [AD-A213218] N90-13762
SILICON OXIDES
SiO overcoating and polishing of CFRP telescope panels N90-13478
Synthesis of inorganic polymers as glass precursors and for other uses. Preceramic block or graft copolymers as potential precursors to nanocomposite materials [AD-A211978] N90-13655
SIMULATION
LORAN C stability integrity assurance [AD-A212663] N90-13364
True covariance simulation of the EUVE update filter N90-13427
Recovery of particle size distribution of ultrafine aerosols from diffusional decay measurements [AD-A213006] N90-13621
Simulation of the control characteristics of an axial piston pump and a flapper-nozzle valve combination N90-13784
Air quality simulation model performance for one-hour averages [PB89-233506] N90-13890
The structural memory: A network model for human perception of serial objects [CWI-CS-R8829] N90-13930
SIMOGEN: An object-oriented language for simulation [AD-A213129] N90-13973
Why stochastic modeling is essential in analyzing interdicted transportation network performance [AD-A213140] N90-14007
Identification of impulsive interference channels [AD-A213154] N90-14009
Global optimization and simulated annealing [MEMO-COSOR-88-21] N90-14025
Analysis of three approaches to qualitative simulation [MEMO-INF-89-32] N90-14035
SIMULATORS
Implementation issues in source coding [NASA-CR-185327] N90-13963
SINGULARITY (MATHEMATICS)
The quadratic matrix inequality in singular H infinity control with state feedback [MEMO-COSOR-89-03] N90-13997
The totally singular linear quadratic problem with indefinite cost [MEMO-COSOR-89-05] N90-13998
The singular zero sum differential game with stability using H infinity control theory [MEMO-COSOR-89-09] N90-13999
The singular H infinity control problem with dynamic measurement feedback [MEMO-COSOR-89-14] N90-14000
SINTERING
Correlation between microstructure and magnetic properties of porous sintered iron and porous iron containing composites [KFK-4522] N90-13647
SIS (SUPERCONDUCTORS)
Far-infrared heterodyne receivers N90-13465
Advances in SIS receiver technology N90-13466
SKIN (STRUCTURAL MEMBER)
Some new techniques for aircraft fuselage skin tests [LR-547] N90-13379
SKIN FRICTION
Skin friction measurements with hot elements N90-13345
SKY SURVEYS (ASTRONOMY)
The detectors N90-13507
Successive iterations of the input catalog N90-13534
Stellar content of the input catalog N90-13535
Ground-based astrometric measurements N90-13536
The compilation of astrometric data N90-13537
Standard stars and photometric calibration N90-13539
Double stars N90-13540
The choice of stars in open clusters N90-13542
The choice of stars in the Magellanic clouds N90-13543
Minor planets and other solar system objects N90-13545
The catalogs produced by the Inca consortium N90-13546
The SIMBAD data base N90-13547
SKYLARK ROCKET VEHICLE
The Skylark sounding rocket program and future launcher developments by British Aerospace (Space Systems) Ltd. N90-13871
SLAGS
Evaluation of copper slag blast media for railcar maintenance [NASA-CR-183744] N90-13681
SLITS
The modulating grid N90-13505
SMOKE
A smoke generator system for aerodynamic flight research [NASA-TM-4137] N90-13372
SODIUM
Diurnal variation of the sodium layer at polar latitudes in summer N90-13869
SOFTWARE ENGINEERING
Processing of undifferences GPS carrier beat phase measurements and adjustment computations [TR-5-1988] N90-13368
Definition of avionics concepts for a heavy lift cargo vehicle, appendix A [NASA-CR-183817] N90-13380
The development of a program analysis environment for Ada [NASA-CR-185860] N90-13962
Software development for avionics SSME control and diagnostics [NASA-CR-184894] N90-13964
Methodology for automating software systems. Task 1 of the foundations for automating software systems [NASA-CR-180499] N90-13965
Software engineering and Ada (Trademark) training: An implementation model for NASA [NASA-CR-186071] N90-13966
Ada task scheduling: A focused Ada investigation [NASA-CR-186072] N90-13967
The APROS software for process simulation and model development [VTT-618] N90-13987
Flight software development for the isothermal dendritic growth experiment [NASA-TM-102412] N90-13988
Applications of artificial intelligence to space station and automated software techniques: High level robot command language [NASA-CR-182997] N90-13991
Executive overview and introduction to the SMAP information system life-cycle and documentation standards [NASA-TM-101785] N90-14134
SOFTWARE TOOLS
Test network Delft [ETN-90-96009] N90-13365
Computer-based tools for assisting air traffic controllers with arrivals flow management [RSRE-88001] N90-13366
Mission simulations N90-13532
On the design of a computer-aided design system for digital circuits N90-13695
Methodology for automating software systems. Task 1 of the foundations for automating software systems [NASA-CR-180499] N90-13965
The APROS software for process simulation and model development [VTT-618] N90-13987
SOIL MAPPING
Physically-based parameterization of spatially variable soil and vegetation using satellite multispectral data [NASA-CR-185957] N90-13879
The use of a deformation model for sampling digitalized stereoscopic images [IMAG-RR-753-I] N90-13884
SOL-GEL PROCESSES
Sol-gel processing science using a Sol-Gel Optics Research Facility (SGORF) [AD-A213056] N90-14095
SOLAR ARRAYS
The Space Station Photovoltaic Panels Plasma Interaction Test Program: Test plan and results [NASA-TM-102474] N90-13581
SOLAR ATMOSPHERE
A high-resolution atlas of the infrared spectrum of the Sun and the Earth atmosphere from space: A compilation of ATMOS spectra of the region from 650 to 4800 cm (2.3 to 16 micron). Volume 1: The Sun [NASA-RP-1224-VOL-1] N90-13893
Rotation of the photospheric magnetic fields: A north-south asymmetry [NASA-CR-186159] N90-14177
SOLAR CELLS
The photovoltaic properties of an Al In As/InP heterojunctions grown by LPE method [NASA-CR-185996] N90-13886
Evolution of the EPR procedure for polycrystalline Si ribbon drawing for photovoltaic cell manufacturing [ISAL-89-0027] N90-13888
SOLAR CORONA
Interplanetary dust close to the Sun (F corona): Its observation in the visible and infrared by a rocket-borne coronagraph N90-13864
Shear-induced inflation of coronal magnetic fields [NASA-CR-186103] N90-14178
SOLAR CYCLES
Rotation of the photospheric magnetic fields: A north-south asymmetry [NASA-CR-186159] N90-14177
SOLAR FLUX DENSITY
Prediction of the 10 cm solar flux index N90-13872
SOLAR GENERATORS
Power generation and distribution N90-13515
SOLAR MAGNETIC FIELD
Rotation of the photospheric magnetic fields: A north-south asymmetry [NASA-CR-186159] N90-14177
Shear-induced inflation of coronal magnetic fields [NASA-CR-186103] N90-14178
SOLAR MAXIMUM MISSION
Temperature dependence of attitude sensor coalignments on the Solar Maximum Mission (SMM) N90-13426
Analysis of the flight dynamics of the Solar Maximum Mission (SMM) off-sun scientific pointing N90-13432
SOLAR PHYSICS
An implementation plan for priorities in solar-system space physics [NASA-CR-185375] N90-14154
Analysis of coordinated observations of a giant stellar flare [NASA-CR-185961] N90-14176
SOLAR POSITION
Launch and early orbit N90-13524
SOLAR RADIATION
Design and technical aspects of the Solly instrument N90-13847
Observation of the solar Lyman-alpha line N90-13868
Senegalese land surface change analysis and biophysical parameter estimation using NOAA AVHRR spectral data [NASA-CR-186120] N90-13883
SOLAR REFLECTORS
LDR structural experiment definition N90-13483

LDR structural technology activities at JPL N90-13488
SOLAR SENSORS
Temperature dependence of attitude sensor coalignments on the Solar Maximum Mission (SMM) N90-13426
Analytical derivation and verification of zero-gyro control for the IUE satellite [NASA-TM-100748] N90-13767
SOLAR SPECTROMETERS
Design and technical aspects of the Solly instrument N90-13847
SOLAR SYSTEM
The German space science program N90-13873
An implementation plan for priorities in solar-system space physics [NASA-CR-185375] N90-14154
SOLAR TERRESTRIAL INTERACTIONS
An implementation plan for priorities in solar-system space physics [NASA-CR-185375] N90-14154
SOLAR X-RAYS
Prediction of the 10 cm solar flux index N90-13872
SOLID ELECTRODES
Metal transfer in gas metal arc welding [AD-A213390] N90-13642
SOLID LUBRICANTS
Evaluation of newly formulated Dow Corning 321 dry film lubricant [NASA-CR-183828] N90-13661
SOLID PROPELLANT COMBUSTION
A theoretical model of double base propellant combustion [ONERA-RTF-23/7128-EY] N90-13672
SOLID PROPELLANT ROCKET ENGINES
Systems tunnel linear shaped charge lightning strike [NASA-CR-183832] N90-13404
SOLID STATE DEVICES
Contribution to the study of a self-protected static switch and its command strategy [ECL-89-002] N90-13711
SOLID STATE LASERS
Development of mid-infrared solid state lasers for spaceborne lidar [NASA-CR-183290] N90-13772
SOLID-SOLID INTERFACES
Numerical analysis of scattering by interface flaws [AD-A212996] N90-13810
SOLIDIFICATION
Containerless Processing of Metals: Undercooling and Solidification [DLR-MITT-89-15] N90-13645
The effects of alloying and thermal factors on the solidification and mechanical properties of gray iron [VTT-619] N90-13651
SOLITARY WAVES
The initial-boundary value problem for the Davey-Stewartson 1 equation; how to generate and drive localized coherent structures in multidimensions [PREPRINT-684] N90-13756
Energy exchange of interacting solitons in multidimensions [PREPRINT-662] N90-14071
SOOT
Transport phenomena and interfacial kinetics in multiphase combustion systems [AD-A212932] N90-13620
SOUND AMPLIFICATION
Propagation of sound in vibrationally excited nitrogen and hydrogen gas mixtures [AD-A213002] N90-14073
SOUND FIELDS
ULF/VLF (0.001 to 50 Hz) Seismo-Acoustic Noise in the Ocean [AD-A212942] N90-13913
SOUND TRANSMISSION
Evaluation of speech intelligibility through a bone conduction stimulator [AD-A212002] N90-13919
SOUND WAVES
Ring source/force excitation of axisymmetric shell structure [ARE-TM(UHA)-88519] N90-14085
SOUNDING ROCKETS
European Rocket and Balloon Programs and Related Research [ESA-SP-291] N90-13826
Swiss scientific balloon and sounding rocket experiments 1987-1989 N90-13827
The Norwegian balloon and sounding rocket program 1989-1992 N90-13829
The Swedish sounding rocket and balloon program N90-13830
The German scientific balloon and sounding rocket program N90-13831
The SN 1987A attitude control system N90-13845
Design and technical aspects of the Solly instrument N90-13847
Preliminary results of the rocket and scatter experiments ROSE: Measurements with the newly designed spherical probe N90-13850
Andoya rocket range: New installations, future plans, and investments N90-13859
Qualification of the 4th stage propulsor of the Brazilian launcher. SLV: A new sounding rocket N90-13860
The Brazilian space program: Actual state of the art N90-13861
Optical observations of interplanetary pick-up ions: The experiment Helly N90-13863
The x ray mirror and the PSPC of the supernova-rocket-project N90-13867
Esrange N90-13876
SOUTHERN HEMISPHERE
Humidity local measurements in the middle atmosphere N90-13833
Long duration balloon flights in the middle stratosphere N90-13874
SPACE ADAPTATION SYNDROME
Preliminary study of pharmacological control of space disease [ETN-90-95015] N90-13927
SPACE COMMERCIALIZATION
Development of a shuttle recovery Commercial Materials Processing in Space (CMPS) program [NASA-CR-183720] N90-13678
Fundamental results from microgravity cell experiments with possible commericial applications N90-13940
Centers for the commercial development of space [NASA-PAM-525] N90-14151
NASA commercial programs [NASA-TM-101853] N90-14152
SPACE ENVIRONMENT SIMULATION
Watchfulness and attention during weightlessness simulations: Use of computerized psychometric tests [REPT-89-TOU-3-1045] N90-13928
SPACE ERECTABLE STRUCTURES
Assembly considerations for large reflectors N90-13480
Hybrid deployable support truss designs for LDR N90-13485
Joints in deployable space truss structures N90-13489
SPACE FLIGHT STRESS
Exercise countermeasures for bed rest deconditioning [NASA-TM-101045] N90-13926
SPACE HABITATS
Measurement of the light flux density patterns from luminaires proposed as photon sources for photosynthesis during space travel [NASA-CR-186124] N90-13916
SPACE INFRARED TELESCOPE FACILITY
Status of direct detector and array development N90-13464
The infrared spectrograph during the SIRTF pre-definition phase [NASA-CR-183234] N90-13759
SOFIA (Stratospheric Observatory For Infrared Astronomy): A 3m class airborne telescope N90-13848
SPACE LABORATORIES
User needs, benefits, and integration of robotic systems in a space station laboratory [NASA-CR-185150] N90-13794
SPACE MISSIONS
A summary of 30 years of space launches [AERONOMICA-ACTA-F-39-1989] N90-13411
Optical properties monitor: Experiment definition phase [NASA-CR-183836] N90-14092
An implementation plan for priorities in solar-system space physics [NASA-CR-185375] N90-14154
SPACE NAVIGATION
GOES I/M image navigation and registration N90-13422
Shuttle relative navigation of a tethered satellite mission with current on board software N90-13423
Impact of tether cutting on onboard navigation during the Tethered Satellite Mission-1 N90-13424
SPACE PROBES
Preliminary results of the rocket and scatter experiments ROSE: Measurements with the newly designed spherical probe N90-13850
SPACE PROCESSING
Development of a shuttle recovery Commercial Materials Processing in Space (CMPS) program [NASA-CR-183720] N90-13678
SPACE PROGRAMS
Development of a shuttle recovery Commercial Materials Processing in Space (CMPS) program [NASA-CR-183720] N90-13678
European Rocket and Balloon Programs and Related Research [ESA-SP-291] N90-13826
SPACE RENDEZVOUS
Active rendezvous between a low-earth orbit user spacecraft and the Space Transportation System (STS) shuttle N90-13436
SPACE SHUTTLE BOOSTERS
Cable coupling lightning transient qualification [NASA-CR-183826] N90-13405
Development of a shuttle plume radiation heating indicator [NASA-CR-183679] N90-13584
Space Transportation Engine Program (STEP). Phase B: Project study and management plan-ingredients for STEP success [NASA-CR-183770] N90-13585
RSRM nozzle fixed housing cooldown test [NASA-CR-183741] N90-13587
Qualification of improved joint heaters [NASA-CR-183827] N90-13594
SPACE SHUTTLE MAIN ENGINE
Computation of viscous incompressible flows [NASA-TM-101090] N90-13329
Space Transportation Engine Program (STEP). Phase B: Project study and management plan-ingredients for STEP success [NASA-CR-183770] N90-13585
SSME LOX post flow analysis/fluid structure interaction. Volume 1: Flow analysis [NASA-CR-183677] N90-13715
SSME LOX post flow analysis/fluid structure interaction. Volume 2: Fluid structure interaction [NASA-CR-183678] N90-13716
Software development for avionics SSME control and diagnostics [NASA-CR-184894] N90-13964
SPACE SHUTTLE MISSION 61-E
Debris/ice/TPS assessment and photographic analysis for Shuttle Mission STS-34 [NASA-TM-102153] N90-13447
SPACE SHUTTLE MISSIONS
Shuttle relative navigation of a tethered satellite mission with current on board software N90-13423
Syncom 4 deploy, LDEF retrieval highlight 10-day Columbia flight [NASA-NEWS-RELEASE-89-180] N90-13448
SPACE SHUTTLE ORBITERS
Debris/ice/TPS assessment and photographic analysis for Shuttle Mission STS-34 [NASA-TM-102153] N90-13447
SPACE SHUTTLE PAYLOADS
Syncom 4 deploy, LDEF retrieval highlight 10-day Columbia flight [NASA-NEWS-RELEASE-89-180] N90-13448
Development of a shuttle recovery Commercial Materials Processing in Space (CMPS) program [NASA-CR-183720] N90-13678
Flight software development for the isothermal dendritic growth experiment [NASA-TM-102412] N90-13988
SPACE SHUTTLES
Active rendezvous between a low-earth orbit user spacecraft and the Space Transportation System (STS) shuttle N90-13436
Space Transportation Engine Program (STEP). Phase B: Project study and management plan-ingredients for STEP success [NASA-CR-183770] N90-13585
Tank pressure control experiment on the space shuttle [NASA-TM-102313] N90-13590
SPACE STATION PAYLOADS
Science and applications on the space station: A strategic vision [NASA-TM-101863] N90-13493
Facilities for microgravity combustion research [NASA-TM-102014] N90-13679
SPACE STATION POLAR PLATFORMS
Science and applications on the space station: A strategic vision [NASA-TM-101863] N90-13493
SPACE STATION POWER SUPPLIES
Space station systems: A bibliography with indexes (supplement 9) [NASA-SP-7056(09)] N90-13580
The Space Station Photovoltaic Panels Plasma Interaction Test Program: Test plan and results [NASA-TM-102474] N90-13581
The US space station and its electric power system [NASA-TM-101974] N90-13596
Modeling of power electronic systems with EMTP [NASA-TM-102375] N90-14060

SPACE STATION PROPULSION
Space station systems: A bibliography with indexes (supplement 9)
[NASA-SP-7056(09)] N90-13580
SPACE STATION STRUCTURES
Space station systems: A bibliography with indexes (supplement 9)
[NASA-SP-7056(09)] N90-13580
SPACE STATIONS
Periodic-disturbance accommodating control of the space station for asymptotic momentum management N90-13416
LDR structural experiment definition N90-13483
Space station gas compressor technology study program, phase 1
[NASA-CR-183758] N90-13491
Space Station Engineering Design Issues
[NASA-CR-185978] N90-13492
Space station systems: A bibliography with indexes (supplement 9)
[NASA-SP-7056(09)] N90-13580
User needs, benefits, and integration of robotic systems in a space station laboratory
[NASA-CR-185150] N90-13794
Exercise countermeasures for bed rest deconditioning
[NASA-TM-101045] N90-13926
Functional decor in the International Space Station: Body orientation cues and picture perception
[NASA-TM-102242] N90-13931
National Aeronautics and Space Administration Multiyear Authorization Act of 1989 N90-14148
National Aeronautics and Space Administration authorization
[S-HRG-101-348] N90-14149
SPACE TRANSPORTATION SYSTEM
On the wings of a dream: The Space Shuttle
[NASA-EP-269] N90-13446
National Aeronautics and Space Administration Multiyear Authorization Act of 1989 N90-14148
National Aeronautics and Space Administration authorization
[S-HRG-101-348] N90-14149
SPACE-TIME FUNCTIONS
Some aspects of curvature in general relativity N90-14122
SPACEBORNE ASTRONOMY
The Voyager Neptune travel guide
[NASA-CR-186108] N90-13412
Interplanetary dust close to the Sun (F corona): Its observation in the visible and infrared by a rocket-borne coronagraph N90-13864
SPACEBORNE EXPERIMENTS
Syncom 4 deploy, LDEF retrieval highlight 10-day Columbia flight
[NASA-NEWS-RELEASE-89-180] N90-13448
Science and applications on the space station: A strategic vision
[NASA-TM-101863] N90-13493
The Norwegian balloon and sounding rocket program 1989-1992 N90-13829
The DYANA campaign 1990 N90-13870
Cells in Space
[NASA-CP-10034] N90-13939
The pituitary growth hormone cell in space N90-13941
Response of lymphocytes to a mitogenic stimulus during spaceflight N90-13942
How to detect when cells in space perceive gravity N90-13946
Gravity and animal embryos N90-13951
Design challenges for space bioreactors N90-13955
SPACEBORNE LASERS
Outline on the future Italian transportable laser ranging station
[CISE-4845] N90-13782
Normal points: Compression of satellite laser ranging data
[ETN-90-96008] N90-14145
SPACEBORNE TELESCOPES
The x ray mirror and the PSPC of the supernova-rocket-project N90-13867
SPACECRAFT CABIN ATMOSPHERES
Refurbishment of one-person regenerative air revitalization system
[NASA-CR-183757] N90-13934
SPACECRAFT COMPONENTS
Electrical testing N90-13520
SPACECRAFT CONTROL
Periodic-disturbance accommodating control of the space station for asymptotic momentum management N90-13416
Simultaneous quaternion estimation (QUEST) and bias determination N90-13417
Spacecraft attitude determination using the earth's magnetic field N90-13429
Analysis of the flight dynamics of the Solar Maximum Mission (SMM) off-sun scientific pointing N90-13432
Optimal trajectories for the aeroassisted flight experiment, 1988-89
[NASA-CR-186132] N90-13443
The dynamics and control of large flexible space structures - 12, supplement 11
[NASA-CR-185966] N90-13494
SPACECRAFT DESIGN
Lifetime predictions for the Solar Maximum Mission (SMM) and San Marco spacecraft N90-13440
SPACECRAFT DOCKING
Active rendezvous between a low-earth orbit user spacecraft and the Space Transportation System (STS) shuttle N90-13436
SPACECRAFT ELECTRONIC EQUIPMENT
Payload electronics and mechanisms N90-13508
SPACECRAFT EQUIPMENT
Overview of the Hipparcos payload N90-13503
SPACECRAFT GUIDANCE
Trajectory optimization and guidance for an aerospace plane
[NASA-CR-185884] N90-13389
Optimal trajectories for the aeroassisted flight experiment, 1988-89
[NASA-CR-186132] N90-13443
SPACECRAFT INSTRUMENTS
The Voyager Neptune travel guide
[NASA-CR-186108] N90-13412
GRADIO: An error analysis of the spaceborne gravity gradiometer
[ETN-90-96010] N90-13901
SPACECRAFT LAUNCHING
A summary of 30 years of space launches
[AERONOMICA-ACTA-F-39-1989] N90-13411
Launch and early orbit N90-13524
The Brazilian space program: Actual state of the art N90-13861
SPACECRAFT MANEUVERS
Analysis of the flight dynamics of the Solar Maximum Mission (SMM) off-sun scientific pointing N90-13432
SPACECRAFT ORBITS
The attitude and orbit control system N90-13516
The in-orbit initialization phase N90-13525
SPACECRAFT POWER SUPPLIES
Power generation and distribution N90-13515
SPACECRAFT PROPULSION
Thin-film sensors for reusable space propulsion systems
[NASA-TM-102383] N90-13595
SPACECRAFT RADIATORS
An improved algorithm for the modeling of vapor flow in heat pipes
[NASA-CR-185179] N90-13748
SPACECRAFT RECOVERY
Syncom 4 deploy, LDEF retrieval highlight 10-day Columbia flight
[NASA-NEWS-RELEASE-89-180] N90-13448
SPACECRAFT SHIELDING
Debris/ice/TPS assessment and photographic analysis for Shuttle Mission STS-34
[NASA-TM-102153] N90-13447
SPACECRAFT STABILITY
The dynamics and control of large flexible space structures - 12, supplement 11
[NASA-CR-185966] N90-13494
SPACECRAFT STRUCTURES
The Hipparcos Mission. Prelaunch status. Volume 1: The Hipparcos satellite
[ESA-SP-1111-VOL-1] N90-13499
The payload structure N90-13510
The spacecraft structure N90-13512
SPACECRAFT TEMPERATURE
Temperature dependence of attitude sensor coalignments on the Solar Maximum Mission (SMM) N90-13426
SPACECRAFT TRACKING
Automation of orbit determination functions for National Aeronautics and Space Administration (NASA)-supported satellite missions N90-13434
Optimum data weighting and error calibration for estimation of gravitational parameters N90-13437
SPACECRAFT TRAJECTORIES
Automation of orbit determination functions for National Aeronautics and Space Administration (NASA)-supported satellite missions N90-13434
Calculation of double-lunar swingby trajectories: I. Keplerian foundation N90-13435
The controllability of the aeroassist flight experiment atmospheric skip trajectory N90-13438
SPACECREWS
Functional decor in the International Space Station: Body orientation cues and picture perception
[NASA-TM-102242] N90-13931
SPALLING
Thermal barrier coating life prediction model development, phase 1
[NASA-CR-182230] N90-13388
SPATIAL DISTRIBUTION
Successive iterations of the input catalog N90-13534
Study of the hydroxyl radical by DRASC resonance in a high pressure flame — Diffusion Raman Anti-Stokes Coherence (DRASC)
[ONERA-RS-53/7131-PY] N90-13632
The relationship between subjective and objective measures of simulator-induced ataxia
[AD-A213095] N90-13922
Data structures for the representation and manipulation of polyhedrons
[IMAG-RR-772-M] N90-14042
SPATIAL FILTERING
Spatiotemporal characteristics of visual localization, phase 2
[AD-A212934] N90-13929
SPATIAL RESOLUTION
Effect of spatial resolution on apparent sensitivity to initial conditions of a decaying flow as it becomes turbulent
[NASA-TM-102377] N90-13719
Role of retinocortical processing in spatial vision
[AD-A210995] N90-13918
SPECIFICATIONS
Multi-level specification and verification of real-time software
[AD-A213227] N90-13975
ERIS: Engineering Resource Information System
[AD-A213357] N90-14144
SPECKLE PATTERNS
Practical systems for speckle velocimetry N90-13341
SPECTRA
Spectral study of a compressible isotropic turbulence
[ECL-88-16] N90-13753
The grand unified photon spectrum: A coherent view of the diffuse extragalactic background radiation
[NASA-CR-186077] N90-14180
SPECTRAL CORRELATION
Reexamination of data from the asteroid/meteoroid detector
[NASA-CR-185997] N90-14175
SPECTRAL REFLECTANCE
Physically-based parameterization of spatially variable soil and vegetation using satellite multispectral data
[NASA-CR-185957] N90-13879
SPECTROMETERS
Spectrometer technology recommendations N90-13468
Three-meter balloon-borne telescope N90-13490
SPECTROSCOPIC ANALYSIS
Study of the hydroxyl radical by DRASC resonance in a high pressure flame — Diffusion Raman Anti-Stokes Coherence (DRASC)
[ONERA-RS-53/7131-PY] N90-13632
Computational studies of structural and transport properties of amorphous solids
[ETN-90-96027] N90-13664
Novel in situ spectroscopic ellipsometer for real time analysis of CVD diamond films
[AD-A213218] N90-13762
SPECTROSCOPY
Ultrafast processes and spectroscopy with free electron lasers
[AD-A212889] N90-13773
Field-effect spectroscopy of interface states
[AD-A212998] N90-14112
SPECTRUM ANALYSIS
Spectral study of a compressible isotropic turbulence
[ECL-88-16] N90-13753
Neutral air turbulence in the middle and upper atmosphere observed during the MAC/EPSILON campaign N90-13855
Archival research on absorption lines in violently star-forming galaxies
[NASA-CR-185960] N90-14163
SPEECH RECOGNITION
Speech reception in quiet and in noisy conditions by individuals with noise-induced hearing loss in relation to their audiogram
[IZF-1989-11] N90-13692
Evaluation of speech intelligibility through a bone conduction stimulator
[AD-A212002] N90-13919
SPHERICAL SHELLS
Ring source/force excitation of axisymmetric shell structure
[ARE-TM(UHA)-88519] N90-14085
SPIN
COBE nonspinning attitude propagation N90-13418
SPIN GLASS
Energy barriers in SK spin-glass model
[PREPRINT-665] N90-14119

SPIN STABILIZATION
Orbit and attitude determination results during launch support operations for SBS-5
[PAPER-7] N90-13420
SPLINE FUNCTIONS
On the recurrence relation for multivariate B-splines with respect to dimension
[MEMO-786] N90-14017
Practice of bivariate quadratic simplicial splines
[MEMO-800] N90-14034
SPORADIC E LAYER
Enhanced electron density layers in the high-latitude lower ionosphere N90-13832
SPRAYED COATINGS
Evaluation of newly formulated Dow Corning 321 dry film lubricant
[NASA-CR-183628] N90-13661
SPREAD F
Auroral and sub-auroral interaction at the F region ionosphere
[AD-A213264] N90-13896
SQUEEZE FILMS
Elasticity effects on cavitation in a squeeze film damper undergoing noncentered circular whirl
[NASA-TM-102392] N90-13786
SQUID (DETECTORS)
Construction of a SQUID magnetometer for investigation of screening properties of high-T(sub c) superconductors
[FOA-C-20765-2.2] N90-13768
Analysis of an R-SQUID noise thermometer
[VTT-PUBL-54] N90-13769
STABILITY
LORAN C stability integrity assurance
[AD-A212663] N90-13364
Synchrotron-betatron parametric instability in free-electron lasers
[AD-A213373] N90-13777
The singular zero sum differential game with stability using H infinity control theory
[MEMO-COSOR-89-09] N90-13999
Stabilizability and detectability of discrete-time time-varying systems
[MEMO-COSOR-88-16] N90-14023
Continuity properties of one-parameter families of linear-quadratic problems without stability
[MEMO-COSOR-88-17] N90-14024
On the output-stabilizable subspace
[MEMO-COSOR-88-27] N90-14027
Another approach to the local disturbance decoupling problem with stability for nonlinear systems
[MEMO-799] N90-14033
On stability of queueing models of local area networks with slotted ring protocols
[MEMO-795] N90-14057
Optical properties monitor: Experiment definition phase
[NASA-CR-183836] N90-14092
STABILIZATION
The output-stabilizable subspace and linear optimal control
[MEMO-COSOR-89-15] N90-14001
STAGNATION FLOW
On catalytic recombination rates in hypersonic stagnation heat transfer N90-13338
STAGNATION POINT
Theory of stagnation point heat transfer in dissociated air N90-13337
STANDARDS
Considerations about the acceptance inspection of HS fasteners intended for controlled tightening
[CRIF-MT-175] N90-13806
Executive overview and introduction to the SMAP information system life-cycle and documentation standards
[NASA-TM-101765] N90-14134
Information system life-cycle and documentation standards, volume 1
[NASA-TM-101856] N90-14135
Management plan documentation standard and Data Item Descriptions (DID). Volume of the information system life-cycle and documentation standards, volume 2
[NASA-TM-101857] N90-14136
Product specification documentation standard and Data Item Descriptions (DID). Volume of the information system life-cycle and documentation standards, volume 3
[NASA-TM-101858] N90-14137
Assurance specification documentation standard and Data Item Descriptions (DID). Volume of the information system life-cycle and documentation standards, volume 4
[NASA-TM-101859] N90-14138
Management control and status reports documentation standard and Data Item Descriptions (DID). Volume of the information system life-cycle and documentation standards, volume 5
[NASA-TM-101860] N90-14139
STANDING WAVES
Influence of RF-parameters on beam lifetime
[NIKHEF-K/AMPS/89-06] N90-14091
STAR CLUSTERS
The Hipparcos Mission. Prelaunch status. Volume 2: The input catalog
[ESA-SP-1111-VOL-2] N90-13529
The choice of stars in open clusters N90-13542
STAR FORMATION
Orion B: Anatomy of a star-forming region N90-14155
STAR TRACKERS
Temperature dependence of attitude sensor coalignments on the Solar Maximum Mission (SMM) N90-13426
Operating principle N90-13500
The modulating grid N90-13505
The detectors N90-13507
The SN 1987A attitude control system N90-13845
STARS
From scientific proposals to the Inca data base N90-13530
The Inca data base N90-13531
The compilation of astrometric data N90-13537
Study of modern instrumentation and methods for astronomic positioning in the field
[AD-A213217] N90-14157
STATIC ELECTRICITY
Cable coupling lightning transient qualification
[NASA-CR-183826] N90-13405
STATIC TESTS
Static and free-vibrational response of semi-circular graphite-epoxy frames with thin-walled open sections
[NASA-CR-186097] N90-13800
STATISTICAL ANALYSIS
Study of the engine bird ingestion experience of the Boeing 737 aircraft
[DOT/FAA/CT-89/16] N90-13360
An introduction via vorticity dynamics and statistical theory --- turbulent shear flows N90-13731
Expected supernovae rates and gravitational waves detection
[NOTA-INTERNA-933] N90-14166
Des Clozeaux's law for strings and galaxies formation. Part 1: Abelian configurations
[ROM1F-89-681-PT-1] N90-14172
STATISTICAL DISTRIBUTIONS
Self-decomposable distributions and branching processes
[MEMO-COSOR-89-06] N90-14052
Note on Urbanik's class L(sub n) --- self-decomposability of functions
[MEMO-COSOR-89-07] N90-14053
Reverse self-decomposability --- for characteristic functions
[MEMO-COSOR-89-08] N90-14054
STATISTICAL MECHANICS
Statistical mechanics of strings and topology
[ROM1F-89-683] N90-14088
Where is an object before you look at it
[NOTA-INTERNA-935] N90-14123
STATISTICAL TESTS
Accuracy and characteristics of the Hipparcos catalog N90-13566
STATORS
Influence of vane sweep on rotor-stator interaction noise N90-13325
STEADY FLOW
Generalized similarity solutions for three dimensional, laminar, steady, compressible boundary layer flows on swept profile cylinders
[DLR-FB-89-34] N90-13725
STEELS
Experimental and numerical investigations of the crack arrest behavior of steels and cast iron materials
[MPA-TWB-88-03] N90-13635
STELLAR ENVELOPES
The winds of high luminosity late-type bright stars
[NASA-CR-182961] N90-14160
STELLAR FLARES
Analysis of coordinated observations of a giant stellar flare
[NASA-CR-185961] N90-14176
STELLAR LUMINOSITY
The winds of high luminosity late-type bright stars
[NASA-CR-182961] N90-14160
STELLAR MAGNITUDE
Proximity effects on adjacent and multiple stars N90-13533
STELLAR MOTIONS
Ground-based astrometric measurements N90-13536
STELLAR PARALLAX
Analysis of the image dissector tube data N90-13550
Analysis of the star mapper data N90-13551
On-ground attitude determination N90-13552
Astrometric parameter determination in FAST N90-13556
STELLAR RADIATION
Analysis of coordinated observations of a giant stellar flare
[NASA-CR-185961] N90-14176
STELLAR SPECTROPHOTOMETRY
New ground-based photometric measurements N90-13538
Standard stars and photometric calibration N90-13539
Double stars N90-13540
Variable stars N90-13541
STELLAR WINDS
The winds of high luminosity late-type bright stars
[NASA-CR-182961] N90-14160
STEREOPHOTOGRAPHY
The use of a deformation model for sampling digitalized stereoscopic images
[IMAG-RR-753-I] N90-13884
STIFFNESS
Field-effect spectroscopy of interface states
[AD-A212998] N90-14112
STIFFNESS MATRIX
Measuring of the complete stiffness matrix for anisotropic laminated materials
[DLR-MITT-89-11] N90-13806
Measuring of the complete stiffness matrix for anisotropic laminated materials
[DLR-MITT-89-12] N90-13807
STIMULANTS
The sensory transduction pathways in bacterial chemotaxis N90-13944
STIMULATION
Evaluation of speech intelligibility through a bone conduction stimulator
[AD-A212002] N90-13919
STOCHASTIC PROCESSES
Test network Delft
[ETN-90-98009] N90-13365
An autopilot design methodology for bank-to-turn missiles
[AD-A213379] N90-13399
Stochastic modelling of EM scattering from foliage
[AD-A213115] N90-13689
First-order Bragg SAR imagery of Kelvin wakes and moving internal wave fields
[AD-A213361] N90-13891
Why stochastic modeling is essential in analyzing interdicted transportation network performance
[AD-A213140] N90-14007
Large deviation estimates in the stochastic quantization of phi sub 2 exp 4
[PREPRINT-666] N90-14050
STOPPING
Stopping rules for a class of random methods for detecting necessary linear inequality constraints
[MEMO-777] N90-13977
On the safe approximation of PROLOG programs
[CWI-CS-R8913] N90-13978
STORAGE RINGS (PARTICLE ACCELERATORS)
Influence of RF-parameters on beam lifetime
[NIKHEF-K/AMPS/89-06] N90-14091
STRAIN GAGES
High temperature capacitive strain gage
[NASA-CR-4266] N90-13760
Development and characterization of PdCr temperature-compensated wire resistance strain gage
[NASA-CR-185153] N90-13761
STRAIN RATE
Anomalous strain rate dependence of the serrated flow in Ni-H and Ni-C-H alloys
[AD-A213244] N90-13641
A slow strain-rate tensile testing machine
[ARL-MAT-TM-399] N90-13764
The Fourth Oxford International Conference on the Mechanical Properties of Materials at High Rates of Strain
[AD-A212293] N90-13809
STRATEGY
Operating principle N90-13500
Electronic warfare: Reliable equipment needed to test Air Force's electronic warfare systems
[AD-A212952] N90-13687
STRATIFIED FLOW
The interaction and variation of waves and turbulence from MST radar data
[AD-A212849] N90-13906
STRATOSPHERE
Humidity local measurements in the middle atmosphere N90-13833
SOFIA (Stratospheric Observatory For Infrared Astronomy): A 3m class airborne telescope N90-13846
A double focusing mass-spectrometer for simultaneous ion measurements in the stratosphere N90-13848

Operational activity in France and a new method of balloon temperature piloting N90-13857
Long duration balloon flights in the middle stratosphere N90-13874
Observations of stratospheric HCl: 1975-1985 [AERONOMICA-ACTA-A-349-1989] N90-13892
The interaction and variation of waves and turbulence from MST radar data [AD-A212849] N90-13906
Meteorological atlas of the Northern Hemisphere lower stratosphere for January and February 1989 during the Airborne Arctic Stratospheric Expedition [NASA-TM-4145] N90-13908

STRESS (PHYSIOLOGY)
Adaptation and resistance of ecosystems to stress [AD-A212999] N90-13889

STRESS ANALYSIS
Probabilistic finite element analysis of dynamic structural response [AD-A213249] N90-13789
Stress intensity factors for cracking metal structures under rapid thermal loading. Volume 2: Theoretical background [AD-A213297] N90-13812
Mean stress and the exhaustion of fatigue-damage resistance [NASA-TM-101311] N90-13819
Application of fracture mechanics and half-cycle method to the prediction of fatigue life of B-52 aircraft pylon components [NASA-TM-8d277] N90-13820
Design and evaluation of a new biaxial testing method for sheet material (SUPERBAT) [LR-548] N90-13824

STRESS CORROSION
Mechanical property characterization of VascoMax T-300 [AD-A212950] N90-13837

STRESS INTENSITY FACTORS
Stress intensity factors for cracking metal structures under rapid thermal loading. Volume 2: Theoretical background [AD-A213297] N90-13812
Unified model of charge build up and annealing of oxide charge and interface states in SiO2 due to stress [HMI-B-465] N90-14120

STRESS-STRAIN RELATIONSHIPS
Anomalous strain rate dependence of the serrated flow in Ni-H and Ni-C-H alloys [AD-A213244] N90-13641
The Fourth Oxford International Conference on the Mechanical Properties of Materials at High Rates of Strain [AD-A212293] N90-13809

STRING THEORY
Scaling in a non Abelian string network [ROM1F-89-676] N90-14066
Configurational statistics of strings, fractals and polymer physics. Part 2: Non Abelian strings [ROM1F-89-680-PT-2] N90-14067
Statistical mechanics of strings and topology [ROM1F-89-683] N90-14068
Observational physics of mirror world [NASA-CR-185923] N90-14076
String correlations and galaxies formation [ROM1F-89-677] N90-14170
Non Abelian string correlations and galaxies formation [ROM1F-89-678] N90-14171
Des Cloizeaux's law for strings and galaxies formation. Part 1: Abelian configurations [ROM1F-89-681-PT-1] N90-14172
Des Cloizeaux's law for strings and galaxies formation. Part 2: Non Abelian configurations [ROM1F-89-682-PT-2] N90-14173

STRUCTURAL ANALYSIS
Constitutive modeling for isotropic materials (HOST) [NASA-CR-179522] N90-13390
Constitutive modeling for isotropic materials (HOST) [NASA-CR-174718] N90-13391
Composite panel development at JPL N90-13458
Control of optical systems N90-13484
Hybrid deployable support truss designs for LDR N90-13485
Effects of joints in truss structures N90-13486
RSRM nozzle fixed housing cooldown test [NASA-CR-183741] N90-13587
Measuring of the complete stiffness matrix for anisotropic laminated materials [DLR-MITT-89-11] N90-13606
Measuring of the complete stiffness matrix for anisotropic laminated materials [DLR-MITT-89-12] N90-13607
Fiber reinforced cementitious composites technology [PB89-227813] N90-13608
Magneto-elastic interactions in conducting structures in transient magnetic fields N90-13686
Probabilistic finite element analysis of dynamic structural response [AD-A213249] N90-13789
Mobility power flow analysis of an L-shaped plate structure subjected to acoustic excitation [NASA-CR-186130] N90-13817
The computational structural mechanics testbed user's manual [NASA-TM-100644] N90-13818

STRUCTURAL BASINS
Late quaternary geomorphology of the Great Salt Lake region, Utah, and other hydrographically closed basins in the western United States: A summary of observations [NASA-CR-185912] N90-13878

STRUCTURAL DESIGN
Efficient methods for integrated structural-aerodynamic wing optimum design N90-13376
Development of an advanced fan blade containment system [DOT/FAA/CT-89/20] N90-13386
Aeroelastic control of composite lifting surfaces: Integrated aeroelastic control optimization N90-13396
Cryogenic systems for the large deployable reflector N90-13470
LDR structural technology activities at JPL N90-13488
Joints in deployable space truss structures N90-13489
Space Station Engineering Design Issues [NASA-CR-185978] N90-13492
Kinematics and control of manipulation robots [WTHD-187] N90-13803

STRUCTURAL ENGINEERING
The adhesive bonding of thermoplastic composites [AD-A213358] N90-13805

STRUCTURAL RELIABILITY
The Fourth Oxford International Conference on the Mechanical Properties of Materials at High Rates of Strain [AD-A212293] N90-13809

STRUCTURAL STABILITY
Space telescope pointing control N90-13454
Comparison of analytical methods for calculation of wind loads [NASA-TM-102782] N90-13813

STRUCTURAL STRAIN
Strain accumulation and surface deformation along the San Andreas, California [NASA-CR-185893] N90-13894

STRUCTURAL VIBRATION
Pointing control for LDR N90-13453
Static and free-vibrational response of semi-circular graphite-epoxy frames with thin-walled open sections [NASA-CR-186097] N90-13600
Probabilistic finite element analysis of dynamic structural response [AD-A213249] N90-13789
Investigation of difficult component effects on finite element model vibration prediction for the Bell AG-1G helicopter. Volume 2: Correlation results [NASA-CR-181916-VOL-2] N90-13814

SUBGROUPS
On distance-transitive graphs and involutions [CWI-PM-R8808] N90-14037

SUBROUTINE LIBRARIES (COMPUTERS)
Extended memory library for AFOS (Automation of Field Operations and Services) applications [PB89-230858] N90-14147

SUBROUTINES
FORTRAN subroutines for the evaluation of the confluent hypergeometric functions [AD-A213308] N90-14012

SUBSONIC FLOW
Effect of suction and cooling on the stability of subsonic and supersonic boundary layers N90-13745

SUBSTRUCTURES
The spacecraft structure N90-13512

SUCTION
Effect of suction and cooling on the stability of subsonic and supersonic boundary layers N90-13745

SULFUR DIOXIDES
Computational solution of chemistry problems [NASA-CR-186000] N90-13618
Air quality simulation model performance for one-hour averages [PB89-233506] N90-13890

SUMMARIES
A summary of 30 years of space launches [AERONOMICA-ACTA-F-39-1989] N90-13411

SUMMER
Observation of wind corners in the middle atmosphere over Andenes (69 N) during winter 1983/84, summer 1987 and summer 1988 N90-13836

SUPERCONDUCTING FILMS
Microwave microstrip resonator measurements of Y1Ba2Cu3O(7-x) and Bi2Sr2Ca1Cu2O(8-y) thin films [NASA-TM-102159] N90-13704

SUPERCONDUCTING MAGNETS
Surface cooled, vacuum impregnated superconducting magnet systems: Design, construction, applications [ETN-90-96014] N90-14072

SUPERCONDUCTING SUPER COLLIDER
Exotic Higgs production at e+e- colliders [PREPRINT-671] N90-14088

SUPERCONDUCTIVITY
Surfaces and interfaces of ceramic materials [AD-A212417] N90-13657
Joint Services Electronics Program [AD-A213015] N90-13699

SUPERCONDUCTORS
Joint Services Electronics Program [AD-A213015] N90-13699

SUPERCRITICAL FLOW
Analysis of experimental data for CAST 10-2/DOA 2 supercritical airfoil at low Reynolds numbers and application to high Reynolds number flow [AD-A211654] N90-13326

SUPERFLUIDITY
Construction of the rotating cryostat ROTA2, its use for zero sound experiments in (3)He-B, and calculations of ion mobility in (3)He-A and (3)He-P [ISBN-952-90091-3-5] N90-13765

SUPERHETERODYNE RECEIVERS
Far-infrared heterodyne receivers N90-13485
Advances in SIS receiver technology N90-13486

SUPERNOVA REMNANTS
Detectable gravitational waves by supernova SN 1987 A pulsar relic [PREPRINT-656] N90-14174

SUPERNOVA 1987A
The SN 1987A attitude control system N90-13845
Project Supernova 1987 N90-13866
SN 1987: A telemetry decoding system N90-13875
Correlation among gravitational wave and neutrino detectors data during SN1987A [NOTA-INTERNA-932] N90-14165

SUPERNOVAE
Expected supernovae rates and gravitational waves detection [NOTA-INTERNA-933] N90-14166
Detectable gravitational waves by supernova SN 1987 A pulsar relic [PREPRINT-656] N90-14174

SUPERSONIC BOUNDARY LAYERS
Effect of suction and cooling on the stability of subsonic and supersonic boundary layers N90-13745

SUPERSONIC COMBUSTION
Numerical solutions of the complete Navier-Stokes equations [NASA-CR-186102] N90-13747

SUPERSONIC CRUISE AIRCRAFT RESEARCH
Study of high-speed civil transports [NASA-CR-4235] N90-13370

SUPERSONIC FLOW
Hot and cold wire applications in supersonic flows: Introductory notes N90-13343
Laser applications in supersonic unsteady flow N90-13344
Computation of Navier-Stokes equations for three-dimensional flow separation [NASA-TM-102268] N90-13353
Application of a two-dimensional unsteady viscous analysis code to a supersonic throughflow fan stage [NASA-TM-4141] N90-13387
Generation of iodine monofluoride in a supersonic multipurpose flowtube facility [AD-A213082] N90-13774

SUPERSONIC NOZZLES
Gas flows in rocket motors, volume 1 [AD-A213348] N90-13591

SUPERSONIC TRANSPORTS
Study of high-speed civil transports [NASA-CR-4235] N90-13370

SURFACE DEFECTS
Surfaces and interfaces of ceramic materials [AD-A212417] N90-13657
Study of surface uniformity of semiconductors 3 to 5 by photoluminescence imagery [ECL-88-15] N90-14116

SURFACE FINISHING
Lightweight composite reflector panels N90-13482
Evaluation of copper slag blast media for railcar maintenance [NASA-CR-183744] N90-13881
GaAs and GaAs:In: Influence of surface treatments and characterization of homogeneity by photoluminescent imagery [ECL-88-24] N90-14118

SURFACE PROPERTIES
Coherent phasing of segmented mirrors N90-13474
Characterization of surfaces cut with a laser beam and thermal model of the process
[ISAL-89-0008] N90-13780
Senegalese land surface change analysis and biophysical parameter estimation using NOAA AVHRR spectral data
[NASA-CR-186120] N90-13883
Study of surface uniformity of semiconductors 3 to 5 by photoluminescence imagery
[ECL-88-15] N90-14116
SURFACE ROUGHNESS
Convective heat transfer measurements from a NACA 0012 airfoil in flight and in the NASA Lewis Icing Research Tunnel
[NASA-TM-102448] N90-13750
SURVIVAL
The human factors relating to escape and survival from helicopters ditching in water
[AGARD-AG-305(E)] N90-13358
SWEDISH SPACE PROGRAM
The Swedish sounding rocket and balloon program N90-13830
SWEPT WINGS
Generalized similarity solutions for three dimensional, laminar, steady, compressible boundary layer flows on swept profile cylinders
[DLR-FB-89-34] N90-13725
Navier-Stokes simulation of the crossflow instability in swept-wing flows
[NASA-CR-186122] N90-13744
SWIMMING
Free swimming organisms: Microgravity as an investigative tool N90-13949
SWINGBY TECHNIQUE
Calculation of double-lunar swingby trajectories: I. Keplerian foundation N90-13435
SWITCHING
Apparatus for cooling electronic components in aircraft
[AD-D014207] N90-13373
Studies of structure and switching dynamics in ferroelectric crystal and liquid crystal thin films
[AD-A212650] N90-14109
SWITCHING CIRCUITS
Contribution to the study of a self-protected static switch and its command strategy
[ECL-89-002] N90-13711
A prototype microprocessor based audiometer for use by the CF (Canadian Forces) medical services for periodic hearing tests
[AD-A212990] N90-13921
Studies of structure and switching dynamics in ferroelectric crystal and liquid crystal thin films
[AD-A212650] N90-14109
SYMMETRY
The algebraic Riccati equation and singular optimal control
[MEMO-COSOR-88-31] N90-14028
R-matrices and higher Poisson brackets for integrable systems
[PREPRINT-669] N90-14069
SYNCHRONOUS SATELLITES
Inexpensive global location and tracking systems using geostationary satellites
[AD-A213025] N90-13498
SYNCHROTRONS
Synchrotron-betatron parametric instability in free-electron lasers
[AD-A213373] N90-13777
SYNCOM SATELLITES
Syncom 4 deploy, LDEF retrieval highlight 10-day Columbia flight
[NASA-NEWS-RELEASE-89-180] N90-13448
SYNTAX
Database interfaces on NASA's heterogeneous distributed database system
[NASA-CR-185420] N90-14133
SYNTHETIC APERTURE RADAR
First-order Bragg SAR imagery of Kelvin wakes and moving internal wave fields
[AD-A213361] N90-13691
Development of a traveling wave tube for the project X-SAR. Construction and testing of a breadboard model
[ETN-90-95900] N90-13713
SYNTHETIC RESINS
A literature survey of inherently conducting polymers
[FOA-C-20763-2.4] N90-13668
SYNTHETIC RUBBERS
Effects of tacky mat contamination on bond degradation for Chemlok/liner and NBR/liner bonds
[NASA-CR-183742] N90-13653
SYSTEM EFFECTIVENESS
A new view of weapon system reliability and maintainability: Executive summary
[AD-A213282] N90-13383
SYSTEM FAILURES
Sufficiency and necessity in reliability modeling
[NASA-CR-186119] N90-13706
SYSTEM IDENTIFICATION
Control of optical systems N90-13484
LDR structural technology activities at JPL N90-13488
Stabilizability and detectability of discrete-time time-varying systems
[MEMO-COSOR-88-16] N90-14023
On the output-stabilizable subspace
[MEMO-COSOR-88-27] N90-14027
SYSTEMS ANALYSIS
Spacelab system analysis: The modified free access protocol: An access protocol for communication systems with periodic and Poisson traffic
[NASA-CR-183805] N90-13497
Research on the controllability of integrated circuits by means of electron beams
[ETN-90-95710] N90-13708
Micro-based fact collection tool user's manual
[NASA-CR-180414] N90-13981
An artificial intelligence approach to analog system diagnosis
[AD-A213135] N90-13992
Analysis of three approaches to qualitative simulation
[MEMO-INF-89-32] N90-14035
On a new integrable Hamiltonian system with nearest neighbors interaction
[PREPRINT-667] N90-14043
Nucleon polarizabilities in the constituent quark model
[NOTA-INTERNA-936] N90-14082
Empirical analysis and refinement of expert system knowledge bases
[AD-A213240] N90-14143
SYSTEMS ENGINEERING
Discretization and model reduction for a class of nonlinear systems N90-13397
Advanced actuation systems development, volume 2
[AD-A213378] N90-13398
Space Station Engineering Design Issues
[NASA-CR-185978] N90-13492
The Hipparcos Mission. Prelaunch status. Volume 1: The Hipparcos satellite
[ESA-SP-1111-VOL-1] N90-13499
The payload structure N90-13510
The spacecraft structure N90-13512
Space Transportation Engine Program (STEP). Phase B: Project study and management plan-ingredients for STEP success
[NASA-CR-183770] N90-13585
Resistive fuses: Analog hardware for detecting discontinuities in early vision
[AD-A211891] N90-13696
On control of manipulators
[ISBN-90-9002789-0] N90-13804
The problem of automation: Inappropriate feedback and interaction, not overautomation
[NASA-CR-186126] N90-13994
On the output-stabilizable subspace
[MEMO-COSOR-88-27] N90-14027
SYSTEMS INTEGRATION
STOVL aircraft simulation for integrated flight and propulsion control research
[NASA-TM-102419] N90-13389
Space station gas compressor technology study program, phase 1
[NASA-CR-183758] N90-13491
User needs, benefits, and integration of robotic systems in a space station laboratory
[NASA-CR-185150] N90-13794
SYSTEMS MANAGEMENT
Information system life-cycle and documentation standards, volume 1
[NASA-TM-101856] N90-14135
Management plan documentation standard and Data Item Descriptions (DID). Volume of the information system life-cycle and documentation standards, volume 2
[NASA-TM-101857] N90-14136
Product specification documentation standard and Data Item Descriptions (DID). Volume of the information system life-cycle and documentation standards, volume 3
[NASA-TM-101858] N90-14137
SYSTEMS SIMULATION
An accurate timing model for fault simulation in MOS circuits
[AD-A213153] N90-13702
Efficient on-line simulations of tree machines and multidimensional turing machines by random access machines
[AD-A213152] N90-13960

T

TARGET RECOGNITION
Efficient detection of small moving objects
[AD-A213314] N90-13690
Compensatory tracking in disturbance tasks and target following tasks. The influence of cockpit motion on performance and control behavior
[LR-511] N90-13933
TARGETS
Analytical derivation and verification of zero-gyro control for the IUE satellite
[NASA-TM-100748] N90-13767
Spatiotemporal characteristics of visual localization, phase 2
[AD-A212934] N90-13929
Some quick and efficient methods for bearing-only target motion analysis
[IMAG-RR-762-M] N90-14049
TASKS
Ada task scheduling: A focused Ada investigation
[NASA-CR-186072] N90-13967
TECHNOLOGY ASSESSMENT
LORAN C stability integrity assurance
[AD-A212663] N90-13364
Study of high-speed civil transports
[NASA-CR-4235] N90-13370
Introduction to the report of the Asilomar 3 LDR workshop N90-13450
Preliminary experiments on filament winding nylon impregnated glass fibers (FIT)
[LR-545] N90-13669
TECHNOLOGY TRANSFER
Centers for the commercial development of space
[NASA-PAM-525] N90-14151
NASA commercial programs
[NASA-TM-101853] N90-14152
TECHNOLOGY UTILIZATION
Aircraft propulsion: Leading the way in aviation
[LR-532] N90-13395
Large heavy duty balloons in Europe N90-13858
Centers for the commercial development of space
[NASA-PAM-525] N90-14151
NASA commercial programs
[NASA-TM-101853] N90-14152
TELECOMMUNICATION
Data handling and telecommunications N90-13514
Optical communication with semiconductor laser diode
[NASA-CR-185886] N90-13770
TELEMETRY
The role of the ground segment N90-13527
The interface with the data reduction consortia N90-13528
SN 1987: A telemetry decoding system N90-13875
TELEOPERATORS
Performance evaluation of a six-axis generalized force-reflecting teleoperator
[NASA-CR-186106] N90-13796
The SN 1987A attitude control system N90-13845
TELESCOPES
A laboratory verification sensor N90-13477
SiO overcoating and polishing of CFRP telescope panels N90-13478
Three-meter balloon-borne telescope N90-13490
SOFIA (Stratospheric Observatory For Infrared Astronomy): A 3m class airborne telescope N90-13846
TEMPERATURE CONTROL
Payload thermal control N90-13511
Spacecraft thermal control N90-13513
TEMPERATURE DEPENDENCE
Temperature dependence of attitude sensor coalignments on the Solar Maximum Mission (SMM) N90-13426
Ultraviolet absorption cross-sections of bromoform in the temperature range 295-240 K
[AERONOMICA-ACTA-A-348-1989] N90-13630
TEMPERATURE DISTRIBUTION
Payload electronics and mechanisms N90-13508
Payload thermal control N90-13511
TEMPERATURE EFFECTS
Large Deployable Reflector (LDR) thermal characteristics N90-13460
Mechanical and thermal testing N90-13521
QM-6 field joint protection system, volume 7
[NASA-CR-183748] N90-13586
Thermal barrier coatings for gas turbine and diesel engines
[NASA-TM-102408] N90-13636
The effects of alloying and thermal factors on the solidification and mechanical properties of gray iron
[VTT-619] N90-13651
Effect of suction and cooling on the stability of subsonic and supersonic boundary layers N90-13745
TEMPERATURE MEASUREMENT
Payload thermal control N90-13511

Spacecraft thermal control N90-13513
Evidence for accurate temperatures from the inflatable falling sphere N90-13835
Near-mesopause temperatures at 69 N latitude in late summer N90-13837
Resonance cone diagnostics in the mid-latitude ionosphere N90-13840
Operational activity in France and a new method of balloon temperature piloting N90-13857

TEMPERATURE MEASURING INSTRUMENTS
Low speed hot and cold wire techniques for unsteady flow N90-13342
Silicon-etalon fiber-optic temperature sensor [NASA-TM-102389] N90-13381

TEMPERATURE PROFILES
Near-mesopause temperatures at 69 N latitude in late summer N90-13837

TEMPLATES
Database interfaces on NASA's heterogeneous distributed database system [NASA-CR-185420] N90-14133

TENSILE PROPERTIES
Fiber reinforced cementitious composites technology [PB89-227813] N90-13608
Mechanical property characterization of VascoMax T-300 [AD-A212950] N90-13637

TENSILE STRENGTH
Contamination removal using various solvents and methodologies [NASA-CR-183747] N90-13652

TENSILE TESTS
Constitutive modeling for isotropic materials (HOST) [NASA-CR-179522] N90-13390
A slow strain-rate tensile testing machine [ARL-MAT-TM-399] N90-13764

TERRAIN ANALYSIS
Reflection indicatrices of natural surfaces for AVHRR channels 1 and 2 [DLR-MITT-89-16] N90-13882

TEST FACILITIES
Dynamic testing techniques and applications for an aeroelastic rotor test facility N90-13406

TEST FIRING
QM-8 field joint protection system, volume 7 [NASA-CR-183748] N90-13586

TETHERED SATELLITES
Shuttle relative navigation of a tethered satellite mission with current on board software N90-13423
Impact of tether cutting on onboard navigation during the Tethered Satellite Mission-1 N90-13424
Shuttle tethered operations: The effect on orbital trajectory and inertial navigation N90-13425

TETHERLINES
Impact of tether cutting on onboard navigation during the Tethered Satellite Mission-1 N90-13424

THAILAND
Applied atmospheric resources research program in Thailand [PB89-235402] N90-13903

THEMATIC MAPPING
Overview of the Hipparcos payload N90-13503
The detectors N90-13507
Standard stars and photometric calibration N90-13539
Analysis of the star mapper data N90-13551
Photometry: Main mission and Tycho N90-13560
Experiments towards a global sphere solution N90-13576
Summaries of the thematic conferences on remote sensing for exploration geology [NASA-CR-185321] N90-13880
The use of LANDSAT-TM data for the management of pine forestations in central Chile [DLR-FB-89-44] N90-13881

THEOREM PROVING
Linear groups and distance-transitive graphs [CWI-PM-R8805] N90-14036
On distance-transitive graphs and involutions [CWI-PM-R8808] N90-14037

THEOREMS
Extension to Eulers's theorem to n-dimensional spaces N90-13431
A new model for the structure of silica glass [AD-A212972] N90-13659
The totally singular linear quadratic problem with indefinite cost [MEMO-COSOR-89-05] N90-13998
Inductive reasoning and Kolmogorov complexity (preliminary version) [CWI-CS-R8915] N90-14062

THEORETICAL PHYSICS
Aspects of the physics of the standard model [PREPRINT-670] N90-14087

THERMAL ANALYSIS
Large Deployable Reflector (LDR) thermal characteristics N90-13460
Feature modeling: The incorporation of a front and eddy map into optimum interpolation-based thermal analysis [AD-A213253] N90-13914

THERMAL CONDUCTIVITY
Metal transfer in gas metal arc welding [AD-A213390] N90-13642

THERMAL CONTROL COATINGS
Thermal barrier coating life prediction model development, phase 1 [NASA-CR-182230] N90-13388
Thermal barrier coatings for gas turbine and diesel engines [NASA-TM-102408] N90-13636

THERMAL EXPANSION
Status of Gr/glass composites technology at UTOS N90-13459
Advanced composite materials for precision segmented reflectors N90-13461

THERMAL PROTECTION
Debris/ice/TPS assessment and photographic analysis for Shuttle Mission STS-34 [NASA-TM-102153] N90-13447
Thermal protection systems for reentry and hypersonic flight [DLR-MITT-89-14] N90-13577
QM-8 field joint protection system, volume 7 [NASA-CR-183748] N90-13586

THERMAL RADIATION
Interaction of radiation with matter: Atomic collision processes occurring in the presence of radiation fields [AD-A213112] N90-14078

THERMAL RESISTANCE
Mechanical and thermal testing N90-13521

THERMAL STABILITY
Report of the Asilomar 3 LDR Workshop [NASA-CR-184656] N90-13449
Status of Gr/glass composites technology at UTOS N90-13459
Advanced composite materials for precision segmented reflectors N90-13461
Payload thermal control N90-13511
Spacecraft thermal control N90-13513

THERMAL STRESSES
Stress intensity factors for cracking metal structures under rapid thermal loading. Volume 2: Theoretical background [AD-A213297] N90-13812

THERMAL VACUUM TESTS
On-ground photometric calibration N90-13523

THERMIONIC CONVERTERS
True asymptotic plasma-sheath matching with an asymptotically correct collisional presheath [AD-A212857] N90-14104

THERMIONIC POWER GENERATION
True asymptotic plasma-sheath matching with an asymptotically correct collisional presheath [AD-A212857] N90-14104

THERMOCHEMISTRY
Evaluation of selected computer models for modeling pyrotechnic and propellant devices [AD-A213003] N90-13671
Thermochemical calculations with inert compounds [FOA-C-20759-2.1] N90-13677
CANOES 2: Dynamics of atmospheric infrared thermochemical excitation, volume 3 [AD-A213343] N90-13899

THERMOCOUPLES
Thin-film sensors for reusable space propulsion systems [NASA-TM-102383] N90-13595

THERMODYNAMIC EQUILIBRIUM
Unitarity limits on the mass and radius of dark matter particles [NASA-CR-186079] N90-14164

THERMODYNAMIC PROPERTIES
The application of cast SiC/Al to rotary engine components [NASA-CR-179610] N90-13385
Large Deployable Reflector (LDR) thermal characteristics N90-13460
Low temperature optical testing of CFRP telescope panels N90-13463
Thin-film sensors for reusable space propulsion systems [NASA-TM-102383] N90-13595
Thermodynamic properties of some metal oxide-zirconia systems [NASA-TM-102351] N90-13666

THERMOMETERS
Analysis of an R-SQUID noise thermometer [VTT-PUBL-54] N90-13769

THERMOPHYSICAL PROPERTIES
Thermophysical properties of buta-1,3-diene [ESDU-89005] N90-13619

THERMOPLASTIC RESINS
The adhesive bonding of thermoplastic composites [AD-A213358] N90-13605
Impact tests on aluminum 2024 T3, aramid and glass reinforced aluminum laminates and thermoplastic composites [LR-534] N90-13613
Crosslinkable polymer [GB-PATENT-2-205-846-A] N90-13663

THERMOPLASTICITY
The adhesive bonding of thermoplastic composites [AD-A213358] N90-13605

THERMOREGULATION
Measurement of mechanical work and energy expenditure in running and bicycling N90-13935

THERMOSPHERE
Neutral air turbulence in the middle and upper atmosphere observed during the MAC/EPSILON campaign N90-13855

THIN FILMS
Thin-film sensors for reusable space propulsion systems [NASA-TM-102383] N90-13595
Evaluation of newly formulated Dow Corning 321 dry film lubricant [NASA-CR-183828] N90-13661
Microwave microstrip resonator measurements of Y1Ba2Cu3O(7-x) and Bi2Sr2Ca1Cu2O(8-y) thin films [NASA-TM-102159] N90-13704
Studies of structure and switching dynamics in ferroelectric crystal and liquid crystal thin films [AD-A212650] N90-14109

THIN WALLED SHELLS
General buckling tests with thin-walled shells [DLR-MITT-89-13] N90-13816

THREE AXIS STABILIZATION
Analysis of the star mapper data N90-13551

THREE DIMENSIONAL BODIES
Comparison of integral and finite-difference methods for predicting the turbulent boundary layer on axisymmetric bodies [ARE-TM(UHA)-88512] N90-13752

THREE DIMENSIONAL BOUNDARY LAYER
Numerical simulation of transition in three-dimensional boundary layers [DLR-FB-89-12] N90-13728

THREE DIMENSIONAL FLOW
Multigrid calculations of 3-D turbulent viscous flows [NASA-CR-185154] N90-13323
Computation of viscous incompressible flows [NASA-TM-101090] N90-13329
Block-structured solution of three-dimensional transonic flows using parallel processing [AD-A212851] N90-13330
Measurement Techniques in Aerodynamics [VKI-LS-1989-05] N90-13339
Practical systems for speckle velocimetry N90-13341
Recent progress in research pertaining to estimates of gas-side heat transfer in an aircraft gas turbine [NASA-TM-102460] N90-13394
A three-dimensional potential flow analysis of dynamic fluid forces acting on a whirling centrifugal impeller bounded by a volute N90-13717
Calculation of flow fields by the solution of the Euler equations using an extended finite volume discretization scheme [DLR-FB-89-38] N90-13729
Application of two-point closures to subgrid scale modeling for homogeneous, 3D turbulence N90-13732
Inviscid 3D solution methods N90-13736
Pressure correction calculation procedures for 3D viscous flow N90-13738
Three D flows in turbine blade rows N90-13739
Model and computation of three-dimensional turbulent jets in a crossflow [ECL-89-007] N90-13755
On the topology of three-dimensional viscous flow structures near a plane wall. A classification and non-hyperbolic singularities on the wall [LR-541] N90-13758

THREE DIMENSIONAL MODELS
Navier-Stokes simulation of the crossflow instability in swept-wing flows [NASA-CR-186122] N90-13744
Interface between MEDUSA and GIFTS for shell structures [LR-553] N90-13985

THRUST VECTOR CONTROL
Aerodynamics of thrust vectoring [NASA-CR-185074] N90-13354

THUNDERSTORMS
A collection of papers related to heavy precipitation forecasting
[PB89-230833] N90-13910
TILT ROTOR AIRCRAFT
A CFD study of tilt rotor flowfields
[NASA-CR-186116] N90-13349
TILTING ROTORS
A CFD study of tilt rotor flowfields
[NASA-CR-186116] N90-13349
TIME
An accurate timing model for fault simulation in MOS circuits
[AD-A213153] N90-13702
TIME OPTIMAL CONTROL
The cellular approach: A new method to speed up simulated annealing for macro placement
[MEMO-COSOR-88-29] N90-13980
TIME SHARING
Waiting times in polling systems with Markovian server routing
[CWI-BS-R8905] N90-13969
Workloads and waiting times in single-server systems with multiple customer classes
[CWI-BS-R8906] N90-14020
Simple appoximations for second moment characteristics of the sojurn time in the M/G/1 processor sharing queue
[CWI-BS-R8907] N90-14055
TIME TEMPERATURE PARAMETER
Gravimetric measurements of materials outgassing applied to graphite-epoxy laminates
[NASA-TM-100753] N90-13609
TITANIUM
Wear-resistant coated object
[EP-PATENT-0-289-173-A1] N90-13643
TITANIUM ALLOYS
The effect of composition and aging treatment on the microstructure and mechanical properties of aluminum-lithium-titanium alloys
[AD-A213144] N90-13640
Threshold for fatigue crack propagation
[DLR-FB-89-33] N90-13815
TITANIUM BORIDES
Toughening of a particulate-reinforced/ceramic-matrix composite
[AD-A213180] N90-13604
TITANIUM NITRIDES
Wear-resistant coated object
[EP-PATENT-0-289-173-A1] N90-13643
TOLERANCES (PHYSIOLOGY)
Generation of free radicals during cold injury and rewarming
[AD-A213088] N90-13915
TOLLMIEN-SCHLICHTING WAVES
Multiple paths to subharmonic laminar breakdown in a boundary layer
[NASA-CR-181948] N90-13722
TOPOLOGY
On the topology of three-dimensional viscous flow structures near a plane wall. A classification and non-hyperbolic singularities on the wall
[LR-541] N90-13758
Scaling in a non Abelian string network
[ROM1F-89-676] N90-14066
Configurational statistics of strings, fractals and polymer physics. Part 2: Non Abelian strings
[ROM1F-89-680-PT-2] N90-14067
Statistical mechanics of strings and topology
[ROM1F-89-683] N90-14068
Some aspects of curvature in general relativity N90-14122
On thick domain walls in general relativity
[NASA-CR-185926] N90-14124
TORPEDOES
Real time image enhancement during underwater recovery operations
[AD-A213139] N90-14097
TORQUE
Autonomous spacecraft attitude control using magnetic torquing only N90-13415
TORSION
Initial test results for the mini-mast N90-13482
TORUSES
Non Abelian string correlations and galaxies formation
[ROM1F-89-678] N90-14171
TOUGHNESS
Toughening of a particulate-reinforced/ceramic-matrix composite
[AD-A213180] N90-13604
TOXICITY
Recovery of particle size distribution of ultrafine aerosols from diffusional decay measurements
[AD-A213006] N90-13621
Novel carbamates, their production and their use as fuels additives
[EP-PATENT-0-298-636-A-1] N90-13676
Adaptation and resistance of ecosystems to stress
[AD-A212999] N90-13889
TOXINS AND ANTITOXINS
Recovery of particle size distribution of ultrafine aerosols from diffusional decay measurements
[AD-A213006] N90-13621
TRACE ELEMENTS
A high-resolution atlas of the infrared spectrum of the Sun and the Earth atmosphere from space: A compilation of ATMOS spectra of the region from 650 to 4800 cm (2.3 to 16 micron). Volume 1: The Sun
[NASA-RP-1224-VOL-1] N90-13893
TRACKING (POSITION)
Inexpensive global location and tracking systems using geostationary satellites
[AD-A213025] N90-13498
Electronic warfare: Reliable equipment needed to test Air Force's electronic warfare systems
[AD-A212952] N90-13687
Compensatory tracking in disturbance tasks and target following tasks. The influence of cockpit motion on performance and control behavior
[LR-511] N90-13933
TRADEOFFS
Space station gas compressor technology study program, phase 1
[NASA-CR-183758] N90-13491
TRAJECTORY ANALYSIS
Shuttle relative navigation of a tethered satellite mission with current on board software N90-13423
Impact of tether cutting on onboard navigation during the Tethered Satellite Mission-1 N90-13424
Some quick and efficient methods for bearing-only target motion analysis
[IMAG-RR-762-M] N90-14049
TRAJECTORY CONTROL
Shuttle tethered operations: The effect on orbital trajectory and inertial navigation N90-13425
TRAJECTORY MEASUREMENT
Some quick and efficient methods for bearing-only target motion analysis
[IMAG-RR-762-M] N90-14049
TRAJECTORY OPTIMIZATION
Trajectory optimization and guidance for an aerospace plane
[NASA-CR-185884] N90-13389
Shuttle tethered operations: The effect on orbital trajectory and inertial navigation N90-13425
Optimal trajectories for the Aeroassisted Flight Experiment. Part 1: Equations of motion in an Earth-fixed system
[NASA-CR-186134] N90-13441
Optimal trajectories for the Aeroassisted Flight Experiment. Part 2: Equations of motion in an inertial system
[NASA-CR-186135] N90-13442
Optimal trajectories for the aeroassisted flight experiment, 1988-89
[NASA-CR-186132] N90-13443
TRANSCONDUCTANCE
The sensory transduction pathways in bacterial chemotaxis N90-13944
TRANSFER ORBITS
GOES-I/M ascent maneuvers from transfer orbit to station N90-13421
Optimal trajectories for the Aeroassisted Flight Experiment. Part 1: Equations of motion in an Earth-fixed system
[NASA-CR-186134] N90-13441
Optimal trajectories for the Aeroassisted Flight Experiment. Part 2: Equations of motion in an inertial system
[NASA-CR-186135] N90-13442
Optimal trajectories for the aeroassisted flight experiment, 1988-89
[NASA-CR-186132] N90-13443
The apogee boost motor N90-13517
Launch and early orbit N90-13524
TRANSFERRING
Model system studies with a phase separated membrane bioreactor N90-13954
Fermentation and oxygen transfer in microgravity N90-13958
TRANSFORMATIONS (MATHEMATICS)
Program transformation with abstract relation algebras
[AD-A213270] N90-14011
Description and manipulation of convex polygons using polarity
[IMAG-RR-771-M] N90-14041
TRANSIENT OSCILLATIONS
Analysis of new phenomena in shear flow of non-Newtonian fluids
[AD-A212893] N90-13721
TRANSIENT RESPONSE
A transient response method for linear coupled substructures
[NASA-TP-2926] N90-13444
TRANSITION PROBABILITIES
Further observations of rotationally excited far infrared OH16 and OH18 emission in Orion-KL: Tighter constraints on the nature of the emitting region
[NASA-CR-186004] N90-14156
TRANSLATIONAL MOTION
Coherent phasing of segmented mirrors N90-13474
TRANSMISSION CIRCUITS
Modeling of power electronic systems with EMTP
[NASA-TM-102375] N90-14060
TRANSMISSION EFFICIENCY
Dynamic workload modeling of high speed token rings in a metropolitan area network
[MEMO-INF-89-21] N90-14059
TRANSMISSION LOSS
Diffraction, chopping, and background subtraction for LDR N90-13476
TRANSMITTER RECEIVERS
Inexpensive global location and tracking systems using geostationary satellites
[AD-A213025] N90-13498
TRANSMITTERS
Optical communication with semiconductor laser diode
[NASA-CR-185886] N90-13770
TRANSONIC FLOW
Block-structured solution of three-dimensional transonic flows using parallel processing
[AD-A212851] N90-13330
Transonic Euler solutions on mutually interfering finned bodies
[AD-A213395] N90-13331
A vapor generator for transonic flow visualization
[NASA-TM-101670] N90-13403
A two-dimensional adaptive-wall test section with ventilated walls in the Ames 2- by 2-foot transonic wind tunnel
[NASA-TM-102207] N90-13407
TRANSONIC WIND TUNNELS
A two-dimensional adaptive-wall test section with ventilated walls in the Ames 2- by 2-foot transonic wind tunnel
[NASA-TM-102207] N90-13407
TRANSPORT PROPERTIES
Transport phenomena and interfacial kinetics in multiphase combustion systems
[AD-A212932] N90-13620
Computational studies of structural and transport properties of amorphous solids
[ETN-90-96027] N90-13664
Turbulent Shear Flows
[VKI-LS-1989-03] N90-13730
Scalar transport in turbulent shear flows N90-13734
Proceedings: US/FRG (Federal Republic of Germany) Workshop on Photochemical Ozone Problem and Its Control: US Experiences and the Situation in Europe
[PB89-233514] N90-13891
TRANSPORT THEORY
A stochastic model for the calculation of multiple scattered lidar returns
[DLR-FB-89-36] N90-13778
TRANSPORTATION NETWORKS
Why stochastic modeling is essential in analyzing interdicted transportation network performance
[AD-A213140] N90-14007
TRAVELING WAVE AMPLIFIERS
Development of a traveling wave tube for the project X-SAR. Construction and testing of a breadboard model
[ETN-90-95900] N90-13713
TRAVELING WAVE TUBES
Development of a traveling wave tube for the project X-SAR. Construction and testing of a breadboard model
[ETN-90-95900] N90-13713
TRAVELING WAVES
Influence of RF-parameters on beam lifetime
[NIKHEF-K/AMPS/89-06] N90-14091
TREES (MATHEMATICS)
Efficient on-line simulations of tree machines and multidimensional turing machines by random access machines
[AD-A213152] N90-13960
TRITONS
The effective (3)He-nucleon force in a microscopic DWBA approach to the (3)He,t charge exchange reaction — Distorted Wave-Borne Approximation (DWBA)
[KVI-763] N90-14077
TROPOSPHERE
The interaction and variation of waves and turbulence from MST radar data
[AD-A212849] N90-13906
TRUSSES
Initial test results for the mini-mast N90-13482
LDR structural experiment definition N90-13483

Hybrid deployable support truss designs for LDR N90-13485
Effects of joints in truss structures N90-13486
Joints in deployable space truss structures N90-13489

TUNING
Advances in SIS receiver technology N90-13466

TURBINE BLADES
Three D flows in turbine blade rows N90-13739
Flows with tip leakage N90-13740

TURBINE ENGINES
Advanced Turbine Technology Applications Project (ATTAP) [NASA-CR-185109] N90-14153

TURBOCOMPRESSORS
Review and evaluation of a turbomachinery throughflow finite element code [AD-A213058] N90-13787

TURBOMACHINERY
Data acquisition in aerodynamic research N90-13340
Application of a two-dimensional unsteady viscous analysis code to a supersonic throughflow fan stage [NASA-TM-4141] N90-13387
Numerical Methods for Flows in Turbomachinery, volume 1 [VKI-LS-1989-06-VOL-1] N90-13735
Numerical Methods for Flows in Turbomachinery, volume 2 [VKI-LS-1989-06-VOL-2] N90-13741
Numerical methods for unsteady turbomachinery flow N90-13743
Probabilistic finite element analysis of dynamic structural response [AD-A213249] N90-13789
An interactive grid generation procedure for axial and radial flow turbomachinery [NASA-CR-185167] N90-13968

TURBOSHAFTS
Development and testing of a contactless static/dynamic shaft seal with little sealing gas requirement [KFK-4599] N90-13802

TURBULENCE
Application of large eddy interaction model to a mixing layer [NASA-CR-185123] N90-13328
Two-dimensional analysis of two-phase reacting flow in a firing direct-injection diesel engine [NASA-TM-102069] N90-13392
Effect of spatial resolution on apparent sensitivity to initial conditions of a decaying flow as it becomes turbulent [NASA-TM-102377] N90-13719

TURBULENCE MODELS
Application of large eddy interaction model to a mixing layer [NASA-CR-185123] N90-13328
SSME LOX post flow analysis/fluid structure interaction. Volume 1: Flow analysis [NASA-CR-183677] N90-13715
Application of two-point closures to subgrid scale modeling for homogeneous, 3D turbulence N90-13732
Numerical Methods for Flows in Turbomachinery, volume 2 [VKI-LS-1989-06-VOL-2] N90-13741
Turbulence modeling and implementation in Navier-Stokes solvers N90-13742
Numerical solutions of the complete Navier-Stokes equations [NASA-CR-186102] N90-13747

TURBULENT BOUNDARY LAYER
Multiple paths to subharmonic laminar breakdown in a boundary layer [NASA-CR-181948] N90-13722
A review of quasi-coherent structures in a numerically simulated turbulent boundary layer [NASA-TM-102191] N90-13723
Comparison of integral and finite-difference methods for predicting the turbulent boundary layer on axisymmetric bodies [ARE-TM(UHA)-88512] N90-13752

TURBULENT DIFFUSION
Application of large eddy interaction model to a mixing layer [NASA-CR-185123] N90-13328
Scalar transport in turbulent shear flows N90-13734

TURBULENT FLOW
Multigrid calculations of 3-D turbulent viscous flows [NASA-CR-185154] N90-13323
Application of large eddy interaction model to a mixing layer [NASA-CR-185123] N90-13328
Reduction of profile drag by modifying the structure next to the wake area [IMFL-88/35] N90-13356
A planar reacting shear layer system for the study of fluid dynamics-combustion interaction [NASA-TM-102422] N90-13393
Effect of spatial resolution on apparent sensitivity to initial conditions of a decaying flow as it becomes turbulent [NASA-TM-102377] N90-13719
The influence of multiple hot-wire probe geometry on the results of measurements in turbulent flows [DLR-FB-89-26] N90-13724
Numerical simulation of transition in three-dimensional boundary layers [DLR-FB-89-12] N90-13728
Turbulent Shear Flows [VKI-LS-1989-03] N90-13730
An introduction via vorticity dynamics and statistical theory — turbulent shear flows N90-13731
Application of two-point closures to subgrid scale modeling for homogeneous, 3D turbulence N90-13732
Coherent structures in a round jet N90-13733
Scalar transport in turbulent shear flows N90-13734
Turbulence modeling and implementation in Navier-Stokes solvers N90-13742
Numerical solutions of the complete Navier-Stokes equations [NASA-CR-186102] N90-13747
Comparison of integral and finite-difference methods for predicting the turbulent boundary layer on axisymmetric bodies [ARE-TM(UHA)-88512] N90-13752
Spectral study of a compressible isotropic turbulence [ECL-88-16] N90-13753
Large eddy simulation of homogeneous turbulence undergoing shear and thermal gradients. Application to one point closing models [ECL-88-23] N90-13754
Model and computation of three-dimensional turbulent jets in a crossflow [ECL-89-007] N90-13755

TURBULENT HEAT TRANSFER
Coherent structures in a round jet N90-13733

TURBULENT MIXING
Numerical solutions of the complete Navier-Stokes equations [NASA-CR-186102] N90-13747

TURING MACHINES
Efficient on-line simulations of tree machines and multidimensional turing machines by random access machines [AD-A213152] N90-13960

TWO DIMENSIONAL BOUNDARY LAYER
The initial-boundary value problem for the Davey-Stewartson 1 equation; how to generate and drive localized coherent structures in multidimensions [PREPRINT-684] N90-13756

TWO DIMENSIONAL FLOW
Measurement Techniques in Aerodynamics [VKI-LS-1989-05] N90-13339
Inviscid 2D solutions on unstructured, adaptive grids N90-13737

TWO DIMENSIONAL MODELS
Two-dimensional analysis of two-phase reacting flow in a firing direct-injection diesel engine [NASA-TM-102069] N90-13392
Analytical and computer-aided models of InP-based MISFETs and heterojunction devices [AD-A211861] N90-14106

TWO PHASE FLOW
Two-dimensional analysis of two-phase reacting flow in a firing direct-injection diesel engine [NASA-TM-102069] N90-13392

U

U.S.S.R. SPACE PROGRAM
Comparison of the space program performance of countries with space programs [ILR-MITT-222] N90-14150

ULTRASONIC FLAW DETECTION
Quantitative non-destructive evaluation using laser generated ultrasonic pulses N90-13805

ULTRAVIOLET ABSORPTION
Ultraviolet absorption cross-sections of bromoform in the temperature range 295-240 K [AERONOMICA-ACTA-A-348-1989] N90-13630

ULTRAVIOLET ASTRONOMY
Deep detection of hot star populations at balloon ultraviolet wavelengths N90-13865
The low-ion QSO absorption-line systems N90-14162

ULTRAVIOLET RADIATION
Interzodiak 2: Observation of EUV-resonance radiation N90-13854
Prediction of the 10 cm solar flux index N90-13872

ULTRAVIOLET REFLECTION
Reflection indicatrices of natural surfaces for AVHRR channels 1 and 2 [DLR-MITT-89-16] N90-13882

ULTRAVIOLET SPECTRA
The low-ion QSO absorption-line systems N90-14162

UNDERWATER ACOUSTICS
ULF/VLF (0.001 to 50 Hz) Seismo-Acoustic Noise in the Ocean [AD-A212942] N90-13913
Ring source/force excitation of axisymmetric shell structure [ARE-TM(UHA)-88519] N90-14085

UNIVERSE
Unitarity limits on the mass and radius of dark matter particles [NASA-CR-186079] N90-14164

UNIVERSITIES
Summary of research academic departments, 1987-1988 [AD-A213252] N90-14183

UNSTEADY AERODYNAMICS
Unsteady forces induced on finite-span cylinders in a cross-flow N90-13746

UNSTEADY FLOW
Blunt-nose inviscid airflows with coupled nonequilibrium processes N90-13336
Low speed hot and cold wire techniques for unsteady flow N90-13342
Laser applications in supersonic unsteady flow N90-13344
Application of a two-dimensional unsteady viscous analysis code to a supersonic throughflow fan stage [NASA-TM-4141] N90-13387
Numerical Methods for Flows in Turbomachinery, volume 2 [VKI-LS-1989-06-VOL-2] N90-13741
Numerical methods for unsteady turbomachinery flow N90-13743

UREAS
Modern biofuel cells for waste recycling in life support systems [NASA-CR-185963] N90-13718

USER MANUALS (COMPUTER PROGRAMS)
MOBILE4 oxygenated fuels version user's guide [PB89-230700] N90-13674
The computational structural mechanics testbed user's manual [NASA-TM-100644] N90-13818
Image enhancement software for underwater recovery operations: User's manual [AD-A212943] N90-14094
Real time image enhancement during underwater recovery operations [AD-A213139] N90-14097

USER REQUIREMENTS
Cryogenics for LDR N90-13471
LDR cryogenics N90-13472
Space Station Engineering Design Issues [NASA-CR-185978] N90-13492
Power generation and distribution N90-13515
User needs, benefits, and integration of robotic systems in a space station laboratory [NASA-CR-185150] N90-13794
Esrange N90-13876
The DOD Gateway Information System: Operational prototype and transition period 1987-1988 [AD-A213044] N90-14141

V

VACUUM APPARATUS
Surface cooled, vacuum impregnated superconducting magnet systems: Design, construction, applications [ETN-90-98014] N90-14072

VALVES
Simulation of the control characteristics of an axial piston pump and a flapper-nozzle valve combination N90-13784

VANADIUM ALLOYS
Threshold for fatigue crack propagation [DLR-FB-89-33] N90-13815

VANES
Influence of vane sweep on rotor-stator interaction noise N90-13325

VAPOR DEPOSITION
Wear-resistant coated object [EP-PATENT-0-289-173-A1] N90-13643
Novel in situ spectroscopic ellipsometer for real time analysis of CVD diamond films [AD-A213218] N90-13762

VAPOR PHASES
Transport phenomena and interfacial kinetics in multiphase combustion systems [AD-A212932] N90-13620

Buoyancy effects on the vapor condensation rate on a horizontal liquid surface
[NASA-TM-102437] N90-13675
Vapor condensation on liquid surface due to laminar jet-induced mixing: The effects of system parameters
[NASA-TM-102433] N90-13751
VAPORIZERS
A vapor generator for transonic flow visualization
[NASA-TM-101670] N90-13403
VAPORS
Thermophysical properties of buta-1,3-diene
[ESDU-89005] N90-13619
Gas identification system using graded temperature sensor and neural net interpretation
[AD-A213359] N90-13627
VARIABLE MASS SYSTEMS
The spacecraft structure N90-13512
VARIABLE STARS
Variable stars N90-13541
VARIABLE THRUST
The apogee boost motor N90-13517
VARIATIONS
The effects of seasonal and latitudinal earth infrared radiance variations on ERBS attitude control N90-13414
Fluctuations of the Lyapunov exponent in disordered systems
[PREPRINT-690] N90-14063
VAX COMPUTERS
Software and hardware description of the helicopter motion equations for VAX computers
[AD-A213248] N90-13375
VECTOR PROCESSING (COMPUTERS)
Implementing the discrete Fourier transform on the hypercube FPS T40
[IMAG-RR-773-I] N90-13983
VEGETATION GROWTH
Effects of microgravity on growth hormone concentration and distribution in plants N90-13947
Gravitropism in plants: Hydraulics and wall growth properties of responding cells N90-13950
VEGETATIVE INDEX
Physically-based parameterization of spatially variable soil and vegetation using satellite multispectral data
[NASA-CR-185957] N90-13879
Reflection indicatrices of natural surfaces for AVHRR channels 1 and 2
[DLR-MITT-89-16] N90-13882
Senegalese land surface change analysis and biophysical parameter estimation using NOAA AVHRR spectral data
[NASA-CR-186120] N90-13883
VELOCITY
Balance laws and centro velocity in dissipative systems
[MEMO-797] N90-13726
Solution of the Boltzmann equation using an energy group method
[AD-A213138] N90-14096
VELOCITY DISTRIBUTION
Practical systems for speckle velocimetry N90-13341
A wall interference assessment/correction interface measurement system for the NASA/ARC 12-ft PWT
[NASA-CR-185474] N90-13401
VELOCITY MEASUREMENT
Measurement Techniques in Aerodynamics
[VKI-LS-1989-05] N90-13339
Practical systems for speckle velocimetry N90-13341
Hot and cold wire applications in supersonic flows: Introductory notes N90-13343
Skin friction measurements with hot elements N90-13345
The 3D LDA techniques in vortex studies and boundary layer surveys N90-13346
Laser two focus techniques N90-13348
The influence of multiple hot-wire probe geometry on the results of measurements in turbulent flows
[DLR-FB-89-26] N90-13724
VERTICAL MOTION
The interaction and variation of waves and turbulence from MST radar data
[AD-A212849] N90-13906
VERTICAL PERCEPTION
The relationship between subjective and objective measures of simulator-induced ataxia
[AD-A213095] N90-13922
VERTICAL TAKEOFF AIRCRAFT
Aircraft/airport compatibility: Some strategic, tactical, and operational issues
[TT-8902] N90-13409
VERY LARGE SCALE INTEGRATION
Resistive fuses: Analog hardware for detecting discontinuities in early vision
[AD-A211891] N90-13696
An accurate timing model for fault simulation in MOS circuits
[AD-A213153] N90-13702
VHSIC (CIRCUITS)
MM and T for VHSIC multichip packages
[AD-A213259] N90-13703
VIBRATION DAMPING
Pointing control for LDR N90-13453
PACOSS program N90-13487
VIBRATION EFFECTS
Pointing control for LDR N90-13453
VIBRATION TESTS
Mechanical and thermal testing N90-13521
Static and free-vibrational response of semi-circular graphite-epoxy frames with thin-walled open sections
[NASA-CR-186097] N90-13600
Identification of equivalent modulus of a composite beam from nonmodal vibratory tests
[ECL-89-001] N90-13821
VIBRATIONAL SPECTRA
Propagation of sound in vibrationally excited nitrogen and hydrogen gas mixtures
[AD-A213002] N90-14073
VIDEO COMMUNICATION
Implementation issues in source coding
[NASA-CR-185327] N90-13963
VIDEO SIGNALS
Image enhancement software for underwater recovery operations: User's manual
[AD-A212943] N90-14094
VISCOELASTICITY
Quadratic dynamical systems describing shear flow of non-Newtonian fluids
[AD-A212892] N90-13720
VISCOUS FLOW
Multigrid calculations of 3-D turbulent viscous flows
[NASA-CR-185154] N90-13323
Hypersonic aerodynamics N90-13335
Application of a two-dimensional unsteady viscous analysis code to a supersonic throughflow fan stage
[NASA-TM-4141] N90-13387
Gas flows in rocket motors. Volume 2, appendix C: Time iterative solution of viscous supersonic flow
[AD-A213349] N90-13592
Pressure correction calculation procedures for 3D viscous flow N90-13738
On the topology of three-dimensional viscous flow structures near a plane wall. A classification and non-hyperbolic singularities on the wall
[LR-541] N90-13758
VISION
Role of retinocortical processing in spatial vision
[AD-A210995] N90-13918
VISUAL PERCEPTION
Computational and psychophysical study of human vision using neural networks
[AD-A213290] N90-13924
Spatiotemporal characteristics of visual localization, phase 2
[AD-A212934] N90-13929
VITON RUBBER (TRADEMARK)
Studies of Aflas fluoroelastomers
[AD-A213046] N90-13622
VITREOUS MATERIALS
Nucleation kinetics in undercooled, glass-forming metallic melts
[DLR-FB-89-32] N90-13644
VOICE COMMUNICATION
Evaluation of speech intelligibility through a bone conduction stimulator
[AD-A212002] N90-13919
Test procedures for the evaluation of helmet and headset mounted active noise reduction systems
[AD-A212991] N90-13937
VOLUME
An algorithm for control volume analysis of cryogenic systems
[AD-A213394] N90-13683
VORTEX BREAKDOWN
A smoke generator system for aerodynamic flight research
[NASA-TM-4137] N90-13372
VORTICES
The 3D LDA techniques in vortex studies and boundary layer surveys N90-13346
A smoke generator system for aerodynamic flight research
[NASA-TM-4137] N90-13372
Feature modeling: The incorporation of a front and eddy map into optimum interpolation-based thermal analysis
[AD-A213253] N90-13914
VORTICITY
An introduction via vorticity dynamics and statistical theory — turbulent shear flows N90-13731
VOYAGER PROJECT
The Voyager Neptune travel guide
[NASA-CR-186108] N90-13412

W

WALL FLOW
Study of the integration of wind tunnel and computational methods for aerodynamic configurations
[NASA-TM-102196] N90-13332
A two-dimensional adaptive-wall test section with ventilated walls in the Ames 2- by 2-foot transonic wind tunnel
[NASA-TM-102207] N90-13407
On the topology of three-dimensional viscous flow structures near a plane wall. A classification and non-hyperbolic singularities on the wall
[LR-541] N90-13758
WALL PRESSURE
A wall interference assessment/correction interface measurement system for the NASA/ARC 12-ft PWT
[NASA-CR-185474] N90-13401
WALLS
Gravitropism in plants: Hydraulics and wall growth properties of responding cells N90-13950
WARNING SYSTEMS
An update to the system safety study of TCAS 2
[DOT/FAA/SA-89/3] N90-13363
Multisensor technologies for low cost methane detection
[PB89-235188] N90-13766
WASTE TREATMENT
Modern biofuel cells for waste recycling in life support systems
[NASA-CR-185963] N90-13718
WASTE WATER
Modern biofuel cells for waste recycling in life support systems
[NASA-CR-185963] N90-13718
WASTES
Space station gas compressor technology study program, phase 1
[NASA-CR-183758] N90-13491
WATER RESOURCES
Activities report of the World Meteorological Organization
[WMO-713] N90-13912
WAVE DRAG
Optimum shape of a blunt forebody in hypersonic flow
[NASA-CR-181955] N90-13351
WAVE FRONTS
Wavefront error sensing for LDR N90-13455
WAVE INTERACTION
Energy exchange of interacting solitons in multidimensions
[PREPRINT-662] N90-14071
WAVE PROPAGATION
Localization of ultrasound in thick composites
[AD-A212994] N90-13602
Electromagnetic wave propagation through circular waveguides containing radially inhomogeneous lossy media
[AD-A213062] N90-13688
Experimental and theoretical study of artificial plasma layers produced by two intersecting beams in a chamber
[NASA-CR-184598] N90-14102
WAVE REFLECTION
Reflection by defective diffusion bonds
[AD-A212995] N90-13638
WAVEGUIDES
An experimental analysis of the waveguide modes in a high-gain free-electron laser amplifier N90-13779
WEAK ENERGY INTERACTIONS
An experiment to search for galactic axions N90-14158
WEAK INTERACTIONS (FIELD THEORY)
Cosmology and the weak interaction
[NASA-CR-186170] N90-14169
WEAPON SYSTEMS
A new view of weapon system reliability and maintainability
[AD-A213281] N90-13382
A new view of weapon system reliability and maintainability: Executive summary
[AD-A213282] N90-13383
Human factors research in aircrew performance and training
[AD-A213285] N90-13938
WEAPONS
Summary of research academic departments, 1987-1988
[AD-A213252] N90-14183
WEAR
The limiting friction force
[ECL-89-005] N90-13801

WEAR RESISTANCE
Wear-resistant coated object
[EP-PATENT-0-289-173-A1] N90-13643
WEATHER
The interaction and variation of waves and turbulence from MST radar data
[AD-A212849] N90-13906
An evaluation of the Smith-Feddes model
[AD-A213237] N90-13907
Activities report of the World Meteorological Organization
[WMO-713] N90-13912
WEATHER FORECASTING
The linear study of zonally asymmetric barotropic flows N90-13902
A collection of papers related to heavy precipitation forecasting
[PB89-230833] N90-13910
Three dimensional analysis of the structure of the atmosphere in polar environments by vertical satellite sounding. Interest for the meteorological forecasts at high latitudes
[ETN-90-95506] N90-13911
WEATHER MODIFICATION
Applied atmospheric resources research program in Thailand
[PB89-235402] N90-13903
WEIGHT REDUCTION
Development of an advanced fan blade containment system
[DOT/FAA/CT-89/20] N90-13386
WEIGHTING FUNCTIONS
Optimum data weighting and error calibration for estimation of gravitational parameters N90-13437
WEIGHTLESSNESS
On the wings of a dream: The Space Shuttle
[NASA-EP-269] N90-13446
Watchfulness and attention during weightlessness simulations: Use of computerized psychometric tests
[REPT-89-TOU-3-1045] N90-13928
WELD STRENGTH
Reflection by defective diffusion bonds
[AD-A212995] N90-13638
WELD TESTS
Metal transfer in gas metal arc welding
[AD-A213390] N90-13642
WELDED JOINTS
Metal transfer in gas metal arc welding
[AD-A213390] N90-13642
Arc current control of a robotic welding system: Modeling and control system design
[AD-A213150] N90-13788
Theoretical evaluation of defects in pressure vessels and pipings
[CRIF-MT-174] N90-13798
WELDING
Activities report of the metallic manufacturing industry
[ISSN-0524-7705] N90-13649
WIND (METEOROLOGY)
Comparison of analytical methods for calculation of wind loads
[NASA-TM-102782] N90-13813
WIND DIRECTION
Observation of wind corners in the middle atmosphere over Andenes (69 N) during winter 1983/84, summer 1987 and summer 1988 N90-13836
WIND PRESSURE
Comparison of analytical methods for calculation of wind loads
[NASA-TM-102782] N90-13813
WIND TUNNEL APPARATUS
A vapor generator for transonic flow visualization
[NASA-TM-101670] N90-13403
High temperature capacitive strain gage
[NASA-CR-4266] N90-13760
WIND TUNNEL MODELS
On the application of modified stepwise regression for the estimation of aircraft stability and control parameters
[REPT-8905] N90-13400
WIND TUNNEL TESTS
Analysis of experimental data for CAST 10-2/DOA 2 supercritical airfoil at low Reynolds numbers and application to high Reynolds number flow
[AD-A211654] N90-13326
Study of the integration of wind tunnel and computational methods for aerodynamic configurations
[NASA-TM-102196] N90-13332
Pressure measurement techniques in use at the Royal Aerospace Establishment N90-13347
Reduction of profile drag by modifying the structure next to the wake area
[IMFL-88/35] N90-13356
A wall interference assessment/correction interface measurement system for the NASA/ARC 12-ft PWT
[NASA-CR-185474] N90-13401
A two-dimensional adaptive-wall test section with ventilated walls in the Ames 2- by 2-foot transonic wind tunnel
[NASA-TM-102207] N90-13407
Helicopter rotor test rig (RoTeSt) in DNW: Application and results
[RAE-TRANS-2171] N90-13408
WIND TUNNEL WALLS
Study of the integration of wind tunnel and computational methods for aerodynamic configurations
[NASA-TM-102196] N90-13332
A wall interference assessment/correction interface measurement system for the NASA/ARC 12-ft PWT
[NASA-CR-185474] N90-13401
A two-dimensional adaptive-wall test section with ventilated walls in the Ames 2- by 2-foot transonic wind tunnel
[NASA-TM-102207] N90-13407
WIND VELOCITY
Meteorological atlas of the Northern Hemisphere lower stratosphere for January and February 1989 during the Airborne Arctic Stratospheric Expedition
[NASA-TM-4145] N90-13908
The winds of high luminosity late-type bright stars
[NASA-CR-182961] N90-14160
WING LOADING
A CFD study of tilt rotor flowfields
[NASA-CR-186116] N90-13349
Advanced actuation systems development, volume 2
[AD-A213378] N90-13398
WING PLANFORMS
Study of forces and moments on wing-bodies at high incidence, volumes 1 and 2 N90-13350
WING PROFILES
Efficient methods for integrated structural-aerodynamic wing optimum design N90-13376
WINGS
Induced drag for non-planar wings
[LR-521] N90-13357
WINTER
Observation of wind corners in the middle atmosphere over Andenes (69 N) during winter 1983/84, summer 1987 and summer 1988 N90-13836
Meteorological atlas of the Northern Hemisphere lower stratosphere for January and February 1989 during the Airborne Arctic Stratospheric Expedition
[NASA-TM-4145] N90-13908
WIRE
Development and characterization of PdCr temperature-compensated wire resistance strain gage
[NASA-CR-185153] N90-13761
WORK
Measurement of mechanical work and energy expenditure in running and bicycling N90-13935
WORK CAPACITY
Exercise countermeasures for bed rest deconditioning
[NASA-TM-101045] N90-13926
WORKSTATIONS
The role of the host in a cooperating mainframe and workstation environment, volumes 1 and 2
[NASA-CR-185463-VOL-1/2] N90-13496
WORLD METEOROLOGICAL ORGANIZATION
Activities report of the World Meteorological Organization
[WMO-713] N90-13912

X

X RAY ASTRONOMY
Project Supernova 1987 N90-13866
The x ray mirror and the PSPC of the supernova-rocket-project N90-13867
X RAY ASTROPHYSICS FACILITY
Project Supernova 1987 N90-13866
X RAY DENSITY MEASUREMENT
Bone mineral measurement using dual energy x ray densitometry N90-13958
X RAY SPECTROSCOPY
Quantitative AES and XPS: Determination of the electron spectrometer transmission function and the detector sensitivity energy dependencies for the production of true electron emission spectra in AES and XPS
[NPL-DMA(A)-194] N90-13634

Y

YAG LASERS
MM and T advanced balancing/machining
[AD-A213103] N90-13775
YTTRIUM COMPOUNDS
Thermal barrier coatings for gas turbine and diesel engines
[NASA-TM-102408] N90-13636
YUKAWA POTENTIAL
Exotic Higgs production at e+e- colliders
[PREPRINT-671] N90-14088

Z

ZERO SOUND
Construction of the rotating cryostat ROTA2, its use for zero sound experiments in (3)He-B, and calculations of ion mobility in (3)He-A and (3)He-P
[ISBN-952-90091-3-5] N90-13765
ZETA PINCH
A solvable self-similar model of the sausage instability in a resistive Z-pinch
[AD-A213137] N90-14006
ZINC SELENIDES
Chemical beam epitaxy of ZnSe
[AD-A213265] N90-13625
ZIRCONIUM COMPOUNDS
Thermal barrier coatings for gas turbine and diesel engines
[NASA-TM-102408] N90-13636
ZIRCONIUM OXIDES
Thermodynamic properties of some metal oxide-zirconia systems
[NASA-TM-102351] N90-13666
ZODIACAL LIGHT
Reexamination of data from the asteroid/meteoroid detector
[NASA-CR-185997] N90-14175
ZONAL FLOW (METEOROLOGY)
The linear study of zonally asymmetric barotropic flows N90-13902

Typical Personal Author Index Listing

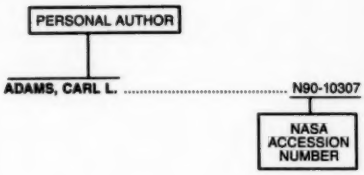

Listings in this index are arranged alphabetically by personal author. The NASA accession number denotes the number by which the citation is identified.

A

AARONS, JULES N90-13896
AARTS, E. N90-14025
ABEYAGUNAWARDENE, S. N90-13421
ABRAHAMSON, K. N90-13324
ACHENBACH, JAN D. N90-13602
N90-13638
N90-13810
ACOURT, RICHARD N90-13676
ADMIRE, J. R. N90-13444
ADOLFSEN, K. N90-13859
AINSWORTH, R. W. N90-13340
AKE, ROBERT L. N90-13618
AKLONIS, J. J. N90-13660
AL-MAAITAH, AYMAN ADNAN N90-13745
ALDRICH, THEODORE B. N90-13938
ALLBRIGHT, CARL A. N90-13398
ALLEGA, A. M. N90-14066
N90-14067
N90-14068
N90-14170
N90-14171
N90-14172
N90-14173
ALLEN, JAMES G. N90-13990
ALLEN, PHILIP CHARLES N90-14099
ALTOZ, F. E. N90-13373
AMIRY, CHARLES N90-14117
AMORETTI, M. N90-13548
N90-13572
ANDERSEN, B. N. N90-13829
ANDERSON, BRUCE ROBERT N90-13779
ANDERSON, JOHN A. N90-13398
ANDERSON, JOHN D., JR. N90-13335
ANDREASEN, G. K. N90-13548
N90-13560
ANGENENT, SIGURD N90-14004
ANSELMET, F. N90-13342
ANTONIADIS, DIMITRI A. N90-13969
ANTONUCCI, E. N90-14177
APT, KRYZYSZTOF R. N90-13978
ARENOU, F. N90-13529
N90-13531
ARGUE, A. N. N90-13529
N90-13544
ARGYROPOULOS, ALEXANDRA N90-13362
ARIJS, E. N90-13848
ARMANDO, IA. N90-13378
ARNOTT, D. R. N90-13764
ARTHUR, C. A. N90-13973
ASHBY, DALE L. N90-13332
ASHILL, P. R. N90-13347
ATHAY, R. GRANT N90-14154
ATKINS, D. J. N90-13752
AUBRUN, JEAN-N. N90-13457
AUPOIX, B. N90-13732
AUTY, DAVID N90-13982
AZAR, MASSOOD TABIB N90-13381

B

BAARSPUL, M. N90-13410
BABAN, FARZAD N90-13746
BACKER, STANLEY N90-13608
BADGLEY, M. B. N90-13794
BADIALI, M. N90-13548
N90-13572
BAHDER, THOMAS B. N90-14110
BAHRI, ABBAS N90-14005
BAILEY, M. C. N90-13694
BAILEY, M. MURRAY N90-13636
BAINUM, PETER M. N90-13494
BAKER, DANIEL N90-14154
BAKKER, P. G. N90-13758
BALLANTYNE, ALEX N90-13775
BANDURSKI, ROBERT S. N90-13947
BANSAL, NAROTTAM P. N90-14108
BAR-ITZHACK, ITZHACK Y. N90-13427
N90-13431
N90-13433
BARASSIN, A. N90-13848
BARBOUR, CHRISTOPHER G. N90-13931
BARNES, PETER JOHN N90-14155
BARTMAN, R. N90-13451
BASCOM, W. D. N90-13599
BASSETT, DAVID ROBINSON, JR. N90-13935
BATTRICK, B. N90-13917
BATUT, T. N90-13499
N90-13504
N90-13505
N90-13506
N90-13509
N90-13523
BAUER, DOUGLAS N90-14003
N90-14013
BEACH, TIMOTHY A. N90-13968
BEC-BORSENBERGER, A. N90-13529
N90-13545
BECKER, K. N90-13891
BECKLIN, ERIC E. N90-14159
BEHEIM, GLENN N90-13381
BELCASTRO, CELESTE M. N90-14061
BELFORTE, P. N90-13548
N90-13551
N90-13552
BENAGE, WILLIAM FRED, JR. N90-13972
BENAMARA, ZINEB N90-14115
BENASSI, P. N90-14100
BENHABIB, R. J. N90-13456
BENNETT, JEAN M. N90-14092
BENNETT, THEODORE J., JR. N90-13914
BENNETT, WILLIAM H. N90-13430
BENO, JOSEPH HENRY, JR. N90-13445
BERI, A. N90-13434
BERKOVITS, AVRAHAM N90-13819
BERMAN, P. R. N90-14078
BERNACCA, P. L. N90-13548
N90-13551
N90-13555
N90-13562
N90-13570
BERNADINI, P. N90-14081
BERTANI, D. N90-13572
BERTHEL, ROBERT O. N90-13907
BERTINO, M. N90-14081
BESKIN, G. M. N90-14076
BETTI, B. N90-13576
BETZ, ALBERT N90-13465
BIEL, E. N90-13631
BINEBRINK, A. L. N90-13439
BIRNBAUM, H. K. N90-13624
N90-13641
BIZOT, ALAIN N90-13672
BJOERKMAN, THOMAS N90-13946
BLACHER, R. N90-14040
BLANKENSHIP, GILMORE L. N90-13689
BLOCK, L. P. N90-13841
BOARDSEN, SCOTT ARNOLD N90-14105
BOCHKAREV, N. E. N90-14076
BOCK, K. D. N90-13499
N90-13521
BOCKRIS, J. OM. N90-13718
BODNER, S. R. N90-13390
N90-13391
BOEHM, BARRY W. N90-13492
BOISON, M. N90-13847
BOL, ROLAND N. N90-13978
BOLJEAU, D. J. N90-13587
BORRELLI, A. N90-14089
BORRIELLO, L. N90-13562
BOS, H. J. N90-13357
BOSCOV, JAYME N90-13860
N90-13861
BOUIZI, ABDELILLAH N90-14075
BOUSMAN, WILLIAM G. N90-13327
BOWLES, DAVID E. N90-13461
BOWLES, TIFFANY N90-13767
BOWMAN, DUANE K. N90-13929
BOXMA, O. J. N90-13989
N90-14020
BOYD, IAIN N90-13578
BOYD, ROBERT W. N90-14093
BRAEUNINGER, H. N90-13867
BRAISTED, W. R. N90-13789
BRAMWELL, JONATHAN RICHARD N90-13884
BRANDENBURG, S. N90-14077
BRAUN, G. N90-13408
BREEMAN, J. H. N90-13410
BREKKE, A. N90-13851
BREWE, DAVID E. N90-13786
BRIEL, U. G. N90-13867
BRIGGS, C. N90-13453
BRINDLEY, WILLIAM J. N90-13636
BROCKMAN, R. A. N90-13789
BROERSMA, H. J. N90-14003
BROOKS, C. J. N90-13358
BROOME, PAUL N90-14011
BROWN, ALLAN H. N90-13948
BROWN, B. A. N90-14077
BROWN, DAVID B. N90-13962
BROWN, H. BENJAMIN, JR. N90-13790
N90-13792
BROWNE, LINDSEY E. N90-13332
BRUCE, ROBERT A. N90-13403
BRUENING, KORNELIA N90-13843
BRUNO, JOHN D. N90-14110
BRUNTY, J. A. N90-13444
BRUSCHI, M. N90-14043
BUCCIARELLI, B. N90-13555
BUETEFISCH, KARL-ALOYS N90-13346
BUFFART, HANS N90-13930
BULLOCK, A. D. N90-14179
BURBECK, CHRISTINA A. N90-13929
BURDETT, JEREMY K. N90-13659
BURGARELLA, D. N90-13865
BURKE, ROGER W. N90-13715
BURKE, W. R. N90-13826
BURKERT, W. N90-13867
BURNETT, L. J. N90-13628
BURROUGHES, JEREMY HENLEY N90-14099
BURROWS, C. J. N90-13499
N90-13501
BUSEN, REINHOLD N90-13882
BUSH, H. N90-13480
BUTLER, E. P. N90-13656
BUTLER, G. F. N90-13995
BYRNE, CATHERINE A. N90-13622

C

CAIRNS, JOHN, JR. N90-13889
CALLAHAN, PAUL X. N90-13939
N90-13940
CALLENDER, E. DAVID N90-14135
N90-14136
N90-14137
N90-14138
N90-14139
CANUTO, E. N90-13551
N90-13552
CAPPUCCI, MARIETTA R. N90-13640
CAPUS, J. N90-13833
CARDARELLI, R. N90-14081
CARDINI, D. N90-13572
CARLIER, THIERRY N90-14042

CARLISLE, HOMER W. N90-13962
CARLUCCI, D. N90-13552
CARLUCCIO, J. R. N90-13385
CARNES, MICHAEL R. N90-13914
CARNEY, CURTIS S. N90-13812
CARON, R. J. N90-13977
CARPENTER, K. G. N90-14150
CARTER, A. L. N90-13820
CASE, EDWIN N90-13703
CASSANDRO, M. N90-13650
CASSENTI, B. N. N90-13391
CASSINELLI, JOSEPH P. N90-14159
CASTRO, DANIEL C. N90-13815
CAVE, B. N90-13764
CAVES, ROBERT N90-13409
CAZALA-HOURCADE, E. N90-13582
CETICA, M. N90-13572
CHAIYAPORN, SOMSAK N90-13821
CHAN, KWAI S. N90-13390
N90-13391
CHAN, Y. Y. N90-13326
CHANG, C. T. N90-13393
CHANG, KAI-HSIUNG N90-13962
CHAPMAN, DAVID K. N90-13953
CHARETON, M. N90-13529
N90-13532
CHATWIN, P. C. N90-13734
CHECHIRLIAN, SERGE N90-13648
CHEN, D. N90-13379
N90-13616
N90-13624
CHEN, L. N90-13718
CHEN, TAO SHINN N90-13695
CHEN, YUN-CHUNG N90-13963
CHIPMAN, RUSSELL A. N90-14092
CHITASHVILI, R. J. N90-14018
CHOI, BYUNG KWON N90-14007
CHOUDRY, A. N90-13964
CHU, D. N90-13418
CHU, PETER L. N90-13690
CIESLINSKI, JAN N90-14030
CINI, MARCELLO N90-14123
CLAFLIN, S. E. N90-13589
CLARK, NOEL A. N90-14109
CLARKE, DAVID ALAN N90-14161
CLAUD, CHANTAL N90-13911
CLAUSEN, K. N90-13499
N90-13502
N90-13524
CLEARWATER, YVONNE A. N90-13931
CLERC, GUY N90-13711
CLIFFORD, P. K. N90-13766
COCHRAN, JOHN E. N90-13419
COHEN, ARJEH M. N90-14036
COLLINS, J. SCOTT N90-13600
COLLIS, P. N. N90-13832
COLOMBANT, D. N90-14096
COLOME, STEVEN D. N90-13920
COMMERE, BRUNO N90-13709
CONSOLI, M. N90-14089
COOK, M. N90-13404
N90-13405
N90-13594
N90-13661
COOK, M. V. N90-13400
COQUART, B. N90-13630
CORNAC, ALAIN N90-13928
COSGROVE, DANIEL J. N90-13950
COSS, RICHARD G. N90-13931
COSTELLO, DANIEL J., JR. N90-13685
COX, J. N90-13811
CRABTREE, R. B. N90-13921
N90-13937
CREZE, M. N90-13529
N90-13532
CRIFO, F. N90-13529
N90-13530
N90-13535
CRISAFULLI, M. N90-14086
CRISANTI, ANDREA N90-14047
CROFT, JOHN N90-13767
CROSBIE, ROSS ANDREW N90-13805
CROSS, JAMES H. N90-13952
CURREY, DONALD R. N90-13878
CURRY, ROBERT E. N90-13372
CUSCHIERI, J. M. N90-13817

D

DAGOSTINI, G. N90-14083
DAHL, A. F. N90-13831
N90-13846
DAHL, FERDINAND N90-13873
DALLMANN, UWE N90-13725
DAM, JACOBUS ADRIANUS MARIA N90-14072
DANCY, R. N90-13825
DANIEL, STEVEN N90-13497
DARDEN, RICHARD B. N90-13959
DAS, DIPAK K. N90-13915
DAVIDSON, FREDERIC N90-13770
DAVIES, C. N90-13324
DAVIES, JOHN N. N90-13895
DAVIES, P. E. N90-13499
N90-13501
DAVIS, MATTHEW N90-13704
DEASON, WILLIAM H. N90-13962
DEBRA, DANIEL B. N90-13492
DECOCK, J. N90-13798
DEFAZIO, R. N90-13421
DEFRIES, DANNY L. N90-13498
DEHAN, E. N90-13806
DEHEN, J. N90-13414
DEISSLER, ROBERT G. N90-13719
DEIWERT, G. S. N90-13324
DEJONG, K. A. N90-13992
DEKKERS, A. N90-14025
DELCLOPEZ, MARIA N90-13375
DEMASI, JEANINE T. N90-13388
DEMAZIERE, M. N90-13892
DEMERJIAN, K. N90-13891
DEMUREN, A. O. N90-14002
DENNIS, A. S. N90-13903
DENYER, PETER BRIAN N90-13961
DESA, SUBHAS N90-13791
N90-13793
DESANCTIS, M. N90-14082
DESBAT, LAURENT N90-13983
DESHPANDE, M. D. N90-13694
DESROSIERS, MARK N90-13947
DEUTSCHMANN, JULIE N90-13433
DEVADAS, SRINIVAS N90-13697
N90-13698
DEVLIN, S. N90-13421
DEWAAL, P. R. N90-14019
DEWEGER, B. M. M. N90-14031
N90-14032
DEWINKEL, M. E. M. N90-13758
DEWITT, KENNETH J. N90-13750
DEYONG, LEO V. N90-13671
DEZWIJGER, H. E. N90-13885
DHERBECOURT, A. N90-13499
N90-13518
DIDELON, P. N90-13575
DIMITRIADES, BASIL N90-13891
DINKELACKER, MICHAEL N90-13629
DISBROW, J. D. N90-13995
DIX, DAVID W. N90-13637
DJOMEHRI, J. N90-13324
DOALI, J. O. N90-13626
DODD, W. R. N90-13794
DODSON, H. C. N90-13589
DOLL, C. E. N90-13434
DOMMANGET, J. N90-13529
N90-13540
DOMPKA, R. V. N90-13814
DONAS, J. N90-13865
DONATI, F. N90-13550
N90-13551
N90-13552
DONNELLAN, MARY E. N90-13639
DORMAN, M. G. N90-13766
DOUGHERTY, HUGH N90-13454
DRACOPOULOS, THEODORE NICOLAS N90-13396
DRAVID, NARAYAN V. N90-14060
DREW, ALICE R. N90-13904
DRIESSEN, THEO N90-14056
DRUMMOND, COLIN K. N90-13389
DUBIN, MAURICE N90-14175
DUBOVITSKY, S. N90-13451
DUC-JACQUET, M. N90-14041
DUFOUR, LOUIS C. N90-13657
DUKE, E. L. N90-13995
DUNLOP, ERIC H. N90-13954
N90-13956
DUPIC, J. N90-13573
DUPREE, ANDREA K. N90-14159
DUSSAUGE, J. P. N90-13343
DWYER, THOMAS A. W., III N90-13430

E

EAGLESON, PETER S. N90-13879
EBERHARD, A. N90-14041
EBERT, WARD L. N90-13415
ECER, AKIN N90-13330
EGELAND, A. N90-13838
EGGEL, H. N90-13499
N90-13507
N90-13508
EGRET, D. N90-13529
N90-13547
N90-13575
EGRY, IVAN N90-13645
EHRFELD, W. N90-13802
EILINGSFELD, FABIAN N90-14150
EKBLAD, ULF N90-13583
ELENA, M. N90-13344
ELIASSON, L. N90-13832
ELKIN, D. N90-13421
ELLIOT, JAMES L. N90-14159
ELLIS, J. A. N90-13871
EMANUELE, A. N90-13572
EMERSON, JERRY N90-13936
ENDLICHER, WILFRIED N90-13881
ENGLUND, J. N90-13876
ENGWERDA, J. C. N90-14023
ENVIA, EDMANE N90-13325
EPPICH, HENRY N90-13775
EREN, K. N90-13367
ERIKSSON, ANDERS I. N90-13842
ERRINGTON, A. N90-13499
N90-13514
ESCHENROEDER, ALAN Q. N90-13336
EUDELL, A. H. N90-13426
EVANS, KURT B. N90-13654
EWALD, R. N90-13846

F

FAELTHAMMAR, C.-G. N90-13841
FAHR, H. J. N90-13854
N90-13863
N90-13866
FAIGLE, U. N90-14015
FALCIONI, MASSIMO N90-14047
FALIN, J. L. N90-13560
N90-13573
FAN, GENGHUA N90-14013
FARGION, DANIELE N90-14174
FARID, BENHAM N90-14121
FARMER, CROFTON B. N90-13893
FASSINO, B. N90-13550
FAST, THOMAS N. N90-13939
N90-13940
FAUCHET, PHILIPPE M. N90-13773
FAUCON, P. N90-13857
FAVRE-MARINET, M. N90-13733
FAY, J. A. N90-13337
FAZIO, G. G. N90-13490
FEJTEK, IAN N90-13349
FELDER, MARIAN C. N90-13581
FELIU, VICENTE N90-13790
N90-13792
FERRARE, RICHARD A. N90-13976
FERRAROTTO, F. N90-13712
FETROW, FRED N90-14183
FICKE, J. M. N90-13820
FIEBRICH, H. K. N90-13515
FIFER, ROBERT A. N90-13626
FIGUERAS, F. N90-13541
FINCH, W. N90-13366
FINDLAY, D. A. N90-13932
FINDLING, ANDREAS N90-13778
FINEMAN, M. A. N90-13628
FINLAYSON, MACK H. N90-13681
FIORE, LUCIEN N90-13812
FIORELLO, J. L., JR. N90-13422
FISK, LENNARD A. N90-14154
FITZ-COY, NORMAN G. N90-13419
FLATICO, JOSEPH M. N90-13381
FLORENCE, G. N90-13927
FOCH, D. N90-13414
FOKAS, A. S. N90-13756
FORICHON, M. N90-13833
FORREST, S. R. N90-14098
FORSHAW, S. E. N90-13921
FORSHAW, STANLY E. N90-13937
FOUNDS, D. N90-13484
FOURNIER, FRANCETTE N90-14074
FOX, WILLIAM JOSEPH N90-13676
FRANCOIS, PHILIPPE N90-14039
FRANKLIN, MATTHEW K. N90-13975
FRASER, MARK E. N90-13897
N90-13898
N90-13899
N90-13900
FRASER, ROBERT S. N90-13976
FRASER, STEPHANIE B. N90-13361
FRAZIER, WILLIAM E. N90-13639
FREDRICKS, ROBERT W. N90-14154
FREEDMAN, GLENN N90-13966
FREELAND, R. E. N90-13462
FRERKING, M. A. N90-13466
FRIEND, RICHARD HENRY N90-14099
FRITSCH, KLAUS N90-13381
FROESCHLE, M. N90-13560
N90-13573

FUJIWARA, M. N90-14077
FULLER, E. R., JR. N90-13656
FUNARO, DANIELE N90-14038
FUSSEN, D. N90-13848

G

GABRIELIAN, ARMEN N90-13975
GALLAGHER, J. S. N90-14163
GALLAVOTTI, G. N90-13650
GALLIGANI, I. N90-13555
GANDHI, K. N90-13660
GARTRELL, CHARLES F. N90-13452
GAUDIOT, JEAN-LUC N90-13970
GEBMAN, J. R. N90-13382
N90-13383
GEDNEY, LARRY D. N90-13895
GEERTS, A. H. W. N90-14001
N90-14027
GEERTS, TON N90-13996
N90-14024
N90-14028
GEIST, ROBERT N90-13706
GELB, A. N90-13897
N90-13898
N90-13899
N90-13900
GELLER, DAVID N90-13416
GENZEL, R. N90-14156
GEORGE, ANNA N90-13915
GEORGE, RUSSELL J. N90-13568
GEORGE, THOMAS F. N90-14113
GERSHWIN, STANLEY B. N90-13969
GHORASHI, B. N90-13393
GHOSH, ABHIJIT N90-13698
GIANIONI, I. N90-13782
GIBBS, NIGEL KEITH N90-13643
GILBERT, NEIL N90-13327
GILES, MICHAEL N90-13743
GILLESSEN, FRIEDHELM N90-13644
GILLOT, RAINER N90-13635
GILLOTAY, D. N90-13630
GLASER, DONALD A. N90-13924
GLAVICH, T. A. N90-13455
GLICKSMAN, MARTIN E. N90-13988
GLOVER, EDWARD L. N90-13674
GLUCK, R. N90-13481
GOETZ, GUENTER N90-14124
GOMEZ, A. N90-13530
N90-13531
N90-13535
GONZALEZ, WAYNE N90-13952
GORINI, E. N90-14081
GOULARD, R. N90-13338
GRAFAREND, E. N90-14157
GRAGG, WILLIAM N90-14012
GRAHAM, ROBERT W. N90-13394
GRANCAGNOLO, F. N90-14081
GRANLUND, S. N90-13705
GRASDIJK, P. N90-14077
GREEN, C. CORDELL N90-13492
GREENE, BRUCE WILLIAM N90-13788
GREENFIELD, M. B. N90-14077
GREENLEAF, JOHN N90-13926
GRENON, M. N90-13530
N90-13538
N90-13539
GREWING, M. N90-13560
GRIEST, KIM N90-14164
GRINDELAND, R. N90-13941
GRISAFFE, SALVATORE J. N90-13597
GUGGISBERG, B. N90-13796
GUNDERSEN, A. N90-13829
GUSTAFSSON, GEORG N90-13842

H

HADAWAY, JAMES B. N90-14092
HADENFELDT, A. C. N90-13963
HAEGGSTROEM, I. N90-13832
HAENNINEN, MARKKU N90-13987
HAFELE, B. W. N90-13491
HAFIZI, B. N90-13777
HAGA, KEVIN D. N90-13962
HAINLEY, DONALD C. N90-13748
HAJJ, IBRAHIM N. N90-14008
HALE, ELGIE N90-13586
HALL, C. N90-13851
N90-13856
HALL, J. GORDON N90-13336
HAMILTON, K. M. N90-13922
N90-13923
HAMLIN, JOHN EDWARD N90-13676
HANDEL, PETER H. N90-14107
HANNA, STEVE N90-13890
HANNAFORD, B. N90-13796
HANSEN, BJORN GARN N90-14052
N90-14053
N90-14054
HANSEN, P. C. N90-13559
HARAKEH, M. N. N90-14077
HARMAN, R. R. N90-13427
HARPER, D. A. N90-13490
HARRIS, JOHN N90-13696
HARRISON, ALAN JOHN N90-14099
HARROD, JOHN F. N90-13655
HARTMAN, K. R. N90-13420
HARVEY, JOHN W. N90-14154
HARVIE, E. N90-13414
HASAN, MOHAMMAD M. N90-13675
N90-13751
HASHEMI-KIA, MOSTAFA N90-13406
HASSAN, H. N90-13499
HASSAN, H. A. N90-13747
HAUTUS, M. L. J. N90-14001
N90-14027
N90-14029
HAVERKORT, BOUDEWIJN R. N90-14059
HAYASHI, S. N90-13604
HAYES, DANIEL G. N90-14181
HEDGEPETH, J. N90-13485
HEEREN, THEODORUS ANTONIUS GERARDUS
N90-13804
HEIJMANS, H. J. A. M. N90-14065
HELGER, A. N90-13876
HELMS, CHARLES A. N90-13774
HELMS, RICH N90-13458
HENDY, K. N90-13923
HENRY, RICHARD C. N90-13492
HEPP, ALOYSIUS F. N90-13595
HERRNSTEIN, J. R. N90-13436
HESLEGRAVE, R. N90-13923
HESS, ROBERT W. N90-13403
HEUERMAN, K. N90-13434
HICKEY, CHARLES F., JR. N90-13637
HIGGINBOTHAM, SCOTT A. N90-13447
HILL, JEFF T. N90-13390
HILL, V. J. N90-14086
HILLERT, W. N90-13855
HIMMES, A. N90-13846
HINDS, H. A. N90-13400
HINDS, WILLIAMS E. N90-13940
HIPPMANN, HORST N90-13866
HOEKSEMA, J. T. N90-14177
HOFFMANN, WILLIAM F. N90-13463
N90-13478
N90-13490
N90-14159
HOFMAN, M. N90-13901
HOG, E. N90-13548
N90-13558
N90-13559
N90-13560
N90-13568
HOLM, LENNART N90-14101
HOLMES, D. GRAHAM N90-13736
N90-13737
HOOPER, H. L. N90-13436
HOPKINS, GERALD J. N90-13374
HOPPE, MARTIN L. N90-13655
HOPPE, U.-P. N90-13852
HORNER, G. N90-13482
HORTA, L. N90-13482
HOSMAN, R. J. A. W. N90-13933
HOUCK, JAMES R. N90-13759
HOUDEVILLE, R. N90-13345
HOVEY, PETER W. N90-13360
HSIEH, E. K. N90-13701
HUANG, GUANG-PING N90-13755
HUANG, SHOU-HSUAN STEPHEN N90-14133
HUC, C. N90-13567
HUDSON, HUGH S. N90-14159
HUEHN, K. N90-13522
HUFF, D. L. N90-13355
HUGGINS, JOHN R. N90-13962
HUGHES, BLYTH A. N90-13691
HUGUENIN, D. N90-13827
N90-13865
HUIJBERTS, H. J. C. N90-14014
HUMMER, LEIGH L. N90-14092
HUNG, CHING-MAO N90-13353
HUNT, J. C. R. N90-13731
HUSSAINI, M. YOUSUFF N90-13722
HYMER, WESLEY C. N90-13941

I

IANO, P. J. N90-13420
IDDINGS, F. A. N90-13359
IDE, ROBERT F. N90-13797
IKEGAMI, R. N90-13486
INGELS, FRANK N90-13497
INGELS, J. N90-13848
IORI, M. N90-14081
IORIO-FILI, D. N90-13572
IWENS, R. P. N90-13456
IZUMI, YUTAKA N90-13907

J

JACOBS, D. N90-13825
JACOBSON, NATHAN S. N90-13666
JAEKEL, E. N90-13508
N90-13510
N90-13511
N90-13512
N90-13513
JAHREISS, H. N90-13537
JALAGUIER, ERIC N90-14114
JAMES, J. H. N90-14085
JAQUES, PETER N90-13920
JASINSKI, MICHAEL F. N90-13879
JEFFRIES, H. N90-13891
JENNEY, GAVIN D. N90-13398
JENOUVRIER, A. N90-13630
JENSEN, PHILIP N90-13947
JENSEN, R. J. N90-13589
JENZER, U. N90-13848
JEPPSEN, J. C. N90-13652
JERACKI, ROBERT J. N90-13352
JEZOUIN, JEAN-LUC N90-13970
JOHN, REJI N90-13812
JOHNSON, ERIC R. N90-13600
JOHNSON, G. A. N90-13350
JOHNSON, G. ALAN N90-13910
JOHNSON, WAYNE N90-13327
JOKIPII, JACK R. N90-14154
JONA-LASINIO, G. N90-13650
N90-14050
JONES, PETER A. N90-13474
JUANG, JER-NAN N90-13807
JUILLEN, J. C. N90-13345
JUNG, G. N90-13520
JUNKER, B. N90-13408
JURA, MICHAEL N90-14159
JUSLIN, KAJ N90-13987

K

KADO, NORMAN Y. N90-13920
KAGAN, DAVID N90-13637
KALBFLEISCH, ALBERT N90-13775
KALIKOW, STEVEN N90-14021
KAMIONKOWSKI, MARC N90-14164
KANTOR, L. N90-13922
N90-13923
KAO, PI-JEN N90-13376
KARLSSON, TOM N90-13668
KARRAY, FAKHREDDINE N90-13430
KATNIK, GREGORY N. N90-13447
KAUFMAN, H. N90-13495
KAUFMAN, YORAM J. N90-13976
KELEHER, WILLIAM R. A. N90-13962
KELLER, W. N90-13802
KELLY, DONALD H. N90-13918
KELLY, K. A. N90-13422
KENNARD, RUTH L. N90-13883
KEPPENNE, C. L. N90-13909
KERN, W. N90-14015
KESSLER, JOHN O. N90-13949
KETCHUM, ELEANOR A. N90-13428
KETTENRING, G. N90-13867
KHAN, KHALID N90-13658
KHLOPOV, M. YA. N90-14076
KHMALADZE, E. Y. N90-14046
KHOUDLI, MOHAMMED N90-13754
KHOUKH, ABDELAZIZ M. N90-14118
KIM, G. N90-13660
KIM, KYONG H. N90-13772
KIM, SUNGHO N90-13702
KIM, WALTER S. N90-13595
KIM, YONG-YIL N90-13791
N90-13793
KIMURA, A. N90-13624
N90-13641
KINDERMANN, M. R. N90-13764
N90-13808
KING, ANDREW MARK N90-13397
KINLOCH, A. J. N90-13605
KIRCHHOF, WERNER N90-13881
KIRKWOOD, S. N90-13832
KITTEL, PETER N90-13471
KIVELSON, MARGARET N90-14154

KLEIN, HERMANN N90-13606
N90-13607
N90-13616
KLEIN, J. R. N90-13432
KLEINMAN, MICHAEL N90-13920
KLIMCHUK, JAMES A. N90-14178
KLINE, S. J. N90-13723
KLINGENBERG, HANS H. N90-13781
KLOP, JAN WILLEM N90-13978
KNEISSEL, B. N90-13864
KNIGHT, LAURA D. N90-14010
KO, W. L. N90-13820
KOBA, RICHARD J. N90-13762
KOBAYASHI, A. S. N90-13804
KOCH, CHRISTOF N90-13696
KODOKIAN, G. K. A. N90-13805
KOHLHASE, CHARLES N90-13412
KOLODZIEJSKI, LESLIE A. N90-13625
KONKEL, C. R. N90-13794
KOPP, E. N90-13848
KOREN, BAREND N90-13727
KOTARU, SATYANARAYANA N90-13579
KOVALEVSKY, J. N90-13533
N90-13548
N90-13549
N90-13562
N90-13564
N90-13565
N90-13573
KOZIARA, MICHAEL N90-13910
KRAITCHMAN, JEROME N90-14144
KRAUSE, R. F., JR. N90-13656
KREBBEKX, J. A. N90-13617
KREJCI, A. N90-14103
KRETZMANN, JANE LEE N90-13974
KRICHBAUMER, WILHELM N90-13778
KRIEGLMEIER, SIGRID N90-13778
KRIKORIAN, ABRAHAM D. N90-13943
KRIMIGIS, STAMATIOS M. N90-14154
KRIZ, D. N90-13660
KROES, F. B. N90-14091
KROLL, NORBERT N90-13333
KRONZON, YIGAL N90-13591
N90-13592
N90-13593
KROUSKY, E. N90-14103
KRUCZYNSKI, DAVID L. N90-13626
KRUEGER, ARLIN J. N90-13908
KU, W. H. N90-14106
KULIKOWSKI, CASIMIR A. N90-14143
KUO, AN-YU N90-13812
KUO, S. P. N90-14102
KURFESS, JAMES N90-14159
KURKI-SUONIO, HANNU N90-14168
KURKI, JORMA N90-13987
KURZAWA, H. N90-13837
N90-13869
KUSMANOFF, ANTONE N90-13496
KUTAY, AYDAN N90-13682
KWAK, DOCHAN N90-13329
KWON, OH JOON N90-13377
KYRIAKOPOULOS, K. J. N90-13495

L

LAAKKONEN, JARI N90-13664
LAAKMANN, JOCHEN N90-13645
LACOLLE, B. N90-14041
LAGARDE, D. P. N90-13927
LAGARDE, S. J. N90-13800
LAGET, M. N90-13665
LAINE, RICHARD M. N90-13655
LAIT, LESLIE R. N90-13908
LALLEMAND, CHRISTIAN N90-14116
LAMBERT, DAVID L. N90-14176
LAMPE, MARTIN N90-14006
N90-14096
LAN, C. EDWARD N90-13354
LANE, ALAN D. N90-13386
LANGER, H.-J. N90-13408
LANGFORD, TED L. N90-13919
LANTOS, P. N90-13872
LANZETTA, KENNETH M. N90-14162
LARDAS, MARK N. N90-13425
LATTANZI, M. N90-13555
N90-13570
LAW, HENRY N90-13910
LAWRENCE, JOHN S. N90-13374
LAY, G. N90-13854
N90-13863
N90-13868
LEAPHART, MARK A. N90-14147
LEE, EUN E. N90-13603
LEE, GEORGE N90-13407
LEE, H. R. N90-14113
LEE, H. S. N90-13835
N90-13849
LEE, JONG SEH N90-13686
LEE, KEVIN A. N90-13423
LEE, MICHAEL H. N90-13428
LEE, W. Y. N90-13441
N90-13442
LEE, Y. D. N90-13660
LEGRAND, SUE N90-13966
N90-13967
LEI, JIH-FEN N90-13761
LEMAIRE, J. N90-14045
LERCH, FRANCIS J. N90-13437
LESTRADE, J. F. N90-13565
LEVAN, NHAN N90-13771
LEVINSON, LAURIE H. N90-13986
LI, FEIYUE N90-13494
LI, MING N90-14062
LI, VICTOR C. N90-13608
N90-13894
LICHTENBERG, CHRISTOPHER L. N90-13704
LIJEWSKI, LAWRENCE E. N90-13331
LILJEGREN, TORSTEN N90-13677
LIM, KYONG BEEN N90-13807
LIN, CHIN-SHUN N90-13675
N90-13751
LINDEGREN, L. N90-13533
N90-13548
N90-13549
N90-13550
N90-13557
N90-13559
N90-13563
N90-13564
N90-13566
N90-13568
LINDHOLM, ULRIC S. N90-13390
N90-13391
LINDLOHR, W. N90-13388
LINDQVIST, P. N90-13705
LIPPENS, C. N90-13892
LIPPERT, GEROLD N90-13713
LORELL, KEN R. N90-13457
LOUI, MICHAEL C. N90-13960
LOVHAUG, U. P. N90-13851
LOWELL, CARL E. N90-13597
LU, YICHI N90-13602
LUEBKEN, F.-J. N90-13855
LUEHR, H. N90-13844
LUGINBUHL, DAVID R. N90-13960
LUGTEN, J. B. N90-14158
LUNDAHL, K. N90-13830
LUNG, F. Y. N90-13789
LUO, JIN N90-13696
LUOVO, ARNO N90-13651
LUPISELLA, M. L. N90-13440
LUSIGNOLI, M. N90-14079
N90-14088
LUTTGES, MARVIN W. N90-13957
LYAN-CHANG, CHAU N90-13591
N90-13592
N90-13593
LYENGAR, JAISIMHA N90-13915
LYLE, JOSEPH A. N90-13374

M

MAAS, R. N90-14091
MACKALL, DALE A. N90-13990
MAEHLUM, B. N. N90-13851
MAESTRELLO, L. N90-13351
MAGEE, L. E. N90-13922
N90-13923
MAGHAMI, PEIMAN N90-13807
MAGILL, S. A. N. N90-13366
MAHONEY, M. J. N90-13449
MAIANI, L. N90-14089
MAIN, GEOFFREY L. N90-14104
MAINARDI, F. N90-13726
MAINS, RICHARD C. N90-13939
MAJOR, C. S. N90-13456
MAKAROVIC, A. N90-14035
MALATERRE, PIERRE N90-13874
MALKUS, DAVID S. N90-13720
N90-13721
MANN, I. N90-13864
MARCUS, L. N90-13876
MARCUS, R. A. N90-14111
MARDIROSSIAN, H. N90-13434
MAREK, C. J. N90-13393
MARIANS, CAROL S. N90-13659
MARION, JEAN-DENIS N90-13753
MARKLEY, F. LANDIS N90-13417
MARRONE, PAUL V. N90-13336
MARSHALL, R. J. N90-13408
MARTIN, NANCY L. N90-13496
MARTINELLI, GUIDO N90-14079
N90-14086
N90-14087
MASON, PETER V. N90-13470
MASSA, F. N90-14081
MATTILA, ANTTI TAPANI N90-13662
MATTOO, SHANA N90-13976
MATTSSON, JOHAN N90-13768
MATVEEV, V. B. N90-14070
MATZNER, RICHARD A. N90-14168
MAYCOCK, PAUL D. N90-13492
MAYER, RICHARD N90-13981
MAYOR, RAMON A. N90-13459
MAZUYER, DENIS N90-13801
MAZZACURATI, V. N90-14100
MCAFFEE, D. N90-13796
MCANULTY, D. M. N90-13938
MCCREIGHT, CRAIG R. N90-13464
MCDEVITT, T. KEVIN N90-13407
MCDONALD, J. F. N90-13977
MCELIGOT, DONALD M. N90-13642
MCELROY, JOHN H. N90-13492
MCELROY, P. M. N90-13462
MCELROY, PAUL N90-13458
MCGUIRE, SAUNDRA Y. N90-14125
MCIVER, D. W. N90-13382
N90-13383
MCKEE, JAMES W. N90-13991
MCLEAN, B. J. N90-13575
MCRUER, DUANE T. N90-13492
MEASE, KENNETH D. N90-13369
MEDINA, J. G. N90-13903
MEERTENS, LAMBERT G. L. T. N90-13979
MELLOTT, DALE B. N90-13665
MELNICK, G. J. N90-14156
MEMIER, M. N90-13884
MENDILLO, MICHAEL N90-13896
N90-14154
MENNESSIER, M. O. N90-13541
MERIENNE, M. F. N90-13630
MERKLE, CHARLES L. N90-13591
N90-13592
N90-13593
MERMILLIOD, J. C. N90-13542
MERZKIRCH, W. N90-13341
MESRATI, NADIR N90-13667
MESSICK, L. J. N90-14106
METZNER, G. N90-13867
MEYER, FRIEDRICH N90-13728
MEYER, STEPHAN N90-13469
MEYER, T. G. N90-13390
MEYERS, L. G. N90-13669
MGHAIETH, RIDHA N90-13888
MICHEL, W. N90-13835
N90-13849
MICOLLET, DOMINIQUE N90-13707
N90-13708
MIELE, A. N90-13441
N90-13442
N90-13443
MIGLIACCIO, F. N90-13576
MIGNANI, R. N90-14080
MIGNARD, F. N90-13560
N90-13562
N90-13573
MIHALOEW, JAMES R. N90-13389
MIKALSEN, P. A. N90-13859
MILHAUD, C. L. N90-13927
MILLER, ROBERT A. N90-13636
MILLIARD, B. N90-13865
MINDERMAN, DONALD J. N90-13813
MISSON, A. N90-14045
MITTER, P. K. N90-14050
MIYAKE, R. N. N90-13460
MOLLS, FRANK B. N90-13719
MONALDI, D. N90-14083
MONTY, CLAUDE N90-13657
MOOR, R. N90-13848
MOORE, G. E. N90-13890
MOORE, JOAN G. N90-13738
MOORE, JOHN N90-13739
N90-13740
MORANDO, B. N90-13563
MORELLI, A. N90-14079
MORIN, D. N90-13531
MORRIS, G. MICHAEL N90-14093
MOSELEY, WARREN N90-13965
MOULINEC, H. N90-13865
MOZO, BEN T. N90-13919
MUELLER, SIEGFRIED N90-13875
MULARZ, E. J. N90-13393
MULDER, J. A. N90-13410
MULLER, C. N90-13892
MURGOLO, F. P. N90-13570
MURPHY, HENRY C. N90-13897
N90-13898

N90-13899
N90-13900
MURRAY, C. A. N90-13548
N90-13550
MURRAY, STEPHEN S. N90-14159
MURTAGH, DONAL P. N90-13834
N90-13853
MURTHY, S. N. B. N90-13328
MUSCHINSKI, A. N90-13844
MUSSER, KEITH L. N90-13415

N

NAGATANI, RONALD M. N90-13908
NAGY, ANDREW F. N90-14154
NAHRA, HENRY K. N90-13581
NAJJAR, WALID N90-13970
NARDONE, M. N90-14100
NASS, H. U. N90-13854
N90-13863
N90-13868
NAST, T. N90-13472
NATALI, RON N90-13703
NEAMTU, M. N90-14017
NEEDLEMAN, A. N90-13601
NELSON, BONITA J. N90-13626
NETA, BENY N90-14012
NEVEJANS, D. N90-13848
NEWMAN, PAUL A. N90-13908
NEWTON, A. RICHARD N90-13698
NEWTON, RON N90-13585
NGUYEN, H. LEE N90-13392
NICHOLS, DONALD K. N90-14084
NICOLET, B. N90-13532
NICOLIS, C. N90-13909
NICOLIS, STAM N90-14063
NIEDERLEHNER, B. R. N90-13889
NIEMEGEERS, IGNAS G. N90-14059
NIEUWPOORT, A. H. M. N90-13410
NO, T. S. N90-13419
NOBACK, R. N90-13371
NOETZOLD, DIRK N90-14124
NOGUES, JEAN-LUC R. N90-14095
NOHEL, JOHN A. N90-13720
N90-13721
NOORMOHAMMADIAN, MASOUD N90-13778
NORMAN, DONALD A. N90-13994
NORMAN, J. P. N90-13385
NORMAN, SUSAN D. N90-13384
NORTON, ROBERT H. N90-13893
NOTENBOOM, RONALD P. N90-13985
NOTTEN, PETRUS HENRICUS LAURENTIUS N90-13633
NOTTROT, R. N90-14016
NYHEIM, I. N90-13859

O

OCONNOR, SEAN PATRICK N90-13676
ODELL, P. C. N90-13921
OEVEL, WALTER N90-14069
OFFERMANN, D. N90-13870
OH, I. H. N90-13422
OLIVE, KEITH A. N90-14168
OPPEL, ULRICH G. N90-13778
ORLADY, HARRY W. N90-13384
ORTIZ, MILTON N90-13388
OSER, H. N90-13917
OSTERYOUNG, JANET G. N90-13623
OTTERBEIN, MANFRED N90-13831
N90-13873
OVARLEZ, H. N90-13833
OVARLEZ, J. N90-13833
OVERDIJK, D. A. N90-13795
OWENS, JOHN N90-13497
OYAMA, K. I. N90-13840

P

PACE, O. N90-13519
N90-13520
PADILLA, A. M. N90-13653
PALADIN, GIOVANNI N90-14063
PALMARA, O. N90-14081
PAN, W.-S. N90-13700
PARK, M. N90-13660
PARTRIDGE, WILLIAM J. N90-14094
N90-14097
PATARINSKI, S. P. N90-13803
PATNAIK, A. N90-13631
PATT, F. S. N90-13426
PATTERSON, JAMES H., JR. N90-13919
PEDROSA, A. C. F. N90-13861
PENFIELD, PAUL, JR. N90-13969
PERRYMAN, M. A. C. N90-13499
N90-13500
N90-13529
N90-13548
N90-13564
PETERSEN, C. N90-13553
N90-13554
N90-13568
N90-13569
PETERSEN, G. R. N90-13954
N90-13955
PETERSON, MIRIAM R. N90-13906
PETOT-ERVAS, GEORGETTE N90-13657
PETRARCA, S. N90-14088
PEZZANITI, LARRY N90-14092
PFEFFERMANN, E. N90-13867
PHENNEGER, M. C. N90-13414
N90-13440
PHOEBUS, PATRICIA A. N90-13914
PIEL, A. N90-13840
PIEPLU, J. L. N90-13567
PIERCE, CHESTER M. N90-13492
PIETERMAN, KAREL N90-14072
PINTO, C. N90-14081
PIPER, LAWRENCE G. N90-13897
N90-13898
N90-13899
N90-13900
PIPITONE, F. J. N90-13992
PIRAPREZ, E. N90-13806
PIRKER, DANA M. N90-13424
PITONE, D. S. N90-13426
N90-13432
PIZZELLA, GUIDO N90-14165
PIZZOLATI, P. L. N90-13782
PLOHR, BRADLEY J. N90-13720
N90-13721
POGLITSCH, A. N90-14156
POINSATTE, PHILIP E. N90-13750
PORKHOLM, KARI N90-13987
POWELL, FEROLYN T. N90-13934
PRESTON, R. A. N90-13585
PREVOT, L. N90-13543
PREZIOSO, N. N90-13562
PROSPERI, D. N90-14082
PRUVOST, J. N90-13356
PUGET, PASCALE N90-13611
PULLES, STEFAN N90-14145
PUSTILNIK, L. A. N90-14076
PUSTILNIK, S. A. N90-14076

Q

QUARTERMAINE, R. W. N90-13408

R

RABINOWITZ, PAUL H. N90-14005
RADOMSKI, M. S. N90-13439
RAGNISCO, ORLANDO N90-14043
N90-14044
N90-14069
RAHN, JEFFREY A. N90-13655
RAJU, M. S. N90-13749
RAMSEYER, H. N90-13848
RANNE, L. N90-13422
RANTALA, TAPIO N90-13651
RAPAGNANI, P. N90-14166
RAPOZO, R. R. N90-13491
RASMUSSEN, R. M. N90-13903
RATIER, G. N90-13504
N90-13505
N90-13506
N90-13509
RATTAN, KULDIP S. N90-13790
N90-13792
RAWLINS, WILSON T. N90-13897
N90-13898
N90-13899
N90-13900
REARDON, JOHN E. N90-13584
REDDY, A. S. S. R. N90-13494
REDDY, T. S. R. N90-13355
REED, HELEN L. N90-13744
REID, ALEXANDER A. N90-13402
REINECKE, MICHAEL N90-13936
REISING, JOHN N90-13936
REMANE, E. N90-13647
RENDALL, ALAN D. N90-14122
RENNER, O. N90-14103
REQUIEME, Y. N90-13536
RESSELL, M. TED N90-14180
RHEA, J. OWEN N90-13910
RHODES, M. N90-13489
RIBEIRO, T. S. N90-13861
RICCARDELLA, PETER C. N90-13812
RICHARDS, K. E., JR. N90-13487
RICHWINE, DAVID M. N90-13372
RIDDELL, F. R. N90-13337
RIEDLINGER, LANCELOT M. N90-13914
RIETVELD, M. T. N90-13851
RILEY, M. J. N90-13327
RIVERA, JOSE A., JR. N90-13403
ROBERTS, LEONARD N90-13349
ROBINSON, JAMES ELLIOTT N90-13662
ROBINSON, S. K. N90-13723
RODRIGUEZ, O. N90-13356
ROEBROEKS, G. H. J. J. N90-13615
ROESER, S. N90-13564
ROESSLER, K. N90-13631
ROETTGER, J. N90-13856
ROLLS, C. N90-13518
RONNEY, PAUL D. N90-13873
RONSE, C. N90-14065
ROSE, G. N90-13850
ROSE, GAYLE E. N90-13352
ROSEMANN, HENNING N90-13724
ROSEN, BENGT N90-13986
ROSNER, DANIEL E. N90-13620
ROSS, HOWARD D. N90-13680
ROSSOW, CORD-CHRISTIAN N90-13729
ROTH, M. N90-14045
ROTH, TIMOTHY N90-14144
ROUAULT, G. N90-13710
RUF, MICHAEL P. N90-14140
RUOCCO, G. N90-14100
RUPPEL, TIMOTHY H. N90-14073
RUSSELL, JOHN C. N90-13915
RUSSELL, R. A. N90-13483
RYLANDS, JULIA M. N90-13937

S

SABINE, KEITH ALLEN N90-13961
SACHRAJDA, C. T. N90-14086
SACHS, EMANUEL M. N90-13969
SACKSTEDER, KURT R. N90-13679
SADOURNY, I. N90-13828
SAGERS, N. W. N90-13681
SALJNIKOV, VIKTOR N90-13725
SALMELIN, RIITTA N90-13765
SALOVEY, R. N90-13660
SAMANTA, SASWATI N90-13915
SAMII, M. V. N90-13434
N90-13439
SANDERS, J. P. N90-13628
SANKAR, N. L. N90-13355
SANSO, F. N90-13576
SANTINI, P. M. N90-13756
N90-14044
N90-14071
SANTONICO, R. N90-14081
SARKAR, SHYAM SUNDAR N90-14146
SATER, BERNARD L. N90-13581
SAVAGE, BLAIR D. N90-14159
SAYOOD, KHALID N90-13963
SCALES, D. N90-13560
SCHAEFER, R. L. N90-13940
SCHAIRER, EDWARD T. N90-13407
SCHERRER, P. H. N90-14177
SCHIJVE, J. N90-13822
SCHIRONE, M. G. N90-13570
SCHMIDLIN, F. J. N90-13835
N90-13849
SCHMITT, M. W. N90-13440
SCHODL, R. N90-13348
SCHOEBERL, MARK R. N90-13908
SCHOEN, ROBERTA S. N90-14141
SCHRAMM, DAVID N. N90-14167
N90-14168
N90-14169
SCHREADLEY, HARRY W. N90-13398
SCHRIJVER, H. N90-13571
SCHULTZ, LARRY L. N90-13813
SCHULZE, AGA N90-13947
SCHURATH, U. N90-13891
SCHUUR, PETER C. N90-13980
N90-13984
SCIALDONE, JOHN J. N90-13809
SCOFIELD, RODERICK A. N90-13910
SCOTT, JAMES F. N90-14109
SEAH, M. P. N90-13634
SEIDEL, D. N90-13802
SENTURIA, STEPHEN D. N90-13969
SEPPA, HEIKKI N90-13769
SERRA, GUY N90-13862
SERVA, MAURIZIO N90-14123
SESHAN, P. K. N90-13954
N90-13955
SETZKE, M. N90-13519
N90-13520

SHEY, A. J. N90-14106
SHULMAN, H. L. N90-13382
N90-13383
SIBONGA, JEAN D. N90-13939
SIEGEL, M. W. N90-13627
SIEMENSMEYER, KONRAD N90-14090
SIGNORELLI, G. N90-14100
SILVENNOINEN, EERO N90-13987
SILVERMAN, B. A. N90-13903
SIMON, P. C. N90-13630
SIMPSON, DAVID G. N90-13429
SIPILAE, MARIKKU N90-13714
SISTO, R. N90-14089
SKELBOE, STIG N90-14006
SKINN, DONALD A. N90-13360
SKOWRONEK, M. S. N90-13823
SMIRNOV, A. O. N90-14070
SMITH, E. A. N90-13440
SMITH, G. C. N90-13634
SMITH, R. L. N90-13977
SMITH, ROGER L. N90-13399
SMITH, STEVEN W. N90-13958
SMOORENBURG, G. F. N90-13692
SNAY, RICHARD A. N90-13904
SOBERMAN, ROBERT K. N90-14175
SODERHJELM, S. N90-13561
SOETHOUDT, J. M. N90-14022
N90-14026
SOLI, GEORGE A. N90-14084
SOLLNER, T. C. L. GERHARD N90-13467
SOMERS, MARCEL ADRIANUS JOHANNES N90-13646
SONNENFELD, GERALD N90-13942
SOTOS, RAYMOND G. N90-13680
SOUBRIER, A. N90-13658
SPALART, P. R. N90-13723
SPEARS, W. M. N90-13992
SPENCER, NED A. N90-13363
SRIVASTAVA, R. N90-13355
STACEY, G. J. N90-14156
STAFFORD, THOMAS P. N90-13492
STALOS, STEPHEN N90-13435
STANTON, MICHAEL B. N90-13683
STARKE, BENJAMIN B. N90-13962
STASKUS, JOHN V. N90-13581
STECKL, A. J. N90-13700
STEEN, A. N90-13877
STEIN, BLAND A. N90-13461
STEINBACHER, JODY N90-14135
N90-14136
N90-14137
N90-14138
N90-14139
STEINKE, RONALD J. N90-13387
STELLA, B. N90-13712
STENCEL, ROBERT E. N90-14160
STENGLE, THOMAS N90-13413
STERRENBURG, W. A. N90-14077
STEUTEL, F. W. N90-14048
STEVENSON, CHARLES G. N90-13447
STEWART, CAROLINE B. N90-13618
STIER, MARK T. N90-13479
STOECKENIUS, T. E. N90-13890
STOLLER, H. M. N90-13385
STONE, DAVID B. N90-13895
STOORVOGEL, A. A. N90-13997
N90-13999
N90-14000
STRADA, P. N90-13516
N90-13517
STREETER, GORDON N90-14181
STRIMITAS, D. N90-13890
SUN, L. N90-13660
SUN, X. N90-13770
SUNDARESAN, MANNUR JAGANATHAN N90-13598
SUTTON, GEORGE H. N90-13913
SYM, ANTONI N90-14030
SYS, A. N90-13799
SZAFRAN, NICOLAS N90-14042

T

TAKEMORI, TOSHIKAZU N90-13627
TALLEY, WILLIAM G. N90-13398
TAM, KWA-SUR N90-14060
TANG, SHU S. N90-13812
TAYA, M. N90-13604
TAYLOR, BARRY L. N90-13944
TAYLOR, DOLORES B. N90-13910
TAYLOR, ROBERT M. N90-13936
TELGEN, J. N90-13977
TESSENDORF, JERRY N90-13905
THERRIEN, CHARLES W. N90-14094
THIEMANN, H. N90-13840
THOMAS, RONALD L. N90-13596
TIIHONEN, OLLI N90-13987
TING, A. N90-13777
TING, L. N90-13351
TINKHAM, MICHAEL N90-13699
TODD, PAUL N90-13945
TOLL, DAVID L. N90-13883
TOMMASINI, T. N90-13555
TOTTON, W. W. N90-13820
TOULMAY, FRANCOIS N90-13327
TOWER, LEONARD K. N90-13748
TOWERS, STEVEN R. N90-13931
TOYAMA, WILSON KATSUMI N90-13860
TRAAS, C. R. N90-14034
TRACY, GENE V. N90-13372
TRENTELMAN, HARRY L. N90-13997
N90-13998
N90-14022
N90-14026
TRESTER, K. N90-13887
TRETOUT, B. N90-13632
TRIBHAWAN, KUMAR N90-13924
TROXEL, DONALD E. N90-13969
TRYSTRAM, DENIS N90-13983
TSAI, SHIR-TAU N90-13784
TSENG, J. B. N90-13354
TUAN, PHAM DINH N90-14049
TUBBS, ELDRED F. N90-13455
TUCKER, THOMAS R. N90-13897
N90-13898
N90-13899
N90-13900
TURAN, G. N90-14015
TURCOTTE, CHARLES N90-13775
TURNER, J. N90-13845
TURNER, MICHAEL S. N90-14180
TURON, C. N90-13529
N90-13530
N90-13533
N90-13534
N90-13535
N90-13542
N90-13546
TWARDY, HARALD N90-13577
TYLER, A. C. F. N90-13366
TYRRELL, DEBRA L. N90-14142
TYSENN, THOMAS N90-13463
TZANAKIS, N. N90-14032

U

UMPLEBY, JEFFREY DAVID N90-13662
N90-13663
UPSON, ROBERT N90-13905

V

VAGHI, S. N90-13500
VALANIS, K. C. N90-13658
VALENTA, FRANK J. N90-13671
VANAREM, B. N90-14057
N90-14058
VANBON, JOHN T. M. N90-14036
N90-14037
VANBUREN, MARK A. N90-13369
VANDAALEN, D. N90-13553
N90-13554
VANDENBERG, J. L. N90-14055
VANDERHA, J. N90-13525
N90-13527
N90-13528
VANDERLAAN, T. N90-13508
N90-13510
N90-13512
VANDERMAREL, H. N90-13553
N90-13554
N90-13564
N90-13569
VANDERMEER, H. N90-13864
VANDERSCHAFT, A. J. N90-13993
VANDERVAART, J. C. N90-13933
VANDERVEGT, JANTIEN N90-13930
VANDERWEGEN, LEO N90-14033
VANDERWERF, S. Y. N90-14077
VANDERWOUDE, J. W. N90-14064
VANDIJK, N. M. N90-14019
VANDOORN, E. A. N90-14058
VANDROMME, DANY N90-13742
VANEYKEN, A. P. N90-13856
VANFOSSEN, G. JAMES N90-13750
VANGROESEN, E. N90-13726
VANKATWIJK, K. N90-13503
VANLEEUWEN, CEES N90-13930
VANLEEUWEN, F. N90-13550
N90-13551
N90-13552
N90-13568
N90-13574
VANMARLE, E. A. N90-14016
VANOOIJEN, W. H. N90-13365
VANOPIJNEN, ROELAND A. N90-13670
VANZYL, JAKOB J. N90-13475
VARGAS, A. N90-13567
VAUDIN, M. D. N90-13656
VAUGHAN, ARTHUR H. N90-13477
VAUGHN, F. J. N90-13440
VELDMAN, HENK JAN N90-14003
N90-14013
VENKATAPATHY, E. N90-13324
VERAVERBEKE, NOEEL N90-14051
VERCHEVAL, J. N90-13411
VERTECHI, D. N90-14119
VIRASORO, M. A. N90-14119
VIRDY, M. N90-13414
VITANYI, PAUL M. B. N90-14062
VLOT, A. N90-13613
N90-13614
VONZAHN, U. N90-13837
N90-13869
VUKOVICH, FRED M. N90-13883
VULPIANI, ANGELO N90-14047
N90-14063
VUORINEN, M. N90-13705

W

WADA, BEN N90-13488
WAELCHLI, U. N90-13848
WAITE, DAVID MARC N90-13717
WALKER, K. P. N90-13391
WALKER, PAUL N. N90-13916
WALKER, SUSAN E. N90-14151
WALTER, H. G. N90-13556
WANG, EDWARD Y. N90-13886
WANG, YOUJIANG N90-13606
WARD, D. T. N90-13440
WARDELL, T. C. N90-13763
WARNATZ, J. N90-13757
WARREN, WAYNE N90-13416
WEBER, E. N90-13847
WEBER, R. M. N90-13390
N90-13391
WEIKEL, JOHN G. N90-13910
WEISS, SHOLOM M. N90-14143
WELCH, JEANNE A. N90-13776
WELSH, B. L. N90-13347
WENGER, M. N90-13547
WESSELIUS, WILLEM N90-14030
WESTSTRATE, J. A. N90-13989
WEY, C. N90-13393
WEY, C. C. N90-13393
WEYRICH, ORVILLE R. N90-13962
WHITES, KEITH W. N90-13688
WHITNEY, DONALD A. N90-13772
WIDDEL, H. U. N90-13836
N90-13839
WIE, BONG N90-13416
WIEDER, H. H. N90-14112
WIKSTROEM, A. N90-13876
WILEY, LYNN M. N90-13951
WILEY, TIMOTHY G. N90-13670
WILKES, DONALD R. N90-14092
WILKINSON, E. T. N90-13366
WILLEKENS, ERIC N90-14051
WILLIAMS, P. J. S. N90-13856
WILLIS, E. A. N90-13749
WILLS, R. D. N90-13501
N90-13502
N90-13526
WILSON, WILLIAM J. N90-13468
WINGET, CHARLES M. N90-13939
N90-13940
WINSA, EDWARD A. N90-13988
WISSER, THOMAS N90-13364
WISSINGER, ALAN B. N90-13479
WITTENBERG, H. N90-13395
WNUK, STEPHEN P., III N90-13760
WNUK, STEPHEN P., JR. N90-13760
WNUK, V. P. N90-13760
WOIDA, PATRICK N90-13463
N90-13478
WOLFE, J. C. N90-13704
WONG, LANWAI N90-13627
WOOD, L. N90-13798
WOOD, R. N90-13438
WOSIK, JAROSLAW N90-13704
WRIGHT, EDWARD L. N90-13476
WU, XIONGHUA N90-13757
WU, Y. C. N90-13460
WUENSCH, WALTER ULRICH N90-14158
WULF, FRIEDRICH N90-14120
WYATT, JOHN N90-13696

X

XU, JIANKE N90-13494
XU, YONGLIN N90-13636
N90-13810

Y

YAM, Y. N90-13453
YANG, YUNFENG N90-13651
YAP, YEN LEE N90-13929
YEE, EUGENE C. N90-13621
YEO, PENG HIAN N90-13787
YOKOTA, JEFFREY W. N90-13323
YOON, H. S. N90-13604
YOUNG, COLIN N90-13327
YOUNG, ERICK T. N90-13473
YOUNG, LAURENCE R. N90-13492
YOUNGDAHL, KAY A. N90-13655
YUAN, BAU-SAN N90-13783
YUAN, SHIFENG N90-13780

Z

ZABIN, SERENA M. N90-14009
ZAK, H. N90-13796
ZAKRAJSEK, JAMES J. N90-13785
ZANG, THOMAS A. N90-13722
ZHANG, Y. S. N90-14102
ZHANG, ZUOJUN N90-13902
ZHAO, Z. Q. N90-13441
N90-13442
ZHU, S. Q. N90-14029
ZHU, YOULAN N90-13757
ZOU, D. N90-13660

Typical Corporate Source Index Listing

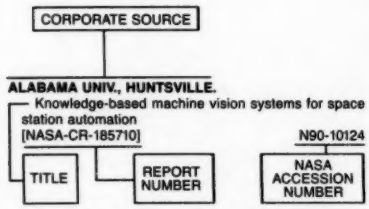

Listings in this index are arranged alphabetically by corporate source. The title of the document provides the user with a brief description of the subject matter. The report number helps to indicate the type of document cited (e.g., NASA report, translation, NASA contractor report). The NASA accession number denotes the number by which the citation is identified. The titles are arranged under each corporate source in ascending accession number order.

A

ABERDEEN UNIV. (SCOTLAND).
Some aspects of curvature in general relativity N90-14122

ACADEMY OF SCIENCES (USSR), MOSCOW.
Observational physics of mirror world
[NASA-CR-185923] N90-14076

ADMIRALTY RESEARCH ESTABLISHMENT, TEDDINGTON (ENGLAND).
Comparison of integral and finite-difference methods for predicting the turbulent boundary layer on axisymmetric bodies
[ARE-TM(UHA)-88512] N90-13752
Ring source/force excitation of axisymmetric shell structure
[ARE-TM(UHA)-88519] N90-14085

ADVANCED STRUCTURES TECHNOLOGY, INC., PHOENIX, AZ.
Development of an advanced fan blade containment system
[DOT/FAA/CT-89/20] N90-13386

ADVISORY GROUP FOR AEROSPACE RESEARCH AND DEVELOPMENT, NEUILLY-SUR-SEINE (FRANCE).
The human factors relating to escape and survival from helicopters ditching in water
[AGARD-AG-305(E)] N90-13358

AEROJET TECHSYSTEMS CO., SACRAMENTO, CA.
Space Transportation Engine Program (STEP). Phase B: Project study and management plan-ingredients for STEP success
[NASA-CR-183770] N90-13585

AERONAUTICAL RESEARCH LABS., MELBOURNE (AUSTRALIA).
A slow strain-rate tensile testing machine
[ARL-MAT-TM-399] N90-13764
A counter gating circuit for acoustic emission monitoring of structures cracking under repetitive alternating loads
[ARL-MAT-TM-398] N90-13808

AIR FORCE ARMAMENT LAB., EGLIN AFB, FL.
An autopilot design methodology for bank-to-turn missiles
[AD-A213379] N90-13399

AIR FORCE AVIONICS LAB., WRIGHT-PATTERSON AFB, OH.
Transonic Euler solutions on mutually interfering finned bodies
[AD-A213395] N90-13331

AIR FORCE GEOPHYSICS LAB., HANSCOM AFB, MA.
An evaluation of the Smith-Feddes model
[AD-A213237] N90-13907

AIR FORCE OFFICE OF SCIENTIFIC RESEARCH, BOLLING AFB, WASHINGTON, DC.
AFOSR technical report summaries
[AD-A213148] N90-14142

AIR FORCE SPACE TECHNOLOGY CENTER, EDWARDS AFB, CA.
Proceedings of the High Energy Density Matter (HEDM) Conference
[AD-A212314] N90-13670

AIR FORCE SYSTEMS COMMAND, KIRTLAND AFB, NM.
Control of optical systems N90-13484

AIR FORCE WEAPONS LAB., KIRTLAND AFB, NM.
Generation of iodine monofluoride in a supersonic multipurpose flowtube facility
[AD-A213082] N90-13774

AIR FORCE WRIGHT RESEARCH AND DEVELOPMENT CENTER, WRIGHT-PATTERSON AFB, OH.
Conference Proceedings of the Human-Electronic Crew: Can They Work Together
[AD-A211871] N90-13936

AIRESEARCH MFG. CO., LOS ANGELES, CA.
Advanced energy system program
[PB89-235170] N90-13887

AIX-MARSEILLES UNIV. (FRANCE).
Low speed hot and cold wire techniques for unsteady flow N90-13342
Hot and cold wire applications in supersonic flows: Introductory notes N90-13343
Laser applications in supersonic unsteady flow N90-13344

ALABAMA A & M UNIV., NORMAL.
Elementary and middle school science improvement project
[NASA-CR-183768] N90-14125

ALABAMA UNIV., HUNTSVILLE.
Software development for avionics SSME control and diagnostics
[NASA-CR-184894] N90-13964
Methodology for automating software systems. Task 1 of the foundations for automating software systems
[NASA-CR-180499] N90-13965
Applications of artificial intelligence to space station and automated software techniques: High level robot command language
[NASA-CR-182997] N90-13991
Optical properties monitor: Experiment definition phase
[NASA-CR-183836] N90-14092
Action languages: Dimensions, effects
[NASA-CR-183388] N90-14181

ALASKA UNIV., FAIRBANKS.
Crustal structure studies utilizing earthquake sequences
[AD-A212916] N90-13895

ALLGEMEINE ELEKTRIZITAETS-GESELLSCHAFT, ULM (GERMANY, F.R.).
Development of a traveling wave tube for the project X-SAR. Construction and testing of a breadboard model
[ETN-90-95900] N90-13713

ALLIED-SIGNAL AEROSPACE CO., PHOENIX, AZ.
Advanced Turbine Technology Applications Project (ATTAP)
[NASA-CR-185109] N90-14153

ALLIED-SIGNAL AEROSPACE CO., TORRANCE, CA.
Space station gas compressor technology study program, phase 1
[NASA-CR-183758] N90-13491

ANACAPA SCIENCES, INC., FORT RUCKER, AL.
Human factors research in aircrew performance and training
[AD-A213285] N90-13938

ARIZONA STATE UNIV., TEMPE.
Navier-Stokes simulation of the crossflow instability in swept-wing flows
[NASA-CR-186122] N90-13744
Unsteady forces induced on finite-span cylinders in a cross-flow N90-13746
The photovoltaic properties of an Al In As/InP heterojunctions grown by LPE method
[NASA-CR-185996] N90-13886

ARIZONA UNIV., TUCSON.
Influence of vane sweep on rotor-stator interaction noise N90-13325
Low temperature optical testing of CFRP telescope panels N90-13463
Development of FIR arrays with integrating amplifiers N90-13473
SiO overcoating and polishing of CFRP telescope panels N90-13478
Three-meter balloon-borne telescope N90-13490
Free swimming organisms: Microgravity as an investigative tool N90-13949

ARMY AEROMEDICAL RESEARCH LAB., FORT RUCKER, AL.
Evaluation of speech intelligibility through a bone conduction stimulator
[AD-A212002] N90-13919

ARMY AVIATION ENGINEERING FLIGHT ACTIVITY, EDWARDS AFB, CA.
Preliminary airworthiness evaluation of the AH-64A equipped with the Air To Air Stinger (ATAS) missile system
[AD-A213030] N90-13374

ARMY AVIATION RESEARCH AND DEVELOPMENT COMMAND, CLEVELAND, OH.
A planar reacting shear layer system for the study of fluid dynamics-combustion interaction
[NASA-TM-102422] N90-13393
Liquid water content and droplet size calibration of the NASA Lewis Icing Research Tunnel
[NASA-TM-102447] N90-13797

ARMY AVIATION SYSTEMS COMMAND, CLEVELAND, OH.
An investigation of gear mesh failure prediction techniques
[NASA-TM-102340] N90-13785

ARMY AVIATION SYSTEMS COMMAND, MOFFETT FIELD, CA.
Correlation of Puma airloads: Lifting-line and wake calculation
[NASA-TM-102212] N90-13327

ARMY CONSTRUCTION ENGINEERING RESEARCH LAB., CHAMPAIGN, IL.
Electromagnetic wave propagation through circular waveguides containing radially inhomogeneous lossy media
[AD-A213062] N90-13688

ARMY LAB. COMMAND, WATERTOWN, MA.
Studies of Aflas fluoroelastomers
[AD-A213046] N90-13622
Mechanical property characterization of VascoMax T-300
[AD-A212950] N90-13637
The effect of composition and aging treatment on the microstructure and mechanical properties of aluminum-lithium-titanium alloys
[AD-A213144] N90-13640

ARMY MILITARY PERSONNEL CENTER, ALEXANDRIA, VA.
Current management for improved railgun performance
[AD-A212887] N90-13445

ARMY TANK-AUTOMOTIVE COMMAND, WARREN, MI.
User's manual for the ride motion simulator
[AD-A212855] N90-13402

ASTRO AEROSPACE CORP., SANTA BARBARA, CA.
Hybrid deployable support truss designs for LDR N90-13485

AUBURN UNIV., AL.
Simulation of spacecraft attitude dynamics using TREETOPS and model-specific computer Codes N90-13419
The development of a program analysis environment for Ada
[NASA-CR-185860] N90-13962

AURORAL OBSERVATORY, TROMSO (NORWAY).
Background electrodynamics measured by EISCAT during the NEED campaign N90-13851

AVCO-EVERETT RESEARCH LAB., MA.
Theory of stagnation point heat transfer in dissociated air N90-13337

B

BALLISTIC RESEARCH LABS., ABERDEEN PROVING GROUND, MD.
The mobile combustion diagnostic fixture and its application to the study of propellant combustion. Part 1: Investigation of the low pressure combustion of LOVA XM39 propellant
[AD-A213272] N90-13626
Program transformation with abstract relation algebras
[AD-A213270] N90-14011
BERN UNIV. (SWITZERLAND).
A double focusing mass-spectrometer for simultaneous ion measurements in the stratosphere N90-13848
BOEING AEROSPACE CO., SEATTLE, WA.
Effects of joints in truss structures N90-13486
BONN UNIV. (GERMANY, F.R.).
Near-mesopause temperatures at 69 N latitude in late summer N90-13837
Interzodiak 2: Observation of EUV-resonance radiation N90-13854
Neutral air turbulence in the middle and upper atmosphere observed during the MAC/EPSILON campaign N90-13855
Optical observations of interplanetary pick-up ions: The experiment Helly N90-13863
Observation of the solar Lyman-alpha line N90-13868
Diurnal variation of the sodium layer at polar latitudes in summer N90-13869
BOSTON UNIV., MA.
Auroral and sub-auroral interaction at the F region ionosphere
[AD-A213284] N90-13896
BRITISH AEROSPACE PUBLIC LTD. CO., BRISTOL (ENGLAND).
The Skylark sounding rocket program and future launcher developments by British Aerospace (Space Systems) Ltd. N90-13871
BRITISH PETROLEUM CO. LTD., LONDON (ENGLAND).
Wear-resistant coated object
[EP-PATENT-0-289-173-A1] N90-13643
Process for producing a shaped, extruded product from a crosslinkable polymeric composition
[GB-PATENT-2-201-677-A] N90-13662
Crosslinkable polymer
[GB-PATENT-2-205-846-A] N90-13663
Novel carbamates, their production and their use as fuels additives
[EP-PATENT-0-298-636-A-1] N90-13676
Memory matrix
[WO-PATENT-88/04096] N90-13961
Optical modulators based on polymers
[EP-PATENT-0-294-061-A1] N90-14099
BROWN UNIV., PROVIDENCE, RI.
Ductile failure
[AD-A212975] N90-13601
BRUNEL UNIV., UXBRIDGE (ENGLAND).
Scalar transport in turbulent shear flows N90-13734
BUREAU OF RECLAMATION, DENVER, CO.
Applied atmospheric resources research program in Thailand
[PB89-235402] N90-13903

C

CALIFORNIA INST. OF TECH., PASADENA.
Reorganization free energy for electron transfers at liquid-liquid and dielectric semiconductor-liquid interfaces
[AD-A212985] N90-14111
CALIFORNIA UNIV., BERKELEY.
Far-infrared heterodyne receivers N90-13465
Computational and psychophysical study of human vision using neural networks
[AD-A213290] N90-13924
CALIFORNIA UNIV., DAVIS.
An experimental analysis of the waveguide modes in a high-gain free-electron laser amplifier N90-13779
Gravity and animal embryos N90-13951
CALIFORNIA UNIV., IRVINE.
Pilot investigation of indoor-outdoor and personal PM10 (thoracic) and associated ionic compounds and mutagenic activity
[PB89-222723] N90-13920
CALIFORNIA UNIV., LOS ANGELES.
Diffraction, chopping, and background subtraction for LDR N90-13476
On-line range prediction system, part 2
[NASA-CR-185889] N90-13771
CALIFORNIA UNIV., SAN DIEGO.
Field-effect spectroscopy of interface states
[AD-A212996] N90-14112
CALIFORNIA UNIV., SAN DIEGO, LA JOLLA.
The problem of automation: Inappropriate feedback and interaction, not overautomation
[NASA-CR-186126] N90-13994
CAMBRIDGE UNIV. (ENGLAND).
An introduction via vorticity dynamics and statistical theory N90-13731
CARNEGIE-MELLON UNIV., PITTSBURGH, PA.
Gas identification system using graded temperature sensor and neural net interpretation
[AD-A213359] N90-13627
The economic impact of automation technology
[AD-A213363] N90-13682
Design and control of a two-degree-of-freedom lightweight flexible arm
[AD-A213335] N90-13790
Acceleration sets of planar manipulators. Part 2: Applications and experiments
[AD-A213336] N90-13791
A new approach to control single-link flexible arms. Part 3: Adaptive control of the tip position with payload changes
[AD-A213337] N90-13792
Definition, determination and characterization of acceleration sets for spatial manipulators
[AD-A213366] N90-13793
ERIS: Engineering Resource Information System
[AD-A213357] N90-14144
CASE WESTERN RESERVE UNIV., CLEVELAND, OH.
Preparation of 110K (Bi, Pb)-Sr-Ca-Cu-O superconductor from glass precursor
[NASA-CR-185162] N90-14108
CENTER FOR MATHEMATICS AND COMPUTER SCIENCE, AMSTERDAM (NETHERLANDS).
The structural memory: A network model for human perception of serial objects
[CWI-CS-R8829] N90-13930
On the safe approximation of PROLOG programs
[CWI-CS-R8913] N90-13978
Constructing a calculus of programs
[CWI-CS-R8914] N90-13979
Waiting times in polling systems with Markovian server routing
[CWI-BS-R8905] N90-13989
On the nonexistence of a strong solution in the boundary problem for a sticky Brownian motion
[CWI-BS-R8901] N90-14018
Monotonicity of performance measures in a processor sharing queue
[CWI-BS-R8902] N90-14019
Workloads and waiting times in single-server systems with multiple customer classes
[CWI-BS-R8906] N90-14020
Random Markov processes and uniform martingales
[CWI-BS-R8908] N90-14021
Linear groups and distance-transitive graphs
[CWI-PM-R8805] N90-14036
On distance-transitive graphs and involutions
[CWI-PM-R8808] N90-14037
Theory of goodness of fit tests and scanning innovation martingales
[CWI-BS-R8904] N90-14046
Simple approximations for second moment characteristics of the sojurn time in the M/G/1 processor sharing queue
[CWI-BS-R8907] N90-14055
Inductive reasoning and Kolmogorov complexity (preliminary version)
[CWI-CS-R8915] N90-14062
A graph theoretic characterization for the rank of the transfer matrix of a structured system
[CWI-OS-R8819] N90-14064
The algebraic basis of mathematical morphology. Part 1: Dilations and erosions
[CWI-AM-R8807] N90-14065
CENTRE D'ESSAIS AERONAUTIQUE TOULOUSE (FRANCE).
Nondestructive analysis of aileron fatigue and aging in a Mirage F1
[REPT-M6-594000] N90-13378
Impact tests of three composite materials with carbon fiber cores
[REPT-M6-582500] N90-13610
CENTRE D'ETUDE SPATIALE DES RAYONNEMENTS, TOULOUSE (FRANCE).
Interstellar medium and infrared emission of the galactic disk N90-13862
CENTRE D'ETUDES ET DE RECHERCHES, TOULOUSE (FRANCE).
Skin friction measurements with hot elements N90-13345
Application of two-point closures to subgrid scale modeling for homogeneous, 3D turbulence N90-13732
CENTRE D'ETUDES ET DE RECHERCHES DE MEDECINE AEROSPATIALE, PARIS (FRANCE).
Preliminary study of pharmacological control of space disease
[ETN-90-95015] N90-13927
CENTRE DE RECHERCHES SCIENTIFIQUES ET TECHNIQUES DE L'INDUSTRIE DES FABRICATIONS METALLIQUES, BRUSSELS (BELGIUM).
Activities report of the metallic manufacturing industry
[ISSN-0524-7705] N90-13649
Theoretical evaluation of defects in pressure vessels and pipings
[CRIF-MT-174] N90-13798
Fatigue resistance of pressure vessels in high strength steels effect of some improvement techniques
[CRIF-MT-176] N90-13799
Considerations about the acceptance inspection of HS fasteners intended for controlled tightening
[CRIF-MT-175] N90-13808
CENTRE NATIONAL D'ETUDES SPATIALES, TOULOUSE (FRANCE).
Choice of a differential method for the attitude restitution in dynamic unbalance
[CNES-CT/DTI/MS/CM/290] N90-13582
Operational activity in France and a new method of balloon temperature piloting N90-13857
Large heavy duty balloons in Europe N90-13858
Long duration balloon flights in the middle stratosphere N90-13874
CENTRE NATIONAL DE LA RECHERCHE SCIENTIFIQUE, DIJON (FRANCE).
Surfaces and interfaces of ceramic materials
[AD-A212417] N90-13657
CENTRE NATIONAL DE LA RECHERCHE SCIENTIFIQUE, PARIS (FRANCE).
The French balloon program and related space research N90-13828
CENTRO INFORMAZIONI STUDI ESPERIENZE, MILAN (ITALY).
Outline on the future Italian transportable laser ranging station
[CISE-4845] N90-13782
CENTRO TECNICO AEROSPACIAL, SAN JOSE DOS CAMPOS (BRAZIL).
Qualification of the 4th stage propulsor of the Brazilian launcher. SLV: A new sounding rocket N90-13860
The Brazilian space program: Actual state of the art N90-13861
CESKOSLOVENSKA AKADEMIE VED, PRAGUE.
Hot spots Ar and Ne gas puff z-pinch
[IPPCZ-289] N90-14103
CHICAGO UNIV., IL.
A new model for the structure of silica glass
[AD-A212972] N90-13659
Cosmology and the weak interaction
[NASA-CR-186170] N90-14169
CINCINNATI UNIV., OH.
Mechanisms in reactive ion etching of silicon carbide thin films
[AD-A213018] N90-13700
CLEMSON UNIV., SC.
Sufficiency and necessity in reliability modeling
[NASA-CR-186119] N90-13706
COCKERHAM (JOHN M.) AND ASSOCIATES, INC., HUNTSVILLE, AL.
Optical properties monitor: Experiment definition phase
[NASA-CR-183836] N90-14092
COLEG PRIFYSGOL CYMRU, ABERYSTWYTH (WALES).
Polar mesosphere summer echoes and associated atmospheric gravity waves N90-13856
COLORADO STATE UNIV., FORT COLLINS.
Fermentation and oxygen transfer in microgravity N90-13956
COLORADO UNIV., BOULDER.
Countermeasures to microgravity N90-13957
Studies of structure and switching dynamics in ferroelectric crystal and liquid crystal thin films
[AD-A212650] N90-14109
COMMITTEE ON COMMERCE, SCIENCE, AND TRANSPORTATION (U.S. SENATE).
National Aeronautics and Space Administration Multiyear Authorization Act of 1989 N90-14148
National Aeronautics and Space Administration authorization
[S-HRG-101-348] N90-14149
COMPUTATIONAL MECHANICS CO., AUSTIN, TX.
SSME LOX post flow analysis/fluid structure interaction. Volume 2: Fluid structure interaction
[NASA-CR-183678] N90-13716
COMPUTER SCIENCES CORP., SILVER SPRING, MD.
The effects of seasonal and latitudinal earth infrared radiance variations on ERBS attitude control N90-13414
COBE nonspinning attitude propagation N90-13418

GOES I/M image navigation and registration N90-13422
Temperature dependence of attitude sensor coalignments on the Solar Maximum Mission (SMM) N90-13426
Analysis of the flight dynamics of the Solar Maximum Mission (SMM) off-sun scientific pointing N90-13432
Calculation of double-lunar swingby trajectories: I. Keplerian foundation N90-13435
Active rendezvous between a low-earth orbit user spacecraft and the Space Transportation System (STS) shuttle N90-13436
Atmospheric drag model calibrations for spacecraft lifetime prediction N90-13439

CONNECTICUT UNIV., FARMINGTON.
Generation of free radicals during cold injury and rewarming
[AD-A213088] N90-13915

CONTROL DATA CORP., MINNEAPOLIS, MN.
The interaction and variation of waves and turbulence from MST radar data
[AD-A212849] N90-13906

CORNELL UNIV., ITHACA, NY.
The infrared spectrograph during the SIRTF pre-definition phase
[NASA-CR-183234] N90-13759

COUNCIL FOR NATIONAL ACADEMIC AWARDS (ENGLAND).
The use of digital signal processing in satellite communication N90-13684

CRANFIELD INST. OF TECH., BEDFORD (ENGLAND).
On the application of modified stepwise regression for the estimation of aircraft stability and control parameters
[REPT-8905] N90-13400

D

DAYTON UNIV., OH.
Study of the engine bird ingestion experience of the Boeing 737 aircraft
[DOT/FAA/CT-89/16] N90-13360
Probabilistic finite element analysis of dynamic structural response
[AD-A213249] N90-13789
Stress intensity factors for cracking metal structures under rapid thermal loading. Volume 2: Theoretical background
[AD-A213297] N90-13812

DEFENCE AND CIVIL INST. OF ENVIRONMENTAL MEDICINE, DOWNSVIEW (ONTARIO).
A prototype microprocessor based audiometer for use by the CF (Canadian Forces) medical services for periodic hearing tests
[AD-A212990] N90-13921
The relationship between subjective and objective measures of simulator-induced ataxia
[AD-A213095] N90-13922
Simulator induced sickness in the CP-140 (Aurora) flight deck simulator
[AD-A213096] N90-13923
Test procedures for the evaluation of helmet and headset mounted active noise reduction systems
[AD-A212991] N90-13937

DEFENCE RESEARCH ESTABLISHMENT PACIFIC, VICTORIA (BRITISH COLUMBIA).
First-order Bragg SAR imagery of Kelvin wakes and moving internal wave fields
[AD-A213361] N90-13691

DEFENCE RESEARCH ESTABLISHMENT SUFFIELD, RALSTON (ALBERTA).
Recovery of particle size distribution of ultrafine aerosols from diffusional decay measurements
[AD-A213006] N90-13621

DEFENSE LOGISTICS AGENCY, ALEXANDRIA, VA.
Total quality management implementation strategy: Directorate of Quality Assurance
[AD-A212863] N90-14127
Total quality management plan: Technical and logistics services
[AD-A212864] N90-14128
Total quality management implementing plan: Office of small and disadvantaged business utilization
[AD-A212865] N90-14129
Total quality management plan: Office of Congressional Affairs
[AD-A212866] N90-14130
Total quality management: Directorate of Contract Management master plan
[AD-A212867] N90-14131
Total quality management plan: Office of Public Affairs
[AD-A212868] N90-14132

DEFENSE TECHNICAL INFORMATION CENTER, ALEXANDRIA, VA.
The DOD Gateway Information System: Operational prototype and transition period 1987-1988
[AD-A213044] N90-14141

DEPARTMENT OF THE NAVY, WASHINGTON, DC.
Apparatus for cooling electronic components in aircraft
[AD-D014207] N90-13373

DEUTSCHE FORSCHUNGS- UND VERSUCHSANSTALT FUER LUFT- UND RAUMFAHRT, COLOGNE (GERMANY, F.R.).
Laser two focus techniques N90-13348

DEUTSCHE FORSCHUNGS- UND VERSUCHSANSTALT FUER LUFT- UND RAUMFAHRT, OBERPFAFFENHOFEN (GERMANY, F.R.).
The SN 1987A attitude control system N90-13845

DEUTSCHE FORSCHUNGS- UND VERSUCHSANSTALT FUER LUFT- UND RAUMFAHRT, STUTTGART (GERMANY, F.R.).
Microwave excited excimer laser
[ETN-90-95909] N90-13781

DEUTSCHE FORSCHUNGSANSTALT FUER LUFT- UND RAUMFAHRT, BRUNSWICK (GERMANY, F.R.).
Computation of flow fields around propellers and hovering rotors based on the solution of the Euler equations
[DLR-FB-89-37] N90-13333
Thermal protection systems for reentry and hypersonic flight
[DLR-MITT-89-14] N90-13577
Measuring of the complete stiffness matrix for anisotropic laminated materials
[DLR-MITT-89-11] N90-13606
Measuring of the complete stiffness matrix for anisotropic laminated materials
[DLR-MITT-89-12] N90-13607
Containerless Processing of Metals: Undercooling and Solidification
[DLR-MITT-89-15] N90-13645
Calculation of flow fields by the solution of the Euler equations using an extended finite volume discretization scheme
[DLR-FB-89-38] N90-13729
General buckling tests with thin-walled shells
[DLR-MITT-89-13] N90-13816

DEUTSCHE FORSCHUNGSANSTALT FUER LUFT- UND RAUMFAHRT, COLOGNE (GERMANY, F.R.).
Nucleation kinetics in undercooled, glass-forming metallic melts
[DLR-FB-89-32] N90-13644
Threshold for fatigue crack propagation
[DLR-FB-89-33] N90-13815
The German scientific balloon and sounding rocket program N90-13831
SOFIA (Stratospheric Observatory For Infrared Astronomy): A 3m class airborne telescope N90-13846
The German space science program N90-13873

DEUTSCHE FORSCHUNGSANSTALT FUER LUFT- UND RAUMFAHRT, GOETTINGEN (GERMANY, F.R.).
The 3D LDA techniques in vortex studies and boundary layer surveys N90-13346
The influence of multiple hot-wire probe geometry on the results of measurements in turbulent flows
[DLR-FB-89-26] N90-13724
Generalized similarity solutions for three dimensional, laminar, steady, compressible boundary layer flows on swept profile cylinders
[DLR-FB-89-34] N90-13725
Numerical simulation of transition in three-dimensional boundary layers
[DLR-FB-89-12] N90-13728

DEUTSCHE FORSCHUNGSANSTALT FUER LUFT- UND RAUMFAHRT, OBERPFAFFENHOFEN (GERMANY, F.R.).
A stochastic model for the calculation of multiple scattered lidar returns
[DLR-FB-89-36] N90-13778
The use of LANDSAT-TM data for the management of pine forestations in central Chile
[DLR-FB-89-44] N90-13881
Reflection indicatrices of natural surfaces for AVHRR channels 1 and 2
[DLR-MITT-89-16] N90-13882

DEUTSCHE FORSCHUNGSANSTALT FUER LUFT- UND RAUMFAHRT, STUTTGART (GERMANY, F.R.).
Gas evolution and bubble formation on electrodes
[DLR-FB-89-35] N90-13629

DIAMOND MATERIALS, INC., STATE COLLEGE, PA.
Novel in situ spectroscopic ellipsometer for real time analysis of CVD diamond films
[AD-A213218] N90-13762

DORNIER SYSTEM G.M.B.H., FRIEDRICHSHAFEN (GERMANY, F.R.).
Design and technical aspects of the Solly instrument N90-13847

DOUGLAS AIRCRAFT CO., INC., LONG BEACH, CA.
Study of high-speed civil transports
[NASA-CR-4235] N90-13370

DREXEL UNIV., PHILADELPHIA, PA.
Big Bang nucleosynthesis and the Quark-Hadron transition
[NASA-CR-186169] N90-14168

DYNAMIC CONTROLS, INC., DAYTON, OH.
Advanced actuation systems development, volume 2
[AD-A213378] N90-13306

E

EASTMAN KODAK CO., ROCHESTER, NY.
Coherent phasing of segmented mirrors N90-13474

ECOLE CENTRALE DE LYON (FRANCE).
Study of fatigue degradation mechanisms in unidirectional composite materials. Application to cumulative damage
[ECL-88-12] N90-13611
Contribution to the fatigue behavior study of composite materials reinforced with unidirectional glass fibers
[ECL-88-20] N90-13612
Implementation and analysis of adhesion in multimaterials of the type Al(Si)-ZrO2 and graphite, metal or ceramics
[ECL-89-004] N90-13667
Elaboration and characterization of MISFET transistors on InP
[ECL-88-19] N90-13709
Design of a power component with IGBT insulated grid. Static and dynamic study
[ECL-88-22] N90-13710
Contribution to the study of a self-protected static switch and its command strategy
[ECL-89-002] N90-13711
Spectral study of a compressible isotropic turbulence
[ECL-88-16] N90-13753
Large eddy simulation of homogeneous turbulence undergoing shear and thermal gradients. Application to one point closing models
[ECL-88-23] N90-13754
Model and computation of three-dimensional turbulent jets in a crossflow
[ECL-89-007] N90-13755
The limiting friction force
[ECL-89-005] N90-13801
Identification of equivalent modulus of a composite beam from nonmodal vibratory tests
[ECL-89-001] N90-13821
A model suitable for predicting the noise associated with the ducted tail rotor of a helicopter
[ECL-88-09] N90-14074
A mixed finite element solution of the linear acoustic equations
[ECL-89-006] N90-14075
Study of metal-insulator-semiconductor structures on indium phosphide, implemented by anodic oxidation
[ECL-88-10] N90-14114
Manufacturing and characterization of insulator-germanium structures
[ECL-88-13] N90-14115
Study of surface uniformity of semiconductors 3 to 5 by photoluminescence imagery
[ECL-88-15] N90-14116
Photoelectrochemical behavior of type n of GaAs in concentrated iodide media and realization of an experimental device
[ECL-88-18] N90-14117
GaAs and GaAs:In: Influence of surface treatments and characterization of homogeneity by photoluminescent imagery
[ECL-88-24] N90-14118

ENDOCHRONICS, INC., VANCOUVER, WA.
A theory of damage in brittle and cementitious materials, part 1
[AD-A212940] N90-13658

ENVIRONMENTAL PROTECTION AGENCY, ANN ARBOR, MI.
MOBILE4 oxygenated fuels version user's guide
[PB89-230700] N90-13674

ENVIRONMENTAL PROTECTION AGENCY, RESEARCH TRIANGLE PARK, NC.
Proceedings: US/FRG (Federal Republic of Germany) Workshop on Photochemical Ozone Problem and Its Control: US Experiences and the Situation in Europe
[PB89-233514] N90-13891

ENVIRONMENTAL RESEARCH INST. OF MICHIGAN, ANN ARBOR.
Summaries of the thematic conferences on remote sensing for exploration geology
[NASA-CR-185321] N90-13880

ESDU INTERNATIONAL LTD., LONDON (ENGLAND).
Thermophysical properties of buta-1,3-diene
[ESDU-89005] N90-13619

ESSEN UNIV. (GERMANY, F.R.).
Practical systems for speckle velocimetry N90-13341
EUROPEAN SPACE AGENCY, PARIS (FRANCE).
The Hipparcos Mission. Prelaunch status. Volume 1: The Hipparcos satellite
[ESA-SP-1111-VOL-1] N90-13499
Operating principle N90-13500
Error allocation and accuracy assessment N90-13501
Overview of the Hipparcos satellite N90-13502
Overview of the Hipparcos payload N90-13503
The telescope mirrors N90-13504
The modulating grid N90-13505
The relay lens systems N90-13506
The detectors N90-13507
Payload electronics and mechanisms N90-13508
The baffles N90-13509
The payload structure N90-13510
Payload thermal control N90-13511
The spacecraft structure N90-13512
Spacecraft thermal control N90-13513
Data handling and telecommunications N90-13514
Power generation and distribution N90-13515
The attitude and orbit control system N90-13516
The apogee boost motor N90-13517
On-board software N90-13518
Assembly, integration, and verification N90-13519
Electrical testing N90-13520
Mechanical and thermal testing N90-13521
Product assurance N90-13522
On-ground photometric calibration N90-13523
Launch and early orbit N90-13524
The in-orbit initialization phase N90-13525
In-orbit payload calibration N90-13526
The role of the ground segment N90-13527
The interface with the data reduction consortia N90-13528
The Hipparcos Mission. Prelaunch status. Volume 2: The input catalog
[ESA-SP-1111-VOL-2] N90-13529
From scientific proposals to the Inca data base N90-13530
The Inca data base N90-13531
Mission simulations N90-13532
Proximity effects on adjacent and multiple stars N90-13533
Successive iterations of the input catalog N90-13534
Stellar content of the input catalog N90-13535
Ground-based astrometric measurements N90-13536
The compilation of astrometric data N90-13537
New ground-based photometric measurements N90-13538
Standard stars and photometric calibration N90-13539
Double stars N90-13540
Variable stars N90-13541
The choice of stars in open clusters N90-13542
The choice of stars in the Magellanic clouds N90-13543
The link to extragalactic objects N90-13544
Minor planets and other solar system objects N90-13545
The catalogs produced by the Inca consortium N90-13546
The SIMBAD data base N90-13547
The Hipparcos Mission. Prelaunch status. Volume 3: The data reductions
[ESA-SP-1111-VOL-3] N90-13548
Overview of the data acquisition and reductions N90-13549
Analysis of the image dissector tube data N90-13550
Analysis of the star mapper data N90-13551
On-ground attitude determination N90-13552
The great circle reductions N90-13553
Great circle interactions: Attitude smoothing and grid-step inconsistencies N90-13554
General and numerical approach to the sphere solution in FAST N90-13555
Astrometric parameter determination in FAST N90-13556
The sphere solution and astrometric parameter determination in NDAC N90-13557
Overview of the Tycho data analysis N90-13558
Tycho astrometry N90-13559
Photometry: Main mission and Tycho N90-13560
Double star reductions in NDAC N90-13561
Double star reductions in FAST N90-13562
The treatment of minor planets and planetary satellites N90-13563
Validation of the Hipparcos catalog N90-13564
Linking Hipparcos to a quasi-inertial system N90-13565
Accuracy and characteristics of the Hipparcos catalog N90-13566
Data processing in the FAST consortium N90-13567
Data processing in the NDAC consortium N90-13568
Great circle reductions: Implementation and simulations N90-13569
Implementation and simulations of the sphere solution in FAST N90-13570
The first-look data analysis at Utrecht N90-13571
Modeling of the Hipparcos optical system N90-13572
Data simulations in the fast consortium N90-13573
Data simulations in the NDAC consortium N90-13574
The Tycho input catalog N90-13575
Experiments towards a global sphere solution N90-13576
European Rocket and Balloon Programs and Related Research
[ESA-SP-291] N90-13826
Life science research in space
[ESA-SP-1105] N90-13917

F

FEDERAL AVIATION ADMINISTRATION, ATLANTIC CITY, NJ.
Study of the engine bird ingestion experience of the Boeing 737 aircraft
[DOT/FAA/CT-89/16] N90-13360
LORAN C stability integrity assurance
[AD-A212663] N90-13364
FERMI NATIONAL ACCELERATOR LAB., BATAVIA, IL.
On thick domain walls in general relativity
[NASA-CR-185926] N90-14124
Unitarity limits on the mass and radius of dark matter particles
[NASA-CR-186079] N90-14164
Nuclear physics and cosmology
[NASA-CR-186166] N90-14167
Big Bang nucleosynthesis and the Quark-Hadron transition
[NASA-CR-186169] N90-14168
Cosmology and the weak interaction
[NASA-CR-186170] N90-14169
The grand unified photon spectrum: A coherent view of the diffuse extragalactic background radiation
[NASA-CR-186077] N90-14180
FLORIDA ATLANTIC UNIV., BOCA RATON.
Mobility power flow analysis of an L-shaped plate structure subjected to acoustic excitation
[NASA-CR-186130] N90-13817

G

GELTECH, INC., ALACHUA, FL.
Sol-gel processing science using a Sol-Gel Optics Research Facility (SGORF)
[AD-A213056] N90-14095
GENERAL ACCOUNTING OFFICE, WASHINGTON, DC.
Electronic warfare: Reliable equipment needed to test Air Force's electronic warfare systems
[AD-A212952] N90-13687
GENERAL DYNAMICS CORP., SAN DIEGO, CA.
Definition of avionics concepts for a heavy lift cargo vehicle, appendix A
[NASA-CR-183817] N90-13380
GENERAL ELECTRIC CO., SCHENECTADY, NY.
Inviscid 3D solution methods N90-13736
Inviscid 2D solutions on unstructured, adaptive grids N90-13737
GENERAL RESEARCH CORP., MCLEAN, VA.
Expert systems for adaptive control of large space structures N90-13452
GENEVA OBSERVATORY (SWITZERLAND).
Swiss scientific balloon and sounding rocket experiments 1987-1989 N90-13827
GEORGIA INST. OF TECH., ATLANTA.
A technique for the prediction of aerodynamics and aeroelasticity of rotor blades N90-13377
Dynamic testing techniques and applications for an aeroelastic rotor test facility N90-13406
Adaptive strategies for controls of flexible arms
[NASA-CR-185866] N90-13783
True asymptotic plasma-sheath matching with an asymptotically correct collisional presheath
[AD-A212857] N90-14104
GRENOBLE-1 UNIV. (FRANCE).
Electron beam sensitive devices for controllability
[IMAG-RR-761-I] N90-13707
The use of a deformation model for sampling digitalized stereoscopic images
[IMAG-RR-753-I] N90-13884
Implementing the discrete Fourier transform on the hypercube FPS T40
[IMAG-RR-773-I] N90-13983
Measurement of arithmetic error and calculation perturbations
[IMAG-RR-767-M] N90-14039
Distribution of a sum of n random variables and a central limit theorem based on moments or on coefficients of polynomial dependence
[IMAG-RR-768-M] N90-14040
Description and manipulation of convex polygons using polarity
[IMAG-RR-771-M] N90-14041
Data structures for the representation and manipulation of polyhedrons
[IMAG-RR-772-M] N90-14042
Some quick and efficient methods for bearing-only target motion analysis
[IMAG-RR-762-M] N90-14049
GRONINGEN RIJKSUNIV. (NETHERLANDS).
The effective (3)He-nucleon force in a microscopic DWBA approach to the (3)He,t charge exchange reaction
[KVI-763] N90-14077

H

HAHN-MEITNER-INST. FUER KERNFORSCHUNG, BERLIN (GERMANY, F.R.).
Unified model of charge build up and annealing of oxide charge and interface states in SiO2 due to stress
[HMI-B-465] N90-14120
HAMPTON INST., VA.
Development of mid-infrared solid state lasers for spaceborne lidar
[NASA-CR-183290] N90-13772
HARRY DIAMOND LABS., ADELPHI, MD.
Elastic impurity scattering in double-barrier resonant tunneling structures
[AD-A212850] N90-14110
HARVARD UNIV., CAMBRIDGE, MA.
Joint Services Electronics Program
[AD-A213015] N90-13699
HEIDELBERG UNIV. (GERMANY, F.R.).
Computation of nonequilibrium gas flow past blunt bodies
[PREPRINT-488] N90-13757
HELSINKI UNIV. OF TECHNOLOGY, ESPOO (FINLAND).
Computational studies of structural and transport properties of amorphous solids
[ETN-90-96027] N90-13664
Parameter estimation for the Gummel-Poon transistor model
[MA-53] N90-13705
Modeling and measurement methods for high speed bipolar transistors
[REPT-11] N90-13714
Construction of the rotating cryostat ROTA2, its use for zero sound experiments in (3)He-B, and calculations of ion mobility in (3)He-A and (3)He-P
[ISBN-952-90091-3-5] N90-13765
HITEC PRODUCTS, INC., AYER, MA.
High temperature capacitive strain gage
[NASA-CR-4266] N90-13780
HOUSTON UNIV., CLEAR LAKE, TX.
Software engineering and Ada (Trademark) training: An implementation model for NASA
[NASA-CR-186071] N90-13966
Ada task scheduling: A focused Ada investigation
[NASA-CR-186072] N90-13967
Micro-based fact collection tool user's manual
[NASA-CR-180414] N90-13981
Ada programming guidelines for deterministic storage management
[NASA-CR-181308] N90-13982
HOUSTON UNIV., TX.
Database interfaces on NASA's heterogeneous distributed database system
[NASA-CR-185420] N90-14133
HOWARD UNIV., WASHINGTON, DC.
The dynamics and control of large flexible space structures - 12, supplement 11
[NASA-CR-185966] N90-13494
Attitude and shape control of optimally designed large space structures N90-13579
HULL UNIV. (ENGLAND).
Quantitative non-destructive evaluation using laser generated ultrasonic pulses N90-13805
HUMAN ENGINEERING LABS., ABERDEEN PROVING GROUND, MD.
Software and hardware description of the helicopter motion equations for VAX computers
[AD-A213248] N90-13375

I

ILLINOIS UNIV. AT URBANA-CHAMPAIGN, SAVOY.
Orion B: Anatomy of a star-forming region N90-14155

ILLINOIS UNIV., URBANA.
Bilinear modeling and nonlinear estimation N90-13430
Effect of adsorbed arsenic on the decomposition rate of nickel hydride [AD-A213245] N90-13624
Anomalous strain rate dependence of the serrated flow in Ni-H and Ni-C-H alloys [AD-A213244] N90-13641
An accurate timing model for fault simulation in MOS circuits [AD-A213153] N90-13702
Arc current control of a robotic welding system: Modeling and control system design [AD-A213150] N90-13788
Efficient on-line simulations of tree machines and multidimensional turing machines by random access machines [AD-A213152] N90-13960
A multilevel parallel solver for block tridiagonal and banded linear systems [AD-A213151] N90-14008
Identification of impulsive interference channels [AD-A213154] N90-14009

IMPERIAL COLL. OF SCIENCE AND TECHNOLOGY, LONDON (ENGLAND).
The adhesive bonding of thermoplastic composites [AD-A213358] N90-13605

INDIANA UNIV.-PURDUE UNIV., INDIANAPOLIS.
Block-structured solution of three-dimensional transonic flows using parallel processing [AD-A212851] N90-13330

INSTITUT D'AERONOMIE SPATIALE DE BELGIQUE, BRUSSELS.
A summary of 30 years of space launches [AERONOMICA-ACTA-F-39-1989] N90-13411
Ultraviolet absorption cross-sections of bromoform in the temperature range 295-240 K [AERONOMICA-ACTA-A-348-1989] N90-13630
Observations of stratospheric HCl: 1975-1985 [AERONOMICA-ACTA-A-349-1989] N90-13892
Climate predictability: A dynamical view [AERONOMICA-ACTA-A-347-1989] N90-13909
An iterative method to solve the nonlinear Poisson's equation in the case of plasma tangential discontinuities [AERONOMICA-ACTA-A-346-1989] N90-14045

INSTITUT DE MECANIQUE DE GRENOBLE (FRANCE).
Coherent structures in a round jet N90-13733

INSTITUT DE MECANIQUE DES FLUIDES DE LILLE (FRANCE).
Reduction of profile drag by modifying the structure next to the wake area [IMFL-88/35] N90-13356

INSTITUT NATIONAL DES SCIENCES APPLIQUEES DE LYON, VILLEURBANNE (FRANCE).
Contribution to the electrochemical study of corrosion in the low conductivity media: Application to the study of the behavior of austenitic stainless steels in concentrated solutions of acetic acid [ISAL-89-0014] N90-13648
Characterization of surfaces cut with a laser beam and thermal model of the process [ISAL-89-0008] N90-13780
Evolution of the EPR procedure for polycrystalline Si ribbon drawing for photovoltaic cell manufacturing [ISAL-89-0027] N90-13888

INSTITUT NATIONAL POLYTECHNIQUE, GRENOBLE (FRANCE).
Research on the controllability of integrated circuits by means of electron beams [ETN-90-95710] N90-13708

INSTITUTE FOR COMPUTER APPLICATIONS IN SCIENCE AND ENGINEERING, HAMPTON, VA.
Optimum shape of a blunt forebody in hypersonic flow [NASA-CR-181955] N90-13351
Multiple paths to subharmonic laminar breakdown in a boundary layer [NASA-CR-181948] N90-13722
Computational aspects of pseudospectral Laguerre approximations [NASA-CR-181934] N90-14038

INSTITUTE FOR PERCEPTION RVO-TNO, SOESTERBERG (NETHERLANDS).
Speech reception in quiet and in noisy conditions by individuals with noise-induced hearing loss in relation to their audiogram [IZF-1989-11] N90-13692

IOWA STATE UNIV. OF SCIENCE AND TECHNOLOGY, AMES.
Simulation of the control characteristics of an axial piston pump and a flapper-nozzle valve combination N90-13784

IOWA UNIV., IOWA CITY.
Dynamics Explorer-1 satellite study of electrostatic ion cyclotron waves N90-14105

J

JET PROPULSION LAB., CALIFORNIA INST. OF TECH., PASADENA.
The Voyager Neptune travel guide [NASA-CR-186108] N90-13412
Report of the Asilomar 3 LDR Workshop [NASA-CR-184656] N90-13449
Introduction to the report of the Asilomar 3 LDR workshop N90-13450
A figure control sensor for the Large Deployable Reflector (LDR) N90-13451
Pointing control for LDR N90-13453
Wavefront error sensing for LDR N90-13455
Composite panel development at JPL N90-13458
Large Deployable Reflector (LDR) thermal characteristics N90-13460
Lightweight composite reflector panels N90-13462
Advances in SIS receiver technology N90-13466
Spectrometer technology recommendations N90-13468
Cryogenic systems for the large deployable reflector N90-13470
Effect of central obscuration on the LDR point spread function N90-13475
A laboratory verification sensor N90-13477
LDR structural technology activities at JPL N90-13488
Performance evaluation of a six-axis generalized force-reflecting teleoperator [NASA-CR-186106] N90-13796
A high-resolution atlas of the infrared spectrum of the Sun and the Earth atmosphere from space: A compilation of ATMOS spectra of the region from 650 to 4800 cm (2.3 to 16 micron). Volume 1: The Sun [NASA-RP-1224-VOL-1] N90-13893
Model system studies with a phase separated membrane bioreactor N90-13954
Design challenges for space bioreactors N90-13955
Use of a krypton isotope for rapid ion changeover at the Lawrence Berkeley Laboratory 88-inch cyclotron [NASA-CR-186107] N90-14084

JOHNS HOPKINS UNIV., BALTIMORE, MD.
Optical communication with semiconductor laser diode [NASA-CR-185886] N90-13770

JOHNS HOPKINS UNIV., LAUREL, MD.
Autonomous spacecraft attitude control using magnetic torquing only N90-13415

K

KANSAS UNIV. CENTER FOR RESEARCH, INC., LAWRENCE.
Aerodynamics of thrust vectoring [NASA-CR-185074] N90-13354

KERNFORSCHUNGSANLAGE, JUELICH (GERMANY, F.R.).
Preparation of binary ice layers by condensation from gas phase [JUEL-2248] N90-13631

KERNFORSCHUNGSZENTRUM G.M.B.H., KARLSRUHE (GERMANY, F.R.).
Correlation between microstructure and magnetic properties of porous sintered iron and porous iron containing composites [KFK-4522] N90-13647
Development and testing of a contactless static/dynamic shaft seal with little sealing gas requirement [KFK-4599] N90-13802

KIEL UNIV. (GERMANY, F.R.).
Resonance cone diagnostics in the mid-latitude ionosphere N90-13840

L

LABORATOIRE D'ASTRONOMIE SPATIALE, MARSEILLE (FRANCE).
Deep detection of hot star populations at balloon ultraviolet wavelengths N90-13865

LABORATOIRE DE METEOROLOGIE DYNAMIQUE DU CNRS, PALAISEAU (FRANCE).
Humidity local measurements in the middle atmosphere N90-13833

LAGOS UNIV. (NIGERIA).
Application of multi-grid methods for solving the Navier-Stokes equations [NASA-TM-102359] N90-14002

LIFE SYSTEMS, INC., CLEVELAND, OH.
Refurbishment of one-person regenerative air revitalization system [NASA-CR-183757] N90-13934

LNK CORP., RIVERDALE, MD.
Novel graph searching methods for image analysis [AD-A213065] N90-13971

LOCKHEED MISSILES AND SPACE CO., HUNTSVILLE, AL.
SSME LOX post flow analysis/fluid structure interaction. Volume 1: Flow analysis [NASA-CR-183677] N90-13715
SSME LOX post flow analysis/fluid structure interaction. Volume 2: Fluid structure interaction [NASA-CR-183678] N90-13716

LOCKHEED MISSILES AND SPACE CO., PALO ALTO, CA.
Segment alignment control system N90-13457
LDR cryogenics N90-13472

LOCKHEED MISSILES AND SPACE CO., SUNNYVALE, CA.
Space telescope pointing control N90-13454
Human factors issues in performing life science experiments in a 0-G environment N90-13952

LOMA LINDA UNIV., CA.
The sensory transduction pathways in bacterial chemotaxis N90-13944

LOUGHBOROUGH UNIV. OF TECHNOLOGY (ENGLAND).
Aircraft/airport compatibility: Some strategic, tactical, and operational issues [TT-8902] N90-13409

LOUISVILLE UNIV., KY.
Response of lymphocytes to a mitogenic stimulus during spaceflight N90-13942

LOWELL OBSERVATORY, FLAGSTAFF, AZ.
Archival research on absorption lines in violently star-forming galaxies [NASA-CR-185960] N90-14163

LUNAR RADIATION CORP., MADISON, WI.
Bone mineral measurement using dual energy x ray densitometry N90-13958

M

MANCHESTER UNIV. (ENGLAND).
Study of forces and moments on wing-bodies at high incidence, volumes 1 and 2 N90-13350

MARTIN MARIETTA AEROSPACE, DENVER, CO.
PACOSS program N90-13487

MARYLAND UNIV., COLLEGE PARK.
Hypersonic aerodynamics N90-13335

MASSACHUSETTS INST. OF TECH., CAMBRIDGE.
A four channel He-3 cooled balloon-borne bolometer radiometer N90-13469
Fiber reinforced cementitious composites technology [PB89-227813] N90-13608
Chemical beam epitaxy of ZnSe [AD-A213265] N90-13625
An algorithm for control volume analysis of cryogenic systems [AD-A213394] N90-13683
Efficient detection of small moving objects [AD-A213314] N90-13690
Resistive fuses: Analog hardware for detecting discontinuities in early vision [AD-A211891] N90-13696
Delay test generation for synchronous sequential circuits [AD-A211917] N90-13697
Test generation for highly sequential circuits [AD-A211932] N90-13698
Numerical methods for unsteady turbomachinery flow N90-13743
Physically-based parameterization of spatially variable soil and vegetation using satellite multispectral data [NASA-CR-185957] N90-13879
Strain accumulation and surface deformation along the San Andreas, California [NASA-CR-185893] N90-13894
Computer-aided fabrication system implementation [AD-A213005] N90-13969
Retrieving and integrating IC fabrication data from dissimilar databases [AD-A211890] N90-14140

MASSACHUSETTS INST. OF TECH., LEXINGTON.
Resonant-tunneling oscillators and multipliers for submillimeter receivers N90-13467

MAX-PLANCK-INST. FUER AERONOMIE, KATLENBURG-LINDAU (GERMANY, F.R.).
Observation of wind corners in the middle atmosphere over Andenes (69 N) during winter 1983/84, summer 1987 and summer 1988 N90-13836
Some remarks on the working principle of the rocketborne nose tip dc probes in the D-region of the ionosphere N90-13839
Preliminary results of the rocket and scatter experiments ROSE: Measurements with the newly designed spherical probe N90-13850

MAX-PLANCK-INST. FUER PHYSIK UND ASTROPHYSIK, GARCHING (GERMANY, F.R.).
Project Supernova 1987 N90-13866
The x ray mirror and the PSPC of the supernova-rocket-project N90-13867
SN 1987: A telemetry decoding system N90-13875
Further observations of rotationally excited far infrared OH16 and OH18 emission in Orion-KL: Tighter constraints on the nature of the emitting region
[NASA-CR-186004] N90-14156

MCDONNELL-DOUGLAS ASTRONAUTICS CO., HOUSTON, TX.
Shuttle relative navigation of a tethered satellite mission with current on board software N90-13423
Impact of tether cutting on onboard navigation during the Tethered Satellite Mission-1 N90-13424
Shuttle tethered operations: The effect on orbital trajectory and inertial navigation N90-13425
The controllability of the aeroassist flight experiment atmospheric skip trajectory N90-13438

MCI TELECOMMUNICATIONS CORP., CLARKSBURG, MD.
Orbit and attitude determination results during launch support operations for SBS-5
[PAPER-7] N90-13420

MICHIGAN STATE UNIV., EAST LANSING.
On the design of a computer-aided design system for digital circuits N90-13695
Effects of microgravity on growth hormone concentration and distribution in plants N90-13947

MISSISSIPPI STATE UNIV., MISSISSIPPI STATE.
Spacelab system analysis: The modified free access protocol: An access protocol for communication systems with periodic and Poisson traffic
[NASA-CR-183805] N90-13497

MISSISSIPPI UNIV., UNIVERSITY.
Propagation of sound in vibrationally excited nitrogen and hydrogen gas mixtures
[AD-A213002] N90-14073

MISSOURI UNIV., SAINT LOUIS.
Fundamental quantum 1/f noise in ultrasmall semiconductor devices and their optimal design principles
[AD-A211947] N90-14107

MITRE CORP., MCLEAN, VA.
National Airspace System airspace management operational concept
[DOT/FAA/DS-89/29] N90-13361
National Airspace System flight planning operational concept
[DOT/FAA/DS-89/30] N90-13362
An update to the system safety study of TCAS 2
[DOT/FAA/SA-89/3] N90-13363

MORTON THIOKOL, BRIGHAM CITY, UT.
QM-6 field joint protection system, volume 7
[NASA-CR-183748] N90-13586
RSRM nozzle fixed housing cooldown test
[NASA-CR-183741] N90-13587
Contamination removal using various solvents and methodologies
[NASA-CR-183747] N90-13652
Effects of tacky mat contamination on bond degradation for Chemlok/liner and NBR/liner bonds
[NASA-CR-183742] N90-13653
Evaluation of a metering, mixing, and dispensing system for mixing polysulfide adhesive
[NASA-CR-183749] N90-13654
Evaluation of copper slag blast media for railcar maintenance
[NASA-CR-183744] N90-13681

MOSAIC INDUSTRIES, INC., MOUNTAIN VIEW, CA.
Multisensor technologies for low cost methane detection
[PB89-235188] N90-13766

N

NATIONAAL INST. VOOR KERNFYSICA EN HOGE ENERGIEFYSICA, AMSTERDAM (NETHERLANDS).
Influence of RF-parameters on beam lifetime
[NIKHEF-K/AMPS/89-06] N90-14091

NATIONAL ACADEMY OF SCIENCES - NATIONAL RESEARCH COUNCIL, WASHINGTON, DC.
Space Station Engineering Design Issues
[NASA-CR-185978] N90-13492
An implementation plan for priorities in solar-system space physics
[NASA-CR-185375] N90-14154
The Explorer program for astronomy and astrophysics N90-14159

NATIONAL AERONAUTICAL ESTABLISHMENT, OTTAWA (ONTARIO).
Analysis of experimental data for CAST 10-2/DOA 2 supercritical airfoil at low Reynolds numbers and application to high Reynolds number flow
[AD-A211654] N90-13326

NATIONAL AERONAUTICS AND SPACE ADMINISTRATION, WASHINGTON, DC.
On the wings of a dream: The Space Shuttle
[NASA-EP-269] N90-13446
Syncom 4 deploy, LDEF retrieval highlight 10-day Columbia flight
[NASA-NEWS-RELEASE-89-160] N90-13448
Science and applications on the space station: A strategic vision
[NASA-TM-101863] N90-13493
Space station systems: A bibliography with indexes (supplement 9)
[NASA-SP-7056(09)] N90-13580
Aerospace medicine and biology: A continuing bibliography with indexes (supplement 330)
[NASA-SP-7011(330)] N90-13925
Ada task scheduling: A focused Ada investigation
[NASA-CR-186072] N90-13967
Small business innovation research: Program solicitation
[NASA-TM-101869] N90-14126
Executive overview and introduction to the SMAP information system life-cycle and documentation standards
[NASA-TM-101765] N90-14134
Information system life-cycle and documentation standards, volume 1
[NASA-TM-101856] N90-14135
Management plan documentation standard and Data Item Descriptions (DID). Volume of the information system life-cycle and documentation standards, volume 2
[NASA-TM-101857] N90-14136
Product specification documentation standard and Data Item Descriptions (DID). Volume of the information system life-cycle and documentation standards, volume 3
[NASA-TM-101858] N90-14137
Assurance specification documentation standard and Data Item Descriptions (DID). Volume of the information system life-cycle and documentation standards, volume 4
[NASA-TM-101859] N90-14138
Management control and status reports documentation standard and Data Item Descriptions (DID). Volume of the information system life-cycle and documentation standards, volume 5
[NASA-TM-101860] N90-14139
Centers for the commercial development of space
[NASA-PAM-525] N90-14151
NASA commercial programs
[NASA-TM-101853] N90-14152

NATIONAL AERONAUTICS AND SPACE ADMINISTRATION. AMES RESEARCH CENTER, MOFFETT FIELD, CA.
Application of a self-adaptive grid method to complex flows
[NASA-TM-102223] N90-13324
Computation of viscous incompressible flows
[NASA-TM-101090] N90-13329
Study of the integration of wind tunnel and computational methods for aerodynamic configurations
[NASA-TM-102196] N90-13332
Computation of Navier-Stokes equations for three-dimensional flow separation
[NASA-TM-102266] N90-13353
Flight deck automation: Promises and realities
[NASA-CP-10036] N90-13384
A two-dimensional adaptive-wall test section with ventilated walls in the Ames 2- by 2-foot transonic wind tunnel
[NASA-TM-102207] N90-13407
Status of direct detector and array development N90-13464
Cryogenics for LDR N90-13471
A review of quasi-coherent structures in a numerically simulated turbulent boundary layer
[NASA-TM-102191] N90-13723
Exercise countermeasures for bed rest deconditioning
[NASA-TM-101045] N90-13926
Functional decor in the International Space Station: Body orientation cues and picture perception
[NASA-TM-102242] N90-13931
Cells in Space
[NASA-CP-10034] N90-13939
Fundamental results from microgravity cell experiments with possible commericial applications N90-13940
The pituitary growth hormone cell in space N90-13941

NATIONAL AERONAUTICS AND SPACE ADMINISTRATION. GODDARD SPACE FLIGHT CENTER, GREENBELT, MD.
Flight Mechanics/Estimation Theory Symposium, 1989
[NASA-CP-3050] N90-13413
Simultaneous quaternion estimation (QUEST) and bias determination N90-13417
GOES-I/M ascent maneuvers from transfer orbit to station N90-13421
True covariance simulation of the EUVE update filter N90-13427
A gyroscope calibration analysis for the Gamma Ray Observatory (GRO) N90-13428
Extension to Euler's theorem to n-dimensional spaces N90-13431
Extended Kalman filter for attitude estimation of the earth radiation budget satellite N90-13433
Automation of orbit determination functions for National Aeronautics and Space Administration (NASA)-supported satellite missions N90-13434
Optimum data weighting and error calibration for estimation of gravitational parameters N90-13437
Lifetime predictions for the Solar Maximum Mission (SMM) and San Marco spacecraft N90-13440
Gravimetric measurements of materials outgassing applied to graphite-epoxy laminates
[NASA-TM-100753] N90-13609
Analytical derivation and verification of zero-gyro control for the IUE satellite
[NASA-TM-100748] N90-13787
Meteorological atlas of the Northern Hemisphere lower stratosphere for January and February 1989 during the Airborne Arctic Stratospheric Expedition
[NASA-TM-4145] N90-13908
Algorithm for atmospheric corrections of aircraft and satellite imagery
[NASA-TM-100751] N90-13976
The winds of high luminosity late-type bright stars
[NASA-CR-182961] N90-14160
Reexamination of data from the asteroid/meteoroid detector
[NASA-CR-185997] N90-14175

NATIONAL AERONAUTICS AND SPACE ADMINISTRATION. HUGH L. DRYDEN FLIGHT RESEARCH FACILITY, EDWARDS, CA.
A smoke generator system for aerodynamic flight research
[NASA-TM-4137] N90-13372
Application of fracture mechanics and half-cycle method to the prediction of fatigue life of B-52 aircraft pylon components
[NASA-TM-86277] N90-13820
A knowledge-based system design/information tool for aircraft flight control systems
[NASA-TM-101704] N90-13990
A knowledge-based flight status monitor for real-time application in digital avionics systems
[NASA-TM-101710] N90-13995

NATIONAL AERONAUTICS AND SPACE ADMINISTRATION. JOHN F. KENNEDY SPACE CENTER, COCOA BEACH, FL.
Debris/ice/TPS assessment and photographic analysis for Shuttle Mission STS-34
[NASA-TM-102153] N90-13447
Comparison of analytical methods for calculation of wind loads
[NASA-TM-102782] N90-13813

NATIONAL AERONAUTICS AND SPACE ADMINISTRATION. LYNDON B. JOHNSON SPACE CENTER, HOUSTON, TX.
Periodic-disturbance accommodating control of the space station for asymptotic momentum management N90-13416
Microwave microstrip resonator measurements of Y1Ba2Cu3O(7-x) and Bi2Sr2Ca1Cu2O(8-y) thin films
[NASA-TM-102159] N90-13704
Action languages: Dimensions, effects
[NASA-CR-183388] N90-14181

NATIONAL AERONAUTICS AND SPACE ADMINISTRATION. LANGLEY RESEARCH CENTER, HAMPTON, VA.
A vapor generator for transonic flow visualization
[NASA-TM-101670] N90-13403
Advanced composite materials for precision segmented reflectors N90-13461
Assembly considerations for large reflectors N90-13480
Initial test results for the mini-mast N90-13482
LDR structural experiment definition N90-13483
Joints in deployable space truss structures N90-13489
Characteristic impedance of microstrip lines
[NASA-TM-101581] N90-13694
A study on the sensitivity and simultaneous adjustment of a hoop-column antenna surface
[NASA-TM-101538] N90-13807

The computational structural mechanics testbed user's manual
[NASA-TM-100644] N90-13818
Laboratory test methodology for evaluating the effects of electromagnetic disturbances on fault-tolerant control systems
[NASA-TM-101665] N90-14061

NATIONAL AERONAUTICS AND SPACE ADMINISTRATION. LEWIS RESEARCH CENTER, CLEVELAND, OH.

Effect of reduced aft diameter and increased blade number on high-speed counterrotation propeller performance
[NASA-TM-102077] N90-13352
Application of an efficient hybrid scheme for aeroelastic analysis of advanced propellers
[NASA-TM-102428] N90-13355
Silicon-etalon fiber-optic temperature sensor
[NASA-TM-102389] N90-13361
Application of a two-dimensional unsteady viscous analysis code to a supersonic throughflow fan stage
[NASA-TM-4141] N90-13387
STOVL aircraft simulation for integrated flight and propulsion control research
[NASA-TM-102419] N90-13389
Two-dimensional analysis of two-phase reacting flow in a firing direct-injection diesel engine
[NASA-TM-102069] N90-13392
A planar reacting shear layer system for the study of fluid dynamics-combustion interaction
[NASA-TM-102422] N90-13393
Recent progress in research pertaining to estimates of gas-side heat transfer in an aircraft gas turbine
[NASA-TM-102460] N90-13394
The Space Station Photovoltaic Panels Plasma Interaction Test Program: Test plan and results
[NASA-TM-102474] N90-13581
Tank pressure control experiment on the space shuttle
[NASA-TM-102313] N90-13590
Thin-film sensors for reusable space propulsion systems
[NASA-TM-102383] N90-13595
The US space station and its electric power system
[NASA-TM-101974] N90-13596
The Materials Division: A case study
[NASA-TM-102380] N90-13597
Thermal barrier coatings for gas turbine and diesel engines
[NASA-TM-102408] N90-13636
Thermodynamic properties of some metal oxide-zirconia systems
[NASA-TM-102351] N90-13666
Buoyancy effects on the vapor condensation rate on a horizontal liquid surface
[NASA-TM-102437] N90-13675
Facilities for microgravity combustion research
[NASA-TM-102014] N90-13679
An investigation of flame spread over shallow liquid pools in microgravity and nonair environments
[NASA-TM-102425] N90-13680
Effect of spatial resolution on apparent sensitivity to initial conditions of a decaying flow as it becomes turbulent
[NASA-TM-102377] N90-13719
Analysis of rotary engine combustion processes based on unsteady, three-dimensional computations
[NASA-TM-102469] N90-13749
Convective heat transfer measurements from a NACA 0012 airfoil in flight and in the NASA Lewis Icing Research Tunnel
[NASA-TM-102448] N90-13750
Vapor condensation on liquid surface due to laminar jet-induced mixing: The effects of system parameters
[NASA-TM-102433] N90-13751
An investigation of gear mesh failure prediction techniques
[NASA-TM-102340] N90-13785
Elasticity effects on cavitation in a squeeze film damper undergoing noncentered circular whirl
[NASA-TM-102392] N90-13786
Liquid water content and droplet size calibration of the NASA Lewis Icing Research Tunnel
[NASA-TM-102447] N90-13797
Mean stress and the exhaustion of fatigue-damage resistance
[NASA-TM-101311] N90-13819
Flight software development for the isothermal dendritic growth experiment
[NASA-TM-102412] N90-13988
Application of multi-grid methods for solving the Navier-Stokes equations
[NASA-TM-102359] N90-14002
Modeling of power electronic systems with EMTP
[NASA-TM-102375] N90-14060

NATIONAL AERONAUTICS AND SPACE ADMINISTRATION. MARSHALL SPACE FLIGHT CENTER, HUNTSVILLE, AL.

A transient response method for linear coupled substructures
[NASA-TP-2926] N90-13444

NATIONAL AERONAUTICS AND SPACE ADMINISTRATION. WALLOPS FLIGHT FACILITY, WALLOPS ISLAND, VA.

Evidence for accurate temperatures from the inflatable falling sphere N90-13835
Application of an optimal filter for inflatable sphere data processing N90-13849

NATIONAL AEROSPACE LAB., AMSTERDAM (NETHERLANDS).

The S.D.G., P.S.D. and the nonlinear airplane
[NLR-MP-88018-U] N90-13371

NATIONAL CENTER FOR ATMOSPHERIC RESEARCH, BOULDER, CO.

An implementation plan for priorities in solar-system space physics
[NASA-CR-185375] N90-14154

NATIONAL INST. OF STANDARDS AND TECHNOLOGY, BOULDER, CO.

Physical phenomena and the microgravity response N90-13945

NATIONAL INST. OF STANDARDS AND TECHNOLOGY, GAITHERSBURG, MD.

Toughening mechanisms in ceramic composites
[PB89-235907] N90-13656

NATIONAL PHYSICAL LAB., TEDDINGTON (ENGLAND).

Quantitative AES and XPS: Determination of the electron spectrometer transmission function and the detector sensitivity energy dependencies for the production of true electron emission spectra in AES and XPS
[NPL-DMA(A)-194] N90-13634

NATIONAL TELECOMMUNICATIONS AND INFORMATION ADMINISTRATION, WASHINGTON, DC.

Long-range plan for management and use of the radio spectrum by agencies and establishments of the Federal Government
[PB89-232367] N90-13693

NATIONAL WEATHER SERVICE, SALT LAKE CITY, UT.

A collection of papers related to heavy precipitation forecasting
[PB89-230833] N90-13910

NATIONAL WEATHER SERVICE, SILVER SPRING, MD.

Extended memory library for AFOS (Automation of Field Operations and Services) applications
[PB89-230858] N90-14147

NAVAL ACADEMY, ANNAPOLIS, MD.

Summary of research academic departments, 1987-1988
[AD-A213252] N90-14183

NAVAL AIR DEVELOPMENT CENTER, WARMINSTER, PA.

Fatigue behavior of silicon carbide Whisker/Aluminum composite
[AD-A213094] N90-13603
Quench sensitivity in Al-Cu-Li alloys
[AD-A213055] N90-13639

NAVAL CIVIL ENGINEERING LAB., PORT HUENEME, CA.

Time domain coupling of the boundary and finite element methods for elastodynamics
[AD-A213243] N90-13811

NAVAL OCEAN RESEARCH AND DEVELOPMENT ACTIVITY, BAY SAINT LOUIS, MS.

Feature modeling: The incorporation of a front and eddy map into optimum interpolation-based thermal analysis
[AD-A213253] N90-13914

NAVAL OCEAN SYSTEMS CENTER, SAN DIEGO, CA.

Using Broyden updates to approximate the Jacobian in a semi-implicit backward differentiation code
[AD-A213239] N90-14010
Analytical and computer-aided models of InP-based MISFETs and heterojunction devices
[AD-A211861] N90-14106

NAVAL ORDNANCE STATION, INDIAN HEAD, MD.

Evaluation of selected computer models for modeling pyrotechnic and propellant devices
[AD-A213003] N90-13671

NAVAL POSTGRADUATE SCHOOL, MONTEREY, CA.

Inexpensive global location and tracking systems using geostationary satellites
[AD-A213025] N90-13498
Review and evaluation of a turbomachinery throughflow finite element code
[AD-A213058] N90-13787
Project ORION microcomputer management system
[AD-A212945] N90-13959
A fault-tolerant software algorithm for a network of transputers
[AD-A213092] N90-13972
Compression of bitmapped graphic data
[AD-A213141] N90-13974
Why stochastic modeling is essential in analyzing interdicted transportation network performance
[AD-A213140] N90-14007
FORTRAN subroutines for the evaluation of the confluent hypergeometric functions
[AD-A213306] N90-14012
Image enhancement software for underwater recovery operations: User's manual
[AD-A212943] N90-14094
Real time image enhancement during underwater recovery operations
[AD-A213139] N90-14097

NAVAL RESEARCH LAB., WASHINGTON, DC.

A review of laser filter materials
[AD-A213134] N90-13776
Synchrotron-betatron parametric instability in free-electron lasers
[AD-A213373] N90-13777
An artificial intelligence approach to analog system diagnosis
[AD-A213135] N90-13992
A solvable self-similar model of the sausage instability in a resistive Z-pinch
[AD-A213137] N90-14006
Solution of the Boltzmann equation using an energy group method
[AD-A213138] N90-14096
NRL (Naval Research Laboratory) Review
[AD-A212886] N90-14182

NEBRASKA UNIV., LINCOLN.

Implementation issues in source coding
[NASA-CR-185327] N90-13963

NEW MEXICO UNIV., ALBUQUERQUE.

A search for the effects of active magnetic fields in extra-galactic radio sources N90-14161

NEW YORK UNIV., NEW YORK.

Interaction of radiation with matter: Atomic collision processes occurring in the presence of radiation fields
[AD-A213112] N90-14078

NORTH CAROLINA STATE UNIV., RALEIGH.

Numerical solutions of the complete Navier-Stokes equations
[NASA-CR-186102] N90-13747

NORTHWESTERN UNIV., EVANSTON, IL.

Localization of ultrasound in thick composites
[AD-A212994] N90-13602
Reflection by defective diffusion bonds
[AD-A212995] N90-13638
Numerical analysis of scattering by interface flaws
[AD-A212996] N90-13810

NORWEGIAN DEFENCE RESEARCH ESTABLISHMENT, KJELLER.

The effects of gravity waves on horizontal layers: Simulation and interpretation N90-13852

NORWEGIAN SPACE CENTER, OSLO.

The Norwegian balloon and sounding rocket program 1989-1992 N90-13829
Andoya rocket range: New installations, future plans, and investments N90-13859

NOTRE DAME UNIV., IN.

Error control techniques for satellite and space communications
[NASA-CR-182751] N90-13685

NOTTINGHAM UNIV. (ENGLAND).

The determinatin of the muon content of EAS from Cygnus X-3 N90-14179

O

OAO CORP., GREENBELT, MD.

Spacecraft attitude determination using the earth's magnetic field N90-13429

OBSERVATOIRE DE PARIS-MEUDON (FRANCE).

Prediction of the 10 cm solar flux index N90-13872

OFFICE NATIONAL D'ETUDES ET DE RECHERCHES AEROSPATIALES, PARIS (FRANCE).

Study of the hydroxyl radical by DRASC resonance in a high pressure flame
[ONERA-RS-53/7131-PY] N90-13632
A theoretical model of double base propellant combustion
[ONERA-RTF-23/7128-EY] N90-13672
Image segmentation for the stereoscopic vision of a mobile robot
[ONERA-RT-1/3692-SY] N90-13800

OHIO STATE UNIV., COLUMBUS.

Aeroelastic control of composite lifting surfaces: Integrated aeroelastic control optimization N90-13396

OLD DOMINION UNIV., NORFOLK, VA.

Computational solution of chemistry problems
[NASA-CR-186000] N90-13818

OSLO UNIV. (NORWAY).
The electrodynamics of the polar ionosphere with special emphasis on the dayside cleft region N90-13838
OXFORD UNIV. (ENGLAND).
Data acquisition in aerodynamic research N90-13340
The Fourth Oxford International Conference on the Mechanical Properties of Materials at High Rates of Strain
[AD-A212293] N90-13809

P

PARIS VI UNIV. (FRANCE).
Three dimensional analysis of the structure of the atmosphere in polar environments by vertical satellite sounding. Interest for the meteorological forecasts at high latitudes
[ETN-90-95506] N90-13911
PDA ENGINEERING, SANTA ANA, CA.
The application of cast SiC/Al to rotary engine components
[NASA-CR-179610] N90-13385
PENNSYLVANIA DEPT. OF TRANSPORTATION, HARRISBURG.
Evaluation of a neoprene latex modified SAMI (Stress Absorbing Membrane Interlayer)
[PB89-226435] N90-13665
PENNSYLVANIA STATE UNIV., UNIVERSITY PARK.
Gas flows in rocket motors, volume 1
[AD-A213348] N90-13591
Gas flows in rocket motors. Volume 2, appendix C: Time iterative solution of viscous supersonic flow
[AD-A213349] N90-13592
Gas flows in rocket motors. Volume 3, appendix D: Computer code listings
[AD-A213350] N90-13593
Measurement of the light flux density patterns from luminaires proposed as photon sources for photosynthesis during space travel
[NASA-CR-186124] N90-13916
Gravitropism in plants: Hydraulics and wall growth properties of responding cells N90-13950
PENNSYLVANIA UNIV., PHILADELPHIA.
Do the design concepts used for the space flight hardware directly affect cell structure and/or cell function ground based simulations N90-13953
PERKIN-ELMER CORP., DANBURY, CT.
Real-time sensing of optical alignment N90-13479
PHYSICAL SCIENCES, INC., ANDOVER, MA.
CANOES 2: Dynamics of atmospheric infrared thermochemical excitation, volume 1
[AD-A213341] N90-13897
CANOES 2: Dynamics of atmospheric infrared thermochemical excitation, volume 2
[AD-A213342] N90-13898
CANOES 2: Dynamics of atmospheric infrared thermochemical excitation, volume 3
[AD-A213343] N90-13899
CANOES 2: Dynamics of atmospheric infrared thermochemical excitation, volume 4
[AD-A213344] N90-13900
PITTSBURGH UNIV., PA.
The low-ion QSO absorption-line systems N90-14162
PLESSEY RESEARCH ROKE MANOR LTD., ROMSEY (ENGLAND).
A guide to reasoning under uncertainty
[REPT-72/87/R486U] N90-13932
POLYTECHNIC UNIV., FARMINGDALE, NY.
Experimental and theoretical study of artificial plasma layers produced by two intersecting beams in a chamber
[NASA-CR-184598] N90-14102
PRATT AND WHITNEY AIRCRAFT, EAST HARTFORD, CT.
Thermal barrier coating life prediction model development, phase 1
[NASA-CR-182230] N90-13388
PRINCETON UNIV., NJ.
Trajectory optimization and guidance for an aerospace plane
[NASA-CR-185884] N90-13369
Experimental and computational study of combustion limits in natural-gas fueled internal combustion engines
[PB89-235196] N90-13673
Magneto-elastic interactions in conducting structures in transient magnetic fields N90-13686
Ultrafast processes and spectroscopy with free electron lasers
[AD-A212889] N90-13773
PURDUE UNIV., WEST LAFAYETTE, IN.
Application of large eddy interaction model to a mixing layer
[NASA-CR-185123] N90-13328
On catalytic recombination rates in hypersonic stagnation heat transfer N90-13338
Discretization and model reduction for a class of nonlinear systems N90-13397

R

RAND CORP., SANTA MONICA, CA.
A new view of weapon system reliability and maintainability
[AD-A213281] N90-13382
A new view of weapon system reliability and maintainability: Executive summary
[AD-A213282] N90-13383
READING UNIV. (ENGLAND).
The linear study of zonally asymmetric barotropic flows N90-13902
REMTECH, INC., HUNTSVILLE, AL.
Development of a shuttle plume radiation heating indicator
[NASA-CR-183679] N90-13584
RENSSELAER POLYTECHNIC INST., TROY, NY.
A practical approach for minimum time control of the Spacecraft Control Laboratory Experiment (SCOLE), appendix A
[NASA-CR-186008] N90-13495
RESEARCH TRIANGLE INST., RESEARCH TRIANGLE PARK, NC.
Senegalese land surface change analysis and biophysical parameter estimation using NOAA AVHRR spectral data
[NASA-CR-186120] N90-13883
RICE UNIV., HOUSTON, TX.
Optimal trajectories for the Aeroassisted Flight Experiment. Part 1: Equations of motion in an Earth-fixed system
[NASA-CR-186134] N90-13441
Optimal trajectories for the Aeroassisted Flight Experiment. Part 2: Equations of motion in an inertial system
[NASA-CR-186135] N90-13442
Optimal trajectories for the aeroassisted flight experiment, 1988-89
[NASA-CR-186132] N90-13443
ROCHESTER UNIV., NY.
Optics and opto-electronics systems
[AD-A212340] N90-14093
An experiment to search for galactic axions N90-14158
ROCKWELL INTERNATIONAL CORP., CANOGA PARK, CA.
LOX/hydrocarbon combustion instability investigation
[NASA-CR-182249] N90-13589
ROME UNIV. (ITALY).
Energy concentration induced by phase transitions in hydrogenated metals
[PREPRINT-672] N90-13650
Low resistivity electrodeless streamer tubes
[PREPRINT-685-89] N90-13712
The initial-boundary value problem for the Davey-Stewartson 1 equation; how to generate and drive localized coherent structures in multidimensions
[PREPRINT-684] N90-13756
On a new integrable Hamiltonian system with nearest neighbors interaction
[PREPRINT-667] N90-14043
A unified algebraic approach to integral and discrete evolution equations
[PREPRINT-668] N90-14044
On the effects of an uncertainty on evolution law in dynamical systems
[PREPRINT-689] N90-14047
Large deviation estimates in the stochastic quantization of phi sub 2 exp 4
[PREPRINT-686] N90-14050
Fluctuations of the Lyapunov exponent in disordered systems
[PREPRINT-690] N90-14063
Scaling in a non Abelian string network
[ROM1F-89-676] N90-14066
Configurational statistics of strings, fractals and polymer physics. Part 2: Non Abelian strings
[ROM1F-89-680-PT-2] N90-14067
Statistical mechanics of strings and topology
[ROM1F-89-683] N90-14068
R-mairices and higher Poisson brackets for integrable systems
[PREPRINT-669] N90-14069
Some comments on the solvable Chiral Potts model
[PREPRINT-673] N90-14070
Energy exchange of interacting solitons in multidimensions
[PREPRINT-662] N90-14071
Lattice QCD estimate of mixing parameters for heavy meson systems
[PREPRINT-687] N90-14079
Nonpotential scattering for the density matrix and quantum gravity
[PREPRINT-688] N90-14080
Performance of resistive plate counters at beam flux up to 140 Hz/cm2
[NOTA-INTERNA-930] N90-14081
Nucleon polarizabilities in the constituent quark model
[NOTA-INTERNA-936] N90-14082
Measurement of the fractional momentum carried by the gluons in the low Q2 photon-gluon fusion events at the ep HERA collider
[NOTA-INTERNA-937] N90-14083
A lattice study of semileptonic decays of D-mesons
[PREPRINT-660] N90-14086
Aspects of the physics of the standard model
[PREPRINT-670] N90-14087
Exotic Higgs production at e+e- colliders
[PREPRINT-671] N90-14088
Model-independent analysis of the Z line shape in e+e- annihilation
[PREPRINT-679] N90-14089
Low frequency polarized and depolarized light scattering in H-bonded liquids: CH3(CH2)n-1OH (n=1,...5)
[PREPRINT-693] N90-14100
Energy barriers in SK spin-glass model
[PREPRINT-665] N90-14119
Where is an object before you look at it
[NOTA-INTERNA-935] N90-14123
Correlation among gravitational wave and neutrino detectors data during SN1987A
[NOTA-INTERNA-932] N90-14165
Expected supernovae rates and gravitational waves detection
[NOTA-INTERNA-933] N90-14166
String correlations and galaxies formation
[ROM1F-89-677] N90-14170
Non Abelian string correlations and galaxies formation
[ROM1F-89-678] N90-14171
Des Cloizeaux's law for strings and galaxies formation. Part 1: Abelian configurations
[ROM1F-89-681-PT-1] N90-14172
Des Cloizeaux's law for strings and galaxies formation. Part 2: Non Abelian configurations
[ROM1F-89-682-PT-2] N90-14173
Detectable gravitational waves by supernova SN 1987 A pulsar relic
[PREPRINT-658] N90-14174
RONDOUT ASSOCIATES, INC., STONE RIDGE, NY.
ULF/VLF (0.001 to 50 Hz) Seismo-Acoustic Noise in the Ocean
[AD-A212942] N90-13913
ROUEN UNIV. (FRANCE).
Turbulence modeling and implementation in Navier-Stokes solvers N90-13742
ROYAL AEROSPACE ESTABLISHMENT, BEDFORD (ENGLAND).
Pressure measurement techniques in use at the Royal Aerospace Establishment N90-13347
ROYAL AIRCRAFT ESTABLISHMENT, FARNBOROUGH (ENGLAND).
Helicopter rotor test rig (RoTeSt) in DNW: Application and results
[RAE-TRANS-2171] N90-13408
ROYAL INST. OF TECH., STOCKHOLM (SWEDEN).
Auroral particle acceleration by dc and low frequency electric fields N90-13841
The auroral current - voltage relationship N90-13843
ROYAL SIGNALS AND RADAR ESTABLISHMENT, MALVERN (ENGLAND).
Computer-based tools for assisting air traffic controllers with arrivals flow management
[RSRE-89001] N90-13366
SIMOGEN: An object-oriented language for simulation
[AD-A213129] N90-13973
RUHR UNIV., BOCHUM (GERMANY, F.R.).
Interplanetary dust close to the Sun (F corona): Its observation in the visible and infrared by a rocket-borne coronagraph N90-13864
RUTGERS - THE STATE UNIV., NEW BRUNSWICK, NJ.
Empirical analysis and refinement of expert system knowledge bases
[AD-A213240] N90-14143

S

SAN DIEGO STATE UNIV., CA.
Nuclear magnetic resonance signatures of nitrogen-containing compounds
[AD-A213375] N90-13628
Integrated optoelectronic receivers
[AD-A213376] N90-14098
SCIENCE APPLICATIONS INTERNATIONAL CORP., TORRANCE, CA.
Gas flows in rocket motors, volume 1
[AD-A213348] N90-13591

Gas flows in rocket motors. Volume 2, appendix C: Time iterative solution of viscous supersonic flow
[AD-A213349] N90-13592
Gas flows in rocket motors. Volume 3, appendix D: Computer code listings
[AD-A213350] N90-13593

SIGMA RESEARCH, INC., LEXINGTON, MA.
Air quality simulation model performance for one-hour averages
[PB89-233506] N90-13890

SOUTHAMPTON UNIV. (ENGLAND).
Modelling of satellite control thruster plumes
N90-13578

SOUTHWEST RESEARCH INST., SAN ANTONIO, TX.
NDI (Nondestructive Inspection) oriented corrosion control for Army aircraft. Phase 1: Inspection methods
[AD-A213368] N90-13359
Constitutive modeling for isotropic materials (HOST)
[NASA-CR-179522] N90-13390
Constitutive modeling for isotropic materials (HOST)
[NASA-CR-174718] N90-13391
The role of the host in a cooperating mainframe and workstation environment, volumes 1 and 2
[NASA-CR-185463-VOL-1/2] N90-13496

SRI INTERNATIONAL CORP., MENLO PARK, CA.
Role of retinocortical processing in spatial vision
[AD-A210995] N90-13918
Spatiotemporal characteristics of visual localization, phase 2
[AD-A212934] N90-13929

STANFORD UNIV., CA.
A CFD study of tilt rotor flowfields
[NASA-CR-186116] N90-13349
Rotation of the photospheric magnetic fields: A north-south asymmetry
[NASA-CR-186159] N90-14177
Shear-induced inflation of coronal magnetic fields
[NASA-CR-186103] N90-14178

STATE UNIV. OF NEW YORK, BUFFALO.
Blunt-nose inviscid airflows with coupled nonequilibrium processes N90-13336
Electrochemistry at very small electrodes
[AD-A213156] N90-13623
Local pairing and antiferromagnetism in high-T sub c superconductors
[AD-A213004] N90-14113

STATE UNIV. OF NEW YORK, STONY BROOK.
Polarity establishment, morphogenesis, and cultured plant cells in space N90-13943

STOCKHOLM UNIV. (SWEDEN).
New calculations of photodissociation cross-sections in the O2 Schumann-Runge system N90-13834
A self-consistent model of the most common nightglow emissions N90-13853

STRUCTUREAL INTEGRITY ASSOCIATES, INC., SAN JOSE, CA.
Stress intensity factors for cracking metal structures under rapid thermal loading. Volume 2: Theoretical background
[AD-A213297] N90-13812

STUTTGART UNIV. (GERMANY, F.R.).
Geodetic network adjustment using GPS triple difference observations and a priori stochastic information
[TR-1-1987] N90-13367
Processing of undifferences GPS carrier beat phase measurements and adjustment computations
[TR-5-1988] N90-13368
Experimental and numerical investigations of the crack arrest behavior of steels and cast iron materials
[MPA-TWB-88-03] N90-13635
Supplementing geodetic data with prior information for crustal deformation in the Imperial Valley, California
[TR-6-1988] N90-13904
Study of modern instrumentation and methods for astronomic positioning in the field
[AD-A213217] N90-14157

SVERDRUP TECHNOLOGY, INC., CLEVELAND, OH.
Multigrid calculations of 3-D turbulent viscous flows
[NASA-CR-185154] N90-13323
An improved algorithm for the modeling of vapor flow in heat pipes
[NASA-CR-185179] N90-13748
Development and characterization of PdCr temperature-compensated wire resistance strain gage
[NASA-CR-185153] N90-13761
An interactive grid generation procedure for axial and radial flow turbomachinery
[NASA-CR-185167] N90-13968

SWEDISH DEFENCE RESEARCH ESTABLISHMENT, LINKOEPING.
Re-entry hazards and cosmos 1900
[FOA-C-30535-9.4] N90-13583
An editor for 3D-models for image analysis
[FOA-C-30534-3.4] N90-13986
Discussion of factors affecting the sensitivity of IR imaging sensors, particularly focal plane mosaic arrays
[FOA-C-30536-3.1] N90-14101

SWEDISH DEFENCE RESEARCH ESTABLISHMENT, STOCKHOLM.
A literature survey of inherently conducting polymers
[FOA-C-20783-2.4] N90-13688
Thermochemical calculations with inert compounds
[FOA-C-20759-2.1] N90-13677
Construction of a SQUID magnetometer for investigation of screening properties of high-T(sub c) superconductors
[FOA-C-20765-2.2] N90-13768

SWEDISH INST. OF SPACE PHYSICS, KIRUNA.
Enhanced electron density layers in the high-latitude lower ionosphere N90-13832
ALIS: An Auroral Large Imaging System in northern Scandinavia N90-13877

SWEDISH INST. OF SPACE PHYSICS, UPPSALA.
Observations of electrostatic hydrogen cyclotron waves and electric field fluctuations near one Hz in auroral acceleration regions N90-13842

SWEDISH SPACE CORP., ESRANGE.
Esrange N90-13876

SWEDISH SPACE CORP., SOLNA.
The Swedish sounding rocket and balloon program
N90-13830

SYSTEMS APPLICATIONS, INC., SAN RAFAEL, CA.
Air quality simulation model performance for one-hour averages
[PB89-233506] N90-13890

SYSTEMS ENGINEERING LABS., INC., GREENBELT, MD.
Stochastic modelling of EM scattering from foliage
[AD-A213118] N90-13689

T

TECHNICAL RESEARCH CENTRE OF FINLAND, ESPOO.
The effects of alloying and thermal factors on the solidification and mechanical properties of gray iron
[VTT-619] N90-13651
Analysis of an R-SQUID noise thermometer
[VTT-PUBL-54] N90-13769
The APROS software for process simulation and model development
[VTT-618] N90-13987

TECHNISCHE UNIV., BERLIN (GERMANY, F.R.).
Investigations of spontaneous nuclear order in copper by neutron diffraction
[ETN-90-96060] N90-14090
Comparison of the space program performance of countries with space programs
[ILR-MITT-222] N90-14150

TECHNISCHE UNIV., BRUNSWICK (GERMANY, F.R.).
High precision rocket attitude reconstruction using star sensor and magnetometer data N90-13844

TECHNISCHE UNIV., DELFT (NETHERLANDS).
Induced drag for non-planar wings
[LR-521] N90-13357
Test network Delft
[ETN-90-96009] N90-13365
Some new techniques for aircraft fuselage skin tests
[LR-547] N90-13379
Aircraft propulsion: Leading the way in aviation
[LR-532] N90-13395
Mathematical model identification for flight simulation, based on flight and taxi tests
[LR-550] N90-13410
Impact tests on aluminum 2024 T3, aramid and glass reinforced aluminum laminates and thermoplastic composites
[LR-534] N90-13613
Buckling of delaminations in ARALL laminates
[LR-535] N90-13614
Constant amplitude fatigue of ARALL-2 laminates
[LR-539] N90-13615
Some aspects of test frequency influence on the fatigue behavior of ARALL
[LR-549] N90-13616
Repair of composites by means of wet-lay-up
[LR-551] N90-13617
Internal and external nitriding and nitrocarburizing of iron and iron-based alloys
[ETN-90-96012] N90-13646
Preliminary experiments on filament winding nylon impregnated glass fibers (FIT)
[LR-545] N90-13669
Multigrid and defect correction for the steady Navier-Stokes equations: Applications to aerodynamics
[ETN-90-96011] N90-13727
On the topology of three-dimensional viscous flow structures near a plane wall. A classification and non-hyperbolic singularities on the wall
[LR-541] N90-13758
Kinematics and control of manipulation robots
[WTHD-187] N90-13803
An evaluation of a fatigue crack growth prediction model for variable-amplitude loading (PREFFAS)
[LR-537] N90-13822
Buckling load analysis for imperfect cylindrical shells, part 1
[LR-543-PT-1] N90-13823
Design and evaluation of a new biaxial testing method for sheet material (SUPERBAT)
[LR-548] N90-13824
The initial imperfection data bank at the Delft University of Technology, part 2
[LR-559-PT-2] N90-13825
Precision of semi-geometrically determined SLR baselines vs. site occupation time
[ETN-90-96007] N90-13885
GRADIO: An error analysis of the spaceborne gravity gradiometer
[ETN-90-96010] N90-13901
Compensatory tracking in disturbance tasks and target following tasks. The influence of cockpit motion on performance and control behavior
[LR-511] N90-13933
Interface between MEDUSA and GIFTS for shell structures
[LR-553] N90-13985
Surface cooled, vacuum impregnated superconducting magnet systems: Design, construction, applications
[ETN-90-96014] N90-14072
Normal points: Compression of satellite laser ranging data
[ETN-90-96006] N90-14145

TECHNISCHE UNIV., EINDHOVEN (NETHERLANDS).
Electrochemical study of the etching of III to V semiconductors
[ETN-90-96015] N90-13633
Conjugate profiles on mating gear teeth
[MEMO-COSOR-89-01] N90-13795
On control of manipulators
[ISBN-90-9002789-0] N90-13804
The cellular approach: A new method to speed up simulated annealing for macro placement
[MEMO-COSOR-88-29] N90-13980
On the asymptotic convergence of the simulated annealing algorithm in the presence of a parameter dependent penalization
[MEMO-COSOR-89-16] N90-13984
A priori results in linear quadratic optimal control theory
[MEMO-COSOR-89-02] N90-13996
The quadratic matrix inequality in singular H infinity control with state feedback
[MEMO-COSOR-89-03] N90-13997
The totally singular linear quadratic problem with indefinite cost
[MEMO-COSOR-89-05] N90-13998
The singular zero sum differential game with stability using H infinity control theory
[MEMO-COSOR-89-09] N90-13999
The singular H infinity control problem with dynamic measurement feedback
[MEMO-COSOR-89-14] N90-14000
The output-stabilizable subspace and linear optimal control
[MEMO-COSOR-89-15] N90-14001
The regular indefinite linear quadratic problem with linear endpoint constraints
[MEMO-COSOR-88-15] N90-14022
Stabilizability and detectability of discrete-time time-varying systems
[MEMO-COSOR-88-16] N90-14023
Continuity properties of one-parameter families of linear-quadratic problems without stability
[MEMO-COSOR-88-17] N90-14024
Global optimization and simulated annealing
[MEMO-COSOR-88-21] N90-14025
Convergence properties of indefinite linear quadratic problems with receding horizon
[MEMO-COSOR-88-25] N90-14026
On the output-stabilizable subspace
[MEMO-COSOR-88-27] N90-14027
The algebraic Riccati equation and singular optimal control
[MEMO-COSOR-88-31] N90-14028
Some remarks on the gap metric
[MEMO-COSOR-88-34] N90-14029
Counterexamples to Robertson's conjecture
[MEMO-COSOR-88-32] N90-14048
Estimation of convolution tail behavior
[MEMO-COSOR-89-04] N90-14051
Self-decomposable distributions and branching processes
[MEMO-COSOR-89-06] N90-14052
Note on Urbanik's class L(sub n)
[MEMO-COSOR-89-07] N90-14053

Reverse self-decomposability
[MEMO-COSOR-89-06] N90-14054
Towards ab initio calculation of electron energies in semiconductors
[ETN-90-90016] N90-14121

TELEDYNE BROWN ENGINEERING, HUNTSVILLE, AL.
User needs, benefits, and integration of robotic systems in a space station laboratory
[NASA-CR-185150] N90-13794

TENNESSEE UNIV., TULLAHOMA.
A wall interference assessment/correction interface measurement system for the NASA/ARC 12-ft PWT
[NASA-CR-185474] N90-13401

TEXAS A&M UNIV., COLLEGE STATION.
Modern biofuel cells for waste recycling in life support systems
[NASA-CR-185963] N90-13718
Estimation of rain rate using spatial and multichannel coherence: Analysis of SSM/I data N90-13905

TEXAS INSTRUMENTS, INC., DALLAS.
MM and T for VHSIC multichip packages
[AD-A213259] N90-13703

TEXAS UNIV., AUSTIN.
Big Bang nucleosynthesis and the Quark-Hadron transition
[NASA-CR-185169] N90-14168
Analysis of coordinated observations of a giant stellar flare
[NASA-CR-185961] N90-14176

TEXAS UNIV., DALLAS.
Architecture and language for a layered relational database N90-14146

TEXTRON BELL HELICOPTER, FORT WORTH, TX.
Investigation of difficult component effects on finite element model vibration prediction for the Bell AG-1G helicopter. Volume 2: Correlation results
[NASA-CR-181916-VOL-2] N90-13814

TEXTRON LYCOMING, STRATFORD, CT.
MM and T advanced balancing/machining
[AD-A213103] N90-13775

THIOKOL CORP., BRIGHAM CITY, UT.
Systems tunnel linear shaped charge lightning strike
[NASA-CR-183832] N90-13404
Cable coupling lightning transient qualification
[NASA-CR-183826] N90-13405
Flight motor set 360L001 (STS-26R). Volume 5: Nozzle component
[NASA-CR-183771] N90-13588
Qualification of improved joint heaters
[NASA-CR-183827] N90-13594
Evaluation of newly formulated Dow Corning 321 dry film lubricant
[NASA-CR-183828] N90-13661
The evaluation of a metered mixer for RTV silicone for RSRM nozzle backfill operations
[NASA-CR-183831] N90-13783

THOMSON-CSF, PALO ALTO, CA.
Multi-level specification and verification of real-time software
[AD-A213227] N90-13975

TOULOUSE UNIV. (FRANCE).
Watchfulness and attention during weightlessness simulations: Use of computerized psychometric tests
[REPT-89-TOU-3-1045] N90-13928

TRW SPACE AND DEFENSE SECTOR, REDONDO BEACH, CA.
Development of high gain three terminal devices - at millimeter wave frequencies
[AD-A213089] N90-13701

TRW SPACE TECHNOLOGY LABS., REDONDO BEACH, CA.
An approach to optical structures control N90-13456
Explicit modeling and concurrent processing in the simulation of multibody dynamic systems N90-13481

U

UMWELTBUNDESAMT, BERLIN (GERMANY, F.R.).
Proceedings: US/FRG (Federal Republic of Germany) Workshop on Photochemical Ozone Problem and Its Control: US Experiences and the Situation in Europe
[PB89-233514] N90-13891

UNITED TECHNOLOGIES CORP., WEST PALM BEACH, FL.
Status of Gr/glass composites technology at UTOS N90-13459

UNIVERSITEIT TWENTE, ENSCHEDE (NETHERLANDS).
Balance laws and centro velocity in dissipative systems
[MEMO-787] N90-13726
Stopping rules for a class of random methods for detecting necessary linear inequality constraints
[MEMO-777] N90-13977
Model reduction of weakly damped mechanical systems
[MEMO-798] N90-13993
On smallest nonhamiltonian regular rough graphs
[MEMO-788] N90-14003
Hamiltonian properties of graphs with large neighborhood unions
[MEMO-779] N90-14013
Using the physical structure of a system for control: An illustration
[MEMO-782] N90-14014
On the performance of on-line algorithms for partition problems
[MEMO-784] N90-14015
Optimal processes described by a parabolic differential equation with control in the coefficients, part 4
[MEMO-785-PT-4] N90-14016
On the recurrence relation for multivariate B-splines with respect to dimension
[MEMO-786] N90-14017
On geometry of inhomogeneous Heisenberg ferromagnet: Nonintegrable case
[MEMO-789] N90-14030
The weighted sum of two S-units being a square
[MEMO-792] N90-14031
Solving a specific Thue-Mahler equation
[MEMO-793] N90-14032
Another approach to the local disturbance decoupling problem with stability for nonlinear systems
[MEMO-799] N90-14033
Practice of bivariate quadratic simplicial splines
[MEMO-800] N90-14034
Analysis of three approaches to qualitative simulation
[MEMO-INF-89-32] N90-14035
The activity selection problem: A network and game theoretic approach
[MEMO-794] N90-14056
On stability of queueing models of local area networks with slotted ring protocols
[MEMO-795] N90-14057
Analysis of a queueing model for slotted ring networks
[MEMO-796] N90-14058
Dynamic workload modeling of high speed token rings in a metropolitan area network
[MEMO-INF-89-21] N90-14059

UNIVERSITY CITY SCIENCE CENTER, PHILADELPHIA, PA.
Gravity receptors and responses N90-13948

UNIVERSITY OF SOUTHERN CALIFORNIA, LOS ANGELES.
Model filled polymers I. Synthesis of crosslinked monodisperse polystyrene beads
[AD-A213228] N90-13860

UNIVERSITY OF SOUTHERN CALIFORNIA, MARINA DEL REY.
Parallelism in the discrete-event simulation algorithm
[AD-A213060] N90-13970

UTAH UNIV., SALT LAKE CITY.
Fractography of composite delamination
[NASA-CR-183291] N90-13599
Late quaternary geomorphology of the Great Salt Lake region, Utah, and other hydrographically closed basins in the western United States: A summary of observations
[NASA-CR-185912] N90-13878

V

VIRGINIA POLYTECHNIC INST. AND STATE UNIV., BLACKSBURG.
Efficient methods for integrated structural-aerodynamic wing optimum design N90-13376
Failure processes in unidirectional composite materials N90-13598
Static and free-vibrational response of semi-circular graphite-epoxy frames with thin-walled open sections
[NASA-CR-186097] N90-13600
Pressure correction calculation procedures for 3D viscous flow N90-13738
Three D flows in turbine blade rows N90-13739
Flows with tip leakage N90-13740
Effect of suction and cooling on the stability of subsonic and supersonic boundary layers N90-13745
Adaptation and resistance of ecosystems to stress
[AD-A212999] N90-13889

VIRGINIA UNIV., CHARLOTTESVILLE.
A three-dimensional potential flow analysis of dynamic fluid forces acting on a whirling centrifugal impeller bounded by a volute N90-13717

VON KARMAN INST. FOR FLUID DYNAMICS, RHODE-SAINT-GENESE (BELGIUM).
An Introduction to Hypersonic Aerodynamics
[VKI-LS-1989-01] N90-13334
Measurement Techniques in Aerodynamics
[VKI-LS-1989-05] N90-13339
Turbulent Shear Flows
[VKI-LS-1989-03] N90-13730
Numerical Methods for Flows in Turbomachinery, volume 1
[VKI-LS-1989-06-VOL-1] N90-13735
Numerical Methods for Flows in Turbomachinery, volume 2
[VKI-LS-1989-06-VOL-2] N90-13741

W

WASHINGTON UNIV., SEATTLE.
Toughening of a particulate-reinforced/ceramic-matrix composite
[AD-A213180] N90-13604
Synthesis of inorganic polymers as glass precursors and for other uses. Preceramic block or graft copolymers as potential precursors to nanocomposite materials
[AD-A211978] N90-13655
How to detect when cells in space perceive gravity N90-13948

WESTINGHOUSE ELECTRIC CORP., MIDDLETOWN, RI.
Metal transfer in gas metal arc welding
[AD-A213390] N90-13642

WISCONSIN UNIV., MADISON.
Quadratic dynamical systems describing shear flow of non-Newtonian fluids
[AD-A212892] N90-13720
Analysis of new phenomena in shear flow of non-Newtonian fluids
[AD-A212893] N90-13721
Measurement of mechanical work and energy expenditure in running and bicycling N90-13935
Parabolic equations for curves on surfaces. 2: Intersections, blow up and generalized solutions
[AD-A212890] N90-14004
Periodic solutions of Hamiltonian systems of 3-body type
[AD-A212891] N90-14005

WORLD METEOROLOGICAL ORGANIZATION, GENEVA (SWITZERLAND).
Activities report of the World Meteorological Organization
[WMO-713] N90-13912

WUPPERTAL UNIV. (GERMANY, F.R.).
The DYANA campaign 1990 N90-13870

WYLE LABS., INC., HUNTSVILLE, AL.
Development of a shuttle recovery Commercial Materials Processing in Space (CMPS) program
[NASA-CR-183720] N90-13678

Y

YALE UNIV., NEW HAVEN, CT.
Transport phenomena and interfacial kinetics in multiphase combustion systems
[AD-A212932] N90-13620

Typical Contract Number Index Listing

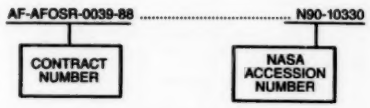

Listings in this index are arranged alphanumerically by contract number. Under each contract number the NASA accession numbers denoting documents that have been produced as a result of research done under that contract are arranged in ascending order. The NASA accession number denotes the number by which the citation is identified.

AF PROJ. 2305 ..... N90-14107
AF PROJ. 2307 ..... N90-13330
AF PROJ. 2308 ..... N90-13620
N90-14104
AF PROJ. 2309 ..... N90-13895
AF PROJ. 2310 ..... N90-13897
N90-13898
N90-13899
N90-13900
AF PROJ. 2312 ..... N90-13889
AF PROJ. 2313 ..... N90-13918
AF PROJ. 2403 ..... N90-13398
AF PROJ. 5730 ..... N90-13670
AF 04(645)-18 ..... N90-13337
AF 49(638)-792 ..... N90-13336
AF-AFOSR-0034-84 ..... N90-13620
AF-AFOSR-0130-85 ..... N90-14107
AF-AFOSR-0141-85 ..... N90-13720
N90-13721
AF-AFOSR-0184-87 ..... N90-13330
AF-AFOSR-0191-87 ..... N90-13720
N90-13721
AF-AFOSR-0202-87 ..... N90-14004
AF-AFOSR-0263-88 ..... N90-13889
AF-AFOSR-0266-85 ..... N90-13895
AF-AFOSR-0375-85 ..... N90-14104
AID/ANE-0337-P-IZ-8021-00 ..... N90-13903
ARB-A6-129-87 ..... N90-13920
ARPA ORDER 4395 ..... N90-14096
ARPA ORDER 5339 ..... N90-13969
BMFT-FK-150-0304-B N90-13635
BMFT-PA4-010-M-86080 ..... N90-13840
BMFT-WRK-90 ..... N90-13839
BMFT-01-OE-610 ..... N90-13836
BMFT-01-OE-8604-6 ..... N90-13855
BMFT-01-OE-86033 ..... N90-13836
BMFT-01-TH-8503-AK/RT N90-13713
BMFT-13-EU-0023/10 ..... N90-13761
DA PROJ. 1L1-61102-AH-45 ..... N90-13393
N90-13786
DA PROJ. 1L1-61102-BH-57 ..... N90-13605
N90-14157
DA PROJ. 1L1-62209-A4-7A N90-13785
DA PROJ. 1L1-62209-A47-A N90-13797
DAAE07-85-C-R163 ..... N90-13775
DAAG29-85-K-0073 ..... N90-14093
DAAH01-88-C-0899 ..... N90-13762
DAAL01-85-C-0442 ..... N90-13703
DAAL03-86-K-0053 ..... N90-14109
DAAL03-86-K-0171 ..... N90-14062
DAAL03-87-K-0036 ..... N90-13720
N90-13721
DAAL03-87-K-0043 ..... N90-14005
DACA88-88-M-1554 ..... N90-13788
DAJA45-84-C-0043 ..... N90-14157
DAJA45-86-C-0037 ..... N90-13605
DAJA45-88-M-0358 ..... N90-13809
DE-AI05-80OR-20679 ..... N90-13656
DEN3-335 ..... N90-14153
DFG-HO-858/1 ..... N90-13837
N90-13889
DLA900-84-C-0910 ..... N90-13359
DRET-BC-88-001-16 ..... N90-13632
DRET-85-1032 ..... N90-13927
DRET-86-34-1390 ..... N90-13672
DRET-87-34-001 ..... N90-13800
DRET-87-003 ..... N90-13356
DTFA01-89-C-00001 ..... N90-13361
N90-13362
N90-13363
DTFA03-88-C-00024 ..... N90-13360
DTRS-57-88-C-00117 ..... N90-13386
EPA-68-02-4352 ..... N90-13890
ERO-DAERO-75-G076 ..... N90-13839
FGD-502-531 ..... N90-14144
F04611-88-C-0014 ..... N90-13591
N90-13592
N90-13593
F19628-85-C-0032 ..... N90-13897
N90-13898
N90-13899
N90-13900
F19628-85-C-0180 ..... N90-13689
F33615-83-C-3600 ..... N90-13398
F33615-85-C-2585 ..... N90-13789
F33615-87-C-3250 ..... N90-13612
F49620-85-C-0144 ..... N90-14051
F49620-86-C-0008 ..... N90-13382
N90-13383
F49620-86-C-0027 ..... N90-13906
F49620-86-C-0120 ..... N90-14095
F49620-87-C-0103 ..... N90-13430
F49620-87-K-0009 ..... N90-13918
F49620-88-C-0038 ..... N90-13658
F49620-88-K-0008 ..... N90-13929
GRI-5084-243-1028 ..... N90-13887
GRI-5087-254-1472 ..... N90-13766
GRI-5088-260-1688 ..... N90-13673
HDL PROJ. AE1951 ..... N90-14110
JPL-956415 ..... N90-13441
N90-13442
MDA903-87-C-0523 ..... N90-13938
MDA904-89-H-2008 ..... N90-14003
MOD-2062/192 ..... N90-13400
NAGW-1321 ..... N90-14124
N90-14167
NAGW-1340 ..... N90-14076
N90-14124
N90-14164
N90-14167
N90-14168
N90-14169
N90-14180
NAGW-1686 ..... N90-13879
NAGW-1782 ..... N90-14175
NAG1-244 ..... N90-13747
NAG1-343 ..... N90-13600
NAG1-515 ..... N90-13495
NAG1-596 ..... N90-13618
NAG1-613 ..... N90-13430
NAG1-623 ..... N90-13783
NAG1-685 ..... N90-13817
NAG1-705 ..... N90-13599
NAG1-755 ..... N90-13706
NAG1-837 ..... N90-13354
NAG1-874 ..... N90-13744
NAG1-877 ..... N90-13772
NAG1-907 ..... N90-13369
NAG2-208 ..... N90-14156
NAG2-303 ..... N90-13771
NAG2-311 ..... N90-14156
NAG2-317 ..... N90-13759
NAG2-551 ..... N90-13401
NAG3-383 ..... N90-13886
NAG3-592 ..... N90-13328
NAG5-203 ..... N90-13976
NAG5-356 ..... N90-13770
NAG5-510 ..... N90-13879
NAG5-557 ..... N90-13685
NAG5-739 ..... N90-14133
NAG5-740 ..... N90-13894
NAG5-797 ..... N90-14160
NAG5-916 ..... N90-13963
NAG5-987 ..... N90-14178
NAG5-989 ..... N90-14163
NAG5-1051 ..... N90-14102
NAG5-1068 ..... N90-13883
NAG8-755 ..... N90-13441
N90-13442
N90-13443
NAG9-181 ..... N90-13942
NAG9-234 ..... N90-13942
NAG9-263 ..... N90-13718
NAG9-341 ..... N90-13496
NAG10-0059 ..... N90-13916
NASA ORDER C-99066-G N90-14002
NASW-3482 ..... N90-14154
NASW-4003 ..... N90-13492
NAS1-17496 ..... N90-13814
NAS1-18378 ..... N90-13370
NAS1-18605 ..... N90-13351
N90-13722
N90-14038
NAS1-18668 ..... N90-13760
NAS3-23925 ..... N90-13390
N90-13391
NAS3-23944 ..... N90-13388
NAS3-24612 ..... N90-13589
NAS3-24847 ..... N90-13385
NAS3-25266 ..... N90-13323
N90-13748
N90-13761
N90-13968
NAS3-25278 ..... N90-13794
NAS5-28753 ..... N90-13878
NAS5-29320 ..... N90-13429
NAS5-30430 ..... N90-13976
NAS5-31500 ..... N90-13414
N90-13418
N90-13421
N90-13426
N90-13428
N90-13432
N90-13434
N90-13435
N90-13436
N90-13439
N90-13440
NAS7-918 ..... N90-13412
N90-13796
N90-13893
N90-14084
NAS8-30490 ..... N90-13404
N90-13405
N90-13586
N90-13587
N90-13588
N90-13594
N90-13652
N90-13653
N90-13654
N90-13661
N90-13681
N90-13763
NAS8-35671 ..... N90-13584
NAS8-36109 ..... N90-13678
NAS8-36277 ..... N90-14125
NAS8-36435 ..... N90-13934
NAS8-36717 ..... N90-13497
NAS8-37361 ..... N90-13715
N90-13716
NAS8-37578 ..... N90-13380
NAS8-37747 ..... N90-13491
NAS8-37755 ..... N90-14092
NAS8-38150 ..... N90-13585
NCC2-213 ..... N90-13942
NCC2-581 ..... N90-13994
NCC3-133 ..... N90-14108
NCC8-13 ..... N90-13964
N90-13965
N90-13991
N90-14181
NCC8-14 ..... N90-13962
NCC9-16 ..... N90-13966
N90-13967
N90-13981
N90-13982

NGL-05-020-272 ..... N90-14178
NGR-05-020-559 ..... N90-14177
NOAA-50-DGNE-6-00003 ..... N90-13422
NR PROJ. 051-855 ..... N90-13623
NSA MDA904-89-H-2008 ..... N90-14013
NSERC-0GP-0036747 ..... N90-14062
NSF AST-88-09616 ..... N90-14164
NSF AST-88-22595 ..... N90-14124
N90-14167
NSF ATM-86-18263 ..... N90-14177
NSF CCR-86-03772 ..... N90-13970
NSF DCR-86-06366 ..... N90-14062
NSF DMS-86-20303 ..... N90-13720
N90-13721
NSF DMS-87-12058 ..... N90-13720
N90-13721
NSF DMS-88-01486 ..... N90-14004
NSF ECE-86-05159 ..... N90-13808
NSF MCS-81-10556 ..... N90-14005
NSF MIP-88-14612 ..... N90-13696
NSG-1414 ..... N90-13494
NSG-7270 ..... N90-13943
N00014-81-K-0605 ..... N90-13700
N00014-82-K-0455 ..... N90-14112
N00014-83-K-0468 ..... N90-13624
N90-13641
N00014-84-C-0149 ..... N90-13702
N90-14008
N90-14009
N00014-84-C-0193 ..... N90-14073
N00014-84-K-0052 ..... N90-13623
N00014-85-K-0213 ..... N90-13969
N00014-85-K-0354 ..... N90-13659
N00014-85-K-0445 ..... N90-14062
N00014-85-K-0570 ..... N90-13960
N00014-85-K-0692 ..... N90-13924
N00014-86-K-0043 ..... N90-14113
N00014-86-K-0085 ..... N90-14177
N00014-86-K-0262 ..... N90-13601
N00014-86-K-0711 ..... N90-13773
N00014-87-C-0689 ..... N90-13971
N00014-87-K-0022 ..... N90-13970
N00014-87-K-0158 ..... N90-13896
N00014-87-K-0303 ..... N90-14078
N00014-87-K-0326 ..... N90-13604
N00014-87-K-0398 ..... N90-14143
N00014-87-K-0825 ..... N90-13696
N90-13697
N90-13698
N90-14140
N00014-88-C-0393 ..... N90-13642
N00014-88-C-2068 ..... N90-13701
N00014-88-K-0134 ..... N90-14005
N00014-88-K-0302 ..... N90-13660
N00014-88-K-0305 ..... N90-13655
N00014-88-K-0546 ..... N90-13915
N00014-88-K-0564 ..... N90-13625
N00014-89-C-0022 ..... N90-13975
N00014-89-J-1023 ..... N90-13699
N00014-89-J-1278 ..... N90-14111
N00014-89-J-1345 ..... N90-13913
N00014-89-J-1362 ..... N90-13602
N90-13638
N90-13810
N00039-87-C-0182 ..... N90-13698
N00228-89-G-0580 ..... N90-13683
N66001-85-C-0422 ..... N90-14106
N66001-85-D-0203 ..... N90-14096
N66001-87-D-0136 ..... N90-13628
OV/RLD-837 ..... N90-13371
PROJ. RS34A50 ..... N90-13639
RR04209 ..... N90-13924
STU-SS-01693P N90-13986
SWRI PROJ. 05-0769 ..... N90-13496
SWRI PROJ. 06-7576 ..... N90-13390
N90-13391
SWRI PROJ. 17-7958-843 ..... N90-13359
142-60-20 ..... N90-13939
199-21-12-07 ..... N90-13626
324-02-00 ..... N90-13760
474-11-10 ..... N90-13596
474-12-10 ..... N90-13581
474-42-10 ..... N90-14060
482-52-21-01 ..... N90-13931
505-43-31 ..... N90-13820
505-60-01 ..... N90-13329
505-60-11 ..... N90-13723
505-61-01 ..... N90-13407
505-62-01 ..... N90-13381
N90-13761
505-62-21 ..... N90-13323
N90-13328
N90-13387
N90-13393
N90-13750
N90-13968
N90-14002
505-62-51 ..... N90-13749
505-62-61 ..... N90-13392
505-62-71 ..... N90-13389
505-63-1A N90-13636
N90-13766
N90-14108
505-63-1B N90-13355
505-63-01-10 ..... N90-13818
505-63-11 ..... N90-13597
505-63-21-09 ..... N90-13403
505-63-51 ..... N90-13785
505-63-51-01 ..... N90-13814
505-66-21-04 ..... N90-14061
505-66-71 ..... N90-13995
505-67-21 ..... N90-13384
505-68-11 ..... N90-13797
505-68-27 ..... N90-13990
505-68-71 ..... N90-13332
N90-13372
505-69-01-01 ..... N90-13370
505-90-01 ..... N90-13719
505-90-21-01 ..... N90-13351
N90-13722
N90-14038
506-40-11 ..... N90-13324
506-44-21-03 ..... N90-13694
506-48-21 ..... N90-13590
510-01-01 ..... N90-13686
533-04-1A N90-13390
N90-13391
535-03-01 ..... N90-13352
551-53-22-301 ..... N90-13444
582-01-11 ..... N90-13595
N90-13819
582-01-31 ..... N90-13589
585-01-21-08 ..... N90-13807
586-01-21 ..... N90-13748
591-23-00 ..... N90-13675
N90-13751
674-22-05 ..... N90-13679
N90-13680
677-22-29-01 ..... N90-13976
694-03-03 ..... N90-13794
694-23-03 ..... N90-13988
889-59-11-31-03 ..... N90-13412
992-21-01 ..... N90-13327

Typical Report Number Index Listing

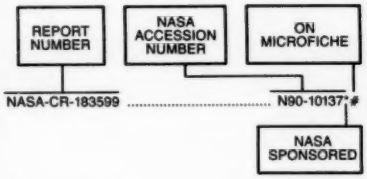

Listings in this index are arranged alphanumerically by report number. The NASA accession number denotes the number by which the citation is identified. An asterisk (*) indicates that the item is a NASA report. A pound sign (#) indicates that the item is available on microfiche.

A-88294 ..... N90-13723* #
A-88315 ..... N90-13926* #
A-89094 ..... N90-13329* #
A-89131 ..... N90-13939* #
A-89148 ..... N90-13332* #
A-89172 ..... N90-13324* #
A-89195 ..... N90-13407* #
A-89196 ..... N90-13384* #
A-89209 ..... N90-13327* #
A-89260 ..... N90-13931* #
A-90036 ..... N90-13353* #

AAR-238-PT-1 ..... N90-13441* #
AAR-239-PT-2 ..... N90-13442* #
AAR-245 ..... N90-13443* #

ACT-108 ..... N90-13960 #

AD-A210995 ..... N90-13918 #
AD-A211654 ..... N90-13326 #
AD-A211861 ..... N90-14106 #
AD-A211871 ..... N90-13936 #
AD-A211890 ..... N90-14140 #
AD-A211891 ..... N90-13696 #
AD-A211917 ..... N90-13697 #
AD-A211932 ..... N90-13698 #
AD-A211947 ..... N90-14107 #
AD-A211978 ..... N90-13655 #
AD-A212002 ..... N90-13919 #
AD-A212293 ..... N90-13809 #
AD-A212314 ..... N90-13670 #
AD-A212340 ..... N90-14093 #
AD-A212417 ..... N90-13657 #
AD-A212650 ..... N90-14109 #
AD-A212663 ..... N90-13364 #
AD-A212849 ..... N90-13906 #
AD-A212850 ..... N90-14110 #
AD-A212851 ..... N90-13330 #
AD-A212855 ..... N90-13402 #
AD-A212857 ..... N90-14104 #
AD-A212863 ..... N90-14127 #
AD-A212864 ..... N90-14128 #
AD-A212865 ..... N90-14129 #
AD-A212866 ..... N90-14130 #
AD-A212867 ..... N90-14131 #
AD-A212868 ..... N90-14132 #
AD-A212886 ..... N90-14182 #
AD-A212887 ..... N90-13445 #
AD-A212889 ..... N90-13773 #
AD-A212890 ..... N90-14004 #
AD-A212891 ..... N90-14005 #
AD-A212892 ..... N90-13720 #
AD-A212893 ..... N90-13721 #
AD-A212916 ..... N90-13895 #
AD-A212932 ..... N90-13620 #
AD-A212934 ..... N90-13929 #
AD-A212940 ..... N90-13658 #
AD-A212942 ..... N90-13913 #
AD-A212943 ..... N90-14094 #
AD-A212945 ..... N90-13959 #
AD-A212950 ..... N90-13637 #
AD-A212952 ..... N90-13687 #
AD-A212972 ..... N90-13659 #
AD-A212975 ..... N90-13601 #
AD-A212985 ..... N90-14111 #
AD-A212990 ..... N90-13921 #
AD-A212991 ..... N90-13937 #
AD-A212994 ..... N90-13602 #
AD-A212995 ..... N90-13638 #
AD-A212996 ..... N90-13810 #
AD-A212998 ..... N90-14112 #
AD-A212999 ..... N90-13889 #
AD-A213002 ..... N90-14073 #
AD-A213003 ..... N90-13671 #
AD-A213004 ..... N90-14113 #
AD-A213005 ..... N90-13969 #
AD-A213006 ..... N90-13621 #
AD-A213015 ..... N90-13699 #
AD-A213018 ..... N90-13700 #
AD-A213025 ..... N90-13498 #
AD-A213030 ..... N90-13374 #
AD-A213044 ..... N90-14141 #
AD-A213046 ..... N90-13622 #
AD-A213055 ..... N90-13639 #
AD-A213056 ..... N90-14095 #
AD-A213058 ..... N90-13787 #
AD-A213060 ..... N90-13970 #
AD-A213062 ..... N90-13688 #
AD-A213065 ..... N90-13971 #
AD-A213082 ..... N90-13774 #
AD-A213088 ..... N90-13915 #
AD-A213089 ..... N90-13701 #
AD-A213092 ..... N90-13972 #
AD-A213094 ..... N90-13603 #
AD-A213095 ..... N90-13922 #
AD-A213096 ..... N90-13923 #
AD-A213103 ..... N90-13775 #
AD-A213112 ..... N90-14078 #
AD-A213114 ..... N90-14177* #
AD-A213118 ..... N90-13689 #
AD-A213129 ..... N90-13973 #
AD-A213134 ..... N90-13776 #
AD-A213135 ..... N90-13992 #
AD-A213137 ..... N90-14006 #
AD-A213138 ..... N90-14096 #
AD-A213139 ..... N90-14097 #
AD-A213140 ..... N90-14007 #
AD-A213141 ..... N90-13974 #
AD-A213144 ..... N90-13640 #
AD-A213148 ..... N90-14142 #
AD-A213150 ..... N90-13788 #
AD-A213151 ..... N90-14008 #
AD-A213152 ..... N90-13960 #
AD-A213153 ..... N90-13702 #
AD-A213154 ..... N90-14009 #
AD-A213156 ..... N90-13623 #
AD-A213180 ..... N90-13604 #
AD-A213217 ..... N90-14157 #
AD-A213218 ..... N90-13762 #
AD-A213227 ..... N90-13975 #
AD-A213228 ..... N90-13660 #
AD-A213237 ..... N90-13907 #
AD-A213239 ..... N90-14010 #
AD-A213240 ..... N90-14143 #
AD-A213243 ..... N90-13811 #
AD-A213244 ..... N90-13641 #
AD-A213245 ..... N90-13624 #
AD-A213248 ..... N90-13375 #
AD-A213249 ..... N90-13789 #
AD-A213252 ..... N90-14183 #
AD-A213253 ..... N90-13914 #
AD-A213259 ..... N90-13703 #
AD-A213265 ..... N90-13625 #
AD-A213270 ..... N90-14011 #
AD-A213272 ..... N90-13626 #
AD-A213281 ..... N90-13382 #
AD-A213282 ..... N90-13383 #
AD-A213284 ..... N90-13896 #
AD-A213285 ..... N90-13938 #
AD-A213290 ..... N90-13924 #
AD-A213297 ..... N90-13812 #
AD-A213308 ..... N90-14012 #
AD-A213314 ..... N90-13690 #
AD-A213335 ..... N90-13790 #
AD-A213336 ..... N90-13791 #
AD-A213337 ..... N90-13792 #
AD-A213341 ..... N90-13897 #
AD-A213342 ..... N90-13898 #
AD-A213343 ..... N90-13899 #
AD-A213344 ..... N90-13900 #
AD-A213348 ..... N90-13591 #
AD-A213349 ..... N90-13592 #
AD-A213350 ..... N90-13593 #
AD-A213357 ..... N90-14144 #
AD-A213358 ..... N90-13605 #
AD-A213359 ..... N90-13627 #
AD-A213361 ..... N90-13691 #
AD-A213363 ..... N90-13682 #
AD-A213366 ..... N90-13793 #
AD-A213368 ..... N90-13359 #
AD-A213373 ..... N90-13777 #
AD-A213375 ..... N90-13628 #
AD-A213376 ..... N90-14096 #
AD-A213378 ..... N90-13398 #
AD-A213379 ..... N90-13399 #
AD-A213390 ..... N90-13642 #
AD-A213394 ..... N90-13683 #
AD-A213395 ..... N90-13331 #

AD-D014207 ..... N90-13373 #

AD-E801979 ..... N90-13399 #

AERONOMICA-ACTA-A-346-1989 ..... N90-14045
AERONOMICA-ACTA-A-347-1989 ..... N90-13909
AERONOMICA-ACTA-A-348-1989 ..... N90-13630
AERONOMICA-ACTA-A-349-1989 ..... N90-13892

AERONOMICA-ACTA-F-39-1989 ..... N90-13411

AFATL-TP-89-18 ..... N90-13331 #

AFATL-TR-89-49 ..... N90-13399 #

AFGL-ERP-1024 ..... N90-13907 #

AFGL-TR-89-0079 ..... N90-13907 #

AFOSR-89-1024TR ..... N90-14107 #
AFOSR-89-1027TR ..... N90-13918 #
AFOSR-89-1212TR-PT-1 ..... N90-13658 #
AFOSR-89-1231TR ..... N90-13895 #
AFOSR-89-1237TR ..... N90-14104 #
AFOSR-89-1238TR ..... N90-14142 #
AFOSR-89-1240TR ..... N90-13620 #
AFOSR-89-1242TR ..... N90-13906 #
AFOSR-89-1244TR ..... N90-13889 #
AFOSR-89-1246TR ..... N90-13929 #
AFOSR-89-1248TR ..... N90-14095 #
AFOSR-89-1256TR ..... N90-13330 #

AFWAL-TR-88-2149 ..... N90-13789 #

AGARD-AG-305(E) ..... N90-13358 #

AIAA-89-0438 ..... N90-13352* #
AIAA-90-0028 ..... N90-13355* #
AIAA-90-0344 ..... N90-13968* #
AIAA-90-0353 ..... N90-13675* #
AIAA-90-0354 ..... N90-13751* #
AIAA-90-0643 ..... N90-13749* #
AIAA-90-0669 ..... N90-13797* #
AIAA-90-0722 ..... N90-13581* #
AIAA-90-0744 ..... N90-13988* #

AL-CP-89-002 ..... N90-13670 #

AL-TR-89-011-VOL-1 ..... N90-13591 #
AL-TR-89-011-VOL-2-APP-C ..... N90-13592 #
AL-TR-89-011-VOL-3-APP-D ..... N90-13593 #

AR-005-647 ..... N90-13808 #
AR-005-648 ..... N90-13784 #

ARB-R-89/397 ..... N90-13920 #

ARE-TM(UHA)-88512 ..... N90-13752 #

ARE-TM(UHA)-88519 N90-14085 #

ARI-TR-858 N90-13938 #

ARL-MAT-TM-398 N90-13806 #
ARL-MAT-TM-399 N90-13764 #

ARO-22758.19-PH N90-14109 #
ARO-22905.14-PH N90-14093 #

ASI-690-319-88 N90-13938 #

AST-89-004 N90-13386 #

AVSCOM-TM-89-C-005 N90-13785* #
AVSCOM-TM-89-C-012 N90-13786* #
AVSCOM-TM-89-C-014 N90-13797* #

AVSCOM-TR-89-C-013 N90-13393* #

BHT-699-099-251-VOL-2 N90-13814* #

BRL-MR-3784 N90-14011 #
BRL-MR-3785 N90-13626 #

BR108415 N90-13752 #
BR108480 N90-13366 #
BR108610 N90-14085 #
BR112013 N90-13408 #

CCMS-89-21 N90-13600* #

CERL-TM-M-89/11 N90-13688 #

CFPA-TH-89-013 N90-14184* #

CISE-4845 N90-13782 #

CMS-TSR-89-24-2 N90-14004 #
CMS-TSR-90-6 N90-13721 #
CMS-TSR-90-7 N90-13720 #
CMS-TSR-90-8 N90-14005 #

CMU-RI-TR-89-11 N90-14144 #
CMU-RI-TR-89-13 N90-13682 #
CMU-RI-TR-89-15-PT-3 N90-13792 #
CMU-RI-TR-89-17-PT-2 N90-13791 #
CMU-RI-TR-89-18 N90-13793 #
CMU-RI-TR-89-20 N90-13627 #
CMU-RI-TR-89-21 N90-13790 #

CNES-CT/DTI/MS/CM/290 N90-13582 #

CRIF-MT-174 N90-13798 #
CRIF-MT-175 N90-13806 #
CRIF-MT-176 N90-13799 #

CSG-106 N90-13702 #

CSSA-ASTRO-89-11 N90-14178* #

CWI-AM-R8807 N90-14065 #

CWI-BS-R8901 N90-14018 #
CWI-BS-R8902 N90-14019 #
CWI-BS-R8904 N90-14046 #
CWI-BS-R8905 N90-13989 #
CWI-BS-R8906 N90-14020 #
CWI-BS-R8907 N90-14055 #
CWI-BS-R8908 N90-14021 #

CWI-CS-R8829 N90-13930 #
CWI-CS-R8913 N90-13978 #
CWI-CS-R8914 N90-13979 #
CWI-CS-R8915 N90-14062 #

CWI-OS-R8819 N90-14064 #

CWI-PM-R8805 N90-14036 #
CWI-PM-R8808 N90-14037 #

D/1989/0238/367 N90-13334 #
D/1989/0238/369 N90-13730 #
D/1989/0238/371 N90-13339 #
D/1989/0238/372-VOL-1 N90-13735 #
D/1989/0238/372-VOL-2 N90-13741 #

DAC-15 N90-14008 #

DC-114 N90-13788 #

DCIEM-89-RR-28 N90-13922 #
DCIEM-89-RR-32 N90-13923 #
DCIEM-89-TR-19 N90-13921 #
DCIEM-89-TR-24 N90-13937 #

DGLR-PAPER-85-113 N90-13408 #

DLR-FB-89-12 N90-13728 #
DLR-FB-89-26 N90-13724 #
DLR-FB-89-32 N90-13644 #
DLR-FB-89-33 N90-13815 #
DLR-FB-89-34 N90-13725 #
DLR-FB-89-35 N90-13629 #
DLR-FB-89-36 N90-13778 #
DLR-FB-89-37 N90-13333 #
DLR-FB-89-38 N90-13729 #
DLR-FB-89-44 N90-13881 #

DLR-MITT-89-11 N90-13606 #
DLR-MITT-89-12 N90-13607 #
DLR-MITT-89-13 N90-13816 #
DLR-MITT-89-14 N90-13577 #
DLR-MITT-89-15 N90-13645 #
DLR-MITT-89-16 N90-13882 #

DMI-TR-89010 N90-13762 #

DOC-89-62095 N90-13867 #

DOE/NASA/0335-1 N90-14153* #

DOT/FAA/CT-TN88/13 N90-13364 #

DOT/FAA/CT-89/16 N90-13360 #
DOT/FAA/CT-89/20 N90-13386 #

DOT/FAA/DS-89/29 N90-13361 #
DOT/FAA/DS-89/30 N90-13362 #

DOT/FAA/SA-89/3 N90-13363 #

DREP-TM-89-13 N90-13691 #

DRES-SR-527 N90-13621 #

DRIC-BR-110829 N90-13973 #

DTIC/TR-89/15 N90-14141 #

E-4224 N90-13786* #
E-4307 N90-13819* #
E-4655 N90-14002* #
E-4674 N90-13596* #
E-4726 N90-13679* #
E-4826 N90-13392* #
E-4837 N90-13352* #
E-4848 N90-13387* #
E-5007 N90-13590* #
E-5049 N90-13785* #
E-5060 N90-13666* #
E-5063 N90-13393* #
E-5109 N90-14060* #
E-5112 N90-13761* #
E-5115 N90-13719* #
E-5116 N90-13323* #
E-5119 N90-13587* #
E-5122 N90-13595* #
E-5130 N90-13381* #
E-5131 N90-14108* #
E-5151 N90-13968* #
E-5160 N90-13636* #
E-5170 N90-13988* #
E-5185 N90-13389* #
E-5190 N90-13680* #
E-5195 N90-13748* #
E-5196 N90-13355* #
E-5201 N90-13751* #
E-5206 N90-13675* #
E-5231 N90-13797* #
E-5232 N90-13750* #
E-5247 N90-13394* #
E-5249 N90-13749* #
E-5261 N90-13581* #

ECL-88-09 N90-14074 #
ECL-88-10 N90-14114 #
ECL-88-12 N90-13611 #
ECL-88-13 N90-14115 #
ECL-88-15 N90-14116 #
ECL-88-16 N90-13753 #
ECL-88-18 N90-14117 #
ECL-88-19 N90-13709 #
ECL-88-20 N90-13612 #
ECL-88-22 N90-13710 #
ECL-88-23 N90-13754 #
ECL-88-24 N90-14118 #
ECL-89-001 N90-13821 #
ECL-89-002 N90-13711 #
ECL-89-004 N90-13667 #
ECL-89-005 N90-13801 #
ECL-89-006 N90-14075 #

ECL-89-007 N90-13755 #

ENDIC-007-AFOSR-1989-PT-1 N90-13658 #

EP-PATENT-APPL-SN-88-303394-6 N90-13643
EP-PATENT-APPL-SN-88-304554-4 N90-14099
EP-PATENT-APPL-SN-88-305799 N90-13676

EP-PATENT-0-289-173-A1 N90-13643
EP-PATENT-0-294-061-A1 N90-14099
EP-PATENT-0-298-636-A-1 N90-13676

EPA/AA/TSS/IM-89/1 N90-13674 #

EPA/600/3-89/071 N90-13890 #
EPA/600/9-89/058 N90-13891 #

ESA-SP-291 N90-13826 #
ESA-SP-1105 N90-13917 #
ESA-SP-1111-VOL-1 N90-13499 #
ESA-SP-1111-VOL-2 N90-13529 #
ESA-SP-1111-VOL-3 N90-13548 #

ESD-TR-89-104 N90-13690 #

ESDU-87021 N90-13619 #
ESDU-89005 N90-13619 #

ETN-89-94604 N90-13635 #
ETN-89-95053 N90-13371 #
ETN-89-95678 N90-14003 #
ETN-89-95745 N90-14077 #
ETN-89-95858 N90-14158* #
ETN-90-94558 N90-13798 #
ETN-90-94559 N90-13806 #
ETN-90-94833 N90-13366 #
ETN-90-94845 N90-13752 #
ETN-90-94846 N90-14085 #
ETN-90-94847 N90-13932 #
ETN-90-95015 N90-13927 #
ETN-90-95051 N90-13333 #
ETN-90-95186 N90-13799 #
ETN-90-95239 N90-14099
ETN-90-95240 N90-13676
ETN-90-95241 N90-13643
ETN-90-95243 N90-13981
ETN-90-95244 N90-13882
ETN-90-95245 N90-13663
ETN-90-95264 N90-13926 #
ETN-90-95265 N90-13780 #
ETN-90-95269 N90-13356 #
ETN-90-95281 N90-13582 #
ETN-90-95327 N90-13631 #
ETN-90-95328 N90-13847 #
ETN-90-95506 N90-13911 #
ETN-90-95513 N90-13648 #
ETN-90-95523 N90-13677 #
ETN-90-95527 N90-13499 #
ETN-90-95528 N90-13529 #
ETN-90-95529 N90-13548 #
ETN-90-95612 N90-14018 #
ETN-90-95613 N90-14019 #
ETN-90-95614 N90-14046 #
ETN-90-95615 N90-13989 #
ETN-90-95616 N90-14020 #
ETN-90-95617 N90-14055 #
ETN-90-95618 N90-14021 #
ETN-90-95657 N90-13978 #
ETN-90-95658 N90-13979 #
ETN-90-95659 N90-14062 #
ETN-90-95668 N90-13977 #
ETN-90-95670 N90-14013 #
ETN-90-95673 N90-14014 #
ETN-90-95675 N90-14015 #
ETN-90-95676-PT-4 N90-14018 #
ETN-90-95677 N90-14017 #
ETN-90-95691 N90-13884 #
ETN-90-95695 N90-13707 #
ETN-90-95696 N90-14049 #
ETN-90-95698 N90-14039 #
ETN-90-95699 N90-14040 #
ETN-90-95700 N90-14041 #
ETN-90-95701 N90-14042 #
ETN-90-95702 N90-13983 #
ETN-90-95706 N90-13888 #
ETN-90-95710 N90-13706 #
ETN-90-95715 N90-13378 #
ETN-90-95716 N90-13610 #
ETN-90-95717 N90-13632 #
ETN-90-95718 N90-13800 #
ETN-90-95737 N90-13334 #
ETN-90-95738 N90-13730 #
ETN-90-95739 N90-13339 #
ETN-90-95740 N90-13735 #
ETN-90-95741 N90-13741 #
ETN-90-95743 N90-13649 #

ETN-90-95760 N90-13826 #
ETN-90-95761 N90-13917 #
ETN-90-95765 N90-14074 #
ETN-90-95766 N90-14114 #
ETN-90-95767 N90-13611 #
ETN-90-95768 N90-14115 #
ETN-90-95769 N90-14116 #
ETN-90-95770 N90-13753 #
ETN-90-95771 N90-14117 #
ETN-90-95772 N90-13709 #
ETN-90-95773 N90-13612 #
ETN-90-95774 N20-13710 #
ETN-90-95775 N90-13754 #
ETN-90-95776 N90-14118 #
ETN-90-95777 N90-13821 #
ETN-90-95778 N90-13711 #
ETN-90-95779 N90-13687 #
ETN-90-95780 N90-13801 #
ETN-90-95781 N90-14075 #
ETN-90-95782 N90-13755 #
ETN-90-95783 N90-14066 #
ETN-90-95784 N90-14170 #
ETN-90-95785 N90-14171 #
ETN-90-95786 N90-14067 #
ETN-90-95787 N90-14172 #
ETN-90-95788 N90-14173 #
ETN-90-95789 N90-14068 #
ETN-90-95790 N90-14174 #
ETN-90-95792 N90-14086 #
ETN-90-95793 N90-14071 #
ETN-90-95794 N90-14119 #
ETN-90-95795 N90-14043 #
ETN-90-95796 N90-14044 #
ETN-90-95797 N90-14069 #
ETN-90-95798 N90-14087 #
ETN-90-95799 N90-14088 #
ETN-90-95800 N90-13650 #
ETN-90-95801 N90-14070 #
ETN-90-95803 N90-14089 #
ETN-90-95804 N90-13756 #
ETN-90-95805 N90-13712 #
ETN-90-95806 N90-14050 #
ETN-90-95807 N90-14079 #
ETN-90-95808 N90-14080 #
ETN-90-95809 N90-14047 #
ETN-90-95810 N90-14063 #
ETN-90-95811 N90-14100 #
ETN-90-95812 N90-14081 #
ETN-90-95814 N90-14165 #
ETN-90-95815 N90-14166 #
ETN-90-95817 N90-14123 #
ETN-90-95818 N90-14082 #
ETN-90-95819 N90-14083 #
ETN-90-95820 N90-14150 #
ETN-90-95826 N90-14120 #
ETN-90-95835 N90-13724 #
ETN-90-95841 N90-13644 #
ETN-90-95842 N90-13815 #
ETN-90-95843 N90-13725 #
ETN-90-95844 N90-13629 #
ETN-90-95845 N90-13606 #
ETN-90-95846 N90-13607 #
ETN-90-95847 N90-13816 #
ETN-90-95848 N90-13577 #
ETN-90-95849 N90-13645 #
ETN-90-95861 N90-13367 #
ETN-90-95863 N90-13368 #
ETN-90-95864 N90-13904 #
ETN-90-95871 N90-13802 #
ETN-90-95875 N90-13757 #
ETN-90-95900 N90-13713 #
ETN-90-95909 N90-13781 #
ETN-90-95919 N90-13668 #
ETN-90-95921 N90-13583 #
ETN-90-95922 N90-14101 #
ETN-90-95928 N90-13672 #
ETN-90-95930 N90-13411
ETN-90-95931 N90-14045
ETN-90-95932 N90-13400 #
ETN-90-95935 N90-13409 #
ETN-90-95936 N90-14022 #
ETN-90-95937 N90-14023 #
ETN-90-95938 N90-14024 #
ETN-90-95939 N90-14025 #
ETN-90-95940 N90-14026 #
ETN-90-95941 N90-14027 #
ETN-90-95942 N90-13980 #
ETN-90-95943 N90-14028 #
ETN-90-95944 N90-14048 #
ETN-90-95945 N90-14029 #
ETN-90-95946 N90-13795 #
ETN-90-95947 N90-13996 #
ETN-90-95948 N90-13997 #
ETN-90-95949 N90-14051 #
ETN-90-95950 N90-13998 #
ETN-90-95951 N90-14052 #
ETN-90-95952 N90-14053 #
ETN-90-95953 N90-14054 #
ETN-90-95954 N90-13999 #
ETN-90-95955 N90-14000 #
ETN-90-95956 N90-14001 #
ETN-90-95957 N90-13984 #
ETN-90-95958 N90-14030 #
ETN-90-95959 N90-14031 #
ETN-90-95960 N90-14032 #
ETN-90-95961 N90-14056 #
ETN-90-95962 N90-14057 #
ETN-90-95963 N90-14058 #
ETN-90-95964 N90-13726 #
ETN-90-95965 N90-13993 #
ETN-90-95966 N90-14033 #
ETN-90-95967 N90-14034 #
ETN-90-95968 N90-14059 #
ETN-90-95969 N90-14035 #
ETN-90-95970 N90-14064 #
ETN-90-95971 N90-14036 #
ETN-90-95972 N90-14037 #
ETN-90-95973 N90-13930 #
ETN-90-95974 N90-14065 #
ETN-90-95975 N90-14091 #
ETN-90-95979 N90-13933 #
ETN-90-95980 N90-13357 #
ETN-90-95981 N90-13395 #
ETN-90-95982 N90-13613 #
ETN-90-95983 N90-13614 #
ETN-90-95984 N90-13822 #
ETN-90-95985 N90-13615 #
ETN-90-95986 N90-13758 #
ETN-90-95987 N90-13823 #
ETN-90-95988 N90-13669 #
ETN-90-95990 N90-13379 #
ETN-90-95991 N90-13824 #
ETN-90-95992 N90-13616 #
ETN-90-95993 N90-13410 #
ETN-90-95994 N90-13617 #
ETN-90-95995 N90-13985 #
ETN-90-95996-PT-2 N90-13825 #
ETN-90-96001 N90-13803
ETN-90-96006 N90-13692
ETN-90-96007 N90-13885 #
ETN-90-96008 N90-14145 #
ETN-90-96009 N90-13365 #
ETN-90-96010 N90-13901 #
ETN-90-96011 N90-13727 #
ETN-90-96012 N90-13846 #
ETN-90-96014 N90-14072 #
ETN-90-96015 N90-13633 #
ETN-90-96016 N90-14121 #
ETN-90-96017 N90-13804 #
ETN-90-96018 N90-13634
ETN-90-96019 N90-13912 #
ETN-90-96020 N90-13768 #
ETN-90-96021 N90-13986 #
ETN-90-96022 N90-13651 #
ETN-90-96023 N90-13987 #
ETN-90-96024 N90-13769 #
ETN-90-96025 N90-13714 #
ETN-90-96026 N90-13765 #
ETN-90-96027 N90-13664 #
ETN-90-96028 N90-13705 #
ETN-90-96030 N90-13782 #
ETN-90-96031 N90-13909
ETN-90-96032 N90-13630
ETN-90-96033 N90-13892
ETN-90-96049 N90-13728 #
ETN-90-96050 N90-13778 #
ETN-90-96052 N90-13729 #
ETN-90-96053 N90-13881 #
ETN-90-96054 N90-13882 #
ETN-90-96060 N90-14090 #

FERMILAB-CONF-89/254-A N90-14167* #
FERMILAB-CONF-89/255-A N90-14169* #

FERMILAB-PUB-89/193-A N90-14076* #
FERMILAB-PUB-89/205-A N90-14164* #
FERMILAB-PUB-89/214-A N90-14180* #
FERMILAB-PUB-89/238-A N90-14124* #
FERMILAB-PUB-89/252-A N90-14168* #

FHWA/PA-87/03+85-107 N90-13685 #

FOA-C-20759-2.1 N90-13677 #
FOA-C-20763-2.4 N90-13666 #
FOA-C-20785-2.2 N90-13786 #
FOA-C-30534-3.4 N90-13986 #
FOA-C-30535-9.4 N90-13583 #
FOA-C-30536-3.1 N90-14101 #

GAO/NSIAD-89-137 N90-13687 #

GARRETT-31-8071(1) N90-14153* #

GB-PATENT-APPL-SN-8703469 N90-13662
GB-PATENT-APPL-SN-8813692 N90-13663

GB-PATENT-2-201-677-A N90-13662
GB-PATENT-2-205-846-A N90-13663

GL-TR-89-0124-VOL-1 N90-13897 #
GL-TR-89-0124-VOL-2 N90-13898 #
GL-TR-89-0124-VOL-3 N90-13899 #
GL-TR-89-0124-VOL-4 N90-13900 #

GPO-99-857 N90-14149 #

GRI-88/0293 N90-13766 #
GRI-89/0080 N90-13887 #
GRI-89/0142 N90-13673 #

H-1383 N90-13820* #
H-1515 N90-13372* #
H-1546 N90-13990* #
H-1566 N90-13995* #

HDL-TR-2162 N90-14110 #

HEL-TN-8-89 N90-13375 #

HMI-B-465 N90-14120 #

IAF-88-355 N90-13679* #

ICASE-89-51 N90-13351* #
ICASE-89-72 N90-14038* #
ICASE-89-78 N90-13722* #

ICOMP-89-24 N90-14002* #

ICS-8904 N90-13994* #

ILR-MITT-222 N90-14150 #

IMAG-RR-753-I N90-13884 #
IMAG-RR-761-I N90-13707 #
IMAG-RR-762-M N90-14049 #
IMAG-RR-767-M N90-14039 #
IMAG-RR-768-M N90-14040 #
IMAG-RR-771-M N90-14041 #
IMAG-RR-772-M N90-14042 #
IMAG-RR-773-I N90-13983 #

IMFL-88/35 N90-13356 #

INT-PATENT-CLASS-B29C-47/08 N90-13662

INT-PATENT-CLASS-C07C-125/06 N90-13676
INT-PATENT-CLASS-C08F-138/02 N90-14099
INT-PATENT-CLASS-C08F-230/08 N90-13663
INT-PATENT-CLASS-C08G-65/32 N90-13676
INT-PATENT-CLASS-C08J-3/24 N90-13662
INT-PATENT-CLASS-C10L-1/22 N90-13676
INT-PATENT-CLASS-C23C-14/02 N90-13643
INT-PATENT-CLASS-C23C-28/00 N90-13643

INT-PATENT-CLASS-G02F-1/35 N90-14099
INT-PATENT-CLASS-G11C-11/34 N90-13961

INT-PATENT-CLASS-H01B-3/44 N90-13662
INT-PATENT-CLASS-H01L-29/28 N90-14099

IPPCZ-289 N90-14103 #

ISAL-89-0008 N90-13780 #
ISAL-89-0014 N90-13648 #
ISAL-89-0027 N90-13888 #

ISBN-0-309-04083-3 N90-13492* #
ISBN-0-85679-676-X N90-13619 #
ISBN-0-904947-14-9 N90-13409 #
ISBN-1-871315-03-4 N90-13400 #
ISBN-90-365-0288-8 N90-14035 #
ISBN-90-370-0020-7 N90-13803
ISBN-90-9002789-0 N90-13804 #
ISBN-92-63-10713-X N90-13912 #
ISBN-92-835-0522-0 N90-13358 #
ISBN-92-9092-006-8 N90-13826 #
ISBN-92-9092-012-2 N90-13917 #
ISBN-92-9092-016-5 N90-13499 #
ISBN-92-9092-016-5 N90-13529 #
ISBN-92-9092-016-5 N90-13548 #
ISBN-951-38-3428-X N90-13651 #
ISBN-951-38-3435-2 N90-13789 #
ISBN-951-38-3468-8 N90-13987 #
ISBN-951-666-282-X N90-13705 #
ISBN-951-754-881-8 N90-13714 #
ISBN-952-90091-3-5 N90-13765 #

ISI/RR-89-227 N90-13970 #

ISSN-0065-3713 ..... N90-13411
ISSN-0065-3713 ..... N90-13630
ISSN-0065-3713 ..... N90-13892
ISSN-0065-3713 ..... N90-13909
ISSN-0065-3713 ..... N90-14045
ISSN-0141-4062 ..... N90-13619 #
ISSN-0143-7313 ..... N90-13634
ISSN-0169-2690 ..... N90-13726 #
ISSN-0169-2690 ..... N90-13977 #
ISSN-0169-2690 ..... N90-13993 #
ISSN-0169-2690 ..... N90-14003 #
ISSN-0169-2690 ..... N90-14013 #
ISSN-0169-2690 ..... N90-14014 #
ISSN-0169-2690 ..... N90-14015 #
ISSN-0169-2690 ..... N90-14016 #
ISSN-0169-2690 ..... N90-14017 #
ISSN-0169-2690 ..... N90-14030 #
ISSN-0169-2690 ..... N90-14031 #
ISSN-0169-2690 ..... N90-14032 #
ISSN-0169-2690 ..... N90-14033 #
ISSN-0169-2690 ..... N90-14034 #
ISSN-0169-2690 ..... N90-14056 #
ISSN-0169-2690 ..... N90-14057 #
ISSN-0169-2690 ..... N90-14058 #
ISSN-0171-1342 ..... N90-13333 #
ISSN-0171-1342 ..... N90-13629 #
ISSN-0171-1342 ..... N90-13644 #
ISSN-0171-1342 ..... N90-13724 #
ISSN-0171-1342 ..... N90-13725 #
ISSN-0171-1342 ..... N90-13728 #
ISSN-0171-1342 ..... N90-13729 #
ISSN-0171-1342 ..... N90-13776 #
ISSN-0171-1342 ..... N90-13815 #
ISSN-0171-1342 ..... N90-13881 #
ISSN-0176-7739 ..... N90-13577 #
ISSN-0176-7739 ..... N90-13606 #
ISSN-0176-7739 ..... N90-13607 #
ISSN-0176-7739 ..... N90-13645 #
ISSN-0176-7739 ..... N90-13816 #
ISSN-0176-7739 ..... N90-13882 #
ISSN-0303-4003 ..... N90-13647 #
ISSN-0303-4003 ..... N90-13802 #
ISSN-0347-3694 ..... N90-13668 #
ISSN-0347-3694 ..... N90-13677 #
ISSN-0347-3694 ..... N90-13768 #
ISSN-0347-3694 ..... N90-13966 #
ISSN-0347-3708 ..... N90-13583 #
ISSN-0347-3708 ..... N90-14101 #
ISSN-0355-2713 ..... N90-13705 #
ISSN-0358-5069 ..... N90-13769 #
ISSN-0358-5077 ..... N90-13651 #
ISSN-0358-5077 ..... N90-13987 #
ISSN-0366-0885 ..... N90-13631 #
ISSN-0377-8312 ..... N90-13334 #
ISSN-0377-8312 ..... N90-13339 #
ISSN-0377-8312 ..... N90-13730 #
ISSN-0377-8312 ..... N90-13735 #
ISSN-0377-8312 ..... N90-13741 #
ISSN-0379-6566 ..... N90-13499 #
ISSN-0379-6566 ..... N90-13529 #
ISSN-0379-6566 ..... N90-13548 #
ISSN-0379-6566 ..... N90-13826 #
ISSN-0379-6566 ..... N90-13917 #
ISSN-0524-7705 ..... N90-13649 #
ISSN-0721-4529 ..... N90-13835 #
ISSN-0783-9448 ..... N90-13714 #
ISSN-0923-1714 ..... N90-14035 #
ISSN-0923-1714 ..... N90-14059 #
ISSN-0933-2839 ..... N90-13367 #
ISSN-0933-2839 ..... N90-13368 #
ISSN-0933-2839 ..... N00-13904 #

IZF-1989-11 ..... N90-13692

JIAA-TR-96 ..... N90-13349* #

JPL-PUBL-88-23 ..... N90-13449* #
JPL-PUBL-89-18 ..... N90-13796* #
JPL-PUBL-89-24 ..... N90-13412* #
JPL-PUBL-89-28 ..... N90-14084* #

JPL-400-370-VOL-1 ..... N90-13893* #

JUEL-2248 ..... N90-13631 #

KFK-4522 ..... N90-13647 #
KFK-4599 ..... N90-13802 #

KSC-DM-3282 ..... N90-13813* #

KVI-763 ..... N90-14077 #

LC-89-62778 ..... N90-13492* #

LLTR-89-3 ..... N90-13878* #

LMSC-HEC-TR-F268618-VOL-1 ..... N90-13715* #
LMSC-HEC-TR-F268618-VOL-2 ..... N90-13716* #

LR-511 ..... N90-13933 #
LR-521 ..... N90-13357 #
LR-532 ..... N90-13395 #
LR-534 ..... N90-13613 #
LR-535 ..... N90-13614 #
LR-537 ..... N90-13822 #
LR-539 ..... N90-13615 #
LR-541 ..... N90-13758 #
LR-543-PT-1 ..... N90-13823 #
LR-545 ..... N90-13669 #
LR-547 ..... N90-13379 #
LR-548 ..... N90-13824 #
LR-549 ..... N90-13616 #
LR-550 ..... N90-13410 #
LR-551 ..... N90-13617 #
LR-553 ..... N90-13985 #
LR-559-PT-2 ..... N90-13825 #

LSI-TR-875-9 ..... N90-13934* #

M/NA/TURB-1 ..... N90-13328* #

MA-53 ..... N90-13705 #

MEMO-COSOR-88-15 ..... N90-14022 #
MEMO-COSOR-88-16 ..... N90-14023 #
MEMO-COSOR-88-17 ..... N90-14024 #
MEMO-COSOR-88-21 ..... N90-14025 #
MEMO-COSOR-88-25 ..... N90-14026 #
MEMO-COSOR-88-27 ..... N90-14027 #
MEMO-COSOR-88-29 ..... N90-13980 #
MEMO-COSOR-88-31 ..... N90-14028 #
MEMO-COSOR-88-32 ..... N90-14048 #
MEMO-COSOR-88-34 ..... N90-14029 #
MEMO-COSOR-89-01 ..... N90-13795 #
MEMO-COSOR-89-02 ..... N90-13996 #
MEMO-COSOR-89-03 ..... N90-13997 #
MEMO-COSOR-89-04 ..... N90-14051 #
MEMO-COSOR-89-05 ..... N90-13998 #
MEMO-COSOR-89-06 ..... N90-14052 #
MEMO-COSOR-89-07 ..... N90-14053 #
MEMO-COSOR-89-08 ..... N90-14054 #
MEMO-COSOR-89-09 ..... N90-13999 #
MEMO-COSOR-89-14 ..... N90-14000 #
MEMO-COSOR-89-15 ..... N90-14001 #
MEMO-COSOR-89-16 ..... N90-13984 #

MEMO-INF-89-21 ..... N90-14059 #
MEMO-INF-89-32 ..... N90-14035 #

MEMO-777 ..... N90-13977 #
MEMO-779 ..... N90-14013 #
MEMO-782 ..... N90-14014 #
MEMO-784 ..... N90-14015 #
MEMO-785-PT-4 ..... N90-14016 #
MEMO-786 ..... N90-14017 #
MEMO-788 ..... N90-14003 #
MEMO-789 ..... N90-14030 #
MEMO-792 ..... N90-14031 #
MEMO-793 ..... N90-14032 #
MEMO-794 ..... N90-14056 #
MEMO-795 ..... N90-14057 #
MEMO-796 ..... N90-14058 #
MEMO-797 ..... N90-13726 #
MEMO-798 ..... N90-13993 #
MEMO-799 ..... N90-14033 #
MEMO-800 ..... N90-14034 #

MIT-324 ..... N90-13879* #

MPA-TWB-88-03 ..... N90-13635 #

MPE-PREPRINT-156 ..... N90-14156* #

MRL-88-0007 ..... N90-13641 #
MRL-89-015 ..... N90-13624 #

MSU-EE-FIN-20A-89 ..... N90-13497* #

MTL-TR-89-69 ..... N90-13622 #
MTL-TR-89-78 ..... N90-13640 #
MTL-TR-89-81 ..... N90-13637 #

MTR-88W115 ..... N90-13363 #

NADC-89037-60 ..... N90-13603 #
NADC-89046-60 ..... N90-13639 #

NAE-AN-60 ..... N90-13326 #

NAS 1.15:4137 ..... N90-13372* #
NAS 1.15:4141 ..... N90-13387* #
NAS 1.15:4145 ..... N90-13908* #

NAS 1.15:86277 ..... N90-13820* #
NAS 1.15:100644 ..... N90-13816* #
NAS 1.15:100748 ..... N90-13767* #
NAS 1.15:100751 ..... N90-13976* #
NAS 1.15:100753 ..... N90-13609* #
NAS 1.15:101045 ..... N90-13926* #
NAS 1.15:101090 ..... N90-13329* #
NAS 1.15:101311 ..... N90-13819* #
NAS 1.15:101538 ..... N90-13807* #
NAS 1.15:101581 ..... N90-13694* #
NAS 1.15:101665 ..... N90-14061* #
NAS 1.15:101670 ..... N90-13403* #
NAS 1.15:101704 ..... N90-13990* #
NAS 1.15:101710 ..... N90-13995* #
NAS 1.15:101765 ..... N90-14134* #
NAS 1.15:101853 ..... N90-14152* #
NAS 1.15:101856 ..... N90-14135* #
NAS 1.15:101857 ..... N90-14136* #
NAS 1.15:101858 ..... N90-14137* #
NAS 1.15:101859 ..... N90-14138* #
NAS 1.15:101860 ..... N90-14139* #
NAS 1.15:101863 ..... N90-13493* #
NAS 1.15:101869 ..... N90-14126* #
NAS 1.15:101974 ..... N90-13596* #
NAS 1.15:102014 ..... N90-13679* #
NAS 1.15:102069 ..... N90-13392* #
NAS 1.15:102077 ..... N90-13352* #
NAS 1.15:102153 ..... N90-13447* #
NAS 1.15:102159 ..... N90-13704* #
NAS 1.15:102191 ..... N90-13723* #
NAS 1.15:102196 ..... N90-13332* #
NAS 1.15:102207 ..... N90-13407* #
NAS 1.15:102212 ..... N90-13327* #
NAS 1.15:102223 ..... N90-13324* #
NAS 1.15:102242 ..... N90-13931* #
NAS 1.15:102266 ..... N90-13353* #
NAS 1.15:102313 ..... N90-13590* #
NAS 1.15:102340 ..... N90-13785* #
NAS 1.15:102351 ..... N90-13666* #
NAS 1.15:102359 ..... N90-14002* #
NAS 1.15:102375 ..... N90-14060* #
NAS 1.15:102377 ..... N90-13719* #
NAS 1.15:102380 ..... N90-13597* #
NAS 1.15:102383 ..... N90-13595* #
NAS 1.15:102389 ..... N90-13381* #
NAS 1.15:102392 ..... N90-13786* #
NAS 1.15:102408 ..... N90-13636* #
NAS 1.15:102412 ..... N90-13988* #
NAS 1.15:102419 ..... N90-13389* #
NAS 1.15:102422 ..... N90-13393* #
NAS 1.15:102425 ..... N90-13680* #
NAS 1.15:102428 ..... N90-13355* #
NAS 1.15:102433 ..... N90-13751* #
NAS 1.15:102437 ..... N90-13675* #
NAS 1.15:102447 ..... N90-13797* #
NAS 1.15:102448 ..... N90-13750* #
NAS 1.15:102460 ..... N90-13394* #
NAS 1.15:102469 ..... N90-13749* #
NAS 1.15:102474 ..... N90-13581* #
NAS 1.15:102782 ..... N90-13813* #
NAS 1.19:269 ..... N90-13446* #
NAS 1.21:7011(330) ..... N90-13925* #
NAS 1.21:7056(09) ..... N90-13580* #
NAS 1.26:4235 ..... N90-13370* #
NAS 1.26:4266 ..... N90-13760* #
NAS 1.26:174718 ..... N90-13391* #
NAS 1.26:179522 ..... N90-13390* #
NAS 1.26:179610 ..... N90-13385* #
NAS 1.26:180414 ..... N90-13981* #
NAS 1.26:180499 ..... N90-13965* #
NAS 1.26:181308 ..... N90-13982* #
NAS 1.26:181916-VOL-2 ..... N90-13814* #
NAS 1.26:181934 ..... N90-14038* #
NAS 1.26:181948 ..... N90-13722* #
NAS 1.26:181955 ..... N90-13351* #
NAS 1.26:182230 ..... N90-13388* #
NAS 1.26:182249 ..... N90-13589* #
NAS 1.26:182751 ..... N90-13685* #
NAS 1.26:182961 ..... N90-14160* #
NAS 1.26:182997 ..... N90-13991* #
NAS 1.26:183234 ..... N90-13759* #
NAS 1.26:183290 ..... N90-13772* #
NAS 1.26:183291 ..... N90-13590* #
NAS 1.26:183388 ..... N90-14181* #
NAS 1.26:183677 ..... N90-13715* #
NAS 1.26:183678 ..... N90-13716* #
NAS 1.26:183679 ..... N90-13584* #
NAS 1.26:183720 ..... N90-13678* #
NAS 1.26:183741 ..... N90-13587* #
NAS 1.26:183742 ..... N90-13653* #
NAS 1.26:183744 ..... N90-13681* #
NAS 1.26:183747 ..... N90-13652* #
NAS 1.26:183748 ..... N90-13586* #
NAS 1.26:183749 ..... N90-13654* #
NAS 1.26:183757 ..... N90-13934* #
NAS 1.26:183758 ..... N90-13491* #

NAS 1.26:183768 ..... N90-14125* #
NAS 1.26:183770 ..... N90-13585* #
NAS 1.26:183771 ..... N90-13588* #
NAS 1.26:183805 ..... N90-13497* #
NAS 1.26:183817 ..... N90-13380* #
NAS 1.26:183826 ..... N90-13405* #
NAS 1.26:183827 ..... N90-13594* #
NAS 1.26:183828 ..... N90-13661* #
NAS 1.26:183831 ..... N90-13763* #
NAS 1.26:183832 ..... N90-13404* #
NAS 1.26:183836 ..... N90-14092* #
NAS 1.26:184598 ..... N90-14102* #
NAS 1.26:184656 ..... N90-13449* #
NAS 1.26:184894 ..... N90-13964* #
NAS 1.26:185074 ..... N90-13354* #
NAS 1.26:185109 ..... N90-14153* #
NAS 1.26:185123 ..... N90-13328* #
NAS 1.26:185150 ..... N90-13794* #
NAS 1.26:185153 ..... N90-13761* #
NAS 1.26:185154 ..... N90-13323* #
NAS 1.26:185162 ..... N90-14108* #
NAS 1.26:185167 ..... N90-13968* #
NAS 1.26:185179 ..... N90-13748* #
NAS 1.26:185321 ..... N90-13880* #
NAS 1.26:185327 ..... N90-13963* #
NAS 1.26:185375 ..... N90-14154* #
NAS 1.26:185420 ..... N90-14133* #
NAS 1.26:185463-VOL-1/2 ..... N90-13496* #
NAS 1.26:185474 ..... N90-13401* #
NAS 1.26:185860 ..... N90-13962* #
NAS 1.26:185868 ..... N90-13783* #
NAS 1.26:185884 ..... N90-13369* #
NAS 1.26:185886 ..... N90-13770* #
NAS 1.26:185889 ..... N90-13771* #
NAS 1.26:185893 ..... N90-13894* #
NAS 1.26:185912 ..... N90-13878* #
NAS 1.26:185923 ..... N90-14076* #
NAS 1.26:185926 ..... N90-14124* #
NAS 1.26:185957 ..... N90-13879* #
NAS 1.26:185960 ..... N90-14163* #
NAS 1.26:185961 ..... N90-14176* #
NAS 1.26:185963 ..... N90-13718* #
NAS 1.26:185966 ..... N90-13494* #
NAS 1.26:185978 ..... N90-13492* #
NAS 1.26:185996 ..... N90-13886* #
NAS 1.26:185997 ..... N90-14175* #
NAS 1.26:186000 ..... N90-13618* #
NAS 1.26:186004 ..... N90-14156* #
NAS 1.26:186008 ..... N90-13495* #
NAS 1.26:186071 ..... N90-13966* #
NAS 1.26:186072 ..... N90-13967* #
NAS 1.26:186077 ..... N90-14180* #
NAS 1.26:186079 ..... N90-14164* #
NAS 1.26:186097 ..... N90-13600* #
NAS 1.26:186102 ..... N90-13747* #
NAS 1.26:186103 ..... N90-14178* #
NAS 1.26:186106 ..... N90-13796* #
NAS 1.26:186107 ..... N90-14084* #
NAS 1.26:186108 ..... N90-13412* #
NAS 1.26:186116 ..... N90-13349* #
NAS 1.26:186119 ..... N90-13706* #
NAS 1.26:186120 ..... N90-13883* #
NAS 1.26:186122 ..... N90-13744* #
NAS 1.26:186124 ..... N90-13916* #
NAS 1.26:186126 ..... N90-13994* #
NAS 1.26:186130 ..... N90-13817* #
NAS 1.26:186132 ..... N90-13443* #
NAS 1.26:186134 ..... N90-13441* #
NAS 1.26:186135 ..... N90-13442* #
NAS 1.26:186159 ..... N90-14177* #
NAS 1.26:186166 ..... N90-14167* #
NAS 1.26:186169 ..... N90-14168* #
NAS 1.26:186170 ..... N90-14169* #
NAS 1.55:3050 ..... N90-13413* #
NAS 1.55:10034 ..... N90-13939* #
NAS 1.55:10036 ..... N90-13384* #
NAS 1.60:2926 ..... N90-13444* #
NAS 1.61:1224-VOL-1 ..... N90-13893* #

NAS-SR-1310 ..... N90-13362 #
NAS-SR-1321 ..... N90-13361 #

NASA-CP-3050 ..... N90-13413* #
NASA-CP-10034 ..... N90-13939* #
NASA-CP-10036 ..... N90-13384* #

NASA-CR-4235 ..... N90-13370* #
NASA-CR-4266 ..... N90-13760* #
NASA-CR-174718 ..... N90-13391* #
NASA-CR-179522 ..... N90-13390* #
NASA-CR-179610 ..... N90-13385* #
NASA-CR-180414 ..... N90-13981* #
NASA-CR-180499 ..... N90-13965* #
NASA-CR-181308 ..... N90-13982* #
NASA-CR-181916-VOL-2 ..... N90-13814* #
NASA-CR-181934 ..... N90-14038* #
NASA-CR-181948 ..... N90-13722* #
NASA-CR-181955 ..... N90-13351* #
NASA-CR-182230 ..... N90-13388* #
NASA-CR-182249 ..... N90-13580* #
NASA-CR-182751 ..... N90-13685* #
NASA-CR-182961 ..... N90-14160* #
NASA-CR-182997 ..... N90-13991* #
NASA-CR-183234 ..... N90-13759* #
NASA-CR-183290 ..... N90-13772* #
NASA-CR-183291 ..... N90-13599* #
NASA-CR-183388 ..... N90-14181* #
NASA-CR-183677 ..... N90-13715* #
NASA-CR-183678 ..... N90-13716* #
NASA-CR-183679 ..... N90-13584* #
NASA-CR-183720 ..... N90-13678* #
NASA-CR-183741 ..... N90-13587* #
NASA-CR-183742 ..... N90-13653* #
NASA-CR-183744 ..... N90-13681* #
NASA-CR-183747 ..... N90-13652* #
NASA-CR-183748 ..... N90-13586* #
NASA-CR-183749 ..... N90-13654* #
NASA-CR-183757 ..... N90-13934* #
NASA-CR-183758 ..... N90-13491* #
NASA-CR-183766 ..... N90-14125* #
NASA-CR-183770 ..... N90-13585* #
NASA-CR-183771 ..... N90-13588* #
NASA-CR-183805 ..... N90-13497* #
NASA-CR-183817 ..... N90-13380* #
NASA-CR-183826 ..... N90-13405* #
NASA-CR-183827 ..... N90-13594* #
NASA-CR-183828 ..... N90-13661* #
NASA-CR-183831 ..... N90-13763* #
NASA-CR-183832 ..... N90-13404* #
NASA-CR-183836 ..... N90-14092* #
NASA-CR-184598 ..... N90-14102* #
NASA-CR-184656 ..... N90-13449* #
NASA-CR-184894 ..... N90-13964* #
NASA-CR-185074 ..... N90-13354* #
NASA-CR-185109 ..... N90-14153* #
NASA-CR-185123 ..... N90-13328* #
NASA-CR-185150 ..... N90-13794* #
NASA-CR-185153 ..... N90-13761* #
NASA-CR-185154 ..... N90-13323* #
NASA-CR-185162 ..... N90-14108* #
NASA-CR-185167 ..... N90-13968* #
NASA-CR-185179 ..... N90-13748* #
NASA-CR-185321 ..... N90-13880* #
NASA-CR-185327 ..... N90-13963* #
NASA-CR-185375 ..... N90-14154* #
NASA-CR-185420 ..... N90-14133* #
NASA-CR-185463-VOL-1/2 ..... N90-13496* #
NASA-CR-185474 ..... N90-13401* #
NASA-CR-185860 ..... N90-13962* #
NASA-CR-185868 ..... N90-13783* #
NASA-CR-185884 ..... N90-13369* #
NASA-CR-185886 ..... N90-13770* #
NASA-CR-185889 ..... N90-13771* #
NASA-CR-185893 ..... N90-13894* #
NASA-CR-185912 ..... N90-13878* #
NASA-CR-185923 ..... N90-14076* #
NASA-CR-185926 ..... N90-14124* #
NASA-CR-185957 ..... N90-13879* #
NASA-CR-185960 ..... N90-14163* #
NASA-CR-185961 ..... N90-14176* #
NASA-CR-185963 ..... N90-13718* #
NASA-CR-185966 ..... N90-13494* #
NASA-CR-185978 ..... N90-13492* #
NASA-CR-185996 ..... N90-13886* #
NASA-CR-185997 ..... N90-14175* #
NASA-CR-186000 ..... N90-13618* #
NASA-CR-186004 ..... N90-14156* #
NASA-CR-186008 ..... N90-13495* #
NASA-CR-186071 ..... N90-13966* #
NASA-CR-186072 ..... N90-13967* #
NASA-CR-186077 ..... N90-14180* #
NASA-CR-186079 ..... N90-14164* #
NASA-CR-186097 ..... N90-13600* #
NASA-CR-186102 ..... N90-13747* #
NASA-CR-186103 ..... N90-14178* #
NASA-CR-186106 ..... N90-13796* #
NASA-CR-186107 ..... N90-14084* #
NASA-CR-186108 ..... N90-13412* #
NASA-CR-186116 ..... N90-13349* #
NASA-CR-186119 ..... N90-13706* #
NASA-CR-186120 ..... N90-13883* #
NASA-CR-186122 ..... N90-13744* #
NASA-CR-186124 ..... N90-13916* #
NASA-CR-186126 ..... N90-13994* #
NASA-CR-186130 ..... N90-13817* #
NASA-CR-186132 ..... N90-13443* #
NASA-CR-186134 ..... N90-13441* #
NASA-CR-186135 ..... N90-13442* #
NASA-CR-186159 ..... N90-14177* #
NASA-CR-186166 ..... N90-14167* #
NASA-CR-186169 ..... N90-14168* #
NASA-CR-186170 ..... N90-14169* #
NASA-EP-269 ..... N90-13446* #

NASA-NEWS-RELEASE-89-180 ..... N90-13448*

NASA-PAM-525 ..... N90-14151* #

NASA-RP-1224-VOL-1 ..... N90-13893* #

NASA-SP-7011(330) ..... N90-13925* #
NASA-SP-7056(09) ..... N90-13580* #

NASA-TM-4137 ..... N90-13372* #
NASA-TM-4141 ..... N90-13387* #
NASA-TM-4145 ..... N90-13908* #
NASA-TM-88277 ..... N90-13820* #
NASA-TM-100644 ..... N90-13818* #
NASA-TM-100748 ..... N90-13767* #
NASA-TM-100751 ..... N90-13976* #
NASA-TM-100753 ..... N90-13609* #
NASA-TM-101045 ..... N90-13926* #
NASA-TM-101090 ..... N90-13329* #
NASA-TM-101311 ..... N90-13819* #
NASA-TM-101538 ..... N90-13807* #
NASA-TM-101581 ..... N90-13694* #
NASA-TM-101665 ..... N90-14061* #
NASA-TM-101670 ..... N90-13403* #
NASA-TM-101704 ..... N90-13990* #
NASA-TM-101710 ..... N90-13995* #
NASA-TM-101765 ..... N90-14134* #
NASA-TM-101853 ..... N90-14152* #
NASA-TM-101856 ..... N90-14135* #
NASA-TM-101857 ..... N90-14136* #
NASA-TM-101858 ..... N90-14137* #
NASA-TM-101859 ..... N90-14138* #
NASA-TM-101860 ..... N90-14139* #
NASA-TM-101863 ..... N90-13493* #
NASA-TM-101869 ..... N90-14126* #
NASA-TM-101974 ..... N90-13596* #
NASA-TM-102014 ..... N90-13679* #
NASA-TM-102069 ..... N90-13392* #
NASA-TM-102077 ..... N90-13352* #
NASA-TM-102153 ..... N90-13447* #
NASA-TM-102159 ..... N90-13704* #
NASA-TM-102191 ..... N90-13723* #
NASA-TM-102196 ..... N90-13332* #
NASA-TM-102207 ..... N90-13407* #
NASA-TM-102212 ..... N90-13327* #
NASA-TM-102223 ..... N90-13324* #
NASA-TM-102242 ..... N90-13931* #
NASA-TM-102266 ..... N90-13353* #
NASA-TM-102313 ..... N90-13590* #
NASA-TM-102340 ..... N90-13785* #
NASA-TM-102351 ..... N90-13666* #
NASA-TM-102359 ..... N90-14002* #
NASA-TM-102375 ..... N90-14060* #
NASA-TM-102377 ..... N90-13719* #
NASA-TM-102380 ..... N90-13597* #
NASA-TM-102383 ..... N90-13595* #
NASA-TM-102389 ..... N90-13381* #
NASA-TM-102392 ..... N90-13786* #
NASA-TM-102408 ..... N90-13636* #
NASA-TM-102412 ..... N90-13988* #
NASA-TM-102419 ..... N90-13389* #
NASA-TM-102422 ..... N90-13393* #
NASA-TM-102425 ..... N90-13680* #
NASA-TM-102428 ..... N90-13355* #
NASA-TM-102433 ..... N90-13751* #
NASA-TM-102437 ..... N90-13675* #
NASA-TM-102447 ..... N90-13797* #
NASA-TM-102448 ..... N90-13750* #
NASA-TM-102460 ..... N90-13394* #
NASA-TM-102469 ..... N90-13749* #
NASA-TM-102474 ..... N90-13581* #
NASA-TM-102782 ..... N90-13813* #

NASA-TP-2926 ..... N90-13444* #

NCEL-TN-1799 ..... N90-13811 #

NIKHEF-K/AMPS/89-06 ..... N90-14091 #

NISTIR-89/4111 ..... N90-13656 #

NLR-MP-88018-U ..... N90-13371 #

NOAA-NWS-TDL-CP-89-3 ..... N90-14147 #

NOAA-TM-NWS-WR-206 ..... N90-13910 #

NORDA-242 ..... N90-13914 #

NOS-IHTR-1279 ..... N90-13671 #

NOSC/TD-1631 ..... N90-14098 #
NOSC/TD-1632 ..... N90-13628 #
NOSC/TD-1652 ..... N90-14010 #

NOTA-INTERNA-930 ..... N90-14081 #
NOTA-INTERNA-932 ..... N90-14165 #
NOTA-INTERNA-933 ..... N90-14166 #
NOTA-INTERNA-935 ..... N90-14123 #
NOTA-INTERNA-936 ..... N90-14082 #
NOTA-INTERNA-937 ..... N90-14083 #

NPL-DMA(A)-194 ..... N90-13634

NPS53-89-014 ..... N90-14012 #
NPS62-89-023 ..... N90-14094 #

NRC-30266 ..... N90-13326 #

NRL-MR-6549 ..... N90-14006 #
NRL-MR-6550 ..... N90-13777 #
NRL-MR-6554 ..... N90-14096 #

NRL-PUB-123-1631 ..... N90-14162 #

NRL-R-9219 ..... N90-13992 #
NRL-R-9226 ..... N90-13776 #

NSF/ENG-89015 ..... N90-13606 #

NTIA-SP-89-22 ..... N90-13693 #

NU-CENTER-QEFP-1989-1 ..... N90-13810 #
NU-CENTER-QEFP-1989-2 ..... N90-13602 #
NU-CENTER-QEFP-1989-3 ..... N90-13638 #

ONERA-RS-53/7131-PY ..... N90-13632 #

ONERA-RT-1/3692-SY ..... N90-13800 #

ONERA-RTF-23/7128-EY ..... N90-13672 #

PAPER-7 ..... N90-13420* #

PARGUM-89-02 ..... N90-14073 #

PB89-222723 ..... N90-13920 #
PB89-226435 ..... N90-13665 #
PB89-227813 ..... N90-13608 #
PB89-230700 ..... N90-13674 #
PB89-230833 ..... N90-13910 #
PB89-230858 ..... N90-14147 #
PB89-232367 ..... N90-13693 #
PB89-233506 ..... N90-13890 #
PB89-233514 ..... N90-13891 #
PB89-235170 ..... N90-13887 #
PB89-235188 ..... N90-13766 #
PB89-235196 ..... N90-13673 #
PB89-235402 ..... N90-13903 #
PB89-235907 ..... N90-13656 #

PDA-86-FR-5303-00-06 ..... N90-13385* #

PREPRINT-488 ..... N90-13757 #
PREPRINT-658 ..... N90-14174 #
PREPRINT-660 ..... N90-14086 #
PREPRINT-662 ..... N90-14071 #
PREPRINT-665 ..... N90-14119 #
PREPRINT-667 ..... N90-14043 #
PREPRINT-668 ..... N90-14044 #
PREPRINT-669 ..... N90-14069 #
PREPRINT-670 ..... N90-14087 #
PREPRINT-671 ..... N90-14088 #
PREPRINT-672 ..... N90-13650 #
PREPRINT-673 ..... N90-14070 #
PREPRINT-679 ..... N90-14089 #
PREPRINT-684 ..... N90-13756 #
PREPRINT-685-89 ..... N90-13712 #
PREPRINT-686 ..... N90-14050 #
PREPRINT-687 ..... N90-14079 #
PREPRINT-688 ..... N90-14080 #
PREPRINT-689 ..... N90-14047 #
PREPRINT-690 ..... N90-14063 #
PREPRINT-693 ..... N90-14100 #

PSI-9032/TR-901-VOL-1 ..... N90-13897 #
PSI-9032/TR-901-VOL-2 ..... N90-13898 #
PSI-9032/TR-901-VOL-3 ..... N90-13899 #
PSI-9032/TR-901-VOL-4 ..... N90-13900 #

PWA-5970-40 ..... N90-13388* #

P89-10180 ..... N90-13448*

R-89-10 ..... N90-13903 #

R/D-4618-EN-01 ..... N90-14157 #
R/D-6143-MS-02 ..... N90-13657 #
R/D-6154-MS-02 ..... N90-13809 #

RADC-TR-89-22 ..... N90-13689 #

RAE-TRANS-2171 ..... N90-13408 #

RAND/R-3604/1-AF ..... N90-13383 #
RAND/R-3604/2-AF ..... N90-13382 #

REPT-M6-582500 ..... N90-13610 #
REPT-M6-594000 ..... N90-13378 #

REPT-11 ..... N90-13714 #
REPT-72/87/R486U ..... N90-13932 #
REPT-89-TOU-3-1045 ..... N90-13928 #
REPT-89-82104(5) ..... N90-13491* #
REPT-89800245 ..... N90-13767* #
REPT-89800261 ..... N90-13413* #
REPT-89800264 ..... N90-13906* #
REPT-90800032 ..... N90-13976* #
REPT-90800039 ..... N90-13609* #
REPT-8905 ..... N90-13400 #

RI/RD-89-179 ..... N90-13589* #

ROM1F-89-676 ..... N90-14066 #
ROM1F-89-677 ..... N90-14170 #
ROM1F-89-678 ..... N90-14171 #
ROM1F-89-680-PT-2 ..... N90-14067 #
ROM1F-89-681-PT-1 ..... N90-14172 #
ROM1F-89-682-PT-2 ..... N90-14173 #
ROM1F-89-683 ..... N90-14068 #

RR-805 ..... N90-14181* #

RSRE-MEMO-4279 ..... N90-13973 #

RSRE-88001 ..... N90-13366 #

RTR-109-02 ..... N90-13584* #

R89-22 ..... N90-13879* #

S-HRG-101-348 ..... N90-14149 #

S-601 ..... N90-13704* #

SBIR-89-1 ..... N90-14126* #

SHEP-88/89-6 ..... N90-14086 #

SIR-89-023-VOL-2 ..... N90-13812 #

SLCET-TR-85-0442-F ..... N90-13703 #

SU-CSSA-ASTRO-89-14 ..... N90-14177* #

SWRI-06-7576/13 ..... N90-13391* #
SWRI-7576/45 ..... N90-13390* #

TACOM-TR-13315 ..... N90-13775 #
TACOM-TR-13464 ..... N90-13402 #

TBE-SSD-P601-89-191 ..... N90-13794* #

TD89-1534 ..... N90-13692

TR-1-1987 ..... N90-13367 #
TR-5-1988 ..... N90-13388 #
TR-6-1988 ..... N90-13904 #
TR-17 ..... N90-13655 #
TR-89-14 ..... N90-13975 #
TR-846 ..... N90-13690 #

TT-8902 ..... N90-13409 #

TWR-PUBL-90197 ..... N90-13661* #

TWR-16417 ..... N90-13654* #
TWR-17272-VOL-5 ..... N90-13568* #
TWR-17591-VOL-7 ..... N90-13586* #
TWR-17796-REV-A ..... N90-13405* #
TWR-18445-REV-A ..... N90-13652* #
TWR-19105 ..... N90-13681* #
TWR-19322 ..... N90-13587* #
TWR-19544 ..... N90-13653* #
TWR-19872 ..... N90-13404* #
TWR-19899 ..... N90-13594* #
TWR-19912 ..... N90-13661* #
TWR-19968 ..... N90-13783* #

UA-REPT-814 ..... N90-13965* #

UAH-RR-803 ..... N90-13991* #
UAH-RR-810 ..... N90-13964* #

UBAFFALO/DC/89/TR-112 ..... N90-14113 #

UC-TR-18 ..... N90-13700 #

UDR-TR-87-130 ..... N90-13789 #
UDR-TR-88-137 ..... N90-13960 #

UILU-ENG-89-2222 ..... N90-13960 #
UILU-ENG-89-2223 ..... N90-14008 #
UILU-ENG-89-2224 ..... N90-14009 #
UILU-ENG-89-2227 ..... N90-13788 #
UILU-ENG-89-2229 ..... N90-13702 #

US-PATENT-APPL-SN-304048 ..... N90-13373 #

USAARL-89-13 ..... N90-13919 #

USAAVSCOM-TR-89-A-006 ..... N90-13327* #

USNA-3910-3-13 ..... N90-14183 #

UT-KBS-89-02 ..... N90-14035 #

UWA/DME/TR-89/2 ..... N90-13604 #

VKI-LS-1989-01 ..... N90-13334 #
VKI-LS-1989-03 ..... N90-13730 #
VKI-LS-1989-05 ..... N90-13339 #
VKI-LS-1989-06-VOL-1 ..... N90-13735 #
VKI-LS-1989-06-VOL-2 ..... N90-13741 #

VLSI-MEMO-89-539 ..... N90-13697 #
VLSI-MEMO-89-551 ..... N90-13696 #
VLSI-MEMO-89-552 ..... N90-14140 #
VLSI-MEMO-89-553 ..... N90-13696 #

VPI-E-89-19 ..... N90-13600* #

VTT-PUBL-54 ..... N90-13769 #

VTT-618 ..... N90-13967 #
VTT-619 ..... N90-13651 #

WL-TR-89-29 ..... N90-13774 #

WMO-713 ..... N90-13912 #

WNSD/HYDRO-89-06 ..... N90-13642 #

WO-PATENT-APPL-SN-PCT/G-B87/00 ... N90-13961

WO-PATENT-88/04096 ..... N90-13961

WRDC-TR-89-3074-VOL-2 ..... N90-13812 #
WRDC-TR-89-3076-VOL-2 ..... N90-13398 #
WRDC-TR-89-7008 ..... N90-13936 #

WTHD-187 ..... N90-13803

Appendix—About STAR

Scientific and Technical Aerospace Reports (STAR) is a major component of a comprehensive National Aeronautics and Space Administration information system covering aeronautics, space, and supporting disciplines. *STAR* is issued on the 8th and 23rd of each month and announces current publications of the following types:

- NASA, NASA contractor, and NASA grantee reports
- Reports issued by other U.S. Government agencies, domestic and foreign institutions, universities, and private firms
- Translations in report form
- NASA-owned patents and patent applications
- Other U.S. Government agency and foreign patents and patent applications
- Domestic and foreign dissertations and theses

Journal, book, and conference literature, cover-to-cover journal translations, and certain foreign dissertations are announced in a companion journal, *International Aerospace Abstracts (IAA),* available on subscription from the American Institute of Aeronautics and Astronautics, Technical Information Service, 555 West 57th Street, 12th Floor, New York, NY 10019.

SUBJECT SCOPE

The subject scope of *STAR* and *IAA* includes all aspects of aeronautics and space research and development, supporting basic and applied research, and applications. Aerospace aspects of earth resources, energy development, conservation, oceanography, environmental protection, urban transportation, and other topics of high national priority are also covered.

OTHER NASA PUBLICATIONS

Other NASA publications and information services are described in the publication, *The NASA Scientific and Technical Information System ... and How to Use It,* available without charge from the NASA Scientific and Technical Information Facility, P.O. Box 8757, BWI Airport, MD 21240.

HOW TO USE *STAR* SUBJECT CATEGORIES

STAR is categorized by 10 major subject divisions broken down further into 76 specific subject categories and one general division/category. The major subject divisions are listed on page ii in the Table of Contents, together with a note for each that defines its scope and provides any cross-references. For example:

AERONAUTICS

Includes aeronautics (general); aerodynamics; air transportation and safety; aircraft communications and navigation; aircraft design, testing and performance; aircraft instrumentation; aircraft propulsion and power; aircraft stability and control; and research and support facilities (air).

For related information see also *Astronautics.*

Each major division is further divided into as many as nine specific categories, which are identified by category numbers.

Abstracts in *STAR* are grouped by subject category, the categories appearing in sequential order. Category breaks in the abstract section are identified by the category number and title, and a scope note. Cross-references to other categories are provided as appropriate. For example:

02 AERODYNAMICS

Includes aerodynamics of bodies, combinations, wings, rotors, and control surfaces; and internal flow in ducts and turbomachinery.

For related information see also *34 Fluid Mechanics and Heat Transfer.*

CROSS-REFERENCES

Individual *STAR* abstracts are not ordinarily cross-referenced, except for certain conference reports or book translations that have had separate abstracts written for their component papers or chapters. Citations and abstracts of the components follow immediately after those of the parent document. When the subject content of a component differs sufficiently from the general content of the parent, a cross-reference citation also is printed at the end of the category to which it normally would have been assigned if it were independent.

DOCUMENTS ON MICROFICHE

Documents on microfiche[1] are designated by a pound sign (#) following the accession number. The pound sign is used without regard to the source or quality of the microfiche.

LIMITED REPRODUCIBILITY

A Note of Limited Reproducibility appears in the citation, if one or a combination of the following factors affect the reproducibility of more than 20% of the document. These factors include: faint or broken type, color photographs, black and white photographs, foldouts, dot matrix print, charts/graphs with script notation, non-Roman alphabet, or some other factor that limits the reproducibility of that document. This notation also appears on the microfiche header, with the specific causing factor checked off on a list visible in the second frame.

AVAILABILITIES

One or more sources from which a document announced in *STAR* is available to the public is given in each citation. The most commonly indicated sources and their acronyms or abbreviations are listed below. If the publication is available from a source other than those listed, the publisher and his address will be displayed on the availability line or in combination with the corporate source line.

Avail: NTIS. Sold by the National Technical Information Service. Prices for hard copy (HC) and microfiche (MF) are indicated by a price code following the letters HC or MF in the *STAR* citation. Current values for the price codes are given in the tables on page A-7.

Initially distributed microfiche under the NTIS SRIM (Selected Research in Microfiche) is available at greatly reduced unit prices. For this service and for information concerning subscription to NASA printed reports, consult the NTIS Subscription Section, Springfield, VA 22161.

NOTE ON ORDERING DOCUMENTS: When ordering NASA publications (those followed by the * symbol), use the N accession number. NASA patent applications (only the specifications are offered) should be ordered by the US-Patent-Appl-SN number. Non-NASA publications (no asterisk) should be ordered by the AD, PB, or other *report number* shown on the last line of the citation, not by the N accession number. It is also advisable to cite the title and other bibliographic identification.

(1) A microfiche is a transparent sheet of film, 105 by 148 mm in size, containing as many as 60 to 98 pages of information reduced to micro images (not to exceed 26:1 reduction).

Avail: SOD (or GPO). Sold by the Superintendent of Documents, U.S. Government Printing Office, in hard copy. The current price and order number are given following the availability line. (NTIS will fill microfiche requests, as indicated above, for those documents identified by a # symbol.)

Avail: BLL (formerly NLL): British Library Lending Division, Boston Spa, Wetherby, Yorkshire, England. Photocopies available from this organization at the price shown. (If none is given, inquiry should be addressed to the BLL.)

Avail: DOE Depository Libraries. Organizations in U.S. cities and abroad that maintain collections of Department of Energy reports, usually in microfiche form, are listed in *Energy Research Abstracts.* Services available from the DOE and its depositories are described in a booklet, *DOE Technical Information Center - Its Functions and Services* (TID-4660), which may be obtained without charge from the DOE Technical Information Center.

Avail: ESDU. Pricing information on specific data, computer programs, and details on Engineering Sciences Data Unit (ESDU) topic categories can be obtained from ESDU International Ltd. Requesters in North America should use the Virginia address while all other requesters should use the London address, both of which are on page A-6.

Avail: Fachinformationszentrum, Karlsruhe. Sold by the Fachinformationszentrum Energie, Physik, Mathematik GMBH, Eggenstein Leopoldshafen, Federal Republic of Germany, at the price shown in deutschmarks (DM).

Avail: HMSO. Publications of Her Majesty's Stationery Office are sold in the U.S. by Pendragon House, Inc. (PHI), Redwood City, CA. The U.S. price (including a service and mailing charge) is given, or a conversion table may be obtained from PHI.

Avail: NASA Public Document Rooms. Documents so indicated may be examined at or purchased from the National Aeronautics and Space Administration, Public Documents Room (Room 126), 600 Independence Ave., S.W., Washington, DC 20546, or public document rooms located at NASA installations, and the NASA Pasadena Office at the Jet Propulsion Laboratory.

Avail: Univ. Microfilms. Documents so indicated are dissertations selected from *Dissertation Abstracts* and are sold by University Microfilms as xerographic copy (HC) and microfilm. All requests should cite the author and the Order Number as they appear in the citation.

Avail: US Patent and Trademark Office. Sold by Commissioner of Patents and Trademarks, U.S. Patent and Trademark Office, at the standard price of $1.50 each, postage free. (See discussion of NASA patents and patent applications below.)

Avail: (US Sales Only). These foreign documents are available to users within the United States from the National Technical Information Service (NTIS). They are available to users outside the United States through the International Nuclear Information Service (INIS) representative in their country, or by applying directly to the issuing organization.

Avail: USGS. Originals of many reports from the U.S. Geological Survey, which may contain color illustrations, or otherwise may not have the quality of illustrations preserved in the microfiche or facsimile reproduction may be examined by the public at the libraries of the USGS field offices whose addresses are listed in this Introduction. The libraries may be queried

concerning the availability of specific documents and the possible utilization of local copying services, such as color reproduction.

Avail: Issuing Activity, or Corporate Author, or no indication of availability. Inquiries as to the availability of these documents should be addressed to the organization shown in the citation as the corporate author of the document.

NASA PATENTS AND PATENT APPLICATIONS

Patents and patent applications owned by NASA are announced in *STAR* under appropriate subject categories and are referenced in the *STAR* indexes. In the Report/Accession Number Index, patents are indexed by the NASA Case Number (which appears in lieu of the report number in other indexes), the U.S. Patent Number, the U.S. Patent Application Serial Number, and the U.S. Patent Class. Patent applications for which patents have not yet been issued are indexed by the NASA Case Number and the U.S. Patent Application Serial Number.

NASA *patent application specifications* are sold in paper copy and microfiche by the National Technical Information Service (NTIS). The US-Patent-Appl-SN- number should be used in ordering either paper copy or microfiche from NTIS. Printed copies of *patents* (which are not microfiched) are available for purchase from:

Commissioner of Patents and Trademarks
U.S. Patent and Trademark Office
Washington, DC 20231

When ordering patents, the U.S. Patent Number should be used, and payment must be remitted in advance, by money order or check payable to the Commissioner of Patents and Trademarks. Prepaid purchase coupons for ordering are also available from the Patent and Trademark Office. The patents and patent applications announced in *STAR* are owned by NASA and are available for royalty-free licensing. Requests for licensing terms and further information should be addressed to:

Associate General Counsel for Intellectual Property/Code GP
National Aeronautics and Space Administration
Washington, DC 20546

ELIGIBILITY AND REGISTRATION FOR NASA INFORMATION PRODUCTS AND SERVICES

A variety of services is available to organizations of the following types that have registered with NASA to receive specific services or products:

1. NASA offices and installations, contractors, subcontractors, grantees, and consultants;
2. Other U.S. Government agencies and their contractors;
3. Libraries in the United States that have arrangements with NASA to maintain collections of NASA documents for public reference;
4. Other organizations in the United States having a need for NASA documents in work related to aeronautics and space research;
5. Organizations abroad that have established reciprocal document exchange arrangements with NASA.

Only the central service points or central points of document acquisition and control within qualified organizations are eligible to register for NASA products and services. Domestic organizations that may be eligible to receive various classes of NASA publications and services should address their requests for registration or for further information to:

NASA Scientific and Technical Information Facility
ATTN: Registration Services
P.O. Box 8757
BWI Airport, MD 21240
301-621-0153

Organizations abroad should direct requests to Manager, International STI Activities, NTT, NASA Headquarters, Washington, DC 20546.

AVAILABILITY OF *STAR* ABSTRACTS ON MICROFICHE

Microfiche of the abstract sections of this issue and other issues of *STAR* are available on annual subscription from NTIS as PB90-911300, Attn: Subscriptions, 5285 Port Royal Road, Springfield, VA 22161. Annual subscription rates are $75.50 North America; $151.00 foreign. Abstract sections for previous years retroactive to 1964 are available at the current rates. Microfiche for individual *STAR* issue abstract sections are not available.

PUBLIC COLLECTIONS OF NASA DOCUMENTS

DOMESTIC: NASA and NASA-sponsored documents and a large number of aerospace publications are available to the public for reference purposes at the library maintained by the American Institute of Aeronautics and Astronautics, Technical Information Service, 555 West 57th Street, 12th Floor, New York, NY 10019

EUROPEAN: An extensive collection of NASA and NASA-sponsored publications is maintained by the British Library Lending Division, Boston Spa, Wetherby, Yorkshire, England, for public access. The British Library Lending Division also has available many of the non-NASA publications cited in *STAR*. European requesters may purchase facsimile copy or microfiche of NASA and NASA-sponsored documents, those identified by both the symbols # and * from ESA - Information Retrieval Service, European Space Agency, 8-10 rue Mario-Nikis, 75738 Paris CEDEX 15, France.

FEDERAL DEPOSITORY LIBRARY PROGRAM

In order to provide the general public with greater access to U.S. Government publications, Congress established the Federal Depository Library Program under the Government Printing Office (GPO), with 51 regional depositories responsible for permanent retention of material, inter-library loan, and reference services. At least one copy of nearly every NASA and NASA-sponsored publication, either in printed or microfiche format, is received and retained by the 51 regional depositories. A list of the regional GPO libraries, arranged alphabetically by state, appears on the inside back cover. These libraries are *not* sales outlets. A local library can contact a Regional Depository to help locate specific reports, or direct contact may be made by an individual.

ADDRESSES OF ORGANIZATIONS

American Institute of Aeronautics and Astronautics
Technical Information Service
555 West 57th Street, 12th Floor
New York, New York 10019

British Library Lending Division,
Boston Spa, Wetherby, Yorkshire,
England

Commissioner of Patents and Trademarks
U.S. Patent and Trademark Office
Washington, DC 20231

Department of Energy
Technical Information Center
P.O. Box 62
Oak Ridge, Tennessee 37830

European Space Agency-Information Retrieval Service
ESRIN
Via Galileo Galilei
00044 Frascati (Rome) Italy

Engineering Sciences Data Unit International
P.O. Box 1633
Manassas, Virginia 22110

Engineering Sciences Data Unit International, Ltd.
251-259 Regent Street
London, W1R 7AD, England

Fachinformationszentrum Energie, Physik, Mathematik
GMBH
7514 Eggenstein Leopoldshafen
Federal Republic of Germany

Her Majesty's Stationery Office
P.O. Box 569, S.E. 1
London, England

NASA Scientific and Technical Information Facility
P.O. Box 8757
BWI Airport, Maryland 21240

National Aeronautics and Space Administration
Scientific and Technical Information Division (NTT)
Washington, DC 20546

National Technical Information Service
5285 Port Royal Road
Springfield, Virginia 22161

Pendragon House, Inc.
899 Broadway Avenue
Redwood City, California 94063

Superintendent of Documents
U.S. Government Printing Office
Washington, DC 20402

University Microfilms
A Xerox Company
300 North Zeeb Road
Ann Arbor, Michigan 48106

University Microfilms, Ltd.
Tylers Green
London, England

U.S. Geological Survey Library National Center
MS 950
12201 Sunrise Valley Drive
Reston, Virginia 22092

U.S. Geological Survey Library
2255 North Gemini Drive
Flagstaff, Arizona 86001

U.S. Geological Survey
345 Middlefield Road
Menlo Park, California 94025

U.S. Geological Survey Library
Box 25046
Denver Federal Center, MS914
Denver, Colorado 80225

NTIS PRICE SCHEDULES

(Effective January 1, 1990)

Schedule A
STANDARD PRICE DOCUMENTS AND MICROFICHE

PRICE CODE	NORTH AMERICAN PRICE	FOREIGN PRICE
A01	$ 8.00	$ 16.00
A02	11.00	22.00
A03	15.00	30.00
A04-A05	17.00	34.00
A06-A09	23.00	46.00
A10-A13	31.00	62.00
A14-A17	39.00	78.00
A18-A21	45.00	90.00
A22-A25	53.00	106.00
A99	*	*
N01	60.00	120.00
N02	59.00	118.00
N03	20.00	40.00

Schedule E
EXCEPTION PRICE DOCUMENTS AND MICROFICHE

PRICE CODE	NORTH AMERICAN PRICE	FOREIGN PRICE
E01	$10.00	$ 20.00
E02	12.00	24.00
E03	14.00	28.00
E04	16.50	33.00
E05	18.50	37.00
E06	21.50	43.00
E07	24.00	48.00
E08	27.00	54.00
E09	29.50	59.00
E10	32.50	65.00
E11	35.00	70.00
E12	38.50	77.00
E13	41.00	82.00
E14	45.00	90.00
E15	48.50	97.00
E16	53.00	106.00
E17	57.50	115.00
E18	62.00	124.00
E19	69.00	138.00
E20	80.00	160.00
E99	*	*

* Contact NTIS for price quote.

IMPORTANT NOTICE

NTIS Shipping and Handling Charges

U.S., Canada, Mexico — ADD $3.00 per TOTAL ORDER

All Other Countries — ADD $4.00 per TOTAL ORDER

Exceptions — Does NOT apply to:

ORDERS REQUESTING NTIS RUSH HANDLING

ORDERS FOR SUBSCRIPTION OR STANDING ORDER PRODUCTS *ONLY*

NOTE: Each additional delivery address on an order requires a separate shipping and handling charge.

FEDERAL REGIONAL DEPOSITORY LIBRARIES

ALABAMA

AUBURN UNIV. AT MONTGOMERY LIBRARY
Documents Department
Montgomery, AL 36193
(205) 279-9110 ext.253

UNIV. OF ALABAMA LIBRARY
Reference Department/Documents
Box S
Tuscaloosa, AL 35486
(205) 348-6046

ARIZONA

DEPT. OF LIBRARY, ARCHIVES, AND PUBLIC RECORDS
Third Floor State Capitol
1700 West Washington
Phoenix, AZ 85007
(602) 255-4121

ARKANSAS

ARKANSAS STATE LIBRARY
Documents Service Section
One Capitol Mall
Little Rock, AR 72201
(501) 371-2090

CALIFORNIA

CALIFORNIA STATE LIBRARY
Govt. Publications Section
914 Capitol Mall
Sacramento, CA 95814
(916) 322-4572

COLORADO

UNIV. OF COLORADO
Norlin Library
Government Publications Division
Campus Box 184
Boulder, CO 80309
(303) 492-8834

DENVER PUBLIC LIBRARY
Govt. Pub. Department
1357 Broadway
Denver, CO 80203
(303) 571-2346

CONNECTICUT

CONNECTICUT STATE LIBRARY
231 Capitol Avenue
Hartford, CT 06106
(203) 566-4971

FLORIDA

UNIV. OF FLORIDA LIBRARIES
Documents Department
Library West
Gainesville, FL 32611
(904) 392-0367

GEORGIA

UNIV. OF GEORGIA LIBRARIES
Government Documents Dept.
Athens, GA 30602
(404) 542-8949

HAWAII

UNIV. OF HAWAII
Hamilton Library
Government Documents Collection
2550 The Mall
Honolulu, HI 96822
(808) 948-8230

IDAHO

UNIV. OF IDAHO LIBRARY
Documents Section
Moscow, ID 83843
(208) 885-6344

ILLINOIS

ILLINOIS STATE LIBRARY
Federal Documents
Centennial Building
Springfield, IL 62756
(217) 782-5012

INDIANA

INDIANA STATE LIBRARY
Serials Section
140 North Senate Avenue
Indianapolis, IN 46204
(317) 232-3686

IOWA

UNIV. OF IOWA LIBRARIES
Government Publications Dept.
Iowa City, IA 52242
(319) 335-5926

KANSAS

UNIVERSITY OF KANSAS
Spencer Research Library
Government Documents
Lawrence, KS 66045
(913) 864-4662

KENTUCKY

UNIV. OF KENTUCKY LIBRARIES
Government Publications/Maps Dept.
Lexington, KY 40506
(606) 257-8400

LOUISIANA

LOUISIANA STATE UNIVERSITY
Middleton Library
Government Documents Dept.
Baton Rouge, LA 70803
(504) 388-2570

LOUISIANA TECHNICAL UNIV.
Prescott Memorial Library
Government Documents Dept.
Ruston, LA 71272
(318) 257-4962

MAINE

UNIVERSITY OF MAINE
Raymond H. Fogler Library
Govt. Documents & Microforms Dept.
Orono, ME 04469
(207) 581-1680

MARYLAND

UNIVERSITY OF MARYLAND
McKeldin Library
Documents/Maps Room
College Park, MD 20742
(301) 454-3034

MASSACHUSETTS

BOSTON PUBLIC LIBRARY
Government Documents Dept.
666 Boylston Street
Boston, MA 02117
(617) 536-5400 ext.226

MICHIGAN

DETROIT PUBLIC LIBRARY
5201 Woodward Avenue
Detroit, MI 48202
(313) 833-1409

LIBRARY OF MICHIGAN
Government Documents
P.O. Box 30007
735 E. Michigan Avenue
Lansing, MI 48909
(517) 373-1593

MINNESOTA

UNIVERSITY OF MINNESOTA
Wilson Library
Government Publications
309 Nineteenth Avenue South
Minneapolis, MN 55455
(612) 373-7813

MISSISSIPPI

UNIV. OF MISSISSIPPI LIB.
Government Documents Dept.
106 Old Gym Bldg.
University, MS 38677
(601) 232-5857

MISSOURI

University of Missouri at Columbia Library
Government Documents
Columbia, MO 65201
(314) 882-6733

MONTANA

UNIV. OF MONTANA
Mansfield Library
Documents Division
Missoula, MT 59812
(406) 243-6700

NEBRASKA

UNIVERSITY OF NEBRASKA - LINCOLN
Love Memorial Library
Documents Department
Lincoln, NE 68588
(402) 472-2562

NEVADA

UNIV. OF NEVADA-RENO LIB.
Govt. Pub. Department
Reno, NV 89557
(702) 784-6579

NEW JERSEY

NEWARK PUBLIC LIBRARY
U.S. Documents Division
5 Washington Street
P.O. Box 630
Newark, NJ 07101
(201) 733-7812

NEW MEXICO

UNIVERSITY OF NEW MEXICO
General Library
Government Publications/Maps Dept.
Albuquerque, NM 87131
(505) 277-5441

NEW MEXICO STATE LIBRARY
325 Don Gaspar Avenue
Santa Fe, NM 87501
(505) 827-3826

NEW YORK

NEW YORK STATE LIBRARY
Documents Sect. Cultural Educ. Ctr.
Empire State Plaza
Albany, NY 12230
(518) 474-5563

NORTH CAROLINA

UNIVERSITY OF NORTH CAROLINA AT CHAPEL HILL
Davis Library 080A
BA/SS Department Documents
Chapel Hill, NC 27514
(919) 962-1151

NORTH DAKOTA

NORTH DAKOTA STATE UNIVERSITY LIBRARY
Government Documents Dept.
Fargo, ND 58105
(701) 237-8352
In cooperation with Univ. of North Dakota, Chester Fritz Library
Grand Forks

OHIO

STATE LIBRARY OF OHIO
Documents Section
65 South Front Street
Columbus, OH 43266
(614) 644-7051

OKLAHOMA

OKLAHOMA DEPT. OF LIBRARIES
Government Documents
200 NE 18th Street
Oklahoma City, OK 73105
(405) 521-2502, ext. 252

OKLAHOMA STATE UNIV. LIB.
Documents Department
Stillwater, OK 74078
(405) 624-0489

OREGON

PORTLAND STATE UNIV.
Millar Library
934 SW Harrison - P.O. Box 1151
Portland, OR 97207
(503) 229-3673

PENNSYLVANIA

STATE LIBRARY OF PENN.
Government Publications Section
Box 1601
Walnut St. & Commonwealth Ave.
Harrisburg, PA 17105
(717) 787-3752

SOUTH CAROLINA

CLEMSON UNIV. COOPER LIB.
Documents Department
Clemson, SC 29634
(803) 656-5174
In cooperation with Univ. of South Carolina, Thomas Cooper Library, Columbia

TEXAS

TEXAS STATE LIBRARY
Public Services Department
P.O. Box 12927 - 1201 Brazos
Austin, TX 78711
(512) 463-5455

TEXAS TECH. UNIV. LIBRARY
Documents Department
Lubbock, TX 79409
(806) 742-2268

UTAH

UTAH STATE UNIVERSITY
Merrill Library & Learning Resources Center, UMC-30
Documents Department
Logan, UT 84322
(801) 750-2682

VIRGINIA

UNIVERSITY OF VIRGINIA
Alderman Library
Government Documents
Charlottesville, VA 22903
(804) 924-3133

WASHINGTON

WASHINGTON STATE LIBRARY
Document Section
Olympia, WA 98504
(206) 753-4027

WEST VIRGINIA

WEST VIRGINIA UNIV. LIB.
Government Documents Section
P.O. Box 6069
Morgantown, WV 26506
(304) 293-3640

WISCONSIN

ST. HIST SOC. OF WISCONSIN LIB.
Government Pub. Section
816 State Street
Madison, WI 53706
(608) 262-2781
In cooperation with Univ. of Wisconsin-Madison, Memorial Library

MILWAUKEE PUBLIC LIBRARY
Documents Division
814 West Wisconsin Avenue
Milwaukee, WI 53233
(414) 278-3065

WYOMING

WYOMING STATE LIBRARY
Supreme Court & Library Bldg.
Cheyenne, WY 82002
(307) 777-5919

National Aeronautics and
Space Administration
Code NTT
Washington, D.C.
20546

Official Business
Penalty for Private Use, $300

SPECIAL FOURTH-CLASS RATE
POSTAGE & FEES PAID
NASA
PERMIT No. G27

NASA

POSTMASTER: If Undeliverable (Section 158
Postal Manual) Do Not Return